Natural Resources Canada | Ressources naturelles Canada

GEOLOGICAL SURVEY OF CANADA
OPEN FILE 7843

TGI 4 – Intrusion Related Mineralisation Project: New Vectors to Buried Porphyry-Style Mineralisation

N. Rogers (ed.)

2015

Canada

GEOLOGICAL SURVEY OF CANADA
OPEN FILE 7843

TGI 4 – Intrusion Related Mineralisation Project: New Vectors to Buried Porphyry-Style Mineralisation

N. Rogers (ed.)

2015

© Her Majesty the Queen in Right of Canada, as represented by the Minister of Natural Resources Canada, 2015

doi:10.4095/296462

This publication is available for free download through GEOSCAN (http://geoscan.nrcan.gc.ca).

Recommended citation
Rogers, N. (ed.), 2015. TGI 4 – Intrusion Related Mineralisation Project: New Vectors to Buried Porphyry-Style Mineralisation; Geological Survey of Canada, Open File 7843, 578 p. doi:10.4095/296462

Publications in this series have not been edited; they are released as submitted by the author.

TGI 4 – Intrusion Related Mineralisation Project:
New Vectors to Buried Porphyry-Style Mineralisation

Edited and compiled by
Neil Rogers

TGI 4 – Intrusion Related Mineralisation Project: A synthesis
N. Rogers 1

Till composition near Cu-porphyry deposits in British Columbia: Highlights for mineral exploration
A. Plouffe and T. Ferbey 15

Till, stream sediment, and stream water geochemical signatures of intrusion-hosted Sn-W deposits: examples from the Sisson W-Mo and Mount Pleasant Sn-W-Mo-Bi-In deposits, New Brunswick
M.B. McClenaghan, M.A. Parkhill, A.G. Pronk, A.A. Seaman, M.W. McCurdy, R.S. Poulin, A.M. McDonald, D.J. Kontak and M.I. Leybourne 39

Tectonostratigraphic controls on the Connaigre Peninsula of south-central Newfoundland and their implications for intrusion-related mineral resources
N. Rogers, D.A. Kellett, V.J. McNicoll, C.R. van Staal, A. Kerr and G. Ruberti 59

Petrographic observations and evaporate mound analysis of quartz-hosted fluid inclusions hosted by granitoid samples from the South Mountain Batholith, Nova Scotia: An exploration tool for vectoring towards mineralized areas in intrusive rocks
F. Tweedale, J.J. Hanley, D.J. Kontak and N. Rogers 79

Controls on indium mineralization in tin-tungsten-base metal deposits of the Canadian Appalachians
C.R. Goeddeke, J.B. Chapman and I.M. Samson 101

Appendix I: TGI 4 – Intrusion Related Mineralisation Project field trip guidebooks 111

Granite-related mineralization and alteration in the Acadian Plutonic Belt: Implications for Sn-W-Mo-Cu exploration in central New Brunswick – TGI 4 Field Guide
N. Rogers, M.B. McClenaghan, K.G. Thorne, L.R. Fyffe, A.A. Seaman, M.A. Parkhill, S.H. McClenaghan, A.G. Pronk, K.L. Beal, D.R. Lentz, R.A. Wilson, J.M. Rice, and C. Lentz 113

The Coast of Bays: Paleozoic tectonic evolution of the Gander margin and adjacent Avalonia in southeastern Newfoundland – TGI 4 Field Guide
C.R. van Staal, G. Ruberti, A. Kerr, J. Conliffe and N. Rogers 205

Appendix II: TGI 4 – Intrusion Related Mineralisation Project presentations.....247

Identifying new vectors to hidden porphyry-style mineralisation
N. Rogers, A. Plouffe, J.B. Chapman, M.B. McClenaghan, D.A. Kellett and R.A. Anderson 249

Glacial stratigraphic, till geochemical, and indicator mineral studies at the Sisson W-Mo and Mount Pleasant Sn-W-Mo-Bi-In polymetallic deposits, southwestern New Brunswick
M.A. Parkhill, M.B. McClenaghan, A.A. Seaman, A.G. Pronk and J.M. Rice 293

Scheelite geochemical signatures and potential for fingerprinting ore deposits
R.S. Poulin, A.M. McDonald, D.J. Kontak and M.B. McClenaghan 317

Geological and structural controls on hydrothermal alteration and W-Mo mineralization in the Sisson deposit, New Brunswick
J.R. Lang, R. Duncan, D.R. Lentz, W. Zhang, A. Bustard, C.R.M. McFarlane and K.G. Thorne 327

Petrologic and geochemical examination of the Early Devonian, Evandale porphyry Cu-Mo-(Au) deposit, southern New Brunswick: Geothermobarometric analysis of petrogenesis
T. White, D.R. Lentz and C.R.M. McFarlane 343

Fluid inclusion and stable isotope evidence for mixing of magmatic – hydrothermal fluids with meteoric water in vein-type Cu-Au-Bi deposits, southern New Brunswick, Canada
J.J. Hanley, F. Tweedale, K. Neyedley, R. Sharpe and M. Fayek 361

Petrographic observations and evaporate mound analysis of quartz-hosted fluid inclusions: Applications to assess metal fertility in granites
F. Tweedale, J.J. Hanley, D.J. Kontak and N. Rogers 369

The south Newfoundland granophile mineral district: Features and opportunities for research on blind deposits
A. Kerr 383

Mineralogy and chemistry of tourmaline in the Woodjam porphyry deposits, British Columbia
J.B. Chapman 403

Gold mineralization in the Cantung W-skarn deposit, Northwest Territories: An examination of distribution, mineralogy, and petrogenesis
E.M. Palmer, C.R.M. McFarlane, D.R. Lentz and H. Falck 415

Feldspar triclinicity, superheating and mineralization
R. Girard, C. Potvin-Doucet, L.P. Bédard and F. Bouchard 429

Chemical fingerprinting of the Archean Côté Gold deposit: A large-tonnage, low-grade intrusion-related deposit system, Ontario, Canada
L.R. Katz, D.J. Kontak, B. Dubé and J.R. Rogers 445

Using biotite composition of the Devonian Lake George granodiorite, New Brunswick, as a case study for W-Mo-Au-Sb mineralized magmatic hydrothermal systems
Z. Azadbakht, D.R. Lentz and C.R.M. McFarlane 459

Trace elements and oxygen isotope of quartz from the Nashwaak Granite and dykes, and quartz veins related to the Sisson Brook W-Mo-Cu deposit, west-central New Brunswick
W. Zhang, D.R. Lentz, C.R.M. McFarlane and K.G. Thorne 475

Are there elephants hiding in the Jurassic of Yukon? A tectonomagmatic perspective on porphyry prospectivity
J.B. Chapman 493

Magmatic evolution in Devonian granitic rocks and relation to granophile mineralization in New Brunswick: Application of biotite trace element mapping with EPMA and LA-ICP-MS
Z. Azadbakht, D.R. Lentz and C.R.M. McFarlane 507

Mineral markers of porphyry processes: regional and local signatures of porphyry prospectivity
J.B. Chapman, A. Plouffe, S.E. Jackson, J.J. Ryan and T. Ferbey 521

Using biotite composition of the Devonian Mount Elizabeth Intrusive Complex, New Brunswick, as a proxy for magma fertility and differentiation in W-Mo-Au-Sb mineralized magmatic hydrothermal systems
Z. Azadbakht, D.R. Lentz and C.R.M. McFarlane 535

Magmatic evolution of the Late Devonian Mount Douglas leucogranites, southwestern New Brunswick, Canada; An example of extreme fractional crystallization
N. Mohammadi and D.R. Lentz 547

Structural and tectonic controls on Devonian intrusion related mineralisation on the Connaigre Peninsula, Newfoundland
G. Ruberti, N. Rogers, D.A. Kellett, C.R. van Staal and J. Hanchar 559

Magmatic mica and its potential as an indicator of magma fertility in the granitoids of New Brunswick
Z. Azadbakht, D.R. Lentz and C.R.M. McFarlane 561

Biotite chemistry as a monitor of magma fertility and mineralisation potential: Results from the Devonian granitoids of New Brunswick
Z. Azadbakht, D.R. Lentz, C.R.M. McFarlane and N. Rogers 563

Magmatic biotite and its use to distinguish barren and mineralized granitic systems in New Brunswick, Canada
Z. Azadbakht, D.R. Lentz and C.R.M. McFarlane 565

Sn-W-Mo polymetallic behaviour during magmatic evolution of Late Devonian Mount Douglas leucogranites, southwestern New Brunswick, Canada
N. Mohammadi, D.R. Lentz and K.G. Thorne 567

Methodology for solute characterization of fluid inclusions by petrographic and SEM/EDS complementary analysis
F. Tweedale, J.J. Hanley, D.J. Kontak and N. Rogers 569

TGI 4: Investigating structural and tectonic controls on Devonian intrusion related mineralisation on the Connaigre Peninsula, Newfoundland
N. Rogers, G. Ruberti, D.A. Kellett, C.R. van Staal and J. Hanchar 571

TGI 4 – Intrusion Related Mineralisation Project: A synthesis

Neil Rogers

Geological Survey of Canada, 601 Booth St., Ottawa, Ontario

Abstract: The Targeted Geoscience Initiative 4 (TGI 4) was a 2010-15 Government of Canada research program to conduct thematic, knowledge-driven ore systems studies aimed at assisting in the discovery of future resources through more effective targeting of buried mineral deposits.

Intrusion related (e.g., porphyry) deposits are the world's most important sources for Cu, Mo, W and Sn, as well as being a major contributor of Au, Ag, and PGEs. Porphyry deposits are typically large, low- to medium-grade deposits in which mineralisation is hosted within and immediately surrounding distinctive intrusive phases within larger intrusive complexes that commonly have prolonged emplacement histories. To develop more effective exploration criteria to identify and evaluate deeply buried and/or hidden fertile intrusive mineralising systems, studies into Cu-Mo/Au and W-Mo-Sn systems are aimed at answering the following questions: i) are there distinctive proximal and distal footprints for deposit types that will allow identification of, and vectoring towards hidden economically viable deposits?; and ii) what are the triggering conditions and indicators of an hydrothermal-magmatic system of size and duration sufficient to develop a large porphyry deposit? To help answer these questions studies are being undertaken at sites associated with the Triassic-Jurassic porphyry deposits of the British Columbia interior and for the array of mineralised Devonian intrusions developed in the Canadian Appalachians.

A common problem facing Cordilleran and Appalachian exploration is how to detect intrusion-related mineralization through the extensive glacial sediment cover. Consequently, research activities are focussing at identifying key geochemical and mineral indicators in till near known mineralisation and their detrital dispersal down-ice. Indicators are being developed for the detection of mineralisation, but also the alteration halos and vein systems associated with mineralization, which represent much larger exploration targets than the actual economic orebody itself. Once identified in till, these indicators can be traced to their bedrock source using reconstructed ice movement vectors.

Structural relationships indicate that Sn-W-Mo mineralised intrusive systems can form due to extension associated with far removed non-orthogonal accretion. Deposits within these bodies form along fluid pathways such as the intersection of high-angle syntectonic breaks. Mineral potential can also be resolved through trace element fingerprinting. Subtle compositional changes in commonly occurring minerals (i.e., biotite) and fluid inclusions provide evidence of chemical variations related to magma fertility and vectors to mineralisation.

Introduction

The Targeted Geoscience Initiative 4 (TGI 4) was a five year (2010-15) collaborative research program instigated by the Government of Canada to develop geoscience knowledge to support enhanced effectiveness of deep exploration. The underlying objectives of the program are to: 1) develop more robust measures of whether a geological system may contain deeply buried ore in order to reduce exploration risk; 2) develop new geoscience knowledge and innovative techniques to model and detect Canada's major mineral systems; and 3) train and mentor students to increase the number of highly-qualified personnel available to the mineral industry. To achieve these objectives the program was constructed to conduct thematic research that was targeted at resolving specific geoscientific problems that inhibit development of effective mineral exploration programs, as opposed to providing additional data to known mineral districts. The intension being that the resulting exploration models will be exportable to new regions and thus facilitate the discovery of the next generation of mineral deposits. In particular that these models will help in the discovery of deeply buried and/or hidden ore (whether it be by a thick sequence of country-rock or a thin veneer of surficial materials) that have defied identification using standard exploration methods.

Research themes within TGI 4 were constructed within "ore systems", which is an approach that focuses of the processes of ore formation, as opposed to the characteristics of specific deposits. The ore system concept is broken down into four parts, namely what terrane to look in, where to look in a terrane, vectors towards ore and detection methods (Fig. 1). The principal questions when determining what terrane to look in are related to tectonic setting and temporal extent, and may include:

- What are the optimal tectonic settings for a particular deposit type?
- How do we recognise these settings?
- Is this deposit type unique to one location and/or time period?

For the second part of where in a terrane to look, then questions are based around lithologic and structural controls, such as:

- Are there optimal rock associations for a particular ore environment?

Corresponding author: Neil Rogers (nrogers@nrcan.gc.ca)

Rogers, N., 2015. TGI 4 – Intrusion Related Mineralisation Project: A synthesis; *in* TGI 4 – Intrusion Related Mineralisation Project: New Vectors to Buried Porphyry-Style Mineralisation, (ed.) N. Rogers; Geological Survey of Canada, Open File 7843, p. 1-13.

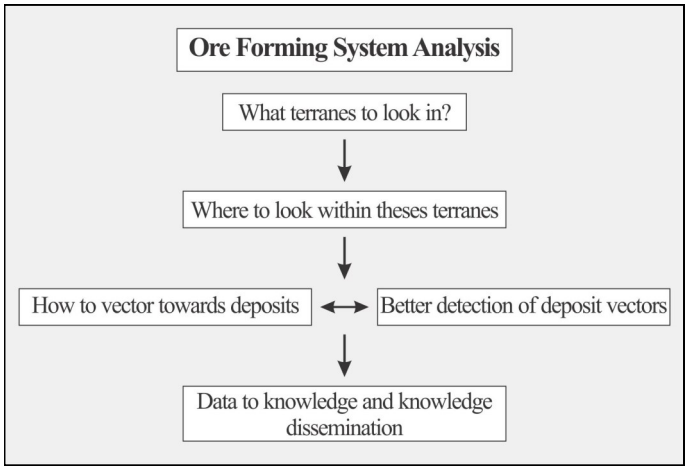

Figure 1 – Ore system conceptual model.

- Are there regional-scale structural controls that focus the ore system?

The third part of the ore system concept is related to vectoring towards ore, which breaks down the individual component parts of how an ore deposit is formed. These aspects are examined to determine whether there are distinctive features that can characterise the potential of or provide directional information to ore. In general the component parts for ore development are as follows:

- Extraction from source – What is the energy driving the system? What are the sources of metals and fluids?
- Migration to trap – How are fluids focussed? What is the nature and extent of fluid pathways?
- Formation of trap – What is the trapping mechanism for ore fluids? Under what conditions do these traps form?
- Deposition of metal – What conditions are necessary for metal precipitation? Are multiple events required to develop ore grade materials?
- Secondary processes – Is post-deposition remobilisation of ore essential in forming economically significant deposits?

The final part of the ore system concept relates to detection methods and techniques, which looks at how improved knowledge on controls of mineralisation can be adapted into enhanced exploration tools and models.

Intrusion related ore system

The term intrusion related ore system is somewhat of a misnomer as it includes two distinct deposit types and does not include all ores generated by intrusive processes. The deposit types under investigation are Cu- and Cu-Mo(-Au) porphyries and post-accretionary granitoid Sn-W-Mo-In deposits. Although these types of mineral deposit form in different tectonic environments and are associated with unrelated varieties of granitoid intrusive rocks, they do share common traits within the mechanisms associated with ore formation that correspond to a single ore system. In a broad sense the common mechanism can be considered as porphyry-style mineralisation, which can be generally envisioned as hydrothermal system driven by intrusive magmatism where the ore metals are temporally and genetically related to the intrusion. Detailed descriptions of porphyry-style mineralisation processes are provided by Sinclair (2007), Sillitoe (2010) and Richards (2011).

The empirical model for porphyry-style mineralisation described by Sinclair (2007) consists of large, low- to medium-grade deposits that are formed in response to extensive, polyphase magmatic-hydrothermal systems developed within and above genetically-related intrusions. Meteoric fluids play a major role in this generic model, as they are typically considered to be largely responsible, though not essential in all cases, for features such as phreatic brecciation that can provide a trap for ore and large-scale alteration (i.e., sericitic alteration) halos (see Sillitoe (2010) and references therein). A modification of the general model has been referred to as the "orthomagmatic" model (Burnham, 1967, 1979; Phillips, 1973; Whitney, 1975, 1984; Sinclair, 2007) where crystallisation produces a volatile phase that transports and concentrates ore metals toward the carapace of the magma chamber (Christiansen et al., 1983; Candela and Holland, 1986; Manning and Pichavant, 1988; Candela, 1989; Cline and Bodnar, 1991; Heinrich et al., 1992). The induced fluid pressure may result in fracturing and rapid escape of the ore bearing fluids into the space provided. The sudden drop in pressure following fracturing causing adiabatic cooling of the fluid phase, which in turn can result in ore precipitation. An addendum to this model has the magmatic processes related to volatile phase generation and transport/ concentration of ore metals causing the upper reaches of a magma chamber to remain largely liquid through-out much of the ore forming process (Shannon et al., 1982; Carten et al., 1988; Kirkham and Sinclair, 1988; Shinohara et al., 1995; Sinclair, 2007).

Porphyry-style mineralisation constitutes the world's most important source for Cu, Mo, W and Sn, as well as representing a major supplier of Au, Ag, and PGEs. Porphyry deposits are typically large generally ranging in size from tens of millions to billions of tonnes of ore (Sinclair, 2007). The grades for economic metals are highly variable between specific deposit types, but are typically low- to medium-grade with ore constituting less than one percent of the mineralised rock (Sinclair, 2007). Porphyry-style mineralisation occurs throughout the world in association with relatively narrow orogenic belts. In Canada the primary terranes correspond to the Triassic and younger orogens of Western Canada (porphyry Cu and Cu-Mo/Au deposits), Devonian sequences of the Canadian Appalachians (Sn-W-Mo-In deposits) and the Archean Superior Provence (porphyry Au). For this project activities have been focussed on the Gibraltar, Highland Valley, Mount Polley and Woodjam deposits of south-central British Columbia (Fig. 2; Plouffe and Ferbey, 2015) and in the Canadian Appalachians the Acadian Plutonic Suite (central New Brunswick), South Mountain Batholith (Nova Scotia) and Connaigre Peninsula (Newfoundland and Labrador) (Fig. 3; Goeddeke et al., 2015; McClenaghan et al., 2015; Rogers et al., 2015a, b; Tweedale et al., 2015; van Staal et al., 2015). Archean porphyry Au deposits were investigated under the auspices of the TGI 4 – Gold project (e.g., De Souza et al., 2014; Gao et al., 2014; Katz et al., 2015).

Sillitoe (2010) argued that porphyry Cu deposits are amongst the most studied and best understood ore deposit type that have enabled advanced exploration programs to be applied (e.g., Kelley et al., 2006; Holliday and Cooke, 2007). Whereas he identified a number of outstanding issues requiring resolution to fully understand the formation and distribution of porphyry Cu deposits, the overall arc tectonic setting (both continental and mature island arc) are well established (e.g., Richards, 2009, 2011). The tectonic setting for post-accretionary Sn-W-Mo-In deposits are far less constrained with several distinct tectonic processes identified as possibly causing such deposits (Richards, 2011), none of which definitively explain the temporal and spatial distribution of such Canadian Appalachian deposits (cf. van Staal et al., 2009, 2014, 2015; Rogers et al., 2014, 2015a, b).

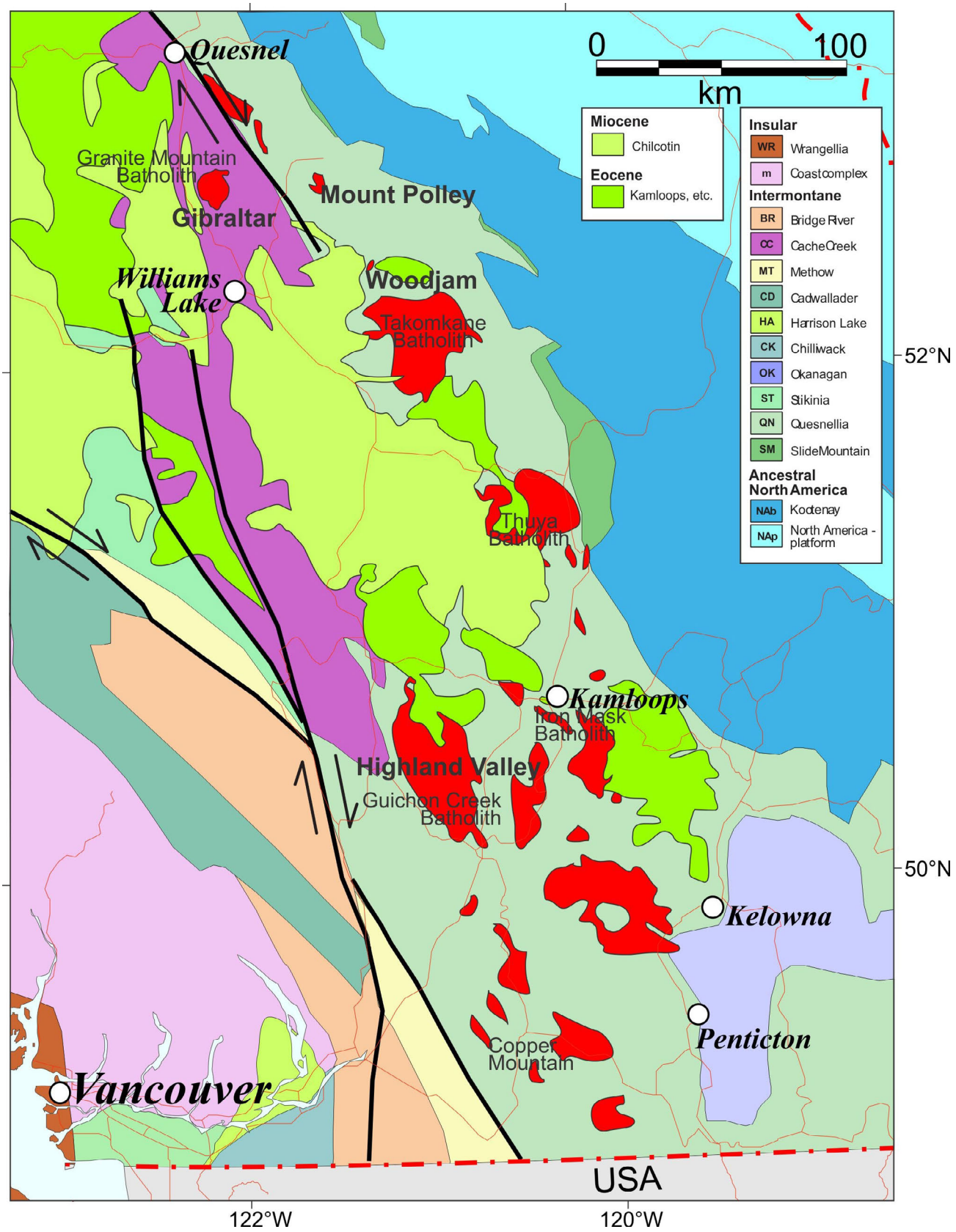

Figure 2 – Simplified bedrock geology map of south-central BC highlighting the location of the Gibraltar, Highland Valley, Mount Polley and Woodjam deposits. Bedrock geology modified after Massey et al. (2005), Erdmer and Cui (2009) and Logan et al. (2010).

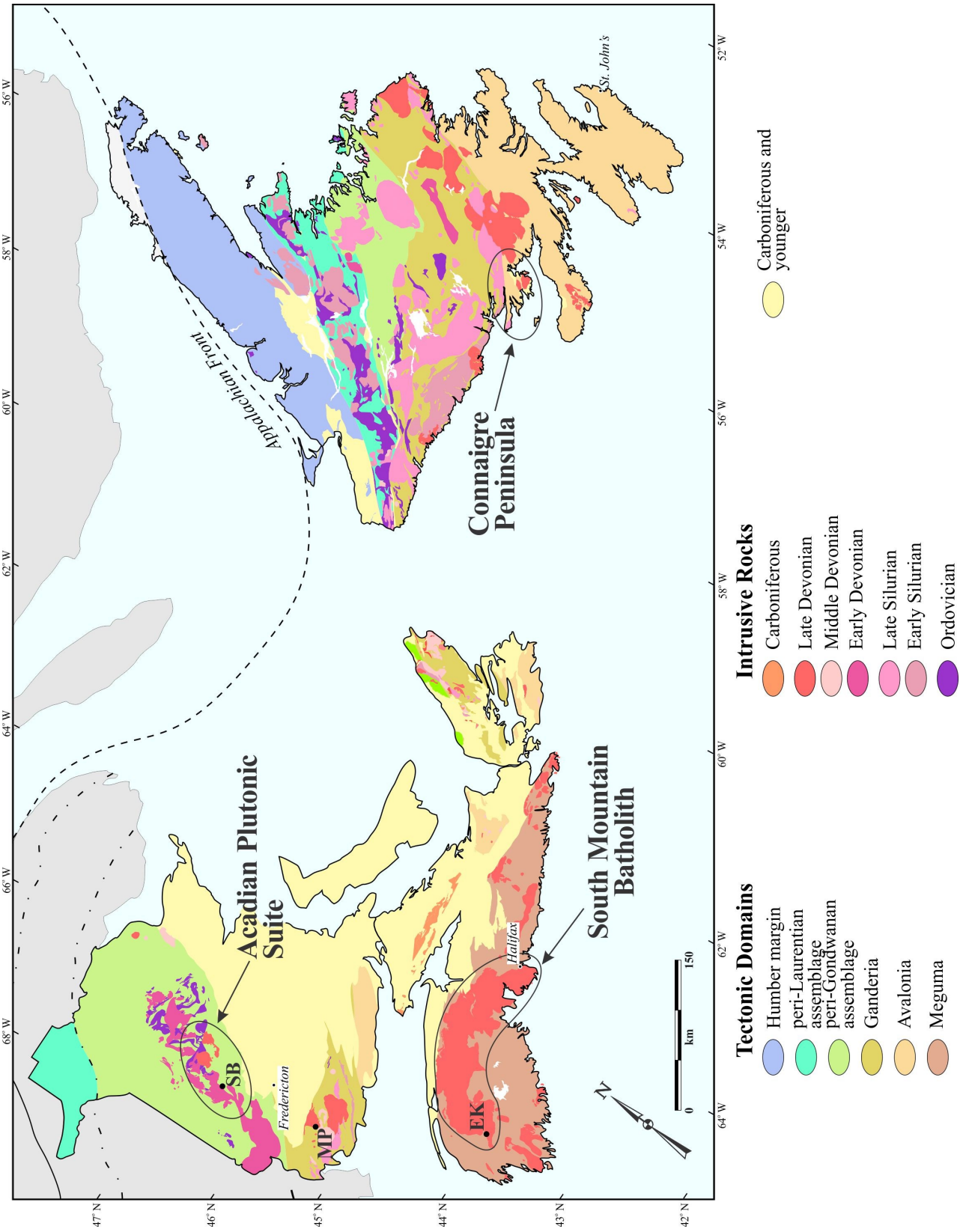

Figure 3 – Distribution of Palaeozoic granitoids and interpreted tectonic subdivisions of the Appalachian Orogen in Newfoundland, New Brunswick and Nova Scotia, highlighting the Acadian Plutonic Suite, South Mountain Batholith and the Connaigre Peninsula. Bedrock geology modified after Hibbard et al. (2006), van Staal et al. (2009), Rogers et al. (2014) and references therein). EK - East Kemptville Mine; MP - Mount Pleasant Mine; SB - Sisson Brook deposit.

Table 1 – Hierarchical hypotheses tested within the TGI 4 - Intrusion Related Mineralisation Project

Primary Hypothesis	Secondary Hypothesis	Tertiary Hypothesis
Tectonic setting, crustal structures and source composition dictate type, metal budget and where porphyry style mineralisation occurs and thus can predict buried/hidden systems	Stratigraphic and structural relations within the country rock are key determinants on the localisation of porphyry-style mineralisation	Intersecting crustal structures present mineralising fluid pathways and thus define high mineral prospectivity zones for deep seated and hidden ore
	W-Mo-Sn mineralization associated with peraluminous granite are oriented by regional stress fields	Sn-W-Mo bearing granite can form by within-plate melting in translational jogs related to oblique subduction
	Barren versus fertile intrusive suites and phases can be differentiated and large mineral systems pinpointed through characterization of late melt and fluid phases	Fertile Sn-W systems contain characteristic fluid inclusions that provide a link to ore potential
		Indium rich systems develop distinctly from typical W-Mo systems and thus late melt charachteristics correlate to In potential
Distinctive geological, mineralogical and geochemical characteristics exist that can differentiate and vector to not only deposit sub-types but also the degree of fertility of hidden/deep mineralization	Geochemical, petrologic and strucural indicators are present that determine whether near surface low grade porphyry-style deposits represent a carapace to higher grade mineralized cores	
	The composition of surficial materials are affected by underlying porphyry deposits such that they provide robust, large-scale and effective exploration vectors to economically viable deposits	Certain elements and minerals are anomalously enriched in glacial materials near porphyry deposits and are indicative of ore fertility
		Epidote abundance within till directly corresponds to entrainment from a mineralised zone
	Indicator mineral profiles are effective economic potential indicators of and vectors towards Sn-W-Mo systems	Scheelite fluorescence under ultraviolet light is an effective pre-screening tool for indicator mineral profiling of till
		On-site portable XRF analysis of till corresponds with indicator mineral vector profiles

Given the objectives behind TGI 4 (above) and the relative knowledge bases for the two types of porphyry-style mineralisation under investigation, activities supported within this project were designed to advance effective exploration for hidden deposits. To that end a hierarchical series of hypotheses were developed for testing (Table 1) that if resolved could reasonably be expected to facilitate advanced exploration models. Within the ore system concept this hypothesis testing largely focussed studies on the source control/system fertility (i.e., distribution and setting of mineralisation) for the post-accretionary deposits across the Canadian Appalachians and on enhanced methods for detecting/vectoring towards buried porphyry deposits (both south-central BC porphyry Cu and Cu-Mo/Au deposits and Appalachian post-accretionary Sn-W-Mo-In deposits). It should be noted that polymetallic, post-accretionary deposits also formed in association with the Western Canadian orogens, and likewise porphyry Cu mineralisation is present within Canadian Appalachian terranes. Although activities were not directed at examples of these specific types of mineralisation within these particular regions, the thematic nature of the ore system concept should enable resulting exploration models to be applicable and exportable to other domains.

Advancements to the intrusion related ore system

Structural and tectonic controls on porphyry-style mineralisation

Studies related to the structural and tectonic controls on porphyry-style mineralisation were primarily aimed at testing the primary hypothesis that "tectonic setting, crustal structures and source composition dictate type, metal budget and where porphyry style mineralisation occurs and thus can predict buried/hidden systems" (Table 1). In the ore system model this relates to helping resolve which terranes are the most prospective and where within these terranes exploration should be focussed.

Spatial and temporal relationships for post-accretionary Sn-W-Mo-In deposits

Although the multiple Palaeozoic accretionary orogens that constitute the Canadian Appalachian resulted in voluminous and widely distributed granitoid magmatism, the bodies that host porphyry-style mineralisation are spatially and temporally restricted (Fig. 3; Kellett et al., 2014; Rogers et al., 2014). These spatial and temporal restrictions closely correspond with pre-existing structures and far removed accretionary orogenic events that the standard tectonic models for post-accretionary polymetallic porphyry development do not readily predict (Rogers et al., 2014). Consequently, a modified tectonic model was proposed that incorporates magma genesis with external orogenic accretionary processes. The first requirement for this model is for the region to have been through at least one orogenic cycle in order to prepare the crust (concentrate ore metals) prior to melting and magma genesis. Crustal melting in the hinterland to an active accretionary margin is subsequently induced in response to non-orthogonal collision causing stress within the upper plate that is dissipated through reactivation of suitably orientated crustal breaks (faults). Depending on the orientation of the accretionary margin, particularly where embayments and promontories are involved, transpressive shear may require crustal scale translational jog to accommodate strain. Such effects can be manifested by crustal thinning and localised extensional basin development such as within the Connaigre Peninsula (Rogers et al., 2015a; van Staal et al., 2015). In this modified model associated pressure and temperature (P-T) transitions in the lower crust, along with potential asthenospheric upwelling, are the drivers for crustal melting, as per standard models for post-collisional granitoid genesis (cf. Richards, 2011). The difference being that the temporal and spatial distributions of mineralised intrusions are explained, and thus the potential prospectivity of a region can be assessed by analysis of the regional tectonic framework.

At a more local scale a spatial association is noted between mineralisation and syn-magmatic faults or lineaments (along which only

minor displacements are present) that intersect at a high angle (Rogers et al., 2014, 2015a, b). The implication is that the intersecting structures provide convenient pathways for ore-bearing fluids, and that motion along them can cause rapid P-T changes which result in ore precipitation due to adiabatic cooling. Essential components of this model are that the syn-magmatic breaks (minor faults, lineaments or well developed joints) be orientated in the extensional field and that associated displacements are minor to facilitate protracted mineralisation/increased ore grade.

Further constraints on the distribution of mineralisation were investigated on the Connaigre Peninsula, south-central Newfoundland (Rogers et al., 2015a; van Staal et al., 2015). This area contains two post-accretionary plutons that were emplaced in the ca. 380 Ma period that corresponds with most of the polymetallic granitoid mineralisation known in Newfoundland (Tuach et al., 1986; Kerr et al., 1993, 1995; Lynch et al., 2009, 2012; Kerr and McNicoll, 2012; Kellett et al., 2014; Kerr, 2014) and where one body hosts several well-developed ore deposits and the other one apparently largely barren (O'Brien et al., 1995; O'Brien, 1998; Rogers et al., 2015a). Although the "barren" intrusion is petrographically distinctive, Rogers et al. (2015a) suggest that the primary factor influencing apparent mineral potential is depth of intrusion. In this case the body that does not contain significant known Mo mineralisation was mostly emplaced virtually at the surface. Notably minor mineralisation does occur within this granite, but its distribution is limited to marginal sections were the emplacement depth (based on the relative stratigraphic position of country-rock) corresponds to the emplacement depth of the adjacent intrusion that hosts multiple ore bodies. The underlying mechanism for this emplacement depth – mineralisation association is interpreted to be related to ore-bearing fluids transgressing a P-T threshold as they migrate upwards, at which point ore minerals are precipitated. The observed spatial association of fluorite with the Mo deposits suggests that ore metals were mostly transported intimately associated with F, either HF complex or redox buffer. Consequently, where P-T conditions are met for fluorite precipitation, ore metals also likely to come out of solution.

Another implication of the above model is that intrusive bodies that evolve by distinct pulses of magma being emplaced at different levels (cf. Vry et al., 2010) can develop zones of mineralisation well within the main granite body in response to changing P-T conditions over time, as opposed to the standard interpretations where ores are restricted towards the top of a pluton (e.g., Tuach et al., 1986). Furthermore, were ore-bearing fluids are transporting metals derived from younger pulses of magma into older granitoid phases, then it is unnecessary for the host granitic rock to be in chemical equilibrium or directly genetically related to ore. An example of this situation is developed within the Acadian Plutonic Suite, central New Brunswick, where the Tin Hill deposit occurs within the Buttermilk Cupola (Rogers et al., 2015b). However, the mineralisation at this site occurs within thick quartz veins that are effectively macroscopic tension gashes accommodating regional strain and competency differences between the granite and adjacent Cambrian to Ordovician clastic sedimentary rocks. Thus, although Sn-W mineralisation is developed within a granitic cupola, this is not an example of idealised orthomagmatic porphyry-style mineralisation (e.g., Sinclair, 2007) as the ore metals are derived from a buried, younger intrusion that is responsible for numerous exogranitic (intrusion related mineralisation not hosted by granitoid rocks) deposits (e.g., Burnt Hill Mine and Two and a Half Mile Brook deposit) within the same structural trend (Rogers et al., 2014, 2015b).

Timing of Cu-Mo mineralisation the Gibraltar Mine, BC

The Gibraltar Mine is one of British Columbia's largest Cu-Mo deposits (Oliver et al., 2009; Anderson et al., 2012). The six ore zones which make up the deposit are hosted by the composite, peraluminous Late Triassic Granite Mountain batholith (Fig. 2; Drummond et al., 1973; Bysouth et al., 1995; Ash et al., 1999a, b; Ash, 2001; Oliver et al., 2009; Schiarizza, 2015). There has been a longstanding debate on the nature of mineralisation at the Gibraltar Mine as the hosting Granite Lake batholith had been interpreted as a part of the Cache Creek terrane (Drummond et al., 1973; Bysouth et al., 1995), in contrast to other Triassic to Jurassic granitoid associated Cu-Mo deposits of south-central BC that form part of the Quesnel terrane (Logan et al., 2010; Nelson et al., 2013). Ash et al. (1999a, b) presented an alternate interpretation that the Granite Mountain batholith was indeed formed within the Quesnel terrane, but was subsequently (inferred as 20 to 30 m.y. after magmatism) juxtaposed by faulting into Cache Creek terrane. Their interpretation was that the structures observed within the Granite Mountain batholith, and associated with ore distribution in the Gibraltar Mine (Fig. 4), were formed by tectonic displacement and thus mineralisation would be unrelated to granite formation (i.e., not a porphyry Cu-Mo deposit). To this end Ash et al. (1999b) stated that for the "cataclastic and mylonitic shear fabrics characterised by retrograde greenschist grade metamorphic assemblages occurred during crystallisation of a magma body is difficult to rationalise", as opposed to the "porphyry with a difference" description of Sutherland Brown (1974).

To test which interpretation of the Cu-Mo mineralisation is correct Re-Os molybdenum age dates from within the Gibraltar Mine were obtained that gave the timing of mineralisation as 215.0 ± 1.0, 212.7 ± 0.9 and 210.1 ± 0.9 Ma (R.G. Anderson, pers. comm., 2012). These ages for the mineralisation are consistent with various crystallisation ages determined for the Granite Lake batholith (217 ± 0.20 Ma – U-Pb zircon TIMS, R. Friedman reported in Schiarizza, 2015; 215 ± 0.8, 212 ± 0.4 Ma – U-Pb zircon(?) reported in Ash and Riveros, 2001; 211.9 ± 4.3, 209.6 ± 6.3 Ma – laser ablation ICP-MS U-Pb zircon, Olivier et al. 2009). Notably these dates are also broadly consistent with those observed for the Guichon Creek batholith that hosts the Highland Valley Cu-Mo porphyry deposits (Fig. 2; McMillan, 1985; McMillan et al., 2009; B. Davis, pers. comm., 2011). These data

Figure 4 – Syn-magmatic ductile deformation of ore rocks within the Gibraltar Mine, BC.

strongly suggest that the mineralisation is syn-magmatic (and by extension so is the deformation, as mineralisation is distributed along both pervasive ductile and later brittle structures), hence this is a porphyry Cu-Mo deposit. It also suggests a genetic correlation between the Gibraltar and Highland Valley deposits. Subsequent mapping (Schiarizza, 2015) has determined that the Granite Mountain batholith does intrude Nicola Group rocks and therefore was emplaced within the Quesnel terrane.

Although the terrane identification for the Gibraltar deposit is important regionally, in the ore system context the recognition of the extent of syn-magmatic deformation that is possible within a porphyry system is of primary importance. These rocks suggest a variation from the standard model for porphyry development is possible whereby a relatively long-lived intrusion can source and transport ore fluid from younger magma phases to older phases that are variably solidified. Concurrent with this, stress can induce pervasive syn-magmatic ductile deformation in portions of the intrusive body that have not crystallised completely and so plastically deform (i.e., act as "soft solid"). As crystallisation continues these phases within the pluton become more rigid and if mineralising fluids are still being produced by deeper and younger magmatic phases then ores are liable to be developed along brittle fractures.

Granitoid ore fertility indicators and vectors to mineralisation

The following studies have focussed on developing new methodologies to chemically test the mineral potential (fertility) and/or divine chemical gradients to (vector towards) mineralisation. In the ore system concept these relate to resolving if there are distinctive chemical markers that indicate that substantive mineralising processes have occurred within an intrusive body, and if so are there directional indicators to an ore body. The standard model for porphyry systems incorporate ore metals being redistributed from a magmatic source and deposited/concentrated elsewhere whether it is within the granitic body (endogranitic) or external to it (exogranitic). Hence, except for circumstances where mineralisation is associated with intense metasomatic alteration, there is no guarantee that the ore component of the system would be in chemical equilibrium to the host (endogranitic) or nearest (exogranitic) granitoid rock. Consequently focus has been on direct measurements of fluid evolution through fluid inclusion decrepitation (Tweedale et al., 2015) or on mineral phases that have low closure temperatures and so act as a proxy for magmatic evolution (Azadbakht, 2015a, b, c). A related study has also been conducted specifically aimed at helping resolve the distinct characteristics that control indium content within certain polymetallic post-accretionary granitoid mineralisation (Goeddeke et al., 2015).

Fluid inclusion utility as a mineral fertility indicator and/or vector to ore

The inherent hydrothermal nature of porphyry-style mineralization means it is only reasonable to expect that a geochemical fingerprint of the mineralizing fluids might be preserved both petrographically and as secondary fluid inclusions in the associated intrusive bodies on a scale equal to or larger than the mineralized zones. A commonly applied technique to investigate fluid inclusion chemistry is microthermometry based on freezing and homogenisation temperature to determine fluid inclusion salinity. However, this technique reports results qualitatively as NaCl equivalent concentration which does not account for other cation and anion solutes that may be significant in porphyry-style mineralising systems. An alternative technique of crush-leach fluid extraction followed by LA-ICP-MS analysis is also potentially inadequate for resolving the evolution of a porphyry system as the results of crush-leach analysis may combine multiple generations of fluids (Chi et al., 2003), and the electronegativity of fluorine, a potentially ore-forming ligand in magmatic-hydrothermal settings (Muecke and Clarke, 1981; Thomas et al., 2006; McPhie et al., 2011) prevents its detection by standard LA-ICP-MS analysis. Given the potential shortfalls of these methods, Tweedale et al. (2015) examined whether fluid inclusion decrepitate analysis techniques (Eadington, 1974; Haynes and Kesler, 1987) can be applied as a cost-effective and time-efficient exploration tool to regionally assess granitoid ore fertility. This method determines semi-quantitatively the composition of solute ions, such as Na, K, Ca, Cl, and F, via scanning electron microscopy/ energy dispersive X-ray spectroscopy analysis of precipitate mounds formed by thermal decrepitation of fluid-inclusions.

Exploration tool potential testing and development was conducted on the South Mountain Batholith of southwestern Nova Scotia (Tweedale et al., 2015). The ca. 380 Ma South Mountain Batholith at ca. 7,300 km^2 is the largest Appalachian batholith and hosts a variety of polymetallic deposits (e.g., East Kemptville and New Ross). Previous detailed mapping has identified 260 discrete granitic bodies that were grouped into 49 map units based on field relations and composition (Keppie, 1979; MacDonald, 2001). These units were assigned to 13 plutons, which in turn are designated as being Stage I (early) or Stage II (later) plutons (MacDonald, 2001). A fundamental aspect of this study was determining if methods can be applied for reconnaissance exploration in such a complex environment (Tweedale et al., 2015). Initial results indicate that reconnaissance studies can efficiently summarise a complex, multi-phase batholith through element distribution maps and identify target areas for detailed follow-up (Tweedale et al., 2014, 2015). In particular the prevalence of F-rich fluids is noteworthy, as this element likely plays a significant role in the potential of fluids to partition, transport and precipitate ore metals (McPhie et al., 2011). The precise role of F in the hydrothermal processes involved in porphyry-style mineralisation remains equivocal, in part due to the most prevalent methods of fluid inclusion analysis not resolving F directly (e.g., Ulrich, 2004; Klemm et al., 2008; Ulrich and Mavrogenes, 2008; Audétat, 2010). Experimental data (e.g., Jackson and Helgeson, 1985; Candela and Holland, 1986; Candela and Bouton, 1990; Keppler and Wyllie, 1991; Hu et al., 2008; Rempel et al., 2008) suggests that Cl-complexes (especially for Cu and Sn), pH and temperature are the main factors on the initial melt-fluid partitioning of metals and their deposition. An indication of the role of F in ore systems developed within the South Mountain Batholith is provided F distribution maps that show a decoupling between the fluid inclusion composition and whole-rock data at fluorite-bearing deposits (Tweedale et al., 2014). The implication here is that fluorite formation depletes the F (and Ca) from the fluid phase, which in turn changes the pH and thus the solubility of ore metals.

In situ mineral analysis and ore system fertility

The Devonian granites of New Brunswick display a wide range of settings from pre-, syn-, late-, to post-tectonic related to the Acadian and Neoacadian orogenies, with affinities from primitive to highly evolved A-, S-, and I-types granitoids and are associated with Sn, Ta, Li, Sb, W, Mo, Cu, and Au, as well as base-metals and U mineralisation (Whalen, 1993; van Staal et al., 2009). To determine whether in situ mineral analysis can differentiate between barren and mineralised granitic systems 42 of New Brunswick's Devonian granitoid intrusions were investigated for the compositional variations in biotite (Azadbakht et al., 2015a, b, c). The choice of biotite for analysis is because it is a common phase to many granitic rocks, is highly sensitive to physico-chemical changes of its host, and continuously re-

equilibrates with host and derivative fluids (Lentz, 1992; Lofersji and Ayuso, 1995; Siahcheshm et al., 2012; Wang et al., 2013). Furthermore biotite is a suitable proxy for the overall magma composition as: 1) it is the most important reservoir of any excess aluminium in granites that do not contain modal garnet, cordierite, or the Al_2SiO_5 polymorphs; therefore, it directly reflects the peraluminosity of the host magma in such rocks; 2) it is the most readily available indicator of oxidation state; and 3) it can provide information about the F and Cl content of the magma. Analyses conducted by electron microprobe and laser ablation ICP-MS have shown major elements are typically constant within biotite grains from core to rim, but can show remarkable trace element zoning. To investigate this zoning further laser ablation ICP-MS trace element maps were also produced where permitted by the size of the biotite, frequency of the mineral inclusions, degree of alteration, and the laser spot size required to achieve sub-ppm detection limits.

Results of this study showed large-ion lithophile element zoning, including Cs, Ba, and Rb, for most of the biotite grains. As these elements are highly incompatible, any zoning can be a result of the magma evolution history recorded within the biotite crystalline structure. For example, biotite grains from the Pleasant Ridge granite show an increase from core to rim for Cs and Sn and a decrease for W and Sc (Fig. 5). Copper is also high along the cleavages where biotite is weakly altered to chlorite. These observations indicate a direct link between the fractional crystallisation of this granite and Sn mineralisation (Azadbakht et al., 2015b). Such correlations indicate that biotite composition can be correlated with magma fertility, but more work needs to be done to define characteristics of different magmatic processes.

Indium is a minor component of some post-accretionary mineralised granitoids in the Canadian Appalachians, but is potentially economically very significant due to high demand for a variety of industrial and technology applications, particularly in electronics (e.g., touch screens). However, indium distribution between deposits is highly uneven, and whereas some deposits contain hundreds of kilograms of the metal at grades sufficient to justify recovery, others are near-barren. At almost 1,000 tonnes combined indicated and inferred contained metal (McCutcheon et al., 2010, 2013), the Mount Pleasant Mine represents possibly the largest documented global indium reserve (Sinclair et al., 2006). In order to investigate the fundamental temperature, mineralogical, spatial and chemical controls on indium mineralisation in the district, a study was undertaken on samples from indium rich and poor occurrences at 10 drilled prospects in southern New Brunswick and southwest Nova Scotia, as well as from the past-producing East Kemptville Mine in Nova Scotia (Goeddeke et al., 2015).

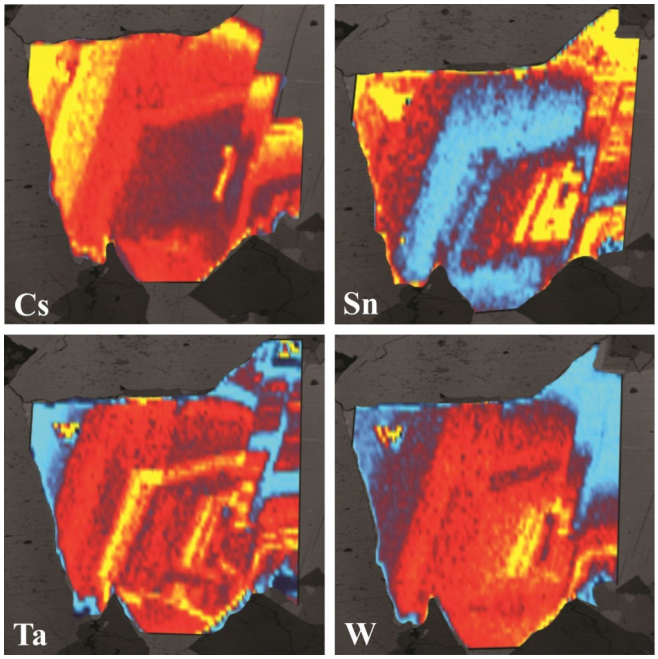

Figure 5 – Laser ablation ICP-MS trace element maps of a biotite crystal from the Pleasant Ridge granite (sample WX-NB-187). After Azadbakht et al. (2015b).

Detailed mineralogical characterization of these materials has shown that, contrary to existing models, within this district, indium is commonly introduced early in the deposit paragenesis, presumably as a component of the initial, high-temperature magmatic-hydrothermal fluids. During this phase of mineralisation, indium is dominantly precipitated within Cu-rich sphalerite, and it is the distribution of this mineral phase that primarily governs the presence or absence of indium within a mineralised body. During later cooling of the deposit a proportion of the indium is exsolved forming lamellae in sphalerite cores zones (Goeddeke et al., 2015).

Surficial vectors towards intrusion related mineralisation

Extensive glacial sedimentation covers many of the prospective regions for porphyry-style mineralisation in Canada. Although these sediments may obscure or completely mask direct bedrock observation of deposits, glacial detrital processes can disperse products associated with ores such that they form a much larger target that can be traced back (vectored) to mineralisation. To develop efficient methodologies and exploration protocols for glaciated terrains, studies were conducted in the vicinity of several major deposits in south-central British Columbia (Plouffe and Ferbey, 2015) and New Brunswick (McClenaghan et al., 2015). These studies were directed towards testing the primary hypothesis of whether "distinctive geological, mineralogical and geochemical characteristics exist that can differentiate and vector to not only deposit sub-types but also the degree of fertility of hidden/deep mineralization" (Table 1). In the ore system concept these activities relate to detection methods and techniques for enhanced exploration.

The utility of till composition in identifying Cu-Mo/Au porphyry deposits buried by glacial sediments was tested in the vicinity of the Gibraltar, Highland Valley and Mount Polley mines and the Woodjam prospect (Fig. 2). The primary objective of this study was to confirm that geochemical and mineralogical indicators of Cu porphyry mineralisation are resolvable in an efficient and cost-effective manor given the typical low to medium ore metal grades of the deposits in question, such that these methods are exportable to the exploration industry. The methods employed involved sampling till and measuring ice-flow indicators from bedrock outcrops following procedures outlined in Spirito et al. (2011) to resolve glacial dispersal patterns and record any chemical or mineral enrichment that could vector to the known deposits (Plouffe and Ferbey, 2015, and references therein).

Key results from this study are that products of porphyry-style mineralisation can be detected over several kilometres both as multi-element chemical enrichment in the clay-sized fraction of till and as identifiable grains of ore related minerals within silt/sand-sized fractions of till (Plouffe and Ferbey, 2015). Comparisons between the various study sites indicates that the actual chemical concentrations or number of grains that define the dispersal trains are not important,

merely that they are anomalous relative to the regional background values. Similarly the areal extent and shape of dispersal trains varies between deposits. In part these features reflect the extent of mineralised bedrock that subject to glacial erosion within individual deposits (Plouffe et al., 2012). The recognition of high abundances of alteration minerals (e.g., epidote) in till down-ice from Cu porphyry deposits can thus be significant, as the alteration zones associated with these types of deposit are much larger than the ore zone itself. Hence, alteration minerals are more likely to be incorporated into till than direct ore products and can potentially represent a larger exploration target (Plouffe and Ferbey, 2015).

Notable ore minerals (e.g., chalcopyrite) are present within the till dispersal trains (Plouffe and Ferbey, 2015). This is significant as other studies elsewhere (e.g., the giant Pebble porphyry Cu-Au-Mo deposit in Alaska – Kelley et al., 2011) have not identified sulphide minerals in tills despite their presence within the ore. The interpretation has been that the absence of chalcopyrite in till reflects sulphide-destructive processes within the surficial environment (Kelley et al., 2011). An alternative explanation for why ore minerals may be precluded from tills is suggested by the observation of ore bodies that are at least partially covered by pre-glacial sedimentation (i.e., the Valley deposit at the Highland Valley Mine). Such relationships would protect mineralised zones from glacial erosion and so impact the potential for ore minerals to be incorporated into till (Fig. 6; Plouffe et al., 2012; Plouffe and Ferbey, 2015). Furthermore, lacustrine deposits can accumulate above ore zones prior to glaciation because the alteration associated with ore generation tends to "weaken" the ore zone relative to its margins, and thus these areas are susceptible to forming palaeotopographic depressions within which sediments may collect.

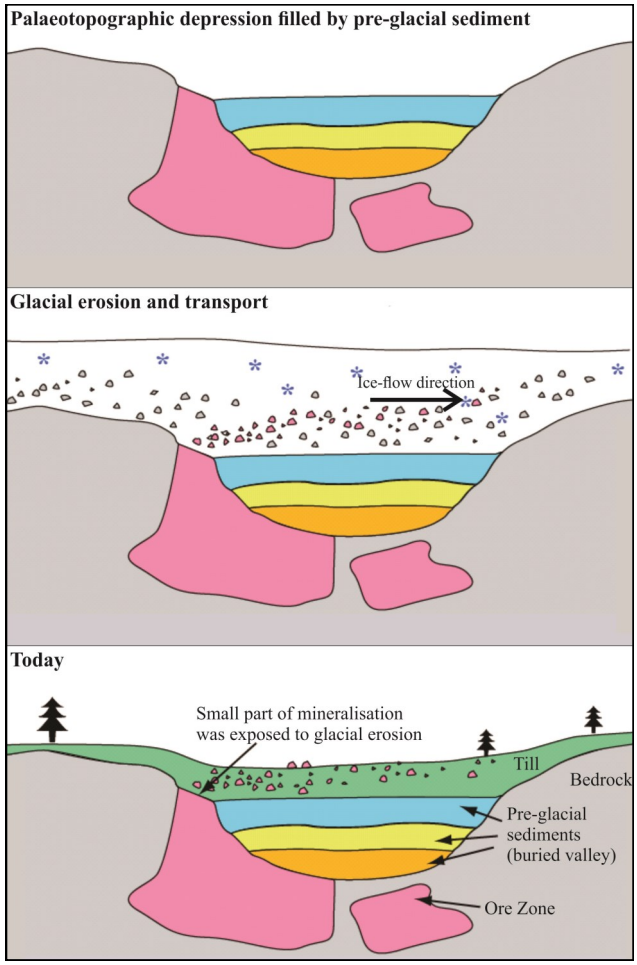

Figure 6 – Diagrammatic representation of how pre-glacial sediments deposited in palaeotopographic depressions can shield Cu porphyry mineralised zones from glacial processes and limit the incorporation of ore into down-ice dispersal trains. Modified from Plouffe et al. (2012).

Surficial signatures for polymetallic, post-accretionary granitoid related mineralisation was examined in the vicinity of the Sisson W-Mo and Mount Pleasant Sn-W-Mo-Bi-In deposits, New Brunswick (McClenaghan et al., 2015 and references therein). Indicator minerals were studied by heavy mineral concentrates from till and stream sediment samples, with chemical analysis (partial and total digestion) were obtained from the silt fraction of till. Indicator/pathfinder trace elements in till includes Sn, W, Mo, Cu, Zn, Pb, Ag, Bi, In, As, Cd, Re, Te, Tl, and Zn. The range of indicator elements reflects the polymetallic nature of the deposits and the broad suite of elements readily available by commercial ICP-MS analysis. The Mount Pleasant deposit contains a significant In resource (Sinclair et al., 2006) and till down-ice from the deposit contains some of the highest In values (13 ppm) ever reported for till, indicating that till geochemistry can be an important exploration tool for In-bearing deposits (McClenaghan et al., 2015). In addition to full chemical analyses, small samples were also examined using a portable XRF. Although the data obtained by portable XRF is not directly comparable in quality or range of elements determined in relation to ICP-MS analysis, its immediacy and potential to analyse many samples make it a valuable tool for directing exploration and reducing the number of samples required to undergo full analysis.

Indicator minerals identified in the medium grain size fraction (0.25-0.5 mm) of till and stream sediment near the Sisson W-Mo deposit include scheelite, wolframite, molybdenite, chalcopyrite, joseite, native Bi, bismutite, bismuthinite, galena, sphalerite, arsenopyrite, spessartine, pyrrhotite, and pyrite. At the Mount Pleasant Sn-W-Mo-In deposit indicator minerals include cassiterite, wolframite, molybdenite, topaz, fluorite, galena, sphalerite, chalcopyrite, galena, arsenopyrite, pyrite, and loellingite. Additional (but rare) secondary indicator minerals at the Mount Pleasant deposit include beudantite, anglesite, and plumbogummite. Indicator minerals present in the coarse (0.5-2.0 mm) heavy mineral fraction of till indicate proximity to the mineralised source. A process to systematically determine scheelite ($CaWO_4$) within heavy mineral concentrates using its short wave ultraviolet light fluorescence was developed and is now commercially available (McClenaghan et al., 2015).

Conclusions

All of the hypotheses listed in Table 1 that underpinned the suite of activities conducted within the auspices of the TGI 4 – Intrusion Related Mineralisation Project have at least partially been confirmed. The resulting advancements to the associated ore system model provide several potential avenues for the application of innovative exploration models for hidden or buried porphyry-style mineralisation. Currently, the improved surficial methods for the detection of intrusion related ore bodies (McClenaghan et al., 2015; Plouffe and Ferbey, 2015) are the most advanced and thus are suitable for immediate adoption by industry as part of a mineral exploration strategy.

Overall the results outlined above provide the basis for predictive models from the regional level of which terrane is most prospective down (tectonic setting/structure) to the small scale with effective vec-

tors to ore (mineral analysis/till composition). A recurring theme within the bedrock related studies has been the significance within the ore system model of the transport of metals via fluid from source to deposition. Granitoid intrusions often develop as a relatively long lived system through multiple intrusive phases and pulses of magma over timescales that can be significantly longer than individual mineralising events. Consequently, there is no inherent reason why host granitoid rocks to a deposit are directly genetically linked (other than by metasomatic alteration) with the ore. In this sense for exploration purposes all porphyry-style deposits should be explored for as if they are exogranitic (hosted externally to the intrusion) even when they form within an intrusion (endogranitic). This principle is particularly relevant in terms of choice of mineralogical analysis as a means to provide vectors to ore, as minerals that remain "open" (liable to constantly re-equilibrate with host and derivative fluids), such as biotite, can be an effective proxy for the whole intrusive system rather than an individual phase that may not be associated with ore genesis. Another implication of this is pluton that develops through multiple pulses of magma can cause recycling and concentration of ore metals through batch processing with ore precipitating at a physico-chemical threshold between or within earlier intrusive phases. This model represents a potential explanation for the increasing grade of ore with depth that is observed in deep levels of some porphyry-style deposits.

Acknowledgements

All of the many people who have diligently worked in the TGI 4 – Intrusion Related Mineralization Project are gratefully acknowledged, with particular thanks going to my Geological Survey of Canada colleagues Alain Plouffe, Beth McClenaghan, Bob Anderson, Cees van Staal, Dawn Kellett, John Chapman and Vicki McNicoll. This project would not have been possible without the active support and collaboration of the geological surveys of British Columbia, New Brunswick, Newfoundland and Labrador, and Nova Scotia. Similarly our academic partners at Laurentian University, Memorial University of Newfoundland, Saint Mary's University, Simon Fraser University, University of British Columbia, University of New Brunswick, University of Victoria, and University of Windsor have been invaluable contributors to project success and suitably appreciated.

References

Anderson, R.G., Plouffe, A., Ferbey, T., and Dunn, C.E., 2012. The search for surficial expressions of buried Cordilleran porphyry deposits; background and progress in a new Targeted Geoscience Initiative 4 activity in the southern Canadian Cordillera, Geological Survey of Canada, Current Research 2012-7, 15 p.

Ash, C.H., 2001. Geology of the Gibraltar copper-molybdenite deposit, east central BC; *in* Geological fieldwork 2000; BC Ministry of Energy and Mines, Paper 2001-1, p. 119-134.

Ash, C.H., and Riveros, C.P., 2001. Geology of the Gibraltar copper molybdenite deposit, east-central British Columbia (93B/9); *in* Geological Fieldwork 2000, British Columbia Ministry of Energy and Mines, British Columbia Geological Survey Paper 2001-1, p. 119-133.

Ash, C.H., Panteleyev, A., MacLennan, K.L., Payne, C.W., and Rydman, M.O., 1999a. Geology of the Gibraltar mine area (NTS 93B/8, 9); British Columbia Geological Survey, Open File OF1999-07, 1 sheet.

Ash, C.H., Rydman, M.O., Payne, C.W., and Panteleyev, A., 1999b. Geological setting of the Gibraltar mine, south central British Columbia (93B/8 and 9); *in* Exploration and mining in BC, 1998, part B – Geological descriptions of selected properties, p. A1-A15.

Audétat, A., 2010. Source and Evolution of Molybdenum in the Porphyry Mo(-Nb) Deposit at Cave Peak, Texas; Journal of Petrology, v. 51, p. 1739-1760.

Azadbakht, Z., Lentz D.R., and McFarlane, C.R.M., 2015a. Magmatic biotite and its use to distinguish barren and mineralized granitic systems in New Brunswick, Canada; *in* TGI 4 – Intrusion Related Mineralisation Project: New Vectors to Buried Porphyry-Style Mineralisation, (ed.) N. Rogers; Geological Survey of Canada, Open File 7843, p. 565-566.

Azadbakht, Z., Lentz D.R., and McFarlane, C.R.M., 2015b. Magmatic evolution in Devonian granitic rocks and relation to granophile mineralization in New Brunswick: Application of biotite trace element mapping with EPMA and LA-ICP-MS; *in* TGI 4 – Intrusion Related Mineralisation Project: New Vectors to Buried Porphyry-Style Mineralisation, (ed.) N. Rogers; Geological Survey of Canada, Open File 7843, p. 507-519.

Azadbakht, Z., Lentz D.R., McFarlane, C.R.M., and Rogers, N., 2015c. Biotite chemistry as a monitor of magma fertility and mineralisation potential: Results from the Devonian granitoids of New Brunswick; *in* TGI 4 – Intrusion Related Mineralisation Project: New Vectors to Buried Porphyry-Style Mineralisation, (ed.) N. Rogers; Geological Survey of Canada, Open File 7843, p. 563-564.

Burnham, C.W., 1967. Hydrothermal fluids at the magmatic stage; *in* Geochemistry of Hydrothermal Ore Deposits, (ed.) H.L. Barnes; Holt, Rinehart and Winston Inc., New York, p. 34-76.

Burnham, C.W., 1979. Magma and hydrothermal fluids; *in* Geochemistry of Hydrothermal Ore Deposits, 2nd edition, (ed.) H.L. Barnes; Wiley Interscience, New York, p. 71-136.

Bysouth, G.D., Campbell, K.V., Barker, G.E., and Gagnier, G.K., 1995. Tonalite-trondhjemite fractionation of peraluminous magma and the formation of syntectonic porphyry copper mineralization, Gibraltar mine, central British Columbia; *in* Porphyry deposits of the northwestern Cordillera of North America, (ed.) T.G. Schroeter; Canadian Institute of Mining and Metallurgy, Special Volume 46, p. 201-213.

Candela, P.A., 1989. Calculation of magmatic fluid contributions to porphyry-type ore system: predicting fluid inclusion chemistries; Geochemical Journal, v. 23, p. 295-305.

Candela, P.A., and Bouton, S.L., 1990. The Influence of oxygen fugacity on tungsten and molybdenum partitioning between silicate melts and ilmenite; Economic Geology, v. 85, p. 633-640.

Candela, P.A., and Holland, H.D., 1986. A mass transfer model for copper and molybdenum in magmatic hydrothermal systems: the origin of porphyry-type ore deposits; Economic Geology, v. 81, p. 1-19.

Carten, R.B., Geraghty, E.P., and Walker, B.M., 1988. Cyclic development of igneous features and their relationship to high-temperature hydrothermal features in the Henderson porphyry molybdenum deposit, Colorado; Economic Geology, v. 83, p. 266-296.

Chi, G., Chou, I.M., and Lu, H., 2003. An overview on current fluid-inclusion research and applications; Acta Petrologica Sinica, v. 19, p. 201-212.

Christiansen, E.H., Burt, D.M., Sheridan, M.F., and Wilson, R.T., 1983. The petrogenesis of topaz rhyolites from the western United States; Contributions to Mineralogy and Petrology, v. 83, p. 16-30.

Cline, J.S., and Bodnar, R.J., 1991. Can economic porphyry copper mineralization be generated by a typical calc-alkaline melt?; Journal of Geophysical Research, v. 96, p. 8113-8126.

De Souza, S., Dubé, B., McNicoll, V.J., Dupuis, C., Mercier-Langevin, P., and Creaser, R., 2014. Fracture-controlled hydrothermal alteration at the Canadian Malartic deposit: Toward a multiphase model for Archean intrusion-related low-grade bulk tonnage gold deposits; Abstracts, Volume 37, Geological Association of Canada – Mineralogical Association of Canada Joint Annual Meeting; Fredericton, NB, p. 70.

Drummond, A.D., Tennant, S.J., and Young, R.J., 1973. The interrelationship of regional metamorphism, hydrothermal alteration and mineralization at the Gibraltar mines copper deposit in BC; Canadian Mining and Metallurgical Bulletin, v. 66, no. 730, p. 48-55.

Eadington, P.J., 1974. Microprobe analysis of the non-volatile constituents of fluid inclusions; Neues Jahebuch für Mineralogie, v. 11, p. 518-525.

Erdmer, P., and Cui, Y., 2009. Geological Map of British Columbia; B.C. Ministry of Energy, Mines and Petroleum Resources, Geoscience Map 2009-1, scale 1:1,500,000.

Gao, J.F., Jackson, S.E., Dubé, B. and De Souza, S., 2014. Gold mineralization in the Canadian Malartic deposit, Canada: Insights from textural and quantitative elemental mapping of pyrite; Abstracts, Volume 37, Geological Association of Canada – Mineralogical Association of Canada Joint Annual Meeting; Fredericton, NB, p. 97-98.

Goeddeke, C.R., Chapman, J.B., and Samson, I.M., 2015. Controls on indium mineralisation in tin-tungsten-base metal deposits of the Canadian Appalachians; *in* TGI 4 – Intrusion Related Mineralisation Project: New Vectors to Buried Porphyry-Style Mineralisation, (ed.) N. Rogers; Geological Survey of Canada, Open File 7843, p. 101-110.

Haynes, F.M., and Kesler, S.E., 1987. Chemical Evolution of Brines during Mississippi Valley-Type Mineralization: Evidence from East Tennessee and Pine Point; Economic Geology, v. 82, p. 53-71.

Heinrich, C.A., Ryan, C.G., Mernach, T.P., and Eadington, P.J., 1992. Segregation of ore metals between magmatic brine and vapor: a fluid inclusion study using PIXE microanalysis; Economic Geology, v. 87, p. 1566-1583.

Hibbard, J., van Staal, C.R., Rankin, D., and Williams, H., 2006. Lithotectonic map of the Appalachian orogen, Canada – United States of America; Geological Survey of Canada, Map 2096A, scale 1:1,500,000.

Holliday, J.R., and Cooke, D.R., 2007. Advances in geological models and exploration methods for copper ± gold porphyry deposits; *in* Proceedings of Exploration 07: Fifth Decennial International Conference on Mineral Exploration, (ed.) B. Milkereit; Prospectors and Developers Association of Canada, p. 791-809.

Hu, X., Bi, X., Hu, R., Shang, L., and Fan, W., 2008. Experimental study on tin partition between granitic silicate melt and coexisting aqueous fluid; Geochemical Journal, v. 42, p. 141-150.

Jackson, K.J., and Helgeson, H.C., 1985. Chemical and thermodynamic constraints on the hydrothermal transport and deposition of tin: I. Calculation of the solubility of cassiterite at high pressures and temperatures; Geochimica et Cosmochimica Acta, v. 49, p. 1-22.

Katz, L.R., Kontak, D.J., Dubé B., and Rogers, J.R., 2015. Chemical fingerprinting of the Archean Côté Gold deposit: A large-tonnage, low-grade intrusion-related deposit system, Ontario, Canada; *in* TGI 4 – Intrusion Related Mineralisation Project: New Vectors to Buried Porphyry-Style Mineralisation, (ed.) N. Rogers; Geological Survey of Canada, Open File 7843, p. 445-458.

Kelley, K.D., Eppinger, R.G., Lang, J., Smith, S.M., and Fey, D.L., 2011. Porphyry Cu indicator minerals in till as an exploration tool: example from the giant Pebble porphyry Cu-Au-Mo deposit, Alaska, USA; Geochemistry: Exploration, Environment, Analysis, v. 11, p. 321-334.

Kelley, D.L., Kelley, K.D., Coker, W.B., Caughlin, B., and Doherty, M.E., 2006. Beyond the obvious limits of ore deposits: The use of mineralogical, geochemical, and biological features for the remote detection of mineralization; Economic Geology, v. 101, p. 729-752.

Kellett, D.A., Rogers, N., McNicoll, V.J., Kerr, A., and van Staal, C.R., 2014. New age data refine extent and duration of Paleozoic and Neoproterozoic plutonism at Ganderia–Avalonia boundary, Newfoundland; Canadian Journal of Earth Sciences, v. 51, p. 943-972.

Keppie, J.D., (comp.) 1979. Geological map of the province of Nova Scotia; Nova Scotia Department of Mines and Energy map, scale 1:500,000.

Keppler, H., and Wyllie, P.J., 1991. Partitioning of Cu, Sn, Mo, W, U, and Th between melt and aqueous fluid in the systems haplogranite-H_2O−HCl and haplogranite-H_2O−HF; Contributions to Mineralogy and Petrology, v. 109, p. 139-150.

Kerr, A., 2014. The south Newfoundland granophile mineral district: Features and opportunities for research on blind deposits; Abstracts, Volume 37, Geological Association of Canada – Mineralogical Association of Canada Joint Annual Meeting; Fredericton, NB, p. 137-138.

Kerr, A., and McNicoll, V.J., 2012. New U-Pb geochronological constraints from mineralized granites in southern Newfoundland; *in* Current Research, Newfoundland Department of Natural Resources, Geological Survey, Report 12-1, p. 21-38.

Kerr, A., Dickson, W.L., Hayes, J.P., and Fryer, B.J., 1993. Devonian postorogenic granites on the southeast margin of the Newfoundland Appalachians: A review of geology, geochemistry, petrogenesis and mineral potential; *in* Current Research, Newfoundland Department of Natural Resources, Geological Survey, Report 93-1, p. 239-279.

Kerr, A., Jenner, G.A., and Fryer, B.J., 1995. Sm-Nd isotopic geochemistry of Precambrian to Paleozoic granitoid suites and the deep-crustal structure of the southeast margin of the Newfoundland Appalachians; Canadian Journal of Earth Sciences, v. 32, p. 224-245.

Kirkham, R.V., and Sinclair, W.D., 1988. Comb quartz layers in felsic intrusions and their relationship to the origin of porphyry deposits; *in* Recent Advances in the Geology of Granite-related Mineral Deposits, (ed.) R.P. Taylor and D.F. Strong; The Canadian Institute of Mining and Metallurgy, Special Volume 39, p. 50-71.

Klemm, L.M., Pettke, T, and Heinrich, C.A., 2008. Fluid and source magma evolution of the Questa porphyry Mo deposit, New Mexico, USA; Mineralium Deposita, v. 43, p. 533-552.

Lentz, D.R., 1992. Petrogenesis and geochemical composition of biotites in rare-element granitic; pegmatites in the southwestern Grenville Province, Canada; Mineralogy and Petrology, v. 46, p. 239-256.

Loferski, P.J., and Ayuso, R.A., 1995. Petrography and mineral chemistry of the composite Deboullie pluton, northern Maine, USA: Implications for the genesis of Cu-Mo mineralization; Chemical Geology, v. 123, p. 89-105.

Logan, J.M., Schiarizza, P., Struik, L.C., Barnett, C., Nelson, J.L., Kowalczyk, P., Ferri, F., Mihalynuk, M.G., Thomas, M.D., Gammon, P., Lett, R., Jackaman, W., and Ferbey, T. (comp.), 2010. Bedrock geology of the QUEST map area, central British Columbia; Geoscience BC Report 2010-5, British Columbia Geological Survey, Geoscience Map 2010-1 and Geological Survey of Canada, Open File 6476, scale 1:500,000.

Lynch, E.P., Selby, D., Feely, M., and Wilton, D.H.C., 2009. New constraints on the timing of molybdenite mineralization in the Devonian Ackley Granite suite, southeastern Newfoundland: Preliminary results from Re-Os geochronology; *in* Current Research, Newfoundland Department of Natural Resources, Geological Survey, Report 09-1, p. 225-235.

Lynch, E.P., Selby, D., and Wilton, D.H.C., 2012. The timing and duration of granite-related magmatic-hydrothermal events in southeastern Newfoundland: Results of Re-Os molybdenite geochronology; Abstracts with Programs, Geological Association of Canada – Mineralogical Association of Canada Joint Annual Meeting. St. John's, Newfoundland.

MacDonald, M.A., 2001. Geology of the South Mountain Batholith, southwestern Nova Scotia; Nova Scotia Department of Natural Resources, Open File Report ME 2001-2, 281 p.

Manning, D.A.C., and Pichavant, M., 1988. Volatiles and their bearing on the behaviour of metals in granitic systems; *in* Recent Advances in the Geology of Granite-related Mineral Deposits, (ed.) R.P. Taylor and D.F. Strong; The Canadian Institute of Mining and Metallurgy, Special Volume 39, p. 13-24.

Massey, N.W.D., MacIntyre, D.G., Desjardins, P.J., and Cooney, R.T., 2005. Geology of British Columbia; British Columbia Ministry of Energy, Mines and Petroleum Resources, British Columbia Geological Survey, Geoscience Map 2005-3, scale 1:1,000,000.

McClenaghan, M.B., Parkhill, M.A., Pronk, A.G., Seaman, A.A., McCurdy, M.W., Poulin, R.S., McDonald, A.M., Kontak, D.J., and Leybourne, M.I., 2015. Till, stream sediment, and stream water geochemical signatures of intrusion-hosted Sn-W deposits: examples from the Sisson W-Mo and Mount Pleasant Sn-W-Mo-Bi-In deposits, New Brunswick; *in* TGI 4 – Intrusion Related Mineralisation Project: New Vectors to Buried Porphyry-Style Mineralisation, (ed.) N. Rogers; Geological Survey of Canada, Open File 7843, p. 39-58.

McCutcheon, S.R., Sinclair, W.D., McLeod, M.J., Boyd, T., and Kooiman, G.J.A., 2010. Part 2: Mount Pleasant Sn–W–Mo–Bi–In Deposit; *in* Polymetallic Deposits Of Sisson Brook And Mount Pleasant, New Brunswick, Canada, (ed.) L.R. Fyffe, and K.G. Thorne; New Brunswick Department of Natural Resources; Lands, Minerals and Petroleum Division, Field Guide No. 3, p. 37-68.

McCutcheon, S., Reddick, J., McKeen, J., Scott, S., El-Rassi, D., and Kociumbas, M., 2013. Amended Technical Report of the Mount Pleasant Property, Including Mineral Resource Estimates, Southwestern New Brunswick, for Adex Mining Inc; Watts, Griffis and McOuat, Toronto. 222 p.

McMillan, W.J., 1985. Geology and ore deposits of the Highland Valley camp; Geological Association of Canada, Mineral Deposits Division, Field Guide and Reference Manual Series, Number 1, 121 p.

McMillan, W.J., Anderson, R.G., Chen, R., and Chen, W., 2009. Geology and mineral occurrences (MINFILE), the Guichon Creek Batholith and Highland Valley porphyry copper district, British Columbia, Geological Survey of Canada, Open File 6079, 2 sheets.

McPhie, J., Kamentsky, V., Allen, S., Ehrig, K., Agangi, A., and Bath, A., 2011. The fluorine link between a supergiant ore deposit and a silicic large igneous province; Geology, v. 39, p. 1003-1006.

Muecke, G.K., and Clarke, D.B., 1981. Geochemical Evolution of the South Mountain Batholith, Nova Scotia: Rare-Earth-Element Evidence; Canadian Mineralogist, v. 19, p. 133-145.

Nelson, J., Colpron, M., and Israel, S., 2013. The Cordillera of British Columbia, Yukon and Alaska: tectonics and metallogeny; *in* Tectonics, Metallogeny, and Discovery - the North American Cordillera and similar accretionary settings, (ed.) M. Colpron, T. Bissig, B. Rusk and J.F.H. Thompson; Society of Economic Geologists, Special Publication 17, p. 53-109.

O'Brien, S.J., 1998. Geology of the Connaigre Peninsula and adjacent areas, southern Newfoundland; Geological Survey, Department of Mines and Energy, Open File Map NFLD/2660; 1:100,000 scale.

O'Brien, S.J., O'Driscoll, C.F., Greene, B.A., and Tucker, R.D., 1995. Pre-Carboniferous geology of the Connaigre Peninsula and the adjacent coast of Fortune Bay, southern Newfoundland; *in* Current Research, Newfoundland Department of Natural Resources, Geological Survey Branch, Report 95-1, p. 267-297.

Oliver, J.L., Crozier, J., Kamionko, M., and Fleming, J., 2009. The Gibraltar mine, British Columbia. A billion tonne deep copper molybdenum porphyry system: structural style, patterns of mineralization and rock alteration; *in* Roundup 2009 program with abstracts; Association for Mineral Exploration British Columbia, Vancouver, British Columbia, p. 35-36.

Phillips, W.J., 1973. Mechanical effects of retrograde boiling and its probable importance in the formation of some porphyry ore deposits; Institute of Mining and Metallurgy Transactions, v. B82, p. 90-98.

Plouffe, A., and Ferbey, T., 2015. Till composition near Cu-porphyry deposits in British Columbia: Highlights for mineral exploration; *in* TGI 4 – Intrusion Related Mineralisation Project: New Vectors to Buried Porphyry-Style Mineralisation, (ed.) N. Rogers; Geological Survey of Canada, Open File 7843, p. 15-37.

Plouffe, A., Ferbey, T., Levson, V.M., and Bond, J.D., 2012. Glacial history and drift prospecting in the Canadian Cordillera: recent developments; Geological Survey of Canada, Open File 7261, 51 p.

Rempel, K.U., Williams-Jones, A.E., and Migdisov, A.A., 2008. The solubility of molybdenum dioxide and trioxide in HCl-bearing water vapour at 350°C and pressures up to 160 bars; Geochimica et Cosmochimica Acta, v. 72, p. 3074-3083.

Richards, J.P., 2009. Postsubduction porphyry Cu-Au and epithermal Au deposits: Products of remelting of subduction-modified lithosphere; Geology, v. 37, p. 247-250.

Richards, J.P., 2011. Magmatic to hydrothermal metal fluxes in convergent and collided margins; Ore Geology Reviews, v. 40, p. 1-26.

Rogers, N., Kellett, D.A., McNicoll, V.J., van Staal, C.R., Kerr, A., and Ruberti, G., 2015a. Tectonostratigraphic controls on the Connaigre Peninsula of south-central Newfoundland and their implications for intrusion-related mineral resources; *in* TGI 4 – Intrusion Related Mineralisation Project: New Vectors to Buried Porphyry-Style Mineralisation, (ed.) N. Rogers; Geological Survey of Canada, Open File 7843, p. 59-78.

Rogers, N., McClenaghan, M.B., Plouffe, A., Kellett, D.A., Chapman, J., Azadbakht, Z., Tweedale, F., Ruberti, G., and Anderson, B., 2014. TGI 4 – Intrusion Related Mineralisation Project: New Vectors to Buried Porphyry-Style Mineralisation; *in* Abstracts 2014:

Exploration, Mining and Petroleum New Brunswick, (ed.) E.A. Keith; New Brunswick Department of Energy and Mines, Geoscience Report 2014–5, p. 31.

Rogers, N., McClenaghan, M.B., Thorne, K.G., Fyffe, L.R., Seaman, A.A, Parkhill, M.A., McClenaghan, S.H., Pronk, A.G., Beal, K.L., Lentz, D.R., Wilson, R.A., Rice, J.M., and Lentz, C., 2015b. Granite-related mineralization and alteration in the Acadian Plutonic Belt: implications for Sn-W-Mo-Cu exploration in central New Brunswick – TGI 4 Field Guide; *in* TGI 4 – Intrusion Related Mineralisation Project: New Vectors to Buried Porphyry-Style Mineralisation, (ed.) N. Rogers; Geological Survey of Canada, Open File 7843, p. 113-204.

Schiarizza, P., 2015. Geological setting of the Granite Mountain batholith, south-central British Columbia; *in* Geological Fieldwork 2014, British Columbia Ministry of Energy and Mines, British Columbia Geological Survey Paper 2015-1, p. 19-39.

Shannon, J.R., Walker, B.M., Carter, R.B., and Geraghty, E.P., 1982. Unidirectional solidification textures and their significance in determining relative ages of intrusions at the Henderson mine, Colorado; Geology, v. 19, p. 293-297.

Shinohara, H., Kazahaya, K., and Lowenstern, J.B., 1995. Volatile transport in a convecting magma column: Implications for porphyry Mo mineralization; Geology, v. 23, p. 1091-1094.

Siahcheshm, K., Calagari, A.A., Abedini, A., and Lentz, D.R., 2012. Halogen signatures of biotites from the Maher-Abad porphyry copper deposit, Iran: characterization of volatiles in syn- to post-magmatic hydrothermal fluids; International Geology Review, v. 54, p. 1353-1368.

Sillitoe, R.H., 2010. Porphyry copper systems; Economic Geology, v. 105, p. 3-41.

Sinclair, W.D., 2007. Porphyry deposits; *in* Mineral Deposits of Canada: A Synthesis of Major Deposit-Types, District Metallogeny, the Evolution of Geological Provinces, and Exploration Methods, (ed.) W.D. Goodfellow; Geological Association of Canada, St. John's, Newfoundland, p. 223–243.

Sinclair, W.D., Kooiman, G.J.A., Martin, D.A., and Kjarsgaard, I.M., 2006. Geology, geochemistry and mineralogy of indium resources at Mount Pleasant, New Brunswick, Canada; Ore Geology Reviews, v. 28, p. 123-145.

Spirito, W., McClenaghan, M.B., Plouffe, A., McMartin, I., Campbell, J.E., Paulen, R.C., Garrett, R.G., and Hall, G.E.M., 2011. Till sampling and analytical protocols for GEM projects: from field to archive; Geological Survey of Canada, Open File 6850, 83 p.

Sutherland Brown, A., 1974. Gibraltar Mine (93B-12, 13); *in* Geology, Exploration and Mining in British Columbia 1973, B.C. Ministry of Energy, Mines and Petroleum Resources, p. 299-318.

Thomas, R., Webster, J.M., Rhede, R., Seifert, W., Rickers, K., Förster, H-J., Heinrich, R., and Davidson, P., 2006. The transition from peraluminous to peralkaline granitic melts: Evidence from melt inclusions and accessory minerals; Lithos, v. 91, p. 137-149.

Tuach, J., Davenport, P.H., Dickson, W.L., and Strong, D.F., 1986. Geochemical trends in the Ackley granite, southeast Newfoundland: Their relevance to magmatic metallogenic processes in high-silica granitic systems; Canadian Journal of Earth Sciences, v. 23, p. 747-765.

Tweedale, F., Hanley, J.J., Kontak, D.J., and Rogers, N., 2014. Petrographic observations and evaporate mound analysis of quartz-hosted fluid inclusions: Applications to assess metal fertility in granites; Abstracts with Programs, Volume 37, Geological Association of Canada – Mineralogical Association of Canada Joint Annual Meeting; Fredericton, NB, p. 275-276.

Tweedale, F., Hanley, J.J., Kontak, D.J., and Rogers, N., 2015. Petrographic observations and evaporate mound analysis of quartz-hosted fluid inclusions hosted by granitoid samples from the South Mountain Batholith, Nova Scotia: An exploration tool for vectoring towards mineralized areas in intrusive rocks; *in* TGI 4 – Intrusion Related Mineralisation Project: New Vectors to Buried Porphyry-Style Mineralisation, (ed.) N. Rogers; Geological Survey of Canada, Open File 7843, p. 79-99.

Ulrich, T., 2004. Molybdenum solubility and transport under hydrothermal-magmatic conditions; *in* Abstracts, 14th Annual Goldschmidt Conference, v. 3, p. 23.

Ulrich, T., and Mavrogenes, J., 2008. An experimental study of the solubility of molybdenum in H_2O and KCl-H_2O solutions from 500°C to 800°C, and 150 to 300 MPa; Geochimica et Cosmochimica Acta, v. 72, p. 2316-2330.

van Staal, C.R., Ruberti, G., Kerr, A., Conliffe, J., Rogers, N., 2015. The Coast of Bays: Paleozoic tectonic evolution of the Gander margin and adjacent Avalonia in southeastern Newfoundland – TGI 4 Field Guide; *in* TGI 4 – Intrusion Related Mineralisation Project: New Vectors to Buried Porphyry-Style Mineralisation, (ed.) N. Rogers; Geological Survey of Canada, Open File 7843, p. 205-245.

van Staal, C.R., Whalen, J.B., Valverde-Vaquero, P., Zagorevski, A., and Rogers, N., 2009. Pre-Carboniferous, episodic accretion-related, orogenesis along the Laurentian margin of the northern Appalachians; *in* Ancient Orogens and Modern Analogues, (ed.) J.B. Murphy, J.D. Keppie and A.J. Hynes; Geological Society, London, Special Publications, v. 327, p. 271-316.

van Staal, C.R., Zagorevski, A., McNicoll, V.J., and Rogers, N., 2014. Time-Transgressive Salinic and Acadian Orogenesis, Magmatism and Old Red Sandstone Sedimentation in Newfoundland; Geoscience Canada, v. 41, p. 138-164.

Vry, V.H., Wilkinson, J.J., Seguel, J., And Millán, J., 2010. Multistage intrusion, brecciation, and veining at El Teniente, Chile: Evolution of a nested porphyry system; Economic Geology, v. 105, p. 119-153.

Wang, R.C., Xie, L., Chen, J., Yu, A., Wang, L., Lu, J., and Zhu, J., 2013. Tin-carrier minerals in metaluminous granites of the western Nanling Range (southern China): Constraints on processes of tin mineralization in oxidized granites; Journal of Asian Earth Sciences, v. 74, p. 361-372.

Whalen, J.B., 1993. Geology, petrography and geochemistry of Appalachian granites in New Brunswick and Gaspesie, Quebec; Geological Survey of Canada, Bulletin 436, 124 p.

Whitney, J.A., 1975. Vapour generation in a quartz monzonite magma: a synthetic model with application to porphyry copper deposits; Economic Geology, v. 70, p. 346-358.

Whitney, J.A., 1984. Volatiles in magmatic systems; in Fluid-mineral Equilibria in Hydrothermal Systems; Reviews in Economic Geology, v. 1, p. 155-175.

Till composition near Cu-porphyry deposits in British Columbia: Highlights for mineral exploration

Alain Plouffe[1] and Travis Ferbey[2]

1. Geological Survey of Canada, 601 Booth St., Ottawa, Ontario

2. British Columbia Geological Survey, 1810 Blanshard St., Victoria, British Columbia

Abstract: Till orientation surveys were completed in the region of four Cu porphyry deposits in British Columbia with the objective of defining geochemical and mineralogical indicators of porphyry mineralisation buried by glacial sediments. We demonstrate that even if those deposits contain low to medium metal grades (e.g., 0.2 to 0.4 % Cu compared to an average crustal abundance of 0.0075 % Cu), they are reflected in the till composition with elevated concentrations of ore metals (Cu, Au, Mo) and pathfinder elements (Hg, Pb, Zn, Ag), and large grain counts of ore minerals (chalcopyrite, gold grains) and alteration minerals (e.g., epidote, andradite garnet, apatite) which are in contrast with surrounding regions devoid of mineralisation. These zones with elevated metal or mineral content in till define glacial dispersal trains that extend several kilometres down-ice from the bedrock mineralised sources. In this study, the shape of the dispersal trains is principally controlled by: 1) the ice-flow directions; and 2) the areal extent of the mineralisation exposed to glacial erosion which can comprise a cluster of sub-economic mineralised zones in the periphery of the main economic deposits. Using those porphyry indicators and existing till composition data sets from a region underlain by Late Triassic to Early Jurassic intrusions within the Quesnel terrane, we postulate that potential for Cu-Au porphyry style mineralisation exists within the Spout Lake pluton to the west of the Takomkane batholith and at the northern end of the Thuya batholith.

Introduction

Porphyry deposits are defined as "large, low- to medium-grade deposits in which primary (hypogene) ore minerals are dominantly structurally controlled and which are spatially and genetically related to felsic to intermediate porphyritic intrusions" (Kirkham, 1972; Sinclair, 2007). In Canada, 40 % of Cu, all Mo and 10 % of Au is produced from porphyry deposits (Sinclair, 2007). Porphyry deposits are predominantly found in orogenic belts and the Canadian Cordillera is no exception to this general rule as it includes a number of porphyry deposits which have been or are still in production (Fig. 1).

A hindrance to exploring for porphyry deposits in broad sectors of the Canadian Cordillera is the presence of an extensive and thick cover of glacial sediments which obscure prospective bedrock geology. Consequently, discoveries made from outcropping mineralisation have become increasingly rare. New efficient methods for detecting buried mineralisation need to be developed in this evolving context. To address this issue, the Geological Survey of Canada in collaboration with the British Columbia Geological Survey implemented an orientation till sampling survey in the region of four Cu-porphyry deposits in the Canadian Cordillera: Highland Valley Copper (Cu-Mo porphyry), Gibraltar (Cu-Mo porphyry) and Mount Polley (Cu-Au-Ag porphyry) mines and the Woodjam prospect (Cu-Mo-Au porphyry) (Fig. 1) . The sampling survey extended over a three year period (2011 to 2013) with the objective of defining key geochemical and mineralogical indicators of porphyry mineralisation that can be identified in till and related to buried mineralisation (Anderson et al., 2012a; Ferbey et al., 2014).

A total of 309 till samples (excluding field duplicate samples) were collected in this study and were geochemically analysed and processed for indicator minerals. Geochemical and mineralogical results were presented on posters and in oral presentations at conferences, and in departmental publications throughout the course of this activity (Anderson et al., 2012a, b, c; Plouffe et al., 2012, 2013a, c, 2014; Ferbey and Plouffe, 2014; Ferbey et al., 2014; Hashmi et al., 2014; Plouffe and Ferbey, 2015a). This paper presents the highlights of the work accomplished to date, provides an overview of the publications to be published in the future as part of this project, and discuss future research avenues that should be pursued to improve and develop mineral exploration methods for porphyry deposits in glaciated areas. As a general overview, we demonstrate that Cu-porphyry deposits with low to medium Cu grades (0.2 to 0.4 % Cu compared to an average crustal abundance of 0.0075 %; Rudnick and Gao, 2004) can be detected using a combination of geochemical and mineralogical analyses of the till matrix.

Porphyry mineralisation setting

Porphyry deposits within the Canadian Cordillera (Cu, Cu-Mo, Cu -Au, Au, W and Mo) occur principally in felsic to intermediate intrusive rocks associated to the Stikine and Quesnel volcanic arc terranes that were accreted to North America in the Middle Jurassic, with fewer porphyry deposits within the Wrangellia terrane (Fig. 1; Logan, 2013). Porphyry deposits formed during two episodes in two general tectonic settings: 1) in an island-arc setting, prior to accretion to North America, in Late Triassic to Middle Jurassic time, and 2) in a continental-arc setting, after accretion, in Late Cretaceous to Eocene time (McMillan and Panteleyev, 1995; McMillan et al., 1995, 1996; Logan, 2013). Logan and Mihalynuk (2014) presented the tectonic controls of a particular prolific period for the formation of Cu porphyry deposits in the Canadian Cordillera centred around 205 Ma when more than 90 % of the Cu deposits were formed.

Corresponding author: Alain Plouffe (aplouffe@nrcan.gc.ca)

Plouffe, A., and Ferbey, T., 2015. Till composition near Cu-porphyry deposits in British Columbia: Highlights for mineral exploration; *in* TGI 4 – Intrusion Related Mineralisation Project: New Vectors to Buried Porphyry-Style Mineralisation, (ed.) N. Rogers; Geological Survey of Canada, Open File 7843, p. 15-37.

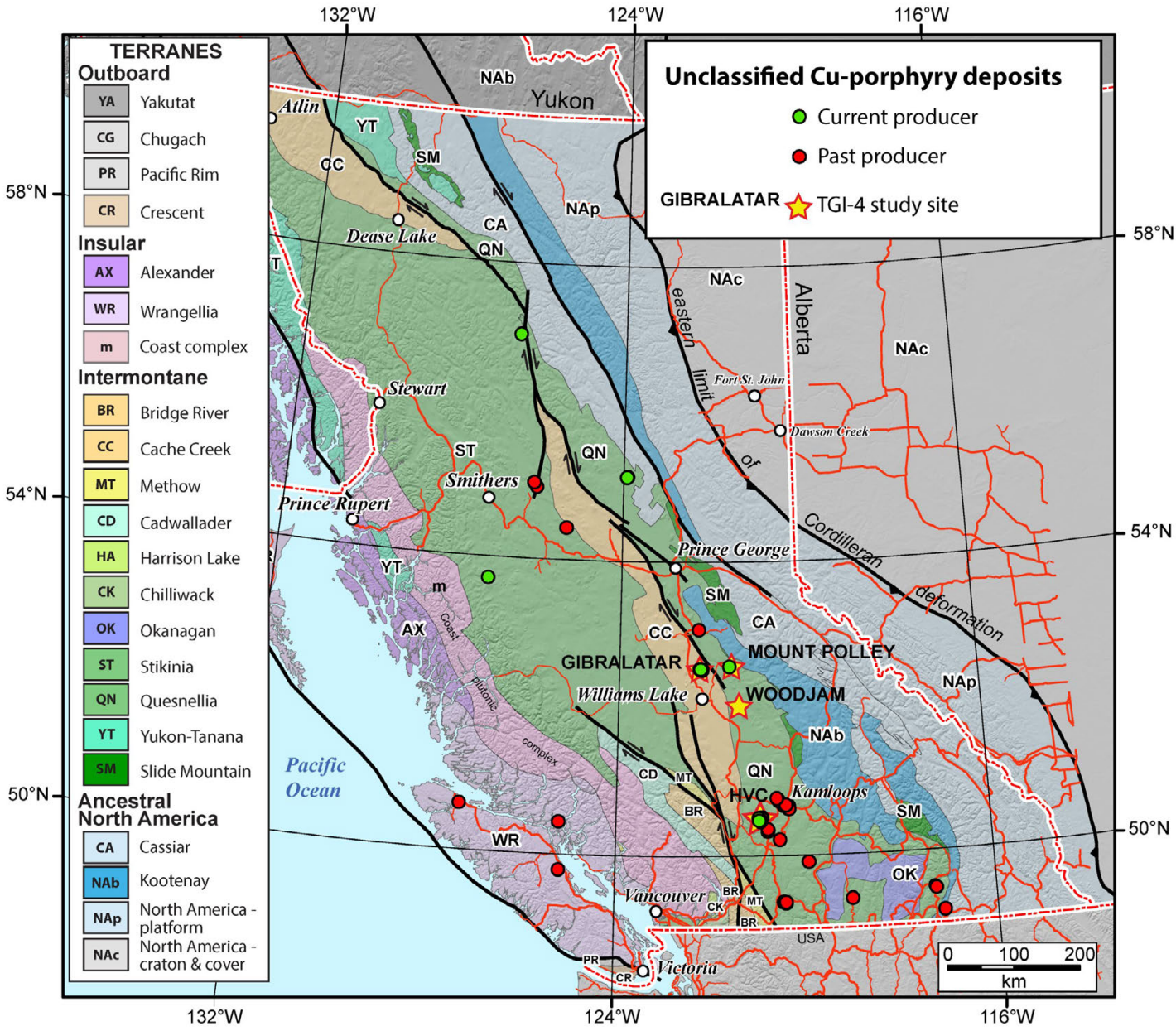

Figure 1 – Location of the four study sites, and of the past-producing and producing unclassified Cu-porphyry deposits (from MINFILE, 2015) depicted on the terrane map of British Columbia (Colpron and Nelson, 2011). HVC- Highland Valley Copper deposit.

The four Cu porphyry deposits investigated as part of this till sampling survey are part of the Quesnel terrane. Copper porphyry mineralisation at the four study sites is hosted in Late Triassic to Early Jurassic calcalkaline (Cu-Mo porphyry) to alkaline (Cu-Au porphyry) intrusions which intruded the coeval Nicola Group volcanic and associated sedimentary rocks. Chalcopyrite is one of the main Cu ore minerals at each site with lesser amounts of bornite. In the calcalkaline deposits, Mo is dominantly hosted in molybdenite.

The Highland Valley Copper Mine includes at least five calcalkaline Cu-Mo porphyry deposits hosted within the Guichon Creek batholith. A total of 1615.16 million tonnes of ore grading 0.40 % Cu and 0.010 % Mo were processed at the mine. In December 2012, the reserves were estimated at 697 million tonnes at 0.29 % Cu and 0.008 % Mo (Byrne et al., 2013).

The Mount Polley Mine is an alkaline Cu-Au-Ag porphyry deposit which has been in operation since 1997 with an interruption period of four years from 2001 to 2005. In addition to the mineralogy typical of Cu-porphyry deposits (i.e., chalcopyrite and bornite), Au and Ag occur as inclusions and as micro-scale grains that co-precipitated with sulfides (Pass, 2010). At this deposit, Au is more enriched in pyrite as compared to the Cu sulphides (Pass, 2010). A total of 80 million tonnes of ore were milled producing 452 million pounds of Cu,

695,000 ounces of Au, and 2.2 million ounces of Ag (Rees, 2013). As of January 2013, the reserves were estimated at 93 million tonnes grading 0.297 % Cu, 0.299 g/t Au, and 0.620 g/t Ag (Rees, 2013).

The Gibraltar Mine is a calcalkaline Cu-Mo porphyry deposit which has been in operation from 1972 to 1988 and from 2004 to present (Liles, 2005; van Straaten et al., 2013). The deposit is hosted within the Granite Mountain batholith. Because of the presence of Cache Creek rocks near the batholith and because of limited bedrock exposure which hinders the interpretation of contact relationship, the batholith was originally interpreted to be part of the Cache Creek terrane, which consists of ocean basin and oceanic arc rocks of Paleozoic to early Mesozoic age (e.g., Drummond et al., 1973, 1976; Bysouth et al., 1995). However, recent mapping has demonstrated that the batholith intrudes Nicola Group volcanic and sedimentary rocks and is part of the Quesnel terrane (Schiarizza, 2014, 2015). Combining past production and current resource, it represents 1.22 billion tonnes of ore with a Cu grade of 0.317 % and an estimated Mo grade of 0.010 % (van Straaten et al., 2013).

The Woodjam prospect includes five mineralised zones associated with emplacement of the Takomkane batholith and accompanying satellite intrusions at the northwestern limit of the batholith: Takom, Megabuck, Deerhorn, Southeast, and Three Firs. None of these zones have been mined. It includes porphyry mineralisation with alkaline and calcalkaline composition (del Real et al., 2013, 2014). To date, inferred resources for three mineralised zones at Woodjam are evaluated at 221.7 million tonnes of ore with Cu grades varying from 0.22 to 0.31 % Cu and 0.26 to 0.49 g/t Au (Sherlock et al., 2013; Sherlock and Trueman, 2013). Calculations of Mo reserves are not publically available for Woodjam.

Glacial sediment cover

The glacial sediment cover varies extensively at the four study sites. At Woodjam, none of the mineralisation is exposed at surface and only a portion of the alteration zone outcrops. Based on drill log data, unconsolidated sediment thickness reaches over 200 m over the deposit (J.W. Morton, pers. comm., 2014; see profiles in del Real et al., 2014). At the Gibraltar, Mount Polley and Highland Valley mines, at pre-mining time, the mineralisation was in large part covered by various thicknesses of glacial sediments (in other words mineralisation was subcropping) but in all cases a small part of the mineralisation was exposed at surface (in other words mineralisation was naturally outcropping) as reported in Rotherham et al. (1972), Casselman et al. (1995), Byrne et al. (2013), and Rees (2013). Any mineralised zone that was protected from glacial erosion represents a limiting factor in the application of till composition for the detection of buried mineralisation (Plouffe et al., 2012). This is the case at Woodjam where one of the mineralised zone (Three Firs) is in part covered by basalt correlated to the Oligocene-Pliocene Chilcotin Group that can be up to 20 m thick (Bissig et al., 2013). At Highland Valley, pre-glacial sediments partly cover the Valley deposit and probably completely cover the J.A. deposit (Bobrowsky et al., 1993; Byrne et al., 2013). The Chilcotin Group basalt at Woodjam and the pre-glacial sediments at Highland Valley acted as a shield which protected part of the mineralisation from glacial erosion. Therefore, none of the protected mineralisation is reflected in the till composition.

Glacial history

The interpretation of the glacial history for the four study sites is based on previous studies plus the current investigation of the ice-flow direction indicators. All of the four sites were covered by the Cordilleran Ice Sheet during the Late Wisconsinan Fraser glaciation. At the onset of glaciation, valley glaciers coalesced into piedmont glaciers in the Coast and Cariboo mountains (Tipper, 1971a, b). Valley glaciers also formed in isolated mountain ranges within the Interior Plateau (e.g., Clague, 1989; Plouffe, 2000). The first glaciers to cover the three northern most study sites were derived from the Cariboo Mountains and were generally advancing to the west to southwest. At glacial maximum, glaciers from the Coast and Cariboo Mountains coalesced over the Interior Plateau forming an east-west ice divide around the 52° latitude from which ice was flowing to the north and south. This ice divide is visible on the provincial compilation map of ice-flow indicators (Ferbey and Arnold, 2013; Ferbey et al., 2013). Consequently, at the three northern sites, there was a second phase of ice flow to the north to northwest which originated from the ice divide. Only in the Gibraltar Mine region, we have found evidence of a third ice movement to the southeast, the origin and timing of which is still unclear. The net implication of these multiple ice-flow movements is that the geochemical or mineralogical signal in till derived from mineralisation might have been transported by any combination of these glacial transport vectors.

Regional surficial geology investigations plus our own field studies in the Highland Valley Copper deposit region, have defined a single vector of ice flow to the south to southeast which was derived principally from the ice divide at the 52° latitude (Fulton, 1975; Ryder, 1976; Bobrowsky et al., 2002; Plouffe et al., 2013a, b).

Methods

Field work involved sampling till, measuring ice-flow indicators on bedrock outcrops and making observations for the production of surficial geology maps. Till sampling was completed following procedures outlined in Spirito et al. (2011) with the objective of obtaining samples not only down-ice but in all directions from the known mineralisation. This approach is used to define the extent of glacial dispersal and to demonstrate that the geochemical or mineralogical enrichment in till which defines a glacial dispersal train stands out above regional background values. Two till samples were collected at each sampling site: a large (ca. 10 kg) and small (ca. 2 kg) sample.

The small sample was shipped to the Sedimentology Laboratory of the Geological Survey of Canada and was processed to separate the silt and clay-sized fraction (<0.063 mm) by dry sieving and the clay-sized fraction (<0.002 mm) by decantation and centrifuging (Girard et al., 2004). Both fractions were submitted for geochemical analyses in a commercial laboratory (ACME Analytical Laboratories, Bureau Veritas Company, Vancouver, BC) which included two analytical packages: 1) 0.2 g aliquots were digested with lithium metaborate/tetraborate, fused at 980°C, dissolved in 5 % HNO_3 and then analysed by inductively coupled plasma emission spectrometry and mass spectrometry (ICP-ES and ICP-MS), and 2) 0.5 of clay sized (<0.002 mm) material and 30 g of silt plus clay sized (<0.063 mm) material were diluted in a HCl and HNO_3 solution (ratio 1:1, modified aqua regia) and analysed by ICP-MS (Fig. 2A). Large silt and clay aliquots (30 g) were submitted for Au analyses by ICP-MS to reduce the nugget effect (Harris, 1982; Stanley, 2008) attributed to fine gold grains heterogeneously distributed in the silt-sized material of the till matrix which generally result in low analytical precision. A combination of field duplicates, laboratory duplicates (blind duplicate) and standards were submitted with the routine samples to monitor sampling site variability, analytical precision and accuracy, respectively.

The large samples were processed to recover the heavy (>3.2 specific gravity (s.g.)) and mid-density (2.8-3.2 s.g.) mineral fractions

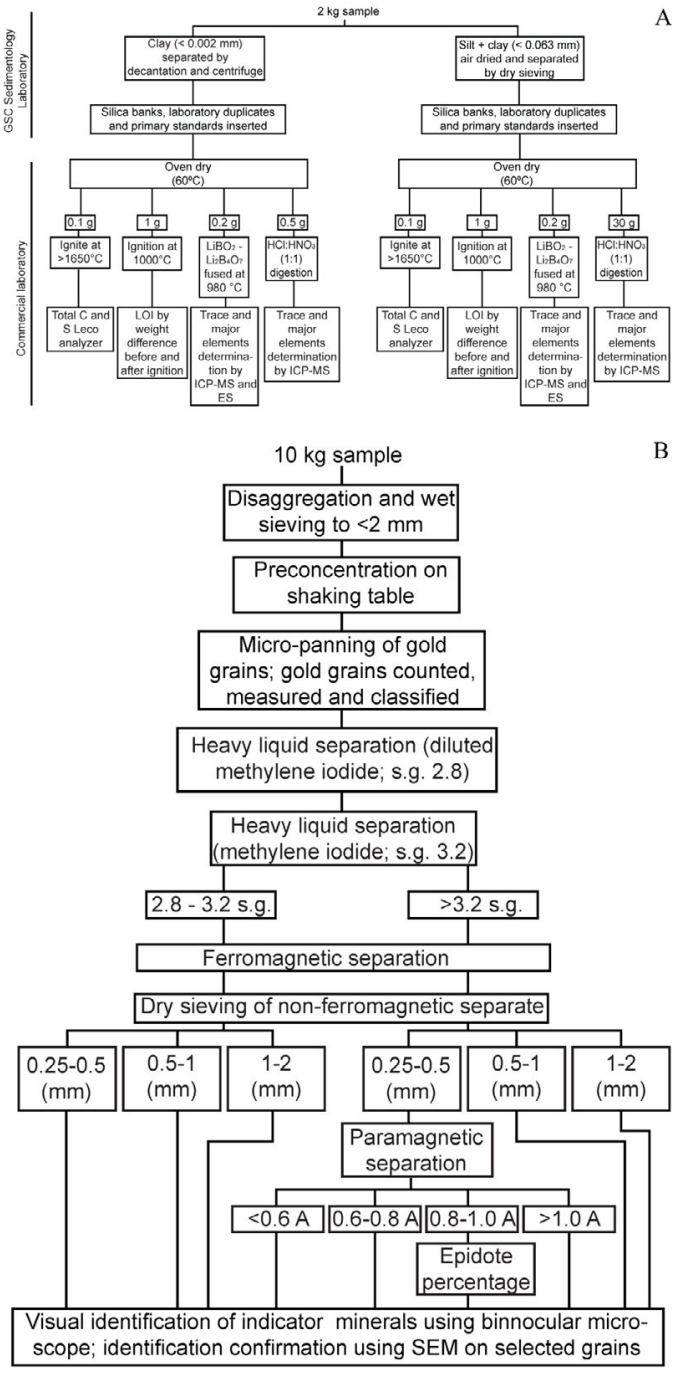

Figure 2 – Flow charts showing the procedures followed for:
(A) geochemical analyses;
(B) heavy mineral separation and indicator mineral identification.

and identify indicator minerals at Overburden Drilling Management Limited (Ottawa, ON) following the protocols adopted at the Geological Survey of Canada (see Plouffe et al. (2013b) for the details of the methodology) and outlined in Figure 2B. Quality assurance and quality control samples were submitted along with the routine samples and included: 1) blank samples from weathered granite to monitor potential cross-contamination, 2) field duplicate samples to monitor sampling site variability, and 3) spiked samples to evaluate the precision of the heavy mineral separation and indicator mineral identification procedures. In addition, a limited number of heavy mineral concentrates were re-numbered and re-submitted for mineral identification to evaluate the precision of the indicator mineral counts.

Geochemical and mineralogical analytical results obtained for this study will be available via an open file report (A. Plouffe and T. Ferbey, work in progress, 2015).

Results and interpretation: an overview

Interpretation of the till geochemical and mineralogical data, taking in consideration the reconstructed ice-flow histories, has important implications for mineral exploration for porphyry deposits in glaciated areas. Key highlights are presented below.

Porphyry mineralisation can be detected based on multi-element enrichment in till.

At the four study sites, Cu-porphyry mineralisation is reflected by a high Cu content in the clay-sized fraction of till down-ice from the mineralised zones (Figs. 3 and 4; Plouffe et al., 2011a, 2013a; Plouffe and Ferbey, 2015a). The high Cu concentrations in till near the known mineralised zones stands out above regional background Cu content of till and reaches concentrations greater than 380 ppm at Gibraltar, Mount Polley and Woodjam, and greater than 990 ppm at Highland Valley Copper. These high Cu concentrations define glacial dispersal trains with various lengths; one to two kilometres at Woodjam but over four kilometres at Mount Polley. The areal extent and shape of the Cu dispersal is in part related to the extent of the bedrock mineralisation exposed to glacial erosion (Plouffe et al., 2012). For example, the large amoeboid dispersal train of Cu in till at Gibraltar is in part related to a cluster of Cu porphyry mineral occurrences in the region that were glacially eroded (Fig. 3).

At calc-alkaline Cu-Mo porphyry deposits, till contains up to 8 ppm Mo (Fig. 5; Plouffe et al., 2014). At Gibraltar, the areas of Mo and Cu rich till are similar in size and shape (Figs. 3 and 5). At the Mount Polley alkaline Cu-Au-Ag porphyry deposit, till contains up to 90 ppb Au defining a Au glacial dispersal train of over 8 km extending down-ice to the northwest (Fig. 6; Hashmi et al., 2014, in press a, b).

High commodity metal contents in till near porphyry deposits can be found in association with high pathfinder element contents. Such is the case at Gibraltar where elevated Ag and Zn (Plouffe et al., 2011a, 2014) and at Mount Polley where elevated Zn and Hg concentrations (Hashmi et al., 2014, in press a) have been identified in till at the periphery of the main deposits. These patterns in the till reflect metal zoning associated to the main mineralisation. These results indicate that porphyry mineralisation that was exposed to glacial erosion and is now partly buried by glacial sediments, can be detected based on elevated multi-element contents in till.

Ore minerals are present in till down-ice from porphyry deposits.

Analogous to high trace element contents identified in till in the region of the porphyry deposits, ore minerals associated with porphyry mineralisation are present in till. Chalcopyrite is a key ore mineral in most Cu porphyry deposits in British Columbia and it has been recovered from till samples at all four study sites (Fig. 7). It is present and

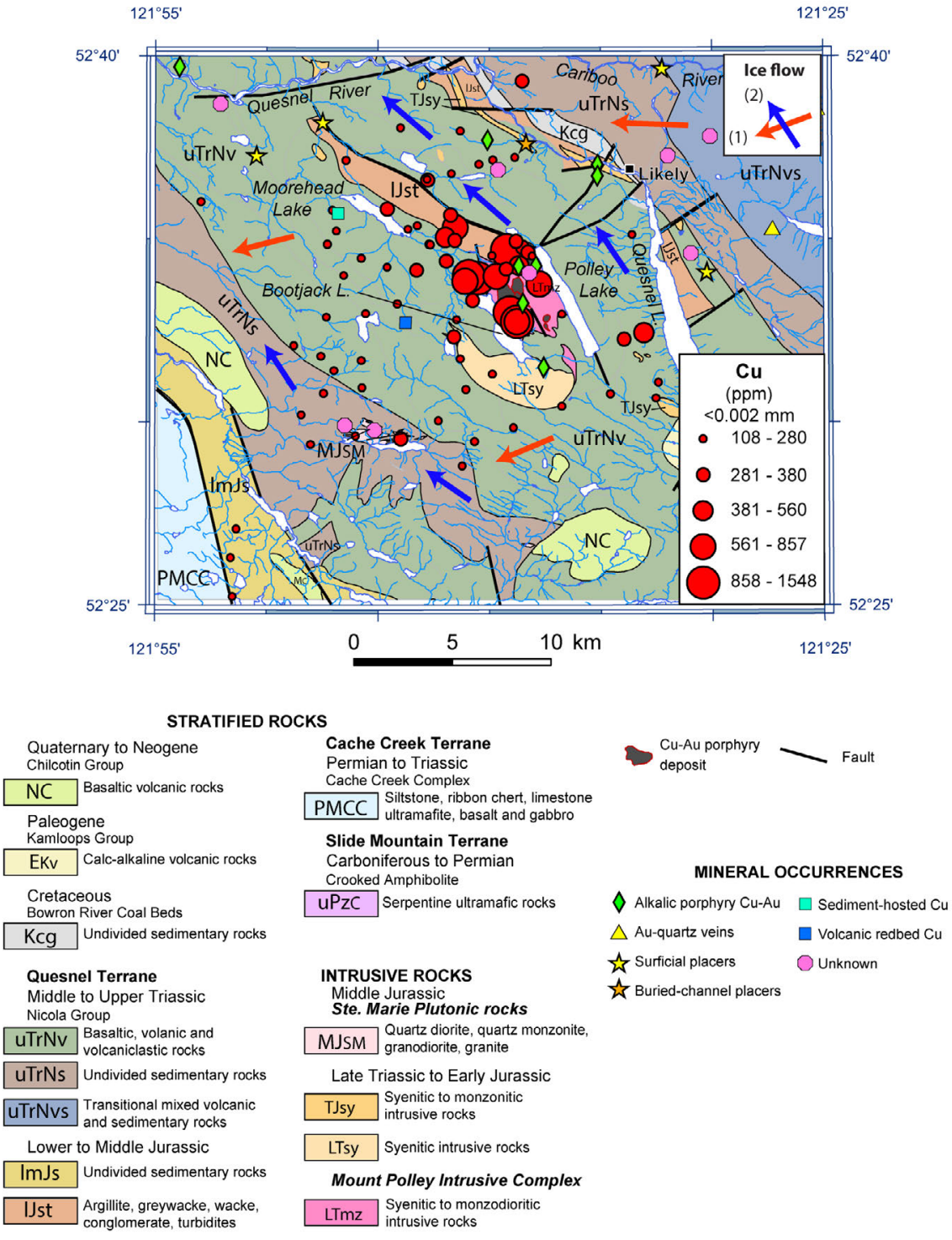

Figure 3 – Copper in the clay-sized fraction of till at the Mount Polley deposit analysed by ICP-MS after an HCl : HNO_3 leach (1:1) (modified from Hashmi et al., in press a). Bedrock geology simplified from Massey et al. (2005) and Logan et al. (2007, 2010).

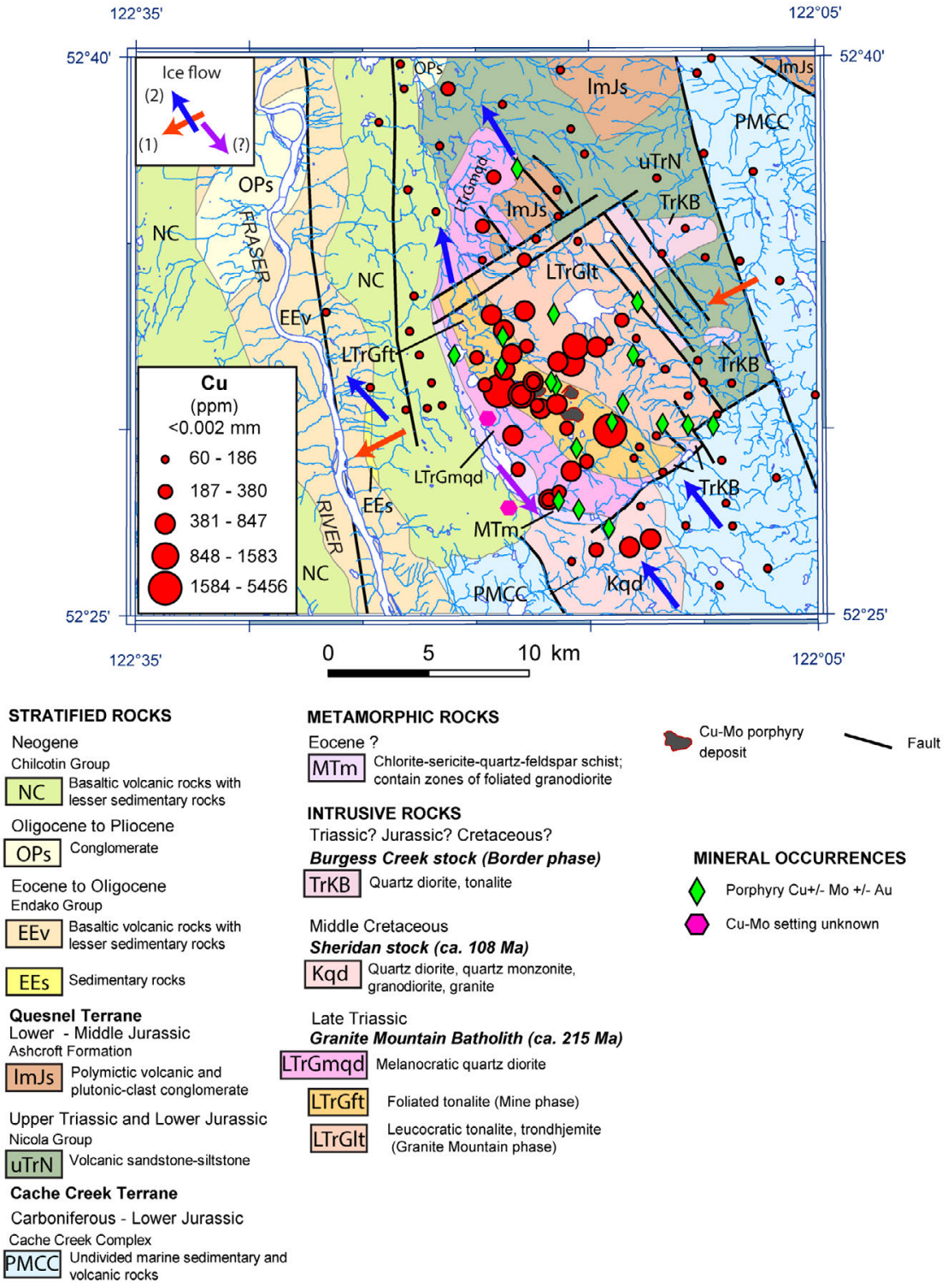

Figure 4 – Copper in the clay-sized fraction of till at the Gibraltar deposit analysed by ICP-MS after an HCl : HNO_3 leach (1:1). Bedrock geology simplified from Ash et al. (1999), Massey et al. (2005) and Schiarizza (2014).

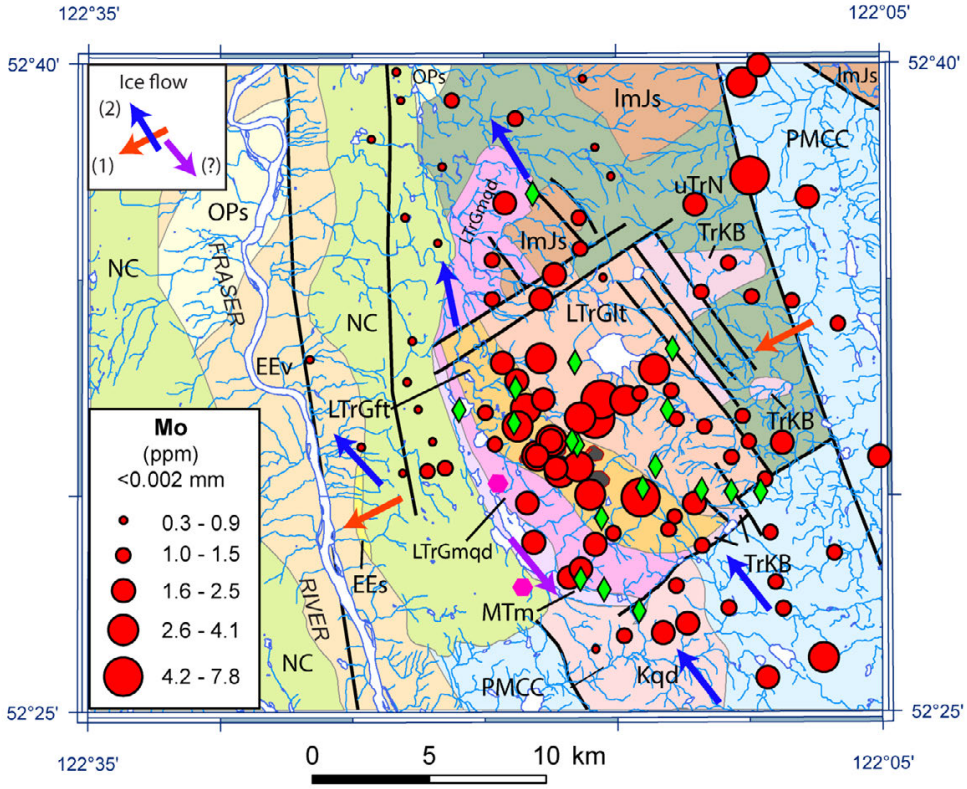

Figure 5 – Molybdenum in the clay-sized fraction of till at the Gibraltar deposit analysed by ICP-MS after an HCl : HNO_3 leach (1:1) (modified from Plouffe et al., 2014). Bedrock geology legend is the same as Figure 4.

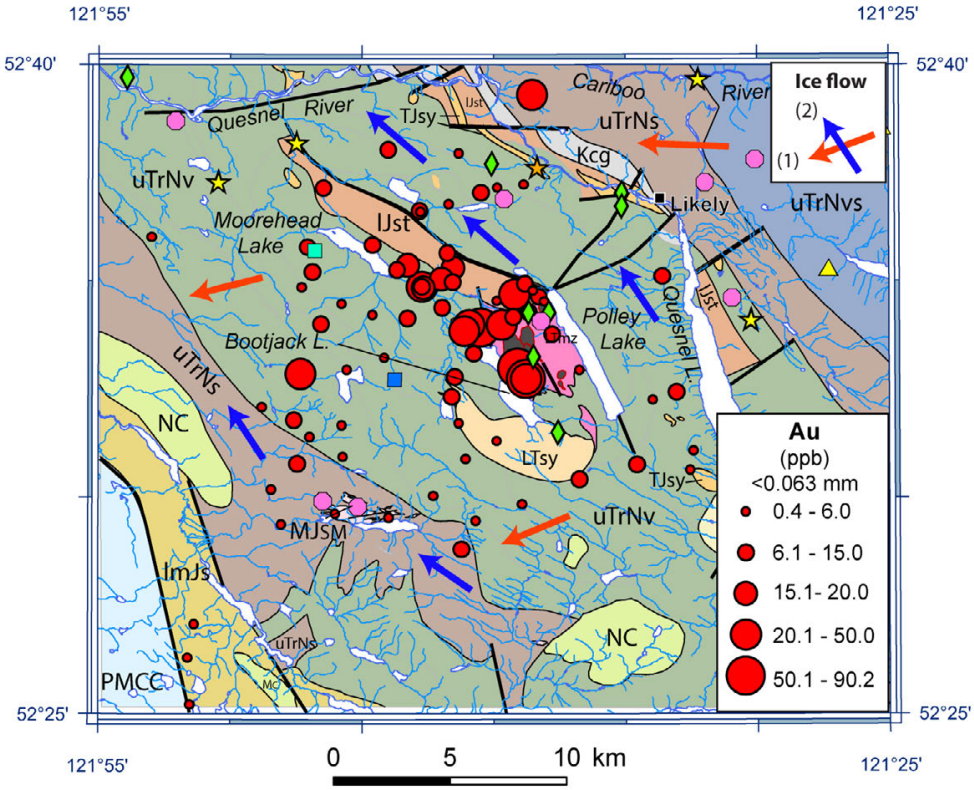

Figure 6 – Gold in the silt plus clay-sized fraction of till at the Mount Polley deposit analysed by ICP-MS after an HCl : HNO_3 leach (1:1) (modified from Hashmi et al., in press a). Bedrock geology legend is the same as Figure 3.

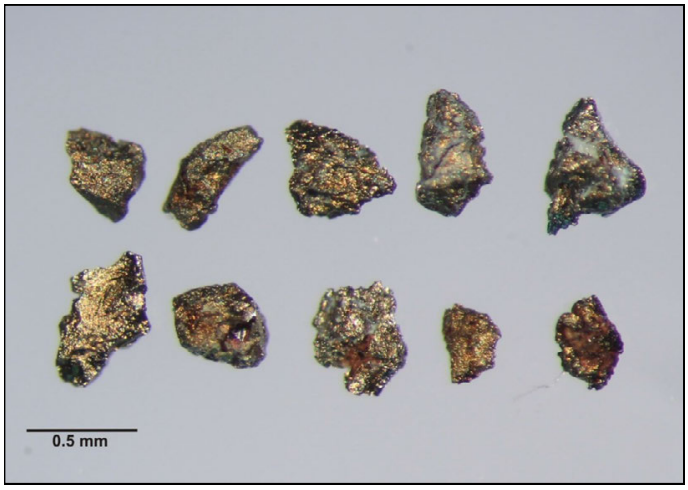

Figure 7 – Chalcopyrite grains (0.25-0.5 mm) recovered from till in the region of the Highland Valley Copper mine (modified from Plouffe et al., 2013a)

more abundant in till down-ice from Cu mineralised zones compared to surrounding regions (Figs. 8 and 9). At Mount Polley, the abundance of chalcopyrite grains in the heavy mineral fraction (0.25-0.5 mm and >3.2 specific gravity) define a dispersal train which extends over six kilometres down-ice (northwest) from the known mineralisation (Fig. 10; Hashmi et al., 2014, in press a, b). At the same site, the Au mineralisation is well reflected in till by a Au grain dispersal train that extends over five kilometres down-ice (Fig. 11). In contrast, molybdenite was not identified in till near any of the Cu-Mo porphyry deposits and consequently, this mineral has limited application for the detection of buried porphyry mineralisation. The absence of molybdenite in till could be related to a combination of the following factors: 1) its weathering in till since deglaciation or 2) its low abundance to absence in the mineralised bedrock that was exposed to glacial erosion and 3) its inability to survive glacial erosion and transportation due to its extreme softness (hardness=1).

The ore mineral chalcopyrite can be considered a key porphyry Cu indicator mineral in till. Likewise, gold grains can be indicative of Cu-Au porphyry mineralisation and can be present along with chalcopyrite grains.

Alteration minerals are present in tills near porphyry deposits.

Porphyry deposits are characterized by the presence of alteration zones that occur peripheral to ore mineralisation (Lowell and Guilbert, 1970). Alteration zones progress outward from a potassic core (K-feldspar, biotite, ± amphibole, ± magnetite, ± anhydrite) which is shelled by phyllic (quartz-sericite-pyrite), argillic (quartz, illite, pyrite, ± kaoloin, ± smectite, ± montmorillonite, ± smectite), and propylitic (epidote-chlorite-calcite, ± albite, ± pyrite) zones (Lowell and Guilbert, 1970; Sinclair, 2007). These alteration zones have been defined at Highland Valley Copper (Casselman et al., 1995; Byrne et al., 2013), Mount Polley (Fraser, 1994; Rees, 2013) and Gibraltar (Drummond et al., 1973, 1976).

Certain alteration minerals are found to be abundant in till down-ice from porphyry deposits. Because the alteration zones in porphyry deposits are larger than the mineralised zones, they potentially represent a larger exploration target and their associated mineralogical signature in till can be aerially extensive. For example, at Gibraltar and Woodjam, large regions extending over 10 km from mineralised zones are characterized by abundant green epidote in till which is in contrast with surrounding regions (Figs. 12, 13, and 14). The epidote in till is thought to be derived at least in part from the propylitic alteration (Plouffe et al., 2013a). On the other hand, at Highland Valley Copper, epidote in till is present in amounts greater than 70 % over a large area probably because of the extensive regional moderate to strong chlorite (epidote) alteration in the Guichon Creek batholith (cf. Casselman et al., 1995; Fig. 15). At Mount Polley, andradite garnet and apatite potentially derived from the porphyry alteration zones (Rees, 2013) are found to be abundant in a limited number of till samples up to at least 2.6 kilometres down-ice (northwest) from the deposit (Hashmi et al., in press a, b). Lastly, jarosite, common in supergene enrichment zones associated with Cu porphyry deposits (e.g., Averill, 2011; Kelley et al., 2011), was identified in till down-ice of mineralised zones at Mount Polley (Hashmi et al., in press a) and Woodjam (Ferbey and Plouffe, 2014).

Minerals common in alteration zones (e.g., epidote, andradite, apatite) or supergene enrichment (e.g., jarosite) associated to porphyry deposits have the potential to become porphyry indicator minerals in till. However, these minerals may not be unique to porphyry deposits and therefore, the physical and compositional attributes of minerals derived from porphyry alteration zones versus other barren sources need to be characterized. Defining the physical and chemical characteristics of alteration minerals will serve to define the presence of buried alteration zones which potentially can represent larger exploration targets compared to the mineralised zone enriched in commodity metals.

Interpretation of till composition needs to take into account reconstruction of local ice-flow history.

The importance of understanding the ice-flow history to interpret till composition as applied to mineral exploration has long been recognized (e.g., DiLabio and Coker, 1989; Kujansuu and Saarnisto, 1990; Bobrowsky et al., 1995; Paulen, 2013). Interpretation of the till geochemical and mineralogical data from this project is no different. For example, the distribution of geochemical and mineralogical porphyry indicators in till at Mount Polley requires consideration of two phases of ice-flow which have formed palimpsest dispersal trains influenced by the first (southwest) and second (northwest) phase of ice movement (Hashmi et al., 2014, in press a, b). At Gibraltar, the extensive amoeboid dispersal trains defined by till geochemistry and mineralogy (Plouffe et al., 2014) reflect, as indicated above, the presence of a cluster of Cu porphyry mineralised zones as well as the complex ice-flow history which included ice movements to the southeast, west and northwest. Amoeboid dispersal trains are known to occur in regions with complex ice-flow histories (e.g., Stea 1989; Shilts, 1993; Trommelen et al., 2013).

Composition of alteration minerals could provide information on porphyry mineralisation source.

At Mount Polley, magnetite-rich hydrothermal alteration is found in close association with Cu mineralisation (Rees, 2013). Magnetite grains from till, the magnetite breccia (mineralised) and the monzonite (unmineralised) from Mount Polley were analysed by laser ablation – inductively coupled plasma mass spectrometry (LA-ICP-MS) at the University of Victoria to test if the hydrothermal magnetite could have a different composition and have different physical characteristic com-

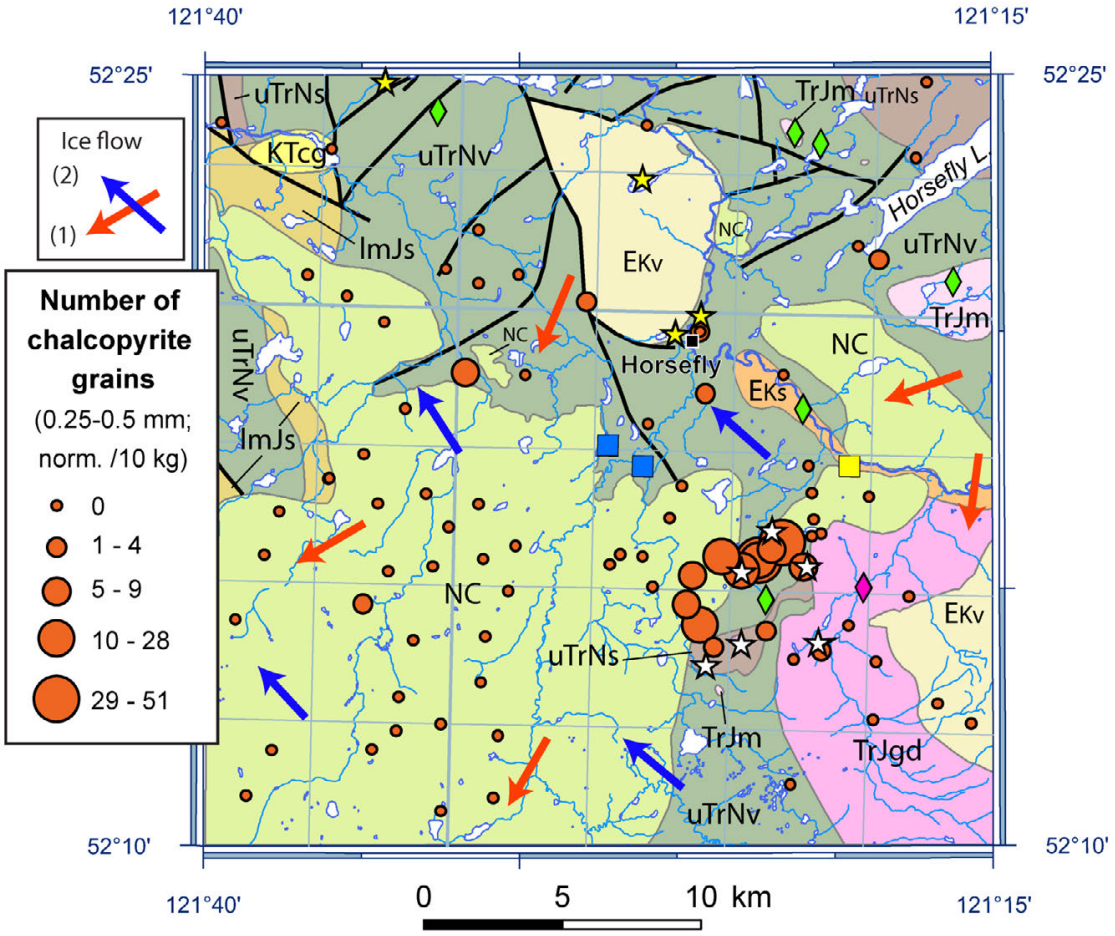

STRATIFIED ROCKS

Oligocene - Pliocene
Chilcotin Group
NC — Basaltic volcanic rocks

Eocene
Kamloops Group
EKs — Shale, siltstone and sandstone
EKv — Andesite, trachyandesite

Tertiary - Cretaceous
KTcg — Undivided sedimentary rocks

Quesnel Terrane
Jurassic
lmJs — Undivided sedimentary rocks
Triassic
Nicola Group
uTrNv — Undivided volcanic rocks
uTrNs — Undivided sedimentary rocks

INTRUSIVE ROCKS
Triassic to Jurassic
TrJm — Syenitic to monzonitic intrusive rocks
Takomkane batholith
TrJgd — Granodioritic intrusive rocks

Mineralized zone
Fault

MINERAL OCCURRENCES
Placer
Volcanic redbed Cu
Alkalic porphyry Au-Cu
Calkalkaline porphyry Cu-Mo-Au
Pumice

Figure 8 – Chalcopyrite grain counts in the 0.25-0.5 mm sized fraction and >3.2 s.g. density fraction of till normalized to 10 kg bulk sediment (<2 mm) at the Woodjam prospect. Bedrock geology simplified from Massey et al. (2005) and Logan et al. (2010).

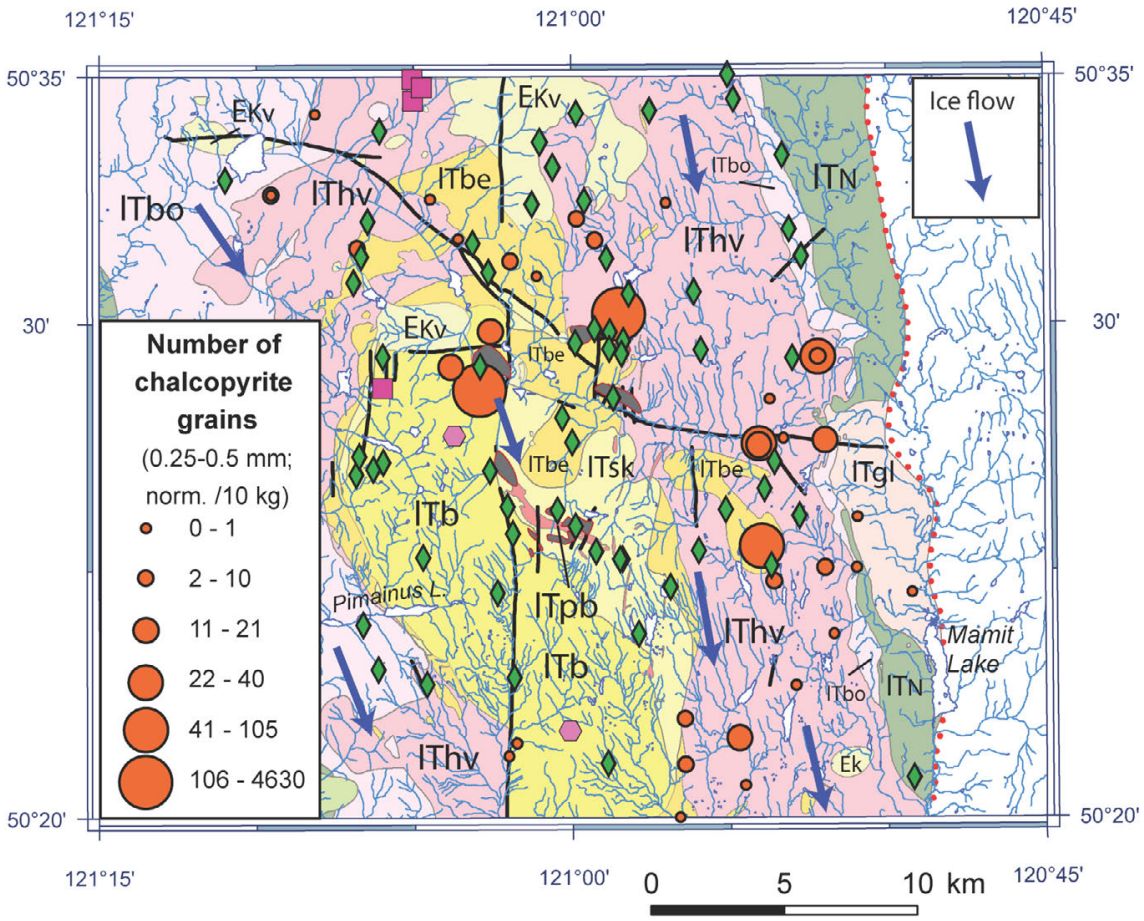

STRATIFIED ROCKS

Eocene and younger (?)

Kamloops Group

Ek — Undivided, predominantly lava flows

Cretaceous

Spences Bridge Group

mKsb — Undivided, mainly lava flows

Quesnel Terrane

Triassic

Nicola Group

ITN — Undivided, mainly volcanic rocks

INTRUSIVE ROCKS

Triassic

Guichon Creek Batholith and associated intrusions

Gump Lake Phase

ITgl — Granodiorite to quartz monzonite

post-Bethseida Phase

ITpb — Porphyry dykes and plugs

Bethseida Phase

ITb — Quartz monzonite to granodiorite

Skeena Variety

ITsk — Intermediate in composition between Bethlehem and Bethseida phase

Bethlehem Phase

ITbe — Granodiorite

Highland Valley Phase

IThv — Granodiorite

Border Phase

ITbo — Quartz diorite to granodiorite

Cu-Mo porphyry deposit

Fault

Limit of bedrock mapping

MINERAL OCCURRENCES

Porphyry Cu+/- Mo +/- Au

Cu+/-Ag veins; porphyry Cu+/-Mo+/-Au

Unknown

Figure 9 – Chalcopyrite grain counts in the 0.25-0.5 mm sized fraction and >3.2 s.g. density fraction of till normalized to 10 kg bulk sediment (<2 mm) at the Highland Valley Copper deposit. Bedrock geology simplified from McMillan et al. (2009).

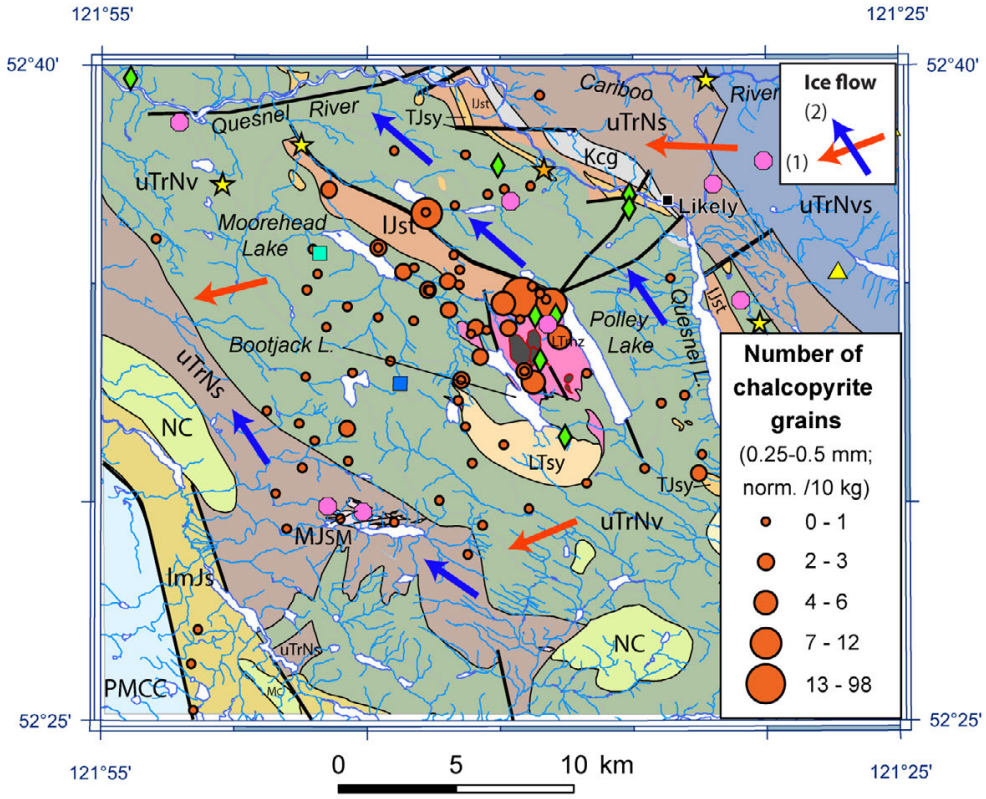

Figure 10 – Chalcopyrite grain counts in the 0.25-0.5 mm sized fraction and >3.2 s.g. density fraction of till normalized to 10 kg bulk sediment (<2 mm) at the Mount Polley deposit. Bedrock geology legend is the same as Figure 3.

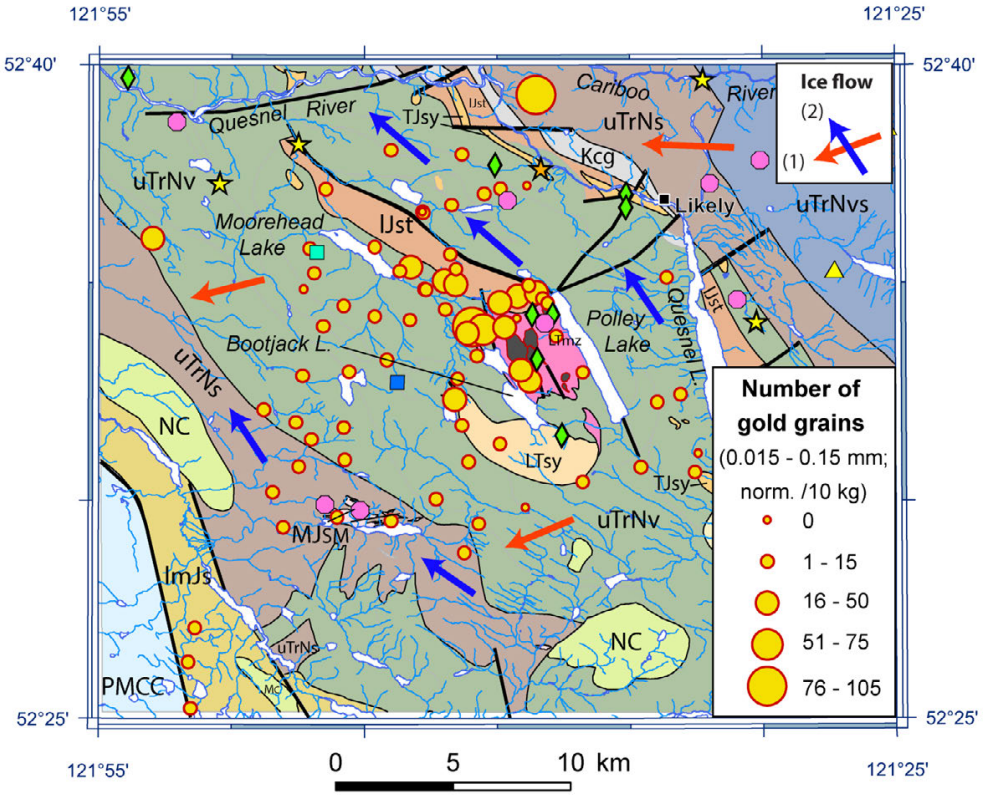

Figure 11 – Gold grain counts with long axis varying from 0.015 to 0.425 mm in the shaking table concentrates normalized to 10 kg bulk sediment (<2 mm) at the Mount Polley deposit. Bedrock geology legend is the same as Figure 3.

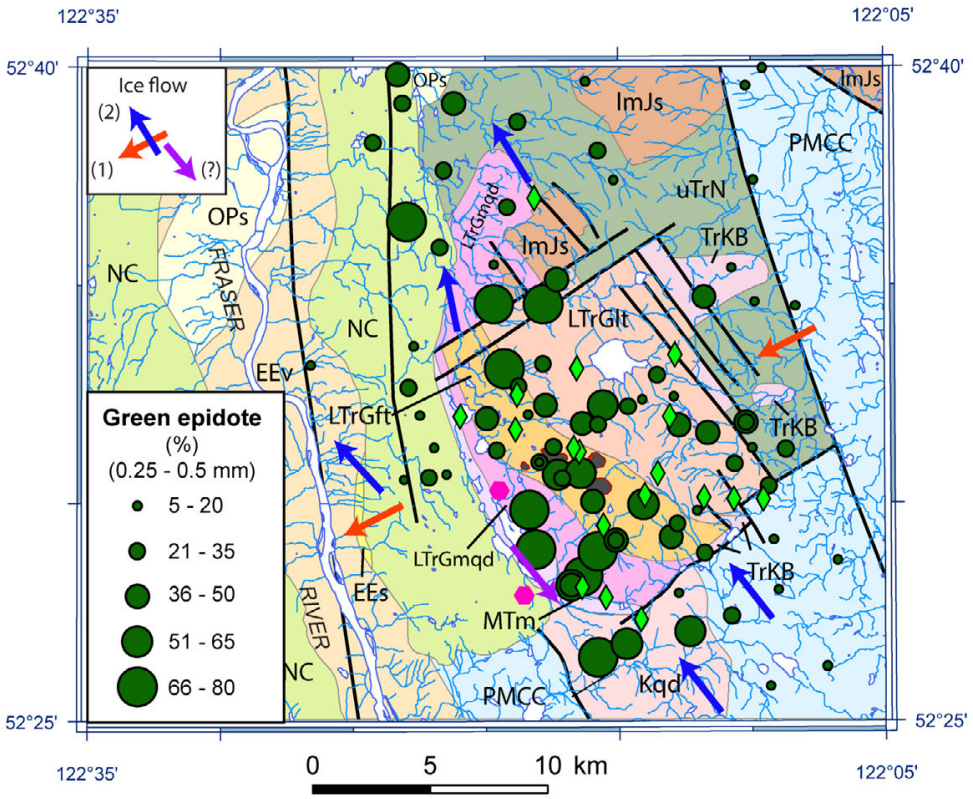

Figure 12 – Green epidote grain counts in the 0.25-0.5 mm sized fraction and >3.2 s.g. density fraction of till normalized to 10 kg bulk sediment (<2 mm) at the Gibraltar deposit. Bedrock geology legend is the same as Figure 4.

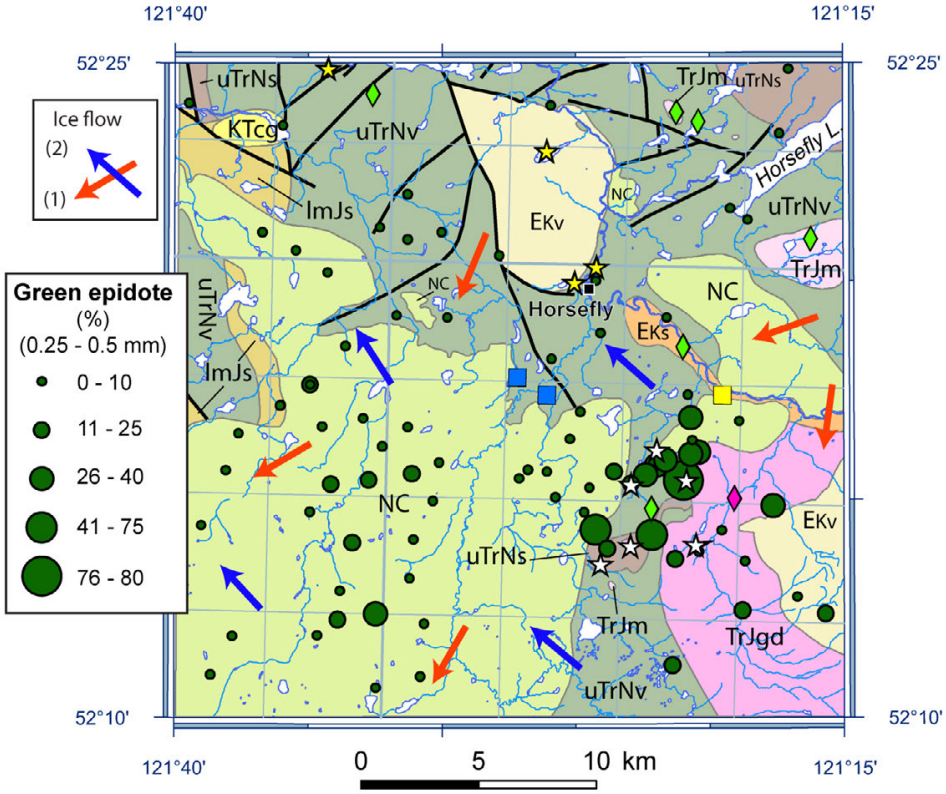

Figure 13 – Green epidote grain counts in the 0.25-0.5 mm sized fraction and >3.2 s.g. density fraction of till normalized to 10 kg bulk sediment (<2 mm) at the Woodjam prospect. Bedrock geology legend is the same as Figure 8.

Figure 14 – Heavy mineral concentrates (0.25-0.5 mm; s.g. >3.2; paramagnetic fraction 0.8 – 1 A; see Figure 2B) from sample 11-PMA-017A-1 collected in the Woodjam area. The amount of epidote in this concentrate is estimated at 80 % (+/- 10 %). Field of view width: 5 mm. Modified from Plouffe et al. (2013a).

pared to the regional magnetite derived from non-mineralised sources. Grondahl (2014) and Piziak et al. (2015) found that the magnetite grains with a Ti and Sn content similar to the Mount Polley magnetite breccia (ca. 0.5 to ca. 3 ppm Sn and 1100-11,000 ppm Ti) can be detected in till up to 6 kilometres to the northwest (down-ice) from the deposit. Beyond this distance, the magnetite grains in till showed no overlapping composition with magnetite from the deposit.

Similar to the magnetite study at Mount Polley, Chapman et al. (2015, in press) studied the composition of tourmaline in till and bedrock at Woodjam to identify the signature of the porphyry mineralised bedrock source. Tourmaline major element compositions were determined by electron microprobe (EPMA) at the University of Ottawa MicroAnalysis Laboratory. Structural formulae were calculated by normalisation on 31 anions and by assuming that Y+Z+T = 15 atoms-per-formula-unit (apfu). Tourmaline from the Takom and Deerhorn zones at Woodjam has compositions typical of tourmaline associated with Cu-porphyry mineralisation as identified by Baksheev et al. (2012). Typically, Mg content is approximately two atoms-per-formula unit and individual analyses are distributed along the $FeAl_{-1}$ substitution vector in a Fe-Mg (apfu) bivariate plot, as well as along the magnesiofoitite-povondraite join in an Fe-Al-Mg ternary plot. The tourmaline abundance in till defines a wide dispersal train which extends approximately 10 km northwest (down-ice) from the Woodjam deposit and the Takomkane batholith (Chapman et al., in press). How-

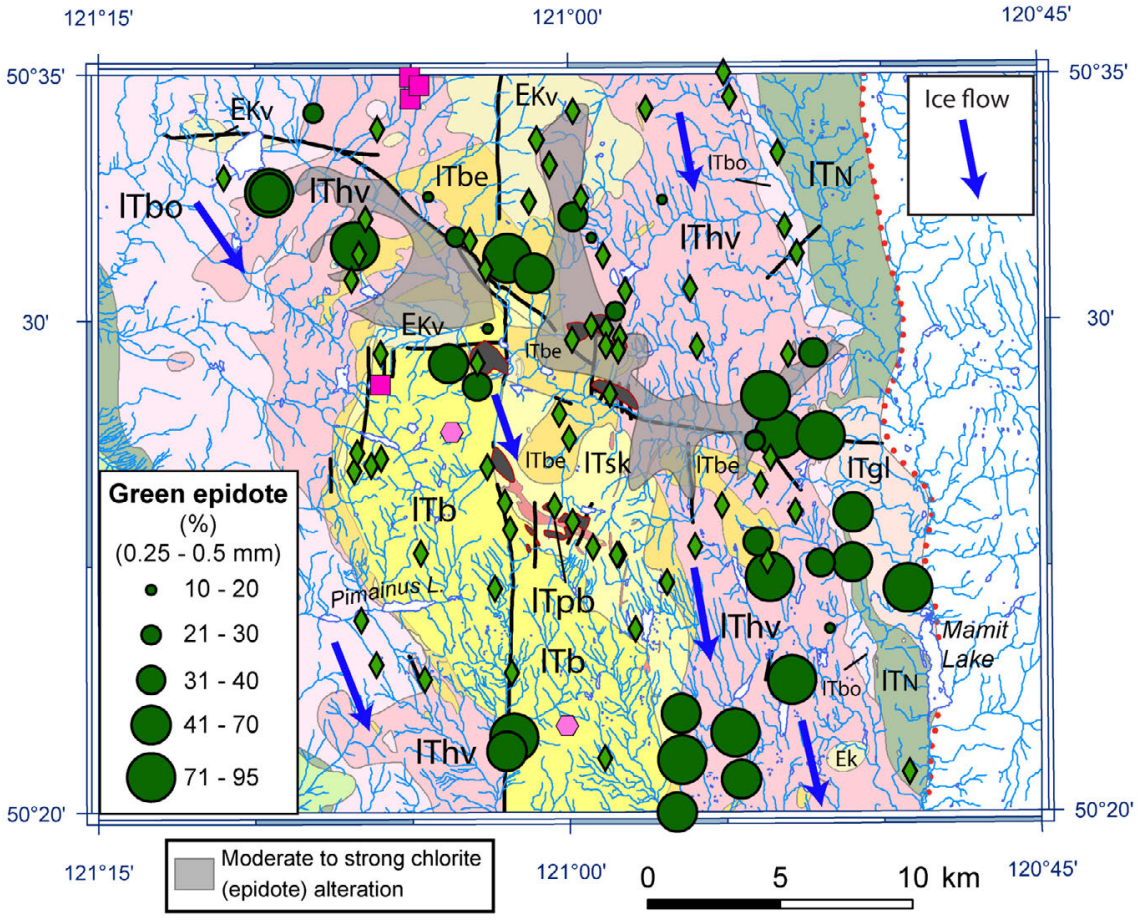

Figure 15 – Green epidote grain counts in the 0.25-0.5 mm sized fraction and >3.2 s.g. density fraction of till normalized to 10 kg bulk sediment (<2 mm) at the Highland Valley Copper deposit. Bedrock geology legend is the same as Figure 9. The mapped extent of chlorite (epidote) alteration is from Casselman et al. (1995).

ever, only tourmaline grains in a till sample located <1 km from Deerhorn have a composition similar to the one in the mineralised source (Chapman et al., in press).

Till indicators of Cu porphyry mineralisation identified as part of this study are used to identify potential exploration targets.

Our study indicates that elevated Cu concentrations along with the presence of chalcopyrite in till can be indicative of Cu porphyry mineralisation. In addition, the presence of elevated Au grain counts or elevated Au concentrations found in association with the Cu indicators could indicate the presence of Cu-Au porphyry mineralisation (Hasmi et al., in press a). Obviously, the interpretation of the till composition needs to take into account the geological setting which needs to be favourable for porphyry mineralisation. In the Quesnel terrane of the Cordillera, a favourable setting for porphyry mineralisation includes Late Triassic to Early Jurassic felsic to intermediate intrusions (McMillan, 1991; McMillan et al., 1991, 1995, 1996; McMillan and Panteleyev, 1995; Logan and Mihalynuk, 2014).

To test the geochemical and mineralogical indicators of Cu-Au porphyry mineralisation identified as part of this study, Plouffe and Ferbey (2015a) have revisited the regional till composition data obtained as part of the Mountain Pine Beetle Program of the Geological Survey of Canada (Plouffe et al., 2009, 2010) for a region which includes two Late Triassic – Early Jurassic intrusions within the Quesnel terrane: the Thuya and Takomkane batholiths. Two vectors of ice-flow movements have been identified in this region by Plouffe et al. (2011b) including a first movement to the west to southwest derived from the Cariboo Mountains which were the source of ice at the onset of the last glaciation. A second flow to the south to southeast originated from an ice divide which formed around the 52 degree latitude following the coalescence of ice from the Coast and Cariboo mountains (Fig. 16). Two regions with elevated Cu concentrations above 359 ppm in the clay-sized fraction of till are defined from this regional data set: one about 30 kilometres south of Woodjam, at the western limit of the Takomkane batholith but underlain by the Late Triassic Spout Lake pluton, and a second one at the northern limit of the Thuya batholith (Fig. 16). Within those two areas, the Au grain content of till is also elevated including numerous adjacent samples with more than 66 Au grains per 10 kg of bulk material (<2 mm) (Fig. 17). A total of 57 samples selected from within and outside the regions with elevated Au and Cu were processed for porphyry Cu indicator minerals identification as part of the Mountain Pine Beetle Program. All samples with more than 3 chalcopyrite grains per 10 kg are located at the northern limit of the Thuya batholith or at the western limit of the Takomkane batholith, above the Spout Lake pluton (Fig. 18). Based on the mineralogical and geochemical indicators of Cu-Au porphyry

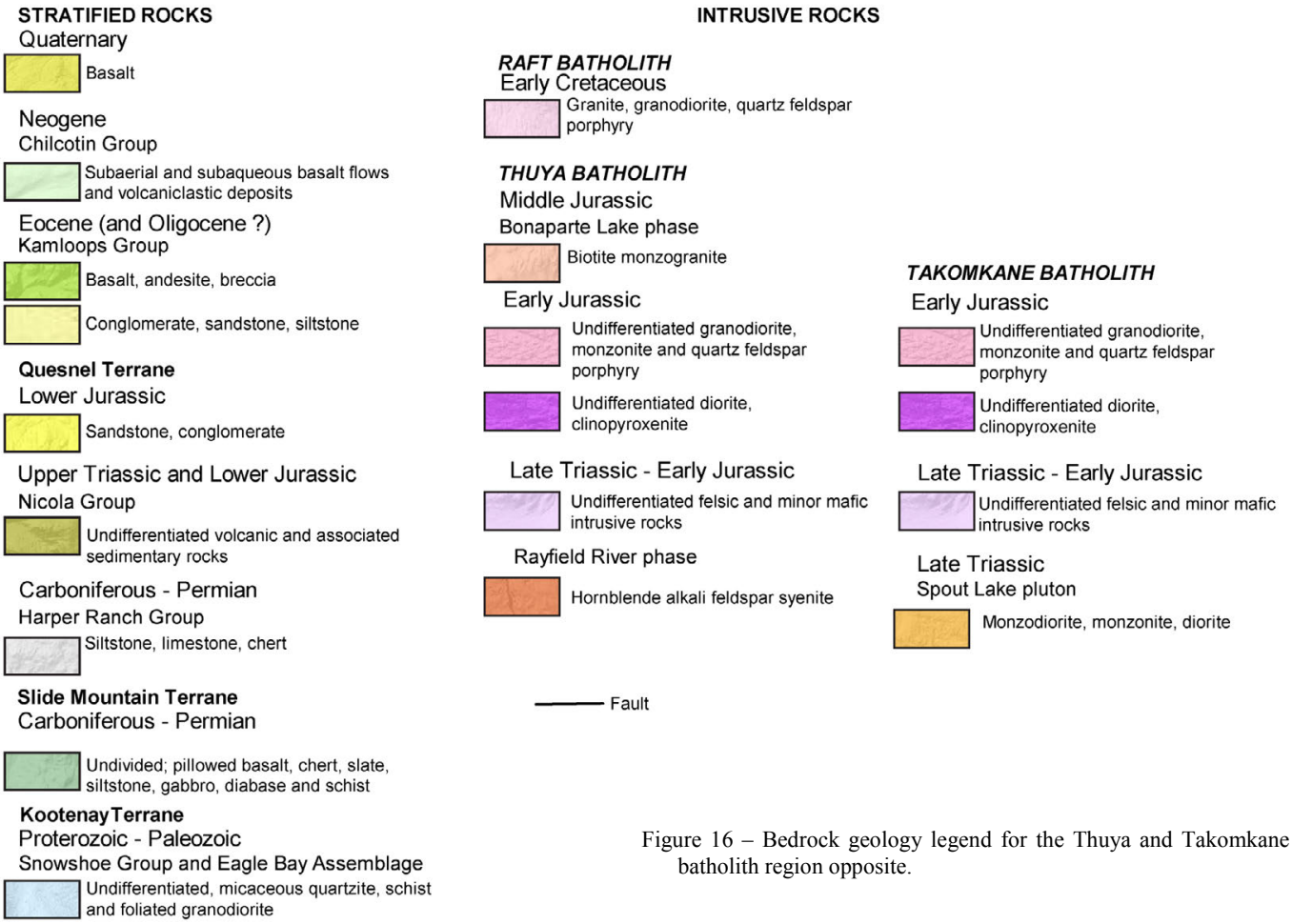

Figure 16 – Bedrock geology legend for the Thuya and Takomkane batholith region opposite.

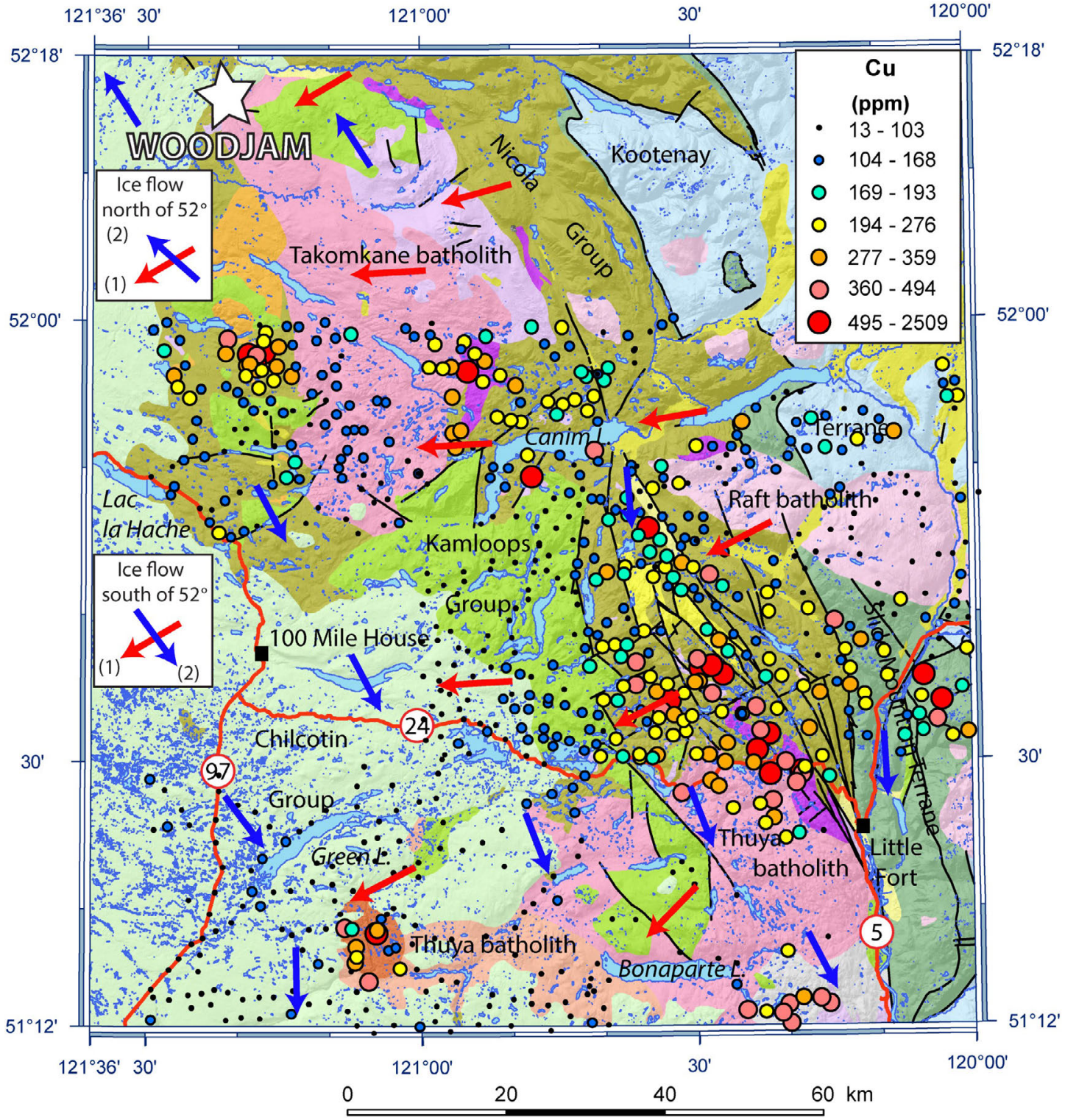

Figure 16 (cont.) – Copper in the clay-sized fraction of till in the region of the Thuya and Takomkane batholiths analysed by ICP-MS after an HCl:HNO3 leach (1:1) . The map includes the region of the Woodjam prospect. Data from Plouffe et al. (2010) and figure modified from Plouffe and Ferbey (2015a). Bedrock geology is simplified from Campbell and Tipper (1971), Schiarizza et al. (2002a, b), Schiarizza and Boulton (2006), Schiarizza and Bligh (2008), and Anderson et al. (2010). Also, it is based on the compilation presented in Plouffe et al. (2011b). Generalized ice flow from Plouffe et al. (2011b) and Ferbey et al. (2013). Note the ice divide around the 52 degree latitude.

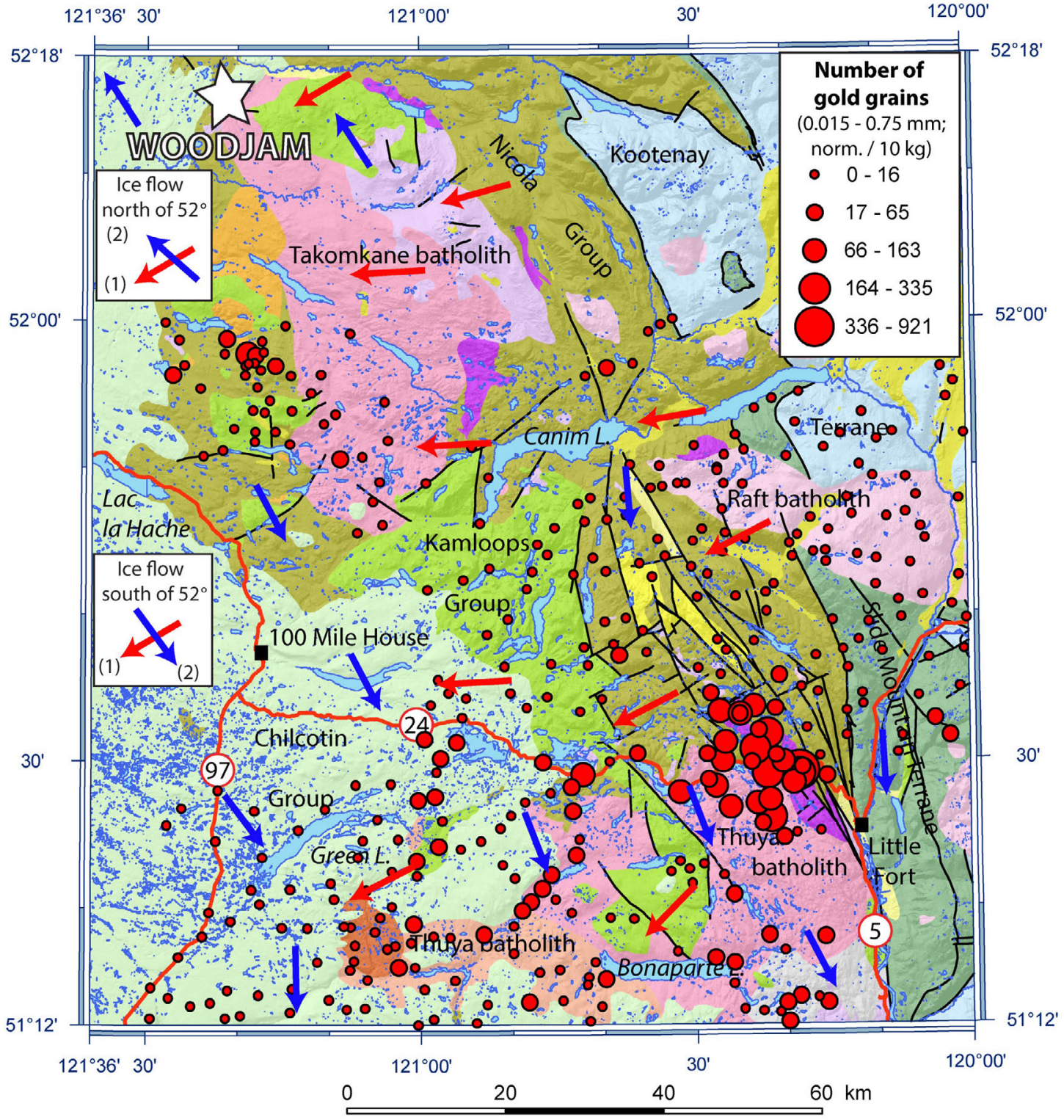

Figure 17 – Gold grain counts with long axis varying from 0.015 to 0.700 mm in the shaking table concentrates normalized to 10 kg bulk sediment (<2 mm) in the region of the Thuya and Takomkane batholiths. Bedrock geology legend is the same as Figure 16.

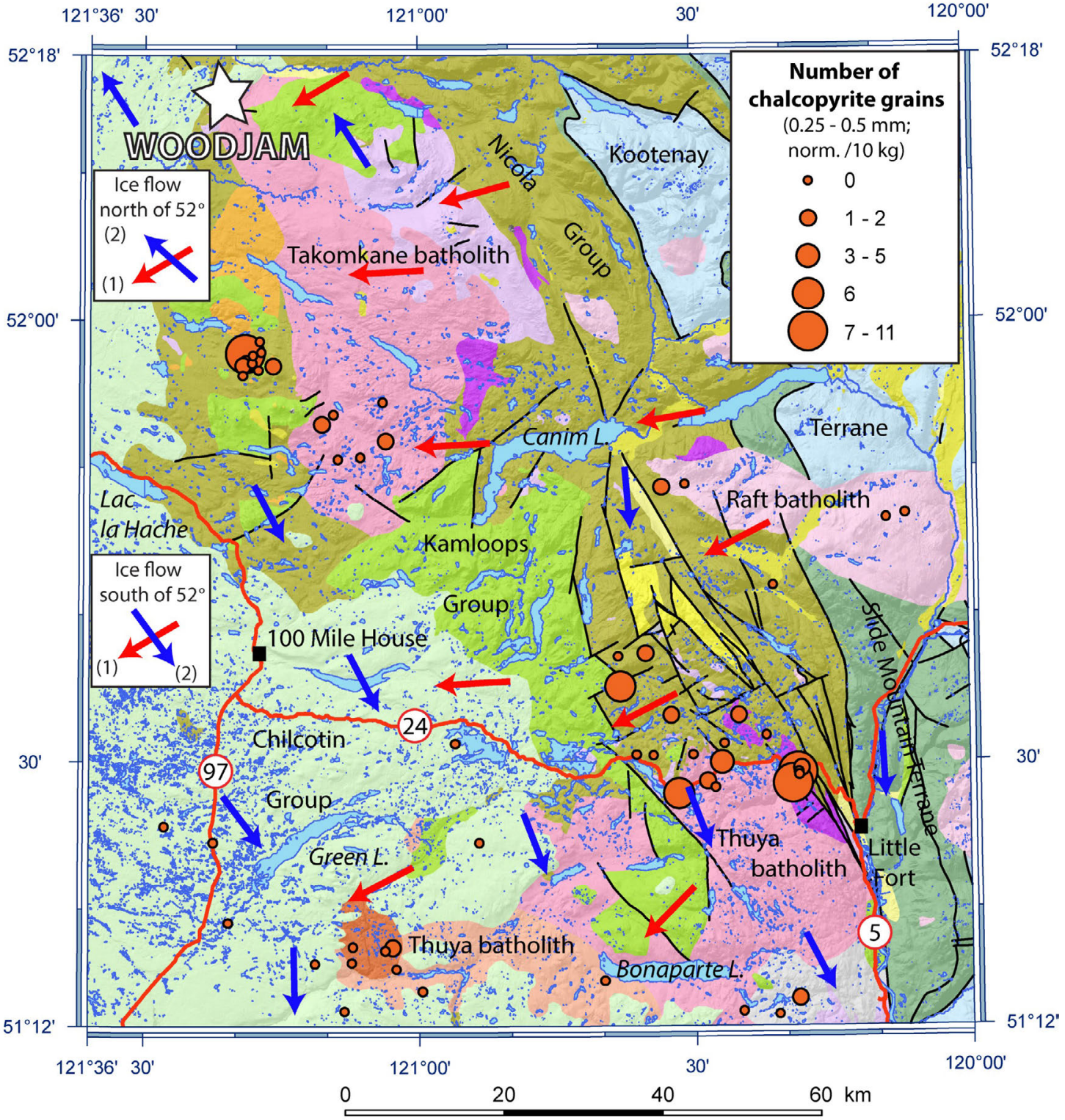

Figure 18 – Chalcopyrite grain counts in the 0.25-0.5 mm sized fraction and >3.2 s.g. density fraction of till normalized to 10 kg bulk sediment (<2 mm) in the region of the Thuya and Takomkane batholiths. Bedrock geology legend is the same as Figure 16..

mineralisation observed in till, we postulate that the northern sector of the Thuya batholith and the western margin of the Takomkane batholith have potential to host porphyry-style Cu-Au mineralisation.

Recommendations for mineral exploration for Cu porphyry mineralisation in glaciated landscape

From the results presented above, we demonstrate that till composition (geochemistry and mineralogy) can reflect the presence of Cu porphyry mineralisation which was exposed to glacial erosion. Geochemical and mineralogical anomalies identified in till can be traced to their bedrock source if the regional ice-flow history (detrital glacial transport direction) is taken into account. Depending on the available funds and the scope of a mineral exploration project (e.g., grass root exploration at a regional scale or detailed follow-up exploration at a property scale) different approaches are recommended.

At a regional scale, till geochemistry based on a sample spacing of one to two kilometres would have defined the presence of elevated concentrations for multiple metals in till at the four study sites (e.g., Cu, Mo, Au, Zn, Hg). In a scenario were there is limited exploration funding available, till geochemistry alone could be sufficient to identify high metal contents or anomalies that could be derived from, and thus indicators of, porphyry mineralisation. This approach would be practical in regions with a high potential for porphyry mineralisation such as the Quesnel and Stikine terranes. Processing all or a selected number of samples for indicator minerals is also recommended since till mineralogy provides additional key information on the mineralogy of the bedrock source. For example, at Mount Polley some till samples with background Au concentrations (<15 ppb in the silt and clay-sized fraction; <0.063 mm) also contained elevated numbers of gold grain (>15 grains per 10 kg) (Hasmi et al., in press a). Furthermore, in an hypothetical scenario where only the alteration zones of a fertile porphyry system were exposed to glacial erosion no high contents of commodity-metals would be detected in till. In this case, only the alteration minerals in the till would be indicative of the presence of buried porphyry mineralisation. Lastly, in a region of thick till such as Woodjam, the geochemical signal in till derived from mineralisation is diluted within a short distance down-ice from the mineralised bedrock source; only two samples located within one kilometre of the mineralisation returned elevated Cu concentrations (> 265 ppm) above concentrations observed in samples throughout the region (Fig. 19). On the other hand, at the same site, 10 samples contain greater than four chalcopyrite grains per 10 kg which is greater than the amounts observed in regional samples (0 to 4 chalcopyrite grains/10 kg; Fig. 8). Plus, samples with elevated chalcopyrite grain counts (> 4 grains / 10 kg) are located up to 3 km from known mineralised zones and define a mineralogical anomaly in till of about 6 by 3 km.

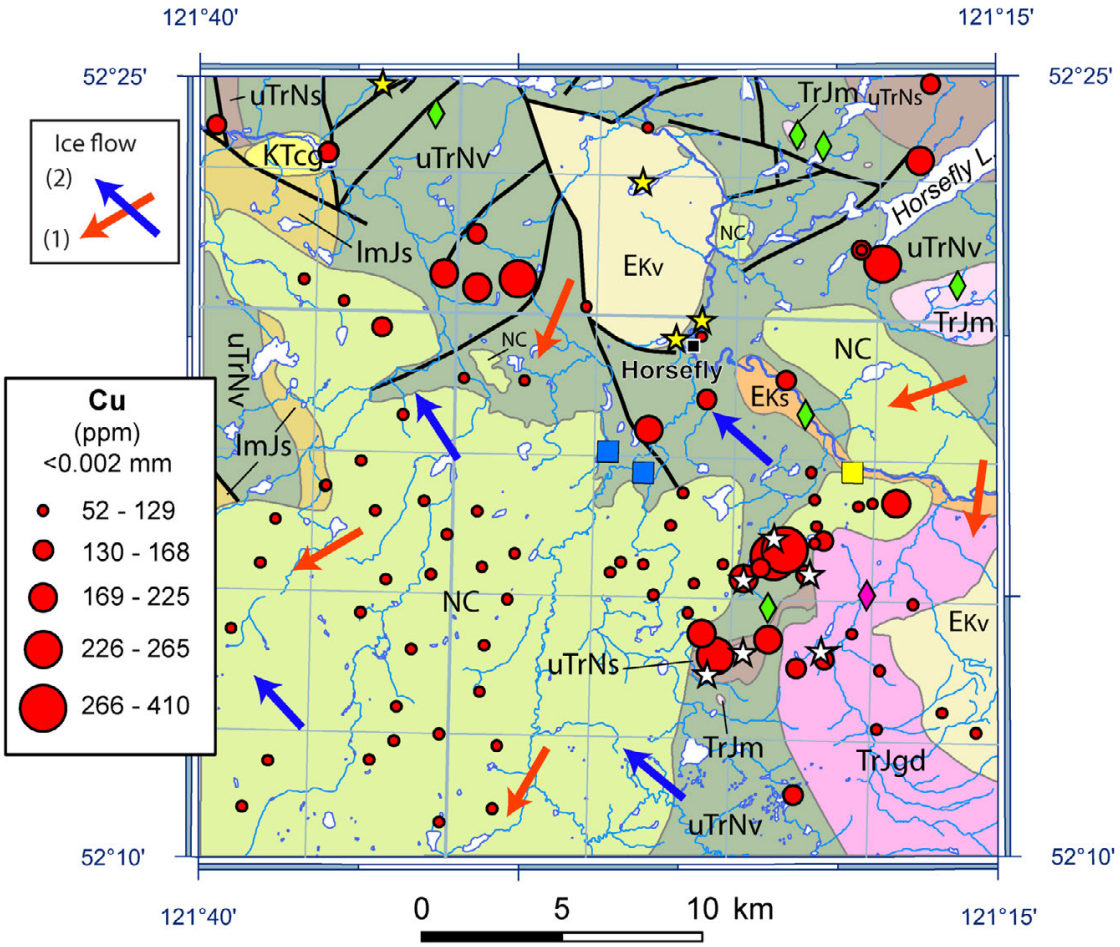

Figure 19 – Copper in the clay-sized fraction of till at the Woodjam prospect analysed by ICP-MS after an HCl : HNO_3 leach (1:1). Bedrock geology legend is the same as Figure 8.

The same approach (that is collecting till samples for geochemical and mineralogical analyses) is recommended at a property scale where the objective might be to locate a bedrock source for advanced exploration activity (e.g., drilling). In such a scenario, the spacing between till samples should be less than one kilometre. The orientation of the till sampling transect and the sample spacing need to take into account the potential shape of the bedrock source and ice-flow direction (e.g., Levson, 2001). Trenching and/or shallow drilling with light equipment might be required to facilitate the sampling of unweathered till at a depth greater than one metre or the sampling of till at various depth intervals if the till is thick (Plouffe, 1995; McMartin and McClenaghan, 2001).

Publications in progress

In addition to the references provided in the text above, a number of publications produced as part of this project have recently been published or are currently in progress. Surficial geology maps at 1:50,000 scale are being prepared for each study site. The surficial geology map for Mount Polley mine area is published (Hashmi et al., 2015) and the one for Highland Valley is in press (Plouffe and Ferbey, 2015b). Surficial geology maps for Gibraltar and Woodjam are in an advance stage of production (i.e., aerial photograph interpretation is completed and data is being prepared for the final map). An open file report with all data on till geochemistry and mineralogy along with all the quality assurance and quality control data is being prepared (A. Plouffe and T. Ferbey, work in progress, 2015). One overview paper on till geochemistry and mineralogy at the four study sites is nearly completed and will be submitted to a peer review scientific journal in 2015. One scientific paper on till geochemistry and mineralogy at Mount Polley is in press (Hasmi et al., in press a). This paper is part of the M.Sc. thesis of S. Hashmi at Simon Fraser University, under the supervision of B.C. Ward. The thesis includes a study of glacial dispersal from the Mount Polley deposit and the reconstructed glacial history of the region based on surficial geology mapping. A paper on glacial dispersal and till composition at the Gibraltar deposit and a second one for the Woodjam deposit are planned with first drafts expected to be completed in 2015.

Future research

Results from this project show how till geochemistry and mineralogy can be used to explore for Cu porphyry mineralisation buried by glacial sediments. As with other research, this work has generated related questions; the answers to which could only further the mineral exploration method. For instance, can the geochemical compositions of porphyry indicator minerals, or their internal textures, be indicative of the bedrock source lithology and the fertility of the ore system? That question was partly addressed by Bouzari et al. (2010, 2011a, b) who demonstrated that apatite derived from unaltered and unmineralised host rock at six porphyry deposits in British Columbia displays yellow to brown colors under cathodoluminescence compared to green and grey apatite in altered and mineralised rocks. The colour of the luminescence is controlled by the composition of apatite; lower Mn/Fe ratios in green apatite (mineralised source) compared to the yellow and brown apatite (unmineralised source). Chlorine, Na and S are also depleted in alteration apatite (Bouzari et al., 2011a).

Similarly, the composition of magnetite (Ti, V, Mn, Ca, Al), a common accessory mineral occurring in a variety of rock types, can serve to discriminate different deposit types (e.g., Dupuis and Beaudoin, 2011). As indicated above, Piziak et al. (2015) and Grondahl (2014) investigated the composition of magnetite in till and bedrock samples from Mount Polley, collected as part of this project. In another study of magnetite composition in porphyry deposits of British Columbia, Bouzari et al. (2011a) demonstrated that in a variety of altered host rocks of porphyry deposits, magnetite grains display a pink core that is replaced by hematite interpreted to reflect the increasing oxidation state of the porphyry system.

The composition of other alteration minerals associated with porphyry mineralisation also has the potential to be tied to bedrock type and fertility. For example, epidote recovered from propylitic alteration zones associated with porphyry and skarn deposits in the Baguio district, Republic of the Philippines, has a chemistry which varies with distance from the deposit centres (Cooke et al., 2014). In their study, epidote contains higher concentrations of Cu, Mo, Au and Sn near the central potassic alteration zone and pathfinder elements (As, Sb, Pb, Zn, Mn) are enriched in epidote up to 1.5 km from the deposit centre. Similarly, given that Cu-sulphides and accessory minerals in supergene zones of porphyry deposits have heavy Cu isotopic signatures (Zhu et al., 2000; Mathur et al., 2009, 2010), the Cu isotopic composition of those minerals recovered from transported sediments could be used to identify a supergene cap source.

This brief overview of recent compositional work conducted on porphyry indicator minerals reveals the great potential of developing exploration methods based on the petrography and chemical composition of a wide variety of alteration and ore minerals associated with porphyry systems. Most of these studies were conducted on minerals recovered from bedrock; the abundance and chemistry of the same minerals in transported glacial and non-glacial sediments needs to be assessed (see also Bouzari et al., 2011a). In other words, do these indicator minerals survive transport in glacial and non-glacial environments and are they present in sufficient amounts in the till to be detected? How extensive is their footprint in the transported medium? The development of indicator minerals for mineral exploration in glaciated and drift covered area should continue for porphyry-style mineralisation but also for other mineral deposit types. The development of new exploration methods in glaciated areas is increasingly important given the increasing demand for a variety of metals and non-metals on global markets and the known difficulty associated to their search in drift covered areas.

Conclusion

Results from the till orientation surveys conducted near four Cu porphyry deposits in British Columbia demonstrate that till geochemistry and mineralogy can detect Cu porphyry mineralisation that was exposed to glacial erosion and is now covered by glacial sediments. The porphyry mineralisation is reflected by the high concentrations of commodity metals (e.g., Cu, Mo, Au), pathfinder elements (e.g., Zn, Ag, Hg), ore minerals (e.g., chalcopyrite, gold grains) and alteration minerals (e.g., epidote, andradite garnet, apatite) in till. These elements and minerals can be dispersed over several kilometres from their bedrock source in the down-ice direction. Resulting dispersal trains have different shapes and lengths which are influenced by transport vectors (i.e., multiple ice-flow events) and in some cases multiple bedrock sources (e.g., cluster of sub-economic mineralised zones peripheral to the zones of economic mineralisation). Future research should include detailed studies on the physical and chemical characteristics of porphyry Cu indicator minerals that are diagnostic of a Cu porphyry source and its potential fertility. The development of mineral exploration methods using the geochemical and mineralogical composition of transported sediments should not be limited to porphyry deposits but should include other mineral deposit types.

Acknowledgements

The research would not have been possible without the support of the mineral exploration and mining companies and their staff who provided enlightening geological discussions, toured us in the field or at the mine site, and ensured our safety while at the mine or project site. These include John Fleming from Taseko Mines Limited (Gibraltar Mine), Tom Schroeter, Ross Sherlock, John Hertel, Jacqueline Blackwell, Amelia Rainbow, and the rest of the field crew from Gold Fields and Consolidated Woodjam Copper Corporation (Woodjam prospect), Gerald Grubisa, Chris LeClair, Mathieu Veillette, and Ron Grayden from Teck Resources Limited (Highland Valley Copper Mine) and, Amber Marko and Chris Rees from Imperial Metals Corporation (Mount Polley Mine). Capable field assistance was provided by H. Arnold, N. Evanoff, C. Grondahl, S. Hashmi, A. Hickin, K.L. Robillard, D. Sacco, and S. van Pelt. We are grateful to the TGI 4 program personnel for enabling the implementation and evolution of this project: N. Rogers (Project Leader), A. Miron (Senior Administrative Assistant), C. Bjerkelund (Project Manager), M. Villeneuve (Program Manager), and C. Hutton (Project Manager – communication with First Nation). R.G. Anderson is acknowledged for his involvement in the preparation for field work, collaboration in the field, and numerous enlightening discussions. Overburden Drilling Management Ltd. (ODM Ltd.) in Ottawa, ON (heavy mineral separation and identification) and Acme Analytical Laboratories, a division of the Bureau Veritas Commodities Canada Limited, in Vancouver, BC (geochemical analyses) are acknowledged for their professional services. This Open File greatly benefited from a critical review completed by M.B. McClenaghan.

References

Anderson, R.G., Plouffe, A., Ferbey, T., and Dunn, C.E., 2012a. The search for surficial expressions of buried Cordilleran porphyry deposits; background and progress in a new TGI-4 activity in the southern Canadian Cordillera; *in* Current Research 2012-7, Geological Survey of Canada, 15 p.

Anderson, R.G., Plouffe, A., Ferbey, T., and Dunn, C.E., 2012b. The search for surficial expressions of buried Cordilleran porphyry deposits; a new TGI4 activity in the southern Canadian Cordillera; Geological Survey of Canada, Open File 7081.

Anderson, R.G., Plouffe, A., Ferbey, T., and Dunn, C.E., 2012c. The search for surficial expressions of buried Cordilleran porphyry deposits; preliminary findings in a new TGI4 activity in the southern Canadian Cordillera; Geological Survey of Canada, Open File 7266, 82 p.

Anderson, R.G., Schiarizza, P., Andrews, G., Breitsprecher, K., Davis, W., Dunn, C.E., Plouffe, A., and Thomas, M.D., 2010. Bedrock, surficial, geophysical and geochemical mapping reveal exploration targets in the Thuya batholith, southern Nicola Arc; *in* TGI-3 Workshop: Public Geoscience in Support of Base Metal Exploration Programme and Abstracts, Geological Association of Canada – Cordilleran Section, http://www.gac-cs.ca/workshops/TGI3/abstracts.shtml, p. 52-57.

Ash, C.H., Panteleyev, A., MacLellan, K.L., Payne, C.W., and Rydman, M.O., 1999. Geology of the Gibraltar Mine area (93B/6&9); British Columbia Ministry of Energy and Mines, Open File 1999-7, scale 1:50,000.

Averill, S.A. 2011. Visible indicator minerals in surficial sediments for two deposit types: Ni-Cu-PGE and porphyry Cu; Geochemistry: Exploration, Environment, Analysis, v. 11, p. 279-291.

Baksheev, I.A., Yu Prokof'ev, V., Zaraisky, G.P., Chitalin, A.F., Yapaskurt, V.O., Nikolaev, Y.N., Tikhomirov, P.L., Nagornaya, E.V., Rogacheva, L.I., Gorelikova, N.V., and Kononov, O.V., 2012. Tourmaline as a prospecting guide for the porphyry-style deposits; European Journal of Mineralogy, v. 24, p. 957-979.

Bissig, T., Heberlein, D.R., and Dunn, C.E., 2013. Geochemical techniques for detection of blind porphyry copper-gold mineralization under basalt cover, Woodjam prospect, south-central British Columbia (NTS93A/03, /06); *in* Geoscience BC Summary of Activities 2012, Geoscience BC, Report 2013-1, p. 63-78.

Bobrowsky, P.T., Cathro, M., and Paulen, R.C., 2002. Quaternary geology reconnaissance studies 92I/2 and 7; *in* Geological Fieldwork 2001, British Columbia Ministry of Energy and Mines, Paper 2002-1, p. 397-401.

Bobrowsky, P.T., Kerr, D.E., Sibbick, S.J., and Newman, K., 1993. Drift exploration studies, Valley Copper Pit, Highland Valley Copper Mine, British Columbia: stratigraphy and sedimentology (92I/6, 7, 10 and 11); *in* Geological Fieldwork 1992, Paper 1993-1, p. 427-437.

Bobrowsky, P.T., Sibbick, S.J., Newell, J.M., and Matysek, P.F. (ed.), 1995. Drift exploration in the Canadian Cordillera; British Columbia Ministry of Energy, Mines and Petroleum Resources, Victoria, British Columbia, Paper 1995-2, 304 p.

Bouzari, F., Hart, C.J.R., Barker, S., and Bissig, T., 2010. Porphyry indicator minerals (PIMs): exploration for concealed deposits in south central British Columbia (NTS 092I/06, 093A/12, 093N/01, /14); *in* Geoscience BC Summary of Activities 2009, Geoscience BC, Report 2010-1, p. 25-32.

Bouzari, F., Hart, C.J.R., Barker, S., and Bissig, T., 2011a. Porphyry indicator minerals (PIMS): a new exploration tool for concealed deposits in south-central British Columbia; Geoscience BC Report 2011-17, 31 p.

Bouzari, F., Hart, C.J.R., Barker, S., and Bissig, T., 2011b. Exploration for concealed deposits using porphyry indicator minerals (PIMs): Application of apatite texture and chemistry; 25th International Applied Geochemistry Symposium, Rovaniemi, Finland, Series B 92-1, p. 89-90.

Byrne, K., Stock, E., Ryan, J., Johnson, C., Nisenson, J., Alva Jimenez, T., Lapointe, M., Stewart, H., Grubisa, G., and Syroka, S., 2013. Porphyry Cu-(Mo) deposits in the Highland Valley district, south-central British Columbia; *in* Porphyry systems of central and southern British Columbia: Tour of central British Columbia porphyry deposits from Prince George to Princeton, (ed.) J.M. Logan and T.G. Schroeter; Society of Economic Geologists, Society of Economic Geologists Field Trip Guidebook, Series 43, p. 99-116.

Bysouth, G.D., Campbell, K.V., Barker, G.E., and Gagnier, G.K., 1995. Tonalite-trondhjemite fractionation of peraluminous magma and the formation of syntectonic porphyry copper mineralization, Gibraltar mine, central British Columbia; *in* Porphyry deposits of the nortwestern Cordillera of North America, (ed.) T.G. Schroeter; Canadian Institute of Mining, Metallurgy and Petroleum, Special Volume 46, Montréal, p. 201-213.

Campbell, R.B., and Tipper, H.W., 1971. Geology, Bonaparte Lake, British Columbia; Geological Survey of Canada, Map 1278A, scale 1:250,000.

Casselman, M.J., McMillan, W.J., and Newman, K.M., 1995. Highland Valley porphyry copper deposits near Kamloops, British Columbia: A review and update with emphasis on the Valley deposit; *in* Porphyry deposits of the northwestern Cordillera of North

America, (ed.) T.G. Schroeter; Canadian Institute of Mining, Metallurgy and Petroleum, Special Volume 46, Montréal, p. 161-191.

Chapman, J., Plouffe, A., and Ferbey, T., in press. Tourmaline: the universal indicator?; 27th International Applied Geochemistry Symposium, Tucson, AZ, Short Course SC02, Application of Indicator Mineral Methods to Mineral Exploration, Association of Applied Geochemists.

Chapman, J.B., Plouffe, A., Jackson, S.E., Ryan, J.J., and Ferbey, T., 2015. Mineral markers of porphyry processes: regional and local signatures of porphyry prospectivity; AMEBC Mineral Exploration Roundup, Vancouver, BC, Abstract volume, p. 24-25.

Clague, J.J., 1989. Cordilleran Ice Sheet; *in* Quaternary geology of Canada and Greenland, (ed.) R.J. Fulton; Geological Survey of Canada, Geology of Canada, no. 1, p. 40-42.

Colpron, M., and Nelson, J.L., 2011. A Digital Atlas of Terranes for the Northern Cordillera; British Columbia Ministry of Energy and Mines, BCGS GeoFile 2011-11,

Cooke, D.R., Baker, M., Hollings, P., Sweet, G., Zhaoshan, C., Danyushevsky, L., Gilbert, S., Zhou, T., White, N., Gemmell, J.B., and Inglis, S., 2014. New advances in detecting the distal geochemical footprints of porphyry systems - epidote mineral chemistry as a tool for vectoring and fertility assessments; *in* Building Exploration Capability for the 21st Century, (ed.) K.D. Kelley and H.C. Golden; Society of Economic Geologists, Special Publication No. 18, Littleton, Colorado, p. 127-152.

del Real, I., Hart, C.J.R., Bouzari, F., Blackwell, J.L., Rainbow, A., and Sherlock, R., 2014. Relationships between calcalkalic and alkalic mineralization styles at the copper-molybdenum Southeast Zone and copper-gold Deerhorn porphyry deposits, Woodjam property, central British Columbia (NTS 093A); *in* Geoscience BC Summary of Activities, Geoscience BC, Report 2014-, p. 63-82.

del Real, I., Hart, C.J.R., Bouzari, F., Blackwell, J.L., Rainbow, A., Sherlock, R., and Skinner, T., 2013. Paragenesis and alteration of the Southeast Zone and Deerhorn porphyry deposits, Woodjam property, central British Columbia (Parts of 093A); *in* Geoscience BC Summary of Activities 2012, Geoscence BC, Report 2013-1, p. 79-90.

DiLabio, R.N.W., and Coker, W.B. (ed.), 1989. Drift prospecting; Geological Survey of Canada, Ottawa, Ontario, Paper 89-20, 169 p.

Drummond, A.D., Sutherland Brown, A., Young, R.J., and Tennant, S.J., 1976. Gibraltar - Regional metamorphism, mineralization, hydrothermal alteration and structural development; *in* Porphyry deposits of the Canadian Cordillera, (ed.) A. Sutherland Brown; Canadian Institute of Mining and Metallurgy, Special Volume 15, p. 195-205.

Drummond, A.D., Tennant, S.J., and Young, R.J., 1973. The interrelationship of regional metamorphism, hydrothermal alteration and mineralization at the Gibraltar mines copper deposit in B.C.; Canadian Mining and Metallurgical Bulletin, v. 66, p. 48-55.

Dupuis, C., and Beaudoin, G., 2011. Discriminant diagrams for iron oxide trace element fingerprinting of mineral deposit types; Mineralium Deposita, v. 46, p. 319-335.

Ferbey, T., and Arnold, H., 2013. Compilation of micro- to macro-scale ice-flow indicators for the Interior Plateau, central British Columbia; British Columbia Ministry of Energy, Mines and Natural Gas, British Columbia Geological Survey, Open File 2013-03, scale 1:900,000.

Ferbey, T., and Plouffe, A., 2014. Lifting the burden of overburden in British Columbia: recent advances in till geochemical surveys; AMEBC Mineral Exploration Roundup, Vancouver, BC, Abstract volume, p. 26-28.

Ferbey, T., Arnold, H., and Hickin, A.S., 2013. Ice-flow indicator compilation, British Columbia; British Columbia Ministry of Energy and Mines, British Columbia Geological Survey, Open File 2013-06, scale 1:1 650,000.

Ferbey, T., Plouffe, A., and Anderson, R.G., 2014. An integrated approach to search for buried porphyry-style mineralization in central British Columbia using geochemistry and mineralogy: a TGI-4 project; *in* Current Research 2014-2, Geological Survey of Canada, 12 p.

Fraser, T.M., 1994. Hydrothermal breccias and associated alteration of the Mount Polley copper-gold deposit; *in* Geological Fieldwork 1993, British Columbia Ministry of Energy, Mines and Petroleum Resources, Paper 1994-1, p. 259-267.

Fulton, R.J., 1975. Quaternary geology and geomorphology, Nicola-Vernon area, British Columbia (82 L W 1/2 and 92 I E 1/2); Geological Survey of Canada, Memoir 380, 50 p.

Girard, I., Klassen, R.A., and Laframboise, R.R., 2004. Sedimentology Laboratory manual, Terrain Sciences Division; Geological Survey of Canada, Open File 4823, 134 p.

Grondahl, C., 2014. Trace elements in magnetite from porphyry deposits: applications in mineral exploration; B.Sc., University of Victoria, Victoria, 83 p.

Harris, J.F., 1982. Sampling and analytical requirements for effective use of geochemistry in exploration for gold; *in* Precious Metals in the Northern Cordillera, (ed.) A.A. Levinson; Association of Exploration Geochemists, Special Publication Number 10, Rexdale, Ontario, p. 53-67.

Hashmi, S., Plouffe, A., and Ward, B.C., 2015. Surficial geology, Bootjack Mountain area, British Columbia, Parts of NTS 93-A/5, NTS 93-A/6, NTS 93-A/11, and NTS 93-A/12; Geological Survey of Canada, Canadian Geoscience Map 209 (preliminary), British Columbia Geological Survey, Geoscience Map 2015-02, scale 1:50,000. doi:10.4095/296029

Hashmi, S., Ward, B.C., Plouffe, A., Ferbey, T., and Leybourne, M.I., 2014. Geochemical and mineralogical dispersal in till from the Mount Polley Cu-Au porphyry deposit, central British Columbia, Canada; Geological Survey of Canada, Open File 7589.

Hashmi, S., Ward, B.C., Plouffe, A., Leybourne, M.I., and Ferbey, T., in press a. Geochemical and mineralogical dispersal in till from the Mount Polley Cu-Au porphyry deposit, central British Columbia, Canada; Geochemistry: Exploration, Environment, Analysis.

Hashmi, S., Ward, B.C., Plouffe, A., Leybourne, M.I., and Ferbey, T., in press b. Till geochemistry and mineralogy in the Mount Polley Cu-Au porphyry deposit region, British Columbia, Canada; International Applied Geochemistry Symposium, Tucson, AZ, Abstract.

Kelley, K.D., Eppinger, R.G., Lang, J., Smith, S.M., and Fey, D.L., 2011. Porphyry Cu indicator minerals in till as an exploration tool: example from the giant Pebble porphyry Cu-Au-Mo deposit, Alaska, USA; Geochemistry: Exploration, Environment, Analysis, v. 11, p. 321-334.

Kirkham, R.V., 1972. Porphyry deposits; *in* Report of Activities Part B, November 1971 to March 1972, (ed.) R.G. Blackadar; Geological Survey of Canada, Paper 72-1B, p. 62-64.

Kujansuu, R., and Saarnisto, M., (ed.), 1990. Glacial indicator tracing; A. A. Balkema, Rotterdam, 252 p.

Levson, V.M., 2001. Regional till geochemical surveys in the Canadian Cordillera: sample media, methods and anomaly evaluation; *in* Drift Exploration in Glaciated Terrain, (ed.) M.B. McClenaghan, P.T. Bobrowsky, G.E.M. Hall and S.J. Cook; Geological Society, Special Publication 185, London, p. 45-68.

Liles, P., 2005. Gibraltar faces restart challenges; Canadian Mining Journal, v. 126, p. 16-17.

Logan, J.M., 2013. Porphyry systems of central and southern BC: Overview and field trip road log; *in* Porphyry systems of central and southern British Columbia: Tour of central British Columbia porphyry deposits from Prince George to Princeton, (ed.) J.M. Logan and T.G. Schroeter; Society of Economic Geologists, Society of Economic Geologists Field Trip Guidebook, Series 43, p. 1-45.

Logan, J.M., and Mihalynuk, M.G., 2014. Tectonic Controls on Early Mesozoic Paired Alkaline Porphyry Deposit Belts (Cu-Au ± Ag-Pt-Pd-Mo) Within the Canadian Cordillera; Economic Geology, v. 109, p. 827-858.

Logan, J.M., Bath, A.B., Mihalynuk, M.G., and Rees, C.J., 2007. Regional geology of the Mount Polley area, central British Columbia; Ministry of Energy, Mines and Petroleum Resources, Geoscience Map 2007-1, scale 1:50,000.

Logan, J.M., Schiarizza, P., Struik, L.C., Barnett, C., Nelson, J.L., Kowalczyk, P., Ferri, F., Mihalynuk, M.G., Thomas, M.D., Gammon, P., Lett, R., Jackaman, W., and Ferbey, T. (comp.), 2010. Bedrock geology of the QUEST map area, central British Columbia; Geoscience BC Report 2010-5, British Columbia Geological Survey, Geoscience Map 2010-1 and Geological Survey of Canada, Open File 6476, scale 1:500,000.

Lowell, J.D., and Guilbert, J.M., 1970. Lateral and vertical alteration-mineralization zoning in porphyry ore deposits; Economic Geology, v. 65, p. 373-408.

Massey, N.W.D., MacIntyre, D.G., Desjardins, P.J., and Cooney, R.T., 2005. Geology of British Columbia; British Columbia Ministry of Energy, Mines and Petroleum Resources, British Columbia Geological Survey, Geoscience Map 2005-3, scale 1:1,000,000.

Mathur, R., Dendas, M., Titley, S., and Phillips, A., 2010. Patterns in the copper isotope composition of minerals in porphyry copper deposits in southwestern United States; Economic Geology, v. 105, p. 1457-1467.

Mathur, R., Titley, S., Barra, F., Brantley, S., Wilson, M., Phillips, A., Munizaga, F., Maksaev, V., Vervoort, J., and Hart, G., 2009. Exploration potential of Cu isotope fractionation in porphyry copper deposits; Journal of Geochemical Exploration, v. 102, p. 1-6.

McMartin, I., and McClenaghan, M.B., 2001. Till geochemistry and sampling techniques in glaciated shield terrain: a review; *in* Drift exploration in glaciated terrain, (ed.) M.B. McClenaghan, P.T. Bobrowsky, G.E.M. Hall and S.J. Cook; Geological Society, Special Publication 185, London, p. 19-43.

McMillan, W.J., 1991. Porphyry deposits in the Canadian Cordillera; British Columbia Ministry of Energy, Mines and Petroleum Resources, Paper 1991-4, p. 253-276.

McMillan, W.J., and Panteleyev, A., 1995. Porphyry copper deposits of the Canadian Cordillera; *in* Porphyry copper deposits of the American Cordillera, (ed.) F.W. Pierce and J.G. Bolm; Arizona Geological Society, Digest 20, p. 203-218.

McMillan, W.J., Anderson, R.G., Chan, R., and Chow, W., 2009. Geology and Mineral Occurrences (minfile), Guichon Creek Batholith and Highland Valley porphyry copper district, British Columbia; Geological Survey of Canada, Open File 6079, scale 1:100,000 and 1:150,000, 2 sheets.

McMillan, W.J., Höy, T., MacIntyre, D.G., Nelson, J.L., Nixon, G.T., Hammack, J.L., Panteleyev, A., Ray, G.E., and Webster, I.C.L., 1991. Ore deposits, tectonics and metallogeny in the Canadian Cordillera; British Columbia Ministry of Energy, Mines and Petroleum Resources, Paper 1991-4, p. 276 p.

McMillan, W.J., Thompson, J.F.H., Hart, C.J.R., and Johnston, S.T., 1995. Regional geological and tectonic setting of porphyry deposits in British Columbia and Yukon Territory; *in* Porphyry deposits of the northwestern Cordillera of North America, (ed.) T.G. Schroeter; Canadian Institute of Mining, Metallurgy and Petroleum, Special Volume 46, Montréal, p. 40-57.

McMillan, W.J., Thompson, J.F.H., Hart, C.J.R., and Johnston, S.T., 1996. Porphyry deposits of the Canadian Cordillera; Geoscience Canada, v. 23, p. 125-134.

MINFILE, 2015. MINFILE British Columbia mineral deposits database; British Columbia Ministry of Energy, Mines and Petroleum Resources, URL http://minfile.gov.bc.ca/SearchBasic.aspx.

Paulen, R.C., 2013. A revised look at Canada's landscape: glacial processes and dynamics; *in* New Frontiers for Exploration in Glaciated Terrain, (ed.) R.C. Paulen and B.M. McClenaghan; Geological Survey of Canada, Open File 7374, p. 5-12.

Pass, H.E., 2010. Breccia-hosted chemical and mineralogical zonation patterns of the Northeast Zone, Mt. Polley Cu-Ag-Au alkalic porphyry deposit, British Columbia, Canada; Ph.D. thesis, The University of Tasmania, Hobart, Australia, 276 p.

Piziak, L.K., Canil, D., Grondahl, C., Plouffe, A., Ferbey, T., and Anderson, R.G., 2015. Magnetite as a porphyry Cu indicator mineral in till: a test using the Mount Polley porphyry Cu-Au deposit, British Columbia; *in* Geoscience BC Summary of Activities 2014, Geoscience BC, Report 2015-1, p. 141-150.

Plouffe, A., 1995. Drift prospecting sampling methods; *in* Drift Exploration in the Canadian Cordillera, (ed.) P.T. Bobrowsky, S.J. Sibbick, J.M. Newell, and P.F. Matysek; British Columbia Ministry of Energy, Mines and Petroleum Resources, Paper 1995-2, p. 43-52.

Plouffe, A., 2000. Quaternary geology of the Fort Fraser and Manson River map areas, central British Columbia; Geological Survey of Canada, Ottawa, Ontario, Bulletin 554, 62 p.

Plouffe, A., and Ferbey, T., 2015a. Discovering buried copper porphyry mineralization: geochemistry and indicator minerals in till; Geological Survey of Canada, Open File 7680, 45 p.

Plouffe, A., and Ferbey, T., 2015b. Surficial geology, Gnawed Mountain area, British Columbia, Parts of NTS 92-I/6, NTS 92-I/7, NTS 92-I/10, and NTS 92-I/11; Geological Survey of Canada, Canadian Geoscience Map 214 (preliminary), British Columbia Geological Survey, Geoscience Map 2015-3, scale 1:50,000. doi:10.4095/296285

Plouffe, A., Anderson, R.G., and Dunn, C.E., 2011a. Till composition and biogeochemistry near a porphyry Cu-Mo deposit: Gibraltar Mine, British Columbia; Geological Survey of Canada, Ottawa, ON, Open File 6755, 25 p.

Plouffe, A., Bednarski, J.M., Huscroft, C.A., Anderson, R.G., and McCuaig, S.J., 2010. Glacial sediments geochemistry of the Bonaparte Lake map area (NTS 92P), south central British Columbia; Geological Survey of Canada, Ottawa, ON, Open File 6440.

Plouffe, A., Bednarski, J.M., Huscroft, C.A., Anderson, R.G., and McCuaig, S.J., 2011b. Late Wisconsinan glacial history in the

Bonaparte Lake map area, south central British Columbia: implications for glacial transport and mineral exploration; Canadian Journal of Earth Sciences, v. 48, p. 1091-1111.

Plouffe, A., Bednarski, J.M., Huscroft, C.A., and McCuaig, S.J., 2009. Gold grain content of till in the Bonaparte Lake map area, south central British Columbia (NTS 92P); Geological Survey of Canada, Ottawa, Open File 6047, CD Rom.

Plouffe, A., Ferbey, T., and Anderson, R.G., 2014. Till composition and ice-flow history in the region of the Gibraltar Mine: developing indicators for the search of buried mineralization; Geological Survey of Canada, Open File 7592.

Plouffe, A., Ferbey, T., Anderson, R.G., Hashmi, S., and Ward, B.C., 2013a. New TGI-4 till geochemistry and mineralogy results near the Highland Valley, Gibraltar, and Mount Polley mines, and Woodjam District: An aid to search for buried porphyry deposits; Geological Survey of Canada, Open File 7473, 58 p.

Plouffe, A., Ferbey, T., Anderson, R.G., Hashmi, S., Ward, B.C., and Sacco, D.A., 2013b. The use of till geochemistry and mineralogy to explore for buried porphyry deposits in the Cordillera - preliminary results from a TGI-4 intrusion-related ore systems project; Geological Survey of Canada, Open File 7367.

Plouffe, A., Ferbey, T., Levson, V.M., and Bond, J.D., 2012. Glacial history and drift prospecting in the Canadian Cordillera: recent developments; Geological Survey of Canada, Open File 7261, 51 p.

Plouffe, A., McClenaghan, M.B., Paulen, R.C., McMartin, I., Campbell, J.E., and Spirito, W.A., 2013c. Processing of glacial sediments for the recovery of indicator minerals: protocols used at the Geological Survey of Canada; Geochemistry: Exploration, Environment, Analysis, v. 13, p. 303-316.

Rees, C., 2013. The Mount Polley Cu-Au deposit, south-central British Columbia, Canada; *in* Porphyry systems of central and southern British Columbia: Tour of central British Columbia porphyry deposits from Prince George to Princeton, (ed.) J.M. Logan and T.G. Schroeter; Society of Economic Geologists, Society of Economic Geologists Field Trip Guidebook, Series 43, p. 67-98.

Rotherham, D.C., Drummond, A.D., and Tennant, S.J., 1972. Exploration of Gibraltar; Western Miner, v. 45, p. 25-28.

Rudnick, R.L., and Gao, S., 2004. Composition of the continental crust; *in* Treatise on Geochemistry, (ed.) H.D. Holland and K.K. Turekian; Elsevier, 3, Amsterdam, p. 1-64.

Ryder, J.M., 1976. Terrain inventory and Quaternary geology Ashcroft, British Columbia; Geological Survey of Canada, Paper 74-49, 17 p.

Schiarizza, P., 2014. Geological setting of the Granite Mountain batholith, host to the Gibraltar porphyry Cu-Mo deposit, south-central British Columbia *in* Geological Fieldwork 2013, British Columbia Ministry of Energy and Mines, British Columbia Geological Survey, Paper 2014-1, p. 95-110.

Schiarizza, P., 2015. Geological setting of the Granite Mountain batholith, south-central British Columbia; British Columbia Geological Ministry of Energy and Mines, GeoFile 2015-5, poster.

Schiarizza, P., and Bligh, J.S., 2008. Geology and mineral occurrences of the Timothy Lake area, south-central British Columbia (NTS 092P/14); *in* Geological Fieldwork 2007, British Columbia Ministry of Energy, Mines and Petroleum Resources, Paper 2008-1, Victoria, B.C., p. 191-211.

Schiarizza, P., and Boulton, A., 2006. Geology of the Canim Lake area, NTS 92P/15; British Columbia Ministry of Energy, Mines and Petroleum Resources, Open File 2006-8, scale 1:50,000.

Schiarizza, P., Heffernan, S., Israel, S., and Zuber, J., 2002a. Geology of the Clearwater - Bowers Lake Area, NTS 092P/9, 10, 15, 16; British Columbia Ministry of Energy, Mines and Petroleum Resources, Open File map 2002-15, scale 1:50,000.

Schiarizza, P., Israel, S., Heffernan, S., and Zuber, J., 2002b. Geology of the Nehalliston Plateau, NTS 092P/7, 8, 9, 10; British Columbia Ministry of Energy and Mines, Open File 2002-4, scale 1:50,000.

Sherlock, R., and Trueman, A., 2013. NI 43-101 technical report for 2012 activities on the Woodjam south property; Gold Fields Horsefly Exploration Group and Consolidated Woodjam Copper Corporation, Cariboo Mining Division, British Columbia, 158 p.

Sherlock, R., Blackwell, J., and Skinner, T., 2013. NI 43-101 technical report for 2012 activities on the Woodjam North property; Gold Fields Horsefly Exploration Group, Consolidated Woodjam Copper Corporation, Cariboo Mining Division, British Columbia, 275 p.

Shilts, W.W., 1993. Geological Survey of Canada's contributions to understanding the composition of glacial sediments; Canadian Journal of Earth Sciences, v. 30, p. 333-353.

Sinclair, W.D., 2007. Porphyry deposits; *in* Mineral Deposits of Canada: A synthesis of Major Deposit-Types, District Metallogeny, the Evolution of Geological Provinces, and Exploration Methods, (ed.) W.D. Goodfellow; Geological Association of Canada, Mineral Deposit Division, Special Publication No. 5, p. 223-243.

Spirito, W., McClenaghan, M.B., Plouffe, A., McMartin, I., Campbell, J.E., Paulen, R.C., Garrett, R.G., and Hall, G.E.M., 2011. Till sampling and analytical protocols for GEM projects: from field to archive; Geological Survey of Canada, Open File 6850, 83 p.

Stanley, C.R., 2008. Missed hits or near misses: determining how many samples are necessary to confidently detect nugget-borne mineralization; Geochemistry: Exploration, Environment, Analysis, v. 8, p. 129-138.

Stea, R.R., Turner, R.G., Finck, P.W., and Graves, R.M., 1989. Glacial dispersal in Nova Scotia: a zonal concept; *in* Drift Prospecting, (ed.) R.N.W. DiLabio and W.B. Coker; Geological Survey of Canada, Paper 89-20, p. 155-169.

Tipper, H.W., 1971a. Multiple glaciations in central British Columbia; Canadian Journal of Earth Sciences, v. 8, p. 743-752.

Tipper, H.W., 1971b. Glacial geomorphology and Pleistocene history of central British Columbia; Geological Survey of Canada, Bulletin 196, 89 p.

Trommelen, M.S., Ross, M., and Campbell, J.E., 2013. Inherited clast dispersal patterns: Implications for palaeoglaciology of the SE Keewatin Sector of the Laurentide Ice Sheet; Boreas, v. 42, p. 693 -713.

van Straaten, B.I., Oliver, J., Crozier, J., and Goodhue, L., 2013. A summary of the Gibraltar porphyry copper-molybdenum deposit, south-central British Columbia, Canada; *in* Porphyry systems of central and southern British Columbia: Tour of central British Columbia porphyry deposits from Prince George to Princeton, (ed.) J.M. Logan and T.G. Schroeter; Society of Economic Geologists, Society of Economic Geologists Field Trip Guidebook, Series 43, p. 55-66.

Zhu, X.K., O'Nions, R.K., Guo, Y., Belshaw, N.S., and Rickard, D., 2000. Determination of natural Cu-isotope variation by plasma-source mass spectrometry: implications for use as geochemical tracers; Chemical Geology, v. 163, p. 139-149.

Till, stream sediment, and stream water geochemical signatures of intrusion-hosted Sn-W deposits: examples from the Sisson W-Mo and Mount Pleasant Sn-W-Mo-Bi-In deposits, New Brunswick

M.B. McClenaghan[1], M.A. Parkhill[2], A.G. Pronk[3], A.A. Seaman[3], M.W. McCurdy[1], R.S. Poulin[4], A.M. McDonald[4], D.J. Kontak[4], and M.I. Leybourne[4]

1. Geological Survey of Canada, 601 Booth Street, Ottawa, Ontario
2. New Brunswick Department of Energy and Mines, Geological Surveys Branch, P.O. Box 50, Bathurst, New Brunswick
3. New Brunswick Department of Energy and Mines, Geological Surveys Branch, P.O. Box 6000, Fredericton, New Brunswick
4. Department of Earth Sciences, Laurentian University, 935 Ramsey Lake Road, Sudbury, Ontario

Abstract: Indicator minerals methods for intrusion-hosted Sn and W deposits were tested at the intrusion-hosted Sisson W-Mo and Mount Pleasant Sn-W-Mo-Bi-In deposits in eastern Canada as part of the Geological Survey of Canada's (GSC) Targeted Geoscience Initiative 4 (TGI 4). The program was a collaborative federal geoscience program with a mandate to provide industry with the next generation of geoscience knowledge and innovative techniques that will result in more effective targeting of buried mineral deposits. The case studies are a collaborative effort between the GSC, the New Brunswick Department of Energy and Mines (NBDEM), and the holders of the Sisson (Northcliff Resources Limited, Hunter Dickinson Inc.) and the Mount Pleasant (Adex Mining Inc.) deposits, and Laurentian University.

The detailed till mineralogical + geochemical study described here is one of the first reported for major Sn-W deposits in glaciated terrain. Indicator minerals were examined in heavy mineral (>3.2 specific gravity) concentrates of bedrock and till samples from both deposits, as well as in stream sediment samples from the Sisson deposit area. The <0.063 mm fraction of till samples from both deposits was analysed geochemically using modified aqua regia (partial) and borate fusion (total) digestions.

Indicator/pathfinder trace elements in till at the Sisson W-Mo deposit includes W, Mo, Cu, Zn, Pb, Ag, Bi, In, As, Cd, Zn, and Te. Indicator/pathfinder trace elements in till at the Mount Pleasant Sn-W-Mo-Bi-In deposit includes Sn, W, Mo, Bi, In, Ag, As, Cd, Cu, Pb, Re, Te, Tl, and Zn. These element suites reflect the polymetallic nature of these deposits and the broader suite of elements that is now available using modern analytical methods such as inductively coupled plasma – mass spectrometry. The Mount Pleasant deposit is a significant source of indium and till down ice of the deposit contains some of the highest indium values (13 ppm) ever reported for till, indicating that till geochemistry can be an important exploration tool for In-bearing deposits. Indicator/pathfinder elements in stream sediment downstream of the Sisson deposit include W, Mo, Ag, As, Bi, Cd, Cu, In, Tl, and Zn. Indicator/pathfinder elements in stream water around the Sisson deposit include W, Mo, As, Cd, Cu, Cs, and Zn.

Indicator minerals of the Sisson deposit identified in the 0.25-0.5 mm fraction of mineralised bedrock, till, and stream sediments include scheelite, wolframite, molybdenite, chalcopyrite, Bi minerals (joseite, native Bi, bismutite, bismuthinite), galena, sphalerite, arsenopyrite, spessartine, pyrrhotite, and pyrite. Indicator minerals of the Mount Pleasant deposit identified in the 0.25-0.5 mm fraction of mineralised bedrock and till include cassiterite, wolframite, molybdenite, topaz, fluorite, galena, sphalerite, chalcopyrite, galena, arsenopyrite, pyrite, and loellingite. Additional but rare secondary indicator minerals of the Mount Pleasant deposit include beudantite, anglesite, and plumbogummite which formed by oxidation and weathering of the galena.

The extensive suite of indicator minerals for both deposits reflects their polymetallic natures and the ability of modern indicator mineral methods to recover these minerals. Indicator minerals present in the coarse (0.5-2.0 mm) heavy mineral fraction of till indicate proximity to the mineralised source. A commercial service is now available to systematically determine the scheelite contents of heavy mineral concentrates using its short wave ultraviolet light fluorescence. This service will provide consistent scheelite results within, and between, heavy mineral sampling surveys. Fluorite abundance was shown to be most abundant in the 3.0-3.2 SG (mid-density) fraction of till and can be readily recovered by including a mid-density heavy liquid separation as part of the processing procedures.

Corresponding author: Beth McClenaghan (bmcclena@nrcan.gc.ca)

McClenaghan, M.B., Parkhill, M.A., Pronk, A.G., Seaman, A.A., McCurdy, M.W., Poulin, R.S., McDonald, A.M., Kontak, D.J., and Leybourne, M.I., 2015. Till, stream sediment, and stream water geochemical signatures of intrusion-hosted Sn-W deposits: examples from the Sisson W-Mo and Mount Pleasant Sn-W-Mo-Bi-In deposits, New Brunswick; *in* TGI 4 – Intrusion Related Mineralisation Project: New Vectors to Buried Porphyry-Style Mineralisation, (ed.) N. Rogers; Geological Survey of Canada, Open File 7843, p. 39-58.

Introduction

Few case studies have been conducted around significant Sn and W deposits to identify their indicator mineral and geochemical signatures in glaciated terrain. The Sisson W-Mo and Mount Pleasant Sn-W-Mo-Bi-In deposits (Fig. 1) in eastern Canada provide ideal sites to test/demonstrate these exploration methods for intrusion-hosted Sn and W deposits. These deposits were chosen because: (1) their bedrock geology is well known; (2) mineralisation was exposed to glacial erosion and they are till covered; and, (3) till geochemical dispersal trains have already been identified down ice from the deposits and thus, zones where metal-rich till occurs at surface are defined and can be targeted for indicator mineral sampling. The two studies were carried out as part of the Geological Survey of Canada's (GSC) Targeted Geoscience Initiative 4 (TGI 4) Program, a collaborative federal geoscience initiative with a mandate to provide industry with the next generation of geoscience knowledge and innovative techniques that will result in more effective targeting of buried mineral deposits. The case studies are a collaborative effort between the GSC, the New Brunswick Department of Energy and Mines (NBDEM), and the holders of the Sisson (Northcliff Resources Limited, Hunter Dickinson Inc.) and the Mount Pleasant (Adex Mining Inc.) deposits, and Laurentian University.

The purpose of this report is to provide an overview of the indicator mineral and geochemical research results for the two deposits. Detailed results are reported in the GSC open files, field guide, and journal paper listed in Table 1. Both deposits are located in the west-central part of New Brunswick and are hosted in Late Silurian to Early Devonian plutonic rocks that form a northeast-trending belt underlying the Miramichi Highlands in central New Brunswick (Fig. 1). In related TGI 4 studies, the GSC also studied indicator mineral and till geochemical signatures for porphyry Cu-Mo-Au deposits in central British Columbia. These results are also reported in this volume (Plouffe and Ferbey, 2015).

Sisson deposit geology

The bedrock geology of the Sisson deposit area is summarized below from Nast and William-Jones (1991), Marr (2009), Fyffe et al. (2008, 2010), Rennie et al. (2013), and Bustard et al. (2013). The deposit occurs at the eastern contact of the Nashwaak Granite and Howard Peak Granodiorite plutons (Fig. 2). The Howard Peak Granodiorite grades eastward into, and becomes intermixed with, gabbro. Granite dykes that are likely offshoots of the Nashwaak Granite transect both the gabbro and granodiorite. East of the Howard Peak Granodiorite are Ordovician Tetagouche Group rocks that include the Turnbull Mountain Formation tuffaceous volcanic and sedimentary rocks, Hayden Lake Formation pyritiferous black shale intercalated with felsic volcanic rocks, and Push and Be Damned Formation mafic volcanic rocks, wacke and shale. Also to the east are the Cambro-Ordovician Miramichi Group quartzite and shale of the Knights Brook Formation.

The Sisson deposit is a bulk tonnage W-Mo intrusion-related deposit that consists of four wide and steeply dipping zones of vein and fracture-controlled W and Mo mineralisation that straddle the strongly sheared eastern contact of the Howard Peak Granodiorite (Figs. 2, 3). Mineralisation is likely related to the presence of a buried granitic stock at depth, which was the heat source for a hydrothermal system and metals. The deposit has elevated concentrations of Cu, Zn, Pb, Bi, and As that are directly related to late quartz-scheelite and sulphide-rich veins. Ore minerals in the deposit include scheelite, minor wolframite, and molybdenite. Other sulphide, oxide and telluride minerals present are listed in Table 2. The Nashwaak occurrence is a small high-grade Pb-Zn-Ag-Sb zone (Fig. 2) that subcrops under thin till cover approximately 900 m east of the Sisson deposit. This occurrence was originally interpreted as a volcanogenic massive sulphide showing but more recently has been interpreted to be a vein-type showing related to the Sisson mineralising system (Marr, 2009; Rennie et al., 2013).

Bedrock outcrops on the Sisson property and surrounding area are rare due to the locally thick and continuous cover of till. Till thickness varies from <2 m to 20 m over the deposit, and is on average 8 m thick. Surface till in the area consist mainly of sandy Early Wisconsinan lodgement till likely deposited by southeast glacial flow during the Caledonia Phase, and possibly reworked by south-southwest glacial flow during the Middle to Late Wisconsinan (Escuminac Phase). This till is discontinuously overlain by up to 2.5 m thick, loose, very sandy till deposited by westward flowing ice during the late-glacial Collins Pond Phase (Younger Dryas) (Seaman and McCoy, 2008; Seaman, 2009; Fyffe et al., 2010; Stea et al., 2011).

As part of a reconnaissance-scale till geochemical survey of central New Brunswick, Lamothe (1992) identified a 10 km long glacial dispersal train trending southeast from the Sisson deposit that was best defined by W, Cu, Pb, Zn, and Mo contents in till. More recently, Seaman (2001, 2002, 2003, 2007, 2012) and Seaman and McCoy (2008) identified elevated concentrations of W, As, Bi, Cd, Cs, Cu, In, Mo, Sn, and Zn in till up to 40 km southeast of the deposit. This glacial dispersal train is discontinuous in places due to local reworking during subsequent Late Wisconsinan glacial phases.

Table 1 – List of publications reporting indicator mineral and till geochemical data for the TGI-4 Sisson and Mount Pleasant deposit case studies: GSC open files, one journal paper, and one field trip guide book.

Deposit	Publication	Source	Content
Sisson	GSC Open File 7387	McClenaghan et al., 2013b	raw indicator mineral data for bedrock, till, stream sediment samples
Sisson	GSC Open File 7430	McClenaghan et al., 2013c	till geochemical data
Sisson	GSC Open File 7431	McClenaghan et al., 2013a	interpretation of indicator mineral data for bedrock samples
Sisson	GSC Open File 7467	McClenaghan et al., 2014c	interpretation of indicator mineral data for till samples
Sisson	GSC Open File 7756	McClenaghan et al., 2015c	geochemical & indicator mineral data for stream sediment and water samples
Sisson	NBDEM Field Guide	Thorne et al., 2014	Sisson field trip guide
Sisson	Atlantic Geology	McClenaghan et al., 2014b	interpretation of till geochemical data
Mount Pleasant	GSC Open File 7573	McClenaghan et al., 2014a	raw indicator mineral data for bedrock and till samples
Mount Pleasant	GSC Open File 7721	McClenaghan et al., 2015a	interpretation of indicator rmineral data for bedrock samples
Mount Pleasant	GSC Open File 7722	McClenaghan et al., 2015b	till geochemical data
Mount Pleasant	GSC Open File 7804	McClenaghan et al., in press	interpretation of indicator rmineral data for till samples

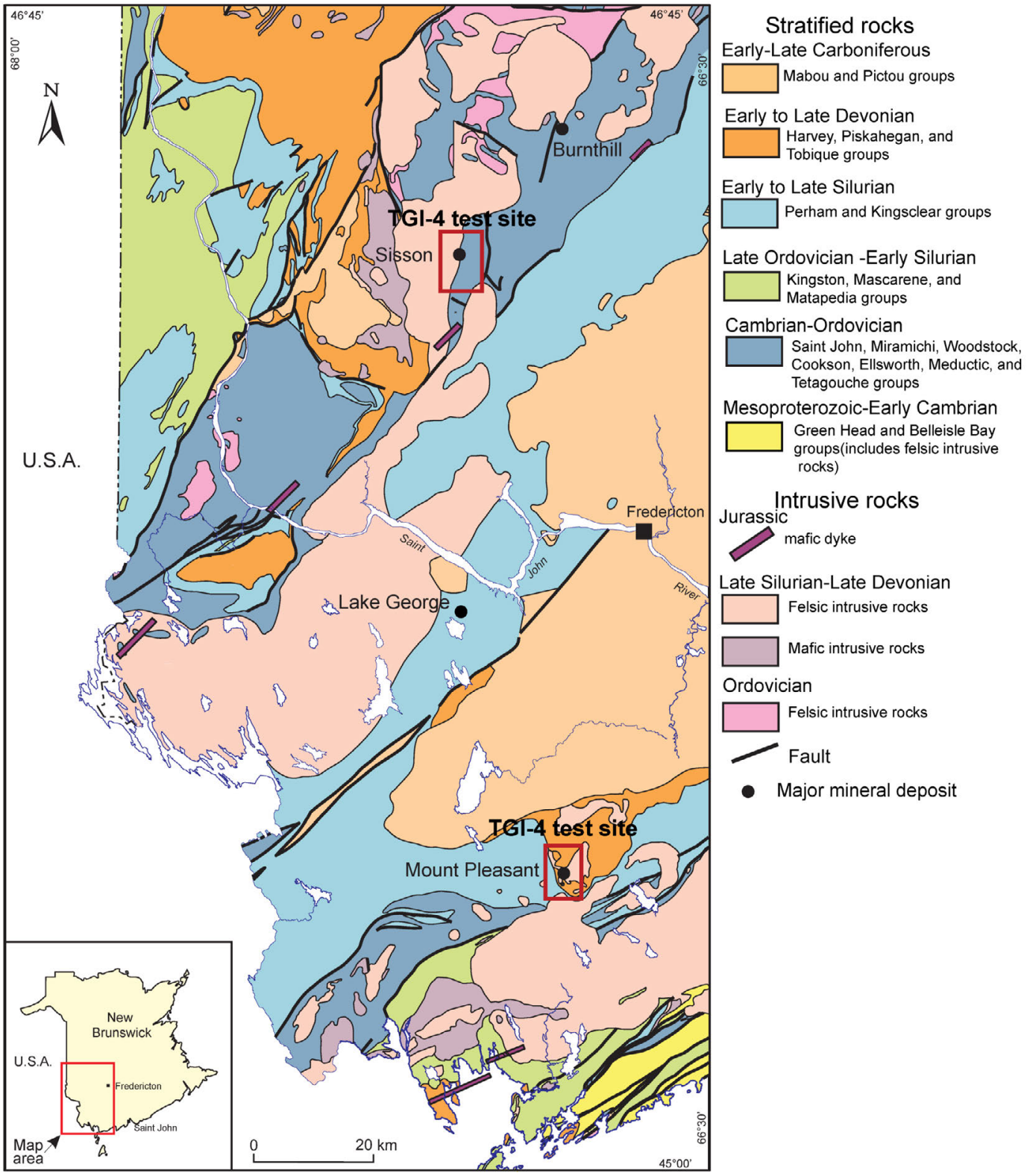

Figure 1 – Bedrock geology of west-central and southern New Brunswick showing the location of the Sisson W-Mo deposit, the Mount Pleasant Sn-W-Mo-Bi-In deposit, and other intrusion-hosted deposits (modified from Fyffe et al., 2010).

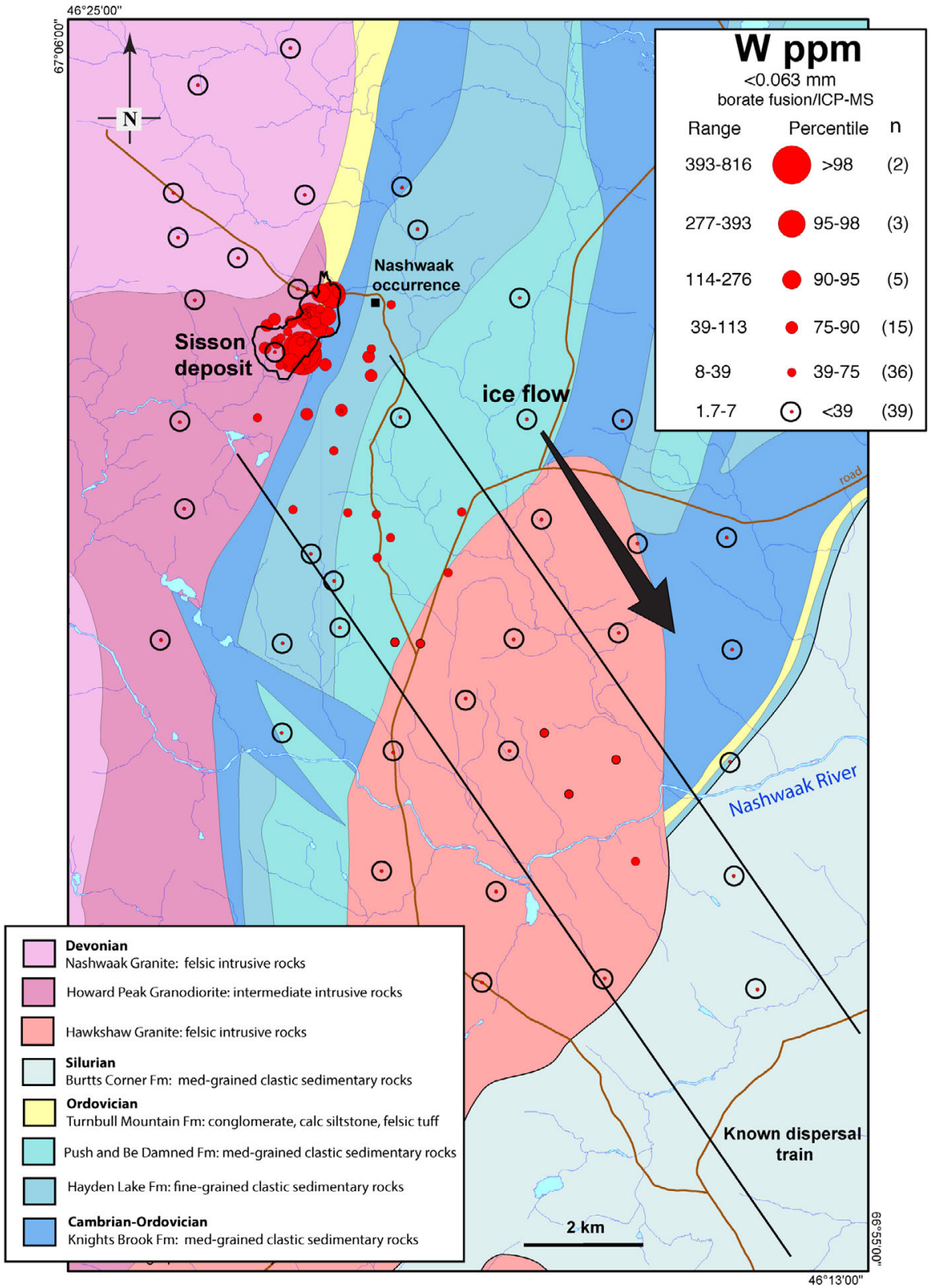

Figure 2 – Proportional dot map of W (borate fusion/ICP-MS) abundance in the <0.063 mm fraction of surface till samples around the Sisson W-Mo deposit. Known dispersal train outlined was identified using data from this study combined with that from Seaman and McCoy (2008). Bedrock geology modified from Smith and Fyffe (2006a, b, c, d). Deposit outline in black is from Rennie et al. (2013) (modified from McClenaghan et al., 2013c, 2014b).

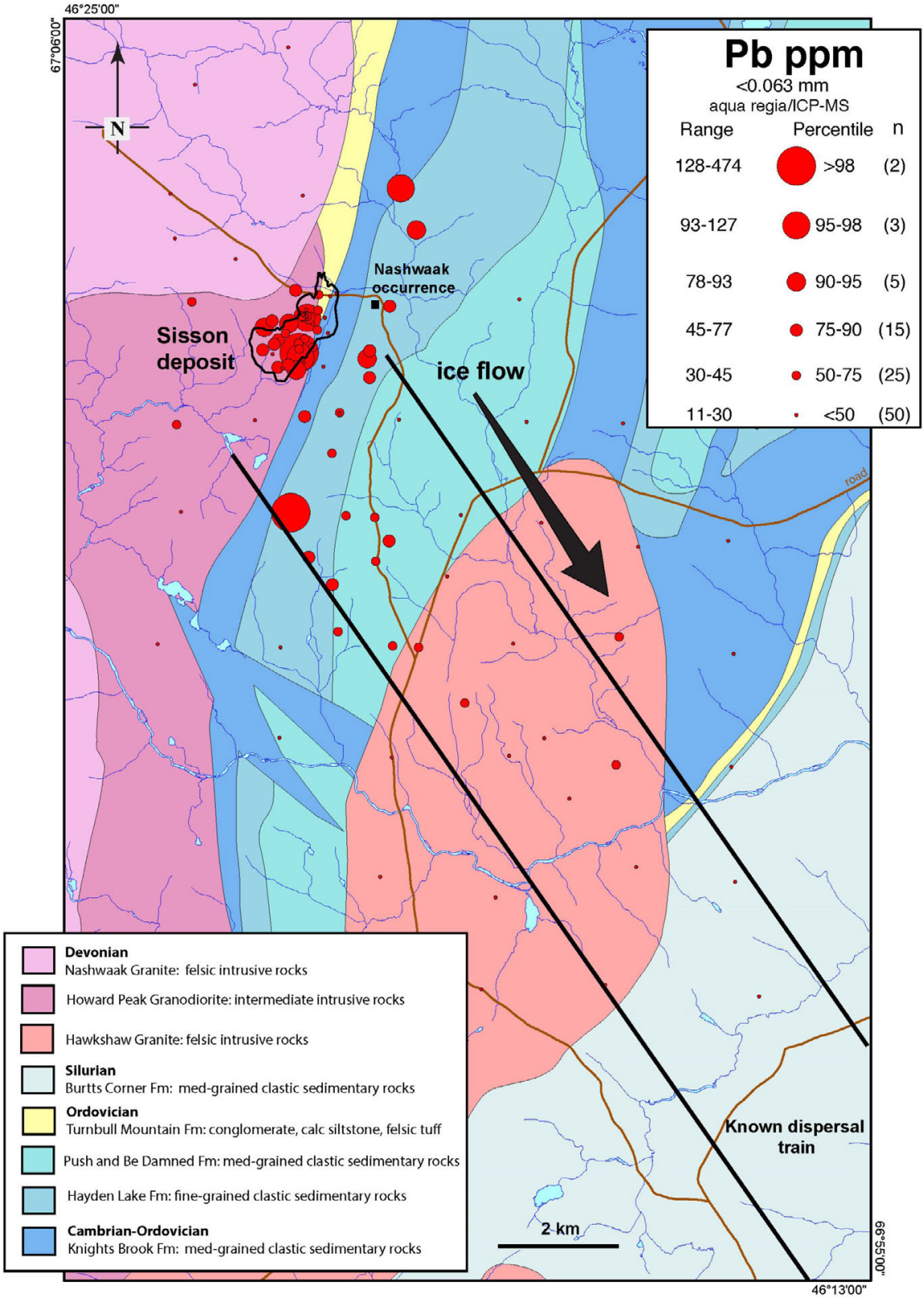

Figure 3 – Proportional dot map of Pb (modified aqua regia /ICP-MS) abundance in the <0.063 mm fraction of surface till samples around the Sisson W-Mo deposit. Bedrock geology modified from Smith and Fyffe (2006a, b, c, d). Deposit outline in black is from Rennie et al. (2013) (modified from McClenaghan et al., 2013c, 2014b).

Table 2 – Indicator minerals in the Sisson W-Mo deposit and those found in till heavy mineral concentrates (HMC) from the TGI-4 study (from McClenaghan et al., 2013a, b).

Mineral	Formula	Specific Gravity	Hardness	Presence in bedrock reported by others	Identified in bedrock PTS in this study	Identified in bedrock HMC in this study	Identified in till HMC in this study
W Minerals							
scheelite	$CaWO_4$	5.9 - 6.1	4-5	Nast & Williams-Jones (1991); Marr (2009)	yes	yes	yes
wolframite	$(Fe,Mn)WO_4$	7.1 - 7.5	4.5	Nast & Williams-Jones (1991); Marr (2009)	yes	yes	yes
Sulphides							
molybdenite	MoS_2	5.5	1.0	Nast & Williams-Jones (1991); Marr (2009)	yes	yes	yes
pyrite	FeS_2	5	6.5	Nast & Williams-Jones (1991); Marr (2009)	yes	yes	yes
chalcopyrite	$CuFeS_2$	4.1 - 4.3	3.5	Nast & Williams-Jones (1991); Marr (2009)	yes	yes	yes
sphalerite	(Zn,Fe)S	3.9 - 4.2	3.5-4	Nast & Williams-Jones (1991); Marr (2009)	yes	yes	yes
galena	PbS	7.2 - 7.6	2.5	Nast & Williams-Jones (1991); Marr (2009)	no	yes	yes
pyrrhotite	$Fe_{(1-x)}S$ (x=0-0.17)	4.6 - 4.7	3.5-4	Nast & Williams-Jones (1991); Marr (2009)	yes	yes	no
arsenopyrite	FeAsS	6.1	5	Nast & Williams-Jones (1991); Marr (2009)	no	yes	yes
Bi Minerals							
bismuthinite	Bi_2S_3	6.8 - 7.2	2.0	no	no	no	yes
bismutite	$Bi_2(CO_3)O_2$	7.0	4.0	no	no	no	yes
native bismuth	Bi	9.7 - 9.8	2-2.5	Nast & Williams-Jones (1991); Marr (2009)	yes	no	yes
joseite	$Bi_4(S,Te)_3$	8.1	2.0	no	no	no	yes
Ag Minerals							
hessite	Ag_2Te	7.2-7.9	1.5-2	Nast & Williams-Jones (1991)	no	no	no
acanthite	Ag_2S	7.2-7.4	2-2.5	Nast & Williams-Jones (1991)	no	no	no

Mount Pleasant deposit geology

The bedrock geology of the Mount Pleasant deposit is summarized below from Kooiman et al. (1986), Invemo and Hutchinson, (2004), Sinclair et al. (2006), McCutcheon et al. (2010), and McCutcheon et al. (2013). The deposit is within two subvolcanic intrusions in the Late Devonian Mount Pleasant Caldera Complex along the north flank of the Saint George Batholith. The McDougall Brook Granitic Suite is related to the early stages of caldera development, and the Mount Pleasant Granitic Suite is related to the late stages of caldera development. The deposit consists of Sn, W, Mo, Bi, and In mineralisation that is genetically related to highly evolved granites of the Mount Pleasant Granitic Suite (Granites I, II and III) that are enriched in incompatible elements F, Li, Rb, Cs, U, Th, and Nb. Granite I and the related breccia hosts W-Mo-Bi mineralisation and Granite II hosts Sn-In mineralisation. Two mineralised zones outcrop or subcrop, the North Zone, and the Fire Tower Zone (Fig. 4), and thus likely contributed mineralised debris to overriding glaciers.

The North Zone consists of older W-Mo mineralisation and younger Sn-In mineralisation, some of which is at or near surface. The Sn-In zones contain cassiterite, arsenopyrite, loellingite, sphalerite, and chalcopyrite as well as the other sulphide minerals listed in Table 3. The Fire Tower Zone contains predominantly large, low-grade W-Mo deposits with some small In-bearing Sn-base metal resources. The main ore minerals are wolframite and molybdenite and minor native bismuth, and bismuthinite. Gangue minerals include cassiterite, arsenopyrite, and loellingite, quartz, topaz, and fluorite. The Fire Tower Zone also contains small In-bearing Sn-base metal zones in irregular veins and breccias consisting mainly of cassiterite and wolframite along with the sulphide minerals listed in Table 3. Indium in the Mount Pleasant deposit occurs mainly as a solid solution between sphalerite and roquesite, but also in chalcopyrite and stannite (Sinclair et al., 2006).

Riddell (1967) was the first to describe the till geochemical signature of the Mount Pleasant deposit. He analysed over 2500 soils developed on till for Sn, Mo, Cu, Pb, and Zn. Metal contents are highest in soils overlying the North and Fire Tower Zones and to the southeast. Distribution patterns reflected glacial dispersal to the southeast from the two zones as well as subsequent mechanical dispersal and/or chemical dispersion of metals down the west and east flanks of the mountain. Szabo et al. (1975), building on the work of Riddell (1967), collected till samples instead of soil samples around the Mount Pleasant deposit. Glacial dispersal southeast from the deposit was best defined by Sn, As, Cu, Pb, and Zn in the 0.5-2.0 mm heavy mineral fraction (>2.95 specific gravity (SG)) of till.

Methods

Sampling

At both deposits, a small suite of mineralised and host rocks, and a larger suite of till samples were collected to examine their indicator mineral content. Till sampling locations, site descriptions, photographs, and sample depth information are reported in McClenaghan et al. (2013b, 2014a, b, 2015b). At each till sample site, three samples were collected: (1) a 8 to 15 kg sample for recovery of indicator minerals; (2) a 3 kg till sample for geochemical analysis of the matrix, textural determinations, and archiving; and, (3) a 200 g sample for in-field testing using a portable XRF. At the Sisson deposit, 61 surface till samples were collected from trenches, road cuts, and hand-dug holes around and within the first 14 km of the known glacial dispersal train to optimize the chances of sampling metal-rich till at varying

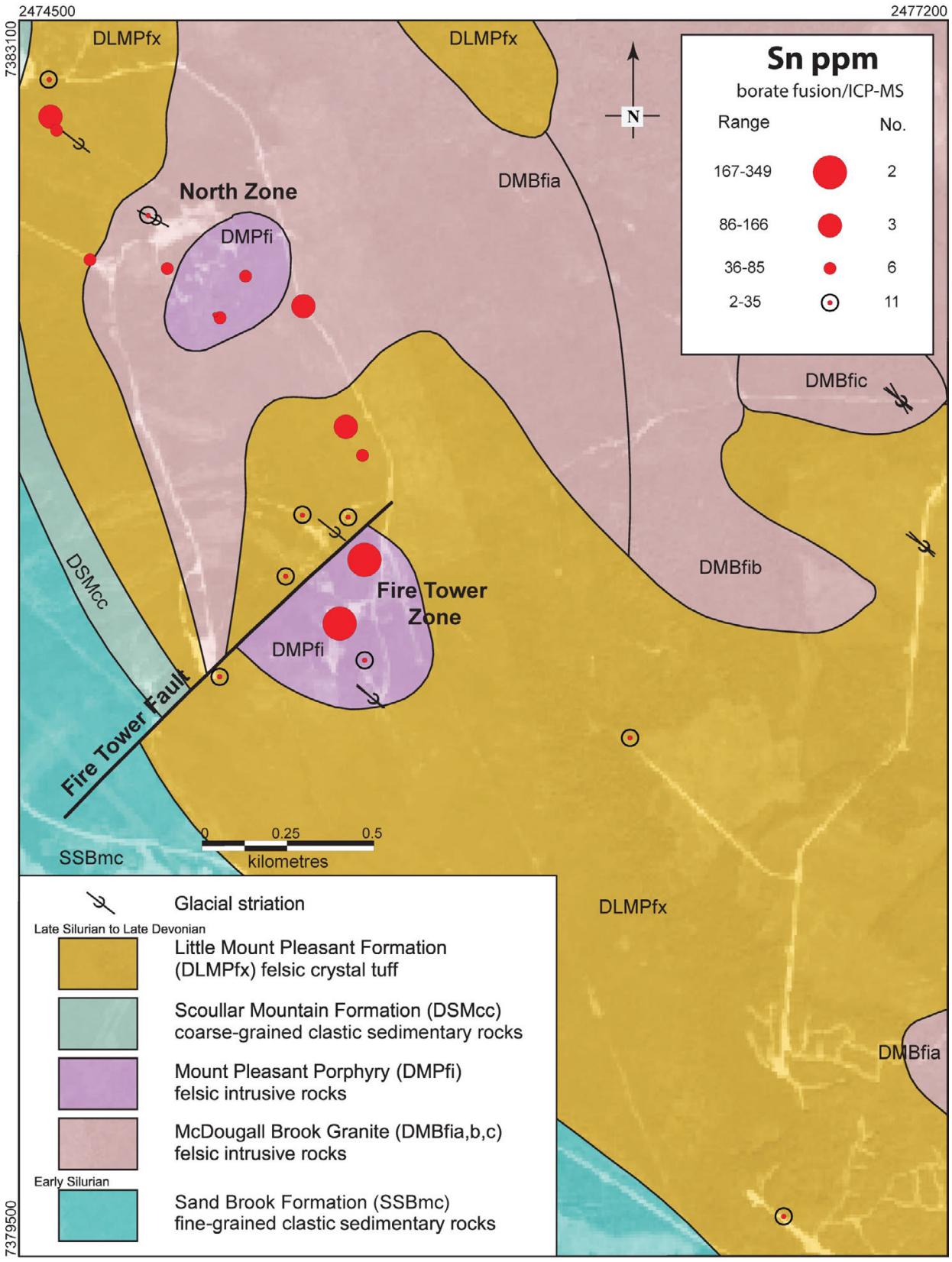

Figure 4 – Proportional dot map of Sn (borate fusion/ICP-MS) abundance in the <0.063 mm fraction of surface till samples around the Mount Pleasant Sn-W-Mo-Bi-In deposit. Bedrock geology from McLeod et al. (2005). (Modified from McClenaghan et al., 2015b).

Table 3 – Indicator minerals in the Mount Pleasant Sn-W-Mo-Bi-In deposit and those found in till heavy mineral concentrates (HMC) from the TGI-4 study (from McClenaghan et al., 2014a, 2015b).

Mineral	Formula	Hardness	Specific Gravity	Presence in bedrock reported by others	Size range in till HMC (mm)
Sn Minerals					
cassiterite	SnO_2	6-7	6.8 - 7	Petruk (1972)	0.25-2.0
stannite	Cu_2FeSnS_4	3.5-4	4.3 - 4.5	Petruk (1972)	not observed
këesterite	$Cu_2(Zn,Fe)SnS_4$	4.5	4.54 - 4.59	Petruk (1972)	not observed
ferrokësterite	$Cu_2(Fe,Zn)SnS_4$	4.0	4.5	Parrish (1977)	not observed
stannoidite	$Cu_8Fe_3Sn_2S_{12}$	4	4.3	Petruk (1972)	not observed
mawsonite	$Cu_6Fe_2SnS_8$	3.5-4	4.7	Petruk (1972)	not observed
W minerals					
scheelite	$CaWO_4$	4-5	5.9 - 6.12	Parrish (1977)	0.25-2.0
wolframite	$(Fe,Mn)WO_4$	4.5	7.1 - 7.5	Petruk (1972)	0.25-2.0
Sulphide and arsenide minerals					
molybdenite	MoS_2	1.0	6	Petruk (1972)	0.25-0.5
pyrite	FeS_2	6.5	5-5.02	Petruk (1972)	0.25-0.5
marcasite	FeS_2	6.0-6.5	4.9	Petruk (1972)	not observed
sphalerite	(Zn,Fe)S	3.5-4	3.9 - 4.2	Petruk (1972)	not observed
pyrrhotite	$Fe_{(1-x)}S$ (x=0-0.17)	3.5-4	4.58 - 4.65	Petruk (1972)	not observed
arsenopyrite	FeAsS	5	6.1	Petruk (1972)	0.25-2.0
loellingite	$FeAs_2$	5.0	7.1 - 7.7	Petruk (1972)	0.25-1.0
ferrimolybdite	$Fe_2(MoO_4)3•8(H_2O)$	2.5-3	4 - 4.5	Parrish (1977)	not observed
scorodite	$Fe(AsO_4)•2(H_2O)$	3.5-4	3.1 - 3.3	Parrish (1977)	not observed
Bi minerals					
bismuthinite	Bi_2S_3	2	6.8 - 7.2	Petruk (1972)	not observed
native bismuth	Bi	2-2.5	9.7 - 9.8	Petruk (1972)	not observed
arsenobismite	$Bi_2(AsO_4)(OH)_3$	3	5.7	Parrish (1977)	not observed
zairite	$Bi(Fe,Al)_3[(OH)_6(PO_4)_2])$	4.5	4.4	not reported	0.25-0.5
Cu minerals					
chalcopyrite	$CuFeS_2$	3.5	4.1 - 4.3	Petruk (1972)	not observed
covellite	CuS	1.5-2.0	4.6 - 4.76	Petruk (1972)	not observed
tennantite	$(Cu,Fe)_{12}As_4S_{13}$	3.5-4	4.6 - 4.7	Petruk (1972)	not observed
bornite	Cu_5FeS_4	3.0	4.9 - 5.3	Petruk (1972)	not observed
chalcocite	Cu_2S	2.5-3	5.5 - 5.8	Parrish (1977)	not observed
roquesite	$CuInS_2$	3.5-4	not reported	Petruk (1973)	not observed
digenite	Cu_9S_5	2.5-3	5.6	Parrish (1977)	not observed
famatinite	Cu_3SbS_4	3-4	4.6	Parrish (1977)	not observed
Pb minerals					
galena	PbS	2.5	7.2 - 7.6	Petruk (1972)	0.25-0.5
wittichenite	Cu_3BiS_3	2.5	6.3 - 6.7	Petruk (1973)	not observed
galenobismutite	$PbBi_2S_4$	2.5-3	6.9 - 7.1	Petruk (1972)	not observed
aikinite	$PbCuBiS_3$	2-2.5	6.1 - 6.8	Petruk (1972)	not observed
cosalite	$Pb_2Bi_2S_5$	2.5-3	6.4 - 6.8	Petruk (1972)	not observed
krupkaite	$PbCuBi_3S_6$	4	7.0	Petruk (1972)	not observed
beudantite	$PbFe_3(AsO_4)(SO_4)(OH)_6$	4.0	4.1-4.3	not reported	0.25-0.5
anglesite	$Pb(SO_4)$	2.5-3	6.3	not reported	0.25-2.0
plumbogummite	$PbAl_3(PO_4)_2(OH)_5H_2O$	4-5	4-5	not reported	0.25-0.5
plumboferrite	$Pb_2Mn_{0.2}Mg_{0.1}Fe_{10.6}O_{18.4}$	5	6	not reported	2.0
Au and Ag Minerals					
freibergite	$(Ag,Cu,Fe)_{12}(Sb,As)_4S_{13}$	3.5-4	4.85 - 5	Petruk (1973)	not observed
pyrargyrite	Ag_3SbS_3	2.5	5.9	Petruk (1973)	not observed
native silver	Ag	2.5-3	10-11	Petruk (1972)	not observed
gold	Au	2.5-3	16-19.3	Parrish (1977)	0.025-0.175
Alteration minerals					
topaz	$Al_2SiO_4(F,OH)_2$	8	3.5 - 3.6	Petruk (1972)	0.25-2.0
fluorite	CaF_2	4	3.01 - 3.25	Petruk (1972)	0.25-1.0
tourmaline (black)	$NaAl_3Al_6(BO_3)_3(Si_6O_{18})(O,OH)_4$	7	3	Petruk (1972)	0.25-1.0
columbite	$(Fe,Mn)(Nb,Ta)_2O_6$	6.0	5.3 - 7.3	Petruk (1972)	not observed

distances down ice (Figs 2, 3). To provide a regional context in which to interpret the new till geochemical data for the Sisson area, the archived <0.063 mm fraction of 39 till samples, previously analysed by NBDEM as part of their regional surveys, were analysed as part of the GSC analytical batch in 2011 and data are reported in McClenaghan et al. (2013c). At the Mount Pleasant deposit, 18 surface till samples were collected from road cuts or hand-dug holes around the North and Fire Tower zones (Fig. 4) within the first 2 km of the known glacial dispersal train.

Stream sediment (silt + fine sand) and stream water samples were collected at 16 sites located upstream, overlying, and downstream (southeast) of the Sisson deposit using GSC National Geochemical Reconnaissance (NGR) sampling protocols (McClenaghan et al., 2015c). At each site, three samples were collected: (1) a 9 to 14 kg stream sediment sample for recovery of indicator minerals; (2) a 200 g fine grained (silt+fine sand) stream sediment sieved to <0.177 mmm for geochemical analysis; and, (3) a 60 ml filtered (0.45 μm) stream water sample for geochemical analysis.

Geochemical analysis

The <0.063 mm (-250 mesh) fraction of till was geochemically analysed at a commercial laboratory (ACME Analytical Laboratories, Bureau Veritas Company, Vancouver, BC), using a modified aqua regia ($HCl:HNO_3$ 1:1) /ICP-MS on 0.5 g, and lithium metaborate/ tetraborate fusion followed by nitric acid digestion/ICP-ES, ICP-MS on 0.2 g. As a result of the lower and variable recovery of W and Sn by the aqua regia digestion in this study (McClenaghan et al., 2013c), only the total W and Sn values determined by fusion/ICP-MS are described and plotted here. Detailed descriptions of analytical methods, monitoring of analytical accuracy and precision using blind duplicates, CANMET certified reference standards, and silica sand blanks along with the data listings are reported in McClenaghan et al. (2013b, c, 2015c).

The <0.177 mm (-80 mesh) fraction of stream sediment was geochemically analysed at a commercial laboratory using modified aqua regia/ICP-MS on 0.5 g and by Instrumental Neutron Activation Analysis (INAA) on ~30 g. Filtered stream water samples were acidified within 48 hours of arrival at GSC with 0.5 ml 8M HNO_3 and analysed for trace metal and major elements at GSC Laboratories, Ottawa. Detailed descriptions of analytical methods, monitoring of analytical accuracy and precision using blind duplicates and CANMET certified reference standards, and data listings for stream sediment and water samples are reported in McClenaghan et al. (2013b, 2015c).

Indicator mineral Analysis

All bedrock, till, and stream sediment samples were processed at the commercial heavy mineral processing laboratory, Overburden Drilling Management Limited (ODM) to recover the heavy mineral concentrate (HMC) and determine the abundance of indicator minerals in each sample. Prior to processing, bedrock samples were disaggregated using an electric pulse disaggregator instead of a conventional rock crusher to preserve natural grain sizes, textures, and shapes. The <2.0 mm fraction of each bedrock, till, and stream sediment sample was processed to produce a non-ferromagnetic HMC for selection of indicator minerals using the tabling and heavy liquid (3.2 SG) procedures outlined in McClenaghan et al. (2013a, b, 2014a, b, c, 2015a, c). The mid-density fraction mineral fraction (3.0-3.2 SG) was also separated for the Mount Pleasant till samples to allow for the determination of fluorite and tourmaline content. The 0.25-0.5, 0.5-1.0, and 1.0-2.0 mm non-ferromagnetic HMC and the 0.25-0.5 mm mid density fractions of samples were then examined. Potential indicator minerals of Sn-W mineralisation were examined and counted and some grains removed for detailed study. In collaboration with ODM, a systematic method was developed to examine individual heavy mineral concentrates inside a black box using short wave ultraviolet light to rapidly and efficiently determine their scheelite content. Under visible light, scheelite has an unremarkable pale yellow colour, but under short wave ultraviolet light it has a diagnostic bright bluish white fluorescence.

Till geochemical results

The term 'indicator element' is used here to refer to an element that is an economically valuable component of the ore being sought and which may be used to detect an orebody. The term 'pathfinder element' refers to non-ore elements associated with the orebody that may be used to detect the orebody (Rose et al., 1979).

Sisson

Indicator elements for the Sisson deposit include W (Fig. 2) and Mo and pathfinder elements include Cu, Zn, Pb, Ag, Bi, In, As, Cd, Zn, and Te. This suite of elements is more extensive than the few elements (W, Mo, Cu, As, and F) identified in earlier studies by Snow and Coker (1987), Lamothe (1992), and Seaman and McCoy (2008). The <0.063 mm fraction of till sampled in this study clearly detects glacial dispersal at least 14 km to the southeast and confirms the observations of a southeast-trending glacial dispersal train reported in the earlier studies. Elevated concentrations of Ag, As, Cu, In, Pb (Fig. 3), Te, and Zn in till east and northeast of the Sisson deposit may reflect (1) glacial dispersal from a more distal expression of the Sisson mineralised system, such as the Nashwaak occurrence, or (2) glacial dispersal from metal-rich Silurian-Ordovician Tetagouche Group sedimentary rocks that are unrelated to the intrusion. These elevated metal concentrations may warrant further investigation to determine their bedrock source.

Mount Pleasant

Indicator elements for the Mount Pleasant deposit include Sn (Fig. 4), W, Mo, Bi, and In (Fig. 5). Pathfinder elements include Ag, As, Cd, Cu, Pb, Re, Te, Tl, and Zn. This suite of elements is significantly larger than (Sn, Mo, Cu, Pb, Zn) that identified by Riddell (1967) and Szabo et al. (1975) in their earlier geochemical studies of the deposit. The <0.063 mm fraction of till sampled in this study is metal-rich at least 1 km to the southeast and confirms the observations of a southeast-trending glacial dispersal train reported by Szabo et al. (1975). Samples 0.5 km to the northwest of the North Zone also have elevated contents of Sn, In, Ag, Cd, Zn, and Pb that likely reflect the presence of a small mineralised zone in this area. The Mount Pleasant deposit is a significant source of In and this study is one of the first to report In-rich till. Three till samples overlying the mineralised zones and one down-ice (southeast) of the North Zone contain 2.79 to 13.08 ppm In (Fig. 5), some of the highest In values ever reported for till.

Stream sediment and water geochemical results

Indicator/pathfinder elements in the <0.177 mm fraction of stream sediment downstream of the Sisson deposit include W, Mo, Ag, As, Bi, Cd, Cu, In, Tl, and Zn. Indicator/pathfinder elements in stream water around the Sisson deposit include W, Mo, As, Cd, Cu, Cs, and Zn (McClenaghan et al., 2015c).

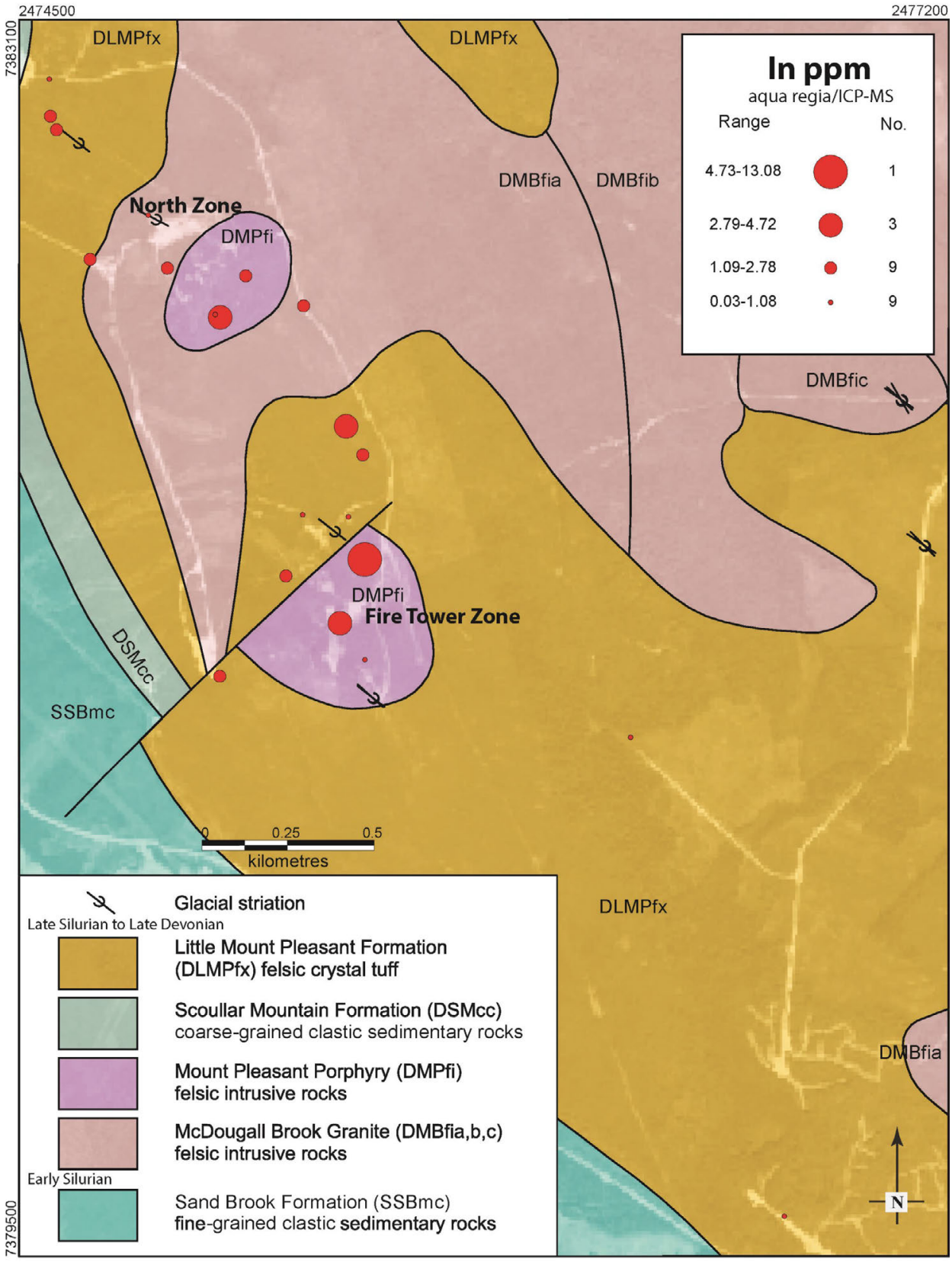

Figure 5 – Proportional dot map of In (modified aqua regia /ICP-MS) abundance in the <0.063 mm fraction of surface till samples around the Mount Pleasant Sn-W-Mo-Bi-In deposit. Bedrock geology from McLeod et al. (2005). (Modified from McClenaghan et al., 2015b).

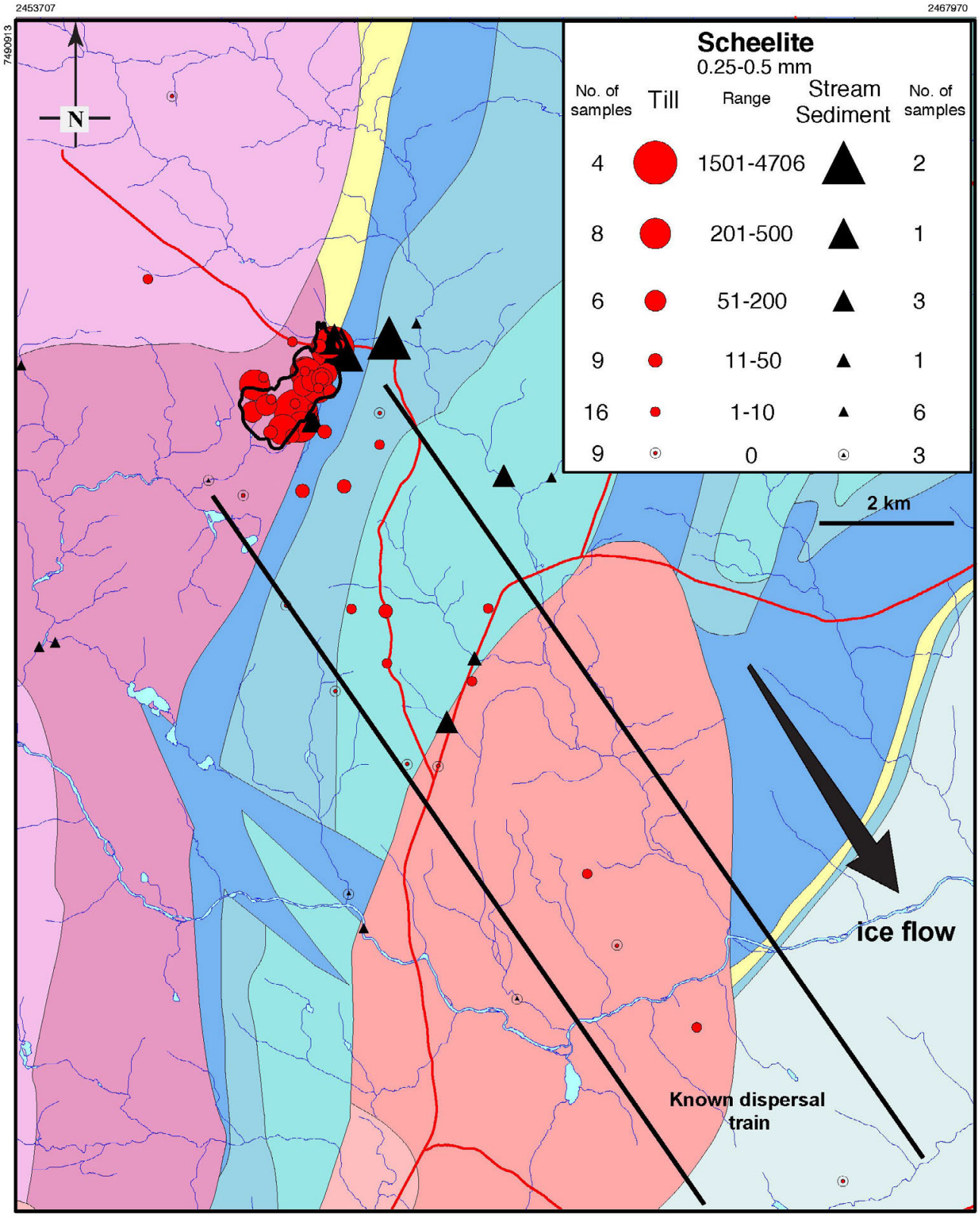

Figure 6 – Proportional symbol map of scheelite abundance in the 0.25-0.5 mm non-ferromagnetic fraction of surface till samples (red dots) and stream sediments (black triangles) around the Sisson W-Mo deposit. Bedrock geology modified from Smith and Fyffe (2006a, b, c, d). Deposit outline in black is from Rennie et al. (2013) (modified from McClenaghan et al., 2014a). Bedrock legend same as in Figure 3.

Indicator mineral results

Sisson

The primary Sisson ore minerals recovered from bedrock, till, and stream sediment samples include scheelite (Fig. 6), wolframite, and molybdenite (Table 2). They are heavy minerals that are visually distinct (Fig. 7) and easily recovered by the common surficial sample processing method that uses tabling + heavy liquids (McClenaghan, 2011). Additional indicator minerals include chalcopyrite, Bi-rich minerals (joseite, native Bi, bismutite, bismuthinite), galena, sphalerite, arsenopyrite, spessartine, pyrrhotite, and pyrite. These minerals are most abundant in the 0.25-0.5 mm fraction of till. Coarse (0.5-2.0 mm) indicator minerals are present in till up to 4 km down ice of the deposit.

Mount Pleasant

Indicator minerals in bedrock and till at the Mount Pleasant deposit (Table 3) include the main ore minerals, cassiterite (Fig. 8), wolframite, and molybdenite, as well as topaz, galena, sphalerite, chalcopyrite, galena, arsenopyrite, pyrrhotite, pyrite, and loellingite in the >3.2 SG fraction of till, and fluorite in the 3.0-3.2 SG fraction (Fig. 9). Useful indicator minerals also include secondary Pb sulphate minerals

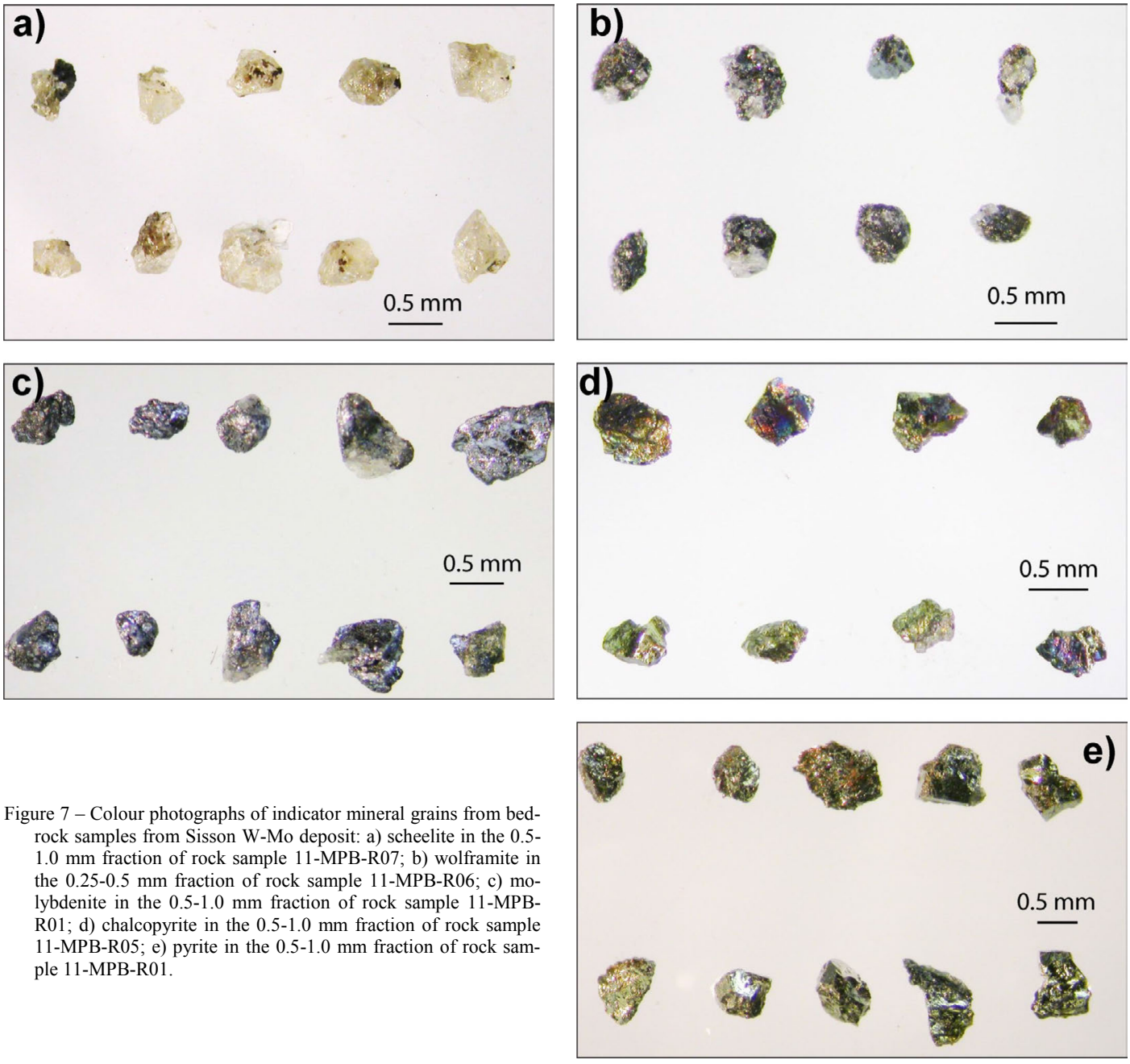

Figure 7 – Colour photographs of indicator mineral grains from bedrock samples from Sisson W-Mo deposit: a) scheelite in the 0.5-1.0 mm fraction of rock sample 11-MPB-R07; b) wolframite in the 0.25-0.5 mm fraction of rock sample 11-MPB-R06; c) molybdenite in the 0.5-1.0 mm fraction of rock sample 11-MPB-R01; d) chalcopyrite in the 0.5-1.0 mm fraction of rock sample 11-MPB-R05; e) pyrite in the 0.5-1.0 mm fraction of rock sample 11-MPB-R01.

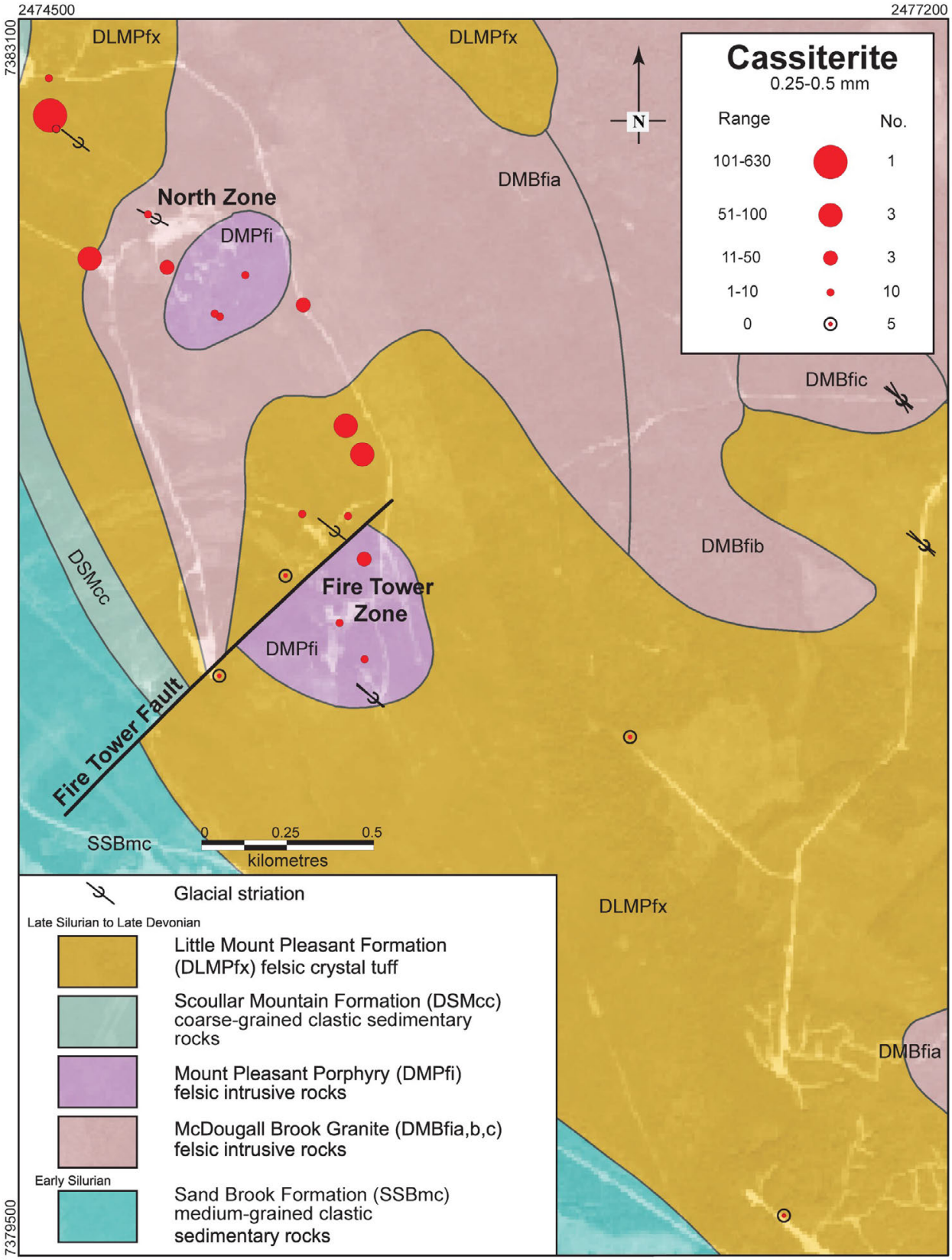

Figure 8 – Proportional dot map of cassiterite abundance in the 0.25-0.5 mm non-ferromagnetic fraction of surface till samples around the Mount Pleasant Sn-W-Mo-Bi-In deposit. Bedrock geology from McLeod et al. (2005).

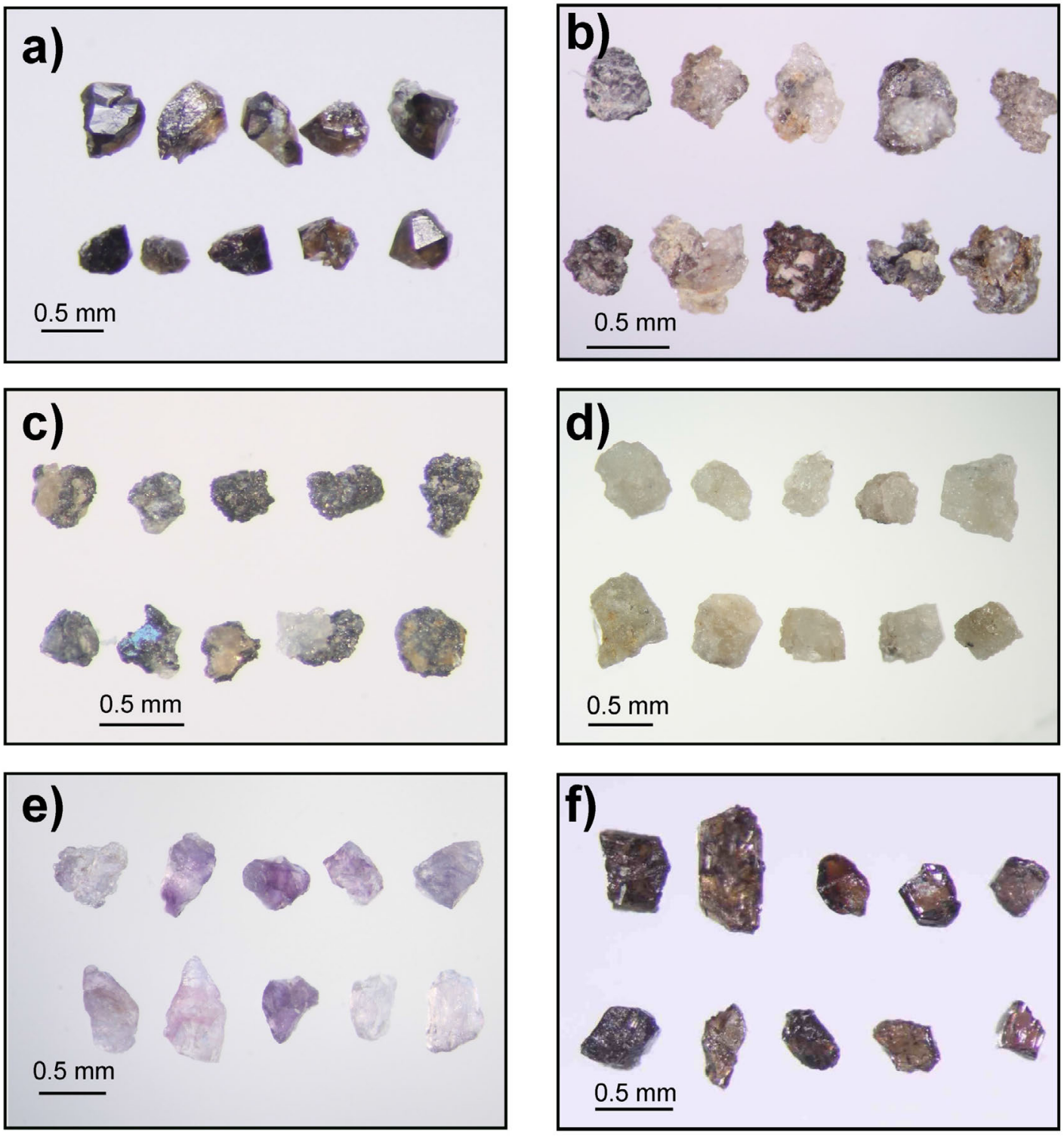

Figure 9 – Colour photographs of indicator mineral grains from till in the Mount Pleasant deposit area: a) prismatic brown cassiterite grains in the 0.25-0.5 mm fraction of sample 12-MPB-1020; b) brown irregular shaped cassiterite grains with adhering quartz in the 0.25-0.5 mm fraction of sample 12-MPB-1020; c) wolframite in the 0.25-0.5 mm fraction of sample 12-MPB-1004; d) topaz in the 0.5-1.0 mm fraction of sample12-MPB-1004; and e) fluorite in the 0.5-1.0 mm fraction of 12-MPB-1008; f) tourmaline in the 0.25-0.5 mm fraction of sample 12-MPB-1007; g) beudantite in the 0.25-0.5 mm fraction of sample 12-MPB-1002; h) anglesite in the 0.25-0.5 mm fraction of sample 12-MPB-1004; i) eulytite in the 0.25-0.5 mm fraction of 12-MPB-1002; j) ziarite in the 0.25-0.5 mm fraction of 12-MPB-1019. Photographs taken by Overburden Drilling Management Ltd.

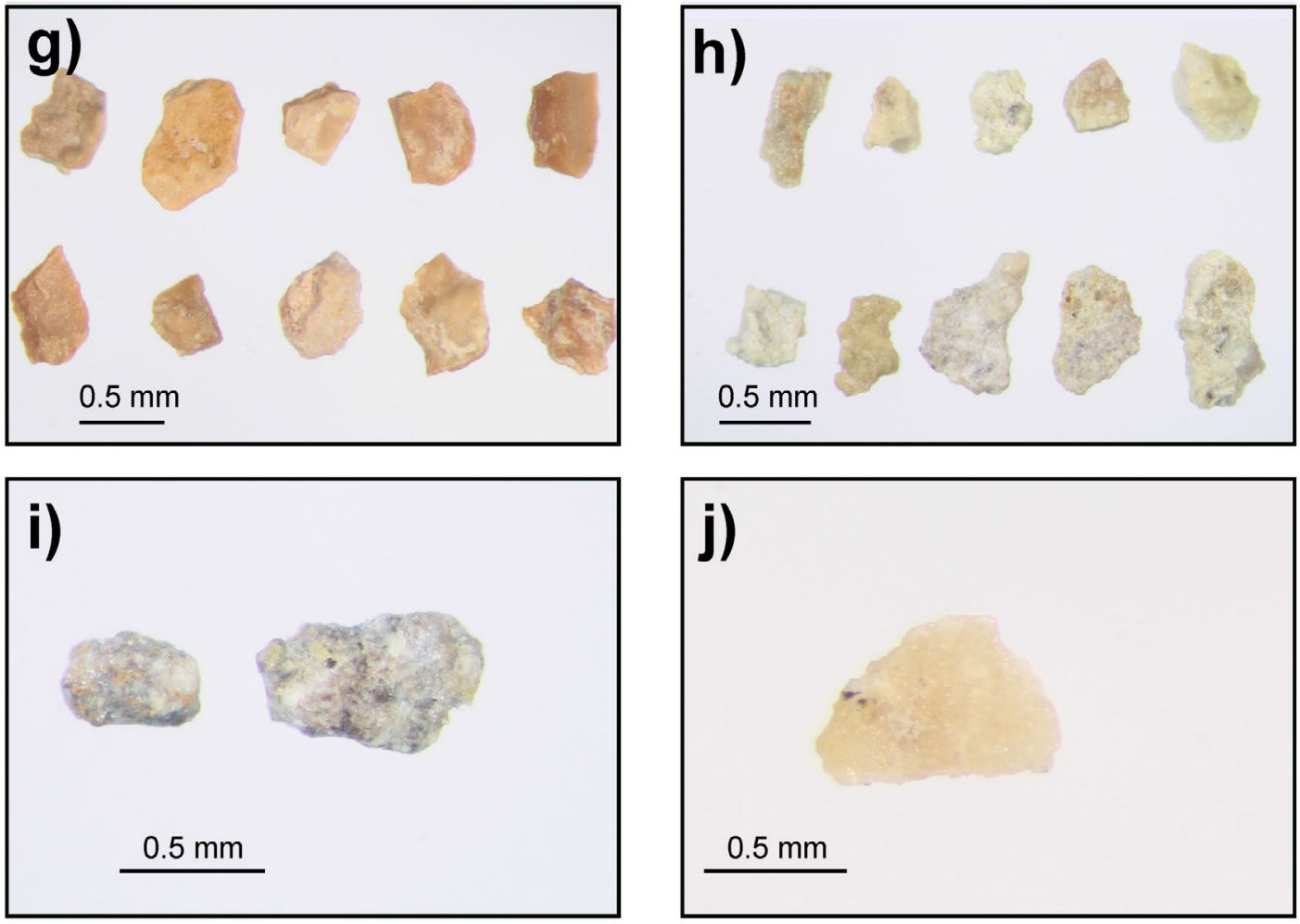

Figure 9 – Continued

beudantite ($PbFe_3(AsO_4)(SO_4)(OH)_6$) and anglesite ($Pb(SO_4)$) and the Pb phosphate mineral plumbogummite ($PbAl_3(PO_4)_2(OH)_5H_2O$), which formed from the oxidation and weathering of galena (Fig. 9). Samples 0.5 km to the northwest of the North Zone also have elevated contents of cassiterite, tourmaline, pyrite and anglesite that likely reflect the presence of a small mineralised zone in this area. Collectively, the indicator minerals identified in this study reflect the presence of Sn mineralisation as well as the polymetallic nature of the deposit. These minerals are most abundant in the 0.25-0.5 mm fraction of till. Coarse (0.5-2.0 mm) indicator minerals are present in till within <1 km down ice of each zone.

Scheelite mineral chemistry

Scheelite ($CaWO_4$) varies from a common to an accessory phase in a variety of hydrothermal ore-deposit settings, including Cu-Mo-W porphyry systems, skarns and vein Sn-W. Scheelite is an economically important source of W, but can also, by association, be an important indicator of ore minerals in other deposit types, such as Au systems (De Smeth, 1985; Robert and Brown, 1986). Because scheelite is a common indicator mineral in surficial sediments (Averill, 2001; Horsnail, 1979; Hosking 1982; Ottensen and Theobald, 1994), a detailed study of scheelite grains from 37 deposits was carried out as part of this TGI 4 study to determine if chemistry of scheelite grains in surficial sediments could be used to identify their ore-deposit setting. This research was carried out at Laurentian University, Sudbury as a M.Sc. thesis supported by the GSC's Research Affiliate Program (RAP). Preliminary results have been reported in numerous conference abstracts, posters, and talks (Poulin et al., 2013a, b, 2014a, b). A variety of analytical methods were used to fully characterize and develop a chemical database (e.g., trace elements, stable isotope ($\delta^{18}O$), cathodoluminescence). Results indicate that scheelite is a chemically complex mineral exhibiting large ranges in the investigated parameters, including: (1) zonation, varying from absent to normal, oscillatory and discordant; (2) minor-element composition, in particular highly variable As and Mo concentrations; (3) trace-element chemistry, specifically the REEs which vary in terms of ∑REEs, degree and type of fractionation pattern observed (flat, convex, concave), and type and magnitude of the Eu anomalies (positive or negative); and (4) isotope chemistry, specifically $\delta^{18}O$ ranging from -4.6 to +9.1‰.

Discussion

Till geochemistry

Most reports describing the use of till geochemistry for Sn and W exploration were published between the 1970s and early 1990s. The analytical methods used for Sn and W in these studies were highly specialized, required a separate and unique method just to determine W or Sn, and added to the cost of routine analytical methods used for other elements. Lithium meta/tetraborate fusion ICP-MS is now routinely used to determine the total concentration of Sn and W in sediments and is a fast and cost effective method.

The extensive suites of indicator/pathfinder trace elements in till and stream sediments at Sisson, and in till at Mount Pleasant, reflect the polymetallic nature of the deposits as well as the ability of modern ICP-MS techniques to determine a broad suite of elements at low detection limits. The indicator/pathfinder element suites are more extensive than previously reported in published till studies around other Sn-W mineralisation (e.g. Steiger, 1977; Matilla and Peuraniemi, 1980; Toverud, 1984; Peuraniemi et al., 1984; Johansson et al., 1986; Coker et al., 1988; Rogers et al., 1990).

Indicator mineral results

Most reports describing the use of indicator minerals for Sn and W exploration were published between the 1970s and early 1990s and were focused on the recovery of scheelite, wolframite, and cassiterite (e.g. Brundin and Bergström, 1977; Ottensen & Theobald, 1994). The heavy mineral recovery methods used in these older studies were highly specialized, specific to each study, not readily available in commercial laboratories, and applied only after a Sn or W-rich samples was geochemically identified.

The extensive list of indicator minerals in till and stream sediments at Sisson and in till at Mount Pleasant, reflect the polymetallic nature of the deposits as well as the ability of modern indicator mineral methods to recover and recognize a broad range of minerals. The indicator minerals identified in these new studies are more extensive than previously published till studies around Sn-W mineralisation (e.g. Szabo et al. 1975; Brundin & Bergstrom 1977; Matilla and Peuraniemi, 1980; Toverud, 1984; Snow and Coker, 1987; Friske et al., 2001).

Recovery of this broad list of indicator minerals is now consistent, routine and fast. The advantages of indicator mineral methods over traditional geochemical analysis of the heavy mineral or the <0.063 mm fraction are that the mineral grains: (1) are visible and can be examined; (2) provide physical evidence of the presence of mineralisation or alteration; (3) provide information about the source that traditional geochemical methods cannot, including nature of the ore, alteration, and proximity to source; (4) equivalent of ppb detection levels when there are just a few grains (Brundin and Bergstrom, 1977; Averill, 2001).

Table 4 – List of indicator mineral short course and workshop presentations given as part of the TGI-4 intrusion-hosted Sn-W research project.

Workshop/Short Course	Date	Topic
Laurentian University, Modular Course in Exploration Geochemistry	December, 2010	Indicator mineral and till geochemical methods for mineral exploration
Association of Applied Geochemists Short Course: Indicator Mineral Methods in Mineral Exploration	August 21, 2011	Modern techniques for the recovery of indicator minerals from surficial sediments
PDAC Student-Industry Mineral Exploration Workshop (S-IMEW)	May 11, 2012	Indicator mineral and till geochemical methods for mineral exploration
Laurentian University, Modular Course in Exploration Geochemistry	December 2012	Modern techniques for the recovery of indicator minerals from surficial sediments
Association for Mineral Exploration British Columbia Short Course:Exploring Through Cover - What Works, What Doesn't & Why	January 26, 2013	Modern techniques for the recovery of indicator minerals from surficial sediments
PDAC Workshop: New Frontiers for Exploration in Glaciated Terrain	March 1, 2013	Quality assuranace and quality control measures for indicator mineral mineral programs
PDAC Student-Industry Mineral Exploration Workshop (S-IMEW)	May 10, 2013	Modern techniques for the recovery of indicator minerals from surficial sediments
Geological Survey of Finland, Green Mining Project Workshop	September 11, 2013	Application of indicator mineral methods to mineral exploration in Canada
Association of Applied Geochemists Short Course: Application of Indicator Mineral Methods to Mineral Exploration	November 17, 2013	Modern analytical techniques for indicator mineral chemistry
Association of Applied Geochemists Short Course: Application of Indicator Mineral Methods to Mineral Exploration	November 17, 2013	Indicator mineral methods for intrusion-hosted W-Mo deposits, with examples from the Sisson deposit
Association for Mineral Exploration British Columbia Short Course: Surficial Geology and Exploration Geochemistry – Know What You Are Sampling & Why	January 24, 2014	Modern techniques for the recovery of indicator minerals from surficial sediments
PDAC Student-Industry Mineral Exploration Workshop (S-IMEW)	May 7, 2014	Modern techniques for the recovery of indicator minerals from surficial sediments
Canadian Institute of Mining and Metallurgy Short Course: Prospecting Under Cover	November 5, 2014	Modern techniques for the recovery of indicator minerals from surficial sediments
Laurentian University, Modular Course in Exploration Geochemistry	December, 2014	Modern techniques for the recovery of indicator minerals from surficial sediments

Comparison of indicator minerals and till geochemistry

In this study, not all till samples that contain cassiterite have corresponding high Sn values in the <0.063 mm fraction. Not all till or stream sediment samples that contain scheelite or wolframite, have high W values. Conversely, samples with elevated Sn or W contents always contain indicator minerals. These patterns suggest that indicator minerals can be more effective than till and/or stream sediment geochemistry for identifying the presence of Sn and W mineralisation.

At Mount Pleasant, Cu, Pb, Zn, Ag, As, and In values are high for many of the till samples, however ore-associated sulphide mineral (e.g. galena, sphalerite, chalcopyrite, arsenopyrite) abundance in the same till samples is low to zero. Pb-bearing secondary minerals beudantite, anglesite, and plumbogummite are present in these same till samples. These patterns indicate that sulphide minerals were either destroyed during pre- or post-glacial oxidation, or both. As a result, till geochemistry and the presence of secondary sulphate or phosphate minerals are useful for identifying the presence and polymetallic (Cu, Pb, Zn, Ag, As, and In) metal-rich debris glacially eroded from the deposit.

Technology transfer

Education and dissemination of information about the application of indicator mineral methods to mineral exploration have been a particular focus of this TGI 4 research activity, with special emphasis on intrusion-hosted Sn-W-Mo exploration. In addition to the publications listed in Table 1, overviews of indicator mineral methods and TGI 4 research results have been presented at numerous workshops and short courses listed in Table 4.

Conclusions and implications for exploration

- The till geochemical + mineralogical studies reported here are among the first detailed studies around major Sn-W deposits in glaciated terrain.
- A broad suite of indicator/pathfinder trace elements for both deposits was identified (Table 5) and these reflect the polymetallic nature of these Sn-W-Mo deposits and the broader suite of elements that is now available using modern ICP-MS techniques. In both case studies, the list of indicator/pathfinder elements is more extensive than previously identified in published soil and till geochemical studies of Sn-W deposits in glaciated terrain.
- The <0.063 mm fraction of till reflects glacial dispersal from both deposits, therefore, use of this till size fraction in regional exploration programs for intrusion-hosted Sn-W-Mo deposits is recommended.
- The Mount Pleasant deposit is a significant source of indium and till down ice of the deposit contains some of the highest indium values ever published for till, indicating that till geochemistry can be an important exploration tool for detecting In-bearing deposits.
- The study compared the efficiency of a modified aqua regia leach versus a lithium metaborate/tetraborate fusion followed by nitric acid digestion (total digestion) for determining metal contents in till. Results indicate that a total digestion is required to report the total concentration of Sn and W in till. The modified aqua regia leach is suitable for determining the other indicator and pathfinder elements.
- Our study identified an area of elevated metal content in till east and northeast of the Sisson deposit overlying Ordovician rocks that warrants further investigation. The bedrock source of the elevated metal contents may be related to a small polymetallic occurrence east of the Sisson deposit or other unknown metal-rich rocks in the area.
- Indicator minerals identified in the 0.25-0.5 mm fraction of mineralised bedrock, till, and stream sediments include a suite of Sn- and W- bearing minerals as well as sulphide, arsenide, telluride, and alteration minerals (Table 5). Additional but rare indicator minerals include beudantite, anglesite, and plumbogummite which formed by oxidation and weathering of the galena. The extensive suite of indicator minerals reflects the polymetallic nature of the deposits and the ability of modern indicator mineral methods to recover these minerals.
- Indicator minerals are also present in the coarse (0.5-2.0 mm) HMC fraction of till samples that are proximal to the deposits, and thus indicator mineral size can provide some insights into glacial transport distance and proximity to the bedrock source.
- Under short wave ultraviolet light, scheelite has a diagnostic bright bluish white fluorescence. A systematic method to rapidly and efficiently determine the scheelite content of heavy mineral concentrate using this fluorescence has been developed and is now commercially available from the laboratory Overburden Drilling

Table 5 – Summary of indicator+pathfinder trace elements in till, stream sediments and stream water, and indicator minerals in bedrock, till and stream sediments at the Sisson W-Mo and Mount Pleasant Sn-W-M-Bi-In deposits.

Deposit	Deposit elements	Media	Indicator/ Pathfinder elements	Indicator Minerals
Sisson	W-Mo	till	W, Mo, Cu, Zn, Pb, Ag, Bi, In, As, Cd, Zn, Te	scheelite, wolframite, molybdenite, chalcopyrite, joseite, native Bi, bismutite, bismuthinite, galena, sphalerite, arsenopyrite, pyrrhotite, pyrite
		bedrock	*not determined*	scheelite, wolframite, molybdenite, chalcopyrite, sphalerite, galena, pyrite, native bismuth
		stream sediment	W, Mo, Ag, As, Bi, Cd, In, Tl, Cu, Zn	scheelite, wolframite, molybdenite, chalcopyrite, sphalerite, arsenopyrite, pyrite
		stream water	W, Mo, As, Cd, Cu, Cs, Zn	
Mount Pleasant	Sn-W-Mo-Bi-In	till	Sn, W, Mo, Bi, In, Ag, As, Cd, Cu, Pb, Re, Te, Tl, Zn	cassiterite, wolframite, molybdenite, topaz, galena, arsenopyrite, loellingite, fluorite, beudantite, anglesite, plumbogummite
		bedrock	*not determined*	cassiterite, molybdenite, sphalerite, chalcopyrite, pyrite, galena, arsenopyrite, fluorite, topaz

Management Limited. This method will provide consistent and comparable scheelite counts for till and stream sediment samples within and between projects.

- Fluorite abundance is greatest in the 3.0-3.2 SG mid-density fraction of till as compared to the >3.2 SG heavy fraction. Thus, when exploring for deposits for which fluorite is an indicator mineral, the mid-density fraction of till should be examined.

Future research

Future studies on the mineral chemistry of scheelite and other physically and chemically robust minerals identified as part of this study (e.g. cassiterite) should be pursued. New indicator mineral recovery and chemical characterization methods are currently being developed to reduce sample size and analytical costs. Ongoing and future research will focus on smaller size fractions of till that currently are not examined (i.e., <0.063 mm) and the applications of new and more accessible analytical instruments to indicator mineral studies (i.e., hyperspectral, mineral liberation analysis (MLA) express) (Layton-Matthews et al., 2014). These developments will ultimately lead to the identification of new and/or improved indicator mineral methods of intrusion-hosted deposits and increased mineral exploration effectiveness.

Acknowledgements

The two case studies were conducted as part of the Geological Survey of Canada's TGI 4 Program and were collaborative research efforts between the Geological Survey of Canada and the New Brunswick Department of Energy and Mines. Kathleen Thorne, New Brunswick Department of Energy and Mines, is thanked for her discussions of the bedrock geology of both deposits and providing Figure 1. For the Sisson study, Rob Duncan, Kandi Gallagher, Will Gilmore, Jim Lang, Megan Little, Charlie Morrisey, Drew Takahashi, and Alexandra Shaw of HDI and Northcliff Resources Limited are thanked for sharing confidential geological information, providing access to the deposit, facilitating field work, and providing bedrock samples. Dave Sinclair (retired GSC Scientist) and John Chapman (GSC) are thanked for providing bedrock samples and geological information about the Mount Pleasant deposit. Adex Mining Inc., in particular Gustaaf Kooiman, are thanked for providing access to the Mount Pleasant mine property. Summer students Jessey Rice, Mike Richards, and Reid van Drecht are thanked for their able field assistance. Alain Plouffe (GSC) is thanked for his review of the manuscript.

References

Averill, S.A., 2001. The application of heavy indicator minerals in mineral exploration with emphasis on base metal indicators in glaciated metamorphic and plutonic terrains; *in* Drift Exploration in Glaciated Terrain, (ed.) M.B. McClenaghan, P.T. Bobrowsky, G.E.M. Hall and S. Cook. Geological Society of London, Special Volume 185, p. 69-81.

Brundin, N.H., and Bergström, J., 1977. Regional prospecting for ores based on heavy minerals in glacial till; Journal of Geochemical Exploration, v. 7, p. 1-19.

Bustard, A., Zhang, W., McFarlane, C.R.M., and Lentz, D., 2013. Tungsten mineralization processes at the Sisson Brook W-Mo-Cu deposit, central New Brunswick: the role of formation of titaniferous phases at reaction fronts; Acta Geologica Sinica (English Edition), 87 Supp., p. 672-675.

Coker, W.B., Robertson J., and Snow, R.J., 1988. Till geo-chemistry at the Great Gull scheelite prospects, Newfoundland, Canada: a case history in orientation and discovery; *in* Prospecting in Areas of Glaciated Terrain – 1988; Canadian Institute of Mining and Metallurgy, p. 587-598.

de Smeth, J.B., Rao, K.S.P., and Schuiling, R.D., 1985. Gold-scheelite mineralization in the Veligallu schist belt, Andhra Pradesh, India; Economic Geology, v. 80, p. 1996-2000.

Friske, P.W.B., Pronk, A.G., McCurdy, M.W., Day, S.J.A., McNeil, R.J., and Boldon, R., 2002. Regional stream sediment and water geochemical data, central New Brunswick; Geological Survey of Canada, Open File 4112.

Fyffe, L.R., Seaman, A., Thorne, K., and Martin, D.A., 2010. Part 1: Sisson Brook W–Mo–Cu deposit; *in* Polymetallic deposits of Sisson Brook and Mount Pleasant, New Brunswick, Canada, (comp.) L.R. Fyffe and K.G. Thorne. New Brunswick Department of Natural Resources, Field Guide No. 3, p. 7-33.

Fyffe, L.R., Thorne, K., Dunning, G.R., and Martin, D.A., 2008. U-Pb geochronology of the Sisson Brook granite porphyry, York County, west-central New Brunswick; *in* Geological Investigations in New Brunswick for 2007, (ed.) G.L. Martin. New Brunswick Department of Natural Resources; Minerals, Policy and Planning Division, Mineral Resource Report 2008-1, p. 35-54.

Horsnail, R.F., 1979. The geology of tungsten; *in* Proceedings of the First Tungsten Symposium, Stockholm, September 5-7, 1979. Mining Journal Books Limited, p. 18-31.

Hosking, K.F.G., 1982. A general review of the occurrence of tungsten in the world; *in* Symposium on Tungsten Geology, Jiangxi, China, (ed.) J.V. Hepsworth. ESCAP/RMRDC Bandung, Indonesia and Geological Publishing House, Be-jing, China, p. 59-86.

Invemo, C.M.C., and Hutchinson, R.W., 2004. Petrochemical discrimination of evolved granitic intrusions associated with Mount Pleasant deposits, New Brunswick, Canada; Institution of Mining and Metallurgy, Transactions, Section B-Applied Earth Sciences, v. 115, p. 23-39.

Johansson, K., Keinänen, V., and Lehmuspelto, P., 1986. Geochemical exploration for tungsten in glaciogenic deposits in Soretiapulju, western Finnish Lapland; *in* Prospecting in Areas of Glaciated Terrain. Institute of Mining and Metallurgy, p. 61-68.

Kooiman, G.J.A., McLeod, M.J., and Sinclair, W.D., 1986. Porphyry tungsten-molybdenum orebodies, polymetallic veins and replacement bodies, and tin-bearing greisen zones in the Fire Tower Zone, Mount Pleasant, New Brunswick; Economic Geology, v. 81, p. 1356-1373.

Lamothe, M., 1992. Pleistocene stratigraphy and till geochemistry of the Miramichi Zone, New Brunswick; Geological Survey of Canada, Bulletin 433, 58 p.

Layton-Matthews, D., Hamilton, C., and McClenaghan, B., 2014. Mineral chemistry: modern techniques and applications to exploration; *in* Application of indicator mineral methods to mineral exploration, (ed.) M.B. McClenaghan, A. Plouffe and D. Layton-Matthews. Geological Survey of Canada, Open File 7553, p. 9-18.

Marr, J.M., 2009. Sisson Brook tungsten molybdenum deposit, New Brunswick, preliminary economic assessment (2009 Technical and Economic Update), National Instrument 43-101 technical; Geodex Minerals Ltd., 106 p.

Matilla, E., and Peuraniemi, V., 1980. On geochemical pro-specting for tin in southern Finland; *in* Methods of the Geochemical Map-

ping and Boulder Prospecting in the Eastern Part of the Baltic Shield; Geological Survey of Finland, Espoo, Finland, p.133-158.

McClenaghan, M.B., 2011. Overview of common processing methods for recovery of indicator minerals from sediment and bedrock in mineral exploration; Geochemistry: Exploration, Environment, Analysis, v. 11, p. 265-278.

McClenaghan, M.B., Parkhill, M.A., Averill, S.A., and Kjarsgaard, I.M., 2013a. Indicator mineral signatures of the Sisson W-Mo deposit, New Brunswick: Part 1 bedrock samples; Geological Survey of Canada, Open File 7431.

McClenaghan, M.B., Parkhill, M.A., Averill, S.A., Pronk, A.G., Boldon, R., Chapman, J., and Rice, J.M., 2014a. Indicator mineral abundance data for bedrock and till from the Mount Pleasant Sn-W-Mo-Bi-In deposit, New Brunswick; Geological Survey of Canada, Open File 7573.

McClenaghan, M.B., Parkhill, M.A., Averill, S.A., Pronk, A.G., Seaman, A.A., Boldon, R., McCurdy, M.W., and Rice, J.M., 2013b. Indicator mineral abundance data for bedrock, till, and stream sediment samples from the Sisson W-Mo de-posit, New Brunswick; Geological Survey of Canada, Open File 7387, 18 p.

McClenaghan, M.B., Parkhill, M.A., Chapman, J.B., and Sinclair, W.D., 2015a. Indicator mineral content of bedrock from the Mount Pleasant Sn-W-Mo-Bi-In deposit, New Brunswick; Geological Survey of Canada, Open File 7721.

McClenaghan, M.B., Parkhill, M.A., Pronk, A.G., Boldon, G.R., Pyne, R.M., and Rice, J.M., 2015b. Till geochemical signatures of the Mount Pleasant Sn-W-Mo-Bi-In deposit, New Brunswick; Geological Survey of Canada, Open File 7722.

McClenaghan, M.B., Parkhill, M.A., Pronk, A.G., Boldon, G.R., Pyne, R.M., and Rice, J.M., in press. Indicator mineral signatures of the Mount Pleasant Sn-W-Mo-Bi-In deposit, New Brunswick; Geological Survey of Canada, Open File 7804.

McClenaghan, M.B., Parkhill, M.A., Pronk, A.G., McCurdy, M.W., Boldon, R., Leybourne, M.I., Pyne, M., and Rice, J.M., 2015c. Geochemical and indicator mineral data for stream sediments and waters around the Sisson W-Mo deposit, New Brunswick (NTS 21J/06, 21J/07); Geological Survey of Canada, Open File 7756.

McClenaghan, M.B., Parkhill, M.A., Seaman, A.A., and Pronk, A.G., 2014b. Till geochemical signatures associated with the Sisson W-Mo deposit, New Brunswick, Canada; Atlantic Geology, v. 50, p. 116-137.

McClenaghan, M.B., Parkhill, M.A., Seaman, A.A., Pronk, A.G., Pyne, M., Rice, J.M., and Hashmi, S., 2013c. Till geochemical signatures of the Sisson W-Mo deposit, New Brunswick; Geological Survey of Canada, Open File 7430, 53 p.

McClenaghan, M.B., Parkhill, M.A., Seaman, A.A., Pronk, A.G., Pyne, M., Rice, R.M., and Pyne, M., 2014c. Indicator mineral signatures of the Sisson W-Mo deposit, New Brunswick: Part 2 till; Geological Survey of Canada, Open File 7467.

McCutcheon, S.R., Reddick, J., McKeen, T., El-Rassi, D. and Kociumbas, M., 2013. Amended technical report of the Mount Pleasant property, including mineral resource estimates, southwestern New Brunswick for Adex Mining Inc.; 43-101 Technical Report, Watts, Griffs and McQuat, SEDAR Website, http://www.sedar.com/

McCutcheon, S.R., Sinclair, W.D., McLeod, M.J., Boyd, T., and Kooiman, G.J.A., 2010. Part 2: Mount Pleasant Sn-W-Mo-Bi-In deposit; *in* Polymetallic deposits of Sisson Brook and Mount Pleasant, New Brunswick, Canada, (compilers) L.R. Fyffe and K.G. Thorne. New Brunswick Department of Natural Resources, Field Guide No. 3, p. 37-68.

McLeod, M.J., Fyffe, L.R., and McCutcheon, S.R., 2005. Bed-rock geology of the McDougall Lake area (NTS 21 G/07), Charlotte County, New Brunswick; New Brunswick Department of Natural Resources, Map Plate MP 2005-30.

Nast, H.J., and Williams-Jones, A.E., 1991. The role of water-rock interaction and fluid evolution in the forming of the porphyry-related Sisson Brook W-Cu-Mo deposit, New Brunswick; Economic Geology, v. 86, p. 302-317.

Ottensen, R.T., and Theobald, P.K., 1994. Chapter 5 - Stream sediments in mineral exploration; *in* Drainage Geochemistry, Handbook of Exploration Geochemistry Volume 6, (ed.) M. Hale and J.A. Plant; Elsevier, Amsterdam, p. 147-185.

Parrish, I.S., 1977. Mineral catalog for the Mount Pleasant deposit of Brunswick Tin Mines; Canadian Mineralogist, v. 15, p. 121-126.

Petruk, W., 1972. The W-Bi-Mo deposit of the Brunswick Tin Mines Limited: its mode of occurrence, mineralogy, and amenability to mineral beneficiation; Department of Energy, Mines and Resources, Mineral Sciences Division, Report MS PP 72-3.

Peuraniemi, V., Mattila, E., Nuutilainen, J., and Autio, H., 1984. Till and bedrock geochemistry in Sn exploration: a case study; Journal of Geochemical Exploration, v. 21, p. 249-259.

Plouffe, A., and Ferbey, T., 2015. Till composition near Cu-porphyry deposits in British Columbia: Highlights for mineral exploration; *in* TGI 4 – Intrusion Related Mineralisation Project: New Vectors to Buried Porphyry-Style Mineralisation, (ed.) N. Rogers; Geological Survey of Canada, Open File 7843, p. 15-37.

Poulin, R.S., McDonald, A.M., Kontak, D.J., and McClenaghan, M.B., 2013a. A crystal-chemical investigation of the suitability of scheelite as a discriminator for different ore-forming settings: Initial results from cathodoluminescence studies; *in* Program with Abstracts, Geological Association of Canada-Mineralogical Association of Canada, Annual Meeting 2013, p. 165.

Poulin, R.S., McDonald, A.M., Kontak, D.J., and McClenaghan, M.B., 2013b. A crystal-chemical study of scheelite from the Sisson W-Mo deposits: Application to exploration; *in* Conference, Program and Abstract Volume, Exploration, Mining and Petroleum New Brunswick, 2013 Conference, p. 63.

Poulin, R.S., McDonald, A.M., Kontak, D.J., and McClenaghan, M.B., 2014a. Scheelite geochemical signatures and potential for fingerprinting ore deposits; *in* Program with Abstracts, Geological Association of Canada – Mineralogical Association of Canada, Annual Meeting 2014, p. 227.

Poulin, R.S., McDonald, A.M., Kontak, D.J., and McClenaghan, M.B., 2014b. Cathodoluminescence of scheelite: Quantifying colour and chemical variations; *in* Program with Abstracts, Geological Association of Canada – Mineralogical Association of Canada, Annual Meeting 2014, p. 226.

Rennie, D.W., Firedman, D., Gray, J., Bolu, M., Pozder, S., and Greskovich, G., 2013. Canadian National Instrument 43-101 technical report on the Sisson Project, New Brunswick, Canada, Samuel Engineering Inc., SEDAR website: DisplayCompanyDocuments.do?lang=EN andissuerNo=00030606

Riddell, J.E., 1967. Geochemical dispersion patterns in soils at Mount Pleasant Mines, Charlotte County, New Brunswick; *in* Proceedings, Symposium on Geochemical Prospecting, (ed.) E.M. Cameron. Geological Survey of Canada, Paper 66-54, p. 233.

Robert, F., and Brown, A.C., 1986. Archean gold-bearing quartz veins at the Sigma mine, Abitibi greenstone belt, Quebec: Part II. Vein paragenesis and hydrothermal alteration; Economic Geology, v. 81, p. 593–616.

Rogers, P.J., Chatterjee, A.K., and Aucott, J.W., 1990. Metallogenic domains and their reflection in regional lake sediment surveys from the Meguma Zone, southern Nova Scotia, Canada; Journal of Geochemical Exploration, v. 39, p. 153-174.

Rose, A.W., Hawkes, H.E., and Webb, J.S., 1979. Geochemistry in Mineral Exploration, Academic Press, London, 657 p.

Seaman, A.A., 2001. Preliminary report - till geochemistry of part of the west half of the Coldstream (NTS 21 J/06) map area, Carleton and York counties, New Brunswick; New Brunswick Department of Natural Resources, Open File 2001-2, 51 p.

Seaman, A.A., 2002. Till geochemistry of the central and eastern parts of the Coldstream (NTS 21 J/06) map area, York and Carleton counties, New Brunswick; New Brunswick Department of Natural Resources, Open File 2002-5, 80 p.

Seaman, A.A., 2003. Follow up till geochemistry, Coldstream (NTS21J/06) map area and part of the adjacent Napadogan (NTS 21 J/07) map area, York and Carleton counties, New Brunswick; New Brunswick Department of Natural Resources, Open File 2003-11.

Seaman, A.A., 2007. Reconnaissance till geochemistry of NTS 21 J/01, J/02, J/07, and J/08 map areas (parts of York, Sunbury, Northumberland, and Queens counties), central New Brunswick: site and geochemical data; New Brunswick Department of Natural Resources, Open File 2007-8, 95 p.

Seaman, A.A, 2009. The Appalachian Glacier Complex, and the Middle to Late Pleistocene history of west-central New Brunswick, Canada; *in* Geological Investigations in New Brunswick for 2008, (ed.) G.L. Martin; New Brunswick Department of Natural Resources, Mineral Resource Report 2009 2, pp. 66 140.

Seaman, A.A., 2012. Till geochemistry of the Burtts Corner, Napadogan, and Hayesville map areas (NTS 21 J/02, 21 J/07 and 21 J/10) west-central New Brunswick; New Brunswick Department of Natural Resources, Open File 2012-3, 42 p.

Seaman, A.A. and McCoy, S.M. 2008. Multiple Wisconsinan tills in the Sisson Brook exploration trench of Geodex Minerals Ltd., York County, west-central New Brunswick; *in* Geological Investigations in New Brunswick for 2007, (ed.) G.L. Martin; New Brunswick Department of Natural Resources, Minerals, Policy and Planning Division, Mineral Resource Report 2008-1, p. 1-34.

Sinclair, W.D., Kooiman, G.J.A., Martin, D.A., and Kjarsgaard, I.M., 2006. Geology, geochemistry and mineralogy of indium resources at Mount Pleasant, New Brunswick, Canada; Ore Geology Reviews, v. 28, p. 123-145.

Smith, E.A., and Fyffe, L.R., (comp.) 2006a. Bedrock geology of the Burtts Corner area (NTS 21 J/02), York County, New Brunswick; New Brunswick Department of Natural Re-sources, Map Plate 2006-3.

Smith, E.A., and Fyffe, L.R. (comp.), 2006b. Bedrock geology of the Millville area (NTS 21 J/03), York and Carleton counties, New Brunswick; New Brunswick Department of Natural Resources, Map Plate 2006-4.

Smith, E.A., and Fyffe, L.R. (comp.), 2006c. Bedrock geology of the Coldstream area (NTS 21 J/06), York and Carleton counties, New Brunswick. New Brunswick Department of Natural Resources, Map Plate 2006-7.

Smith, E.A., and Fyffe, L.R. (comp.), 2006d. Bedrock geology of the Napadogan area (NTS 21 J/07), York and Carleton counties, New Brunswick; New Brunswick Department of Natural Resources, Map Plate 2006-8.

Snow, R.J., and Coker, W.B., 1987. Overburden geochemistry related to W-Cu-Mo mineralization at Sisson Brook, New Brunswick, Canada: an example of short- and long-distance glacial dispersal; *in* Geochemical Exploration 1985, (ed.) R.G. Garrett; Journal of Geochemical Exploration, v. 28, p. 353-368.

Stea, R.R., Seaman, A.A., Pronk, T., Parkhill, M.A., Allard, S., and Utting, D., 2011. Chapter 48: The Appalachian Glacier Complex in Maritime Canada; *in* Quaternary Glaciations - Extent and Chronology - A Closer Look; *in* Developments in Quaternary Science, 15, (ed.) J. Ehlers, P.L. Gibbard, and P.D. Hughes. Elsevier, Amsterdam, p. 631 659.

Steiger, R. 1977. Prospecting for lithium and tungsten in Ireland; *in* Prospecting in Areas of Glaciated Terrain 1977. Institution of Mining and Metallurgy, London, p. 14-24.

Szabo, N.L., Govett, G.J.S., and Lajtai, E.Z., 1975. Dispersion trends of elements and indicator pebbles in glacial till around Mt. Pleasant, New Brunswick, Canada; Canadian Journal of Earth Sciences, v. 12, p. 1534-1556.

Thorne, K.G., Fyffe, L.R., Seaman, A.A., Parkhill, M.A., Pronk, A.G., McClenaghan, M.B, Rogers, N., Rice, J.M., Beal, K-L., Lentz, D.R., and McClenaghan, S.H., 2014. Field guide to granite-related mineralization at the Sisson W-Mo deposit and the Zealand Station Be-Mo-W prospect, New Brunswick; Geoscience Report GR 2014-3, New Brunswick Department of Minerals and Petroleum.

Toverud, Ö., 1984. Dispersal of tungsten in glacial drift and humus in Bergslagen, south central Sweden; Journal of Geochemical Exploration, v. 21, p. 261-272.

Tectonostratigraphic controls on the Connaigre Peninsula of south-central Newfoundland and their implications for intrusion-related mineral resources

Neil Rogers[1], Dawn A. Kellett[1], Vicki J. McNicoll[1], Cees van Staal[2], Giorgio Ruberti[3] and Andrew Kerr[4]

1. Geological Survey of Canada, 601 Booth St., Ottawa, Ontario
2. Geological Survey of Canada, 625 Robson St., Vancouver, British Columbia
3. Department of Earth Sciences, Memorial University of Newfoundland, St. John's, Newfoundland and Labrador
4. Geological Survey of Newfoundland and Labrador, PO Box 8700, St. John's, Newfoundland and Labrador

Abstract: The Connaigre Peninsula of south-central Newfoundland has long been considered to be amongst the most complete and best exposed sections of Neoacadian and older Avalonian rocks in the Appalachians. The rocks of this region range from the Cryogenian volcano-sedimentary rocks of the Tickle Point Formation (ca. 682 Ma rhyolite) to the Middle to Upper Devonian clastic sedimentary rocks of the Great Bay De L'Eau and Poole's Cove formations and Late Devonian Belleoram Granite and Old Woman Stock (ca. 380 Ma). However the recent age determination of the Pass Island Granite that shows it as Silurian (423 ± 4 Ma), contradicts earlier interpretations that the whole of the Connaigre Peninsula formed on the Avalonian microcontinent. It is now evident that the eastern portion exhibits a distinct Neoproterozoic to Lower Palaeozoic tectonostratigraphy.

Five distinct phases of granitoid emplacement are recorded across the Connaigre Peninsula. The oldest of these is the Furby's Cove Intrusive Suite (ca. 673 Ma) that intruded the Tickle Point Formation prior to deposition of the Connaigre Bay Group. The later unit is in turn cut by the ca. 620 Ma Simmons Brook Intrusive Suite. All of these units are cut by a series of ca. 570 Ma intrusive bodies belonging to the Grole and Hardy's Cove intrusive suites and Harbour Breton Granite. At the southern end of Hermitage Bay, Grole Intrusive Suite rocks are intruded by the Silurian Pass Island Granite. All of these units are restricted to a region between the Hermitage Bay Fault to the west and the White Horse – East Bay fault to the east. The youngest intrusive rocks in the region are the Late Devonian Belleoram and Old Woman granitic bodies, as well as a series of mafic sills and/or flows on the Boxey Point Promontory, and several minor granitic dykes and small bodies that are considered offshoots of the Belleoram Granite. These Late Devonian intrusions are only known to cut the Ediacaran Long Harbour Group, Latest Ediacaran to Upper Cambrian Young's Cove Group and Devonian Cinq Isles, Poole's Cove and Great Bay De L'Eau formations, which are restricted to (or in the case of the Cinq Isles and Poole's Cove formations partly overlap) the areas to the east of the White Horse – East Bay fault. Given the different pre-Devonian tectonostratigraphies on either side of the White Horse – East Bay fault, the Connaigre Peninsula is herein informally divided into the Deadman's Bight (western) and Wreck Cove (eastern) domains.

Intrusion related mineralisation on the Connaigre Peninsula is largely restricted to Mo +/- Cu and fluorite occurrences associated with the Old Woman Stock. Similar Mo deposits occur within the coeval Ackley Pluton to the north-east and the associated minor intrusion on Belle Island. However to date no Mo mineralisation has been identified within the age equivalent Belleoram Granite, although minor fluorite occurrences are observed.

Introduction

The Connaigre Peninsula is situated on the south-central coast of Newfoundland between Fortune and Hermitage bays. These rocks have previously been assigned as Avalonian (e.g., O'Brien et al., 1995; O'Brien, 1998), with the Hermitage Bay, which defines the north-western margin of the peninsula, considered as marking the Avalonia – Ganderia boundary zone in southern Newfoundland (Figs. 1 and 2). The terms "Ganderia" and "Avalonia" are generally (but not completely) synonymous with the Gander and Avalon zones, respectively, in the original terminology of Williams (1979) for the principle tectonostratigraphic divisions of the Appalachians in Newfoundland. As originally defined the Avalon Zone is situated to the east of the Appalachian "mobile belts" and represented the largest section of Proterozoic peri-Gondwanan rocks (Williams, 1979; O'Brien et al., 1990).

The Palaeozoic provenance and tectonic relationships between Avalonia and Ganderia remain a fundamental problem in understanding the geological development of the Appalachians. Recent studies were conducted in this area as part of TGI 4 by the Geological Survey of Canada, in conjunction with the Geological Survey of Newfoundland and Labrador (GSNL), as the bounding region between these blocks contains a number of intrusive bodies that have greisen style

Corresponding author: Neil Rogers (nrogers@nrcan.gc.ca)

Rogers, N., Kellett, D.A., McNicoll, V.J., van Staal, C.R., Ruberti, G., and Kerr, A., 2015. Tectonostratigraphic controls on the Connaigre Peninsula of south-central Newfoundland and their implications for intrusion-related mineral resources; *in* TGI 4 – Intrusion Related Mineralisation Project: New Vectors to Buried Porphyry-Style Mineralisation, (ed.) N. Rogers; Geological Survey of Canada, Open File 7843, p. 59-78.

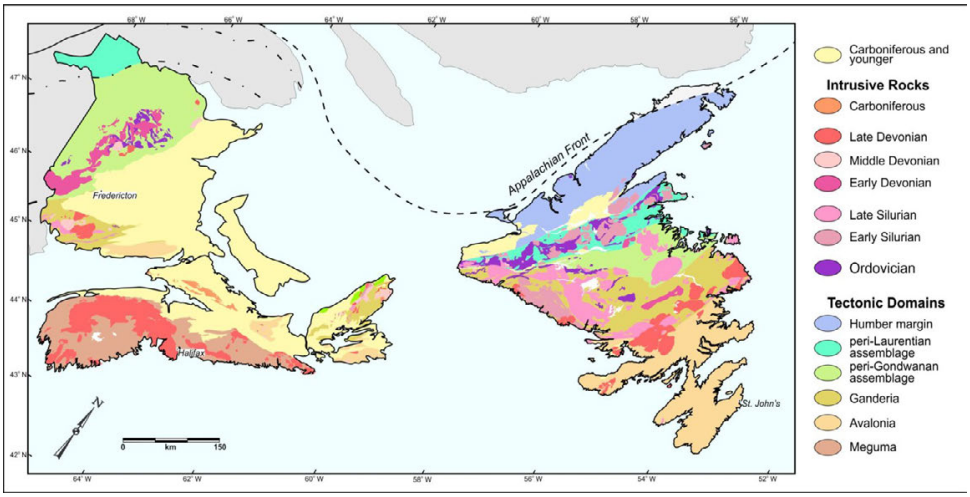

Figure 1 – Distribution of Palaeozoic granitoids and interpreted tectonic subdivisions of the Appalachian Orogen in Newfoundland, New Brunswick and Nova Scotia (modified after Hibbard et al. (2006), van Staal et al. (2009), Rogers et al. (2014) and references therein).

mineralisation. These studies will better document and help determine the tectonic evolution of Ganderia and Avalonia during the Silurian and Devonian, and place a tectonic context on the formation of Late Silurian and Devonian magmatic rocks, and their accompanying mineralisation, and thus help define an advanced framework for targeted exploration for intrusion related Sn-W-Mo deposits.

Geological framework

The Newfoundland Appalachians form part of the Appalachian-Caledonian Orogen that extends along the eastern margin of North America through the British Isles and Scandinavia into central Europe. It resulted from the Palaeozoic accretion of multiple terranes (arcs, microcontinents, oceanic material) to the eastern Laurentian margin during progressive closures of the Iapetus, Tornquist and Rheic ocean basins (van Staal et al. 1998; 2009). Tectonic amalgamation in Newfoundland was completed with the arrival of Avalonia by ca. 420 Ma, but the spatial relationship of the Avalon Zone to the remainder of the orogen at that time remains uncertain; deformation and reorganization continued into the Devonian and later with the Acadian and Neoacadian orogenies (van Staal et al. 2009).

Several Paleozoic intrusive suites were emplaced both into the Laurentian margin and into the outboard accreted terranes or zones during and after terrane accretion (Figs. 1 and 2). Appalachian-cycle magmatism in Newfoundland was voluminous, and in broad terms appears to young towards the southeast (Fig. 3). Ordovician intrusive rocks are predominantly exposed in the peri-Laurentian and, to a limited extent, peri-Gondwanan accretionary tracts (Notre Dame and Exploits subzones of Williams et al., 1988). Silurian to Early Devonian intrusive rocks are abundant to the west of the Dover and Hermitage faults. Late Early to Late Devonian intrusive rocks are primarily localised along eastern Ganderia and western Avalonia (e.g., Williams et al. 1989; Kerr 1997; Figs. 2 and 3).

This study focuses on the timing and distribution of plutonic suites exposed on the Connaigre Peninsula to the immediate south-east of the Hermitage Bay Fault (Fig. 3). Granitoid rocks are abundant on both sides of the Hermitage Bay Fault (Fig. 3). To the northwest, these are largely Palaeozoic in age (Silurian (e.g., Galtois Granite – 421 ± 2 Ma; Dunning et al., 1990) to Devonian (e.g., Indian Point Granite – ca. 403 Ma; G.R. Dunning unpublished age reported by O'Brien,

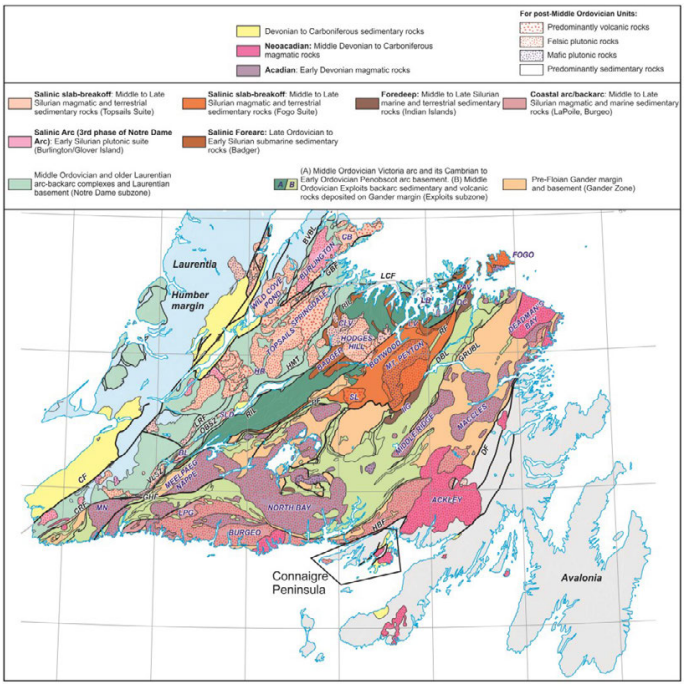

Figure 2 – Thematic map of the geology of Newfoundland (modified after Hibbard et al., 2006), showing the Connaigre Peninsula. BL – Boogie Lake pluton; BVBL – Baie Verte-Brompton Line; CB – Cape Brule porphyry; CF – Cabot Fault; CLV – Charles Lake volcanics; CRF – Cape Ray Fault; DBL Dog Bay Line; DC – Duder Complex; DF – Dover Fault; GHF – Gunflap Hills Fault; GRB – Green Bay Fault; GRUBL – Gander River Ultrabasic Belt Line; HBF – Hermitage Bay Fault; HMT – Hungry Mountain Thrust; HR – Harry's River; IIG – Indian Islands Group; LB – Loon Bay pluton; LCF – Lobster Cove Fault; LPG – La Poile Group; LRF – Lloyds River Fault; LV – Launceton volcanic; MN – Meelpaeg Nappe; OBSZ – Otter Brook shear zone; PAV – Port Albert volcanic; PF – Pine Falls Formation; RF – Reach Fault; SL – Stony Lake volcanics; RIL – Red Indian Line; SLD – Star Lake Dam; VLSZ – Victoria Lake Shear Zone. NOTE: not all of the above features are referenced in the text of this field guide.

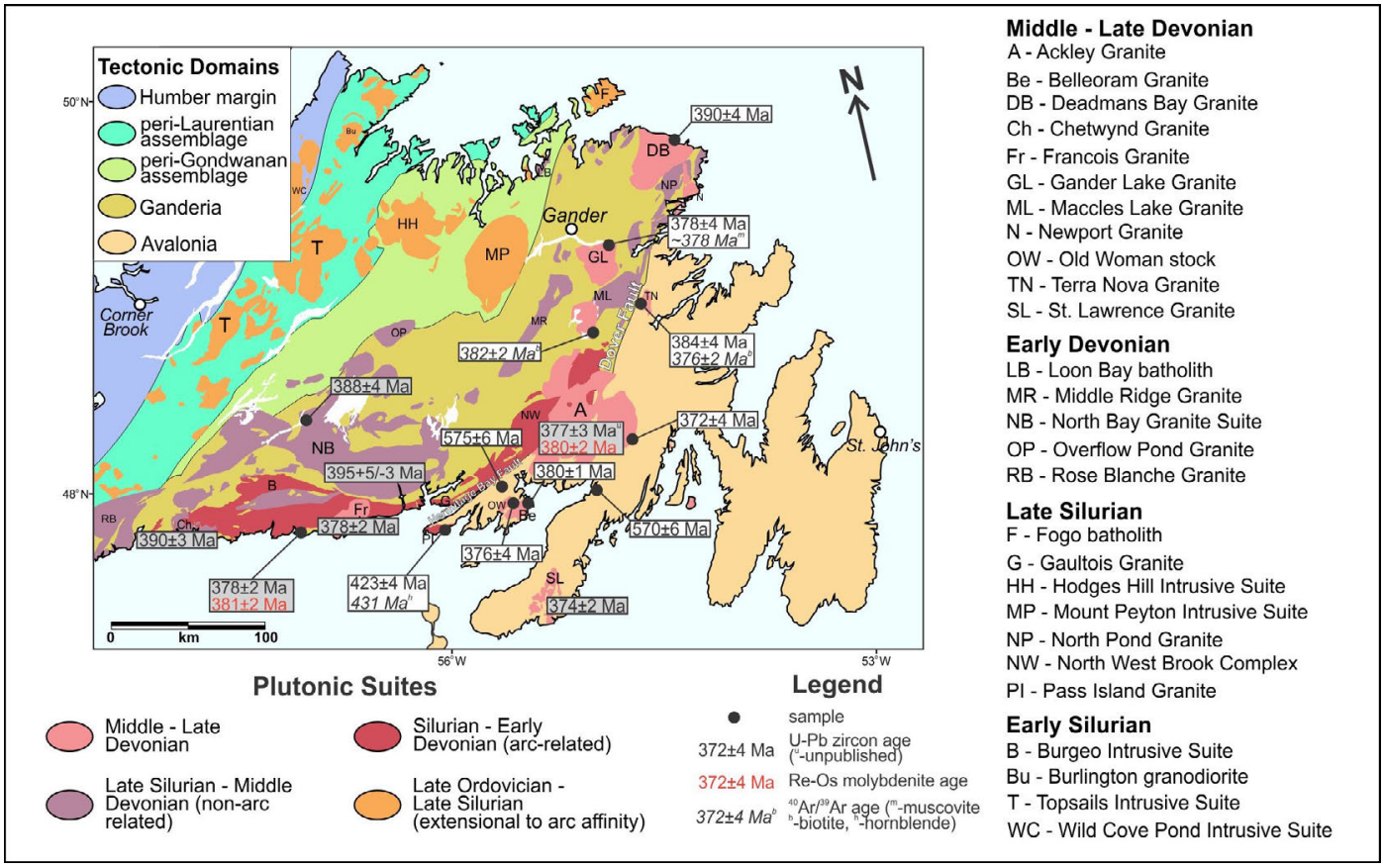

Figure 3 – Outline geological map of Newfoundland showing tectonic zones after Williams (1979) and Siluro–Devonian plutonic suites. Sample locations and ages are shown. Ages in white boxes are new data; grey boxes are previously published data (see text for references). Map is modified from Rogers et al. (2014) and references therein, after Hibbard et al. (2006) and van Staal et al. (2009).

1998)), but to the east of the fault there are several generations ranging in age from Neoproterozoic (ca. 620 Ma) to Late Devonian (ca. 375 Ma). Some of the granitoid rocks in the region remain undated and field characteristics/geochemistry have proven to be insufficient to distinguish them from one another. This is illustrated by Harbour Breton Granite as originally defined by Widmer (1950) and mapped by Green and O'Driscoll (1976), prior to radiometric dating, including ca. 620 Ma Simmons Brook and ca. 476 Ma Old Woman granites in addition to the ca. 570 Ma granite at Harbour Breton.

The Ganderian rocks (Gander Zone of Williams, 1979) to the west of the Dover and Hermitage faults consists of Cambrian to Ordovician clastic metasedimentary rocks that are poly-deformed and variably metamorphosed to greenschist facies and locally higher metamorphic grade, and intruded by the two voluminous granitic suites of Silurian and Devonian age. Well-developed deformation fabrics locally preserved in granitic rocks, particularly at the northeastern extent of onshore Ganderia, indicate that much of this deformation and metamorphism occurred during the Silurian, as a result of the Salinic orogeny (e.g., Dunning et al. 1990; Holdsworth, 1994; Schofield and D'Lemos 2000; van Staal 1994; van Staal et al. 2008; 2009).

In contrast, Avalonia (Avalon Zone of Williams, 1979) contains sub-greenschist facies Neoproterozoic volcanic, plutonic and sedimentary rocks overlain by Cambrian-Ordovician platform cover sequences. Avalonia was generally affected by open folding during the latest Silurian to Devonian Acadian orogeny (Williams, 1993), but deformation is locally complex near the Ganderia – Avalonia boundary. Here tight folds and associated thrusts formed under greenschist-facies conditions are locally preserved (Williams et al., 1995).

In Newfoundland, the boundary between the Ganderia and Avalonia has been correlated to the major shear zones of the Dover and Hermitage Bay faults (Fig. 2; Blackwood and Kennedy, 1975; Blackwood and O'Driscoll, 1976). The Dover Fault is a shear zone up to 25 km wide that has two documented phases of movement (Silurian ductile, sinistral transpressive and Devonian or younger brittle-ductile, dextral; Dallmeyer et al., 1981; Hanmer, 1981; Holdsworth, 1994; D'Lemos et al., 1997). Seismic reflection studies indicate this to be a crustal-scale structure that offsets the Moho (Keen et al., 1986; Marillier et al., 1989; Stockmal et al., 1990). Southwest of the Ackley Granite, the Hermitage Bay Fault forms a prominent brittle fault zone that has been interpreted as the continuation of the Ganderia - Avalonia boundary (e.g., Blackwood and O'Driscoll, 1976), but has a more subtle expression in seismic reflection data (Quinlan et al. 1992).

U-Pb geochronology

Four samples from the Connaigre Peninsula were collected for U-Pb geochronology as part of a larger study of Silurian to Devonian magmatism in central and southern Newfoundland (Kellett et al., 2014). These supplement previous U-Pb zircon ages presented in O'Brien et al. (1995), O'Brien (1998) and references therein (Fig. 4)

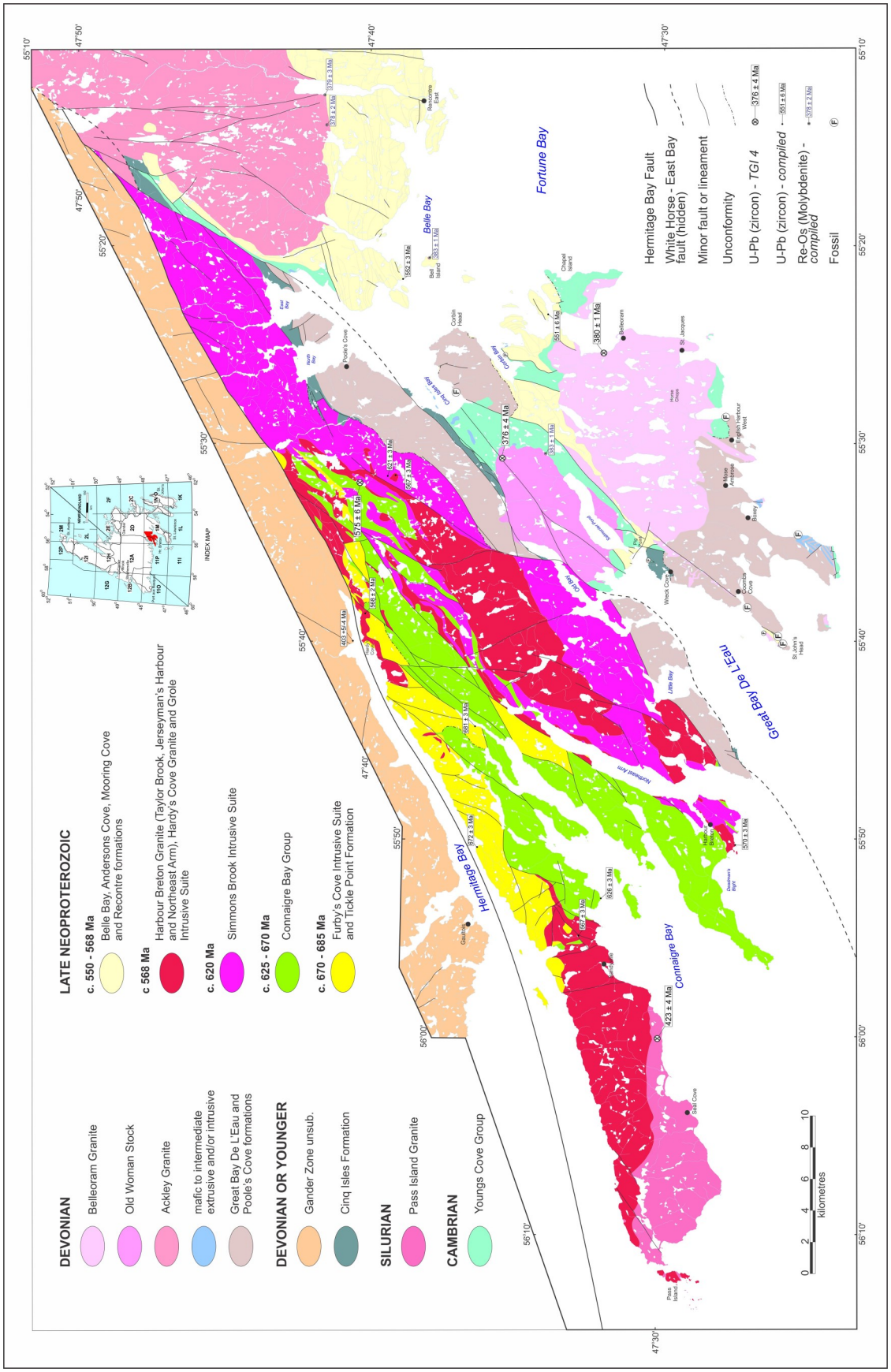

Figure 4 – Simplified geological map of the Connaigre Peninsula modified after O'Brien et al. (1995), O'Brien (1998), Lynch et al. (2009), Kellett et al. (2014) and Rogers et al. (2014).

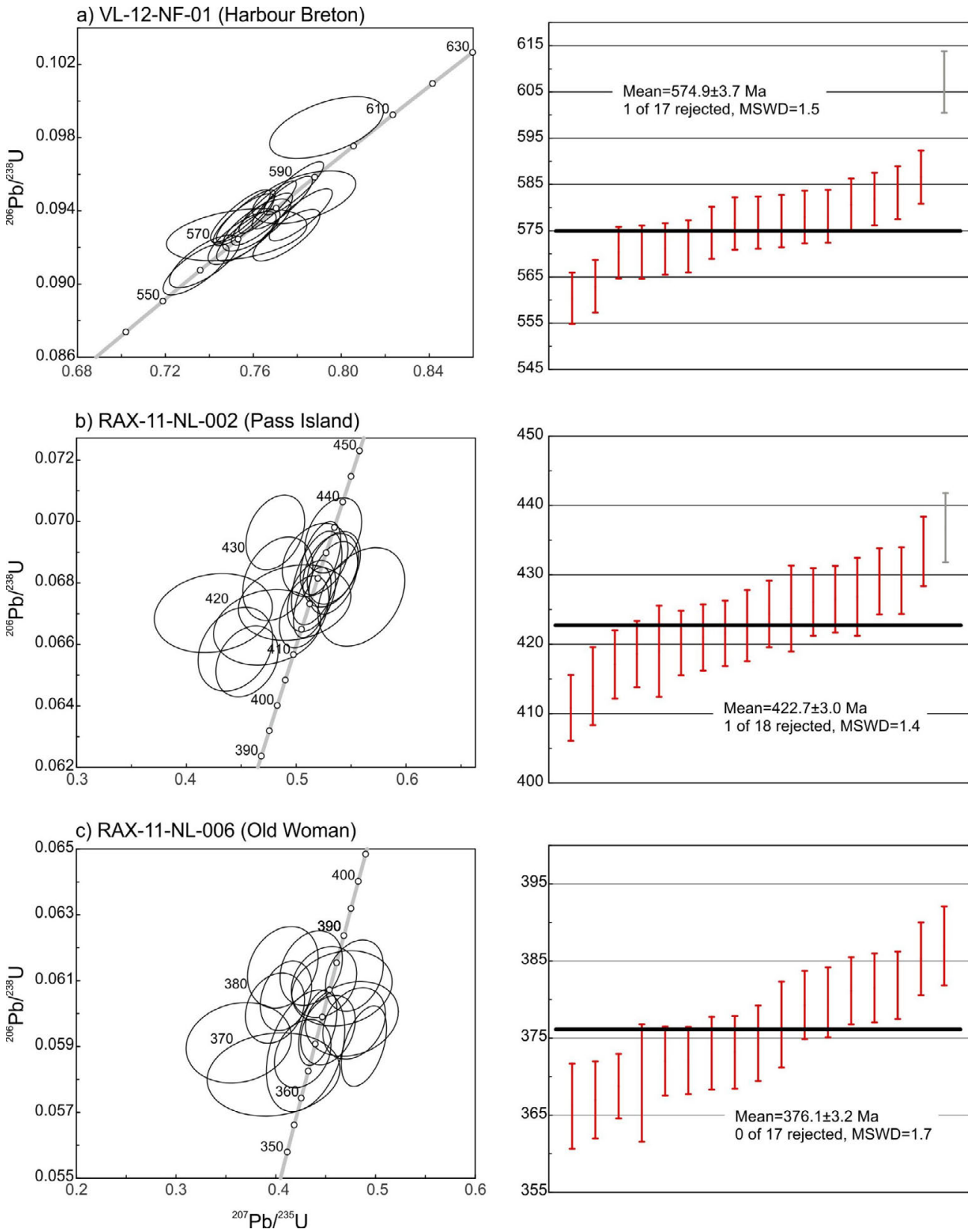

Figure 5 – Zircon U–Pb dating results for (a) VL-12-NF-01 (Taylor Brook Stock, Harbour Breton Granite); (b) RAX-11-NL-002 (Pass Island Granite); and (c) RAX-11-NL-006 (Old Woman stock). The left column displays concordia plots, and the right column displays weighted mean age plots and results. Error ellipses in the concordia plots are at the 2σ level, error bars are at the 1σ level.

and Re-Os decay molybdenite ages of Lynch et al. (2009; 2012) obtained on the Leonard's Find Mo Showing in the Old Woman Stock and at the Belle Island Mo showing off the east coast of the peninsula (Fig. 4).

Age determinations for samples RAX-11-NL-002, RAX-11-NL-006 and VL-12-NF-01 are also presented in Kellett et al. (2014).

Analytical techniques

Sensitive High-Resolution Ion MicroProbe (SHRIMP II)

Samples RAX-11-NL-002, RAX-11-NL-006 and VL-12-NF-01 were comminuted and density separated using methylene iodide heavy liquid. A Frantz™ magnetic separator was used to isolate a non-magnetic, zircon-rich separate. Zircons were hand-picked from this fraction and cast in 2.5 cm diameter epoxy mounts along with fragments of the GSC laboratory standard zircon (z6266, with $^{206}Pb/^{238}U$ age = 559 Ma). The mid-sections of the zircons were exposed using 9, 6 and 1 µm diamond compound, and mount surfaces were evaporatively coated with 10 nm of high purity Au. The internal features of the zircons (zoning, alteration, inclusions, etc.) were characterized using back-scattered electrons (BSE), as well as cathodoluminescence (CL) for zircon separates that exhibited zoning in CL, using a Zeiss Evo® 50 scanning electron microscope (Kellett et al., 2014).

Spot selections, guided by BSE and CL-SEM images, were made to avoid fractures and inclusions, as well as to sample both core and rim regions of grains. SHRIMP analytical procedures followed those described by Stern (1997) for the SHRIMP installed at the Geological Survey of Canada in Ottawa, with standards and U-Pb calibration methods following Stern and Amelin (2003). Between 17 and 27 spots were sampled on 16 to 23 grains for each sample (Table 1; Fig. 5). Long-term external reproducibility of secondary standards on the SHRIMP is 1 % at the 2σ level, thus ages are reported with a 2σ external error of 1 %.

Thermal ionization mass spectrometry

Heavy minerals were concentrated from geochronology sample RAX-11-NL-005 using standard crushing, grinding, and separation on a Wilfley table and by heavy liquid techniques. Mineral separates were sorted by magnetic susceptibility using a Frantz™ isodynamic separator and hand-picked using a binocular microscope. Analyses were performed using single zircon grains that were chemically abraded following the techniques of Mattinson (2005), including annealing for 48 hours at 1000°C prior to leaching with HF at 180°C for 16 hours. Details of zircon morphology and quality are summarized in Table 2. U-Pb isotope dilution thermal ionization mass spectrometry (ID-TIMS) techniques utilized in this study are modified after Parrish et al. (1987) with treatment of analytical errors after Roddick (1987). Procedural blank levels were generally on the order of 0.5-1.0 pg for Pb. U-Pb ID-TIMS analytical result age uncertainties are presented at the 2σ level (Table 2).

Harbour Breton Granite (Taylor Brook Stock) – 47°40'36.21" N, 55°31'55.92" W

Sample VL-12-NF-01 was collected from an intrusive body exposed north of Hwy-362, approximately 7.8 km east of Poole's Cove. The exposure was mapped by O'Brien (1998) as part of the Neoproterozoic Taylor Brook Stock of the Harbour Breton Granite (Figs. 4 and 6). At the sample locality, it is a fine-grained, deformed and foliated, pink-red, altered plagioclase-porphyritic monzogranite containing quartz phenocrysts and hornblende. The granite is pervasively cut by epidote-bearing veins. Locally the granite intrudes hornblende-bearing diorite, likely belonging to the Late Neoproterozoic Simmons Brook Intrusive Suite (O'Brien, 1998).

Figure 6 – Salmon pink to orange, feldspar porphyritic granite of the Neoproterozoic Taylor Brook Stock of the Harbour Breton Granite.

The Late Neoproterozoic age of the Harbour Breton Granite (O'Brien et al., 1995 and references therein) was confirmed by sample VL-12-NF-001 yielding an age of 575 ± 6 Ma (Fig. 5a; Table 1). Potential inheritance in this sample is indicated by a single ca. 604 Ma grain (Fig. 5a; Kellett et al., 2014).

Pass Island Granite – 47°30'6.22" N, 55°59'46.03" W

Sample RAX-11-NL-002 was collected from the Pass Island Granite, which occupies the southwestern tip of the Connaigre Peninsula between Connaigre and Hermitage bays. At the sampling site, a disused dimension-stone quarry, medium- to coarse-grained monzogranite containing hornblende and biotite outcrops (Figs. 4 and 7). Kerr et al. (1993b) commented on the lithological and geochemical similarity between the Pass Island Granite and the Francois Granite on the south coast of Newfoundland (Fig. 3); on this basis the Pass Island Granite was consigned as Devonian. The granite is also petrographically and compositionally similar to several other intrusions from

Figure 7 - Homogeneous orange to pink, coarse-grained, equigranular biotite-hornblende granite exposed in a disused dimension-stone quarry of the Late Silurian Pass Island Granite.

Table 1 – SHRIMP U-PB zircon results for samples RAX-11-NL-002, RAX-11-NL-006 and VL-12-NF-01.

Spot name	U (ppm)	Th (ppm)	Th/U	$^{206}Pb^*$ (ppm)	$^{204}Pb/^{206}Pb$	% ±	f(206)^{204} %	$^{208*}Pb/^{206*}Pb$	% ±	$^{207*}Pb/^{235}U$	% ±	$^{206*}Pb/^{238}U$	% ±	Corr Coeff	$^{207*}Pb/^{206*}Pb$	% ±	Apparent Ages (Ma) $^{206}Pb/^{238}U$	±$^{206}Pb/^{238}U$	$^{207}Pb/^{206}Pb$	±$^{207}Pb/^{206}Pb$	Disc. (%)
VL-12-NF-01, Harbour Breton pluton																					
10923-75.1	622	270	0.45	53	0.00031	21	0.54	0.140	1.6	0.793	2.2	0.0986	1.1	0.5	0.0584	1.8	607	7	544	40	-12
10923-88.1	642	347	0.56	50	0.00012	19	0.20	0.157	1.5	0.738	1.4	0.0912	1.0	0.7	0.0586	1.0	563	6	554	21	-2
10923-79.1	1256	702	0.58	103	0.00001	32	0.02	0.179	1.0	0.778	1.2	0.0952	1.0	0.9	0.0593	0.6	587	6	577	12	-2
10923-83.1	1096	451	0.42	87	0.00020	12	0.34	0.135	1.2	0.775	1.3	0.0927	1.0	0.8	0.0607	0.8	570	6	627	18	+9
10923-37.1	535	257	0.50	43	-0.00001	90	-0.01	0.141	1.8	0.755	1.4	0.0925	1.0	0.8	0.0592	0.9	570	6	574	19	+1
10923-91.1	1107	455	0.43	88	0.00050	16	0.87	0.118	1.2	0.752	2.8	0.0927	1.0	0.4	0.0589	2.6	572	6	562	57	-2
10923-17.1	1448	726	0.52	116	0.00016	11	0.28	0.149	1.0	0.756	1.2	0.0935	1.0	0.8	0.0586	0.7	577	6	552	15	-5
10923-93.1	1703	877	0.53	138	0.00003	25	0.04	0.169	0.9	0.766	1.1	0.0942	1.0	0.9	0.0590	0.5	581	6	567	11	-2
10923-15.1	806	334	0.43	63	0.00008	27	0.13	0.130	1.5	0.734	1.4	0.0908	1.0	0.8	0.0586	0.9	560	6	553	19	-1
10923-23.1	1528	1386	0.94	123	0.00020	9	0.34	0.237	0.8	0.764	1.2	0.0936	1.0	0.8	0.0592	0.7	577	6	575	14	-0
10923-57.1	1659	1527	0.95	134	0.00014	11	0.25	0.299	0.7	0.754	1.2	0.0937	1.0	0.8	0.0584	0.6	578	6	543	14	-7
10923-87.1	1258	547	0.45	100	0.00017	12	0.29	0.135	1.1	0.758	1.3	0.0927	1.0	0.8	0.0593	0.8	571	6	579	16	+1
10923-62.1	1586	914	0.60	129	0.00036	14	0.63	0.191	0.8	0.783	2.0	0.0947	1.0	0.5	0.0599	1.7	583	6	602	37	+3
10923-19.1	1094	443	0.42	88	0.00008	16	0.14	0.130	1.3	0.782	1.2	0.0938	1.0	0.8	0.0604	0.7	577	6	619	15	+7
10923-97.1	1155	455	0.41	92	0.00033	8	0.57	0.119	1.2	0.762	1.3	0.0932	1.0	0.7	0.0592	0.9	575	6	576	19	+0
10923-81.1	1294	512	0.41	104	0.00005	20	0.09	0.126	1.2	0.757	1.2	0.0937	1.0	0.9	0.0586	0.6	578	6	550	13	-5
10923-96.1	1707	931	0.56	138	0.00018	9	0.31	0.174	0.9	0.773	1.2	0.0945	1.0	0.9	0.0594	0.6	582	6	581	13	-0
RAX-11-NL-002, Pass Island pluton																					
10648-56.1	304	158	0.54	17.1	0.00023	23	0.41	0.169	7.3	0.455	4.1	0.0654	1.2	0.3	0.0504	4.0	411	5	216	92	-92
10648-30.1	290	206	0.73	16.4	0.00038	19	0.67	0.253	6.9	0.445	5.0	0.0658	1.4	0.3	0.0490	4.8	414	6	147	114	-186
10648-21.1	258	177	0.71	14.8	0.00045	41	0.78	0.211	7.3	0.474	6.8	0.0666	1.2	0.2	0.0516	6.7	417	5	268	154	-57
10648-29.1	664	282	0.44	38.3	0.00009	25	0.15	0.134	6.5	0.507	2.9	0.0671	1.2	0.4	0.0549	2.7	419	5	406	60	-3
10648-28.1	170	90	0.55	9.9	0.00000	100	0.00	0.180	9.9	0.559	4.7	0.0675	1.6	0.3	0.0601	4.4	419	7	606	95	+31
10648-14.1	1114	1166	1.08	64.4	0.00000	100	0.00	0.300	3.9	0.515	2.2	0.0674	1.1	0.5	0.0554	1.9	420	5	429	42	+2
10648-32.1	434	126	0.30	25.1	0.00018	125	0.31	0.093	8.2	0.499	6.8	0.0674	1.2	0.2	0.0537	6.7	421	5	358	151	-18
10648-33.1	737	348	0.49	42.8	-0.00005	83	-0.08	0.151	5.7	0.514	2.8	0.0676	1.1	0.4	0.0552	2.6	422	5	419	58	-1
10648-11.1	387	233	0.62	22.3	0.00079	26	1.37	0.194	7.5	0.425	8.4	0.0670	1.3	0.2	0.0459	8.3	423	5	-5	199	+8148
10648-54.1	508	212	0.43	29.8	0.00000	100	0.00	0.138	6.3	0.534	2.7	0.0682	1.1	0.4	0.0568	2.5	424	5	484	55	+12
10648-55.1	628	293	0.48	36.8	0.00000	100	0.00	0.151	6.0	0.519	2.9	0.0682	1.5	0.5	0.0552	2.5	425	6	420	56	-1
10648-17.1	470	187	0.41	27.6	0.00011	33	0.18	0.114	7.4	0.531	3.1	0.0684	1.2	0.4	0.0563	2.9	426	5	466	65	+9
10648-57.1	479	219	0.47	28.2	0.00010	27	0.17	0.139	6.5	0.534	3.0	0.0685	1.1	0.4	0.0566	2.8	426	5	475	61	+10
10648-31.1	222	57	0.27	13.0	0.00000	100	0.00	0.076	13.4	0.483	4.4	0.0681	1.3	0.3	0.0514	4.2	427	6	261	95	-65
10648-16.1	1269	518	0.42	75.0	0.00070	16	1.21	0.124	4.1	0.517	3.8	0.0688	1.1	0.3	0.0546	3.6	429	5	395	82	-9
10648-50.1	986	368	0.39	58.3	0.00008	31	0.14	0.131	4.7	0.522	2.3	0.0688	1.1	0.5	0.0550	2.0	429	5	414	45	-4
10648-12.1	384	144	0.39	23.0	0.00000	100	0.00	0.134	7.5	0.534	3.2	0.0696	1.2	0.4	0.0557	3.0	433	5	439	66	+1
10648-13.1	377	335	0.92	22.5	0.00013	32	0.22	0.277	5.3	0.481	3.7	0.0696	1.2	0.3	0.0501	3.5	437	5	199	81	-122
RAX-11-NL-006, Old Woman pluton																					
10639-13.1	146	123	0.87	7.3	0.00042	34	0.73	0.280	9.9	0.398	11.0	0.0582	1.4	0.1	0.0496	11.0	366	6	177	256	-109
10639-45.1	509	384	0.78	25.8	0.00000	100	0.00	0.244	5.4	0.488	3.1	0.0590	1.4	0.4	0.0600	2.7	367	5	605	59	+40
10639-30.1	779	416	0.55	39.4	0.00031	38	0.53	0.142	5.9	0.427	4.4	0.0588	1.2	0.3	0.0527	4.2	369	4	315	96	-17
10639-29.1	192	403	2.16	9.7	0.00000	100	0.00	0.670	6.3	0.430	6.0	0.0589	2.1	0.3	0.0530	5.7	369	8	327	129	-13
10639-42.1	265	178	0.69	13.6	-0.00008	91	-0.13	0.220	7.7	0.479	4.3	0.0597	1.2	0.3	0.0581	4.2	372	4	535	91	+31
10639-43.1	267	183	0.71	13.7	0.00001	92	0.02	0.201	7.8	0.452	4.0	0.0595	1.2	0.3	0.0551	3.8	372	4	418	85	+11
10639-20.1	155	285	1.90	8.0	0.00038	33	0.66	0.692	5.8	0.476	6.5	0.0598	1.3	0.2	0.0577	6.3	373	5	520	139	+29
10639-47.1	589	488	0.86	30.1	0.00000	100	0.00	0.290	4.4	0.442	2.9	0.0596	1.3	0.4	0.0538	2.6	373	5	364	58	-3
10639-49.1	237	213	0.93	12.0	0.00064	37	1.11	0.290	7.1	0.363	9.6	0.0591	1.4	0.1	0.0445	9.5	374	5	-82	233	+566
10639-21.1	76	109	1.49	4.0	-0.00116	61	-2.00	0.466	11.8	0.613	15.1	0.0615	1.8	0.1	0.0722	15.0	377	6	993	304	+63
10639-46.1	282	217	0.80	14.6	0.00029	26	0.51	0.239	6.9	0.399	4.9	0.0602	1.2	0.2	0.0481	4.8	379	4	105	113	-265
10639-9.1	223	196	0.91	11.6	0.00007	299	0.12	0.267	7.5	0.466	7.1	0.0608	1.2	0.2	0.0557	7.0	380	5	439	156	+14
10639-48.1	350	248	0.73	18.2	0.00027	23	0.46	0.226	6.0	0.410	4.1	0.0605	1.2	0.3	0.0491	4.0	381	4	155	93	-149
10639-2.1	271	263	1.00	14.2	0.00000	100	0.00	0.383	5.8	0.479	4.0	0.0612	1.2	0.3	0.0568	3.8	382	4	483	84	+21
10639-3.1	412	484	1.22	21.6	0.00027	44	0.47	0.380	4.6	0.448	4.8	0.0610	1.2	0.2	0.0533	4.7	382	4	344	106	-11
10639-39.1	222	186	0.87	11.7	0.00012	36	0.21	0.270	7.3	0.436	4.7	0.0614	1.2	0.3	0.0515	4.6	385	5	262	105	-48
10639-4.1	206	64	0.32	10.9	0.00027	33	0.46	0.095	19.8	0.407	5.7	0.0614	1.3	0.2	0.0481	5.6	387	5	103	132	-280

Notes (see Stern, 1997):

Spot name follows the convention x-y.z; where x = sample number, y = grain number and z = spot number. Multiple analyses in an individual spot are labelled as x-y.z.z

Uncertainties are reported at 1s and are calculated by using SQUID 2.23.08.10.21, rev. 21 Oct 2008

f(206)^{204} refers to mole percent of total ^{206}Pb that is due to common Pb, calculated using the ^{204}Pb-method; common Pb composition used is the surface blank (4/6: 0.05770; 7/6: 0.89500; 8/6: 2.13840)

* refers to radiogenic Pb (corrected for common Pb)

Disc: Discordance given as difference between measured $^{206}*Pb/^{238}U$ ratio and the expected $^{206}*Pb/^{238}U$ ratio at t=207*/206* age, in percent.

Calibration standard 6266; U = 910 ppm; Age = 559 Ma; $^{206}Pb/^{238}U$ = 0.09059

Error in $^{206}Pb/^{238}U$ calibration 1.5% (included)

Standard Error in Standard calibration was 0.34% (not included in above errors but required when comparing data from different mounts).

$^{206}Pb/^{238}U$ apparent age is corrected for common Pb using ^{207}Pb.

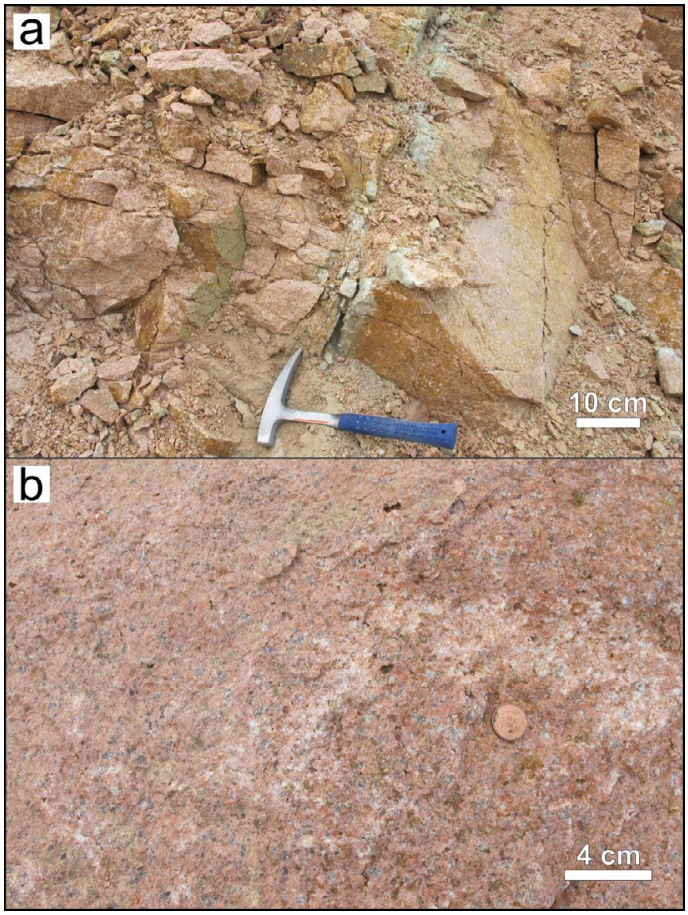

Figure 8 – Late Devonian Old Woman Stock, orange to red microgranite containing localised Mo mineralisation (Road Cut Showing). (a) Mineralisation associated with a metasomatically altered joint surface that forms part of a series with a generally northwest – southeast to north-northwest – south-southeast orientation. (b) Mo mineralisation as fine-grained disseminations and larger crystals associated with small vugs.

central Newfoundland, including the Devonian Terra Nova and Ackley granites.

Contrary to the previous interpretations, this sample yielded a Silurian crystallization age of 423 ± 4 Ma (Fig. 5b; Table 1; Kellett et al., 2014).

Old Woman Stock – 47°35'37.84" N, 55°30'39.64" W

RAX-11-NL-006 was collected from the Road Cut Showing of the Old Woman Stock, a granite body that is exposed in the central part of the Connaigre Peninsula between Old Bay and Salmonier Pond. The Old Woman Stock at the sampling location, a large quarry adjacent to Hwy-362, is medium-grained, pink, K-feldspar-rich granite (Figs. 4 and 8). The equigranular granite contains abundant vesicles or cavities, many of which are filled with epidote + quartz. The outcrops in the general area show strong sericitization and possible clay-mineral alteration (Kerr et al., 1993b). Sporadic molybdenite mineralization is developed within the granite.

Zircon from the Old Woman Stock sample yielded a U-Pb age of 376 ± 4 Ma (Fig. 5c; Table 1; Kellett et al., 2014).

Belleoram Granite – 47°32'04.44" N, 55°25'17.3" W

Sample RAX-11-NL-005 was obtained from an outcrop of the Belleoram Granite located on a trail approximately 300 m north of the community of Belleoram (Fig. 4). At the sampling site the Belleoram Granite consists of medium to fine grained, grey to light pink granodiorite (Fig. 9). The most distinctive feature of the Belleoram Granite is the presence of mm- to cm-scale, spheroidal mafic magmatic enclaves (Fig. 9b) that occur throughout the intrusion as well as within several dykes and minor intrusive bodies that have been correlated with the Belleoram Granite (O'Brien et al., 1995).

The granite sample yielded a large number of high quality prismatic zircon crystals. Analysis of six single-grain fractions yielded two discordant analyses and a cluster of data overlapping concordia. U-Pb ID-TIMS analytical results are presented in Table 2 and displayed in a concordia plot (Fig. 10), where age uncertainties are presented at the 2σ level. A weighted average of the $^{206}Pb/^{238}U$ ages of the overlapping concordant to near-concordant analyses is calculated to be 380.1 ± 1.0 Ma (MSWD=1.7, n=4), which is interpreted to be the crystallization age of the Belleoram granite. Analyses A16-4 and B16-1 are interpreted to contain inherited components.

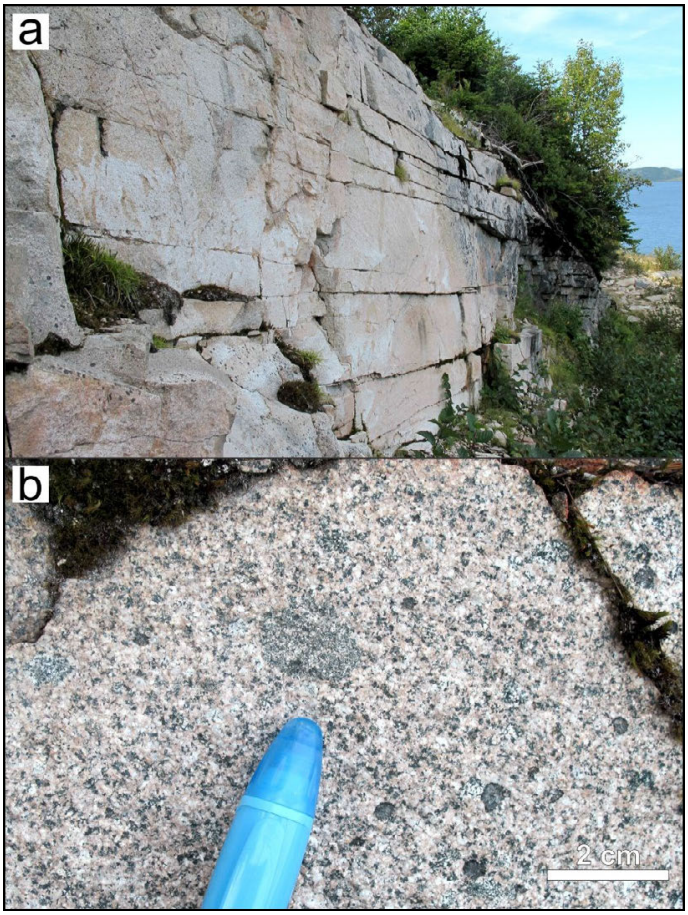

Figure 9 – Equigranular grey to pink, granodiorite, featuring mm- to cm-scale, spheroidal mafic magmatic enclaves, of the Late Devonian Belleoram Granite.

Table 2 – U-Pb zircon ID-TIMS result for sample RAX-11-NL-005.

Fraction[1]	Description[2]	Wt.	U	Pb[3]	$^{206}Pb/^{204}Pb$[4]	Pb^{5}	Isotopic Ratios[6]								Ages (Ma)[8]						
							$^{208}Pb/^{206}Pb$	$^{207}Pb/^{235}U$	±1SE Abs	$^{206}Pb/^{238}U$	±1SE Abs	Corr.[7] Coeff.	$^{207}Pb/^{206}Pb$	±1SE Abs	$^{206}Pb/^{238}U$	±2SE	$^{207}Pb/^{235}U$	±2SE	$^{207}Pb/^{206}Pb$	±2SE	% Disc
		ug	ppm	ppm		pg															
RAX-11-NL-05 (Z11127;1); UTM NAD83, zone 21, E-N																					
A16-1 (Z:1)	Co,Clr,Eu,Pr,fIn,CA16	2.1	77	5	545	1.1	0.30	0.45806	0.00266	0.06093	0.00013	0.550	0.05452	0.00027	381.3	1.5	382.9	3.7	392.7	22.2	3.0
A16-2 (Z:1)	Co,Clr,Eu,Pr,fIn,CA16	1.7	58	4	175	2.4	0.30	0.45274	0.00951	0.06060	0.00024	0.589	0.05418	0.00103	379.3	2.9	379.2	13.3	378.6	82.9	-0.2
A16-3 (Z:1)	Co,Clr,Eu,Pr,fIn,CA16	3.0	212	14	1064	2.3	0.22	0.45411	0.00183	0.06051	0.00019	0.759	0.05442	0.00014	378.8	2.3	380.2	2.6	388.7	11.8	2.6
A16-4 (Z:1)	Co,Clr,Eu,Pr,rIn,CA16	1.8	56	4	282	1.4	0.29	0.47822	0.00510	0.06269	0.00023	0.591	0.05532	0.00050	392.0	2.8	396.8	7.0	425.3	39.7	8.1
B16-1 (Z:1)	Co,Clr,Eu,Pr,fIn,fFr,CA16	4.9	36	3	813	0.9	0.31	0.49745	0.00203	0.06482	0.00009	0.483	0.05566	0.00020	404.9	1.1	410.0	2.8	438.8	16.0	8.0
B16-2 (Z:1)	Co,Clr,Eu,Pr,fIn,CA16	4.0	61	5	432	2.2	0.39	0.45647	0.00283	0.06054	0.00020	0.637	0.05469	0.00026	378.9	2.4	381.8	3.9	399.5	21.5	5.3

Notes:

[1]Z=zircon. Number in bracket refers to the number of grains in the analysis.

[2]Fraction descriptions: Co=Colourless,Clr=Clear, Pr=Prismatic, fFr=Few Fractures, rIn=Rare Inclusions, fIn=Few Inclusions, CA16=Chemically Abraded for 16 hours.

[3]Radiogenic Pb

[4]Measured ratio, corrected for spike and fractionation

[5]Total common Pb in analysis corrected for fractionation and spike

[6]Corrected for blank Pb and U and common Pb, errors quoted are 1 sigma absolute: procedural blank values for this study ranged from <0.1- 0.1 pg for U and 0.5-1 pg for Pb; Pb blank isotopic composition is based on the analysis of procedural blanks; corrections for common Pb were made using Stacey and Kramers (1975;1) compositions

[7]Correlation Coefficient

[8]Corrected for blank and common Pb, errors quoted are 2 sigma in Ma

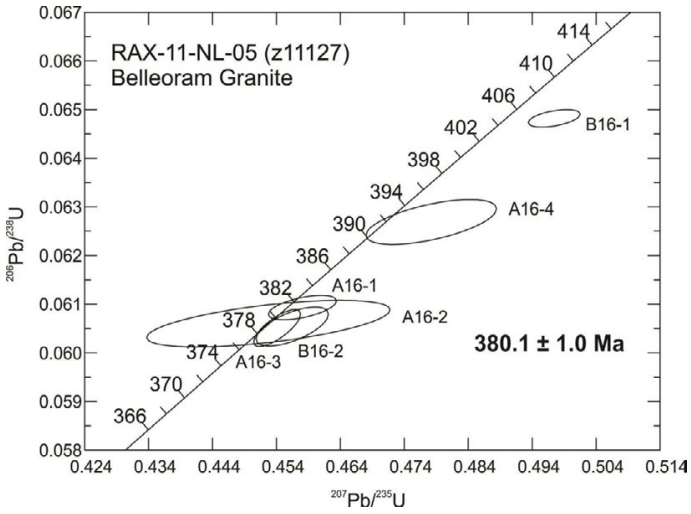

Figure 10 – Zircon U–Pb concordia plot for the Belleoram Granite (sample RAX-11-NL-05), where age uncertainties are presented at the 2σ level.

Updated tectonostratigraphy of the Connaigre Peninsula

Tickle Point Formation

The oldest known sequence on the Connaigre Peninsula is the Cryogenian, low-grade, arc-related volcanic rocks of the Tickle Point Formation (O'Driscoll, 1977; O'Brien et al., 1995; O'Brien, 1998). The distribution of the Tickle Point Formation is restricted to the western side of the peninsula (Fig. 4). This formation is primarily characterised by massive, calc-alkaline rhyolite flows, along with minor fine-grained felsic pyroclastic rocks and autobrecciated and/or flow-banded rhyolite. Mafic volcanic and clastic sedimentary rocks are also present, but have limited distribution. Towards the top of the formation, a distinctive unit of finely laminated to banded and internally brecciated carbonate rock is locally preserved (O'Brien et al., 1995). This unit is often host to, or associated with, significant Zn- and Cu-rich VMS-style mineralization (Sears, 1990; O'Brien and O'Driscoll, 1994). Rhyolite flows from the type locality have yielded a U-Pb zircon age of 681 ± 3 Ma (Fig. 4; O'Brien, 1998, and references therein).

Furby's Cove Intrusive Suite

The Cryogenian Furby's Cove Intrusive Suite (672 ± 3 Ma; O'Brien et al., 1992a; O'Brien, 1998) intruded the Tickle Point Formation prior to deposition of the Connaigre Bay Group (Fig. 4; O'Brien et al., 1995). The suite includes locally sheet-like granite and gabbro phases, with a pink to white, equigranular, blue-quartz granite and granodiorite being the most distinctive unit. The felsic and mafic units are locally intimately mixed and likely comagmatic. Near the Tickle Point Formation contact, the granite is affected by intense ductile shearing (O'Brien et al., 1995). The Furby's Cove Intrusive Suite also includes a bimodal dyke swarm that consists of hundreds of dykes cross-cutting the main granite and gabbro bodies and Tickle Point country rocks. It is likely that at least some of these dykes are related to the region's extensive younger (Late Neoproterozoic?) magmatism.

Connaigre Bay Group

The Tickle Point Formation and Furby's Cove Intrusive Suite rocks were deformed and exhumed prior to deposition of the lower Ediacaran Connaigre Bay Group (O'Brien et al., 1992a; 1995), such that the Connaigre Bay Group unconformably overlies various structural levels of both units. However, in most cases, the contact is tectonised or masked by younger intrusions. The distribution of the Connaigre Bay Group is mainly limited to the immediate area around and to the north-east of Connaigre Bay in the central-west part of the peninsula (Fig. 4).

The base of the Connaigre Bay Group is represented by marine siliciclastic rocks of the Sam Head Formation (Colman-Sadd et al., 1979). This formation is mostly fine- grained, graded sandstone and argillite, except at its base, where coarse-grained cobble conglomerate and breccia lie unconformably on basement (O'Driscoll, 1977; O'Brien et al., 1995).

The Sam Head Formation is conformably overlain by the tholeiitic basaltic and andesitic flows and volcanic breccias of the Doughball Point Formation (O'Driscoll, 1977; O'Brien et al., 1995). Minor interlayered rhyolitic rocks have provided a U-Pb zircon age of 626 ± 3 Ma (R.D. Tucker, unpublished data; O'Brien et al., 1994). The top of the Connaigre Bay Group is represented by red to grey, terrestrial, clastic

sedimentary rocks of the Downs Point Formation (O'Driscoll, 1977; Colman-Sadd et al., 1979).

Simmons Brook Intrusive Suite

The calc-alkaline Simmons Brook Intrusive Suite consists of grey, medium-grained, equigranular, hornblende-biotite granodiorite and tonalite, along with dark-grey to green, fine- to medium-grained diorite and (to a lesser extent) gabbro (O'Driscoll, 1977; O'Driscoll and Strong, 1979; O'Brien et al., 1995). Minor pink to red, locally porphyritic, alaskitic granite, which is effectively petrographically indistinguishable from younger intrusive rocks in the region, is also present within the suite (Fig. 11). A U-Pb zircon age of 621 ± 3 Ma has been obtained from foliated granodiorite (Fig. 4; R.D. Tucker, unpublished data; O'Brien et al., 1994).

The Simmons Brook Intrusive Suite forms a 5- to 10-km-wide band, extending from Harbour Breton in the south, northeastward across the Connaigre Peninsula (Fig. 4). It intrudes Tickle Point Formation and Connaigre Bay Group rocks, with its eastern limit marked by an unconformable or faulted contact with younger units.

Figure 11 – Simmons Brook Intrusive Suite pink to red, alaskitic granite.

Harbour Breton Granite and Grole and Hardy's Cove intrusive suites

Distribution of the middle Ediacaran Harbour Breton Granite and Grole and Hardy's Cove intrusive suites are restricted to the western side of the Connaigre Peninsula, between the Hermitage Bay and White Horse – East Bay faults (Fig. 4; O'Brien et al., 1995; O'Brien, 1998). They are intrusive into all of the older sequences; transecting structures indicating that there was likely to have been at least one phase of regional deformation in the period between the deposition of the Connaigre Bay Group and emplacement of the Simmons Brook Intrusive Suite and the intrusion of these units.

The Harbour Breton Granite is the most aerially extensive of these three intrusive units, and is primarily emplaced into Simmons Brook Intrusive Suite rocks, and to a lesser extent into the Connaigre Bay Formation. It shares faulted contacts with the older Tickle Point and younger Poole's Cove formations in the vicinity of Northeast Arm and Little Bay, respectively (Fig. 4; O'Brien, 1998). As originally defined, the Harbour Breton Granite (Widmer, 1950; Greene, 1975; Greene and O'Driscoll, 1976; Colman-Sadd et al., 1979) was considered to consist of two main and several smaller granitic bodies that were Devonian or younger. Subsequent studies determined that these granites were not all related and required division, such that only the Old Woman Stock is known to be Devonian (see later; O'Brien et al., 1995 and references therein). The remaining units of the revised Harbour Breton Granite (O'Brien et al., 1992b; 1995; O'Brien, 1998) are distributed between the Jerseyman's Harbour, Northeast Arm and Taylor Brook bodies (O'Brien, 1998) that occur at the north end of Northeast Arm between Little Bay and Harbour Breton, , and to the north of Old Bay, respectively (Fig. 4). Prior to this study only the Jerseyman's Harbour body had been dated, with a U-Pb zircon age of 570 ± 3 Ma (G.R. Dunning unpublished age reported in O'Brien et al., 1995). This has now been supplemented by the addition of the 575 ± 6 Ma age for the Taylor Brook Stock (Figs. 4 and 5a; Kellett et al., 2014).

The Harbour Breton Granite is comprised of mostly fine- to medium-grained, equigranular, red and orange alaskite and biotite (± hornblende) granite (Fig. 6), with minor microgranitic and medium-grained, porphyritic granite/monzogranite regions.

The Hardy's Cove Intrusive Suite (Elias and Strong, 1982) is an elongate, northeast-trending pluton that intrudes Tickle Point Formation and Connaigre Bay Group rocks near the head of Hermitage Bay (Fig. 4; O'Brien, 1998). The suite comprises pink to orange, medium-grained equigranular (± biotite) granite, along with minor buff to grey, medium-grained granodiorite, and grey to green, medium-grained diorite.

The Grole Intrusive Suite (O'Brien et al., 1992a) is mostly located between Connaigre and Hermitage bays (Fig. 4), although a few small, correlated bodies intrude Simmons Brook rocks to the north of Old Bay. This unit consists of black and dark-green to grey, medium- to coarse-grained gabbro with dark-grey, medium-grained quartz-diorite and diorite. Both the main body and one of the correlated bodies have been dated at 567 ± 3 Ma (O'Brien et al., 1994; R.D. Tucker, unpublished data).

Long Harbour Group

The middle to upper Ediacaran Long Harbour Group (568 ± 5 Ma to 552 ± 3 Ma (O'Brien et al., 1994; R.D. Tucker, unpublished data)) is restricted to the east of the White Horse – East Bay fault on the Connaigre Peninsula (Fig. 4; Williams, 1971; O'Brien et al., 1995; O'Brien, 1998). In this area the Long Harbour Group consists of the Belle Bay, Mooring Cove and Rencontre formations that have in part experienced contact metamorphism from adjacent Devonian intrusions (O'Brien, 1998).

The basal Belle Bay Formation comprises a thick succession of bimodal volcanic and epiclastic sedimentary rocks. In the type locality, north of Fortune Bay, these rocks are conformably overlain by the sedimentary Anderson's Cove Formation that in turn is conformably overlain by bimodal volcanic rocks of the Mooring Cove Formation. The local absence of the Anderson's Cove Formation, as is the case on the Connaigre Peninsula, has been interpreted as indicating a regional disconformity (H. Williams, personal communication reported in O'Brien et al., 1995). The uppermost unit in the group is represented by the conformably to disconformably overlying clastic sedimentary rocks of the Rencontre Formation.

Young's Cove Group

The Young's Cove Group form a thick sequence (in excess of 1000m) that range from the latest Ediacaran to Early Cambrian Chapel Island Formation to the Late Cambrian Salmonier Cove Formation;

the later unit consisting predominantly of black shale (White, 1939; Williams, 1971; Narbonne et al., 1987; O'Brien et al., 1995; O'Brien, 1998). The high sedimentation rate associated with the relatively slight palaeobathymetric variation (Myrow and Hiscott, 1993) suggests that these rocks formed in an extensional basin on the Avalonian passive margin. It is not known if the hiatuses within the group reflect local tectonic and/or global sea-level effects.

The typically grey, micaceous siltstone and thin-bedded siliceous sandstone of the Chapel Island Formation conformably overlies the Long Harbour Group. Locally the unit contains abundant Lower Cambrian trace fossils (Crimes and Anderson, 1985; Myrow, 1987; Narbonne et al., 1987) and is believed to transect the Proterozoic – Palaeozoic boundary (Narbonne et al., 1987). Notably, the Chapel Island Formation, together with the Devonian granitic rocks of the Old Woman Stock, define a ca. 2 to 4 km wide boundary zone between the Devonian sedimentary Great Bay De L'Eau and Poole's Cove formations (see later; O'Brien, 1998). In this area pyritiferous gossans are locally well developed within the Chapel Island Formation, likely in relation to metasomatism/mineralisation effects from the adjacent Old Woman intrusion.

The Chapel Island Formation is transitionally/conformably overlain by the primarily white, cross-bedded orthoquartzite of the Random Formation. This unit is also believed to be Lower Cambrian in age (O'Brien et al., 1995). On the Connaigre Peninsula the Random Formation occurs as unconformable and/or fault bounded blocks near Blue Pinion Cove, Otter Cove Point and Boxey Point (Fig. 4; O'Brien, 1998). At these sites and elsewhere the Random Formation is disconformably overlain by the early Middle Cambrian Chamberlain's Brook Formation (O'Brien et al., 1995). This disconformity is locally represented by a section of pebble conglomerate.

The black shale and minor grey, fine-grained sandstone of the Upper Cambrian Salmonier Cove Formation (Widmer, 1950) is restricted in distribution to a few small blocks on the shores of the Great Bay De L'Eau (O'Brien, 1998). These rocks contain *Agnostis pisiformis, Olenus* and *Peltura* zone fauna, as well as inarticulate brachiopods (Widmer, 1950; Hutchinson, 1962; Greene, 1975). The apparent lack of upper Middle Cambrian in the Connaigre Peninsula/Fortune Bay areas could reflect the presence of a disconformity at the base of the Upper Cambrian (O'Brien et al., 1995).

Pass Island Granite

The Late Silurian Pass Island Granite, dated at 423 ± 4 Ma (Figs. 4 and 5b; Kellett et al., 2014), intrudes the Ediacaran Grole Intrusive Suite at the southwestern tip of the peninsula between Hermitage and Connaigre bays. The Pass Island Granite is a homogeneous orange and pink, medium- to coarse-grained, equigranular or locally K-feldspar phyric, biotite-hornblende granite. The granite locally hosts numerous mafic and rhyolitic dykes that have been considered unrelated to Pass Island magmatism (O'Brien et al., 1995).

Cinq Isles Formation

The Cinq Isles Formation consists of red to grey micaceous sandstone, pebble conglomerate, shale and limestone (Figs. 4 and 12; Williams, 1971; Calcutt, 1973; Greene, 1975; O'Brien, 1998). The formation unconformably overlies the Young's Cove Group (and possibly very locally directly overlies the Long Harbour Group as well) to the east of the White Horse – East Bay fault and the Simmons Brook Intrusive Suite to the west. Although no direct age constraints exist for this unit, it is unconformably overlain by the Upper Devonian Great Bay De L'Eau Formation, and the local development of sedimentary mélange suggest it was deposited coincident with the Early Devonian docking of Avalonia to the composite Laurentian margin.

Figure 12 – Sedimentary mélange developed in red to grey micaceous sandstone of the Early Devonian Cinq Isles Formation.

Great Bay De L'Eau and Poole's Cove formations

The Middle to Upper Devonian, largely fluvial, sandstone to boulder conglomerates of the Poole's Cove and Great Bay De L'Eau formations represent the youngest stratified units on the Connaigre Peninsula. They are distributed over a broad swathe from East Bay to Great Bay De L'Eau and Boxey Point (Fig. 4). The precise age relationship between the formations is unknown, as no direct dating or fossils have been reported from the Poole's Cove Formation. Both sequences disconformably to unconformably overlie the Cinq Isles Formation (Fig. 13a) that is presumed to be pre-Middle Devonian, and both are cut by Late Devonian magmatism. They are, however, never found in direct contact, with the Poole's Cove Formation overlapping and to the west of the White Horse – East Bay fault and the Great Bay De L'Eau Formation to the south-east and separated by a zone of older rocks (Chapel Island Formation plus Cinq Isles Formation and Long Harbour Group). Although previous studies have presented the Great Bay De L'Eau Formation as the younger unit (i.e., O'Brien et al., 1998 and references therein), for the purposes of this study they are considered as effectively coeval.

The Poole's Cove Formation has been divided into several mappable units (Williams, 1971; Greene, 1975; O'Brien, 1998), the base of which consists of red, coarse-grained boulder conglomerate containing rounded heterolithic clasts interpreted to be derived from the adjacent Simmons Brook Intrusive Suite and Harbour Breton Granite (Fig. 13). Large clasts of Cinq Isles limestone are also reported indicating tectonic uplift occurred post-Cinq Isles Formation deposition. The upper units consist of variable, thickly to very thickly bedded units of buff to orange arkosic sandstone and conglomerate to bolder conglomerate. Rare, very thin beds of laminated mudstone likely represent localised lacustrine deposition. The upper conglomerate contains clasts, up to boulder size, of banded gneiss, amphibolite and megacrystic/ muscovite granite (Fig. 13b; O'Brien et al., 1995) suggesting a source area extending to Ganderian mid-crustal rocks uplifted during Acadian and/Neoacadian deformation. There is a noticeable tendency for boulder-sized granitoid clasts that were likely derived from the Harbour Breton Granite (± Simmons Brook Intrusive Suite) to be more angular

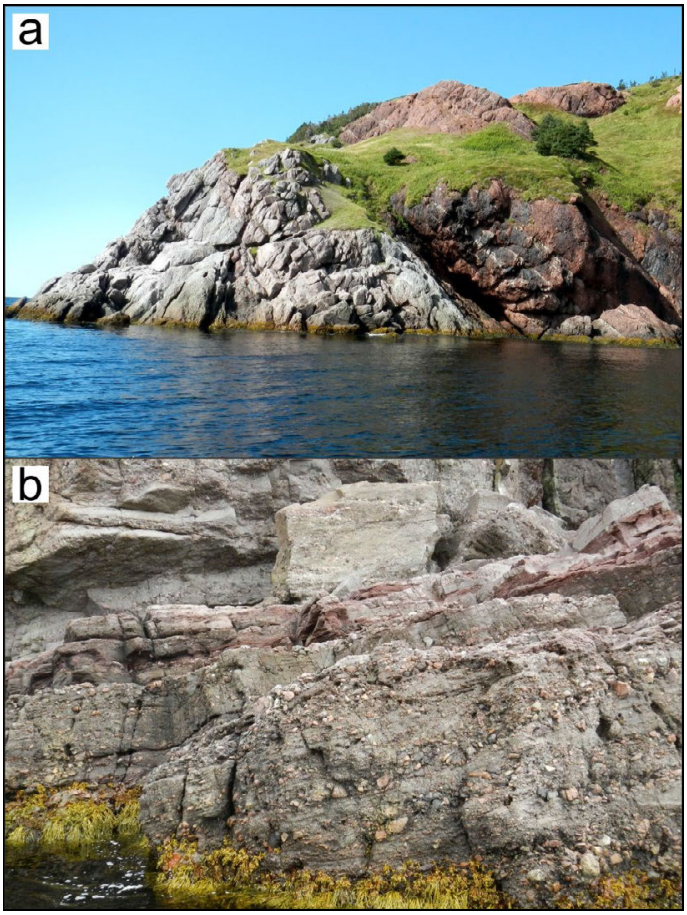

Figure 13 – Middle to Upper Devonian, largely fluvial, sandstone to boulder conglomerates of the Poole's Cove Formation. (a) Fault modified, unconformity separating the Poole's Cove Formation from limestone of the Cinq Isles Formation at the mouth of Little Bay. (b) Thin to thickly bedded fluvial red bedded sandstone to boulder conglomerate of the Poole's Cove Formation from Devil's Island in Great Bay De L'Eau.

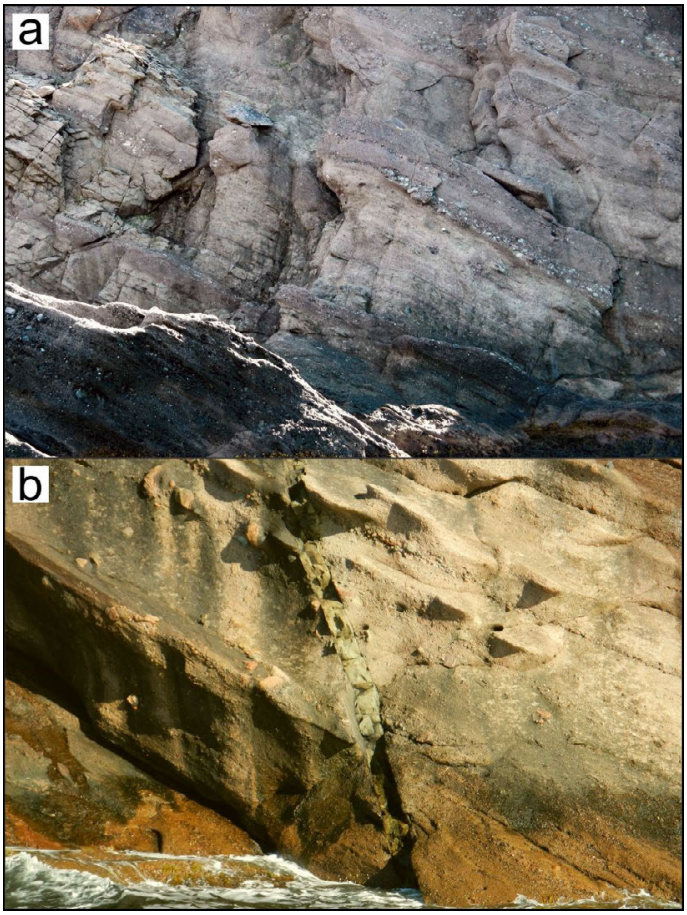

Figure 14 – Middle to Upper Devonian, fluvial redbed sandstone to conglomerate of the Great Bay De L'Eau Formation.

at the southern end of the formation relative to type locality at Poole's Cove. This is interpreted to be directly related to transport extent prior to deposition.

The Great Bay De L'Eau Formation (Widmer, 1950) comprises red to buff, pebble to boulder conglomerate and lesser amounts of green conglomerate and red and black shale (Fig 14). Basaltic hypabyssal intrusions or flows crop out towards the upper reaches of the formation at Boxey Point, and have been correlated with basaltic rocks that form the Cinq Isles and that intrude the nearby Chapel Island Formation (Fig 4; O'Brien, 1998).

In the Coomb's Cove – St. John's Head area black bituminous shale contains plant fossils including *Eospermatopteris* and *protolepidodendron* (Widmer, 1950). Although not a precise time marker, these fossils correspond to flora preserved from the Givetian fossil forest at Gilboa, New York (Grierson and Bonamo, 1979; Driese et al., 1997; Retallack and Huang, 2011; Stein et al., 2012) suggesting that the Great Bay De L'Eau Formation was likely deposited ca. 390 to ca. 385 Ma.

Old Woman Stock

The Late Devonian Old Woman Stock is an elliptical granitoid body primarily made up of plagioclase-phyric granite, locally cut by microgranite and K-feldspar porphyry, with orange to red microgranite, aplite and fine- to medium-grained hornblende-biotite granite towards its margins (Fig. 8). It is located at the head of Great Bay De L'Eau, between Old Bay and Salmonier Pond, where it primarily intrudes into the Chapel Island Formation and locally the Cinq Isles and Poole's Cove formations (Figs. 4 and 15). Along its southwestern margin it has been thrust northwards beneath the Simmons Brook Intrusive Suite along a fault surface that was likely formed as a reactivation splay of the pre-Cinq Isles Formation (Lower Devonian or older) White Horse – East Bay Fault.

There are a number of small Mo (+ fluorite) mineral occurrences around the margins of the Old Woman Stock and in association with minor, northeast – southwest trending, brittle extensional faults and/lineaments that transect the body (Fig. 4). Mineralisation is typically associated with quartz veins and metasomatically altered joint surfaces (Fig. 8a), which at the Road Cut Showing have a generally northwest – southeast to north-northwest – south-southeast orientation. It also occurs as fine-grained disseminations and crystals up to 2.5 cm in diameter associated with vugs and/or as irregular masses.

Figure 15 - Orange to red medium-grained hornblende-biotite granite of the Old Woman Stock intruding into the Chapel Island Formation at the head of Great Bay De L'Eau.

The Old Woman Stock has been dated at the Road Cut Showing at 376 ± 4 Ma (SHRIMP U-Pb zircon; Kellett et al., 2014) and yielded a Re-Os decay molybdenite age of 383 ± 1 Ma (Lynch et al., 2012) from the Leonard's Find Showing.

Belleoram Granite

The Belleoram Granite forms a near circular body approximately 12 km in diameter that intrudes the Ediacaran to Cambrian Long Harbour and Young's Cove groups, as well as the Early to Middle Devonian Cinq Isles and Great Bay De L'Eau formations in the southeastern portion of the Connaigre Peninsula (Figs. 4 and 16). The unit consists primarily of equigranular grey to pink, quartz monzonite to granodiorite and red, feldspar-phyric microgranite, which has been dated herein at 380.1 ± 1.0 Ma (Figs. 9 and 10). Also associated with this granite are quartz-feldspar porphyry dykes that extend into country rocks locally for more than 8 km from the main body (Fig. 4). The largest of these forms a prominent ridge that extends from near the centre of the main granite body at Horse Chops to the coast at English Harbour Back Cove, making the dyke at least 7 km long by 350 m wide.

The main distinguishing characteristic of the Belleoram Granite is the presence of mm- to cm-scale, spheroidal mafic magmatic enclaves that are distributed throughout the unit and represent the determinant for linking the quartz-feldspar porphyry dykes and minor intrusive bodies to the Belleoram Granite main body (Fig. 9b). Such ubiquitous enclaves are unique to the Belleoram Granite in comparison to the other granitoids of the Connaigre Peninsula, irrespective of age, and further afield the largely contemporaneous Ackley Pluton to the northeast.

Figure 16 – Strongly jointed Belleoram Granite.

Mineralisation is largely restricted to some minor fluorite and barite occurrences, typically along the outer margins of the Belleoram Granite (i.e., the Chapel Island Fluorite and Mose Ambrose Barite showings; Furey, 1985; O'Driscoll et al., 1995; O'Brien, 1998). Very minor galena and sphalerite have been recognised at the Chapel Island showings, whereas chalcopyrite-bearing quartz veins within hornfelsed Long Harbour Group rocks near Pig Point (i.e., Southern Salmonier Cove Showing) are purported to be epithermal (Berrange, 1955).

Discussion

Tectonostratigraphic domains of the Connaigre Peninsula

Although the Connaigre Peninsula has been considered amongst the most comprehensive examples of Devonian and older Avalonian sequences, it is apparent from recent age determinations that the region actually consists of two domains that have clearly different pre-Devonian tectonostratigraphic histories. These domains, separated by the White Horse – East Bay fault, are informally referred to herein as the Deadman's Bight and Wreck Cove domains (respectively west of and east of the fault). In this scheme, the Deadman's Bight domain contains the Tickle Point and Connaigre Bay formations, all Neoproterozoic intrusive rocks and the Silurian Pass Island Granite (Figs. 4 and 17). The Wreck Cove domain, in contrast, contains the various sedimentary and volcanic rocks of the Long Harbour and Young's Cove groups (Figs. 4 and 17). The boundary zone between these domains is mostly hidden beneath the Lower (?) Devonian Cinq Isles Formation and younger rocks. Thus it is interpreted that the two domains were separate through the Late Neoproterozoic and Lower Palaeozoic, but were together by the latest Silurian/early Devonian, which corresponds to the timing for the onset of the Acadian Orogeny (van Staal et al., 1998).

Direct correlatives to the Deadman's Bight domain Neoproterozoic rocks have not been described elsewhere in Newfoundland. This could in part be due to insufficient age determinations hampering comparisons. An illustration of this is Berry Hill Granite on the northern Burin Peninsula that prior to recent dating at 570 ± 6 Ma (Kellett et al., 2014) had been interpreted as Devonian (e.g., Kerr et al. 1993b). At the current level of precision, this intrusion is coeval to the Ediacaran Harbour Breton Granite and Hardy's Cove and Grole intrusive suites in the Deadman's Bight domain, but also to the much larger Swift Current Granite situated approximately 50 km to the northeast of it (Blackwood et al., 1984; O'Driscoll et al., 1995; O'Brien et al., 1999). However, in the Burin section these intrusions cut the ca. 590 Ma to ca. 565 Ma Marystown Group and associated rocks and are reported as overlain by the Long Harbour Group (O'Brien et al., 1999 and references therein); such sequences and relationships are not present within the Deadman's Bight domain. Furthermore, there are no known equivalents to the Tickle Point Formation in the Burin section. A similar situation occurs within the area south of Conception Bay where granitoid rocks that are contemporary to the Simmons Brook Intrusive Suite of the Deadman's Bight domain occur (Holyrood Intrusive Suite – King, 1988; Krogh et al., 1988). Although both intrusive suites are emplaced within early Ediacaran supracrustal rocks,

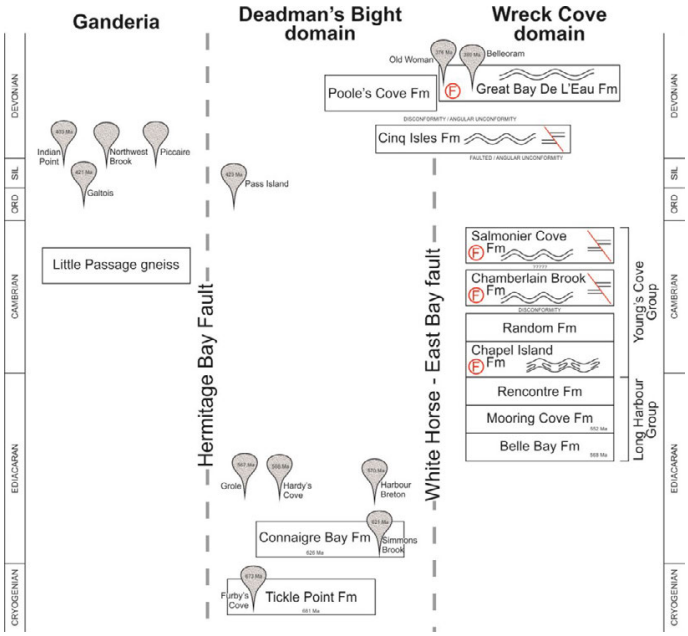

Figure 17 – Timing and distribution of tectonostratigraphic units within the Connaigre Peninsula.

their stratigraphies and tectonic settings are profoundly different (cf., O'Brien et al., 1997). Additionally, early Edicaran intrusive rocks at Conception Bay are unconformably overlain by Cambrian sedimentary rocks (King, 1988; O'Brien et al., 1997).

A Neoproterozoic sequence that potentially correlates to that present within the Deadman's Bight domain occurs within the Stirling belt of the Mira Terrane in Cape Breton, Nova Scotia (Barr, 1993; Macdonald and Barr, 1993). It should be noted, however, that there are no known equivalents to the Silurian Pass Island Granite within the Stirling belt, and that the Neoproterozoic sequences of the Stirling belt are unconformably overlain by Cambrian sedimentary rocks (Kelvin Glen Group; Barr et al., 1992, 1996; Reynolds et al., 2009). However, isotopic analysis of detrital zircon and muscovite have demonstrated that whereas the Kelvin Glen Group is contemporaneous with the Young's Cove Group, as developed in the Wreck Cove domain of the Connaigre Peninsula, they are not equivalents (Reynolds et al., 2009; Willner et al., 2013). Young's Cove Group equivalents are present, along with the underlying Long Harbour Group correlatives, in the adjacent, fault bounded Coastal belt of the Mira Terrane (Weeks, 1954; Landing, 1996; Barr et al., 1992, 1996). Macdonald and Barr (1993) interpreted the Sterling belt to have formed as a Neoproterozoic intra-arc or back-arc basin, with the Coastal belt developing as a late Ediacaran continental margin arc. These different belts were interpreted to represent separate parts of an extended magmatic arc or series of arcs and intra-arc basins (Barr, 1993; Barr et al., 1996) that were juxtaposed between 620 to 575 Ma by margin parallel strike-slip faulting (Macdonald and Barr, 1993; Barr, 2010). Detrital zircon population studies have subsequently indicated that these belts were not joined until much later (post-Kelvin Glen Group deposition; Willner et al., 2013), but presumably by the Cambrian MacCodrum Formation deposition, as this unit is mapped across both belts (Hutchinson, 1952; Barr et al., 1996; Willner et al., 2013). The absence of any evidence for Kelvin Glen Group or MacCodrum Formation rocks on the Connaigre Peninsula might indicate that tectonic development of the Sterling belt and Deadman's Bight domain diverged during the Ediacaran or Lower Cambrian as a consequence of the reorganisation of tectonostratigraphic blocks within composite Avalonia (Barr, 1993; Kerr et al., 1995; Barr et al., 1996).

The Late Silurian age of the Pass Island Granite within the Deadman's Bight domain is unusual, as it represents the first evidence for Silurian granitoid magmatism within the Avalonian portion of the Canadian Appalachians (Kellett et al., 2014). Existing tectonic models for the timing of tectonism and assembly of the Canadian Appalachians (e.g., Barr, 2010; van Staal et al., 2014) do not include a mechanism to explain such magmatism in Avalonia, sensu stricto, at this point in time prior to its accretion to composite Laurentia and the associated onset of the Acadian Orogeny. One possibility is that following the reorganisation of tectonostratigraphic blocks along the western margin (current coordinates) of composite Avalonia, the Deadman's Bight domain became positioned within the Acadian Seaway that separated Ganderia and Avalonia (van Staal et al., 2009, 2012; van Staal and Barr, 2012) as either a distinct microcontinental sliver or a promontory. In this scenario, during Silurian closure of the Acadian Seaway, this block could have docked to the leading edge of composite Laurentia at some time before the arrival of the main Avalonian continental block. This would enable the Deadman's Bight domain to be positioned in the upper plate setting during the Late Silurian formation of the Fogo suite (informal name; van Staal et al., 2014) of granitoid rocks that are otherwise restricted to Ganderia (Elliott et al. 1991; Dunning, 1992, 1994; Aydin, 1995; Sandeman and Malpas, 1995; Currie, 2003; van Staal et al., 2014). Van Staal et al. (2014) proposed that the Fogo suite was formed due to slab steepening and eduction associated with break-off of the Salinic slab created a progressively widening asthenospheric window beneath the foreland of the Salinic Orogen (i.e., Ganderia) that, in this scenario, would include the accreted Deadman's Bight domain (Fig. 18). Further study is required to determine whether this model is valid, or if another mechanism can explain the generation of the Pass Island Granite.

One consequence of the above model would be that the Hermitage Bay Fault would not, sensu stricto, represent the southern extent of the Ganderia – Avalonia bounding structure in Newfoundland (i.e., continuation of the Dover Fault). Instead, the arrival of the main tract of Avalonia would have occurred along the White Horse – East Bay fault, the pre-Early Devonian history of which is largely hidden beneath the Cinq Isles Formation and younger units. Even though the main, domain bounding movement(s) on the White Horse – East Bay fault occurred prior to Cinq Isles Formation deposition, it is apparent that there was a protracted history of fault reactivations that influenced Devonian sedimentation and likely intrusion-related mineralisation (see later). This is most clearly illustrated by the presence of Cinq Isles Formation limestone incorporated as clasts within boulder conglomerates in the overlying upper Poole's Cove Formation. Given the fault-modified, transgressive basal conglomerate deposition along the unconformity between the Cinq Isles and Poole's Cove formations and the Simmons Brook Intrusive Suite, and the fault bounded blocks of Young's Cove and Long Harbour groups between Cinq Isles Bay and Salmonier Pond and the Great Bay De L'Eau Formation on the Corbin Head Promontory, it is apparent that the White Horse – East Bay fault zone was a locus for horsts and grabens during the Middle to Late Devonian. Post Avalonian accretion reactivation of terrane bounding faults is also apparent for the Hermitage Bay Fault, where fault gouge at Hardy's Cove containing abundant chlorite and epidote related to pervasive brittle faulting was dated by K/Ar at 350 ± 7 Ma (D.A. Kellett, unpublished data, 2015). The timing of this movement corresponds with the brittle reactivation of sutures across much of

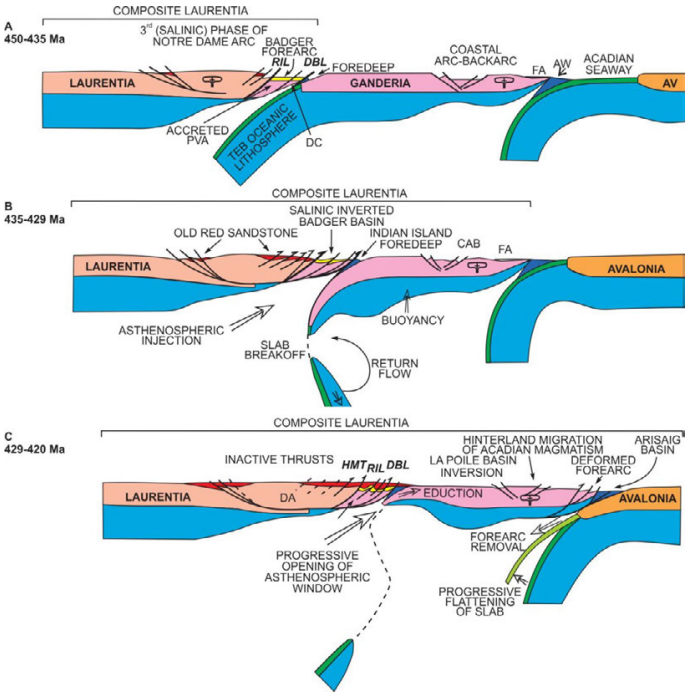

Figure 18 - Tectonic model for Salinic and Acadian subduction and orogenesis after van Staal et al., 2014.

(A) Late Ordovician to Early Silurian closure of the Tetagouche – Exploits back-arc basin (TEB) and start of the Salinic collision of composite Laurentia with leading edge of Gander margin. Waning Salinic-related arc magmatism took place to the west of the Red Indian Line (RIL). Salinic collision was coeval with and hence, may have been the cause of initiation of subduction in the Acadian seaway beneath the trailing edge of Gander margin, forming the Coastal arc – back-arc system (CAB). Red bed molasse sedimentation (shown in red) initiated in basins that formed during early Salinic thrusting and uplift in the hinterland of orogen. Marine sedimentation took place in the Badger forearc basin. The Badger forearc progressively grew eastwards due to accretion of buoyant blocks such as the Duder Complex (DC), which formed in the TEB. A marine foredeep accumulated Badger-like clastic sedimentary rocks and sedimentary rocks of the younger Indian Island Group on the leading edge of the Gander margin of Ganderia.

(B) Progressive steepening of the Gander margin slab during and/or following tearing (break-off) of the TEB oceanic slab. Red bed sedimentation reached the Red Indian Line (RIL), while the adjacent marine Badger forearc basin was inverted. DBL: Dog Bay Line.

(C) Eduction of the Gander margin and eastward expansion of an asthenospheric window beneath the Salinic orogen. Red bed sedimentation had now overstepped onto all parts Ganderia. Start of Acadian collision at ca. 420 Ma at the trailing edge of the Gander margin (now the leading edge of composite Laurentia) due to the entrance of Avalonia at the trench. Progressive flattening of the down-going slab following the start of collision produced a hinterland migrating retro-arc deformation zone and terminated in expulsion of the mantle wedge and extinction of Acadian magmatism during the Emsian. AW: accretionary wedge; DA: Dashwoods; FA: forearc; PVA: Popelogan – Victoria arc.

Newfoundland, such as the Red Indian Line (Lissenberg et al., 2005; Rogers et al., 2005) where small syn-tectonic extensional basins contain terrestrial fossils correlated to the Late Famennian to Tournaisian Horton Group in Nova Scotia (Newhouse, 1931; Belt, 1969; Kean, 1978; Rygel et al., 2006).

Intrusion related mineralisation on the Connaigre Peninsula

Kellett et al. (2014) reviewed the spatial and temporal distribution of Mo, W, and F mineralisation in Newfoundland. Dated plutons that are known to contain such mineralisation are ca. 380 Ma (Kerr et al., 1993a, 1993b, 1995; Kerr and McNicoll 2012, Kellett et al., 2014), with the exception of Granite Lake, where Mo-W-F mineralisation and associated granites are dated at ca. 387 and 388 Ma, respectively (Kerr and McNicoll, 2012; Lynch et al. 2012). These relationships are taken as indicating that the spatial distribution of mineralisation is related to the timing of pluton emplacement during an extended period of regional exhumation. Kellett et al. (2014) noted that the near concordance of $^{40}Ar/^{39}Ar$ ages and U-Pb crystallization ages supported the interpretation that rapid regional uplift and exhumation occurred concurrently with pluton emplacement.

An unusual feature of Connaigre Peninsula is that the Belleoram Granite and Old Woman Stock represent effectively coeval magmatism, emplaced in the ca. 380 Ma primary window for Mo-W-F mineralisation, where one body is largely barren and the other hosts several well-developed ore deposits. The main distinguishing characteristic of the Belleoram Granite is the pervasive, small mafic enclaves that delineate hybrid magmatism. However, this petrographic distinction is not believed to be a controlling factor for mineral potential, considering the presence of minor fluorite, barite, galena, sphalerite and chalcopyrite mineralisation near the outer margins of the Belleoram Granite and the evidence for metasomatism and thermal overprint in adjacent country rocks (O'Brien et al., 1995; O'Brien, 1998), all of which indicate that ore-forming fluids were present to some degree within the system.

The most likely variant to influence mineral potential between the Belleoram Granite and Old Woman Stock is the depth of intrusion. The Old Woman Stock is primarily emplaced into the Chapel Island Formation (Figs. 4 and 15), with only a small portion cutting the overlying Devonian sedimentary rocks. In stark contrast, the Belleoram Granite is positioned high in the Great Bay De L'Eau Formation (estimated to have been ca. 300 m thick; O'Brien et al., 2005 and references therein), such that that the magmatic body was emplaced virtually at the surface. This corresponds with the general hypabyssal/subvolcanic petrographic appearance of much of the body. Notably, most of the sparse mineralisation in the Belleoram Granite occurs in sections that intrude Young's Cove and older rocks (i.e., the Chapel Island Fluorite and Southern Salmonier Cove showings). The underlying mechanism is related to the Tuach et al. (1986) model for Ackley Pluton mineralisation, where the distribution of ore deposits is dictated by the depth of erosion across the granite (Fig. 19A). In that case, zones of mineralisation at randomly distributed cupolas developed throughout the upper reaches of the granite body, some of which were subsequently eroded. However in the case of the Belleoram Granite, mineralisation may have focussed where ore-bearing fluids precipitated metals upon reaching a pressure – temperature threshold (Fig. 19B). A corollary of this model is that intrusive bodies that evolve by distinct pulses of magma being emplaced at different levels can develop zones of mineralisation well within the main granite body in response to changing P-T conditions over time, as opposed to the tradi-

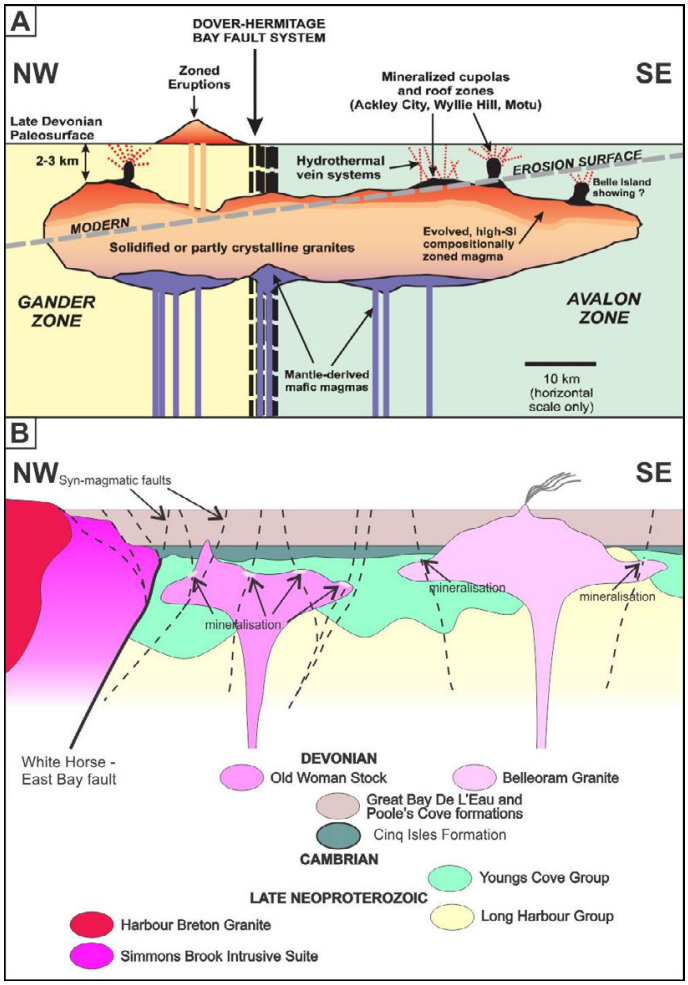

Figure 19 – (A) Conceptual model from Tuach et al. (1986) for the Ackley Granite of southeastern Newfoundland, showing the modern erosion surface and its relationship to the original plutonic architecture, and evolved magmas concentrated near the roof of the magma chamber. (B) Conceptual model for the Late Devonian emplacement of the Belleoram Granite and Old Woman Stock into the Connaigre Peninsula and relationship between location of mineralisation, emplacement depth and syn-magmatic faulting associated with reactivation of the White Horse – East Bay fault that juxtaposes the Deadman's Bight (NW) and Wreck Cove (SE) domains.

tional interpretations where ores are restricted towards the top of a pluton.

The presence of fluorite at each of the Mo deposits, and the association between fluoride-rich fluid inclusions and mineral potential (Rogers et al., 2014; Tweedale et al., 2014, 2015) suggests that ore metals are primarily transported as HF complexes. Once P-T conditions are met for fluorite to precipitate, often at ca. 2 km depth, ore metals also come out of solution. The opposite situation is observed in the Acadian Plutonic Suite of central New Brunswick (Rogers et al., 2014, 2015) wherein the apparently barren Juniper Barrens Pluton is interpreted as representing a significantly deeper section through Late Devonian granitoids than the adjacent Burnthill and Dungarvon plutons that are associated with numerous mineral occurrences. It is also significant that the zones of mineralisation in the Old Woman Stock are typically associated with syn-magmatic faults or lineaments along which only minor displacements are apparent, intersecting at a high angle. This may imply that they provided convenient fluid pathways, and that motion along them could have caused rapid P-T changes inducing ore precipitation. A similar correspondence between minor syn-magmatic breaks and loci of intrusion associated greisen-style mineralisation has also been observed in the Acadian Plutonic Suite (Rogers et al., 2014). Consequently, determining a region's tectonic history may be utilised as a primary exploration model, as prospectivity is a combination of overall tectonic setting, distribution of syn-magmatic structures, and emplacement depth.

Fortune Bay hydrocarbon potential

This new model for the tectonostratigraphic development of the Connaigre Peninsula may also have some implications for on-shore to near off-shore (Fortune Bay) hydrocarbon potential. The variably indurated Poole's Cove and Great Bay De L'Eau formations have a high potential as a reservoir. Traps and seals are possible (Enachescu, 2006), as these sequences display open, typically large wavelength folding and warping, and are locally transected by syn- to post-depositional faulting. Stratigraphic inversions are present, such as at Blue Pinion Cove, where Early Cambrian orthoquartzite tectonically overlies Great Bay De L'Eau conglomerate (Fig. 4). Onshore examples of potential hydrocarbon source rocks are less prevalent than potential reservoirs. However, near Coomb's Cove a sequence of black bituminous shale occurs within the Great Bay De L'Eau Formation (Fig. 4) from which a likely Givetian fossil assemblage has been reported. This sequence could be equivalent to known source rocks within the Horton Group in Nova Scotia and New Brunswick. In addition, there is untested potential in minor shales within the Cinq Isles Formation and the black shale of the earlier Salmonier Cove Formation. Another factor that might influence hydrocarbon potential is the high heat-flow associated with underplating of Upper Devonian intrusions (i.e., Belleoram Granite) that could potentially help drive hydrocarbon generation as an atypical petroleum system (cf., Tasmin Basin – Bendall et al., 2000; Neuquen Basin, Argentina – Monreal et al., 2009). This high heat-flow is potentially significant as the North Sydney Basin, and in particular Fortune Bay, is largely under explored as the depth of sedimentation in this part of the basin is considered insufficient for standard hydrocarbon generation.

Conclusions

The Connaigre Peninsula provides a key region in determining the timing and nature of Avalonia's accretion to the composite Laurentian margin and the onset of the Acadian Orogeny. Two distinct pre-Devonian tectonostratigraphies occur in the region, separated by a largely blind fault that is masked by younger sedimentary and intrusive rocks and by Devonian to Carboniferous rifting-related fault reactivations, forming a series of horsts and grabens. These distinct blocks (referred to herein as the Deadman's Bight and Wreck Cove domains) correspond closely with the Stirling and Coastal belts of the Mira Terrane in Cape Breton, NS. These belts were until recently believed to have been juxtaposed during the Neoproterozoic, but recent isotopic studies have suggested they were not together until the Lower Palaeozoic. Unlike the Stirling belt, the Deadman's Bight domain does not preserve Lower Palaeozoic sedimentation. It is possible that such sedimentary rocks were eroded during the Devonian when the Deadman's Bight domain was uplifted and excised along the White Horse – East Bay fault. However such rocks have not been recognised within the clast populations of the Devonian conglomerates that were sourced

from this uplift, in stark contrast to the Neoproterozoic Harbour Breton Granite and Simmons Brook Intrusive Suite that dominate the clasts. Also, the recognition of Silurian magmatism in the Deadman's Bight domain indicates a possibility that this particular block was not part of composite Avalonia until the final stages of Avalonia's accretion to the composite Laurentian margin in the Latest Silurian. Furthermore this indicates that this domain was, at least for part of the time, in the upper plate position with respect to the subduction and closure of the Acadian Seaway. In turn this raises questions on the nature of the Hermitage Bay Fault and if it should be ascribed as the fundamental suture for Avalonian accretion in this region.

The adjacent ca. 380 Ma granitoid intrusions of the Belleoram Granite and Old Woman Stock provide a rare opportunity to compare contemporary mineralised and largely barren bodies in close proximity. Although the Belleoram Granite is one of the very few petrographically distinctive granitoids not just on the Connaigre Peninsula but in central Newfoundland as a whole, indications are that the primary influence for ore development is depth of intrusion. It is interpreted that the Belleoram Granite was emplaced at too shallow a depth for associated fluids to have maintained and transported a significant metal content. Since it is clear that the Belleoram Granite is a composite body featuring several, distinct pulses of magma intruding into itself, this raises the possibility that volatile-rich fluids could have precipitated metals at deeper depths within the intrusion.

Acknowledgements

We gratefully acknowledge laboratory assistance from Nancy Joyce, Tom Pestaj, Nicole Rayner, Julie Peressini and Bill Davis. This activity was conducted as part of the Government of Canada's 2010-15 Intrusion Related Mineralization Project of the Targeted Geoscience Initiative 4 research program, in collaboration with the Geological Survey of Newfoundland & Labrador and Memorial University of Newfoundland. In particular, Prof. John Hanchar (MUN) is thanked for his contribution to the success of this activity. Alex Zagorevski is thanked for his constructive review of this manuscript.

References

Aydin, N.S., 1995. Petrology of the composite mafic – felsic rocks of the Fogo Island batholith: A window to mafic magma chamber processes and the role of mantle in the petrogenesis of granitoid rocks; Unpublished Ph.D. thesis, Memorial University of Newfoundland, St. John's, NL, 191 p.

Barr, S.M., 1993. Geochemistry and tectonic setting of late Precambrian volcanic and plutonic rocks in southeastern Cape Breton Island, Nova Scotia; Canadian Journal of Earth Sciences, v. 30, p. 1147-1154.

Barr, S.M., 2010. Granites and terranes in Cape Breton Island; *in* Eurogranites 2010: Field excursion guidebook - Nova Scotia, (ed.) D.B. Clarke; Atlantic Geoscience Society Special Publication Number 37, Acadia University, Wolfville, NS, p. 63-88.

Barr, S.M., White, C.E., and Macdonald, A.S., 1992. Revision of Upper Precambrian – Cambrian stratigraphy, southeastern Cape Breton Island, Nova Scotia; *in* Current Research, Part D, Geological Survey of Canada, Paper 92-1D, p. 21–26.

Barr, S.M., White, C.E., and Macdonald, A.S., 1996. Stratigraphy, tectonic setting, and geological history of Late Precambrian volcanic – sedimentary – plutonic belts in southeastern Cape Breton Island, Nova Scotia; Geological Survey of Canada Bulletin 468, 84p.

Belt, E.S., 1969. Newfoundland Carboniferous stratigraphy and its relation to the Maritimes and Ireland; *in* North Atlantic Geology and Continental drift, (ed.) M. Kay; American Association of Petroleum Geology Memoir 12, p. 734–753.

Bendall, M.R., Burrett, C.F., and Askin, H.J., 2000. Petroleum systems in Tasmania's frontier onshore basins; Journal of Australian Petroleum Production and Exploration Association, v. 1, p. 26-38.

Berrange, J.P., 1955. Field report on Salmonier Cove Pond area, Newfoundland; Newfoundland and Labrador Corporation Limited unpublished report.

Blackwood, R.F., and Kennedy, M.J., 1975. The Dover Fault: western boundary of the Avalon zone in northeastern Newfoundland; Canadian Journal of Earth Sciences, v. 12, p. 320-325.

Blackwood, R.F., and O'Driscoll, C.F., 1976. The Gander – Avalon boundary in southeastern Newfoundland; Canadian Journal of Earth Sciences, v. 13, p. 1155-1159.

Blackwood, R.F., Colman-Sadd, S.P., O'Brien, S., Hibbard, J., Meyer, J., Tomlin, S., and Green, R., 1984. Mineral Occurrence Map, Gander Lake, Newfoundland; Government of Newfoundland and Labrador, Department of Mines and Energy, Mineral Development Division, Map 84-045, scale: 1:250,000.

Calcutt, M.J., 1973. The stratigraphy and sedimentology of the Cinq Isles Formation, Fortune Bay, Newfoundland. Unpublished M.Sc. thesis, Memorial University of Newfoundland, St. John's, Newfoundland, 68 p.

Colman-Sadd, S.P., Greene, B.A., and O'Driscoll, C.F., 1979. Gaultois map area; Newfoundland Department of Mines and Energy, Mineral Development Division, Open File Map 79-104.

Crimes, T.P., and Anderson, M.M., 1985. Trace fossils from Late Precambrian-Early Cambrian of southeastern Newfoundland (Canada): temporal and environmental implications; Journal of Paleontology, v. 59, p. 310-343.

Currie, K.L., 2003. Emplacement of the Fogo Island Batholith, Newfoundland; Atlantic Geology, v. 39, p. 79-96.

D'Lemos, R.S., Schofield, D.I., Holdsworth, R.E., and King, T.R., 1997. Deep crustal and local rheological controls on the siting and reactivation of fault and shear zones, northeastern Newfoundland; Journal of the Geological Society, v. 154, p. 117-121.

Dallmeyer, R.D., Blackwood, R.F., Odom, A.L., 1981. Age and origin of the Dover Fault: tectonic boundary between the Gander and Avalon Zones of the northeastern Newfoundland Appalachians; Canadian Journal of Earth Sciences, v. 18, p. 1431-1442.

Driese, S.G., Mora, C.I., and Elick, J.M., 1997. Morphology and Taphonomy of Root and Stump Casts of the Earliest Trees (Middle to Late Devonian), Pennsylvania and New York, U.S.A.; Palaios, v. 12, p. 524-537.

Dunning, G.R., 1992. U–Pb geochronological research agreement final report for the Newfoundland Department of Mines and Energy; Unpublished report.

Dunning, G.R., 1994. U–Pb geochronological research agreement final report for the Newfoundland Department of Mines and Energy; Unpublished report.

Dunning, G.R., O'Brien, S.J., Colman-Sadd, S.P., Blackwood, R.F., Dickson, W.L., O'Neill, P.P., and Krogh, T.E., 1990. Silurian orogeny in the Newfoundland Appalachians; Journal of Geology, v. 98, p. 895-913.

Elias, P.N., and Strong, D.F., 1982. Timing of arrival of the Avalon Zone in the northeastern Appalachians: a new look at the Strad-

dling Granite. Canadian Journal of Earth Sciences, v. 19, p. 1088-1094.

Elliott, C.G., Dunning, G.R., and Williams, P.F., 1991. New U/Pb zircon age constraints on the timing of deformation in north-central Newfoundland and implications for early Paleozoic Appalachian orogenesis; Geological Society of America Bulletin, v. 103, p. 125–135.

Enachescu, M., 2006. Petroleum Exploration Opportunities in Western Newfoundland Offshore and Sydney Basin; Call for Bids NL08-3 and 4, Sydney Basin: Government of Newfoundland and Labrador, Department of Natural Resources.

Furey, D., 1985. Geology of the Belleoram pluton, southeast Newfoundland; Current Research, Part A, Geological Survey of Canada, Paper 85-IA, p. 151-156.

Greene, B.A., 1975. Harbour Breton, Newfoundland; Newfoundland Department of Mines and Energy, Mineral Development Division, Open File Map.

Greene, B.A., and O'Driscoll, C.F., 1976. Gaultois map area; *in* Report of Activities, Newfoundland Department of Mines and Energy, Mineral Development Division, Report 75-1, p. 3-9.

Grierson, J.D., and Bonamo, P.M., 1979. *Leclerquia complexa*: earliest ligulate lycopod (Middle Devonian); American Journal of Botany, v. 66, p. 474-476.

Hanmer, S., 1981. Tectonic significance of the northeastern Gander Zone, Newfoundland: an Acadian ductile shear zone; Canadian Journal of Earth Sciences, v. 18, p. 120-135.

Hibbard, J., van Staal, C.R., Rankin, D., and Williams, H., 2006. Lithotectonic map of the Appalachian orogen, Canada – United States of America; Geological Survey of Canada, Map 2096A, scale 1:1,500,000.

Holdsworth, R.E., 1994. Structural evolution of the Gander – Avalon terrane boundary: a reactivated transpression zone in the NE Newfoundland Appalachians; Journal of the Geological Society, London, v. 151, p. 629-646.

Hutchinson, R.D., 1952. The stratigraphy and trilobite faunas of the Cambrian sedimentary rocks of Cape Breton Island, Nova Scotia; Geological Survey of Canada Memoir 263.

Hutchinson, R.D., 1962. Cambrian stratigraphy and trilobite faunas of southeastern Newfoundland; Geological Survey of Canada, Bulletin 88, 156 p.

Kean, B.F., 1978. Geology of the Star Lake east half sheet (12A/11E), Newfoundland; *in* Report of Activities for 1977, Mineral Development Division, Department of Mines and Energy, Government of Newfoundland and Labrador, Report 78-1, p. 129-134.

Keen, C.E., Keen, M.J., Nichols, B., Reid, I., Stockmal, G.S., Colman-Sadd, S.P., O'Brien, S.J., Miller, H., Quinlan, G., Williams, H., and Wright, J., 1986. Deep seismic reflection profile across the northern Appalachians. Geology, v. 14, p. 141-145.

Kellett, D.A., Rogers, N., McNicoll, V.J., Kerr, A., and van Staal, C.R., 2014. New age data refine extent and duration of Paleozoic and Neoproterozoic plutonism at Ganderia – Avalonia boundary, Newfoundland; Canadian Journal of Earth Sciences, v. 51, p. 943-972.

Kerr, A., 1997; Space-time composition relationships among Appalachian-cycle plutonic suites in Newfoundland; *in* The Nature of Magmatism in the Appalachian Orogen, (ed.) A.K. Sinha, J.B. Whalen and J.P. Hogan; Geological Society of America Memoir 191, p. 193-219.

Kerr, A., and McNicoll, V.J., 2012. New U-Pb geochronological constraints from mineralized granites in southern Newfoundland; *in* Current Research, Newfoundland Department of Natural Resources, Geological Survey, Report 12-1, p. 21-38.

Kerr, A., Dickson, W.L., Hayes, J.P., and Fryer, B.J., 1993a. Devonian postorogenic granites on the southeast margin of the Newfoundland Appalachians: A review of geology, geochemistry, petrogenesis and mineral potential; *in* Current Research, Newfoundland Department of Natural Resources, Geological Survey, Report 93-1, p. 239-279.

Kerr, A., Dunning, G.R., and Tucker, R.D., 1993b. The youngest Paleozoic plutonism of the Newfoundland Appalachians: U-Pb ages from the St. Lawrence and François granites; Canadian Journal of Earth Sciences, v. 30, p. 2328-2333.

Kerr, A., Jenner, G.A., and Fryer, B.J., 1995. Sm-Nd isotopic geochemistry of Precambrian to Paleozoic granitoid suites and the deep-crustal structure of the southeast margin of the Newfoundland Appalachians; Canadian Journal of Earth Sciences, v. 32, p. 224-245.

King, A.F., 1988. Geology of the Avalon Peninsula, Newfoundland; Newfoundland Department of Mines, Mineral Development Division, Map 88-01.

Krogh, T.E., Strong, D.F., O'Brien, S.J., and Papezik, V.S., 1988. Precise U-Pb zircon dates from the Avalon Terrane in Newfoundland; Canadian Journal of Earth Sciences, v. 25, p. 442-453.

Landing, E., 1996. Avalon: Insular continent by the latest Precambrian; *in* Avalonian and related peri-Gondwanan terranes of the circum-North Atlantic, (ed.) R.D. Nance and M.D. Thompson. Geological Society of America, Special Publication 304, p. 29–63.

Lissenberg, C.J., Zagorevski, A., Rogers, N., van Staal, C.R., and Whalen, J.B., 2005. Geology, Star Lake, Newfoundland and Labrador; Geological Survey of Canada, Open File 1669, 1 sheet; 1 CD-ROM.

Lynch, E.P., Selby, D., Feely, M., and Wilton, D.H.C., 2009. New constraints on the timing of molybdenite mineralization in the Devonian Ackley Granite suite, southeastern Newfoundland: Preliminary results from Re-Os geochronology; *in* Current Research, Newfoundland Department of Natural Resources, Geological Survey, Report 09-1, p. 225-235.

Lynch, E.P., Selby, D., and Wilton, D.H.C., 2012. The timing and duration of granite-related magmatic-hydrothermal events in southeastern Newfoundland: Results of Re-Os molybdenite geochronology; Abstracts with Programs, Geological Association of Canada – Mineralogical Association of Canada Joint Annual Meeting. St. John's, Newfoundland.

Macdonald, A.S., and Barr, S.M., 1993. Geological setting and depositional environment of the Stirling Group of southeastern Cape Breton Island, Nova Scotia; Atlantic Geology, v. 29, p. 137-147.

Marillier, F., Keen, C.E., Stockmal, G.S., Quinlan, G., Williams, H., Colman-Sadd, S.P., and O'Brien, S.J., 1989. Crustal structure and surface zonation of the Canadian Appalachians: implications of deep seismic reflection data; Canadian Journal of Earth Sciences, v. 26, p. 305-321.

Mattinson, J.M., 2005. Zircon U–Pb chemical abrasion (CA-TIMS) method; combined annealing and multi-step partial dissolution analysis for improved precision and accuracy of zircon ages; Chemical Geology, v. 220, p. 47–66.

Monreal, F.R., Villar, H.J., Baudino, R., Delpino, D., and Zencich, S., 2009. Modelling an atypical petroleum system: A case study of hydrocarbon generation, migration and accumulation related to

igneous intrusions in the Neuquen Basin, Argentina; Marine and Petroleum Geology, v. 26, p. 590-605.

Myrow, P.M., 1987. Sedimentology and depositional history of the Chapel Island Formation (Late Precambrian to Early Cambrian), southeast Newfoundland; Unpublished Ph.D. thesis, Memorial University of Newfoundland, St. John's, Newfoundland, 512 p.

Myrow, P., and Hiscott, R., 1993. Depositional history and sequence stratigraphy of the Precambrian-Cambrian boundary stratotype, Chapel Island Formation, southeast Newfoundland; Palaeogeography, Palaeoclimatology, Palaeoecology, v. 104, p. 13-35.

Narbonne, G.M., Myrow, P., Landing, E., and Anderson, M.M., 1987. A candidate stratotype for the Precambrian – Cambrian boundary, Fortune Head, Burin Peninsula, southeast Newfoundland; Canadian Journal of Earth Sciences, v. 24, p. 1277-1293.

Newhouse, W.H., 1931. The geology and ore deposits of Buchans, Newfoundland; Economic Geology, v. 26, p. 399-414.

O'Brien, S.J., 1998. Geology of the Connaigre Peninsula and adjacent areas, southern Newfoundland; Geological Survey, Department of Mines and Energy, Open File Map NFLD/2660; 1:100,000 scale.

O'Brien, S.J., and O'Driscoll, C.F., 1994. Geology of the western Connaigre Peninsula, Newfoundland; Department of Natural Resources, Geological Survey, Map 94-243.

O'Brien, S.J., Dubé, B., and O'Driscoll, C.F., 1999. High-sulphidation, epithermal-style hydrothermal systems in Late Neoproterozoic Avalonian rocks on the Burin Peninsula, Newfoundland: Implications for gold exploration; *in* Current Research, Newfoundland Department of Mines and Energy, Geological Survey Branch, Report 99-1, p. 275-296.

O'Brien, S.J., King, A.F., O'Driscoll, C.F., 1997. Late Neoproterozoic geology of the central Avalon Peninsula, Newfoundland, with an overview of mineralization and hydrothermal alteration; *in* Current Research, Newfoundland Department of Natural Resources, Geological Survey Branch, Report 97-1, p. 257-282.

O'Brien, S.J., O'Driscoll, C.F., Greene, B.A., and Tucker, R.D., 1995. Pre-Carboniferous geology of the Connaigre Peninsula and the adjacent coast of Fortune Bay, southern Newfoundland; *in* Current Research, Newfoundland Department of Natural Resources, Geological Survey Branch, Report 95-1, p. 267-297.

O'Brien, S.J., O'Driscoll, C.F., and Tucker, R.D., 1992a. A reinterpretation of the geology of parts of the Hermitage Peninsula, southwestern Avalon Zone, Newfoundland; *in* Current Research, Newfoundland Department of Mines and Energy, Geological Survey Branch, Report 92-1, p. 185-194.

O'Brien, S.J., Strong, D.F., and King, A.F., 1990. The Avalon Zone type area: southeastern Newfoundland Appalachians; *in* Avalonian and Cadomian Geology of the North Atlantic, (ed.) R.A. Strachan and G.K. Taylor; Blackie and Son, Ltd., Glasgow, p. 166-194.

O'Brien, S.J., Tucker, R.D., Dunning, G.R., and O'Driscoll, C.F., 1992b. Four-fold subdivision of the Late Precambrian magmatic record of the Avalon Zone type area (east Newfoundland): nature and significance; Abstracts with Programs, Volume 17, Geological Association of Canada – Mineralogical Association of Canada Joint Annual Meeting; Wolfville, NS, p. A85.

O'Brien, S.J., Tucker, R.D., and O'Driscoll, C.F., 1994. Neoproterozoic basement-cover relationships and the tectono-magmatic record of the Avalon Zone on the Hermitage Peninsula and environs, Newfoundland; *in* New Perspectives in the Appalachian-Caledonian Orogen, Geological Association of Canada NUNA Conference, Program with Abstracts, p. 21-22.

O'Driscoll, C.F., 1977. Geology, petrology and geochemistry of the Hermitage Peninsula, Southern Newfound land; Unpublished M.Sc. thesis, Memorial University of Newfoundland, St. John's, Newfoundland, 144 p.

O'Driscoll C.F., and Strong, D.F., 1979. Geology and geochemistry of the Late Precambrian volcanic and intrusive rocks of the southwestern Avalon Zone in Newfoundland; Precambrian Research, v. 8, p. 19-48.

O'Driscoll, C.F, Stapleton, G.J., and King, D.W., 1995. Mineral occurrence map, Belleoram/St Lawrence, Newfoundland; Newfoundland and Labrador Mineral Development Division, Map 95-016.

Parrish, R.R., Roddick, J.C., Loveridge, W.D., and Sullivan, R.W., 1987. Uranium-lead analytical techniques at the Geochronology Laboratory, Geological Survey of Canada; Geological Survey of Canada, Paper 87-2, p. 3-7.

Quinlan, G.M., Hall, J., Williams, H., Wright, J.A., Colman-Sadd, S.P., O'Brien, S.J., Stockmal, G.S., and Marillier, F., 1992. Lithoprobe onshore seismic reflection transects across the Newfoundland Appalachians; Canadian Journal of Earth Sciences, v. 29, p. 1865-1877.

Retallack, G.J., and Huang, C., 2011. Ecology and evolution of Devonian trees in New York, USA; Palaeogeography, Palaeoclimatology, Palaeoecology, v. 299, p. 110–128.

Reynolds, P.H., Barr, S.M., and White, C.E., 2009. Provenance of detrital muscovite in Cambrian Avalonia of Maritime Canada: $^{40}Ar/^{39}Ar$ ages and chemical compositions; Canadian Journal of Earth Sciences, v. 46, p. 169-180.

Roddick, J.C., 1987. Generalized numerical error analysis with applications to geochronology and thermodynamics; Geochimica et Cosmochimica Acta, v. 51, p. 2129-2135.

Rogers, N., McClenaghan, M.B., Plouffe, A., Kellett, D.A., Chapman, J., Azadbakht, Z., Tweedale, F., Ruberti, G., and Anderson, B., 2014. TGI 4 – Intrusion Related Mineralisation Project: New Vectors to Buried Porphyry-Style Mineralisation; *in* Abstracts 2014: Exploration, Mining and Petroleum New Brunswick, (ed.) E.A. Keith; New Brunswick Department of Energy and Mines, Geoscience Report 2014–5, p. 31.

Rogers, N., McClenaghan, M.B., Thorne, K.G., Fyffe, L.R., Seaman, A.A, Parkhill, M.A., McClenaghan, S.H., Pronk, A.G., Beal, K.L., Lentz, D.R., Wilson, R.A., Rice, J.M., and Lentz, C., 2015. Granite-related mineralization and alteration in the Acadian Plutonic Belt: implications for Sn-W-Mo-Cu exploration in central New Brunswick – TGI 4 Field Guide; *in* TGI 4 – Intrusion Related Mineralisation Project: New Vectors to Buried Porphyry-Style Mineralisation, (ed.) N. Rogers; Geological Survey of Canada, Open File 7843, p. 113-204.

Rogers, N., van Staal, C.R., McNicoll, V.J., Squires, G.C., Pollock, J., and Zagorevski, A., 2005. Geology, Lake Ambrose and part of Buchans, Newfoundland and Labrador; Geological Survey of Canada, Open File 4544, 1 sheet; 1 CD-ROM.

Rygel, M.C., Calder, J.H., Gibling, M.R., Gingras, M.K., and Melrose, C.S.A., 2006. Tournaisian forested wetlands in the Horton Group of Atlantic Canada; Geological Society of America Special Papers, v. 399, p. 103-126.

Sandeman, H.A., and Malpas, J., 1995. Epizonal I- and A-type granites and associated ash-flow tuffs, Fogo Island, northeast Newfoundland; Canadian Journal of Earth Sciences, v. 32, p. 1835–1844.

Schofield, D.I., and D'Lemos, R.S., 2000. Granite petrogenesis in the Gander Zone, NE Newfoundland: mixing of melts from multiple

sources and the role of lithospheric delamination; Canadian Journal of Earth Sciences, v. 37, p. 535-547.

Sears, W.A., 1990. A geochemical, petrographic and metallogenic analysis of volcanogenic sulphide deposition within the Connaigre Bay Group, Hermitage Peninsula, Southern Newfoundland; Unpublished M.Sc. thesis, Memorial University of Newfoundland, St. John's, Newfoundland, 282 p.

Stein, W.E., Berry, C.M., VanAller Hernick, L., and Mannolini, F., 2012. Surprisingly complex community discovered in the mid-Devonian fossil forest at Gilboa; Nature, v. 483, p. 78–81.

Stern, R.A., 1997. The GSC Sensitive High-Resolution Ion Microprobe (SHRIMP): analytical techniques of zircon U-Th-Pb age determinations and performance evaluation; *in* Current Research, Part F, Geological Survey of Canada, p. 1-31.

Stern, R.A., and Amelin, Y., 2003. Assessment of errors in SIMS zircon U-Pb geochronology using a natural zircon standard and NIST SRM 610 glass; Chemical Geology, v. 197, p. 111-142.

Stockmal, G.S., Colman-Sadd, S.P., Keen, C.E., Marillier, F., O'Brien, S.J., and Quinlan, G.M., 1990. Deep seismic structure and plate tectonic evolution of the Canadian Appalachians; Tectonics, v. 9, p. 45-62.

Tuach, J., Davenport, P.H., Dickson, W.L., and Strong, D.F., 1986. Geochemical trends in the Ackley granite, southeast Newfoundland: Their relevance to magmatic metallogenic processes in high-silica granitic systems; Canadian Journal of Earth Sciences, v. 23, p. 747-765.

Tweedale, F., Hanley, J.J., Kontak, D.J., and Rogers, N., 2014. Petrographic observations and evaporate mound analysis of quartz-hosted fluid inclusions: Applications to assess metal fertility in granites; Abstracts with Programs, Volume 37, Geological Association of Canada – Mineralogical Association of Canada Joint Annual Meeting; Fredericton, NB, p. 275-276.

Tweedale, F., Hanley, J.J., Kontak, D.J., and Rogers, N., 2015. Petrographic observations and evaporate mound analysis of quartz-hosted fluid inclusions hosted by granitoid samples from the South Mountain Batholith, Nova Scotia: An exploration tool for vectoring towards mineralised areas in intrusive rocks; *in* TGI 4 – Intrusion Related Mineralisation Project: New Vectors to Buried Porphyry-Style Mineralisation, (ed.) N. Rogers; Geological Survey of Canada, Open File 7843, p. 79-99.

van Staal, C.R., 1994. The Brunswick subduction complex in the Canadian Appalachians: record of the Late Ordovician to Late Silurian collision between Laurentia and the Gander margin of Avalon; Tectonics, v. 13, p. 946-962.

van Staal, C.R., and Barr, S.M., 2012. Lithospheric architecture and tectonic evolution of the Canadian Appalachians and associated Atlantic margin; *in* Tectonic Styles in Canada: The LITHOPROBE perspective, (ed.) J.A. Percival, F.A. Cook and R.M. Clowes; Geological Association of Canada Special Paper 49, p. 41–95.

van Staal, C.R., Barr, S.M., and Murphy, J.B., 2012. Provenance and tectonic evolution of Ganderia: Constraints on the evolution of the Iapetus and Rheic oceans; Geology, v. 40, p. 987–990.

van Staal, C.R., Currie, K.L., Rowbotham, G., Rogers, N., and Goodfellow, W., 2008. Pressure-temperature paths and exhumation of Late Ordovician-Early Silurian blueschists and associated metamorphic nappes of the Salinic Brunswick subduction complex, northern Appalachians; Geological Society of America Bulletin, v. 120, p. 1455-1477.

van Staal, C.R., Dewey, J.F., Mac Niociall, C., and McKerrow, W.S., 1998. The Cambrian-Silurian tectonic evolution of the northern Appalachians and British Caledonides: History of a complex, west and southwest Pacific-type segment of Iapetus; Geological Society, London, Special Publication, v. 143, p. 197-242.

van Staal, C.R., Whalen, J.B., Valverde-Vaquero, P., Zagorevski, A., and Rogers, N., 2009. Pre-Carboniferous, episodic accretion-related, orogenesis along the Laurentian margin of the northern Appalachians; *in* Ancient Orogens and Modern Analogues, (ed.) J.B. Murphy, J.D. Keppie and A.J. Hynes; Geological Society, London, Special Publications, v. 327, p. 271-316.

van Staal, C.R., Zagorevski, A., McNicoll, V.J., and Rogers, N., 2014. Time-Transgressive Salinic and Acadian Orogenesis, Magmatism and Old Red Sandstone Sedimentation in Newfoundland; Geoscience Canada, v. 41, p. 138-164.

Weeks, F.J., 1954. Southeast Cape Breton Island, Nova Scotia; Geological Survey of Canada, Memoir 277, 112 p.

White, D.E., 1939. Geology and molybdenite deposits of the Rencontre East area, Fortune Bay, Newfoundland; Unpublished Ph.D. thesis, Princeton University, Princeton, New Jersey, 19 p.

Widmer, K., 1950. The geology of the Hermitage Bay area, Newfoundland; Unpublished Ph.D. thesis, Princeton University, Princeton, New Jersey, 439 p.

Williams, H., 1971. Geology of the Belleoram map area, Newfoundland; Geological Survey of Canada, Paper 70-65, 39 p.

Williams, H., 1979. Appalachian Orogen in Canada; Canadian Journal of Earth Sciences, v. 16, p. 792-807.

Williams, H., 1993. Acadian orogeny in Newfoundland; *in* The Acadian Orogeny: Recent Studies in New England, Maritime Canada, and the Autochthonous Foreland, (ed.) D.C. Roy and J.W. Skehan; Geological Society of America Special Paper, v. 275, p. 123-133.

Williams, H., Colman-Sadd, S.P., and Swinden, H.S., 1988. Tectonic-stratigraphic subdivisions of central Newfoundland; Geological Survey of Canada Paper 88-1B, p. 91–98.

Williams, H., Dickson, W.L., Currie, K.L., Hayes, J.P., and Tuach, J., 1989. Preliminary report on a classification of Newfoundland granitic rocks and their relations to tectonostratigraphic zones and lower crustal blocks; *in* Current Research, Part B, Geological Survey of Canada Paper 89-1B, p. 47-53.

Williams, H., O'Brien, S.J., King, A.F., and Anderson, M.M., 1995. Avalon Zone – Newfoundland; *in* The Geology of North America (Vol. 2), Geology of the Continental Margin of Eastern Canada, (ed.) M.J. Keen and G.L. Williams, Geological Society of America, p. 226-237.

Willner, A.P., Massonne, H.J., Barr, S.M., and White, C.E., 2013. Very low- to low-grade metamorphic processes related to the collisional assembly of Avalonia in SE Cape Breton Island (Nova Scotia, Canada); Journal of Petrology, v. 54, p. 1849-1874.

Petrographic observations and evaporate mound analysis of quartz-hosted fluid inclusions hosted by granitoid samples from the South Mountain Batholith, Nova Scotia: An exploration tool for vectoring towards mineralised areas in intrusive rocks

Fergus Tweedale[1], Jacob J. Hanley[1], Dan J. Kontak[2] and Neil Rogers[3]

1. Department of Geology, Saint Mary's University, 923 Robie St., Halifax, Nova Scotia
2. Department of Earth Sciences, Laurentian University, 935 Ramsey Lake Rd., Sudbury, Ontario
3. Geological Survey of Canada, 601 Booth St., Ottawa, Ontario

Abstract: The ca. 380 Ma South Mountain Batholith (SMB) of Nova Scotia is a large (ca. 7,300 km^2), mesozonal granitoid intrusion that consists of 13 coalesced plutons of granodiorite to leucomonzogranitic composition which host a variety of mineralised zones (e.g., Sn-Zn-Cu-Ag, Mo, Mn-Fe-P, U, Cu-Ag). Given the hydrothermal nature of this mineralisation, it is expected that a fingerprint of the mineralizing fluids might be manifested both petrographically and by the chemistry of secondary, quartz-hosted fluid inclusions in the granites on a scale equal to or larger than the mineralised centres. In order to assess the potential of using the petrographic and chemical fingerprints as vector for exploration, a study integrating both these methods was investigated. The protocol involved in the study included the following: (1) completing a detailed petrographic study of hundreds of archived thin section samples that focused on the extent and degree of alteration that reflect fluid-rock interaction. The indices included: (i) type and abundance of perthite, (ii) chloritic alteration of biotite, (iii) plagioclase alteration, (iv) amount of secondary white mica, and (v) abundance of secondary fluid inclusions in quartz; and (2) determining the fluid chemistry of quartz-hosted fluid inclusions in samples (n = 66) collected from the SMB. For this study, a detailed protocol was developed to address specific analytical considerations, including decrepitation temperature, oven versus stage heating, EDS calibration, EDS acquisition time, representative sampling and raster versus point mode of analysis. Thus, in this study, quartz chips were heated to 500ºC and a maximum of 16 mounds per sample were analysed (60 seconds) in raster mode, the latter to circumvent chemical variation related to elemental fractionation during mound formation. To date, the results indicate that the fluids from Phase 1 samples are dominated by a Na-F-Cl-Ca fluid. In contrast, fluids from Phase 2 samples are dominated by two fluid inclusion populations: a Na-K fluid and a F-Na-Cl-Ca fluid.

Introduction

Fluid inclusions are microscopic (i.e., <50 μm) samples of paleofluids that circulated at some time during the hydrothermal history of the host mineral, and in mineralised areas, may be associated with hydrothermal ore deposits. The composition of fluid inclusions therefore, provides chemical data that is relevant to the modelling of ore deposits and the design of exploration strategies (Roedder and Bodnar, 1997). A problem associated with categorizing large granitoid intrusions that host ore deposits is the simultaneous management of environmental and economic costs and the collection of data that is representative of the entire system. To address this problem, we propose the development and testing of a cost-effective and time-efficient exploration technique that is a useful for regional-scale characterization of fluid-rock interaction, called evaporate mound analysis. The technique involves the controlled decrepitation (i.e., bursting) of quartz-hosted fluid inclusions and chemical analysis of the resultant evaporate mounds with an electron probe equipped with a high resolution imaging system. The ca. 7,300 km^2, mineralised South Mountain Batholith (SMB), Nova Scotia, is largest granitoid intrusion in the northern Appalachians (Fig. 1). The SMB is also one of the most intensively studied peraluminous granitoid complexes in the world (Chatterjee and Clarke, 1985), and the abundance of accessible outcrop, as well as the preservation of archived thin section and slab collections housed by the Nova Scotia Department of Natural Resources, make the SMB an ideal testing ground for evaporate mound analysis. Additionally, SMB quartz hosts abundant liquid-rich secondary fluid inclusions. This paper provides a framework describing the methodology behind SEM-EDS analysis, including step-by-step details regarding sample preparation, artificial decrepitation procedures, SEM-EDS analytical protocols, application of calibration standards, EDS data-reduction considerations, and data-display options. The methodology was refined through examination of a suite of granitoid samples collected from the contiguous and fertile SMB. This research evaluates fluid chemistry in an effort to better characterize a fertile metal system by providing a regional-scale assessment that can guide future studies. The results of this work will help determine if evaporate mound analysis, when combined with petrographic work, is a viable exploration tool. This Targeted Geoscience Initiative 4 (TGI 4) funded work is a

Corresponding author: Fergus Tweedale (fergus.tweedale@gmail.com)

Tweedale, F., Hanley, J.J., Kontak, D.J., and Rogers, N., 2015. Petrographic observations and evaporate mound analysis of quartz-hosted fluid inclusions hosted by granitoid samples from the South Mountain Batholith, Nova Scotia: An exploration tool for vectoring towards mineralised areas in intrusive rocks; *in* TGI 4 – Intrusion Related Mineralisation Project: New Vectors to Buried Porphyry-Style Mineralisation, (ed.) N. Rogers; Geological Survey of Canada, Open File 7843, p. 79-99.

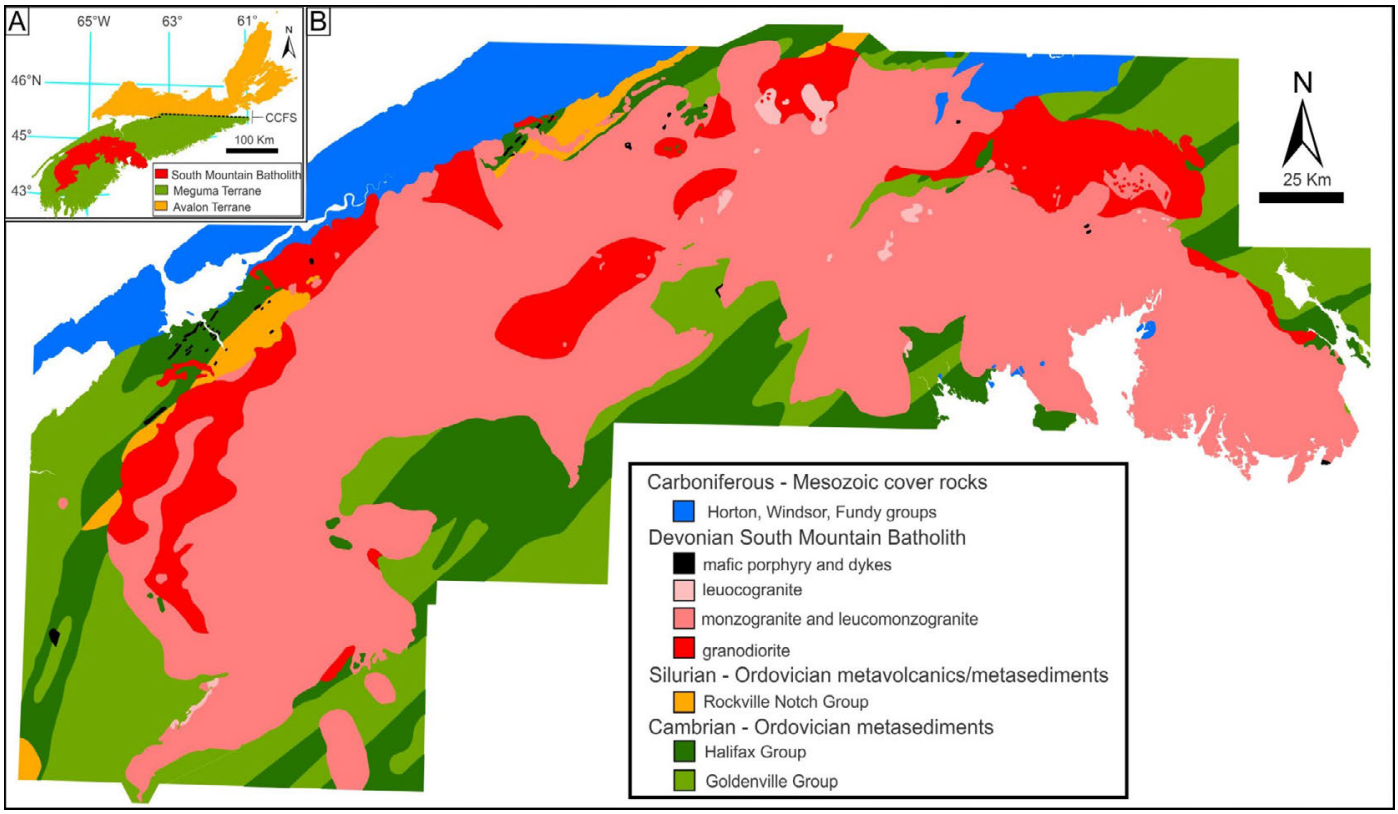

Figure 1 – Geological map of study area. (A) Index map showing simplified geology of Nova Scotia, showing the two terrane units separated by the Cobequid Chedbucto Fault System (CCFS). The South Mountain Batholith (SMB) intrudes the Meguma terrane, the most outboard terrane of the Appalachian Orogen. (B) Geological map of the SMB. Map boundaries from the Nova Scotia Department of Natural Resources.

test case and is the first of its kind conducted on a batholithic scale, with the resulting methodological protocols being readily exportable for mineral fertility assessment of other areas

Relevance of analytical technique

Fluid-filled cavities in minerals, called fluid inclusions, are trapped samples of the ambient fluid that circulated during mineral growth (i.e., primary fluid inclusions) or during post-crystallisation alteration (i.e., secondary fluid inclusions; Timofeeff et al., 2000; Ménez et al., 2002). Aqueous fluid inclusions therefore provide an opportunity to directly analyse the chemical composition and evolution of fluids involved with magmatic-hydrothermal ore deposition. Microthermometry is the most frequently used technique to evaluate fluid inclusion salinity, but results reported in equivalent wt% NaCl units can provide only qualitative detail, and cannot account for undetermined cation and anion solutes. Metastability affecting phase change behaviour also invites caution (Kontak, 2004). Other conventional methods used for solute analysis of fluid inclusions include crush-leach techniques to extract the fluid followed by LA-ICP-MS compositional analysis. However, the results obtained from crush-leach analysis reflects multiple generations of fluids (Chi et al., 2003), and the electronegativity of fluorine, a potential ore metal complexation ligand in magmatic-hydrothermal fluids (McPhie et al., 2011; Thomas et al., 2006; Wilkinson, 2001; Muecke and Clarke, 1981) precludes application of standard LA-ICP-MS analysis (Bu et al., 2003). Scanning electron microscopy/energy dispersive X-ray spectroscopy (SEM-EDS) evaporate mound analysis, is a cost effective alternative method to obtain in-situ solute analysis of fluid inclusions (Kontak, 2004).

Previous studies

By employing relatively low-cost equipment and time-efficient methodology, evaporate mound analysis is an effective approach for characterizing fluid inclusion solute chemistry in a variety of magmatic-hydrothermal settings. Previous work indicates that SEM-based methods produce semi-quantitative chemical analyses of fluid inclusions hosted in minerals in a variety of geologic settings, including volcanogenic massive sulphide deposits (Zaw et al., 2003), Mississippi Valley-type deposits (Haynes and Kesler, 1987; Savard and Chi, 1998), carbonitite-hosted deposits (Samson et al., 1995), metamorphosed strata-bound copper depsoits (Heinrich and Cousens, 1989), and granite-hosted mineral deposits (Chryssoulis and Wilkinson, 1983; Kontak et al., 1999; Carruzzo et al., 2000; Kontak, 2004).

Of the numerous techniques used to analyse fluid inclusion solute chemistry (see Chi et al. (2003) for a summary review), only crush-leach ion chromatography, laser ablation inductively coupled plasma mass spectrometry (LA-ICP-MS) and SEM-EDS evaporate mound analysis are comparable in terms of sensitivity to solute cations and anions. Many other techniques used in fluid inclusion research are analytically challenging (i.e., time-inefficient) and/or provide data expressed in relative units (i.e., wt% NaCl). For example, secondary ion mass spectrometry (SIMS) analysis can, in principle, provide detection for all elements (Diamond et al., 1990), but the analytical complexity (Ménez et al, 2002) and the prohibitive cost (Gleeson, 2003) of

this technique impair its practicality as an exploration tool. Other microbeam-based techniques including synchrotron X-ray fluorescence (SXRF), proton-induced X-ray emission (PIXE) and proton-induced gamma emission (PIGE) require time-consuming sample preparation and long analytical times (Ménez et al., 2002; Anderson and Mayanovic, 2003). Additionally, PIXE and PIGE mostly yield only cation data (Gleeson, 2003), and solute concentration measurements using SXRF demand tedious measurement of the microscopic volume of the inclusions (Frantz et al., 1988).

It should also be emphasized that SEM-EDS analysis has advantages over LA-ICP-MS and bulk crush-leach techniques. Crush-leach analyses integrate a protracted hydrothermal history (i.e., solute compositions of fluid inclusion assemblages and single inclusions are not resolvable). Although costly in terms of time and equipment, LA-ICP-MS is a highly sensitive technique, but electronegativity issues regarding some halogens (i.e., metal ligands) makes some (e.g., F) elements undetectable (e.g., Bu et al., 2003).

Geological setting of the South Mountain Batholith

The mineralised SMB, located within the Meguma Zone of the Appalachian Orogen, is a post-tectonic granitoid complex of Devonian age (ca. 380 Ma; Clarke and Halliday, 1980; Reynolds et al., 1981). The batholith intrudes the regionally metamorphosed (greenschist-amphibolite facies) Cambrian to Ordovician Meguma Supergroup (MS) and the overlying Ordovician to Silurian Rockville Notch Group (RNG). The MS comprises a thick (>10 km) sequence of folded metasedimentary strata that includes the lower, sandstone-dominated Goldenville Group and the overlying siltstone-dominated Halifax Group. The SMB contact with the RNG trends NE-SW and is overlain in some areas by Carboniferous cover rocks. The RNG comprises mixed volcanic, volcanoclastic and metasedimentary rocks, and the overlying cover rocks include the coarse-clastic terrestrial sedimentary rocks, evaporites sequences and volcanoclastic rocks of the Mississippian Horton, and the Triassic Windsor and Fundy groups, respectively (Fig 1). In general terms, the SMB is a composite intrusion of granodiorites, monzogranites, leucomonzogranites and leucogranites, locally cut by metre-scale pegmatite dykes and aplite sheets. Outcrop-scale structures within the SMB (Fig. 2) provide clear evidence that late-stage fluid flow is part of the hydrothermal history of the batholith.

Based on field relationships and compositional variations identified during research conducted by the NSDNR (MacDonald, 2001) SMB rock units are grouped into 13 plutons, which include five Stage 1 plutons and eight Stage 2 plutons (Fig. 3). The earlier Stage 1 plutons mainly consist of biotite granodiorite and biotite monzogranite. Stage 2 plutons intrude Stage 1 plutons. Stage 2 plutons mainly consist of two-mica monzogranite, fine- and coarse-grained leucomonzogranite and muscovite leucogranite. Internal contacts can be either intrusive or gradational (MacDonald, 2001).

Known Mineralisation within the South Mountain Batholith

The SMB is host to the past-producing East Kemptville (Sn-Zn-Cu-Ag) and New Ross Manganese (Mn-Fe-P) mines, the Millet Brook (U-Cu-Ag) deposit, as well as numerous other polymetallic prospects and occurrences (Fig. 4).

Four main deposit types occur within the SMB: greisen, vein, breccia and pegmatite. Although associated with the SMB, peribatho-

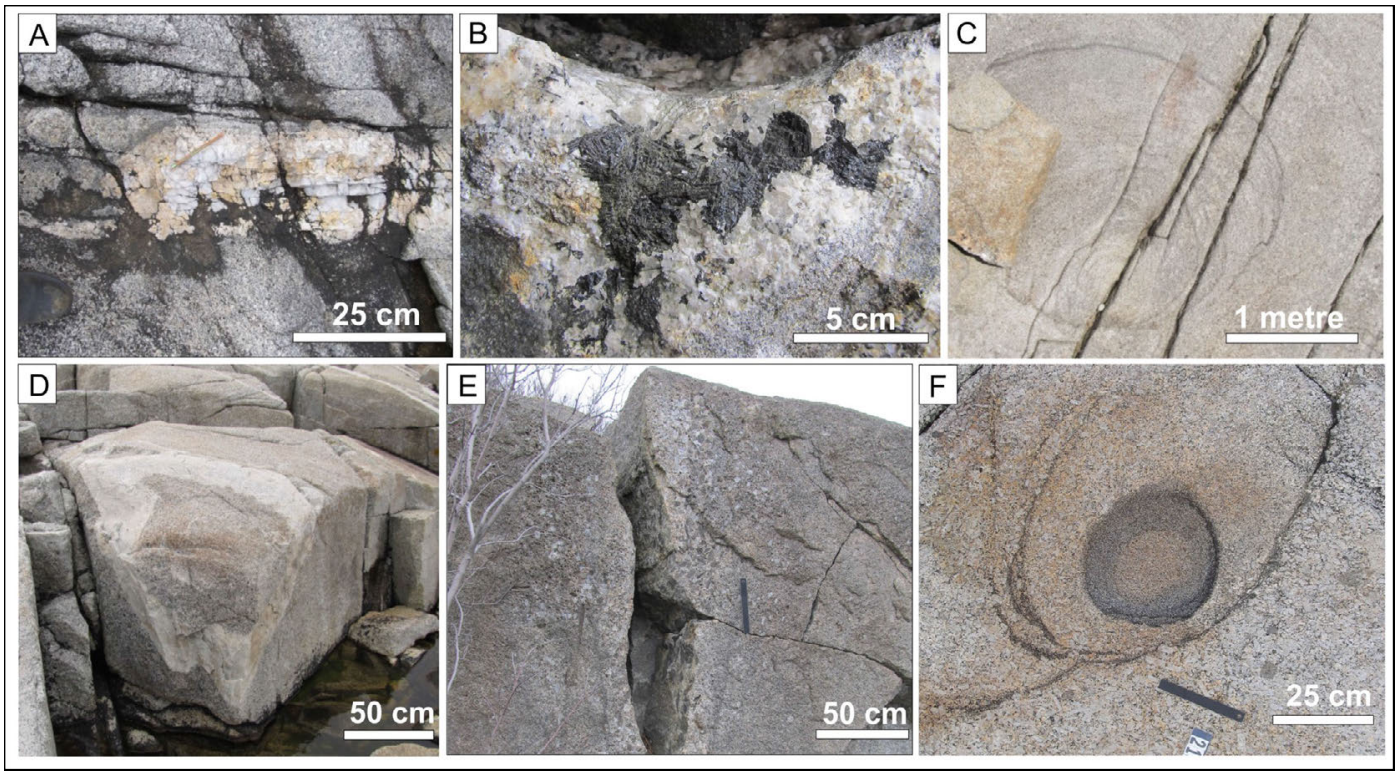

Figure 2 – Macroscopic-scale evidence of hydrothermal fluid flow in the SMB. (A) Miarolitic cavity near Aspotogan Point in Lunenburg County. (B) Tourmaline clot in the Halifax Pluton. (C) Ring schlieren at Pennant Point, Halifax County. (D) Aplite sheet at Peggy's Cove. (E) Breccia pipe in highway outcrop near Halifax. (F) Biotite schlieren near municipality of Prospect.

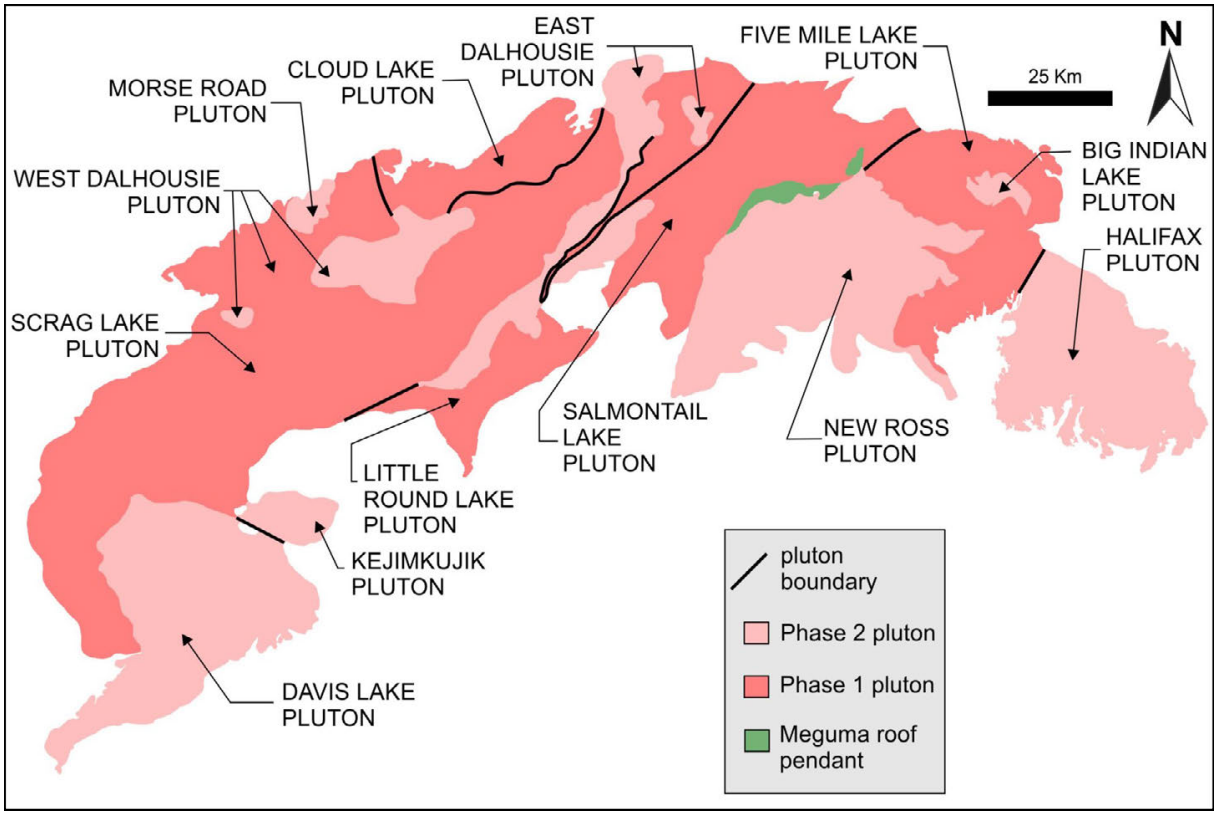

Figure 3 –Map of South Mountain Batholith pluton boundaries Phase 1 plutons are generally biotite-granodiorites and biotite monzogranites. Later Phase 2 plutons are generally 2 mica monzogranites, leucomonzogranites and leucogranites (MacDonald, 2001).

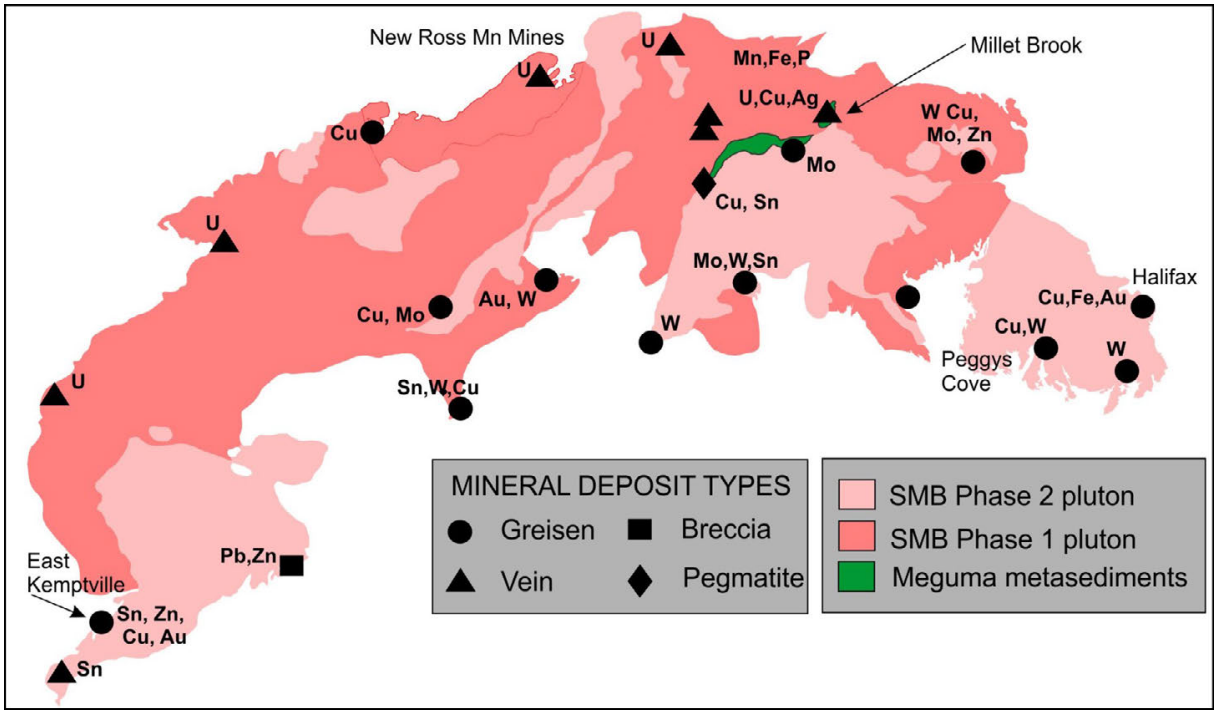

Figure 4 – Locations of major known mineral deposits hosted by the South Mountain Batholith (modified from MacDonald, 2001). The great diversity in style (e.g., greisen, vein, breccia and pegmatite) and in metal assemblages (e.g., Sn-Zn-Cu-Ag, Mo, Mn-Fe-P, U, Cu-Ag) of SMB mineralised centres are the result of post-crystallisation hydrothermal processes.

lithic (endogranitic) deposits (MacDonald et al., 2002; Kontak, 1990) occurring near contact areas with the Meguma rocks are not discussed. Brief details of each of the SMB deposit types are discussed below.

Greisen deposits (Sn-W-Mo-As-Cu-Pb-Zn-F-Au-Ag)

Greisen occurs in SMB rocks that range in composition from the least-evolved granodioritic phases (e.g., Sandwich Point prospect) to the most evolved muscovite-leucocratic phases (e.g., East Kemptville deposit), and tends to occur primarily in the Stage 2 plutons. Typically SMB greisens are spatially associated with major structural features. However, the underlying genetic relationship between major structural features and ore deposition associated with greisen occurrence remains unclear. Whereas the SMB greisens are distributed throughout the batholith, the largest greisen-style mineral occurrences are typically proximal to shallow-dipping contact zones between the granite and Meguma metasedimentary rocks. The past-producing East Kemptville Sn-Zn-Cu-Ag occurrence is the largest known economic SMB-hosted deposit, and it occurs at the SMB-Meguma contact within the regional East Dalhousie East Kemptville Shear Zone (EKEDSZ). Greisen associated with the Long Lake Mo-W-Cu prospect west of the municipality of Chester Grant in Lunenburg County, and the W-Sn-Mo-Cu-Zn-Ag-Au prospect at Westfield in Queen's County are proximal to granite-metasediment contacts that are not associated with major faults (O'Reilly, 2011, 2013; Cormier, 1988). However, greisen mineralisation is also associated with vein-type deposits, including the Sandwich point prospect that occurs adjacent to vein mineralisation (Au-Bi-Sb-Cu-Zn) that cuts SMB monzogranite near the Meguma – SMB contact (Kontak and Kyser, 2011). From this, it appears evident that greisen form preferentially near SMB-metasedimentary contact zones that are proximal to fault zones.

Of particular relevance for fluid inclusion studies, past research suggests that SMB greisens are intimately associated with hydrothermal fluids. For example, Clarke et al. (1993) interpret the results of field, petrologic and geochemical studies to suggest that hydrothermal alteration of fine-grained leucomonzogranites produced the muscovite -leucogranites greisens and associated mineralised centres of the Long Lake prospect. From an evaluation of compositional and mineralogical changes in a zoned greisen, Halter et al. (1996) substantiated the role of fluid–rock interaction in forming the East Kemptville deposit. Elevated concentrations of Bi and Au are a unique chemical signature of the Inglisville greisens, which MacDonald and O'Reilly (1989) associate with the circulation of hydrothermal fluids through the Meguma metasediments proximal to their contact with the SMB. Understanding the solute chemistry of fluid inclusions may provide information that is helpful in resolving the development of these deposits.

Vein deposits (U-Cu-Mn-P-F-Ag)

Whereas greisen deposits tend to occur in Stage 2 plutons, vein deposits of economic interest occur dominantly in Stage 1 plutons. Most of the past-producing vein deposits are within the interior of the batholith, including the New Ross Manganese Mines that are hosted by the Stage 1 Salmontail Lake Pluton. In contract to the greisen deposits, U and Mn are economically significant commodities of vein deposit mineralisation (MacDonald, 2001).

The Millet Brook U-Cu-Ag deposit occurs near a Meguma roof pendant in Lunenburg County. Pitchblende is the dominant ore mineral, but minor chalcopyrite, bornite, covellite, chalcocite, proustite, galena, sphalerite and wolframite also occur (MacDonald, 2001). The en-echelon distribution of the mineralised veins (i.e., ore zones) suggests structural influence. Hematization (i.e., turbid feldspar) and chloritization of biotite are closely associated with some ore-zones,

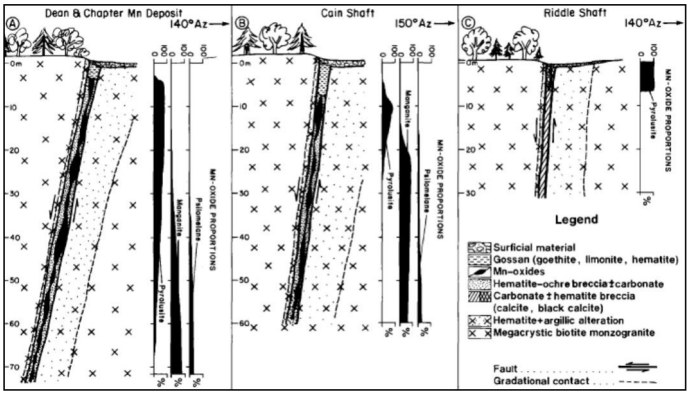

Figure 5 – Cross section schematic of the New Ross Manganese Mines (copied from O'Reilly, 1992). Ore minerals at the Dean & Chapter and Cain & Riddle mines include manganite (MnO(OH), Pyrolusite (MnO_2), Psilomelane ($Ba,H_2O)_2$ Mn_5O_{10}, fluoroapatite $Ca_5(PO_4)_3F$ and manjiroite $(Na,K)(Mn^{4+},Mn^{2+})_8O_{16}.n(H_2O)$.

suggesting that fluid–rock interaction played a role in ore deposition at Millet Brook (MacDonald, 2001).

Similarly, the most pervasive alteration associated with the economic mineralisation at the New Ross Manganese Mines (Mn-Fe-P) is hematization, but desilification, albitization and sericitization are also observed (O'Reilly, 1992). Located near the municipality of New Ross, in Lunenburg County, the New Ross Manganese Mines include the past-producing Cain and Riddle Mine and the Dean and Chapter Mine. At these mine sites, ore bodies occur along steeply dipping faults that are interpreted as being localised along pre-existing structural features (Fig. 5). Several types of hydrothermal alteration have been observed. Hematization and sericitization are well developed in the ore veins, and the co-precipitation of fluoroapatite and Mn-oxides suggests the presence of a phosphate-bearing fluid at low temperature (O'Reilly, 1992). Moreover, and adding pertinence to this fluid inclusion study, O'Reilly (1992) suggested that the alteration sequence at the New Ross Mines could be part of an evolving, and potentially regional, hydrothermal system, which suggests a potential for as yet undiscovered deposits of granophile mineralisation (Smith and Turek, 1976).

Breccia deposits (Pb-Zn-Ba-Au-Ag)

Known SMB breccia deposits (Pb, Zn, Ba, Au, Ag) are spatially restricted to the area proximal to the Tobeatic fault zone (TFZ) in the southwest portion of the batholith, where exploration efforts are hindered by poor outcrop control and metre-scale overburden (Giles, 1985). Extending approximately 8 km in length, and averaging 100 m in width (Giles, 1985), the TFZ coincides with the southern extent of the larger Tobeatic Lake Shear Zone (Horne et al., 1992). Disseminated combinations of galena, sphalerite, barite, chalcopyrite, arsenopyrite and pyrite have been observed in brecciated boulders (MacDonald, 2001). Based on anomalous high concentrations of Zn, Pb, Sn, W and Au in regional till samples, Corey and Horne (1989) suggest the area to be a prime base metal and precious metal exploration target.

Pegmatite deposits (Sn-W-U-Cu-Zn-Ag)

The New Ross Pluton hosts all the reported pegmatite mineral deposits within the SMB, but unmineralised pegmatites are associated

with the East Kemptville deposit, the Gaspereau Lake U-P-F prospect and the Long Lake deposit (MacDonald, 2001, and references therein). Coarse-grained leucomonzogranites and leucogranites host the known pegmatite deposits. Although previous exploration did not indicate a significant resource potential for SMB pegmatite deposits, two known prospects draw particular interest as they have not been subjected to detailed exploration, and thus have unknown economic potential. Firstly, the Keddy Mo-Ta-Nb prospect, hosted in the Keddy-Reeves muscovite-topaz leucogranite, occurs near the boundary between the Stage 1 Salmontail Lake Pluton and the Stage 2 New Ross Pluton. Secondly, the spodumene- and tourmaline-bearing pegmatites of the Brazil Lake prospect are considered to have economic potential for Be and Li (Corey, 1994).

Methodology

Sampling strategy

The objective for this regional-scale research is to obtain a sample set that represents the entire SMB study area. We use a grid system to systematically divide the study area into a number of sampling targets. A 10 x 10 km^2 grid was superimposed on the SMB map pattern (Fig. 6) and an ideal sample set would include one sample from each grid square. However, samples in some grid locations are inaccessible due to poor outcrop exposure due to glacial overburden (e.g., the Scrag Lake Pluton), therefore, grid sampling in principal provides only a general guideline. In some cases, where several rock types occur in a given grid square, a sample of each rock type was collected.

Evaporate Mound Analysis

Indices of Alteration

Characterizing the extent and degree of fluid-rock interaction and locating quartz grains that host abundant fluid inclusions are the objectives of the petrographic work which must be completed prior to evaporate mound analysis. Following identification of alteration assemblages that occur in the study area, the degree or extent of the alteration is qualitatively assessed. Assessment is measured on a nominal scale where a value of '1' represents the lowest degree or extent of alteration and '10' represents an extreme or high degree of alteration. For the SMB appropriate indices include (i) chloritization of biotite, (ii) abundance and type of perthite, (iii) sericitization and (iv) saussuritization (Fig. 7), (v) the abundance of white mica (Fig. 8), and the abundance of fluid inclusions hosted by quartz (Fig. 9).

Preparation of fluid inclusion wafers

The preparation of double polished thick sections requires the cutting and grinding of slab samples into ca. 150 µm fluid inclusion wafers that are bonded to glass slides for petrographic examination. Sections (i.e., chips) that include target mineral grains are cut from the wafer using a fine circle blade appropriate for cutting small centimetre -scale chips. Following the experience from cutting hundreds of sections, we recommend a minimum section size of 1 cm^2 for ease of handling during further processing (Fig. 10).

Mound generation and decrepitation temperature

Published results of other evaporate mound research report a range of decrepitation temperatures (Table 1). However, there are no published reports that assess the effect of decrepitation temperature on mound generation, mound size, and mound composition. To address these issues, we selected a small subset of samples (n = 3) and prepared three chips from each sample for experimental heating. Three temperatures, 325°C, 400°C and 500°C (one grain/sample for each temperature) were selected. In addition we compare results from mounds generated by heating in an oven and a heating-freezing stage. The oven heating rate was 1°C/minute and the stage heating rate was 20°C/minute. The oven is Thermacraft clamshell furnace and the stage

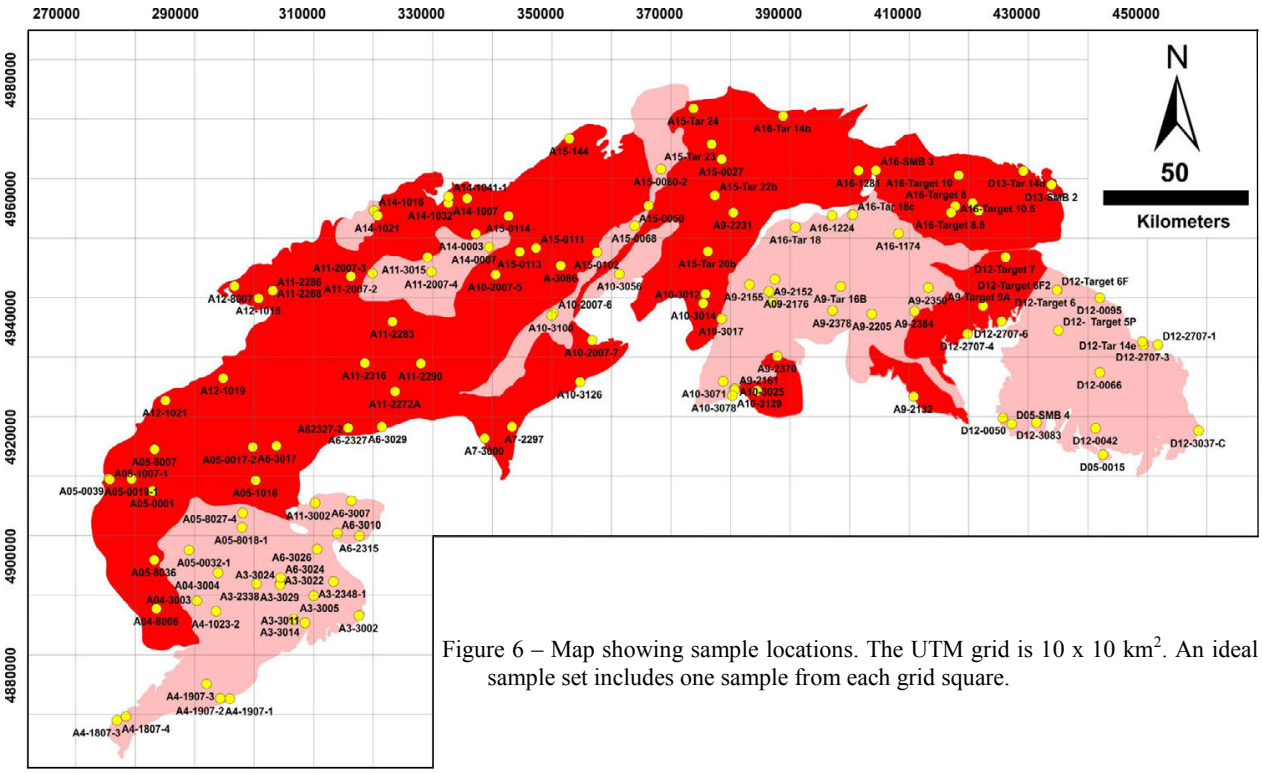

Figure 6 – Map showing sample locations. The UTM grid is 10 x 10 km^2. An ideal sample set includes one sample from each grid square.

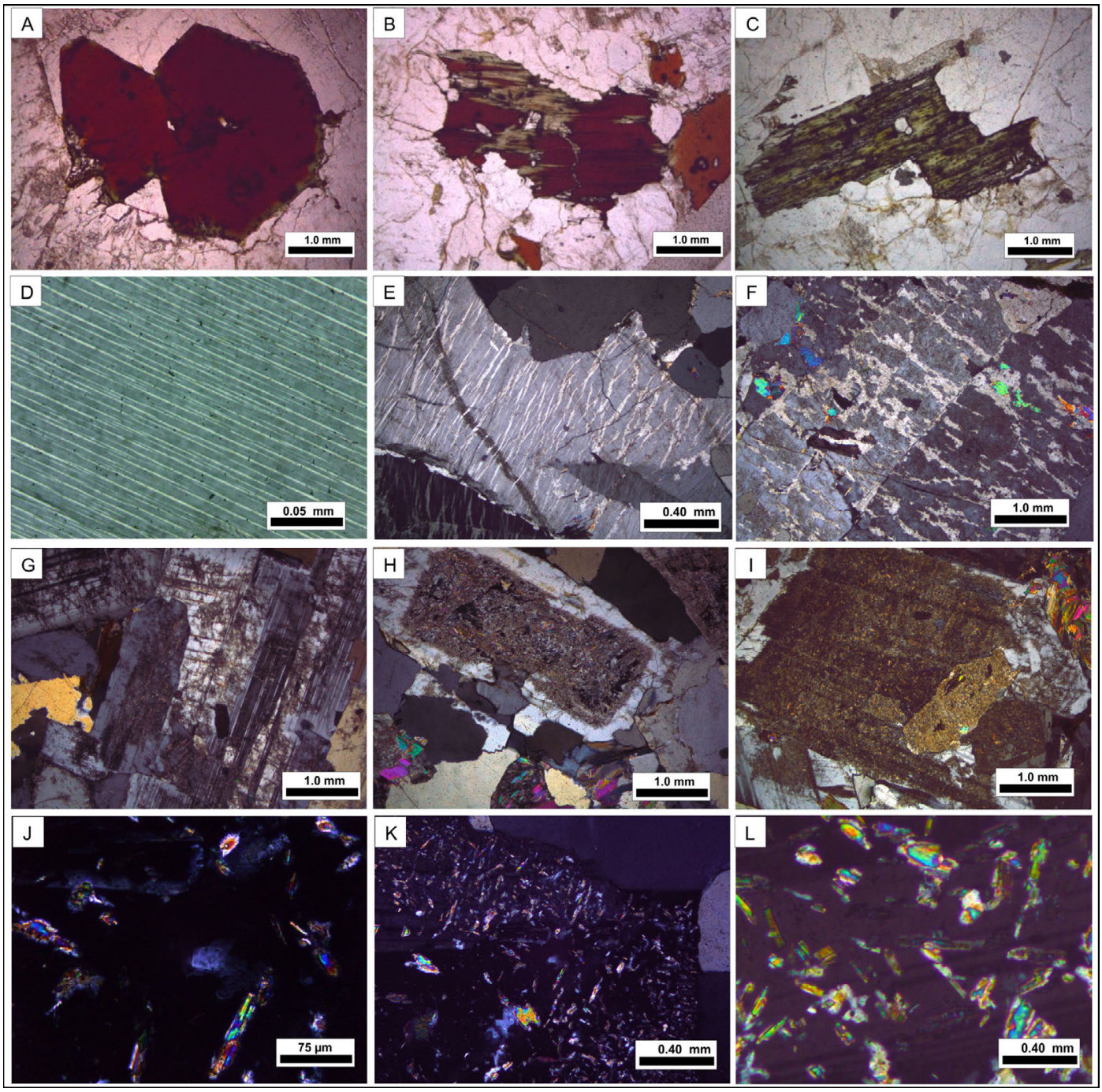

Figure 7 – Photomicrograph images of alteration indices used to determine the degree of fluid–rock interaction in SMB granitoid samples. (A-C) Chloritization of biotite. (D-F) Perthite. (G-I) Sericite. (J-L) Saussuritization. In all four indices, fluid–rock interaction increases from a minimum in the left photomicrograph to a maximum in the right photomicrograph.

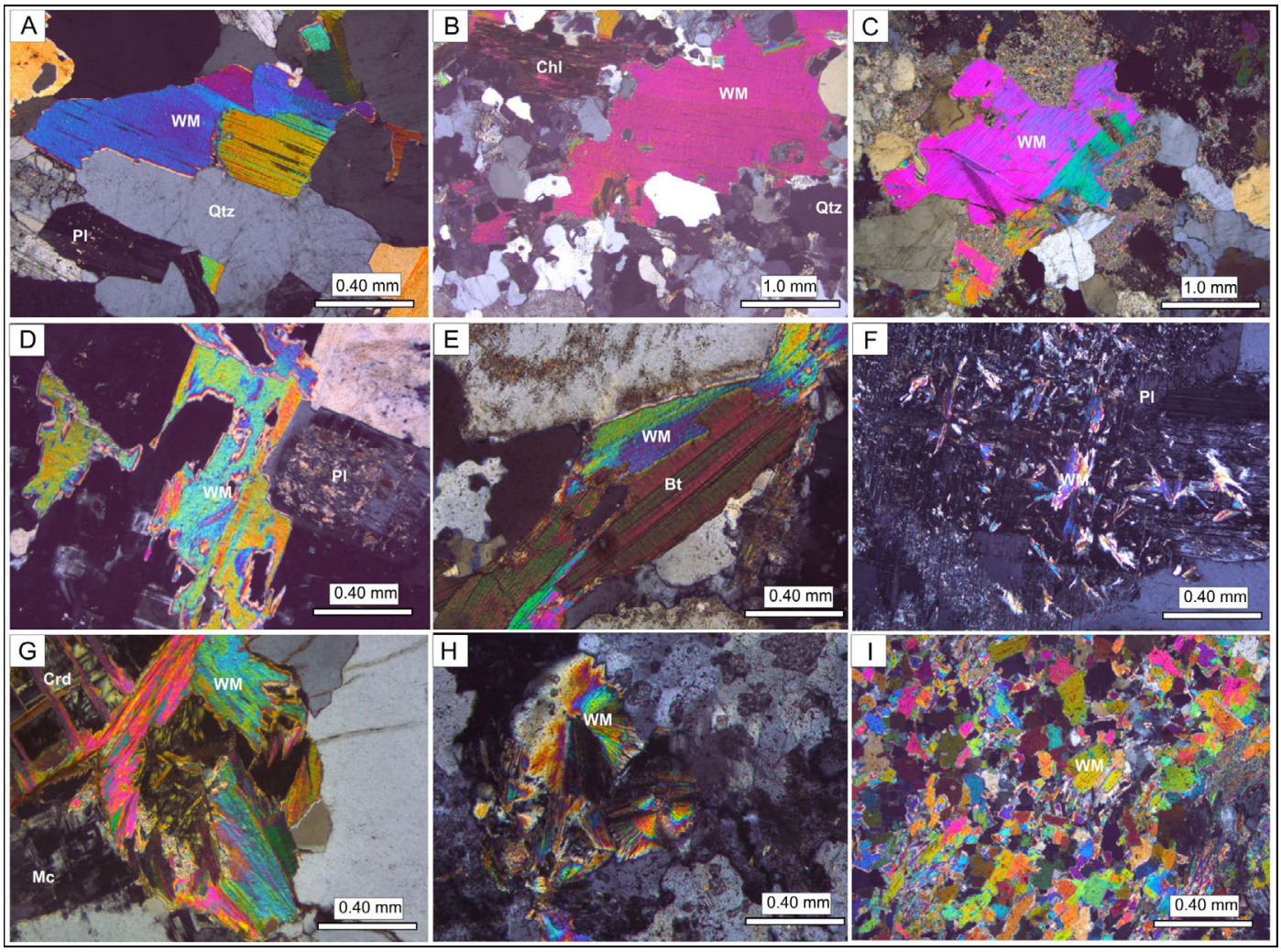

Figure 8 – Photomicrographs of thin sections displaying white mica varieties in SMB granitoid samples. Mineral abbreviations: Crd: cordierite; Mc: microcline; Pl: plagioclase; Qtz: quartz; WM: white mica. (A) Sample LU87-4: coarse-grained, euhedral and equant white mica grain displaying sharp crystal boundaries in equigranular leucomonzogranite. (B) Sample D12-0124-3: coarse-grained, subhedral white mica in quartz matix showing extensive development of sutured grain boundaries and allotriomorphic texture. Biotite grain adjacent to white mica is extensively chloritized. (C) Sample A09-2229: prominent kink in crystal face (001) of coarse-grained white mica that shows extensive sericite alteration along embayed grain boundary. (D) Sample A09-2211-2: white mica overgrowth on alkali feldspar grain. (E) Sample D05-3105: white mica replacing an earlier biotite phase. Note both mica phases share common optical orientation. (F) Sample BILP-3: medium-grained white mica clusters on an earlier plagioclase phase. (G) Sample D05-3105: white mica replacement of cordierite adjacent to microcline. (H) Sample D12-0122-2: clusters of white mica rosettes in altered granite from the Halifax pluton. (I) Sample A15-0008-4: white mica greisens.

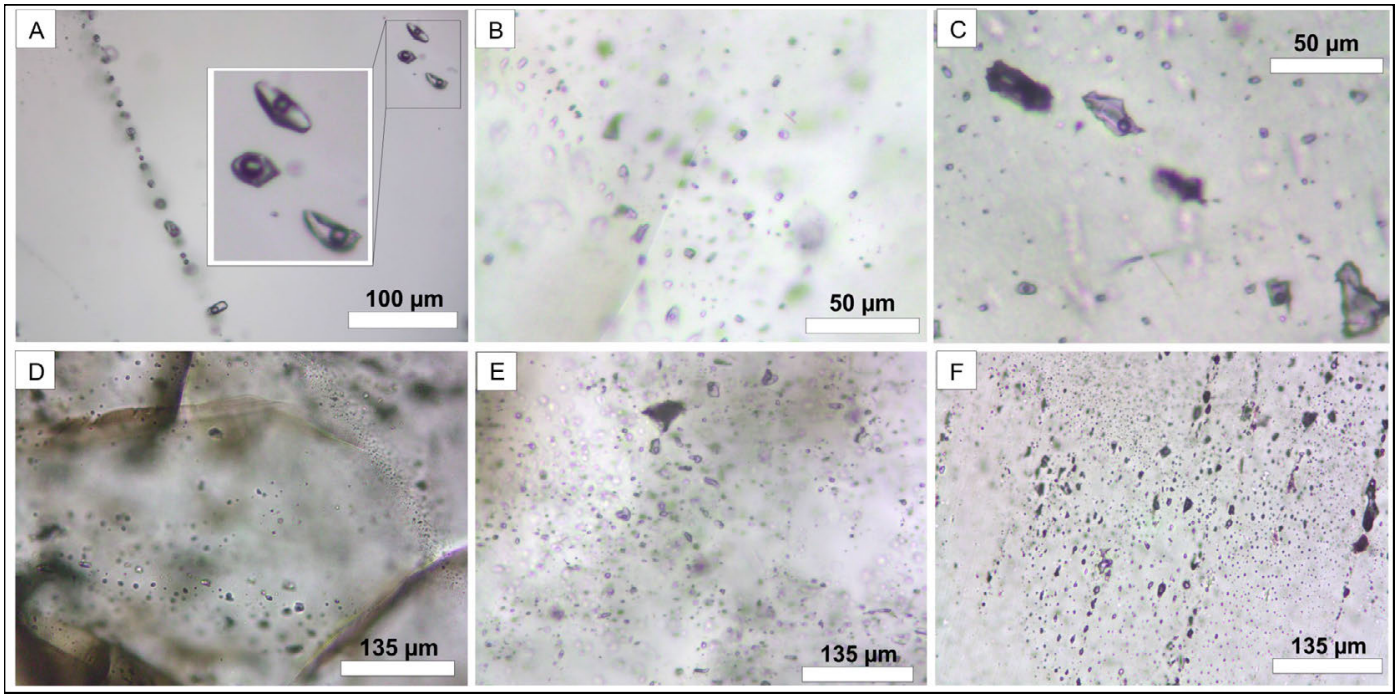

Figure 9 – Photomicrographs of thin sections displaying secondary fluid inclusions in annealed quartz in SMB granitoid samples. (A) Sample A09-0045: two-phase LV-type fluid inclusions forming linear arrays and isolated fluid inclusion assemblages in quartz. (B) Sample A03-3024-2: Inundation of variably-sized two-phase (LV) and monophase (L) fluid inclusions. (C) Sample A04-3004-2: large (15 µm), irregularly-shaped fluid inclusions with common long-axis orientation. (D) Sample A09-3024: fluid inclusion arrays showing orientations that do not coincide with grain boundary orientations. (E) Sample A09-2378: fluid inclusion inundation hosted by quartz in a monzogranite sample from the New Ross pluton. (F) Sample A16-1400: 2-phase (L-V) and monophase (V) fluid inclusions. Note large range in fluid inclusion size.

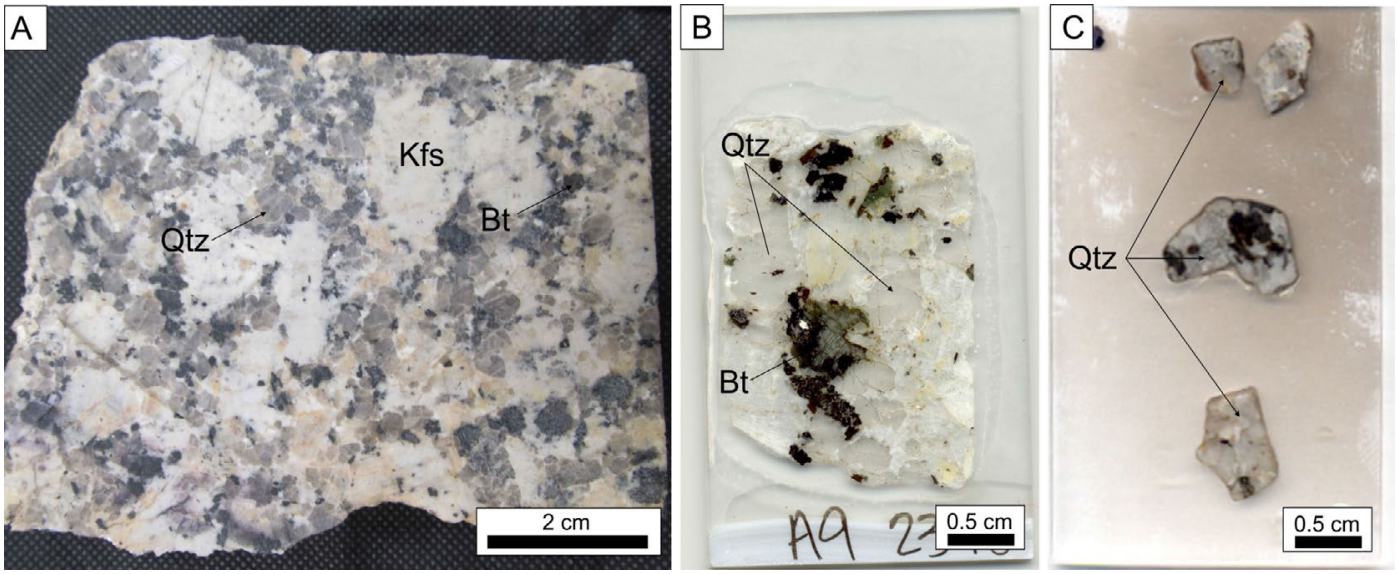

Figure 10 – Preparation of samples for SEM-EDS analysis. (A) A slab sample for each grid square covering the study area is collected. (B) Fluid inclusion wafers are prepared for petrographic evaluation and identifying of targeted fluid inclusions. (C) Chips containing fluid inclusion host mineral, quartz, are cut from wafer and immediately carbon coated (10 – 20 µm veneer). Carbon mitigates charge build-up during SEM-EDS analysis.

Table 1 – Decrepitation temperature ranges used in other evaporate mound research.

Host rock	Host mineral	Dominant fluid inclusion type	Decrepitaion temp. range(°C)	Reference
n/a	*synthetic quartz*	*2-phase L-V*	*360 - 420*	*Haynes et al., 1988*
altered granite, pegmatite, greisen, veins	*quartz*	*L-V, L-V-H, L-V-H-Sylvite*	*350 - 500*	*Kontak 2004*
granitoid	*quartz*	*L-rich, V-rich, L-V, L-V±S, L-V-H*	*400 - 420*	*Carruzzo et al., 2000*
carbonitite	*apatite, calcite*	*L-V, L-V-H*	*400 - 500*	*Samson et al., 1995*
carbonate	*calcite, dolomite, sphalerite*	*not given*	*420*	*Savard and Chi, 1998*
breccia/quartz syenite	*fluorite, quartz, bastnaesite, barite*	*L-V-S, L-V, A-C*	*400*	*Williams-Jones et al., 2000*
quartz-kaolinite breccia	*quartz*	*L-V*	*450 - 600*	*Kontak and Kyser, 2011*
veins hosted in granite	*quartz*	*V-rich, L-rich, L-S, V-S*	*up to 570*	*Chryssoulis and Wilkinson, 1983*
brecciated carbonate	*sphalerite and dolomite*	*not specified*	*325 - 350*	*Haynes and Kesler, 1987*
rhyolite/sedimentary	*quartz*	*L-V*	*350-400*	*Zaw et al., 2003*
vein infill	*quartz, sphalerite*	*L(H_2O-CO_2-CH_4)-S*	*500*	*Walsh et al., 1988*
metasedimentary	*quartz*	*L-V*	*300 - 350*	*Heinrich and Cousens, 1989*

Abbreviations for fluid inclusion types: aqueous-carbonic, A-C; halite, H; liquid, L; solid, S; vapour, V.

is a Linkham MDS600 heating –freezing stage mounted on a standard petrographic microscope stage. Following decrepitation, all samples are immediately carbon coated and stored in a desiccation chamber until taken to the SEM.

SEM-EDS operating conditions and acquisition time

The LEO 1450VP SEM used in this study was operated with a tungsten filament saturated at 3.2-3.3 A, an accelerating voltage of 25 keV and a working distance range of 17 to 21 mm. The SEM imaging system is equipped with an Oxford Instrument INCA X-max 80 mm^2 silicon drift detector (SDD) EDS analyser linked to a desktop computer (INCA software). In this experimental study, point mode was used to analyse small (i.e., < 5 µm diameters) mounds, and raster mode used to analyse large, irregularly shaped mounds. Results obtained using point and raster modes are reported here. A 60 second acquisition time was used for all analyses. However, in an effort to determine maximum efficiency with the technique, we collected EDS data using a range of acquisition times (5, 10 and 30 second) to assess the effect of run time on results. In this sample, six mounds were analysed three times using 5, 10 and 30 second acquisition times. Thirdly, and again to maximize the technique's efficiency, we conducted analyses to investigate how to determine the minimum number of samples required to obtain results that represent the actual solute composition (s) of a fluid inclusion population. The number of analysis required to collected representative data is assessed by comparing results collected from samples for which we analyse 4, 8, 16 and 32 evaporate mounds.

SEM-EDS instrument calibration and synthesis of standards

To assess the performance of the EDS detector, we synthesized and analysed a series of salt standards. Standards are synthesized with salts composed of the major cation and anion species identified in mounds analysed during preliminary testing (i.e., mounds generated for evaluation of decrepitation temperature). To prepare synthetic salts, laboratory-standard NaCl and fluorite crystals were crushed and hand mortared to a very fine granular texture. Next, salt compounds were mixed to form a simple series of ratios that range from pure NaCl and pure fluoride salt (Table 2). Ideally, the matrix effects associated with these compounds chosen to make the synthetic mounds are similar to the matrix effects associated with evaporate mounds in SMB samples. In this study, F, Na, Cl, K and Ca are major solute species, and we corrected EDS data for F, Na, Cl and Ca using calibration curves constructed from the analysis of standards (Fig. 11).

Results

Petrography

Extent and degree of fluid–rock interaction in the South Mountain Batholith

To some extent, alteration assemblages occur in all SMB samples examined in this study. Petrographic observation of hundreds of SMB

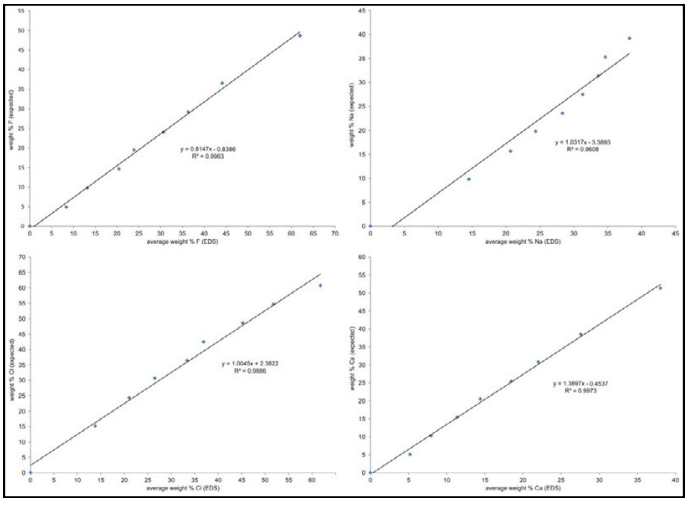

Figure 11 – Calibration curves for major cation and anion species in SMB mounds.

Table 2 – Composition of synthetic mounds. The compositional range of salt standards includes the expected compositional range of major solutes in evaporate mounds formed by decrepitation of fluid inclusions hosted in samples from study area.

Standard label	Mass (g)			Weight (mg)					Weight %				
	NaCl	CaF_2	Total	Na	Cl	Ca	F	Total	%Na	%Cl	%Ca	%F	Total
0	0.101	0.000	0.101	39.63	61.37	0.00	0.00	101.00	39.24	60.76	0.00	0.00	100.00
10	0.090	0.010	0.100	35.32	54.68	5.13	4.87	100.00	35.32	54.68	5.13	4.87	100.00
20	0.080	0.020	0.100	31.39	48.61	10.27	9.73	100.00	31.39	48.61	10.27	9.73	100.00
30	0.070	0.030	0.100	27.47	42.53	15.40	14.60	100.00	27.47	42.53	15.40	14.60	100.00
40	0.060	0.040	0.100	23.55	36.45	20.53	19.47	100.00	23.55	36.45	20.53	19.47	100.00
50	0.051	0.050	0.101	20.01	30.99	25.67	24.33	101.00	19.82	30.68	25.41	24.09	100.00
60	0.040	0.060	0.100	15.70	24.30	30.80	29.20	100.00	15.70	24.30	30.80	29.20	100.00
75	0.025	0.075	0.100	9.81	15.19	38.50	36.50	100.00	9.81	15.19	38.50	36.50	100.00
100	0.000	0.101	0.101	0.00	0.00	51.85	49.15	101.00	0.00	0.00	51.33	48.67	100.00

thin sections, it is known that alteration in SMB granitoids ranges from essentially unaltered samples (Fig. 12) to pervasively altered samples (Fig. 13). However, location data for samples in the western half of the batholith is not preserved, so mapping of petrographic data is limited to the eastern half of the batholith (Fig. 14). Several general patterns emerge from this data. Firstly, fluid inclusions occur in abundance throughout the batholith. Secondly, perthitic feldspar is much more abundant as patch perthite as compared to film and flame perthite. Thirdly, saussuritization, or the replacement of plagioclase by epidote occurs in much lower abundance than sericite (replacement of feldspar by clay minerals.

Evaporate Mound Analysis

Decrepitation temperature

The number of mounds generated during three oven heating runs at 325°C, 400°C and 500°C suggests a 500°C decrepitation temperature is preferable for mound generation. Within the experimental temperature range, mound size is largest in samples heated to 500°C and smallest in samples heated to 325°C (Fig. 15A) Further, results demonstrate that decrepitation temperature does not impact composition of evaporate mounds (Fig. 15B). The shape (i.e., morphology) and chemical diversity of mounds generated through the oven-decrepitation of SMB samples is displayed in Fig.16.

Oven versus stage heating and acquisition time

Decrepitation of chips from two samples (A09-2378 and A09-2370), using both oven and stage heating, produced Na-K rich mounds (Fig. 17). The median concentrations of Na, Cl and K in mounds generated by both methods in sample A09-2370 are comparable. However, the median concentration of Na, Cl and K in mounds in sample A09-2378 are consistently higher in stage-generated mounds.

Two important results emerge from the preliminary assessment of EDS analysis collected using 5, 10 and 30 second acquisition times. Firstly, the number of major solute species detected increases with acquisition time. The EDS signals for 5 second acquisition time includes four major solute species (F, Na, Cl and Ca), whereas 10 and 30 second acquisition times detected five major solute species (F, Na,

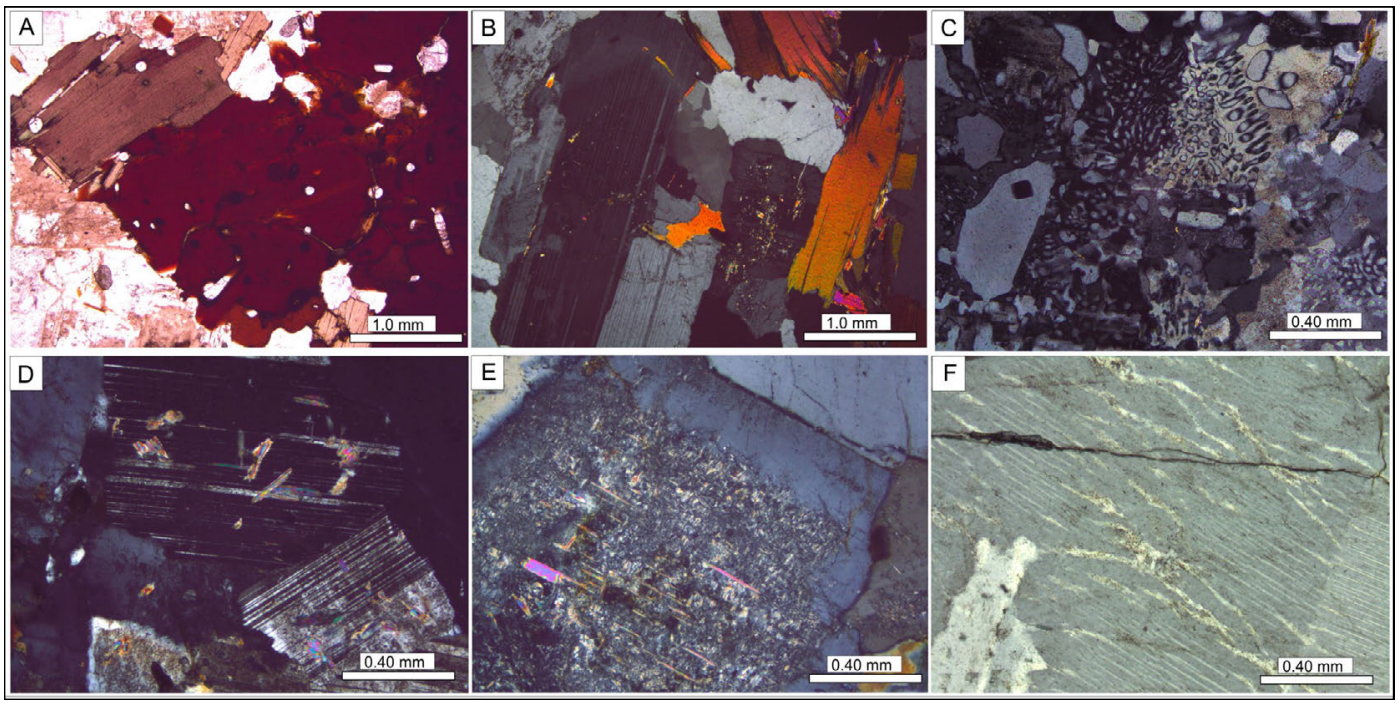

Figure 12 – Photomicrograph images of textures in unaltered SMB granitoids. (A) Sample D13-2-8-10: glomeroporphyritic texture defined by fresh reddish-brown biotite grains displaying numerous apatite inclusions. (B) Sample D13-2004: hypidomorphic granodiorite displaying coarse-grained (>0.5 mm), euhedral, tabular, zoned plagioclase phenocryst with incipient sericitization. (C) Sample D12-0121-1-C: pervasive graphic texture defined by blebby intergrowths of quartz and feldspar of inequigranular leucogranite consisting of fine- to medium-grained matrix minerals and coarse-grained unaltered quartz. (D) Sample A09-2095: incipient saussuritization and partial sericitization in euhedral plagioclase in holocrystalline granodiorite. (E) Sample D12-3074: seritization of zoned euhedral plagioclase displaying incipient muscovite development along cleavage planes. Note fluid inclusion trails hosted in along fracture planes in adjacent coarse-grained quartz. (F) Sample D05-0015: orthoclase megacryst displaying film and flame perthite.

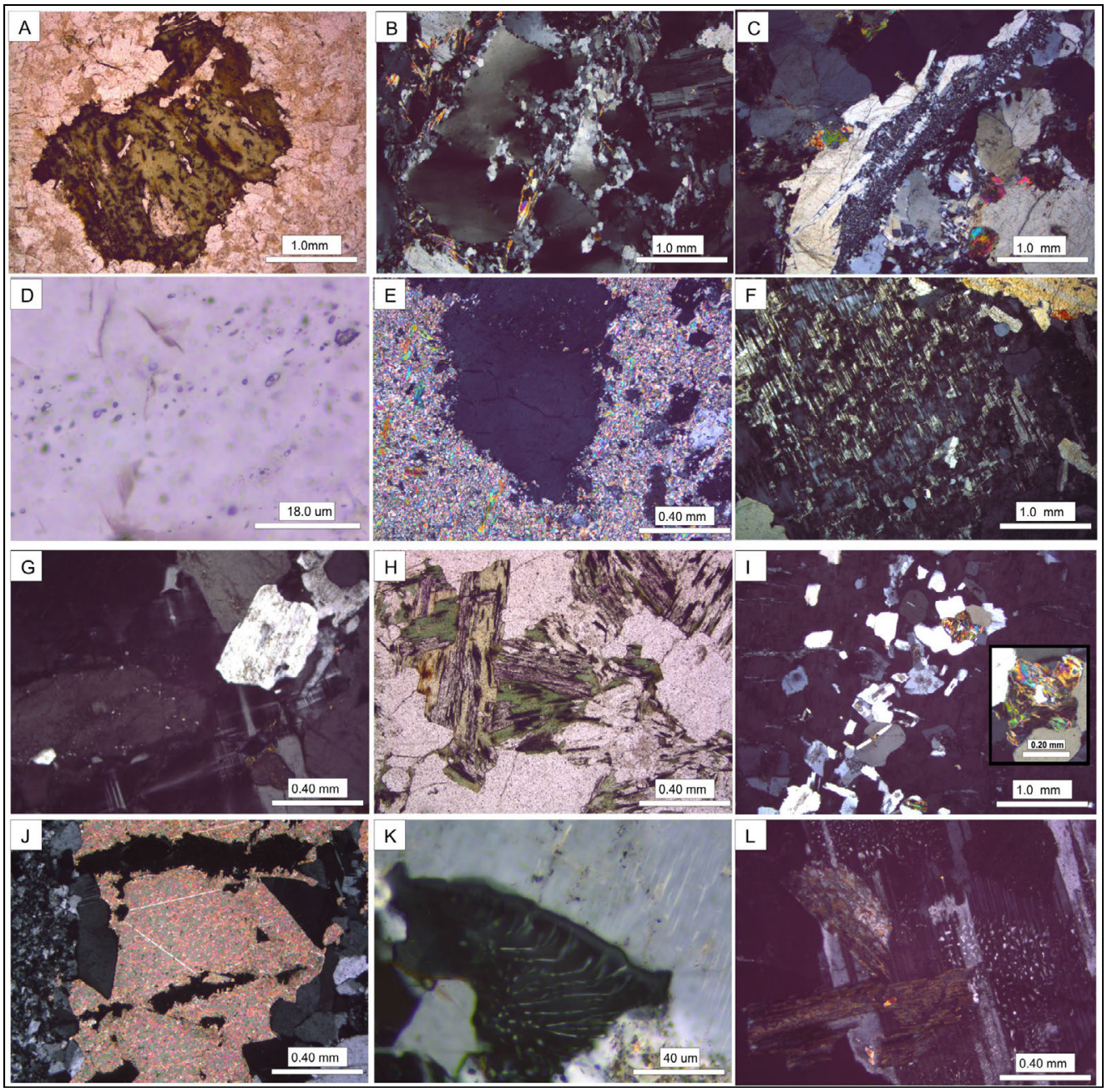

Figure 13 – Photomicrographs of thin sections of pervasively altered SMB granitoid samples. (A) Sample D13-2065. Extreme chloritization of biotite with abundant fine-grained opaque inclusions. Note sericitization of adjacent feldspar. (B) Sample A04-1054: Porphyritic granitoid displaying coarse-grained quartz phenocrysts with undulose texture and medium-grained plagioclase phenocrysts displaying kinked polysynthetic twin planes. Interstitial space filled with secondary fine-quartz grains and white mica. (C) Sample A09-2141: Fine-grained quartz grain filling fracture between quartz and feldspar phenocrysts. Quartz grain clearly inundated with fluid inclusions and graphic textures matrix displays pockets of white mica. (D) Sample A09-2141: high magnification photomicrograph of quartz-hosted fluid inclusions in hydrothermally altered granite. Inclusions are predominately 2-phase types with a liquid/vapour ratio of 95/5. (E) Extreme hydrothermal alteration texture. Primary feldspar components are hydrothermally altered, which results in crystallisation of fine-grained epidote and white mica. (F) Corse-grained perthitic feldspar displaying patchy albite and orthoclase. (G) Microcline domains adjacent to adjacent to subhedral quartz and feldspar grains in hypidomorphic granitoid. (H) Sample D12-0113-2: Chloritization of biotite glomerocryst and inundation of fluid inclusions through all mineral phases evidenced by dusty texture. (I) Sample D12-3071: Coarse-grained poikilitic feldspar with blebby quartz inclusions and sparse pinitized cordierite (inset). (J) Euhedral fluorite (isometric) grains ingrown with calcite (high relief) in pervasively altered granitoid. (K) Sample D12-0039. Myrmekitic texture with fine-grained vermicular quartz included in plagioclase adjacent to alkali feldspar. Note flame perthite in feldspar. (L) Sample D12-0113-1. Myrmekitic texture in albitic plagioclase defined by vermicular intergrowths of quartz. Note also the chloritized biotite intergrown into the plagioclase.

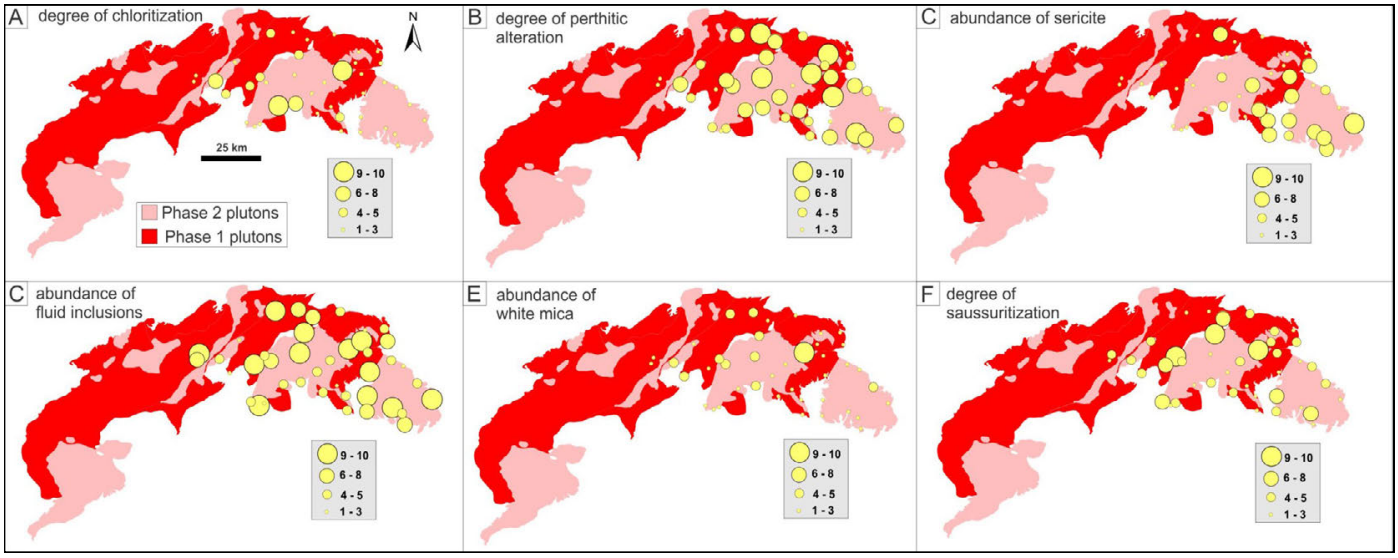

Figure 14 – Proportional symbol plot showing distributions of hydrothermal alteration textures in SMB granitoids. (A-F) Proportional circle sizes represent the degree of alteration assemblages and the abundance of sericite, white mica and fluid inclusions. Scales are qualitative (no units) and grouped into three categories: minimal alteration (1-4), moderate (5-7) and pervasive (8-10).

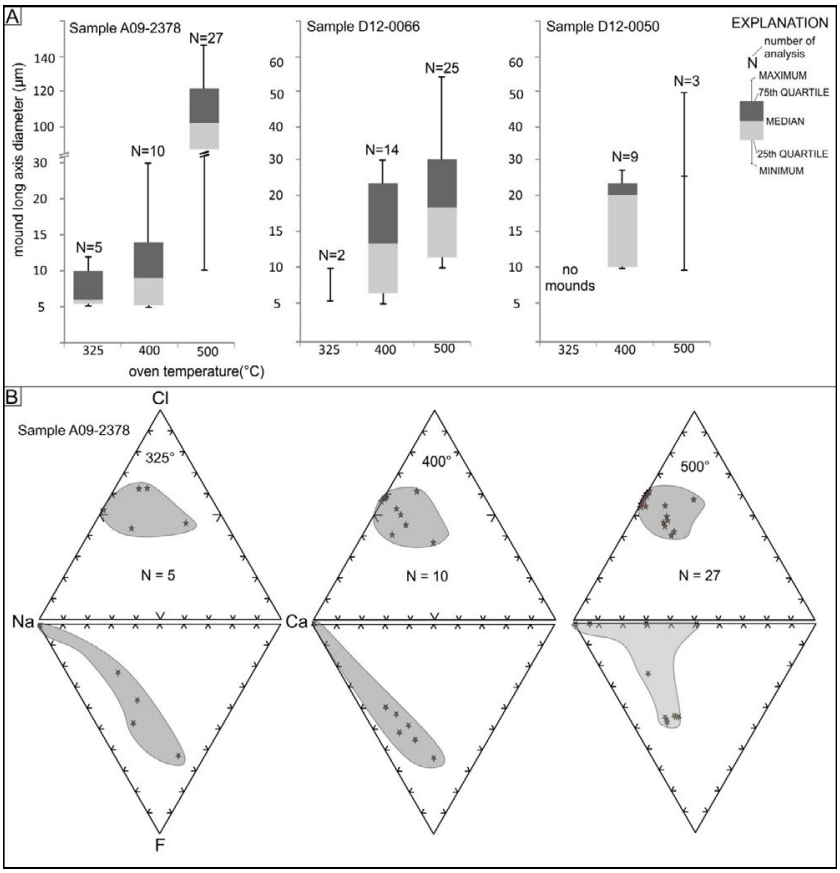

Figure 15 – (A) Box and whisker plots of observable mound size versus decrepitation temperature. The important observation is that the mounds generated by heating quartz grains to 500°C are larger and more abundant than mounds generated at 325°C and 400°C. (B) Ternary plots of major cation species concentration (normalised wt%) in mounds generated by heating to 325°C, 400°C and 500°C. The important point is that mound composition is unaffected by decrepitation temperature.

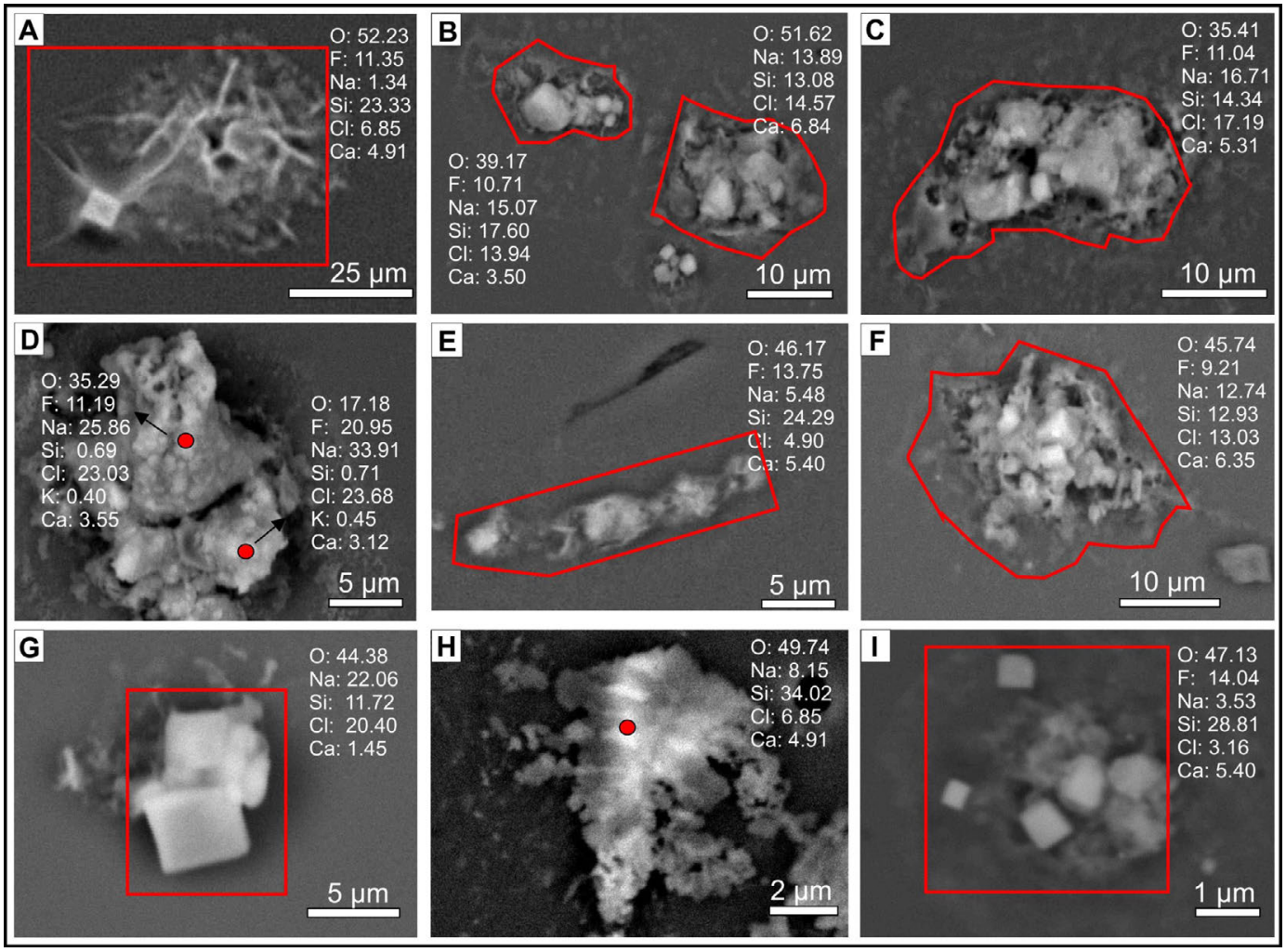

Figure 16 – Evaporate mounds generated through decrepitation (500°C) of SMB fluid inclusions hosted by quartz. (A – I) Chemical composition of mounds analysed in raster mode (outlined by red boxes) or point mode (red dots). Units for chemical composition are atomic concentrations in mound (normalised to 100%).

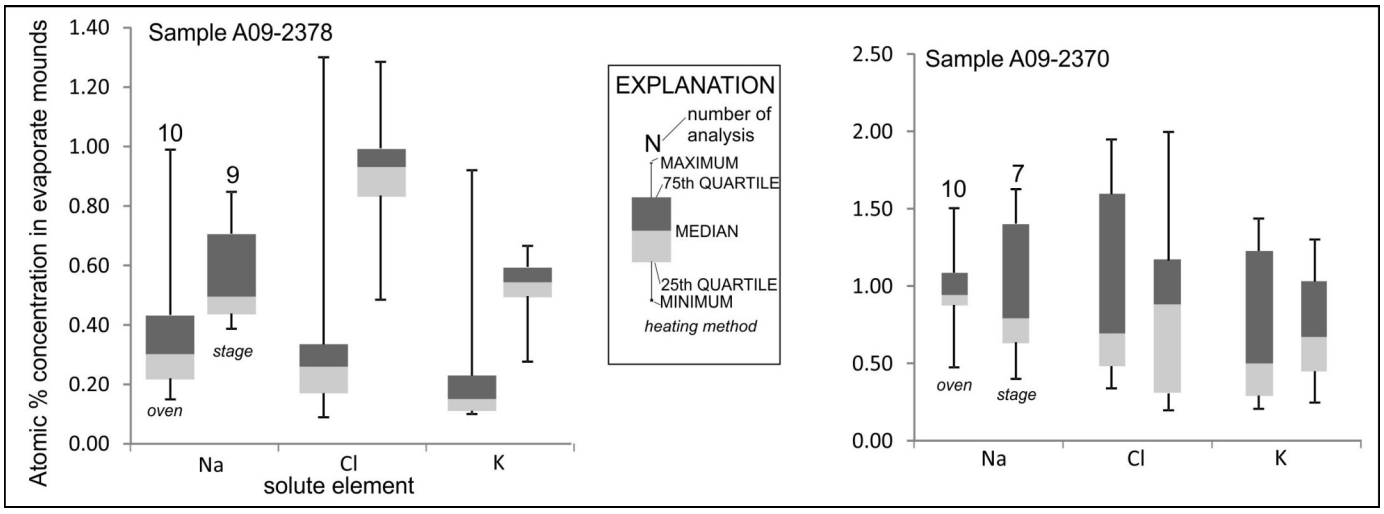

Figure 17 – Box plots comparing results from EDS analysis of oven- and stage-heated samples. The number of Na-Cl-K mounds generated by these methods is comparable, suggesting that heating rate does not have an effect on mound generation.

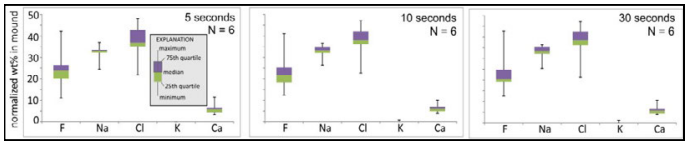

Figure 18 – Box plots of major solute concentration versus EDS acquisition time. Concentrations of major solute species in mounds EDS data generated using 5, 10 and 30 second run times are consistent.

Cl, K and Ca). Secondly, the concentrations of major solute species in the results for 5, 10 and 30 second acquisition times are consistent (Fig.18).

Calibration for major solute species

An assessment of default-calibrated data and custom-calibrated data are shown in Fig. 19. Comparing the two data sets reveals a distinct trend: default EDS settings result in an over-reporting of fluorine and sodium, and an under-reporting for chlorine and calcium. The discrepancy between default- and custom-calibrated data is greatest in F and Ca.

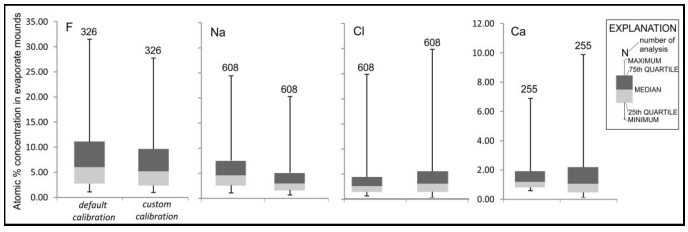

Figure 19 – Box plots of element concentration in evaporate mounds for major solutes in SMB quartz-hosted fluid inclusions. The EDS analyser used in this research, a correction needed to be applied due to an overestimation of F and Na and an under estimation for Cl and Ca.

Number of analyses

From the assessment of results obtained from two samples in which 4, 8, 16 and 32 mounds were analysed, there is consistent number of major solute species detected. The concentration range of major solute species however does vary with number of analysis. However, this variation shows no consistent pattern in F, Na and Cl. However, the median values and range in Ca concentrations appears to be less variable than other major solute species (Fig. 20).

Raster vs. point analysis

Two important points emerge from assessing EDS data obtained from raster- and point-mode analysis of evaporate mounds. Firstly, both point-mode analyses substantiate mound heterogeneity (Fig. 21) Point analysis reveals that the solute composition of mounds is not uniform as elements tend to concentrate in discrete domains within the mound. Secondly, point mode analysis reveals elements that are not detectable in raster analysis (Fig. 22). Although multiple point analyses can provide average compositions for major solute species that are comparable to raster analysis results (Fig 22), minor solute components (e.g., S) may not be detected. In addition, X-ray maps reveal that sodium chloride and calcium fluoride salts are the dominant salt compounds in SMB decrepitate mounds (Fig. 23).

Identifying different fluids

Following screening of the initial data set for internal consistency, 517 good mound analyses were retained for further analysis. Of these, 133 are from Phase 1 samples (n = 20) and 384 are from Phase 2 samples (n = 46). The chemical composition of Phase 1 pluton fluid inclusions is clearly dominated by F-Na-Cl-Ca fluid. In addition, Phase 1 pluton samples host fluid inclusions that contain trace concentrations of S, Zn, Fe, Mo and V (Fig 24A). Conversely, the chemical composition of Phase 2 pluton fluid inclusions include two populations: a Na-K fluid and a F-Na-Cl-Ca fluid. Phase 2 pluton hosted fluid inclusions carry trace concentrations of S, F, Mo, Mn, Sn and Yb (Fig. 24B).

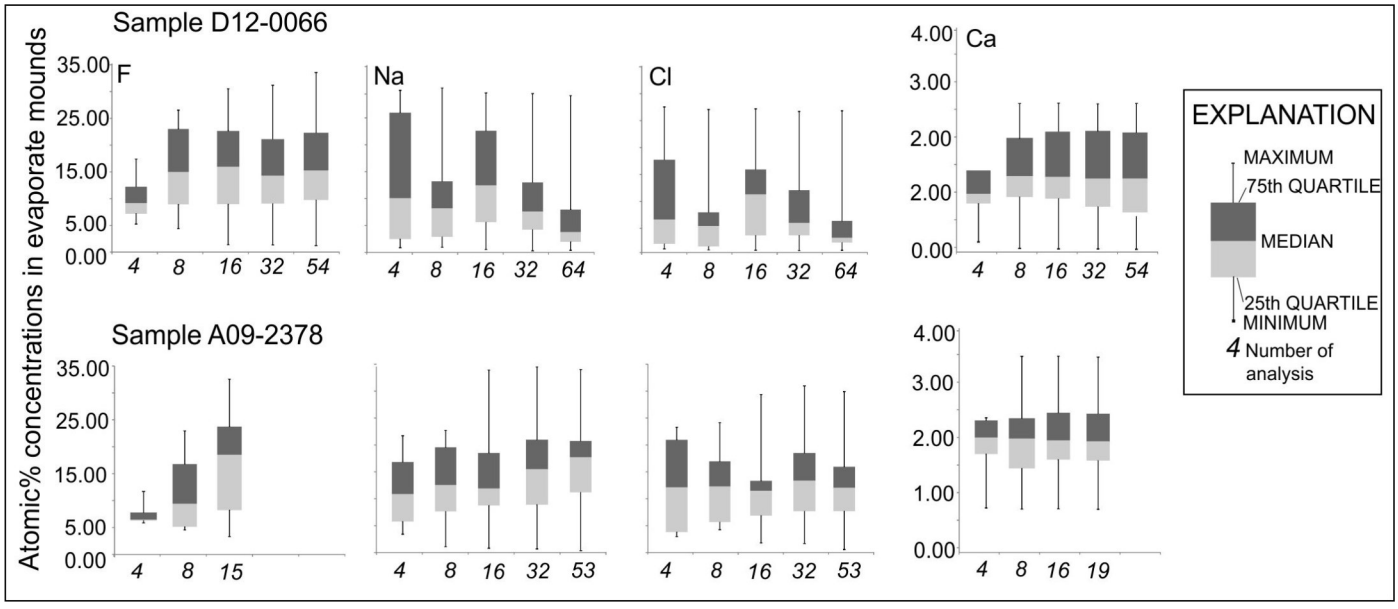

Figure 20 – Box plots of major element concentrations in mounds verses number of analysis.

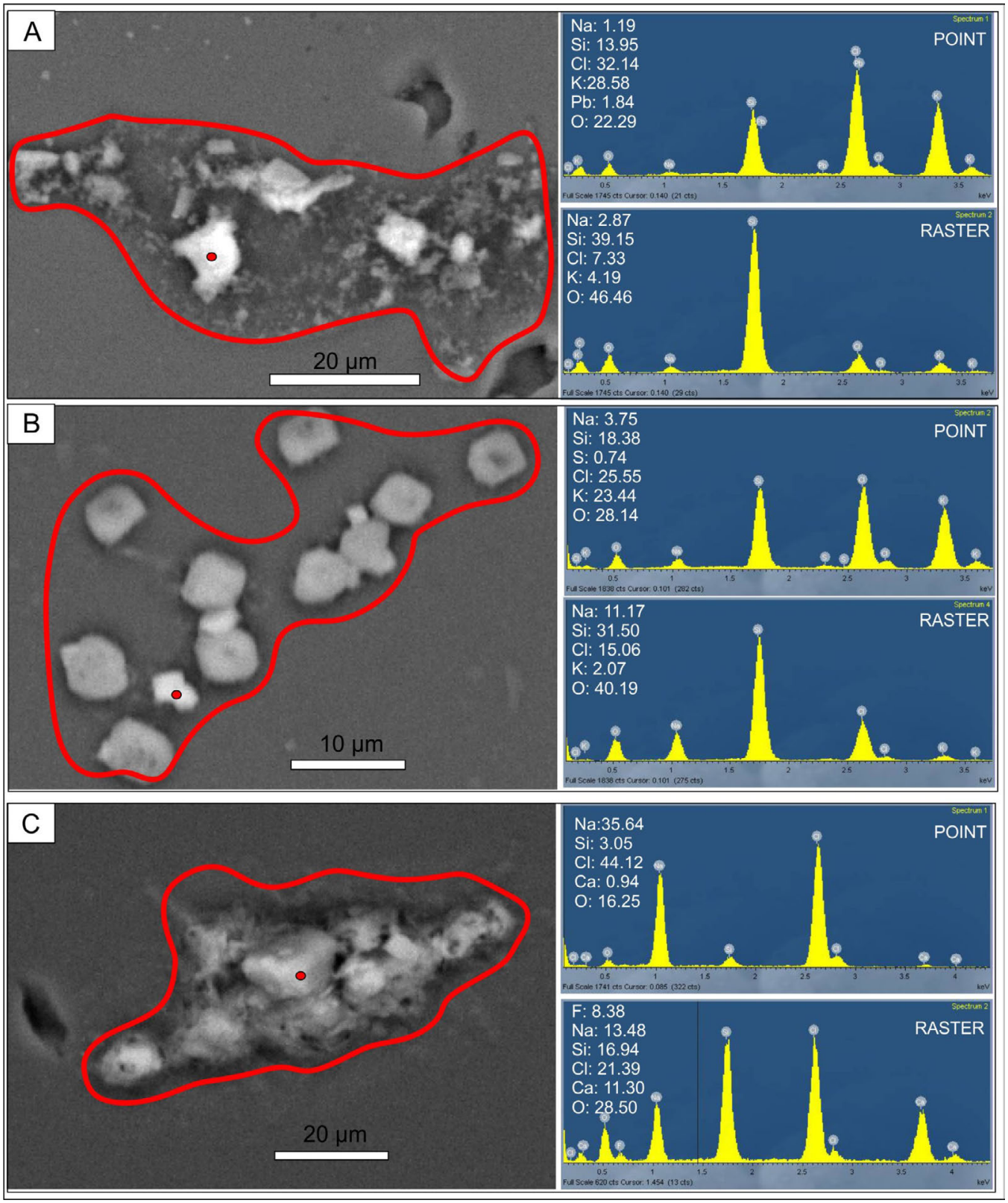

Figure 21 – Backscattered electron (BSE) images of evaporate mounds and corresponding EDS signals. (A) Na-Cl-K rich mound piled next to empty vugs (i.e., evacuated fluid inclusion pit). Point analysis histogram also reveals presence of lead decrepitate. (B) Cubic-shaped Na-Cl rich evaporate mounds. Point analysis reveals presence of sulphur residue. (C) F-Na-Cl-Ca rich evaporate mound. Note that presence of F and Ca is not resolved in point analysis. Elemental abundance for solute species in mounds in atomic concentrations.

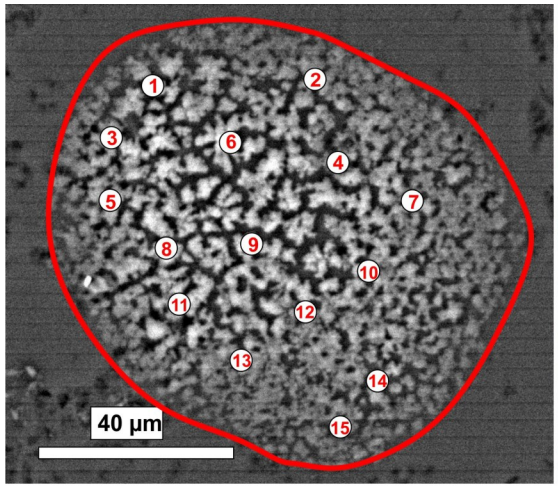

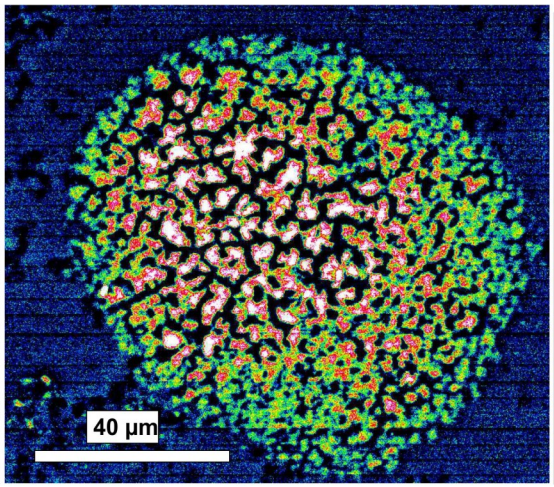

Point	O	Na	Si	Cl	K	Ca
1	66.08	2.85	29.71	1.21	0.15	
2	60.69	6.48	27.20	4.49	1.14	
3	46.95	14.88	29.05	8.83	0.30	
4	58.62	6.53	31.24	3.61		
5	53.08	6.70	33.31	5.33	1.59	
6	47.81	14.74	26.83	9.93	0.70	
7	50.40	16.08	23.76	8.92	0.63	0.21
8	58.59	4.80	34.17	2.44		
9	48.79	11.82	32.22	6.86	0.32	
10	43.92	13.65	34.07	7.83	0.53	
11	41.25	15.18	33.31	9.82	0.44	
12	47.13	15.81	27.34	9.00	0.54	0.18
13	56.65	10.32	27.46	5.57		
14	51.46	16.90	22.16	9.14	0.35	
15	53.50	10.86	28.93	6.41	0.30	
Average	52.33	11.17	29.38	6.63	0.47	0.03
Raster	53.19	11.73	28.61	6.10	0.38	

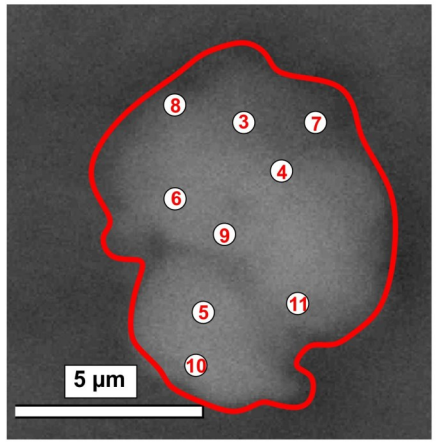

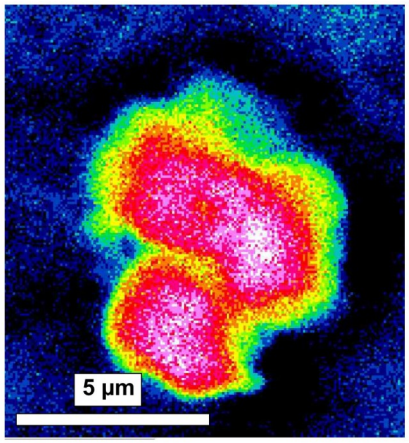

Point	O	F	Na	Al	Si	S	Cl	K	Ca	Cu	Pb
3	30.99	19.01	20.15		13.02	0.09	14.47		2.27		
4	29.51	17.00	25.32	0.15	9.31		16.45		2.26		
5	40.28	10.50	23.35		10.22	0.06	14.48	0.05	1.06		
6	27.07	14.76	27.39		10.94		18.35		1.49		
7	40.08	14.25	10.57		22.19		10.23		2.51	0.16	
8	38.23	19.69	14.42		16.31	0.13	9.36		1.86		
9	32.77	20.68	20.38		12.09	0.13	12.03		1.93		
10	39.21	16.62	16.45		9.57		7.98		1.06		
11	40.47	11.42	14.14		20.18		11.51		2.20		0.07
Average	35.40	15.99	19.13	0.02	13.76	0.05	12.76	0.01	1.85	0.02	0.01
Raster	36.79	15.96	19.38		13.92		12.32		1.64		

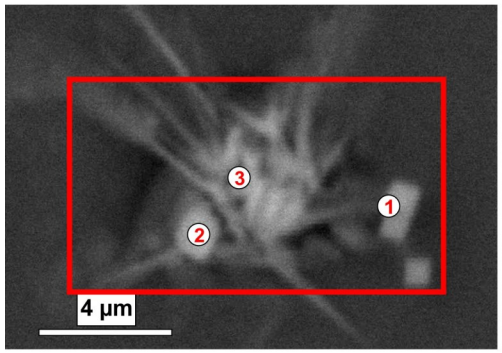

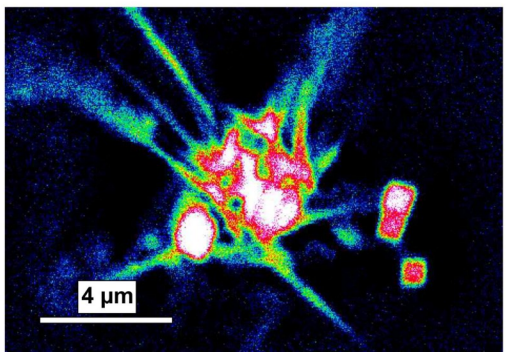

Point	O	F	Na	Si	S	Cl	Ca
1	52.21	7.53	9.3	23.86	0	5.87	1.23
2	22.73	16.24	16.38	26.94	0.41	13.21	4.08
3	30.61	23.61	8.58	24.78	0	7.24	5.18
Average	35.18	15.79	11.42	25.19	0.14	8.77	3.50
Raster	40.04	21.06	2.63	30.29		2.28	3.7

Figures 22 – Backscattered electron (BSE) images (grey scale and false-colour scale) of evaporate mounds and corresponding EDS data. Note that heavier (i.e., metallic) solutes are readily imaged using this technique, and EDS point mode provides better resolution of minor solute components compared to raster mode. Mound compositions and point analyses given in atomic concentrations.

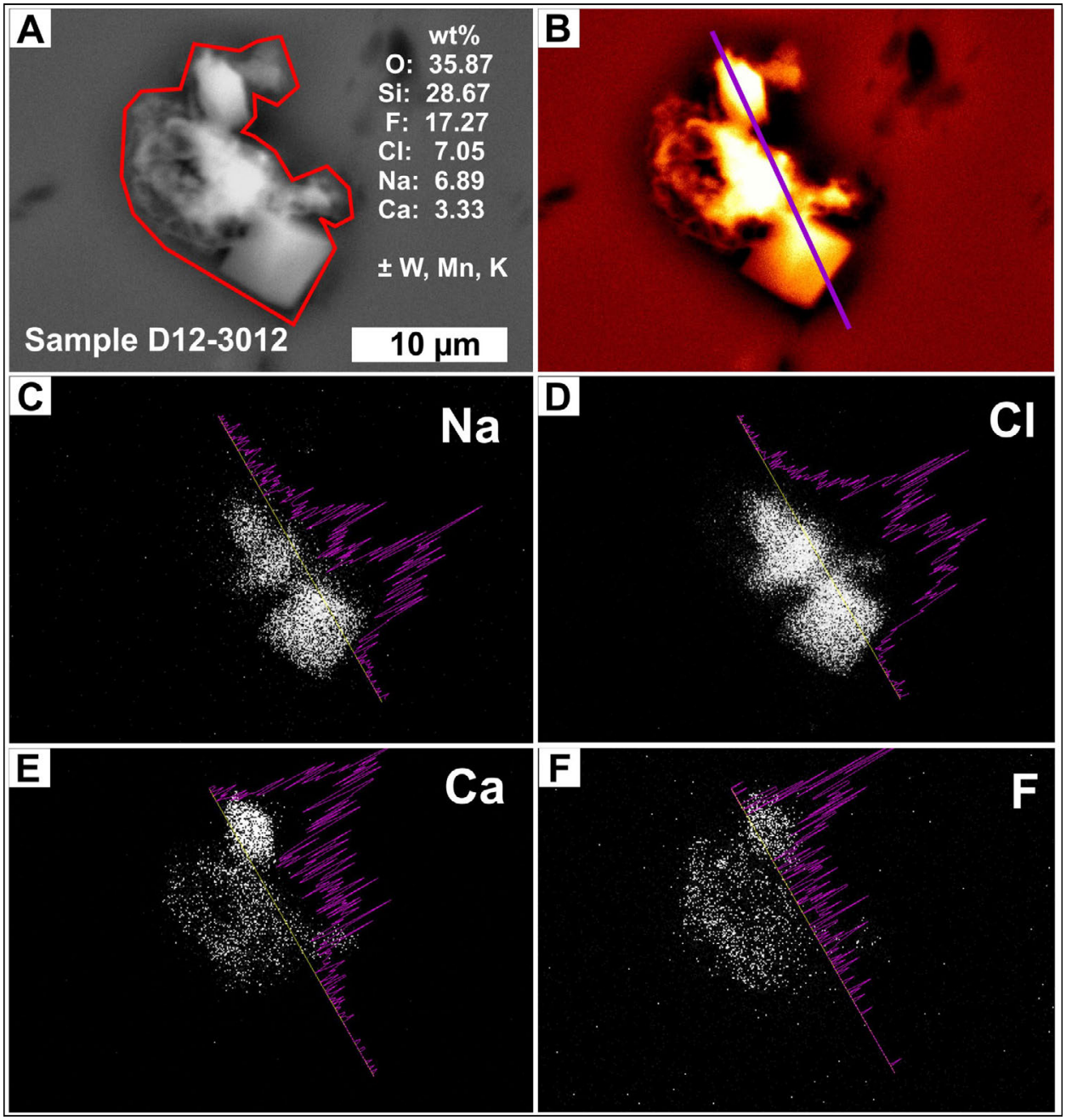

Figure 23 – BSE image and X-ray map analysis of evaporate mound. (A) BSE image of evaporate mound showing raster area in red outline. (B) False-colour BSE image of evaporate mound showing X-ray transect. (C-D) X-ray maps of sodium and chlorine. Light-coloured (i.e., bright) areas correspond to areas of high concentration of corresponding element. (E-F) X-ray maps of calcium and fluorine. These images show the chemical composition of salt compounds that compose evaporate mounds.

Discussion

In-situ fluid inclusion composition analysis

All magmatic-hydrothermal mineral deposits share a common history, which includes magma fractionation, evolution of an aqueous, multi-component fluid phase, partitioning of the fluid phase, fluid migration into new T-P-X environments, and eventual precipitations of metals. Evaluating the chemistry of magmatic-hydrothermal fluids is useful for understanding mineral crystallisation if the bulk solute composition of the mineralizing fluid(s) is accurately determined. Evaporate mound analysis is a unique analytical technique because it permits in-situ solute characterization of the mineralizing fluids preserved as fluid inclusions in rock-forming minerals. Furthermore, this method resolves the presence of different fluids within single coarse-grained quartz by analysing solutes in evaporate mounds formed during the decrepitation of variable-sized (i.e., 1 to >30 µm long-axis diameters) fluid inclusions in a cost-effective and time efficient manner.

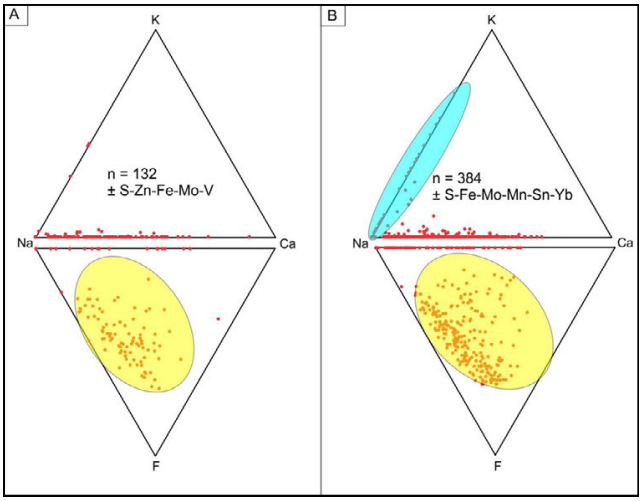

Figure 24 – Ternary plots of SMB fluid inclusion solute compositions. (A) Phase 1 fluid inclusions compositional data. A fluid inclusion population consisting of F-Na-Cl-Ca highlighted. (B) Phase 2 fluid inclusion compositional data. Two fluid inclusion populations highlighted: one consisting of Na-K and another consisting of F-Na-Cl-Ca.

Significance of resolving fluid compositions

The SEM-EDS methodology described herein resolves the solute composition of fluid inclusions using simple and effective analytical procedures. The results produced from the analysis of SMB quartz-hosted fluid inclusions in this study provide average solute compositions for a large number (n = 66) of samples. These data record the presence of elevated Ca, including those from the chemically evolved, therefore calcium-depleted, rocks, and the pervasive occurrence of fluorine in samples that are distal to any known mineralisation. The Ca-bearing fluid may be considered to reflect the petrographic observation of extensive albitization of plagioclase, which occurs in all samples. This alteration process could involve a coupled dissolution-precipitation reaction (which leaves a distinctive pitted texture in the altered the feldspar and liberated calcium to the fluid (Putnis, 2002). The process is attributed to the reaction of an orthomagmatic fluid with already crystallised granite, although it does not preclude some Ca contribution from a wall-rock metamorphic fluid, as indicated from stable isotopes (Kontak and Kyser, 2011).

Another point worthy of further discussion is the unexpected enrichment of F in the fluid inclusion F-Na-Ca population, which is likely the first recognition of this phenomenon in granitic bodies on such a scale anywhere. The pervasive occurrence of F in the sample set suggests that the generation of this F-rich fluid is part of the natural evolution of the system and consistent with the presence of topaz in the most evolved magmatic rocks and as part of mineralised greisens. Finally, that F enrichment occurs in the same fluid with Ca indicates a possible cause and effect relationship which we suggest relates to the reactive capacity of the original exsolved Na-F fluid.

Future studies

Outstanding questions about the technique should guide the direction of future work. Firstly, in order to relate alteration assemblages to fluid-inclusion compositions, petrographic work on samples for which we have mound data must be completed. Secondly, more work is required to explain the variation in data between oven-generated mounds and stage-generated mounds. Thirdly, we have grouped samples by pluton, which is the broadest rock classification identified in the SMB. NSDNR mapping identifies 260 mappable SMB rock units, which is an available mapping guide for future evaporate mound analysis work.

The usefulness of the technique as an exploration tool for vectoring towards areas of mineralisation is not yet known. Application of evaporate mound analysis to a local-scale study area (i.e., 1 or 2 km^2 area) would provide an opportunity to assess how the technique may be useful to industry.

Acknowledgments

This fluid inclusion study was supported by the Canadian Federal Government's Research Affiliate Program and contributes towards the fulfilment of objectives for the Targeted Geoscience Initiative 4. This component of the project also represents the academic and professional research that can be generated by formal cooperation between the Geological Survey of Canada and Saint Mary's University Department of Geology. This work provides an example of the complementarity between these two institutions. Well-beyond formal commitments, this project owes its success and to the dedicated initiatives of Dr Jacob Hanley (Saint Mary's University, Halifax), Dr Dan Kontak (Laurentian University, Sudbury) and Dr Neil Rogers (Geological Survey of Canada, Ottawa). A summary of the raw data generated by the study is presented in this report, and the complete data set is available to anyone who may wish to view it, and is available from the Magmatic Ore Deposits Laboratory, Department of Geology, Saint Mary's University, 923 Robie Street, Halifax, Nova Scotia.

The first author would like to express his many thanks to Drs Jacob Hanley and Daniel Kontak for conceiving this project and giving freely of their time in assisting with the design and execution of this project. And a great deal of thanks is owed to Dr Neil Rogers for guidance during field work in Yarmouth County and the New Ross area, as well as help with various reports produced throughout the past two years. Tracy Lenfesty, Dr Chris White, Dr Bob Ryan and Mick O'Neill are acknowledged for providing access to samples at the Nova Scotia Department of Natural Resources (NSDNR).

References

Anderson, A.J., and Mayanovic, R.A., 2003. Electron, nuclear and X-ray probe microanalysis of fluid inclusions; *in* Fluid Inclusions: Analysis and Interpretation, (ed.) I. Samson, A.J. Anderson and D. Marshall; Mineralogical Association of Canada Short Course Publication, p. 323-352.

Bu, X., Wang, T., and Hall, G., 2003. Determination of halogens in organic compounds by high resolution inductively coupled mass spectrometry; Journal of Analytical Atomic Spectrometry, v. 18, p. 1443-1451.

Carruzzo, S., Kontak, D.J., and Clarke, D.B., 2000. Granite-hosted mineral deposits of the New Ross area, South Mountain Batholith, Nova Scotia, Canada: Constraints of fluids using fluid inclusion thermometry and decrepitate analysis; Transactions of the Royal Society of Edinburgh: Earth Sciences, v. 91, p. 303-319.

Chatterjee, A.K., and Clarke, D.B., 1985. Physical and chemical processes in the South Mountain Batholith; *in* Recent Advances in the Geology of Granite-Related Mineral Deposits, Proceed-

ings of the CIM Conference on Granite-Related Mineral Deposits, (ed.) R.P. Taylor and D.F. Strong; The Canadian Institute of Mining and Metallurgy: Special volume 39, p. 223-233.

Chi, G., Chou, I.M., and Lu, H., 2003. An overview on current fluid-inclusion research and applications; Acta Petrologica Sinica, v. 19, p. 201-212.

Chryssoulis, S., and Wilkinson, N., 1983. High silver content of fluid inclusions in quartz from Guadalcazar Granite, San Luis Potosi, Mexico: A contribution to ore-genesis theory; Economic Geology, v. 78, p. 302-318.

Clarke, D.B., and Halliday, A.N., 1980. Strontium isotope geology of the South Mountain Batholith, Nova Scotia; Geochimica et Cosmochimica Acta, v. 44, p. 1045-1058.

Clarke, D.B., MacDonald, M.A., Reynolds, P.H., and Longstaffe, F.J., 1993. Leucogranites from the eastern part of the South Mountain Batholith, Nova Scotia; Journal of Petrology v. 34, p. 653-679.

Corey, M.C., 1994. Diamond-drilling of rare element pegmatites in southwestern Nova Scotia; *in* Mines and Minerals Branch, Report of Activities 1993, (ed.) D.R. MacDonald; Nova Scotia Department of Natural Resources, Report 94-01, p. 65-79.

Corey, M.C., and Horne, R.J., 1989. Polymetallic-precious metal potential of the Tobeatic fault zone in southwestern Nova Scotia; Nova Scotia Department of Mines and Energy Report 89-1, p. 27-36.

Cormier, C.F.M., 1988. Greisenization and metasomatism associated with the Meguma – South Mountain Batholith contacts, Inglisville, Nova Scotia; unpublished BSc thesis, Saint Francis Xavier University, Antigonish, Nova Scotia, 81 p.

Diamond, L.W., Marshall, D.D., Jackman, J.A., and Skippen, G.B., 1990. Elemental analysis of individual fluid inclusions in minerals by Secondary Ion Mass Spectrometry (SIMS): Application to cation ratios of fluid inclusions in an Archaean mesothermal gold-quartz vein; Geochimica et Cosmochimica Acta, v. 54, p. 545-552.

Frantz, J.D., Mao, H.K., Zhang, Y-G., Wu, Y., Thompson, A.C., Underwood, J.H., Giauque, R.D., Jones, K.W., and Rivers, M.L., 1988. Analysis of fluid inclusions by X-ray fluorescence using synchrotron radiation; Chemical Geology, v. 69, p. 235-244.

Giles, P.S., 1985. A major post-Visean sinistral shear zone – New perspectives on Devonian and Carboniferous rocks of Southern Nova Scotia; *in* Guide to Granites and Mineral Deposits of Southwestern Nova Scotia, (ed.) A.K. Chatterjee and D.B. Clarke; Nova Scotia Department of Mines and Energy, paper 85-3, p. 233-248.

Gleeson, S., 2003. Bulk analysis of volatiles in fluid inclusions; *in* Fluid Inclusions: Analysis and Interpretation, (ed.) I. Samson, A.J. Anderson and D. Marshall; Mineralogical Association of Canada Short Course Publication, p. 247-278.

Halter, W.F., Williams-Jones, A.E., and Kontak, D.J., 1996. The role of greisenization in cassiterite precipitation at the East Kemptville Tin Deposit, Nova Scotia; Economic Geology, v. 91, p. 368-385.

Haynes, F.M., and Kesler, S.E., 1987. Chemical evolution of brines during Mississippi Valley-type mineralization: evidence from East Tennessee and Pine Point; Economic Geology, v. 82, p. 53-71.

Haynes, F.M., Sterner, S.M., and Bodnar, R.J., 1988. Synthetic fluid inclusions in natural quartz. IV. Chemical analyses of fluid inclusions by SEM/EDA: Evaluation of method; Geochimica et Cosmochimica Acta, v. 52, p. 969-977.

Heinrich, C.A., and Cousens, D.R., 1989. Semi-quantitative electron microprobe analysis of fluid inclusion salts from the Mount Isa copper deposit (Queensland, Australia); Geochimica et Cosmochimica Acta, v. 53, p. 21-28.

Horne, R.J., MacDonald, M.A., Corey, M.C., and Ham, L.J., 1992. Structure and emplacement of the South Mountain Batholith, southwestern Nova Scotia; Atlantic Geology, v. 28, p. 29-50.

Kontak, D.J., 1990. The East Kemptville muscovite-topaz leucogranite. I. Geological setting and whole rock geochemistry; Canadian Mineralogist, v. 28, p. 787-825.

Kontak, D.J., 2004. Analysis of Evaporate mounds as a compliment to fluid-inclusion – thermometric data: case studies from granitic environments in Nova Scotia and Peru; Canadian Mineralogist, v. 42, p. 1315-1327.

Kontak, D.J., and Kyser, K., 2011. A fluid inclusion and isotopic study of an intrusion-related gold deposit (IRGD) setting in the 380 Ma South Mountain Batholith, Nova Scotia, Canada: evidence for multiple reservoirs; Mineralium Deposita, v. 46, p. 337-363.

Kontak, D.J., Ansdell, K., and Archibald, D., 1999. New constraints on the age and origin of the Dunbrack Pb-Cu-Zn-Ag deposit, Musquodoboit Batholith, southern Nova Scotia; Atlantic Geology, v. 35, p. 19-42.

MacDonald, M.A., 2001. Geology of the South Mountain Batholith, southwestern Nova Scotia; Nova Scotia Department of Natural Resources, Open File Report ME 2001-2, 281 p.

MacDonald, M.A., and O'Reilly, G.A., 1989. Gold enrichment associated with post-magmatic processes in the South Mountain batholith, southwestern Nova Scotia; Nova Scotia Department of mines and Energy Report 89-1, p. 13-25.

MacDonald, L.A., Barr, S.M., White, C.E., and Ketchum, J.W.F., 2002. Petrology, age, and tectonic setting of the White Rock Formation, Meguma terrane, Nova Scotia: evidence for Silurian continental rifting; Canadian Journal of Earth Sciences, v. 39, p. 259-277.

McPhie, J., Kamentsky, V., Allen, S., Ehrig, K., Agangi, A., and Bath, A., 2011. The fluorine link between a supergiant ore deposit and a silicic large igneous province; Geology, v. 39, p. 1003-1006.

Ménez, B., Phillippot, P., Bonnin-Mosbah, M., Simionovici, A., and Gibert, F., 2002. Analysis of individual fluid inclusions using synchrotron X-ray fluorescence microprobe: Progress toward calibration for trace elements; Geochimica et Cosmochimica Acta, v. 66, p. 561-576.

Muecke, G.K., and Clarke, D.B., 1981. Geochemical evolution of the South Mountain Batholith, Nova Scotia: Rare-Earth-Element evidence; Canadian Mineralogist, v. 19, p. 133-145.

O'Reilly, G.A., 1992. Petrographic and geochemical evidence for a hypogene origin of granite-hosted, vein-type Mn mineralization at the New Ross Mn deposits, Lunenburg County, Nova Scotia, Canada; Economic Geology, v. 87, p. 1275-1300.

O'Reilly, G.A., 2011. The Long Lake Mo-W-Cu greisens: A classic example of greisen development. Nova Scotia Department of Natural Resources Minerals Update Newsletter 28, p. 5.

O'Reilly, G.A., 2013. Granite- and metasediment-hosted W-Sn-Mo-Cu-Zn-Ag-Au at Westfield, Queens County; Nova Scotia Department of Natural Resources Minerals Update Newsletter 30, p. 4.

Putnis, A., 2002. Mineral replacement reaction: from macroscopic observations to microscopic mechanisms; Mineralogical Magazine, v. 66, p. 689-708.

Reynolds, P. H., Zentilli, M., and Muecke, G.K., 1981. K-Ar and $^{40}Ar/^{39}Ar$ geochronology of granitoid rocks from southern Nova Scotia: Its bearing on the geochemical evolution of the Meguma Zone of the Appalachians; Canadian Journal of Earth Sciences, v. 18, p. 386-394.

Roedder, E., and Bodnar, B., 1997. Fluid inclusion studies of hydrothermal ore deposits; *in* Geochemistry of Hydrothermal Ore Deposits, Third edition, (ed.) H.L. Barnes; p. 657-698.

Samson, I.M., Williams-Jones, A.E., and Lui, W., 1995. The chemistry of hydrothermal fluids in carbonitites: Evidence from leachate and SEM-decrepitate analysis of fluid inclusions from Oka, Quebec, Canada; Geochimica et Cosmochimica Acta, v. 59, p. 1979-1989.

Savard, M.M., and Chi, G., 1998. Cation study of fluid inclusion decrepitates in the Jubilee and Gays River (Canada) Zn-Pb deposits – characterization of ore-forming brines; Economic Geology, v. 93, p. 920-931.

Smith, T.E., and Turek, A., 1976. Tin-bearing potential of some Devonian granitic rocks in S.W. Nova Scotia; Mineralium Deposita, v. 11, p. 234-245.

Thomas, R., Webster, J.M., Rhede, R., Seifert, W., Rickers, K., Förster, H.J., Heinrich, R., and Davidson, P., 2006. The transition from peraluminous to peralkaline granitic melts: Evidence from melt inclusions and accessory minerals; Lithos, v. 91, p. 137-149.

Timofeeff, M.N., Lowenstein, T.K., and Blackburn, W.H., 2000. ESEM-EDS: an improved technique for major element chemical analysis of fluid inclusions; Chemical Geology, v. 164, p. 171-182.

Walsh, J.F., Kesler, S.E., Duff, D., and Cloke, P.L., 1988. Fluid inclusion geochemistry of high-grade, vein-hosted gold ore at Pamour Mine; Porcupine Camp, Ontario; Economic Geology, v. 83, p. 1347-1367.

Wilkinson, J.J., 2001. Fluid inclusions in hydrothermal ore deposits; Lithos, v. 55, p. 229-272.

Williams-Jones, A.E., Samson, I.M., and Olivo, G.R., 2000. The genesis of hydrothermal fluorite-REE deposits in the Gallinas Mountains, New Mexico; Economic Geology, v. 95, p. 327-342.

Zaw, K., Hunns, S.R., Large, R.R., Gemmell, J.B., Ryan, C.G., and Mernagh, T.P., 2003. Microthermometry and chemical composition of fluid inclusions from the Mt Chalmers volcanic-hosted massive sulphide deposits, central Queensland, Australia: implications for ore genesis; Chemical Geology, v. 194, p. 225-244.

Controls on indium mineralisation in tin-tungsten-base metal deposits of the Canadian Appalachians

Christopher R. Goeddeke[1], John B. Chapman[2] and Iain M. Samson[1]

1. Department of Earth and Environmental Sciences, University of Windsor, 401 Sunset Av., Windsor, Ontario

2. Geological Survey of Canada, 625 Robson St., Vancouver, British Columbia

Abstract: Indium is a minor but potentially economically significant component of the ore metal tenor of many porphyry-style, stockwork and polymetallic vein-type Sn-W and Sn-base metal deposits of the Canadian Appalachians. However, indium distribution between deposits is highly uneven, and whereas some deposits contain hundreds of kilograms of the metal at grades sufficient to justify recovery, others are near-barren. In order to investigate the fundamental temperature, mineralogical, spatial and chemical controls on indium mineralisation in the district, this study has taken samples from indium rich and poor occurrences at 10 drilled prospects in southern New Brunswick and southwest Nova Scotia, as well as from the past-producing East Kemptville Mine in Nova Scotia.

Detailed mineralogical characterization of these materials has shown that, contrary to existing models, within this district indium is commonly introduced early in the deposit paragenesis, presumably as a component of the initial, high-temperature magmatic-hydrothermal fluids. During this phase of mineralisation, indium is dominantly precipitated within copper-rich sphalerite, and it is the distribution of this mineral phase that primarily governs the presence or absence of indium within a mineralised body. During later cooling of the deposit a proportion of the indium is exsolved from sphalerite during recrystallization, and forms lamellae of a sulphide mineral that resembles sakuraiite in the core zones of many individual sphalerite.

Introduction

Indium has seen a dramatic rise in demand in recent years due to the variety of industrial and technology applications it can be put to, particularly in electronics. Devices such as touch screens, superconductors and solar panels incorporate significant quantities of indium, and at present there is no practicable or cost-effective substitute available.

Within the provinces of New Brunswick and Nova Scotia, rocks of the Appalachian Orogen (Fig. 1) contain numerous porphyry- and granitoid-related tin, tungsten and base metal deposits that are variably enriched with indium, particularly in the vicinity of the past-producing Mount Pleasant mine in Charlotte County, NB (Fig. 2), and East Kemptville mine near Yarmouth, NS (Fig. 3). In many cases, indium content within a deposit may be only slightly enriched above regional background levels and does not contribute significantly to the economic potential of the deposit. However, at other deposits indium can be present in quantities great enough that it comprises a significant proportion of the economic ore tenor. At almost 1000 tonnes combined indicated and inferred contained metal (McCutcheon et al., 2013), the porphyry tungsten-tin-base metal deposits of the Mount Pleasant mine represent possibly the largest documented global indium reserve (Sinclair et al., 2006).

These documented occurrences represent an opportunity to study the mechanisms and controls on indium deposition in known indium enriched and barren ore forming systems of otherwise similar genesis. The objective of the work described herein is to characterize these processes in order to provide improved genetic context and exploration targeting criteria. Samples recovered from archival diamond drill core taken at a variety of deposits across the region were used to characterize the mineralogy and paragenesis of indium-rich and indium-poor ore assemblages, to determine the mineralogical controls on indium distribution, and to characterize possible mechanisms controlling the transport and concentration of indium into viable ore deposits.

Geology, geochemistry and mineralogy of indium

Geochemistry

Indium, in its native form, is a soft, lustrous metal that is highly malleable and ductile. In the natural environment, however, the most common oxidation state of indium is +3, where its outer valence shell comprises a full complement of ten d-orbital electrons. This electron configuration leads to a greater degree of covalent bonding and greater stability when forming chloride complexes than other elements in the same periodic group (Wood and Samson, 2005). The high charge and moderate ionic radius of the In^{3+} ion make it a hard acid, that should preferentially form complexes with hard bases (e.g., OH^-, F^-) and organic ligands bonding through oxygen (Wood and Samson, 2005). The In^{3+} ion is larger than similar cations of like charge, which results in greater tendency to form complexes with chloride and bisulfide (Wood and Samson, 2005).

Indium is not found in significant quantities in common natural waters as strong complexation or highly acidic conditions are required to solubilize indium at low temperatures (Wood and Samson, 2005); for example, indium concentrations are less than 1.7 parts per trillion in Japanese freshwater systems that have been exposed to significant anthropogenic indium (Nozaki et al., 2000). Higher concentrations of

Corresponding author: John Chapman (jchapman@nrcan.gc.ca)

Goeddeke, C.R., Chapman, J.B., and Samson, I.M., 2015. Controls on indium mineralisation in tin-tungsten-base metal deposits of the Canadian Appalachians; *in* TGI 4 – Intrusion Related Mineralisation Project: New Vectors to Buried Porphyry-Style Mineralisation, (ed.) N. Rogers; Geological Survey of Canada, Open File 7843, p. 101-110.

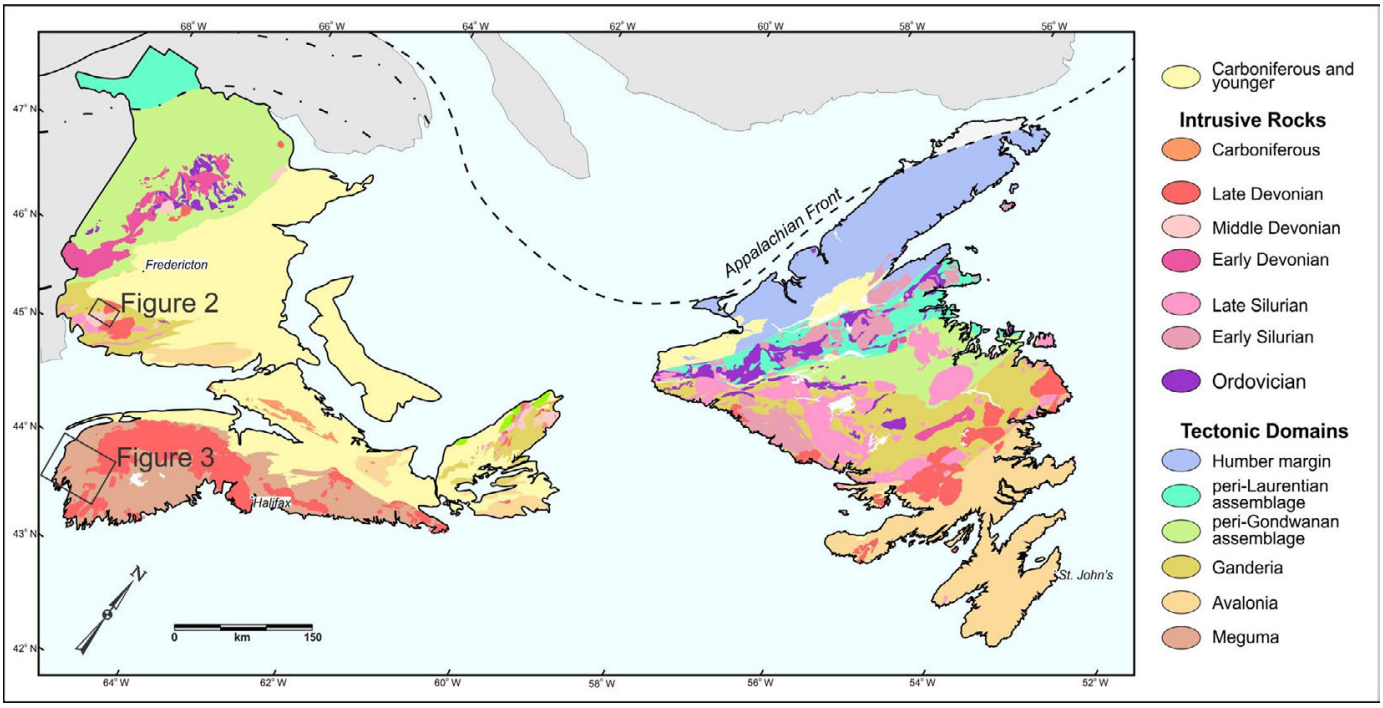

Figure 1 – Simplified lithotectonic map of the Appalachian Orogen in Canada. Positions of Figures 2 and 3 are indicated by solid boxes. Modified after Hibbard et al. (2006), van Staal et al. (2009), Rogers et al. (2014) and references therein.

indium, reaching several hundred parts per million, have been documented from active undersea vent fluids, however (Schwarz-Schampera and Herzig, 2002). In acidic, fluoride-rich solutions, indium fluoride complexes may play role in the hydrothermal transport of indium, but this may be limited by the low solubility of fluorite and topaz (Wood and Samson, 2005). Experimental investigations have indicated that the only indium chloride species present in a 0.1 mol HCl solution at 350°C is the tetrahedrally coordinated $InCl_4^-$ ion (Seward et al., 2000; Wood and Samson, 2005). The existence of hydrothermal enrichments of indium demonstrate that conditions exist under which the element is relatively soluble, but at present these are only sparsely documented in nature.

Mineralogy

Indium can be contained within a variety of minerals, either as a major structural constituent or as a trace element substitution (Tables 1 and 2; Schwarz-Schampera and Herzig, 2002). Minerals within which indium is an essential, structural element are rarely found in substantial quantities, and indium most commonly occurs in base metal sulphides such as sphalerite, chalcopyrite, stannite and stannoidite through a range of elemental substitutions. Sphalerite is the most economically significant source of indium, with indium-rich sphalerite occurs in various types of deposits around the world (Schwarz-Schampera and Herzig, 2002). The bulk of indium production at present is achieved as a by-product of the mining of zinc-rich volcanogenic massive sulphide (VMS) deposits, such as at the giant Kidd Creek deposit in Ontario (Cook et al., 2011a). Other deposits within which indium occurs in economically viable quantities also contain sphalerite, and indium generally shows a positive grade correlation with zinc and copper in bulk analyses (Schwarz-Schampera and Herzig, 2002), and a possible negative correlation with iron (Cook et al., 2009) consistent with the bulk of the indium residing within sphalerite

Table 1 – Minerals into which indium displays significant natural substitution

Mineral	Ideal formula	Dominant substitution
Sphalerite	(Zn,Fe)S	Zn, Fe
Stannite	Cu_2FeSnS_4	Sn, Fe
Kesterite	$Cu_2(Zn,Fe)SnS_4$	Sn
Mawsonite	$Cu_6Fe_2SnS_8$	Sn, Fe
Stannoidite	$Cu_6^+Cu_2^{2+}(Fe^{2+},Zn)_3Sn_2S_{12}$	Sn, Zn, Fe
Cassiterite	SnO_2	(Sn), Fe
Digenite	Cu_9S_5	Cu
Enargite	Cu_3AsS_4	Cu, As
Tetrahedrite	$(Cu,Fe)_{12}Sb_4S_{13}$	Cu, Sb, (As)
Tennantite	$(Cu,Ag,Fe,Zn)_{12}As_4S_{13}$	Cu, As, (Sb)

Table 2 – Indium minerals

Mineral	Ideal formula	Common association
Roquesite	$CuInS_2$	Spahlerite, chalcopyrite
Sakuraiite	$(Cu,Zn,Fe)_3(In,Sn)S_4$	Spahlerite, chalcopyrite
Dzhalindite	$In(OH)_3$	Sphalerite
Indite	$FeIn_2S_4$	Linnaeite
Laforetite	$AgInS_2$	Chalcopyrite
Petrukite	$(Cu,Fe,Zn,Ag)_3(Sn,In)S_4$	Stannite
Ishiharite	(Cu,Ga,Fe,In,Zn)S	Sphalerite

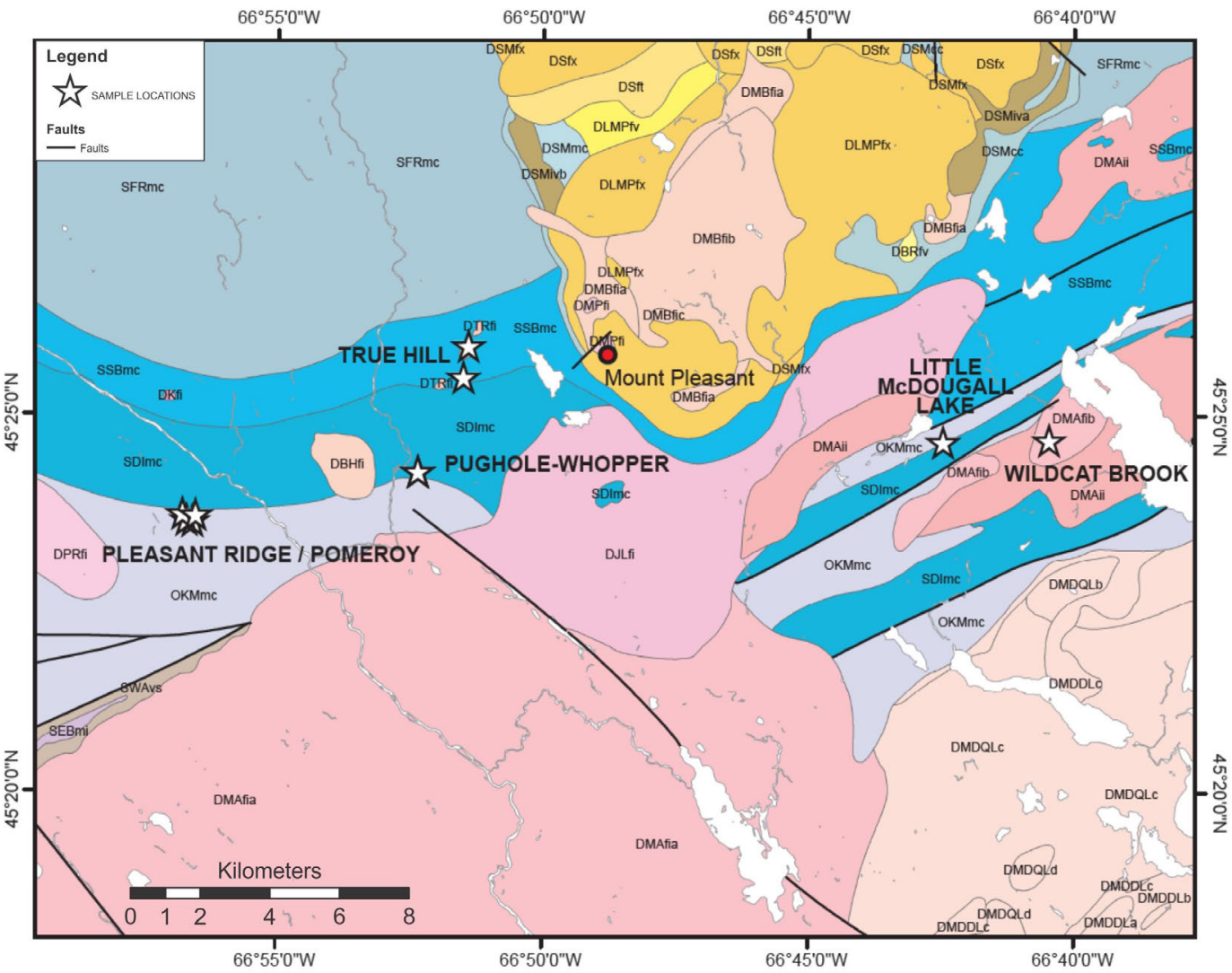

Bailey Rock Rhyolite (DBRfv)
Beech Hill Granite (DBHfi)
Digdeguash Formation (SDlmc)
East Branch Brook Gabbro (SEBmi)
Flume Ridge Formation (SFRmc)
John Lee Brook Granite (DJLfi)
Kedron Stream Granite (DKfi)
Kendall Mountain Formation (OKMmc)
Little Mount Pleasant Formation (DLMPfv) felsic volcanic rocks
Little Mount Pleasant Formation (DLMPfx) felsic crystal tuff
Magaguadavic Granite (DMAfia)
Magaguadavic Granite (DMAfib)
Magaguadavic Granite (DMAii)
McDougall Brook Granite (DMBfia)
McDougall Brook Granite (DMBfib)
McDougall Brook Granite (DMBfic)
Mount Douglas Granite (DMDDLa) Disappointment Lake Phase
Mount Douglas Granite (DMDDLb) Disappointment Lake Phase
Mount Douglas Granite (DMDDLc) Disappointment Lake Phase
Mount Douglas Granite (DMDQLb) Queens Lake Phase
Mount Douglas Granite (DMDQLc) Queens Lake Phase
Mount Douglas Granite (DMDQLd) Queens Lake Phase
Mount Pleasant Porphyry (DMPfi)
Pleasant Ridge Granite (DPRfi)
Sand Brook Formation (SSBmc)
Scoullar Mountain Formation (DSMcc) coarse-grained clastic sedimentary rocks
Scoullar Mountain Formation (DSMfx) felsic crystal tuff
Scoullar Mountain Formation (DSMiva)
Scoullar Mountain Formation (DSMivb) intermediate volcanic rocks
Scoullar Mountain Formation (DSMmc)
Seelys Formation (DSft) felsic tuff
Seelys Formation (DSfx) felsic crystal tuff
True Hill Granite (DTRfi)
Waweig Formation (SWAvs)

Figure 2 – Sample location map of the Mount Pleasant tin-tungsten district, Charlotte County, New Brunswick. Bedrock geology after McLeod et al. (2005).

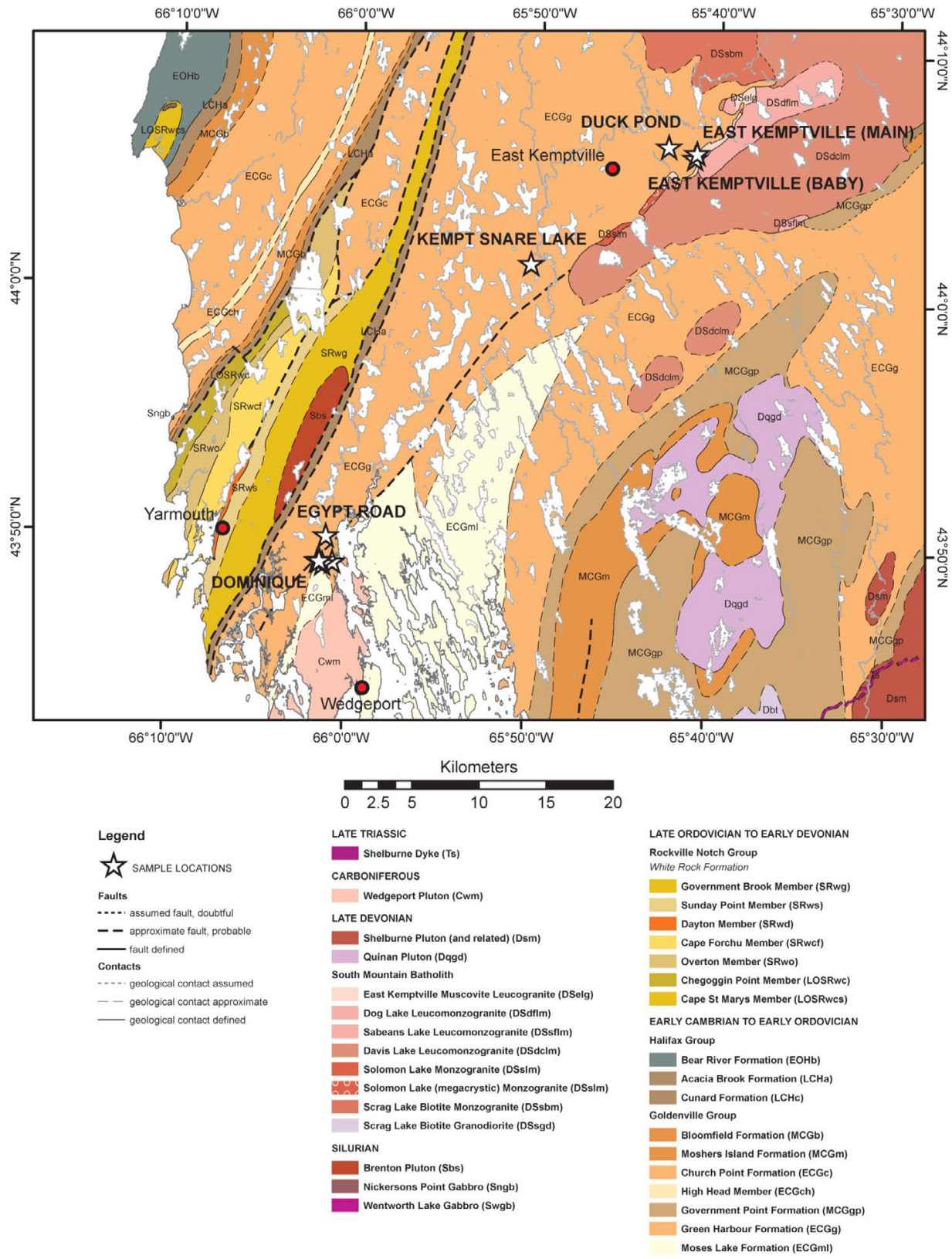

Figure 3 – Sample location map of the southwest Nova Scotia tin domain, Yarmouth County, Nova Scotia. Bedrock geology after White et al. (2012).

and copper sulphide minerals. This distribution is observed at the Mount Pleasant deposits, where sphalerite is the most important indium host, with chalcopyrite the second most significant host (Sinclair et al., 2006).

Formation of indium-rich sphalerite may occur as part of primary mineralisation or may be part of later alteration, with a possible positive correlation between high temperatures of formation or alteration and indium content within sphalerite (Cook et al., 2011b). Indium-rich sphalerite has been associated with elevated copper content. Secondary alteration processes, such as those associated with 'chalcopyrite disease', have been associated with the formation of iron rich and indium-bearing sphalerite (Barton and Bethke, 1987; Eldridge et al., 1988; Schwarz-Schampera and Herzig, 2002). Incomplete or 'disordered' solid solution series have been suggested between sphalerite and roquesite [$CuInS_2$], and between sphalerite and stannite [$Cu_2(Fe,Zn)SnS_4$] (Sinclair et al., 2006; Cook et al., 2011b). The solid solution between sphalerite and stannite encompasses the stannite-group mineral sakuraiite [$(Cu,Fe,Zn)_2(Sn,In)S_4$].

Indium substitutes for either zinc or iron in the lattice of sphalerite, usually in conjunction with copper through a charge-balanced coupled substitution mechanism. This substitution requires that $Cu^{+}+In^{3+}$ replaces $2(Zn^{2+},Fe^{2+})$. Replacement zones in experimentally synthesized sphalerite crystals indicate that iron was preferentially replaced by indium, rather than zinc (Bente and Doering 1995). How this process varies as a function of temperature is not fully understood, although it has been theorized that indium substitution occurs in sphalerite over the relatively narrow temperature range of 350-400°C (Cook et al., 2011b).

Chalcopyrite can also host significant indium, and in some occurrences has higher indium content than coexisting sphalerite (Schwarz-Schampera and Herzig, 2002). Stannite and stannoidite have also been documented as hosts for indium, as have tennantite-tetrahedrite, cassiterite, and a variety of other minerals (Table 1; Cook et al., 2011b). The formation of roquesite, and other minerals within which indium is a required structural component, has been interpreted to occur only where the availability of minerals containing indium-replaceable elements (e.g., iron in sphalerite) is limited (Cook et al., 2011b).

Deposit associations

Indium is commonly associated with zinc-rich sulphide deposits such as VMS, sedimentary exhalative (SEDEX) and skarn types, but is also concentrated in tin porphyry, stockwork vein, and epithermal systems (Schwarz-Schampera and Herzig, 2002). The average crustal abundance of indium is ca. 0.1 ppm, but concentrations within known deposits can range up to ca. 3000 ppm (reported from polymetallic veins; Murao et al., 2008). The majority of present global production is from zinc-rich VMS deposits, whereby indium is recovered as a by-product of zinc processing. However, the majority of known indium reserves reside in porphyry-related deposits such as that those found at the Mount Pleasant mine in New Brunswick (Jorgenson and George, 2004). Previous models for the formation of the Mount Pleasant deposits suggested that indium-bearing mineral assemblages were superimposed on earlier tungsten-iron-tin-molybdenum or zinc-bearing assemblages at temperatures in excess of 350°C (Schwarz-Schampera and Herzig, 2002). However, in light of recent detailed studies of indium mineralogy and inter-mineral partitioning by Cook et al. (2011b), observations of coexisting indium-poor sphalerite and roquesite within the North Zone at Mount Pleasant suggest that indium introduction was not solely a late stage phenomenon.

Deposit geology

Within the Canadian Appalachian region a number of different ore deposit styles occur that contain significant indium, including porphyry, stockwork vein, and epithermal types and many of the VMS deposits of the Bathurst Mining Camp in New Brunswick contain extractable indium (e.g., Brunswick #12). Assay data from the porphyry and stockwork deposits at Mount Pleasant, Pleasant Ridge/Pomeroy, Pughole and True Hill in New Brunswick (Fig. 2) indicate enrichments of indium of potentially economic significance. The largest of these is 620 tonnes of contained indium metal identified within the Mount Pleasant deposits (Sinclair et al., 2006). In Nova Scotia, the East Kemptville, Dominique, Duck Pond and Egypt Road deposits (Fig. 3) have also been identified as potential indium resources. During the late 1970s and early 1980s, extensive diamond drilling of these deposits was carried out and recovered drill core from many were assayed for indium at that time. Technology-driven demand for indium in more recent times has led to reassessment of these materials and their potential at providing a means to resolve the mode of occurrence and controls on indium endowment within these provinces.

Most of the deposits within the Canadian Appalachians documented as hosting economically significant indium contents (>60 ppm; Sinclair et al., 2006) were formed during the Devonian to Early Carboniferous Acadian and Neoacadian orogenies (van Staal et al., 2009, and references therein). Of those indium-rich deposits linked to magmatism associated with granitoid emplacement, the Mount Pleasant in Charlotte County, south-western New Brunswick, has attracted the most detailed academic investigation. Here, indium occurs mainly in sphalerite but is also associated with chalcopyrite. The indium potential of deposits within the Southwest Nova Scotia Tin domain, including the past-producing East Kemptville mine, is less well understood. Multiple replacement and mineralisation events are common to the deposits, with mineralisation occurring as pockets in veins and along the interface between veins and their host lithologies. Greisen-style alteration is commonly associated with tin and indium deposition, but not exclusively. Not all areas subject to greisen alteration contain elevated indium, but indium-rich sphalerite is largely associated with greisen alteration (Halter et al., 1998; Sinclair et al., 2006).

New Brunswick indium deposits

Mount Pleasant

The Mount Pleasant deposit comprises two discrete centres of porphyry-style intrusive mineralisation, located at the south-western margin of the late Devonian Mount Pleasant Caldera Complex (Fig. 2; McCutcheon et al., 2010). These two centres, each cored by magmatic-hydrothermal breccia, are the Fire Tower Zone and the North Zone. Of these, the Sn-Zn-dominated North Zone contains most of the significant indium mineralisation (Fig. 4; Sinclair et al., 2006), while the W-Mo-Bi-rich Fire Tower Zone is less strongly enriched in indium, and its distribution within this zone is irregular. Within the Mount Pleasant deposits, indium mineralisation is strongly correlated to zinc abundance and, to a lesser extent, copper (Sinclair et al., 2006). There is also a weaker correlation between indium and tin, and little to no correlation between indium and cadmium. Indium is dominantly hosted within sphalerite (ca. 90 %) and chalcopyrite (ca. 9 %), with minor quantities contained within stannite group minerals (to ca. 1 %) and sparse indium minerals such as roquesite (<<1 %). Whole-rock indium concentrations from Mount Pleasant range from 1 to 3690 ppm, with a median value of 58 ppm (Sinclair et al., 2006).

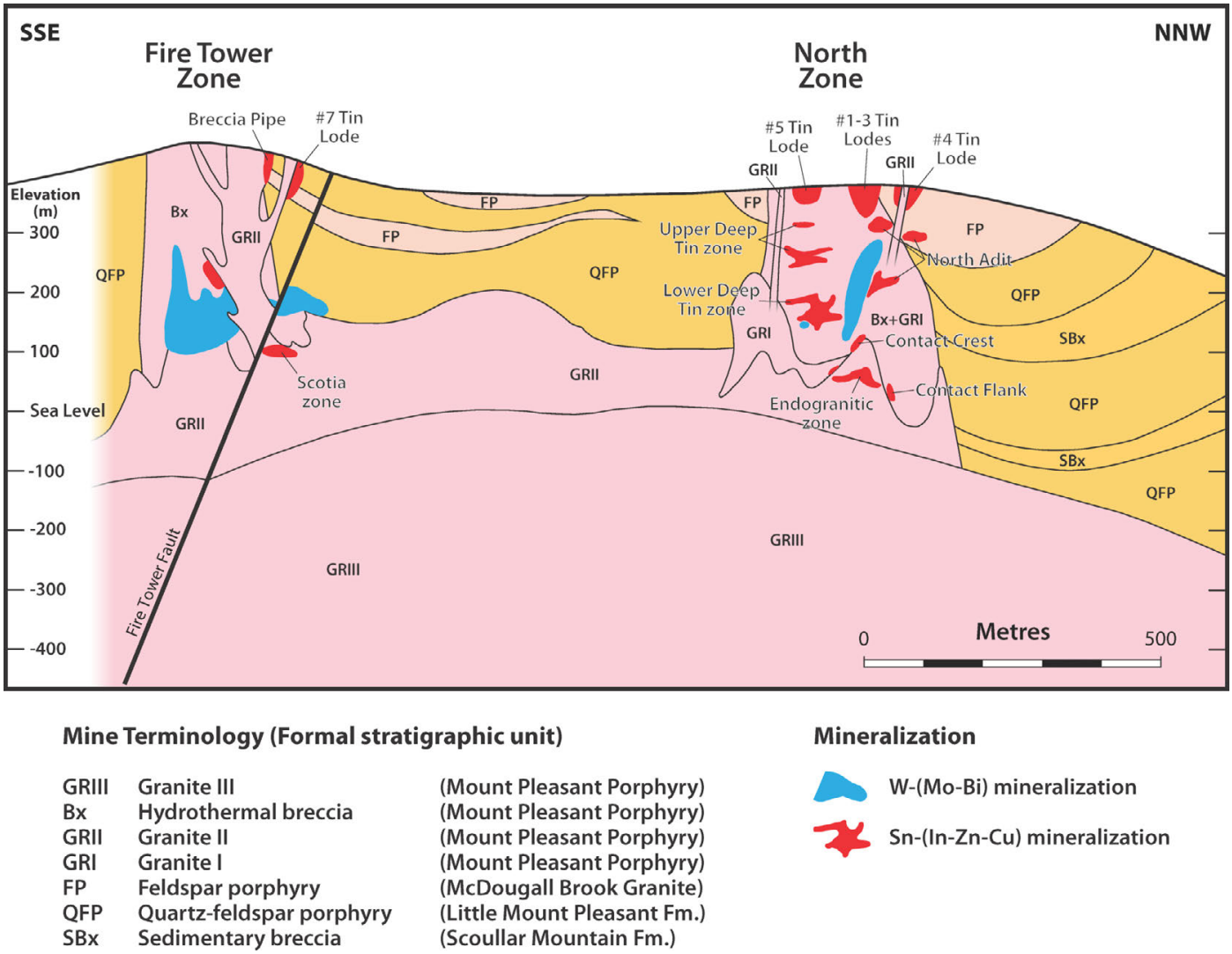

Figure 4 – Schematic cross section through the Fire Tower Zone and North Zone at the Mount Pleasant mine, New Brunswick (Fig. 2), facing southwest. Each zone comprises a cluster of W-(Mo-Bi) and Sn-(In-Zn-Cu) mineralised bodies centred on a near-vertical plug of magmatic-hydrothermal breccia associated with the second phase of intrusion of the Mount Pleasant Porphyry complex (Granite II) into older rocks of the Mount Pleasant Caldera complex. Annotation nomenclature used is the informal mine terminology, but formal unit names given in parentheses and colour scheme are per Figure 2. Modified from McCutcheon et al. (2010; 2013) and Sinclair et al. (2006).

The North Zone mineralisation is hosted within stockwork bodies contained within a cluster of breccia pipes and subvolcanic granite plutonic bodies. The granitic phases have been subdivided into three main sequences, which from oldest to youngest are designated Granites I, II and III. These have been interpreted as representing the cooling stages of a single parent magma body (McCutcheon et al., 2010). Granite I is associated with low-grade tungsten and molybdenum mineralisation, and was brecciated and altered by fluids released during subsequent emplacement of Granite II beneath it. Individual intrusive bodies of Granite II are approximately cone-shaped, and contain breccia pipes in their upper portions. These breccia pipes are thought to be of magmatic-hydrothermal origin, caused by the exsolution of magmatic fluids from the cooling plutonic bodies. Metallic mineral precipitation was likely caused by a combination of rapid cooling and increasing pH within the magmatic fluids, as a consequence of their interaction and mixing with groundwater (Sinclair et al., 2006).

The North Zone is itself divided into several sub-zones that exhibit different alteration and mineralisation characteristics. Of particular interest for their indium content are a high-sulphide near surface zone (HSNSZ) of breccia and vein-hosted lodes, the Upper and Lower Deep Tin Zones (UDTZ and LDTZ), and the Endogranitic Zone (EZ; Sinclair et al., 2006). Within HSNSZ deposits, cassiterite, arsenopyrite, lollingite and sphalerite are the major ore minerals present, associated with lesser stannite, marcasite, pyrite, galena, wolframite, molybdenite, tennantite, chalcocite, bornite, native bismuth, bismuthinite and wittichenite. Sinclair et al. (2006) report indium grades of the #4 Lode from within this zone of up to 91 g/t. The Sn-base metal deposits of the UDTZ are associated with the highest indium tonnages, reported as 1.7 Mt of ore, grading 280 g/t indium at a cut-off grade of 60 g/t (Sinclair et al., 2006). Within veins and breccia bodies of the UDTZ, major ore minerals observed are sphalerite, chalcopyrite, arsenopyrite

and cassiterite, with minor roquesite, lollingite, tennantite, stannite, stannoidite and wittichenite. The UDTZ forms a near-horizontal to steeply dipping body of highly silicified and brecciated early Granite II, adjacent to a local cupola of a later phase of Granite II. The genetically associated LDTZ bodies are situated beneath and outward of the UDTZ mineralisation. In contrast to UDTZ bodies, the LDTZ exhibits relatively low indium concentrations, commonly assayed at between 5 and 20 g/t (Sinclair et al., 2006), and mineralisation is dominantly hosted within cassiterite and arsenopyrite veinlets within greisen (quartz-topaz) and chlorite-biotite alteration. Mineralisation within the EZ is compositionally and mineralogically similar to the LDTZ, but major mineralised interval in this zone was preceded by two additional phases of hydrothermal alteration, comprising pervasive sericitic alteration cross-cut by fracture-controlled chloritic alteration. The EZ is a large, tabular body containing 1.4 Mt of ore grading an average of 45 g/t indium.

Pleasant Ridge/Pomeroy

Although the Mount Pleasant deposits are the most studied in the area, the surrounding district contains numerous additional deposits of similar age and genetic character associated with smaller granitoid intrusive and plutonic bodies. Claim groups including True Hill and Pleasant Ridge (later Pomeroy) have been assayed and shown to contain elevated indium. Of these, the Pleasant Ridge/Pomeroy deposit in particular has significantly elevated indium concentrations, together with geological characteristics and similar zinc and copper mineral associations that appear similar in nature to the Mount Pleasant North Zone deposits (Watters and Martin, 2009).

Nova Scotia indium deposits

Southwest Nova Scotia has been subject to exploration interest for tin and tungsten deposits since the mid-1970s, following the discovery of mineralised granite and metasedimentary rocks near Wedgeport in Yarmouth County (O'Reilly, 2012). Intensive exploration has delineated a broad swathe of deposits from a zone south and east of Yarmouth itself, north-eastward along the margin of the late Devonian South Mountain Batholith, to the East Kemptville deposits, a distance of approximately 50 km. Within the Southwest Nova Scotia Tin Domain the various granite- and metasediment-hosted deposits have highly variable indium content.

East Kemptville

The East Kemptville deposit occurs along the northeast-trending East Kemptville Shear Zone at the margin of the Davis Lake Pluton of the South Mountain Batholith. The deposit is hosted partly within peraluminous granite and partly within Meguma Group metasedimentary rocks. Magmatic aqueous fluids exsolved from the cooling intrusion, enriched in tin, iron, zinc, sulphur and fluorine, were focused along fault planes and interacted with wall rocks, creating greisen-style alteration and mineralisation. Two main zones of greisen mineralisation have been defined within the East Kemptville property: the Main and Baby zones. Both are linked to leucogranite bodies of similar composition, and are dominated by greisen-style mineralisation developed both within the granites and their surrounding metasedimentary rocks.

The Main Zone deposit at East Kemptville is a well-documented example of greisen tin mineralisation, that locally has been subdivided into 'massive' and 'zoned' styles (Halter et al., 1996). Massive greisens formed from overlapping of individual alteration halos in highly fractured zones (Halter et al., 1998). Zoned greisens are confined to individual veins that were subject to multiple stages of alteration (Halter et al., 1996). In each case, leucogranite was initially altered to a quartz-sericite greisen assemblage through the replacement of feldspars by muscovite, which in turn was altered to quartz-topaz greisen that is associated with development of significant cassiterite and sulphide mineralisation (Halter et al., 1998). Zonation developed through overprinting of alteration developed by successive pulses of fluid infiltration. The Baby Zone is centred on a separate cupola-like intrusion some 200 m to the southwest of the Main Zone, and only displays the zoned greisen mineralisation style (O'Reilly and Kontak 1992). Mineralisation within the Baby Zone is almost exclusively within quartz-topaz greisens, and is more concentrated than within the Main Zone (Halter et al., 1998).

The East Kemptville mine was developed during the 1980s as North America's first primary tin producer, based solely on the deposit's tin resource, but was forced to close in the early years of the 1990s due to the collapse of the tin price (O'Reilly, 2012). Recent re-examination of assay data taken during initial development of the property coupled with analysis of additional diamond-drill core material from recent and archived drilling programs within the East Kemptville footprint and from prospects in the immediate vicinity has revealed intervals containing indium at concentrations of up to 81 g/t (Avalon Rare Metals Inc., 2010).

Duck Pond

The Duck Pond prospect is located approximately 2 km to the west of the East Kemptville deposit, within the East Kemptville Shear Zone. Mineralisation at Duck Pond occurs in three distinct styles: strata-bound, quartz-chlorite-sulphide veins, and silicified/sericitised zones. Metallic minerals associated with this deposit occur primarily within the quartz-chlorite veins and strata-bound zones. The Duck Pond host rocks are primarily metawacke and meta-argillite sequences of the Goldenville Formation (Pitre and Richardson, 1989). The mineral hosting veins have been attributed to repeated hydrostatic fracturing of the country rocks by volatiles released from underlying magmatic intrusions. Multiple intrusive tin-porphyries within the Duck Pond property are assumed to occur as a result of deformation associated with the formation of the East Kemptville Shear Zone (Pitre and Richardson, 1989). Although the deposits within the Duck Pond property are compositionally similar to the East Kemptville deposits, they occur in different host strata and have some significant geochemical and mineralogical differences to the larger deposit to the east. Fluorine-bearing and tin sulphide minerals are unknown at Duck Pond, whereas trace tourmaline is reported by Pitre and Richardson (1989) that is not present at East Kemptville. Iron-, copper- and arsenic-rich mineralisation occurs within zones associated with argillic alteration at Duck Pond, whereas alkalic alteration zones have associated muscovite, and chloritized zones are associated with elevated cassiterite, chalcopyrite and sphalerite (Pitre and Richardson, 1989).

Dominique

The Dominique deposit occurs within metasedimentary strata of the Goldenville Formation ca. 40 km southwest of the East Kemptville and Duck Pond deposits. Although the mineralisation styles are similar, the multiple granitoid intrusions in this area, such as the Early Carboniferous Wedgeport Pluton, are interpreted as significantly younger than the Late Devonian Davis Lake Pluton associated with the tin mineralisation in the vicinity of East Kemptville (McLean et al., 2003). Mineralised zones at Dominique are hosted primarily within chloritic shear zones, as replacements, and within quartz-carbonate

veins developed within altered calcareous wacke and black slate. Three separate, east-trending zones of altered and mineralised host rocks were identified during exploration by Shell Canada and Votix Corporation, and subsequent follow-up work conducted by the Nova Scotia Department of Natural Resources (O'Reilly and Kontak, 1992). Although indium distribution within the various zones of the Dominique prospect is highly variable (indium content reach ca. 90 g/t within the most northerly zone; O'Reilly and Kontak, 1992), a strong correlation with zinc content has been identified.

Sampling and methods

Samples of mineralisation at each described location were recovered from surface outcrop locations (where available) and archival diamond-drill core materials held within the New Brunswick and Nova Scotia provincial government repositories, plus additional East Kemptville samples from recent exploration drill core from Avalon Rare Metals. Samples recovered are described in brief in Table 3. Samples were chosen to illustrate the greatest range of mineralisation and alteration associations possible from within those deposits known to be enriched in indium, or those of economic significance apparently bereft of indium. Data sources used to select core intervals for sampling include archived assay and core logs available through public records in both provinces, and those archived alongside core materials at warehousing facilities in Sussex, NB, and Stellarton, NS.

These samples were subsequently used to prepare polished sections for mineralogical analysis and geochemical investigation. Sample mineralogy and paragenesis were thoroughly characterized using a combination of optical and scanning electron microscopy techniques, including cathodoluminescence imagery, and quantitative mineral chemistry was determined using electron probe microanalysis (EPMA).

Results and discussion

Detailed analysis of material from the Pomeroy deposit has indicated that existing models for the incorporation of indium within tin-tungsten-base metal mineralisation likely need revisiting. Pomeroy is associated with the Pleasant Ridge Granite and contains sulphide-rich intersections (characterized by arsenopyrite, cassiterite, chalcopyrite, galena, hematite, magnetite, pyrite, and sphalerite) containing up to 15 wt% zinc and 1 wt% tin. An indium-rich phase that is tentatively interpreted as sakuraiite occurs as exsolution lamellae in sphalerite that also exhibits chalcopyrite disease (Fig. 5). Globally, indium is principally reported as a trace component in sphalerite, although indium minerals such as roquesite ($CuInS_2$) and sakuraiite ($(Cu,Fe,Zn)_3(In,Sn)S_4$) have been described from a variety of deposits (Schwarz-Schempera and Herzig, 2002). A solid solution has been proposed between both roquesite and sphalerite (Cook et al., 2009) and sakuraiite and sphalerite (Murao et al., 2008). It has been proposed that indium can either be incorporated into sphalerite during initial precipitation or through secondary alteration during interaction with copper-rich, high temperature (200-400°C) fluids, the latter being associated with the development of chalcopyrite disease.

The indium mineral lamellae at Pomeroy are restricted to the centres of sphalerite crystals (Fig. 5b, c), suggesting that the initial stages of sphalerite crystallization incorporated significant indium and copper, which were subsequently exsolved as the unknown mineral (sakuraiite?). The outer parts of the sphalerite crystals incorporated less copper and indium, presumably reflecting a decrease in the copper and indium concentrations in the fluid as a result of changes at

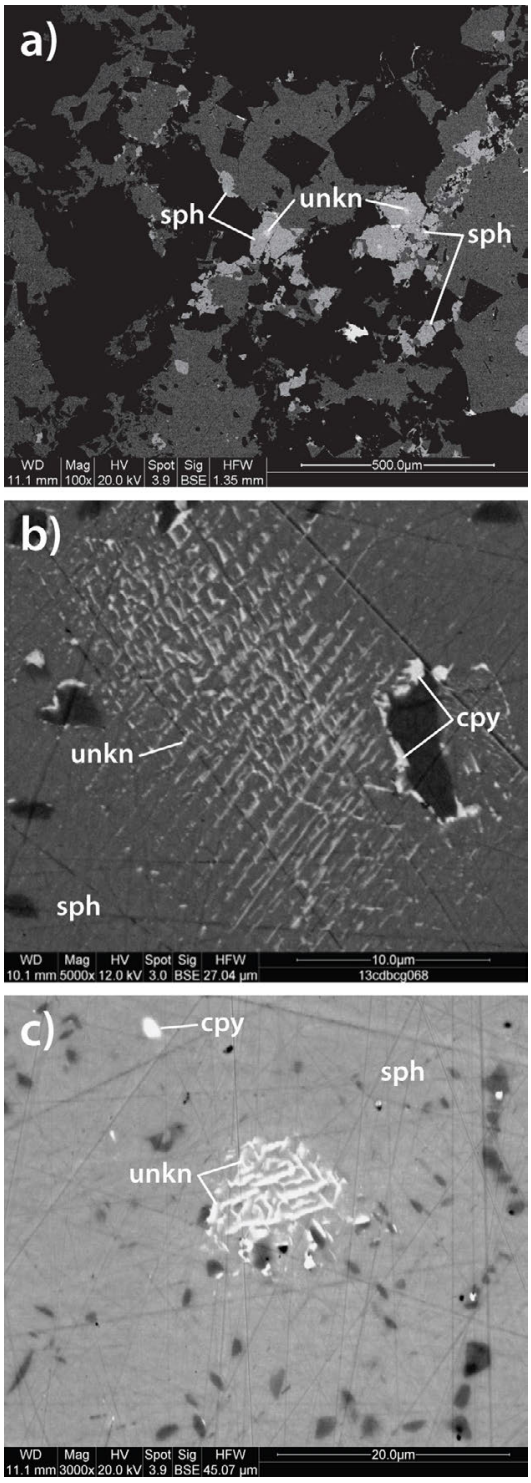

Figure 5 – Backscattered electron photomicrograph images of indium-rich sulphide assemblages from the Pomeroy deposit, New Brunswick: a) aggregate of granular sphalerite (sph) crystals with high-reflectivity cores; b) high magnification image of a high-reflectivity zone in the core of a sphalerite grain. Cross-cutting exsolution lamellae of an unknown sulphide mineral (unk), likely sakuraiite, and associated peripheral chalcopyrite blebs; c) high magnification image of putative sakuraiite (unk) exsolution lamellae in sphalerite, formed along three cleavage planes.

Table 3 – Summary of deposits included in this study

Name	Province	Type	Host rocks	Max. indium assay (ppm)	Dominant metallic minerals
Dominique	NS	Polymetallic vein	Greywacke, argillite	120	Pyrite, sphalerite, chalcopyrite
Duck Pond	NS	Polymetallic vein	Argillite, quartzite	n/a	Sphalerite, pyrite, cassiterite
East Kemptville	NS	Polymetallic vein, stockwork	Greywacke, brecciated greywacke, greisenized granit	81	Cassiterite, disseminated sphalerite
Egypt Road	NS	Polymetallic vein in boulders	Metasediment	38	Sphalerite
Kempt Snare Lake	NS	Polymetallic vein	Graphite-bearing greisenized leucogranite	n/a	Sphalerite, galena
Little McDougall Lk.	NB	Polymetallic vein, skarn	Hornfelsed wacke	n/a	Pyrite
Pleasant Ridge	NB	Polymetallic vein	Feldspathic wacke, mudstone, black shale	1000	Sphalerite, magnetite, cassiterite
Pomeroy	NB	Polymetallic vein	Quartzose arenite	1520	Sphalerite, magnetite, cassiterite
Pughole	NB	Polymetallic vein, stockwork	Shale, lithic and feldspathis wacke, silty mudstone	356	Sphalerite, galena, chalcopyrite
True Hill	NB	Sn-porphyry	Feldspathic wacke, silty mudstone	59	Sphalerite, galena
Wildcat Brook	NB	Vein/disseminated, float boulders	Greisenized wacke, argillite	n/a	Molybdenite, wolframite

source, or locally due to the incorporation of these elements into early-formed sphalerite. Regardless, these observations demonstrate that late addition of indium (and copper) to sphalerite is not a viable model for this assemblage at Pomeroy.

Elemental analysis of all the major phases present in the Pomeroy mineralisation was conducted by EPMA. Copper, Fe, Zn, In and Sn data are summarized as a ternary plot in Figure 6. This plot displays an evident solid solution straight line array between sphalerite and the unknown exsolution mineral. Although the grain sizes of the lamellae are too small to allow unambiguous mineralogical determinations, the trend of the solid solution is toward the stoichiometric composition of sakuraiite, reinforcing the postulated initial mineralogical interpretation. In addition, analyses of grains more certainly known to be sakuraiite show that there is a significant excess of copper within their composition, relative to the stoichiometric ideal composition of that mineral. This may be a simple substitution rather than a solid solution relationship between sakuraiite and chalcopyrite, as the scatter in these data within the ternary plot do not vector toward the chalcopyrite stoichiometric composition. Solid solution between sakuraiite and another, more copper-rich, sulphide phase (possibly bornite; Fig. 6) cannot be discounted but the data herein are not sufficient to confirm the existence of this relationship at present.

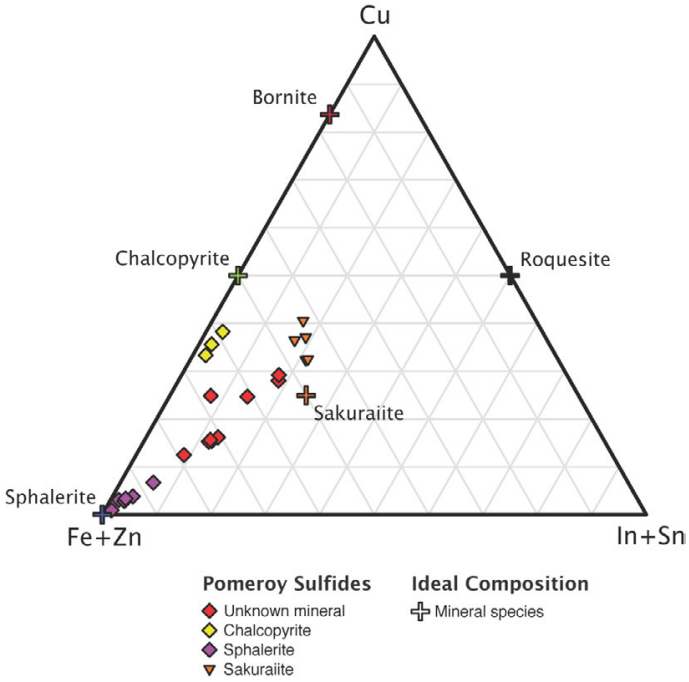

Figure 6 – Cu–(Fe+Zn)–(In+Sn) ternary plot of sulphide compositions for samples taken from the Pomeroy deposit, New Brunswick, determined by electron probe microanalysis.

Conclusions

Detailed mineralogical characterization of these materials has shown that within this district indium is commonly introduced early in the deposit paragenesis, presumably as a component of the initial, high-temperature magmatic-hydrothermal fluids. During this phase of mineralisation, indium is dominantly precipitated within copper-rich sphalerite, and it is the distribution of this mineral phase the primarily governs the presence or absence of indium within a mineralised body. During later cooling of the deposit a proportion of the indium is exsolved from sphalerite during recrystallization, and forms lamellae of a sulphide mineral that resembles sakuraiite in the core zones of many individual sphalerite crystals.

The identification of indium as a part of the initial, high-temperature, magmatic-hydrothermal ore fluid composition, and the trapping mechanism suggested by the presence of the putative sakuraiite lamellae within sphalerite, all indicate that indium concentration should be maximised closest to the centre of hydrothermal activity. Hence, although apparently unpredictable, indium content may be a useful indicator of and vector toward the position of porphyry and granite intrusion cupolas.

Acknowledgements

We would like to thank the many people who contributed to this project, who provided much helpful discussion and advice, and who assisted in and facilitated the sampling campaigns: the staff of the Nova Scotia Department of Natural Resources, in particular Mick O'Neill; the staff of the New Brunswick Department of Energy and Mines, particularly Kay Thorne, Mike Parkhill, Maurice Mazerolle and Sue Johnson; John Wightman of Annapolis Valley Goldfields Inc.; Bill Mercer of Avalon Rare Metals Inc.; Derek Thomas, consulting geologist; and Michele Wamboldt of Rio Algom Ltd. We are particularly indebted to Neil Rogers for providing the original idea that sparked this project, and for his thorough and thoughtful review which greatly improved the quality of this manuscript.

References

Avalon Rare Metals Inc., 2010. Avalon Provides Progress Report on East Kemptville Tin Indium Project, Yarmouth County, Nova Scotia; News Release No. 10-23, Avalon Rare Metals Inc., Toronto.

Barton Jr., P.B., and Bethke, P.M., 1987. Chalcopyrite disease in sphalerite: pathology and epidemiology; American Mineralogist, v. 72, p. 451-467.

Bente, K., and Doering, T., 1995. Experimental studies on the solid state diffusion of Cu + In in ZnS and on "Disease", DIS (Diffusion Induced Segregations), in sphalerite and their geological applications; Mineralogy and Petrology, v. 53, p. 285-305.

Cook, N.J., Ciobanu, C.L., Pring, A., Skinner, W., Shimizu, M., Danyushevsky, L., Saini-Eidukat, B., and Melcher, F., 2009. Trace and minor elements in sphalerite: A LA-ICPMS study; Geochimica et Cosmochimica Acta, v. 73, p. 4761-4791.

Cook, N.J., Ciobanu, C.L., and Williams, T., 2011a. The mineralogy and mineral chemistry of indium in sulphide deposits and implications for mineral processing; Hydrometallurgy, v. 108, p. 226-228.

Cook, N.J., Sundblad, K., Valkama, M., Nygård, R., Ciobanu, C.L., and Danyushevsky, L., 2011b. Indium mineralisation in A-type granites in southeastern Finland: Insights into mineralogy and partitioning between coexisting minerals; Chemical Geology, v. 284, p. 62-73.

Eldridge, C.S., Bourcier, W.L., Ohmoto, H., and Barnes, H.L., 1988. Hydrothermal inoculation and incubation of the chalcopyrite disease in sphalerite; Economic Geology, v. 83, p. 978-989.

Halter, W.E., Williams-Jones, A.E., and Kontak, D.J., 1996. The role of greisenization in cassiterite precipitation at the East Kemptville tin deposit, Nova Scotia; Economic Geology, v. 91, p. 368-385.

Halter, W.E., Williams-Jones, A.E., and Kontak, D.J., 1998. Origin and evolution of the greisenizing fluid at the East Kemptville tin deposit, Nova Scotia, Canada; Economic Geology, v. 93, p. 1026-1051.

Hibbard, J., van Staal, C.R., Rankin, D., and Williams, H., 2006. Lithotectonic map of the Appalachian orogen, Canada – United States of America; Geological Survey of Canada, Map 2096A, scale 1:1,500,000.

Jorgenson, J.D., and George, M.W., 2004. Mineral Commodity Profile: Indium; US Geological Survey, Open-File Report 2004-1300, 20 p.

MacLean, N.J., Barr, S.M., White, C.E., and Ketchum, J.W.F., 2003. New U-Pb (zircon) age and geochemistry of the Wedgeport pluton, Meguma terrane, Nova Scotia; Atlantic Geology, v. 39, p. 239-253.

McCutcheon, S.R., Sinclair, W.D., McLeod, M.J., Boyd, T., and Kooiman, G.J.A., 2010. Part 2: Mount Pleasant Sn–W–Mo–Bi–In Deposit; in Polymetallic Deposits Of Sisson Brook And Mount Pleasant, New Brunswick, Canada, (ed.) L.R. Fyffe, and K.G. Thorne; New Brunswick Department of Natural Resources; Lands, Minerals and Petroleum Division, Field Guide No. 3, p. 37-68.

McCutcheon, S., Reddick, J., McKeen, J., Scott, S., El-Rassi, D., and Kociumbas, M., 2013. Amended Technical Report of the Mount Pleasant Property, Including Mineral Resource Estimates, Southwestern New Brunswick, for Adex Mining Inc; Watts, Griffis and McOuat, Toronto. 222 p.

McLeod, M.J., Fyffe, L.R., and McCutcheon, S.R., 2005. Bedrock geology of the McDougall Lake area (NTS 21 G/07), Charlotte County, New Brunswick; New Brunswick Department of Energy and Mines, Map Plate MP 2005-30.

Murao, S., Deb, M., and Furuno, M., 2008. Mineralogical evolution of indium in high grade tin-polymetallic hydrothermal veins - A comparative study from Tosham, Haryana state, India and Goka, Naegi district, Japan; Ore Geology Reviews, v. 33, p. 490-504.

Nozaki, Y., Lerche, D., Alibo, D.S., and Tsutsumi, M., 2000. Dissolved indium and rare earth elements in three Japanese rivers and Tokyo Bay: evidence for anthropogenic Gd and In; Geochimica et Cosmochimica Acta, v. 64/23, p. 3975-3982.

O'Reilly, G.A., 2012. The East Kemptville Tin Deposit: Jewel of the Southwest Nova Scotia Tin Domain; Nova Scotia Minerals Update, v. 29, p. 3.

O'Reilly, G.A., and Kontak, D.J., 1992. The East Kemptville tin deposit and the southwest Nova Scotia tin domain; in Mines and Minerals Branch Report of Activities 1991, (ed.) D.R. MacDonald; Nova Scotia Department of Natural Resources, Report 92-1, p. 65-74.

Pitre, C.V., and Richardson, J.M., 1989. Paragenesis of veins of the Duck Pond tin prospect, Meguma Group, East Kemptville, Nova Scotia; Canadian Journal of Earth Sciences, v. 26, p. 2032-2043.

Rogers, N., McClenaghan, M.B., Plouffe, A., Kellett, D.A., Chapman, J., Azadbakht, Z., Tweedale, F., Ruberti, G., and Anderson, B., 2014. TGI 4 – Intrusion Related Mineralisation Project: New Vectors to Buried Porphyry-Style Mineralisation; in Abstracts 2014: Exploration, Mining and Petroleum New Brunswick, (ed.) E.A. Keith; New Brunswick Department of Energy and Mines, Geoscience Report 2014–5, p. 31.

Schwarz-Schampera, U., and Herzig, P.M., 2002. Indium: Geology, Mineralogy, and Economics; Springer-Verlag, Berlin, Heidelberg, New York, 257 p.

Seward, T.M., Henderson, C.M.B., and Charnock, J.M., 2000. Indium (III) chloride complexing and solvation in hydrothermal solutions to 350°C: an EXAFS study; Chemical Geology, v. 167, p. 117-127.

Sinclair, W.D., Kooiman, G.J.A., Martin, D.A., and Kjarsgaard, I.M., 2006. Geology, geochemistry and mineralogy of indium resources at Mount Pleasant, New Brunswick, Canada; Ore Geology Reviews, v. 28, p. 123-145.

van Staal, C.R., Whalen, J.B., Valverde-Vaquero, P., Zagorevski, A., and Rogers, N., 2009. Pre-Carboniferous, episodic accretion-related, orogenesis along the Laurentian margin of the northern Appalachians; in Ancient Orogens and Modern Analogues, (ed.) J.B. Murphy, J.D. Keppie and A.J. Hynes; Geological Society, London, Special Publications, v. 327, p. 271-316.

Watters, S., and Martin, D.A., 2009. Report of Diamond Drilling, Geological Observations and Ground Geophysical Orientation Surveys (Gravity, Induced Polarization an Electro-Magnetic), June 2006 to April 2008, Pleasant Ridge Claim Group (Assessment Report #476814); Geodex Minerals Ltd. For Champlain Mineral Ventures Ltd., 19 p.

White, C.E., Fisher, B.E., McKinnon, J.S. and Ehler, A.L., 2012. Digital Geological Data Generated as Part of Geological Mapping of the Meguma Terrane of Southwestern Nova Scotia (1998-2010), Shelburne, Digby, Yarmouth, Annapolis, Queens, and Lunenberg Counties, Nova Scotia; Nova Scotia Department of Natural Resources, Mineral Resources Branch, Digital Product DP ME 127, Version 1.

Wood, S.A., and Samson, I.M., 2006. The aqueous geochemistry of gallium, germanium, indium and scandium; Ore Geology Reviews, v. 28, p. 57-102.

Appendix I:

TGI 4 – Intrusion Related Mineralisation Project field trip guidebooks

Compiled by

Neil Rogers

Granite-related mineralization and alteration in the Acadian Plutonic Belt: Implications for Sn-W-Mo-Cu exploration in central New Brunswick – TGI 4 Field Guide

Neil Rogers[1], M. Beth McClenaghan[1], Kathleen G. Thorne[2], Leslie R. Fyffe[2], Allen A. Seaman[2], Michael A. Parkhill[3], Sean H. McClenaghan[4], Antonius G. Pronk[2], Kristy-Lee Beal[5], David R. Lentz[5], Reg A. Wilson[3], Jessey M. Rice[6], and Carlin Lentz[5]

1. Geological Survey of Canada, 601 Booth St., Ottawa, Ontario
2. New Brunswick Department of Energy and Mines, Geological Surveys (Branch), P.O. Box 6000, 1350 Regent St., Fredericton, New Brunswick
3. New Brunswick Department of Energy and Mines, Geological Surveys North (Section), P.O. Box 50, 495 Riverside Dr., Bathurst, New Brunswick
4. Geology Department, Museum Building, Trinity College Dublin, Dublin, Ireland
5. Department of Earth Sciences, University of New Brunswick, P.O. Box 4400, Fredericton, New Brunswick
6. Department of Earth and Environmental Sciences, University of Waterloo, 200 University Ave. W, Waterloo, Ontario

Guide based on the Geological Association of Canada/Mineralogical Association of Canada (GAC/MAC) Joint Annual Meeting 2014 Field Trip B1, May 24-26, 2014 and Exploration, Mining and Petroleum Conference Field Trip, November 1, 2014

Corresponding author: Neil Rogers (nrogers@nrcan.gc.ca)

Rogers, N., McClenaghan, M.B., Thorne, K.G., Fyffe, L.R., Seaman, A.A, Parkhill, M.A., McClenaghan, S.H., Pronk, A.G., Beal, K.L., Lentz, D.R., Wilson, R.A., Rice, J.M., and Lentz, C., 2015. Granite-related mineralization and alteration in the Acadian Plutonic Belt: implications for Sn-W-Mo-Cu exploration in central New Brunswick – TGI 4 Field Guide; *in* TGI 4 – Intrusion Related Mineralisation Project: New Vectors to Buried Porphyry-Style Mineralisation, (ed.) N. Rogers; Geological Survey of Canada, Open File 7843, p. 113-204.

Table of contents

Table of contents 114
List of figures 117
Safety issues 120
Acknowledgements 120

Geological setting of the Acadian Plutonic Complex in the Miramichi Highlands, central New Brunswick 122
Introduction 122
Regional geology 122
Tectonic history 126
Trousers Lake Metamorphic Suite 127
Acadian Plutonic Belt 127
Becaguimec Lake Gabbro 128
Howard Peak Intrusive 128
Juniper Barrens Pluton 128
Nashwaak Pluton 129
Lost Lake Pluton 129
Burnthill Pluton 129
Dungarvon Pluton 129
Metallogeny 131
Glacial history 132

Sisson W-Mo Deposit 135
Exploration history 135
Geological setting 137
Structural geology 139
Deposit geology 141
Mineralisation 143
Resource estimates 144
Indicator mineral, till geochemical, and stream sediment geochemical signatures 145

Burnthill W-Sn-Mo Deposit 149
Exploration history 149
Deposit description 151

Zealand Station beryl prospect 153
Exploration history 153
Geological setting 155
Geochemistry 156
Geochronology 157
Beryl mineralisation 157
Molybdenum and tungsten mineralisation 158
Deposit model 158

Trip 1 – Sisson Brook and Zealand Station 159
Itinerary 159
Stop 1-01: Hayden Lake Formation 159
Stop 1-01A: Ferromanganiferous mudstones 159
Stop 1-01B: Black graphitic and pyritic shales 160
Stop 1-02: Miramichi Group 161
Stop 1-03: Intense greisen alteration, Nashwaak Granite 162
Stop 1-04: Alteration zone in Nashwaak Granite 163
Stop 1-05A: Nashwaak Granite 164
Stop 1-05B: Nashwaak Granite 165
Stop 1-06: Howard Peak Granodiorite 165
Stop 1-07: Sisson Brook Zone I trench 166
Stop 1-08: Howard Peak Granodiorite 168
Stop 1-09: Sisson Brook Zone III trench 169
Stop 1-10: Ablation till 173
Stop 1-11: Zealand Station beryl prospect 173

Trip 2 – Tin Hill 175
Itinerary 175
Stop 2-01: Western domain of Nashwaak Granite 175
Stop 2-02: Eastern domain of Nashwaak Granite 176
Stop 2-03: Knight's Brook Formation 177
Stop 2-04: Push and Be Damned Formation 178
Stop 2-05: Two and a Half Mile Brook Occurrence 180
Stop 2-06: Burnthill Granite 180
Stop 2-07: Tin Hill 181

Stop 2-07A: Buttermilk Brook Cupola 183
Stop 2-07B: Tin Hill Sn-W-Mo Occurrence 183
Stop 2-08: Knight's Brook Formation (hornfels) 184
Stop 2-09: Burnthill Granite 184
Stop 2-10: McKiel Lake Orthogneiss 186
Stop 2-11: Trousers Lake Migmatite 187
Stop 2-12: Juniper Barrens Granite 188

Trip 3 – Burnthill 189
Itinerary 189
Stop 3-01: Hayden Lake Formation 189
Stop 3-02: Knight's Brook Formation W-Sn-Mo mineralisation 190
Stop 3-03: Burnthill Mine site 192
Stop 3-03A: Adit portal 192
Stop 3-03B: Exogranitic W-Sn-Mo mineralisation 193
Stop 3-03C: Decommissioned headframe 194
Stop 3-03D: Drill core 194
Stop 3-04: Todd Mountain Sn Occurrence 194

References 197

List of figures

Figure 1 – Radarsat image of New Brunswick and Maine, showing relief of the Miramichi Highlands and the location of the Acadian Plutonic Belt.

Figure 2 – Geology of west-central and southwestern New Brunswick, showing the location of the Sisson Brook, Burnthill and Zealand Station deposits.

Figure 3 – Regional geology map highlighting the various Late Silurian to Late Devonian Acadian Plutonic Belt intrusions.

Figure 4 – Simplified geological map of New Brunswick and adjacent Maine.

Figure 5 – Various styles of mineralisation found in the Acadian Plutonic Belt, central New Brunswick.

Figure 6 – Space/time stratigraphical summary of central and southern New Brunswick.

Figure 7 – Orientation of regional and local ice-flow phases in south-central New Brunswick.

Figure 8 – Geology map of the Sisson Brook area showing the location of mineralised zones at the Sisson deposit.

Figure 9 – Boudinaged granitic dyke and dykelets cross-cutting foliated gabbro of the Howard Peak Granodiorite along the western margin of the Sisson W-Mo deposit.

Figure 10 – Massive, fine-grained granite porphyry dyke containing quartz and feldspar phenocrysts.

Figure 11 – Granitic dykes cross-cutting gabbroic rocks of the Howard Peak Granodiorite.

Figure 12 – Granodiorite cross-cut by a diabase dyke that is offset along a set of prominent west-northwest-trending microfaults (Sisson Zone I trench).

Figure 13 – Gabbro containing plagioclase porphyroclasts in the trenched exposure at Sisson Zone III. Note the deformed granitic dykes and the cross-cutting northwest-trending quartz vein.

Figure 14 – Sinistral offset of an east-trending quartz-feldspar vein along a north-trending fault along the southern margin of the trench at Sisson Zone III.

Figure 13 – Gabbro containing plagioclase porphyroclasts in the trenched exposure at Sisson Zone III. Note the deformed granitic dykes and the cross-cutting northwest-trending quartz vein.

Figure 14 – Sinistral offset of an east-trending quartz-feldspar vein along a north-trending fault along the southern margin of the trench at Sisson Zone III.

Figure 15 – A) Fracture-controlled scheelite mineralisation mantled by an alteration halo of biotite alteration. B) Molybdenite mineralisation along the margins of a quartz vein.

Figure 16 – Scheelite in the 0.25-0.5 mm size fraction of till in the vicinity of the Sisson W-Mo deposit.

Figure 17 – Scheelite in the 0.25-0.5 mm size fraction of stream sediments in the vicinity of the Sisson W-Mo deposit.

Figure 18 – Molybdenite in the 0.25-0.5 mm size fraction of till in the vicinity of the Sisson W-Mo deposit.

Figure 19 – Headframe at the former Burnthill Tungsten Mine (ca. 1960s).

Figure 20 – Bedrock geology of the Burnthill area showing the location of the Burnthill Mine in relation to the other mineral occurrences in the region.

Figure 21 – Cross-section displaying drillhole intersections of Burnthill mineralisation and their relationship with the underlying Burnthill Pluton.

Figure 22 – Paragenetic sequence for the Burnthill deposit.

Figure 23 – Geological setting of the Zealand Station beryl prospect.

Figure 24 – Photographs of the various granitic phases of the Hawkshaw Granite at the Zealand Station prospect.

Figure 25 – A) Disseminated beryl within granite at the Zealand Station prospect. B) Subhedral to euhedral beryl crystals from the Zealand Station prospect.

Figure 26 – Fe- and Mn-rich shale of the Hayden Lake Formation in the pit at Stop 1-01A.

Figure 27 – Contact between black pyritic shale (left) and maroon siltstone of the Hayden Lake Formation at Stop 1-01B.

Figure 28 – Field photograph of the quartzose sandstone beds of the Miramichi Group at Stop 1-02.

Figure 29 – Calcite filled pod rimmed by drusy quartz within the Nashwaak Granite at Stop 1-04.

Figure 30 – Field photograph of the Nashwaak Granite outcrop along the edge of the Nashwaak River at Stop 1-05A.

Figure 31 – Field photographs of an aplitic dyke cutting equigranular biotite granite of the Nashwaak Granite at Stop 1-05A.

Figure 32 – Howard Peak Granodiorite: medium- to coarse-grained plagioclase-rich diorite/granodiorite, cross-cut by fine- to medium-grained biotite-bearing felsic dykes interpreted to be derived from the Nashwaak Granite (Stop 1-06).

Figure 33 – Schematic diagram of the trench at Zone I.

Figure 34 – Field photograph showing the faulted contact between metasedimentary rocks and granodiorite in the trench at Zone I (Stop 1-07).

Figure 35 – C-S fabric developed in silicified metasedimentary units in the trench at Zone I, Sisson deposit (Stop 1-07).

Figure 36 – Foliated Howard Peak Granodiorite cross-cut by northerly-trending granitic dykelets, which in turn are cross-cut by west-northwesterly trending, molybdenite-bearing quartz veins (Stop 1-08).

Figure 37 – Foliated Howard Peak Granodiorite cross-cut by granite pegmatite dyke at Stop 1-08.

Figure 38 – Exploration trench at Zone III of the Sisson deposit at Stop 1-09.

Figure 39 – Intersecting, molybdenite-bearing quartz veins in the Zone III trench at Stop 1-09, Sisson deposit.

Figure 40 – Till sections in the Zone III trench of the Sisson W-Mo deposit.

Figure 41 – Geology map of the trenched exposure at the Zealand Station prospect (Stop 1-11).

Figure 42 – Bedrock Geology map in the areas covered by Stops 2-01 and 2-02.

Figure 43 – Exposed outcrop of migmatite (Trousers Lake Metamorphic Suite) pendant enclosed within the Nashwaak Granite (Stop 2-01).

Figure 44 – Porphyroblast development in the metamorphic aureole of the Nashwaak Pluton (Stop 2-02)

Figure 45 – Bedded quartzose wacke and siltstone exhibiting a prominent S1 fabric and metamorphic spotting (Stop 2-03).

Figure 46 – Middle Ordovician Hayden Lake Formation massive siltstone and lithic wacke with rare tuffaceous ash beds (Stop 2-04).

Figure 47 – Exo-contact mineralisation of the Two and a Half Mile Brook occurrence (Stop 2-05).

Figure 48 – Coarse-grained granite of the Burnthill Pluton (Stop 2-06).

Figure 49 – Simplified geology of the Burnthill region.

Figure 50 – Endogranitic quartz veins and greisen hosting Sn-W-Mo mineralisation of the Tin Hill occurrence (Stop 2-07).

Figure 51 – Endogranitic quartz veins and greisen hosting Sn-W-Mo mineralisation of the Tin Hill occurrence (Stop 2-07).

Figure 52 – Cordierite-spotted and hornfelsed metasedimentary rocks (siltstone and wacke) of the Knight's Brook Formation, Miramichi Group (Stop 2-08).

Figure 53 – Multiple phases of the Burnthill Pluton – medium to coarse-grained, seriate to equigranular textured biotite granite is cut by pods of the porphyritic quartz-feldspar microgranite (Stop 2-09).

Figure 54 – Rapakivi texture developed in the Burnthill Pluton at Stop 2-09.

Figure 55 – Coarse-grained feldspar augen granite (orthogneiss) of the McKiel Lake Suite (Stop 2-10).

Figure 56 – Migmatite of the Trousers Lake Metamorphic Suite cut by Devonian pegmatite veins (Stop 2-11).

Figure 57 – Coarse-grained biotite granite of the Juniper Barrens Pluton (Stop 2-12).

Figure 58 – Small, roadbed outcrop of Hayden Lake Formation aphanitic rhyolite (Stop 3-01).

Figure 59 – Cordierite-spotted siltstone and quartzose wacke of the Knight's Brook Formation, Miramichi Group, cut by numerous wolframite-bearing quartz veins (Stop 3-02).

Figure 60 – Composite plan map of underground workings at the Burnthill Mine.

Figure 61 – Quartz veins and W-Sn-Mo mineralisation related to the nearby Burnthill Mine Property (Stop 3-02).

Figure 62 – Exogranitic mineralisation developed in metasedimentary rocks of the Knight's Brook Formation at the adit portal of the Burnthill Mine (Stop 3-03A).

Figure 63 – Molybdenite mineralisation and bladed wolframite associated with quartz veins and greisen at the Burnthill Mine.

Figure 64 – Bedrock geology of the Burnthill and Dungarvon areas showing the location of the Todd Mountain occurrence in relation to mineral occurrences throughout the region.

Figure 65 – Locally garnetiferous metasedimentary rocks of the Knight's Brook Formation, Miramichi Group, at the Todd Mountain Sn Occurrence (Stop 3-04).

Figure 66 – Contrasting mineralisation styles at the Todd Mountain deposit. A) Arsenopyrite along widely spaced fracture cleavage. B) Cassiterite-bearing greisen.

Safety issues

Field trips such as this may involve hazards to the leaders and participants. The organizers recommend steel-toed safety boots when working around road cuts, cliffs, or other locations where there is a potential hazard from falling objects. Some field trip stops require sturdy hiking boots for safety.

The weather in New Brunswick can be unpredictable, and participants should be prepared for a wide range of temperatures and conditions, and so always take suitable clothing.

Above all, field trip participants are responsible for acting in a manner that is safe for themselves and their co-participants. This responsibility includes using personal protective equipment (PPE) when necessary. We will be working in a granitic terrain, with very hard splintery rocks (granites and hornfels). At all outcrops please be careful if taking samples; make sure you have safety glasses and that those around you are aware of what you are doing.

Acknowledgements

We would like to thank JD Irving Ltd. for access to the Irving Deersdale woodlands, as well as Northcliff Resources Ltd. and Cadillac Ventures Ltd., for permission to visit their properties and view drill core. Lyman Lawrence is also thanked for allowing access to his mineral collection and the Zealand property. The New Brunswick Department of Energy and Mines has provided maps, printable materials and logistics for the excursion. The Geological Survey of Canada has provided financial support to mapping activities in the region. We would like to acknowledge L.R. Fyffe, R.A. Wilson, D. Lentz, H.E. MacLellan, C. St Peter, C. Lentz, G.W. Crouse, R.R. Irrinki, J.B. Whalen, C.R. van Staal, W.H. Poole, W. Zhang, R. Boldon, M. Richards, R. van Drecht and W. Gilmore for their contributions to the resolving the geology of the area and producing this field guide.

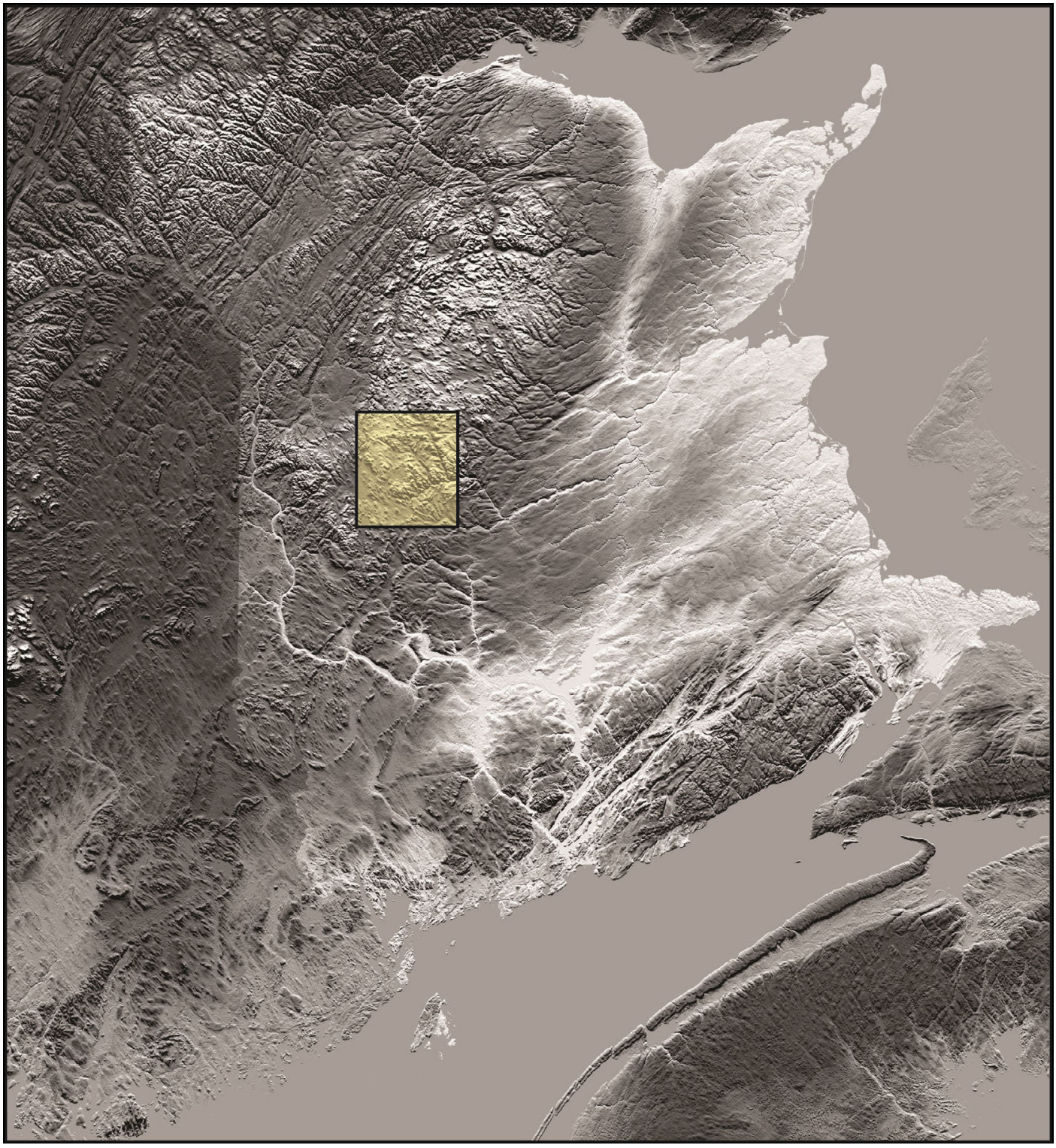

Figure 1 – Radarsat image of New Brunswick and Maine, showing relief of the Miramichi Highlands and the location of the Acadian Plutonic Belt.

Geological Setting of the Acadian Plutonic Complex in the Miramichi Highlands, Central New Brunswick

Introduction

The Acadian Plutonic Belt is a region of widespread Late Silurian to Late Devonian plutonism and associated mineral occurrences that are principally exposed in the Juniper region of central New Brunswick (Figs. 1 and 2). This belt contains voluminous plutons of varying age and composition that formed during the Acadian and Neoacadian orogenies (ca. 420-360 Ma), which intrude the high-grade migmatites and variably metamorphosed (greenschist to amphibolite) volcanic and sedimentary rocks of the central Miramichi Highlands (Fig. 2). The Acadian Plutonic Belt (Fig. 3) is host to a variety of endogranitic and exogranitic deposits of Sn, W, Mo, Sb, Cu, Au, Ag, and rare earth elements, as well as numerous beryl and tourmaline pegmatite occurrences. In the eastern half of the Acadian Plutonic Belt, the Late Devonian Burnthill and Dungarvon granites are among the most prolific plutons for generating Sn-W-Mo mineralisation, including the past producing Burnthill W Mine. Early Devonian plutons in the western half of the belt intrude high-grade migmatites of the Ordovician Trousers Lake Metamorphic Suite and are typically barren of any Sn-W-Mo-Cu mineralisation. In contrast, the Early Devonian Nashwaak Granite that occurs to the east of the Trousers Lake Metamorphic Suite contains numerous zones of greisen-style and potassic alteration and is potentially the source for the exogranitic W-Mo mineralisation at Sisson, the largest known W-Mo deposit in the entire Acadian Plutonic Belt. The age of the Sisson mineralisation is however only poorly constrained as syn- to post-intrusive in relation to the main body of the Nashwaak Granite (ca. 422-416 Ma) and predating post- deformational biotite-granite dykes dated at ca. 364 Ma.

Overall, Devonian plutonism is considered to be the source of widespread Sn-W-Mo-Cu mineralisation throughout the Acadian Plutonic Belt, with timing (age), local geology, and mode of emplacement significantly constraining mineralisation.

Regional Geology

The Miramichi Highlands of central New Brunswick (Figs. 2 and 3) are characterized by Cambrian to Early Ordovician quartzose sedimentary rocks of the Miramichi Group and overlying Middle Ordovician volcanic and sedimentary rocks that are correlated to the Tetagouche Group, as defined for the Bathurst Mining Camp approximately 100 km to the northeast (van Staal and Fyffe, 1991, 1995a, 1995b; van Staal et al., 1992; Fyffe et al., 1997). The Miramichi Group in the Sisson Brook area comprise a deep-water, turbiditic sequence of interbedded quartzose sandstone and shale that are allocated to the Knights Brook Formation. The base of the Tetagouche Group in the central Miramichi Highlands is marked by a thin unit of conglomerate and interbedded calcareous siltstone and felsic tuff (Turnbull Mountain Formation). The calcareous siltstone in the Turnbull Mountain Formation in central New Brunswick and correlative Vallée Lourdes Formation in the Bathurst area of northeastern New Brunswick contain Early Ordovician (Arenigian) brachiopods (Fyffe, 1976; Neuman, 1984; Fyffe et al., 1997; Poole and Neuman, 2003). The upper part of the Tetagouche Group in central New Brunswick comprises the Hayden Lake Formation, which consists of ferromanganiferous cherty siltstone, black chert and shale interbedded with mafic volcanic rocks, along with minor felsic volcanic rocks, which in turn is overlain by wacke and shale of the Ordovician Push and Be Damned Formation. The bimodal volcanic rocks of the Tetagouche Group are interpreted, on the basis of their geochemical composition, to have been generated in an intra-arc rift to back-arc basin transitional setting (van Staal, 1987; van Staal et al., 1991, 2003; van Staal and Fyffe, 1995a).

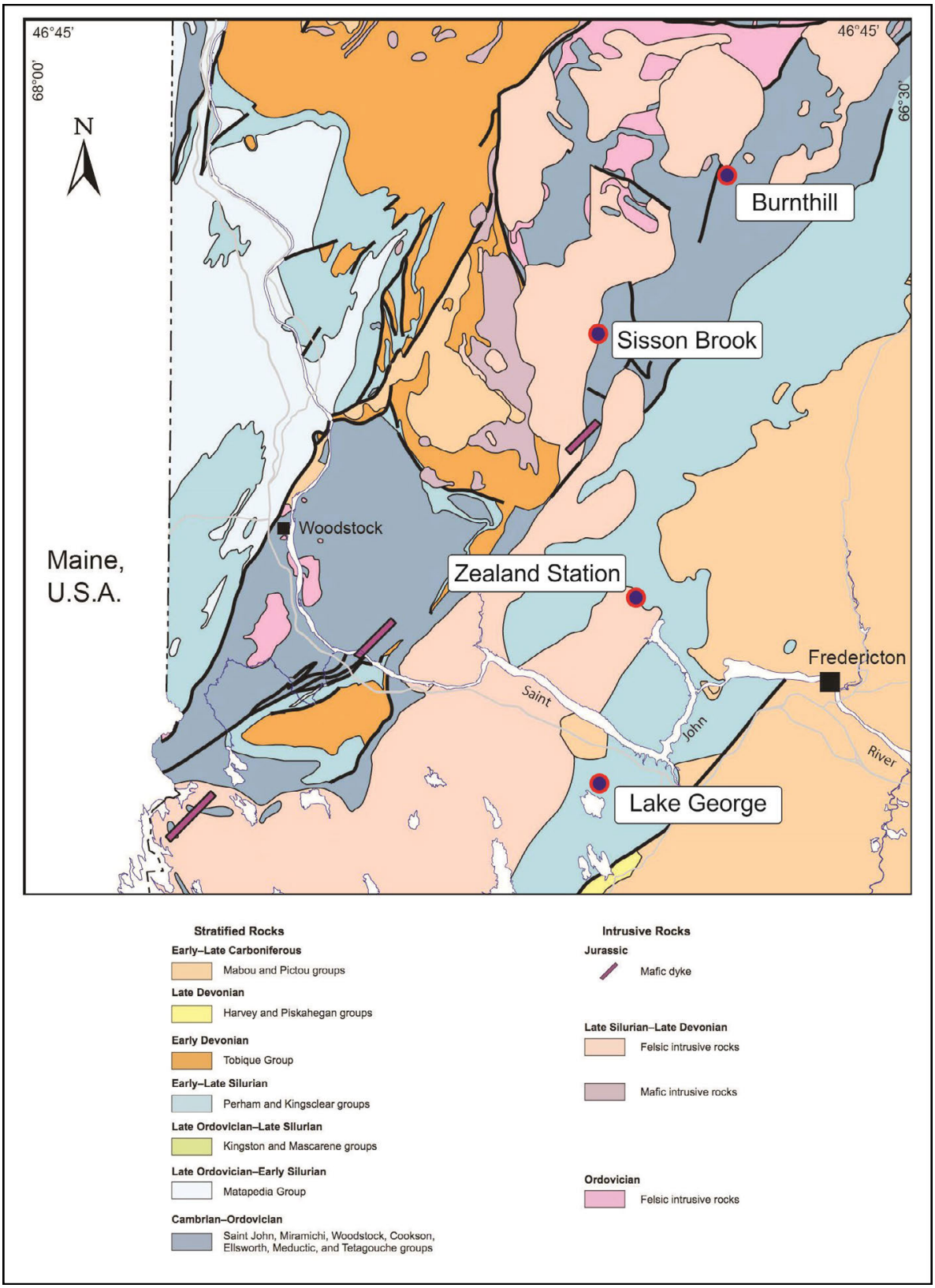

Figure 2 – Geology of west-central and southwestern New Brunswick, showing the location of the Sisson Brook, Burnthill and Zealand Station deposits (after Fyffe et al., 2010).

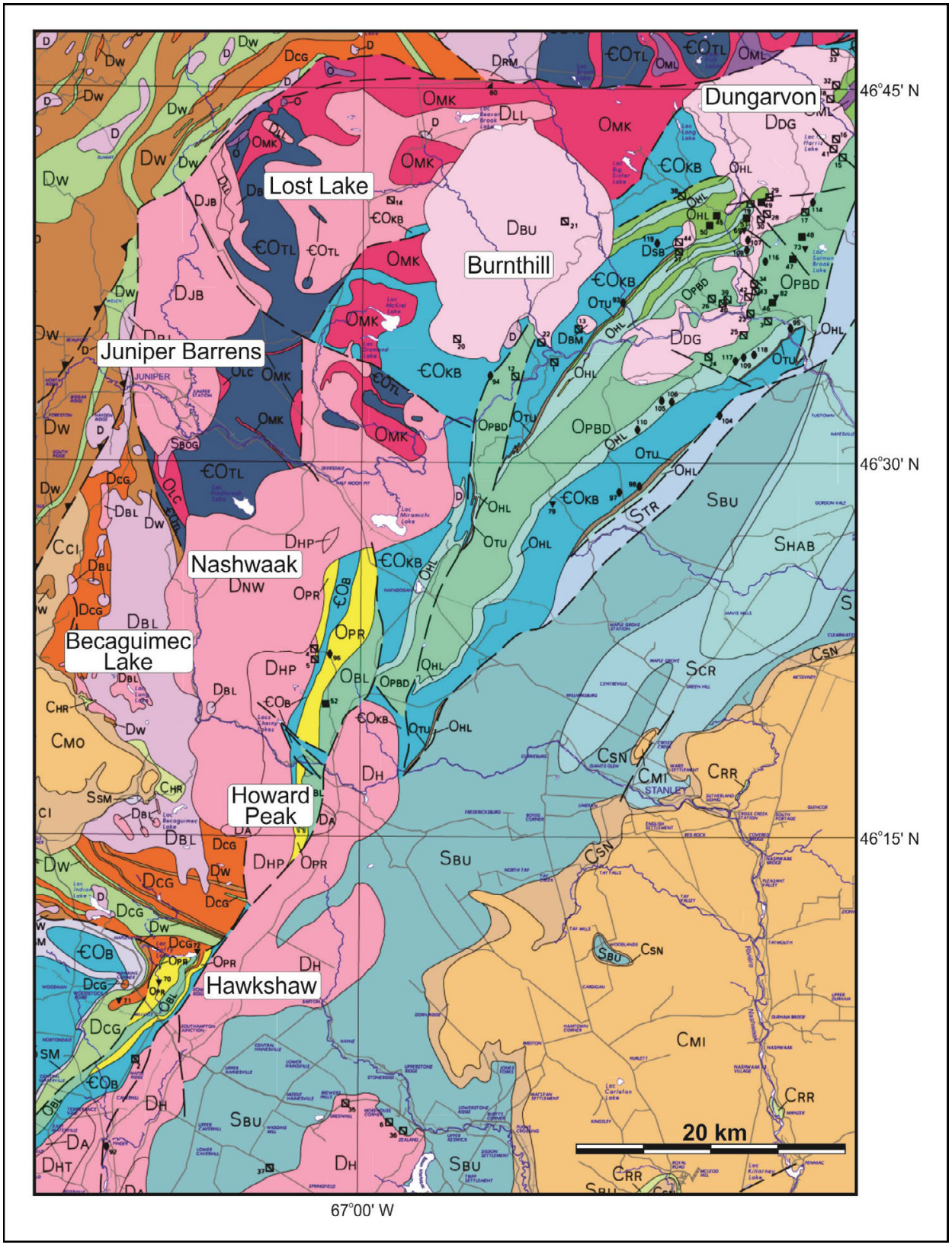

Figure 3 – Regional geology map highlighting the various Late Silurian to Late Devonian Acadian Plutonic Belt intrusions (after Smith and Fyffe, 2006).

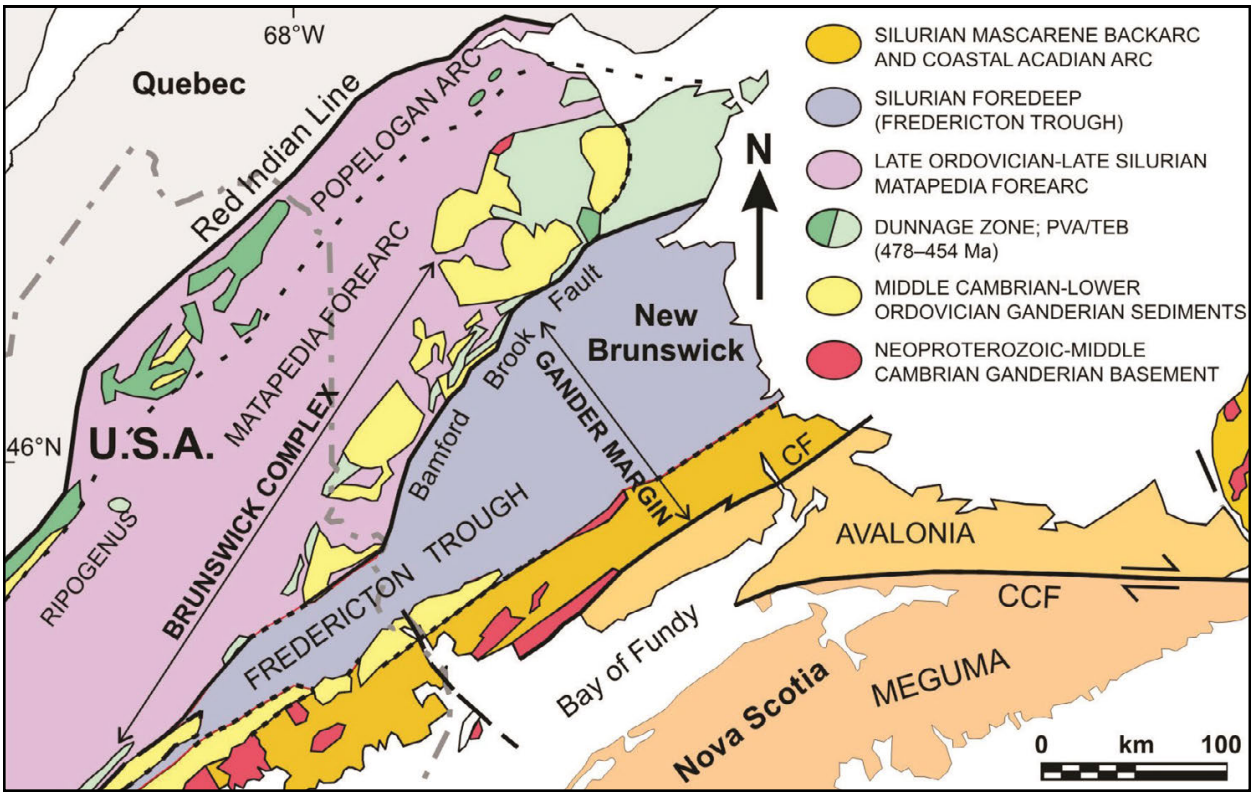

Figure 4 – Simplified geological map of New Brunswick and adjacent Maine displaying the exposed remnants of the Brunswick subduction complex and other Ordovician–Silurian Ganderian tectonic elements (van Staal et al., 2008).

Pre-Silurian rocks in the Miramichi Highlands can be broadly divided into four lithostratigraphic groups (Figs. 3 and 4), namely the Miramichi and Woodstock groups of the Gander Zone and Tetagouche and Meductic groups of the Dunnage Zone (van Staal, 1987; van Staal and Fyffe, 1991; van Staal et al., 2003).

The Miramichi Group consists of a continentally derived turbidite sequence of quartz wacke, quartzite, siltstone, and shale of Early Cambrian to Early Ordovician age, consistent with the presence of Tremadocian graptolites in black shale of the Woodstock Group (Fyffe et al., 1983). The Miramichi Group has been divided into three formations; from oldest to youngest, they are: 1) a lower sequence of thick-bedded quartzose sandstone (Chain of Rocks Formation); 2) a middle sequence of medium-bedded quartzose sandstone and shale (Knights Brook Formation); and an upper sequence of medium- bedded feldspathic wacke and shale (Patrick Brook Formation). The major distinguishing feature between the Knights Brook and Patrick Brook formations is the colour and composition of sandstone, whereas the Chain of Rocks Formation is dominated by coarser-grained clasts, sandstone and greywacke (van Staal and Fyffe, 1991; van Staal et al., 2003).

Along the western margin of the Acadian Plutonic Belt, the Trousers Lake Metamorphic Suite occurs as a dismembered slice of high-grade amphibolite-facies migmatite in thrust contact with lower-grade (middle-greenschist) sedimentary rocks of the Miramichi Group (Fyffe et al., 1988). The Trousers Lake Metamorphic Suite rocks exhibit a distinct paragneiss texture that has been interpreted as migmatitic melts of a sedimentary protolith equivalent to the Cambro-Ordovician Miramichi Group.

At the onset of Ordovician volcanic activity (Dunnage Zone), sedimentary rocks of the Gander Zone were subjected to Ordovician plutonism (gabbro to granite) that is, in part related to volcanism associated with the Tetagouche-Exploits back-arc basin and associated arc terranes. Ordovician plutons are found throughout the Miramichi highlands and likely represent late melts from the magma chambers that fed these very large volcanic events. In the vicinity of Juniper these Ordovician granite plutons have been assigned to either the Little Clearwater or McKiel Lake suites.

In the core of the Miramichi Highlands, Cambro-Ordovician siliciclastic rocks of the Gander Zone (Miramichi and Woodstock groups) are overlain by remnants of the Dunnage Zone represented by Middle Ordovician volcanic arc and back-arc rocks of the Meductic and Tetagouche groups (van Staal and Fyffe, 1991, 1995a, 1995b; van Staal et al., 1992; Fyffe et al., 1997). The upper part of the Tetagouche Group in central New Brunswick comprises a sequence of ferromanganiferous cherty siltstone, black chert and shale interbedded with aphanitic to feldspar-phyric felsic volcanic rocks and pillowed mafic volcanic rocks of the Hayden Lake Formation. Overall, bimodal volcanic rocks of the Tetagouche Group are interpreted, on the basis of their geochemical composition, to have been generated in an intra-arc rift to extensional back-arc basin transitional setting (van Staal, 1987; van Staal et al., 1991, 2003; van Staal and Fyffe, 1995a). Recent lithogeochemistry of aphyric felsic rocks of the Hayden Lake Formation outcropping in the Renous River to the north reveal an alkaline (comenditic) composition and are likely contemporaneous with the eruption of comenditic rocks of the Boucher Brook Formation (Bathurst Mining Camp) during the later stages of rifting in the Tetagouche-Exploits back-arc basin. Following the waning of volcanic activity, the region was covered by a thick sequence of lithic wackes, mudstones, shale, calcareous siltstone and rare conglomerates that constitute the Late Ordovician Push and Be Damned Formation. The area was subsequently intruded by several Late Silurian- to Late Devonian-aged plutons of the Acadian Plutonic Belt.

Tectonic History

Sinistral-oblique convergence of the Popelogan – Victoria Lake Arc during the Middle to Late Ordovician, followed by collision with Laurentia ca. 455-450 Ma, marked the end of the Taconic orogenic cycle (van Staal et al., 2003, 2008). Further convergence between Laurentia and Ganderia was accommodated by northwest-directed (present coordinates) subduction of ensimatic to ensialic crustal segments of the Tetagouche – Exploits back-arc basin beneath the Popelogan Arc from the Late Ordovician (Caradocian) to late Early Silurian (van Staal et al., 2003). The resulting accretionary wedge, referred to as the Brunswick Subduction Complex, developed by obduction of thrust nappes onto the Ganderian continental margin, and was accompanied by polyphase deformation and lower to upper-greenschist metamorphism (van Staal et al., 2003) throughout the Miramichi Highlands. However, in the Trousers Lake Metamorphic Suite in the southern Miramichi Highlands (i.e., Juniper – Sisson area), metamorphism reaches amphibolite grade (van Staal et al., 2008). Development of the accretionary wedge was characterized by imbrication into numerous thrust nappes and panels that were subsequently folded into shallow and steep structures (van Staal et al., 2003). In central New Brunswick, this has had the effect of juxtaposing a narrow, dismembered slice of amphibolite-grade migmatite of the Trousers Lake Metamorphic Suite (see below) with lower-grade (middle -greenschist) metasedimentary rocks of the Miramichi Group (Fyffe et al., 1988).

Subduction of Tetagouche – Exploits back-arc crust ended with collision of Ganderia and composite Laurentia (Salinic Orogeny) in the late Early Silurian (ca. 430 Ma; van Staal et al., 2003, 2009). Slab break-off and a subsequent influx of asthenospheric mantle resulted in uplift in the adjacent Matapedia forearc and Silurian to Devonian bimodal volcanism. Devonian sedimentary and volcanic rocks were deposited in both subaerial and submarine settings within an extensional/transtensional tectonic regime (e.g., Dostal et al. 1989). Large scale folding, cleavage

development, and brittle faulting in the Early to Middle Devonian accompanied southeast-to-northwest migration of the Acadian deformation front during dextral oblique convergence of Avalonia with composite Laurentia. The Acadian Orogeny led to inversion of the Silurian Mascarene Back-arc Basin behind coastal Acadian volcanic arcs, and progressive Early Devonian uplift in northern New Brunswick culminating in subaerial volcanism and fluvio-lacustrine sedimentation. Middle to Late Devonian, post-Acadian tectonics were dominated by large-scale dextral transpression throughout much of New Brunswick (van Staal et al., 2008).

Trousers Lake Metamorphic Suite

At the western end of the Acadian Plutonic Belt, a dismembered slice of high-grade amphibolite-facies migmatites (Trousers Lake Metamorphic Suite) sits in thrust contact with lower-grade (middle-greenschist) metasedimentary rocks of the Miramichi Group (Figs. 2 and 3; Fyffe et al., 1988). Contacts are obscured by sedimentary and volcaniclastic rocks (Tobique Group) and by synorogenic granites and gabbros, which tend to intrude along these natural breaks. These rocks exhibit a distinct paragneiss texture, which has been interpreted as migmatitic melts of a sedimentary protolith coeval with the Cambro-Ordovician Miramichi Group. Migmatites of the Trousers Lake Metamorphic Suite are remarkably consistent in appearance featuring a leucosome melt composed of quartz and feldspar and a melanocratic residuum that is rich in biotite. The migmatites can frequently include preserved paleosome that resembles metamorphosed quartzite and siltstone of the Miramichi Group. Amphibolite units occur frequently within the migmatites, likely representing Ordovician mafic intrusive rocks, which reflect the higher metamorphic grades (Fyffe et al., 1988). Ordovician granites of the McKiel Lake Suite exhibit an intimate relationship with the migmatites and are found throughout the Trousers Lake Metamorphic Suite. Ordovician granite bodies of both the Little Clearwater and McKiel Lake granites exhibit distinct orthogneiss textures, having been subjected to tectonism of the Salinic Orogeny. To date, Ordovician plutons throughout the Juniper region have been largely assigned to the McKiel Lake and Clearwater Suites (Fig. 2). Compositionally, several distinct plutonic suites are found in the region, indicating this nomenclature is simplistic and in need of revision.

Acadian Plutonic Belt

Devonian magmatism has resulted in prolific granite and gabbroic intrusions throughout the Miramichi Highlands (Fyffe et al., 1981; Bevier and Whalen, 1990; Whalen, 1993; Whalen et al., 1996). Recent radiometric dating has partially resolved the timing of granitoid emplacement in the Acadian Plutonic Belt, revealing two broad episodes of plutonism. An Early Devonian (ca. 420-410 Ma) episode is concurrent with the main phase of the Acadian orogeny, resulting in elongate intrusive bodies aligned with Acadian structural grain, and stitching boundaries between various structural breaks within the Miramichi Highlands. Internally, syn-orogenic granites exhibit varying degrees of tectonic fabric development, with the most intense of these fabrics best developed along the edges of plutons. A second Late Devonian (ca. 380 Ma) episode resulted in the emplacement of post-orogenic plutons at higher crustal levels in the Miramichi Highlands and is coeval with Neoacadian orogenesis. The timing of these events reflects the progressive accretion of peri-Gondwanan micro-continental terranes onto composite Laurentia. Ganderia, of which the Miramichi Highlands are a part, was the first block accreted to Laurentia at ca. 455 Ma following the closure of the Iapetus Ocean. The ca. 420 Ma oblique (dextral) accretion of Avalonia to the eastern margin of Ganderia induced the Acadian Orogeny (effects of which are most intense in southern New Brunswick). This was subsequently followed by the emplacement of Meguma and the associated Neoacadian Orogeny. Although the Acadian Plutonic Belt rocks are within- plate, "anorogenic" granites, and far removed from the active arc-back-arc magmatism the coincidental timing of events indicates a relationship. The most likely being that the non-orthogonal accre-

tion resulted in large-scale dextral transpression throughout the Miramichi Highlands (van Staal et al., 2008), which in turn triggered the granitoid magmatism.

The main plutons in the Sisson Brook area include the Howard Peak Granodiorite and the Nashwaak Granite. The Howard Peak Granodiorite consists of hornblende-biotite granite grading into gabbro that is intensely sheared and cataclastic in nature along its eastern margin. It exhibits a penetrative fabric as well as abundant elongated, schistose xenoliths derived from the adjacent folded country rocks (Lutes, 1981; Venugopal, 1982). Both the granodiorite and gabbro are intruded by the Nashwaak Granite, the largest pluton in the region. It also intrudes both the Trousers Lake Metamorphic Suite and meta-sedimentary rocks of the Miramichi Group, obscuring much of the structural boundary between these two distinct terranes.

Becaguimec Lake gabbro

The Becaguimec Lake gabbro (Fig. 3) is a medium to coarse-grained ophitic gabbro troctolite that is accompanied by numerous stocks and dykes of hornblende-biotite felsic porphyry and is most prevalent along the southwest margin of the Acadian Plutonic Belt. The gabbro cuts migmatites of the Trousers Lake Metamorphic Suite and Devonian cover rocks of the Wapske Formation (Tobique Group), but is intruded by the Devonian Juniper Barrens Granite making this gabbro one of the earliest of the Devonian intrusive phases in the region.

Howard Peak Intrusive

The Early Devonian Howard Peak granodiorite (Fig. 3) is a medium-grained, hornblende – biotite granodiorite that grades into a dark grey, medium-grained ophitic gabbro. The eastern margin of the pluton is intensely sheared and cataclastic in nature, and exhibits a penetrative fabric as well as abundant elongated, schistose xenoliths derived from the adjacent folded country rocks (Lutes, 1981; Venugopal, 1982). Both the granodiorite and gabbro are cut by granitic dykes related to the intruding Nashwaak Pluton.

Juniper Barrens Pluton

The Juniper Barrens Pluton (Fig. 3) consists of a medium to coarse-grained equigranular biotite granite and biotite-muscovite, which exhibits a mild tectonic fabric consistent with its emplacement during the Acadian Orogeny. The Juniper Barrens granite has been dated at 415.8 ± 0.3 Ma (U-Pb Zircon; TIMS) and has been reassigned to include adjoining phases of the Beadle Mountain granite, which is similar in composition and texture, and yielded an age of 416.1 ± 0.5 Ma (U-Pb Zircon; TIMS). Both the Juniper Barrens granite and formerly Beadle Mountain granite intrude cover rocks of the Wapske Formation in the west as indicated by contact hornfels alteration of sedimentary rocks and excessive potassic alteration in the region. The Juniper Barrens granite is not known to host Sn-W-Mo mineralisation, with only rare garnetiferous aplite, small pods of tourmaline-muscovite pegmatite, and veins of massive tourmaline identified along its margins.

On the southern fringes of the Juniper Barrens granite, several occurrences of granodiorite exhibiting mild fabrics had been mapped as a distinct pluton (Bogans Brook), and interpreted as Silurian in age (based on K-Ar dating of muscovite). Recent work indicates that this intrusive likely represents partially digested pendants of Trousers Lake migmatite and (or) meta-sediments on the peripheries of the Juniper Barrens granite.

Nashwaak Pluton

One of the largest plutons in the region, the Nashwaak Pluton intrudes both the Trousers Lake Metamorphic Suite and meta-sedimentary rocks of the Miramichi Group, obscuring much of the structural boundary between these two distinct terranes (Fig. 3). The Nashwaak Pluton consists of medium-grained, sub-porphyritic biotite granite, which grades into a two mica, muscovite-biotite granite in the north. The Nashwaak granite exhibits a mild tectonic fabric consistent with its syn-tectonic emplacement in the Early Devonian. The Nashwaak Pluton differs from many of the Early Devonian Plutons, as it is host to a large the world-class W-Mo deposit. The Sisson Brook deposit (Figs. 2 and 5) consists of exo-contact W-Mo-Cu mineralisation along the eastern intrusive contact with the Howard Peak diorite/gabbro and metasedimentary and volcanic rocks of the Miramichi and Meductic Groups, respectively. Elsewhere in the Acadian Plutonic Belt, the Nashwaak granite is host minor occurrences of garnet, beryl and tourmaline-bearing pegmatite.

Lost Lake Pluton

The Lost Lake Pluton (Fig. 3) is a distinctly polyphase intrusion occurring in the north of the region and has been dated at 409.7 ± 0.5 Ma (U-Pb Zircon; TIMS). The granitic phase consists of a medium to coarse-grained, mildly foliated, equigranular, muscovite and biotite-bearing granite. The subordinate intermediate granodiorite phase of the Lost Lake Pluton is typically fine-grained and biotite-dominant. The Lost Lake granite generates abundant coarse-grained pegmatites, more than any other pluton in the region, with several notable veins containing vitreous green beryl and tourmaline (Fig. 5).

Burnthill Pluton

The Burnthill Pluton (Fig. 3) is well exposed in the Miramichi Highlands and as a result has been well documented. MacLellan et al. (1990) mapped the polyphase Burnthill Pluton in the greatest detail, characterizing several prominent phases. Medium to coarse-grained seriate biotite granite comprises the main phase of the Burnthill granite and is distributed throughout the pluton. Late stage porphyritic microgranite is found to occur sporadically throughout the pluton, but is best developed on the pluton peripheries. Rare fine-grained melanocratic biotite granite pods occur in several isolated areas and are hosted entirely by the coarse-grained main phase. The Burnthill Pluton has been dated at 380.6 ± 0.3 Ma (U-Pb Zircon; TIMS), approximately 35 m.y. younger than the Juniper Barrens Pluton and consistent with post-orogenic emplacement or near the end of the Acadian Orogeny.

The Burnthill Pluton is surrounded by numerous occurrences of exogranitic contact mineralisation including the McLean Brook and the Two and a Half Mile Brook Sn-W prospects, as well as the past-producing Burnthill Tungsten (W-Mo) Mine (Figs. 2 and 5). The small (2 km diameter) isolated Buttermilk Brook Granite consists of coarse-grained porphyritic granite, which likely represents a small cupola of the main Burnthill Pluton to the northwest. The Buttermilk phase is host to endogranitic Sn-W-Mo greisen mineralisation of the Tin Hill deposit; drilling has intersected a similar cupola beneath the Burnthill Mine.

Dungarvon Pluton

To the west lies the highly irregularly shaped Dungarvon pluton (Fig. 3), its distribution controlled largely by late reactivated faults proceeding emplacement. The Late Devonian Dungarvon Pluton is petrogenetically similar to the Burnthill Pluton, comprising medium to coarse-grained seriate biotite granite with late-stage porphyritic microgranite pods occurring sporadically throughout the pluton. Nearby, the small (3 km diameter) Sisters Brook gran-

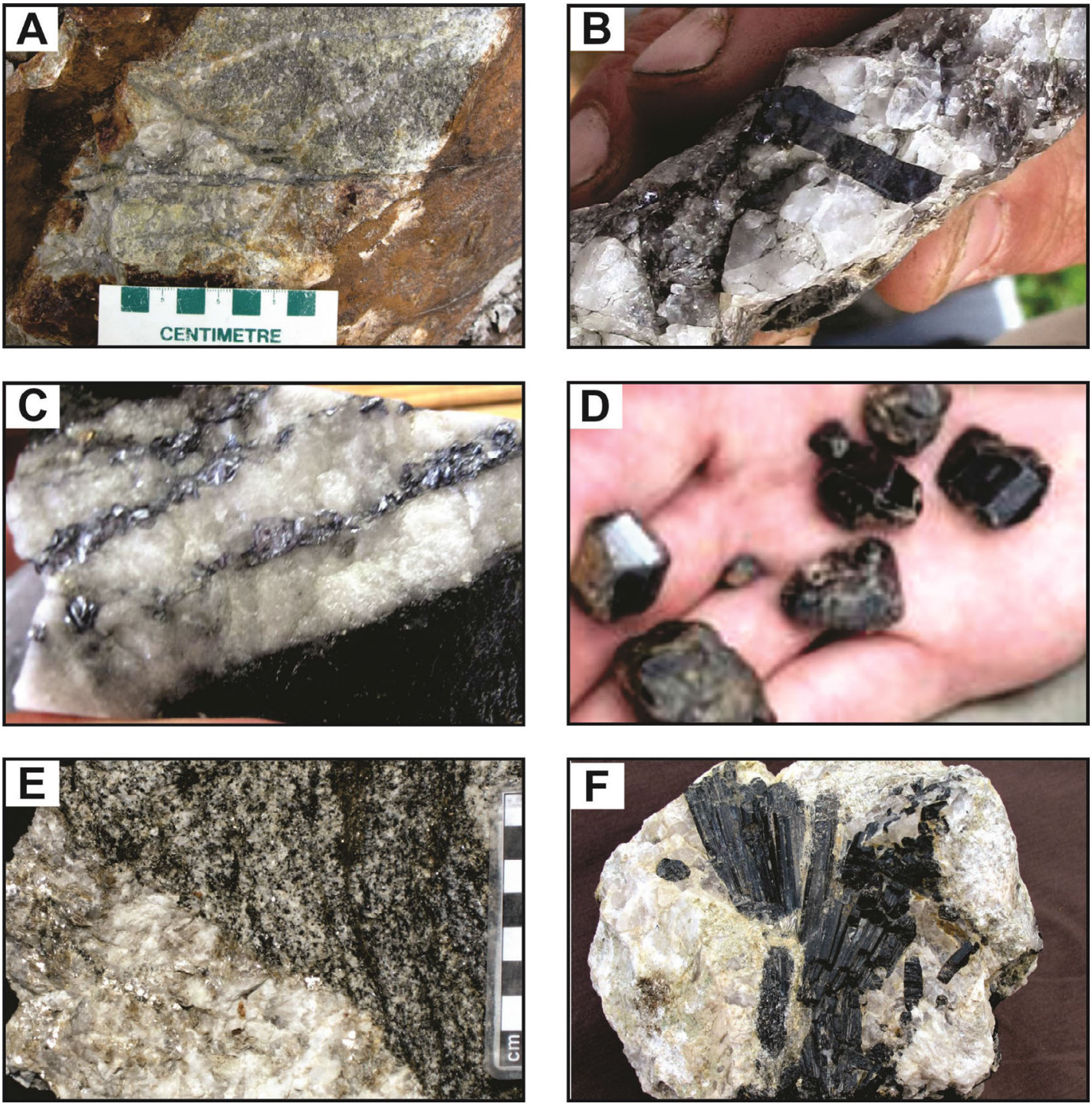

Figure 5 – Various styles of mineralisation found in the Acadian Plutonic Belt, central New Brunswick. A) Exo-contact alteration and mineralisation from the Two And A Half Mile Brook Occurrence; B) Bladed wolframite from the Sisson Brook deposit; C) Veinlets of molybdenite in quartz vein from the Sisson Brook deposit; D) Cassiterite grains from endogranitic greisen of the Tin Hill deposit; E) Coarse-grained pegmatite originating from the Lost Lake Pluton; F) Tourmaline crystals from pegmatite typical of the Lost Lake Pluton.

ite is exposed along Sisters Brook, and likely represents an exposed cupola of the larger irregularly shaped Dungarvon pluton. The Dungarvon Pluton is host to numerous occurrences of endogranitic and contact mineralisation with notable anomalous base metals, Sn-W-Mo, REE and Au. These include the Fall Brook, Peaked Mountain, Dungarvon, Cleveland, Four Mile Brook, Sisters Brook, Todd Mountain, Trout Lake and Anomaly 100.

Metallogeny

Devonian granite plutons in the Acadian Plutonic Belt are metaluminous to moderately peraluminous and exhibit I-type characteristics with some A-type affinities. The geochemical and isotopic characteristics of Devonian and Ordovician plutons in the Acadian Plutonic Belt are remarkably close. These granites all exhibit within-plate signatures that are transitional to volcanic arcs, likely due to partial melting of Proterozoic continental basement (Whalen, 1993).

Polymetallic mineral deposits within intra-plate continental settings are typically associated with late-stage, highly evolved granitic magmas enriched in lithophile elements such as silica, rubidium, lithium, beryllium, boron, and fluorine. The occurrence of these granite-related polymetallic mineral deposits in post-tectonic, intra- plate settings can be attributed to the existence of a continental crust thickened by previous orogenesis. Extension of this thickened crust can lead to underplating by mafic magma and to the production of large volumes of granitic melt in upper crustal magma chambers. Volatiles, including fluorine, emanating from the underplated mafic magmas can infiltrate the granitic melts and become further enriched in small volumes of melt through the fractionation process (Carten et al., 1993).

The presence of a fluxing agent such as fluorine in a silicate melt is of particular importance in the formation of polymetallic mineral deposits in that it lowers the crystallisation temperature and allows the melt more time to evolve and rise higher into the crust. During this process, metals such as tungsten, molybdenum, and tin become concentrated in the late-stage melts and hydrothermal fluids. Release of fluid pressure and quenching of silica-rich melts results in the evolution of metalliferous fluids (Strong, 1981). These fluids can proceed along pre-existing structures within the granite pluton and form endogranitic quartz vein hosted deposits with an enveloping greisen alteration of the granite host. Furthermore, the elements such as fluorine that helped in the original metallic enrichment of the magma, can form complexes to facilitate the transport and concentration of metals (Tweedale et al., 2014, 2015). Metalliferous fluids commonly breach the pluton and infiltrate the surrounding country rocks, resulting in disseminations, breccia fillings, stockwork veinlets, and massive quartz-vein systems near the contact of a granite pluton. Mineralisation may also take advantage of pre-existing structures in the country rock, especially where there are lineaments and/or faults (preferable with minor syn-magmatic extensional motions) intersecting at high angles (Rogers et al., 2014, 2015) leading to, typically, quartz vein-hosted deposits at considerable distances from the source intrusion.

The most common style of mineralisation associated with Devonian granite intrusions (Fig. 5) of the Acadian Plutonic Belt comprises small exo-contact greisen alteration zones within meta-sedimentary rocks. Mineralisation consists of intense silicification and associated potassic alteration (sericite) that is accompanied by disseminated pyrite- arsenopyrite with anomalous values (ppm) of Sn-W-Mo. In other instances Sn-W-Mo mineralisation can take the form of coarse-grained quartz-vein hosted cassiterite, wolframite, scheelite and molybdenite as both endogranitic and exo-contact deposits. Quartz-feldspar-muscovite-biotite pegmatites are also seen to cut through both granites and migmatites in the Acadian Plutonic Belt. These veins are coarse grained and may also contain garnet, scheelite, rare tourmaline, and a vitreous green beryl.

Glacial history

Presumably west-central New Brunswick was glaciated many times during the Pleistocene (Fig. 6). Previously all known glacial deposits in New Brunswick were interpreted to have been deposited during the Wisconsinan Stage (e.g., Lamothe, 1992; Seaman, 2004; Fyffe et al., 2009) (approximately 75 ka to 11.5 cal ka BP). [Note: all dates cited in this section are expressed as 'ka BP', i.e., thousands of years before present, with those lying within the range of radiocarbon dating (<50 ka) calibrated to be approximately equivalent to calendar years, i.e., cal ka BP.] However, a new date obtained for the organic-bearing fluviatile sediments at the Half Moon Pit section of Lamothe (1992) indicates that these sediments, originally interpreted to have been deposited during a Middle Wisconsinan interstadial, were instead deposited prior to the Wisconsinan glaciation. Hence, they were interpreted to be of Sangamonian lnterglaciation age (approximately 128 to 75 ka BP). Consequently, the stratigraphically underlying Lower Till of Lamothe (1992) is of pre-Wisconsinan rather than Early Wisconsinan age, while the immediately overlying Upper Till is of Early Wisconsinan age rather than Late Wisconsinan age (Seaman, 2009). This reinterpretation brings the Quaternary stratigraphy of New Brunswick into accord with that of Nova Scotia, where ice cover was continuous throughout the Wisconsinan (Stea et al., 1998, 2011).

The glacial history of the Maritime Provinces is now described in terms of seven glacial phases (Seaman et al., 2011; Stea et al., 2011; Seaman, 2013) (Figs. 6 and 7). Pre- Wisconsinan glacial deposits, including the lower till at Sisson (Seaman and McCoy, 2008) and elsewhere (e.g., Lamothe, 1992), the Carlisle dispersal train (Seaman, 2004, 2009), and locally preserved sub-till glaciofluvial deposits (Seaman, 2013) are assigned to the Northumberland Phase, and interpreted to have been deposited during the lllinoian Stage, approximately 200 to 130 ka BP (Seaman,

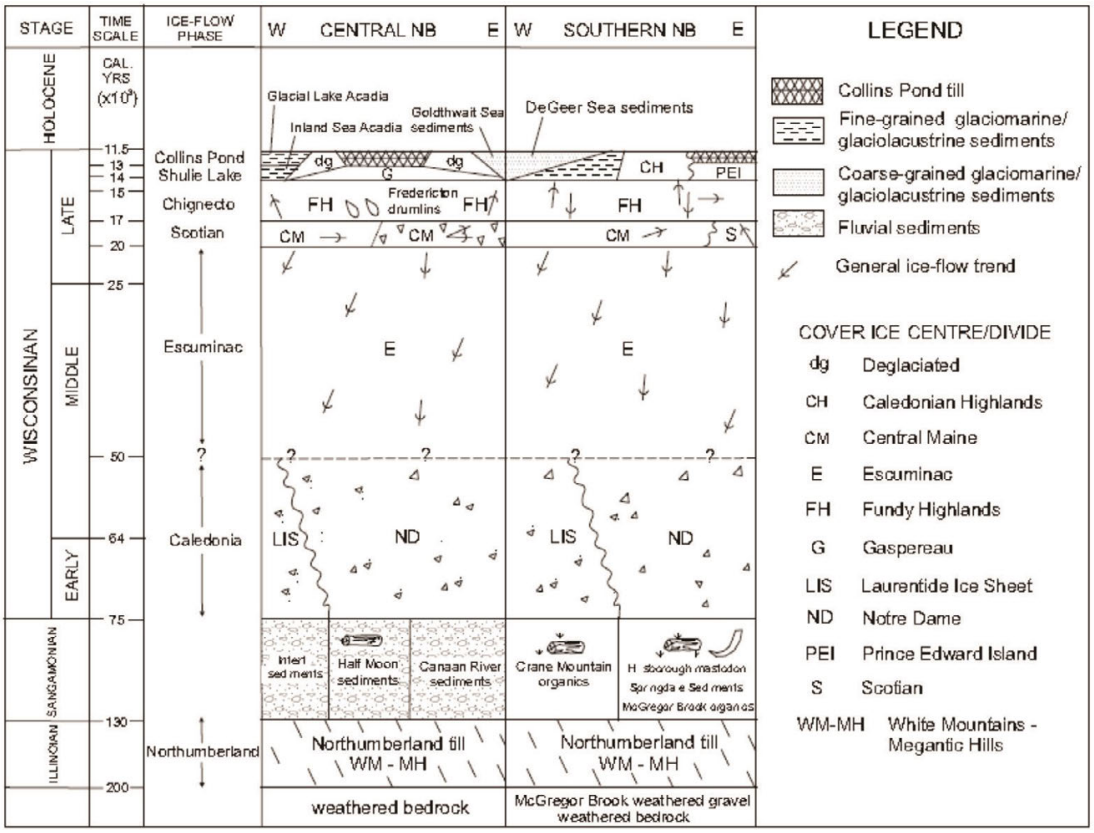

Figure 6 – Space/time stratigraphical summary of central and southern New Brunswick (from Seaman, 2013).

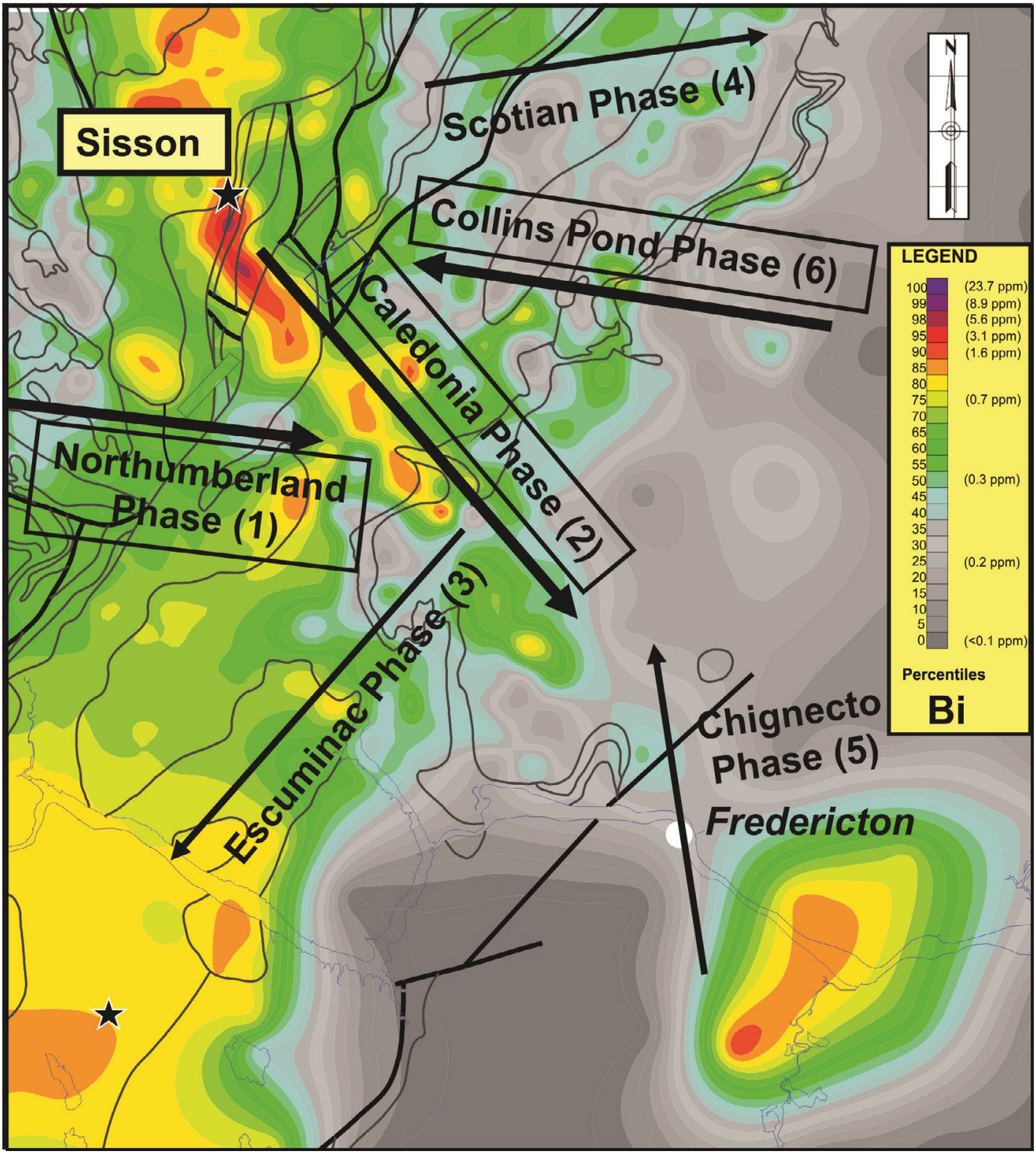

Figure 7 – Orientation of regional and local ice-flow phases in south-central New Brunswick. Note the main bismuth (Bi) in till dispersal train, down-ice from the Sisson W-Mo deposit, paralleling the Caledonia Phase. Till geochemical concentrations are from the <0.063 mm fraction of basal till.

2009, 2013). These deposits were produced by east to east-southeast flow from the White Mountains-Megantic Hills Ice Divide of the Appalachian Glacier Complex (AGC). The apparently old glacial striae of similar trend that were reported by Rampton et al. (1984) from west-central New Brunswick are also attributed to the Northumberland Phase, as are muted, large-scale glacially streamlined landforms (Seaman, 2009). Non-glacial fluvial sediments, as described by Rampton et al. (1984) and Lamothe (1992), and preserved between the Northumberland till (informal name) and the overlying Wisconsinan till, are assigned to the Sangamonian Interglacial Stage.

The Early to Middle Wisconsinan Caledonia Phase began, approximately 75 ka BP, with incursion of the south-east-flowing Laurentide Ice Sheet (LIS) into the Saint John River valley area, accompanied by parallel flow of the Notre Dame glacier of the AGC (Seaman, 2009). The latter glacier had its source in the Notre Dame Ice Divide, located over the Notre Dame Mountains of the Gaspe Peninsula (Rampton et al., 1984). The difference in power between these two glaciers is evident in the contrast between the glacially sculpted bedrock topography of southwestern New Brunswick (Seaman, 2004) compared to the evidence for minimal subglacial erosion in east-central New Brunswick during the Wisconsinan (Seaman, 2013). Dispersal trains in basal till throughout central and southern New Brunswick indicate that most of the surface till was deposited by southeast to south-southeast glacier flow (Seaman, 2009, 2013). Consequently, it is interpreted to be Caledonia till (informal name).

The Caledonia Phase glaciers extended to the edge of the continental shelf (Stea et al., 1998, 2011). Contradictory cross cutting relationships between southeast and south- southeast-trending glacial striae indicate that the ice flow fluctuated between these limits several times during the course of the Caledonia Phase (Seaman, 2009). The Caledonia Phase terminated approximately 40 ka BP, during the Middle Wisconsinan (64 ka to 25 cal ka BP). In Nova Scotia it was followed by a period of inactive ice cover (Stea et al., 2011). However, in New Brunswick the AGC remained active, with the Caledonia Phase transitioning into the Escuminac Phase during the Middle Wisconsinan (Seaman et al., 2011). The LIS withdrew to the north of the St. Lawrence River valley, never to return to New Brunswick, and the AGC adapted to its departure by a stepwise shift in ice flow from the south-southeast of the Caledonia Phase to the south-southwest of the Escuminac Phase. This shift in ice-flow trend was influenced by three factors:

- the flow of the Notre Dame glacier into the area vacated by the withdrawal of the LIS;
- the gradual shift in the dominant AGC ice flow centre from the Notre Dame Ice Divide to the Escuminac Ice Centre, located to the north of Prince Edward Island in the area of the current Gulf of St. Lawrence (Rampton et al., 1984); and
- the development of a calving bay in the Gulf of Maine and adjacent Bay of Fundy (Stea et al., 1998), causing drawdown of the Escuminac glacier toward the southwest (Seaman et al., 2011).

With the onset of the Late Wisconsinan cooling, approximately 25 cal ka BP, the Escuminac glacier advanced across the Bay of Fundy and Nova Scotia and terminated at the edge of the continental shelf by the late-glacial maximum, approximately 20 cal ka BP.

Subsequent glacial phases were related to the gradual retreat and dissipation of the AGC during the Late Wisconsinan, during which ice-flow directions changed dramatically in response to the reorganization of flow patterns (Seaman, 2009; Stea et al., 2011; Seaman et al., 2011). These phases were:

- the Scotian Phase (20-17 cal ka BP), with the AGC margin at the Scotian Moraine, offshore of Nova Scotia ;
- the Chignecto Phase (15.9-14.7 cal ka BP), with the ice margin established along the shores of the Bay of Fundy;

- the Shulie Lake Phase (approximately 14 cal ka BP), a short-lived readvance of the AGC, primarily at the upper end of the Bay of Fundy, correlative with the Older Dryas Stadial; and
- the Collins Pond Phase (12.8-11.5 cal ka BP), correlative with the Younger Dryas Stadia!, involving the readvance of remnant ice masses that had survived the initial deglaciation, or, less likely, the initiation of new ice centres.

In west-central New Brunswick the Escuminac and subsequent glaciers generally exhibited limited power. Locally they reworked the previously deposited Caledonia till into a hybrid till (e.g., Allard and Pronk, 2003), reorienting its fabric and generating a confusing plethora of glacial striae where their influence extended to the bedrock surface (Seaman, 2009). Glacier flow was initially eastward during the Scotian Phase, and then transitioned to northeastward in response to the development of a high velocity ice stream in the Curventon – Bathurst valley. During the Chignecto and Shulie Lake phases, glacier flow was toward the northwest to northeast. The Shulie Lake Phase was followed by significant deglaciation, with the local deposition of large volumes of ablation till and glaciofluvial sediment. However, remnant ice masses probably persisted over the highlands and the western part of the New Brunswick Lowlands. With the onset of the Younger Dryas cooling, these ice masses rapidly readvanced, or were regenerated. Of these Collins Pond Phase glaciers, the Gaspereau Ice Centre (Seaman, 2006) in central New Brunswick advanced toward the west to northwest, depositing the late-glacial till at Todd Mountain (Lamothe, 1992) and the uppermost of the three tills at Sisson (Seaman and McCoy, 2008). The disintegration of the Gaspereau glacier resulted in the deposition of the extensive ablation till deposits (hummocky disintegration moraine) noted in the Sisson Brook area by Snow and Coker (1987). Deglaciation was probably complete by the beginning of the Holocene (11.5 cal ka BP).

Sisson W-Mo Deposit

The Sisson tungsten-molybdenum deposit, discovered in 1979 by Texasgulf Inc., is located in the Coldstream map area (NTS 21 J/06) of west-central New Brunswick, approximately 60 km northwest of Fredericton (Fig. 2). Like many polymetallic deposits, the mineralisation at Sisson is closely associated with felsic igneous rocks. The deposit at Sisson is divided into three mineralised zones – Zone I and Zone II, which contain mainly wolframite and chalcopyrite; and Zone III, in which scheelite and molybdenite are predominant (Fig. 8).

Exploration history

Texasgulf Inc. staked claims in the Sisson Brook area in 1978 to cover ground where Penarroya Canada Ltd had intersected tungsten-copper mineralisation in three holes drilled in 1969 (Rabinovich, 1969; Moore, 1979). Regional geochemical surveys conducted by the New Brunswick Department of Natural Resources in 1972 also indicated that stream silts in the area contained anomalous molybdenum values (Austria and Chork, 1976).

Diamond drilling (11 holes) conducted by Texasgulf in 1979 to test geophysical anomalies in the central portion of its claim group resulted in the discovery of the Zone I and Zone II tungsten-copper mineralisation at Sisson (Mann, 1981a). The following year, another 12 holes were drilled to delineate the extent of the two known zones (Mann, 1980). Kidd Creek Mines Ltd. drilled an additional nine holes south of the known zones in 1981, which led to the discovery of tungsten-molybdenum mineralisation in Zone III. One of these 1981 holes (SSN-26) intersected dykes of massive granite porphyry (Mann, 1981b). Another eight holes were drilled in the following year to test Zone III along strike and at depth (Mann, 1982).

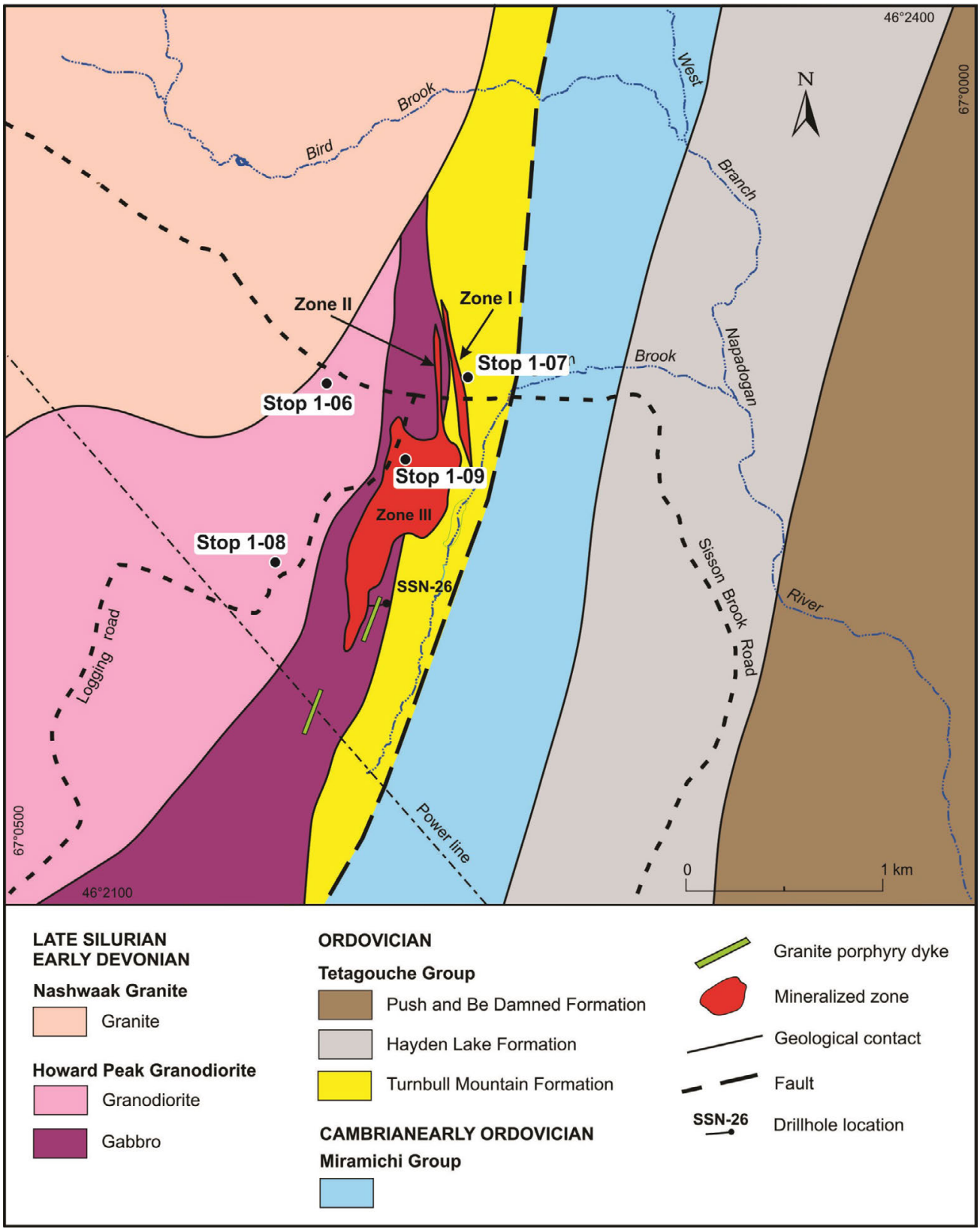

Figure 8 – Geology map of the Sisson Brook area showing the location of mineralised zones at the Sisson

Champlain Resources Inc. staked ground in the Sisson Brook area in 1997. Government regional till geochemical sampling (2 km grid) was carried out in the area encompassing Sisson Brook in 2001 (Seaman, 2002), with follow-up sampling the following year to confirm the anomalies and the limits of the identified glacial dispersal train (Seaman, 2003). Geodex Minerals Ltd. optioned the Sisson Brook claim group from Champlain Resources in 2004. In the following year, Geodex carried out geological mapping, prospecting, soil sampling, geophysical surveys, and drilling (nine holes) on the property. Geodex subsequently conducted a fence-drilling program on Zone III to calculate National Instrument 43-101, Standards of Disclosure for Mineral Projects resources for the deposit (Martin, 2006; Ozturk, 2007; Geodex Minerals Ltd., 2008). This drill program comprised 30 holes totalling 7,784 m in 2006, and 83 holes totalling 20,178 m in 2007, which included two metallurgical holes. In 2008 Geodex conducted 11,800 m of both infill and exploration drilling on adjacent targets as well as geotechnical, environmental, and community studies. A positive Preliminary Economic Assessment report was completed by Geodex in 2009. In the fall of 2010, Northcliff Resources acquired an interest in the property and now holds controlling interest. They have completed a positive feasibility study of the deposit and have submitted an Environmental Impact Assessment report to the Provincial and Federal regulators for regulatory and public review. They are currently awaiting feedback on whether they can proceed to the mine development stage where they would extract the ore by open pit mining methods, construct a mill to process the ore, and build an ammonium-paratungstate plant-the first of its kind in Canada. The mine is expected to operate for 27 years.

This portion of the fieldtrip will visit road and trench exposures to examine the glacial deposits that overlie the deposit, the geological setting and style of mineralisation at Sisson, and discuss a possible genetic model based on the unique structural characteristics of the Sisson deposit.

Geological setting

The Sisson deposit is situated along the eastern margin of the Late Silurian to Late Devonian Acadian Plutonic Belt that occurs within the Miramichi Highlands of central New Brunswick (Fig. 2). The plutonic rocks were emplaced into a variety of country rocks, including sedimentary rocks of the Cambrian to Early Ordovician Miramichi Group; Ordovician volcanic and sedimentary rocks correlated with the Tetagouche Group; and deformed Ordovician plutonic rocks (Fyffe, 1982a, b; van Staal and Fyffe, 1991). The two main Acadian Plutonic Belt intrusions in the immediate vicinity of the Sisson deposit (Figs. 3 and 8) are the Howard Peak Granodiorite and Nashwaak Granite (Fyffe et al., 1981), although younger granitic dykes suggest a more protracted intrusive history.

The country rocks immediately adjacent to the Howard Peak and Nashwaak plutons are an intercalated sequence of fine- to medium-grained, medium- to thick-bedded, light grey crystal tuft; layers of 1 m thick, dark green, banded amphibolitic mafic tufts; and light grey to greyish purple, medium-bedded, biotite-rich psammite (Lutes, 1981). The age of this westernmost volcanic-bearing sequence in the Sisson Brook area is not known with certainty (Fyffe et al., 1988), but it has been correlated with the Turnbull Mountain Formation of the Tetagouche Group. Medium- to thick-bedded, light grey, fine- grained quartzite and greyish green shale lying immediately east of the volcanic- bearing sequence are assigned to the Miramichi Group (Fig. 8). The quartzose sequence of the Miramichi Group is conformably overlain to the east by a lower section of pyritiferous black shale intercalated with minor flow -banded and brecciated felsic volcanic rocks, and fragmental mafic volcanic rocks correlated with the Hayden Lake Formation; and an upper section of thin- to medium-bedded feldspathic to lithic wacke, and dark grey shale correlated with the Push and Be Damned Formation (Potter, 1969; Lutes, 1981). Lutes (1981) considered the quartzose sedimentary rocks of the Miramichi Group in the Sisson Brook area to lie in the core of an anticline, flanked to the east and west by conformably overlying volcanic-bearing sequences. However, to the east, volcanic rocks of the Hayden

Lake Formation are interbedded with black shale, whereas to the west, they contain interbeds that are predominantly psammitic. Fyffe et al. (1988) agreed that both volcanic sequences may be correlatives of the Middle Ordovician Tetagouche Group but, on the basis of abundant quartz-flooding observed near the unexposed contact, interpreted the western sequence to be faulted against the Miramichi Group. The presence of such a fault on the western limb of the proposed anticline is consistent with the intensely sheared nature of rocks hosting the Sisson mineralisation.

Mann (1980, 1981b) reports - based on observations of graded bedding and flame structures in drill core -that the western volcanic-bearing sequence youngs to the east. The western sequence is herein tentatively correlated with the tuffaceous felsic and mafic rocks of the Turnbull Mountain Formation, which conformably underlies the Hayden Lake Formation northeast of Sisson Brook in the Napadogan area (Poole and Neuman, 2003). It is possible that a considerable amount of stratigraphic section is missing across the fault separating the Turnbull Mountain and Hayden Lake formations.

The Howard Peak Granodiorite is a medium-grained, foliated, hornblende-biotite granodiorite that grades eastward into, and becomes intermixed with, dark grey, medium-grained ophitic gabbro (Fig. 8). Both the granodiorite and gabbro are transected by dykes of massive to foliated, light greyish pink, equigranular granite (Fig. 9). The eastern margin of the pluton is intensely sheared and cataclastized, and it contains an abundance of elongated, schistose xenoliths derived from the adjacent folded country rocks (Lutes, 1981; Venugopal, 1982). Recent dating of the Howard Peak Granodiorite by Bustard (2013) yielded a U-Pb (titanite) age of 432 ± 2 Ma.

Figure 9 – Boudinaged granitic dyke and dykelets cross-cutting foliated gabbro of the Howard Peak Granodiorite along the western margin of the Sisson W-Mo deposit.

The Nashwaak Granite is a massive, light greyish pink, medium-grained, equigranular to subporphyritic biotite granite that varies to muscovite-biotite granite in the north. This granite has yielded a Rb-Sr muscovite age of 422 ± 4 Ma and a K-Ar muscovite age of 386 ± 5 Ma (Whalen and Theriault, 1990). The granitic dykes cutting the Howard Peak Granodiorite are probably offshoots of the Nashwaak Granite (Fig. 9). The Nashwaak Granite exhibits a mild tectonic fabric consistent with its syn-tectonic emplacement in the Early Devonian.

Massive, fine-grained, granite porphyry dykes were intersected in drillhole SSN-26 near the southern end of Zone III of the Sisson deposit (Fig. 8). The massive dykes (Fig. 10) were intruded post-tectonically into foliated gabbro of the Howard Peak Granodiorite and have been interpreted as offshoots of an assumed deeply buried stock that generated the mineralising hydrothermal fluids at Sisson (Mann, 1981b; Nast, 1985; Nast and Williams-Jones, 1991). A sample of porphyry from drillhole SSN-26 yielded a U-Pb age of 364.5 ± 1.3 Ma (Fyffe et. al., 2008) and was therefore emplaced during the Famennian Stage of the Late Devonian.

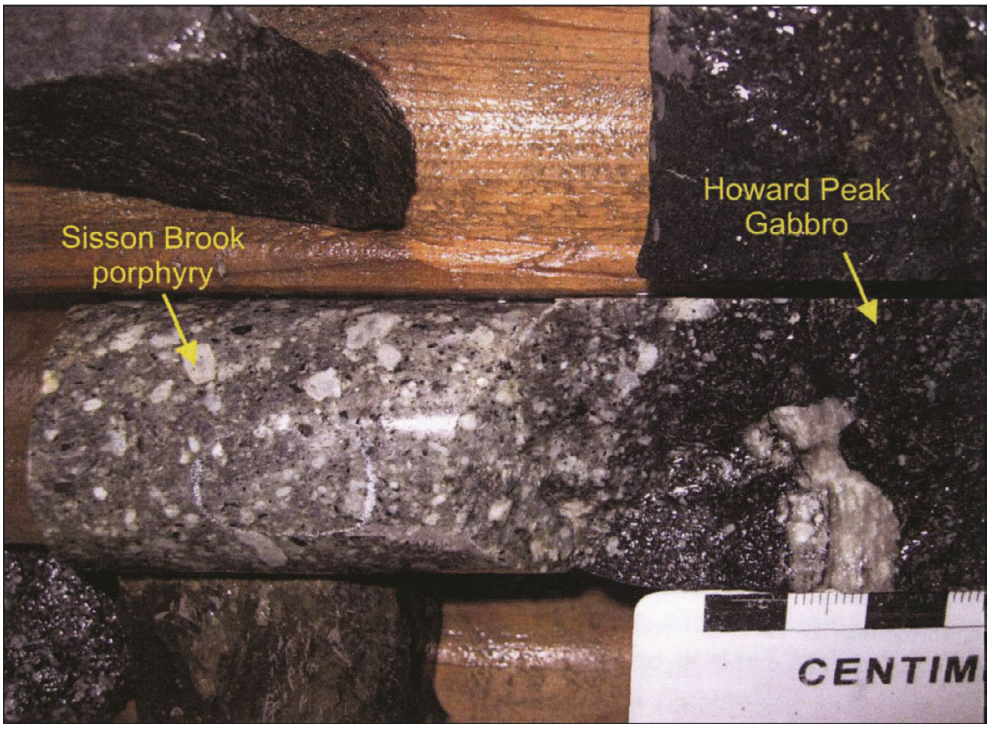

Figure 10 – Massive, fine-grained granite porphyry dyke containing quartz and feldspar phenocrysts. Core from drillhole SSN-26 (see Fig. 8).

Structural geology

The stratigraphic sequences in the Sisson Brook area are folded into a series of north- northeast-trending anticlines and synclines, plunging 30° to the south (Lutes, 1981; Fyffe, 1982a, b). A steep, northwest-dipping axial planar, crenulation cleavage (S2) developed during this event. There has been no recognition of folding associated with an earlier slaty cleavage (S1), defined by fine-grained muscovite and chlorite oriented subparallel to bedding (Lutes, 1981). A late northwest-trending, steeply dipping fracture cleavage (S3) is associated with steeply plunging kink bands. Porphyroblasts of cordierite, andalusite, and garnet in the thermal aureole of the Nashwaak Granite overprint S1 and S2 but are overprinted by S3 (Lutes, 1981; Nast, 1985).

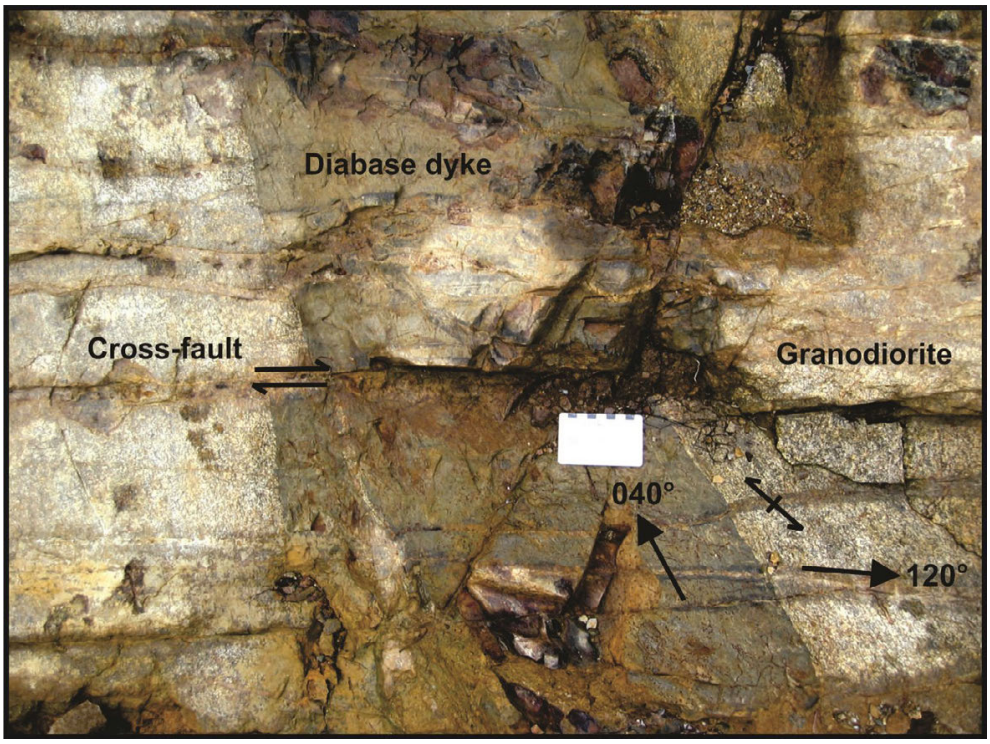

Figure 11 – Granitic dykes cross-cutting gabbroic rocks of the Howard Peak Granodiorite (Stop 1-07; scale in cm).

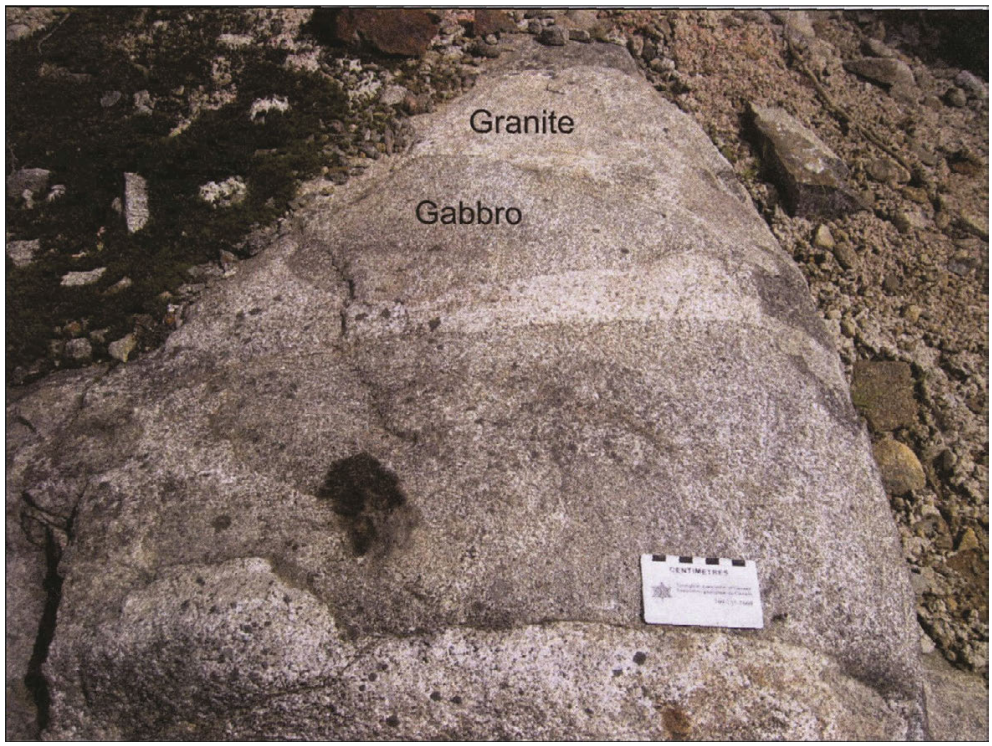

Figure 12 – Granodiorite cross-cut by a diabase dyke that is offset along a set of prominent west-northwest-trending microfaults (Sisson Zone I trench; scale in cm).

The gabbroic rocks of the Howard Peak Granodiorite along the western margin of the Sisson deposit (Fig. 8) possess a foliation defined by prominent melanocratic and leucocratic bands or by weakly aligned plagioclase and amphibole crystals (Lutes, 1981; Nast, 1985). As the foliation trends subparallel to the S2 fabric of the country rocks along the eastern boundary of the pluton, the Howard Peak has been interpreted as synchronous with S2 (Fyffe and Thorne, 2010). Granitic dykes transecting and partially assimilating the gabbroic rocks vary from weakly foliated to massive (Fig. 11). Differing orientations of the foliation in some of the engulfed gabbroic xenoliths indicate that they were rotated during their incorporation into the granite. The granitic dykes likely are offshoots of the Nashwaak pluton, which must therefore have been emplaced during the waning stage and after the cessation of D2 deformation. A prominent set of joints oriented at 120° transects the foliation in the plutonic rocks (Fig. 12). These tensional joints have developed parallel to the maximum stress direction in the region (Lajtai and Stringer, 1981).

A number of major, north- to north-northeast-trending faults that displace D2 fold structures have been mapped in central New Brunswick (Fyffe, 1982a, b). One such fault has been interpreted to truncate the stratigraphic section on the western limb of the anticline in the Sisson Brook area (Fyffe et al., 2008). The north-northeast lineament controlling the course of Sisson Brook may mark the main trace of this fault (Fig. 8). In addition to the evidence of a missing section in the stratigraphy, an increase in intensity of the structural fabrics from west to east across the area supports the existence of a high-strain zone located in the immediate vicinity of the Sisson deposit.

Although bedrock exposure is sparse in the area, it appears that the weak foliation observed in the plutonic rocks to the west of the deposit develops into a strong cataclastic fabric further to the east. In Zone III of the Sisson deposit (Fig. 8) gabbroic rocks, possessing a penetrative foliation and a granulated fine-grained matrix containing small porphyroblasts of plagioclase, are cut by granitic dykes exhibiting a prominent cataclastic foliation along which augen of feldspar are aligned (Fig. 13). The development of this localized high-strain zone apparently provided permeable pathways for the introduction of hydrothermal fluids that were the mechanism for mineralisation at Sisson. Any major movement along this north-northeast-trending shear in Zone III must have taken place prior to the injection of a set of the cross cutting, west-northwest-trending, molybdenite-bearing quartz veins. However, there is evidence of some late, minor sinistral displacement of these veins (Fig. 14). Late sinistral displacement occurs in Zone I at the northern end of the Sisson deposit. Schistosity-shear fabrics indicate that an interbedded sequence of siltstone and tuff of the Turnbull Mountain Formation has been juxtaposed against granodioritic rocks of the Howard Peak Granodiorite along a north- northwest-trending sinistral shear zone. The shear abruptly truncates a west-northwest- trending joint set prominently displayed in the granodiorite, indicating that a considerably greater amount of late sinistral movement has occurred in Zone I compared to Zone III. Some limited movement along the joint set is shown by small dextral displacement of the margins of two trap dykes cutting the granodiorite (Fig. 12). The minor dextral and dominant sinistral movement were likely caused by the same stress field given that the previously developed joint set was oriented near to the conjugate shear direction of the principal stress axis. The north-northwest-trending shear zone exposed in the trench at Zone I is interpreted to be a horsetail splay off of the main north-northeast-trending high- strain shear zone that occurs along the eastern margin of the Howard Peak Granodiorite in Zone III.

Deposit geology

The mineralisation at Sisson occurs in a series of structurally controlled quartz veins in highly silicified shear zones along the eastern margin of the Howard Peak Granodiorite (Fig. 8). Zones I and II at the north end of the deposit strike north-northwest and dip steeply to the west, parallel to the trend of a late sinistral shear. Zone I is hosted by a thin-bedded sequence of dark grey siltstone and tuff. The bedding trends to the north- northeast and dips steeply

Figure 13 – Gabbro containing plagioclase porphyroclasts in the trenched exposure at Sisson Zone III. Note the deformed granitic dykes and the cross-cutting northwest-trending quartz vein (coin is 2.7 cm in diameter).

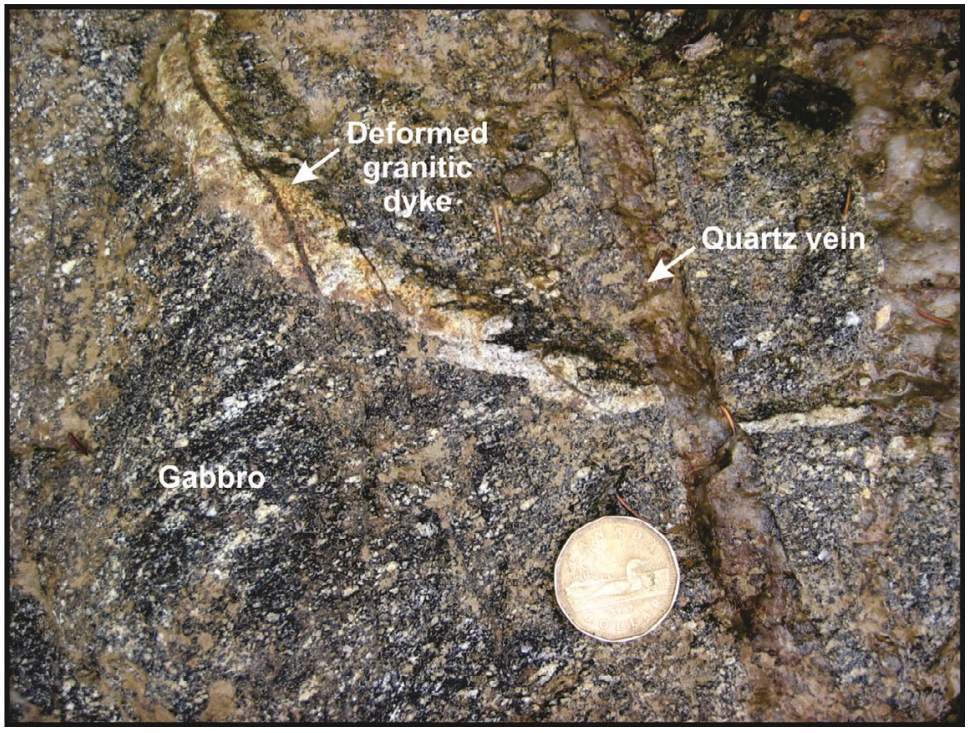

Figure 14 – Sinistral offset of an east-trending quartz-feldspar vein along a north-trending fault along the southern margin of the trench at Sisson Zone III (looking north; coin is 2.7 cm in diameter).

to the east. The mineralisation in Zone I has been traced along strike for about 950 m and varies in thickness from 2 m to 36 m. Zone II is hosted in gabbroic rocks about 100 m west of Zone I and has been traced along strike for 400 m. Quartz veins associated with the mineralisation in Zones I and II range in width from about 0.5 cm to 3 cm.

Zone III strikes north-northeast and dips steeply to the northwest (Mann, 1980, 1981a, b, 1982), parallel to the trend of a major shear zone. The mineralisation is hosted by sheared and silicified gabbroic rocks of the Howard Peak Granodiorite and associated cataclastically deformed granitic dykes that likely represent offshoots of the Nashwaak Granite. Zone III has been traced along strike for 1100 m with a maximum thickness of about 400 m (Geodex Minerals Ltd., 2008).

Mineralisation

Ore minerals at Sisson consist mainly of wolframite and chalcopyrite in Zones I and II, and scheelite and molybdenite in Zone III. According to Nast and Williams-Jones (1991), a low fluid-rock ratio governed the style of mineralisation at Sisson. Thus, precipitation of scheelite was controlled by the composition of the calcium-rich, gabbroic wall rocks of Zone III; whereas, precipitation of wolframite was governed by the calcium-poor, sedimentary wall rocks of Zone I.

Scheelite in Zone III tends to be concentrated in quartz veins (Fig. 15A) that parallel the north-northeast-trending shear fabric; conversely, molybdenite (Fig. 15B) is concentrated in cross cutting quartz veins oriented between 120° to 140°. This latter trend is approximately parallel to the prominent set of joints in the less deformed gabbroic and granitic rocks along the western margin of Zone III. Similar molybdenite-bearing quartz veins occur in brittle fractures transecting the Late Devonian granite porphyry observed in drill core from the southern part of Zone III.

The mineralisation has been traced over a strike length of 1900 m with an average width of 650 m and 350 m depth (Samuel Engineering, 2013). Paragenetic studies and field relations suggest that there was an early barren to weakly mineralised alteration event preceded by an early stage of tungsten mineralisation, an intermediate stage of molybdenum +/- tungsten mineralisation, and a late stage of polymetallic mineralisation whereby tungsten was accompanied by base metals (Lang, 2010).

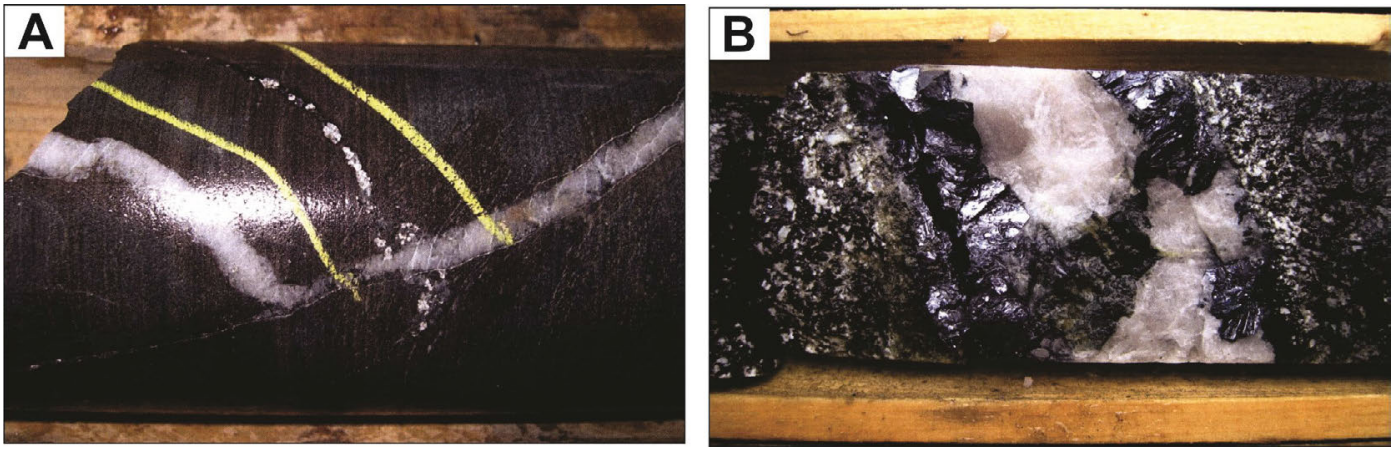

Figure 15 – A) Fracture-controlled scheelite mineralisation (outlined by yellow marks) mantled by an alteration halo of biotite alteration cutting metasedimentary host rocks. B) Molybdenite mineralisation along the margins of a quartz vein.

Resource estimates

Calculations by Texasgulf Inc. indicated that Zone I contains an estimated 6.8 Mt of 0.21% W03 and 0.35% Cu, and that Zone II contains an estimated 1.4 Mt of 0. 14% W03 and 0.09% Cu (Mann, 1980; Martin, 2006). A mineral resource estimate for Zone III (Table 1) was calculated on the basis of assay results from the 2008 drilling program (Geodex Minerals Ltd., 2009). A mineral resource estimate was also calculated for the Ellipse Zone, located a few hundred meters south of Zone III within the diorite (Table 2; Geodex Minerals Ltd., 2009). Mineral reserves for the deposit are shown in Table 3.

Table 1. Mineral resource estimate for Zone III, Sisson deposit.

Threshold Equivalent WO_3 %	Measured Tonnes (Mt)	WO_3 %	Mo %	Indicated Tonnes (Mt)	WO_3 %	Mo %	Inferred Tonnes (Mt)	WO_3 %	Mo %
0.025	26.6	0.072	0.025	257.3	0.062	0.019	223.6	0.055	0.018
0.075	19.4	0.086	0.030	151.1	0.082	0.026	118.7	0.073	0.027
0. 125	11.0	0.109	0.037	69.1	0.107	0.034	47.8	0.097	0.036
0.175	5.1	0.135	0.044	26.7	0.131	0.045	5.9	0.120	0.049
0.225	1.8	0.168	0.053	9.3	0.152	0.058	5.4	0.138	0.064

Note: $W0_3$ equivalent = $W0_3$ % + 2.02 Mo %

Table 2. Mineral resource estimate for Ellipse Zone, Sisson deposit.

Threshold Equivalent WO_3 %	Measured Tonnes (Mt)	WO_3 %	Mo %	Indicated Tonnes (Mt)	WO_3 %	Mo %	Inferred Tonnes (Mt)	WO_3 %	Mo %
0.025	1.1	0.082	0.023	28.3	0.072	0.024	36.5	0.061	0.019
0.075	0.9	0.092	0.027	22.5	0.081	0.027	23.4	0.073	0.026
0.125	0.5	0.112	0.034	10.4	0.105	0.038	8.6	0.091	0.041
0.175	0.2	0.135	0.044	4.6	0.121	0.05	3.4	0.102	0.057
0.225	0.1	0.146	0.068	1.5	0. 139	0.067	0.9	0.094	0.094

Note: $W0_3$ equivalent = $W0_3$ % + 2.02 Mo %

Table 3. Mineral reserves, Sisson deposit (January 2013)

Categories	Tonnes	NSR ($/t)	WO_3 %	Mo %	W (M mtu)	Mo (M lb)
Proven	105,415,000	25.48	0.069	0.023	7.3	53.0
Probable	228,948,000	23.54	0.065	0.020	14.9	101.7
Total	334,363,000	24. 15	0.066	0.021	22.2	154.8

Indicator mineral, till geochemical, and stream sediment geochemical signatures

During the Geological Survey of Canada's (GSC) Targeted Geoscience Initiative (TGl-4; 2010-2015), GSC and the New Brunswick Department of Energy and Mines (NBDEM) conducted indicator mineral case studies around the Sisson W-Mo and Mount Pleasant Sn-W-Mo-Bi-ln polymetallic deposits in New Brunswick. The objective is to document glacial dispersal patterns of W, Mo, Sn, and In-bearing indicator minerals and matrix geochemical signatures in till and stream sediments at varying distances down-ice of the deposits, in support of exploration in New Brunswick and other glaciated terrains. This is the first study to document glacial dispersal of W-bearing minerals around a significant W deposit.

At Sisson, 3 tills are present: lllinoian Northumberland till, Early to Middle Wisconsinan Caledonia till, and the geochemically barren, Younger Dryas, Collins Pond till (Seaman, 2009; Stea et al., 2011). This presented sampling challenges as the tills were deposited by ice flows from different source areas and are geochemically distinct but not easy to distinguish in the field. At Sisson, 79 bulk till samples were collected up-ice, overlying, and up to 14 km down-ice (SE) of the deposit. The distribution of sample sites was guided by previous sampling by Kidd Creek Mines (Snow and Coker, 1987) and the NBDEM (Seaman, 2002, 2003; Seaman and McCoy, 2008). Stream water, silt, and bulk samples were collected at 16 sites at Sisson to characterize scheelite abundance, size, and shape for comparison with grains in the till. Results for all of the TGl-4 sampling are contained in several GSC Open File Reports (McClenaghan et al., 2013a, b, c, d). The till geochemical signatures of the TGl-4 work in the area of the Sisson deposit are also presented in McClenaghan et al. (2014).

Till sampling was optimized by first collecting sixty-one 200 g till samples and determining W, Mo, Sn, Bi, and Cu concentrations, using a portable XRF (pXRF) spectrometer. At Sisson, anomalous pXRF concentrations match previously known NBDEM anomalies in the glacial dispersal train extending 14 km to the SE, and correlate well with subsequent borate fusion and aqua regia/ICP-MS analyses of the <0.063 mm fraction of till (up to 815 ppm W, 65 ppm Mo, and 978 ppm Cu). Till, stream, and a suite of bedrock samples were processed to produce heavy mineral concentrates for assessment of indicator minerals and to characterize the indicator mineral signature of the Sisson deposit (McClenaghan et al., 2013a, b, c, d). Scheelite is abundant in the deposit, and a significant indicator mineral in till up to 10 km down-ice (Fig. 16) and in stream sediments up to 8 km downstream (Fig. 17). Other indicator minerals of the Sisson deposit include molybdenite, chalcopyrite, wolframite, Bi minerals, sphalerite, and galena. Note that there is minimal glacial dispersal of molybdenite (hardness 1) at Sisson because it is much softer than scheelite (hardness 4-5) and therefore does not survive glacial transport (Fig. 18). The pathfinder elements in till for the Sisson deposit are W, Mo, Cu, Bi, As, Sn, Cd, Ag, In, Zn, Pb and it is recommended that till geochemistry be used in combination with indicator minerals methods (McClenaghan et al., 2013a, b, c, d, 2014).

The implications for exploration resulting from the TGl-4 project are as follows.

- Scheelite is an indicator mineral of W mineralisation, in till and stream sediments; Northcliff Resources Ltd. is currently using the methodology developed in this project.
- Scheelite is physically robust and survives glacial and fluvial transport.
- Silt to sand sized presence of coarse scheelite (>0.5 mm) is an indicator of proximity to source.
- Scheelite is abundant (100s to 1000s of grains proximal to source).
- This project developed a systematic method for scheelite grain counting under UV light, now a new service being offered at a commercial heavy mineral lab.
- Wolframite, molybdenite, bismuth minerals, chalcopyrite, and arsenopyrite are also present.

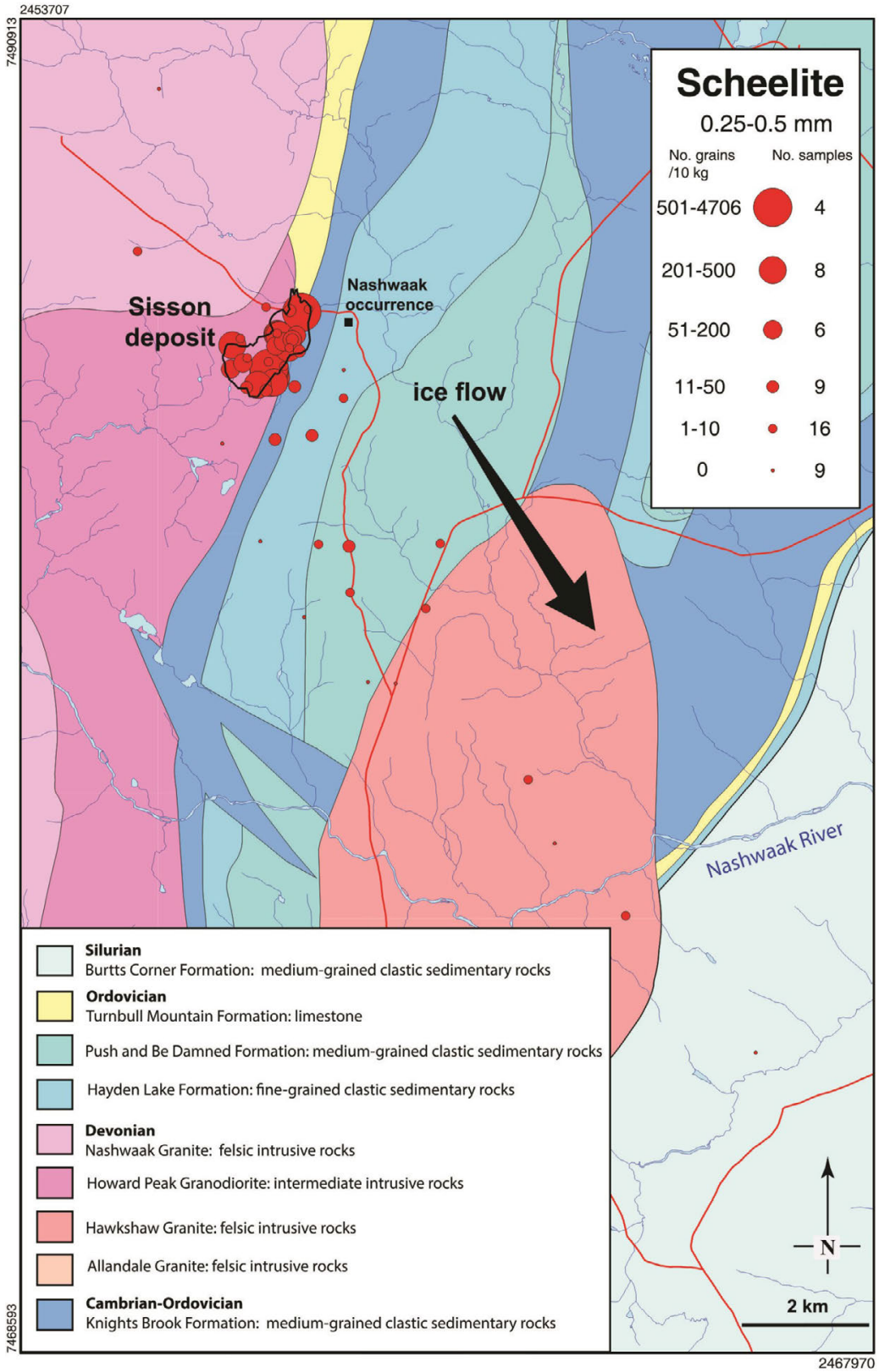

Figure 16 – Scheelite in the 0.25-0.5 mm size fraction of till in the vicinity of the Sisson W-Mo deposit (McClenaghan et al., 2013d).

- Scheelite is easily detectable and efficient results are obtained with a sample density of one per 5 km^2.
- Physical evidence for the presence of mineralisation, grain morphology, and chemistry provide information about distance to, and nature of, the bedrock source.

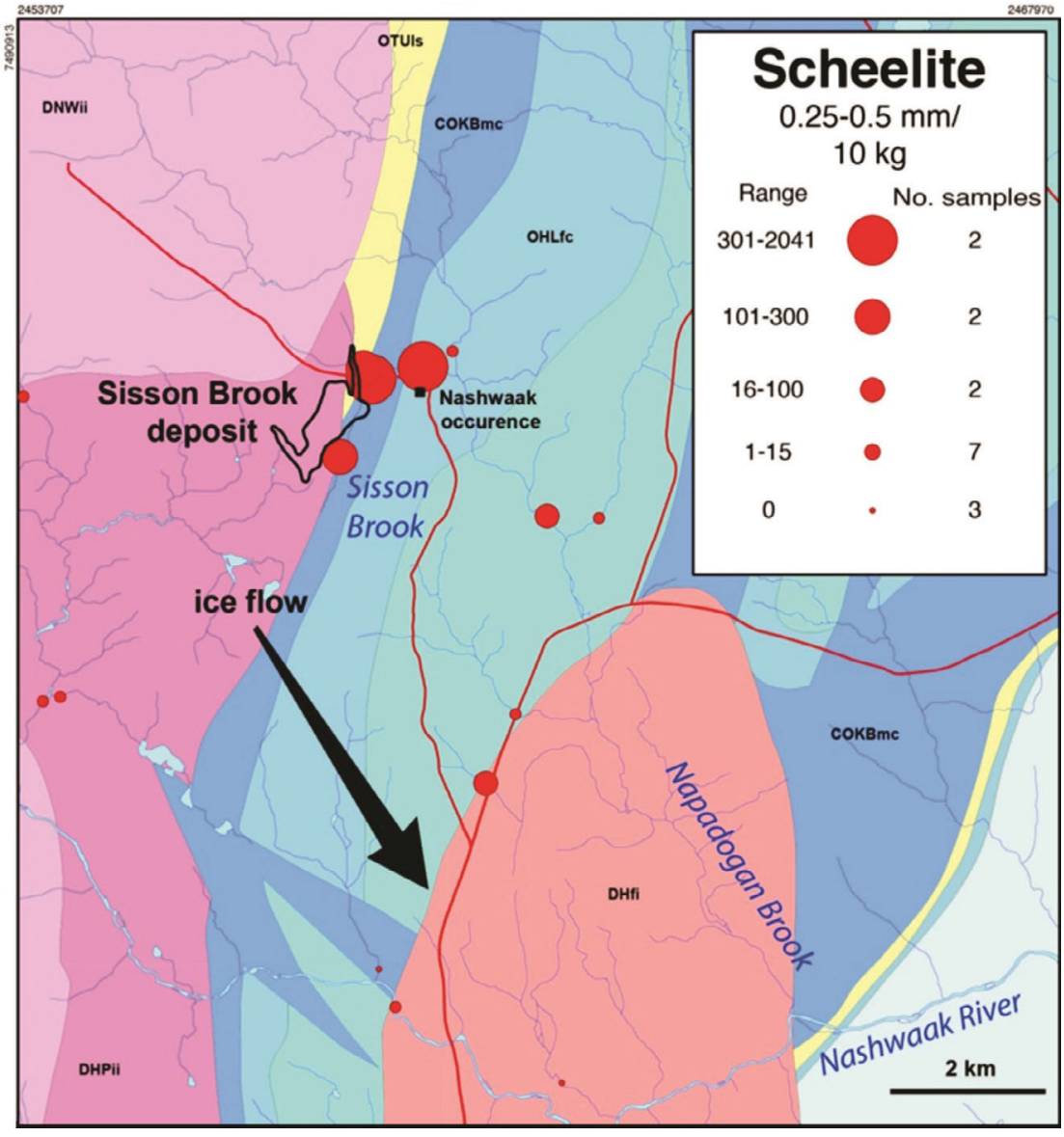

Figure 17 – Scheelite in the 0.25-0.5 mm size fraction of stream sediments in the vicinity of the Sisson W-Mo deposit (McClenaghan et al., 2013d).

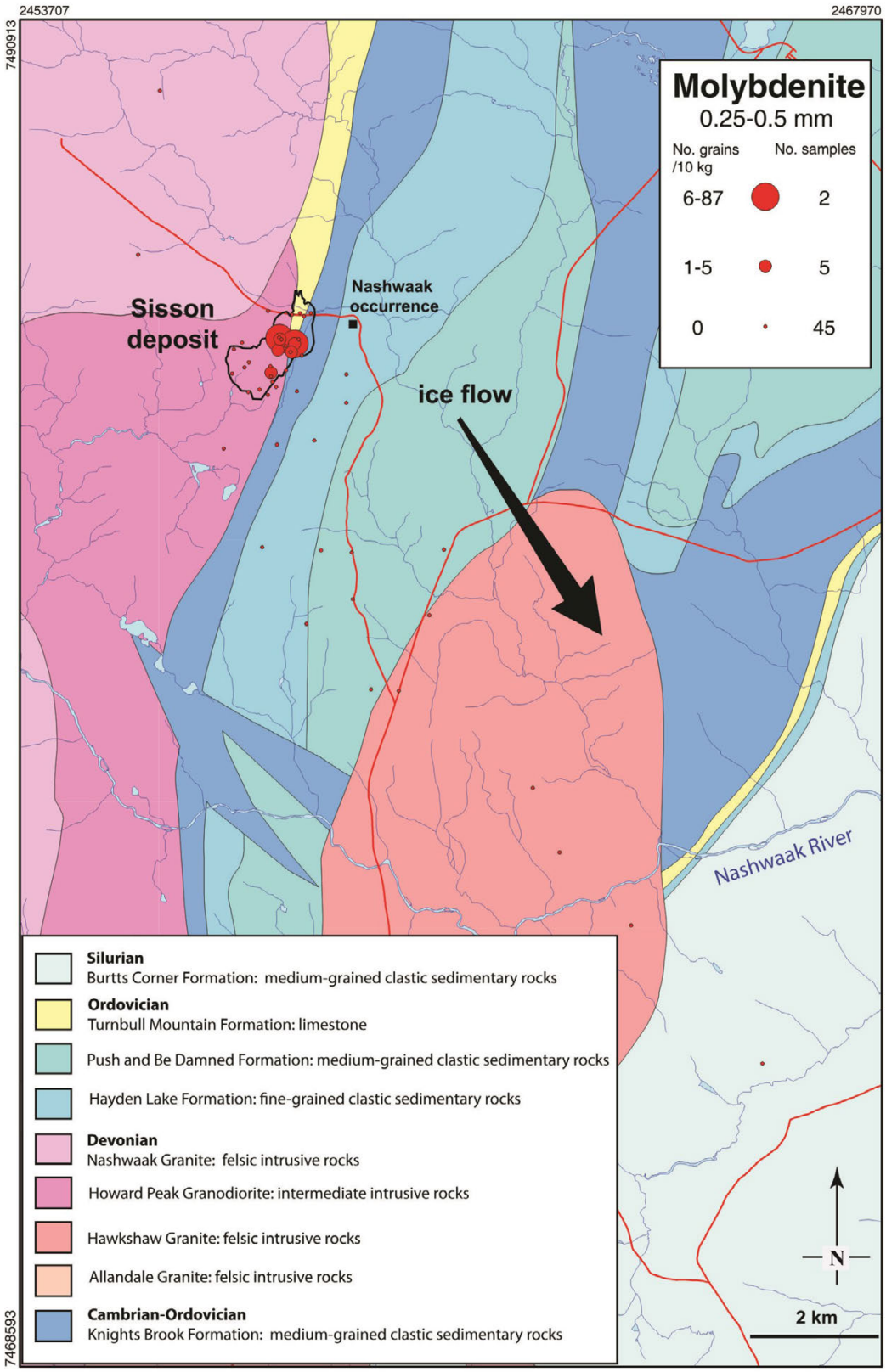

Figure 18 – Molybdenite in the 0.25-0.5 mm size fraction of till in the vicinity of the Sisson W-Mo deposit (McClenaghan et al., 2013d).

Burnthill W-Sn-Mo Deposit

The Burnthill Mine is located approximately 70 km NNW of Fredericton, along the southern flank of the Southwest Miramichi River. The past-producing tungsten mine (Fig. 19) occurs within rocks that comprise the Miramichi Terrane in central New Brunswick. The area is underlain by a northeast-trending belt of Cambro-Ordovician rocks that comprise the Tetagouche and Miramichi groups, which have been intruded by a number of post-orogenic Late Silurian to Early Devonian granites. These intrusions are thought to have played a major role in the mineralising processes that generated the various types of mineralisation in that area (Fig. 20).

Figure 19 – Headframe at the former Burnthill Tungsten Mine (ca. 1960s).

Exploration history

Much of the exploration history summarized in this section is taken from that presented in Burns et al. (2008). Molybdenite mineralisation in quartz veins was first discovered by Dr Charles Robb in 1868 at the mouth of Burnthill Brook along the northern side of the Southwest Miramichi River. In 1910, Mr Samuel Freeze discovered additional mineralisation in the same general vicinity. His samples were sent to Dr T.L. Walker of the Mines Branch in Ottawa, who later identified wolframite within the samples. Mr Freeze continued to explore the area and was confident that there were millions of tonnes of tungsten in the area. Mr Freeze, together with Mr Matthew Lodge and Mr A.E. Williams, formed the Acadia Tungsten Mines Ltd. Surface drilling and trenching was conducted on the site and eventually a shaft was sunk. Minor production took place at the mine site in October 1915 and by mid-1916, the company had delineated a resource of 47.2 tonnes of concentrate at a grade of 65% WO_3. Besides tungsten ore, the mine also produced topaz - some of which were ground for use as a polisher in place of emery powder or diamond dust. In 1917, the shaft was deepened from 18 m to 51 m but in December 1917, the mine was closed down because of the inability of the milling equipment to concentrate the complex wolframite and sulphide ore (Victor, 1957).

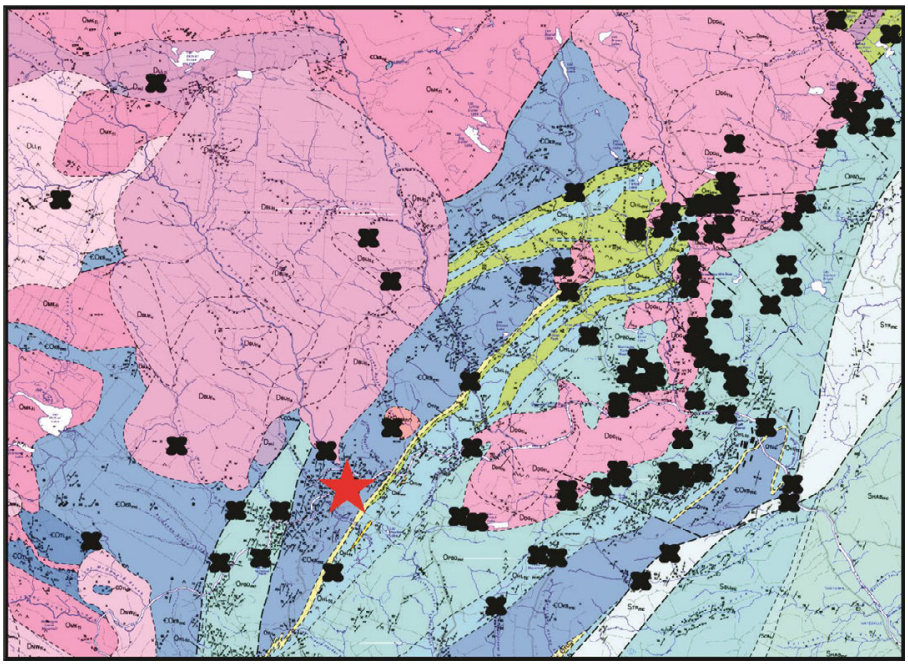

Figure 20 – Bedrock geology of the Burnthill area showing the location of the Burnthill Mine in relation to the other mineral occurrences in the region.

Between 1941 and 1942 Consolidated Mining and Smelting conducted an extensive trenching program. Bulk samples were collected from two of their seven trenches, which yielded grades of 2.97% WO_3 and 1.3% WO_3 over a length of 15.5 m. At the time, Mr J.M. Black reported an approximate resource of 31,752 tonnes of tungsten ore. Burnt Hill Tungsten Mines Limited secured the property in 1952-1956. A 290 m adit was driven on the property and both surface and subsurface drilling programs were conducted. A 150 tpd mill was erected on the property as well as a number of other buildings, the remnants of which can still be seen. Production of tungsten concentrates begun in the early fall of 1954. 50,128 lbs of concentrate grading 69% WO_3 and 3.5% Sn were shipped. At this time three "ore blocks" were estimated to contain a mineable resource of 252,000 tons grading 1.63% WO_3. It was also estimated that the tungsten concentrate would contain 4% recoverable Sn. It appears that only the No. 2 and No. 3 veins were used for the estimate, which was based on underground workings and drillhole data. At the then (1956) prevailing price of US$ 100 per mtu of WO_3 or US$ 5.00 per lb the value of the tungsten mineralisation is reported "to be worth $75 per ton of ore."

Between 1963 and 1964, surface drilling was conducted by Burnthill Tungsten and Metallurgical Limited to depths of 152.4 m below the adit. Extensive exploration and development were carried out during 1967, which included re-opening of the west portal close to the 1915 shaft, underground surveying and mapping of the adit and drifts, 334.4 m of subsurface drilling in 5 drill holes, and 700 m of surface drilling in 8 holes. A new shaft was sunk on the property in 1969 to a vertical depth of 72.5 m. Several drifts were excavated to the southwest and northwest.

In 1972, McPhar Geophysics conducted an IP survey over the Burnthill Mine site on behalf of Miramichi Lumber Company. From 1978-1980, Miramichi Lumber Company began an extensive mine evaluation program that began with the dewatering of the 1969 shaft in 1978. Additional drifts were excavated at the 150 ft level and a sample was sent to Ore Sorters Canada Ltd. for pre-concentration testing.

In 1979, 70 tons of materials were shipped to Lakefield Research of Canada Ltd for processing and testing. A surface-drilling program was also carried out in that year and an indicated ore reserve of 2,820,900 tons grading

0.147% WO_3 was calculated (ACA Howe International). In 1980, a 365.8 m decline was driven, which was located just to the west of the 1969 shaft. A 12,341 tonne bulk sample was collected and treated at an on- site pilot plant, which consisted of ore storage, crushing, screening, and sampling sections. A photometric ore sorter was also used to separate white mineralised quartz vein material from the darker meta-sedimentary waste rock. From this point, a mine plan was proposed but was never carried out. In 1981, following the 1979 and 1980 underground and pilot plant programs, and using the results of underground sampling (100 level (adit level), 150 level and 150 old level), surface and underground diamond drilling and bulk samples from the adit decline, A.C.A. Howe International Limited estimated unclassified mineral resources at Burnt Hill, totalling 2,820,900 tons grading 0.147% WO_3 (Brewster, 1981). It should be emphasized that the reserves report by Burnt Hill Tungsten Mines Limited, was based on only three mineable blocks and did not include any resources/reserves beyond the immediate mine development area. The resources reported by Brewster (1981), on the other hand, represent an unconstrained estimate based on mineralisation along a strike length of 440 m and over a vertical depth of 240 m. A summary of the historical resource estimates (non 43-101 compliant) for the Burnt Hill deposit are given in Table 4 (from Brewster, 1981).

The deposit is currently held by Noront Resources who have a joint venture with Cadillac Ventures Inc. (the chief operators). Over the past couple of years, Cadillac Ventures Inc. has further explored the deposits (i.e., geological mapping, sampling, and drilling) in order to bring the resource estimates up to NI 43- 101 standards.

Table 4. Unclassified Historical Resource estimates Burnt Hill Tungsten deposit

Company	Year	Tonnage (tons)	Grade WO_3 %	Estimated contained W (lbs WO_3)
Burnt Hill Tungsten Mines	1956	252,000	1.63	5,544,000
A.C.A. Howe (Brewster)	1981	2,821,000	0.147	9,123,000

Deposit description

The Burnthill deposit consists of numerous W-Sn-Mo-Be-F bearing quartz veins that occur within and above the apical portion of a cupola of the Burnthill pluton (Fig. 21). This cupola is located in the subsurface 1 km to the south of the surface exposure of the Burnthill pluton, and has been intersected in previous drill programs. Wolframite, the main ore mineral, is found in en echelon sets of steeply dipping quartz veins that range in width from a few centimetres to several meters. These cut the cupola granite, its host rocks, and an earlier set of barren, bedding-parallel quartz veins.

In addition to the mineralisation hosted within the quartz veins, the underlying granite also contains mineralisation. Quartz-greisen and greisen veins contain molybdenite and cassiterite. Mineralisation is concentrated in four main quartz veined zones collectively occupying an area approximately 335 m long by 152 m wide to a depth of 285 m (Potter, 1969; Puritch et al., 2005). The veins strike approximately 300° and have a variable dip (usually moderate to steeply northeast-dipping) (Potter, 1969). This trend is identical to the mode of the trends of the major joint set in the Burnthill pluton. In addition to wolframite and quartz, these veins also contain variable proportions of scheelite, cassiterite, beryl, topaz, fluorite, and bismuth as well as molybdenite, pyrite, and arsenopyrite. Trace amounts of ga-

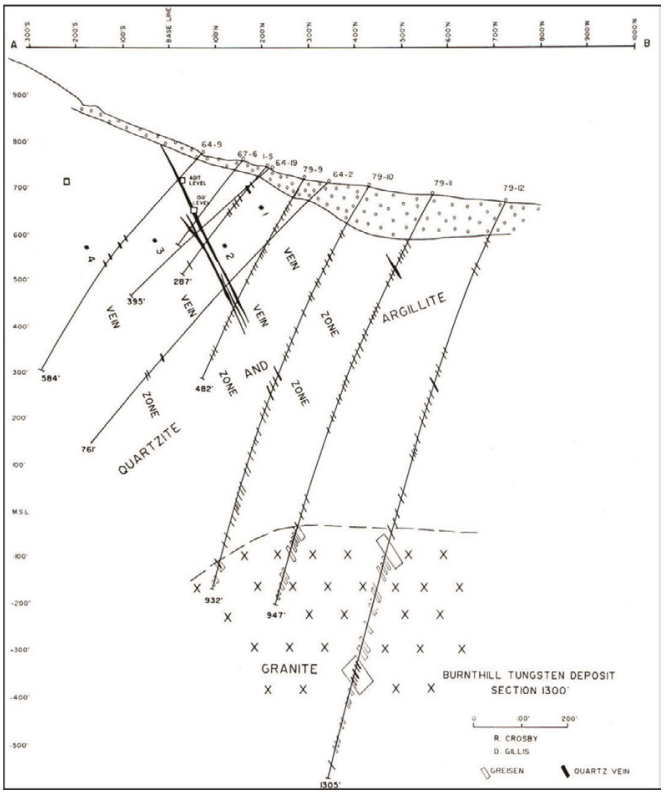

Figure 21 – Cross-section displaying drillhole intersections of Burnthill mineralisation and their relationship with the underlying Burnthill Pluton.

lena, native bismuth, scheelite, helvite, rutile, anatase, apatite and calcite have also been identified. Gold mineralisation (up to 1.9 git Au) was reported in a sample collected from the tailings piles by Fyffe and MacLellan (1988).

Early paragenetic studies by Victor (1957) are presented in Figure 22. Lyon (1988) also proposed a paragenetic sequence of the vein mineralogy and divided it into three stages as determined from mineral growth patterns (i.e., as mutual intergrowths, inclusions, replacements, vein selvages, vein and fracture fillings, etc.): 1) an early oxide-silicate stage; 2) sulphide stage; and 3) late vein stage.

Potter (1969) described two different types of mineralised quartz veins both of which correspond to Lyon's (1988) oxide-silicate stage. The first type contains quartz and muscovite with minor beryl, molybdenite, scheelite, wolframite, fluorite, and cassiterite. This, the most abundant vein type, commonly occurs along joints and faults striking 100° to 120°. The second type comprises quartz and topaz with minor wolframite, pyrrhotite, chalcopyrite, pyrite, arsenopyrite, fluorite, molybdenite, beryl, native bismuth, anatase and cassiterite. Iron-rich chlorite (chamosite) and helvite (beryllium silicate mineral) have also been identified (R.M. Crosby, pers. comm., 1985). Sulfides from the second stage extensively replace the first stage minerals (Victor, 1957; Lyon, 1988). The complex paragenesis and structural relationships of the Burnthill veins suggest a protracted history of vein mineralisation possibly taking place over a considerable range of temperatures (Victor, 1957).

Wolframite occurs as shiny jet black (brown when weathered) individual prisms up to 5 cm in diameter, as coarse bladed crystal aggregates, and in massive form (Sabina, 1992). Pyrrhotite is commonly dark brown and massive, molybdenite occurs in platy masses, arsenopyrite is normally crystalline and massive, and pyrite occurs as cubes and irregular masses (Sabina, 1992).

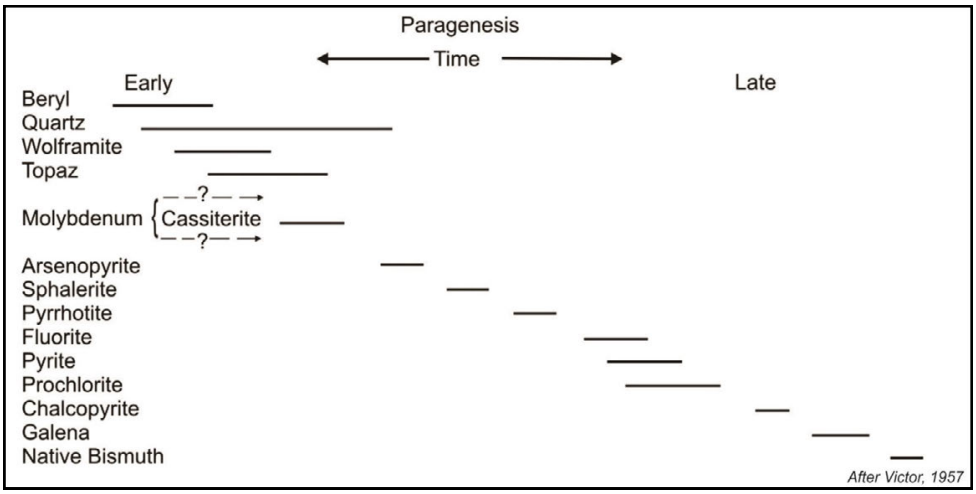

Figure 22 – Paragenetic sequence for the Burnthill deposit (from Victor, 1957).

According to Sabina (1992), the quartz associated with the mineralisation is commonly vitreous, milky, or massive with some crystals reaching a length of 5 cm. The topaz can be massive, nearly square, often striated, prismatic crystals (up to 2.5 cm wide) of translucent to turbid, white, yellow, dull green and smoky to grey in colour. Gem quality topaz has been reported from the deposit but is rare. Most topaz contains tiny inclusions of wolframite thus producing a turbid, cloudy appearance. The beryl that has been observed is light green, transparent, slender crystals (generally 0.5 cm wide and 3.5 to 5 cm long) and sometimes occurs as radiating crystal masses. Fluorite can be massive or crystalline, colourless, purple or green (less commonly pink, blue, yellow or white). Chlorite occurs as dark green, flaky or scaly masses whereas calcite is pearly- white foliated, brownish white platy and massive white. Orthoclase is colourless to white in small, platy, aggregates. Apatite is massive and crystalline and fluoresces a deep yellow under 'short' ultraviolet rays. Muscovite occurs as scaly to flaky masses. These minerals are generally associated with each other and with the metallic minerals but their paragenesis is not presently known. Many of them occur in vugs in quartz, e.g. fluorite and/or quartz crystals coated with crystals of pyrite and chlorite; and topaz and quartz crystals, in places studded with cassiterite crystals. The pink fluorite (chlorophane) is phosphorescent and fluorescent (bright green) under short wave ultraviolet light; when heated it phosphoresces brilliant aquamarine. Secondary sulphates that were identified include jarosite (yellow, powdery encrustation on sulfides and on the host rock) and rozenite (white, powdery patches and coatings on pyrrhotite).

Zealand Station beryl prospect

The Zealand Station beryl prospect is located 30 km northwest of Fredericton, NB in York County (Fig. 2). The mineralised zone occurs in a stripped area approximately 100 m by 200 m along a major northwest-trending power line. Access to the property can be obtained via Lawrence Lane off Highway 104.

Exploration history

Initial interest in the Zealand Station area was in the early 1950s when molybdenite was first discovered in quartz veins by a Mr. Perkins. Attempts to uncover significant Mo mineralisation in two test pits were unsuccessful; however, the presence of a "blue rock" in the trench was mentioned. In 1957, M.J. Boylen staked the area in search

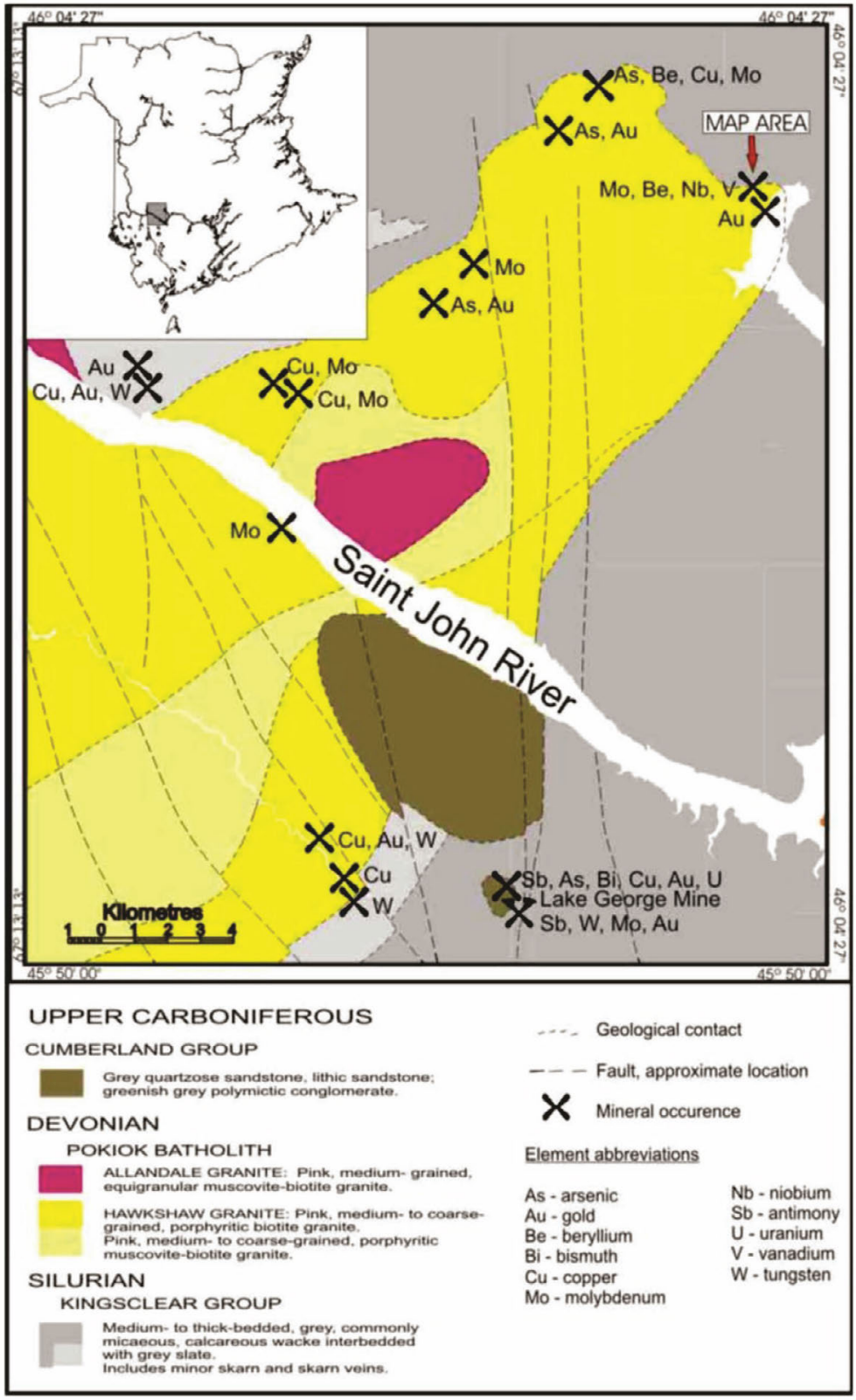

Figure 23 – Geological setting of the Zealand Station beryl prospect (modified from Caron, 1996).

of beryl mineralisation. Mapping in the area was conducted by A.B. Baldwin in 1959 and during the summer of 1961, trenching and a berylometer test were conducted. Positive results were obtained but the project was terminated. Latam Explorations Ltd. staked the area in 1962 and conducted diamond drilling (5 holes totalling ca. 47 m), channel sampling, soil sampling, and geological mapping. Limited Mo mineralisation as molybdenite in quartz was discovered in the drilling as well as beryl mineralisation that was reported to be of uneconomic proportions at the time (Latam Explorations Ltd., 1962). An additional three drill holes were completed in 1964 by Fred J. Smith, which showed significant mineralisation over a 2.4 m interval in two of the three holes (Smith, 1964).

Brunswick Mining and Smelting Corporation Ltd. staked the property in 1982 for its molybdenum, tungsten, and uranium potential. They conducted geochemical surveys (including soil and stream sediments) and geological mapping. Only two W anomalies were identified in soils but it was noted that W and U concentrations in the stream sediments increased up stream (Brunswick Mining and Smelting Corporation Ltd., 1982).

In 1985, geological mapping, channel sampling, trenching, and a magnetometer survey were carried out on the property by Shediac Bay Resources Inc. Three trenches were dug in the main stripped area where rock and channel sampling took place. Results of the 120 samples collected yielded only ten samples that had BeO concentrations above 100 ppm: one sample contained 980 ppm BeO (Shediac Bay Resources Inc., 1985). Additional sampling, trenching, and mapping were done in the area of the main Be mineralisation. Grab samples collected from the area ranged from 0.003 to 7.18% BeO. A resource estimate was calculated for the area by Dr. Rainer Stahlberg, which consisted of 133,329 tonnes (147,000 tons) grading 0.74% BeO (Shediac Bay Resources Inc., 1986).

Further exploration and mapping were conducted in the vicinity of the main Be showing. A detailed map of the area was produced along with additional grab sampling and a berylometer analysis (Shediac Bay Resources Inc., 1986). The average grade of the beryl mineralisation was reported to be between 0.01 to 0.1% BeO, which was considered to be uneconomic at the time (Shediac Bay Resources Inc., 1987). Since then, the property has only seen limited exploration activity.

Geological setting

The Zealand Station beryl prospect is situated along the northeastern cusp of the multiphase Devonian Pokiok Batholith (Fig. 23) that intrudes the metasedimentary rocks of the Fredericton Trough in southwestern New Brunswick. The Pokiok Batholith intrudes the southern end of the Miramichi Highlands and underlies an area of approximately 1,500 km^2. The batholith is divided into four units, which from oldest to youngest comprise: i) Hartfield Tonalite (Venugopal, 1979): grey, medium-grained, foliated, hornblende-biotite tonalite; ii) Hawkshaw Granite (Lutes, 1979): light grey to pink, medium- to coarse-grained, equigranular to megacrystic, biotite granite to granodiorite ; iii) Skiff Lake Granite (Lutes, 1979): light grey, coarse- to medium-grained, porphyritic to equigranular, muscovite-biotite granite; and iv) Allandale Granite (Ruitenberg and Fyffe, 1982): pink to grey, fine-to medium-grained, equigranular to seriate, muscovite biotite granite. A buried granodiorite intrusion in the underground workings at the Lake George Antimony deposit is considered to be part of the Pokiok Batholith (Seal et al., 1987, 1988; Yang et al., 2002, 2008). Bevier and Whalen (1990) presented Early Devonian U-Pb zircon ages ranging from 415 ± 1 Ma to 402 ± 1 Ma for the main intrusive phases.

The particular granitic phase that contains the beryl mineralisation at Zealand Station was mapped as the Hawkshaw Granite by Caron (1996), which was dated at 411 ± 1 Ma (U-Pb titanite; Whalen, 1993). The surrounding country rocks consist of metasedimentary rocks of the Early Silurian Kingsclear Group.

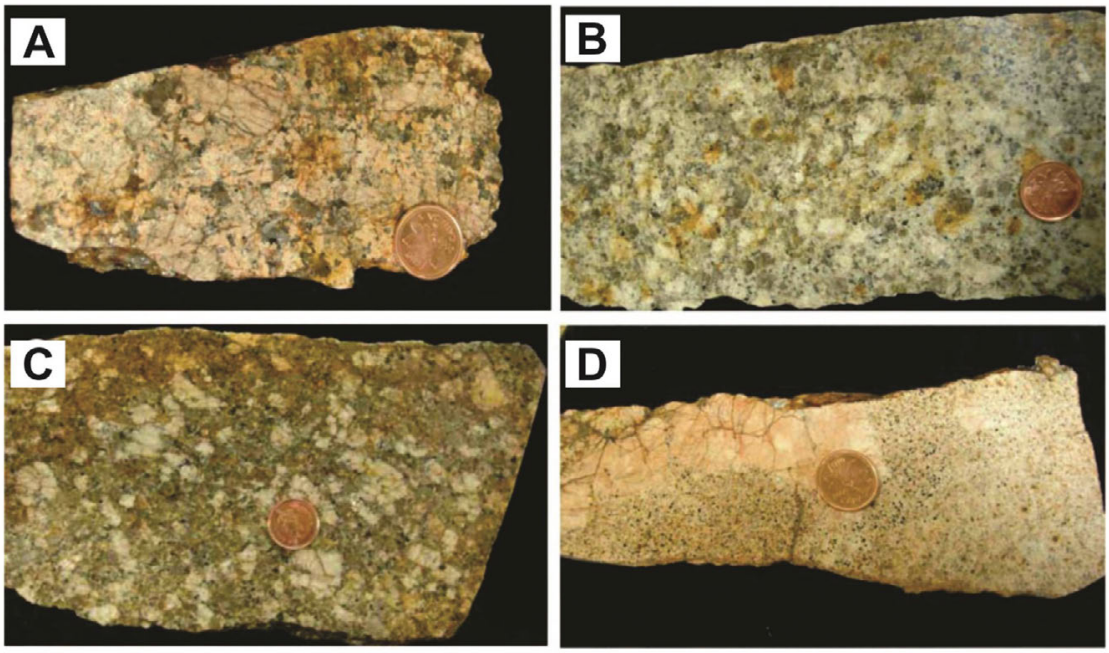

Figure 24 – Photographs of the various granitic phases of the Hawkshaw Granite at the Zealand Station prospect (after Beal et al., 2009). A) Pink granite; B) White granite; C) Biotite granite; and D) quartz

The Hawkshaw Granite is generally characterized by pink to grey feldspar porphyritic, medium-grained biotite granite to granodiorite; however, at Zealand Station the rocks are medium-grained granite with local textural and accessory mineral variations (Fig. 24). A late-stage, southeast-trending weakly porphyritic aplite dyke cross cuts the granite. It is in places pegmatitic, and locally has abundant blue beryl (aquamarine) occurrences in the aplitic groundmass, as well as in association with very coarse K-feldspar crystals (Fig. 25). To the east-southeast of the main trenched exposure is a pegmatite dyke that consists predominantly of muscovite, quartz, and orthoclase with crystals reaching close to 30 cm in size.

Contact metamorphosed hornfels of the Silurian Burtts Corner Formation (Kingsclear Group) are exposed in small outcrops on the property. They consist of metamorphosed very fine-grained grey shale, which contain variable quantities of cordierite, biotite, and minor subhedral pyrite.

Geochemistry

The host granite and cross cutting dyke have a granitic composition with $Si0_2$ contents within the range of 67.5 to 82.4 wt%. Using the Frost et al. (2001) classification, the FeO*/(FeO*+MgO) ratio is from 0.09 to 0.95, which shows that these granites are predominantly magnesian and slightly potassic. The modified alkali-lime index (MALI) diagram of Frost et al. (2001) shows that the host granite and porphyritic aplite dyke is calc-alkaline with strong peraluminosity (ASI = 1.23 to 3.76), enhanced by greisenization.

In comparison, the samples collected from the granite and aplitic dyke have partially overlapping compositions. The trace-element data have elemental characteristics of S-, fractionated I-, and crustal A-type granites. Geochemical data indicates that the dyke and granite source composition is either S-type or fractionated I-type that has been

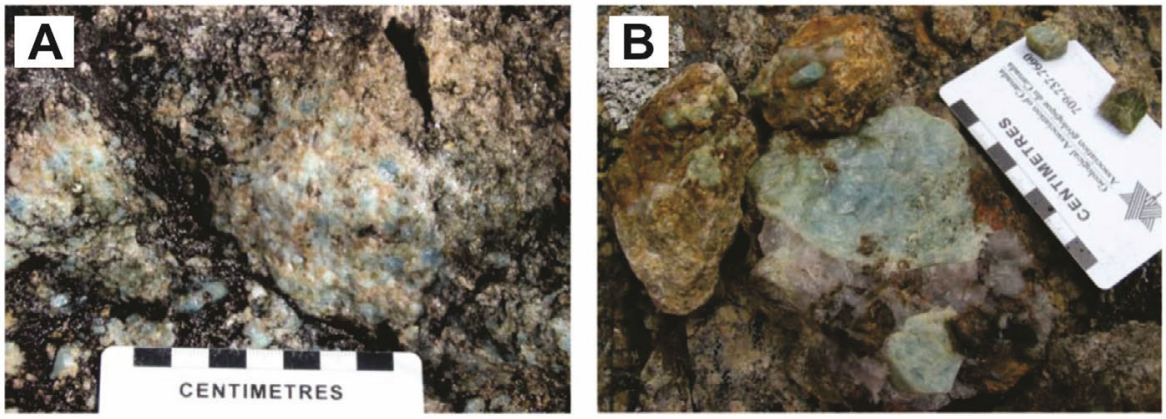

Figure 25 – A) Disseminated beryl within granite at the Zealand Station prospect. B) Subhedral to euhedral beryl crystals from the Zealand Station prospect.

contaminated by assimilation and mixing. The latter classification is more likely the case as there is evidence of assimilation of surrounding metasedimentary rocks (i.e., xenoliths) near the granite-hornfels contact.

The geotectonic discrimination diagrams of Pearce et al. (1984) indicate that in all cases, the data from both the host granite and the aplitic pegmatite dykes plot near the triple point between within-plate granites, volcanic arc granites, and syn-collisional granites.

Geochronology

The porphyritic aplite dyke provided an age of 400.5 ± 1.2 Ma (TIMS U-Pb zircon; Beal, 2007), whereas an age of 404 ± 8 Ma was obtained using the U-Pb in magmatic monazite by the EPMA technique (Beal, 2007). These ages link the aplitic dyke to the Allandale Granite phase, previously dated at 402 ± 1 Ma (Whalen, 1993). The Allandale phase is the youngest defined phase of the Pokiok Batholith.

Beryl mineralisation

At the Zealand Station beryl (aquamarine) occurrence, the host granite is altered to greisen in pockets (<3 m wide) and along the margins of veins that have associated molybdenite booklets and beryl locally. The quartz-rich veins have two predominant orientations: 135°/90°, and 010°/75°W. They are <5 cm wide with rare molybdenite-rich pockets (<1.5 cm thick) and can be traced along strike for up to 30 cm. The greisen pods show no preferred orientation, although they are suggested by Chrzanowski and Elliot (Shediac Bay Resources Inc., 1986) to be associated with nearby fracture orientations in the granite. The veins and greisen pods contain up to 5.61 wt% BeO. In addition to the secondary beryl in the granite, there is up to 20 vol% beryl in a portion of the aplitic phase of the dyke. Other samples from the aplitic dyke and pegmatite contain up to 79 ppm Be.

Beryl crystals at the Zealand Station prospect are up to 4 cm in length and 2 cm in diameter (Fig. 25). The crystals are clear to milky, light to medium blue in colour, and are commonly euhedral to subhedral. Zoning can be seen in some specimens where the core is dark blue and the rims are light blue. The crystals found on the property all have microfractures; however, there is the possibility of gem quality aquamarine crystals occurring beneath the zone of deep weathering (Beal, 2007).

Molybdenum and tungsten mineralisation

Throughout the main exposure at the Zealand property, molybdenum (molybdenite) and tungsten (scheelite and wolframite) mineralisation has been found as disseminations within altered granite, associated with greisen alteration, as well as in quartz veins and fractures. A pegmatite exposed in a 2 m by 2 m outcrop along the eastern margin of the property does not contain any beryl but does contain tungsten mineralisation in the form of wolframite (Beal and Lentz, 2010; Beal et al., 2010). The pegmatite has a distinctive border zone, intermediate zone and a core dominated by quartz and plagioclase crystals up to 15 cm in diameter. In addition, there are biotite booklets up to 3 cm wide and wolframite crystals up to 3 cm long in the core zone. The border and intermediate zones primarily contain orthoclase, albite, quartz, and muscovite with trace amounts of biotite, zircon, rutile, monazite, chlorite, calcite, and iron-oxides (Beal and Lentz, 2010; Beal et al., 2010). The property has never been systematically evaluated for its molybdenum- tungsten potential.

Deposit model

Beal (2007) proposes that the deposition of beryl mineralisation at the Zealand Station prospect requires that there were elevated quantities of Be present during the fractionation of the A-type granite. During ascension, local assimilation of the country rocks cause Be and other incompatible rare element enrichment of the magma until such time as a separate magmatic fluid phase exsolves. Saturation within the volatile phase occurs as the magma cools and the resulting rare-earth element hybrid-type pegmatite and aplite dykes are formed. Within this evolved magma-fluid system, the separate fluid phase allows crystallisation of beryl within local pegmatitic pockets. The magmatically derived fluids also infiltrate the host rock fracture network precipitating beryl in quartz veins and surrounding greisen pockets. Beryl compositions are consistent with crystallisation between 600°C to 660°C at 2.5 kbar (Beal, 2007).

Trip 1 – Sisson Brook and Zealand Station

Itinerary

Trip 1 will focus on the geology of the Sisson Brook W-Mo deposit and minor occurrences associated with the Nashwaak Pluton; several stops will highlight regional stratigraphy, which is host to much of the exo-contact Sn-W-Mo-Cu mineralisation throughout the region. The day will finish with a visit to the Zealand Station beryl prospect that occurs along the northeastern margin of the multiphase Pokiok Batholith.

Stop 1-01: Hayden Lake Formation

Stop 1-01A: Ferromanganiferous Mudstones (46°22'55.46" N, 66°53'42.45" W)

Route: *From downtown Fredericton, head north on the Westmorland Street Bridge. Proceed through the lights at the Ring Road-Maple Street intersection and then again at the Ring Road – Brookside Drive intersection. Take Exit 620 on the right and head towards Stanley. Turn right onto Hwy-620, and continue on this road until reaching the Village of Stanley (42.1 km). Turn left onto Hwy-107 and proceed through the village for approximately 3.7 km. Turn left and head toward Florenceville – Bristol. Turn right onto a logging road at 16.2 km and proceed to the pit area 300 m on the road to the right.*

Hazards: *Please watch your step in the rubbly areas and exercise caution along the small ridge.*

Figure 26 – Fe- and Mn-rich shale of the Hayden Lake Formation in the pit at Stop 1-01A.

The exposure in this pit consists primarily of maroon iron- and manganese-enriched mudstone and siltstone of the Ordovician Hayden Lake Formation (Fig. 26). It is one of three formations that make up the Ordovician Tetagouche Group in the Deersdale – Nashwaak River area. The Hayden Lake Formation is conformably underlain by a sequence of felsic tuffs and interbedded, brachiopod-bearing, calcareous siltstone of the Early Ordovician (Arenigian) Turnbull Mountain Formation, and is conformably overlain by a sequence of interbedded wacke, siltstone and minor conglomerate of the Push-and- Be-Damned Formation. The Tetagouche Group extends some 200 km to the northeast where it hosts the world-class volcanogenic massive base-metal sulphide deposits of the Bathurst Mining Camp. The reddish coloured beds in the pit are intercalated with green mudstones; manganese staining is evident along fracture surfaces. Black chert and graphitic shale comprising the upper part of the Hayden Lake Formation are exposed in the quarry at Stop 1-01B.

Stop 1-01B: Black Graphitic and Pyritic Shales (46°22'50.90" N, 66°53'46.86" W)

Route: *Walk 100 m back toward the main road and stop at the pit area on the left.*

Hazards: *At the east side of the quarry, the walls are steep and unstable so please do not get too close to the edge.*

The west side of the quarry (closest to the logging road) consists of black graphitic and pyritic shales of the Ordovician Hayden Lake Formation. The east side of the quarry (farthest from the logging road) consists of medium grey to maroon siltstone like those seen in the previous stop. The contact between the maroon and black sequences is

Figure 27 – Contact between black pyritic shale (left) and maroon siltstone (right) of the Hayden Lake Formation at Stop 1-01B.

marked by a rusty, 20 m wide zone of fault gouge and abundant barren quartz veins (Fig. 27). Graptolites in black shale of the Hayden Lake Formation in the Turnbull Mountain area range in age from the *Glyptograptus terretiusculus* Zone of the Middle Ordovician to the *Nemagraptus glacilis* Zone of the Upper Ordovician (Poole, 1963; lrrinki, 1980; van Staal and Fyffe, 1991, 1995a).

Stop 1-02: Miramichi Group (46°25'14.93" N, 67°01'25.23" W)

Route: *From Stop 1-01B, return to the main road and turn right. Continue along Hwy-107 for 9.4 km. Turn left onto the dirt road (Road 19). At 1.7 km, keep right at the intersection. Proceed for 2.7 km from the intersection and stop at the outcrop on the right hand side of the road.*

Hazards: *The outcrop may be unstable in certain sections. Please exercise caution while examining the outcrop. Also, please be aware of those around you before hammering the rocks.*

The rocks of the Cambrian to Early Ordovician Miramichi Group in the Sisson area consist of deep-water, turbiditic sequence of interbedded quartzose sandstone and shale. This sequence was deposited on the Ganderian continental slope along the south-eastern side of the Iapetus Ocean (Rice and van Staal, 1992). In the local area, the rocks of Miramichi Group form the core of a north-northeast-trending antiform; they are in faulted contact with the Early Ordovician Turnbull Mountain Formation of the Tetagouche Group to the west and are overlain unconformably by the Hayden Lake Formation of the Tetagouche Group to the east. The outcrop at this stop consists of laminated

Figure 28 – Field photograph of the quartzose sandstone beds of the Miramichi Group at Stop 1-02.

quartzose sandstone interbedded with slate (Fig. 28). Sandstones of the Miramichi Group are typically light grey but the purplish brown hue in this exposure is due to the presence of biotite formed as a result of hornfelsization; minor barren quartz veins cross-cut the bedding.

Stop 1-03: Intense greisen alteration, Nashwaak Granite (46°29'33.99" N, 67°02'51.42" W)

Route: *From Stop 1-02 backtrack to Hwy-107. Turn left and continue along Hwy-107 for 9.0 km. Outcrop on the left (south) side of the road.*

Hazards: *This is a busy road/or logging trucks. Please park well of/to the side of the road and watch for traffic.*

At this location, alteration of the Nashwaak Granite is much more intense, a result of sericitization and silicification and accompanied by disseminated pyrite-arsenopyrite mineralisation. Similar greisen alteration is found within the Nashwaak Granite to the north and south for a considerable distance and is coincident with a steeply dipping fracture cleavage (029/74° E) that is prominent in the western domain of the Nashwaak pluton.

Figure 29 – Calcite filled pod rimmed by drusy quartz within the Nashwaak Granite at Stop 1-04.

Stop 1-04: Alteration zone in Nashwaak Granite (46°29'39.06" N, 67°03'10.97" W)

Route: *Continue 400 m west along Hwy-107 and stop at the outcrop on the south-west side of the Deersdale intersection.*

Hazards: *This is a busy intersection for logging trucks. Please park well off to the side of the road and watch for traffic.*

At this location, the greenish alteration of the biotite-muscovite phase of the Nashwaak Granite is a result of local sericitization. Pods of calcite with rims of drusy quartz are present within the granite (Fig. 29), as are xenoliths that range up to 5 cm in length.

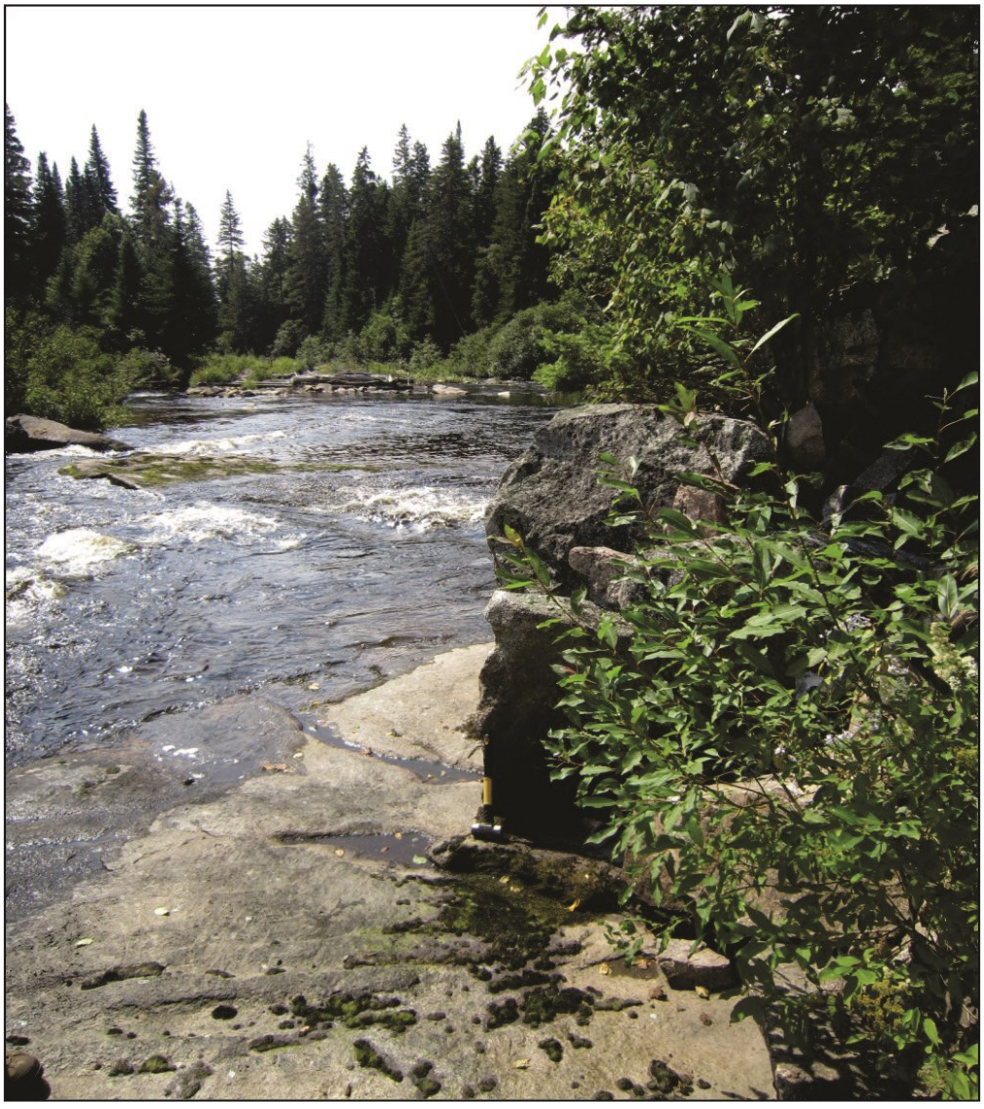

Figure 30 – Field photograph of the Nashwaak Granite outcrop along the edge of the Nashwaak River at Stop 1-05A.

Stop 1-05A: Nashwaak Granite
(46°24'40.12" N, 67°09'38.06" W)

Route: *Turn south on dirt road at Deersdale intersection. Continue on dirt road for 15.6 km. At 3-way junction turn right. Proceed for 300 m and park at the ATV rest area. Walk 300 m down the trail to the river.*

Hazards: *Stumps and rocks may pose tripping hazards along the trail to the river. Please exercise extreme caution at this stop. The river is deep with a swift current at this location and the smooth outcrop along the edge of the river can be very slippery when wet.*

The outcrop is located along the west side of the Nashwaak River and once formed the abutment of an old bridge that crossed the river at this location (Fig. 30). The Early Devonian Nashwaak Granite at this location consists of orangey pink to light grey equigranular to seriate textured biotite granite. Medium orange coloured aplitic dykes cross-cutting the granite are discernible in some of the angular boulders at this location (Fig. 31).

Figure 31 – Field photographs of an aplitic dyke cutting equigranular biotite granite of the Nashwaak Granite at Stop 1-05A.

Stop 1-05B: Nashwaak Granite (46°24'28.28" N, 67°09'37.11" W)

Route: *Return to the main road via the trail. Proceed back to the intersection (300 m).*

Hazards: *This is a busy intersection for logging trucks. Please park well off to the side of the road and watch for traffic.*

Outcrop is exposed as several subcrops at the road intersection. The Early Devonian Nashwaak Granite at this location consists of orangey pink to light grey equigranular to seriate textured biotite granite.

Stop 1-06: Howard Peak Granodiorite (46°22'28.03" N, 67°03'02.90" W)

Route: *At intersection and turn left. Proceed for 2.2 km and turn right. Follow the dirt road for 4.6 km and turn right at the stop sign. At 4.3 km; stop at the outcrop on the right side of the road.*

Hazards: *This outcrop is near a blind knoll on a busy logging road. Please park well off the road and be sure to stay well off the road in case a logging truck comes over the hill. Please exercise caution along the steep edges of the outcrop and beware of those around you when hammering the rocks.*

The outcrop on the south side of the road consists of the Early Devonian Howard Peak Granodiorite that forms the host rocks to a portion of the Sisson W-Mo deposit. This medium- to coarse-grained plagioclase-rich diorite/

Figure 32 – Howard Peak Granodiorite: medium- to coarse-grained plagioclase-rich diorite/granodiorite, cross-cut by fine- to medium-grained biotite-bearing felsic dykes interpreted to be derived from the Nashwaak Granite (Stop 1-06).

granodiorite is medium grey on the weathered surface and dark grey on the fresh surface (Fig. 32). Light orange, fine- to medium-grained biotite-bearing felsic dykes up to 30 cm wide that locally crosscut the granodiorite are interpreted to be derived from the Nashwaak Granite.

Stop 1-07: Sisson Brook Zone I trench (46°22'23.53" N, 67°02'29.72" W)

Route: *Return to the vehicles and proceed down the road another 700 m. Park along the side of the road. The trench is located on the left hand side of the road, down a small trail.*

Hazards: *Park well off to the side of this busy logging road. Please watch for logging trucks before you cross the road. The short trail to the trench has uneven sections that may pose tripping hazards. The smooth sections of the trench may be slippery when wet. Please be aware of others when hammering the rocks.*

The bedrock in the northeastern part of the trench at Zone I (Fig. 8) comprises an interbedded sequence of dark grey siltstone and light grey felsic tuff of the Turnbull Mountain Formation. The beds range from 1 cm to 10 cm in thickness, strike 020° and dip 60° E. The bedded sequence is in contact with granodioritic rocks of the Howard Peak pluton along a north-northwesterly trending fault exposed in the southwestern part of the trench. A medium-grained, north-northwesterly trending dyke intrudes the bedded sequence in the northern part of the trench and is truncated to the south by an east-west-trending cross fault. Movement on this cross-fault was dextral, assuming that the gabbroic dyke observed on the southern side of the fault represents the displaced continuance of the same dyke (Fig. 33).

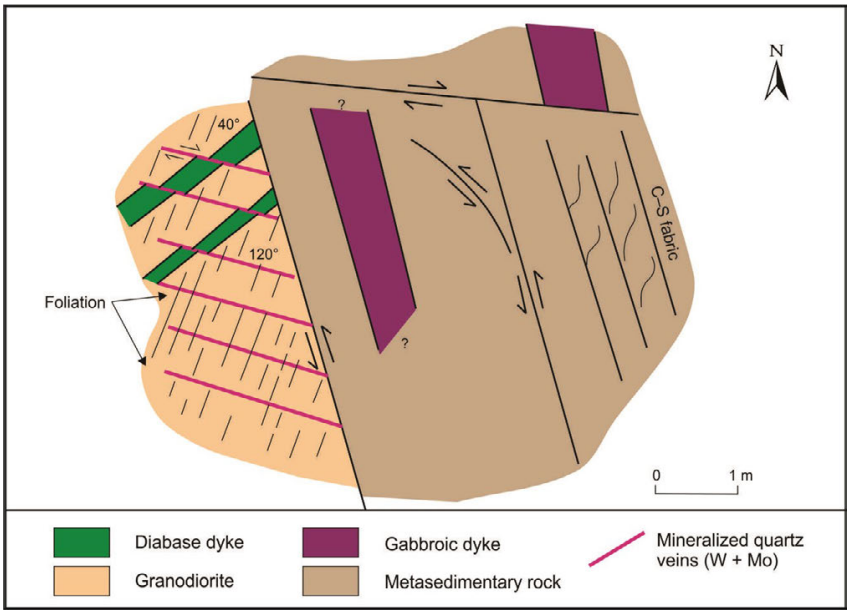

Figure 33 – Schematic diagram of the trench at Zone I (from Fyffe and Thorne, 2010).

Granodiorite of the Howard Peak pluton shows a steep foliation that strikes about 030°. Both the foliation and a prominent, west-northwesterly trending (300°-310°) joint set in the granodiorite are abruptly truncated by the north-northwesterly trending fault that marks the boundary with the bedded rocks to the northeast (Figs. 33 and 34). Schistosity-shear fabrics in the bedded sequence indicate sinistral movement along this fault zone (Fig. 35). Some move-

Figure 34 – Field photograph showing the faulted contact between metasedimentary rocks and granodiorite in the trench at Zone I (Stop 1-07).

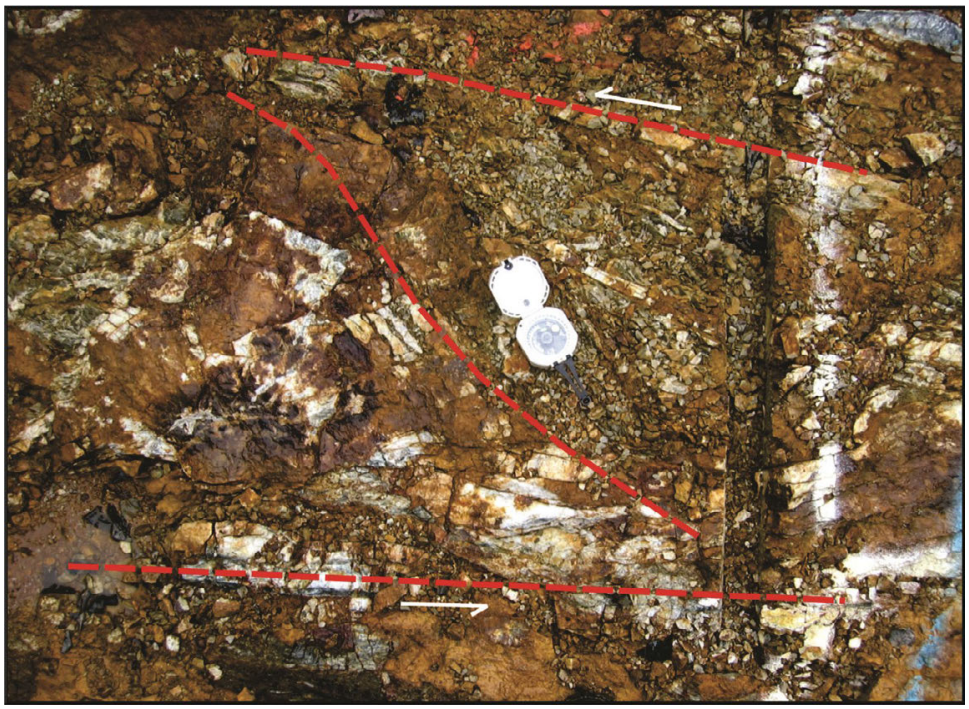

Figure 35 – C-S fabric developed in silicified metasedimentary units in the trench at Zone I, Sisson deposit (Stop 1-07). View looking northwest.

ment also took place along the west-northwesterly trending joint set, as indicated by small dextral displacement of the margins of two 30 cm thick, northeasterly trending diabase dykes cutting the granodiorite (Fig. 11). Narrow quartz veins containing pyrite, chalcopyrite, wolframite, and molybdenite follow the strike of bedding, the fault zone, and the joint set. The fault zone exposed in the trench at Zone I is interpreted to be a horsetail splay off the main north-northeasterly trending, high-strain shear zone that lies along the eastern margin of the Howard Peak pluton on Zone III.

Stop 1-08: Howard Peak Granodiorite (46°21'54.13" N, 67°03'13.63" W)

Route: *Return to the vehicles and proceed to the bottom of the hill and turn around at the logging road on the left (100 m). Head back up the hill for 400 m and turn left onto the logging road Proceed for 1.3 km and park along the side of the road at the comer. The outcrop is located in the ditch on the right side of the road.*

Hazards: *Smooth surfaces of the outcrop may be slippery when wet. Please be aware of others around you when hammering rocks.*

Outcrops on the west side of the logging road consist of foliated granodiorite of the Howard Peak pluton. Foliation in the northerly part of the exposure strikes between 15° and 30° and dips approximately 80° SE. Granitic dykelets strike 175° and dip 80° E (Fig. 36). Quartz veins at this location range from 0.5 cm to 1 cm in width and strike between 130° and 140° and dip 65° SW. The quartz veins cross-cut the foliation and dextrally offset the gra-

Figure 36 – Foliated Howard Peak Granodiorite cross-cut by northerly-trending granitic dykelets, which in turn are cross-cut by west-northwesterly trending, molybdenite-bearing quartz veins (Stop 1-08).

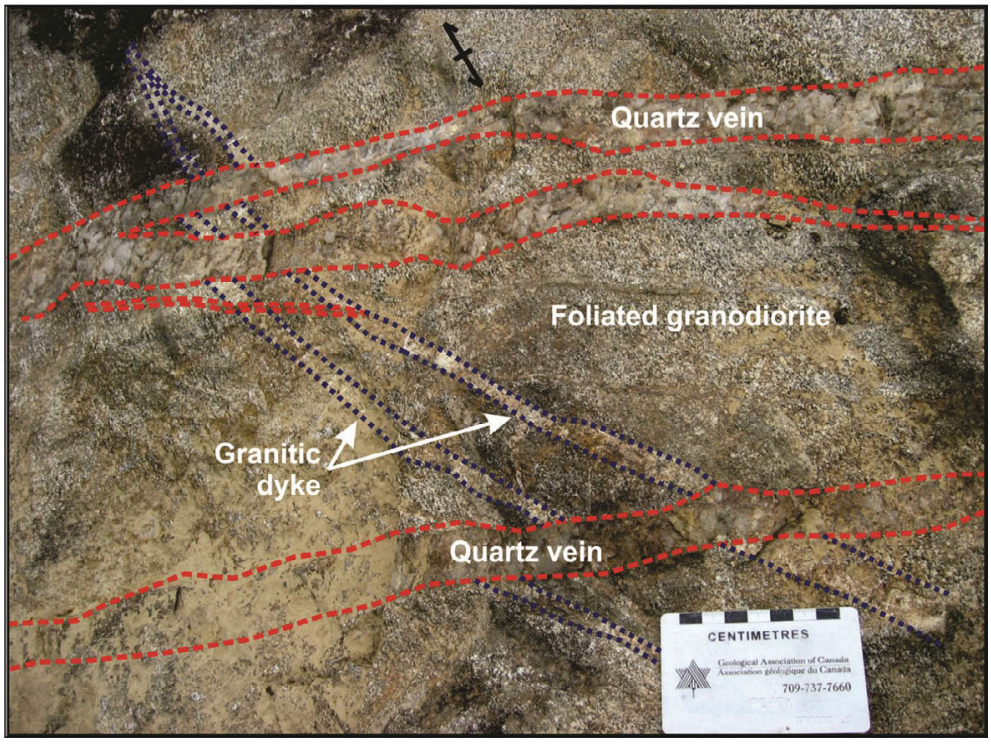

Figure 37 – Foliated Howard Peak Granodiorite cross-cut by granite pegmatite dyke at Stop 1-08.

nitic dykelets. Blebs of molybdenite are locally present in the quartz veins. Granitic dykelets in the southerly part of the exposure are overprinted by the foliation and are folded; however, a pod of granite pegmatite is undeformed (Fig. 37).

Stop 1-09: Sisson Brook Zone III trench (46°22'10.06" N, 67°02'49.93" W)

Route: *Return to the vehicles and turn around. Proceed back out the road for approximately 800 m and park on the right side of the road by the spoil piles at the west end of the large trench at Zone III.*

Hazards: *The walls of the trench are steep and unstable in places so please stay well back from the edge and exercise extreme caution. Be aware of those around you when hammering rocks.*

The stockpiles at the beginning of the trench were bulk sampled and excavated at 5 m intervals from along the length of the trench prior to flooding. The variation in lithologies (cut by Mo- and W-mineralised veins) can be seen amongst the piles. Molybdenite-bearing veins were more prevalent at the eastern end of the trenches whereas scheelite is more abundant at the western end and the grade increases toward the western limits of the trench. These veins were cut by north to northwesterly-dipping veins carrying quartz-chalcopyrite-wolframite veins.

Bedrock at the eastern end of the trench at Zone III (Fig. 38) is a fine-grained silicified gabbro that possesses a prominent foliation trending 003° and dipping 55° W. Chalcopyrite and pyrite are present in 10 cm thick silicified zones and quartz veins that follow the foliation trend. A later set of quartz veins (about 2 cm thick), striking 125°

Figure 38 – Exploration trench at Zone III of the Sisson deposit at Stop 1-09 (looking west).

and dipping 80° SW, transects the foliation in the gabbro and contains abundant molybdenite. Westward along the south wall of the trench, a 2 cm thick quartz vein with a 095° strike and 60° S dip is intersected at a low angle by a 4 cm thick quartz vein with a 135° strike and 85° SW dip. In places, the veins are sinistrally offset by a few centimetres along the northerly trending foliation plane (Fig. 13). Granitic dykes from 10 cm to 15 cm thick cut the gabbro and possess a strong northerly trending, cataclastic foliation along which feldspar augen are aligned. The top of the north wall of the trench features a strongly foliated, fine-grained gabbro containing plagioclase porphyroclasts about 2 cm in length (Fig. 14). The gabbro is cut by a vertical, northerly trending granite pegmatite dyke that is about 5 cm thick and cut by two intersecting, molybdenite-bearing quartz veins. The earlier quartz vein (V1) is about 0.5 cm thick, strikes 110° and dips 65° SW; the later quartz vein (V2) is about 2 cm thick, strikes 140° and dips 60° SW (Fig. 39).

As originally exposed in 2007, the trench was excavated as a series of benches about 0.5 to 1 m high (Fig. 38). Over the Mo-zone (Fig. 40A), to the east, there were two benches in till, with the bedrock surface comprising a third. To the west, over the W-zone, the till was thicker, with five benches in till and then the bedrock surface (Fig. 40B). The excavation did not reach the bedrock surface at the far western end of the trench, where two visibly different basal tills were observed. The lower till was slightly yellower in colour, and characterized by significant clay (ca. 25 %) in the matrix and an east-southeast-trending fabric. This till was assigned to the Early Caledonia Phase by Seaman and McCoy (2008). However, following redating of the buried organic materials at the Half Moon Pit section of Lamothe (1992), this lower till – stratigraphically equivalent to his Lower Till – was reassigned to the Northumberland Phase, of probable Illinoian age (Seaman, 2009).

Figure 39 – Intersecting, molybdenite-bearing quartz veins in the Zone III trench at Stop 1-09, Sisson deposit (looking east).

The upper till exposed in the trench appeared to be the sandy basal till typical of the surface till of the area. However, geochemical and till fabric investigations revealed that there were two sandy tills present (Seaman and McCoy, 2008). The lower of these (i.e., the middle till at this site) is the regional surface till, correlative with the Upper Till of Lamothe (1992); it is now assigned to the Early Wisconsinan Caledonian Phase glaciation (Seaman, 2009), which was characterised by southeast to south-southeast ice flow. Its geochemical signature strongly reflects the mineralisation in the underlying bedrock. The uppermost till is the stratigraphic equivalent to the late-glacial till identified at Todd Mountain by Lamothe (1992). At Sisson this till is comprised of a mix of material reworked from the underlying till diluted with unmineralised material from late-glacial ablation till and glaciofluvial, glaciolacustrine, and organic deposits by westward flow of the late-glacial Gaspereau Ice Centre - Collins PondPhase; Younger Dryas Stadial (Seaman, 2009). The late-glacial till effectively masks the geochemical signature of the subcropping bedrock at Sisson. For example, in samples from a section overlying the Mo-zone (Fig. 40A), the late-glacial till contained no detectable Mo (<1 ppm), while duplicate samples from the underlying Caledonia till averaged 39 ppm Mo (very anomalous), and a sample of underlying gossanous till contained 260 ppm Mo (Seaman and McCoy, 2008).

During the Targeted Geoscience Initiative 4 (TGI 4) indicator mineral and till and stream sediment geochemical sampling project (McClenaghan et al., 2013a, b, c , d, 2014; Parkhill et al., 2014) several back hoe pits were excavated in the area of the Zone III trench. Scrub piles from several of these pits are still present in the west end of the

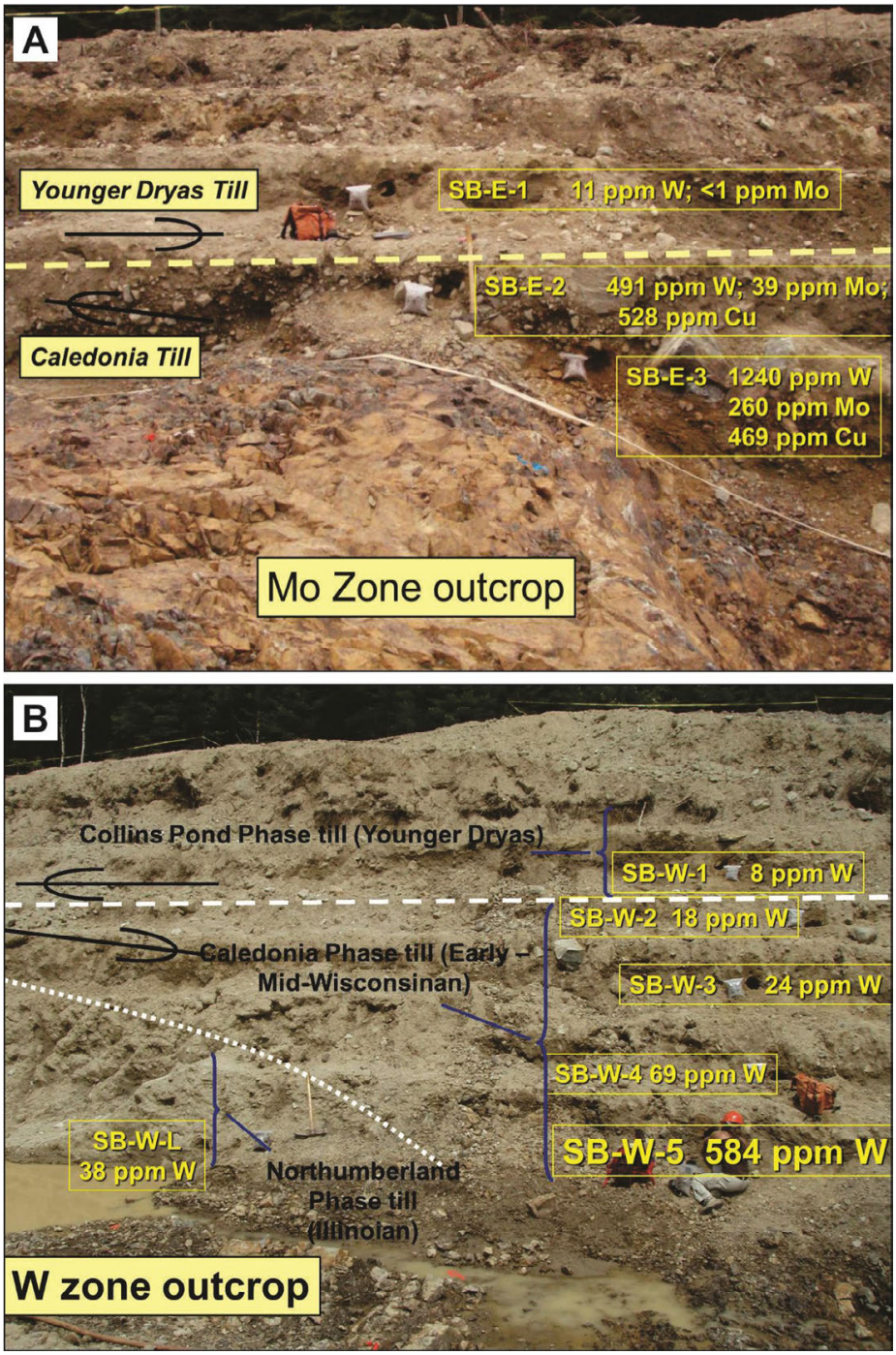

Figure 40 – A) Till section in the south face of the east end of trench at Zone III (SB-N) of the Sisson W-Mo deposit, overlying the Mo-zone; sample from the upper lift (beside the pack) is Younger Dryas till (CS-SB-E-1); middle sample is Caledonia till (CS-SB-E-2); lower sample is gossanous (?) Caledonia till (CS-SB-E-3). Till geochemical concentrations are from the <0.063 mm fraction of basal till (Seaman and McCoy, 2008). Note arrows indicating the direction of ice flow for the 2 tills. View looking south. B) Till section (sample CS-SB-W) above the W-zone in the western part of the trench at Zone III of the Sisson W-Mo deposit. Till geochemical concentrations are from the <0.063 mm fraction of basal till (Seaman and McCoy, 2008). Note arrows indicating the direction of ice flow in the 2 tills. View looking north.

trench. This will provide an opportunity to see the textural differences between the Northumberland and Caledonia tills.

Stop 1-10: Ablation till (46°14'21.10" N, 67°02'03.59" W)

Route: Proceed to the intersection (500 m) and turn right onto the Sisson Brook Road. Continue for 8.0 km. Bear right (south) onto the Nackawic Haulage Road and continue south, crossing the Nashwaak River in 2.8 km. Continue south for 4.6 km to the Keswick River Bridge. Just before the bridge note the large road cut on the left that consists of the medium-grained, red equigranular muscovite-bearing Hawkshaw granite phase of the Pokiok Batholith. Proceed for 1.5 km from the Keswick River Bridge and stop at the gravel pit on the right side of the road.

Hazards: There are a number of logging trucks that use this road. Please be aware of the truck traffic and stay well off to the side of the road.

This roadside borrow pit exposes up to 5 m of ablation till in a hummocky disintegration moraine. This material, deposited during the final melting of a stagnant glacier, comprises material that was transported in the englacial or supraglacial zones (within the glacier or on top of it, respectively), and deposited during final meltout of the glacier. It is commonly derived from a different direction or source than the basal till formed beneath an active glacier, and therefore comprises a different geochemical population. In this area, the basal till was formed by the Late Wisconsinan Escuminac Phase glacier, with a southeast to south-southeast flow, that partially reworked an older till formed by the east-southeastward flowing Early Caledonia Phase (Early Wisconsinan) glacier. In contrast, the ablation till was either deposited at the end of the Chignecto Phase, following a period of northeastward ice flow, or during the Collins Pond Phase (Younger Dryas), near the western margin of the Gaspereau Ice Centre in central New Brunswick (Seaman, 2006).

Stop 1-11: Zealand Station beryl prospect

Note: *At the request of the mineral claim holder, we ask that you please refrain from sample collecting at this location.*

Route: *From Stop 1-10 drive south along the Nackawic Haulage Road for 19.4 km to Hwy-104 junction. Turn left and follow Hwy-104 for 17.5 km to Morehouse Corner. Turn right onto Lawrence Lane and drive up the hill 600 m to the end of the paved road. Park at the last house on the road and obtain permission from the land owner to proceed along the dirt road to the trenched exposure on the power line.*

Hazards: *The surface of the trenched exposure is very irregular in places and locally has patches of loose gravel, so please watch your step.*

Within the trenched exposure, the unconformable/intrusive contact between the Hawkshaw Granite of the Pokiok Batholith and the metasedimentary rocks of the Kingsclear Group can be seen in the northern part of the area (Figs. 2, 23 and 41). There are several variations of granite associated with the Hawkshaw Granite phase in this area including white granite, pink granite, biotite granite, and alkali feldspar aplite-porphyry. The distribution of these units is shown in Fig. 41. The alkali feldspar aplite-porphyry unit locally contains blue beryl. Aquamarine coloured beryl can be found throughout all of the phases of granite present within the area of the trench. In addition there are also pockets of muscovite-quartz greisen and Mo mineralisation occur throughout the trench.

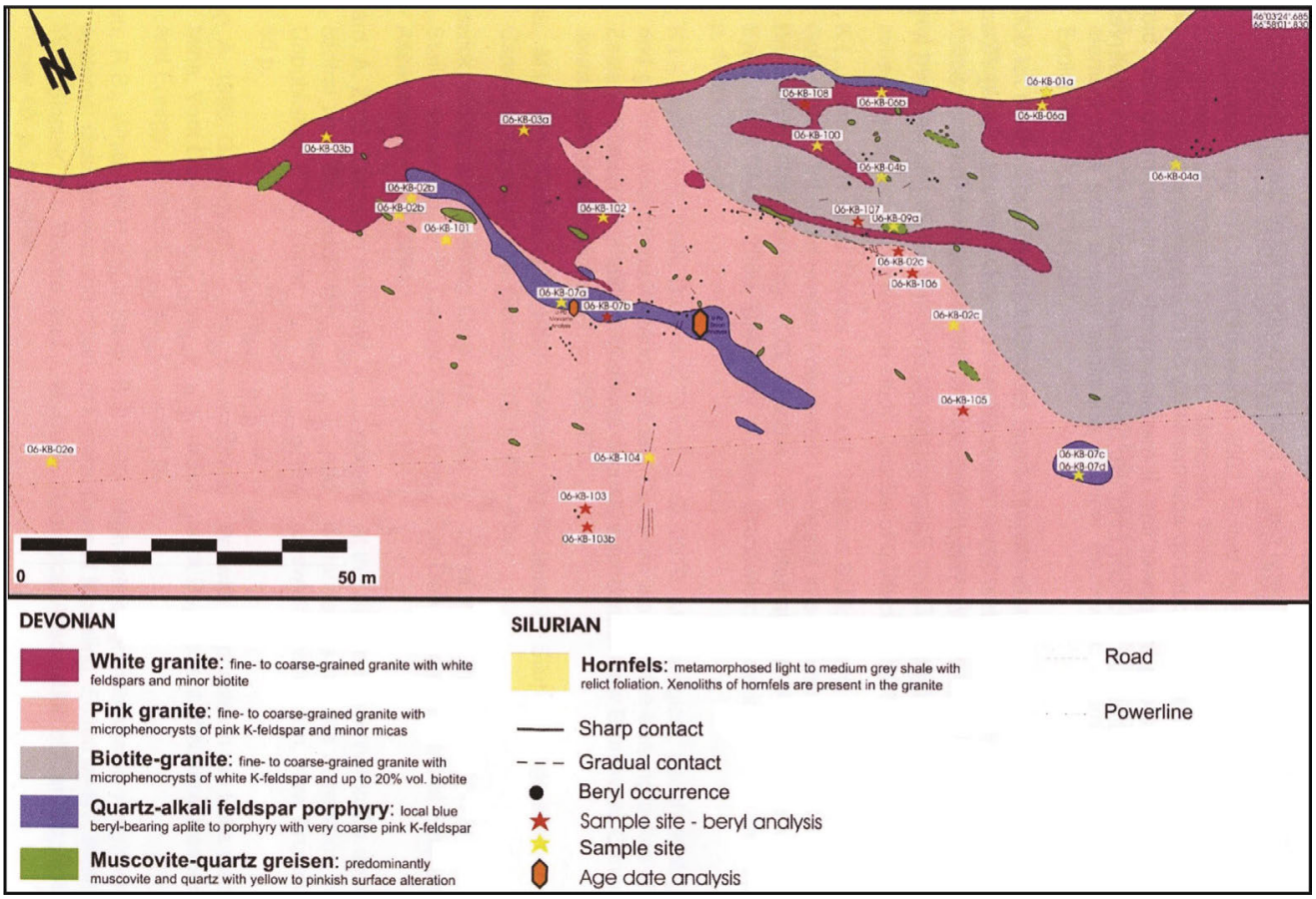

Figure 41 – Geology map of the trenched exposure at the Zealand Station prospect (Stop 1-11; after Beal et al., 2009).

End of the Day: *Backtrack to Hwy-104 and turn right (east) and proceed for 16.5 km. At T-junction, turn left onto Hwy-105 and proceed east for 18.2 km to Fredericton.*

Trip 2 – Tin Hill

Itinerary

Trip 2 will focus on a number of mineralisation styles in the Acadian Plutonic Belt, highlighted by a visit to the Tin Hill Sn-W deposit, which is associated with the large Burnthill Pluton. A number of field stops will highlight the regional geology of country rocks surrounding granite plutons and contact metamorphic effects.

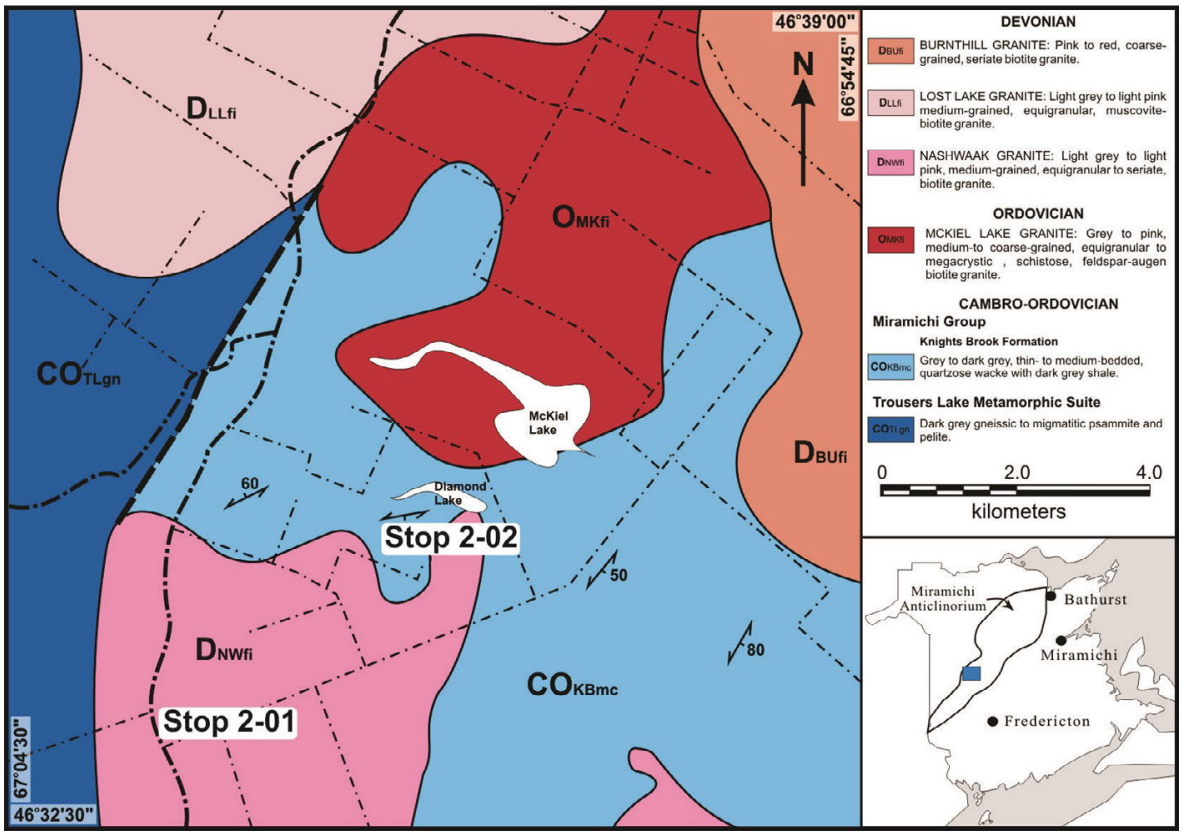

Figure 42 – Bedrock Geology map in the areas covered by Stops 2-01 and 2-02.

Stop 2-01: Western domain of Nashwaak Granite (46°33'07.06" N, 67°02'17.13" W)

Route: *From downtown Fredericton, head north on the Westmorland Street Bridge. Proceed through the lights at the Ring Road-Maple Street intersection and then again at the Ring Road – Brookside Drive intersection. Take Exit 620 on the right and head towards Stanley. Turn right onto Hwy-620, and continue on this road until reaching the Village of Stanley (42.1 km). Turn left onto Hwy-107 and proceed through the village for approximately 3.7 km. Turn left and head toward Florenceville – Bristol. Turn right onto a logging road at the Deersdale intersection (34.9 km) and head north for 600 m across the Miramichi River towards the Deersdale Mill. Vehicles are required to sign in at the guardhouse, and CB radios (channel 1) will be mandatory while in the Deersdale Woodlands. While proceeding through the property, vehicles are required to state their position at each mile marker and indicate their direction of travel. For safety purposes, field trip vehicles will yield to all oncoming traffic, and pull over towards*

the shoulder. Proceed north 5.5 km along the main Deersdale road; turn right (east) on road G and proceed 500 m up the hill to an exposed outcrop on the roadbed.

***Hazards:** This is a blind hill and prone to fast moving trucks. Please park well off to the side of the road and watch for traffic.*

The outcrop on the roadbed consists of a large raft of high-grade migmatite (Trousers Lake Metamorphic Suite) resting within the western domain of the Early Devonian Nashwaak Pluton (Fig. 42). The migmatite features leucosome melt comprising quartz and feldspar with a melanocratic residuum that is rich in biotite (Fig. 43). This outcrop is typical of the Trousers Lake Complex throughout the region, but these migmatites can include preserved paleosome that resemble metamorphosed quartzite and siltstone. This migmatite likely represents a large pendent within the Nashwaak Pluton, nevertheless fabrics are orientated roughly N – S, parallel to the inferred contact between the Trousers Lake Suite and Miramichi Group. An adjacent outcrop in the ditch on the north side of the road features greisen alteration similar to that found at Stop 1-03. The greisen consists of a zone of intense silicification accompanied by disseminated pyrite-arsenopyrite mineralisation.

Figure 43 – Exposed outcrop of migmatite (Trousers Lake Metamorphic Suite) pendant enclosed within the Nashwaak Granite (Stop 2-01).

Stop 2-02: Eastern domain of Nashwaak Granite (46°34'40.17" N, 66°59'43.85" W)

***Route:** Continue in an easterly direction for 2.7 km, turn left (north) on road G-65 and proceed 1.6 km around a dogleg bend in the road; turn right (north) on road H-10, proceed another 1.4 km to a T-junction; turn left (north) and proceed 400 m to Stop 2-02.*

Figure 44 – Porphyroblast development in the metamorphic aureole of the Nashwaak Pluton (Stop 2-02)

An outcrop on the roadside exposes the intrusive contact between the Nashwaak granite and quartzo-feldspathic meta-sedimentary rocks of the Miramichi Group. In this locality, the Nashwaak Granite comprises a medium-grained, light pink, locally garnetiferous biotite-muscovite leucogranite and most likely represents a late evolved phase within the Nashwaak Pluton. Where the granite intrudes meta-sedimentary rocks, a contact metamorphic aureole is well developed with meta-pelitic rocks closest to the contact dominated by cordierite porphyroblasts, which are now pseudomorphs with minor andalusite phases (Fig. 44).

Stop 2-03: Knight's Brook Formation (46°35'47.29" N, 66°57'09.96" W)

Route: *Return the 3.4 km to road G intersection and turn left (east) onto road G. Proceed 5.3 km to the intersection of road G and Q-69. Turn left on road Q-69 and proceed to the northwest; at 700 m make a sharp turn to the north-east; proceed 800 m to Stop 2-03.*

Rocks of the Cambrian to Early Ordovician Miramichi Group in the region consist of a deep-water, turbiditic sequence of interbedded quartzose sandstone and shale. In this locality, quartzose wackes and siltstone of the Knight's Brook Formation are unconformably overlain by volcaniclastic rocks of the Hayden Lake formation and thick- bedded lithic wacke and silty mudstone of the Push and Be Damned Formation. Regionally, the Miramichi Group has been metamorphosed to greenschist facies and forms the core of a large north-northeast-trending anti-form. The outcrop at this stop consists of bedded quartzose wacke and siltstone exhibiting a prominent S1 fabric (022/62° NW) and spotting of siltstone bands. The area has been affected by local metamorphic effects of the Ordo-

Figure 45 – Bedded quartzose wacke and siltstone exhibiting a prominent S1 fabric and spotting due to local metamorphic effects of the Ordovician McKiel Lake Granite and Devonian Nashwaak and Burnthill plutons (Stop 2-03).

vician McKiel Lake Granite and Devonian Granites of the Nashwaak and Burnthill Plutons (Fig. 45). Minor quartz veins and alteration occur at the east end of the outcrop, and are common throughout the region.

Stop 2-04: Hayden Lake Formation (46°34'20.27" N, 66°50'50.28" W)

Route: *Proceed 1.7 km to a T-junction with between road Q-69 and Q-X Turn left (northeast) and proceed 200 m to another intersection; make a hard right turn, then an immediate left and proceed northeast on road Q-50. Proceed 2.9 km around several turns; make a right turn at the intersection with road Q-59 and proceed southeast 5.7 km, stopping at the east gate. Proceed through the east gate and travel 400 m to a T-junction. Turn right and proceed southeast 2.3 km on Spider Brook road, turning right (southwest) on a small side road. Proceed 1.4 km to the southwest around a bend to the outcrop at Stop 2-04.*

Siltstones and wackes of the Cambrian to Ordovician Knights Brook Formation are unconformably overlain by more massive thick-bedded silty mudstone and lithic wacke of the Middle Ordovician Hayden Lake Formation. To the north, these siltstones are conformably underlain by pillowed basalt and rhyolite that also form part of the Hayden Lake Formation. An outcrop in the ditch consists of massive siltstone and rare tuffaceous ash beds (Fig. 46) that have undergone the effects contact metamorphism from the adjacent Burnthill Pluton, approximately 2 km to the north. These silty-mudstones host several small exogranitic quartz veins and greisen Sn-W-Mo occurrences. At the north end of the outcrop, occur greisen and quartz veins with minor wolframite that cut the altered siltstone.

Figure 46 – Middle Ordovician Hayden Lake Formation massive siltstone and lithic wacke with rare tuffaceous ash beds that have undergone the effects contact metamorphism from the adjacent Burnthill Pluton (Stop 2-04).

Figure 47 – Exo-contact mineralisation of the Two and a Half Mile Brook occurrence (Stop 2-05).

Stop 2-05: Two and a Half Mile Brook Occurrence (46°33'35.51" N, 66°51'06.04" W)

Route: *Switch to 4x4 drive. Return to Spider Brook road, turn right and proceed 3.4 km around a large bend and across Two and a Half Mile Brook. Turn right and proceed north 350 m, parking vehicles at a fork in the road Walk 350 m up the hill to the outcrop at Stop 2-05.*

Hazards: *Smaller side roads do not have shoulders and can plunge several meters into the rough brush. Use extreme caution when manoeuvring vehicles.*

Trenching and stripping of areas anomalous (soil) for Sn, W and Mo in the Two and a Half Mile Brook area exposed quartz veins containing arsenopyrite, pyrite, chalcopyrite, wolframite, cassiterite and stannite. An outcrop in a ditch on the north side of the road consists of siltstones of the Push and Be Damned Formation cut by quartz-vein hosted exogranitic mineralisation (Fig. 47). The mineralisation trends 093/24° N and is likely controlled by regional jointing (118/47° N and 110/67° N). Mineralisation and contact metamorphism are a result of the underlying Burnthill Pluton; apophyses of greisenized granite occur in the local area.

Stop 2-06: Burnthill Granite (46°36'49.26" N, 66°49'47.25" W)

Route: *Return to the Spider Brook road, turn left and proceed 5.7 km back across Two and a Half Mile Brook and around the large bend. Continue in a northerly direction and at the T-junction proceed north 3 km down into the valley, over Burnthill Brook and up the hill to Stop 2-06 on the right (east) side of the road.*

Figure 48 – Coarse-grained granite of the Burnthill Pluton (Stop 2-06).

Hazards: *The road into the Burnthill Brook valley is very steep. Please control your speed and keep a safe distance from other vehicles.*

The outcrop is located along the south side of the road offers exposure of the main intrusive phase of the middle Devonian Burnthill granite. The Burnthill granite at this location (Fig. 48) consists of a medium to coarse-grained, biotite granite. The outcrop has been extensively eroded by local run off; the eroded appearance of the granite is typical of the Burnthill pluton, which is easily degraded to fine sandy deposits across the region.

Stop 2-07: Tin Hill (46°35'27.72" N, 66°47'26.97" W)

Route: *Continue northeast 1.6 km and make a hard right onto a small side road. Proceed south 3.4 km to a T-junction; turn left (northeast) and proceed 860 m turning right (south) at another T-junction. Continue south around several bends and at the sharp bend in the road at 840 m continue straight on the rough inclined side road. Proceed 200 m up the small hill; turn left (east) and continue 150 m to Stop 2-07.*

Figure 49 – Endogranitic quartz veins and greisen hosting Sn-W-Mo mineralisation of the Tin Hill occurrence (Stop 2-07).

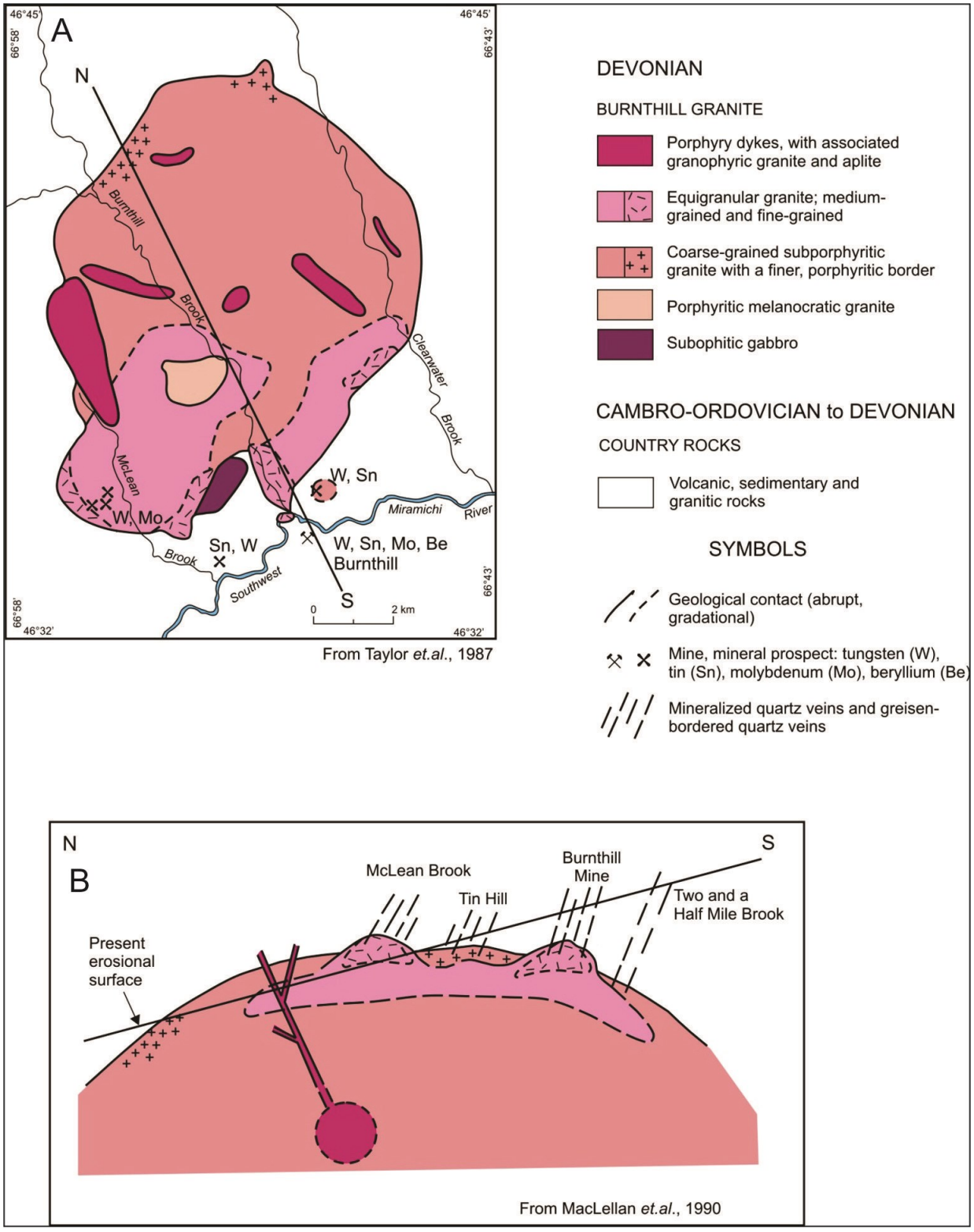

Figure 50 – A) Simplified geology of the Burnthill region highlighting the McLean Brook, Two and a Half Mile Brook, Tin Hill, and Burnthill deposits. B) Idealized section through the Burnthill Pluton (modified from Taylor et al., 1987; MacLellan et al., 1990).

Hazards: *The roads in this area are soft, with very steep road edges. Please exercise caution, control your speed and keep a safe distance from other vehicles.*

Stop 2-07A: Buttermilk Brook Cupola

The Tin Hill site has been largely cleared of vegetation and has been stripped to expose the Buttermilk Brook granite (Figs. 49 and 50). The Buttermilk Granite is largely composed of a coarse-grained porphyritic phase of the Burnthill Pluton, which forms small cupolas exposed at Tin Hill; the cupola can include equigranular to seriate phases at the north end. The granite has incurred shearing (139/82° W), potassic alteration (K-feldspar), and has been penetrated by large quartz veins with associated greisen and mineralisation (Figs. 49 and 51).

Figure 51 – Endogranitic quartz veins and greisen hosting Sn-W-Mo mineralisation of the Tin Hill occurrence (Stop 2-07).

Stop 2-07B: Tin Hill Sn-W-Mo Occurrence

Prospecting and soil anomalies on the Grid 7 property by the Miramichi Lumber and subsequent mapping and trenching uncovered a series of quartz veins and associated greisen cutting the granite (Figs. 50 and 51); later stripping of the site uncovered the full extent of mineralisation. There are over 10 large (up to 1 m) quartz veins trending between 123° and 167° veins intersect and coalesce in areas. Cassiterite and wolframite are the dominant form of mineralisation at tin hill, but also includes scheelite, molybdenite, magnetite, pyrite, galena, sphalerite, fluorite and

topaz. Mineralisation and quartz veins terminate at the edges of the cupola where it is in intrusive contact with metasedimentary rocks of the Knight's Brook Formation.

Stop 2-08: Knight's Brook Formation (hornfels) (46°36'01.76" N, 66°47'42.33" W)

Route: *Proceed 350 m back down the small hill; continue straight (north) 1 km to stop 2-08, a small outcrop on the left side of the road.*

Hazards: *The roads in this area are very soft and possibly muddy, vehicles must remain in 4x4 drive. Please exercise caution, control your speed and keep a safe distance from other vehicles.*

The outcrop on the left (northwest) side of the road consists of cordierite-spotted and hornfelsed metasedimentary rocks (siltstone and wacke) of the Knight's Brook Formation, Miramichi Group (Fig. 52). These rocks have been subjected to intense alteration from the Burnthill pluton, which is likely situated just beneath this sedimentary enclave and outcropping a few meters to the north.

Figure 52 – Cordierite-spotted and hornfelsed metasedimentary rocks (siltstone and wacke) of the Knight's Brook Formation, Miramichi Group (Stop 2-08).

Stop 2-09: Burnthill Granite (46°39'48.05" N, 66°46'12.62" W)

Route: *Proceed 2.8 km back to the main road; turn right (northeast) and continue 7.5 km east, down a steep meandering road, over Clearwater Brook and up the hill on the other side of the valley. Stop 2-09 is on the right side of the road.*

Figure 53 – Multiple phases of the Burnthill Pluton – medium to coarse-grained, seriate to equigranular textured biotite granite is cut by pods of the porphyritic quartz-feldspar microgranite (Stop 2-09).

Figure 54 – Rapakivi texture (large ovoids of K-feldspar mantled by a rim of plagioclase) developed in

Hazards: *The roads in this area are very soft and possibly muddy, vehicles must remain in 4x4 drive. Please exercise caution, control your speed and keep a safe distance from other vehicles.*

The long exposed outcrop on the right (east) side of the road offers continuous exposure of multiple phases of the Burnthill Pluton (Figs. 53 and 54). The granite at this location consists of a medium to coarse-grained, seriate to equigranular textured biotite granite; a pod of the porphyritic quartz-feldspar microgranite (biotite) phase of the Burnthill Pluton is exposed on the hillside. These late porphyry phases are related to the Buttermilk cupola and are distributed throughout the Burnthill pluton, although there is a tendency for them to be more abundant near the edges of the pluton.

Stop 2-10: McKiel Lake Orthogneiss (46°41'25.28" N, 66°57'41.83" W)

Route: *Backtrack 10 km in a southwest direction along the main road; turn right (north) on road GG. Proceed through the gate and continue for 14 km north to a T-junction with the Deersdale road. Turn left and proceed west 10.8 km, turning right on road U. Proceed 670 m in a northwest direction turning left again on road U-2. Stop 2-10 consists of an outcrop on the side of the road.*

Hazards: *Exercise caution when turning vehicles around on the main road.*

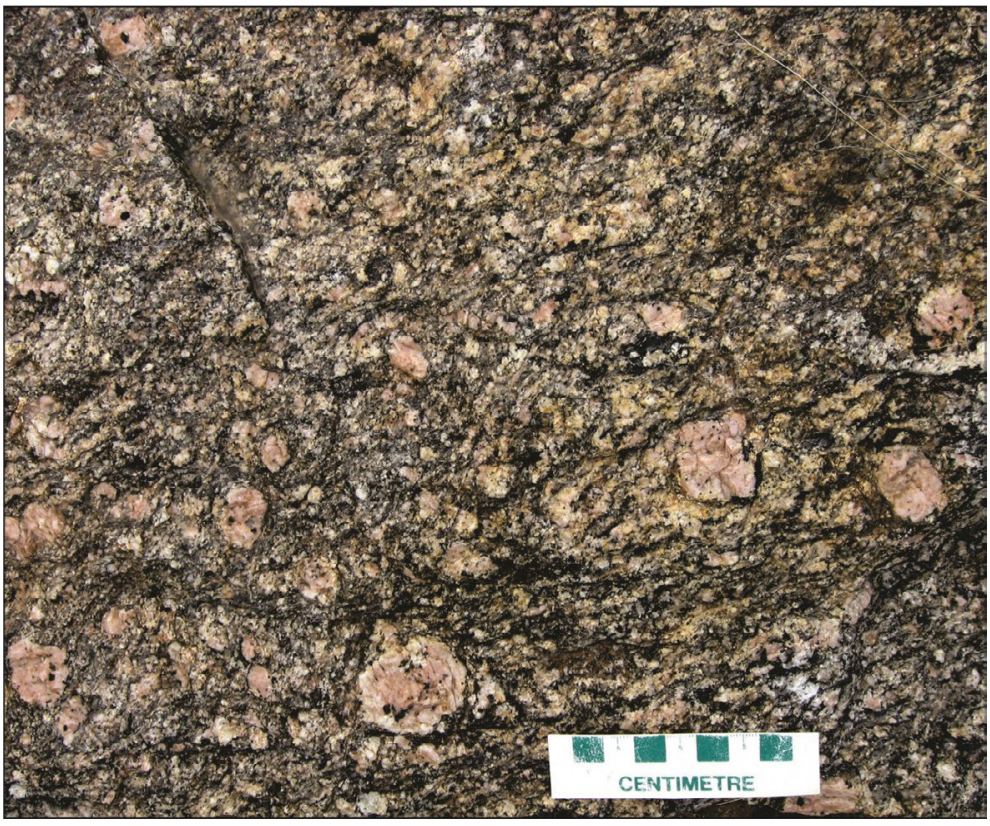

Figure 55 – Coarse-grained feldspar augen granite (orthogneiss) of the McKiel Lake Suite (Stop 2-10).

The outcrop consists of medium to coarse-grained feldspar-augen biotite granite of the McKiel Lake granite suite (Fig. 55). A number of quartz-feldspar-muscovite pegmatites are seen to cut through the migmatite and can contain garnet and beryl; these pegmatitic stocks can be sourced to the nearby Devonian Lost Lake Pluton.

Stop 2-11: Trousers Lake Migmatite (46°42'11.85" N, 67°02'46.71" W)

Route: *Backtrack to the main road; turn right and proceed south 3.5 km and turn right on road S (Miramichi Deadwater). Continue northwest 5.2 km to the outcrop on the left side of the road.*

The outcrop on the south side of the road consists of a large exposure of high-grade migmatite of the Trousers Lake Metamorphic Suite (Fig. 56), which dominates the western half of the Acadian Plutonic Belt; metasedimentary rocks of the Miramichi Group are not found in this region with the exception of preserved paleosome material resembling metamorphosed quartzite and siltstone.

Trousers Lake migmatites have been intruded by the Nashwaak, Juniper Barrens and Lost Lake Devonian plutons as well as a number of Ordovician granitoids, which exhibit a distinctly orthogneissic texture. The migmatite in this outcrop features leucosome melt comprising quartz and feldspar with a melanocratic residuum that is rich in biotite. A band of amphibolite likely represents a mafic dyke or sill; elsewhere in the belt, these bodies are Ordovician in age and are tholeiitic in composition. A number of quartz-feldspar-muscovite pegmatites are seen to cut through the migmatite and can contain rare tourmaline, scheelite and a vitreous green beryl; these pegmatitic stocks can be sourced to the nearby Devonian Lost Lake Pluton.

Figure 56 – Migmatite of the Trousers Lake Metamorphic Suite cut by Devonian pegmatite veins (Stop 2-11).

Stop 2-12: Juniper Barrens Granite (46°34'56.03" N, 67°07'57.22" W)

Route: *Backtrack 5.2 km to the main Deersdale road. Turn right (south) and proceed for 18.5 km; turn right (west) on road D and proceed 9.1 km northwest. Turn right on road D-40, proceed 600 m to an outcrop on the right side of the road.*

The outcrop on the right side of the road consists of fine to medium-grained biotite muscovite granite (Fig. 57) of the Juniper Barrens Pluton near its contact with the surrounding Trousers Lake Suite. The Devonian Juniper Barrens granite was emplaced along the western boundary of the Acadian Plutonic Belt and intrudes both the Ordovician migmatites of the Miramichi Terrane and the Devonian cover sequence to the west.

Figure 57 – Coarse-grained biotite granite of the Juniper Barrens Pluton (Stop 2-12).

End of the Day: *Backtrack 4.8 km to road D, turn right and proceed west for 3.7 km, across the bridge over the North Branch of the Little Southwest Miramichi River (Yield: One Lane). At the T-junction (airport), turn left (south) and proceed for 7.5 km through the Juniper gate, over the railroad tracks and into the town of Juniper. At the junction with Hwy-107, turn left and return to Fredericton via Hwy-107 and Hwy-620 (ca. 100 km).*

Trip 3 – Burnthill

Itinerary

Trip 3 will focus primarily on W-Sn-Mo mineralisation at the Burnthill Mine, investigating local stratigraphy and exposures of mineralisation on the now decommissioned mine site. The field trip will wrap up with a visit to the Todd Mountain Sn occurrence, associated with the Dungarvon granite to the east of Burnthill.

Stop 3-01: Hayden Lake Formation (46°30'50.93" N, 66°50'32.24" W)

Route: *From downtown Fredericton, head north on the Westmorland Street Bridge. Proceed through the lights at the Ring Road-Maple Street intersection and then again at the Ring Road – Brookside Drive intersection. Take Exit 620 on the right and head towards Stanley. Turn right onto Hwy-620, and continue on this road until reaching the Village of Stanley (42.1 km). Turn left onto Hwy-107 and proceed through the village for approximately 3.7 km. Turn left and head toward Florenceville – Bristol. Turn right at Napadogan (20.8 km) and head north on the Irving Lumber road to the gate at the 2.5 km mark. Proceed another 14.8 km along the meandering road in a generally northeasterly direction to a fork in the road; veer to the left (north) and proceed another 1.1 km north to a small outcrop on the road surface.*

Hazards: *This is a busy road for logging trucks. Please park well off to the side of the road and watch for traffic.*

Figure 58 – Small, roadbed outcrop of Hayden Lake Formation aphanitic rhyolite that

The small exposure in the roadbed is consists of an outcrop of aphanitic rhyolite that has been silicified and altered to sericite (Fig. 58). This is one of only a few rare outcrops of felsic volcanic rocks of the Hayden Lake Formation which tend to form semi-continuous beds and isolated pods along a horizon dominated by ferromanganiferous mudstone, chert and shale. The Hayden Lake Formation is dominated by pillowed mafic volcanic rocks in northern regions of the belt and is underlain by thin to medium-bedded shale and quartzose wacke of the Knight's Brook Formation (Miramichi Group); a discontinuous unit of calcareous siltstone intercalated with felsic tuff sits stratigraphically between the two units.

Stop 3-02: Knight's Brook Formation: W-Sn-Mo mineralisation (46°34'8.40" N, 66°49'5.50" W)

Route: *From Stop 1 proceed another 7.4 km along the main road to Stop 3-02. Please note that the road meanders considerably and has numerous branches and crossroads.*

Hazards: *Stop 3-02 is on a blind turn in the road, participants should exercise caution when exiting vehicles.*

The outcrop on the right (southeast) side of the road is part of a larger exposure of bedrock and loose rubble at the northwest end of the Burnthill Mine Property (Fig. 59). The original 1916 shaft is approximately 175 m to the southeast with an underground mining adit (150' level drift) extending close to the present location at a depth of 45 m (Fig. 60). The outcrop consists of cordierite-spotted meta-sedimentary rocks (siltstone and quartzose wacke) of the Knight's Brook Formation (Miramichi Group) cut by numerous wolframite-bearing quartz veins. An early bed-

Figure 59 – Exposure of bedrock and loose rubble at the northwest end of the Burnthill Mine Property comprising of cordierite-spotted siltstone and quartzose wacke of the Knight's Brook Formation, Miramichi Group, cut by numerous wolframite-bearing quartz veins (Stop 3-02).

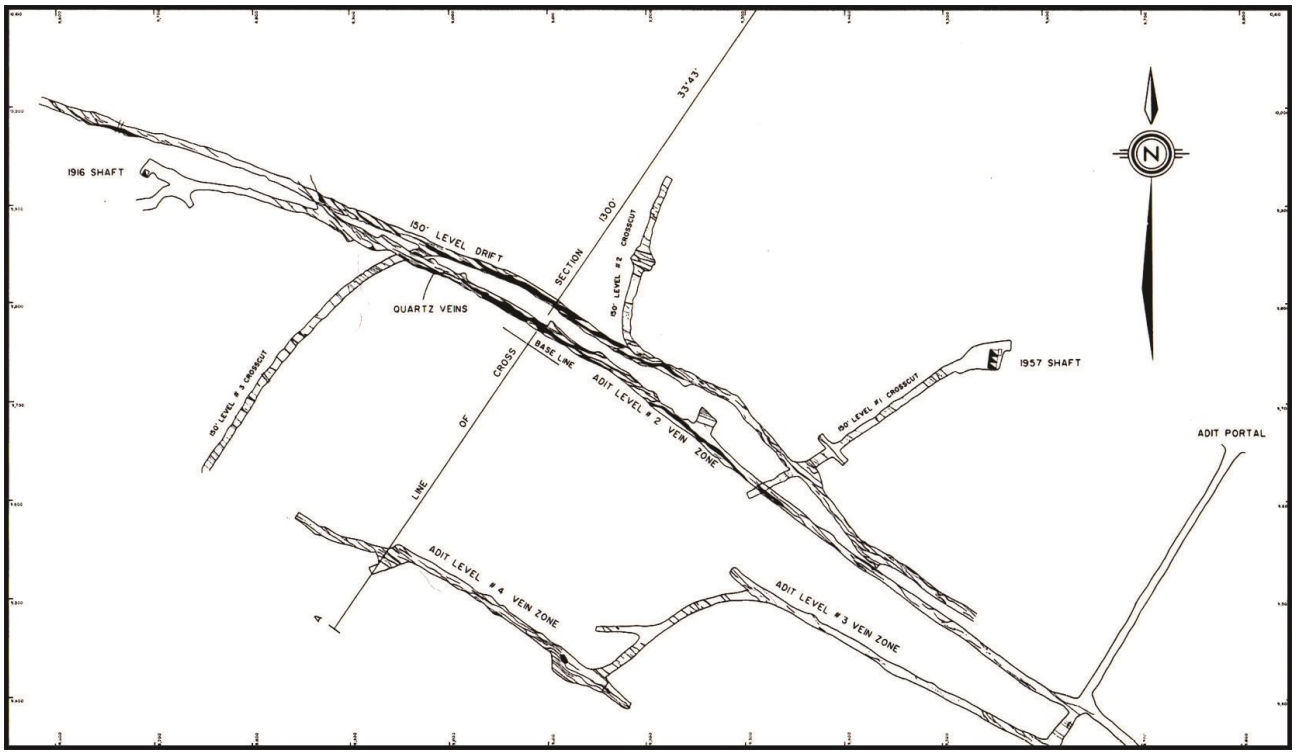

Figure 60 – Composite plan map of underground workings at the Burnthill Mine.

Figure 61 – Quartz veins and W-Sn-Mo mineralisation related to the nearby Burnthill Mine Property (Stop 3-02).

ding parallel foliation (S0/S1) strikes between 020° and 030° and has a dip of 61° NW. A steeply dipping (124/78° NE) joint set (fracture cleavage) features dilatant quartz veins and W-Sn-Mo mineralisation (Fig. 61).

Stop 3-03: Burnthill Mine site (46°34'10.75" N, 66°48'36.35" W)

Route: *Continue 400 m to the east from Stop 2-02 and park vehicles at the main gate for the Burnthill Mine. Participants will walk 400 m to the on the mine road to the Burnthill Mine site and present exploration office for Cadillac Ventures.*

Hazards: *While on the mine site, do not approach unstable rock faces and overhangs; hard hats and safety glasses must be worn at all times.*

Stop 3-03A: Adit portal

The adit's portal provides excellent exposure of exogranitic mineralisation and the nature of its relationship with the host metasedimentary rocks of the Knight's Brook Formation (Fig. 62). Endogranitic mineralisation is found at depth (approx. 300 m), where a cupola of the Burnthill granite pluton is cut by endogranitic quartz veins and greisen with notable molybdenite and cassiterite. Within the Burnthill Mine, W-Sn-Mo mineralisation is concentrated along four main quartz vein zones collectively occupying an area approximately 335 m long by 152 m wide and extending

Figure 62 – Exogranitic mineralisation developed in metasedimentary rocks of the Knight's Brook Formation at the adit portal of the Burnthill Mine (Stop 3-03A).

Figure 63 – Molybdenite mineralisation and bladed wolframite associated with quartz veins and greisen at the Burnthill Mine.

to a depth of 285 m (Potter, 1969; Puritch et al., 2005). At surface, mineralisation consists of steeply dipping dilatant quartz veins found in en echelon sets and orientated parallel to a regional joint set (120/80° NE). Wolframite is the main ore mineral found in the quartz veins and consists of bladed crystals radiating inward from quartz vein boundaries; these veins also contain scheelite, cassiterite, beryl, topaz, fluorite, native bismuth, molybdenite, pyrite, and arsenopyrite (Fig. 63).

Stop 3-03B: Exogranitic W-Sn-Mo mineralisation

Carefully climb the hill above the adit portal by using the drilling access road, which meanders, up the hillside. Just above the adit portal and near the fence lies an outcrop of cordierite-spotted meta-sedimentary rocks of the Knight's Brook Formation (Miramichi Group) cut by W-bearing quartz veins of the Burnthill ore zone. On the exposure, the late quartz veins are seen to cut an early fabric (S0/S1 030/74° NE) along a prominent joint set trending

122/76° NE. Bladed wolframite crystals and molybdenite (rare?) can be found in the quartz veins and concentrated along their margins in contact with the metasedimentary host rock.

Stop 3-03C: Decommissioned headframe

Carefully proceed to the east, past the safety fence and up the hill to old mill remnants and a decommissioned mine shaft. This represents one of several shafts installed on the mine site to hoist ore to surface for production. The area has many remnant pieces of Burnthill ore, ideal for collection.

Stop 3-03D: Drill core

Carefully proceed down the hill along the path and drilling access road to the Cadillac Ventures exploration office. A recent drill hole collared on the Burnthill Mine Site will be on display at the drill core racks. The drill hole is seen to intersect exogranitic quartz veins in meta-sedimentary rocks of the Knight's Brook Formation (Miramichi Group) as well as the cupola of the Burnthill granite pluton.

Stop 3-04: Todd Mountain Sn Occurrence (46°32'30.85" N, 66°42'04.98" W)

Route: *Return to vehicles at the Main Gate and backtrack 8.9 km to the first fork in the road (near Stop 2-01). Continue in a south-easterly direction for 23 km until you reach a significant crossroads. Turn left and proceed north on this very curly road, veering left at 3.9 km and veering right at 8.4 km. At 15.7 km make a hard left turn and proceed west up the hill for 700 m. Park and exit vehicles; follow trail through the woods for 400 m to the Todd Mountain occurrence.*

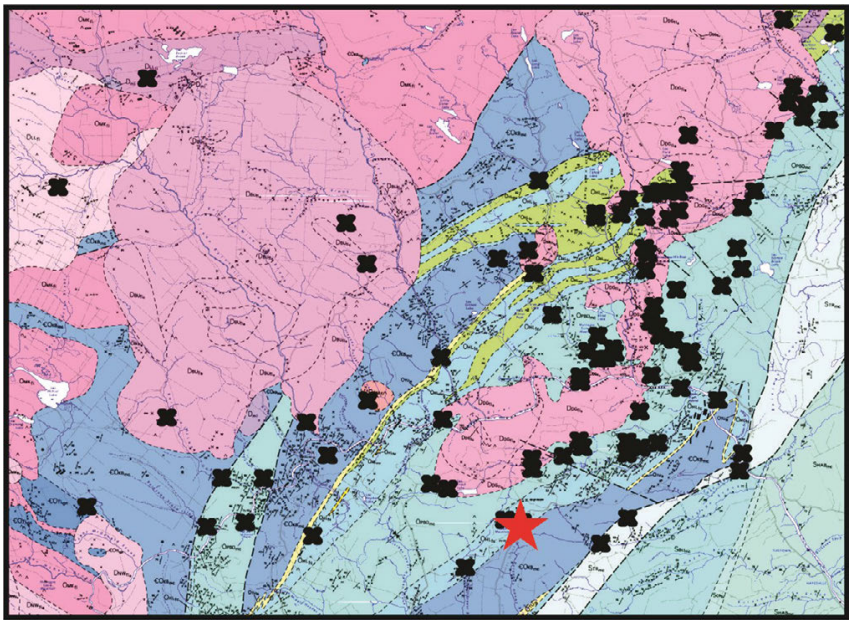

Figure 64 – Bedrock geology of the Burnthill and Dungarvon areas showing the location of the Todd Mountain occurrence in relation to mineral occurrences throughout the region.

Figure 65 – Locally garnetiferous metasedimentary rocks (siltstone and quartzose wacke) of the Knight's Brook Formation, Miramichi Group, at the Todd Mountain Sn Occurrence (Stop 3-04).

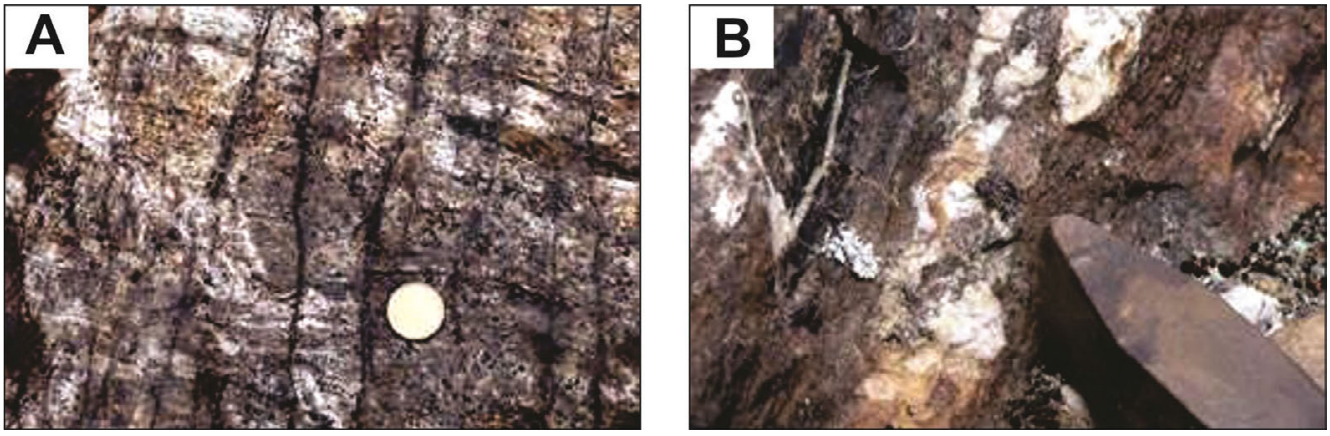

Figure 66 – Contrasting mineralisation styles at the Todd Mountain deposit. A) Arsenopyrite along widely spaced fracture cleavage. B) Cassiterite-bearing greisen.

Hazards: *This is a rough road, and in places may have incurred erosion and washouts from spring runoff. Drive carefully and follow the path of the lead vehicle.*

The Todd Mountain site (Fig. 64) has been largely cleared of vegetation and in areas is stripped and trenched to expose local bedrock. Mineralisation is hosted within locally garnetiferous meta-sedimentary rocks (siltstone and quartzose wacke) of the Knight's Brook Formation (Miramichi Group), and sits above the Dungarvon Granite (Figs. 65 and 66). Examination of outcrops on the site will reveal two contrasting styles of mineralisation. Steeply dipping cassiterite-bearing quartz veins and associated chlorite-muscovite greisen trends 025° (NE-SW) sub-parallel to a penetrative S0/S1 fabric trending 045/47° SE. A second hydrothermal event resulted in sericite alteration and disseminated arsenopyrite mineralisation along a widely spaced fracture cleavage that is orthogonal to S0/S1 fabrics and trends 112/88° NE. In 1983, Billiton drilled a fence of nine holes at the Todd Mountain occurrence and had favourable drill intersections of 0.67 % Sn over 1.5 m and 0.18 % Sn over 15 m (Lutes, pers. Comm., 1988).

End of the Day: *Backtrack to the crossroads at 23 km and turn left (east) proceeding 5.1 km to the Gordon Vale Gate. Exit the Irving Woodlands, continue east; make a hard right at 9 km, proceed south for another 2 km. At the T-junction, turn left and proceed east for 7.6 km. At the junction with Hwy-8, turn right (south) proceed ca. 65 km to Fredericton.*

References

Allard, S., and Pronk, A.G., 2003. Glacial history of southwestern New Brunswick: challenges to drift prospecting; *in* Current Research 2002, (ed.) B.M.W. Carroll. New Brunswick Department of Natural Resources; Minerals, Policy and Planning Division, Mineral Resource Report 2003-4, p. 1-11.

Austria, V., and Chork, C.Y., 1976. A study of the application of regression analysis for trace element data from stream sediments in New Brunswick; Journal of Geochemical Exploration, v. 6, p. 211-232.

Beal, K.L., 2007. The Zealand Station beryl (aquamarine) deposit, west-central NB: mineralogic, geochronologic, and petrogenetic constraints; unpublished B.Sc. Honours thesis, University of New Brunswick, Fredericton, New Brunswick, 153 p.

Beal, K.L., and Lentz, D.R., 2010. Aquamarine beryl from Zealand Station, Canada: a mineralogical and stable isotope study; Journal of Geosciences, v. 55, p. 57-67.

Beal, K.L., Lentz, D.R., Hall, D.C., and Dunning, G., 2010. Mineralogical, geochronological and geochemical characterization of Early Devonian aquamarine-bearing dykes of the Zealand Station beryl and molybdenite deposit, west central New Brunswick; Canadian Journal of Earth Sciences, v. 47, p. 859-874.

Beal, K.L., Lentz, D.R., and Thorne, K.G., 2009. Zealand Station beryl prospect; *in* Field Trip Guide Book: Intrusion-related Polymetallic Deposits in southwestern and Central New Brunswick, (comp.) K.G. Thorne. 24th International Applied Geochemistry Symposium (IAGS) 2009, University of New Brunswick, Fredericton, New Brunswick, p. 1-9.

Bevier, M.L., and Whalen, J.B., 1990. Tectonic significance of Silurian magmatism in the Canadian Appalachians; Geology, v. 18, p. 411-414.

Dostal, J., Wilson, R.A., and Keppie, J.D., 1989. Geochemistry of Siluro-Devonian Tobique volcanic belt in northern and central New Brunswick (Canada): Tectonic implications; Canadian Journal of Earth Sciences, v. 26, p. 1282-1296.

Brewster, N.E., 1981. Sum of work program 1980/1981 on the Burnt Hill project for Canadian International Paper Limited; A.C.A. Howe International Limited, Report No. 432.

Brunswick Mining and Smelting Corp. Ltd., 1982. Report of Work Project 440(175) Zealand Station (prepared by P. Cooper); New Brunswick Department of Natural Resources, Assessment File 472894.

Burns, J.G., Willoughby, N., P & E Mining Consultants, 2008. NI 43-101 Technical report for the Burnt Hill property, Stanley Parish, York County, Central New Brunswick, Canada.

Bustard, A., 2013. Tungsten mineralisation processes at the Sisson Brook W-Mo-Cu deposit, central New Brunswick: the role of formation of titaniferous phases at reaction front; unpublished B.Sc. Thesis, University of New Brunswick, Fredericton, New Brunswick, 65 p.

Caron, A., 1996. Geology of the Pokiok Batholith aureole, with emphasis on the Lake George Mine, York County, New Brunswick; New Brunswick Department of Natural Resources and Energy, Geoscience Report 94-2, 91 p.

Carten, R.B., White, W.H., and Stein, S.J., 1993. High-grade, granite-related molybdenum systems: classification and origin; *in* Mineral Deposit Modeling, (ed.) RV. Kirkham, W.D. Sinclair, R.I. Thorpe and J.M. Duke. Geological Association of Canada Special Paper 40, p. 521-554.

Frost, B.R., Barnes, C.G., Collins, W.J., Arculus, R.J., Ellis, D.J., and Frost, C.D., 2001. A geochemical classification for granitic rocks; Journal of Petrology, v. 42, p. 2033-2048.

Fyffe, L.R., 1976. Correlation of geology in the southwestern and northern parts of the Miramichi Zone; *in* 13th Annual Report of the Department of Natural Resources of the Province of New Brunswick for the Year Ended 31st March 1976; The Government of the Province of New Brunswick, Fredericton, p. 137-141.

Fyffe, L.R., 1982a. Taconian and Acadian structural trends in central and northern New Brunswick; *in* Major Structural Zones and Faults of the Northern Appalachians, (ed.) P. St-Julien and J. Beland. Geological Association of Canada, Special Paper 24, p. 117-130.

Fyffe, L.R., 1982b. Geology of Woodstock (sheet 21J). New Brunswick Department of Natural Resources; Mineral Resources Division, Map NR-4 (with marginal notes).

Fyffe, L.R., and MacLellan, H.E., 1988. Lithogeochemistry (including gold) of altered and mineralised samples from the Burnthill Brook area (NTS 21J/10) of central New Brunswick; New Brunswick Department of Natural Resources and Energy, Minerals and Energy Division, Geoscience Report 88-1, 92 p.

Fyffe, L.R., and Thorne, K.G., (comp.) 2010. Polymetallic deposits of Sisson Brook and Mount Pleasant, New Brunswick, Canada; New Brunswick Department of Natural Resources; Lands, Minerals and Petroleum Division, Field Guide No. 3, 68 p.

Fyffe, L.R., Barr, S.M., and Bevier, M.L., 1988. Origin and U-Pb geochronology of amphibolite-facies metamorphic rocks, Miramichi Highlands, New Brunswick. Canadian Journal of Earth Sciences, v. 25, p. 1674-1686.

Fyffe, L.R., Forbes, W.H., and Riva, J., 1983. Graptolites from the Benton area of west- central New Brunswick and their regional significance; Maritime Sediments and Atlantic Geology, v. 19, p. 117-125.

Fyffe, L.R., McCutcheon, S.R., and Wilson, R.A., 1997. Miramichi – Tetagouche stratigraphic relationships, Bathurst Mining Camp, northern New Brunswick; *in* Current Research 1996, (ed.) B.M.W. Carroll. New Brunswick Department of Natural Resources and Energy; Minerals and Energy Division, Mineral Resource Report 97-4, p. 37-51.

Fyffe, L.R., Pajari, G.E., and Cherry, M.E., 1981. The Acadian plutonic rocks of New Brunswick; Maritime Sediments and Atlantic Geology, v. 17, p. 23-36.

Fyffe, L.R., Seaman, A., Thorne, K.G., and Martin, D., 2009. Bedrock and surficial geology of the Sisson Brook W-Mo (-Cu) deposit; *in* Field Trip Guide Book: Intrusion-related Polymetallic Deposits in southwestern and Central New Brunswick, (comp.) K.G. Thorne. 24th International Applied Geochemistry Symposium (IAGS) 2009, University of New Brunswick, Fredericton, New Brunswick, p. 10-46.

Fyffe, L.R., Seaman, A., Thorne, K., and Martin, D.A., 2010. Part 1: Sisson Brook W–Mo–Cu deposit; *in* Polymetallic deposits of Sisson Brook and Mount Pleasant, New Brunswick, Canada, (comp.) L.R. Fyffe and K.G. Thorne; New Brunswick Department of Natural Resources, Field Guide No. 3, p. 7-33.

Fyffe, L.R., Thorne, K.G., Dung, G.R., and Martin, D.A., 2008. U-Pb geochronology of the Sisson Brook Granite Porphyry, York County, west-central New Brunswick; *in* Geological Investigations in New Brunswick for 2007, (ed.) G.L. Martin. New Brunswick Department of Natural Resources; Minerals, Policy and Planning Division, Mineral Resource Report 2008-1, p. 35-54.

Geodex Minerals Ltd., 2008. Geodex resource model increases Sisson Brook tungsten-molybdenum-copper deposit to 243.9 million tonnes 'measured and indicated' and 154.4 million tonnes 'inferred'; http://ww.sortweb.com/cwsimages/Miscfiles/6244_June-5-08-News-Release.pdf Accessed June 2008.

Geodex Minerals Ltd., 2009. Geodex updates Zone II resource model at Sisson Brook, New Brunswick and adds new resources from the adjacent 'Ellipse Zone'; http://www.sortweb.com/cwsimages/ Miscfiles/6761_NRM& IResourceModel27January09.pdt. Accessed April 2009.

lrrinki, R.R., 1980. Geology of Kennedy Lakes-Little Dungarvon and South Renous rivers region (map areas M-13, M-14, M-15 and Part of M-16); New Brunswick Department of Natural Resources, Mineral Resources Branch, Map Report 80-2, 39 p.

Lang, J.R., 2010. Geological due diligence of the Sisson Brook deposit, New Brunswick, Canada. Part A: hydrothermal characteristics, influence on mineral processing and geotechnical evaluation, and logistical considerations; Report to Northcliff Exploration Limited, 27 p.

Lajtai, E.Z., and Stringer, P., 1981. Joints, tensile strength and prefer fracture orientation in sandstones, New Brunswick and Prince Edward Island, Canada; Maritime Sediments and Atlantic Geology, v. 17, p. 70-87.

Lamothe, M., 1992. Pleistocene stratigraphy and till geochemistry of the Miramichi zone, New Brunswick; Geological Survey of Canada, Bulletin 433, 58 p.

Latam Explorations Ltd., 1962. Zealand Station Beryllium prospect; New Brunswick Department of Natural Resources, Assessment File 470218.

Lutes, G.G., 1979. Geology of Fosterville-North and Eel lakes, map-area G-23, and Canterbury-Skiff Lake, map-area H-23; New Brunswick Department of Natural Resources, Mineral Resources Branch, Map Report 79-3, 22 p.

Lutes, G.G., 1981. Geology of Deersdale-Head of Nashwaak River, map area J-17, and upper parts of Nashwaak River-McBean and Sisters brooks, map area J-18; New Brunswick Department of Natural Resources; Mineral Resources, Map Report 81-4, 26 p.

Lyon, S.B., 1988. Mineralogy and paragenesis of the Burnt Hill tungsten deposit, New Brunswick; unpublished B.Sc. thesis, Carleton University, Ottawa, Ontario, Canada.

MacLellan, H.E., Taylor, R.P., and Gardiner, W.W., 1990. Geology and geochemistry of Middle Devonian Burnthill granites and related tin-tungsten deposits, York and Northumberland counties, New Brunswick; New Brunswick Department of Natural Resources and Energy; Mineral Resources Branch, Mineral Resource Report 4, 95 p.

Mann, R., 1980. Report on diamond drilling at Sisson Brook; unpublished company report, Texasgulf Minerals Exploration Office, Fredericton, New Brunswick, 32 p.

Mann, R., 1981a. Report on diamond drilling at Sisson Brook; unpublished company report, Kidd Creek Mines Ltd., Fredericton, New Brunswick, 36 p.

Mann, R., 1981b. Assessment work report on Sisson Brook Claim Group; Texasgulf Inc. New Brunswick Department of Natural Resources; Mineral Resources Branch, Assessment Report 472669, 17 p.

Mann, R., 1982. Report on diamond drilling at Sisson Brook; unpublished company report, Kidd Creek Mines Ltd., Fredericton, New Brunswick, 26 p.

Martin, D.A., 2006. Report of geological compilation, line-cutting, soil sampling, geological mapping and prospecting, magnetic and induced polarization surveys, and drilling, 2005, Sisson Brook Claim Group, York County, New Brunswick; Geodex Minerals for Champlain Resources Inc., License No. 15088. New Brunswick Department of Natural Resources; Minerals, Policy and Planning Division, Assessment Report 476311, 17 p.

McClenaghan, M.B., Parkhill, M.A., Averill, S.A., and Kjarsgaard, l.M., 2013a. Indicator mineral signatures of the Sisson W-Mo deposit, New Brunswick: Part 1 bedrock samples; Geological Survey of Canada, Open File 7431.

McClenaghan, M.B., Parkhill, M.A., Averill, S.A., Pronk, A.G., Seaman, A.A., Boldon, R., McCurdy, M.W., and Rice, J.M., 2013b. Indicator mineral abundance data for bedrock, till, and stream sediment samples from the Sisson W-Mo deposit, New Brunswick; Geological Survey of Canada, Open File 7387, 18 p.

McClenaghan, M.B., Parkhill, M.A., Seaman, A.A., Pronk, A.G., Pyne, M., and Rice, J.M., 2013c. Indicator mineral signatures of the Sisson W-Mo deposit, New Brunswick: Part 2 till; Geological Survey of Canada, Open File 7467.

McClenaghan, M.B., Parkhill, M.A., Seaman, A.A., Pronk, A.G., Pyne, M., Rice, J.M., and Hashmi, S., 2013d. Till geochemical signatures of the Sisson W-Mo deposit, New Brunswick; Geological Survey of Canada, Open File 7430.

McClenaghan, M.B., Seaman, A.A., Parkhill, M.A., and Pronk, A.G., 2014. Till geochemical signatures associated with the Sisson W-Mo deposit, New Brunswick, Canada; Atlantic Geology, v. 50 p. 116-137.

Moore, R.L., 1979. Geochemical report on Sisson Brook claims, New Brunswick (NTS 21J/16E); New Brunswick Department of Natural Resources; Mineral Resources Branch, Assessment Report 472393, 22 p.

Nast, H.J., 1985. The geology and petrochemistry of the Sisson Brook W-Cu-Mo deposit, New Brunswick; unpublished M.Sc. thesis, McGill University, Montreal, Quebec, 196 p.

Nast, H.J., and Williams-Jones, A.E., 1991. The role of water-rock interaction and fluid evolution in forming the porphyry-related Sisson Brook W-Cu-Mo deposit, New Brunswick; Economic Geology, v. 86, p. 302-317.

Neuman, R.B., 1984. Geology and paleobiology of islands in the Iapetus Ocean: review and implications; Geological Society of America Bulletin, v. 95, p. 1188-1201.

Ozturk, H., 2007. Technical report on the Sisson Brook project, New Brunswick, Canada; unpublished report, Wardrop Engineering, 32 p.

Pearce, J.A., Harris, N.B.W., and Tindle, A.G., 1984. Trace element discrimination diagrams for the tectonic interpretation of granitic rocks; Journal of Petrology, v. 25, p. 956-984.

Poole, W.H., 1963. Geology, Hayesville, New Brunswick; Geological Survey of Canada, Map 6-1963 (with marginal notes).

Poole, W.H., and Neuman, R.B., 2003. Arenig volcanic and sedimentary strata, central New Brunswick and eastern Maine. Atlantic Geology, v. 38, p. 109-134.

Potter, R.R., 1969. The geology of the Burnt Hill area and ore controls of the Burnt Hill tungsten deposit; unpublished Ph.D. thesis, Carleton University, Ottawa, Ontario, 199 p.

Puritch, E., Kuehnbaum, R.M., and Ewert, W.D., 2005. Geological report and preliminary resource estimate on the Burnt Hill Tungsten Deposit, Claim Group #3785, Stanley Parish, York County, New Brunswick, Canada; for Noront Resources Ltd., ACA Howe Report No. 879, 88 p.

Rabinovich, M., 1969. Region de Napadogan, Campagne d'hiver 1969-sondages; New Brunswick Department of Natural Resources, Assessment Report 470269, 6 p.

Rampton, V.N., Gauthier, R.C., Thibault, J., and Seaman, A.A., 1984. Quaternary geology of New Brunswick; Geological Survey of Canada, Memoir 416, 77 p.

Ruitenberg, A.A., and Fyfe, L.R., 1982. Mineral deposits associated with granitoid intrusions and related subvolcanic stocks in New Brunswick and their relationship to Appalachian tectonic evolution; Canadian Institute of Mining and Metallurgy Bulletin, v. 75, p. 83-97.

Rogers, N., McClenaghan, M.B., Plouffe, A., Kellett, D.A., Chapman, J., Azadbakht, Z., Tweedale, F., Ruberti, G., and Anderson, B., 2014. TGI 4 – Intrusion Related Mineralisation Project: New Vectors to Buried Porphyry-Style Mineralisation; *in* Abstracts 2014: Exploration, Mining and Petroleum New Brunswick, (ed.) E.A. Keith; New Brunswick Department of Energy and Mines, Geoscience Report 2014–5, p. 31.

Rogers, N., Kellett, D.A., McNicoll, V.J., van Staal, C.R., Kerr, A., and Ruberti, G., 2015. Tectonostratigraphic controls on the Connaigre Peninsula of south-central Newfoundland and their implications for intrusion-related mineral resources; *in* TGI 4 – Intrusion Related Mineralisation Project: New Vectors to Buried Porphyry-Style Mineralisation, (ed.) N. Rogers; Geological Survey of Canada, Open File 7843, p. 59-78.

Sabina, A.P., 1992. Rocks and minerals for the collector: Estrie and Gaspesie, Quebec: and parts of New Brunswick; Geological Survey of Canada Miscellaneous Report 46, 156 p.

Samuel Engineering, 2013. Canadian National Instrument 43-101 Technical Report on the Sisson Project, New Brunswick Canada; Prepared for Northcliff Resources, 302 p.

Seal II, R.R., Clark, A.H., and Morrissy, C.J., 1987. Stockwork tungsten (scheelite) - molybdenum mineralisation, Lake George, southwestern New Brunswick; Economic Geology, v. 82, p. 1259-1282.

Seal II, R.R., Clark, A.H., and Morrissy, C.J., 1988. Lake George southwestern New Brunswick: a Silurian, multi-stage, polymetallic (Sb-W-Mo-Au-base metal) hydrothermal centre; *in* Recent Advances in the Geology of Granite-Related Mineral Deposits, (ed.) R.P. Taylor and D.F. Strong. Canadian Institute of Mining and Metallurgy Conference on Granite-Related Mineral Deposits Special Volume 39, p. 252-264.

Seaman, A.A., 2002. Till geochemistry of the central and eastern parts of the Coldstream (NTS 21J/06) map area, York and Carleton counties, New Brunswick; New Brunswick Department of Natural Resources and Energy; Minerals, Policy and Planning Division, Open File 2002-5, 80 p.

Seaman, A.A., 2003. Follow-up till geochemistry, Coldstream (NTS 21J/06) map area and part of the adjacent Napadogan (NTS 21J/07) map area, York and Carleton counties, New Brunswick; New Brunswick Department of Natural Resources and Energy; Minerals, Policy and Planning Division, Open File 2003- 11, 103 p.

Seaman, A.A., 2004. Late Pleistocene history of New Brunswick, Canada; *in* Quaternary Glaciations-Extent and Chronology, Part II: North America, (ed.) J. Ehlers and P.L. Gibbard. Developments in Quaternary Science, 2b, Elsevier, Amsterdam, p. 151-167.

Seaman, A.A., 2006. A new interpretation of the late glacial history of central New Brunswick: the Gaspereau Ice Centre as a Younger Dryas ice cap; *in* Geological Investigations in New Brunswick for 2005, (ed.) G.L. Martin. New Brunswick Department of Natural Resources; Minerals, Policy and Planning Division, Mineral Resource Report 2006-3, p. 1-36.

Seaman, A.A., 2009. The Appalachian Glacier Complex and the Middle to Late Pleistocene history of west-central New Brunswick, Canada; *in* Geological Investigations in New Brunswick for 2008, (ed.) G.L. Martin. New Brunswick Department of Natural Resources; Minerals, Policy and Planning Division, Mineral Resource Report 2009-2, p. 66-140.

Seaman, A.A., 2013. Buried sand and gravel deposits in central and southern New Brunswick, Canada: implications for the glacial history of the Maritimes; New Brunswick Department of Energy and Mines; Geological Surveys Branch, Mineral Resource Report 2013-1, 52 p.

Seaman, A.A., and McCoy, S.M., 2008. Multiple Wisconsinan tills in the Sisson Brook exploration trench of Geodex Minerals Ltd., York County, west-central New Brunswick; *in* Geological Investigations in New Bruns-

wick for 2007, (ed.) G.L. Martin. New Brunswick Department of Natural Resources; Minerals, Policy and Planning Division, Mineral Resource Report 2008-1, p. 1-34.

Seaman, A.A., Stea, R.R., and Allard, S., 2011. The Appalachian Glacier Complex in the Canadian Maritime Provinces during the Illinoian and Wisconsinan; Proceedings, GeoHydro 2011, Quebec, Quebec, doc-2097, 8 p.

Shediac Bay Resources Inc., 1985. Report on 1985 exploration program, Zealand Station property, NB (prepared by P.A. Hartwick. and R.W. Woolham). New Brunswick Department of Natural Resources and Energy, Assessment File 473228.

Shediac Bay Resources Inc., 1986. Report on Zealand Station property, NB (prepared by T.L. Warner); New Brunswick Department of Natural Resources, Assessment File 473251.

Shediac Bay Resources Inc., 1987. Progress report beryllium, Zealand Station, NB (prepared by M.J. Chrzanowski and C.G. Elliot); New Brunswick Department of Natural Resources, Assessment File 473350.

Smith, F.J., 1964. Keswick Claims prospecting report; New Brunswick Department of Natural Resources, Assessment File 470219.

Smith, E.A., and Fyffe, L.R., 2006. Bedrock geology of central New Brunswick (NTS 21J); New Brunswick Department of Natural Resources; Minerals, Policy and Planning Division, Plate NR-4, 2nd edition.

Snow, R.J., and Coker, W.B., 1987. Overburden geochemistry related to W-Cu-Mo mineralisation at Sisson Brook, New Brunswick, Canada: an example of short- and long-distance glacial dispersal; Journal of Geochemical Exploration, v. 28, p. 353-368.

Stea, R.R., Piper, D.J.W., Fader, G.B.J., and Boyd, R., 1998. Wisconsinan glacial and sea-level history of Maritime Canada and the adjacent continental shelf: a correlation of land and sea events; Geological Society of America Bulletin, v. 110, p. 821-845.

Stea, R.R., Seaman, A.A., Pronk, T., Parkhill, M.A., Allard, S., and Utting, D., 2011. The Appalachian Glacier Complex in Maritime Canada; *in* Quaternary Glaciations – Extent and Chronology – A closer look, (ed.) J. Ehlers, P.L. Gibbard and P.O. Hughes. Developments in Quaternary Science 15. Elsevier, Amsterdam, Chapter 48, p. 631-659.

Strong, D.F., 1981. Ore deposit models – 5. A model for granophile mineral deposits. Geoscience Canada, v. 8, p. 155-161.

Taylor, R.P., Lux, D.R., MacLellan, H.E., and Hubacher, F., 1987. Age and genesis of granite-related W-Sn-Mo mineral deposits, Burnthill, New Brunswick, Canada; Economic Geology, v. 82, p. 2187-2198.

Tweedale, F., Hanley, J.J., Kontak, D.J., and Rogers, N., 2014. Petrographic observations and evaporate mound analysis of quartz-hosted fluid inclusions: Applications to assess metal fertility in granites; Abstracts with Programs, Volume 37, Geological Association of Canada – Mineralogical Association of Canada Joint Annual Meeting; Fredericton, NB, p. 275-276.

Tweedale, F., Hanley, J.J., Kontak, D.J., and Rogers, N., 2015. Petrographic observations and evaporate mound analysis of quartz-hosted fluid inclusions hosted by granitoid samples from the South Mountain Batholith, Nova Scotia: An exploration tool for vectoring towards mineralized areas in intrusive rocks; *in* TGI 4 – Intrusion Related Mineralisation Project: New Vectors to Buried Porphyry-Style Mineralisation, (ed.) N. Rogers; Geological Survey of Canada, Open File 7843, p. 79-99.

van Staal, C.R., 1987. Tectonic setting of the Tetagouche Group in northern New Brunswick: implications for plate tectonic models of the northern Appalachians; Canadian Journal of Earth Sciences, v. 24, p. 1329-1351.

van Staal, C.R., and Fyffe, L.R., 1991. Dunnage and Gander zones, New Brunswick: Canadian Appalachian Region; New Brunswick Department of Natural Resources; Minerals, Policy and Planning Division, Geoscience Report 91-2, 39 p.

van Staal, C.R., and Fyffe, L.R., 1995a. Gander Zone – New Brunswick; *in* Geology of the Appalachian-Caledonian Orogen in Canada and Greenland, Chapter 3, (ed.) H. Williams. Geological Survey of Canada, Geology of Canada, No. 6, p. 216-223.

van Staal, C.R., and Fyffe, L.R., 1995b. Dunnage Zone-New Brunswick; *in* Geology of the Appalachian-Caledonian Orogen in Canada and Greenland, Chapter 3, (ed.) H. Williams. Geological Survey of Canada, Geology of Canada, No. 6, p. 166-178.

van Staal, C.R., Currie, K.L., Rowbotham, G., Rogers, N., and Goodfellow, W., 2008. Pressure-temperature paths and exhumation of Late Ordovician-Early Silurian blueschists and associated metamorphic nappes of the Salinic Brunswick subduction complex, northern Appalachians; Geological Society of America Bulletin, v. 120, p 1455-1477.

van Staal, C.R., Fyffe, L.R., Langton, J.P., and McCutcheon, S.R., 1992. The Ordovician Tetagouche Group, Bathurst Camp, northern New Brunswick. Exploration and Mining Journal, v. 2, p. 93-103.

van Staal, C.R., Whalen, J.B., Valverde-Vaquero, P., Zagorevski, A., and Rogers, N., 2009. Pre-Carboniferous, episodic accretion-related, orogenesis along the Laurentian margin of the northern Appalachians; *in* Ancient Orogens and Modern Analogues (ed.) J.B. Murphy, J.D. Keppie and A.J. Hynes; Geological Society of London Special Publication 327, p. 271-316.

van Staal, C.R., Wilson, R.A., Rogers, N., Fyffe, L.R., Langton, J.P., McCutcheon, S.R., McNicoll, V.J., and Ravenhurst, C.E., 2003. Geology and tectonic history of the Bathurst Supergroup, Bathurst Mining Camp, and its relationships to coeval rocks in southwestern New Brunswick and adjacent Maine-a synthesis; *in* Massive Sulfide Deposits of the Bathurst Mining Camp, New Brunswick and Northern Maine, (ed.) W.D. Goodfellow, R.R. McCutcheon and J.M. Peter. Economic Geology Monograph 11, p. 37-60.

van Staal, C.R., Winchester, J.A., and Bedard, J.H., 1991. Geochemical variations in Middle Ordovician volcanic rocks of the northern Miramichi Highlands and their tectonic significance; Canadian Journal of Earth Sciences, v. 28, p. 1031-1049.

Victor, I., 1957. Burnt Hill Wolframite deposit, New Brunswick; Economic Geology, v. 52, p. 149-168.

Venugopal, D.V., 1979. Geology of Debee Junction-Gibson Millstream-Temperance Vale-Meductic region, map-areas G-21, H-21, 1-21, and H-22 (Parts of 21 J/3, 21 J/4, 21 G/13, 21 G/14); New Brunswick Department of Natural Resources, Mineral Resources Branch, Map Report 79-5, 36 p.

Venugopal, D.V., 1982. Geology of upper parts of Becaguimec, Keswick and Nashwaak rivers, Cloverdale-Millville map-areas 1-19, J-19, J-20 (Parts of 21J/3, 21J/6); New Brunswick Department of Natural Resources; Mineral Resources, Map Report 82-2, 35 p.

Whalen, J.B., 1993. Geology, petrography and geochemistry of Appalachian granites in New Brunswick and Gaspesie, Quebec; Geological Survey of Canada, Bulletin 436, 124 p.

Whalen, J.B., and Theriault, R., 1990. K-Ar and Rb-Sr geochronology of granites, Miramichi terrane, New Brunswick; *in* Radiogenic Age and Isotopic Studies, Report 3. Geological Survey of Canada, Paper 89-2, p. 101-107.

Whalen, J.B., Jenner, G.A., Longstaffe, F.J., and Hegner, E., 1996. Nature and evolution of the eastern margin of lapetus: geochemical and isotopic constraints from Siluro-Devonian granitoid plutons in the New Brunswick Appalachians; Canadian Journal of Earth Sciences, v. 33, p. 140-155.

Yang, X.M., Lentz, D.R., and Chi, G., 2002. Petrochemistry of Lake George granodiorite stock and related gold mineralisation, York County, New Brunswick; Geological Survey of Canada, Current Research 2002-07, 10 p.

Yang, X.M., Lentz, D.R., Chi, G., and Thorne, K.G., 2008. Geochemical characteristics of gold-related granitoids in southwestern New Brunswick, Canada; Lithos, v. 104, p. 355-377.

The Coast of Bays: Paleozoic tectonic evolution of the Gander margin and adjacent Avalonia in southeastern Newfoundland – TGI 4 Field Guide

Cees van Staal[1], Giorgio Ruberti[2], Andrew Kerr[3], James Conliffe[3] and Neil Rogers[4]

1. Geological Survey of Canada, 625 Robson Street, Vancouver, British Columbia
2. Department of Earth Sciences Memorial University of Newfoundland, St. John's, Newfoundland and Labrador
3. Geological Survey of Newfoundland and Labrador, Department of Natural Resources, PO Box 8700, St. John's, Newfoundland and Labrador
4. Geological Survey of Canada, 601 Booth Street, Ottawa, Ontario

Guide based on the Geological Association of Canada - Newfoundland and Labrador Section 2014 Fall Field Trip, September 25th – 28th, 2014

This field trip was developed on behalf of the Geological Association of Canada's Newfoundland and Labrador Section as their 2014 Fall Field Trip. This trip took place from September 25th to 28th, 2014. The Geological Association of Canada's Newfoundland and Labrador Section, and specifically Andy Kerr are thanked for their contribution in developing the logistics to hold this trip. This guide has been modified for consistency of formatting (e.g., using geographic coordinates for locations), with the original stand-alone field guide, plus other associated guides the Geological Association of Canada's Newfoundland and Labrador Section have previously sponsored related to the south-central Newfoundland region, are available for download at www.gac-nl.ca.

Corresponding author: Neil Rogers (nrogers@nrcan.gc.ca)

van Staal, C.R., Ruberti, G., Kerr, A., Conliffe, J., and Rogers, N., 2015. The Coast of Bays: Paleozoic tectonic evolution of the Gander margin and adjacent Avalonia in southeastern Newfoundland – TGI 4 Field Guide; *in* TGI 4 – Intrusion Related Mineralisation Project: New Vectors to Buried Porphyry-Style Mineralisation, (ed.) N. Rogers; Geological Survey of Canada, Open File 7843, p. 205-245.

Table of contents

Table of contents 206
List of figures 208
About this field trip 209
Acknowledgements 210
Safety information 211

Part 1: Geological setting of the Coast of Bays region, southeastern Newfoundland 213
Introduction 213
Regional setting and general geology 213
Overview of geology and outstanding problems 216
Ganderia: Geology and evolution 219
Western Avalonia: Geology and evolution 225
Hermitage Bay Fault 228

Part 2: Field trip itinerary 229

Day One: A transect through Baie d'Espoir Group and Little Passage Gneiss, along the Baie d'Espoir Highway 229
Stop 1.1: Ultramafic rocks of the Great Bend Ophiolite 229
Stop 1.2: Conglomerates of the Baie d'Espoir Group 229
Stop 1.3: Twillick Brook Member of the St. Josephs Cove Formation 230
Stop 1.4: St. Josephs Cove Formation 230
Stop 1.5: Day Cove fault 230
Stop 1.6: Pelitic schists and psammite of the Little Passage gneiss 231
Stop 1.7: Northeastern extremity of the Gaultois Granite 232
Stop 1.8: Northwest Brook Complex granite 232
Stop 1.9: Hermitage Bay fault in Northwest Brook granite 232
Stop 1.10: Sheared mafic volcanic rocks of Avalonian affinity 232

Day Two: Paleozoic evolution of the Avalonian rocks of northern Fortune Bay and the Connaigre Peninsula 233
Stop 2.1: Simmons Brook Intrusive Suite 233
Stop 2.2: Devonian dykes intruding the Pool's Cove Formation 233
Stop 2.3: Basal unconformity of the Pool's Cove Formation 234
Stop 2.4: Pool's Cove Formation – conglomerates with plutonic boulders 234

Stop 2.5: Deformed rocks of the Chapel Island Formation 234
Stop 2.6: Unconformity beneath the Great Bay de l'Eau Formation 235
Stop 2.7: Belleoram Granite 236
Stop 2.8: Porphyritic phase of the Belleoram Granite 237
Stop 2.9: The Boxey Trail Section 237
Stop 2.10: Acadian folding and thrusting of the Cinq Isles Formation 237
Stop 2.11: Mineralization and alteration in the Old Woman Stock 238

Day Three: Some miscellaneous outcrops along Route 360 239
Stop 3.1: Tungsten-bearing skarns and granite veins 239
Stop 3.2: Chromite and magnesite in the Great Bend Ophiolite 240
Stop 3.3: Sedimentary structures in the Botwood Group 240

References.....241

List of figures

Figure 1 – Subdivisions of the Appalachian Orogen in Newfoundland, Atlantic Canada and the adjacent USA, showing the context of the field trip area.

Figure 2 – Thematic map of the geology of Newfoundland (modified from Hibbard et al., 2006), showing the area of this field trip.

Figure 3 – Tectono-stratigraphic columns and structural relationships of the various elements of Ganderia and Avalonia (modified from van Staal et al., 2014). The peri-Gondwanan terranes are bounded to the west by the Red Indian Line, which separates these from the peri-Laurentian terranes.

Figure 4 – Tectonic model for Salinic and Acadian subduction and orogenesis (modified from van Staal et al., 2014).

Figure 5 – Tectonic elements of the Newfoundland Appalachians expanded to show seaways that occurred outboard of the Humber margin (modified from van Staal and Zagorevski, 2012). Closure of these seaways during the Cambrian-Devonian progressively expanded composite Laurentia (van Staal and Barr, 2014) towards the east and resulted in punctuated orogenic events (Taconic, Salinic and Acadian) in Newfoundland.

Figure 6 – Cambrian-Early Ordovician tectonic evolution of Ganderia (after van Staal and Zagorevski, 2012). A – Magmatic arc is built on Ganderia, concurrent with the development of the Rheic Ocean (van Staal et al., 2012); B – Rifting and drift of Ganderia further opening the Rheic Ocean, and the development of the Penobscot backarc basin within Ganderia; C – Closure of the Penobscot back-arc basin and obduction of ophiolites on to the Gander Margin.

Figure 7 – Simplified geological map of the field trip area, derived from the 1:1 million scale map of Newfoundland, showing the approximate locations of field trip stops for Day 1 and Day 3. For the locations of field trip stops on Day 2 see Figure 8.

Figure 8 – Field trip stops for Day 2. Geology after O'Brien (1998).

Figure 9 – Generalized stratigraphic column for the area of northern Fortune Bay (partly after O'Brien et al, 1996; O'Brien, 1998).

Plate 1 – F1 and F2 folding in rocks assigned to the Chapel Island Formation, along Route 361 (Stop 2.5).

Plate 2 – Angular unconformity between Cambrian (Chapel Island and Chamberlain Brook formations) and Devonian sedimentary rocks of the Great Bay de l'Eau Formation at Blue Pinion Cove.

Table 1 – Stratigraphic nomenclature for the lower Paleozoic, showing currently used terminology from the International Commission on Stratigraphy (ICS) in comparison to terminology used in most previous accounts of the field trip area (DNAG time scale; Palmer, 1984). Ages refer to the base of the Epoch or Stage in question.

About This Field Trip

The region around Baie d'Espoir and northern Fortune Bay, known colloquially as the "Coast of Bays" has long been on the agenda for GAC-NL field trips, and was previously visited on trips in the late 1970s and early 1980s, when the logistics were more complex than those of today. In the 30 years that followed these trips, our knowledge of the evolution of the Appalachians in Newfoundland has grown by leaps and bounds, and our interpretative models are more detailed by at least an order of magnitude. However, our knowledge of the later episodes in the Appalachian-Caledonian Wilson Cycle, in particular the Silurian-Devonian Acadian Orogeny, remains vague compared to what we now know about Ordovician events. The Baie d'Espoir and northern Fortune Bay area is critical to understanding these events, with a major fault system separating regions now known as Ganderia and Avalonia which retain evidence for complex Paleozoic deformation and magmatism,. It is in this context that the established relationships and map patterns are re-evaluated and re-assessed in the light of new geochronological data and a more focused examination of Paleozoic rocks in Avalonia. Like many previous GAC-NL field trips, it is not our intention to present one interpretation as if it were fact, but rather to foster discussion about multiple possibilities and missing information that might be acquired through future work.

In addition to its geological interest, this is a scenically spectacular part of our province, with high rugged hills, deep fiords and picturesque communities. It is admittedly somewhat remote and little-known as a destination, and we are happy to offer a field trip that will expose a new audience to its physical beauty and scientific challenges.

Acknowledgements

The organization of field trips is both a scientific and a logistical challenge, and it has some financial aspects to it as well. The support of the Geological Survey of Newfoundland and Labrador (part of the Department of Natural Resources) in terms of time and organization, support for participation, and assistance with vehicle support is gratefully acknowledged. Without this, such ventures could rarely happen. The Department of Earth Sciences at Memorial University provided valuable subsidies to encourage student participation, which is an important aspect of these excursions. GAC-NL also wishes to acknowledge direct financial support for the 2014 trip from Anaconda Mining Inc. (operators of the Pine Cove gold mine) and from the Geoscience Education Trust of Newfoundland and Labrador (GET-NL), established from revenues accrued from National GAC-MAC meetings in 1988, 2001 and 2012. GET-NL previously operated under the name “St. John’s 88-01 Trust Fund” but has now been rebranded.

Assistance from the staff at the Vancor Motel in Baie d’Espoir is greatly appreciated, as is the culinary expertise and fresh fish supplies of April’s Place in English Harbour West, Fortune Bay. Editorial assistance from Chris Pereira with the final version of this field trip guide is greatly appreciated. Steve Colman-Sadd is thanked for generously sharing his knowledge of local geology and problems throughout the planning and execution of the field trip. We hope that this will become a useful document relating to Newfoundland geology, as many other guides of its type have eventually proven to be.

Safety Information

General Information

Field trips such as this may involve hazards to the leaders and participants. The organizers recommend steel-toed safety boots when working around road cuts, cliffs, or other locations where there is a potential hazard from falling objects. Some field trip stops require sturdy hiking boots for safety.

The weather in Newfoundland is often unpredictable, and participants should be prepared for a wide range of temperatures and conditions. Always take suitable clothing. A rain suit, sweater, and sturdy footwear are essential at almost any time of the year. Gloves and a warm hat could prove invaluable if it is cold and wet, and a sunhat and sunscreen might be just as essential. It is not impossible for all such clothing items to be needed on the same day.

Above all, field trip participants are responsible for acting in a manner that is safe for themselves and their co-participants. This responsibility includes using personal protective equipment (PPE) when necessary.

Specific Hazards

Some of the stops on this field trip are in coastal localities. Access to the coastal sections may require short hikes, in some cases over rough, stony or wet terrain. Participants should be in good physical condition and accustomed to exercise. The coastal sections contain saltwater pools, seaweed, mud and other wet areas; in some cases it may be necessary to cross brooks or rivers. There is a strong possibility that participants will get their feet wet, and we recommend waterproof footwear. We also recommend footwear that provides sturdy ankle support, as localities may also involve traversing across beach boulders or uneven rock surfaces. On some of the coastal sections that have boulders or weed-covered sections, participants may find a hiking stick a useful aid in walking safely.

Coastal localities present some specific hazards, and participants must behave appropriately for the safety of all. High sea cliffs are extremely dangerous, and falls at such localities would almost certainly be fatal. Participants must stay clear of the cliff edges at all times. Coastal sections elsewhere may lie below cliff faces, and participants must

be aware of the constant danger from falling debris. Please stay away from any overhanging cliffs or steep faces, and do not hammer any locations immediately beneath the cliffs. In all coastal localities, participants must keep a safe distance from the ocean, and be aware of the magnitude and reach of ocean waves. Participants should be aware that unusually large "freak" waves present a very real hazard in some areas. If you are swept off the rocks into the ocean, your chances of survival are negligible. If possible, stay on dry sections of outcrops that lack any seaweed or algal deposits, and stay well back from the open water. Remember that wave-washed surfaces may be slippery and treacherous, and avoid any area where there is even a slight possibility of falling into the water. If it is necessary to ascend from the shoreline, avoid unconsolidated material, and be aware that other participants may be below you. Take care descending to the shoreline from above.

Other field trip stops are located on or adjacent to roads. At these stops, participants should make sure that they stay off the roads, and pay careful attention to traffic. Participants should be extremely cautious in crossing roads, and ensure that they are visible to any drivers. Roadcut outcrops present hazards from loose material, and they should be treated with the same caution as coastal cliffs; be extremely careful and avoid hammering beneath any overhanging surfaces.

The hammering of rock outcrops, which is in most cases completely unnecessary, represents a significant "flying debris" hazard to the perpetrator and other participants. For this reason, we ask that outcrops not be assaulted in this way; if you have a genuine reason to collect a sample, inform the leaders, and then make sure that you do so safely and with concern for others. Many locations on trips contain outcrops that have unusual features, and these should be preserved for future visitors. Frankly, our preference is that you leave hammers at home or in the field trip vans.

Subsequent sections of this guidebook contain the stop descriptions and outcrop information for the field trip. In addition to the general precautions and hazards noted above, the introductions for specific localities make note of specific safety concerns such as traffic, water, cliffs or loose ground. Field trip participants must read these cautions carefully and take appropriate precautions for their own safety and the safety of others.

Part 1: Geological setting of the Coast of Bays region, southeastern Newfoundland

Introduction

Overview of the fieldtrip

This three day field trip will mainly focus on the geology of the Avalonian rocks in northern Fortune Bay, and the adjacent Ganderian rocks situated between the Hermitage Bay fault and the Baie d'Espoir area (Figs. 1 and 2). The terms "Ganderia" and "Avalonia" are to a large extent (but not completely) synonymous with the Gander and Avalon zones in the original terminology of Williams (1979). Emphasis is placed on the effects, regional distribution and tectonic setting of the Salinic and Acadian orogenies in this part of Newfoundland. In addition, we will make a few stops along the Baie d'Espoir highway including parts of the Early-Middle Cambrian Coy Pond-Great Bend ophiolite (Kean, 1974; Colman-Sadd and Swinden, 1982; Sandeman et al., 2012) and other miscellaneous localities of geological interest.

The Paleozoic provenance and tectonic relationships between Avalonia and Ganderia remain one of the outstanding problems in Appalachian geology. Recent studies were conducted in this area as part of TGI 4 by the Geological Survey of Canada, in conjunction with work by the Geological Survey of Newfoundland and Labrador (GSNL). Current work by GSNL is aimed largely at Quaternary geology and till geochemistry (D. Brushett, unpublished data), but the area was of interest in the context of previous regional projects investigating granitoid magmatism (e.g., Kerr et al., 1995; Kerr, 1997), and geological mapping in Avalonia east of the Hermitage Bay fault (e.g., O'Brien et al., 1996, O'Brien, 1998). Mapping in the metamorphic and igneous rocks of Ganderia west of the fault was completed in the late 1970s and early 1980s, and is summarized by Colman-Sadd and Swinden (1982) and Colman-Sadd (1979; 1985). The current TGI 4 project in Newfoundland is intended to better document and understand the tectonic evolution of Ganderia and Avalonia during the Silurian and Devonian, and unravel the details of their interaction. This will also improve our knowledge of the tectonic setting responsible for the formation of Late Silurian and Devonian magmatic rocks, and accompanying mineralization, and hopefully also outline new targets for exploration.

Regional setting and general geology

The area of the field trip lies in south-central Newfoundland, and encompasses parts of Baie d'Espoir, Hermitage Bay, and northern Fortune Bay; inland areas along the Baie d'Espoir highway are mostly part of the Gander River drainage basin. In the zonal terminology of Williams (1979) this includes the southwestern Avalon Zone and parts of the Gander Zone and structurally overlying Dunnage Zone (Exploits Subzone). In the synthesis of Williams et al. (1988), the Dunnage Zone rocks were viewed as tectonically juxtaposed above the largely metasedimentary rocks of the Gander Zone, with the latter forming several prominent tectonic "windows" (Fig. 1). Although not exposed within the field trip area, Neoproterozoic (Ediacaran) plutonic and volcanic rocks are present in central Newfoundland, and a basement of similar character is inferred to exist at depth throughout the eastern part of the Central Mobile Belt (Figs. 1 and 2). To the southeast of the Hermitage Bay fault, the geology is dominated by Neoproterozoic volcanic, sedimentary and plutonic rocks that have a complex history, and which are overlain by sedimentary rocks of latest Ediacaran to Cambrian age. The youngest sedimentary rocks in the area are shallow-marine to terrestrial sequences of Devonian age, which are of local extent, but are potentially important in understanding tectonic evolution.

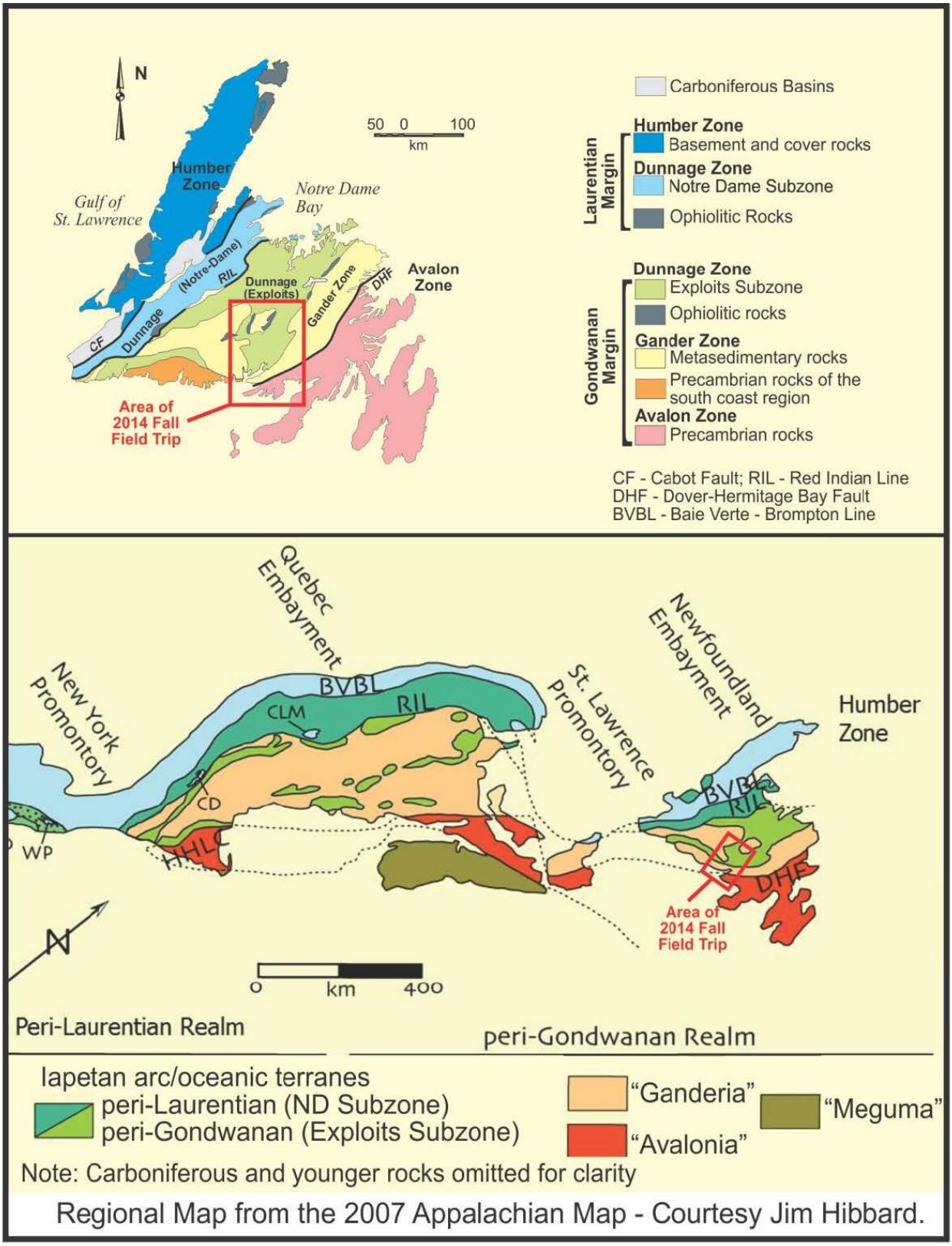

Figure 1 – Subdivisions of the Appalachian Orogen in Newfoundland, Atlantic Canada and the adjacent USA, showing the context of the field trip area.

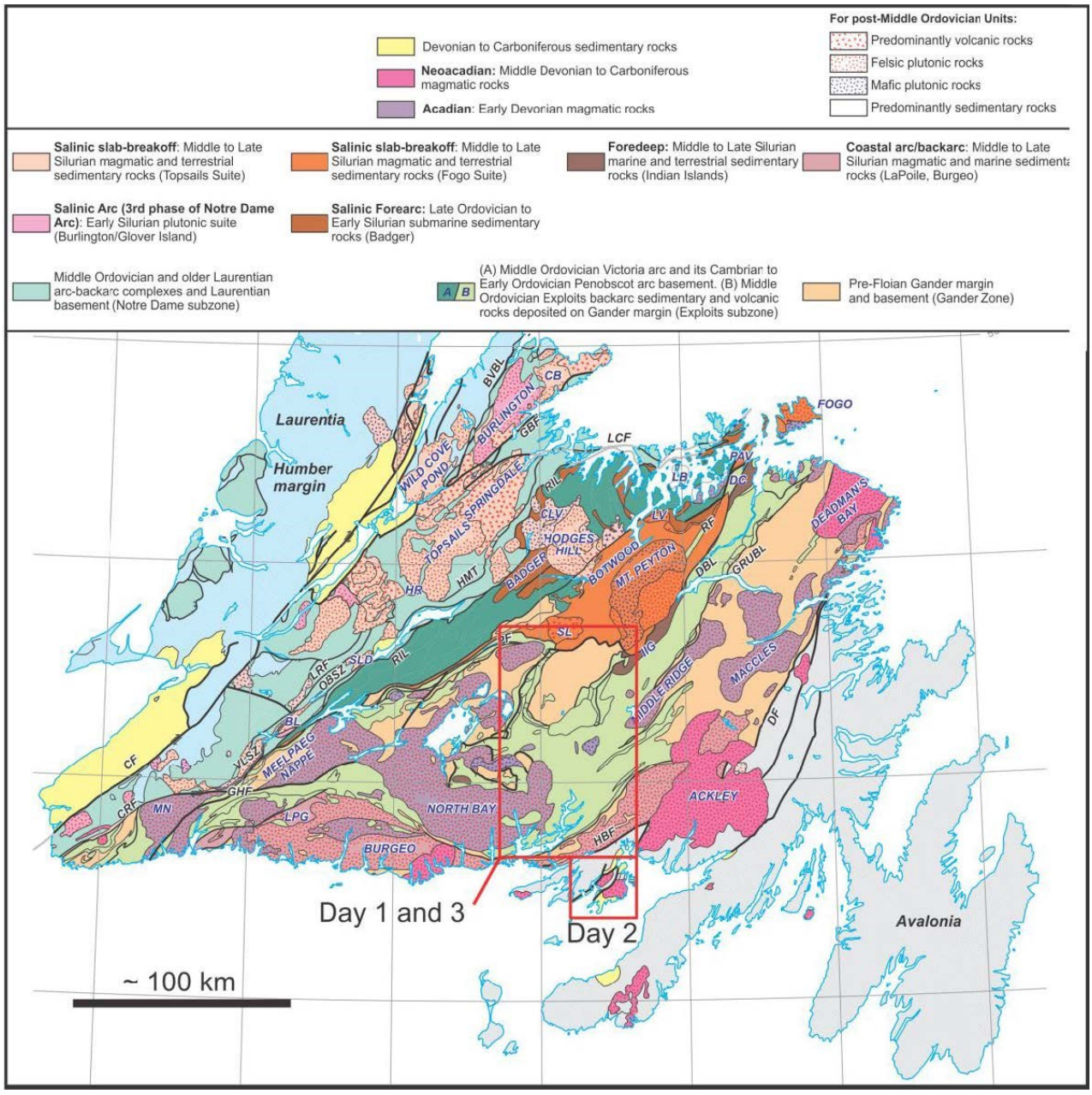

Figure 2 – Thematic map of the geology of Newfoundland (modified from Hibbard et al., 2006), showing the area of this field trip. BL – Boogie Lake pluton; BVBL – Baie Verte-Brompton Line; CB – Cape Brule porphyry; CF – Cabot Fault; CLV – Charles Lake volcanics; CRF – Cape Ray Fault; DBL Dog Bay Line; DC – Duder Complex; DF – Dover Fault; GHF – Gunflap Hills Fault; GRB – Green Bay Fault; GRUBL – Gander River Ultrabasic Belt Line; HBF – Hermitage Bay Fault; HMT – Hungry Mountain Thrust; HR – Harry's River; IIG – Indian Islands Group; LB – Loon Bay pluton; LCF – Lobster Cove Fault; LPG – La Poile Group; LRF – Lloyds River Fault; LV – Laurenceton volcanic; MN – Meelpaeg Nappe; OBSZ – Otter Brook shear zone; PAV – Port Albert volcanic; PF – Pine Falls Formation; RF – Reach Fault; SL – Stony Lake volcanics; RIL – Red Indian Line; SLD – Star Lake Dam; VLSZ – Victoria Lake Shear Zone. NOTE: not all of the above features are referenced in the text of this field guide.

Granitoid rocks are abundant on both sides of the Hermitage Bay fault (Fig. 2). To the northwest, these are of largely Paleozoic age (Silurian to Devonian), but east of the fault there are several generations ranging in age from Neoproterozoic (ca. 620 Ma) to Late Devonian (ca. 375 Ma). Not all such granitoid rocks are dated, and field characteristics or geochemistry alone are not sufficient to distinguish them from one another. The large Ackley Granite, dated at 380-377 Ma (O'Brien, 1998; Lynch et al., 2009) crosscuts the Hermitage Bay fault and is traditionally regarded as a "stitching pluton" that constrains the final amalgamation of the bounding terranes.

The deformation histories on both sides of the Hermitage Bay fault are complex, and various aspects of these events form a major focus for this field trip.

Overview of geology and outstanding problems

Geological background

The rocks of the Gander Zone and intimately associated parts of the Dunnage Zone (Exploits subzone) share at least in part, a common provenance and Proterozoic basement (see above) and will be referred to herein as Ganderia. The rocks of the Avalon Zone will be referred to herein as Avalonia (cf. van Staal and Barr, 2012 and references therein). Avalonia and Ganderia are two Gondwanan-derived terranes that originated on different parts of the eastern margin of the Iapetus Ocean and travelled across Iapetus to arrive at the margin of composite Laurentia during the Early and Late Silurian respectively (van Staal et al., 2012; Figs. 3 and 4). These two terranes are separated by the Dover-Hermitage Bay fault system in Newfoundland (Figs. 2 and 3). This fault zone is a major structure that at least locally appears to cut the entire lithosphere along its northern extension (Keen et al., 1986). The Dover fault zone accommodated both strike-slip as well southeast-directed oblique reverse movements (Holdsworth, 1994; van der Velden et al., 2004). The Paleozoic evolution of Ganderia and Avalonia is markedly different until the late Early Devonian, when red sandstones and conglomerates (a molasse sequence termed the "Old Red Sandstone" in the British Caledonides) overstepped onto Avalonia (Fig. 3; Williams and O'Brien, 1995; O'Brien et al., 1996; van Staal et al., 2014). This supports other lines of evidence that these terranes remained isolated from each other until their successive accretion to composite Laurentia (van Staal and Barr, 2012). However, exactly how convergence was accommodated between Ganderia and Avalonia is poorly constrained at present, because obvious remnants of an intervening ocean have nowhere been preserved along their boundary in Newfoundland. Nevertheless, Silurian arc-like plutons and associated volcanic rocks in southern Newfoundland (e.g., ca. 429 Ma Burgeo Intrusive Suite; Dickson et al., 1985; Dunning et al., 1990; Kerr et al., 1995; Kerr, 1997) suggest that subduction of intervening oceanic lithosphere is a possible model to explain convergence and amalgamation of these terranes (Fig. 4). If so, this oceanic basin (Acadian seaway of Hibbard et al., 2006; van Staal et al., 2009) was probably narrow, because arc-backarc magmatism associated with its closure was relatively short-lived (Dunning et al., 1990; O'Brien et al., 1991). Subduction-driven convergence and collision between Ganderia and Avalonia also provides an attractive causative mechanism for the penetrative Late Silurian-Early Devonian Acadian orogeny between 419 and 395 Ma (van Staal et al., 2009; Fig. 4). Old and dense oceanic lithosphere is generally not expected to be preserved during terrane convergence driven by subduction. Hence, the absence of preserved remnants is not definitive evidence against the former existence of oceanic crust between Ganderia and Avalonia. For example, all that is left of the Luzon arc – China convergence in the collision zone in central Taiwan is a strongly-deformed accretionary prism, mainly made up of sedimentary rocks scraped off from the down-going Eurasian continental margin. The latter was juxtaposed in central Taiwan against rocks forming part of the Luzon arc-forearc system built upon the overriding Philippine Sea plate. No igneous rocks representing the intervening South China Sea oceanic lithosphere have been preserved and most of the forearc terrane was probably underthrusted beneath the Luzon arc (Tang and Chemenda, 2000). This

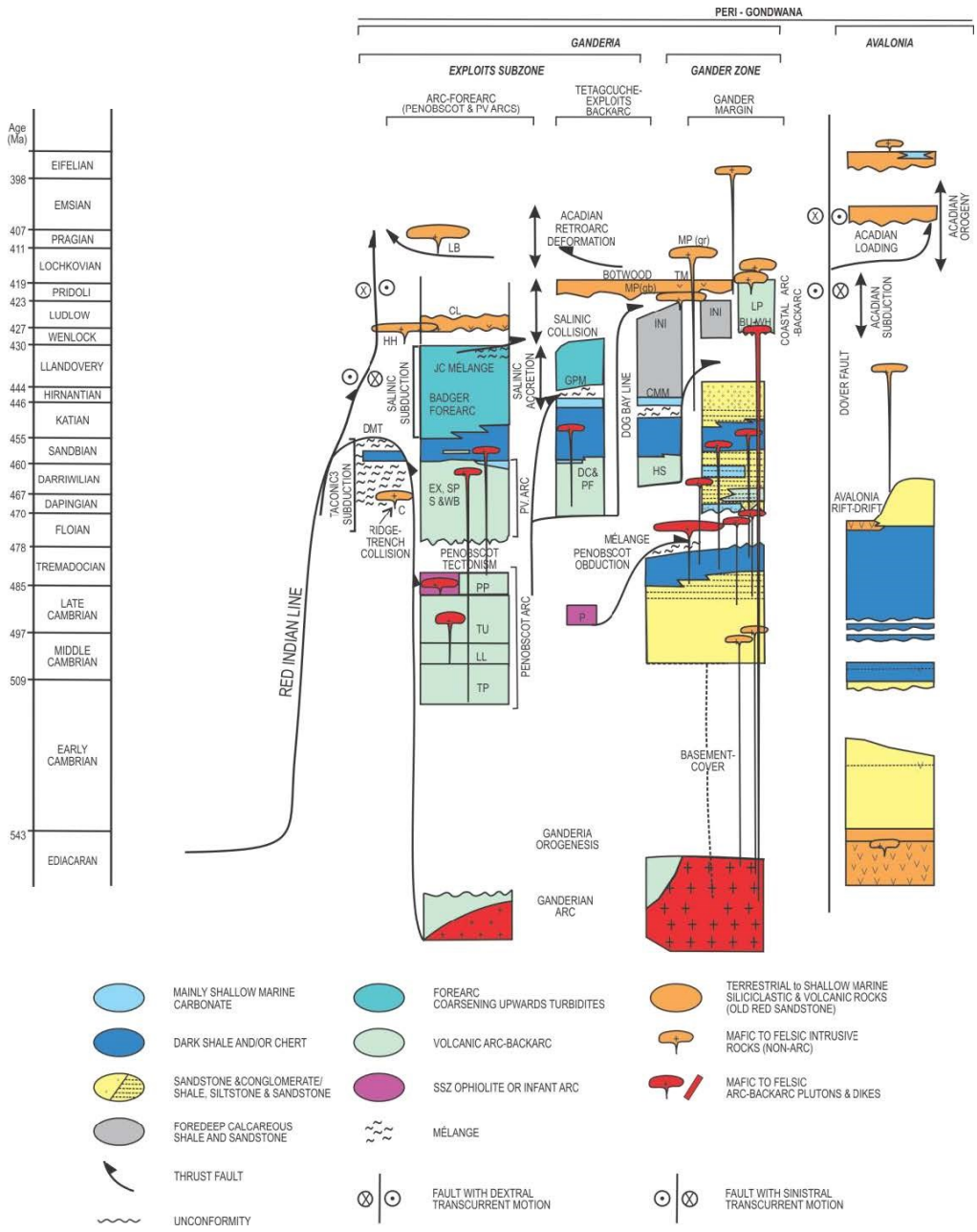

Figure 3 – Tectono-stratigraphic columns and structural relationships of the various elements of Ganderia and Avalonia (modified from van Staal et al., 2014). The peri-Gondwanan terranes are bounded to the west by the Red Indian Line, which separates these from the peri-Laurentian terranes (not shown here). BU – Burgeo Intrusive Suite; C – Coaker Porphyry; CL – Charles Lake volcanics; CMM – Carmanville melange ; DC – Duder Complex; EX – Exploits Groups; GPM – Garden Point melange; HH – Hodges Hill Complex; HS – Hamitlon Sound Group ; INI – Indian Islands Group; JC – Joey's Cove; LB – Loon Bay pluton; LL – Long Lake Group; LP – La Poile Group; MPgb – gabbro phase of Mount Peyton pluton; MPgr – late granite phase of Mount Peyton pluton ; P – Pipestone Pond Complex; PF – Pine Falls Formation; PP – Pats Pond Group; PV – Popelogan-Victoria; S – Summerford Group; SP – Sutherlands Pond group; TM – Ten Mile Formation; TP – Tally Pond Group; TU – Tulks Group; WB – Wild Bight Group; WH – Western Head granite. NOTE: Not all of these features are referenced in the text of this field guide

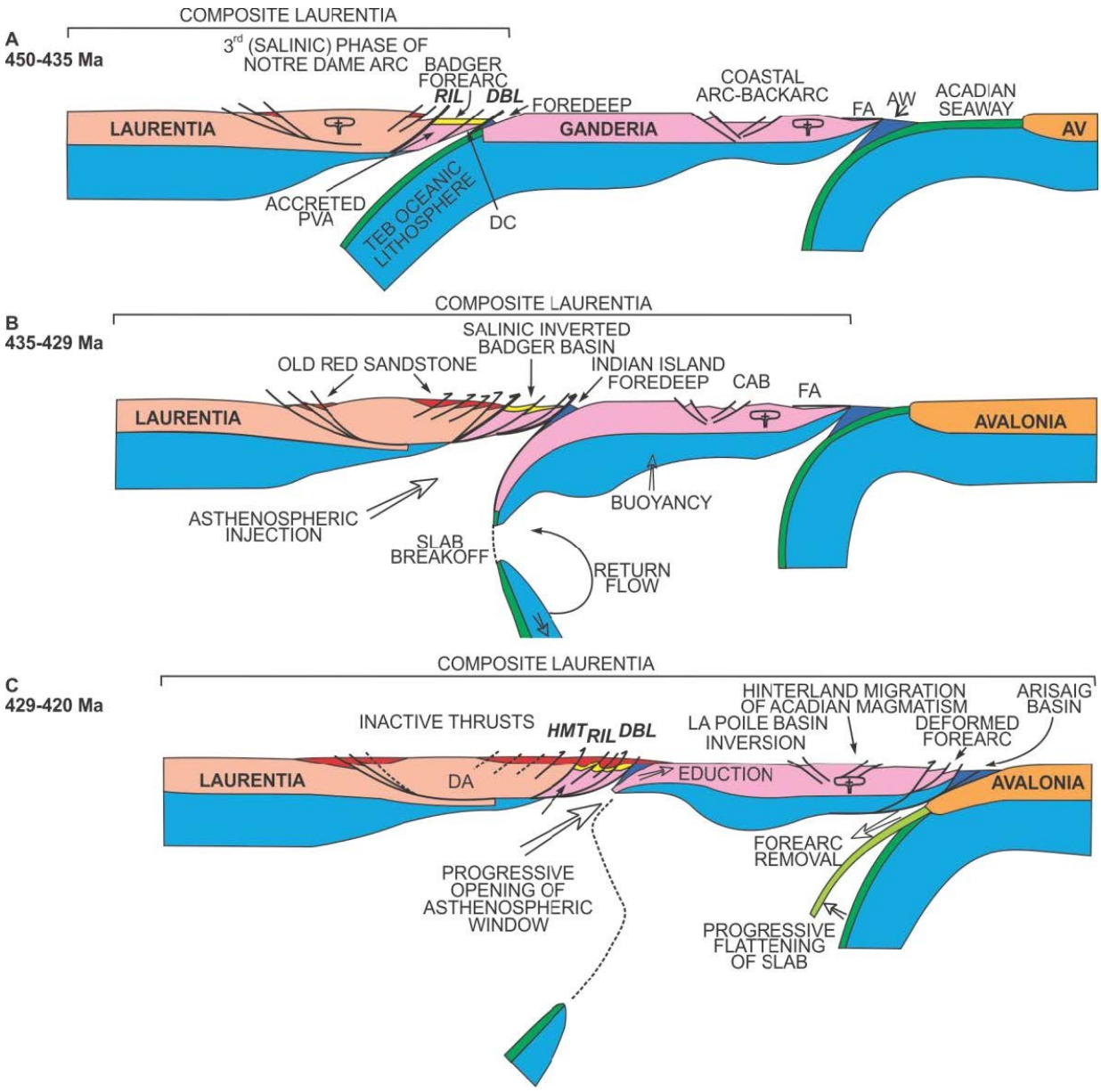

Figure 4 – Tectonic model for Salinic and Acadian subduction and orogenesis (modified after van Staal et al., 2014). (A) Late Ordovician-Early Silurian closure of the Tetagouche – Exploits back-arc basin (TEB) and start of the Salinic collision of composite Laurentia with the leading edge of the Ganderia. Salinic collision was coeval with (and hence may have caused) initiation of subduction in the Acadian seaway beneath the trailing edge Ganderia, forming the coastal arc – back-arc system (CAB). Red bed molasse sedimentation was initiated in basins that formed during early Salinic thrusting and uplift in the hinterland of the orogeny. Marine sedimentation took place in the Badger forearc basin. A marine foredeep accumulated Badger-like clastic sedimentary rocks and sedimentary rocks of the younger Indian Islands Group. (B) Progressive steepening of the Gander margin slab during and/or following break-off of the TEB oceanic slab. (C) Eduction of the Gander margin and eastward expansion of an asthenospheric window beneath the Salinic orogeny. Acadian collision (leading edge of Avalonia enters the trench) starts at ca. 420 Ma. Avalonia is subducted beneath composite Laurentia, now represented by the accreted Gander margin. Progressive flattening of the down-going slab following collision produced a hinterland migrating retro-arc deformation zone and terminated in mantle expulsion.

model of subduction-related convergence through consumption of a narrow oceanic realm (seaway) provides a working model (Figs. 4 and 5) that can be tested through detailed geological studies.

Ganderia: Geology and evolution

The geological elements of Ganderia vary from west to east (Figs. 2, 3 and 5). In the west, it comprises Cambrian-Ordovician ensialic island arc sequences and associated sedimentary rocks (e.g., Victoria Lake Supergroup), which formed on a Late Ediacaran volcanic – plutonic substrate (Rogers et al., 2006; Zagorevski et al., 2010). In the east, it is dominated by Cambrian-Ordovician sedimentary and associated minor volcanic rocks (mainly felsic) that collectively define the Gander margin (see further discussion below) (Colman-Sadd, 1980; van Staal, 1994). Inheritance and isotope studies combined with relationships established in other parts of the Canadian Appalachians suggest that the Gander margin is underlain by Proterozoic basement containing rocks of a similar nature to those known to be present beneath the Paleozoic island arc sequences further to the west (Kerr et al., 1995; van Staal and Barr, 2012 and references therein; Fig. 3). Both halves of Ganderia are also characterised by similar Lower to Mid-

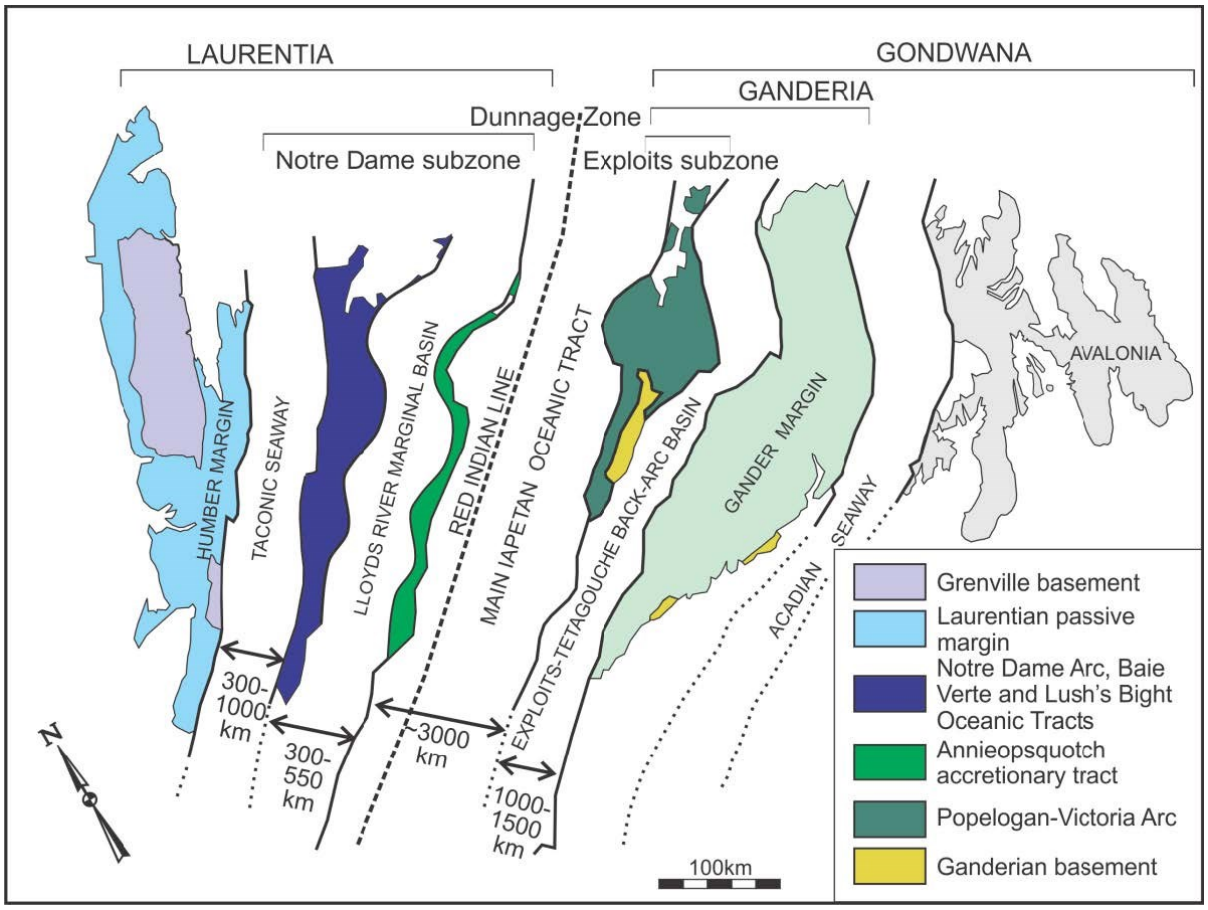

Figure 5 – Tectonic elements of the Newfoundland Appalachians expanded to show seaways that occurred outboard of the Humber margin (modified from van Staal and Zagorevski, 2012). Closure of these seaways during the Cambrian-Devonian progressively expanded composite Laurentia (van Staal and Barr, 2014) towards the east and resulted in punctuated orogenic events (Taconic, Salinic and Acadian) in Newfoundland.

dle Ordovician (Floian – Darriwilian) fossil faunas (Williams et al., 1995; Harper et al., 2009). For reference purposes, the various stratigraphic subdivisions and absolute ages for Lower Paleozoic periods and their boundaries are indicated in Table 1; this guide uses the International Commission on Stratigraphy (ICS) terminology, rather than subdivisions based upon the DNAG time scale (Palmer, 1984), employed in most older publications. Models for the evolution of Ganderia during the Lower Paleozoic are suggested in Figure 6. Figure 7 summarizes the geological units and the field trip stops.

Table 1 – Stratigraphic nomenclature for the lower Paleozoic, showing currently used terminology from the International Commission on Stratigraphy (ICS) in comparison to terminology used in most previous accounts of the field trip area (DNAG time scale; Palmer, 1984). Ages refer to the base of the Epoch or Stage in question.

Era	Period	Epoch	DNAG Scale (1983)	354	Current Scale (2014)	359
PALEOZOIC	DEVONIAN	Upper	Famennian	364	Famennian	374.5
			Frasnian	370	Frasnian	385.3
		Middle	Givetian	381	Givetian	391.8
			Eifelian	391	Eifelian	397.5
		Lower	Emsian	400	Emsian	407
			Segennian	412	Pragian	411.2
			Geddinnian	417	Lochkovian	416
	SILURIAN	Upper	Pridoli	419	Pridoli	418.7
			Ludlovian	423	Ludfordian	421.3
					Gorstian	422.9
		Lower	Wenlockian	428	Homerian	426.2
					Sheinwoodian	428.2
			Llandoverian	443	Telychian	436.1
					Aeronian	439
					Rhuddanian	443.7
	ORDOVICIAN	Upper	Ashgillian	449	Hirnantian	445.6
			Caradocian)	458	Katian	455.8
					Sandbian	460.9
		Middle	Llandeilian	464	Darriwillian	468.1
			Llanvirnian	470	Dapingian	471.8
		Lower	Arenigian	485	Floian	478.6
			Tremadocian	495	Tremadocian	488.3
	CAMBRIAN	Upper 505			(Stage 10)	~492
					(Stage 9)	~496
					Paibian	~499
		Middle 518			Guzhangian	~503
					Drumian	~506.5
					(Stage 5)	~510
		Lower 545			(Stage 4)	~515
					(Stage 3)	~521
					(Stage 2)	~528
					Fortunian	~542
NEOPROT-EROZOIC	EDIACARAN 635					
	CRYOG-ENIAN 850					

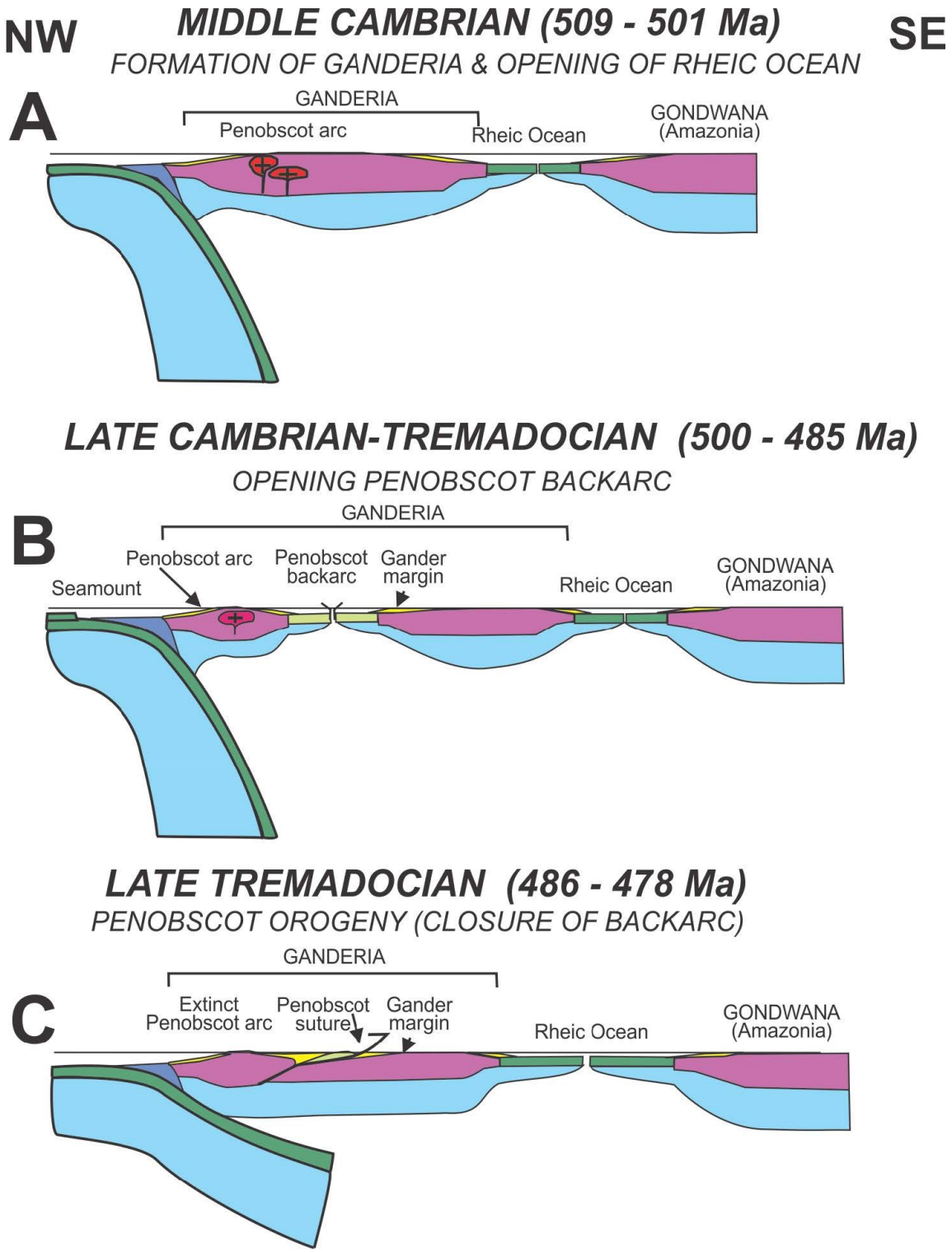

Figure 6 – Cambrian-Early Ordovician tectonic evolution of Ganderia (after van Staal and Zagorevski, 2012). A – Magmatic arc is built on Ganderia, concurrent with the development of the Rheic Ocean (van Staal et al., 2012); B – Rifting and drift of Ganderia further opening the Rheic Ocean, and the development of the Penobscot back-arc basin within Ganderia; C – Closure of the Penobscot back-arc basin and obduction of ophiolites on to the Gander Margin.

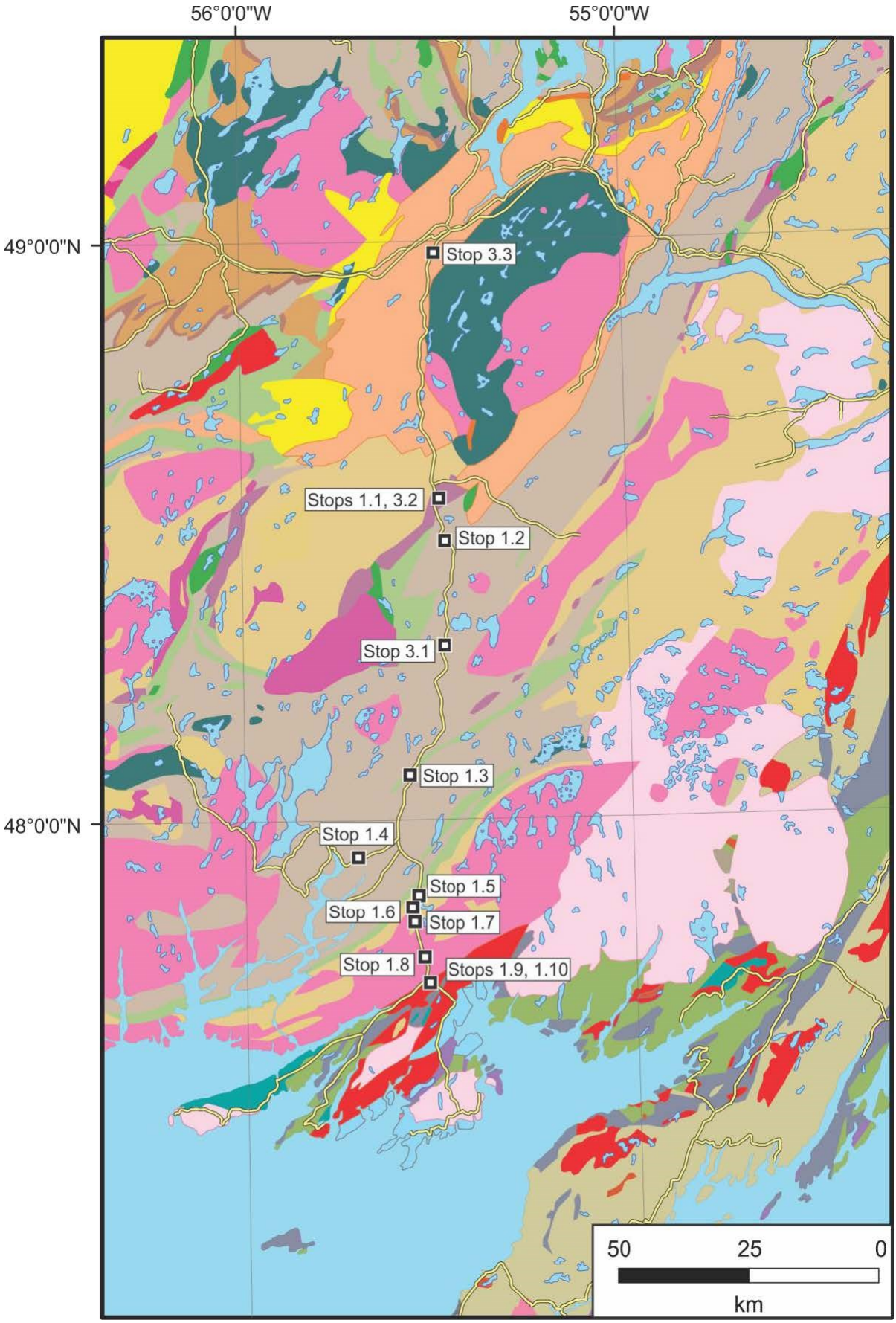
56°0'0"W
55°0'0"W
49°0'0"N
48°0'0"N
Stop 3.3
Stops 1.1, 3.2
Stop 1.2
Stop 3.1
Stop 1.3
Stop 1.4
Stop 1.5
Stop 1.6
Stop 1.7
Stop 1.8
Stops 1.9, 1.10
50
25
0
km

Figure 7 – Simplified geological map of the field trip area, derived from the 1:1 million scale map of Newfoundland, showing the approximate locations of field trip stops for Day 1 and Day 3. For the locations of field trip stops on Day 2 see Figure 8.

In southeastern Newfoundland, the Gander margin is dominated by Cambrian to Ordovician marine sedimentary rocks, which were metamorphosed from greenschist facies to upper amphibolite facies conditions, and locally formed migmatites suggestive of partial melting processes. These rocks have been divided into the Baie d'Espoir Group and the Little Passage gneiss, which are separated by the Day Cove fault (Colman-Sadd, 1976; 1980). The Little Passage gneiss is thought to represent the high-grade and migmatised equivalents of the Baie d'Espoir group (Blackwood, 1985), consistent with the presence locally of coticule beds and pyritiferous schist of probable volcanogenic origin in paragneisses. However, it may also include some high-grade equivalents of the quartz-rich sandstones and shales of the Gander Group, which is located along strike to the northeast.

The Ordovician Baie d'Espoir Group ranges in age from Lower Ordovician (Floian) to Upper Ordovician (Katian). On the basis of sparse fossil evidence; this corresponds to a range in age from ca. 479 Ma to ca. 456 Ma. It mainly comprises a series of sandstones, siltstones and shales, in part representing deep water turbidites (Colman-Sadd, 1980), which together with correlatives along strike (e.g., Davidsville Group) in turn unconformably to conformably overlie Cambrian to Lower Ordovician (?) metasandstones and shales of the Gander Group (O'Neill and Blackwood, 1989; Colman-Sadd et al., 1992; Valverde-Vaquero et al., 2006). Both units were interpreted to have been deposited on a northwest-facing (present coordinates) continental margin by Colman-Sadd (1980), which is consistent with the nature of the sedimentary rocks and paucity of volcanic rocks in both the Gander and Baie d'Espoir groups and correlatives elsewhere (van Staal et al., 1996; van Staal and Barr, 2012). For this reason these rocks were collectively termed the Gander margin by van Staal (1994; 2007). Passive margin sedimentation was interrupted for a short period during the earliest Ordovician (Tremadocian to Floian; 483-478 Ma), at least in the western parts of the Gander margin, by the obduction of ophiolites such as the Coy Pond and Pipestone Pond complexes onto the Gander Group (Colman-Sadd et al., 1992). This event is now generally termed the Penobscot Orogeny (Fig. 6), and is broadly synchronous with the better known Taconic events on the Laurentian margin of Iapetus. Passive margin sedimentation terminated during the Late Ordovician and Early Silurian and was replaced by marine foreland basin deposits following the onset of Salinic tectonism (van Staal and Barr, 2012; van Staal et al., 2014). It is significant that volcanic-derived sandstones in the Baie d'Espoir Group (North Steady Pond Formation) become more pronounced and coarsen upwards towards the northwest (Colman-Sadd, 1980), which suggests that the Gander margin probably represents the passive margin of a backarc rather than a true oceanic basin throughout its history. This back-arc basin (Jenner and Swinden, 1993; Zagorevski et al., 2008; 2010) was sandwiched between the Cambrian to Middle Ordovician (515-458 Ma) island arc volcanic rocks such as the Victoria Lake Supergoup at the northwestern (leading) edge of Ganderia and the Gander margin to the southeast. The short-lived Penobscot obduction destroyed most evidence of the Cambrian-Early Ordovician opening phase of the back-arc basin adjacent to the Gander margin, but back-arc rifting and spreading resumed after 476 Ma and led to the opening of the Exploits back-arc basin (Fig. 4). These latter events were concurrent with deposition of the Baie d'Espoir Group and its correlatives (e.g. Davidsville and Harbour Le Cou groups) on its passive southeast margin (van Staal, 1994; Schofield et al., 1997; Valverde-Vaquero et al., 2006; Zagorevski et al., 2010).

Closure of the Exploits backarc basin eventually led to Late Ordovician - Early Silurian accretion of the Gander margin to composite Laurentia, which subjected the Baie d'Espoir Group and its underlying basement to the Salinic orogeny (Fig. 4). The Salinic orogeny in southeastern Newfoundland culminated in formation of the Little Passage gneiss and generation of spatially associated syn-tectonic biotite-bearing granitoid rocks between 423 and 421 Ma. Observations by CVS and GR confirmed that unfoliated veins of the K-feldspar porphyritic Gaultois granite (421 ± 2 Ma) cut foliated tonalitic and granodioritic veins and neosomes that make up the bulk of the migmatitic phase of the Little Passage gneiss dated at 423+5/-3 Ma (Colman-Sadd, 1976; Dunning et al., 1990). The Salinic orogeny was

thus in its waning stages when the Gaultois granite intruded, which is consistent with age relationships deduced in northeastern Newfoundland (van Staal et al., 2014).

The products of Salinic deformation and metamorphism (D1 – M1) in turn were overprinted by structures generated during the Early Devonian Acadian orogeny (Figs. 3 and 4). The Acadian tectonism led to SE-vergent D2 folds, sinistral oblique SE-directed reverse faults (e.g. Day Cove fault) and low- to medium-pressure metamorphism (M2), which is coeval with generation of syn-to post D2 biotite-muscovite granites (Colman-Sadd, 1976, 1979, 1980; Piasecki, 1988) of the Early Devonian (417-396 Ma) North Bay granite suite (Dickson, 1990; Dunning et al., 1990). D2-related shear localised in ductile faults (e.g., Day Cove fault) caused retrogression of high-grade metamorphic assemblages in the shear zones and emplaced relatively low-grade (biotite zone) Acadian metamorphic tectonites above higher-grade gneisses and schists of the Little Passage gneiss that record the earlier Salinic Orogeny (Colman-Sadd, 1976; Piasecki, 1988). Shear sense indicators observed by CVS and GR are consistent with the structural interpretations of Piasecki (1988) that the Day Cove fault probably accommodated a reverse component of movement in addition to sinistral strike-slip shear. The accumulated finite strain led to intense flattening, marked by "chocolate-tablet" boudinage (see later field stop descriptions) in the sheared rocks, which suggests that movements may have been polyphase and complex. This phase of shearing followed earlier exhumation of the high-grade Salinic metamorphic rocks and probably took place late during D2. These relationships are consistent with a model in which the Salinic and Acadian orogenies represent two kinematically-unrelated tectonic events, separated by a phase of latest Silurian – Early Devonian uplift and exhumation (van Staal et al., 2014; Figs. 3 and 4).

Western Avalonia: Geology and evolution

The Avalonian rocks of the northern Fortune Bay area (Figs. 8 and 9) comprise a series of Cryogenian to Ediacaran (685-550 Ma) sedimentary and volcanic rocks; the latter are considered to be predominantly arc-related. In ascending order, these rocks are assigned to the Tickle Cove Formation, the Connaigre Bay Group and the Long Harbour Group and associated coeval intrusive suites (O'Brien et al., 1996; O'Brien, 1998). The Cryogenian (685-670 Ma) rocks of the Tickle Point Formation and Furby's Cove intrusive suite are separated from the younger Ediacaran units by a phase of deformation that predates intrusion of c. 620 Ma granitoid rocks of the Simmons Brook intrusive suite. Another phase of deformation locally affected these c. 620 Ma plutonic rocks prior to intrusion of younger Ediacaran intrusive suites after 590 Ma (O'Brien et al., 1996; O'Brien, 1998). The causes and tectonic significance of the various Neoproterozoic events in Avalonia remain poorly understood, but are probably related to convergence and progressive amalgamation of the various volcanic arc terranes that together make up Avalonia. The Neoproterozoic volcanic and sedimentary rocks in the east of the Fortune Bay area are overlain by Ediacaran to Lower Paleozoic (Cambrian) sedimentary rocks of the Youngs Cove Group (Figs. 8 and 9), which based on observations by CVS and GR were complexly folded and involved in thrusting prior to deposition of redbeds of the Middle to Upper Devonian Great Bay de L'Eau Formation, which in turn was deposited prior to intrusion of the Middle to Late Devonian Belleoram granite (Williams, 1971; O'Brien et al., 1996; O'Brien, 1998). The sub-middle Devonian unconformity marks the Acadian orogeny in this part of Newfoundland. Observations by CVS and GR confirm earlier conclusions by Williams and O'Brien (1995) that Lower to Middle Devonian red beds and minor limestone of the Cinq Isles and Pool's Cove formations were locally complexly deformed, involving Acadian upright to recumbent folding and thrusting. The red beds comprise a thick sequence of sandstone and conglomerate and probably represent the fill of a late Acadian molasse basin (van Staal et al., 2014) that captured detritus form the rising Acadian mountains in adjacent Ganderia (Williams and O'Brien, 1995; Fig. 3). All data thus confirm earlier inferences (Williams, 1995 and references therein) that the Acadian Orogeny affected both Ganderia and Avalonia, even though collision-related metamorphic and igneous rocks are principally concentrated in Ganderia. These relation-

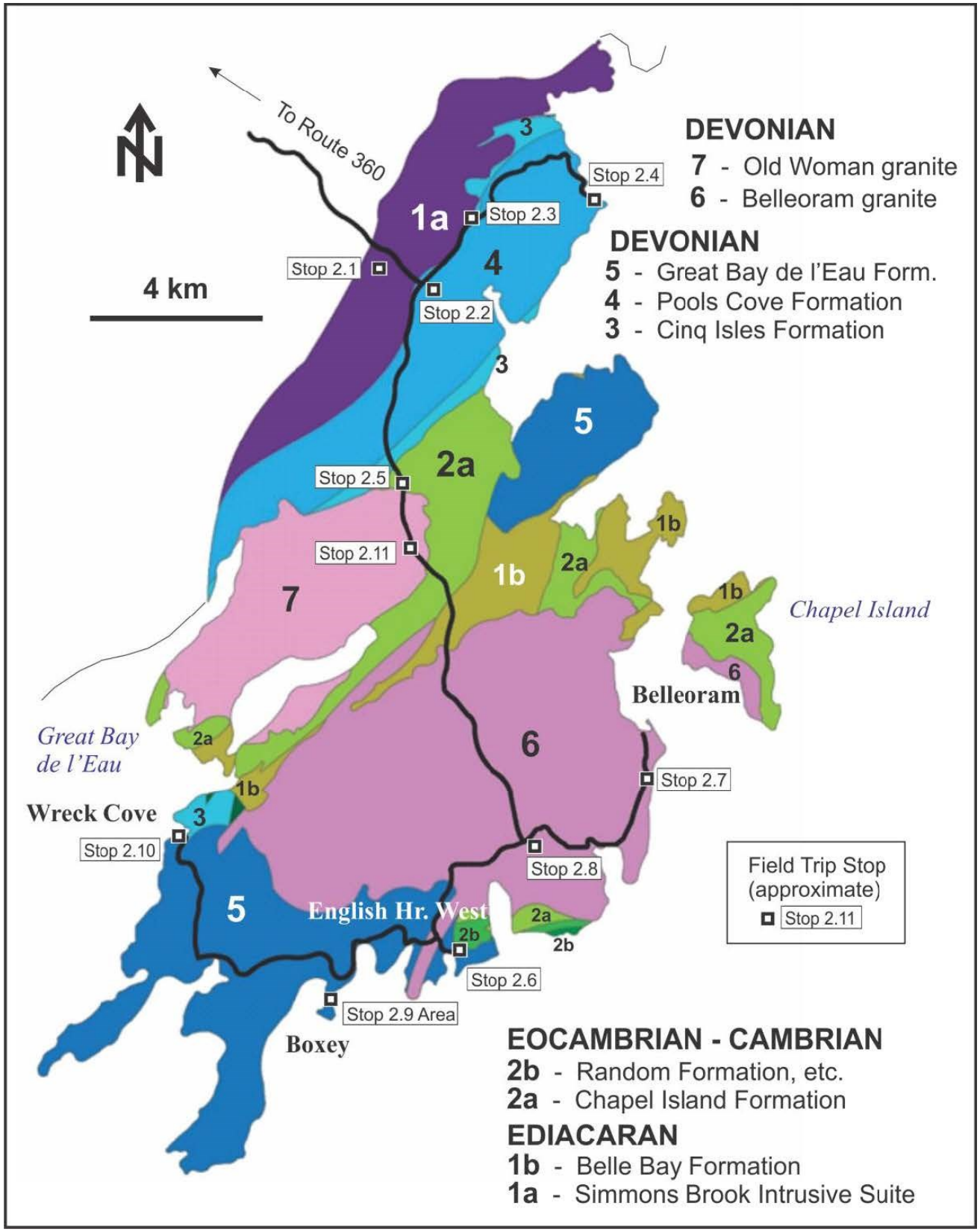

Figure 8 – Field trip stops for Day 2. Geology after O'Brien (1998).

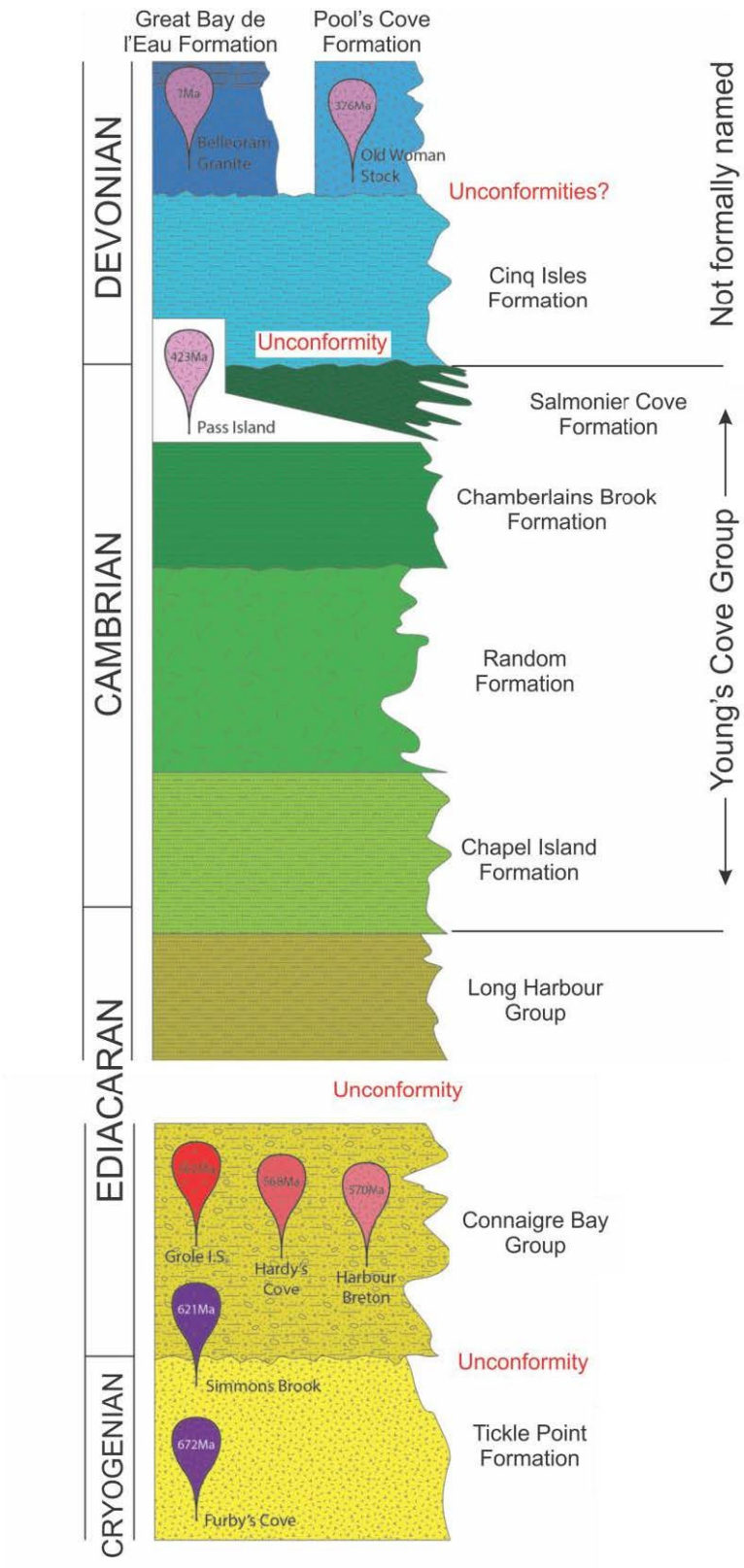

Figure 9 – Generalized stratigraphic column for the area of northern Fortune Bay (partly after O'Brien et al, 1996; O'Brien, 1998).

ships support a tectonic model in which Ganderia was situated on the upper plate, as implied also by the presence of Silurian arc-type magmatic rocks in the Hermitage flexure (Fig. 4). Avalonia, on the other hand, represented the lower plate during Acadian convergence and collision between these two terranes (Fig. 4).

An interesting new problem is posed by geochronological data from the Pass Island granite at the southwestern tip of the Connaigre Peninsula (Fig. 2), which has always been assumed to be a Devonian pluton of similar age to other prominent examples such as the Ackley Granite and Francois Granite (Kerr et al., 1993). However, a Late Silurian (ca. 423 Ma) crystallization age now forces some reconsideration of this link (Kellett et al., 2014). Granitic plutons of ca. 423 Ma age are previously unknown in Avalonia in Newfoundland or Atlantic Canada, but such late Silurian magmatism is important throughout Ganderia. The age from Pass Island raises questions as to whether all of the Precambrian rocks of northern Fortune Bay are truly part of Avalonia and, if not, whether the Hermitage Bay fault actually represents the true terrane boundary along its whole length.

Hermitage Bay Fault

The Hermitage bay fault is inferred to mark the Ganderia-Avalonia boundary in southeastern Newfoundland (Figs. 2 and 3; Fig. 7). The fault juxtaposes Upper Silurian to Lower Devonian K-feldspar-porphyritic granites such as the ca. 421 Ma Gaultois granite and leucocratic granites of the Northwest Brook Complex in Ganderia against Neoproterozoic rocks of the Tickle Point Formation, Connaigre Bay Group, Simmons Brook intrusive suite and Harbour Breton granite in Avalonia (O'Brien, 1998). The fault zone is characterised by ductile-brittle chlorite- rich shears and belts of cataclasite. The absence of ductile shears in contrast to the wide zone of fault-related tectonites associated with the Dover fault along strike to the northeast (Holdsworth, 1994), suggest that different crustal levels of the structure are exposed, and that the Hermitage Bay fault accommodated mainly higher-level movements. It is also possible that ductilely sheared rocks akin to those of the Dover fault zone are largely masked in southeastern Newfoundland by granitoid rocks of the Northwest Brook Complex, which forms a composite pluton elongated along the fault zone's western margin. This is supported by evidence suggesting that the ca. 403 Ma Indian Point granite (O'Brien, 1998), (formerly called the Straddling granite; Colman-Sadd, 1980), which is a member of the Northwest Brook Intrusive Complex, intruded late into the brittle fault zone. Red aplite of the Indian Point granite cuts strongly foliated Gaultois-type granite along the western margin of Hermitage Bay, but the Indian Point granite itself is only weakly foliated or transformed into narrow zones of chlorite-bearing feldspar-porphyroclastic cataclasite along the trace of the Hermitage Bay fault. The Avalonian rocks incorporated in the Hermitage Bay fault zone on the other hand are much more penetratively deformed into cataclasite than the Indian Point granite. These observations collectively suggest that the main brittle movements accommodated by the Hermitage Bay fault zone took place before ca. 403 Ma. If the strongly foliated parts of the Gaultois granite record early ductile deformation associated with development of the Hermitage Bay fault zone, movements along the had started by at least by ca. 421 Ma. The orientation of subsidiary shears, lineations and scarce shear sense indicators suggest the Hermitage Bay fault subsequently accommodated a long and complex movement history involving both strike-slip as well dip-slip motions.

Part 2: Field trip itinerary

The field trip itinerary is broken into two full days, followed by a partial day including selected stops en route from Baie d'Espoir to the Trans-Canada Highway. Day One focuses on rocks within Ganderia, and terminates at outcrops representing the Hermitage Bay fault. Day Two follows the same route initially, but focuses on the area of Avalonia located southeast of the fault, around the communities of Pool's Cove, Belleoram, English Harbour West and Wreck Cove. Day Three includes three general interest stops on the Baie d'Espoir highway.

Field trip stops for Day One and Day Three are indicated in Figure 7, and the field trip stops for Day Two are indicated in Figure 8.

Day One: A transect through Baie d'Espoir Group and Little Passage Gneiss, along the Baie d'Espoir Highway.

Stop 1.1: Ultramafic rocks of the Great Bend Ophiolite (48°33'24.26" N, 55°29'24.94" W)

Join Highway 360 just east of the Exploits River bridge outside Bishop's Falls. Check to see if there is adequate fuel in the tank! Watch for moose, and also for moose hunters! Continue for about 55.9 km, to Stop 1.1, which is a large quarry located on the east (left) side of the road, 3.0 km south of the bridge over the Northwest Gander River.

This locality reveals varied, serpentinized, ultramafic rocks of the Great Bend ophiolite complex, one of several such units that separate the higher-grade metasedimentary rocks of the Gander Group and equivalents from volcanic and sedimentary rocks assigned to the Dunnage Zone. The emplacement of these ophiolites records the earliest Paleozoic orogenic event in the field trip area, the Ordovician Penobscot Orogeny. The timing of this event, which emplaced arc-type volcanic sequences developed within the Iapetus Ocean above the siliciclastic rocks of the Gander Group and its equivalents, is constrained by the ca. 464 Ma U-Pb ages obtained from leucocratic granites that cut both the metasedimentary rocks and the ophiolites (Colman-Sadd et al., 1992).

The ultramafic rocks here contain minor chromite, and at a nearby locality more abundant chromite and also magnesite (Magnesium Carbonate) are present. The latter is a product of hydrothermal alteration processes, and has attracted some economic evaluation. These areas of mineralogical interest within the Great Bend ophiolite will be visited on the return trip on Day Three (see Stop 3.2). Stop 1.1 is dominated by massive peridotite, and represents material from the uppermost mantle, below the Moho.

Stop 1.2: Conglomerates of the Baie d'Espoir Group (48°29'18.02" N, 55°28'58.78" W)

These roadcut outcrops are located in roadcuts about 8.2 km south of Stop 1.1, and are described in a previous field trip guide by Colman-Sadd and Swinden (1983; Stop 14).

The conglomerates at this locality include varied clasts of sedimentary, plutonic and volcanic rock types. The conglomerate is interpreted to be a channel fill deposit within a larger turbidite fan, i.e., not of shallow-water origin. It is closely associated with volcanogenic sandstones that resemble those seen at Stop 1.3 (see below). Although this outcrop has always been regarded as part of the Ordovician Baie d'Espoir Group, an outcrop located along strike to the northeast yielded Silurian fossils in blocks (W.L. Dickson, unpublished data) raising questions about its true age

and relationships. Sedimentary rocks of the latest Ordovician to Silurian Badger and Botwood groups are present in locations to the northeast, but paucity of outcrop renders stratigraphic relationships rather uncertain, to say the least.

Stop 1.3: Twillick Brook Member of the St. Josephs Cove Formation, Baie d'Espoir Group (48°04'24.43" N, 55°34'31.97" W)

From Stop 1.2, continue south on Route 360 for another 52.1 km, to roadcut outcrops located on the west (right) side of the road, around 1.6 km south of the bridge over Twillick Brook. The exposure continues in a gravel pit also located on the west side of the road. The stop is described in a previous guidebook by Colman-Sadd and Swinden (1983; Stop 13).

The Twillick Brook Member contains Dapingian – Darriwilian (468 ± 2 Ma) felsic pyroclastic rocks (e.g., quartz-feldspar crystal tuff) and represents one of the few volcanic rocks deposited on the Gander margin in this part of Newfoundland (Colman-Sadd et al., 1992). In these outcrops, the metavolcanic rocks are in contact with graphitic slates to the south, and also include sedimentary lenses. These rocks all form part of the St. Josephs Cove Formation, which mainly comprises fine grained, low energy turbidites and is conformably and gradually overlain by black shale (Colman-Sadd, 1979, 1980); poorly-preserved graptolites in this were consistent with a Darriwillian – Sandbian age in current terminology (Williams et al., 1992). Significantly, the Twillick Brook Member appears to be in direct contact with the Gander Group further to the northeast (Blackwood and Green, 1982), such that the underlying turbidites are cut out, hinting that here there may be a cryptic fault, or a disconformity (or a combination of both) between the Gander and Baie d'Espoir groups. This quarry is the site of geochronology sampling by Colman-Sadd et al., 1992, who obtained an age of 468 ± 2 Ma (Darriwilian in current stratigraphic terminology).

Stop 1.4: St. Josephs Cove Formation, Trout Hole Falls Park, Head of Baie d'Espoir (47°55'53.18" N, 55°43'17.94" W)

Continue south on Route 360 from Stop 1.3 for 12.5 km, and then turn right on Route 361 towards Head of Baie d'Espoir. Continue for 9.8 km to Trout Hole Falls Municipal Park, located on the right (west) side of the road. The outcrop is also described in the Traveller's Guide to the Geology of Newfoundland and Labrador (Colman-Sadd and Scott, 1994; Stop 47).

Prominent beds of sandstone and shale here form a natural dam, creating a lovely swimming hole and an excellent lunch stop. The beds are nearly vertical, and well-cleaved. These steeply-dipping thinly-bedded greenschist facies sedimentary rocks contain a S1 cleavage that is nearly parallel to bedding. Both the beds and S1 are folded into nearly symmetrical recumbent F2 folds with a shallowly-dipping S2 crenulation cleavage. The F2 structures are situated near the hinge of a large SE-verging F2 fold according to Colman-Sadd (1976). The outcrop is extremely instructive in terms of understanding how complex structural patterns develop through multiple periods of deformation.

Stop 1.5: Day Cove fault (47°50'0.69" N, 55°35'12.89" W)

From Stop 1.4, return to Route 360 (9.8 km), and turn south. The outcrops representing the fault zone are about 16.8 km south of from the Route 360/361 junction. The outcrop is described in an earlier field trip guide by Colman-Sadd

and O'Driscoll (1978; Stop 9); it reveals the basal fault, slide or detachment zone (or whatever you choose to call it) of the Baie d'Espoir Group.

This outcrop was visited by C. van Staal in 2001 with S. Colman-Sadd and comprises mylonitic rocks developed in felsic volcanic or volcanogenic sedimentary rocks of the Isle Galet Formation (Colman-Sadd, 1976, 1980). Near Barasway de Cerf the same formation contains a trilobite pygidium of possibly Late Cambrian or Early Ordovician age (Colman-Sadd, 1976). A fossil locality on nearby Conne River contains trilobites of Early to Middle Ordovician (Floian to Dapingian) age (S. Colman-Sadd, pers. comm., 2001). Boudinage of veins indicate a strong oblique down-dip stretching lineation. Structural investigations of this fault zone along strike along the shores of Baie d'Espoir show juxtaposition of moderately NW-dipping dark greenschist facies phyllite and phyllonitic felsic volcanic rocks of the Isle Galet Formation with mylonitic schists of the Little Passage gneiss (see Stop 1.6 below). The shear zone-related mylonitic foliation contains intrafolial isoclines of quartz veins, which in turn are overprinted by two generation of mesoscopic folding. "Chocolate-tablet boudinage" seen in veins suggests the fault accommodated a high flattening strain. Shear-sense indicators are ambiguous, but are consistent with a reverse component. Not all of the features discussed above are readily visible in these roadcut outcrops, but the fault zone is marked by a prominent topographic depression (seen to the northwest) which links to the coastal outcrops; the metamorphic rocks of the Little Passage gneiss, to the south, show a marked topographic and vegetation contrast with the terrain underlain by the lower-grade sedimentary and volcanic rocks.

Stop 1.6: Pelitic schists and psammite of the Little Passage gneiss injected by muscovite-bearing leucocratic granite veins (47°49'19.00" N, 55°35'9.11" W)

This stop is located a short distance south of the Day Cove fault, about 1.3 km from Stop 1.6. The rocks contrast strongly with all outcrops seen previously, and a previous description given by Colman-Sadd and O'Driscoll (1978; Stop 10) is augmented below.

The rocks are paragneisses and schists consisting of quartz, mica and feldspar, and contain variable amounts of garnet, staurolite and sillimanite, and also tourmaline and pyrite. Complex folding is obvious, and no primary sedimentary structures are reported. These pelitic schists interlayered with thin bedded psammite were folded into SE-overturned F_2 folds, which are accompanied by a fanning S2 crenulation cleavage of S1. S1 is axial planar to intrafolial F1 folds in the psammite. The leucocratic granite veins likely belong to the Early Devonian North Bay granite suite, which contains rocks of similar aspect (Colman-Sadd, 1976; Dickson, 1990) and occur in two orientations: one set is roughly parallel to S2 and weakly foliated; the other set is roughly parallel to S1 and was folded, albeit less strongly than the host, and contains a well-developed S2 fabric. Apparently the veins intruded in several orientations, and those with an orientation in the shortening field of the strain ellipsoid were folded and well-cleaved, whereas those that intruded in the extensional field were not, but developed a weak cleavage and were instead boudinaged. These relationships suggest that intrusion took place during F2, consistent with other lines of evidence that F2 is related to the Acadian orogeny, assuming that the early Devonian age inferred for the granite veins is correct. There is presently no direct geochronological information on the granitoid veins, but this would obviously be important information.

Stop 1.7: Northeastern extremity of the Gaultois Granite (here of dioritic composition) (47°48'16.54" N, 55°35'39.08" W)

From Stop 1.6, continue approximately 2.2 km south on Route 360. These outcrops were previously described by Colman-Sadd and O'Driscoll (1978; Stop 11); this material is augmented below.

The outcrops consist of foliated, melanocratic diorite. Although these outcrops are not typical of the Gaultois Granite as a whole, mapping indicates that this unit is continuous with, and grades into, more typical megacrystic granitoid rocks to the southwest. The diorite is cut by veins of leucogranite containing minor garnet and tourmaline, which are equated with the rocks at Stop 1.7 below (S. Colman-Sadd, pers. comm.)

Stop 1.8: Northwest Brook Complex granite close to Hermitage Bay fault (47°44'31.28" N, 55°32'53.31" W)

From Stop 1.7, continue approximately 8.2 km south to prominent outcrops located in roadcuts and gravel pits on the right (west) side of Highway 360. These outcrops were previously described by Colman-Sadd and O'Driscoll (1978; Stop 13); this material is augmented below.

The red K-feldspar porphyritic muscovite-biotite granite, locally containing minor garnet, is dissected by numerous brittle faults and joints. Locally it also contains a weak shear fabric with structures suggesting dextral strike-slip movement. The shear fabric formed under greenschist facies or lower conditions, as feldspar shows no recrystallization. Cross-cutting pegmatite zones in these outcrops contain garnet and tourmaline.

Stop 1.9: Hermitage Bay fault in Northwest Brook granite (47°41'53.89" N, 55°34'19.32" W)

From Stop 1.8, continue southward on Route 360 for 6.2 km to the Junction for Route 362. The road descends into the deep valley that marks the trace of the Hermitage Bay fault. Turn left on Route 362, and shortly afterwards (275 m), turn left into large gravel pits located in the bottom of the valley.

In these outcrops, K-feldspar porpyritic granite akin to that observed at Stop 1.6 is chloritized and deformed into a subvertical cataclasite and associated minor ductile-brittle shears. Lineation is shallowly plunging and indicates the fault here accommodated mainly strike-slip movements. No reliable shear-sense indicators have been observed.

Stop 1.10: Sheared mafic volcanic rocks of Avalonian affinity on the other side of the Hermitage Bay fault (47°41'51.34" N, 55°34'13.03" W)

From Stop 1.9, return to Route 362, and drive westward to the first prominent set of roadcut outcrops (c. 250 m).

We have now crossed into Avalonia. The original rock type for these outcrops is not easily resolved due to their extensive brittle deformation overprint, but the dark colour and abundance of chlorite and epidote strongly suggests a mafic volcanic protolith, and they are assigned to the Doughball Point Formation (part of the Connaigre Bay Group) of O'Brien (1998).

Day Two: Paleozoic evolution of the Avalonian rocks of northern Fortune Bay and the Connaigre Peninsula

The Day Two field stops are all located in the area between Highway 360 and the communities of Pool's Cove, Belleoram, English Harbour West and Wreck Cove (Fig. 8). Some adjustment of stop order may be needed for time-management purposes.

Stop 2.1: Simmons Brook Intrusive Suite and possible Devonian granite dykes (47°39'55.85" N, 55°31'19.36" W)

From Baie d'Espoir, proceed along Route 361 to Route 360, and drive southward past previous from Day One, and then turn left onto Route 362, passing Stop 1.9 from Day One. Follow Route 362 (signed for Pool's Cove and Belleoram) for a distance of 5.8 km from its junction with Route 360, and turn right (south) on to a gravel road that leads to a nearby communication tower. The road may be rough and difficulty to turn on, but the outcrops can easily be accessed on foot from the junction with Route 362.

The Simmons Brook Intrusive Suite consists of hornblende ± biotite bearing granodiorite to quartz-diorite quartz with lesser amounts of granite and gabbro. These rocks extend from Harbour Breton in the southwest to East Bay in the northeast, forming a 5- to 10-km wide band bounded by the East Bay-White Horse fault in the south and the Hermitage Bay in the North. In the East, the Simmons Brook Suite is unconformably overlain by the Pool's Cove Formation (Stop 2-3), and in that locality it has been dated at 621 ± 3 Ma (O'Brien et al., 1995). It is intruded by K-feldspar porphyritic hornblende granite, grouped with the Harbour Breton Granite, which yielded a preliminary U-Pb zircon age of ca. 575 Ma (Kellett et al., 2014). The outcrops in the road show the typical homogeneous and hornblende-rich character of this unit, and also contain dykes of pink felsic granite to porphyry, which clearly intrude the granodiorite. Visually, these rocks resemble some variants of the "Old Woman Stock", a Devonian granite to be visited later in the day, and they are thought to be of the same age. However, given the lack of direct age data and the presence of several generations of granitoid rocks in this part of Avalonia, other interpretations cannot be ruled out.

The Simmons Brook Intrusive Suite has an unusually evolved Nd isotope signature (ƐNd of -6.3 to -8.2 at 600 Ma) compared to other intrusive rocks across Avalonia in Newfoundland, which almost all have "juvenile" Nd isotopic signatures (ƐNd of +1 to +6) . This result suggests an older crustal component in the area of northern Fortune Bay that is not reflected amongst intrusive rocks of equivalent age to the east (Kerr et al., 1995). More data are required to confirm and possibly extend this pattern, and to assess its significance in the light of other new results, such as the Silurian age for the Pass Island Granite (Kellett et al., 2014; see earlier discussion).

Stop 2.2: Devonian dykes intruding the Pool's Cove Formation (47°39'18.50" N, 55°30'7.60" W)

From Stop 2.1, return to Route 362, and continue east to the junction where the road to Pool's Cove diverges, a distance of about 1.9 km.

This location introduces the terrestrial sedimentary rocks of the Pool's Cove Formation. The red conglomerate is intruded by several porphyritic felsic dykes, which are probably offshoots of the ca. 376 Ma Old Woman Stock granite pluton (see stop 2.11 below).

The dykes have prominent contact metamorphic aureoles, despite their narrow widths. The extent of the metamorphic aureole suggests that the intrusion of the Middle Devonian dykes took place whilst the conglomerate was still wet, and that the water contained in the sediments acted as a heat carrier. If the correlation with the Old Woman stock is correct, the Pool's Cove Formation is late Early to Middle Devonian. Closely similar dykes are also found along the coast of the Cinq Isles, consistent with their correlation with the nearby Old Woman Stock pluton.

Stop 2.3: Basal unconformity of the Pool's Cove Formation (47°39'48.53" N, 55°29'20.04" W)

From Stop 2.2, continue 1.4 km east towards Pool's Cove, and examine outcrops exposed in Simmons Brook to the left (north) of the road; a short access trail is located just before the bridge. This locality is also described in the Traveller's Guide to the Geology of Newfoundland and Labrador (Colman-Sadd and Scott, 1994; Stop 49).

The outcrop about 30 m upstream shows the near-vertical unconformity at the base of the Lower to Middle Devonian Pool's Cove Formation, which here is in contact with granitoid rocks of the Simmons Brook Intrusive Suite. The granitoid rocks are cut by narrow diabase dykes, and pebbles of the older unit are included within the basal layers of the younger sedimentary unit. In other locations similar conglomerate is in tectonic contact with older rocks, or lies disconformably (Greene and O'Driscoll, 1976; Williams and O'Brien, 1995) upon the Cinq Isles Formation, which hence is older and probably Lower Devonian. The Cinq Isles Formation appears to have been subjected to more intense deformation, including cleavage formation, consistent with the presence of an unconformity within the Devonian sedimentary sequence (see stop 2-10 for further discussion)

Stop 2.4: Pool's Cove Formation – conglomerates with plutonic boulders (47°40'35.74" N, 55°25'37.22" W)

From Stop 2.3, continue 7.6 km to Pool's Cove, and stop by the fish warehouse facility close to the end of the road.

In this location, the Pool's Cove Formation consists of boulder conglomerates, with strata dipping at about 30° to the southwest; aside from the tilting, deformation is absent. The boulders are mainly of plutonic composition and derived from the adjacent Neoproterozoic intrusive suites that were being eroded at that time. Elsewhere, the conglomerate also contains sedimentary, metamorphic, and volcanic cobbles, and also quartz clasts probably derived from vein materials.

The deformation of the Pool's Cove Formation is very heterogeneous and its attitude varies from nearly horizontal to moderately- or steeply-dipping, due to upright folding. Foliations are locally developed, and deformation seems to increase in intensity adjacent to faults.

Stop 2.5: Deformed (folded) rocks of the Chapel Island Formation (47°35'49.09" N, 55°30'40.14" W)

From Stop 2.4, return from Pool's Cove to the junction at Stop 2.2 (about 9 km), and continue on the road towards Belleoram for approximately 6.9 km. Outcrops on both sides of the road show rusty weathering.

The sedimentary rocks mapped as part of late Ediacaran to Early Cambrian Chapel Island Formation by O'Brien et al. (1995). These sedimentary rocks conformably overlie shallow marine sediments assigned to the Rencontre

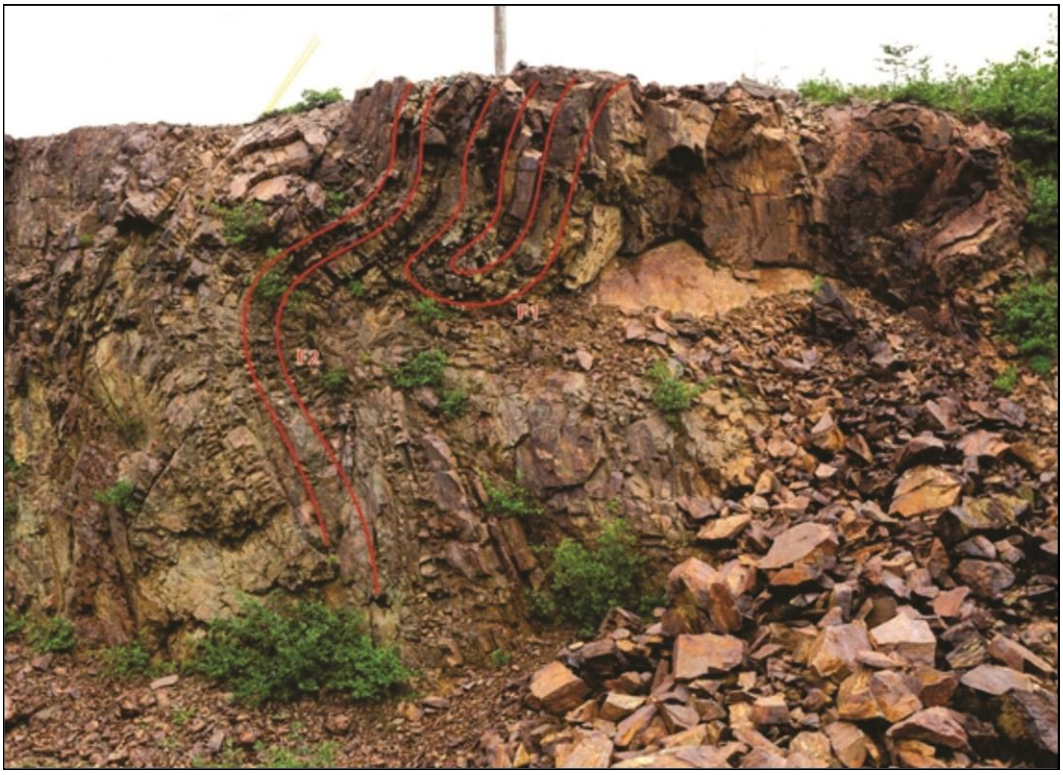

Plate 1 – F1 and F2 folding in rocks assigned to the Chapel Island Formation, along Route 361 (Stop 2.5).

Formation. Sedimentation was essentially continuous across the Precambrian-Cambrian boundary, as seen also on the southern part of the Burin Peninsula, across Fortune Bay. This outcrop comprises sandstones, siltstones and dark shales, which are complexly folded and locally cleaved (Plate 1). Along the coast, folding in this unit is associated with small thrust zones, and the development of broken formations (are these tectonic melanges?). The intensity of deformation in these older rocks is generally more intense and complex compared to the heterogeneous and localized deformation observed in the Cinq Isles and Pool's Cove formations. The outcrop suggests that the Chapel Island Formation was subjected to a complex deformation involving folding and faulting, both of which are inferred to have occurred during the Early Devonian Acadian orogeny. The polarity and asymmetry of folds in these outcrops suggests that they are southeast-verging.

Stop 2.6: Unconformity beneath the Great Bay de l'Eau Formation (47°27'42.51" N, 55°29'33.35" W)

From Stop 2.5, continue south for 13 km on Route 362, and then turn right at the intersection. Continue on Route 363 for 4.9 km, and then turn left at the junction for English Harbour West. After about 0.9 km, turn left again at the Stop sign, and continue for another 0.6 km.

These outcrops show moderately to steeply south-dipping white quartzite assigned to the Cambrian Random Formation, which conformably overlies clastic sedimentary rocks assigned to the Chapel Island Formation. The Random quartzite in turn is overlain by red and green shale, mudstone and minor sandstone assigned to the Chamberlains Brook Formation. The Ediacaran to Cambrian succession is unconformably overlain by the gently south-

Plate 2 – Angular unconformity between Cambrian (Chapel Island and Chamberlain Brook formations) and Devonian sedimentary rocks of the Great Bay de l'Eau Formation at Blue Pinion Cove.

dipping Great Bay de l'Eau Formation (visible from the other side of the bay), which in turn is intruded by the Middle to Late Devonian Belleoram granite (O'Brien, 1998; see Plate 2). The relationships suggest that the Great Bay de l'Eau Formation is probably Middle to Upper Devonian in age, and probably was deposited during the last stages of the Acadian orogenic episode; the angular unconformity is inferred to mark the uplift and exhumation of Avalonia following the deformation induced during the main phase of the Acadian Orogeny.

Stop 2.7: Belleoram Granite (47°30'43.33" N, 55°24'33.16" W)

From Stop 2.6, return to Route 363, and drive back to the intersection with Route 362. Continue on Route 363 towards Belleoram for about 6.2 km to roadside outcrops located high on a hillside above the water, with spectacular views across to Chapel Island.

These outcrops are typical of the Belleoram Granite. In clear weather, the view across to Chapel Island reveals a cross-section through the roof zone of the granite, and granitic and composite mafic-felsic dykes cutting country rocks of the Chapel Island Formation.

The Belleoram Granite represents one two Devonian granitoid intrusions in the area; the other is represented by the Middle Devonian (ca. 376 Ma) Old Woman Stock (see Stop 2.11). The two Devonian intrusions comprise equigranular grey to pink, quartz monzonite to granodiorite, and red feldspaphyric microgranite (O'Brien et al., 1995). The Belleoram Granite is presently undated (work is in progress) but its age is constrained by the fact that it intrudes both the Chapel Island and Pool's Cove formations. The Belleoram Granite is characterized by the widespread presence of rounded, fine-grained mafic enclaves. By comparison with similar features described from many other granite plutons, such as the Fogo Island Intrusion, these are interpreted as frozen globules of coexisting mafic

or hybrid magmas (e.g., Kerr, 2013). Nd isotope investigations of these inclusions and their host granites (Morrissey, 1993; Kerr et al., 1995) show that they have the same signatures (ƐNd of around +2) indicating that the mafic and felsic magmas either had similar sources or that inclusions were isotopically homogenized with surrounding magma.

Stop 2.8: Porphyritic phase of the Belleoram Granite (47°29'36.04" N, 55°27'45.10" W)

From Stop 2.7, a short scenic excursion towards Belleoram may be possible; the views of this picturesque community and the surrounding steep mountains are spectacular. Returning via Route 363, Stop 2.8 is a small quarry is located on the left (south) of the road, approximately opposite the junction with Route 362.

Optional stop that reveals a high-level porphyritic variant of the Belleoram Granite.

Stop 2.9: The Boxey Trail Section (47°27'21.61" N, 55°32'35.38" W)

From Stop 2.8, return to Route 363, and continue southwest for about 10 km, to the signpost for the "Boxey Trail", which diverges to the left to access the shore along a small peninsula. The Stop contains two parts, accessed by a short hike.

The first outcrop (Stop 2.9A; 47°26'49.84" N, 55°32'41.70" W) shows gently-dipping red conglomerates of the Great Bay de l'Eau Formation, which here dip gently to the southeast. The second outcrop (Stop 2.9B; 47°26'40.79" N, 55°32'58.98" W) shows complex intrusive relationships, where granitic dykes intrude the conglomerate. There are also basaltic units here, which are interpreted as sills; these are probably equivalent to basaltic volcanics that occur within higher parts of the Great Bay de l'Eau Formation (Williams, 1971; O'Brien, 1998). The granitic rocks are undated, but equated with the Belleoram Granite; the mafic sills and flows also remain undated.

Stop 2.10: Acadian folding and thrusting of the Cinq Isles Formation at Wreck Cove (47°29'49.89" N, 55°36'31.89" W)

From Stop 2.9, return to Route 363, and continue south for 5.5 km, and then turn right on the road to Wreck Cove. Drive for 4.5 km, then turn left just before Cox's Grocery Store, and park by the wharf to walk along the shore.

Gently-dipping sedimentary rocks of the Cinq Isles Formation, the oldest Devonian sedimentary unit in the area, are here affected by a variety of structural complications. The Cinq Isles Formation is the oldest unit incorporating Devonian terrestrial and/or shallow marine sedimentary rocks ("Old Red Sandstone") in the northern Fortune Bay area. It comprises red micaceous sandstone, quartz-pebble conglomerate, red mudstone and red and grey limestone. The latter forms a distinctive part of this unit. The Cinq Isles Formation unconformably overlies the Simmons Brook intrusive suite west of Pool's Cove. It is commonly more intensely and complexly deformed than the overlying Middle-Upper (?) Devonian red beds, suggestive of an important Early-Middle Devonian (Acadian) unconformity within the Devonian sequence. The Cinq Isles Formation is interpreted as a foredeep molasse sequence that was deposited at a relatively early stage of the Acadian orogeny, as a result of the progressive tectonic loading of Avalonia by Ganderian rocks.

Stop 2.11: Mineralization and alteration in the granite of the Old Woman Stock (47°35'37.84" N, 55°30'39.64" W)

This stop is located 12.5 km north of the Route 362/Route 363 intersection, within a large area of quarries and gravel pits located on the right (east) side of Route 362.

The outcrops consist of variably altered and bleached granite and quartz-feldspar porphyry, with localized fresh areas where original textures are well-preserved. The alteration includes abundant sericite, and is suspected to also include clay-mineral alteration such as kaolinite and dickite. Alteration of this type is typical of high-level mineralized granites. Mineralization is sporadic at this locality, and consists of disseminated splashes of molybdenite and patches of interstitial fluorite; there is also widespread very-fine-grained pyrite in many areas. A larger molybdenite showing including both disseminated and vein-hosted molybdenite mineralization (Leonard's Find) is located less than 1 km to the southwest, and several other molybdenite and fluorite indications are noted in the area.

The Old Woman Stock was originally included with the Harbour Breton Granite, but was recognized as a discrete younger unit by O'Brien (1998). The presence of narrow granite veinlets in the adjacent Pool's Cove conglomerate in the northern part of the intrusion (O'Brien et al., 1995) and the presence of probable consanguineous porphyritic dikes at Stop 2.2 suggest that the pluton might extend much further to the northeast at depth. Kellett et al. (2014) report a U-Pb zircon age of 376 ± 3 Ma for the Old Woman Stock, which provides a younger age constraint for the Pool's Cove Formation. Lynch et al. (2012) report a slightly older Re-Os molybdenite age of ca. 382 Ma for the nearby Leonard's Find showing.

This is the final stop for Day Two. From here, return to Route 360 and to Baie d'Espoir.

Day Three: Some miscellaneous outcrops along Route 360.

The Stops for Day Three are of general interest, and two have connections to economic geology and mineral potential. Other Stops are of general geological interest for students. Locations for these stops are shown in Figure 7.

Stop 3.1: Tungsten-bearing skarns and granite veins, Great Gull Lake area (48°16'31.12" N, 55°28'39.86" W)

From Baie d'Espoir, return to Route 360, and turn north towards Bishops Falls and the Trans-Canada Highway. Drive northward for approximately 38.8 km, to a series of quarry pits located on the right (east) side of the road. If coming in the opposite direction, the location is about 2.4 km south of a gravel access road to a communication tower, which branches off to the east about 8 km south of where Route 360 passes the shores of Little Gull Lake, These outcrops may be partially flooded and not fully accessible in all areas; participants should take care around steep slopes located above flooded areas. A general description of these outcrops is given in the Traveller's Guide to the Geology of Newfoundland and Labrador (Colman-Sadd and Scott, 1994; Stop 46); this is augmented below.

These outcrops are located in metasedimentary rocks of the Baie d'Espoir Group, which probably form part of the North Steady Pond Formation, dominated by grey-green shale, slate and sandstone, locally calcareous, and rusty-weathering due to disseminated pyrite. Bedding in the sedimentary rocks here dips gently to moderately southwest, but in some areas appears steep, suggesting that folds are present. These sedimentary host rocks are partially replaced by massive white material dominated by carbonates and calc-silicates; these zones are quite striking and have a gneiss-like appearance in some areas, presumably because relict bedding is preserved as dark streaks. The replacement zones contain disseminated pyrrhotite bands, and also a pale green mineral that resembles malachite (but may not be). Locally, they contain clinopyroxene, garnet and the tungsten-bearing mineral scheelite ($CaWO_4$). Scheelite is difficult to identify on the basis of appearance, and is commonly present in small amounts; its best diagnostic property is blue fluorescence under short-wave UV light, which we will not be able to demonstrate. The outcrop is cut by numerous veins of texturally variable muscovite-bearing granite, pegmatite and aplite, and surrounding outcrops also contain numerous quartz veins. Some of the quartz veins are also reported to contain scheelite, and one loose sample of vein material examined by A. Kerr in 2009 contained a black mineral thought to be the similar mineral wolframite ($(Fe,Mn)WO_4$). No detailed mineralogical, petrological or geochemical work has ever been conducted on these occurrences, but they would make an excellent undergraduate thesis topic for the right individual.

These zones are believed to be skarns, developed through the interaction of hydrothermal fluids from nearby granitoid intrusions with calcareous and pyritiferous rocks of the Baie d'Espoir Group. They have been explored on a limited scale (see Kerr et al., 2009, for a review and references), but both channel sampling and three reconnaissance drill holes yielded only sporadic low-grade material, forming multiple narrow zones (typically a few cm thick) containing < 1 % WO_4. The best intersection was 0.2 m of 2.7 % WO_4. The drill core has not been examined or sampled, but descriptions suggest that scheelite is not always present in altered material. The granite and pegmatite veins that are common in these outcrops are interpreted to indicate the presence of an underlying intrusion, perhaps part of the Middle Ridge Granite, an extensive leucogranite body that has given an early Devonian U-Pb monazite age (410 ± 3 Ma; R. Tucker, quoted by Kerr (1997). The mineralization known in this area likely has no economic potential, but it represents the only skarn-type granophile mineralization yet reported in Newfoundland; the surrounding areas may have potential for further exploration, given interest in tungsten as a commodity.

Stop 3.2: Chromite and magnesite in the Great Bend Ophiolite (48°32'54.16" N, 55°29'43.30" W)

From Stop 3.1, continue 33.3 km northward, to the area of the Great Bend ophiolite (also visited on Day One). This stop is located a short distance (0.8 km) south of the large quarry visited at Stop 1.1, close to an open area located on the right (east) side of the road. An abandoned road leads to a smaller quarry, a few hundred metres from the road. It is described by Colman-Sadd and Swinden (1983; Stop 15) and Colman-Sadd and Scott (1994; Stop 45).

The ultramafic rocks in this area lie close to the transition into gabbroic rocks exposed to the south, and have been pervasively altered to magnesite ($MgCO_3$), which is associated with white quartz. The magnesite weathers brown, but is white on fresh surfaces. Magnesite-rich zones occur in other Newfoundland ophiolites at approximately the same stratigraphic level, between the ultramafic rocks and overlying gabbroic material. The outcrops also contain chromite pods, which appear to have resisted the alteration that generated the magnesite. This area has been investigated for its potential as a magnesium source, but appears to be too small as presently defined. Information on previous work is contained in MODS file 002D/11/Mg008 and Kean (1974).

Stop 3.3: Sedimentary structures in the Botwood Group (48°58'26.21" N, 55°29'39.07" W)

From Stop 3.2, continue 51.8 km north on Route 360, back into rocks of the Dunnage Zone (Exploits Subzone).

These roadside outcrops are red and green sandstones of the Silurian Botwood Group. They display well-developed ripple marks and locally have bedding surfaces that display mud cracks suggesting periodic desiccation. The description is taken from Colman-Sadd and Swinden (1983).

From Bishop's Falls, the field trip returns to Gander and St. John's.

References

Blackwood, R.F., 1985. Geology of the Grey River area, southwest coast of Newfoundland; in Current Research: Newfoundland Department of Mines and Energy, Mineral Development Division, Report 85-1, p. 198-209.

Blackwood, R.F., and Green, L., 1982. Geology of the Great Gull Lake – Dead Wolf Pond area (2D/06, 2D/10); Newfoundland Department of Mines and Energy, Mineral Development Division, Report 82-1, p. 51-64.

Colman-Sadd, S.P., 1976. Geology of the St. Alban's Map area, Newfoundland (1M/13); Newfoundland Department of Mines and Energy, Mineral Development Division, Report 76-4, 19 p.

Colman-Sadd, S.P., 1979. Geology of the Twillick Brook Map area, Newfoundland (2D/4); Newfoundland Department of Mines and Energy, Mineral Development Division, Report 79-2, 23 p.

Colman-Sadd, S.P., 1980. Geology of south-central Newfoundland and evolution of the eastern margin of Iapetus; American Journal of Science, v. 280A, p. 991-1017.

Colman-Sadd, S.P., 1985. Geology of the Burnt Hill map area, Newfoundland. Newfoundland; Newfoundland and Labrador Department of Mines and Energy, Mineral Development Division, Report 85-3, 94 p.

Colman-Sadd, S.P., and O'Driscoll, C.F., 1978. Field trip guide for Baie d'Espoir and Hermitage Peninsula; Geological Association of Canada, Newfoundland and Labrador Section, Fall Field trip for 1978. Available from www.gac-nl.ca.

Colman-Sadd, S. P., and Scott, S., 1994. Traveller's Guide to the Geology of Newfoundland and Labrador; Map and guide to stops of interest; Geological Association of Canada, Newfoundland and Labrador Section. Available from www.gac-nl.ca.

Colman-Sadd, S.P., and Swinden, H.S., 1982. Geology and mineral potential of south-central Newfoundland; Newfoundland Department of Mines and Energy, Mineral Development Division, Report 82-8, 102 p.

Colman-Sadd, S.P., and Swinden, H.S., 1983. Road log and stop descriptions for Baie d'Espoir field trip; Geological Association of Canada, Newfoundland Section, Fall Field Trip 1983. Available at www.gac-nl.ca.

Colman-Sadd, S.P., Dunning, G.R., and Dec, T., 1992. Dunnage-Gander relationships and Ordovician orogeny in central Newfoundland: a sediment provenance and U/Pb study; American Journal of Science, v. 292, p. 17-355.

Dickson, W.L., 1990. Geology of the North Bay Granite Suite and metasedimentary rocks in southern Newfoundland (NTS 11P/15E, 11P/16 and 12A/2E); Newfoundland Department of Mines and Energy, Geological Survey Branch, Report 90-3, 101 p.

Dickson, W.L., Delaney, P.W., and Poole, J.C., 1985. Geology of the Burgeo Intrusive Suite and associated rocks in the Ramea (11P/11) and La Hune (11P/10) map areas; Geological Survey of Canada, Paper 85-1B, p. 601-608.

Dunning, G., O'Brien S.J., Colman-Sadd, S.P., Blackwood, R., Dickson, W.L., O'Neill, P.P., and Krogh T.E., 1990. Silurian orogeny in the Newfoundland Appalachians; Journal of Geology, v. 98, p. 895-913.

Greene, B.A., and O'Driscoll, C.F., 1976. Gaultois Map Area; Newfoundland Department of Mines and Energy, Mineral Development Division, Report 75-1, p. 3-9.

Harper, D.A.T., Owen, A.W., and Bruton, D.L., 2009. Ordovician life around the Celtic fringes: diversifications, extinctions and migrations of brachiopod and trilobite faunas at middle latitudes; *in* Early Paleozoic Gond-

wanan Terranes: New Insights from Tectonics and Biogeography, (ed.) M.G. Basset; Geological Society London Special Publication, v. 325, p. 157-170.

Hibbard, J., van Staal, C.R., Rankin, D., and Williams, H., 2006. Lithotectonic map of the Appalachian orogen, Canada – United States of America; Geological Survey of Canada, Map 2096A, scale 1:1 500 000.

Holdsworth, R.E., 1994. Structural evolution of the Gander-Avalon terrane boundary: a reactivated transpression zone in the NE Newfoundland Appalachians; Journal of the Geological Society, London, v. 151, p. 629-646.

Jenner, G.A., and Swinden, H.S., 1993. The Pipestone Pond Complex, central Newfoundland: complex magmatism in an eastern Dunnage Zone ophiolite; Canadian Journal of Earth Sciences, v. 30, p. 434-448.

Kean, B.F., 1974. Notes on the geology of the Great Bend and Pipestobe Pond ultramafic bodies; Newfoundland Department of Mines and Energy, Mineral Development Division, Report 74-1, p. 33-42.

Keen, C.E., Keen, M.J., Nichols, B., Reid, I., Stockmal, G.S., Colman-Sadd, S.P., O'Brien, S.J., Miller, H., Quinlan, G., Williams, H., and Wright, J., 1986. Deep seismic reflection profile across the Northern Appalachians; Geology, v. 14, p. 141-145.

Kellett, D.A., Rogers, N., McNicoll, V., Kerr, A., and van Staal, C.R., 2014. New age data refine extent and duration of Paleozoic and Neoproterozoic plutonism at Ganderia – Avalonia boundary, Newfoundland; Canadian Journal of Earth Sciences, v. 51, p. 943-972. doi:10.1139/cjes-2014-0090.

Kerr, A., 1997. Space-time composition relationships among Appalachian-cycle plutonic suites in Newfoundland; *in* The Nature of Magmatism in the Appalachian Orogen, (ed.) K. Sinha, J.B. Whalen, and J.P. Hogan; Geological Society of America, Memoir, v. 191, p. 193-220.

Kerr, A., 2013. The Fogo process from a geologist's perspective: a discussion of models and research problems; Newfoundland and Labrador Department of Natural Resources, Geological Survey, Report 2013-1, p. 233-267.

Kerr, A., Dickson, W.L., Hayes, J.P., and Fryer, B.J., 1993. Devonian post-orogenic granites on the southeast margin of the Newfoundland Appalachians: A review of geology, geochemistry and mineral potential; Newfoundland and Labrador Department of Mines and Energy, Geological Survey, Report 93-1, p. 239-279.

Kerr, A., Jenner, G.J., and Fryer, B.J., 1995. Sm-Nd isotopic geochemistry of Precambrian to Paleozoic granitoid suites and the deep-crustal structure of the southeast margin of the Newfoundland Appalachians; Canadian Journal of Earth Sciences, v. 32, p. 224-245.

Kerr, A., van Nostrand, T., Dickson, W.L., and Lynch, E.P., 2009. Molybdenum and tungsten in Newfoundland: A geological overview and a summary of recent exploration developments; Newfoundland and Labrador Department of Natural Resources, Geological Survey, Report 2009-1, p. 43-81.

Lynch, E.P., Selby, D., Feely, M., and Wilton, D.H.C., 2009. New constraints on the timing of molybdenite mineralization in the Devonian Ackley Granite suite, southeastern Newfoundland; preliminary results from Re-Os geochronology; Newfoundland and Labrador Department of Natural Resources, Geological Survey, Report 2009-1, p. 225-235.

Lynch, E.P., Selby, D., Feely, M., and Wilton, D.H.C., 2012. The timing and duration of granite- related magmatic-hydrothermal events in southern Newfoundland; results of Re-Os geochronology; GAC-MAC joint annual meeting, St, John's, 2012, Abstract.

Morrisey, R., 1993. The Belleoram granite, southern Newfoundland: petrology and geochemistry of magmatic inclusions; Unpublished B.Sc. thesis, Memorial University.

O'Brien, B., O'Brien, S., and Dunning, G.R., 1991. Silurian cover, Late Precambrian-Early Ordovician basement, and the chronology of Silurian orogenesis in the Hermitage Flexure (Newfoundland Appalachians); American Journal of Science, v. 291, p. 760-799.

O'Brien, S.J. (comp.), 1998. Geology of the Connaigre Peninsula and adjacent areas, southern Newfoundland; Geological Survey, Department of Mines and Energy, Open file Map NFLD/2660; 1: 100 000 scale.

O'Brien, S.J., O'Brien, B.H., Dunning, G.R., and Tucker, R.D., 1996. Late Neoproterozoic Avalonian and related peri-Gondwanan rocks of the Newfoundland Appalachians; *in* Avalonian and Related Peri-Gondwanan Terranes of the Circum-North Atlantic, (ed.) R. Nance, and M.D. Thompson; Geological Society of America, Special Paper 304, p. 9-28.

O'Brien, S.J., O'Dricoll, C.F., Greene, B.A., and Tucker, R.D, 1995. Pre Carboniferous geology of the Connaigre Peninsula and the adjacent coast of Fortune Bay, Southern Newfoundland; Newfoundland Department of Natural Resources, Report, 95-1, p. 267-297.

O'Neill, P.P., and Blackwood, R.F., 1989. A proposal for revised stratigraphic nomenclature of the Gander and Davidsville Groups and the Gander River ultrabasic belt of northeast Newfoundland; Newfoundland Department of Mines and Energy, Mineral Development Division, Report 89-1, p. 121-127.

Palmer, A.R., 1984. The Decade of North American Geology 1983 time scale; Geology, v. 11, p. 503-504.

Piasecki, M.A.J., 1988. A major ductile shear zone in the Bay d'Espoir area, Gander terrane, southeastern Newfoundland; Newfoundland Department of Mines and Energy, Mineral Development Division, Report 88-1, p. 135-144.

Rogers, N., van Staal, C.R., McNicoll, V., Pollock, J., Zagorevski, A., and Whalen, J., 2006. Neoproterozoic and Cambrian arc magmatism along the eastern margin of the Victoria Lake Supergroup: A remnant of Ganderian basement in central Newfoundland?; Precambrian Research, v. 148, p. 320-341.

Sandeman, H., McNicoll, V., and Evans, D.T., 2012. U-Pb geochronology and lithogeochemistry of the host rocks to the Reid Brook gold deposit, central Newfoundland; Newfoundland Department of Natural Resources, Geological Survey Branch Report 2012-1, p. 85-102.

Schofield, D., van Staal, C.R., and Winchester, J., 1997 Tectonic setting and regional significance of the Port aux Basques Gneiss, SW Newfoundland; Journal of the Geological Society London, v. 155, p. 323-334.

Tang, J.C., and Chemenda, A.I., 2000. Numerical modelling of arc-continent collision: application to Taiwan. Tectonophysics, v. 325, p. 23-42.

Valverde, P., Dunning, G., and van Staal, C.R., 2000. The Margaree orthogneiss (Port aux Basques Complex, SW Newfoundland): evolution of a peri-Gondwanan, Mid Arenig-Early Llanvirn, mafic-felsic igneous complex; Canadian Journal of Earth Sciences, v. 37, p. 1691-1710.

Valverde-Vaquero, P., van Staal, C.R., McNicoll, V., and Dunning, G., 2006. Middle Ordovician magmatism and metamorphism along the Gander margin in Central Newfoundland; Journal of the Geological Society, London, v. 163, p. 347-362.

Van der Velden, A.J., van Staal, C.R., and Cook, F.A., 2004. Crustal structure, fossil subduction and the tectonic evolution of the Newfoundland Appalachians: Evidence from a reprocessed seismic reflection survey; Geological Society America Bulletin, v. 116, p. 1485–1498.

van Staal, C.R., 1994. The Brunswick subduction complex in the Canadian Appalachians: Record of the Late Ordovician to Late Silurian collision between Laurentia and the Gander margin of Avalon; Tectonics, v. 13, p. 946-962.

van Staal, C.R., 2007. Pre-Carboniferous tectonic evolution and metallogeny of the Canadian Appalachians; *in* Mineral deposits of Canada: A Synthesis of Major Deposit-Types, District Metallogeny, the Evolution of Geological Provinces, and Exploration Methods, (ed.) W.D. Goodfellow; Geological Association of Canada, Mineral Deposits Division, Special Publication 5, p. 793-818.

van Staal, C.R., and Barr, S., 2012. Lithospheric Architecture and Tectonic Evolution of the Canadian Appalachians and Associated Atlantic Margin; *in* Tectonic Styles in Canada: the LITHOPROBE Perspective, (ed.) R. Clowes, J. Percival and F. Cook; Geological Association of Canada Special Paper 49, p. 41-95.

van Staal, C.R., and Zagorevski, A., 2012. Accreted Terranes of the Appalachian Orogen in Newfoundland: In the Footsteps of Hank Williams; Geological Association of Canada, Field Trip Guidebook A1, 2012; 118 p.

van Staal, Murphy, J.B., and Barr, S.M., 2012. Provenance and tectonic evolution of Ganderia: constraints on the evolution of the Iapetus and Rheic oceans; Geology, v. 40, p. 987-990.

van Staal, C.R., Sullivan, R.W., and Whalen, J.B., 1996. Provenance and tectonic history of the Gander Margin in the Caledonian/Appalachian Orogen: Implications for the origin and assembly of Avalonia; *in* Avalonian and Related Peri- Gondwanan Terranes of the Circum-North Atlantic, (ed.) R.D. Nance and M.D. Thompson; Geological Society of America, Special Paper 304: p. 347-367.

van Staal, C.R., Whalen, J.B., Valverde-Vaquero, P., Zagorevski, A., and Rogers, N., 2009. Pre-Carboniferous, episodic accretion-related, orogenesis along the Laurentian margin of the northern Appalachians; *in* Ancient Orogens and Modern Analogues, (ed.) J.B. Murphy, J.D. Keppie and A.J. Hynes; Geological Society of London Special Publications 327, p. 271-316.

van Staal, C.R., Zagorevski, A., McNicoll, V., and Rogers, N., 2014. The time transgressive Salinic and Acadian orogenesis, magmatism and old red sandstone sedimentation in Newfoundland; Geoscience Canada, v. 41, p. 138-164.

Williams, H., 1971. The geology of the Belleoram map area, Newfoundland; Geological Survey of Canada, Paper 70 -65, 39 p.

Williams, H., 1979. Appalachian Orogen in Canada; Canadian Journal of Earth Sciences, v. 16, p. 792-807.

Williams, H., 1995. The Appalachian/Caledonian Orogen: Canada and Greenland; Geological Survey of Canada, Geology of Canada Series no. 6, 944 p.

Williams, H., and O'Brien, S.J., 1995. Fortune Belt; in The Appalachian/Caledonian Orogen: Canada and Greenland, (ed.) H. Williams; Geological Survey of Canada, Geology of Canada, 6, p. 423-425 (also Geological Society of America, the Geology of North America, F- 1).

Williams, H., Colman-Sadd, S.P., and Swinden, H.S., 1988. Tectonostratigraphic subdivisions of central Newfoundland; *in* Current Research, Part B. Geological Survey of Canada, Paper, 88-1B, p. 91-98.

Williams, S.H., Boyce, W.D., and Colman-Sadd, S.P., 1992, A new Lower Ordovician (Arenig) faunule from the Coy Pond Complex, central Newfoundland, and a refined understanding of the closure of the Iapetus Ocean; Canadian Journal of Earth Sciences, v. 29, p. 2046-2057.

Williams, S.H., Harper, D.A.T., Neuman, R.B., Boyce, W.D., and MacNiocaill, C.,1995. Lower Paleozoic fossils from Newfoundland and their importance in understanding the history of the Iapetus Ocean; *in* Current Per-

spectives in the Appalachian-Caledonian Orogen, (ed.) J.P. Hibbard, C.R. van Staal and P.A. Cawood; Geological Association of Canada Special Paper 41, p. 115-126.

Zagorevski, A., van Staal, C.R., McNicoll, V., Rogers, N., and Valverde-Vaquero, P., 2008. Tectonic architecture of an arc-arc collision zone, Newfoundland Appalachians; *in* Formation and Applications of the Sedimentary Record in Arc-Collision Zones, (ed.) P. Clift and A. Draut; Geological Society of America, Special Paper 346, p. 309-334.

Zagorevski, A., van Staal, C.R., Rogers, N., McNicoll, V.J., and Pollock, J.C., 2010. Middle Cambrian to Ordovician arc-backarc development on the leading edge of Ganderia, Newfoundland Appalachians; Geological Society of America Memoir 206, p. 367-396.

Appendix II:

TGI 4 – Intrusion Related Mineralisation Project presentations

Compiled by

Neil Rogers

Identifying new vectors to hidden porphyry-style mineralisation

N. Rogers[1], A. Plouffe[1], J.B. Chapman[2], M.B. McClenaghan[1], D.A. Kellett[1] and R.A. Anderson[2]

1 Geological Survey of Canada, 601 Booth St. Ottawa, Ontario

2. Geological Survey of Canada, 605 Robson St., Vancouver, British Columbia

Abstract: Intrusion related (e.g., porphyry) deposits are the most important sources for Cu, Mo, W and Sn, along with Au, Ag, and PGEs. Porphyry deposits are large, low- to medium-grade deposits in which mineralisation is hosted within and immediately surrounding distinctive intrusive phases within larger intrusive complexes that commonly have prolonged emplacement histories. To develop more effective exploration criteria to identify and evaluate deeply buried and/or hidden fertile intrusive mineralizing systems, studies into Cu-Mo/Au and W-Mo-Sn systems are aimed at answering the following questions: i) Are there distinctive proximal and distal footprints for each deposit type that will allow identification of, and vectoring towards hidden economic deposits?; ii) Is there evidence of fertility within the root system of intrusions, i.e. what are the triggering conditions and indicators of an hydrothermal-magmatic system of size and duration sufficient to develop a large porphyry deposit? To help answer these questions studies are being undertaken at sites associated with the Triassic-Jurassic porphyry deposits of the British Columbia interior and for the array of mineralised Canadian Appalachian Siluro-Devonian intrusions, for which the fundamental geoscience knowledge is often lacking.

A common problem facing Cordilleran and Appalachian exploration is how to detect intrusion-related mineralization through the extensive glacial sediment cover. Consequently, research activities are focussing at identifying key geochemical and mineral indicators in till near known mineralization and their detrital dispersal down-ice. Indicators are being developed for the detection of mineralization, but also the alteration halos and vein systems associated with mineralization, which represent much larger exploration targets than the actual economic orebody itself. Once identified in till, these indicators can be traced to their bedrock source using reconstructed ice movement vectors.

Structural relationships indicate that Sn-W-Mo mineralised intrusive systems can form due to extension associated with far removed non-orthogonal accretion. Deposits within these bodies form along fluid pathways such as the intersection of high-angle syntectonic breaks. Mineral potential can also be resolved through trace element fingerprinting. Subtle compositional changes in commonly occurring minerals (i.e., biotite) and fluid inclusions provide evidence of chemical variations related to magma fertility and vectors to mineralisation.

Originally presented Fredericton 2014: Geological Association of Canada - Mineralogical Association of Canada Joint Annual Meeting, Special Session 3: Discovering the Next Generation of Porphyry Deposits: Advancements in Locating and Understanding Hidden Intrusion-related Mineralization. May 21, 2014.

Corresponding author: Neil Rogers (nrogers@nrcan.gc.ca)

Rogers, N., Plouffe, A., McClenaghan, M.B., Kellett, D.A., Anderson, R.A., 2015. Identifying new vectors to hidden porphyry-style mineralisation; *in* TGI 4 – Intrusion Related Mineralisation Project: New Vectors to Buried Porphyry-Style Mineralisation, (ed.) N. Rogers; Geological Survey of Canada, Open File 7843, p. 249-291.

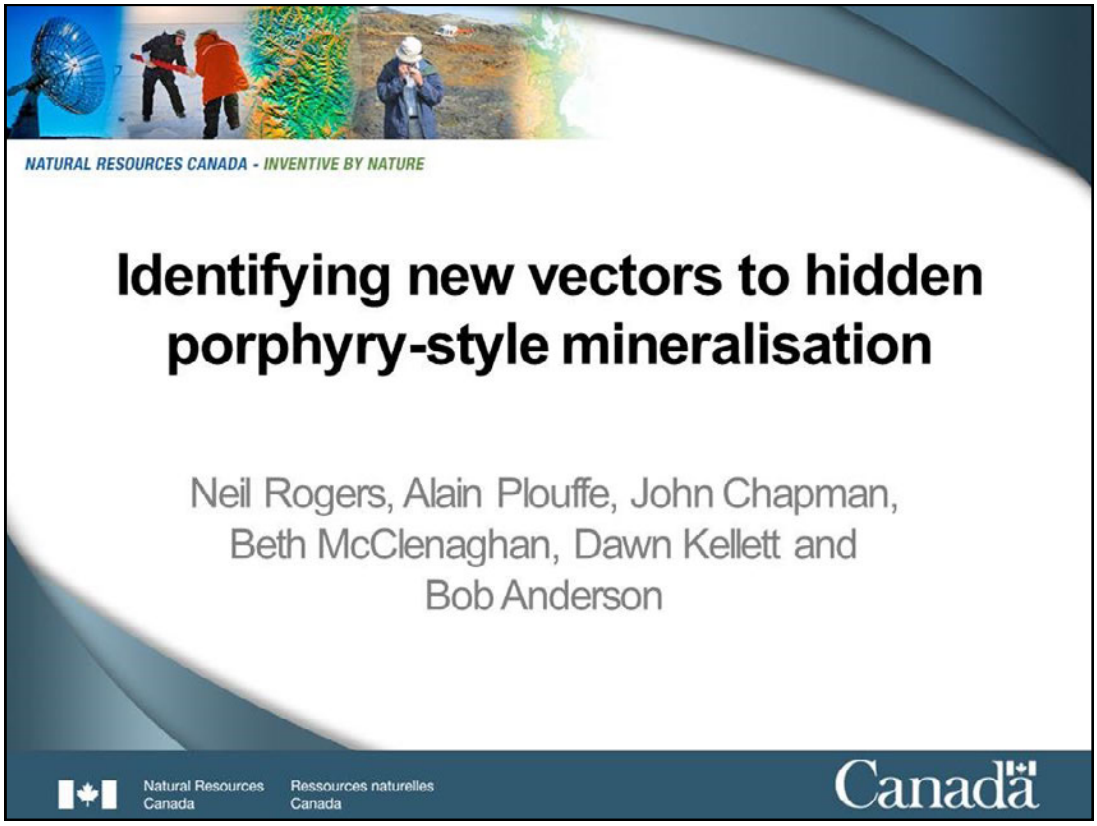

Fredericton 2014

Wednesday, 21 May

SS3: Discovering the Next Generation of Porphyry Deposits: Advancements in Locating and Understanding Hidden Intrusion-related Mineralization

Neil Rogers (Neil.Rogers@NRCan-RNCan.gc.ca), Bob Anderson, John Chapman, Dawn Kellett, Beth McClenaghan, Alain Plouffe

MacLaggan Hall, Room 53

Porphyry-style deposits are the world's foremost sources for Cu, Mo, W and Sn, plus major sources of Au, Ag, and PGEs. They are typically large, low- to medium-grade deposits hosted within and near distinctive intrusive phases. Metal content is diverse and reflects tectonic settings; Cu and Cu-Mo deposits are relatively abundant in island- and continental-arc terranes, whereas Mo and W-Mo deposits are associated with extension of continental crust. This Special Session will investigate their genetic controls and distal footprints that identify hidden economic porphyry-style deposits by highlighting new ways to predict, identify, model, and evaluate fertile intrusive mineralizing systems. Themes will include tectonic settings, structural controls, mineral and fluid inclusion compositions, and surficial and biogeochemical indicators of covered and deep porphyry deposits.

Natural Resources Canada Ressources naturelles Canada Canada

TGI 4 Objectives

"Geoscience knowledge to support enhanced effectiveness of deep exploration"

Natural Resources Canada Ressources naturelles Canada

Canada

TGI 4 Objectives

"Geoscience knowledge to support enhanced effectiveness of deep exploration"

1) Develop more robust measures of whether a geological system may contain deeply buried ore (**system fertility**), as well as indicators that provide the direction to that ore (**exploration vectors**), in order to reduce exploration risk

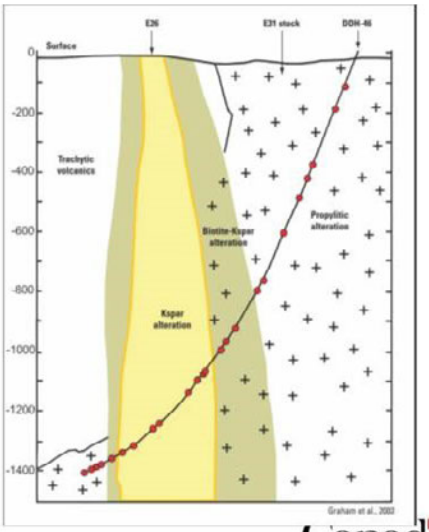

Natural Resources Canada Ressources naturelles Canada

Canada

TGI 4 Objectives

"Geoscience knowledge to support enhanced effectiveness of deep exploration"

2) Develop new geoscience knowledge and innovative techniques to model and detect Canada's major mineral systems.

Natural Resources Canada Ressources naturelles Canada

Canada

TGI 4 Objectives

"Geoscience knowledge to support enhanced effectiveness of deep exploration"

3) Train and mentor students to increase the number of HQP available to the mineral industry.

Natural Resources Canada Ressources naturelles Canada

Canada

Ore system approach to project definition

- **Base Metals:**
  - **Intrusion-related (Cu-Mo, Cu-Au, Mo-W, Sn-In)**
  - Ni-Cu-(PGE)-Cr
  - Pb-Zn SEDEX
  - Polymetallic VMS
- **Precious Metals:**
  - Lode Gold
  - (Ni-Cu)-PGE
- **Other:**
  - Uranium
  - Specialty Metals
- **Method Development**

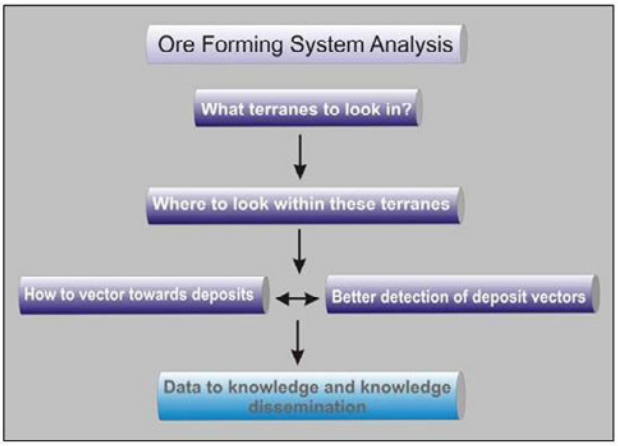

Ore Systems focus on processes of formation, not characteristics of ore deposits

Natural Resources Canada Ressources naturelles Canada

Canada

TGI 4 Intrusion-Related Mineralisation Project

Porphyry-style deposits

2 sub-projects

- *Arc related Cu- and Cu-Au porphyries*
- *Post-accretionary Sn – W – Mo – In*
- Objective to assist in the discovery/development of next generation (hidden/buried) deposits
- Hypothesis driven activities
  - Hierarchical nested hypotheses
- Porphyry ore-system components are: source controls; transport; deposition; and discovery
  - Activities focused on source control and discovery

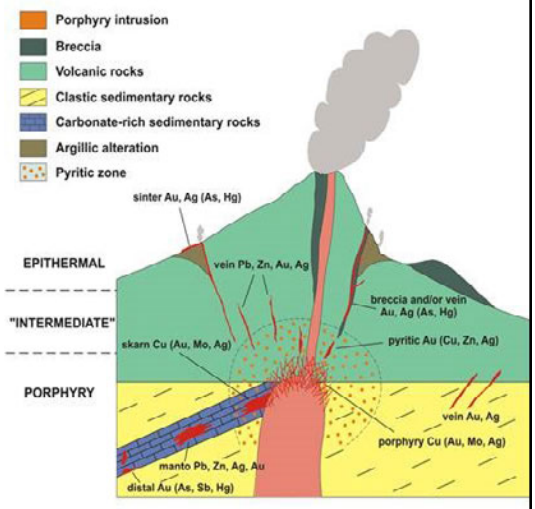

Canada

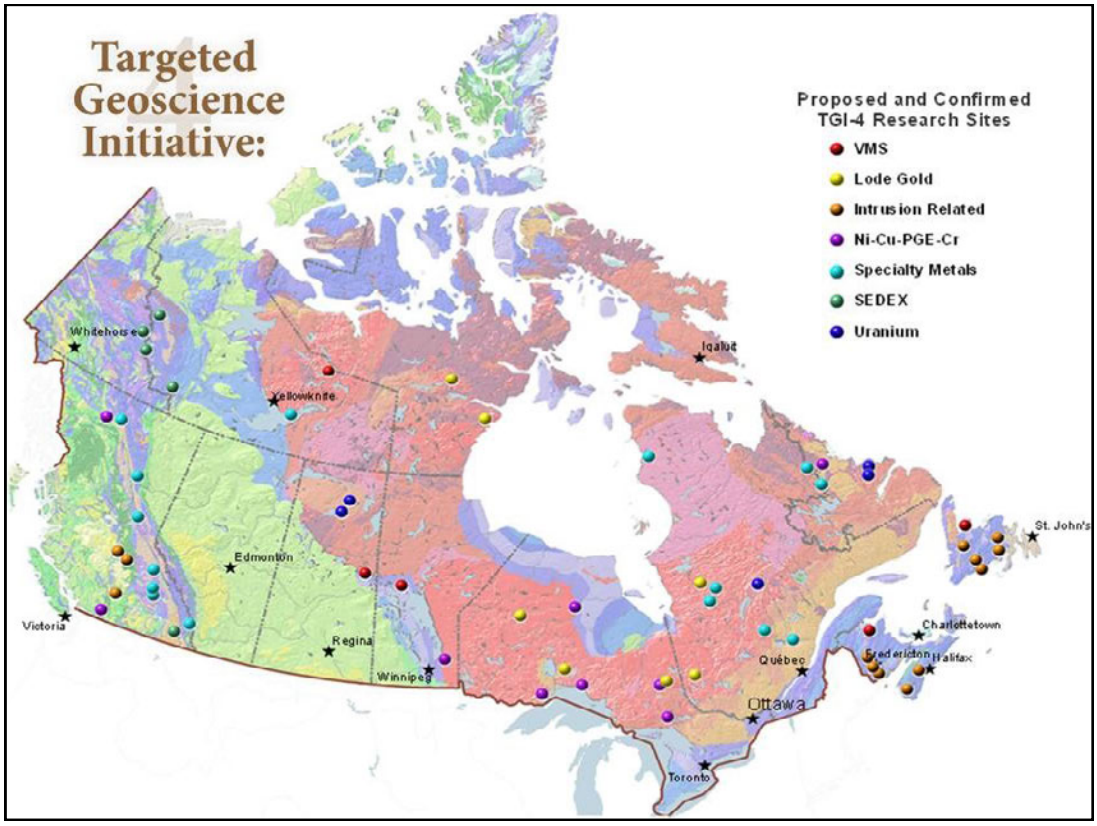
Targeted
Geoscience
Initiative:
Proposed and Confirmed
TGI-4 Research Sites
VMS
Lode Gold
Intrusion Related
Ni-Cu-PGE-Cr
Specialty Metals
SEDEX
Uranium
Whitehorse
Yellowknife
Iqaluit
Edmonton
Victoria
Regina
Winnipeg
Québec
Ottawa
Toronto
St. John's
Charlottetown
Fredericton
Halifax

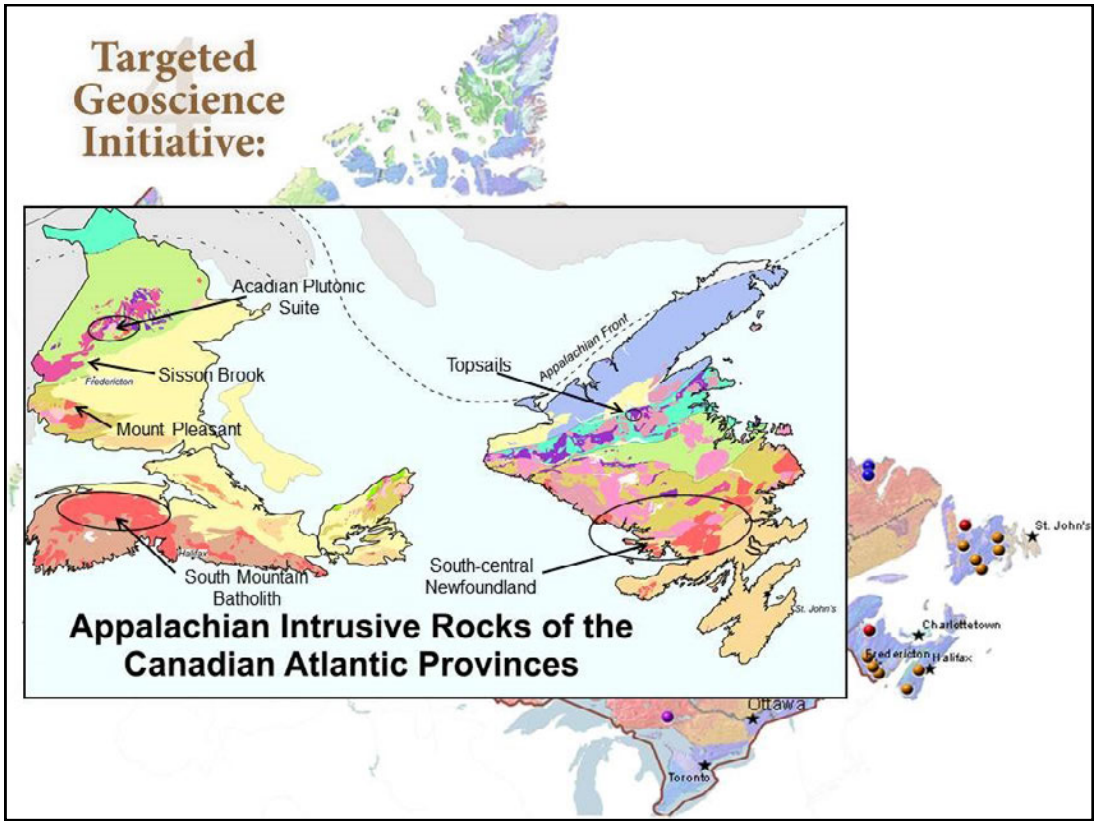
Targeted
Geoscience
Initiative:
Acadian Plutonic
Suite
Sisson Brook
Mount Pleasant
South Mountain
Batholith
Topsails
Appalachian Front
South-central
Newfoundland
Appalachian Intrusive Rocks of the
Canadian Atlantic Provinces
Ottawa
Toronto
St. John's
Charlottetown
Fredericton
Halifax

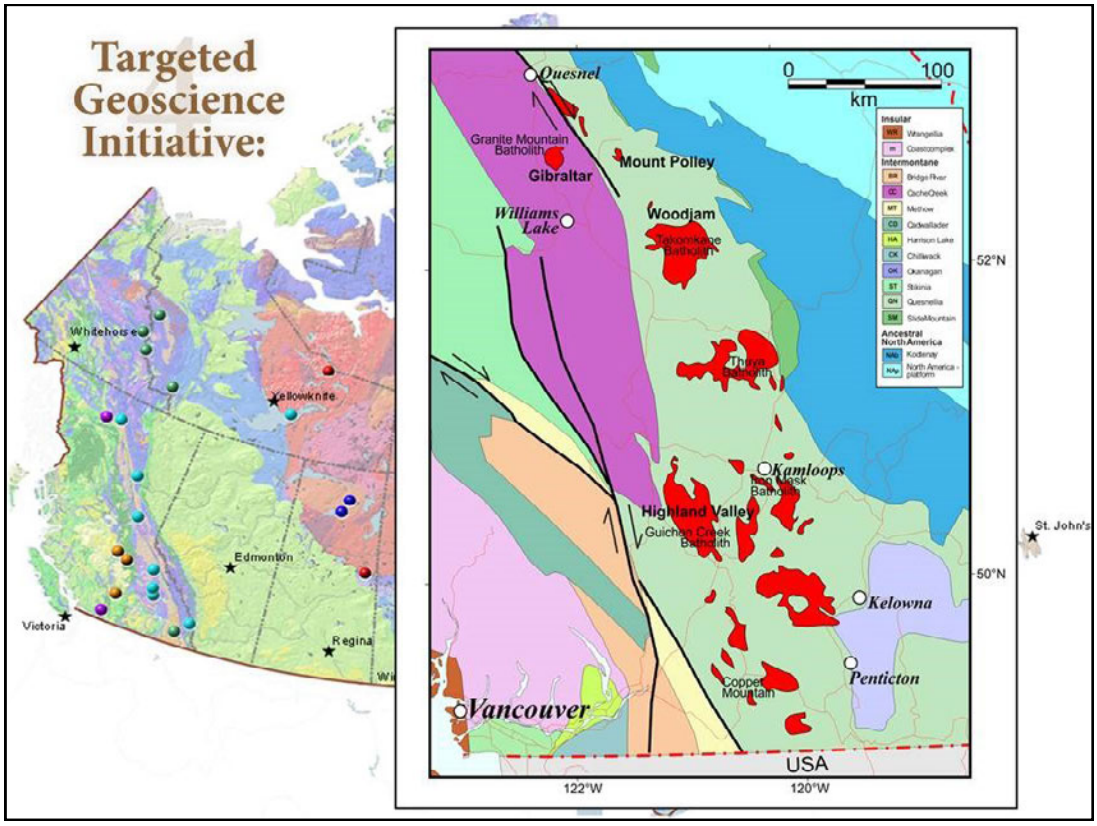
Targeted Geoscience Initiative:
Whitehorse
Yellowknife
Edmonton
Victoria
Regina
Quesnel
Granite Mountain Batholith
Gibraltar
Mount Polley
Williams Lake
Woodjam
Takomkane Batholith
Thuya Batholith
Kamloops
Iron Mask Batholith
Highland Valley
Guichon Creek Batholith
Kelowna
Penticton
Copper Mountain
Vancouver
USA
0
100
km
Insular
Intermontane
Ancestral North America
52°N
50°N
St. John's
122°W
120°W

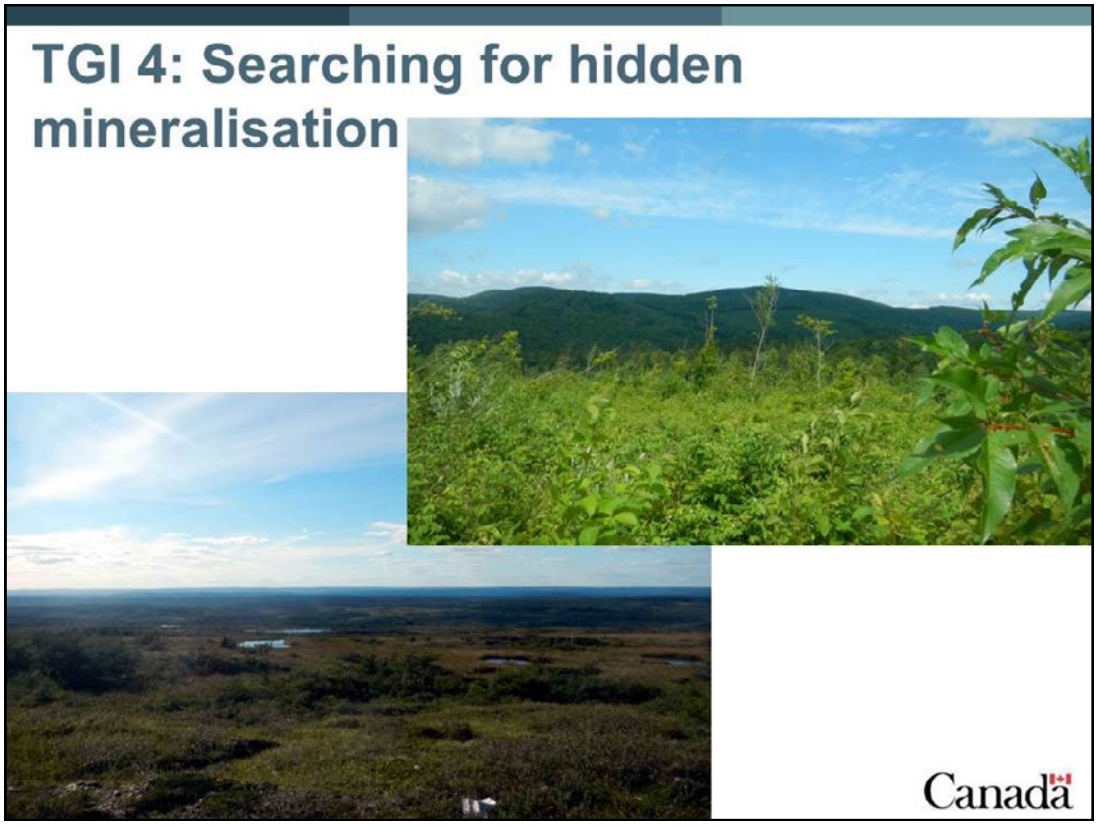
TGI 4: Searching for hidden mineralisation
Canada

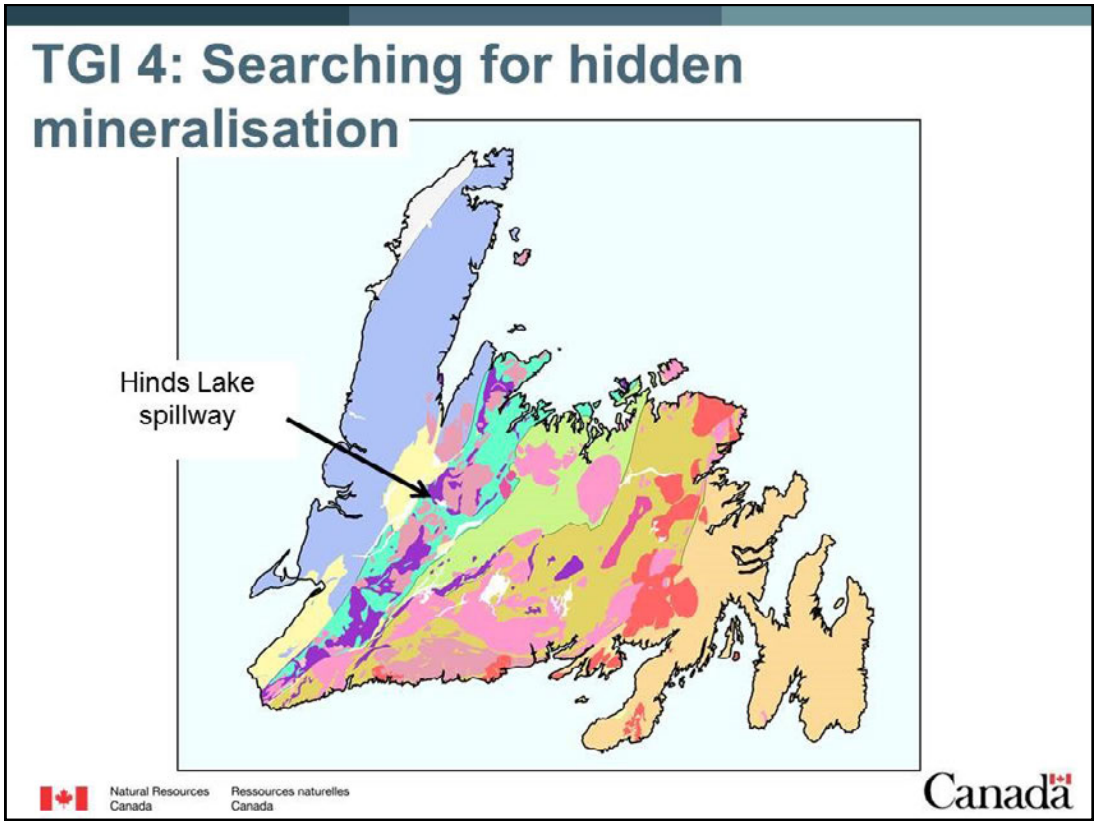
TGI 4: Searching for hidden mineralisation
Hinds Lake spillway
Natural Resources Canada
Ressources naturelles Canada
Canada

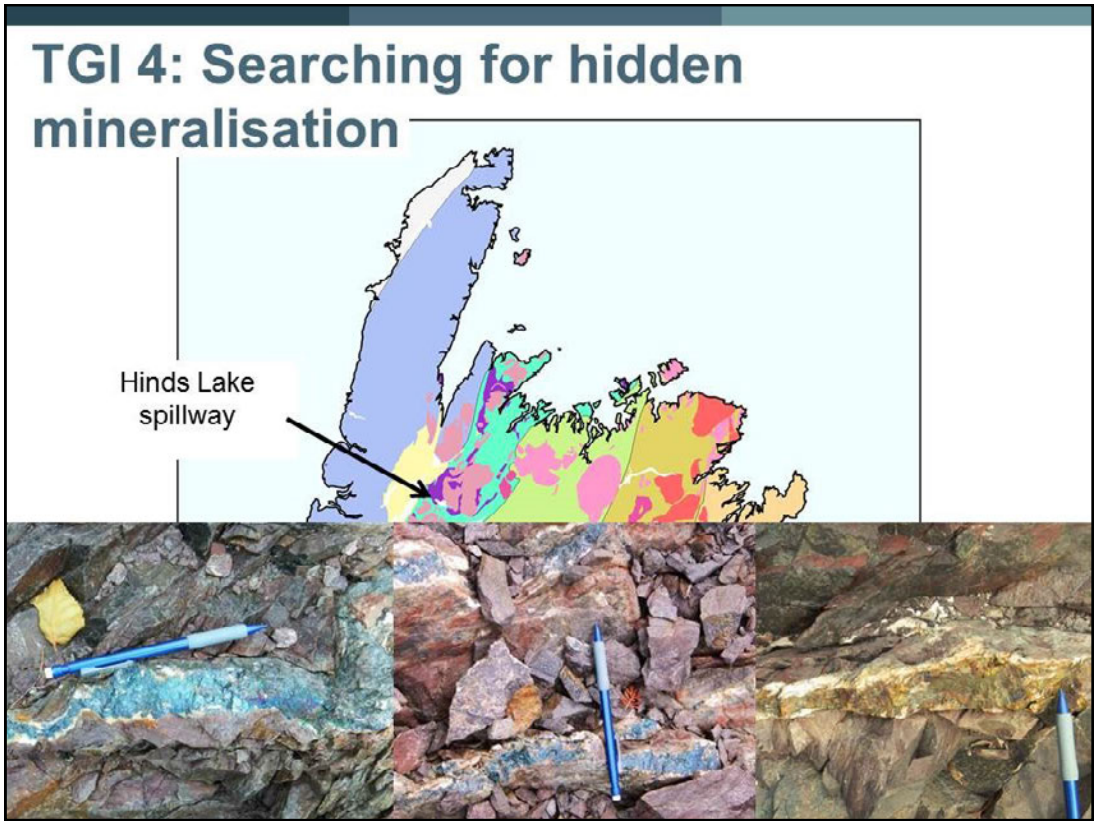
TGI 4: Searching for hidden mineralisation
Hinds Lake spillway

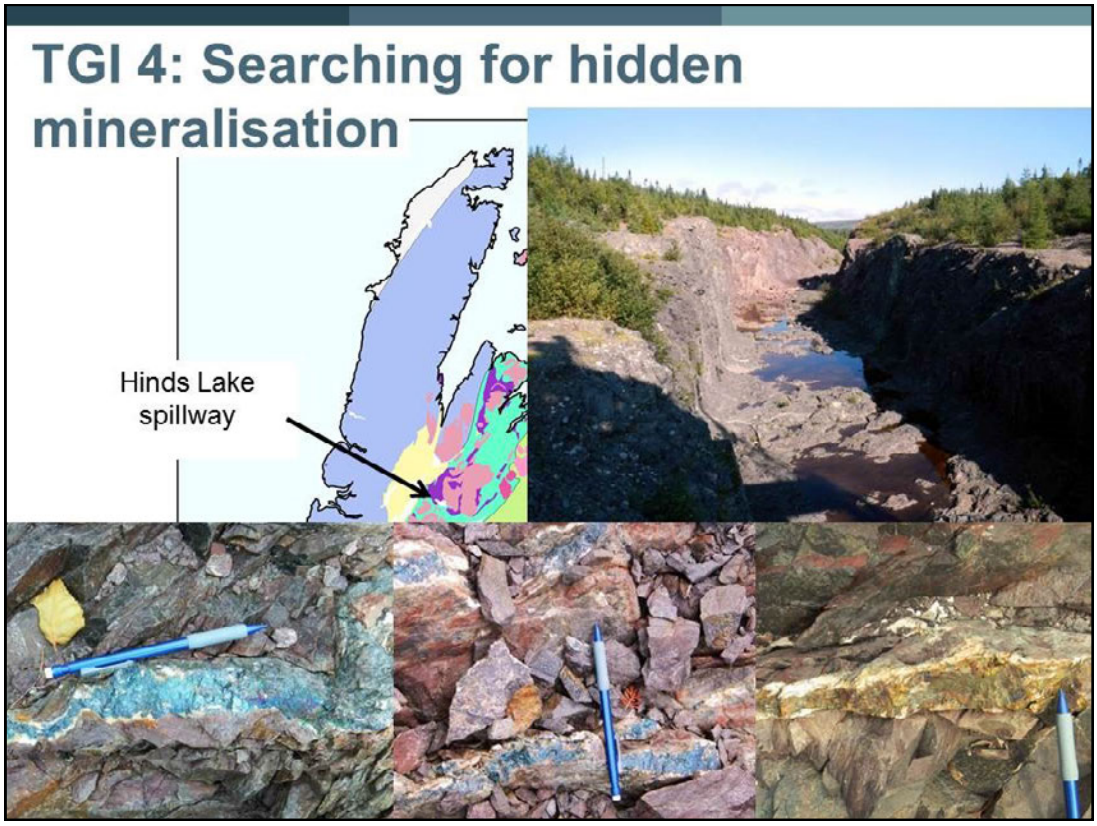
TGI 4: Searching for hidden mineralisation
Hinds Lake spillway

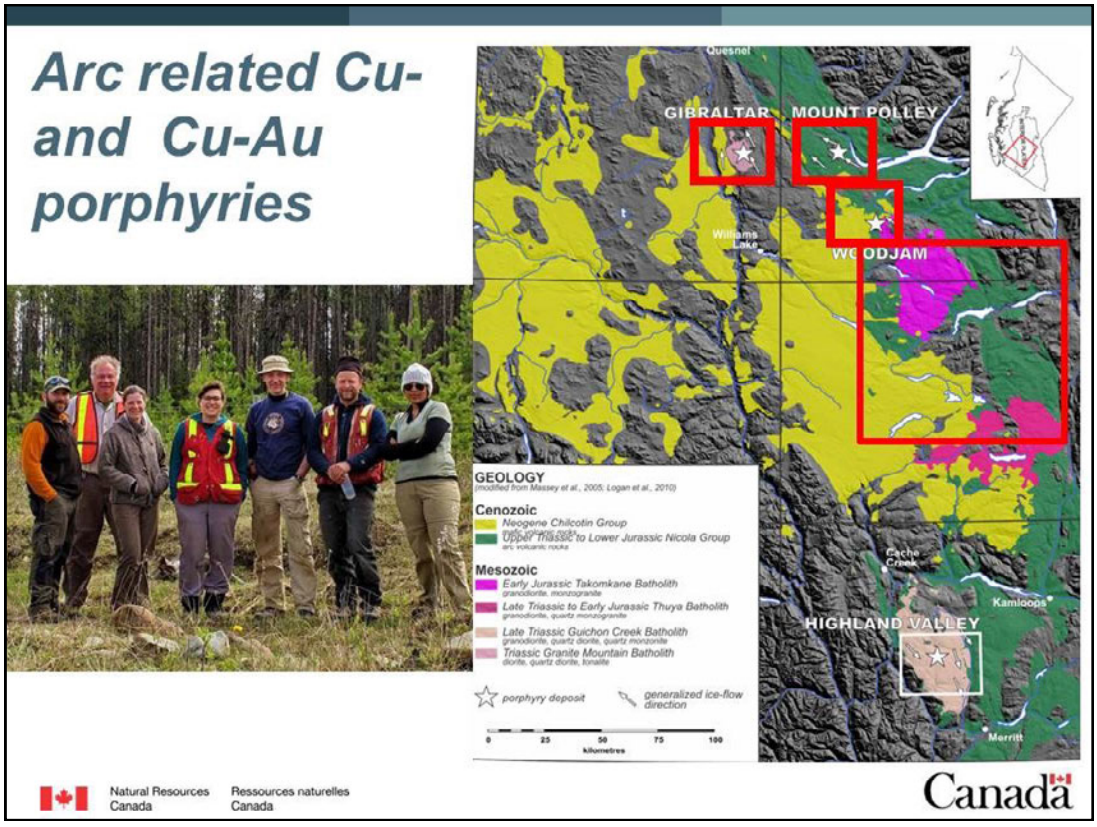
Arc related Cu- and Cu-Au porphyries
GIBRALTAR
MOUNT POLLEY
Williams Lake
WOODJAM
HIGHLAND VALLEY
Kamloops
Merritt
GEOLOGY
Cenozoic
Neogene Chilcotin Group
Upper Triassic to Lower Jurassic Nicola Group
Mesozoic
Early Jurassic Takomkane Batholith
Late Triassic to Early Jurassic Thuya Batholith
Late Triassic Guichon Creek Batholith
Triassic Granite Mountain Batholith
porphyry deposit
generalized ice-flow direction
kilometres
Natural Resources Canada
Ressources naturelles Canada
Canada

Gibraltar: Integrated bedrock, surficial and biogeochemical mapping

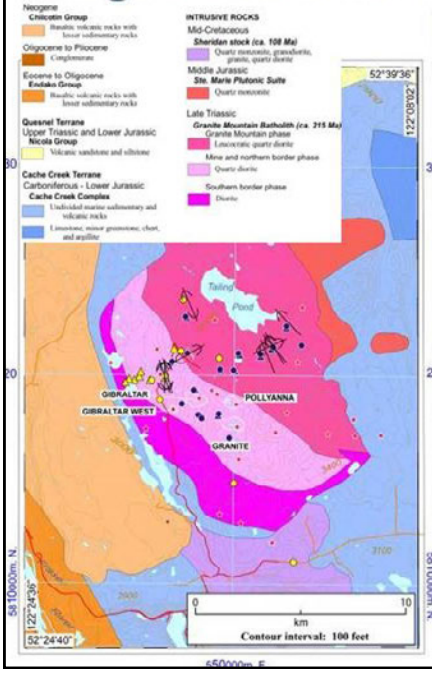

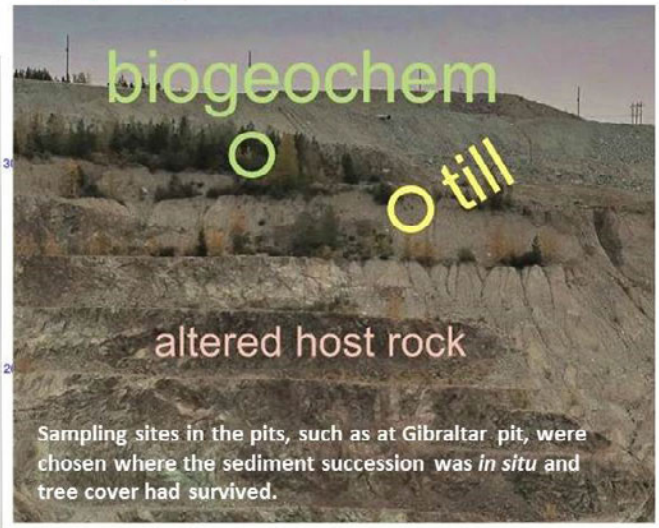

Open pit
Glacial striations (movement direction: known, unknown)

Geology from: Ash et al., 1999

2008 samples (GSC OF 6755)
tree bark
till
2011 samples
tree bark
till
Minfile occurrence

Canada

Gibraltar: Moly Re-Os dates

Location	Rock Type	Structure	Alteration	Mineralization

Re-Os age: 215.0 +/- 1.0 Ma

Granite	Tonalite	Weakly to moderately foliated	Weak to moderate QS +/- Chl	Weak to moderate

Re-Os age: 212.7 +/- 0.9 Ma

Granite	Tonalite	Weakly to moderately foliated	Moderate CQ	Strong

Re-Os age: 210.1 +/- 0.9 Ma

Gibraltar	Tonalite	Weakly to moderately foliated	Weak to Moderate QSC	Weak

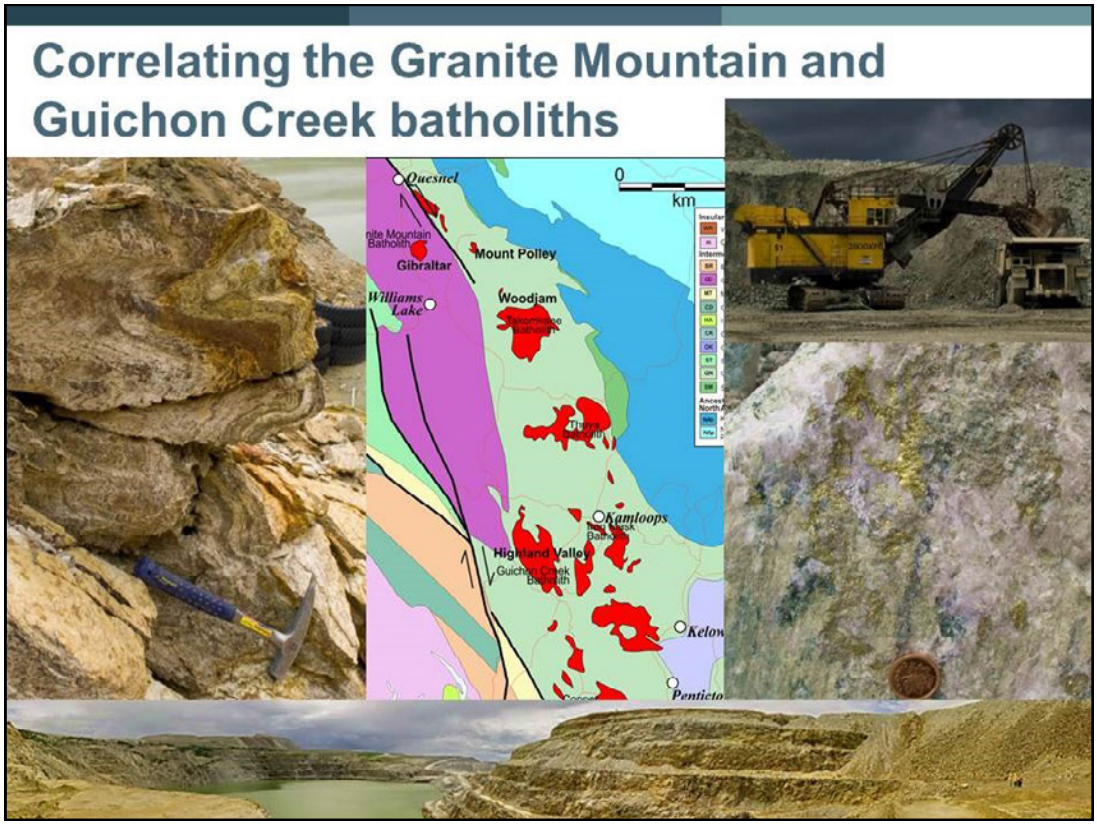
Correlating the Granite Mountain and Guichon Creek batholiths
Quesnel
0
km
Mount Polley
Gibraltar
Williams Lake
Woodjam
Kamloops
Highland Valley
Kelow
Pentict

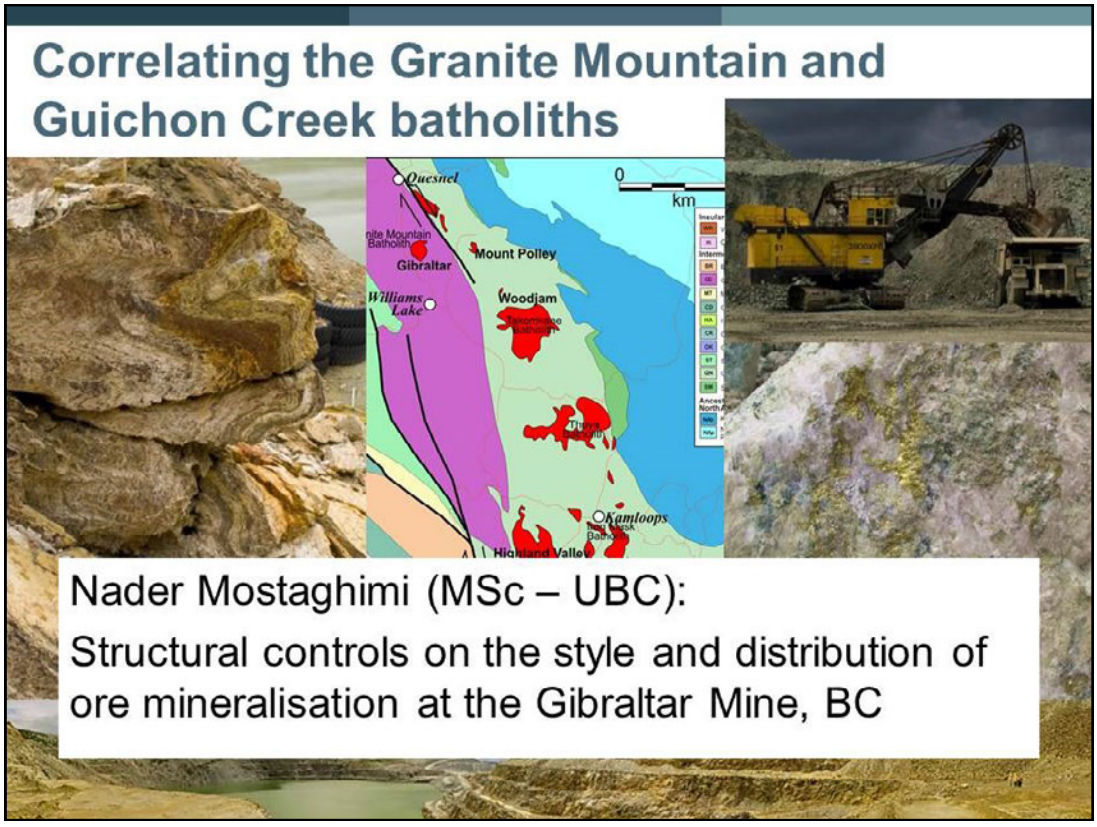
Correlating the Granite Mountain and Guichon Creek batholiths
Quesnel
0
km
Mount Polley
Gibraltar
Williams Lake
Woodjam
Kamloops
Nader Mostaghimi (MSc – UBC):
Structural controls on the style and distribution of ore mineralisation at the Gibraltar Mine, BC

Correlating the Granite Mountain and Guichon Creek batholiths

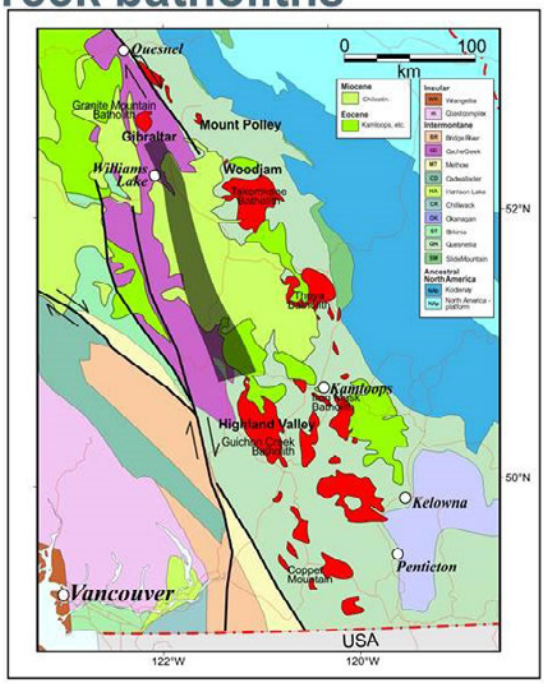

Correlating the Granite Mountain and Guichon Creek batholiths

High prospectivity zones?

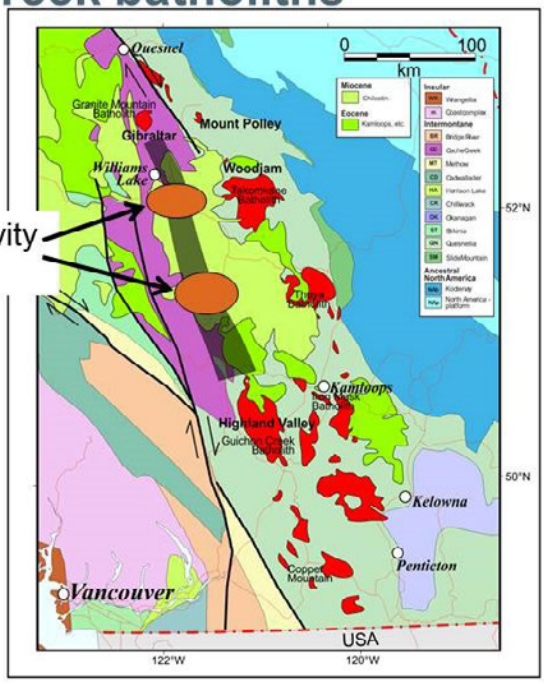

Glacial Processes: Profile of a glacier

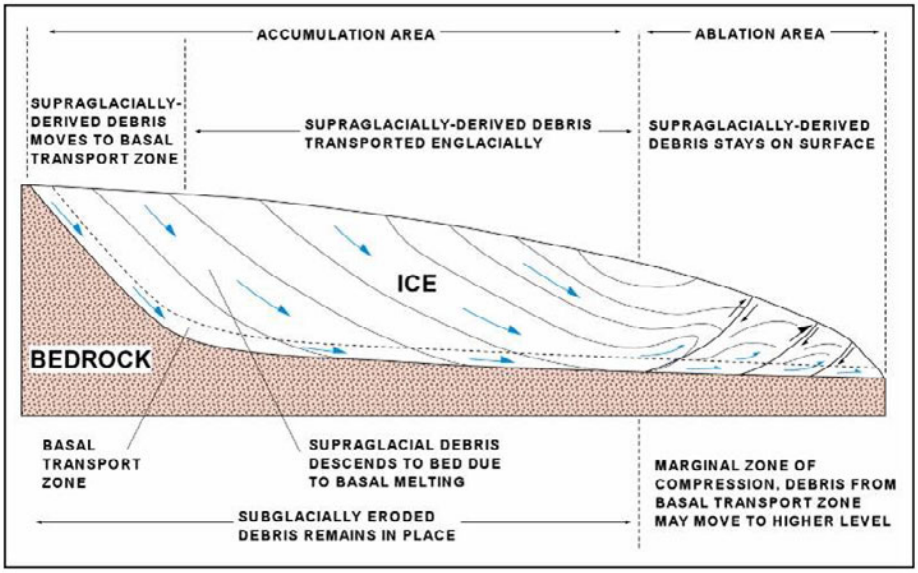

Boulton (1996)

Natural Resources Canada Ressources naturelles Canada

Canada

Glacial transport and dispersal train

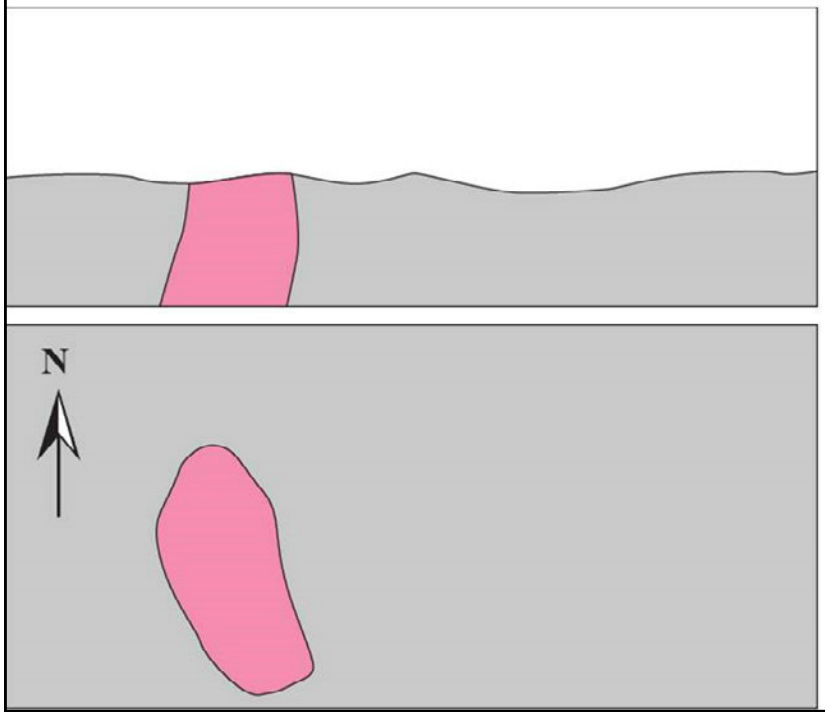

Modified from Drake (1983), Miller (1984), McClenaghan and Kjarsgaard (2007)

No scale

Canada

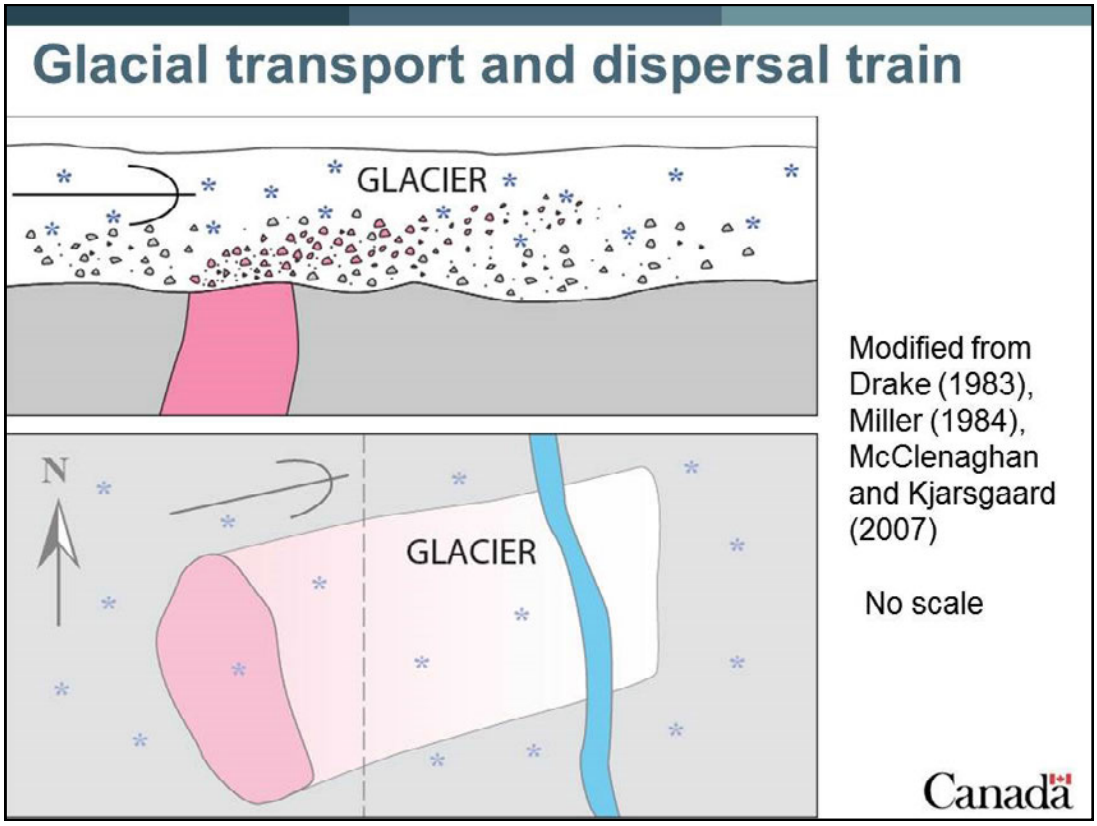
Glacial transport and dispersal train
GLACIER
N
GLACIER
Modified from Drake (1983), Miller (1984), McClenaghan and Kjarsgaard (2007)
No scale
Canada

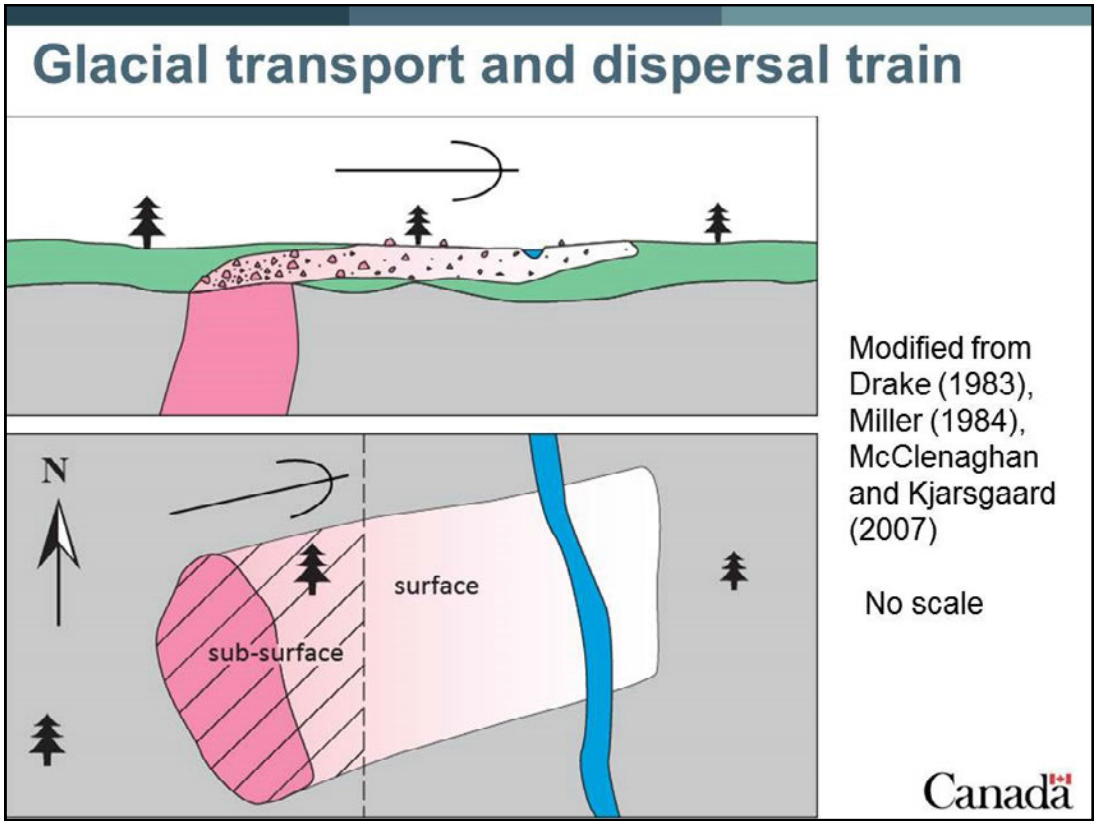
Glacial transport and dispersal train
N
surface
sub-surface
Modified from Drake (1983), Miller (1984), McClenaghan and Kjarsgaard (2007)
No scale
Canada

Ice-flow history: Bonaparte Lake area

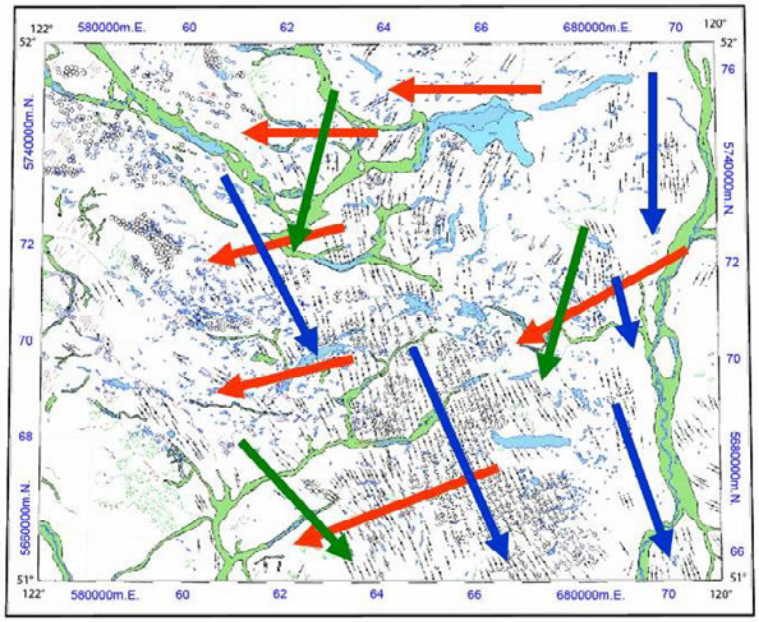

(Plouffe et al., 2011, CJES)

Ice-flow Indicators

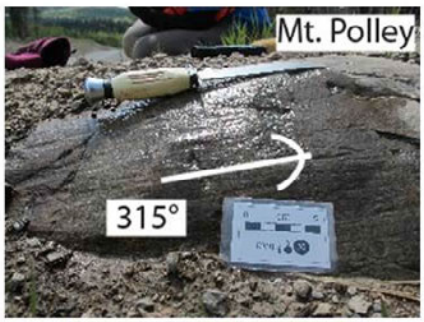

Ice-divide Migration and effect on glacial dispersal

Based on dispersal at Huckleberry Mine

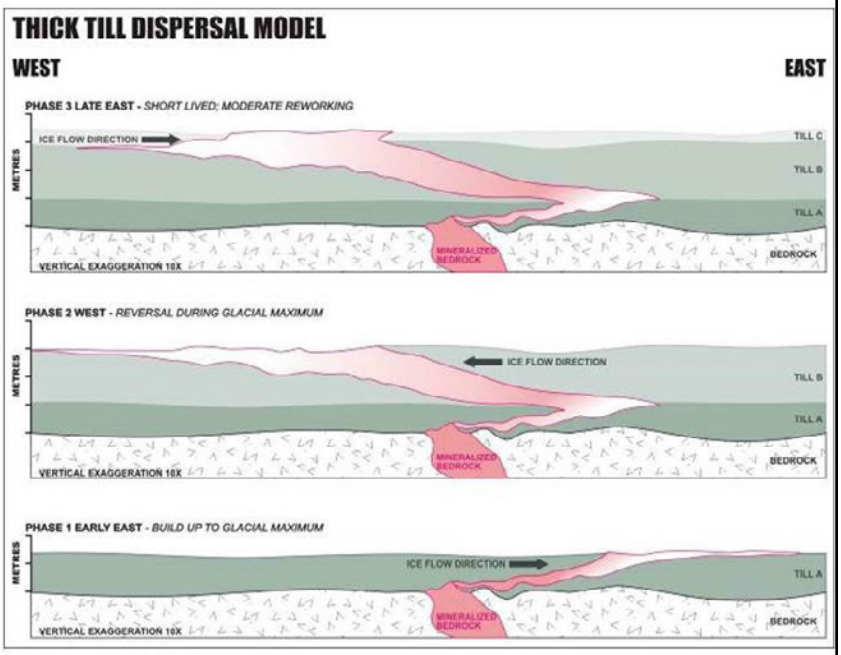

Ferbey et al. (2012; BCGS Open File 2012-02)

Palaeo-topography and till

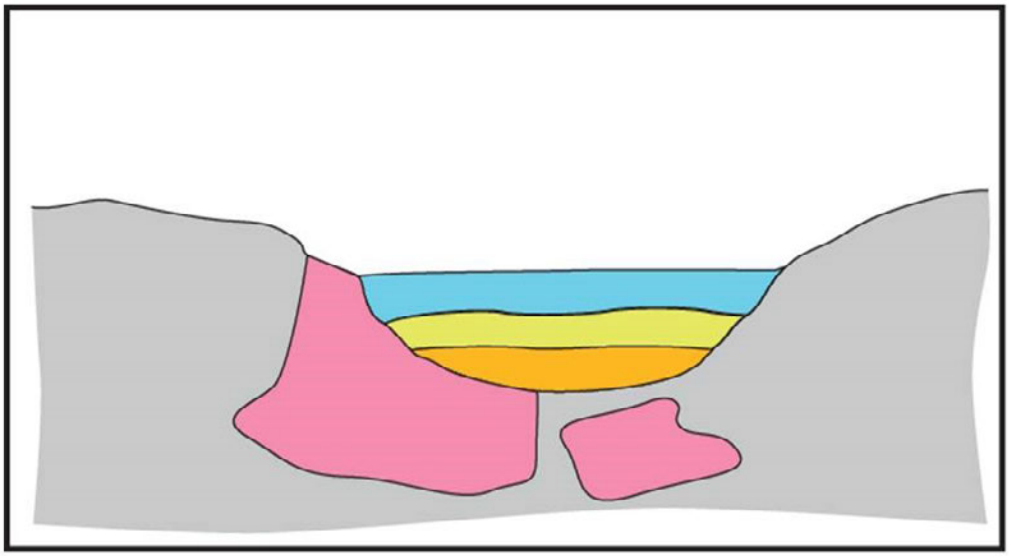

Natural Resources Canada Ressources naturelles Canada

Canada

Palaeo-topography and till

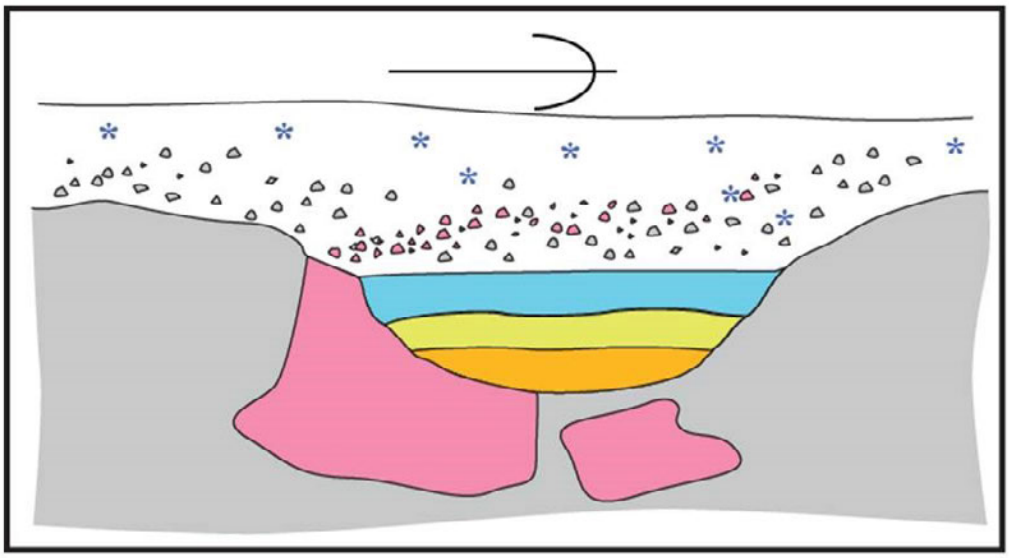

Natural Resources Canada Ressources naturelles Canada

Canada

Palaeo-topography and till

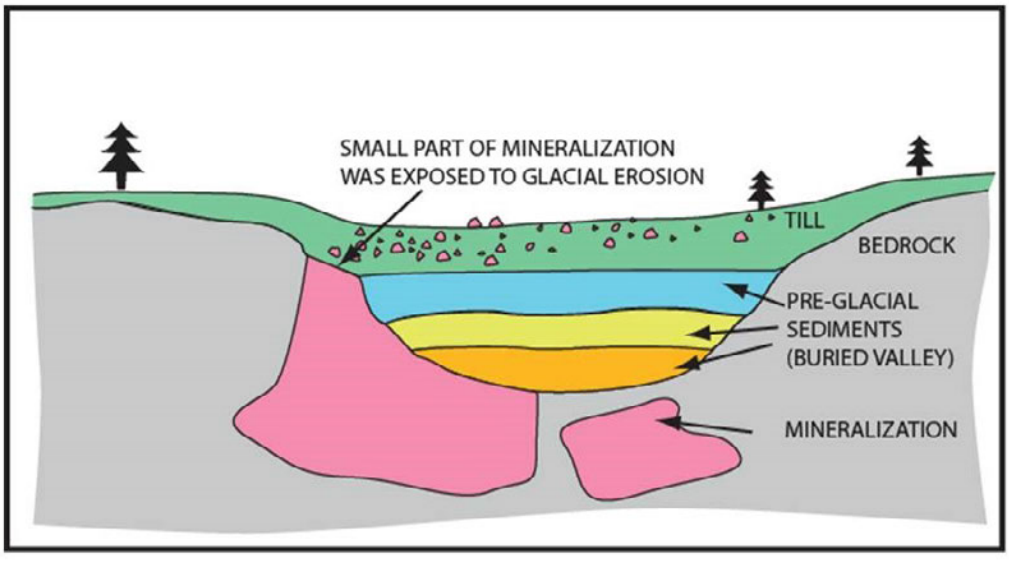

e.g. Highland Valley Mine

Natural Resources Canada Ressources naturelles Canada

Canada

Highland Valley Mine: Valley Pit

Natural Resources Canada Ressources naturelles Canada

Canada

Porphyry Indicator Minerals (PIM) – Woodjam

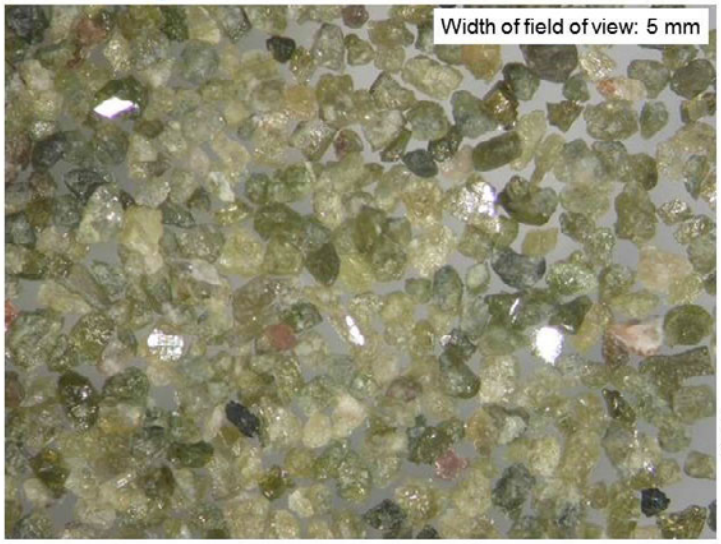

Sample 11PMA-017A-1 (WOODJAM)

80% Epidote (0.25-0.50 mm)

Source: ODM, March 2012; modal estimates +/-10% precision

Percentage of epidote in HMC of till could provide a key indication of the presence of propylitic alteration; this could become a regional indicator mineral for buried porphyry mineralization

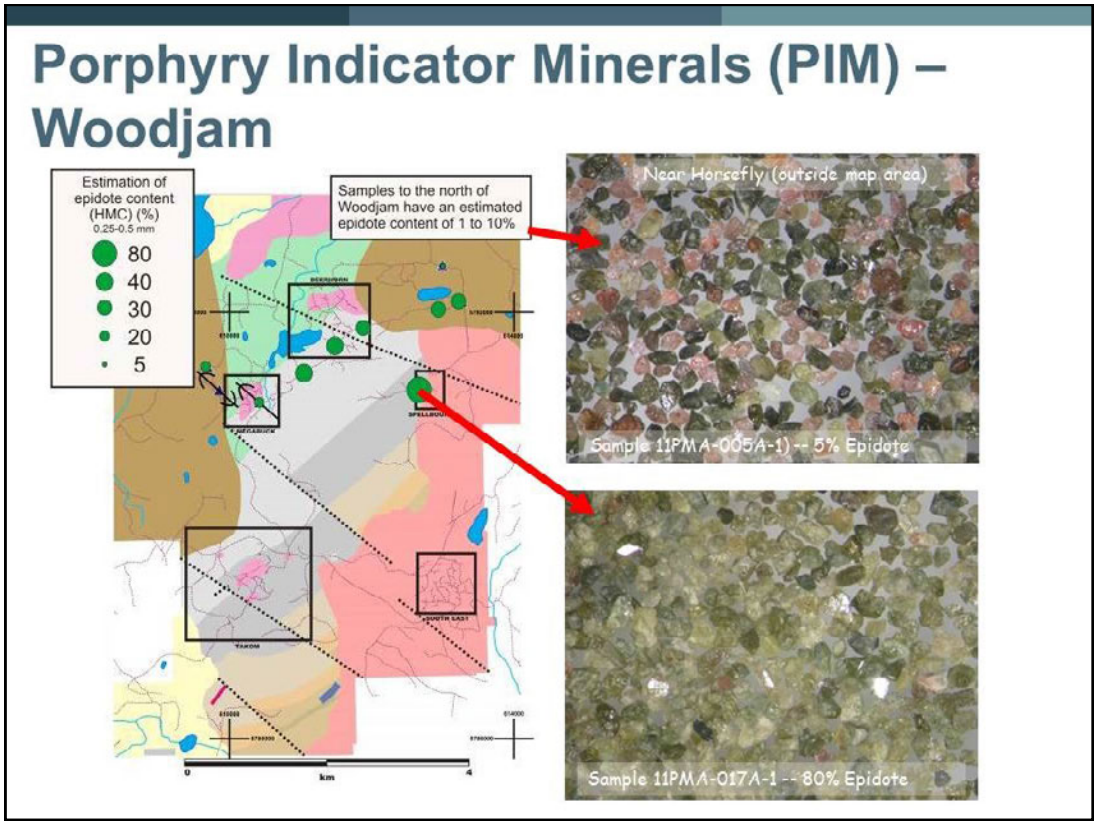
Porphyry Indicator Minerals (PIM) – Woodjam
Estimation of epidote content (HMC) (%)
0.25-0.5 mm
80
40
30
20
5
Samples to the north of Woodjam have an estimated epidote content of 1 to 10%
Near Horsefly (outside map area)
Sample 11PMA-005A-1) -- 5% Epidote
Sample 11PMA-017A-1 -- 80% Epidote
km

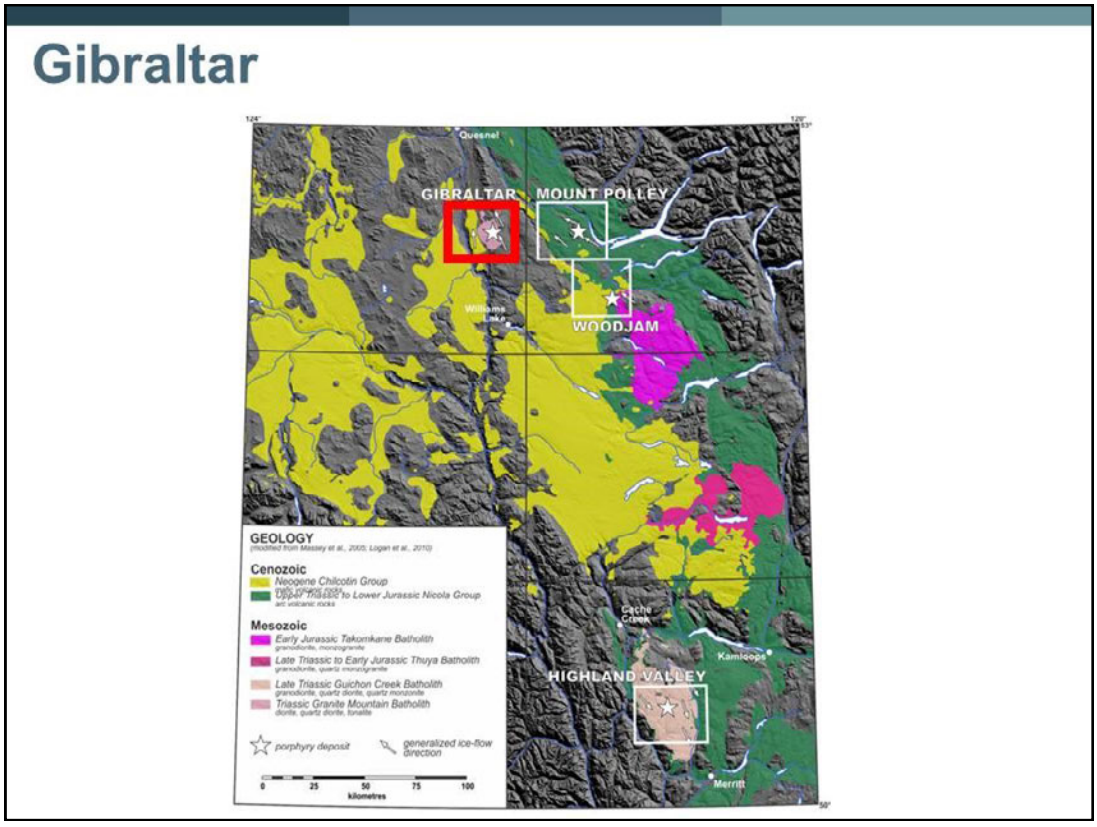
Gibraltar
GIBRALTAR
MOUNT POLLEY
WOODJAM
HIGHLAND VALLEY
Quesnel
Williams Lake
Cache Creek
Kamloops
Merritt
GEOLOGY
Cenozoic
Neogene Chilcotin Group
Mesozoic
Early Jurassic Takomkane Batholith
Late Triassic to Early Jurassic Thuya Batholith
Late Triassic Guichon Creek Batholith
Triassic Granite Mountain Batholith
porphyry deposit
generalized ice-flow direction
kilometres

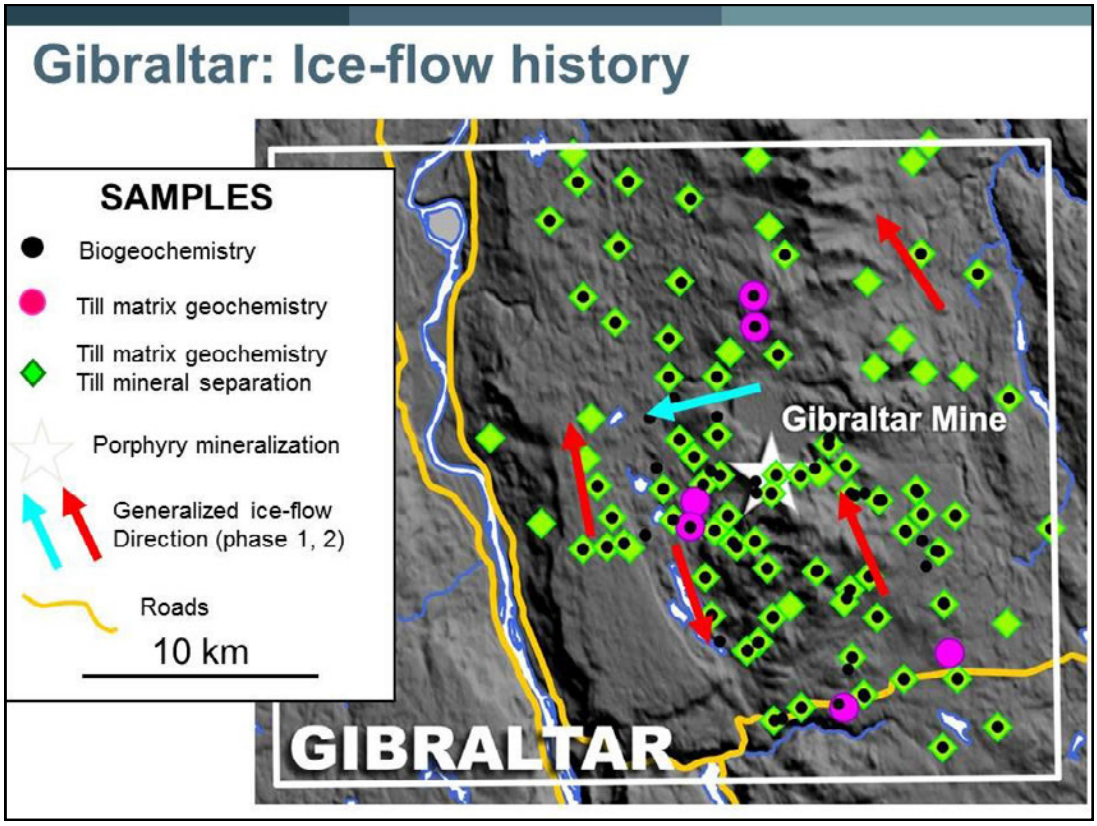
Gibraltar: Ice-flow history
SAMPLES
Biogeochemistry
Till matrix geochemistry
Till matrix geochemistry
Till mineral separation
Porphyry mineralization
Generalized ice-flow
Direction (phase 1, 2)
Roads
10 km
Gibraltar Mine
GIBRALTAR

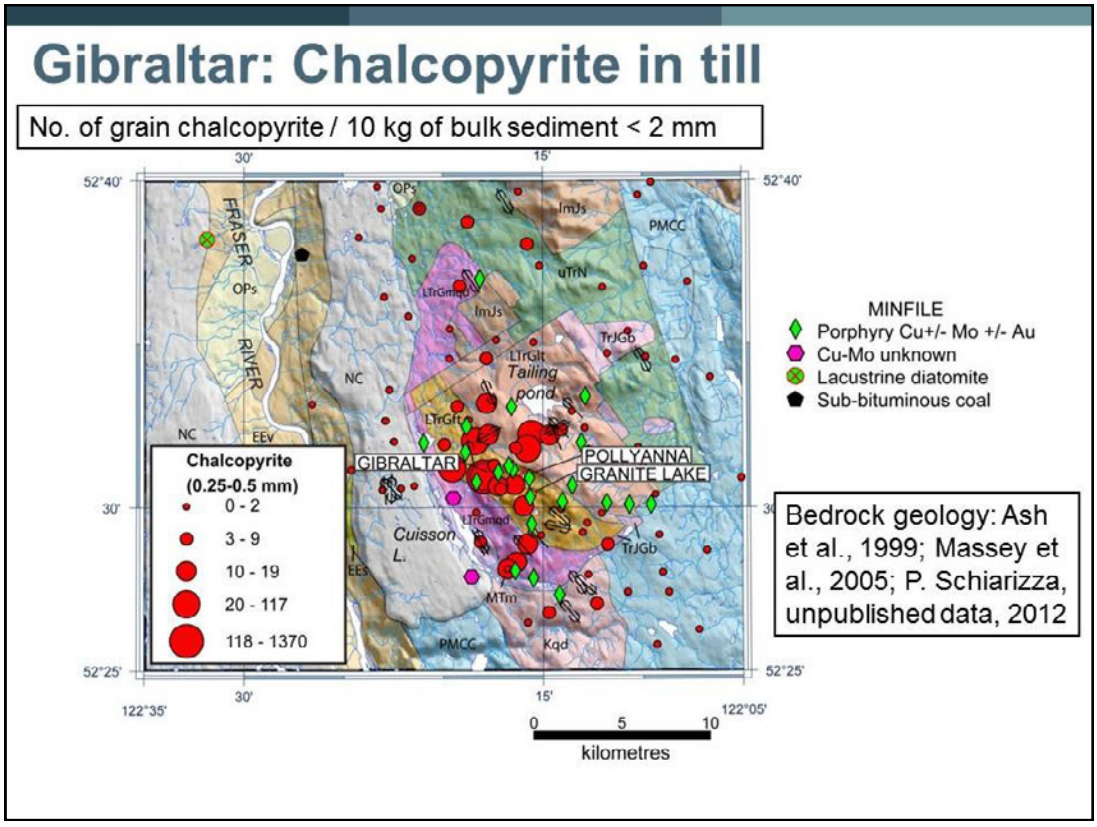
Gibraltar: Chalcopyrite in till
No. of grain chalcopyrite / 10 kg of bulk sediment < 2 mm
Chalcopyrite
(0.25-0.5 mm)
0 - 2
3 - 9
10 - 19
20 - 117
118 - 1370
MINFILE
Porphyry Cu+/- Mo +/- Au
Cu-Mo unknown
Lacustrine diatomite
Sub-bituminous coal
GIBRALTAR
POLLYANNA
GRANITE LAKE
Cuisson L.
Tailing pond
FRASER RIVER
Bedrock geology: Ash et al., 1999; Massey et al., 2005; P. Schiarizza, unpublished data, 2012
kilometres

Gibraltar: Cu in clay from till

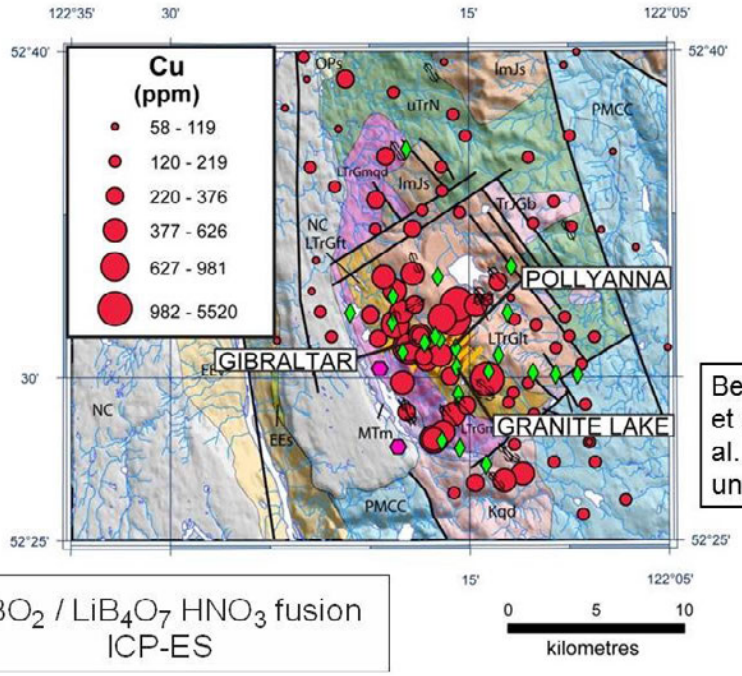

Bedrock geology: Ash et al., 1999; Massey et al., 2005; P. Schiarizza, unpublished data, 2012

$LiBO_2$ / LiB_4O_7 HNO_3 fusion
ICP-ES

Mount Polley

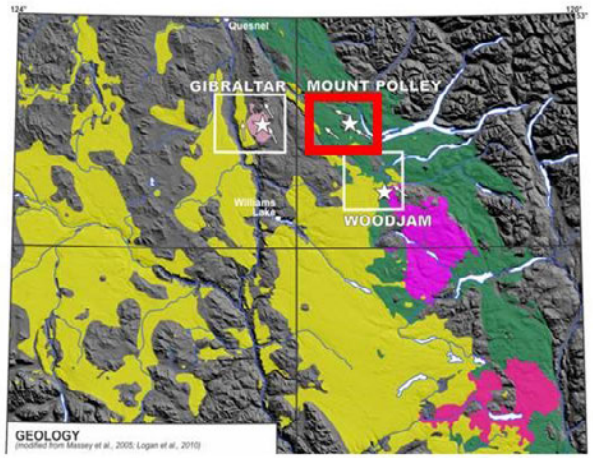

Sarah Hashmi (MSc – SFU):

Geochemical and mineralogical dispersal in till from the Mount Polley Cu-Au porphyry deposit, central British Columbia, Canada

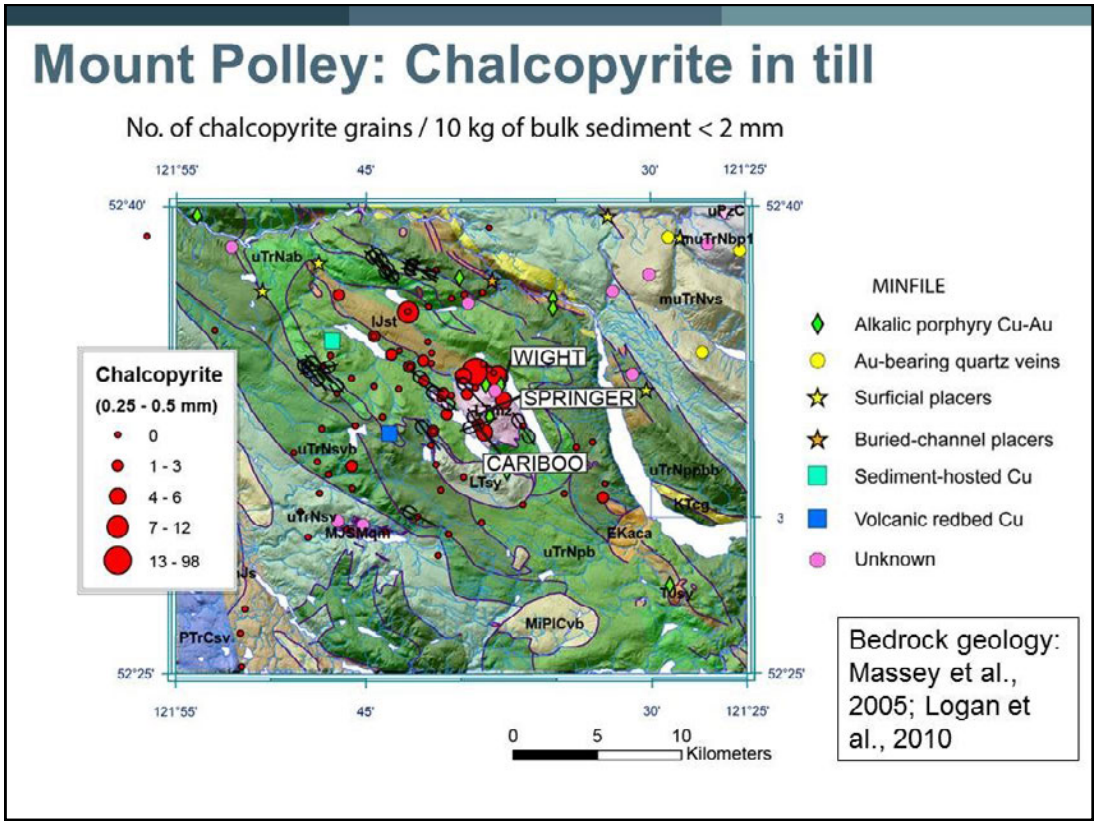
Mount Polley: Chalcopyrite in till
No. of chalcopyrite grains / 10 kg of bulk sediment < 2 mm
Chalcopyrite
(0.25 - 0.5 mm)
0
1 - 3
4 - 6
7 - 12
13 - 98
MINFILE
Alkalic porphyry Cu-Au
Au-bearing quartz veins
Surficial placers
Buried-channel placers
Sediment-hosted Cu
Volcanic redbed Cu
Unknown
WIGHT
SPRINGER
CARIBOO
Bedrock geology: Massey et al., 2005; Logan et al., 2010
0 5 10 Kilometers

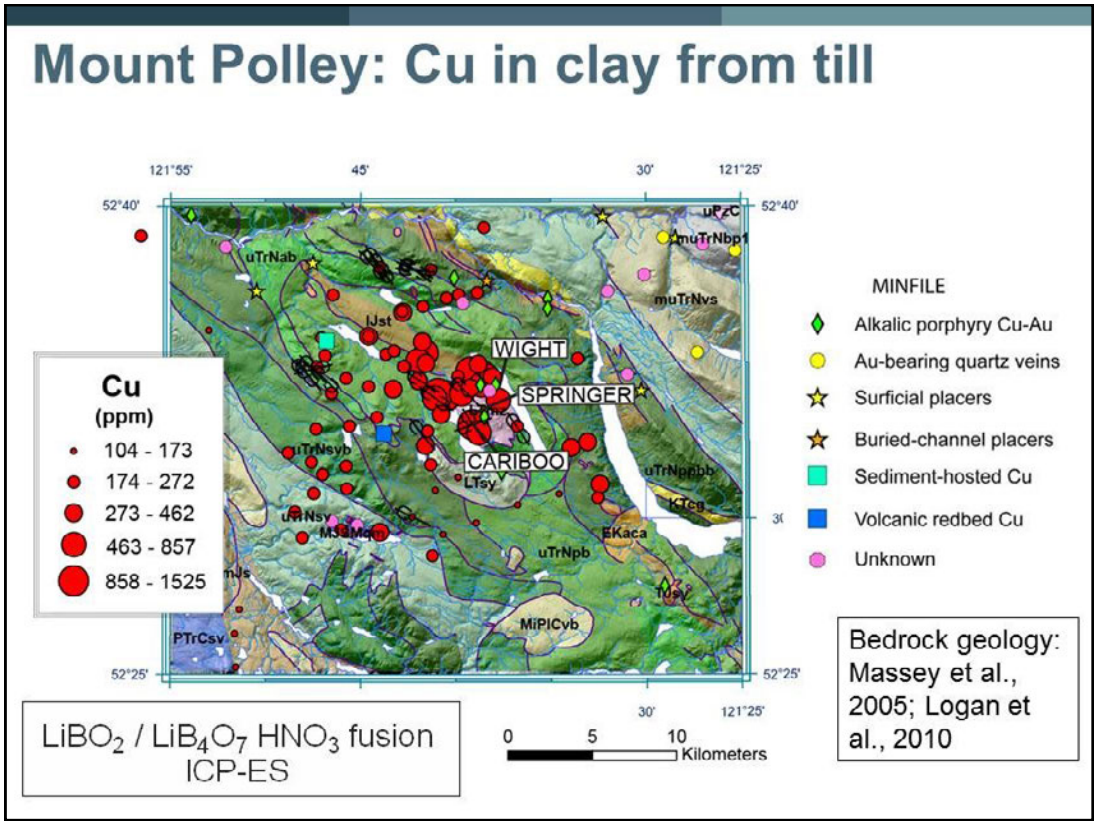
Mount Polley: Cu in clay from till
Cu
(ppm)
104 - 173
174 - 272
273 - 462
463 - 857
858 - 1525
MINFILE
Alkalic porphyry Cu-Au
Au-bearing quartz veins
Surficial placers
Buried-channel placers
Sediment-hosted Cu
Volcanic redbed Cu
Unknown
WIGHT
SPRINGER
CARIBOO
Bedrock geology: Massey et al., 2005; Logan et al., 2010
LiBO2 / LiB4O7 HNO3 fusion
ICP-ES
0 5 10 Kilometers

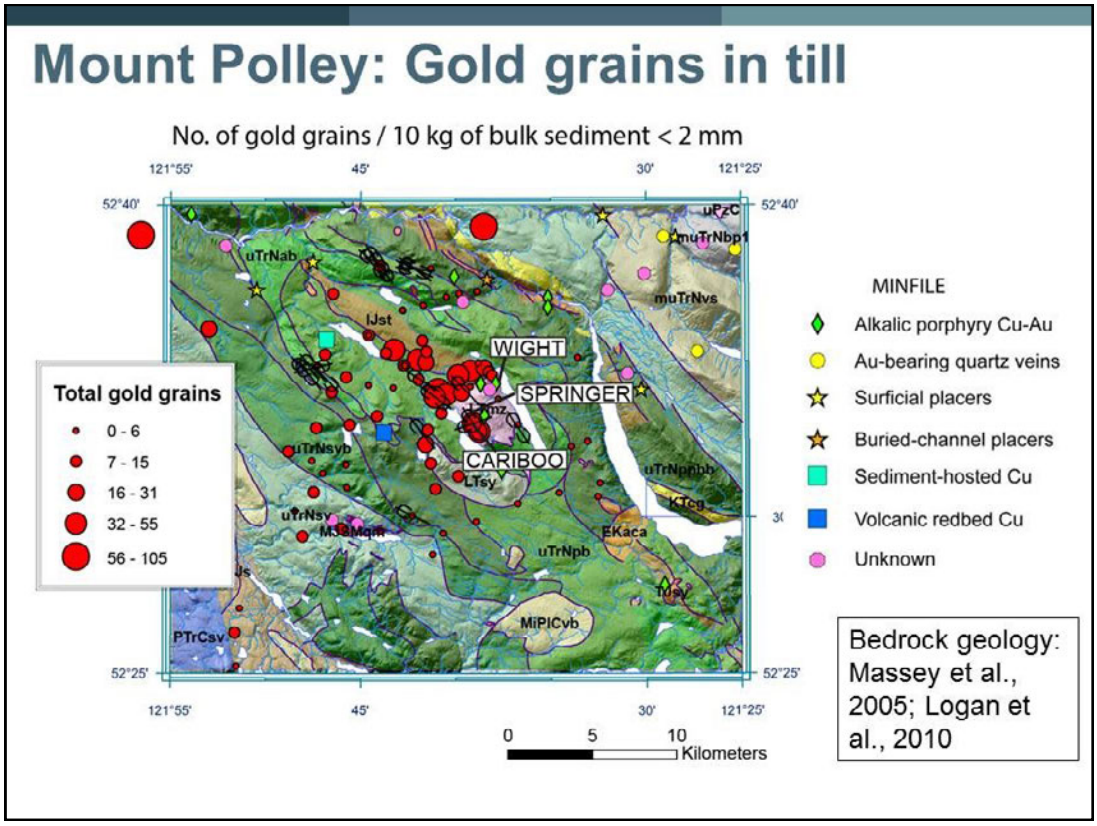
Mount Polley: Gold grains in till
No. of gold grains / 10 kg of bulk sediment < 2 mm
121°55'
45'
30'
121°25'
52°40'
52°25'
uTrNab
lJst
WIGHT
SPRINGER
CARIBOO
uTrNsyb
LTsy
uTrNsy
uTrNpb
EKaca
MiPlCvb
PTrCsv
uPzC
muTrNbp1
muTrNvs
uTrNpnhb
lKTcg
Total gold grains
0 - 6
7 - 15
16 - 31
32 - 55
56 - 105
MINFILE
Alkalic porphyry Cu-Au
Au-bearing quartz veins
Surficial placers
Buried-channel placers
Sediment-hosted Cu
Volcanic redbed Cu
Unknown
Bedrock geology: Massey et al., 2005; Logan et al., 2010
0
5
10
Kilometers

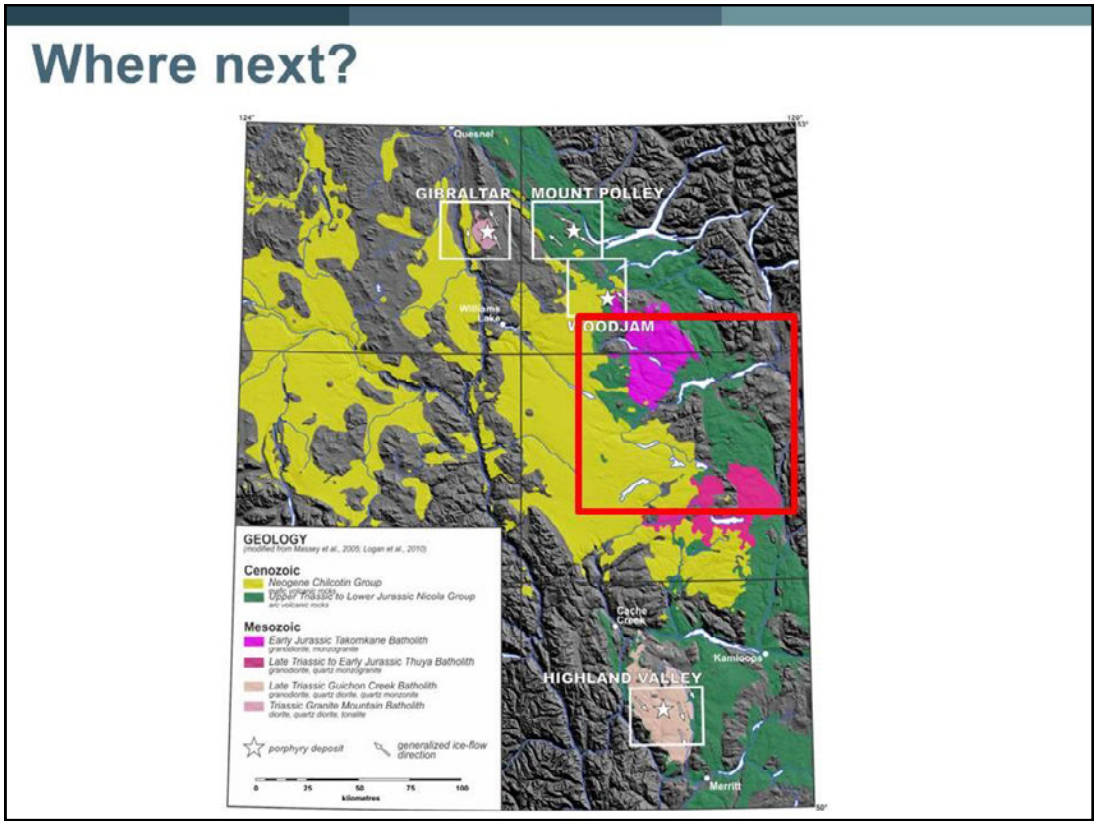
Where next?
Quesnel
GIBRALTAR
MOUNT POLLEY
WOODJAM
Williams Lake
Cache Creek
Kamloops
HIGHLAND VALLEY
Merritt
GEOLOGY
Cenozoic
Neogene Chilcotin Group
Mesozoic
Early Jurassic Takomkane Batholith
Late Triassic to Early Jurassic Thuya Batholith
Late Triassic Guichon Creek Batholith
Triassic Granite Mountain Batholith
porphyry deposit
generalized ice-flow direction

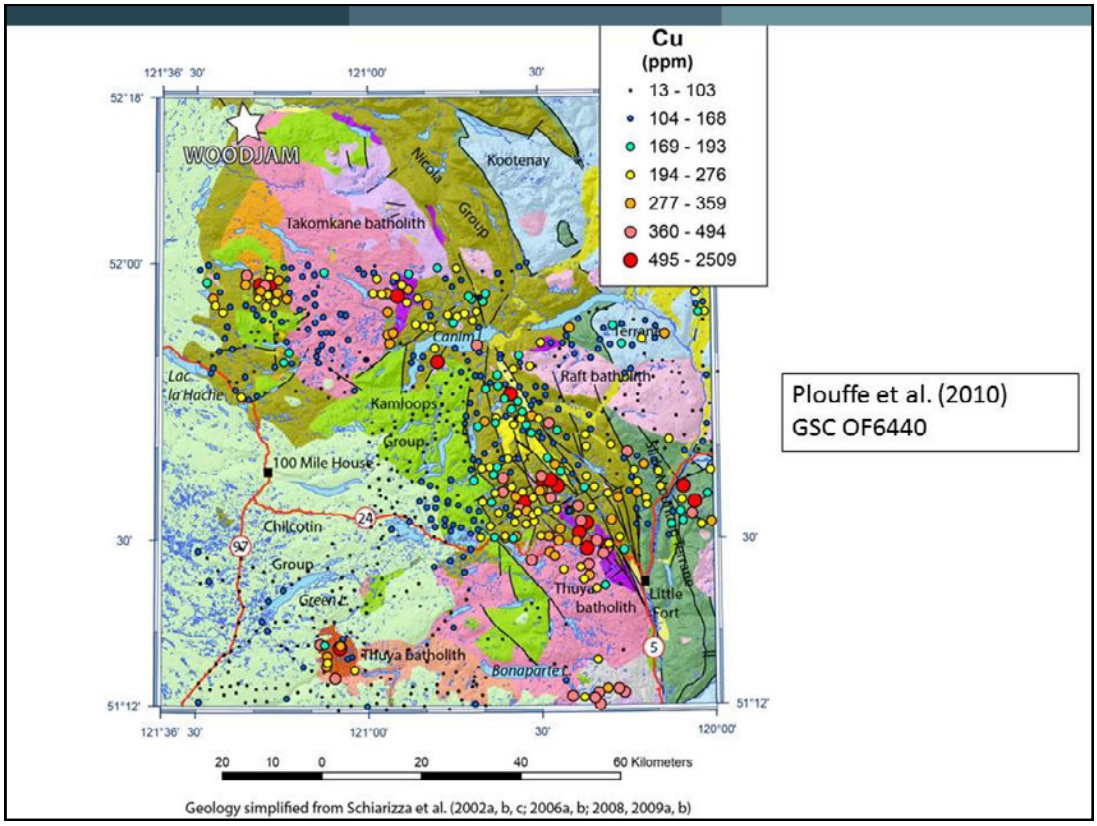
Cu
(ppm)
13 - 103
104 - 168
169 - 193
194 - 276
277 - 359
360 - 494
495 - 2509
WOODJAM
Nicola
Group
Kootenay
Takomkane batholith
Canim L.
Terrane
Raft batholith
Lac la Hache
Kamloops
Group
100 Mile House
Chilcotin
Group
Green L.
Thuya batholith
Bonaparte L.
Little Fort
Fennell Terrane
121°36' 30'
121°00'
30'
120°00'
52°18'
52°00'
51°12'
30'
97
24
5
20 10 0 20 40 60 Kilometers
Plouffe et al. (2010)
GSC OF6440
Geology simplified from Schiarizza et al. (2002a, b, c; 2006a, b; 2008, 2009a, b)

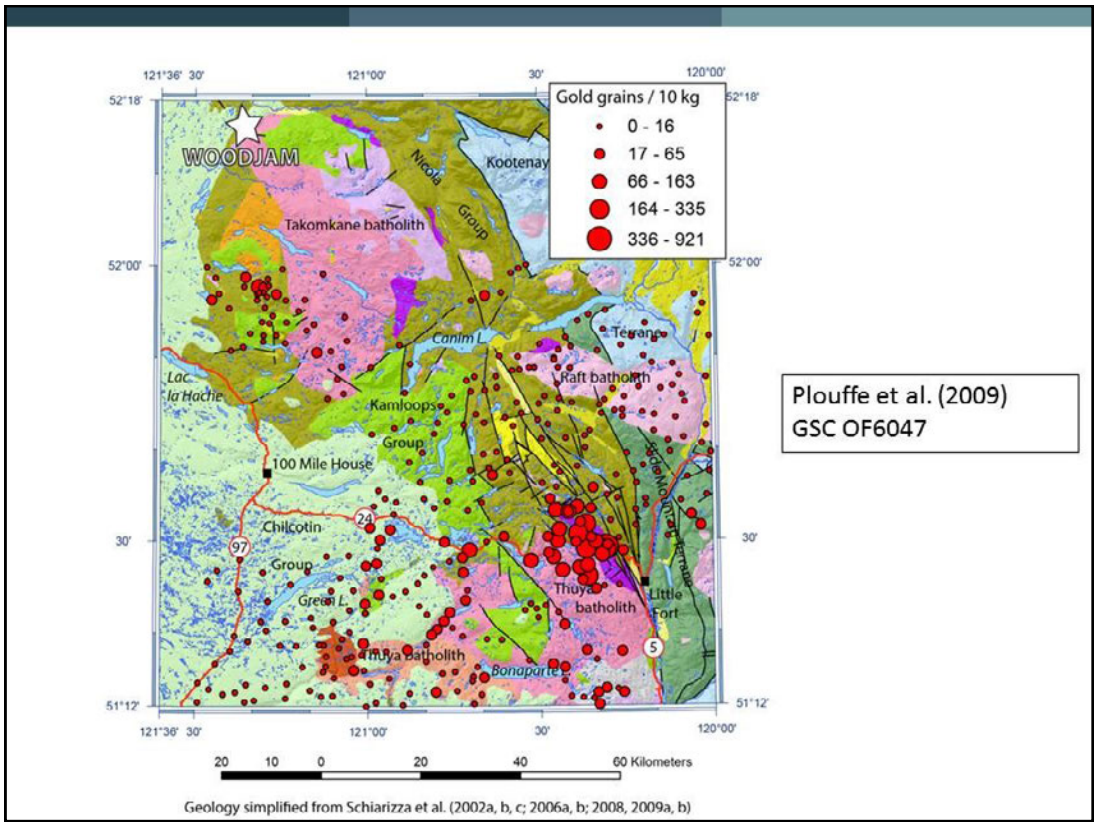
Gold grains / 10 kg
0 - 16
17 - 65
66 - 163
164 - 335
336 - 921
WOODJAM
Nicola
Group
Kootenay
Takomkane batholith
Canim L.
Terrane
Raft batholith
Lac la Hache
Kamloops
Group
100 Mile House
Chilcotin
Group
Green L.
Thuya batholith
Bonaparte L.
Little Fort
Fennell Terrane
121°36' 30'
121°00'
30'
120°00'
52°18'
52°00'
51°12'
30'
97
24
5
20 10 0 20 40 60 Kilometers
Plouffe et al. (2009)
GSC OF6047
Geology simplified from Schiarizza et al. (2002a, b, c; 2006a, b; 2008, 2009a, b)

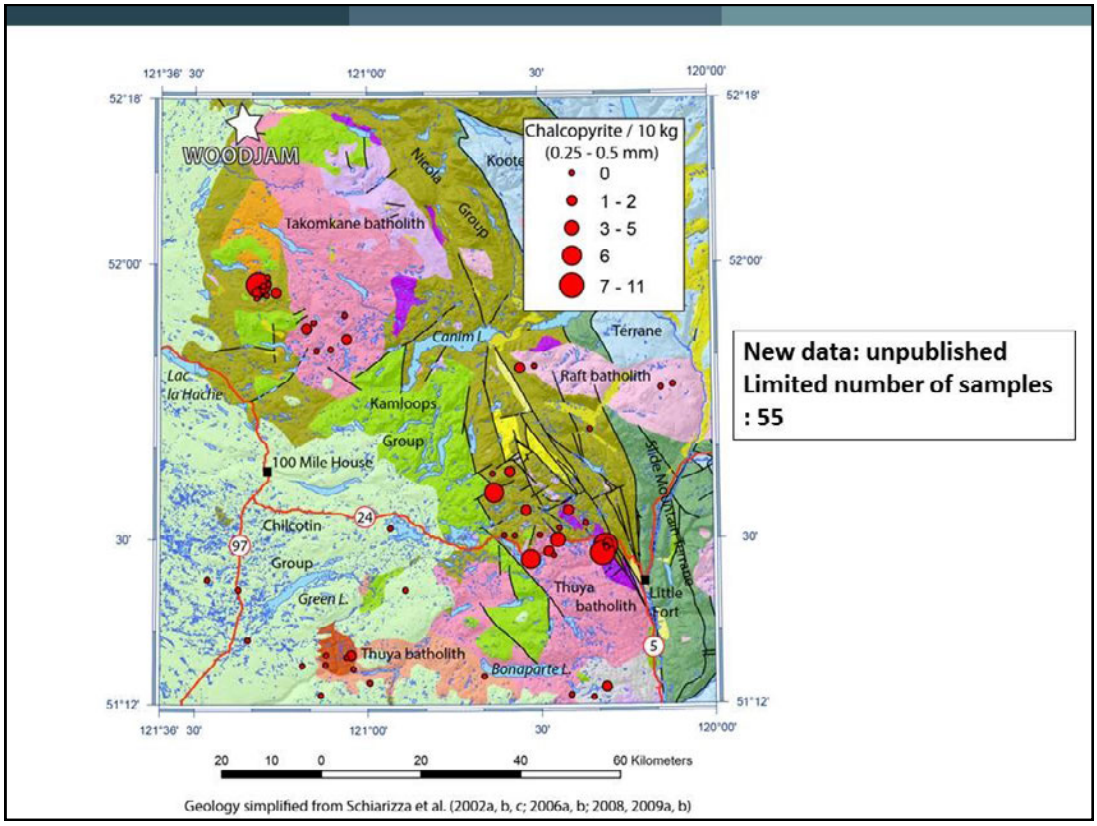

8:40 Parkhill, M.A.*, McClenaghan, M.B., Seaman, A.A., Pronk, A.G. and Rice, J.M. Glacial stratigraphic, till geochemical, and indicator mineral studies at the Sisson W-Mo and Mount Pleasant Sn-W-Mo-Bi-In polymetallic deposits, southwestern New Brunswick

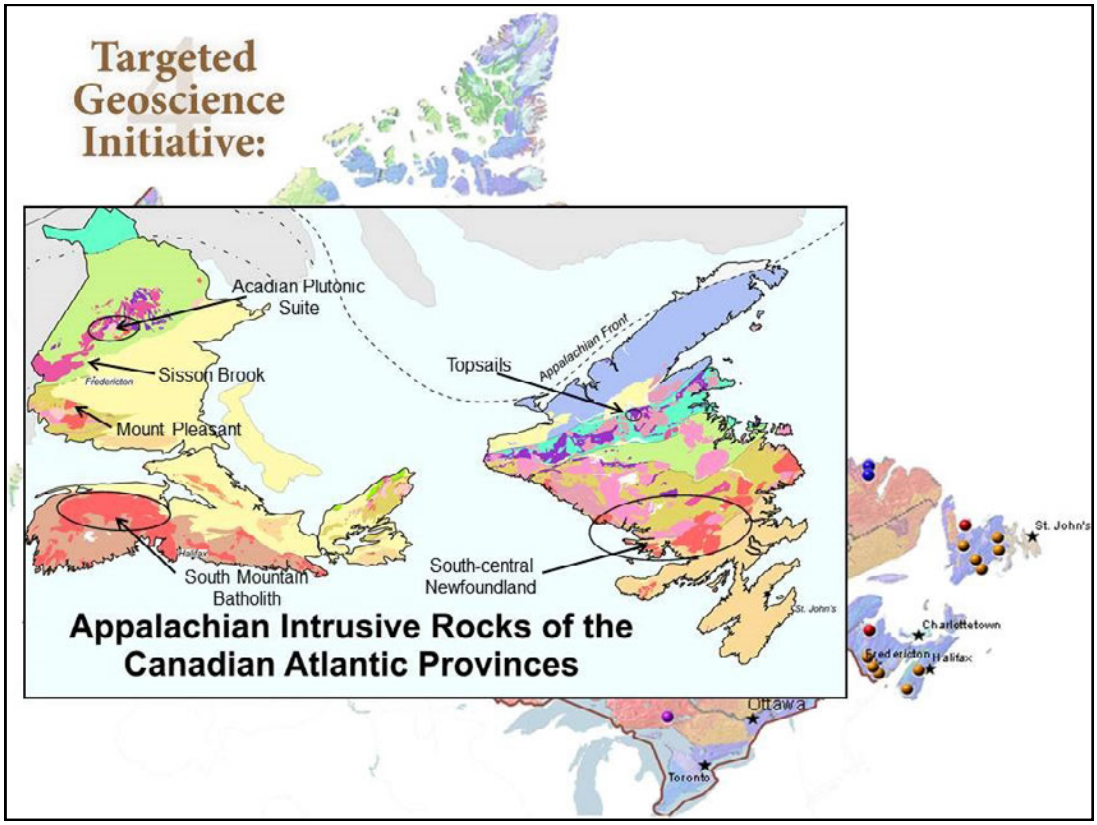
Targeted
Geoscience
Initiative:
Acadian Plutonic
Suite
Sisson Brook
Mount Pleasant
Topsails
Appalachian Front
South Mountain
Batholith
South-central
Newfoundland
Appalachian Intrusive Rocks of the
Canadian Atlantic Provinces
St. John's
Charlottetown
Fredericton
Halifax
Ottawa
Toronto

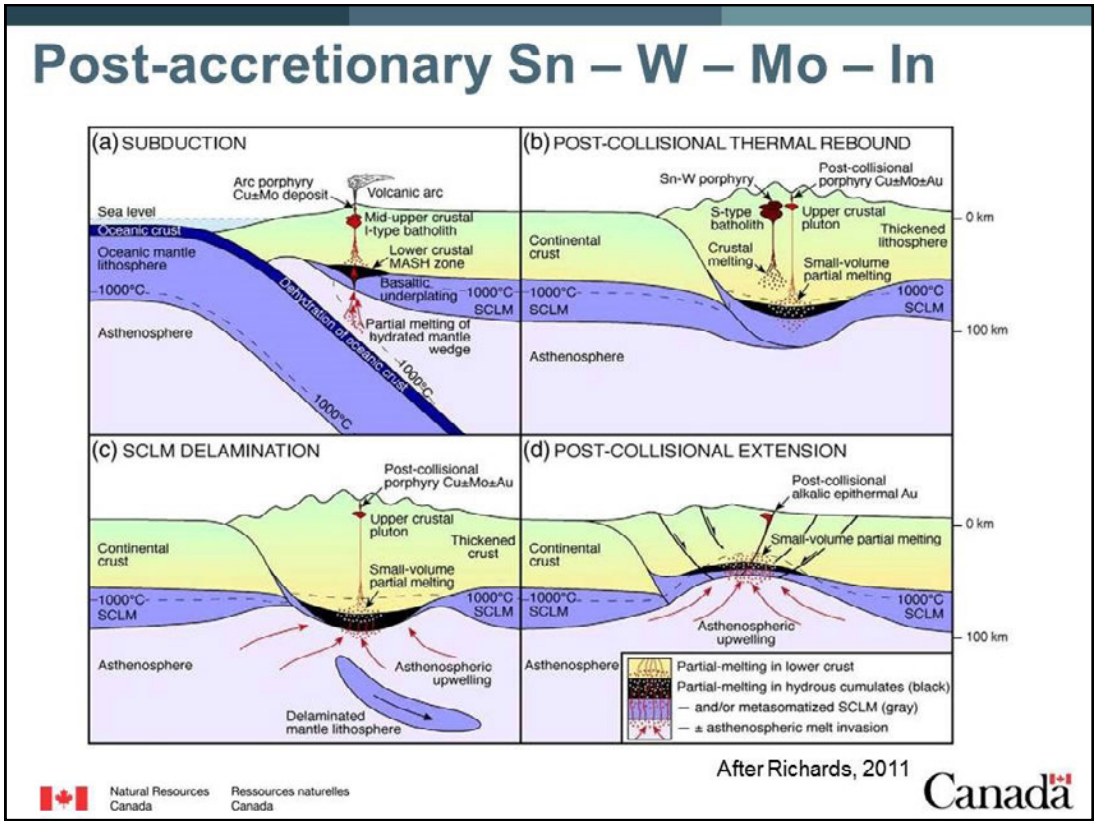
Post-accretionary Sn – W – Mo – In
(a) SUBDUCTION
Arc porphyry
Cu±Mo deposit
Volcanic arc
Sea level
Oceanic crust
Mid-upper crustal
I-type batholith
Oceanic mantle
lithosphere
Lower crustal
MASH zone
1000°C
Basaltic
underplating
1000°C
SCLM
Partial melting of
hydrated mantle
wedge
Asthenosphere
Dehydration of oceanic crust
100°C
1000°C
(b) POST-COLLISIONAL THERMAL REBOUND
Sn-W porphyry
Post-collisional
porphyry Cu±Mo±Au
S-type
batholith
Upper crustal
pluton
Thickened
lithosphere
Continental
crust
Crustal
melting
Small-volume
partial melting
0 km
1000°C
SCLM
1000°C
SCLM
100 km
Asthenosphere
(c) SCLM DELAMINATION
Post-collisional
porphyry Cu±Mo±Au
Upper crustal
pluton
Thickened
crust
Continental
crust
Small-volume
partial melting
1000°C
SCLM
1000°C
SCLM
Asthenosphere
Asthenospheric
upwelling
Delaminated
mantle lithosphere
(d) POST-COLLISIONAL EXTENSION
Post-collisional
alkalic epithermal Au
0 km
Small-volume partial melting
Continental
crust
1000°C
SCLM
1000°C
SCLM
Asthenospheric
upwelling
100 km
Asthenosphere
Partial-melting in lower crust
Partial-melting in hydrous cumulates (black)
– and/or metasomatized SCLM (gray)
– ± asthenospheric melt invasion
After Richards, 2011
Natural Resources
Canada
Ressources naturelles
Canada
Canada

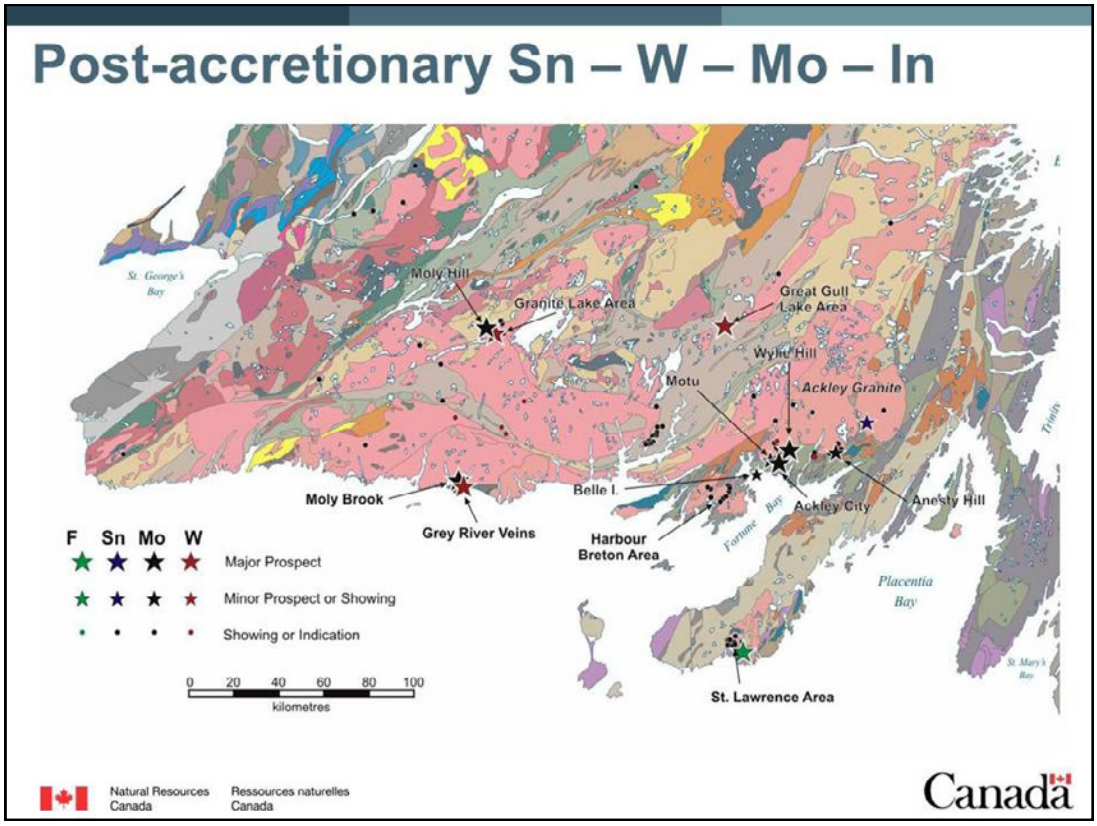
Post-accretionary Sn – W – Mo – In
St. George's Bay
Moly Hill
Granite Lake Area
Great Gull Lake Area
Wylie Hill
Motu
Ackley Granite
Moly Brook
Grey River Veins
Belle I.
Harbour Breton Area
Fortune Bay
Ackley City
Anesty Hill
Placentia Bay
St. Lawrence Area
F Sn Mo W
Major Prospect
Minor Prospect or Showing
Showing or Indication
0 20 40 60 80 100
kilometres
Natural Resources Canada
Ressources naturelles Canada
Canada

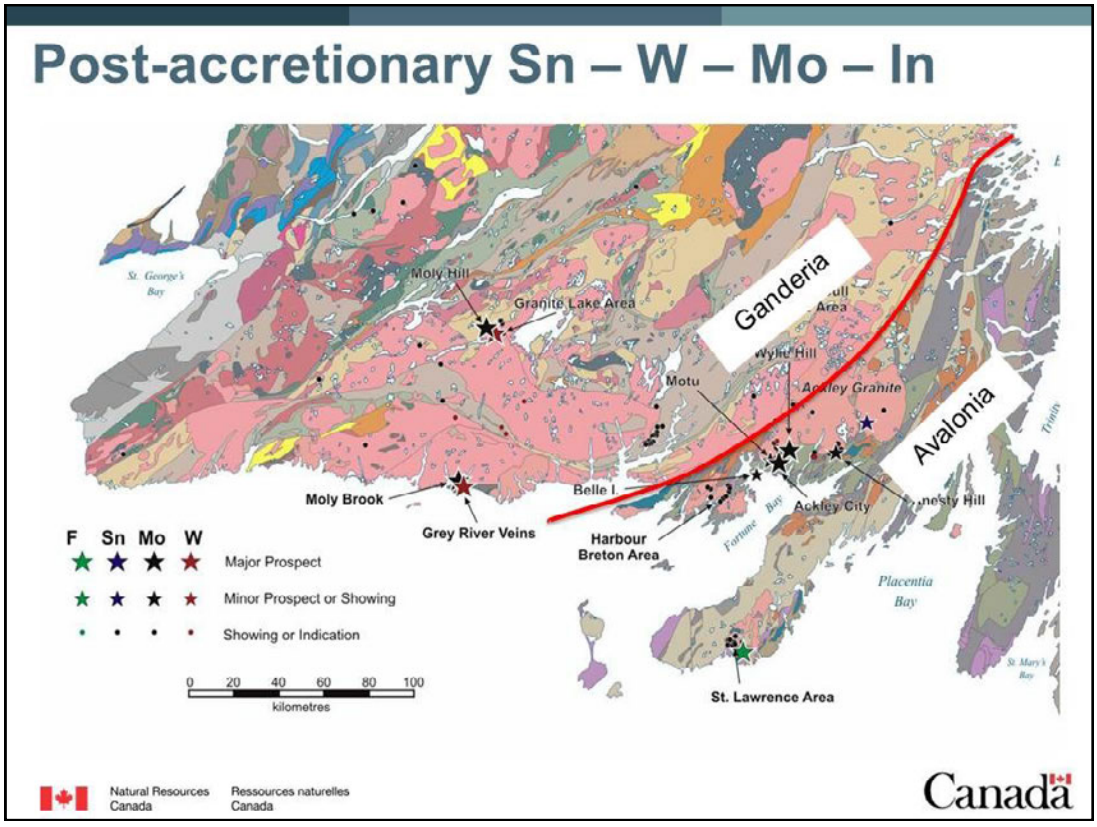
Post-accretionary Sn – W – Mo – In
St. George's Bay
Moly Hill
Granite Lake Area
Ganderia
Wylie Hill
Motu
Ackley Granite
Avalonia
Moly Brook
Grey River Veins
Belle I.
Harbour Breton Area
Fortune Bay
Ackley City
Placentia Bay
St. Lawrence Area
F Sn Mo W
Major Prospect
Minor Prospect or Showing
Showing or Indication
0 20 40 60 80 100
kilometres
Natural Resources Canada
Ressources naturelles Canada
Canada

Post-accretionary Sn – W – Mo – In

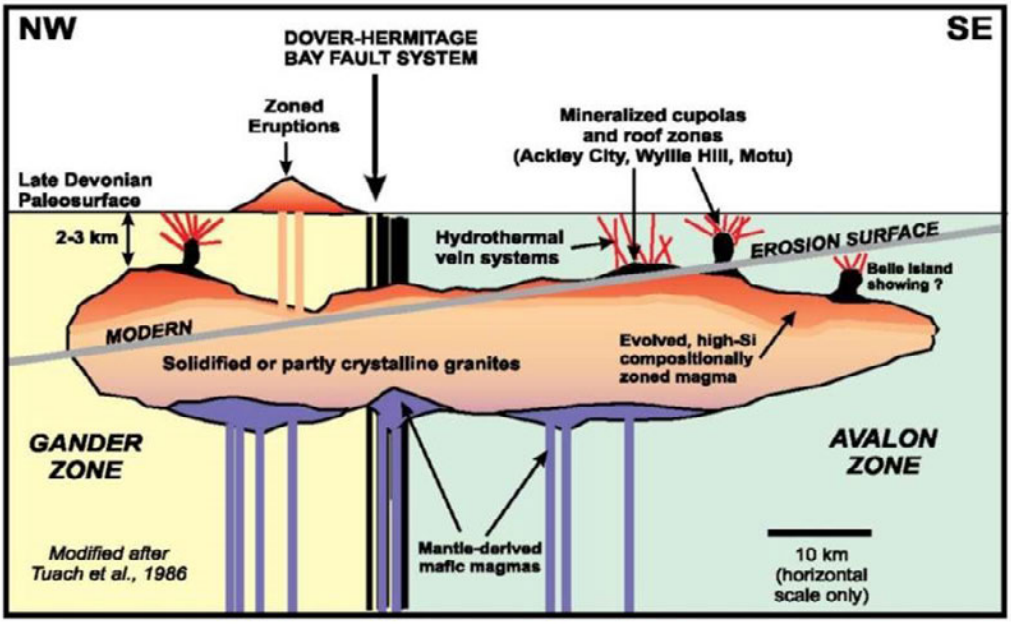

Natural Resources Canada Ressources naturelles Canada

Canada

Post-accretionary Sn – W – Mo – In

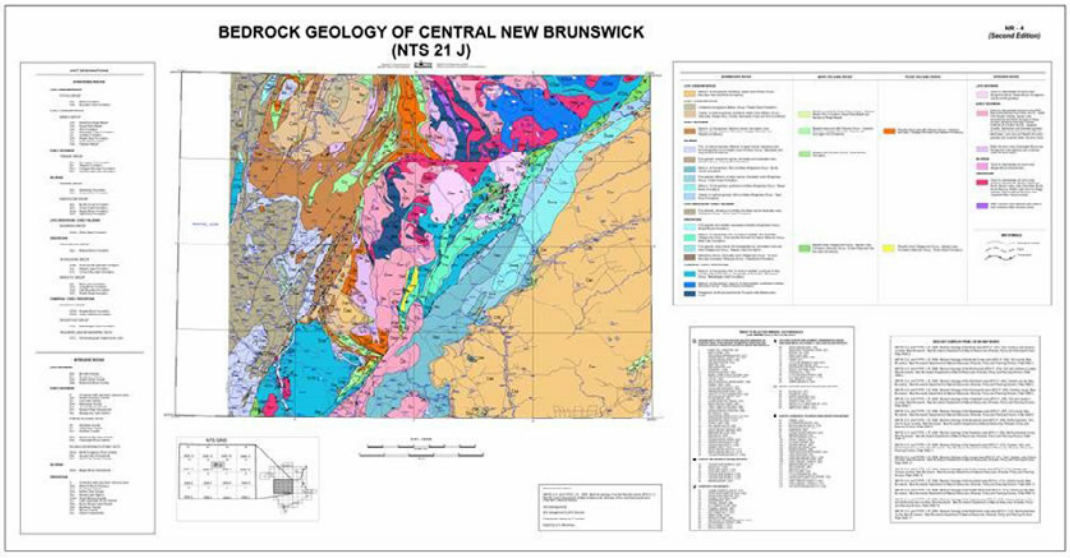

Natural Resources Canada Ressources naturelles Canada

Canada

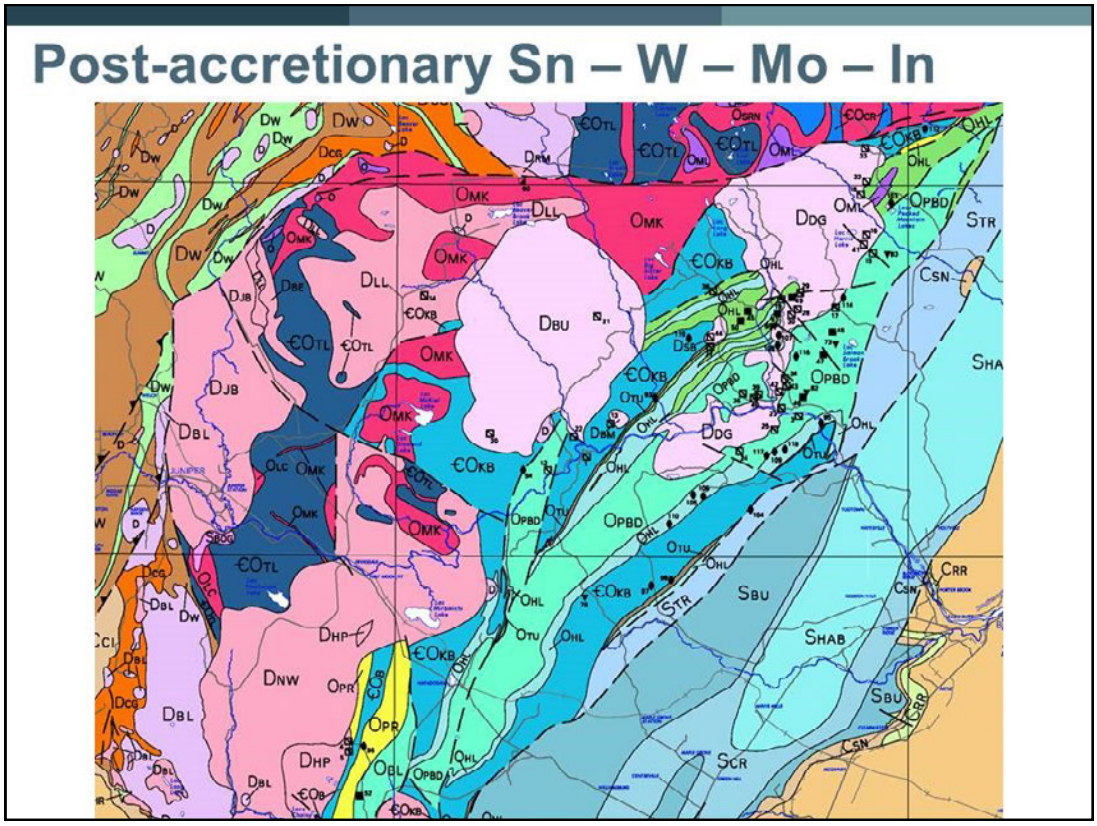
Post-accretionary Sn – W – Mo – In

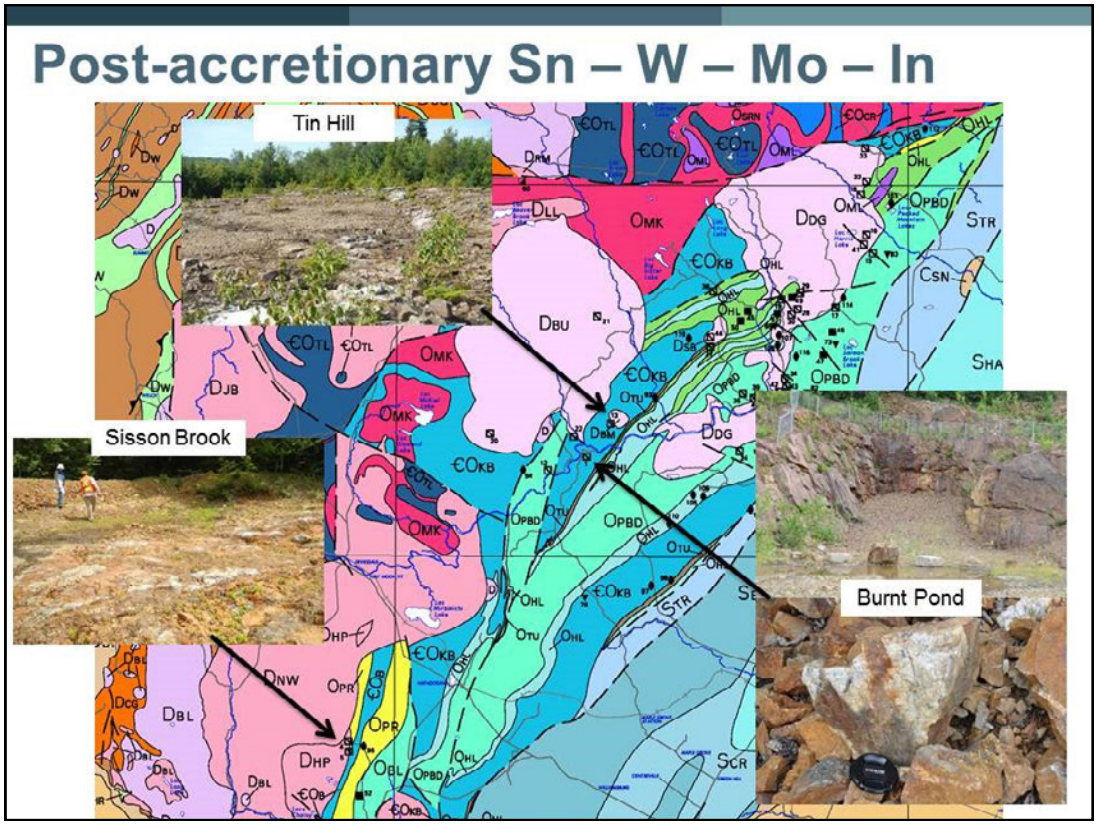
Post-accretionary Sn – W – Mo – In
Tin Hill
Sisson Brook
Burnt Pond

Post-accretionary Sn – W – Mo – In

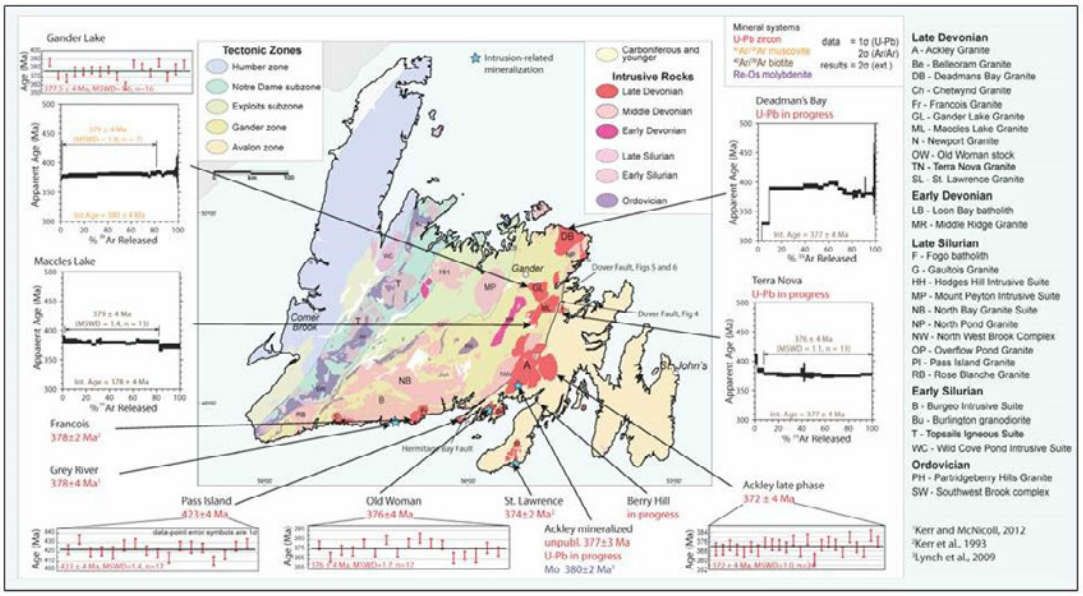

Natural Resources Canada Ressources naturelles Canada

Canada

Connaigre Peninsula, NL

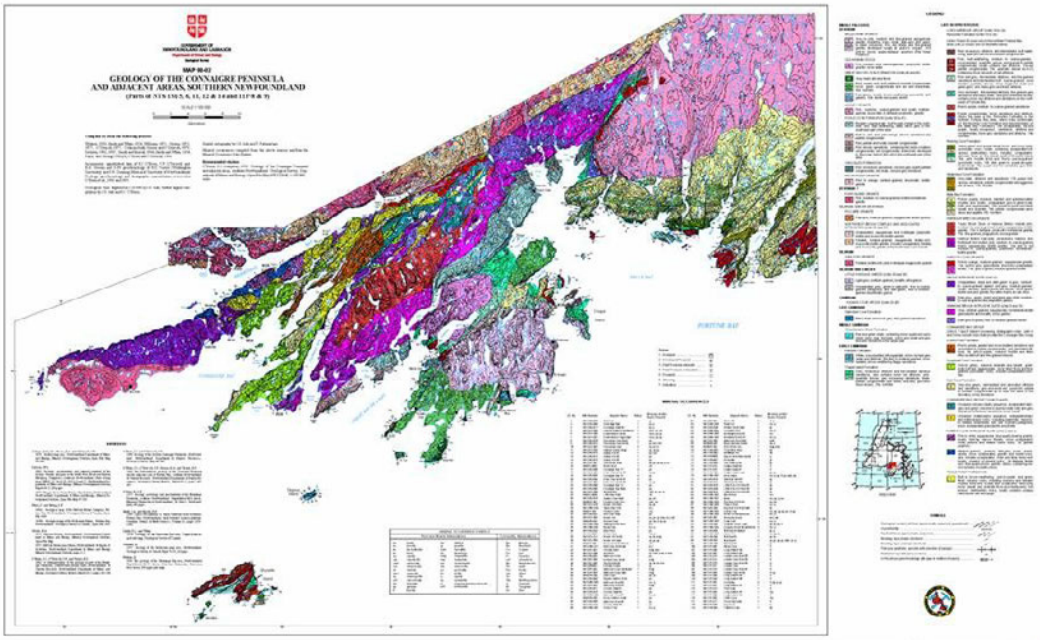

Natural Resources Canada Ressources naturelles Canada

Canada

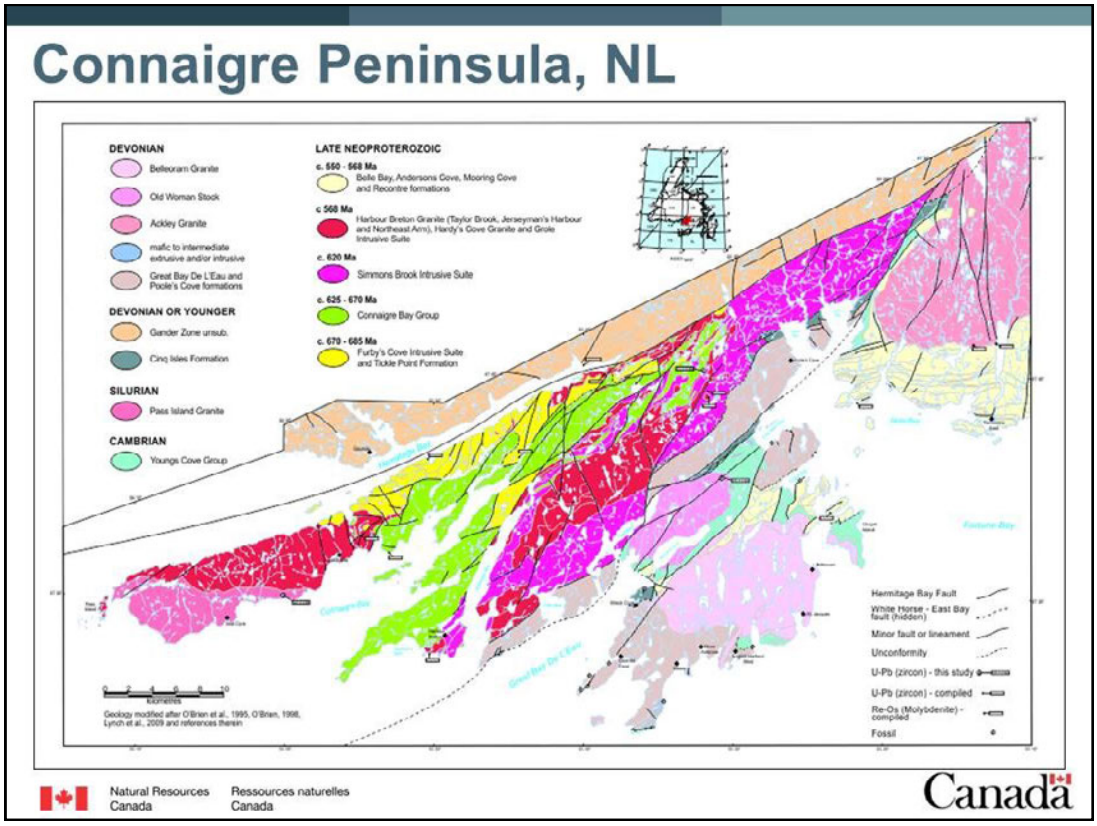
Connaigre Peninsula, NL
DEVONIAN
Belleoram Granite
Old Woman Stock
Ackley Granite
mafic to intermediate extrusive and/or intrusive
Great Bay De L'Eau and Poole's Cove formations
DEVONIAN OR YOUNGER
Gander Zone unsub.
Cinq Isles Formation
SILURIAN
Pass Island Granite
CAMBRIAN
Youngs Cove Group
LATE NEOPROTEROZOIC
c. 550 - 568 Ma
Belle Bay, Andersons Cove, Mooring Cove and Recontre formations
c 568 Ma
Harbour Breton Granite (Taylor Brook, Jerseyman's Harbour and Northeast Arm), Hardy's Cove Granite and Grole Intrusive Suite
c. 620 Ma
Simmons Brook Intrusive Suite
c. 625 - 670 Ma
Connaigre Bay Group
c. 670 - 685 Ma
Furby's Cove Intrusive Suite and Tickle Point Formation
Hermitage Bay Fault
White Horse - East Bay fault (hidden)
Minor fault or lineament
Unconformity
U-Pb (zircon) - this study
U-Pb (zircon) - compiled
Re-Os (Molybdenite) - compiled
Fossil
Geology modified after O'Brien et al., 1995, O'Brien, 1998, Lynch et al., 2009 and references therein
Natural Resources Canada
Ressources naturelles Canada
Canada

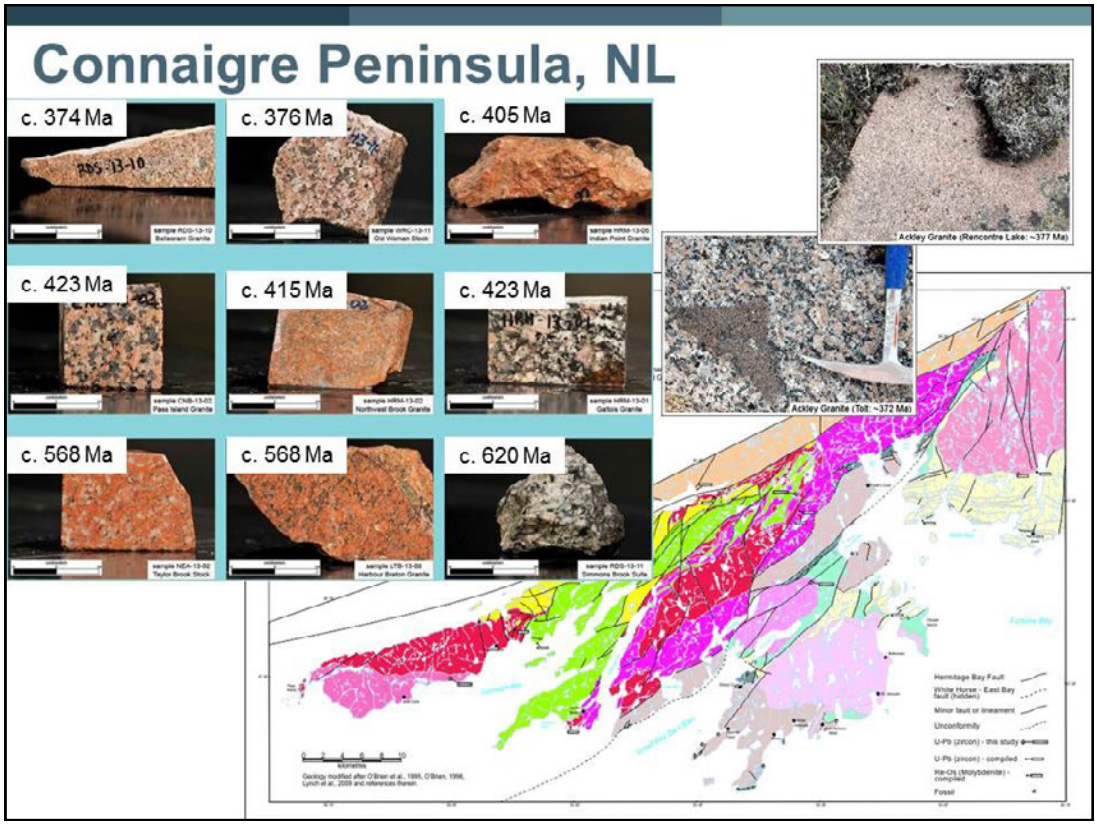
Connaigre Peninsula, NL
c. 374 Ma
c. 376 Ma
c. 405 Ma
c. 423 Ma
c. 415 Ma
c. 423 Ma
c. 568 Ma
c. 568 Ma
c. 620 Ma
Ackley Granite (Rencontre Lake: ~377 Ma)
Ackley Granite (Toll: ~372 Ma)

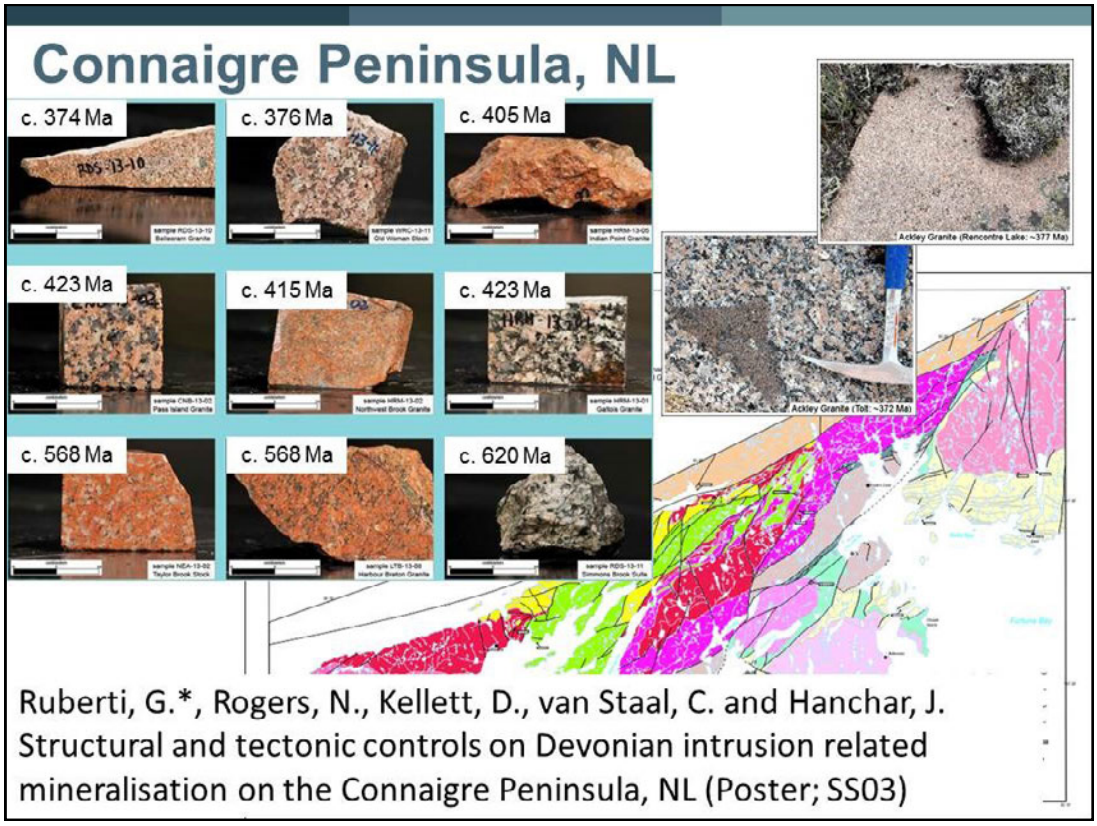
Connaigre Peninsula, NL
c. 374 Ma
c. 376 Ma
c. 405 Ma
c. 423 Ma
c. 415 Ma
c. 423 Ma
c. 568 Ma
c. 568 Ma
c. 620 Ma
Ackley Granite (Rencontre Lake: ~377 Ma)
Ackley Granite (Toll: ~372 Ma)
Ruberti, G.*, Rogers, N., Kellett, D., van Staal, C. and Hanchar, J.
Structural and tectonic controls on Devonian intrusion related
mineralisation on the Connaigre Peninsula, NL (Poster; SS03)

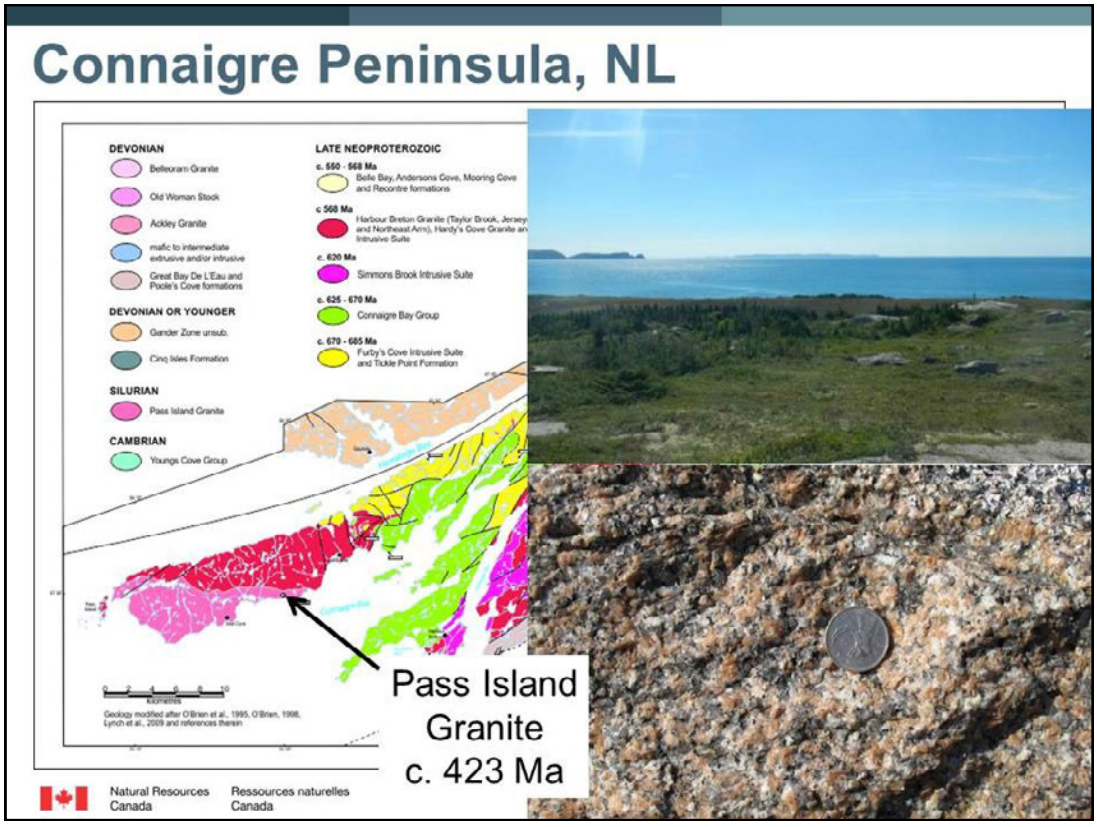
Connaigre Peninsula, NL
DEVONIAN
Belleoram Granite
Old Woman Stock
Ackley Granite
mafic to intermediate extrusive and/or intrusive
Great Bay De L'Eau and Poole's Cove formations
DEVONIAN OR YOUNGER
Gander Zone undiv.
Cinq Isles Formation
SILURIAN
Pass Island Granite
CAMBRIAN
Youngs Cove Group
LATE NEOPROTEROZOIC
c. 550 - 568 Ma
Belle Bay, Andersons Cove, Mooring Cove and Recontre formations
c 568 Ma
Harbour Breton Granite (Taylor Brook, Jersey and Northeast Arm), Hardy's Cove Granite an Intrusive Suite
c. 620 Ma
Simmons Brook Intrusive Suite
c. 625 - 670 Ma
Connaigre Bay Group
c. 670 - 685 Ma
Furby's Cove Intrusive Suite and Tickle Point Formation
Pass Island Granite
c. 423 Ma
Natural Resources Canada
Ressources naturelles Canada

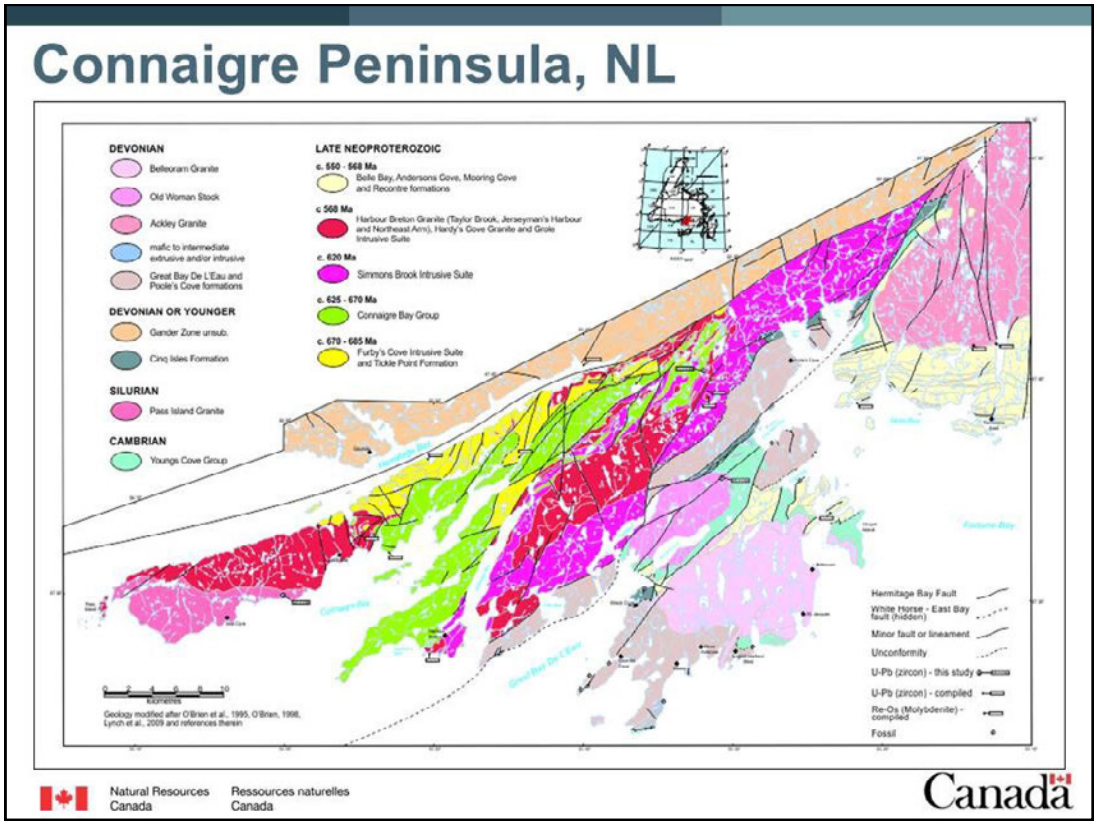
Connaigre Peninsula, NL
DEVONIAN
Belleoram Granite
Old Woman Stock
Ackley Granite
mafic to intermediate extrusive and/or intrusive
Great Bay De L'Eau and Poole's Cove formations
DEVONIAN OR YOUNGER
Gander Zone unsub.
Cinq Isles Formation
SILURIAN
Pass Island Granite
CAMBRIAN
Youngs Cove Group
LATE NEOPROTEROZOIC
c. 550 - 568 Ma
Belle Bay, Andersons Cove, Mooring Cove and Recontre formations
c 568 Ma
Harbour Breton Granite (Taylor Brook, Jerseyman's Harbour and Northeast Arm), Hardy's Cove Granite and Grole Intrusive Suite
c. 620 Ma
Simmons Brook Intrusive Suite
c. 625 - 670 Ma
Connaigre Bay Group
c. 670 - 685 Ma
Furby's Cove Intrusive Suite and Tickle Point Formation
Hermitage Bay Fault
White Horse - East Bay fault (hidden)
Minor fault or lineament
Unconformity
U-Pb (zircon) - this study
U-Pb (zircon) - compiled
Re-Os (Molybdenite) - compiled
Fossil
Kilometres
Geology modified after O'Brien et al., 1995, O'Brien, 1998, Lynch et al., 2009 and references therein
Natural Resources Canada
Ressources naturelles Canada
Canada

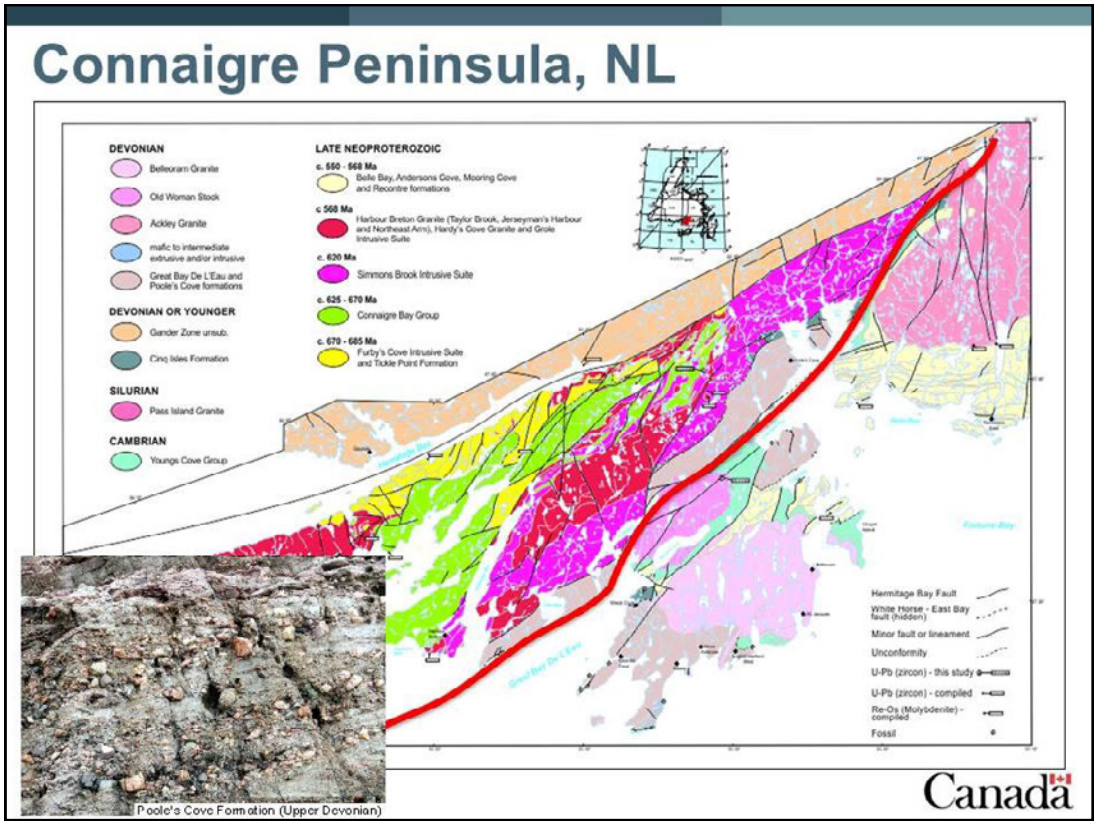
Connaigre Peninsula, NL
DEVONIAN
Belleoram Granite
Old Woman Stock
Ackley Granite
mafic to intermediate extrusive and/or intrusive
Great Bay De L'Eau and Poole's Cove formations
DEVONIAN OR YOUNGER
Gander Zone unsub.
Cinq Isles Formation
SILURIAN
Pass Island Granite
CAMBRIAN
Youngs Cove Group
LATE NEOPROTEROZOIC
c. 550 - 568 Ma
Belle Bay, Andersons Cove, Mooring Cove and Recontre formations
c 568 Ma
Harbour Breton Granite (Taylor Brook, Jerseyman's Harbour and Northeast Arm), Hardy's Cove Granite and Grole Intrusive Suite
c. 620 Ma
Simmons Brook Intrusive Suite
c. 625 - 670 Ma
Connaigre Bay Group
c. 670 - 685 Ma
Furby's Cove Intrusive Suite and Tickle Point Formation
Hermitage Bay Fault
White Horse - East Bay fault (hidden)
Minor fault or lineament
Unconformity
U-Pb (zircon) - this study
U-Pb (zircon) - compiled
Re-Os (Molybdenite) - compiled
Fossil
Poole's Cove Formation (Upper Devonian)
Canada

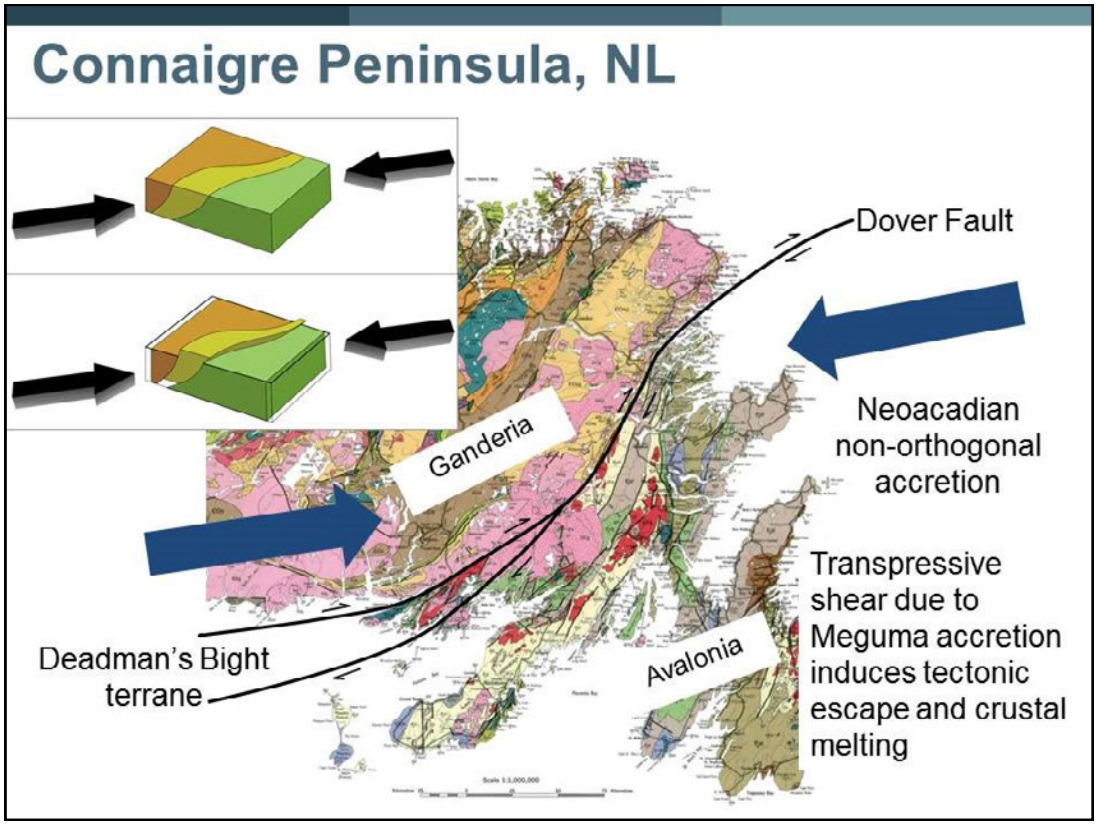
Connaigre Peninsula, NL
Dover Fault
Neoacadian non-orthogonal accretion
Ganderia
Transpressive shear due to Meguma accretion induces tectonic escape and crustal melting
Deadman's Bight terrane
Avalonia

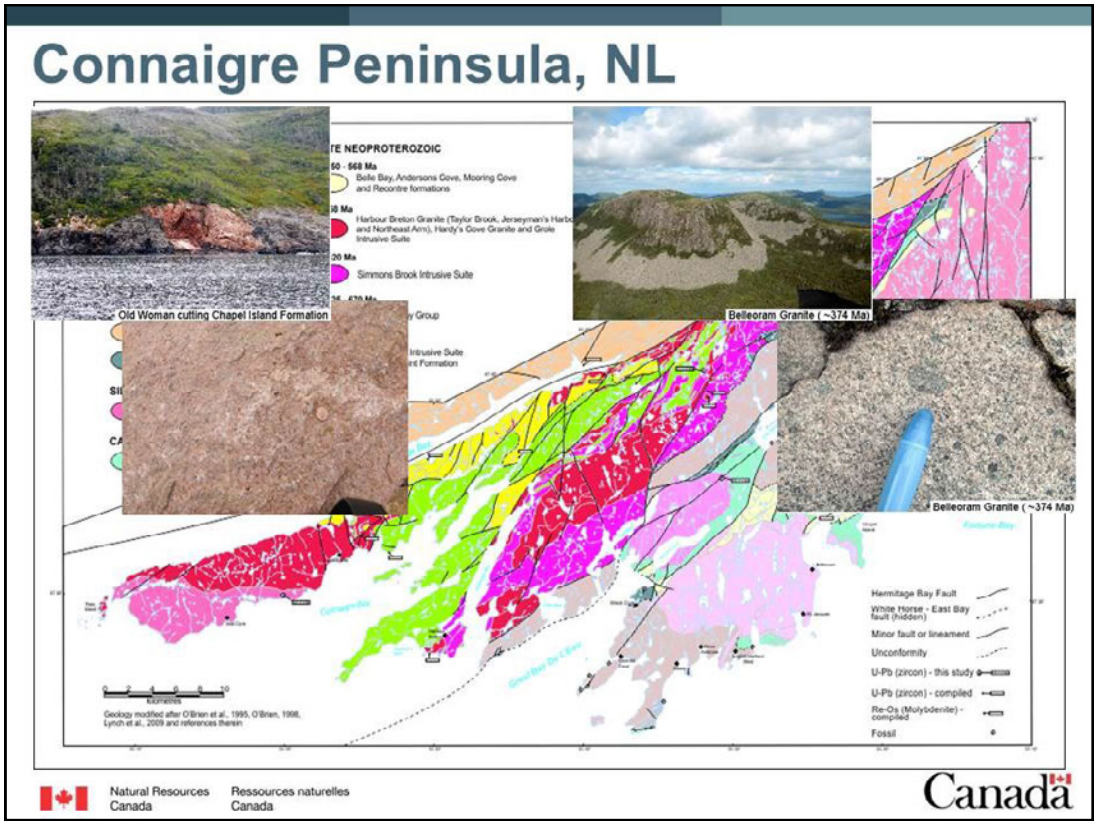
Connaigre Peninsula, NL
Old Woman cutting Chapel Island Formation
Belleoram Granite (~374 Ma)
Belleoram Granite (~374 Ma)
Simmons Brook Intrusive Suite
Hermitage Bay Fault
Minor fault or lineament
Unconformity
U-Pb (zircon) - this study
U-Pb (zircon) - compiled
Fossil
Natural Resources Canada
Ressources naturelles Canada
Canada

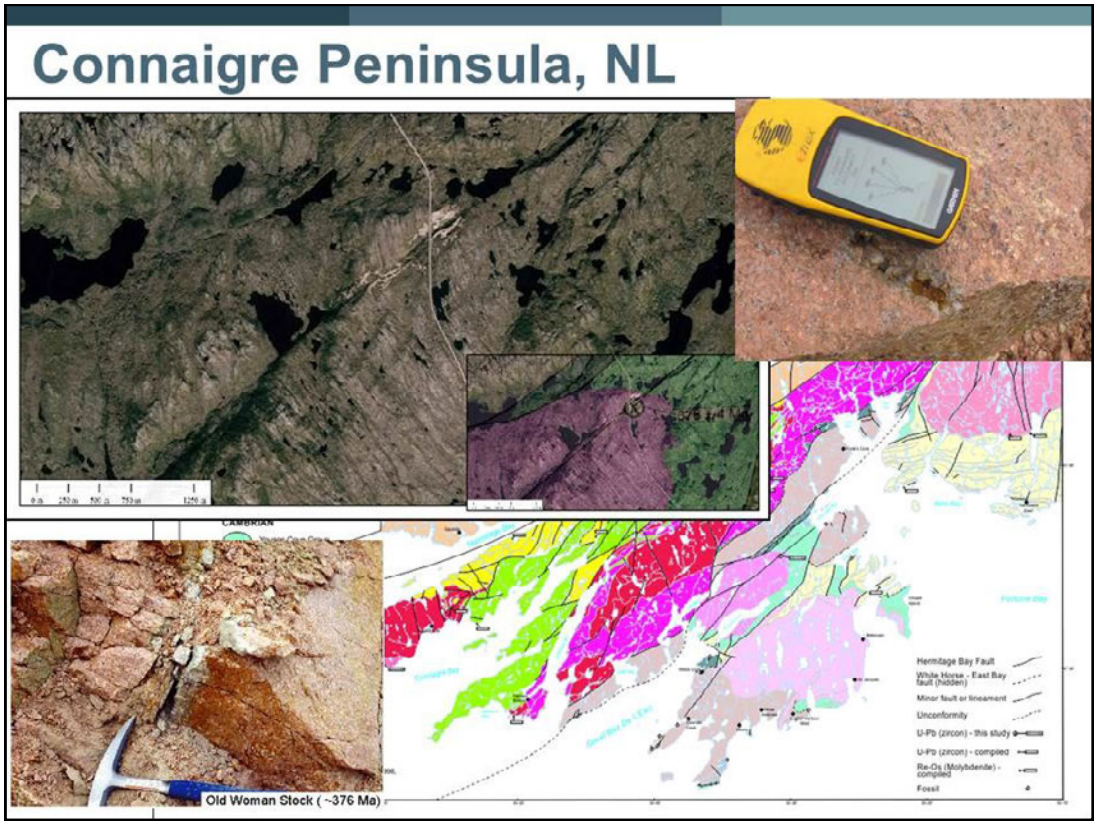
Connaigre Peninsula, NL
Old Woman Stock (~376 Ma)
Hermitage Bay Fault
White Horse - East Bay fault (hidden)
Minor fault or lineament
Unconformity
U-Pb (zircon) - this study
U-Pb (zircon) - compiled
Re-Os (Molybdenite) - compiled
Fossil

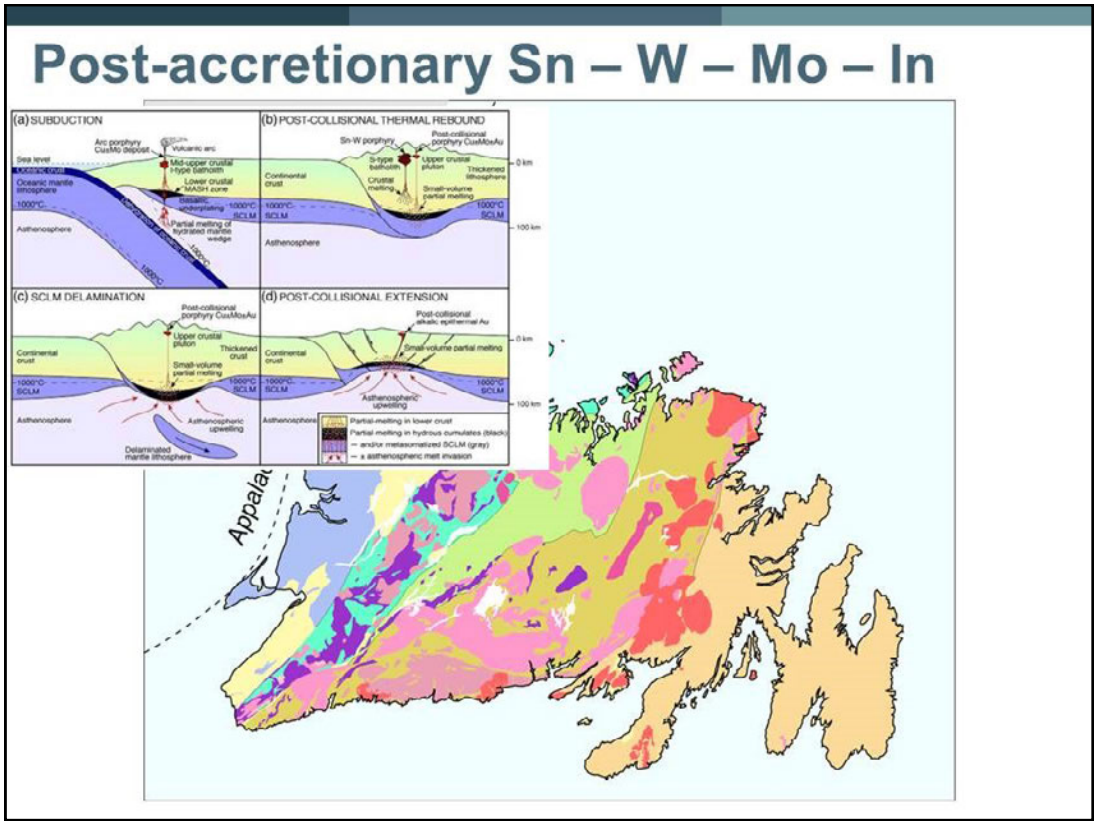
Post-accretionary Sn – W – Mo – In
(a) SUBDUCTION
(b) POST-COLLISIONAL THERMAL REBOUND
(c) SCLM DELAMINATION
(d) POST-COLLISIONAL EXTENSION
Appala

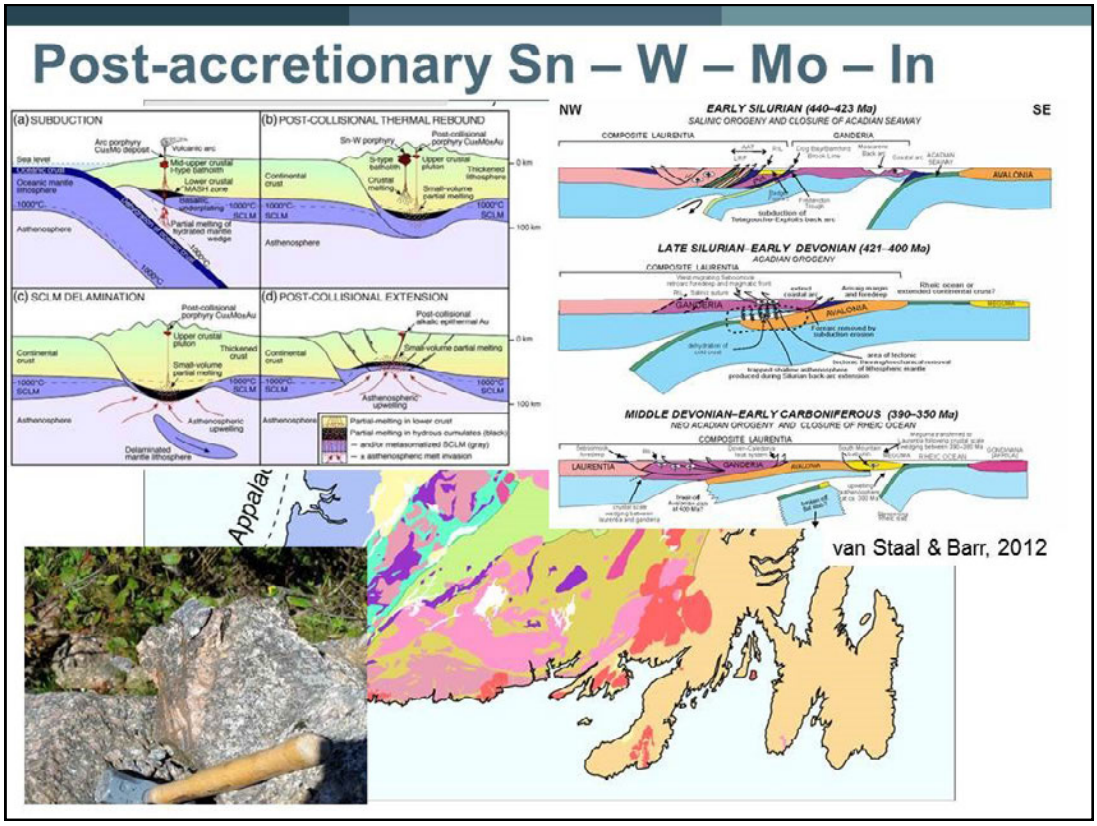
Post-accretionary Sn – W – Mo – In
(a) SUBDUCTION
(b) POST-COLLISIONAL THERMAL REBOUND
(c) SCLM DELAMINATION
(d) POST-COLLISIONAL EXTENSION
NW
SE
EARLY SILURIAN (440–423 Ma)
SALINIC OROGENY AND CLOSURE OF ACADIAN SEAWAY
LATE SILURIAN–EARLY DEVONIAN (421–400 Ma)
ACADIAN OROGENY
MIDDLE DEVONIAN–EARLY CARBONIFEROUS (390–350 Ma)
NEO ACADIAN OROGENY AND CLOSURE OF RHEIC OCEAN
van Staal & Barr, 2012

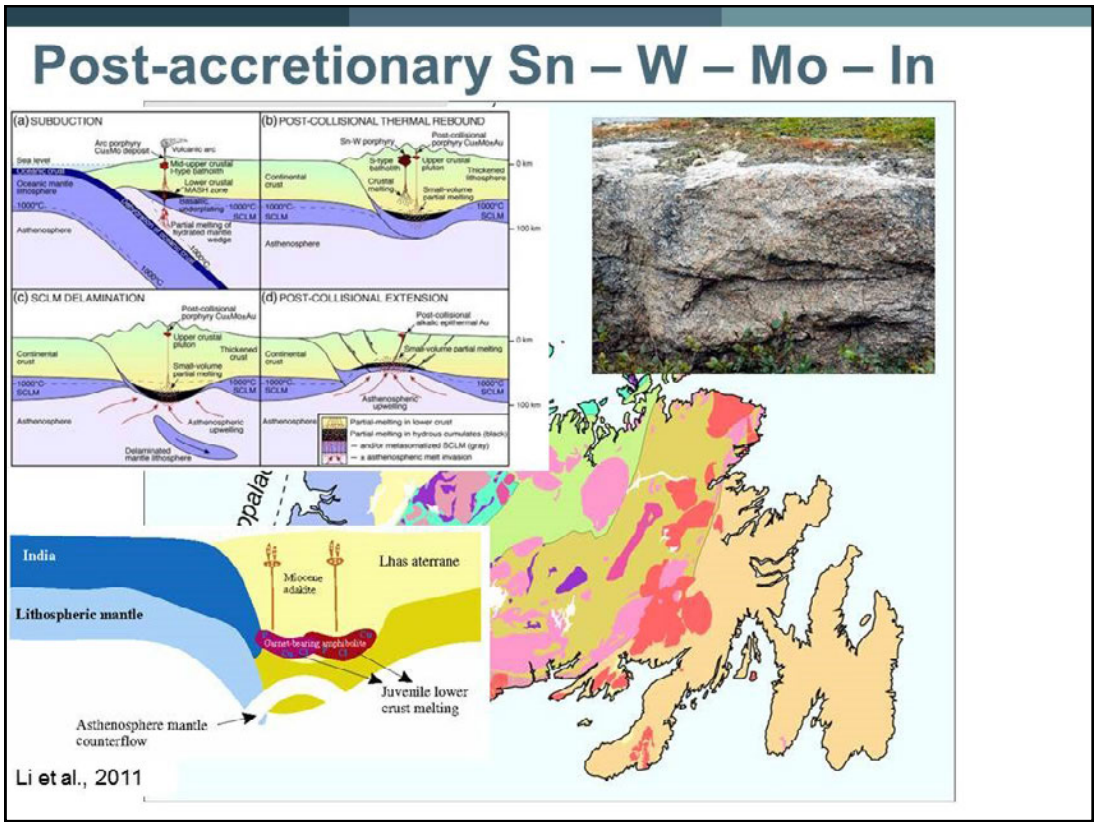
Post-accretionary Sn – W – Mo – In
India
Lithospheric mantle
Lhas aterrane
Miocene adakite
Quartet-bearing amphibolite
Juvenile lower crust melting
Asthenosphere mantle counterflow
Li et al., 2011

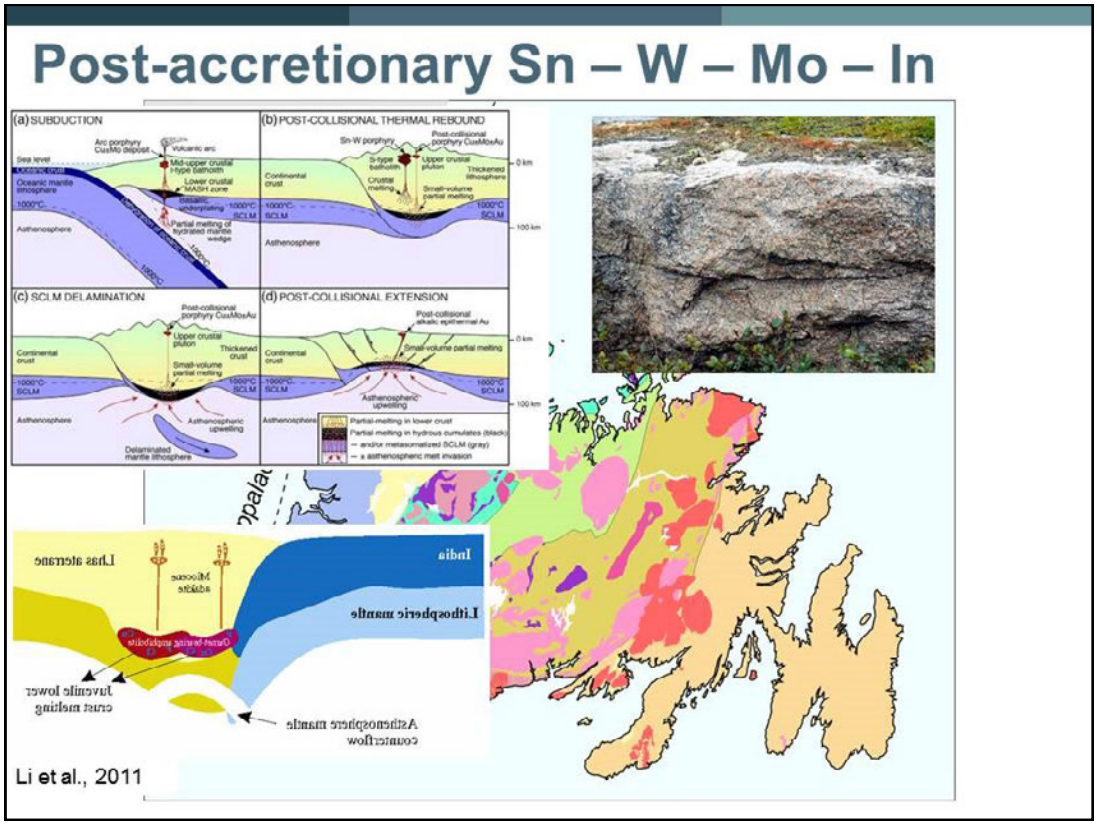
Post-accretionary Sn – W – Mo – In
(a) SUBDUCTION
(b) POST-COLLISIONAL THERMAL REBOUND
(c) SCLM DELAMINATION
(d) POST-COLLISIONAL EXTENSION
Li et al., 2011

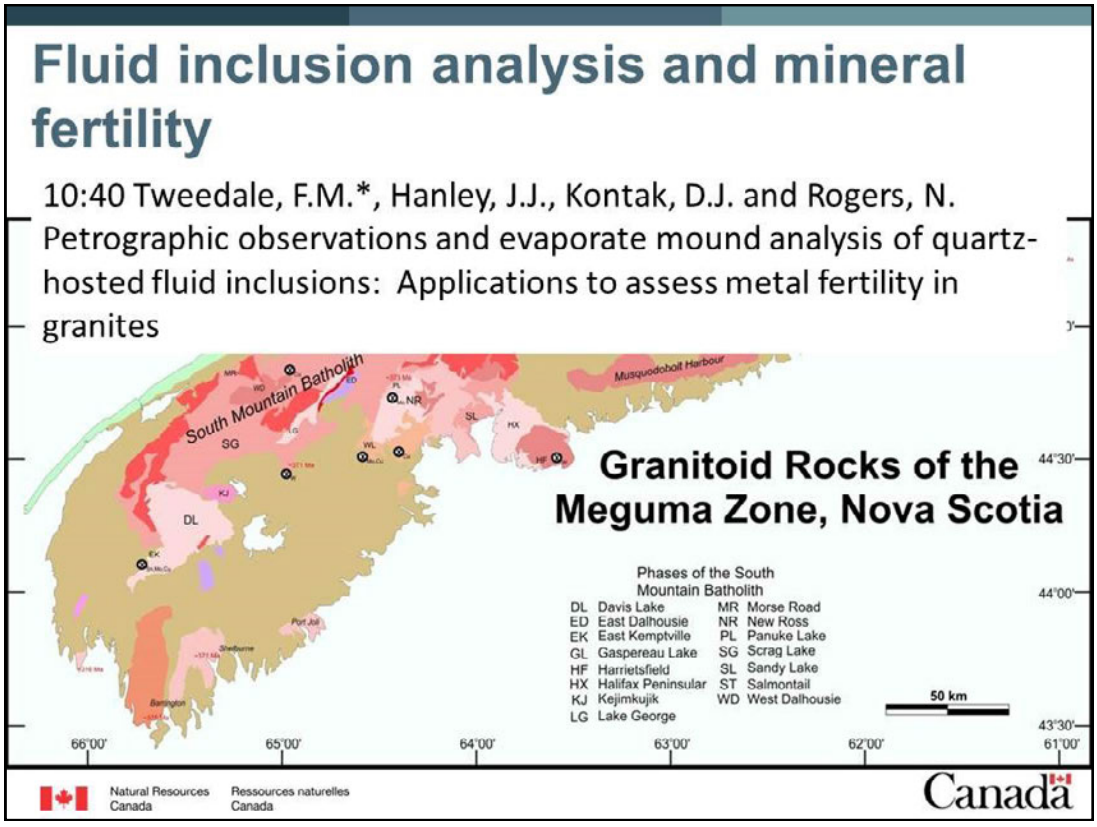
Fluid inclusion analysis and mineral fertility
10:40 Tweedale, F.M.*, Hanley, J.J., Kontak, D.J. and Rogers, N. Petrographic observations and evaporate mound analysis of quartz-hosted fluid inclusions: Applications to assess metal fertility in granites
South Mountain Batholith
Musquodoboit Harbour
Granitoid Rocks of the Meguma Zone, Nova Scotia
Phases of the South Mountain Batholith
DL Davis Lake
ED East Dalhousie
EK East Kemptville
GL Gaspereau Lake
HF Harrietsfield
HX Halifax Peninsular
KJ Kejimkujik
LG Lake George
MR Morse Road
NR New Ross
PL Panuke Lake
SG Scrag Lake
SL Sandy Lake
ST Salmontail
WD West Dalhousie
50 km
66°00'
65°00'
64°00'
63°00'
62°00'
61°00'
44°30'
44°00'
43°30'
Natural Resources Canada
Ressources naturelles Canada
Canada

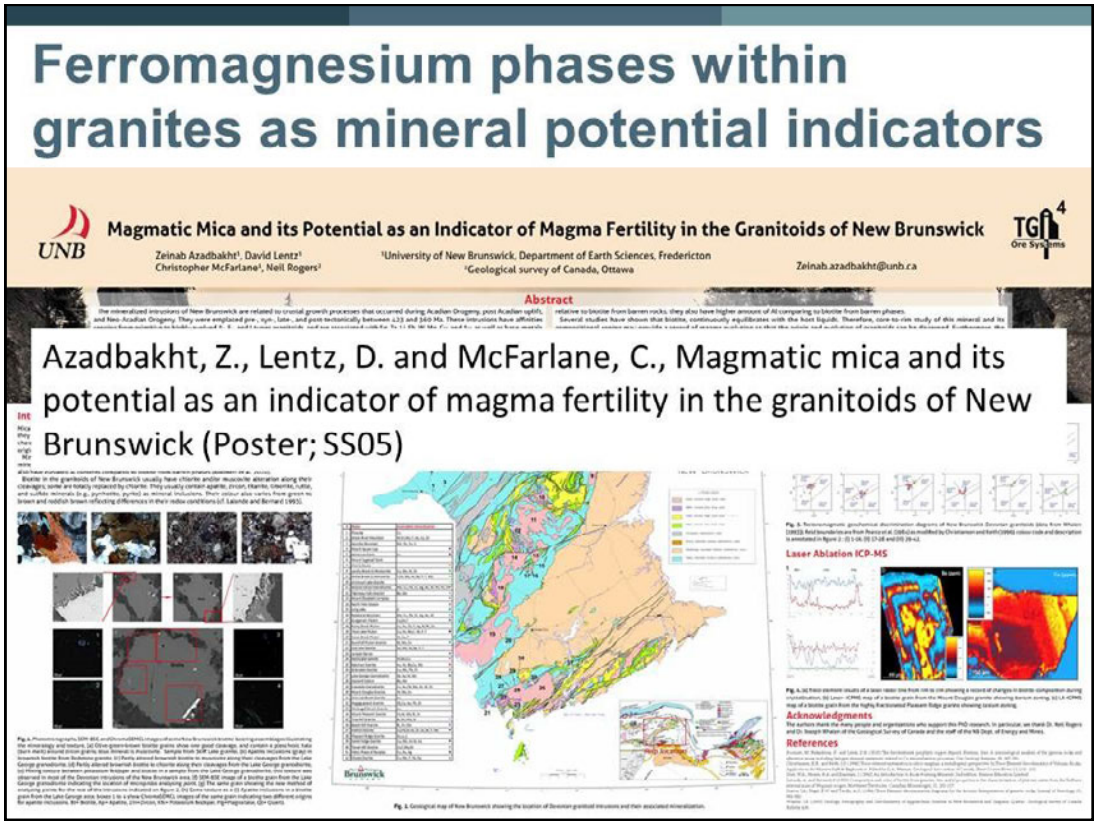
Ferromagnesium phases within granites as mineral potential indicators
Magmatic Mica and its Potential as an Indicator of Magma Fertility in the Granitoids of New Brunswick
Zeinab Azadbakht[1], David Lentz[1]
Christopher McFarlane[2], Neil Rogers[2]
[1]University of New Brunswick, Department of Earth Sciences, Fredericton
[2]Geological survey of Canada, Ottawa
Zeinab.azadbakht@unb.ca
Abstract
Azadbakht, Z., Lentz, D. and McFarlane, C., Magmatic mica and its potential as an indicator of magma fertility in the granitoids of New Brunswick (Poster; SS05)
Laser Ablation ICP-MS
Acknowledgments
References

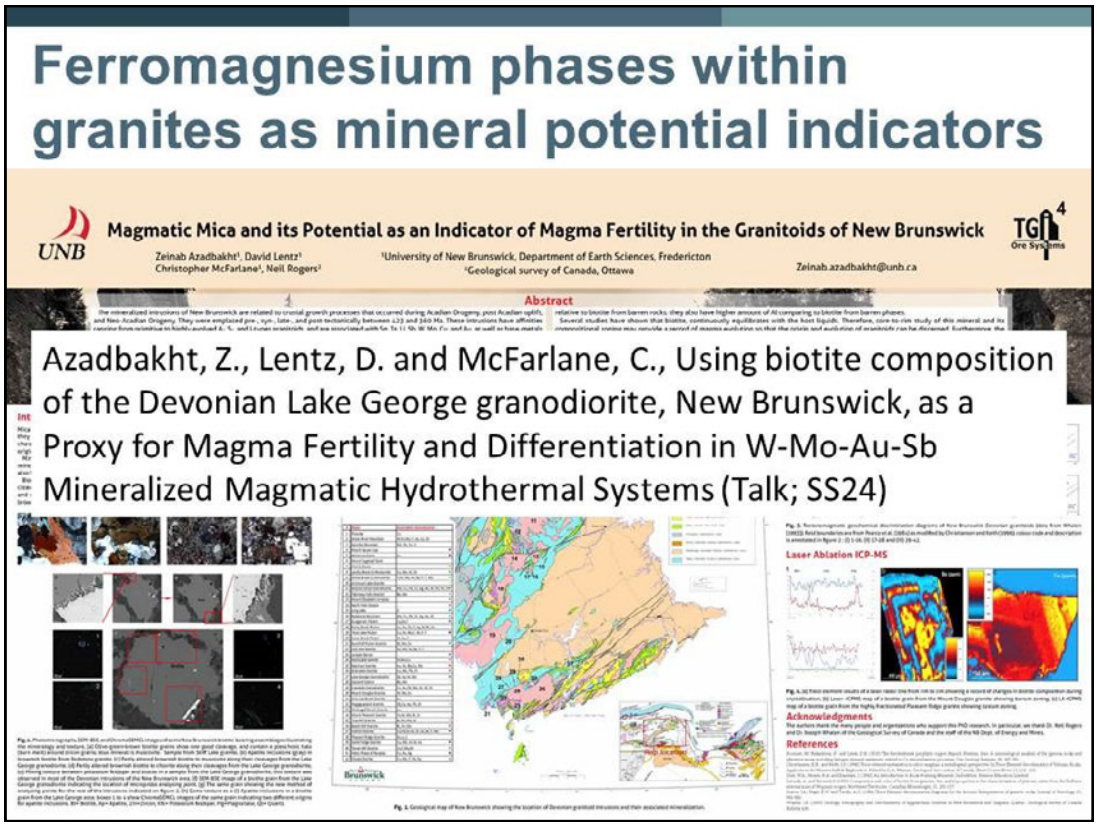
Ferromagnesium phases within granites as mineral potential indicators
Magmatic Mica and its Potential as an Indicator of Magma Fertility in the Granitoids of New Brunswick
Zeinab Azadbakht[1], David Lentz[1]
Christopher McFarlane[2], Neil Rogers[2]
[1]University of New Brunswick, Department of Earth Sciences, Fredericton
[2]Geological survey of Canada, Ottawa
Zeinab.azadbakht@unb.ca
Abstract
Azadbakht, Z., Lentz, D. and McFarlane, C., Using biotite composition of the Devonian Lake George granodiorite, New Brunswick, as a Proxy for Magma Fertility and Differentiation in W-Mo-Au-Sb Mineralized Magmatic Hydrothermal Systems (Talk; SS24)
Laser Ablation ICP-MS
Acknowledgments
References

Distribution and controls on indium within Sn-W-base metal mineralization

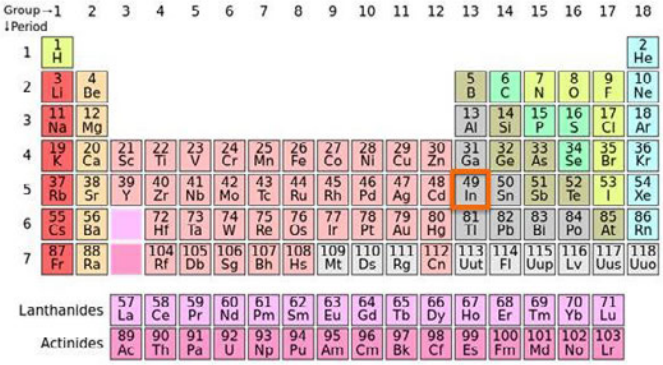

- Atomic number: 49
- Relative atomic mass: 114.8
- Melt point: 156.6 °C
- Post-transition or poor metal
- Discovered in Freiburg, Saxony, in 1863 by Reich and Richter
- First isolated in 1864
- Named for **indigo** spectral line

Natural Resources Canada Ressources naturelles Canada

Canada

Distribution and controls on indium within Sn-W-base metal mineralization

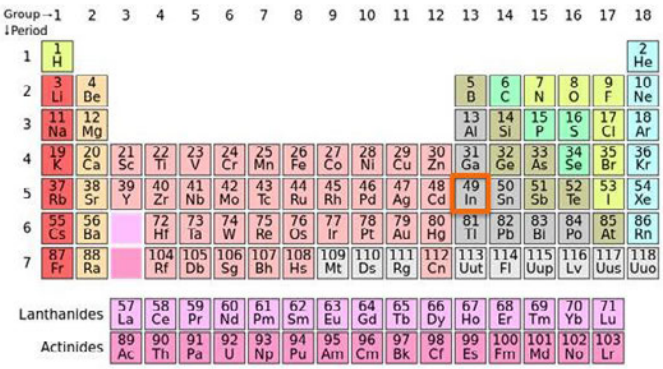

Chris Goeddeke (MSc – University of Winsor):

Controls on Indium content within post-collisional intrusive systems of the Canadian Appalachians

Natural Resources Canada Ressources naturelles Canada

Canada

Uses of Indium

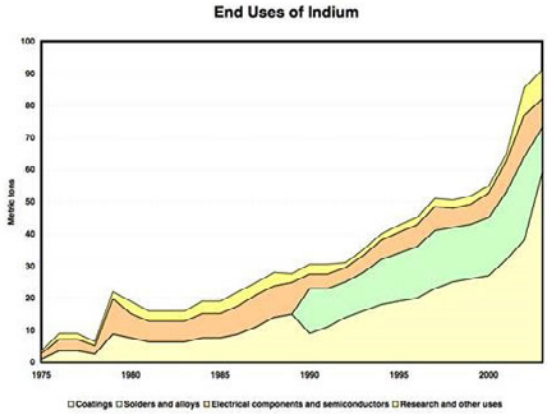

- The primary use of indium is for thin film coatings, principally indium-tin oxide (ITO)
  - Approximately 85% of global indium consumption
  - ITO is commonly 90% In_2O_3 and 10% SnO
  - Transparent, electrically conductive, low IR transmissibility

Second greatest use is for specialist solders and low melt-point alloys (≈ 8%)

Natural Resources Canada Ressources naturelles Canada

Canada

Indium Supply

- Global primary ≈ 670 t/yr
- Recycling ≈ 850 t/yr
- 55-60% from China
- Canada 2nd largest producer
- Teck Trail Smelter (BC) produces ≈ 75 t/yr
- Falconbridge (latterly Xstrata) Kidd Met. Site (ON) produced ≈ 40 t/yr
- Adex pilot trials produced Zn concentrate with 5310 ppm In, and hydrometallurgical indium sponge at 96.25%

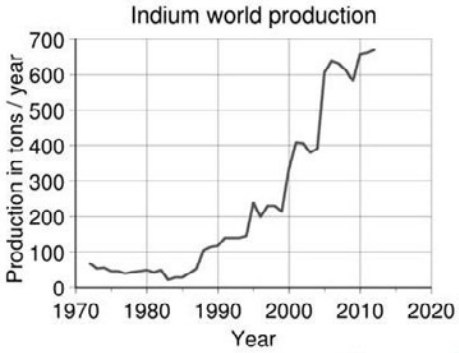

Natural Resources Canada Ressources naturelles Canada

Canada

Indium Mineralogy

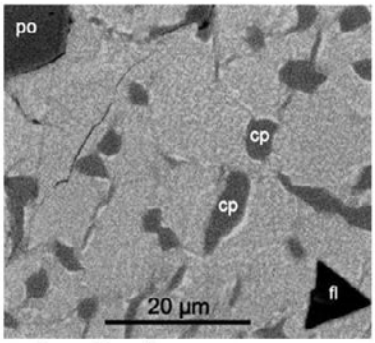

Sinclair *et al.* (2006)

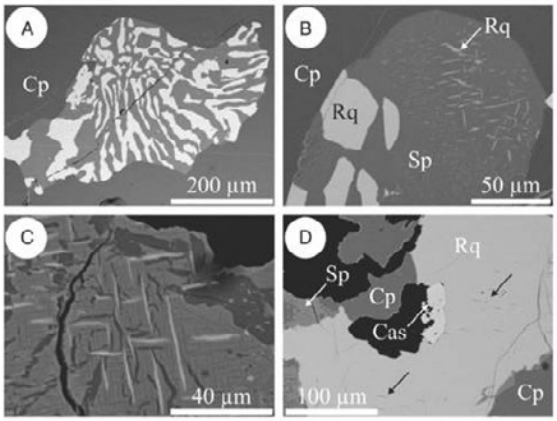

Cook *et al.* (2011)

- Most In sequestered into sphalerite, coupled substitution:
- $2(Zn^{2+},Fe^{2+}) \Leftrightarrow In^{3+} + Cu^{+}$
- Rapidly quenched high-temperature sphalerite has been shown to contain up to 14 wt.% In
- Slow cooling rates allow almost complete exsolution

Indium in Charlotte County

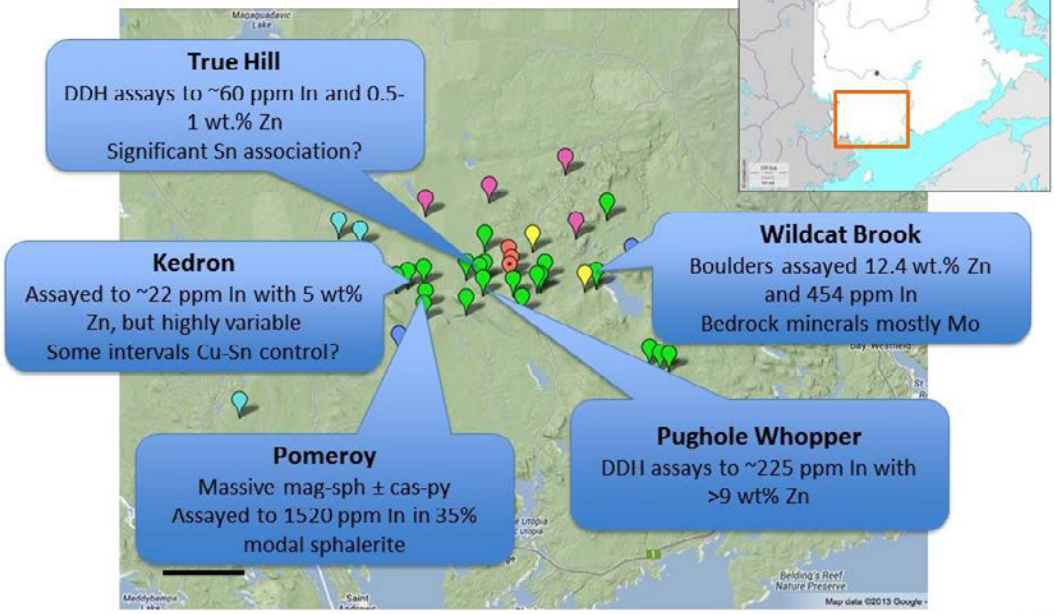

Indium in the Mount Pleasant Deposits

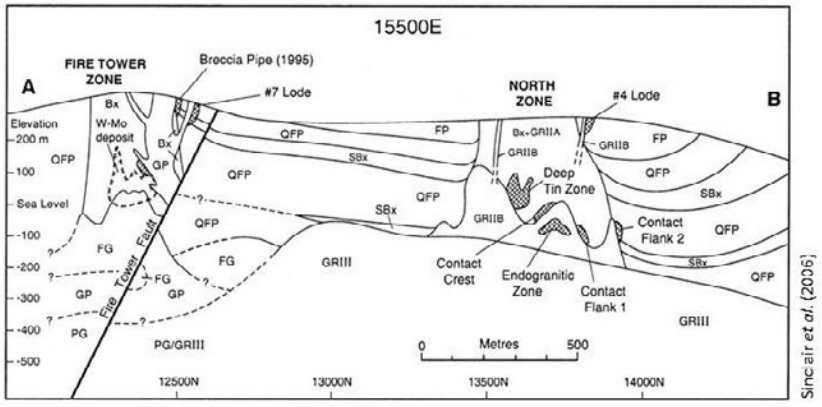

- Updated 2012 NI 43-101 indium resource estimate:
  - Indicated = 12.4 Mt @ 64 ppm
  - Inferred = 2.8 Mt @ 70 ppm
- Total contained In metal ≈ 987,000 kg ($0.6 – 0.7 bn)

Natural Resources Canada Ressources naturelles Canada

Canada

Indium in SW Nova Scotia

East Kemptville - Baby
Granite-hosted massive greisen. Abundant sphalerite and chalcopyrite, but little In

Duck Pond
Metasediment-hosted qtz-sulfide veins and greisen. Zn to wt% levels, no In data

Gardners Meadow
Metasediment-hosted qtz-sulfide veins. DDH assays to 26 ppm In with 1.07 wt% Zn

Kempt Snare Lake
Metasediment-hosted qtz-sulfide veins. Zn to wt% levels but little/no In

Dominique
Metasediment-hosted greisen Sn-Zn. DDH assays to 120 ppm In with 1.2 wt% Zn

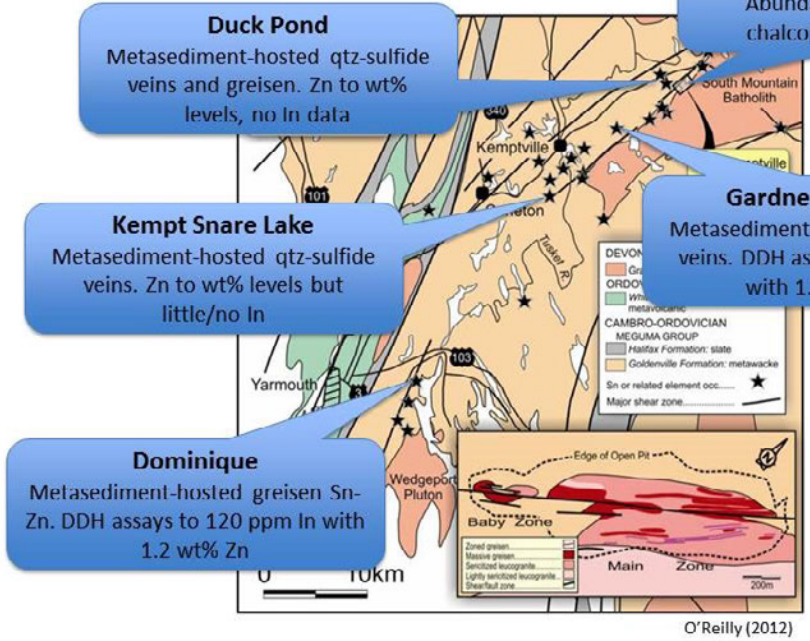

O'Reilly (2012)

Natural Resources Canada Ressources naturelles Canada

Canada

Project Outline

- What controls indium distribution within granite-associated Sn-W-Zn-Cu mineralization?
  - Do indium-rich zones simply reflect indium-rich fluid sources?
  - Is indium sequestration controlled by abundance of other elements (e.g. Cu, S, Zn) or a particular PT window?
  - Do high In+Cu zones reflect proximity to heat and fluid sources?
  - PTX conditions during mineral precipitation determined by fluid inclusion microthermometry and single inclusion LA-ICP-MS

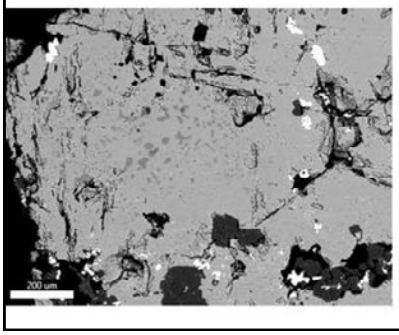

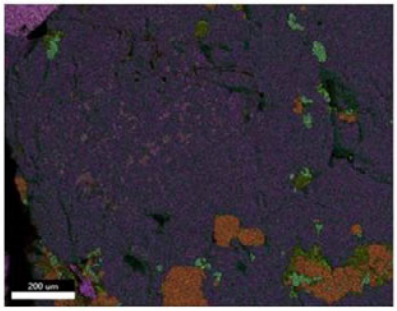

Canada

Project Outline

- In distribution is decoupled from W mineralisation, and likely from the main phase of Sn mineralisation
- Decoupling suggests that secondary enrichment/metasomatism by late stage In-rich, Zn-poor fluids are a primary control
- Kesterite is thought to be the mineral giving the best indication of high-temperature, high-copper fluids most conducive to the high-indium content
  - Kesterite - $Cu_2(Zn,Fe)SnS_4$

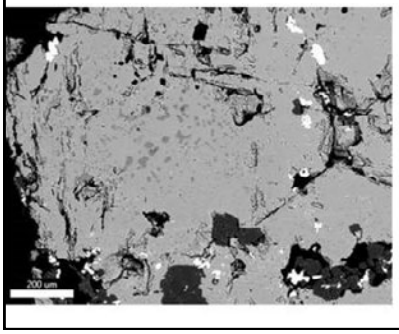

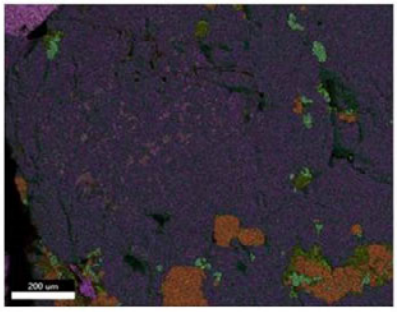

Canada

Glacial stratigraphic, till geochemical, and indicator mineral studies at the Sisson W-Mo and Mount Pleasant Sn-W-Mo-Bi-In polymetallic deposits, southwestern New Brunswick

M.A. Parkhill[1], M.B. McClenaghan[2], A.A. Seaman[3], A.G. Pronk[3] and J.M. Rice[4]

1. Geological Surveys Branch, New Brunswick Department of Energy and Mines, PO Box 50, Bathurst, New Brunswick

2. Geological Survey of Canada, 601 Booth St, Ottawa, Ontario

3. Geological Surveys Branch, New Brunswick Department of Energy and Mines, PO Box 6000, Fredericton, New Brunswick

4. Department of Earth Sciences, Brock University, 500 Glenridge Ave., St. Catharines, Ontario

Abstract: During the Geological Survey of Canada's (GSC) Targeted Geoscience Initiative (TGI 4; 2010-2015), GSC and the New Brunswick Department of Energy and Mines (NBDEM) conducted indicator mineral case studies around the Sisson W-Mo and the Mount Pleasant Sn-W-Mo-Bi-In polymetallic deposits in New Brunswick. The objective is to document glacial dispersal patterns of W, Mo, Sn, and In-bearing indicator minerals and matrix geochemical signatures in till at varying distances down-ice of the deposits, in support of exploration in New Brunswick and other glaciated terrains. This is the first study to document glacial dispersal of W-bearing minerals around a significant W deposit.

At Sisson, 3 tills are present: Illinoian Northumberland till, Early-Middle Wisconsinan Caledonia till, and the geochemically barren, Younger Dryas, Collins Pond till. This presented sampling challenges as the tills are deposited by ice flows from different source areas and are geochemically distinct but not easy to distinguish. At Sisson, 79 bulk till samples were collected up-ice, overlying, and up to 14 km down-ice (SE) of the deposit. The distribution of sample sites was guided by previous sampling by Kidd Creek Mines and the NBDEM. Stream water, silt, and bulk samples were collected at 16 sites at Sisson to characterize scheelite abundance, size, and shape for comparison with grains in the till. At the Adex-owned Mount Pleasant deposit, 22 bulk till samples were collected. Here, sampling was guided by previous work conducted by N. Szabo (University of New Brunswick) and the NBDEM.

Till sampling was optimized by first collecting 200 g till samples (61 at Sisson and 50 at Mount Pleasant) and determination of W, Mo, Sn, Bi, Sn, and Cu concentrations, using a portable XRF (pXRF) spectrometer. At Sisson, anomalous pXRF concentrations match previously known NBDEM anomalies in the glacial dispersal train extending 14 km to the SE, and correlate well with subsequent borate fusion and aqua regia/ICP-MS analyses of the <0.063 mm fraction of till (up to 815 ppm W, 65 ppm Mo, and 978 ppm Cu). Till, stream, and a suite of bedrock samples have been processed to produce heavy mineral concentrates for assessment of indicator minerals and to characterize the indicator mineral signature of each deposit. Scheelite is abundant in both deposits, and a significant indicator mineral in till down-ice. Other indicator minerals of the Sisson deposit include molybdenite, chalcopyrite, wolframite, Bi minerals, sphalerite, and galena. Cassiterite, topaz, beudantite, anglesite, and wolframite are indicators of the Mount Pleasant deposit.

Originally presented Fredericton 2014: Geological Association of Canada - Mineralogical Association of Canada Joint Annual Meeting, Special Session 3: Discovering the Next Generation of Porphyry Deposits: Advancements in Locating and Understanding Hidden Intrusion-related Mineralization. May 21, 2014.

Corresponding author: Mike Parkhill (Michael.Parkhill@gnb.ca)

Parkhill, M.A, McClenaghan, M.B., Seaman, A.A., Pronk, A.G., and Rice, J.M., 2015. Glacial stratigraphic, till geochemical, and indicator mineral studies at the Sisson W-Mo and Mount Pleasant Sn-W-Mo-Bi-In polymetallic deposits, southwestern New Brunswick; *in* TGI 4 – Intrusion Related Mineralisation Project: New Vectors to Buried Porphyry-Style Mineralisation, (ed.) N. Rogers; Geological Survey of Canada, Open File 7843, p. 293-316.

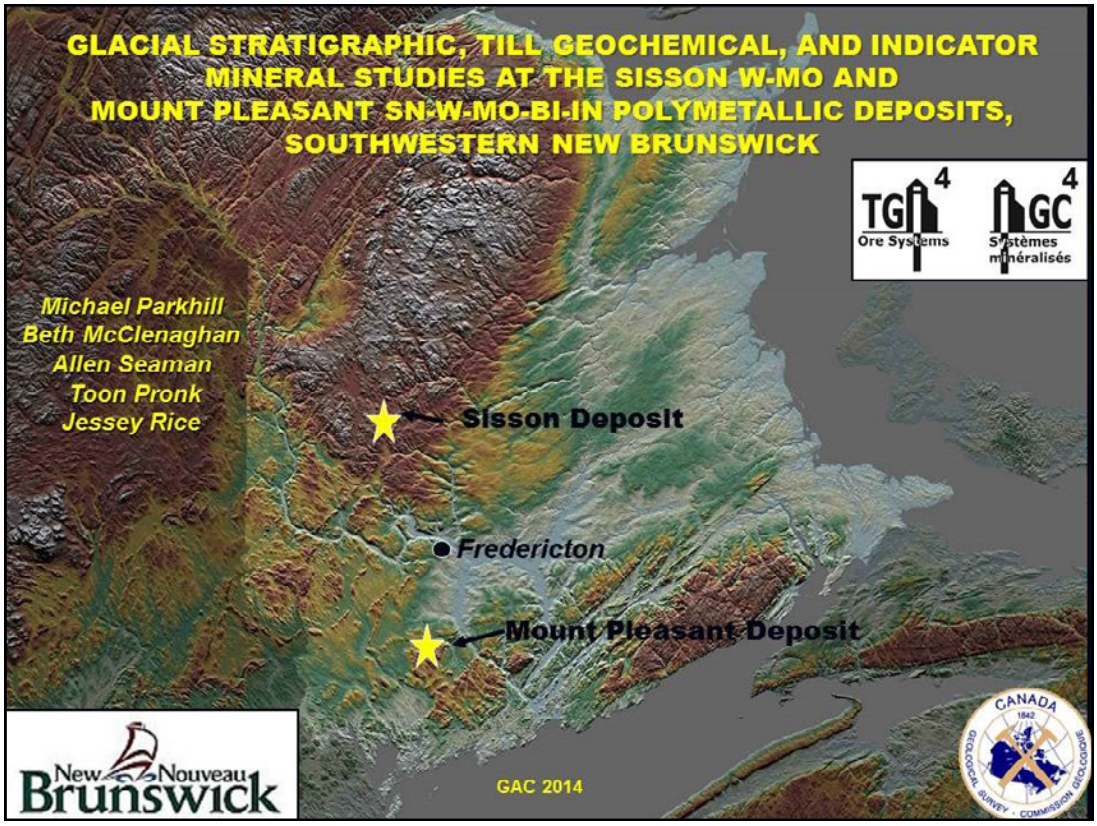
GLACIAL STRATIGRAPHIC, TILL GEOCHEMICAL, AND INDICATOR MINERAL STUDIES AT THE SISSON W-MO AND MOUNT PLEASANT SN-W-MO-BI-IN POLYMETALLIC DEPOSITS, SOUTHWESTERN NEW BRUNSWICK
TGI 4 Ore Systems
GC 4 Systèmes minéralisés
Michael Parkhill
Beth McClenaghan
Allen Seaman
Toon Pronk
Jessey Rice
Sisson Deposit
Fredericton
Mount Pleasant Deposit
New Nouveau Brunswick
GAC 2014
CANADA 1842 GEOLOGICAL SURVEY · COMMISSION GÉOLOGIQUE

New Nouveau Brunswick
Acknowledgements
CANADA 1842 GEOLOGICAL SURVEY · COMMISSION GÉOLOGIQUE
Geological Survey of Canada – Targeted Geoscience Initiative (TGI-4)
New Brunswick Geological Surveys Branch - Ordinary Budget
HDI Northcliff (Jim Lang, Will Gilmore, Rob Duncan, Drew Takahashi, Charlie Morrissy, Kandi Gallagher, Megan Little, Monique Morin, Jesse Spilman, Kyle McIntosh, Justin Giggee)
Adex Mining
Rex Boldon, Reid van Drecht, Mike Richards, Sarah Hashmi
Overburden Drilling Mgnt. Ltd.
TGI 4 Ore Systems
GC 4 Systèmes minéralisés

TGI-4 Indicator Mineral and Till Geochemical Dispersal Studies

OBJECTIVE:
Document indicator mineral dispersal in till and stream sediments from various deposit types to provide industry with a proven indicator mineral methodology for exploration.

NEW BRUNSWICK PROJECTS

1. Intrusion hosted Sn-W-Mo deposits:
   - Sisson
   - Mount Pleasant
2. Cu-Pb-Zn VMS deposits:
   Bathurst Mining Camp
   - Halfmile Lake, TGI-3 & TGI-4

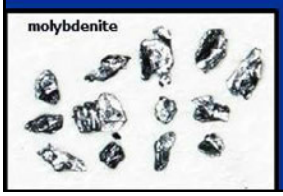

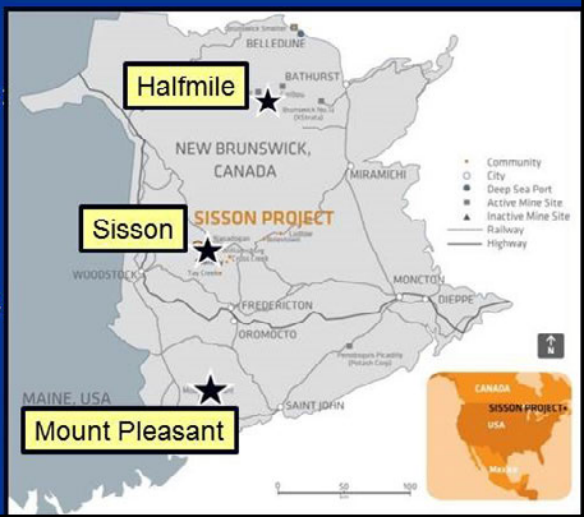

Properties of an Indicator Mineral

- Source-specific – deposit, bedrock
- Visually and chemically distinct
- Heavy (moderate to high density)
- Survives weathering and clastic transport
- Indicator minerals are silt to sand sized

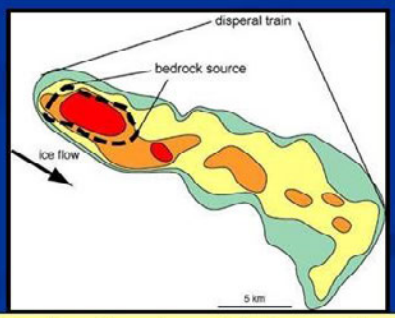

(Averill, 2007)

Exploration target is larger than mineralized bedrock source

Rationale for Sisson/Mount Pleasant Study:

- Geology well documented
- Glacier eroded ore zone
- Access to deposit – Northcliff and Adex
- Till covered

- Glacial history and glacial dispersal trains outlined during NBGSB till geochemical surveys;
  a guide to sampling of metal-rich till for indicator mineral studies
- No indicator mineral case studies have been published that document glacial dispersal from significant tungsten or tin deposits

"Sisson is the first tungsten (W) case study"

Sisson Exploration History

Pre-1978	**W geochem anomalies**
1978 - 1984	**Kidd Creek Mines (TexasGulf)** ▪ Outlined 3 mineralized zones and W and Mo rich till up to 8 km down-ice
2004 - 2009	**Geodex Minerals;** ▪ 46,500m of drilling ▪ Increased resource; ▪ Preliminary environmental, metallurgical, engineering studies and economic assessment
2010 - 2012	**Geodex Joint venture with Northcliff 2010** ▪ 11,000 m drilling in 2010-2011 ▪ Initiated feasibility and EIA studies
2013 - 2014	**100% Northcliff owned; mining plan underway**

Lang 2011

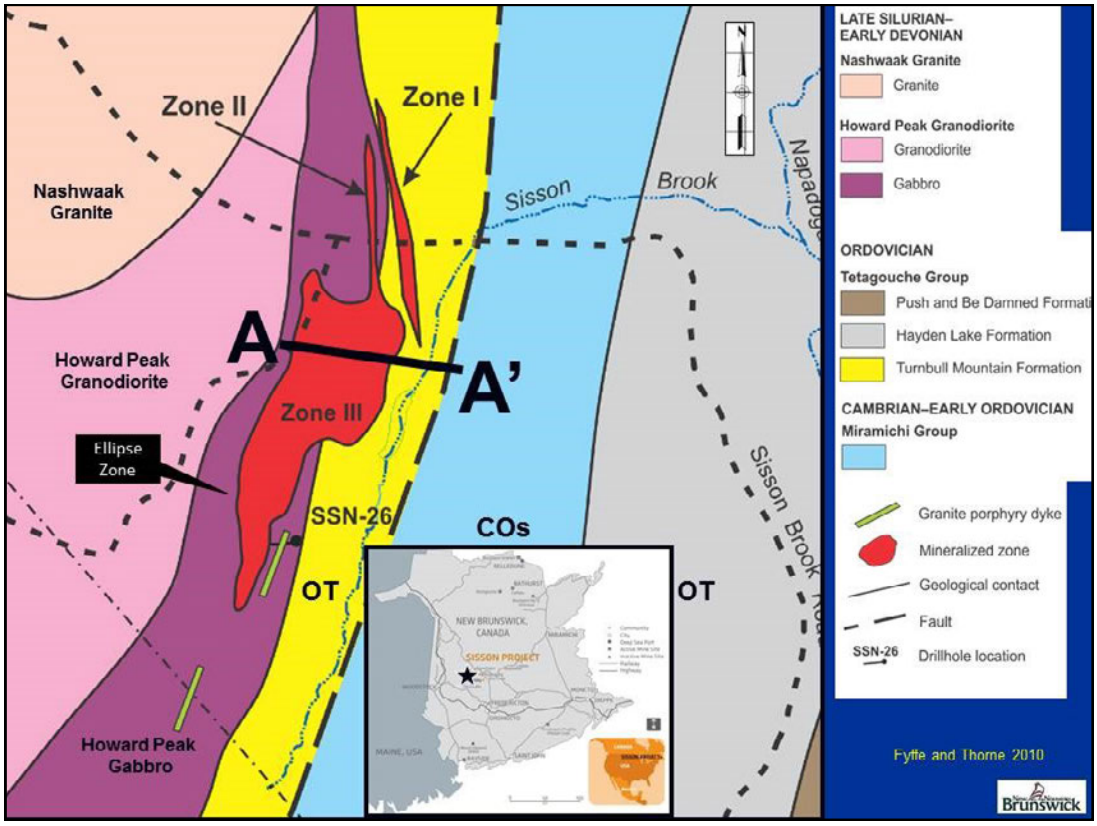
Zone II
Zone I
Nashwaak Granite
Sisson Brook
Howard Peak Granodiorite
A
A'
Zone III
Ellipse Zone
SSN-26
COs
OT
OT
Howard Peak Gabbro
Sisson Brook
LATE SILURIAN–EARLY DEVONIAN
Nashwaak Granite
Granite
Howard Peak Granodiorite
Granodiorite
Gabbro
ORDOVICIAN
Tetagouche Group
Push and Be Damned Formati
Hayden Lake Formation
Turnbull Mountain Formation
CAMBRIAN–EARLY ORDOVICIAN
Miramichi Group
Granite porphyry dyke
Mineralized zone
Geological contact
Fault
SSN-26
Drillhole location
Fyffe and Thorne 2010
Brunswick

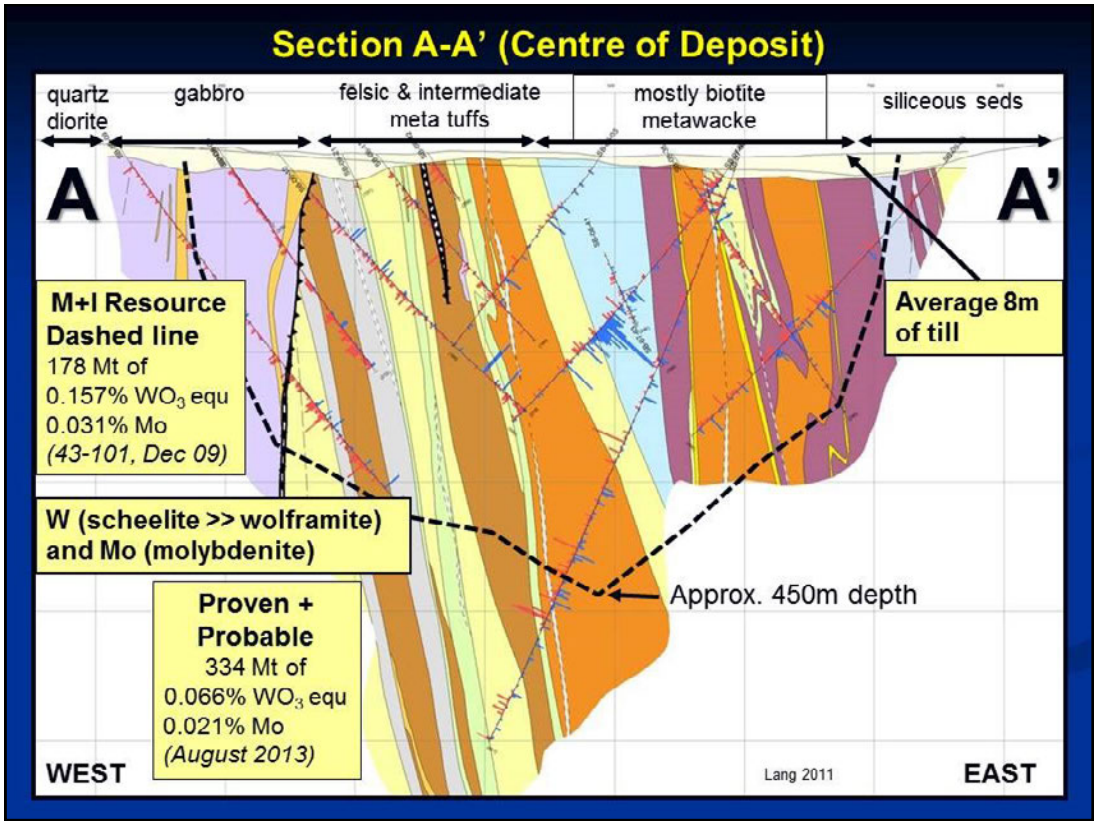
Section A-A' (Centre of Deposit)
quartz diorite
gabbro
felsic & intermediate meta tuffs
mostly biotite metawacke
siliceous seds
A
A'
M+I Resource
Dashed line
178 Mt of
0.157% WO3 equ
0.031% Mo
(43-101, Dec 09)
Average 8m of till
W (scheelite >> wolframite) and Mo (molybdenite)
Approx. 450m depth
Proven + Probable
334 Mt of
0.066% WO3 equ
0.021% Mo
(August 2013)
WEST
Lang 2011
EAST

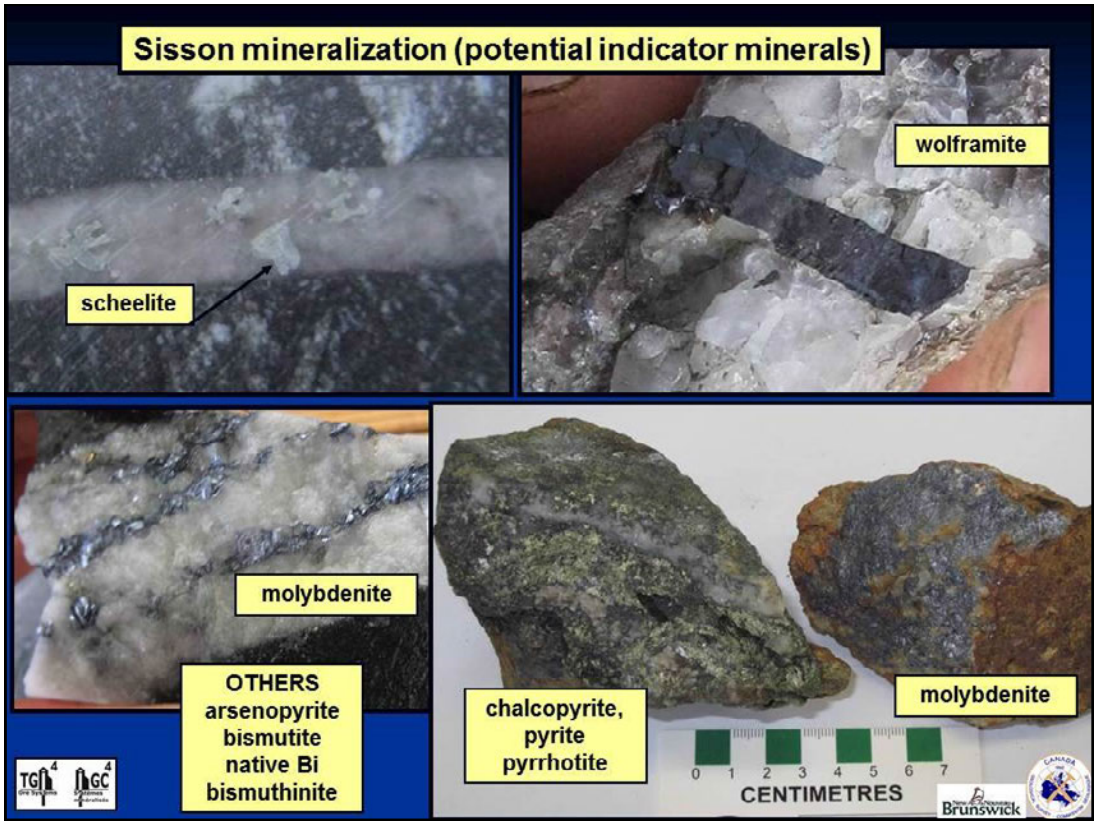
Sisson mineralization (potential indicator minerals)
scheelite
wolframite
molybdenite
OTHERS
arsenopyrite
bismutite
native Bi
bismuthinite
chalcopyrite,
pyrite
pyrrhotite
molybdenite
0 1 2 3 4 5 6 7
CENTIMETRES
Brunswick

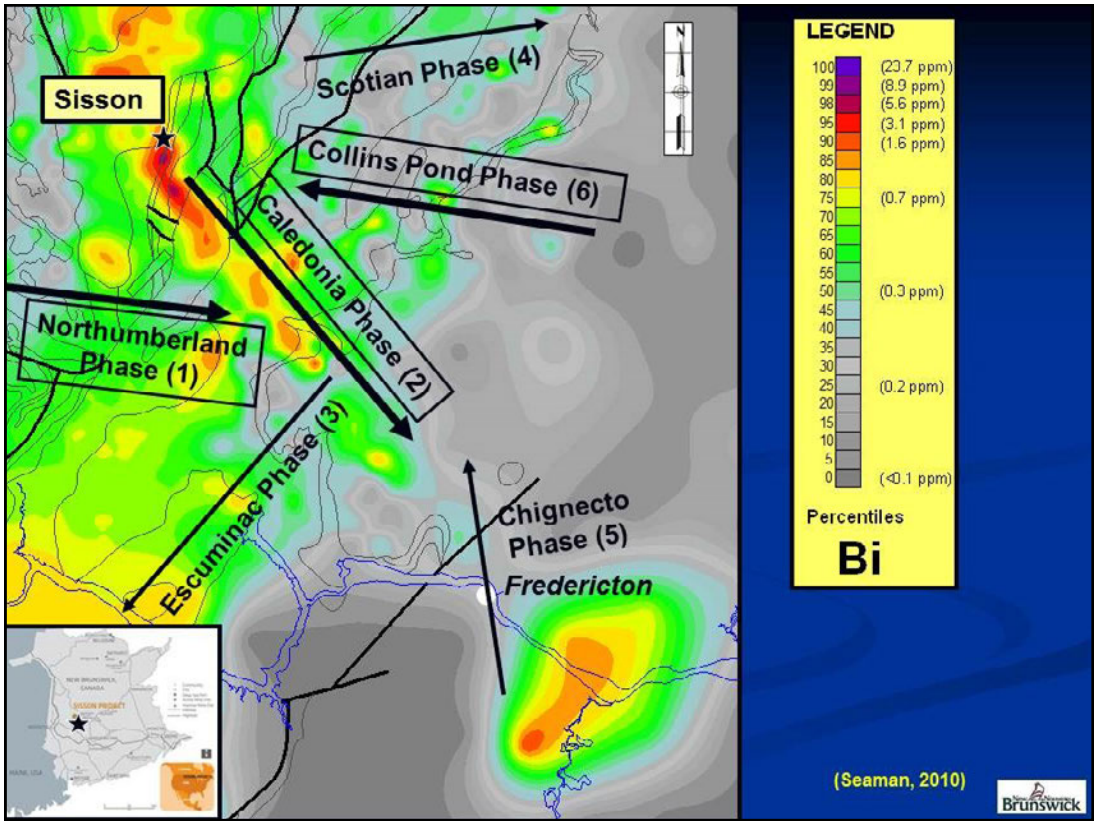
Sisson
Scotian Phase (4)
Collins Pond Phase (6)
Caledonia Phase (2)
Northumberland
Phase (1)
Escuminac Phase (3)
Chignecto
Phase (5)
Fredericton
LEGEND
100 (23.7 ppm)
99 (8.9 ppm)
98 (5.6 ppm)
95 (3.1 ppm)
90 (1.6 ppm)
75 (0.7 ppm)
50 (0.3 ppm)
25 (0.2 ppm)
0 (<0.1 ppm)
Percentiles
Bi
(Seaman, 2010)
Brunswick

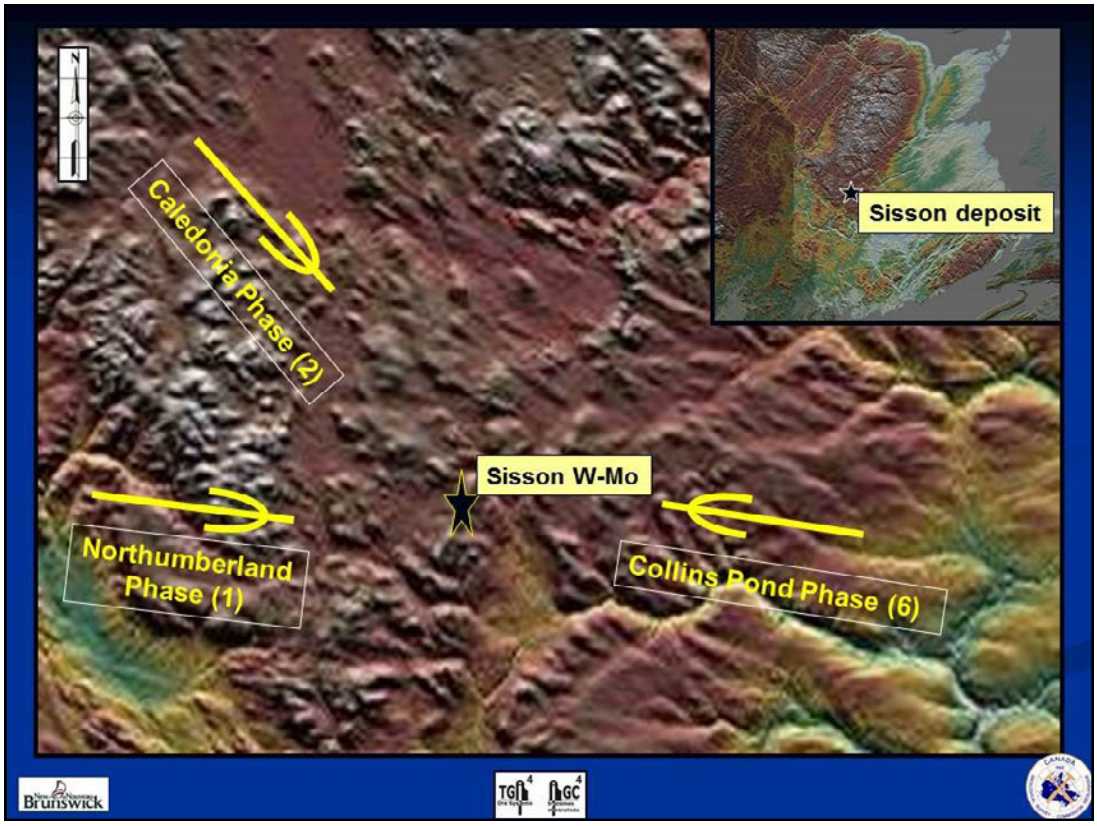
N
Caledonia Phase (2)
Sisson deposit
Sisson W-Mo
Northumberland Phase (1)
Collins Pond Phase (6)

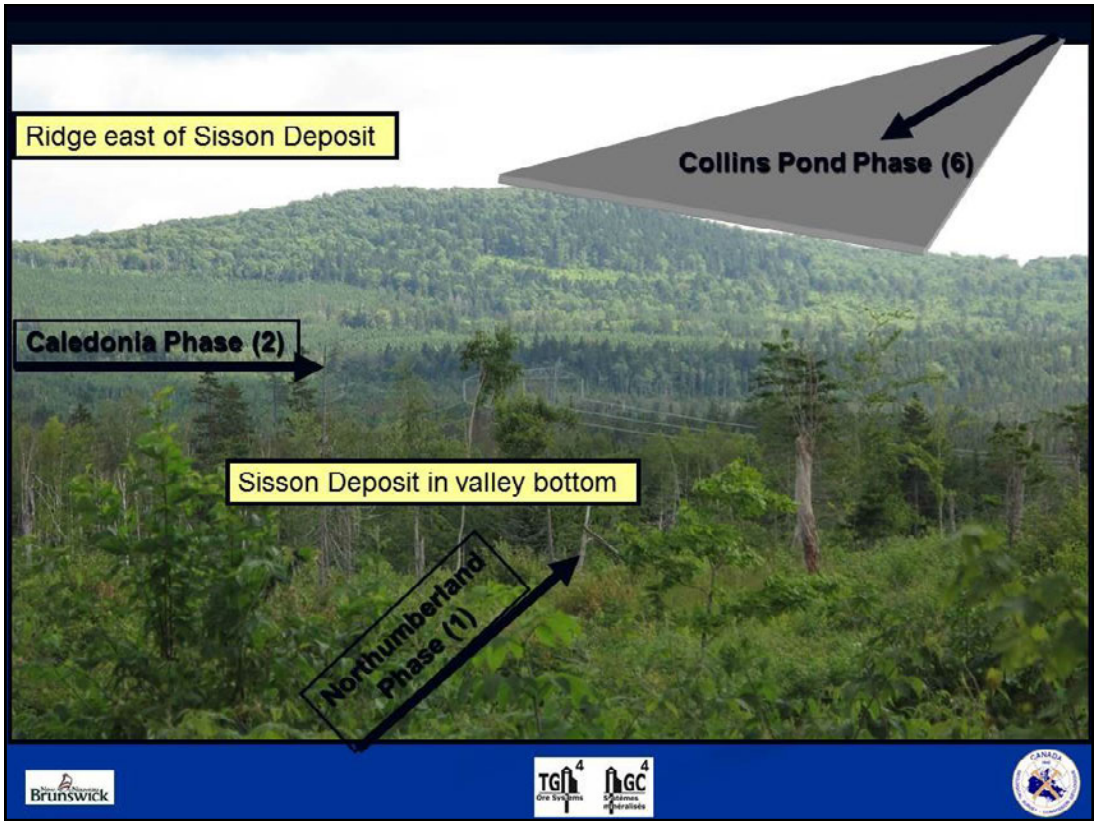
Ridge east of Sisson Deposit
Collins Pond Phase (6)
Caledonia Phase (2)
Sisson Deposit in valley bottom
Northumberland Phase (1)

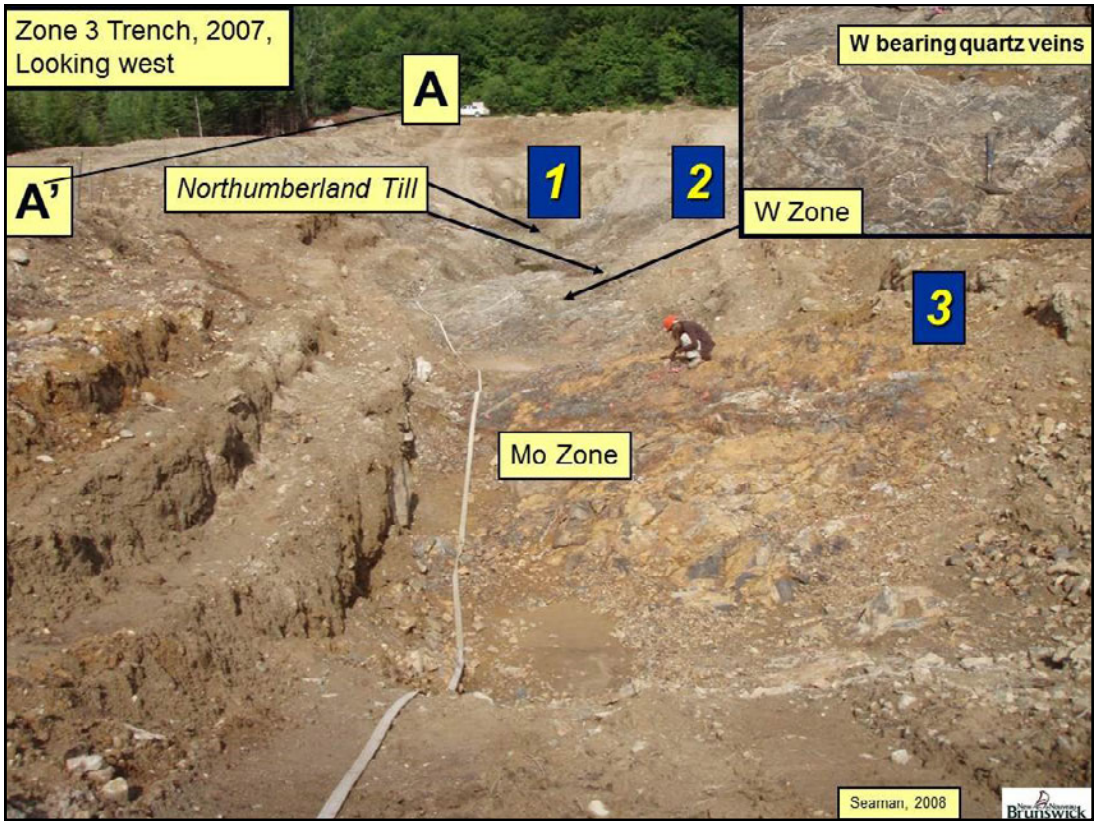
Zone 3 Trench, 2007,
Looking west
A
A'
Northumberland Till
1
2
W bearing quartz veins
W Zone
3
Mo Zone
Seaman, 2008
New Brunswick

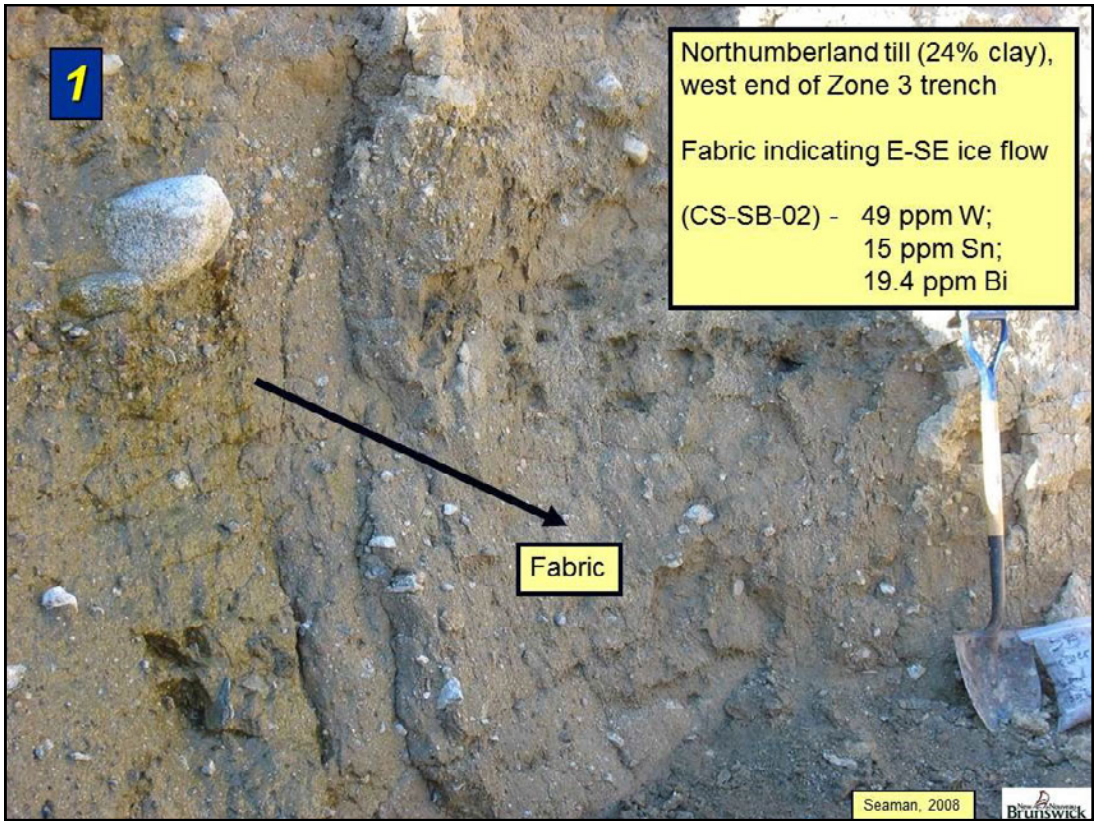
1
Northumberland till (24% clay),
west end of Zone 3 trench
Fabric indicating E-SE ice flow
(CS-SB-02) - 49 ppm W;
15 ppm Sn;
19.4 ppm Bi
Fabric
Seaman, 2008
New Brunswick

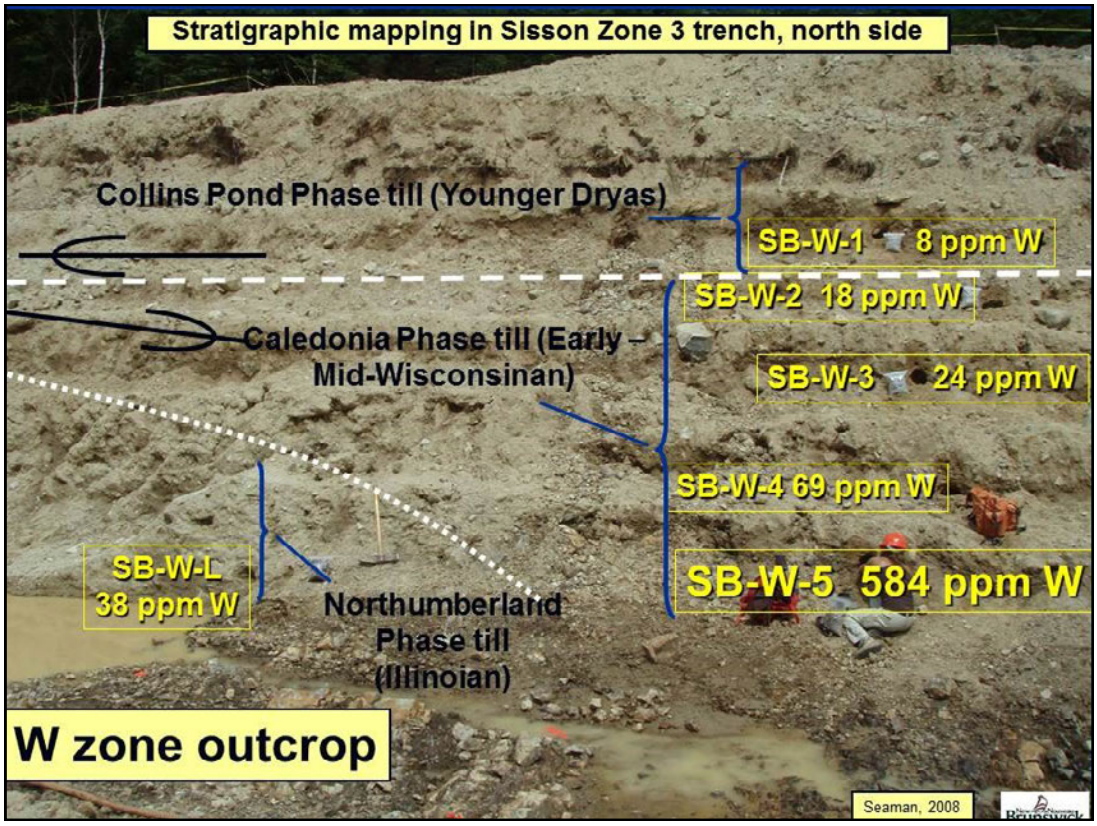
Stratigraphic mapping in Sisson Zone 3 trench, north side
Collins Pond Phase till (Younger Dryas)
SB-W-1 8 ppm W
SB-W-2 18 ppm W
Caledonia Phase till (Early – Mid-Wisconsinan)
SB-W-3 24 ppm W
SB-W-4 69 ppm W
SB-W-5 584 ppm W
SB-W-L 38 ppm W
Northumberland Phase till (Illinoian)
W zone outcrop
Seaman, 2008

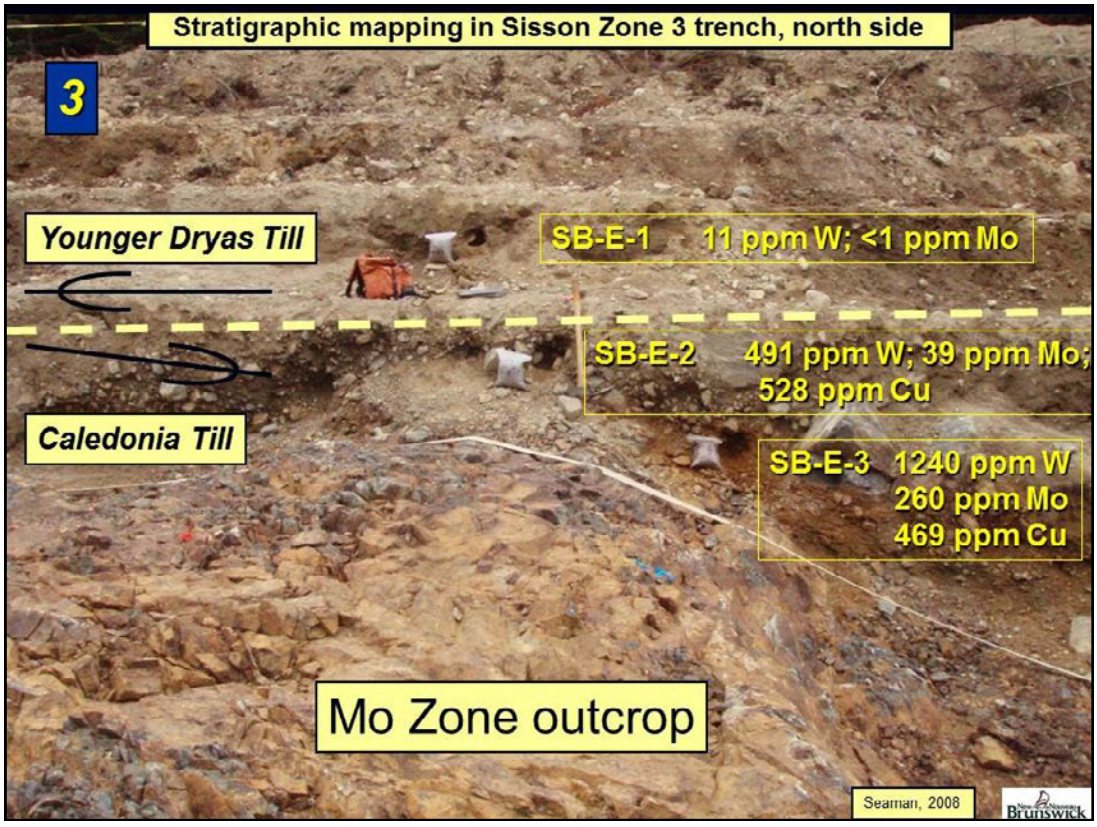
Stratigraphic mapping in Sisson Zone 3 trench, north side
3
Younger Dryas Till
SB-E-1 11 ppm W; <1 ppm Mo
SB-E-2 491 ppm W; 39 ppm Mo; 528 ppm Cu
Caledonia Till
SB-E-3 1240 ppm W 260 ppm Mo 469 ppm Cu
Mo Zone outcrop
Seaman, 2008

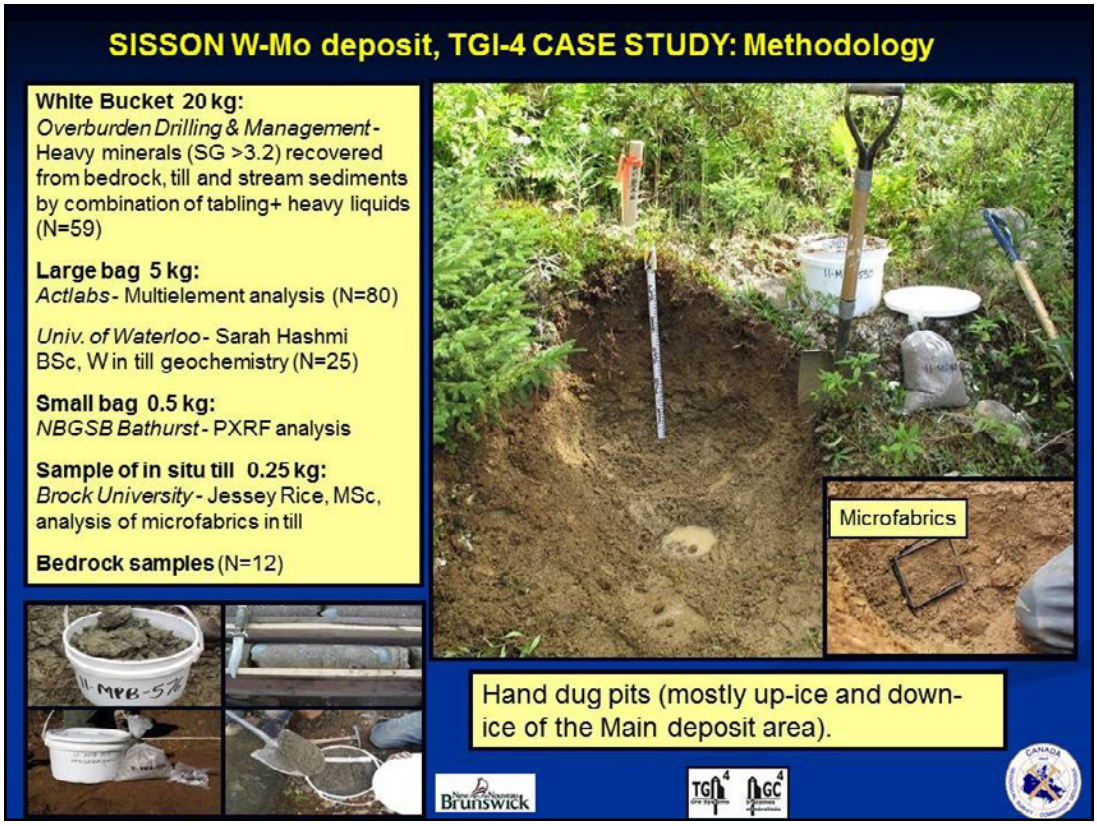
SISSON W-Mo deposit, TGI-4 CASE STUDY: Methodology
White Bucket 20 kg:
Overburden Drilling & Management - Heavy minerals (SG >3.2) recovered from bedrock, till and stream sediments by combination of tabling+ heavy liquids (N=59)
Large bag 5 kg:
Actlabs - Multielement analysis (N=80)
Univ. of Waterloo - Sarah Hashmi BSc, W in till geochemistry (N=25)
Small bag 0.5 kg:
NBGSB Bathurst - PXRF analysis
Sample of in situ till 0.25 kg:
Brock University - Jessey Rice, MSc, analysis of microfabrics in till
Bedrock samples (N=12)
Microfabrics
Hand dug pits (mostly up-ice and down-ice of the Main deposit area).

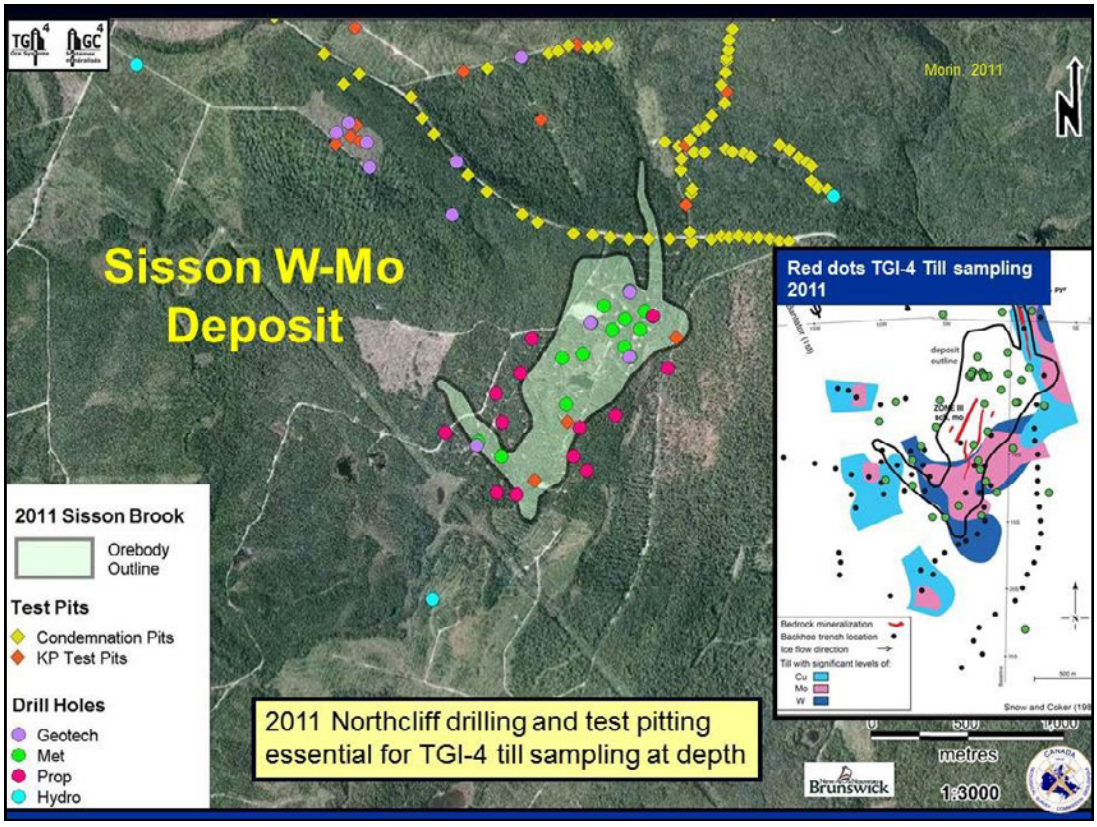
Monn 2011
Sisson W-Mo Deposit
Red dots TGI-4 Till sampling 2011
2011 Sisson Brook
Orebody Outline
Test Pits
Condemnation Pits
KP Test Pits
Drill Holes
Geotech
Met
Prop
Hydro
2011 Northcliff drilling and test pitting essential for TGI-4 till sampling at depth
metres
1:3000

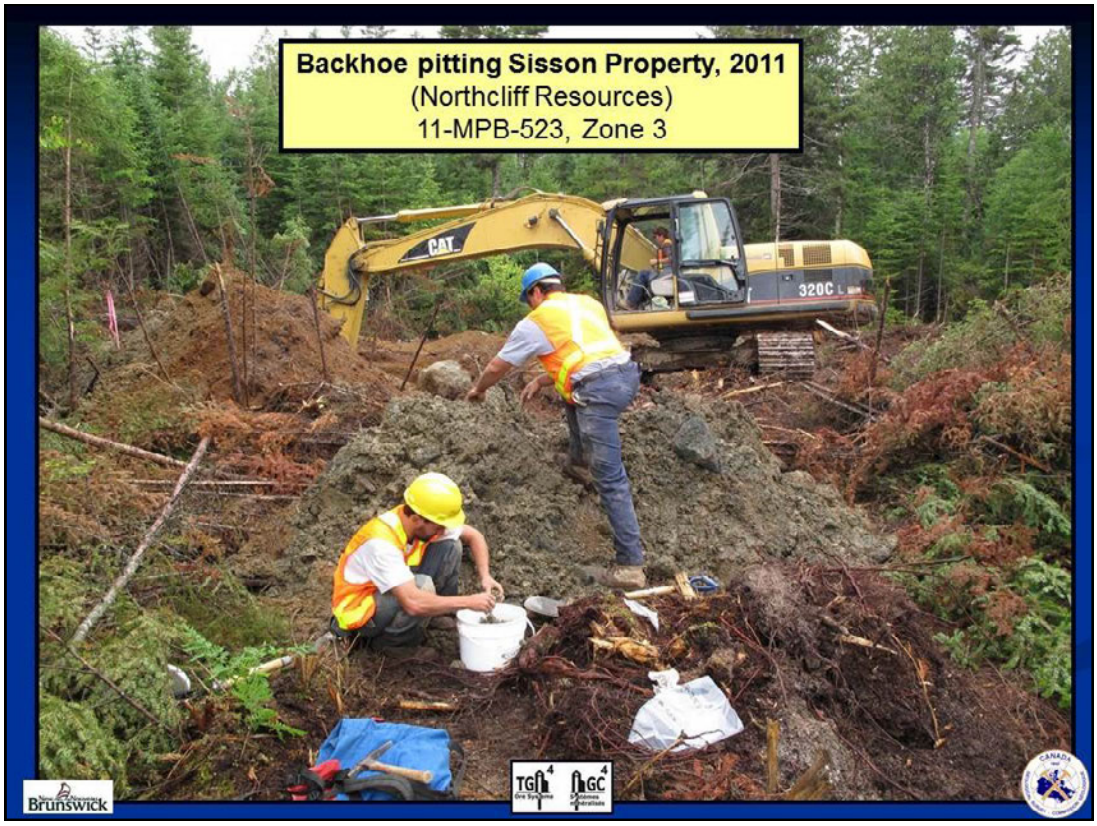
Backhoe pitting Sisson Property, 2011
(Northcliff Resources)
11-MPB-523, Zone 3
CAT
320C

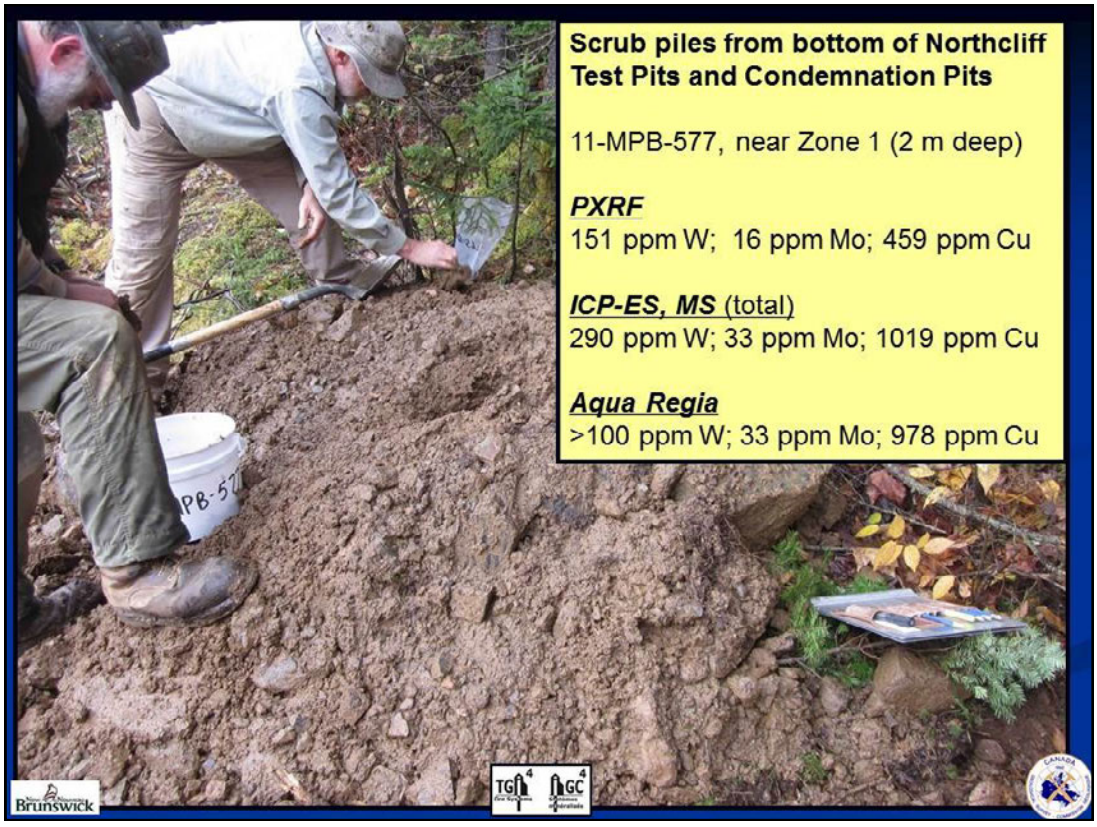
Scrub piles from bottom of Northcliff Test Pits and Condemnation Pits
11-MPB-577, near Zone 1 (2 m deep)
PXRF
151 ppm W; 16 ppm Mo; 459 ppm Cu
ICP-ES, MS (total)
290 ppm W; 33 ppm Mo; 1019 ppm Cu
Aqua Regia
>100 ppm W; 33 ppm Mo; 978 ppm Cu

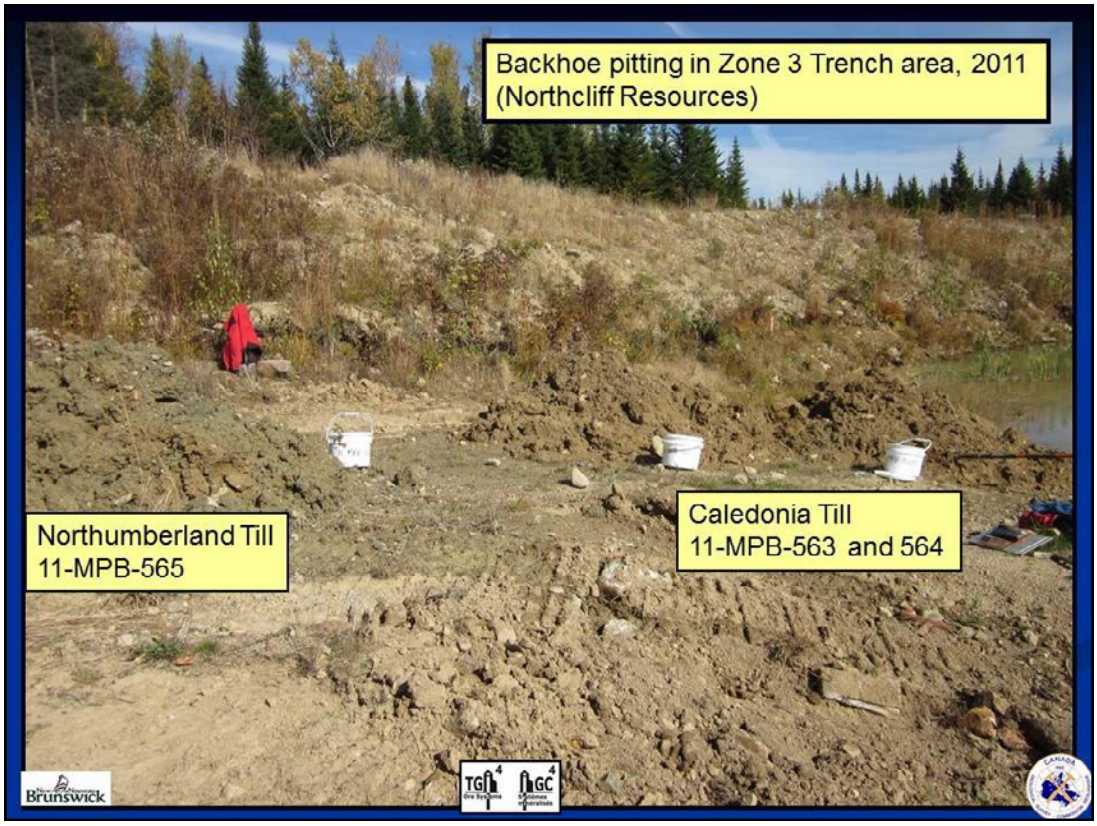
Backhoe pitting in Zone 3 Trench area, 2011
(Northcliff Resources)
Northumberland Till
11-MPB-565
Caledonia Till
11-MPB-563 and 564

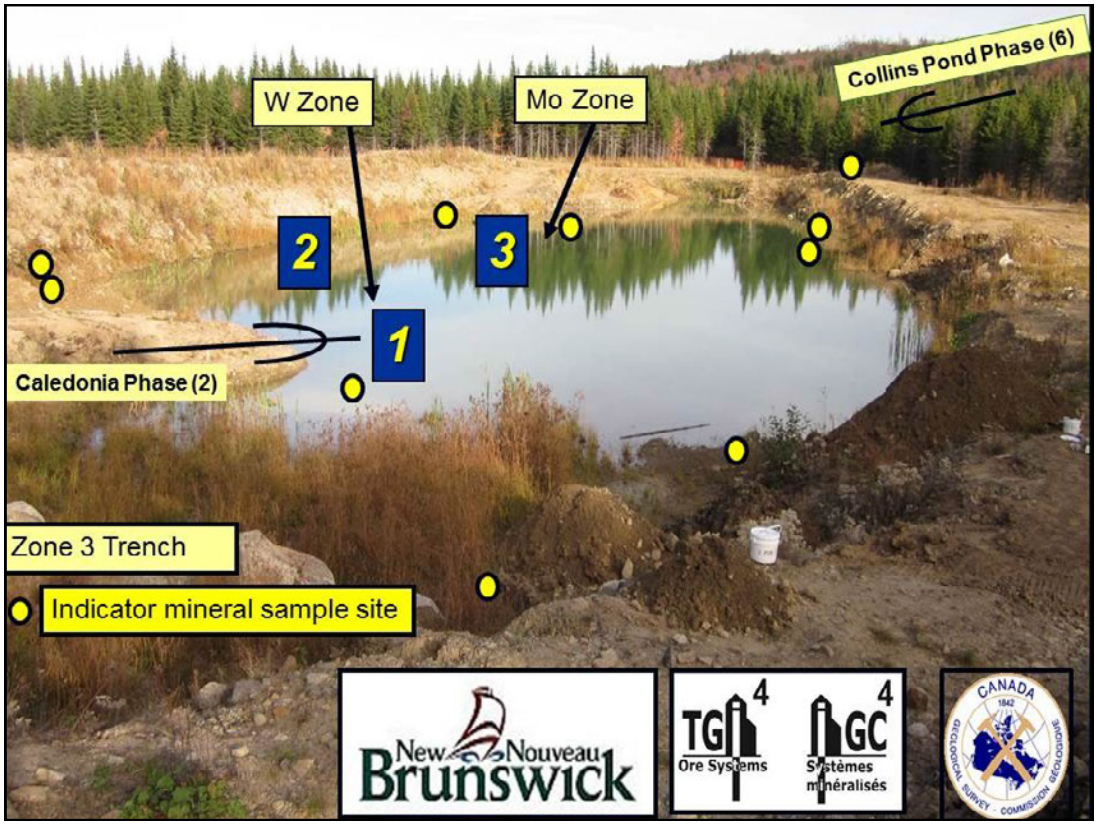
W Zone
Mo Zone
Collins Pond Phase (6)
2
3
1
Caledonia Phase (2)
Zone 3 Trench
Indicator mineral sample site
New Nouveau Brunswick
TGI4 Ore Systems
GSC Systèmes minéralisés
CANADA 1842 GEOLOGICAL SURVEY COMMISSION GÉOLOGIQUE

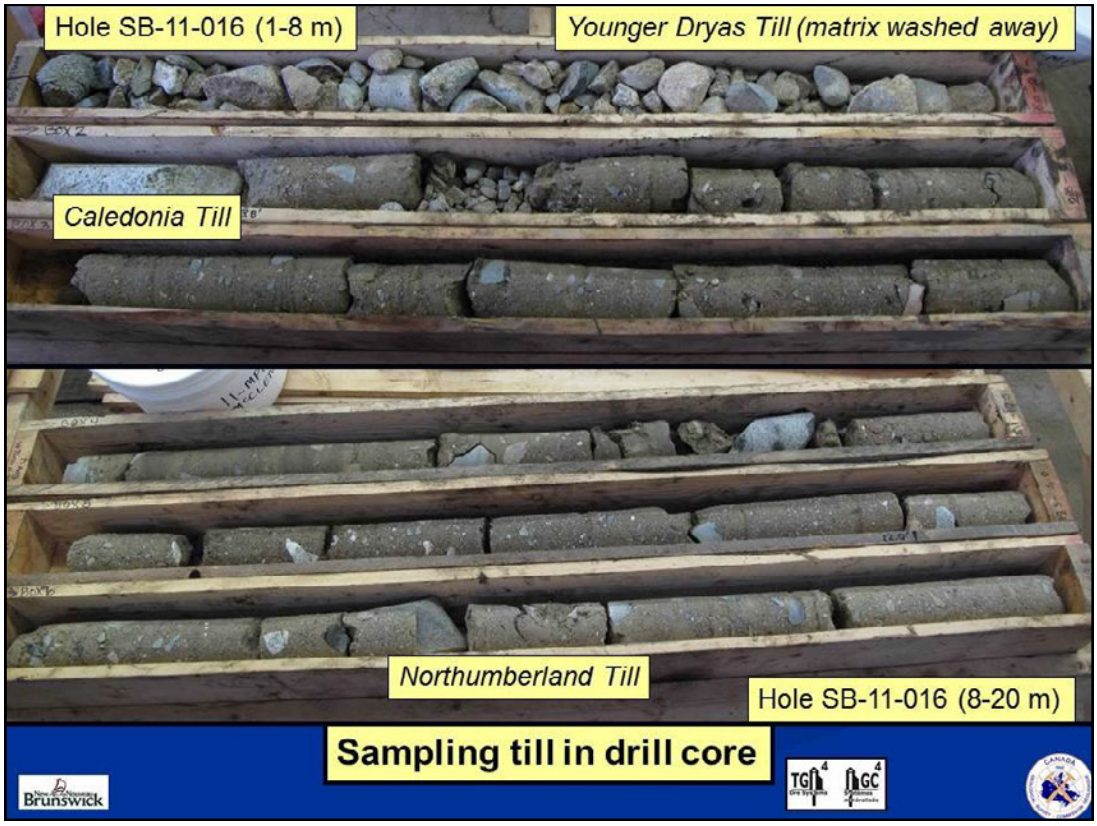
Hole SB-11-016 (1-8 m)
Younger Dryas Till (matrix washed away)
Caledonia Till
Northumberland Till
Hole SB-11-016 (8-20 m)
Sampling till in drill core

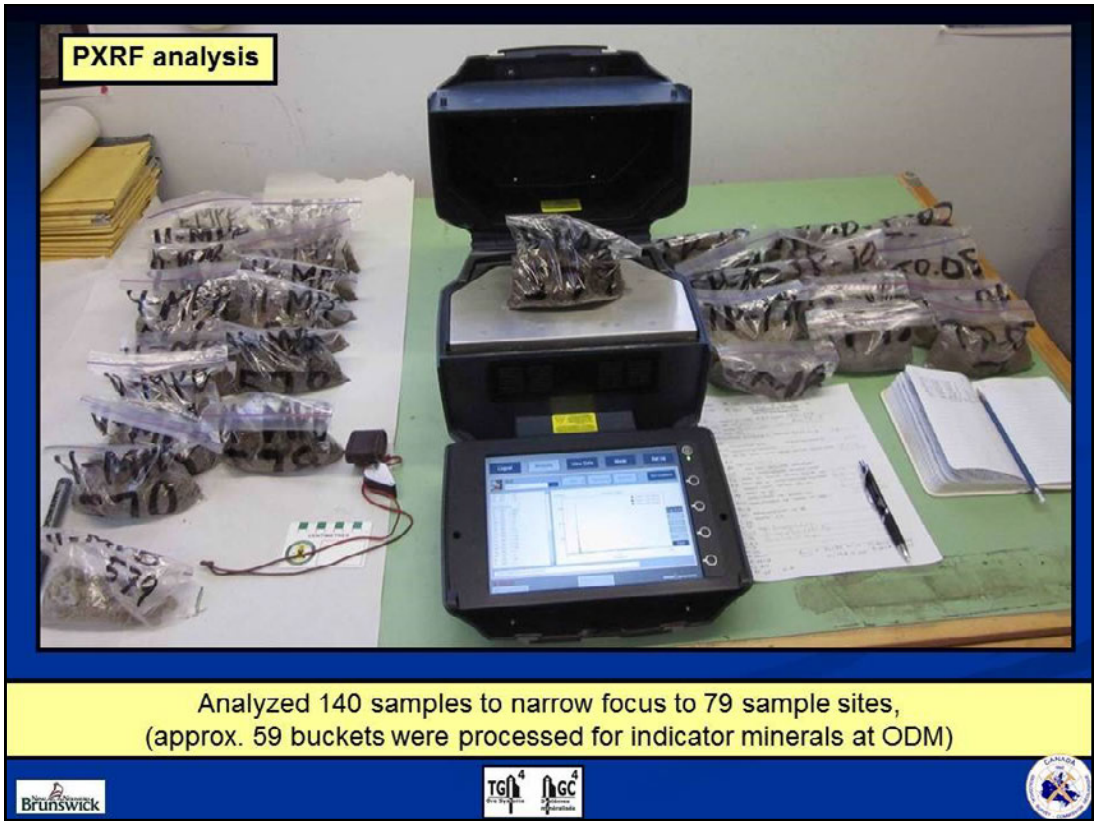
PXRF analysis
Analyzed 140 samples to narrow focus to 79 sample sites,
(approx. 59 buckets were processed for indicator minerals at ODM)

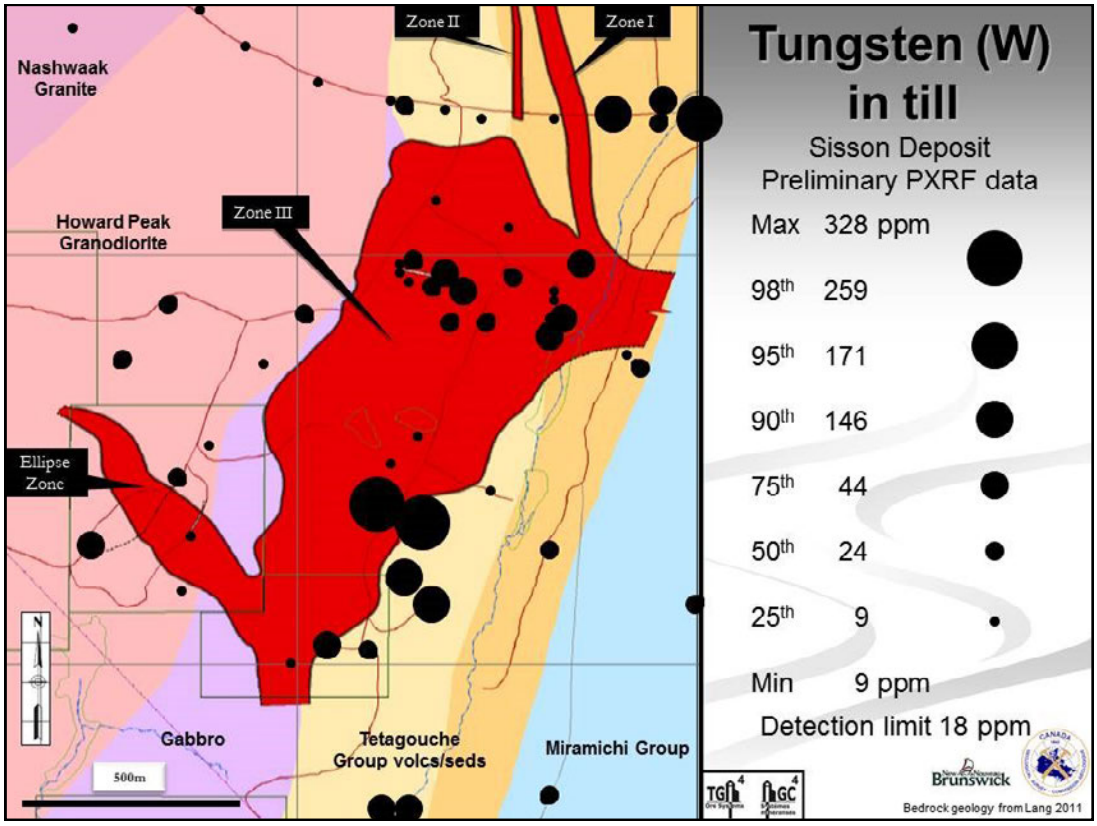
Zone II
Zone I
Nashwaak Granite
Howard Peak Granodiorite
Zone III
Ellipse Zone
Gabbro
Tetagouche Group volcs/seds
Miramichi Group
500m
Tungsten (W) in till
Sisson Deposit
Preliminary PXRF data
Max 328 ppm
98th 259
95th 171
90th 146
75th 44
50th 24
25th 9
Min 9 ppm
Detection limit 18 ppm
Bedrock geology from Lang 2011

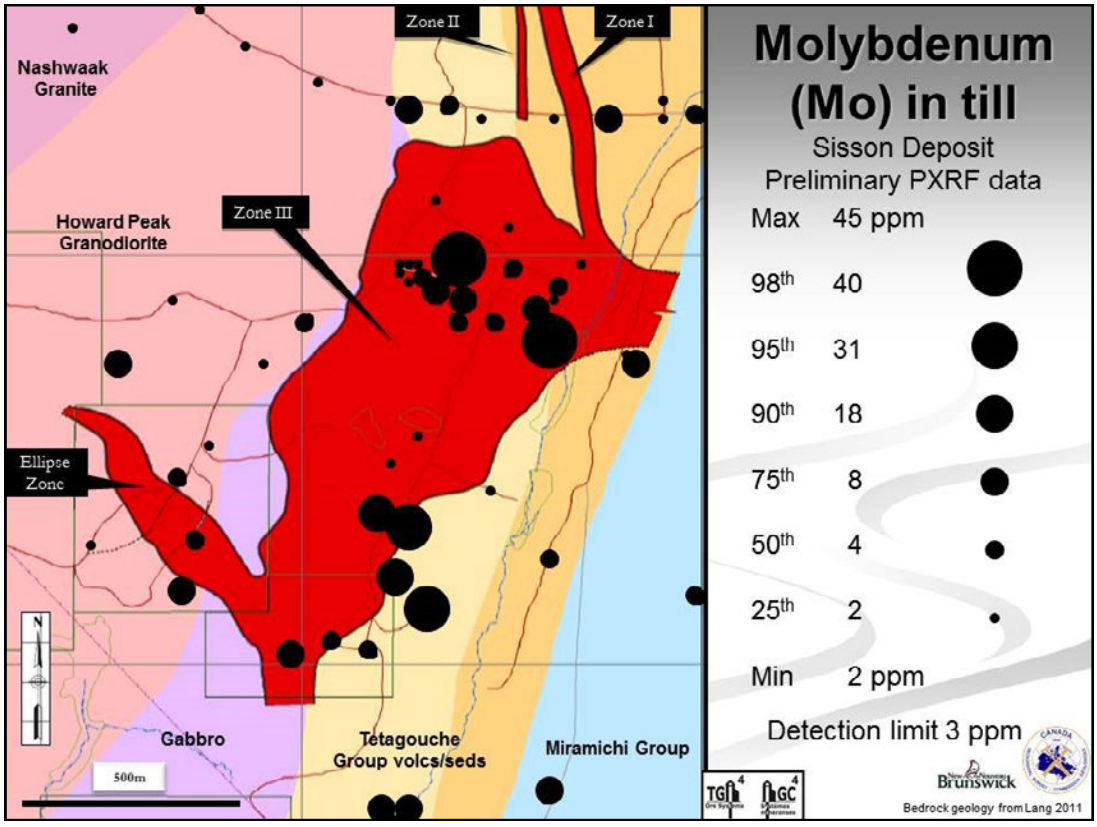
Zone II
Zone I
Nashwaak Granite
Howard Peak Granodiorite
Zone III
Ellipse Zone
Gabbro
Tetagouche Group volcs/seds
Miramichi Group
500m
Molybdenum (Mo) in till
Sisson Deposit
Preliminary PXRF data
Max 45 ppm
98th 40
95th 31
90th 18
75th 8
50th 4
25th 2
Min 2 ppm
Detection limit 3 ppm
Bedrock geology from Lang 2011

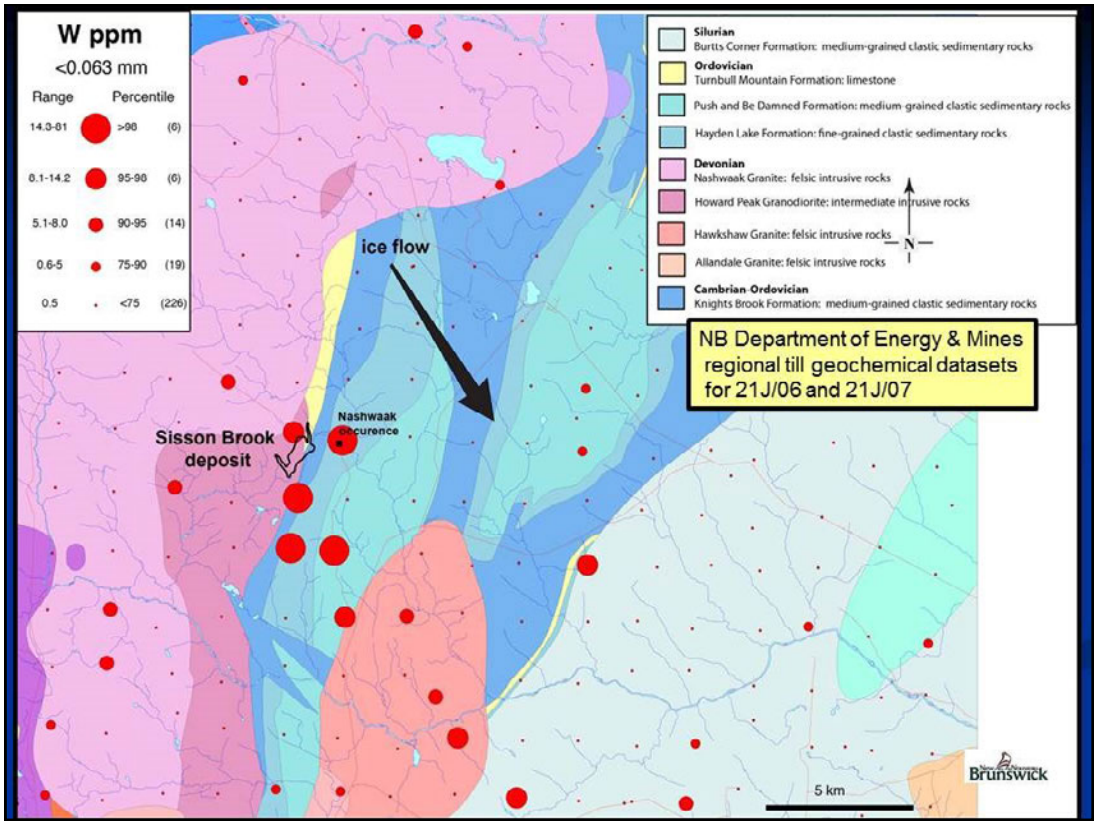
W ppm
<0.063 mm
Range
Percentile
14.3-81
>90
(6)
0.1-14.2
95-90
(6)
5.1-8.0
90-95
(14)
0.6-5
75-90
(19)
0.5
<75
(226)
Silurian
Burtts Corner Formation: medium-grained clastic sedimentary rocks
Ordovician
Turnbull Mountain Formation: limestone
Push and Be Damned Formation: medium-grained clastic sedimentary rocks
Hayden Lake Formation: fine-grained clastic sedimentary rocks
Devonian
Nashwaak Granite: felsic intrusive rocks
Howard Peak Granodiorite: intermediate intrusive rocks
Hawkshaw Granite: felsic intrusive rocks
Allandale Granite: felsic intrusive rocks
Cambrian-Ordovician
Knights Brook Formation: medium-grained clastic sedimentary rocks
N
ice flow
Sisson Brook deposit
Nashwaak occurence
NB Department of Energy & Mines regional till geochemical datasets for 21J/06 and 21J/07
5 km
Brunswick

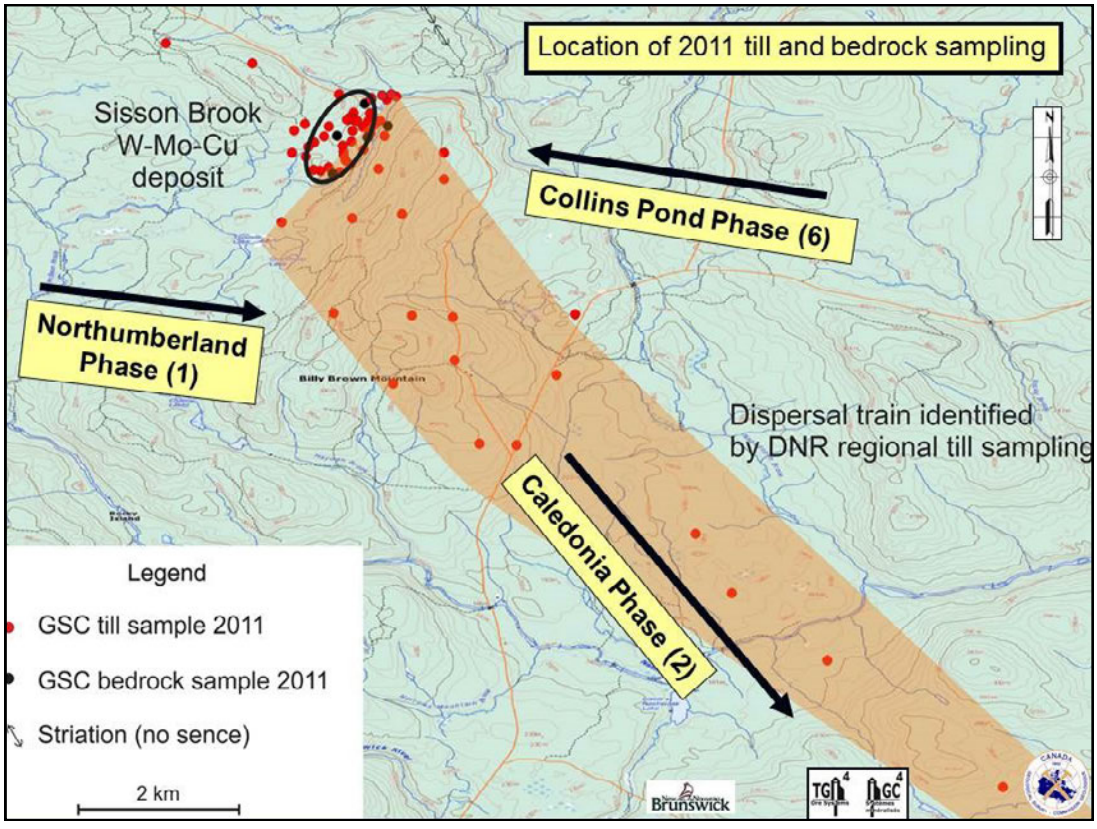
Location of 2011 till and bedrock sampling
Sisson Brook W-Mo-Cu deposit
Collins Pond Phase (6)
Northumberland Phase (1)
Billy Brown Mountain
Dispersal train identified by DNR regional till sampling
Caledonia Phase (2)
N
Legend
GSC till sample 2011
GSC bedrock sample 2011
Striation (no sence)
2 km
Brunswick

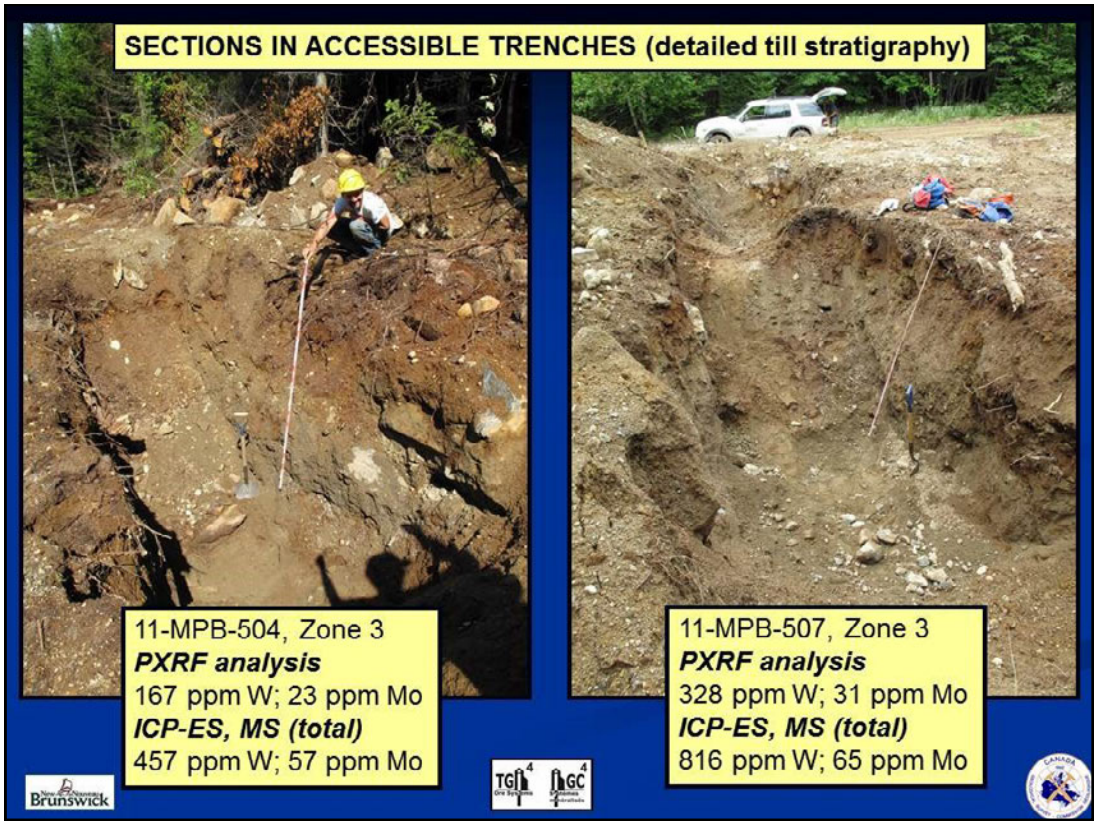
SECTIONS IN ACCESSIBLE TRENCHES (detailed till stratigraphy)
11-MPB-504, Zone 3
PXRF analysis
167 ppm W; 23 ppm Mo
ICP-ES, MS (total)
457 ppm W; 57 ppm Mo
11-MPB-507, Zone 3
PXRF analysis
328 ppm W; 31 ppm Mo
ICP-ES, MS (total)
816 ppm W; 65 ppm Mo

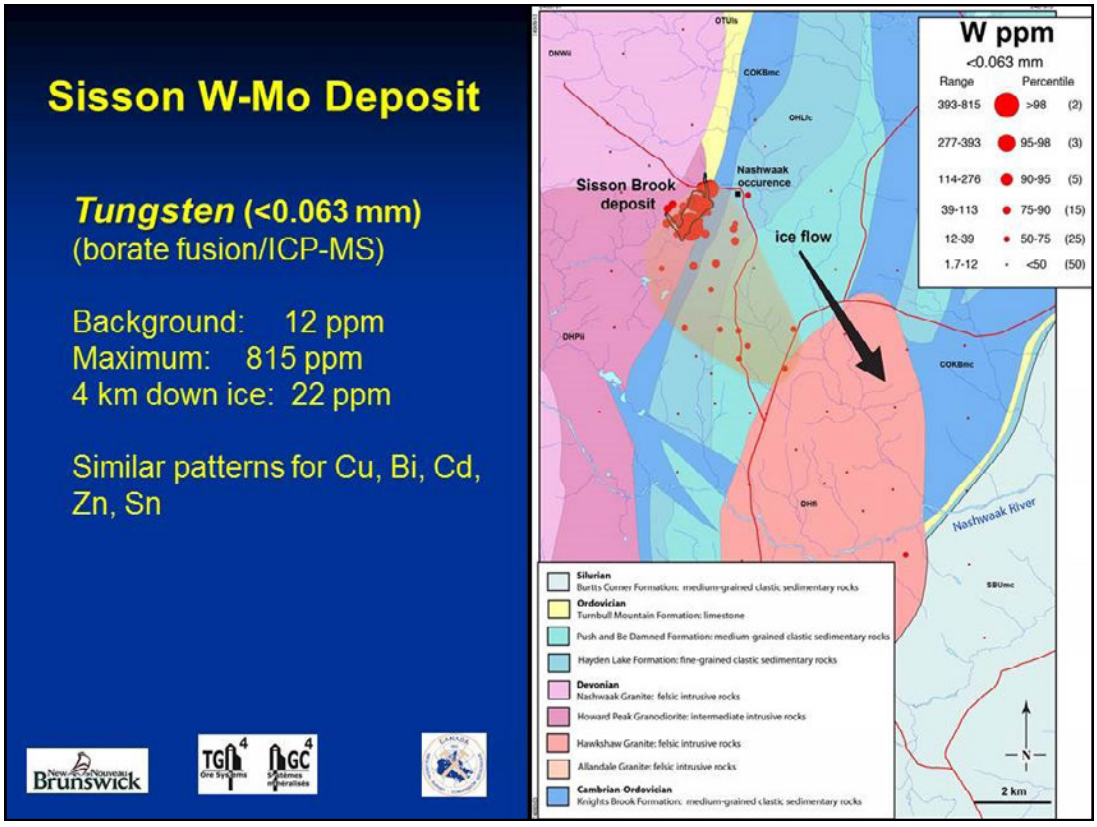
Sisson W-Mo Deposit
Tungsten (<0.063 mm)
(borate fusion/ICP-MS)
Background: 12 ppm
Maximum: 815 ppm
4 km down ice: 22 ppm
Similar patterns for Cu, Bi, Cd, Zn, Sn
W ppm
<0.063 mm
Range
Percentile
393-815 >98 (2)
277-393 95-98 (3)
114-276 90-95 (5)
39-113 75-90 (15)
12-39 50-75 (25)
1.7-12 <50 (50)
Sisson Brook deposit
Nashwaak occurence
ice flow
Nashwaak River
Silurian
Burtts Corner Formation: medium-grained clastic sedimentary rocks
Ordovician
Turnbull Mountain Formation: limestone
Push and Be Damned Formation: medium-grained clastic sedimentary rocks
Hayden Lake Formation: fine-grained clastic sedimentary rocks
Devonian
Nashwaak Granite: felsic intrusive rocks
Howard Peak Granodiorite: intermediate intrusive rocks
Hawkshaw Granite: felsic intrusive rocks
Allandale Granite: felsic intrusive rocks
Cambrian-Ordovician
Knights Brook Formation: medium-grained clastic sedimentary rocks
2 km

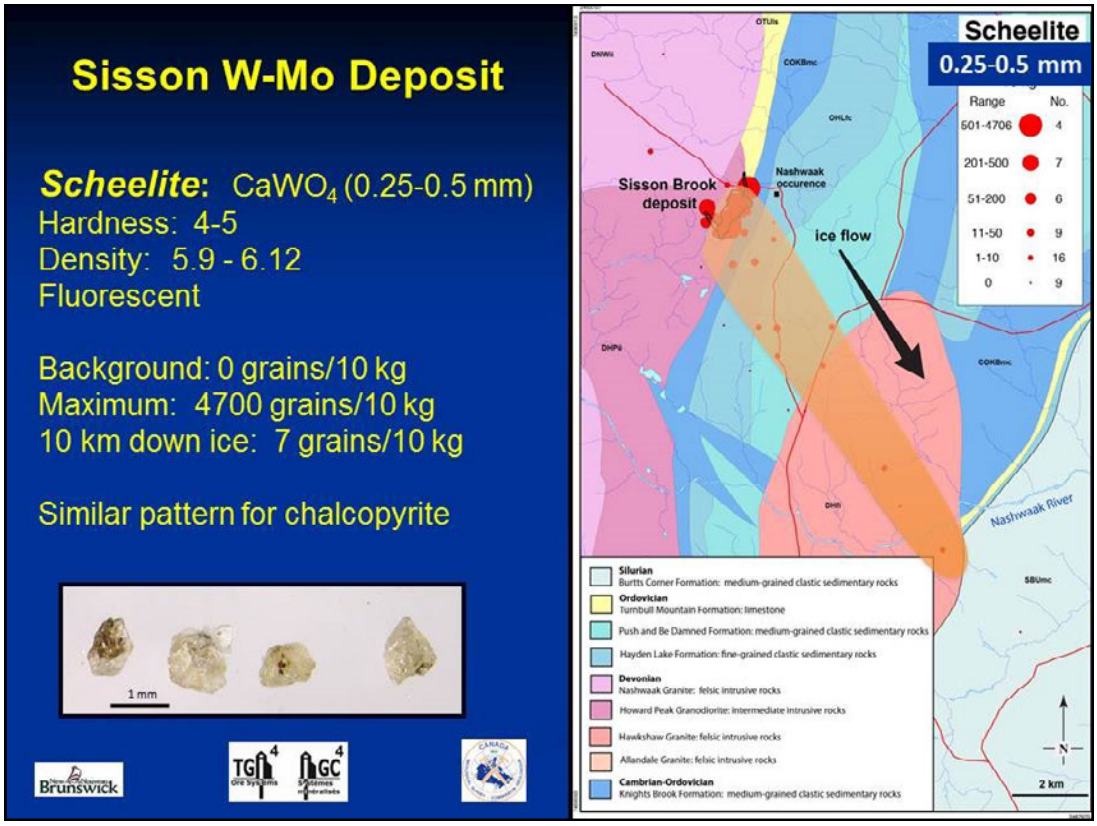
Sisson W-Mo Deposit
Scheelite: CaWO4 (0.25-0.5 mm)
Hardness: 4-5
Density: 5.9 - 6.12
Fluorescent
Background: 0 grains/10 kg
Maximum: 4700 grains/10 kg
10 km down ice: 7 grains/10 kg
Similar pattern for chalcopyrite
1 mm
Scheelite
0.25-0.5 mm
Range
No.
501-4706 4
201-500 7
51-200 6
11-50 9
1-10 16
0 9
Sisson Brook deposit
Nashwaak occurence
ice flow
Nashwaak River
Silurian
Burtts Corner Formation: medium-grained clastic sedimentary rocks
Ordovician
Tumbull Mountain Formation: limestone
Push and Be Damned Formation: medium-grained clastic sedimentary rocks
Hayden Lake Formation: fine-grained clastic sedimentary rocks
Devonian
Nashwaak Granite: felsic intrusive rocks
Howard Peak Granodiorite: intermediate intrusive rocks
Hawkshaw Granite: felsic intrusive rocks
Allandale Granite: felsic intrusive rocks
Cambrian-Ordovician
Knights Brook Formation: medium-grained clastic sedimentary rocks
N
2 km

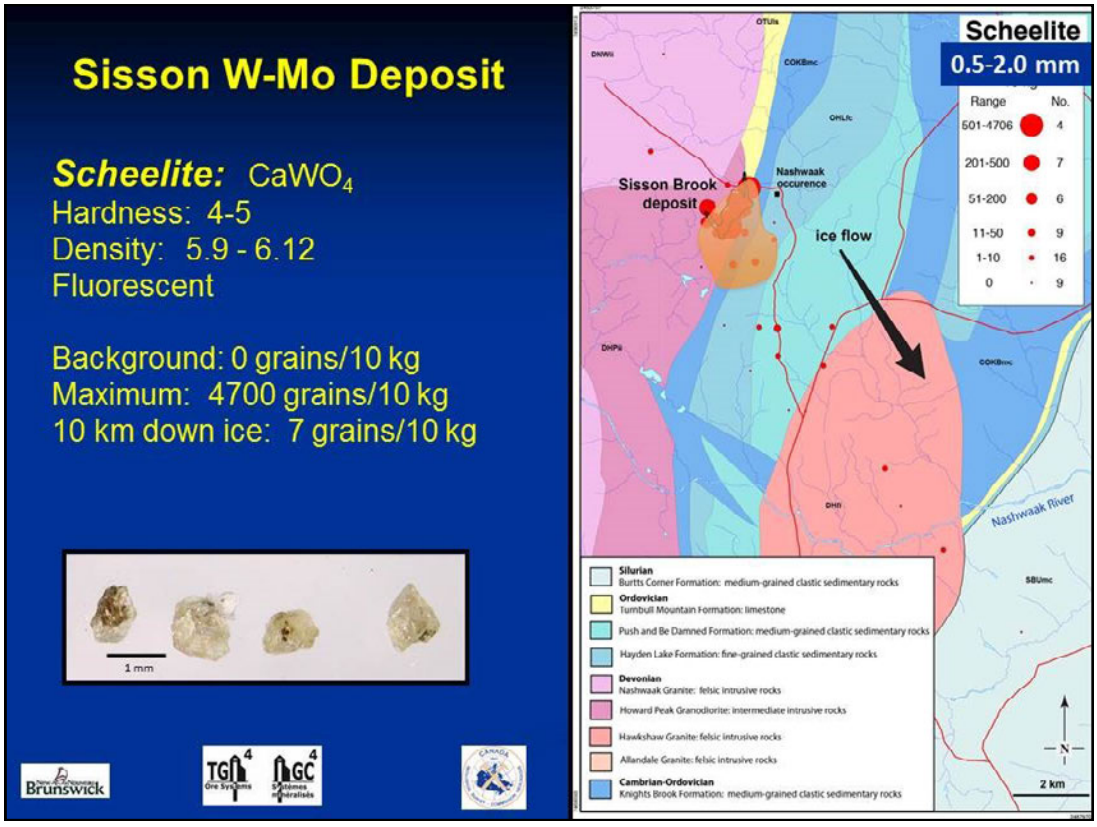
Sisson W-Mo Deposit
Scheelite: CaWO4
Hardness: 4-5
Density: 5.9 - 6.12
Fluorescent
Background: 0 grains/10 kg
Maximum: 4700 grains/10 kg
10 km down ice: 7 grains/10 kg
1 mm
Scheelite
0.5-2.0 mm
Range
No.
501-4706 4
201-500 7
51-200 6
11-50 9
1-10 16
0 9
Sisson Brook deposit
Nashwaak occurence
ice flow
Nashwaak River
Silurian
Burtts Corner Formation: medium-grained clastic sedimentary rocks
Ordovician
Tumbull Mountain Formation: limestone
Push and Be Damned Formation: medium-grained clastic sedimentary rocks
Hayden Lake Formation: fine-grained clastic sedimentary rocks
Devonian
Nashwaak Granite: felsic intrusive rocks
Howard Peak Granodiorite: intermediate intrusive rocks
Hawkshaw Granite: felsic intrusive rocks
Allandale Granite: felsic intrusive rocks
Cambrian-Ordovician
Knights Brook Formation: medium-grained clastic sedimentary rocks
N
2 km

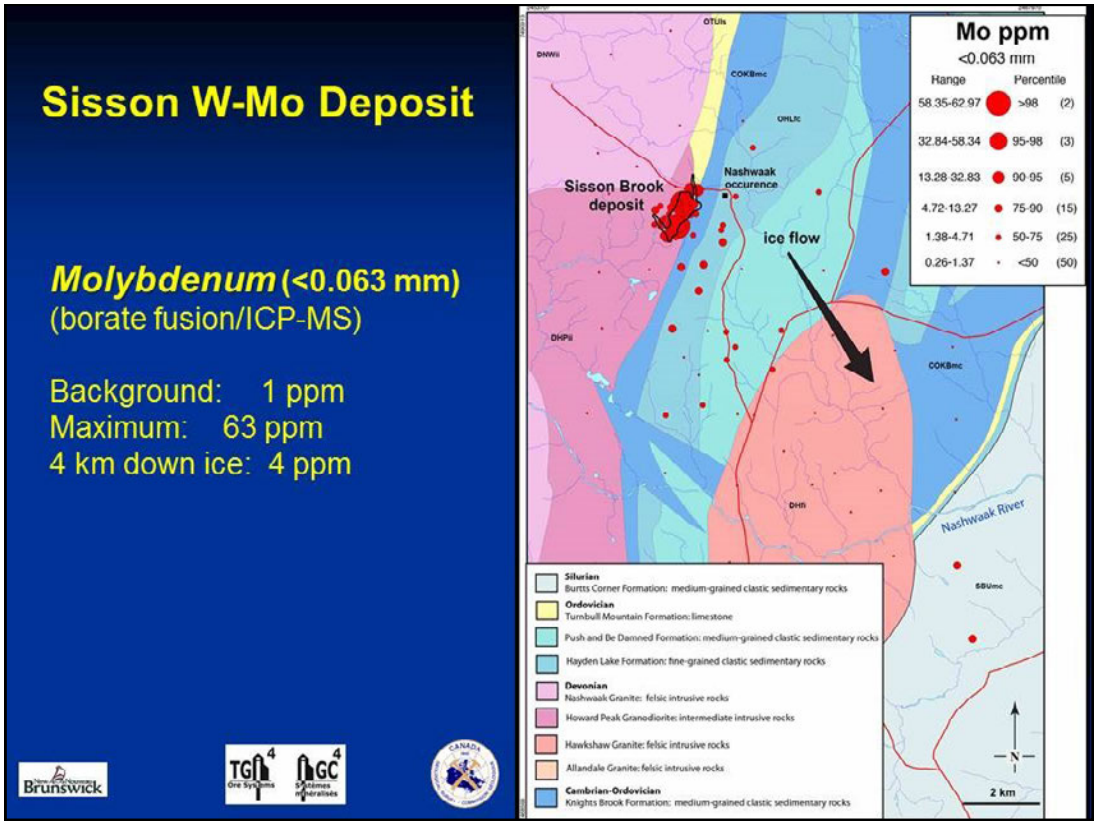
Sisson W-Mo Deposit
Molybdenum (<0.063 mm)
(borate fusion/ICP-MS)
Background: 1 ppm
Maximum: 63 ppm
4 km down ice: 4 ppm
Mo ppm
<0.063 mm
Range
Percentile
58.35-62.97 >98 (2)
32.84-58.34 95-98 (3)
13.28-32.83 90-95 (5)
4.72-13.27 75-90 (15)
1.38-4.71 50-75 (25)
0.26-1.37 <50 (50)
Sisson Brook deposit
Nashwaak occurence
ice flow
Nashwaak River
2 km
Silurian
Burtts Corner Formation: medium-grained clastic sedimentary rocks
Ordovician
Turnbull Mountain Formation: limestone
Push and Be Damned Formation: medium-grained clastic sedimentary rocks
Hayden Lake Formation: fine-grained clastic sedimentary rocks
Devonian
Nashwaak Granite: felsic intrusive rocks
Howard Peak Granodiorite: intermediate intrusive rocks
Hawkshaw Granite: felsic intrusive rocks
Allandale Granite: felsic intrusive rocks
Cambrian-Ordovician
Knights Brook Formation: medium-grained clastic sedimentary rocks

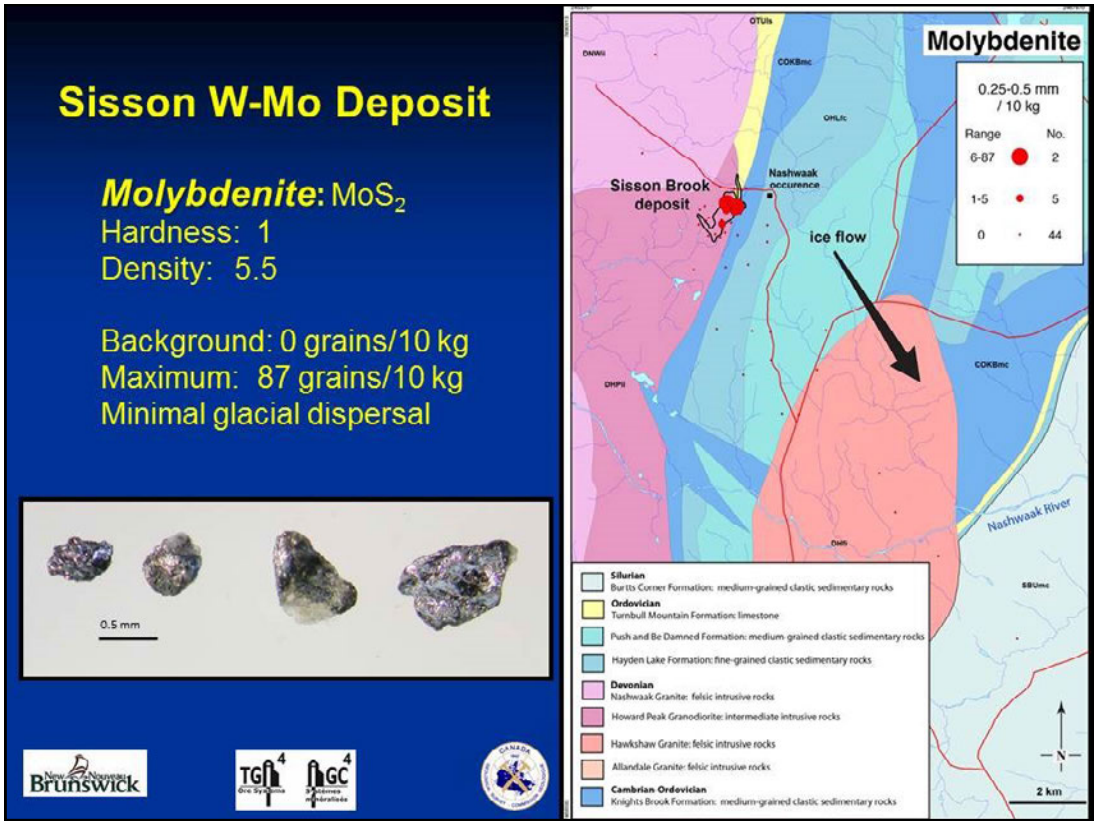
Sisson W-Mo Deposit
Molybdenite: MoS_2
Hardness: 1
Density: 5.5
Background: 0 grains/10 kg
Maximum: 87 grains/10 kg
Minimal glacial dispersal
0.5 mm
Molybdenite
0.25-0.5 mm
/ 10 kg
Range
No.
6-87 2
1-5 5
0 44
Sisson Brook deposit
Nashwaak occurence
ice flow
Nashwaak River
2 km
Silurian
Burtts Corner Formation: medium-grained clastic sedimentary rocks
Ordovician
Turnbull Mountain Formation: limestone
Push and Be Damned Formation: medium-grained clastic sedimentary rocks
Hayden Lake Formation: fine-grained clastic sedimentary rocks
Devonian
Nashwaak Granite: felsic intrusive rocks
Howard Peak Granodiorite: intermediate intrusive rocks
Hawkshaw Granite: felsic intrusive rocks
Allandale Granite: felsic intrusive rocks
Cambrian-Ordovician
Knights Brook Formation: medium-grained clastic sedimentary rocks

Sisson W-Mo Deposit

Bismuth Minerals:
Hardness: 2 to 4
Density: 6.8 to 9
Colour: silver grey-dark grey

Background: 0 grains/10 kg
Maximum: 14 grains/10 kg
4 km down ice: 4 grains/10 kg

Native Bismuth Bi
Bismuthinite Bi_2S_3
Bismutite $Bi2(CO_3)O_2$
Joseite $Bi_4(S,Te)_3$

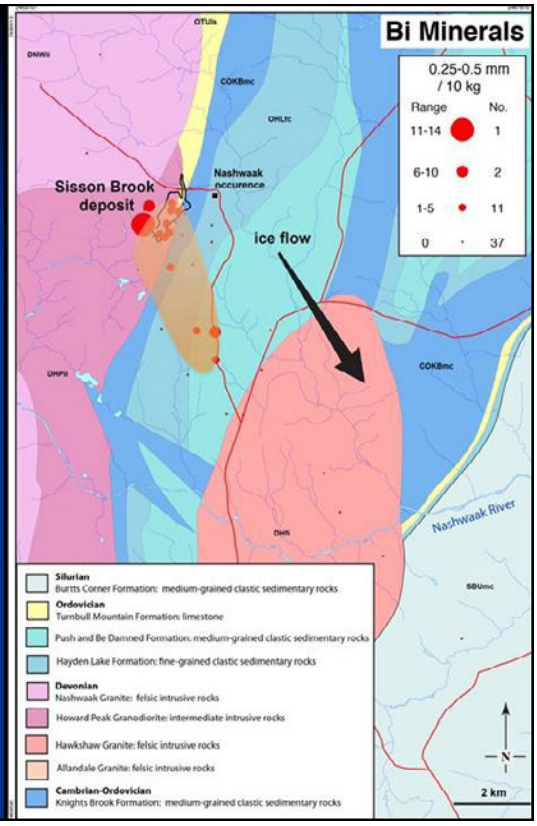

Sisson W-Mo Deposit

Silver **(<0.063 mm)**
(aqua regia/ICP-MS)

Background: 72 ppb
Maximum: 708 ppb

- Similar patterns for: Pb, As, In

- Distal expression of intrusion?
or
- Mineralization from a different source in Ordovician-Silurian Tetagouche sedimentary rocks?

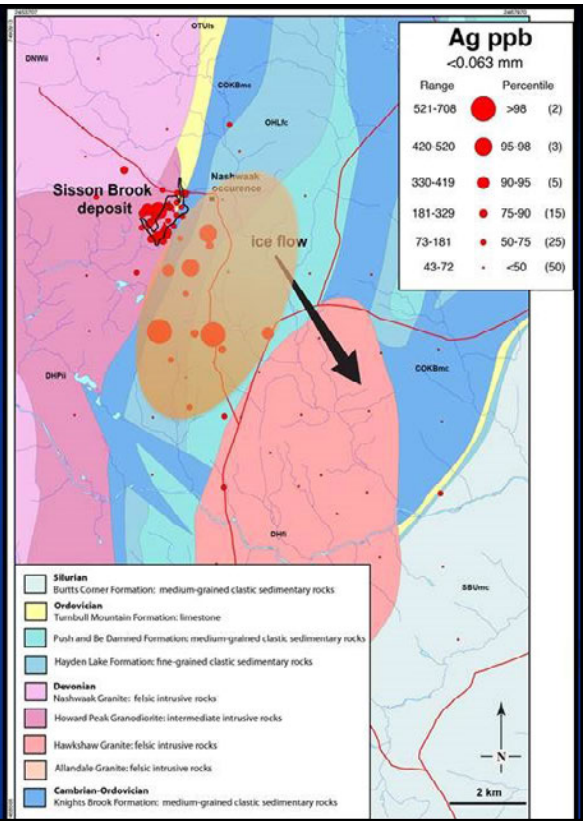

Stream Sediment Sampling Sisson 2012

- Stream samples collected at 16 sites up stream, overlying, and up to 8 km down stream from the deposit
- Collected stream water, silt, and bulk sample (10-12 kg) for heavy minerals
- Characterize scheelite abundance, size and shape for comparison with grains in till

Sisson W-Mo Deposit

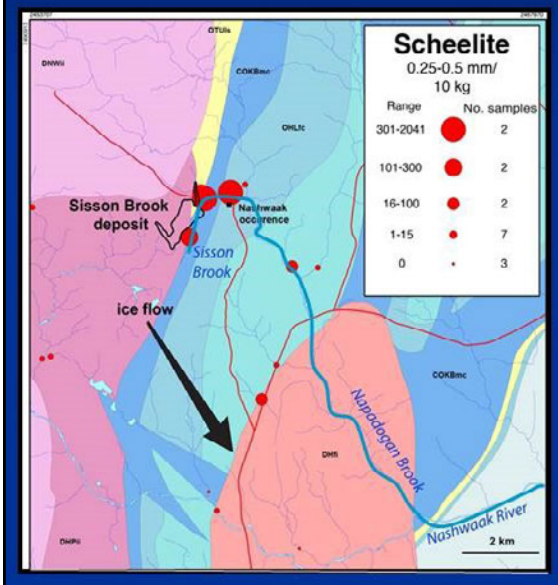

Stream Sediment Sampling

Well developed scheelite signature in stream sediments at least 4 km down stream

Background: 0 - 8 grains/10 kg
Maximum: 2041 grains/10 kg

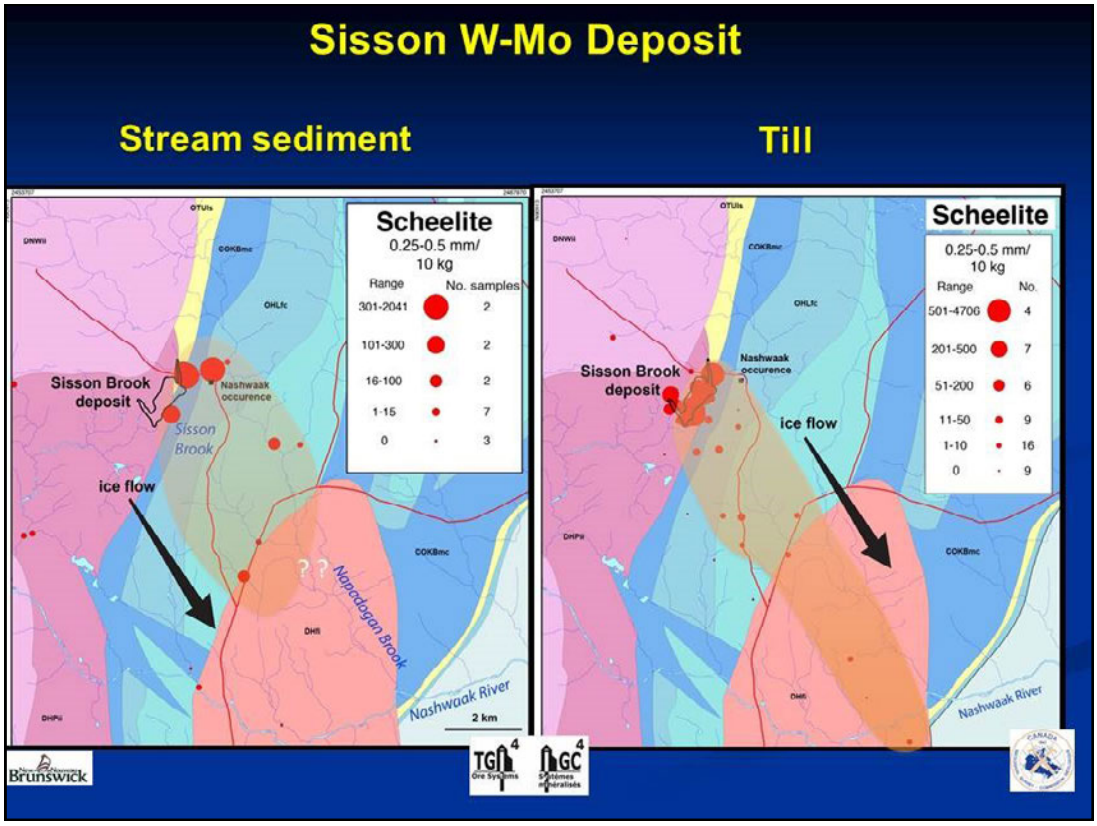
Sisson W-Mo Deposit
Stream sediment
Till
Scheelite
0.25-0.5 mm/
10 kg
Range
No. samples
301-2041
101-300
16-100
1-15
0
Sisson Brook deposit
Nashwaak occurence
Sisson Brook
ice flow
Napadogan Brook
Nashwaak River
2 km
Scheelite
0.25-0.5 mm/
10 kg
Range
No.
501-4700
201-500
51-200
11-50
1-10
0

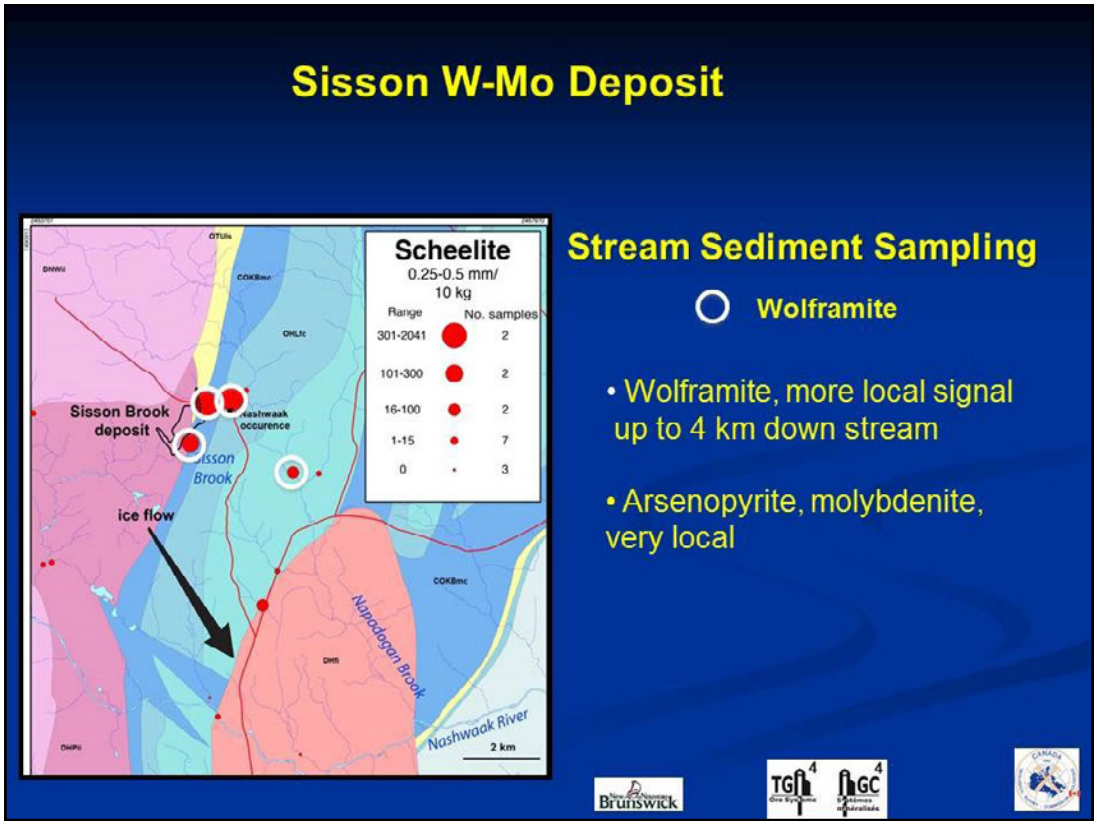
Sisson W-Mo Deposit
Scheelite
0.25-0.5 mm/
10 kg
Range
No. samples
301-2041
101-300
16-100
1-15
0
Sisson Brook deposit
ice flow
Napadogan Brook
Nashwaak River
2 km
Stream Sediment Sampling
Wolframite
• Wolframite, more local signal up to 4 km down stream
• Arsenopyrite, molybdenite, very local

Implications for Exploration - Sisson

SCHEELITE

- Indicator mineral of W mineralization, in till and stream sediments; Northcliff is currently using the methodology developed in this project.
- Physically robust, survives glacial and fluvial transport
- Silt to sand sized presence of coarse scheelite (>0.5 mm) indicator of proximity to source
- Abundant, 100s to 1000s of grains proximal to source
- Developed systematic method for scheelite grain counting under UV light, new service at commercial heavy mineral lab
- Wolframite, molybdenite, bismuth minerals, chalcopyrite, arsenopyrite also present
- Sample density: detectable and efficient at 5 km^2
- ADVANTAGES: physical evidence of the presence of mineralization, morphology, and chemistry provide information about distance to, and nature of, bedrock source

Photo: Scheelite grains under UV light

Implications for Exploration - Sisson

TILL GEOCHEMISTRY

- Pathfinder elements for Sisson: W, Mo, Cu, Bi, As, Sn, Cd, Ag, In, Zn, Pb
- Recommend till geochemistry be used in combination with indicator minerals methods

NASHWAAK OCCURRENCE (900 m E of Sisson Deposit)

- Multi-element till geochemical anomaly overlying Tetagouche Group rocks, may be related to the intrusion? or other mineralization?
- Warrants further investigation

Mount Pleasant Sn-W-Mo-Bi-In Deposit

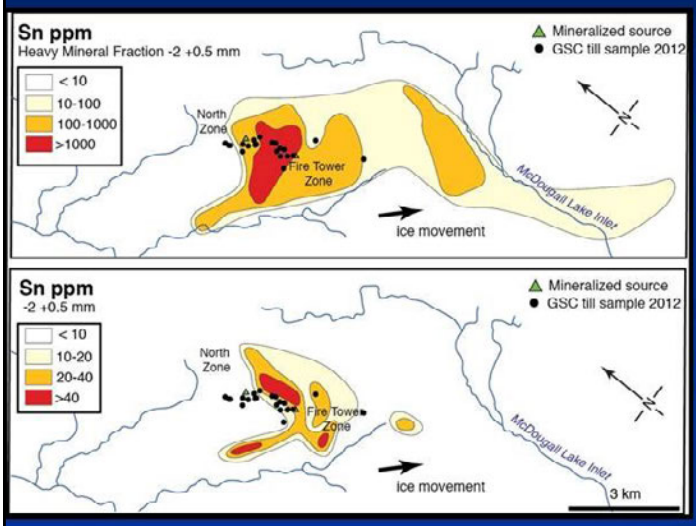

(Szabo, 1975)

Glacial dispersal train identified by Szabo (1975) using till geochemistry: Sn, Cu, Pb, Zn, As

Dispersal train best defined by till geochemistry of heavy mineral fraction

Polymetallic deposit, ideal test site for indicator mineral study of an intrusion-hosted deposit, focus on cassiterite and scheelite

Ideal test site for till geochemical study of indium

Mount Pleasant Sn-W-Mo-Bi-In Deposit

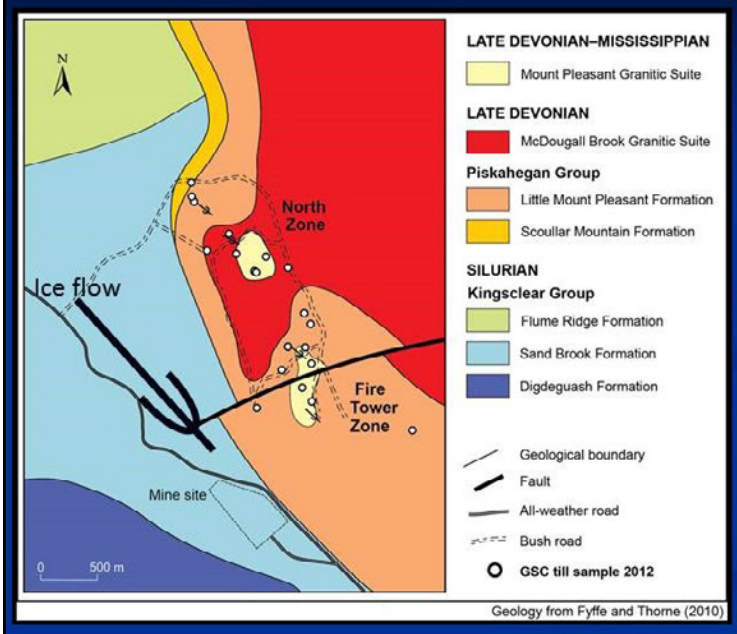

2012 Till Sampling

25 till samples (15 kg)

Up-ice, overlying and down-ice of North Zone

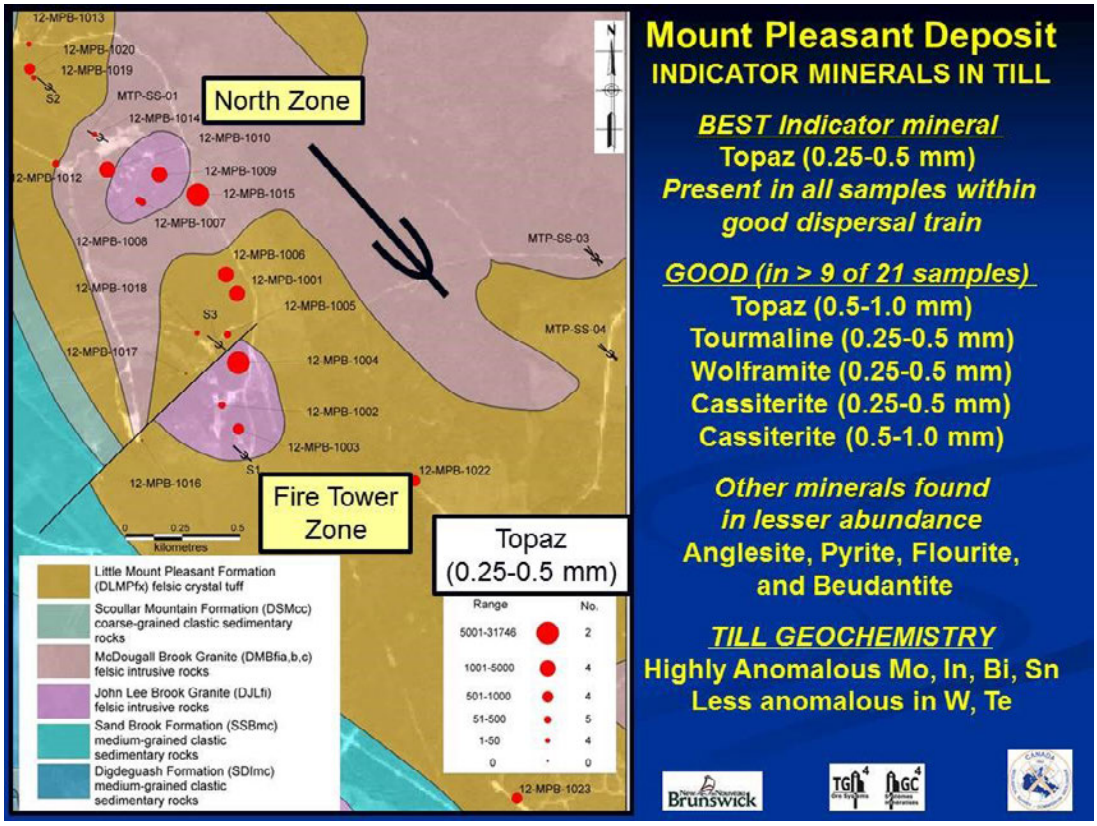
Mount Pleasant Deposit
INDICATOR MINERALS IN TILL
BEST Indicator mineral
Topaz (0.25-0.5 mm)
Present in all samples within good dispersal train
GOOD (in > 9 of 21 samples)
Topaz (0.5-1.0 mm)
Tourmaline (0.25-0.5 mm)
Wolframite (0.25-0.5 mm)
Cassiterite (0.25-0.5 mm)
Cassiterite (0.5-1.0 mm)
Other minerals found in lesser abundance
Anglesite, Pyrite, Flourite, and Beudantite
TILL GEOCHEMISTRY
Highly Anomalous Mo, In, Bi, Sn
Less anomalous in W, Te
North Zone
Fire Tower Zone
Topaz (0.25-0.5 mm)
Range
No.
5001-31746
2
1001-5000
4
501-1000
4
51-500
5
1-50
4
0
0
kilometres
Little Mount Pleasant Formation (DLMPfx) felsic crystal tuff
Scoullar Mountain Formation (DSMcc) coarse-grained clastic sedimentary rocks
McDougall Brook Granite (DMBfia,b,c) felsic intrusive rocks
John Lee Brook Granite (DJLfi) felsic intrusive rocks
Sand Brook Formation (SSBmc) medium-grained clastic sedimentary rocks
Digdeguash Formation (SDImc) medium-grained clastic sedimentary rocks
12-MPB-1013
12-MPB-1020
12-MPB-1019
S2
MTP-SS-01
12-MPB-1014
12-MPB-1010
12-MPB-1012
12-MPB-1009
12-MPB-1015
12-MPB-1007
12-MPB-1008
MTP-SS-03
12-MPB-1006
12-MPB-1001
12-MPB-1018
12-MPB-1005
S3
MTP-SS-04
12-MPB-1017
12 MPB-1004
12-MPB-1002
12-MPB-1003
S1
12-MPB-1022
12-MPB-1016
12-MPB-1023

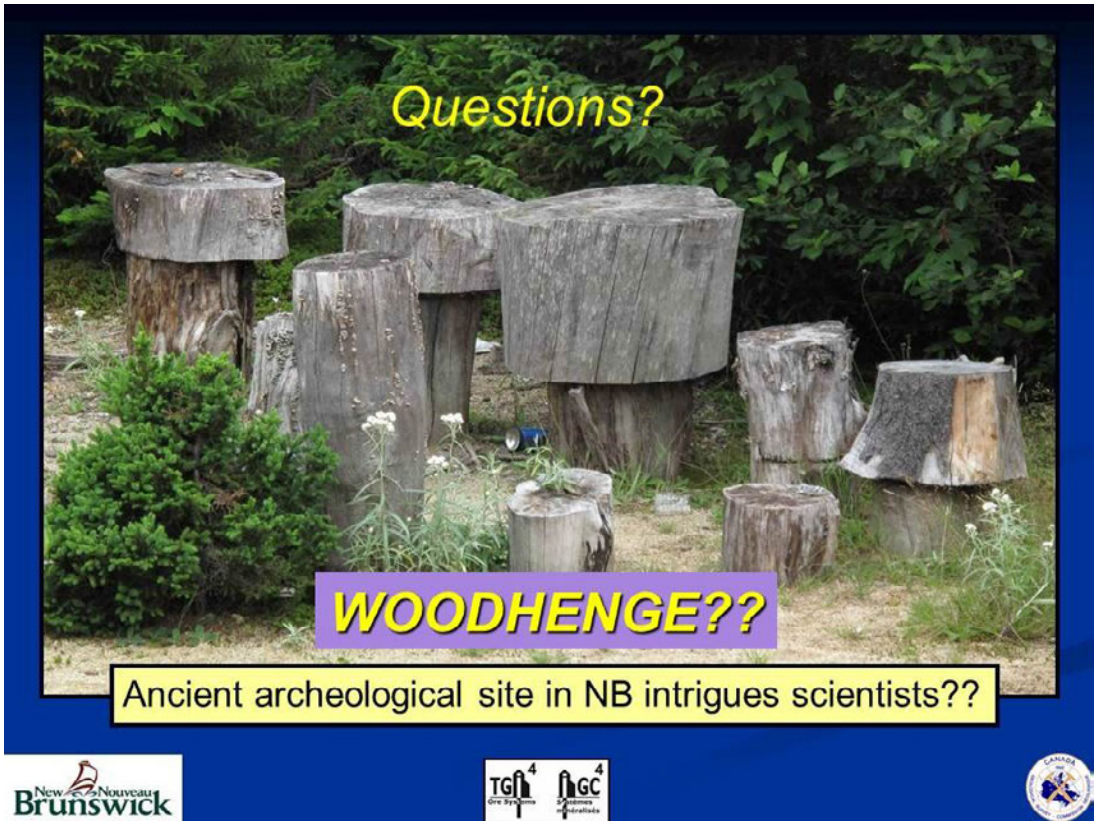
Questions?
WOODHENGE??
Ancient archeological site in NB intrigues scientists??

Scheelite geochemical signatures and potential for fingerprinting ore deposits

R.S. Poulin[1], A.M. McDonald[1], D.J. Kontak[1] and M.B. McClenaghan[2]

1. Department of Earth Sciences, Laurentian University, 935 Ramsey Lake Road, Sudbury, Ontario

2. Geological Survey of Canada, 601 Booth Street, Ottawa, Ontario

Abstract: Scheelite ($CaWO_4$) is a common accessory mineral found in a variety of geologically diverse ore-deposit settings, including vein/stockwork, skarn, porphyry, epithermal and strata-bound. As part of the Geological Survey of Canada's (GSC) Targeted Geoscience Initiative (TGI 4) program, the project reported on here was developed to investigate the potential for discriminating scheelite originating from different ore-deposit types. The study investigated whether crystal-chemical features of scheelite, such as cathodoluminescence (CL), trace-element chemistry, and isotopic signature (O), could be used independently or together as deposit-type discriminators, thereby assessing the feasibility of using scheelite for provenance studies in regional till-sampling programs. Here we report on the geochemical data obtained using the LA ICP-MS method on scheelite to see if it could be used to geochemically fingerprint its environment of formation. The samples used come from the granite-related, world-class Sisson W-Mo porphyry-type deposit, NB, along with forty-one scheelite samples from a range of deposit types that constituted the suite used in the broader crystal-chemical study. The protocol used was twofold: (1) collect data using line traverses and integrate the data over intervals showing uniform chemistry; and (2) generate element maps for a select few scheelite grains which displayed complex zoning patterns revealed through CL imaging. Despite using an extensive element list (e.g., LILEs, alkalies, transition metals, HFSEs), only Mo, As and the REEs, which follow crystal growth patterns, showed significant levels of elemental enrichment (i.e., > 1.0 ppm). The correlation of As and Mo indicate only a small intra-deposit variance, but the large inter-deposit variation offers the potential to use this element pair to discriminate deposit types. The results for the REEs indicate: (1) a lack of apparent correlation between REEs and the type of CL observed despite previous suggestions to the contrary; (2) considerable variation in the ∑REEs amongst the sample suite used; (3) most samples are dominated by a single chondrite-normalized (CN) pattern, but rarely a second pattern is present; although the type of CN REE patterns vary (e.g., convex MREE, LREE enrichment), there is a similarity among deposit types; and 5) both positive and negative Eu anomalies are observed. These initial results suggest that the minor and trace-element chemistry of scheelite along with CL imaging, may offer the potential to discriminate and identify deposit types based on its geochemical fingerprinting.

Originally presented Fredericton 2014: Geological Association of Canada - Mineralogical Association of Canada Joint Annual Meeting, Special Session 3: Discovering the Next Generation of Porphyry Deposits: Advancements in Locating and Understanding Hidden Intrusion-related Mineralization. May 21, 2014.

Corresponding author: Rémy S. Poulin (RY_Poulin@laurentian.ca)

Poulin, R.S., McDonald, A.M., Kontak, D.J., and McClenaghan, M.B., 2015. Scheelite geochemical signatures and potential for fingerprinting ore deposits; *in* TGI 4 – Intrusion Related Mineralisation Project: New Vectors to Buried Porphyry-Style Mineralisation, (ed.) N. Rogers; Geological Survey of Canada, Open File 7843, p. 317-326.

Scheelite geochemical signatures and potential for fingerprinting ore deposits

Poulin, R.S.[1], McDonald, A.M. [1], Kontak, D.J.[1] and McClenaghan, M.B.[2]

[1]*Department of Earth Sciences, Laurentian University*
[2]*Geological Survey of Canada*

Overview

- Scheelite as an indicator mineral
- Cathodoluminescence
- REE patterns
  - Simple
  - Mixed
  - Evolved
- $\delta^{18}O$ isotopes
- Distinguishing ore types
- Summary and conclusions

Why scheelite as an indicator mineral?

- Scheelite ($CaWO_4$)
  - Hardness (4.5-5 Moh's)
- Highly fluorescent
- Ease of identification and recovery from surficial sediments

Santa Cruz, Sonora Mexico;
Scheelite, Quartz & Tourmaline

- The previous success with geochemical fingerprinting of minerals (KIMs, rutile, titanite, etc.) from a range of ore deposits suggests that scheelite could be used in a similar manner.

Scheelite (cont.)

- Occurs as ore-grade to minor phases in mineral deposits across the world.
  - World's current production of tungsten is from :
    - skarn (48%)
    - vein/stockwork (44%)
    - strata bound (5%)
    - pegmatite (2%)
    - breccia (1%)
- Occurs in a wide range of geologic ages and proximal to orogenic belts.
  - Rockies/Andes, Pyrenees, Alps, Hercynian and Caledonian
- Focus on differentiation from skarns versus quartz veins

Werner & *al.* 1998

Cathodoluminescence
Quartz Veins

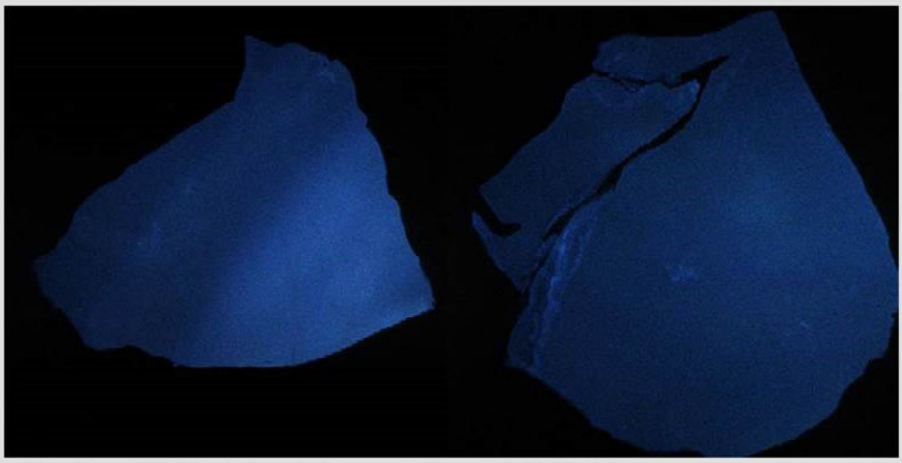

Kazlas, YT (Left) and Sigma Mine Qc (Right)

Cathodoluminescence
Skarns

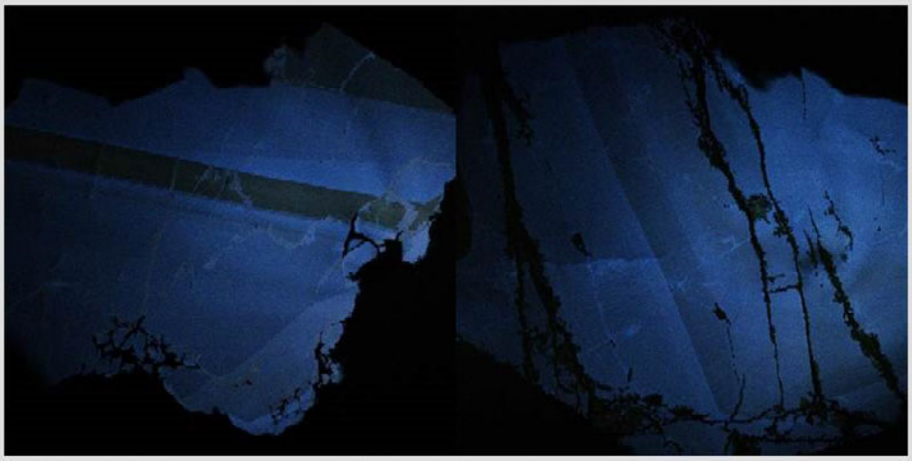

Kum Bel, Kyrgyzstan (Left) and Darwin, US-CA (Right)

- Difficulties discerning deposit type solely on the CL response

Geochemical Fingerprinting

- Devoid of major element changes (Na, Mg, Fe, K, etc.)
- Elemental changes occur with Mo, Sr & As.
  - Mo ranges from ≤LOD to 10 wt%
  - As ranges from ≤LOD to 2300 ppm
  - Sr ranges from ≤LOD to 1.1 wt%*

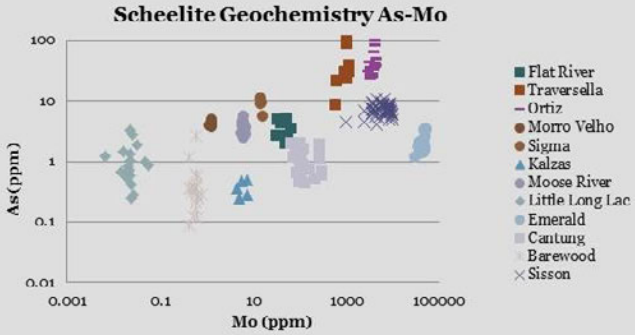

- Mo and As show narrow range between samples from a single locale.

Incorporation of REE

- LREE are preferentially incorporated within the Ca^{2+} in the [8]-coordinated site in relation to HREE.
  - Positive Eu anomalies (Eu occurring in 2+ state, from a reduced fluid)
  - HREE relatively depleted (fluid source has fractionated HREE or enriched in LREE)

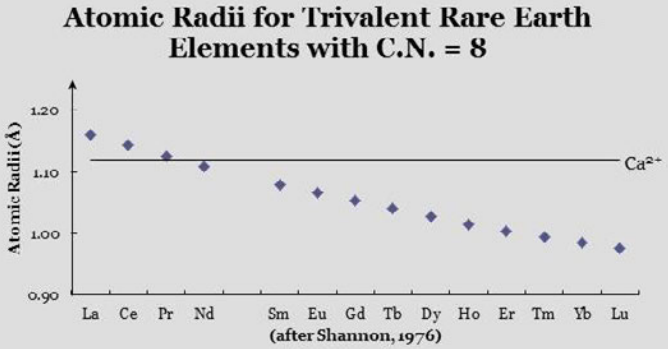

- Three styles of patterns are generally observed;
  - Simple, Evolved and Mixed

REE Patterns - Simple

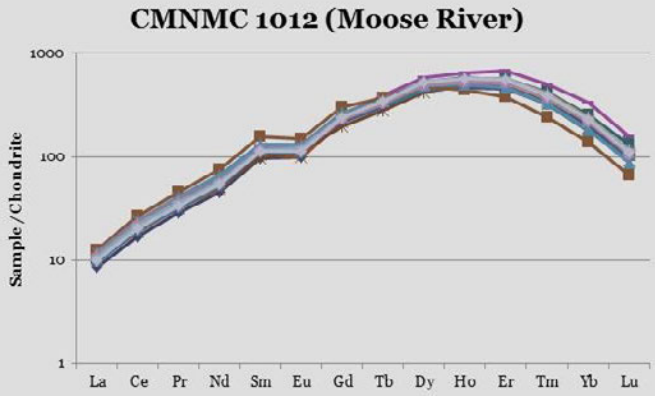

- When a sample is dominated by a single chondrite normalized pattern.
- This stratabound/vein type pattern is consistent with 19 measurements.

Multiple Signatures...

- In some cases the overall REE pattern is not dominated by a single pattern.
- In these cases a second pattern exists in conjunction with the primary pattern.
- *Two proposed models*
  1) Fluid **mixing** resulting in two patterns. (Ghaderi *et al.* 1999)
  2) Fluid **evolution** from one type of pattern to another. (Brugger *et al.* 2000)
- No single model is favoured for scheelite mineralization

REE Patterns - Evolved

- Kalzas, YT (Vein)
  - Type I pattern: as the LREE is preferentially incorporated within scheelite, a subsequent LREE depleted pattern is developed.

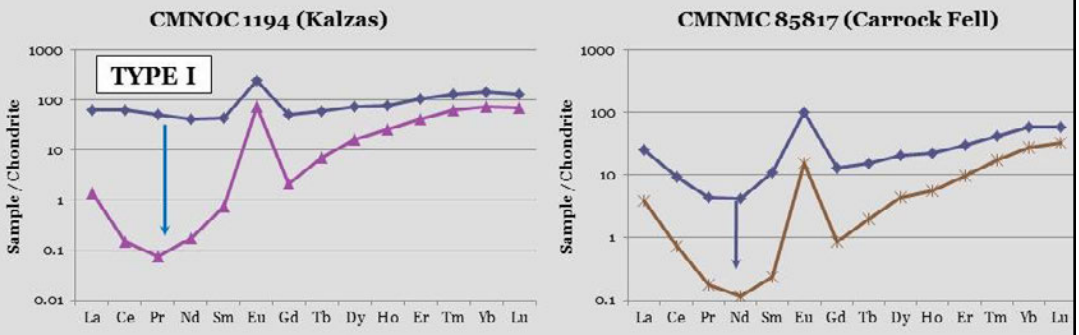

- Carrock Fell, UK (Vein)
  - This pattern shows a similar pattern to the LREE depleted pattern observed at Kalzas, however the original fluid pattern is absent.

REE Patterns – Evolved

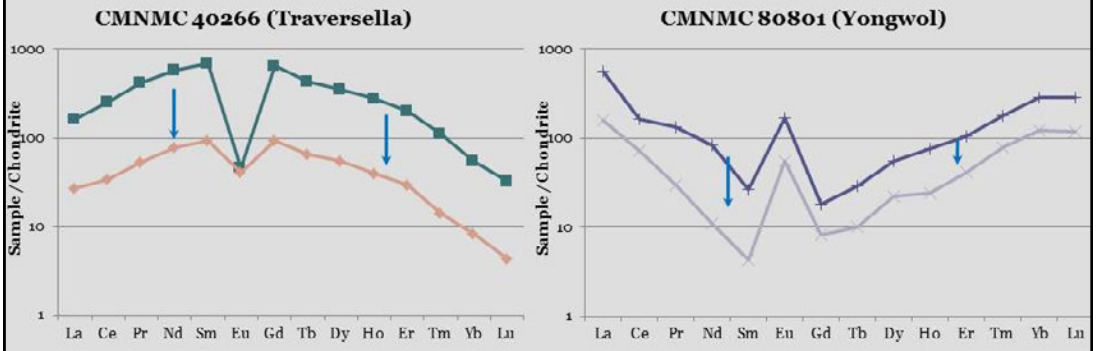

- Traversella, Italy and Yongwol, South Korea (Skarns)
  - Each of these patterns show a uniform depletion of REE within the fluid.
- Different patterns may arise for a similar ore deposit settings

REE patterns – Mixed

- In some instances, such as Silverton, US-CO (Vein) two distinctly different patterns are apparent.
- Fluid mixing?
  - As scheelite mineralized, it inherited the geochemical signatures of both fluids as they homogenized.

$\delta^{18}O$ values

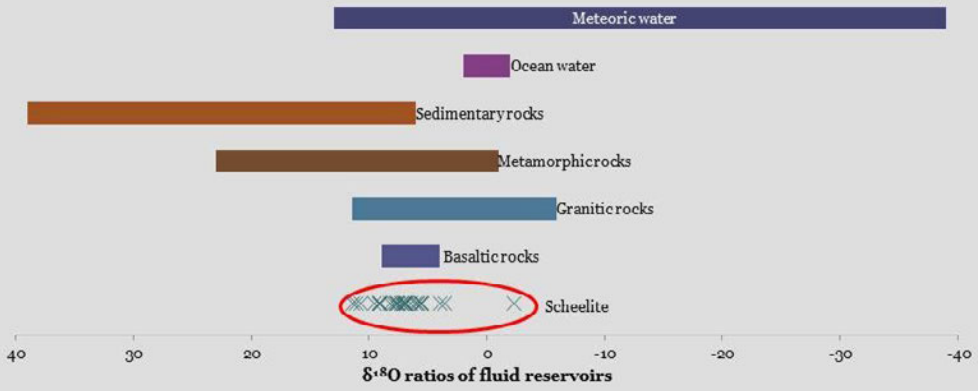

- Fluid source(s)?
  - The range for scheelite varies on average from 3.6 to 11.4 ‰ with an outlier of -2.3‰.
  - Different fluids (magmatic, metamorphic and meteoric) are involved in scheelite mineralization.
  - The presence of different fluid signatures demonstrate the importance of $\delta^{18}O$ data with regards to interpreting REE and trace element data correctly.

Distinguishing ore types

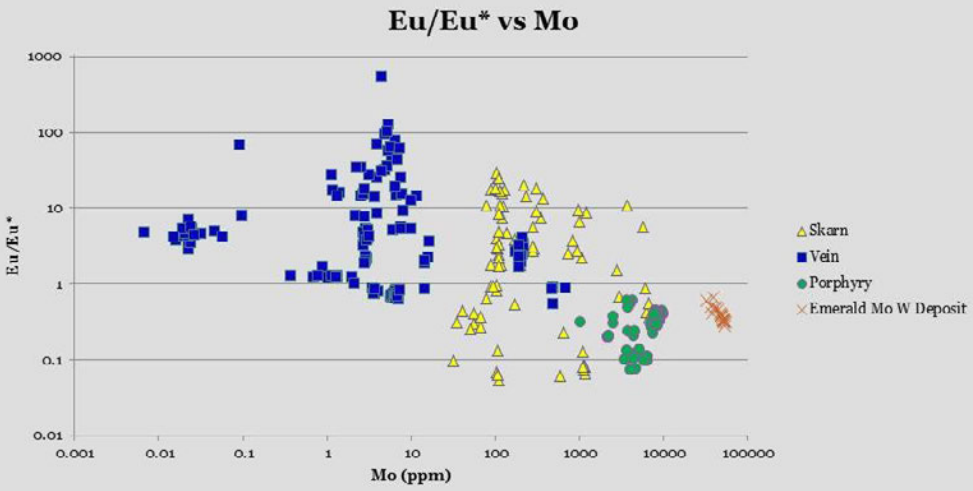

- By combining the minor and trace element data, this enables the potential to discriminate and identify deposit types

Summary and Conclusions

- In some cases, the deposit type of scheelite can be distinguished based on the CL response.
  - This is dependent on crystal orientation and field of view.
- REE patterns vary between scheelites from similar and different ore deposit settings.
  - Patterns however are generally homogenous within a single deposit.
  - Eu/Eu* anomalies; are particularly sensitive to small variations in pH during mineral formation and the onset of fluid-rock interactions.
- The variability of REE patterns between deposit types and the presence of fluid mixing and/or evolution adds complexity to determining deposit settings.
- $\delta^{18}O$ isotopes is an important factor in order to correctly interpret the REE patterns.
- Using Eu/Eu* vs. Mo suggests a potential tool to discriminate and identify deposit types in a regional till sampling tests.

Acknowledgments
• Joe Petrus, Laurentian University
• Michel Picard, Canadian Museum of Nature
• Mark Badham, Miller Museum, Queen's University
• Northcliff Resources Ltd.
• Overburden Drilling Management Ltd.
Questions?
LaurentianUniversity
UniversitéLaurentienne
ODM
HDINORTHCLIFF
CANADA
TGI 4
Ore Systems

Geological and structural controls on hydrothermal alteration and W-Mo mineralization in the Sisson deposit, New Brunswick

J.R. Lang[1], R. Duncan[2], D.R. Lentz[3], W. Zhang[3], A. Bustard[3], C.R.M. McFarlane[3] and K.G. Thorne[4]

1. Hunter Dickinson Inc., 1040 West Georgia Street, Vancouver, British Columbia

2. Mineral Deposit Research Unit, University of British Columbia, Vancouver, British Columbia

3. University of New Brunswick, Fredericton, New Brunswick

4. Geological Surveys Branch, New Brunswick Department of Natural Resources, Fredericton, New Brunswick

Abstract: The Sisson deposit is a Late Devonian, structurally-controlled, intrusion-related W-Mo deposit located in west-central New Brunswick. Resources are estimated at 383 Mt grading 0.067 % WO_3 and 0.021 % Mo (measured/indicated) and 178 Mt grading 0.051 % WO_3 and 0.021 % Mo (inferred). Host rocks to Sisson include quartz diorite and gabbro phases (432 Ma; U-Pb on titanite) of the Howard Peak intrusion on the west, which are in fault contact across the vertical, north-trending Sisson shear zone with north-northwest-striking, steeply east-dipping metavolcanic and metasedimentary rocks of the Cambrian to Ordovician Tetagouche and Miramichi Groups on the east. Re-Os dates of ca. 378 Ma on molybdenite overlap U-Pb dates on zircon from narrow granite dykes within the deposit, which are likely related to the Late Devonian Nashwaak Granite batholith located immediately northwest of the deposit. The deposit is cut by narrow, undeformed, barren granite porphyry dykes dated at ca. 364 Ma (U-Pb on zircon).

The Sisson deposit obliquely straddles the Sisson shear zone. Hydrothermal activity comprises: (1) early, weakly to unmineralized amphibole veinlets with albite alteration envelopes and small, erratically-distributed zones of biotite±pyrite alteration; (2) quartz- scheelite veinlets with biotite envelopes; (3) quartz-molybdenite±scheelite veinlets with sericite envelopes; (4) mostly late but possibly long-lived, larger and more continuous, polymetallic quartz-shear veins with broad sericite envelopes and associated sulphide-rich veinlets, which also introduced minor Cu, Bi, Sb, As, Pb and Zn to the deposit; and (5) rare endoskarn with scheelite mineralization of uncertain timing in narrow granite dykes intersected only at depths of >400 metres. Alteration is mostly restricted to the envelopes which enclose veinlets. Scheelite mineralization occurs primarily in quartz veinlets and their alteration envelopes, molybdenite is restricted to quartz veinlets, and minor ferberitic wolframite, mostly replaced by scheelite, occurs in some quartz-scheelite veinlets and in most quartz-shear veins.

Veins throughout the deposit form a sheeted array with consistent northwest strike and steep to moderate southwest dips. The nature and geometry of the vein sets are most compatible with formation during crustal extension, which was synchronous with sinistral, syn-hydrothermal displacement across the north-trending Sisson shear zone. The structural plumbing system focused ascent of W-mineralizing fluids from intrusions at depth, the presence of which is indicated by syn-hydrothermal granite dykes within the deposit. Precipitation of W and Mo mineralization resulted from chemical interactions between hydrothermal fluids and wall rock at a low fluid to rock ratio, and from changes in sulphur and oxygen fugacity.

Originally presented Fredericton 2014: Geological Association of Canada - Mineralogical Association of Canada Joint Annual Meeting, Special Session 3: Discovering the Next Generation of Porphyry Deposits: Advancements in Locating and Understanding Hidden Intrusion-related Mineralization. May 21, 2014.

Corresponding author: James R. Lang (jimlang@hdimining.com)

Lang, J.R., Duncan, R., Lentz, D.R., Zhang, W., Bustard, A., McFarlane, C.R.M., and Thorne, K.G., 2015. Geological and structural controls on hydrothermal alteration and W-Mo mineralization in the Sisson deposit, New Brunswick; *in* TGI 4 – Intrusion Related Mineralisation Project: New Vectors to Buried Porphyry-Style Mineralisation, (ed.) N. Rogers; Geological Survey of Canada, Open File 7843, p. 327-341.

HDI NORTHCLIFF
The Sisson W-Mo Project, New Brunswick: Deposit Geology, Ore Controls & Exploration Methods
Authors: Lang, J.; Duncan, R.; Lentz, D.; Zhang, W.; Bustard, A.; McFarlane, C.; Thorne, K

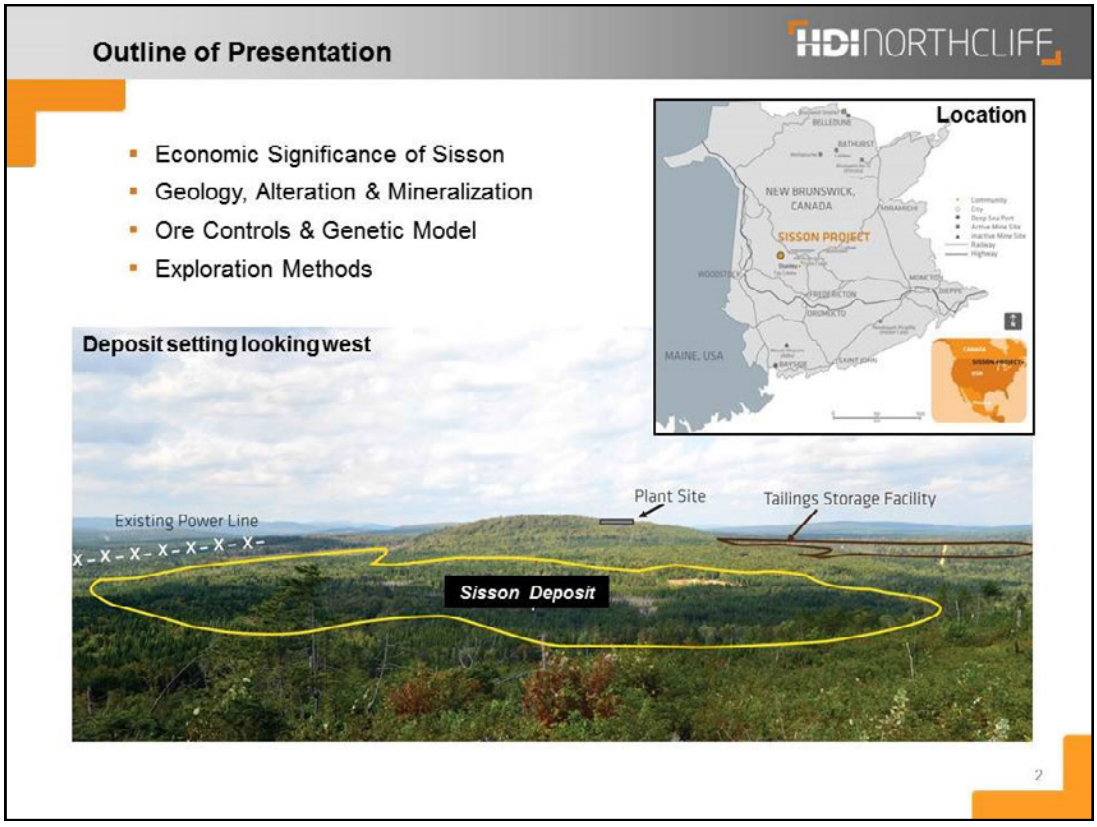
Outline of Presentation
HDI NORTHCLIFF
Economic Significance of Sisson
Geology, Alteration & Mineralization
Ore Controls & Genetic Model
Exploration Methods
Location
NEW BRUNSWICK, CANADA
SISSON PROJECT
MAINE, USA
Deposit setting looking west
Plant Site
Tailings Storage Facility
Existing Power Line
Sisson Deposit
2

Reserves & Mining Plan

HDI NORTHCLIFF

Sisson is one of the most significant tungsten reserves outside of China
(2013 Northcliff Feasibility Study)

Sisson Deposit 43-101 Mineral Reserves (January 2013 at $8.83/tonne NSR cutoff[1])

Category	Cut-Off Grade (NSR $/t)	Tonnes (Mt)	NSR ($/t)	WO_3 (%)	Mo (%)	Tungsten (WO_3) (million MTUs)	Contained Mo (Mlb)
Proven	8.83	105.4	25.48	0.069	0.023	7.3	53.0
Probable	8.83	228.9	23.54	0.065	0.020	14.9	101.7
Total	8.83	334.4	24.15	0.066	0.021	22.2	154.8

[1]Contained within Ultimate Pit Limit. Metal Prices: WO_3=US$350/metric tonne unit (mtu), Mo=US$15/lb; Assumed Concentrator Recoveries: WO_3=variable with feed grade, Mo=82%; APT Plant Recovery of WO_3=97%; USD$:CDN$0.9:1; NSR=(WO_3% * NSP WO_3*Recovery WO_3*22.046)+(Mo%*NSP Mo Recovery Mo*22.046); Net Smelter Price (NSP) WO_3=CDN$17.46/lb; Mo=CDN$14.50/lb.

FEASIBILITY PRODUCTION PLAN:

- Mine life of 27 years
- Average annual production:
  - 557,000 MTU/yr WO_3 (MTU = 10 kg contained WO_3)
  - 4.1M lbs/yr Mo
- First ammonium paratungstate (APT) plant in Canada

3

Sisson Project History

HDI NORTHCLIFF

1978 – 1984
- Discovery by Kidd Creek Mines (TexasGulf)

2004 – 2009
- Geodex Minerals advanced and largely delineated the deposit

2010 – Present
- Northcliff Resources
  - Initial JV with Geodex in late 2010
  - Acquired 100% of project in June 2012
  - Positive feasibility study completed January 2013
  - EIA submitted mid-2013

4

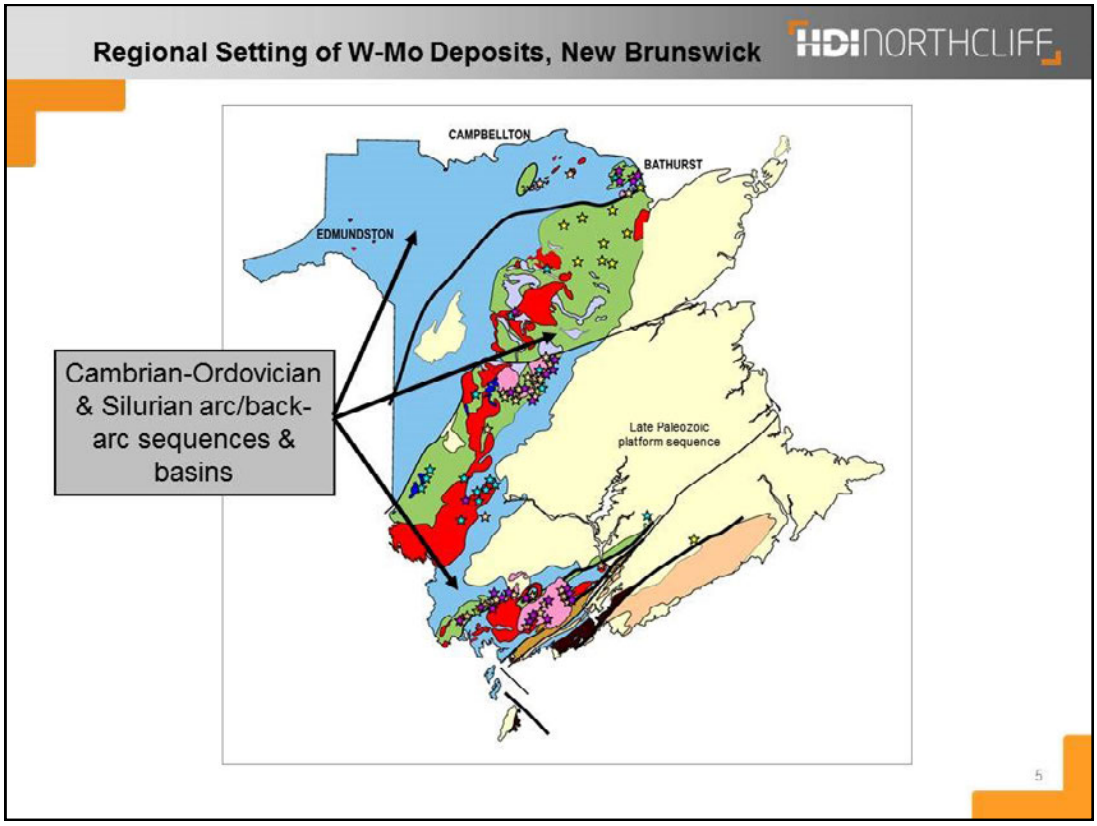
Regional Setting of W-Mo Deposits, New Brunswick
HDI NORTHCLIFF
CAMPBELLTON
BATHURST
EDMUNDSTON
Late Paleozoic platform sequence
Cambrian-Ordovician & Silurian arc/back-arc sequences & basins
5

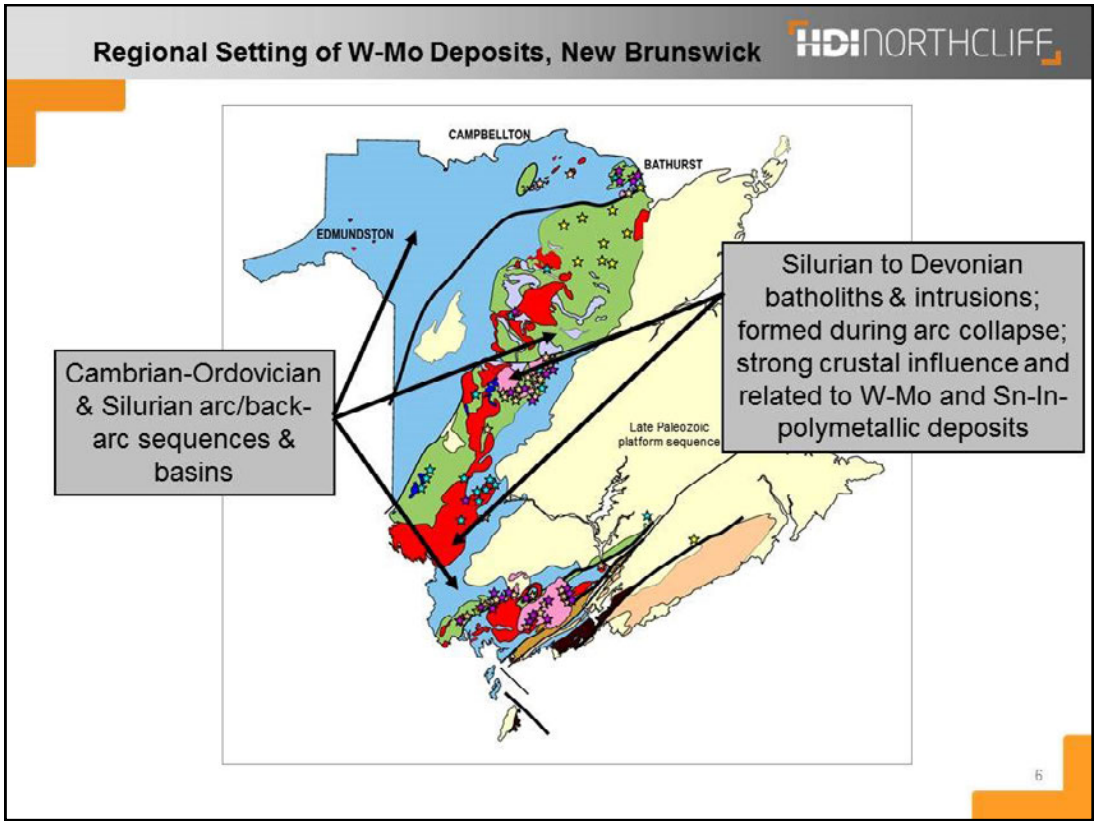
Regional Setting of W-Mo Deposits, New Brunswick
HDI NORTHCLIFF
CAMPBELLTON
BATHURST
EDMUNDSTON
Late Paleozoic platform sequence
Cambrian-Ordovician & Silurian arc/back-arc sequences & basins
Silurian to Devonian batholiths & intrusions; formed during arc collapse; strong crustal influence and related to W-Mo and Sn-In-polymetallic deposits
6

Regional Setting of W-Mo Deposits, New Brunswick

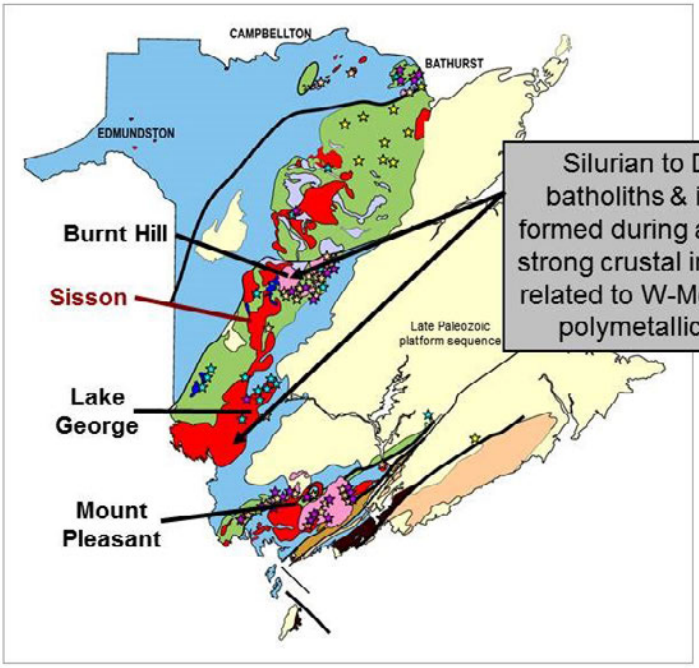

W-Mo Deposits

Silurian to Devonian batholiths & intrusions; formed during arc collapse; strong crustal influence and related to W-Mo and Sn-In-polymetallic deposits

Mineralized Zones & District Geology

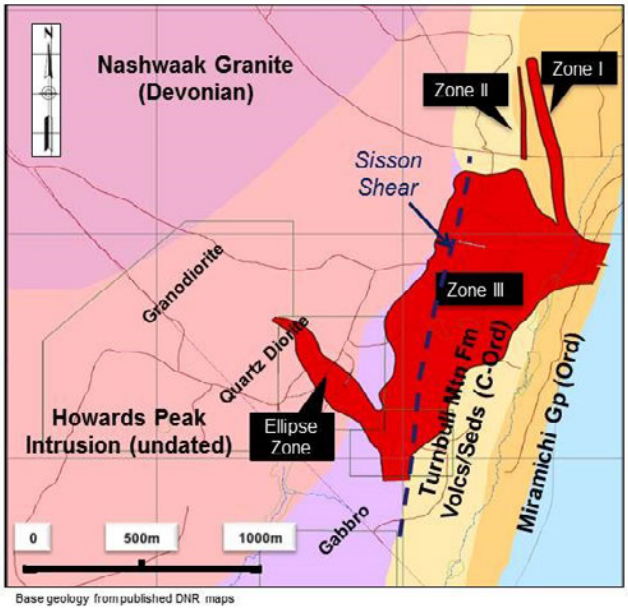

Base geology from published DNR maps

General Setting:

- W-Mo min'l comprises four contiguous zones (377.5 Ma by Re-Os on molybdenite)
- Min'l obliquely spans the vertical, sinistral Sisson Shear
- Separates C-Ord metaseds/volcs of the Turnbull Mtn Fm (east) from Howard Peak gabbro (west; U-Pb = 432 Ma)
- Acadian Nashwaak Granite batholith 500 m west (poorly dated; U-Pb = 376-422 Ma)

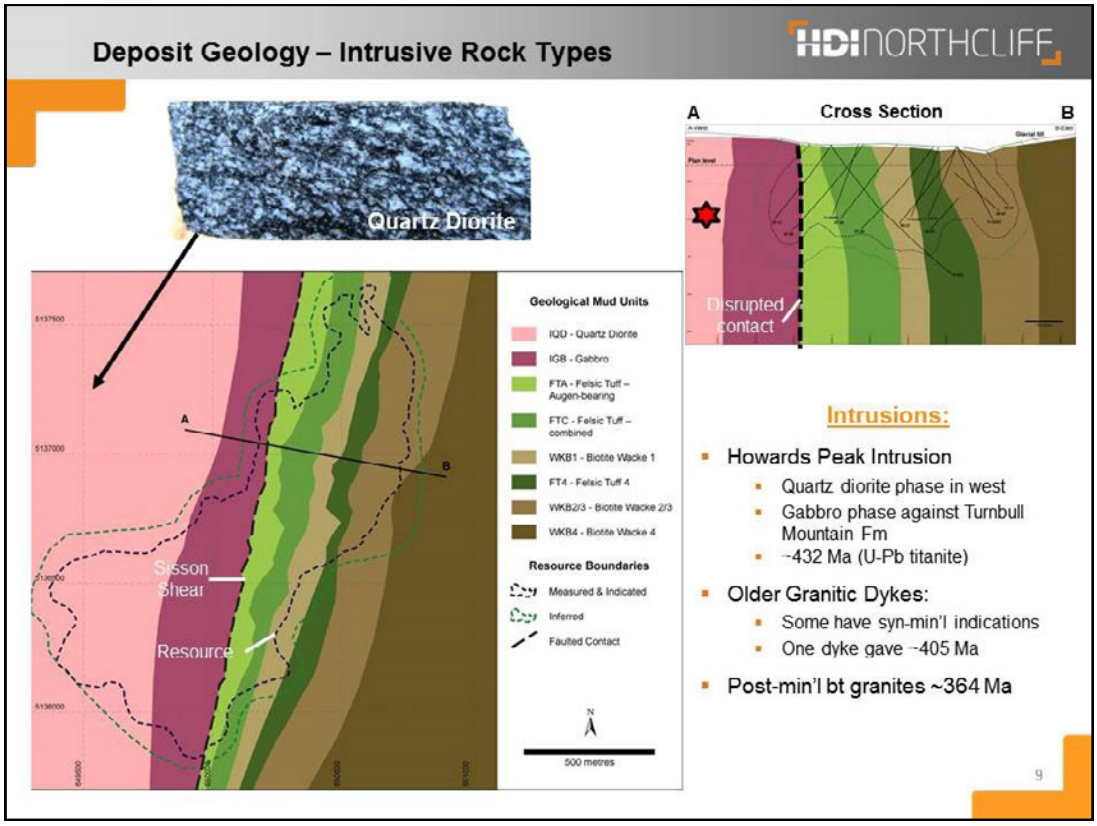
Deposit Geology – Intrusive Rock Types
HDI NORTHCLIFF
Quartz Diorite
Cross Section
A
B
Disrupted contact
Geological Mud Units
IQD - Quartz Diorite
IGB - Gabbro
FTA - Felsic Tuff – Augen-bearing
FTC - Felsic Tuff – combined
WKB1 - Biotite Wacke 1
FT4 - Felsic Tuff 4
WKB2/3 - Biotite Wacke 2/3
WKB4 - Biotite Wacke 4
Resource Boundaries
Measured & Indicated
Inferred
Faulted Contact
Sisson Shear
Resource
500 metres
Intrusions:
Howards Peak Intrusion
Quartz diorite phase in west
Gabbro phase against Turnbull Mountain Fm
~432 Ma (U-Pb titanite)
Older Granitic Dykes:
Some have syn-min'l indications
One dyke gave ~405 Ma
Post-min'l bt granites ~364 Ma
9

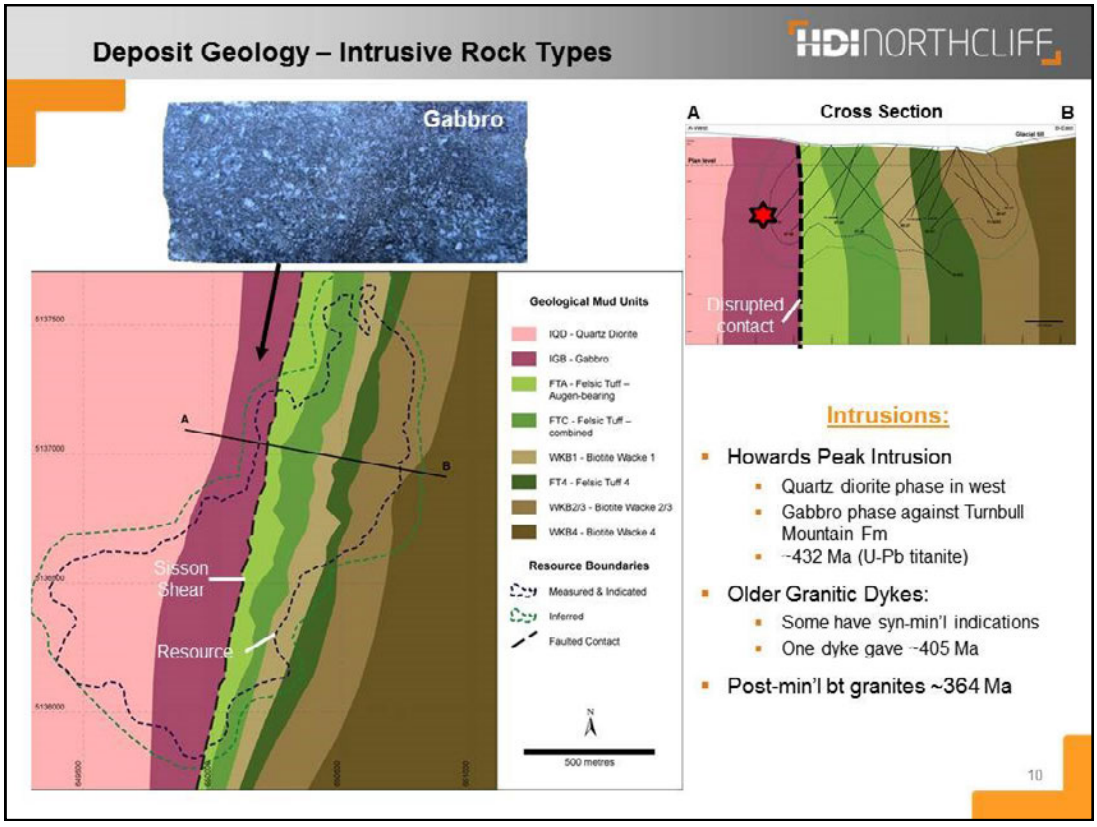
Deposit Geology – Intrusive Rock Types
HDI NORTHCLIFF
Gabbro
Cross Section
A
B
Disrupted contact
Geological Mud Units
IQD - Quartz Diorite
IGB - Gabbro
FTA - Felsic Tuff – Augen-bearing
FTC - Felsic Tuff – combined
WKB1 - Biotite Wacke 1
FT4 - Felsic Tuff 4
WKB2/3 - Biotite Wacke 2/3
WKB4 - Biotite Wacke 4
Resource Boundaries
Measured & Indicated
Inferred
Faulted Contact
Sisson Shear
Resource
500 metres
Intrusions:
Howards Peak Intrusion
Quartz diorite phase in west
Gabbro phase against Turnbull Mountain Fm
~432 Ma (U-Pb titanite)
Older Granitic Dykes:
Some have syn-min'l indications
One dyke gave ~405 Ma
Post-min'l bt granites ~364 Ma
10

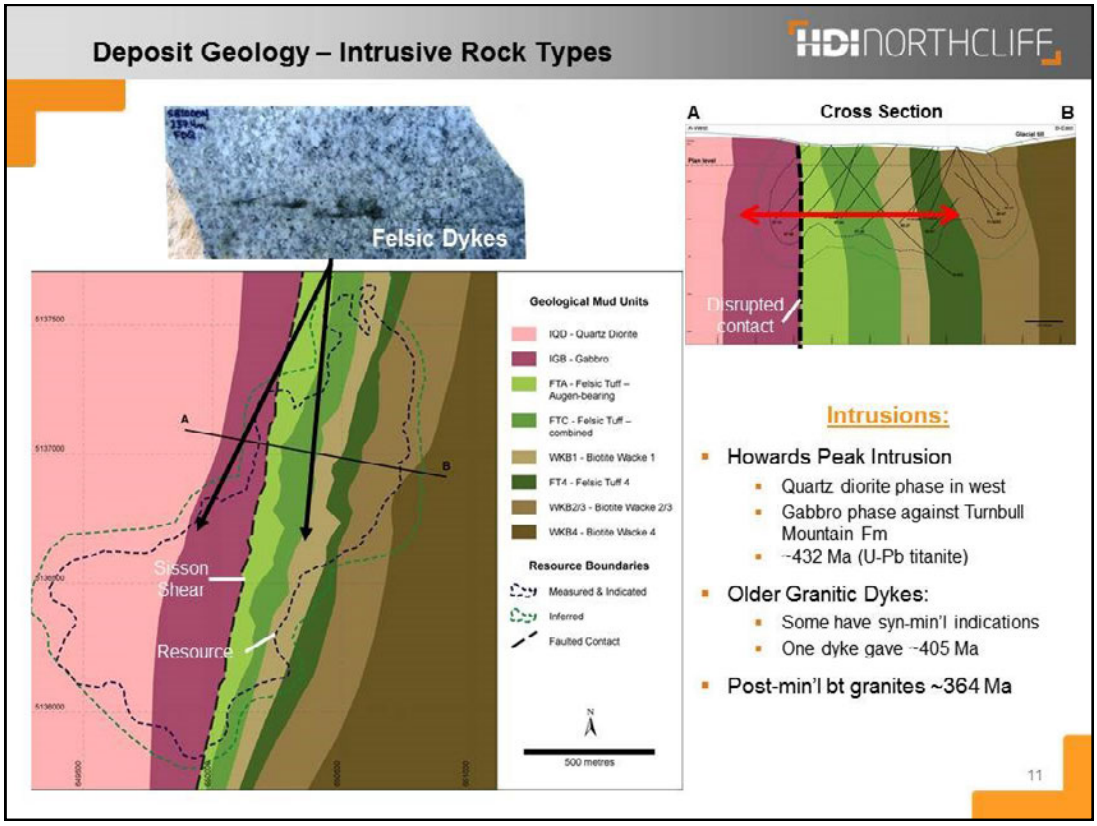
Deposit Geology – Intrusive Rock Types
HDI NORTHCLIFF
Felsic Dykes
A
Cross Section
B
Disrupted contact
Geological Mud Units
IQD - Quartz Diorite
IGB - Gabbro
FTA - Felsic Tuff – Augen-bearing
FTC - Felsic Tuff – combined
WKB1 - Biotite Wacke 1
FT4 - Felsic Tuff 4
WKB2/3 - Biotite Wacke 2/3
WKB4 - Biotite Wacke 4
Resource Boundaries
Measured & Indicated
Inferred
Faulted Contact
Sisson Shear
Resource
N
500 metres
Intrusions:
Howards Peak Intrusion
Quartz diorite phase in west
Gabbro phase against Turnbull Mountain Fm
~432 Ma (U-Pb titanite)
Older Granitic Dykes:
Some have syn-min'l indications
One dyke gave ~405 Ma
Post-min'l bt granites ~364 Ma
11

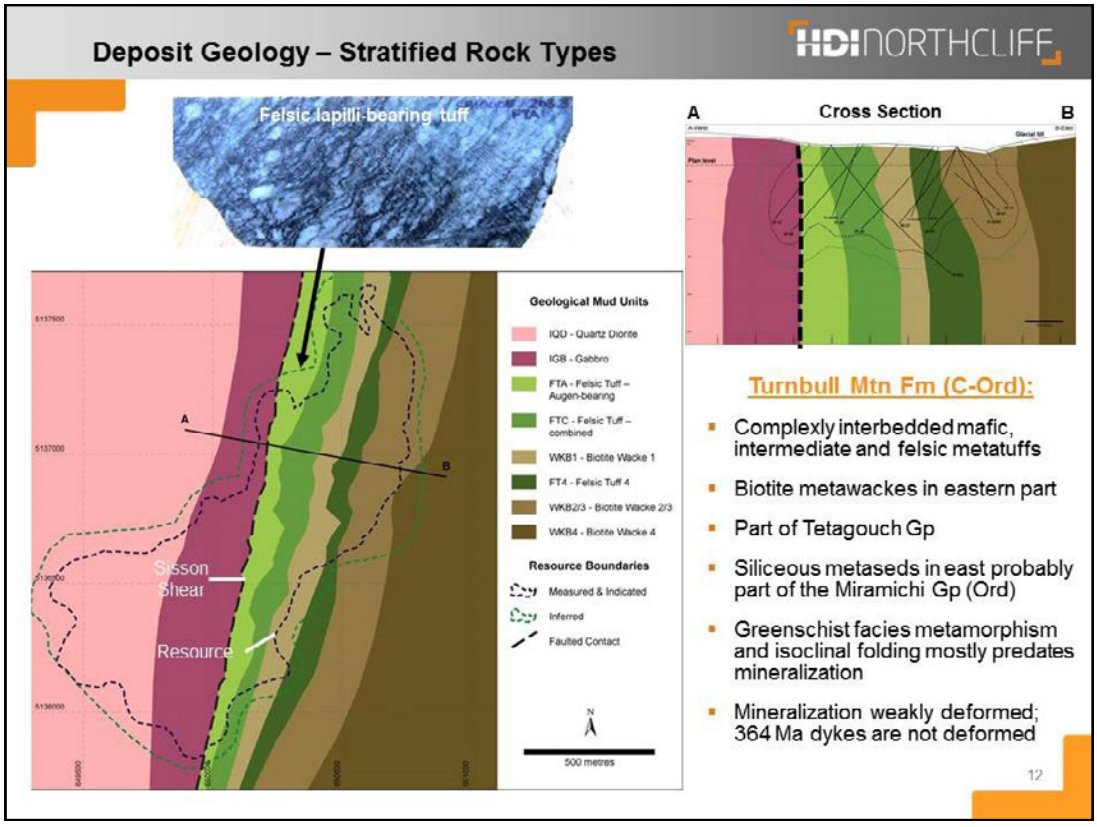
Deposit Geology – Stratified Rock Types
HDI NORTHCLIFF
Felsic lapilli-bearing tuff
A
Cross Section
B
Geological Mud Units
IQD - Quartz Diorite
IGB - Gabbro
FTA - Felsic Tuff – Augen-bearing
FTC - Felsic Tuff – combined
WKB1 - Biotite Wacke 1
FT4 - Felsic Tuff 4
WKB2/3 - Biotite Wacke 2/3
WKB4 - Biotite Wacke 4
Resource Boundaries
Measured & Indicated
Inferred
Faulted Contact
Sisson Shear
Resource
N
500 metres
Turnbull Mtn Fm (C-Ord):
Complexly interbedded mafic, intermediate and felsic metatuffs
Biotite metawackes in eastern part
Part of Tetagouch Gp
Siliceous metaseds in east probably part of the Miramichi Gp (Ord)
Greenschist facies metamorphism and isoclinal folding mostly predates mineralization
Mineralization weakly deformed; 364 Ma dykes are not deformed
12

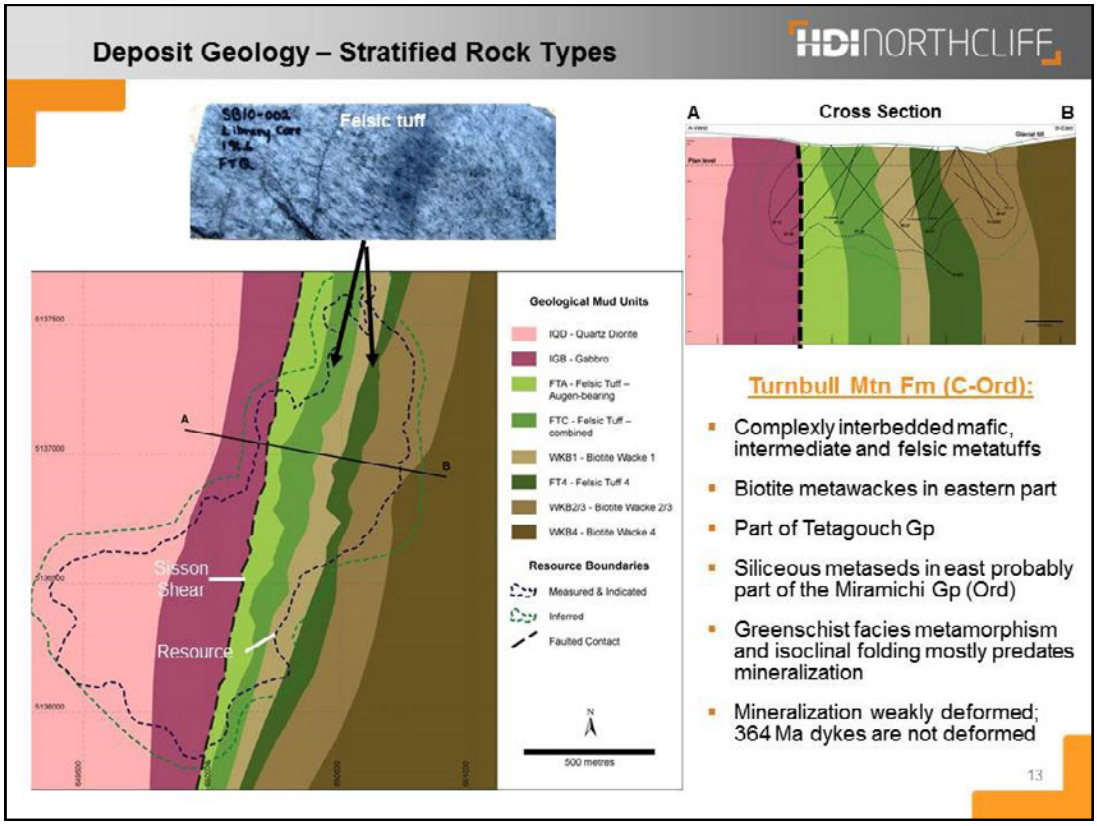
Deposit Geology – Stratified Rock Types
HDI NORTHCLIFF
Felsic tuff
A
Cross Section
B
Geological Mud Units
IQD - Quartz Diorite
IGB - Gabbro
FTA - Felsic Tuff – Augen-bearing
FTC - Felsic Tuff – combined
WKB1 - Biotite Wacke 1
FT4 - Felsic Tuff 4
WKB2/3 - Biotite Wacke 2/3
WKB4 - Biotite Wacke 4
Resource Boundaries
Measured & Indicated
Inferred
Faulted Contact
Sisson Shear
Resource
500 metres
Turnbull Mtn Fm (C-Ord):
Complexly interbedded mafic, intermediate and felsic metatuffs
Biotite metawackes in eastern part
Part of Tetagouch Gp
Siliceous metaseds in east probably part of the Miramichi Gp (Ord)
Greenschist facies metamorphism and isoclinal folding mostly predates mineralization
Mineralization weakly deformed; 364 Ma dykes are not deformed
13

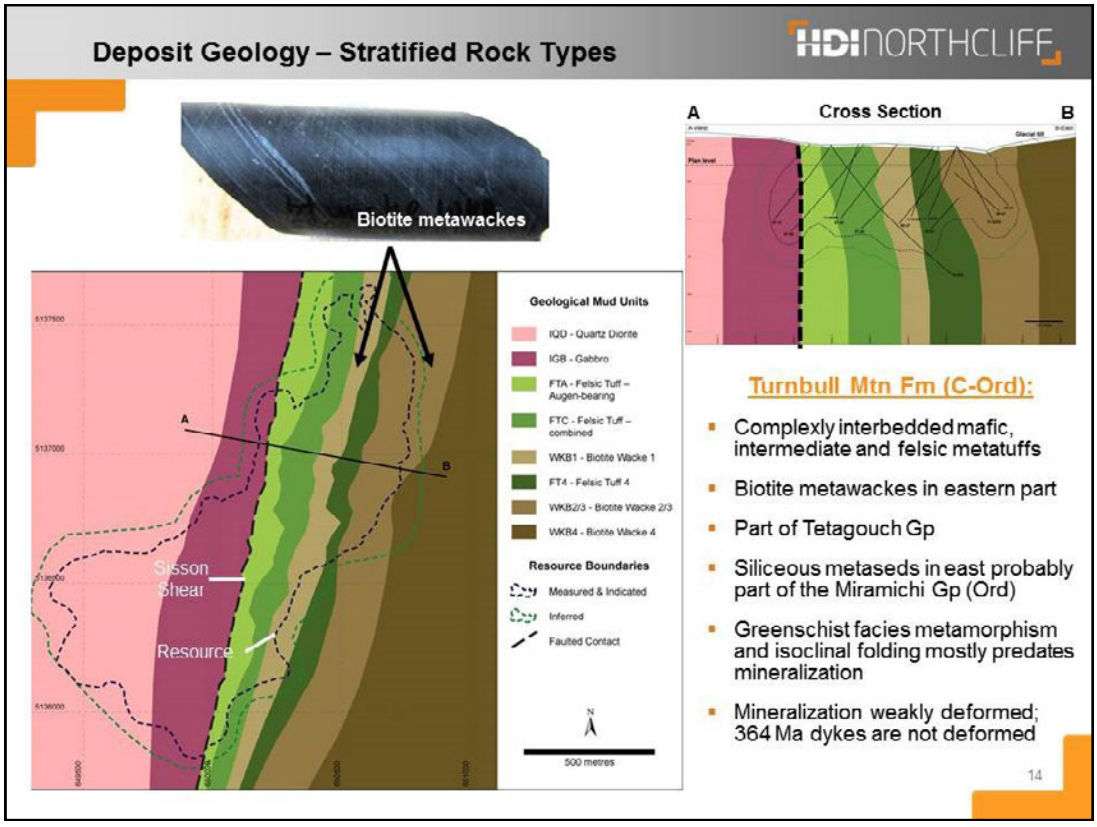
Deposit Geology – Stratified Rock Types
HDI NORTHCLIFF
Biotite metawackes
A
Cross Section
B
Geological Mud Units
IQD - Quartz Diorite
IGB - Gabbro
FTA - Felsic Tuff – Augen-bearing
FTC - Felsic Tuff – combined
WKB1 - Biotite Wacke 1
FT4 - Felsic Tuff 4
WKB2/3 - Biotite Wacke 2/3
WKB4 - Biotite Wacke 4
Resource Boundaries
Measured & Indicated
Inferred
Faulted Contact
Sisson Shear
Resource
500 metres
Turnbull Mtn Fm (C-Ord):
Complexly interbedded mafic, intermediate and felsic metatuffs
Biotite metawackes in eastern part
Part of Tetagouch Gp
Siliceous metaseds in east probably part of the Miramichi Gp (Ord)
Greenschist facies metamorphism and isoclinal folding mostly predates mineralization
Mineralization weakly deformed; 364 Ma dykes are not deformed
14

Deposit Geology – Stratified Rock Types

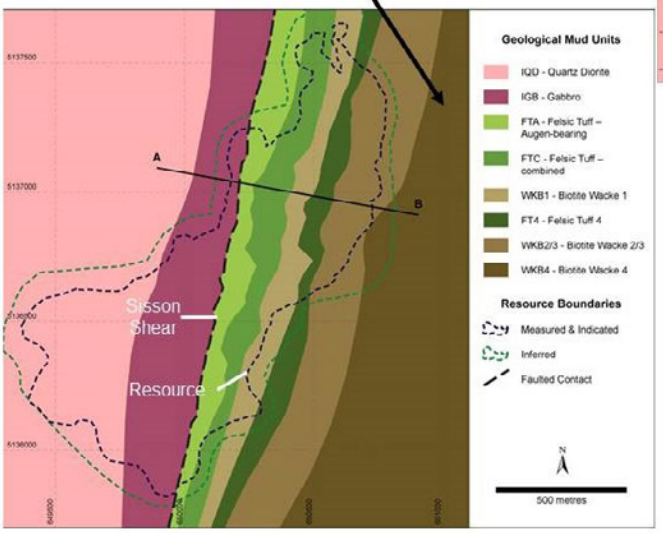

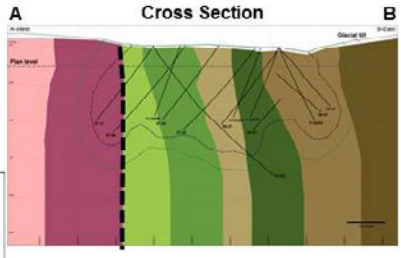

Turnbull Mtn Fm (C-Ord):

- Complexly interbedded mafic, intermediate and felsic metatuffs
- Biotite metawackes in eastern part
- Part of Tetagouch Gp
- Siliceous metaseds in east probably part of the Miramichi Gp (Ord)
- Greenschist facies metamorphism and isoclinal folding mostly predates mineralization
- Mineralization weakly deformed; 364 Ma dykes are not deformed

15

Early Alteration & Veins

Na-Ca Alt'n & Amphibole Veins

- Albite-actinolite envelopes
- Mostly in gabbro
- No significant mineralization

Biotite±Pyrite Alteration

- Pervasive
- Erratic, volumetrically minor
- No significant mineralization

Calc-Silicate Alteration

- Rare, small, deep
- Moderate scheelite min'l
- Possibly in felsic dykes
- *Relative timing unknown*

16

W & Mo Mineralization Mostly in Quartz Veins

HDI NORTHCLIFF

Early Qtz-Scheelite Veins	Intermediate Qtz-Molybdenite Veins	(Mostly Late) Qtz-Shear Veins & Sulphide-Rich Fractures
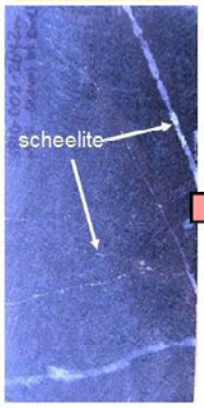	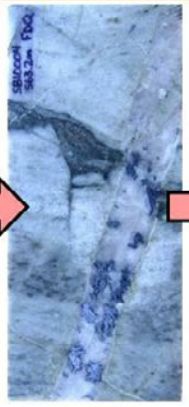	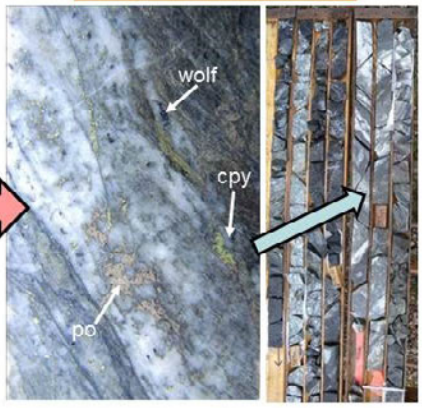
Strong W Minor to no Mo Decrease with depth Low sulphide Narrow biotite alt'n envelopes	Most of the Mo Low to high-grade W Extend to great depth Low sulphide Rare, narrow sericite alt'n envelopes	Complex, episodic growth Wide, sulphide-rich shear veins and narrow, sulphide-rich fractures High grade W, no Mo High sulphide; host most of the Cu, Zn, As, Bi Wide sericite-pyrite-pyrrhotite alt'n envelopes

17

Veins, Alteration & Mineralization

HDI NORTHCLIFF

Vein density is low & domains between veinlets are nearly unaltered

Hydrothermal system was weak or largely confined to fractures/veinlets

18

Characteristics of Tungsten Mineralization

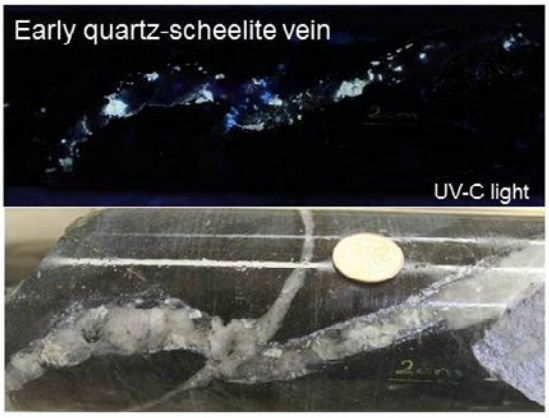

Tungsten Mineralization

- Dominated by scheelite (blue fluorescence)
- Molybdoscheelite (yellow fluorescence) contains <4 wt% Mo
- Mostly in veins & fractures
- Lesser in alteration envelopes
- Minor ferberitic wolframite typically replaced by scheelite

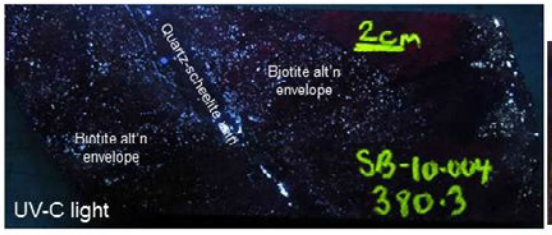

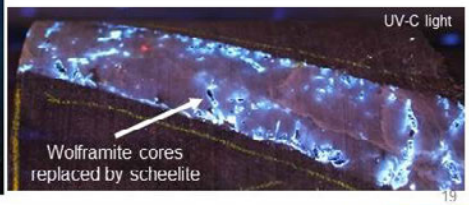

19

Metal Distribution and Zoning

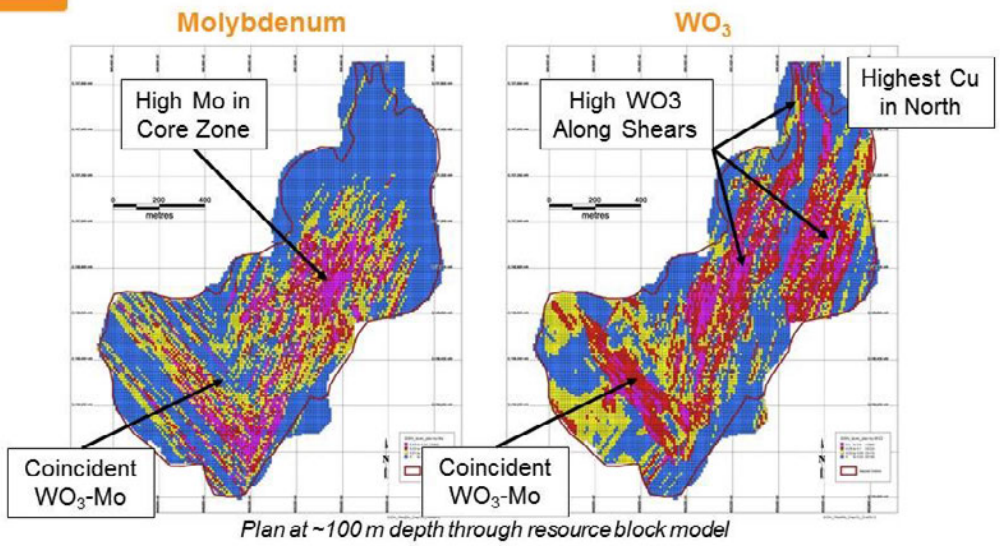

Plan at ~100 m depth through resource block model

- **Vertically:**
  - WO_3 min`l extends to 200 m in north, 350 m in south – base plunges south
  - Molybdenite min`l extends deeper to the limit of drilling at >550 m depth

20

Vein Structural Relationships

HDI NORTHCLIFF

- ***Larger shear veins*** – NNE-striking, ~vertical, sinistral movement
- ***Sheeted veinlet arrays*** – NW-striking, SW-dipping, mineralized fractures and extension veins

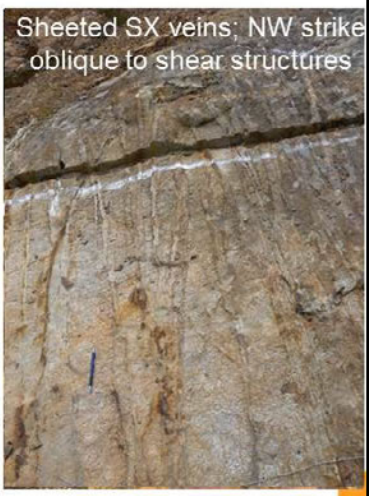

21

Sheeted Vein Arrays Are Ubiquitous

HDI NORTHCLIFF

Veins in Ellipse Zone Trench

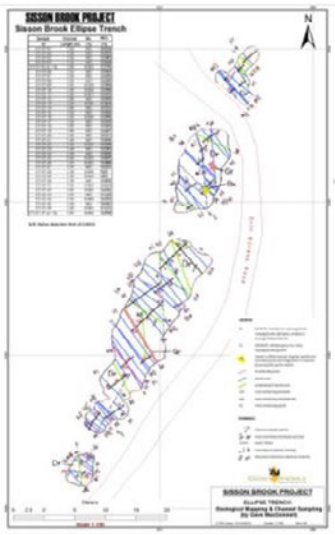

Veins in Oriented Drill Core

Qtz-Scheelite Veins **Qtz-Molybdenite Veins** **Qtz-Shear Veins**

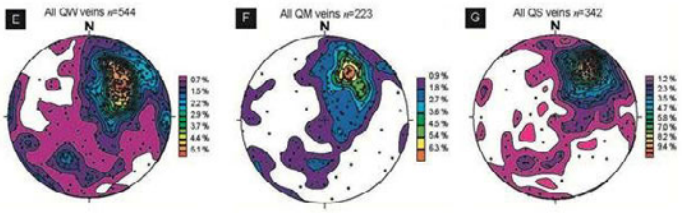

Vein Orientations:

- Strong preferred NW strike for all vein types
- Steep dips, mostly to the SW
- A few wide veins strike N in mapped trenches
- Sheeted vein array likely located between larger sinistral shear zones

22

Magmatic-Hydrothermal-Structural Model

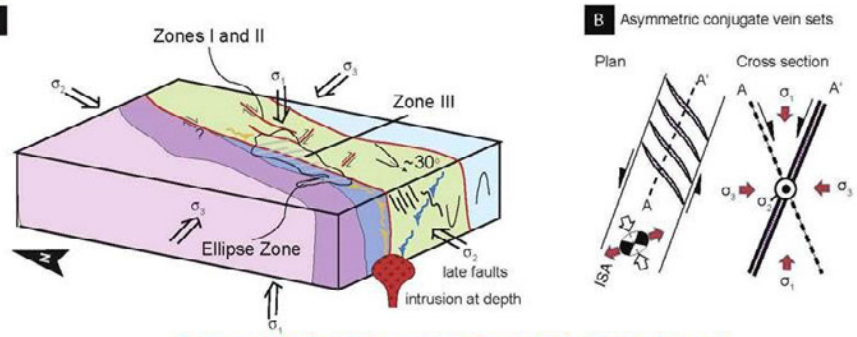

Structural Control & Provisional Genetic Model:

- **Timing.** Late Acadian trans-tensional stress
- **Plumbing System.** Vertical, NNE sinistral faults (wide QS veins) which control intervening sheeted vein sets (QW, QM, sulphidic fractures)
- **Fluids.** Magmatic origin supported by $\delta^{18}O$ in vein quartz and rare endoskarn in granite dykes
- **Source.** Probably a late, marginal phase related to the Nashwaak Granite at depth, controlled by same structural regime
- **Fluid Flux.** Low or confined, indicated by weak alteration & low vein density
- **Conditions.** Fluid inclusions (Nast, 1985) indicate WO_3 min'l at 370-430°C and 500 bars.

23

Controls on Scheelite Precipitation

- Fluid – wall rock interaction probably critical:
  - Alteration mostly confined to vein envelopes – low or very confined fluid flux.
  - **Fluid-mineral reactions and local chemical component availability (Ca, Ti).**
  - Destabilized $HKWO_3$ complexes = scheelite ppt'n
  - Other proposals: prograde versus retrograde temperature regimes, fluid mixing, changes in fS_2
  - More study required

Ca availability in mafic host rocks during biotite alteration

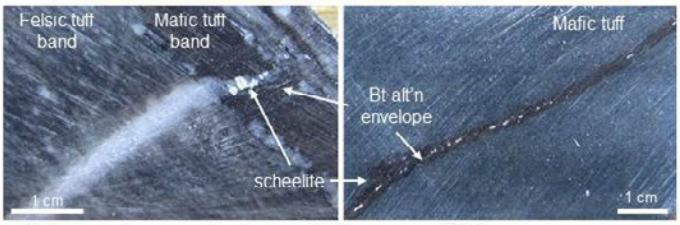

- Major control proposed by Nast and Williams-Jones (1991)
- See this W-matic (Ca) relationship at many scales at Sisson

Reactions involving Ti-bearing minerals

Bustard (2013)

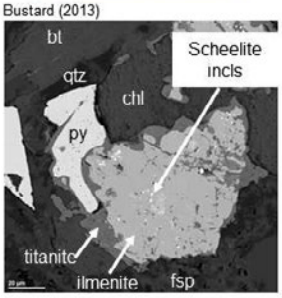

Simplified reactions:

Hbl + Plag + Ti (aq) + $2HKWO_3$ = Bt + 2Scheelite + Ilmenite

&

Bt + Ilmenite + Ca + S = Titanite + Py + Chl

24

Methods for Exploration Through Glacial Cover

HDI NORTHCLIFF

- Potential tools for exploration through glacial cover at Sisson:
  - Soil gas hydrocarbon analysis (proprietary method of Actlabs)
  - Geochemical patterns of W and other metals in basal tills
  - Heavy indicator minerals, such as scheelite, in basal tills

25

Exploration – Soil Gas Hydrocarbon (SGH) Surveys

HDI NORTHCLIFF

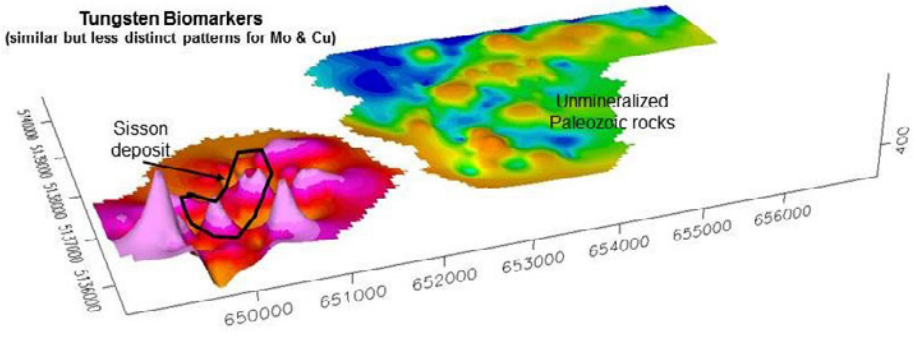

- Soil gas hydrocarbon analysis (proprietary method from Actlabs)
- Based on groups of hydrocarbons (biomarkers) released by dying microbes which had interacted with ore minerals at depth
- Used basic soil sampling methods
- In a blind study SGH successfully highlighted Sisson using W, Mo & Cu biomarkers
- SGH also recognized internal metal zoning between W, Mo & Cu

26

Basal Till – Geochemistry & Heavy Indicator Minerals

HDI NORTHCLIFF

Scheelite Grain Counts

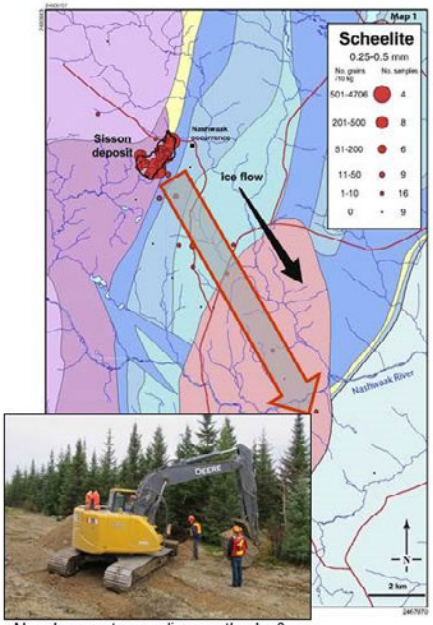

Need correct sampling methods & QA/QC control – can be expensive

W by Borate Fusion ICP-MS on <0.063 mm Size Fraction (Similar for Sn, Mo, Cu, Bi, As, Zn & Ag)

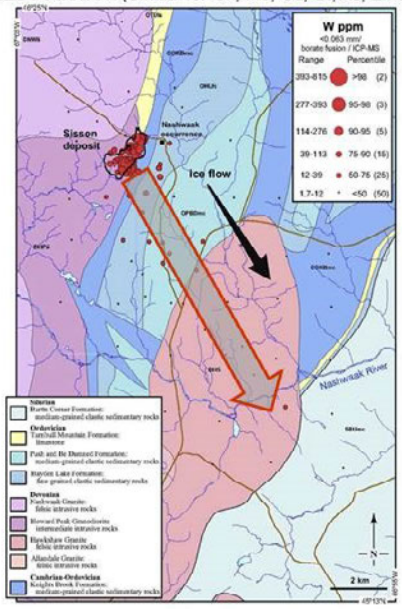

Maps from McClenaghan et al. (2013 & 2014; **TGI-4**)

27

Key Points

HDI NORTHCLIFF

- Sisson is a very large, intrusion-related, structurally-controlled, bulk-tonnage W-Mo deposit.
- Mineralization occurs in a sheeted vein array controlled by larger, well-mineralized, sinistral shear zones active in the Late Devonian.
- The fracture network focused upflow of fluids from an underlying felsic intrusion represented within the deposit by granitic dykes.
- Intrusions associated with min'l were plausibly Late Devonian, marginal phases of the nearby Nashwaak Granite batholith.
- Geochemical and heavy indicator mineral surveys in basal till are excellent regional exploration tools.
- Soil gas hydrocarbon surveys may further focus local exploration.

28

Petrologic and geochemical examination of the Early Devonian, Evandale porphyry Cu-Mo-(Au) deposit, southern New Brunswick: Geothermobarometric analysis of petrogenesis

T. White, D.R. Lentz and C.R.M. McFarlane

University of New Brunswick, Fredericton, New Brunswick

Abstract: Porphyry Cu-Mo-(Au) systems associated with the granitoid rocks in eastern North American orogenic belts have been researched using current deposit models; however, relatively few studies have examined the potential for late stage fine-grained porphyritic to aplitic intrusive phases being host to mineralization. The Evandale Granodiorite is an example of a well- preserved Mid-Devonian (U-Pb zircon age of 391.2 ± 3.2 Ma for the coarser granitoid, and 390.2 ± 1.6 Ma for the aplite) polyphase pluton intruding through deformed Silurian sedimentary and mafic volcanic rocks of the Mascarene Basin in southern New Brunswick. The two intrusive phases have been identified as I type granites with a minor sedimentary component. The pluton is separated both petrochemically and texturally into two distinct phases. The coarser phase ranges from medium- to coarse-grained seriate to porphyritic granodiorite to monzogranite and the later finer stage layered aplite ranges from a monzogranite to syeno-granite. INAA analysis of each phase found that the highest concentrations of Cu and Au (108 ppm Cu, and 33 ppb Au) are associated with pyrite, chalcopyrite, and arsenopyrite within the aplitic dykes sampled, whereas concentrations of up to 6 ppm Mo were detected within the c.g. granite. Current models suggest that the transport of metals (particularly Cu and Au) are sourced from secondary two-phase fluids at shallow depths (approximately 2 kb), and is controlled primarily by Cl fugacity of the magma. Analyses of biotite phenocrysts from both the aplite and granite contain an average of 0.21 wt% Cl, which is similar to other high grade Cu-Mo-(Au) porphyry deposits. Average zircon saturation temperatures were calculated to be 818°C for the aplite and 787°C for the granitoid. Average apatite saturation temperatures were found to be 880°C for the aplite and 934°C for the granitoid phase. Hornblende-plagioclase thermometry revealed the crystallization temperature of the granite to be 642°C and 600°C for the aplite, cooler than most deposits of the same type. Al in hornblende geobarometery indicates crystallization depths of ~2.1 kb for hornblende in the aplite and ~0.7 kb for the c.g. granite. The aplitic dykes were subject to higher crystallization pressures and lower crystallization temperatures suggesting that their formation may either be a result of pressure quenching of the melt during rapid ascent or by the sub-solidus recrystallization of the melt as pyroclastic flows.

Originally presented Fredericton 2014: Geological Association of Canada - Mineralogical Association of Canada Joint Annual Meeting, Special Session 3: Discovering the Next Generation of Porphyry Deposits: Advancements in Locating and Understanding Hidden Intrusion-related Mineralization. May 21, 2014.

Corresponding author: Travis White (Travis.White@unb.ca)

White, T., Lentz, D.R., and McFarlane, C.R.M., 2015. Petrologic and geochemical examination of the Early Devonian, Evandale porphyry Cu-Mo-(Au) deposit, southern New Brunswick: Geothermobarometric analysis of petrogenesis; *in* TGI 4 – Intrusion Related Mineralisation Project: New Vectors to Buried Porphyry-Style Mineralisation, (ed.) N. Rogers; Geological Survey of Canada, Open File 7843, p. 343-360.

The Early Devonian, Evandale Porphyry Cu-Mo-(Au) Deposit, Southern New Brunswick

Petrologic, Geochemical, Geothermobarometric, and Geochronologic Characterization of the Host Rocks and its Origin

By: Travis White
Supervised by: Dr. David Lentz

Outline

- Current Model
- Evandale Introduction
- Geochronology
- Geochemistry
- Mineral Saturation Temperatures
- Geothermometry
- Geobarometry
- Conclusion

The Porphyry Copper Model

- Porphyry copper deposits mostly contain copper, with minor amounts of molybdenum and gold
- Porphyry stocks are usually between 0.1 to 1 km in diameter (John, *et al.,* 2010; Sillitoe, 2010)
- Stocks normally crystalize at depths of 2-5 km
- Hypogene ore zones can reach up to 1.5 km depth, with supergene ore at <300 m (John, *et al.,* 2010)

The Porphyry Copper Model

- Linked to the evolution of magmatic arcs along convergent plate margins (John, *et. al.,* 2010)

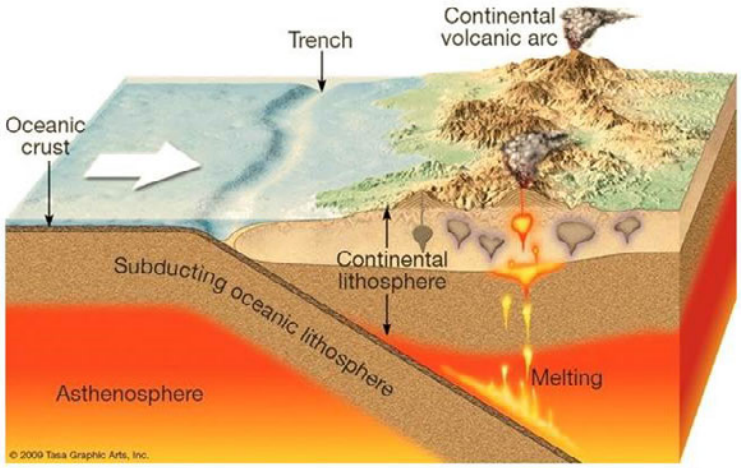

Fig. 01: Diagram of a Convergent Margin (http://tasaclips.com/illustrations.html)

The Porphyry Copper Model

- Crystallization progresses inwards, increasing volatile pressures and fracturing the surrounding rock (Sillitoe, 2010)

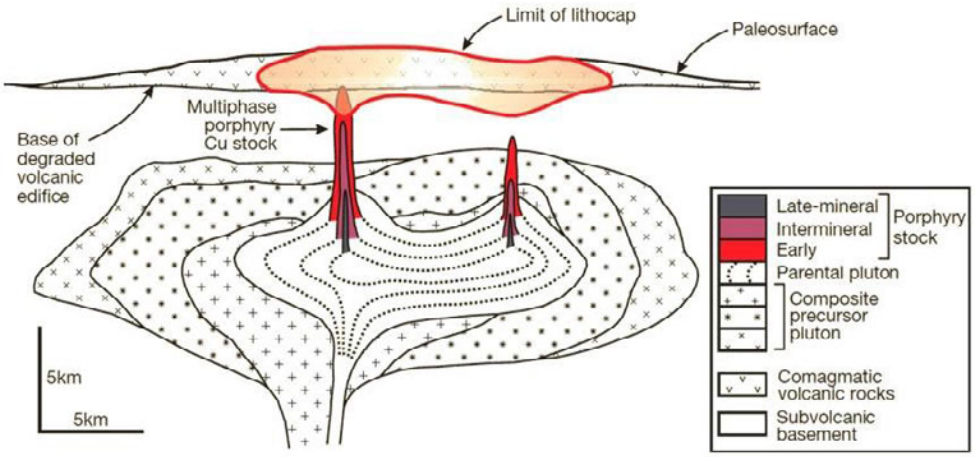

Fig. 02: Conceptual model of a porphyry stocks, in relation to the underlying pluton (Sillitoe, 2010).

The Porphyry Copper Model

- Escaping Fluids move outward from the stock cooling to about 350°C start precipitating metals
  - Cu+Mo → Zn+Pb with Au occurring throughout
- Fluid escape occurs in multiple phases and each phase typically decreases in grade (John, *et. al.,* 2010)
  - Early Porphyries (most mineralization)
  - Intermineral porphyries (less mineralized)
  - Late mineral porphyries (typically barren)
- Typical low grade ore is between 0.5-1.5% Cu, <0.04% Mo, and <1.5g/t Au (Sillitoe, 2010)

The Porphyry Copper Model

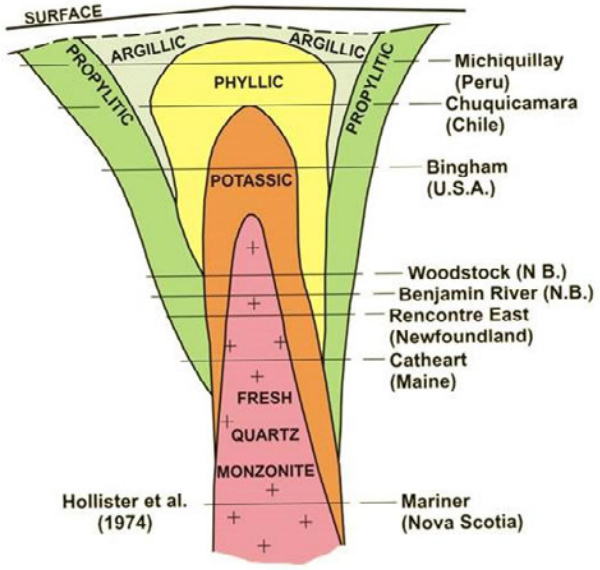

Fig. 03: Conceptual model of a porphyry stock, with examples of current exposure levels (Hollister et al., 1974).

Intro to Evandale

- The Evandale Porphyry Cu-Mo-(Au) deposit is located 30km North of Saint John
- 2.5 km diameter cylindrical stock granite stock intruding through deformed Silurian aged sedimentary and mafic-volcanic rocks
- A 60m greenschist grade contact aureole surrounds the stock
- Mineralization occurs as:
  - Gold bearing quartz veinlets (NW trending)
  - Phenocrysts of chalcopyrite and pyrite within both the coarser granite and the aplite phase of the deposit

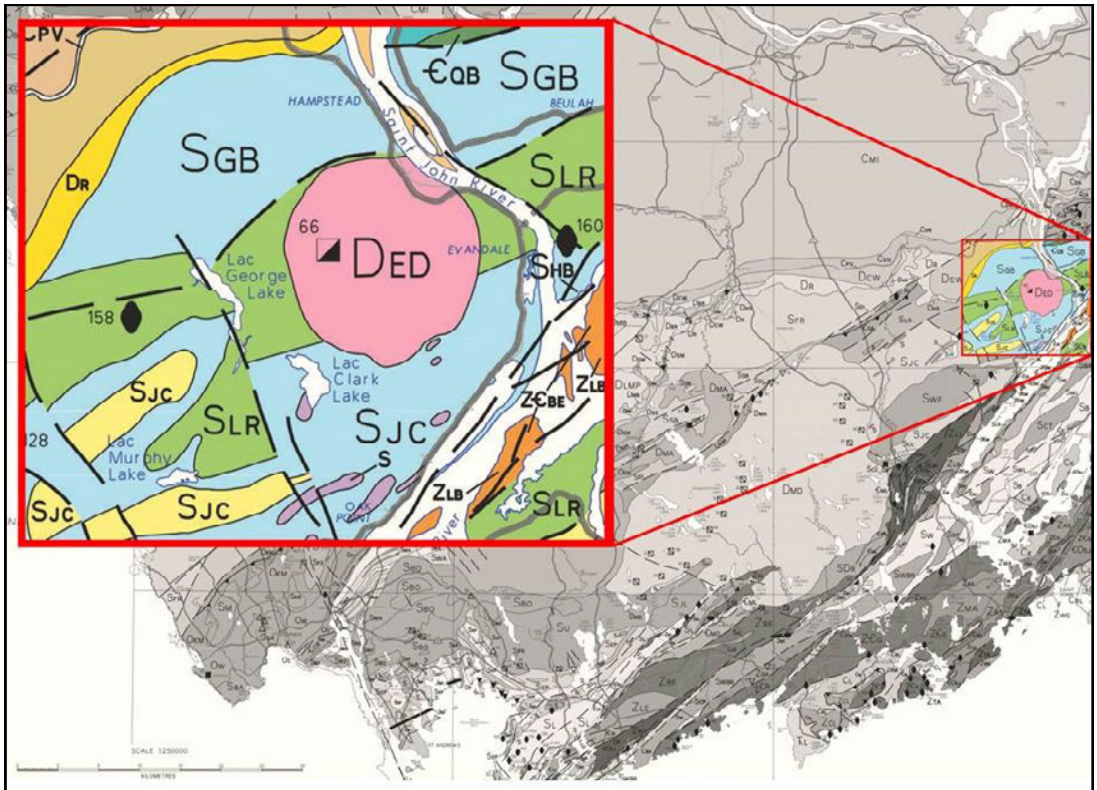

Fig. 04: Surficial Geology Map of New Brunswick with claim area modified from DNR-5.

Previous Exploration

- Discovered in 1967 by Rio Tinto Canadian Exploration Limited
- 1979 a 13 hole diamond drilling program totaling 1619 m
  - Best intersection was 0.7ft containing 14.7ppm Au, 293.8ppm Ag, 2.41% Cu, 6.67% Zn, 0.07% Mo, 0.02% WO3
- 1989 a total field magnetic survey, very low frequency electro-magnetic survey, and a gravity survey
  - Four conductive areas were defined, exploration continued but did not return any promising results
- All exploration programs concluded that the mineralization was not great enough to be considered economic

Petrology

- Samples were collected from drill core and grab samples from out crop
  - 15 thin sections were prepared
    - 12 from the diamond drill core
    - 3 from a rock quarry in the northern region of the deposit
- Examination of thin sections shows there are two primary intrusive phases based on texture
  - The seriate to porphyritic medium grained hbl-bt granite; and
  - The equigranular to porphyritic aplite

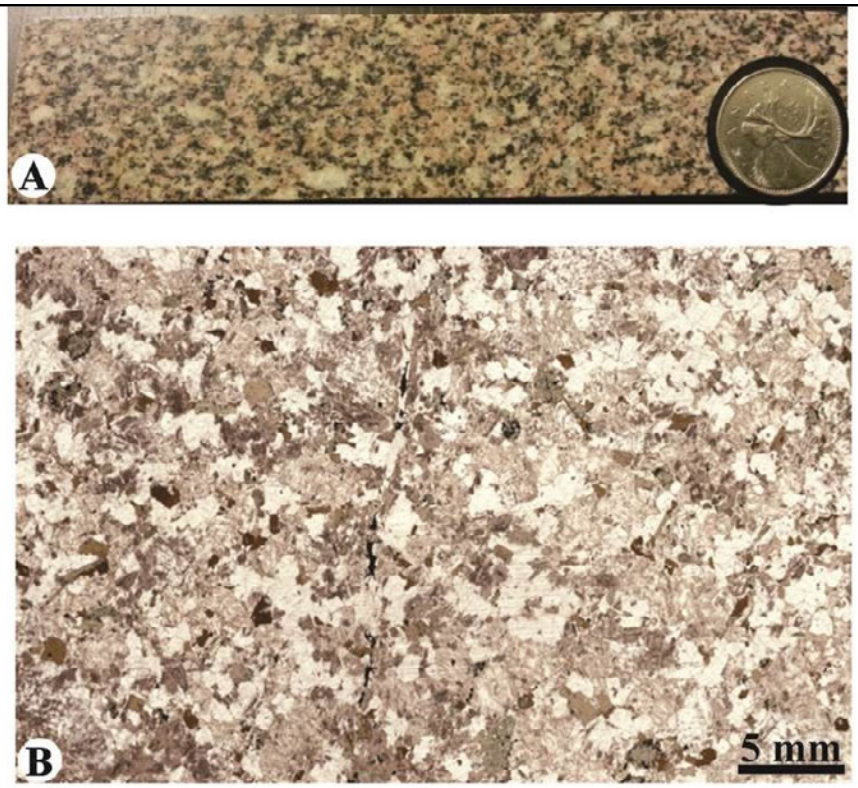

Fig. 05: Sample CB06 Polished slab (A) and respective thin section scan (B) of the seriate granite phase, at the Evandale stock.

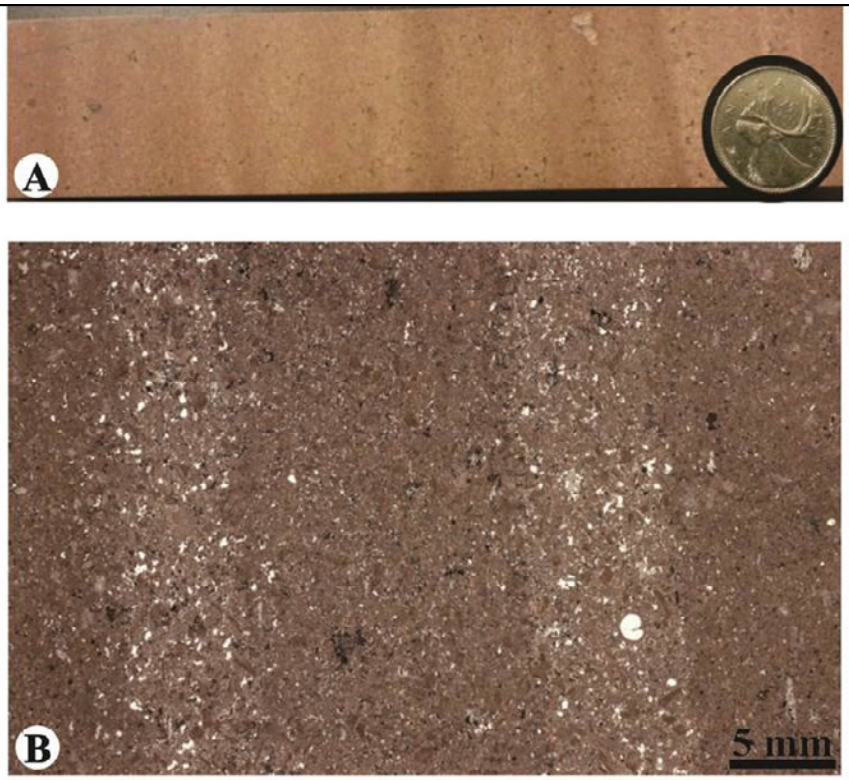

Fig. 06: Sample CB08 Polished slab (C) and respective thin section scan (D) of the fine grained aplite phase, at the Evandale stock.

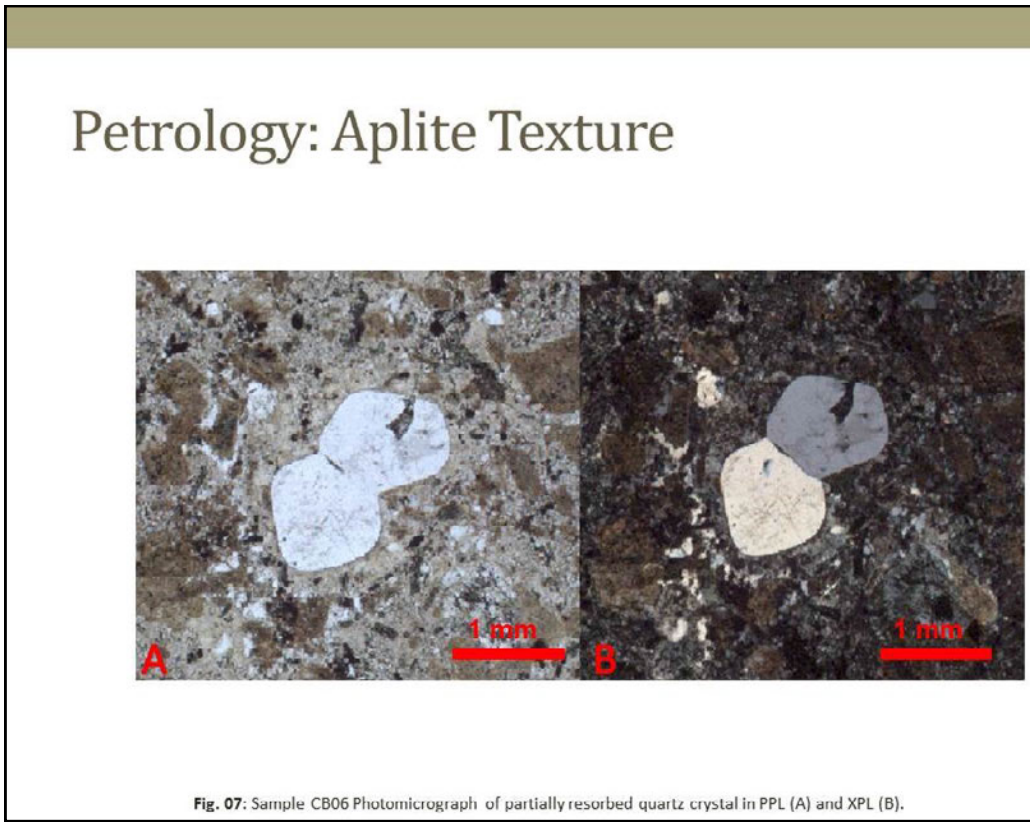

Fig. 07: Sample CB06 Photomicrograph of partially resorbed quartz crystal in PPL (A) and XPL (B).

Petrology: Mineralization

- Chalcopyrite mineralization occurs in both the granitic and aplitic phases
  - Within the granite it usually occurs as fracture fills, with associated hydrous iron oxides
  - Within the aplite it occurs typically as up to 5 mm phenocrysts
- Sulfide mineralization becomes pyrite dominated at shallower depths

Petrology: Chalcopyrite

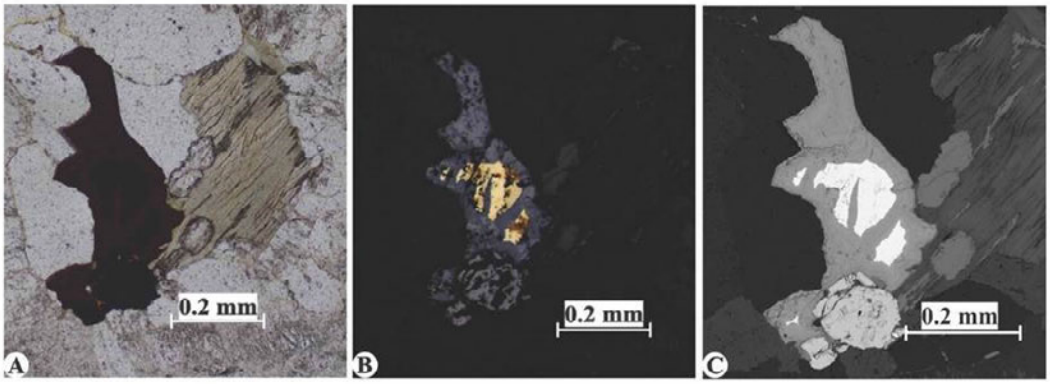

Fig. 08: Photomicrograph of a chalcopyrite grain (35.5% Cu) enveloped by a hydrous iron phase (14.65% Cu), from sample CB03 (granite phase). (A) Image taken in PPL. (B) Image taken in reflected light (RL). (C) Backscatter electron Image taken on scanning electron microscope (SEM).

Geochronology

- U-Pb dating of zircons using Laser Ablation Inductively Coupled Plasma-Mass Spectrometry (LA ICP-MS)
- Two representative samples from each textural phase, covering a total of 16 grains
- Two distinct ages were found:
  - 391.2 ±3.2 Ma for the granite (CB02 & CB03); and
  - 390.2 ±1.6 Ma for the aplite (CB12 & CB15)

Geochronology: Granite

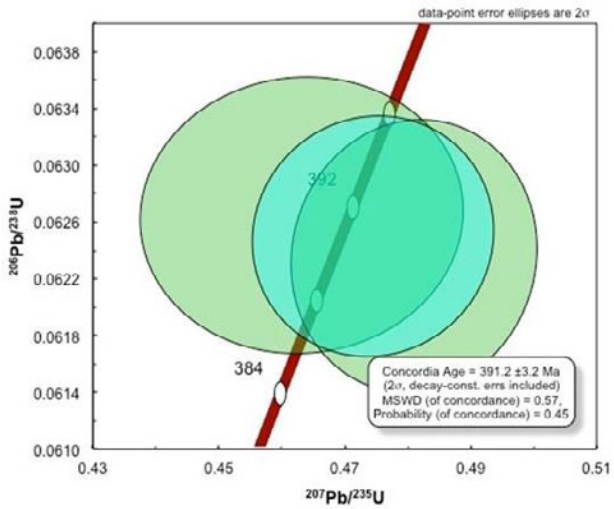

Fig. 09: Concordia diagram for samples CB02 and CB03, age is concordant, all samples plotted along the Concordia line suggesting a zircons within this system cogenetic.

Geochronology: Aplite

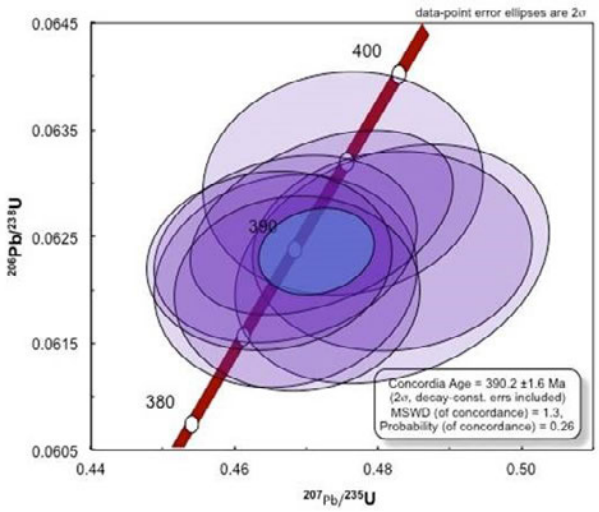

Fig. 10: Concordia diagram for samples CB12 and CB15, age is concordant, all samples plotted along the Concordia line suggesting a zircons within this system cogenetic.

Geochemsitry

- 15 samples were crushed to 200-mesh at UNB and prepared for the each analytical method used
- Analyses Conducted:
  - X-Ray Fluorescence (Memorial University)
  - Instrumental Neutron Activation Analysis (Actlabs)
  - Inductively Coupled Plasma – Mass Spectrometry (Actlabs)

QAP Classification

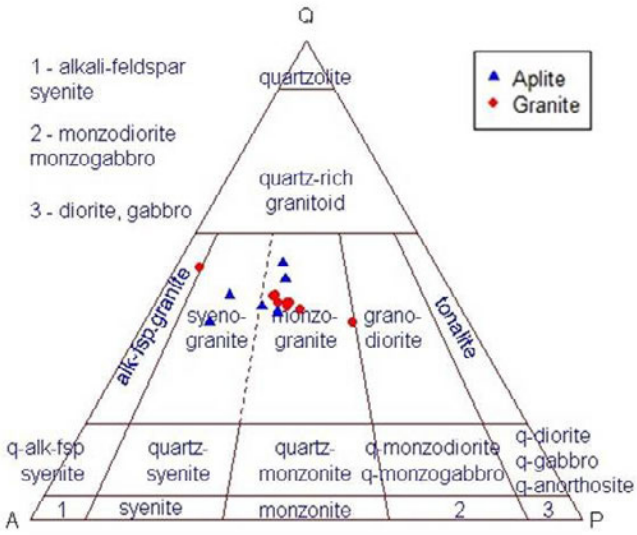

Fig. 11: QAP diagram by Streckeisen (1974), with samples norms calculated from XRF whole rock analyses. Diagram created using GCDkit, version 3.0 (Janoušek *et al.* 2006).

Classification: Fe-Number

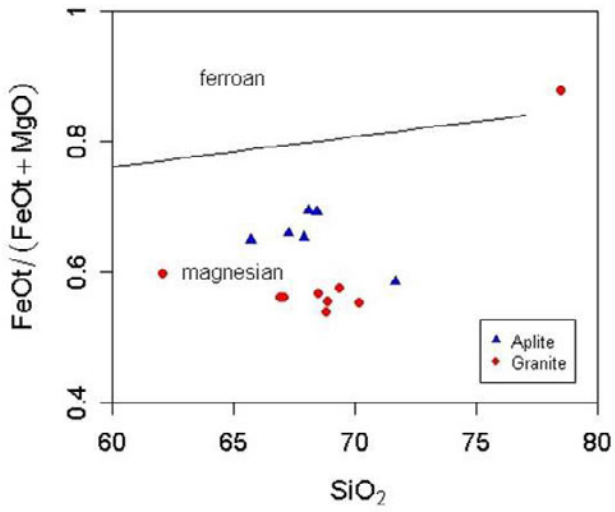

Fig. 12: (FeO/FeO+MgO) versus SiO2 (wt. %) discrimination diagram from Frost et al. (2001). This diagram describes the differentiation history and is used to distinguish between granitoids from different tectonic environments. Created using GCDkit, version 3.0 (Janoušek et al. 2006).

Classification: MALI

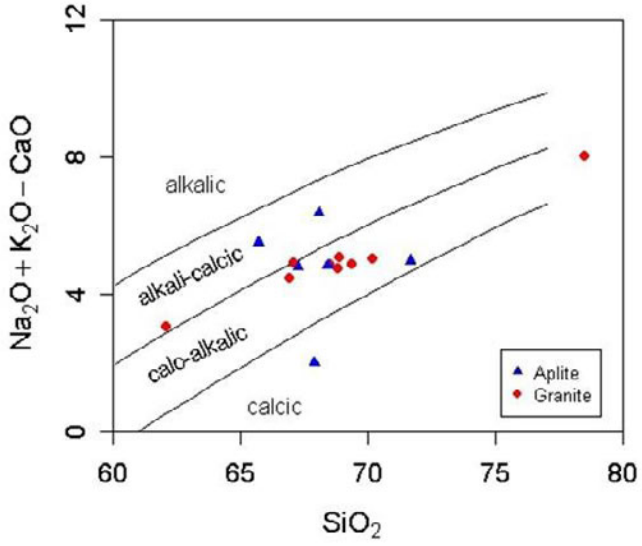

Fig. 13: The Modified Alkali Lime Index (MALI) diagram (Na2O + K20 – CaO versus SiO2) from Frost (2001). Created using GCDkit, version 3.0 (Janoušek et al. 2006).

Classification: ASI

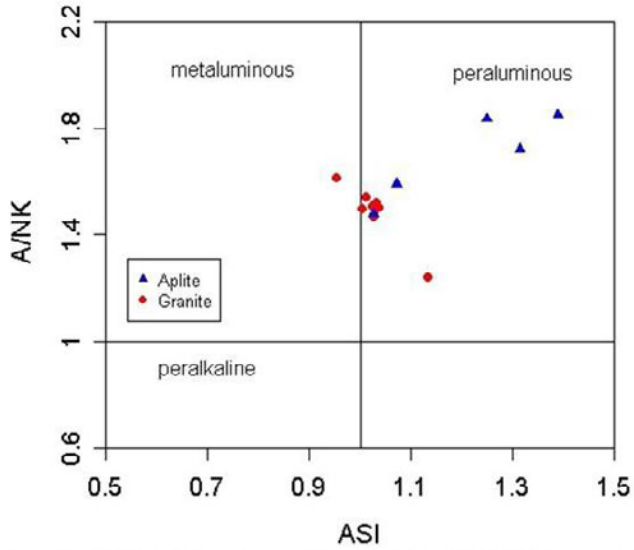

Fig. 14: ASI versus A/NK. Where ASI = [Al/(Ca-1.61P+Na+K)] , and A/NK = [Al_2O_3/(Na_2O+K_2O)]. This diagram identifies whether the rock is metaluminous, peraluminous or peralkaline. Calculations and plot created using GCDkit, version 3.0 (Janoušek *et al.* 2006).

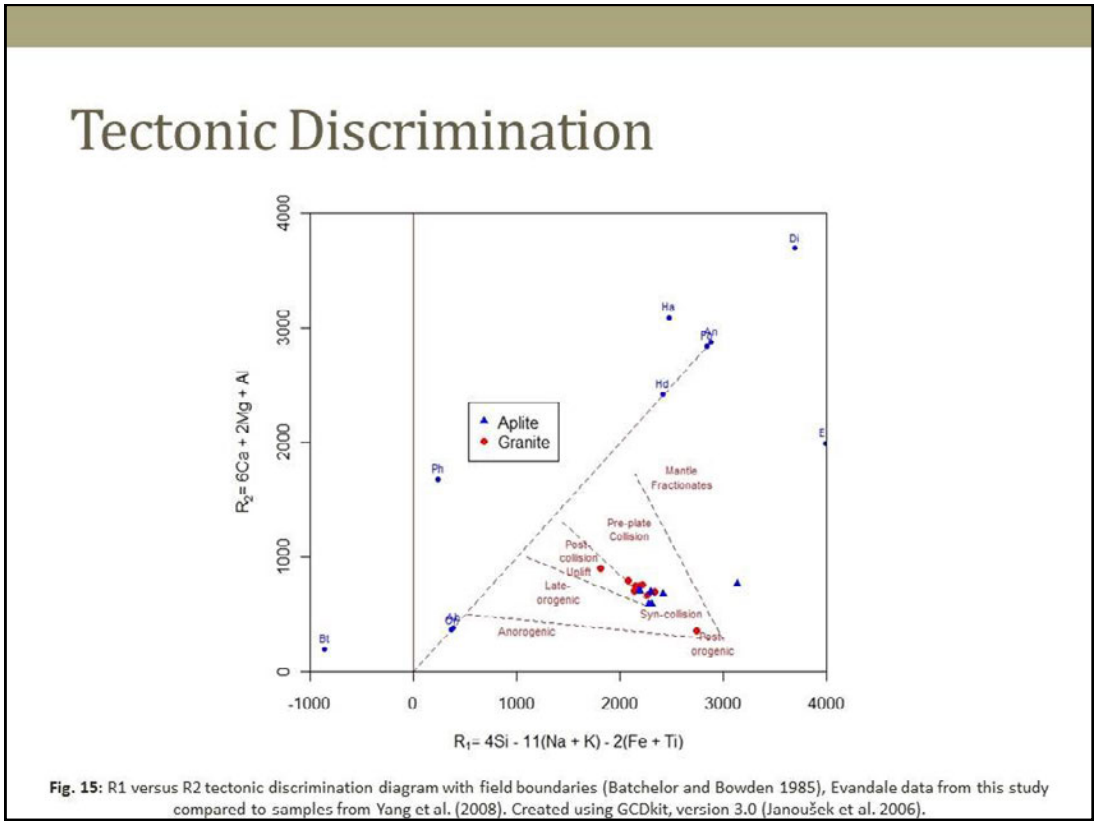

Fig. 15: R1 versus R2 tectonic discrimination diagram with field boundaries (Batchelor and Bowden 1985), Evandale data from this study compared to samples from Yang et al. (2008). Created using GCDkit, version 3.0 (Janoušek et al. 2006).

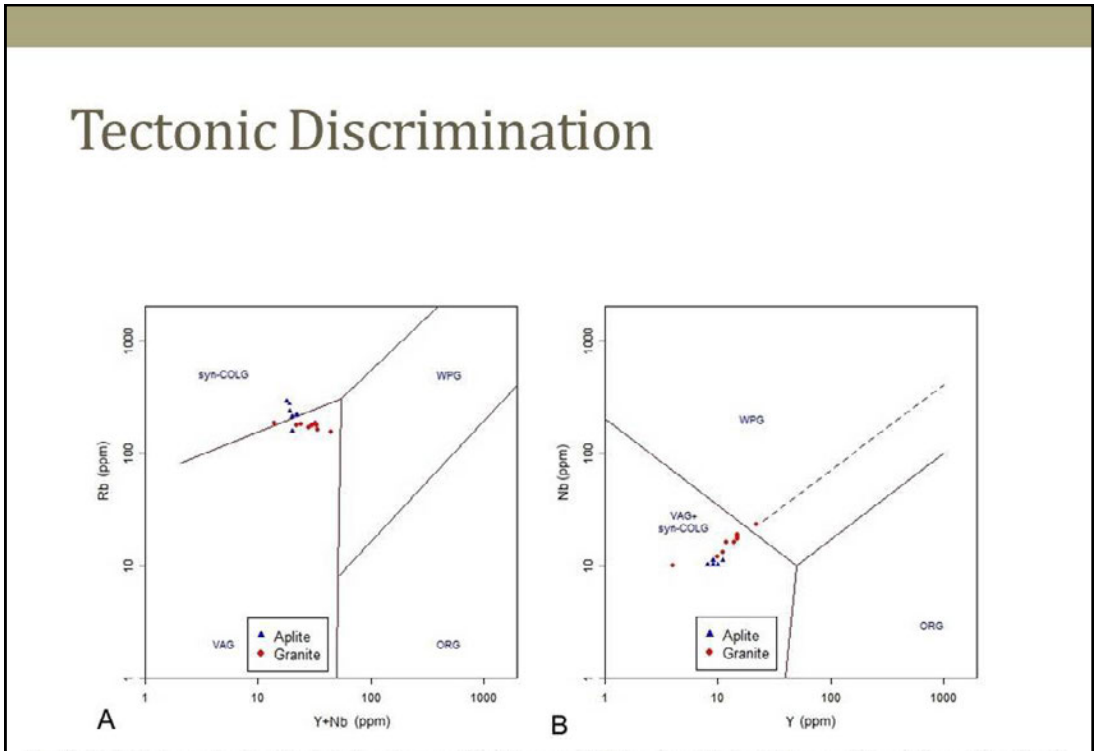

Fig. 16: Geotectonic geochemical discrimination diagrams: (Top) Rb versus Y+Nb (ppm), and (bottom) Nb versus Y (ppm). Ocean Ridge Granite (ORG); Within Plate Granite (WPG); Volcanic Arc Granite (VAG); and Syn- and Post-collision Granite (syn-COLG and post-COLG). Field boundaries are from Pearce et al. (1984). Created in GCDkit (Janoušek et al. 2006).

Zircon & Apatite Saturation

- Calculated used the model from Watson and Harrison (1984)
- Zircon saturation temperatures:
  - 787°C for the granite
  - 818°C for the aplite
- Apatite saturation temperatures:
  - 880°C for the granite
  - 934°C for the aplite

Geothermometry

- Hbl-Pl thermometer developed by Blundy and Holland (1990)
- Electron Microprobe Analyses of hornblende
  - Total of 54 spot measurements over 18 grains

$$T = \frac{0.677P[\text{kb}] - 48.98}{-0.0429 - 0.008314 \ln\left\{\left(\frac{\text{Si}-4}{8-\text{Si}}\right) X_{\text{Ab}}^{\text{Pl}}\right\}}$$

Equation 1: Si = atoms per formula unit (a.f.u.), X(pl/ab) = mole fraction of albite in plagioclase.

Geothermometry

- Previous calculations found combined average temperatures of:
  - 617 degrees Celsius (Yang, 2005)
  - 648 degrees Celsius (Godbout, 1997)
- Results from this study, average for each phase:
  - 642°C for the granite
  - 600°C for the aplite

Geobarometry

- Al in Hbl geobarometry is done using the methods from Anderson and Smith (1995)
- Previous results from Yang and Lentz (2005):
  - 0.6 kbar (60 MPa) for the granite
  - 1.5 kbar (150 MPa) for the aplite
- Present Study:
  - 0.7 kbar (70 MPa) for the granite
  - 2.1 kbar (210 MPa) for the aplite

Conclusion

- Textures and banding within the aplite suggest it may have formed as pyroclastic flows.
- Geochronology indicates both the granite pluton and the aplite are cogenetic forming after the Taconic Orogeny.
- Evandale pluton formed in a post collisional tectonic setting, predominantly I type with a moderate sedimentary component.
- Crystallization temperatures and pressures, volatile concentrations in the melt (Yang and Lentz, 2005) are similar to that of many other porphyry Cu forming systems.

Acknowledgements

- Dr. Chris McFarlane for assistance with U-Pb zircon data;
- NB Department of Energy and Mines for funding and support; and
- Dr. David Lentz for funding, and the continued support to make this project possible.

References

- Burton, D. M. (1989). Report of Geophysical Surveys, Evandale Option, NovaGold Resources Inc. *NB Assessment Report , 473643*.
- Fournier, R. O. (1999). Hydrothermal processes related to movement of fluid from plastic into brittle rock in the magmatic-epithermal environment. *Economic Geology , 94*, 1193-1211.
- Fyffe, L. R., Pajari, G. E., & Cherry, M. E. (1981). The Acadian Plutonic Rocks of New Brunswick. *Maritime Sediments and Atlantic Geology , 17*, 23-36.
- Giggie, K. V. (1991). Report of Drilling and Trenching, Evandale Option, NovaGold Resources Inc. *NB Assessment Report , 473996*.
- Govett, G. J., & Atherden, P. R. (1988). Applications of Rock Geochemistry to Productive plutons and Volcanic Sequences. *Journal of Geochemical Exploration , 30*, 223-242.
- Harris, N. (1996). Radiogenic isotopes and the interpretation of granitic rocks. *Episodes , 19* (4), 107-113.
- Meinert, L. D., Hedenquist, J. W., Satoh, H., & Matsuhisa, Y. (2003). Formation of anhydrous an dhydrous skarn in Cu-Au ore deposits by magmatic fluids. *Economic Geology , 98*, 147-156.
- Meinert, L. D., Hefton, K. K., Mayes, D., & Tasiran, I. (1997). Geology, zonation, and fluid evolution of the Big Gossan Cu-Au skarn deposit, Ertsberg district, Irian Jaya. *Economic Geology , 92*, 509-534.
- Ossandón, G., Fréraut, R., Gustafson, L. B., Lindsay, D. D., & Zentilli, M. (2001). Geology of the Chuquicamata mine: A progress report. *Economic Geology , 96*, 249-270.
- Shewman, R. (1968). Geological Report on the Evandale Stock. *NB Assessment Report , 470171*.
- Sillitoe, R. H. (2010). Porphry Copper Systems. *Society of Economic Geologists , 105*, 3-41.
- Taylor, W. R. (1979). Report on Diamond Drilling, Evandale Project, Dome Exploration Ltd. *NB Assessment Report , 472550*.
- Whalen, J., Jenner, G., Longstaffe, F., & Hegner, E. (1996). Nature and Evolution of the Eastern Margin of Lapetus: Geochemical and Isotopic Constraints from Siluro-Devonian granitoid plutons in the New Brunswick Appalachians. *Canadian Journal of Earth Sciences , 33*, 140-155.

Fluid inclusion and stable isotope evidence for mixing of magmatic – hydrothermal fluids with meteoric water in vein-type Cu-Au-Bi deposits, southern New Brunswick, Canada

J.J. Hanley[1], F. Tweedale[1], K. Neyedley[1], R. Sharpe[2] and M. Fayek[2]

1. Department of Geology, Saint Mary's University, 923 Robie Street, Halifax, Nova Scotia

2. Department of Geological Sciences, University of Manitoba, 125 Dysart Road, Winnipeg, Manitoba

Abstract: Vein-type Cu-Au-Ag-Bi mineralization in the Caledonian Highlands, southern NB, Canada, is hosted within quartz-carbonate-rich shear zones cutting felsic lithic tuffs, intermediate intrusives and interbedded felsic and mafic flows of the Neoproterozoic Broad River Group. Mineralization in the veins consists of bornite-chalcocite-hematite, coprecipitated with electrum and bismuthinite; ore minerals post-date quartz and REE-rich carbonates in the veins, with later supergene oxidation and hydration of the ores to cuprite-malachite. Wall-rock alteration is characterized by albitization and paragonitization. Replacement of bornite by chalcocite- hematite indicates changes in fluid redox with mineralization progression.

Trails of secondary fluid inclusions in the quartz veins are two-phase liquid-vapour at room temperature. Homogenization occurs by vapour bubble disappearance between 150-270°C for all assemblages; individual assemblages show relatively narrow ranges (e.g., 173-191°C, n=22). Bulk salinities from final ice melting range from 4 to 13 wt% NaCl eq. with individual assemblages showing similarly narrow ranges.

Stable isotope data (bulk separates, and in-situ by secondary ion mass spectrometry [SIMS]) for vein-stage quartz ($\delta^{18}O_{bulk}$ = 13.7-15.1‰; $\delta^{18}O_{SIMS\text{-}qtz}$ = 10.8±1.5‰, 1ζ, n=32) and carbonate ($\delta^{13}C_{bulk}$ = -4.4 to -4.6 ‰) combined with microthermometric data rule out unmodified, heated seawater and meteoric water as the dominant fluid components, and suggest that the metal-bearing fluids were magmatic in origin or represented saline formation waters modified through fluid-rock interaction with the host volcanic rocks (calculated $\delta^{18}O_{fluid}$ ~ 6-7 ‰). However, significant variations in $\delta^{18}O_{SIMS\text{-}qtz}$ are observed within single quartz crystals across growth zones and in massive quartz texturally predating sulfides and gold (from as low as 8.2 ‰ to 14.8 ‰ in quartz enclosed entirely within bornite-chalcocite). This indicates either (i) localized mixing of the metal-bearing fluid with low latitude meteoric water (calculated $\delta^{18}O$ = -1.0 to 0 ‰), or (ii) fluctuations in fluid temperature during vein formation, with the lowest T portions of the vein associated with base metal-gold precipitation, or (iii) both. The isotopic composition of coeval quartz-carbonate predict a crystallization/final equilibration T of vein-stage at ~250- 270°C; if inclusions are primary, then a maximum $P_{trapping}$ = ~1.5 kbar, based on the lowest T assemblages, is estimated.

Significant fluctuations in fO_2, fluid temperature or fluid composition during vein precipitation highlight the importance of fluid mixing for mineralization. These characteristics, combined with the style of mineralization, link these deposits in NB genetically to much larger vein Cu deposits worldwide (e.g., Churchill, Davis-Keays, and Mamainse Point, Canada; Inyati, Zimbabwe; Copper Hills, Australia; Messina, South Africa; Cornwall, UK).

Originally presented Fredericton 2014: Geological Association of Canada - Mineralogical Association of Canada Joint Annual Meeting, Special Session 3: Discovering the Next Generation of Porphyry Deposits: Advancements in Locating and Understanding Hidden Intrusion-related Mineralization. May 21, 2014.

Corresponding author: Jacob J. Hanley (jacob.hanley@smu.ca)

Hanley, J.J., Tweedale, F., Neyedley, K., Sharpe, R., and Fayek, M., 2015. Fluid inclusion and stable isotope evidence for mixing of magmatic – hydrothermal fluids with meteoric water in vein-type Cu-Au-Bi deposits, southern New Brunswick, Canada; *in* TGI 4 – Intrusion Related Mineralisation Project: New Vectors to Buried Porphyry-Style Mineralisation, (ed.) N. Rogers; Geological Survey of Canada, Open File 7843, p. 361-368.

Fluid inclusion and stable isotope evidence for mixing of magmatic-hydrothermal fluids with meteoric water in vein-type Cu-Au-Bi deposits, southern New Brunswick, Canada

Jacob Hanley, Fergus Tweedale, Kevin Neyedley
Dept. of Geology
Saint Mary's University, Halifax, Nova Scotia

Ryan Sharpe, Mostafa Fayek
Dept. of Geology
University of Manitoba, Winnipeg, Manitoba

SAINT MARY'S UNIVERSITY Since 1802
One University. One World. Yours.

MINERAL EXPLORATION & ORE FLUIDS LABORATORY

UNIVERSITY OF MANITOBA

Quartz-carbonate Cu-Au vein deposits in southern NB

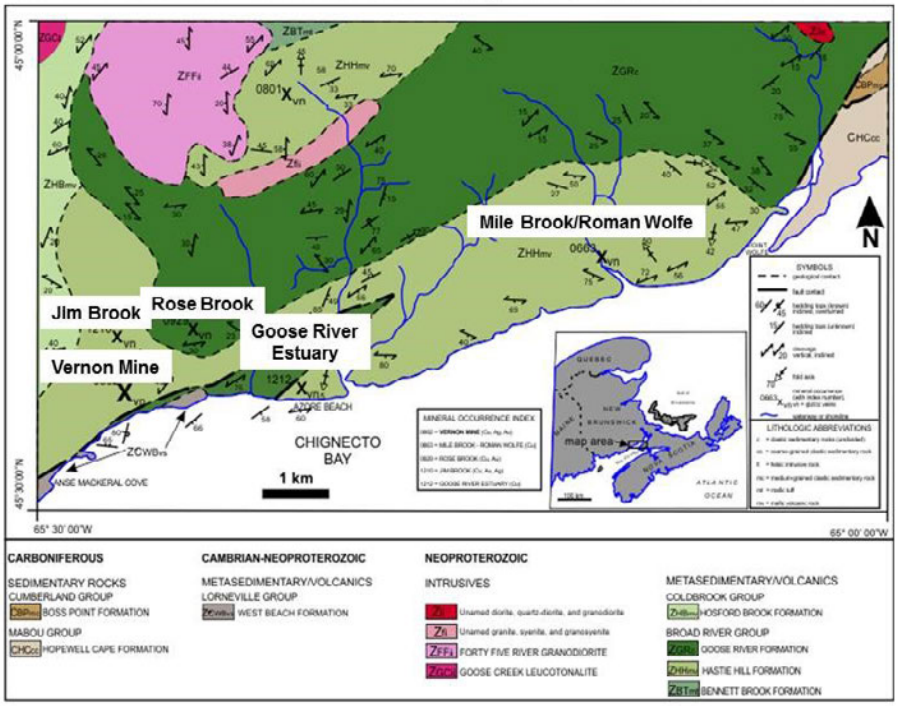

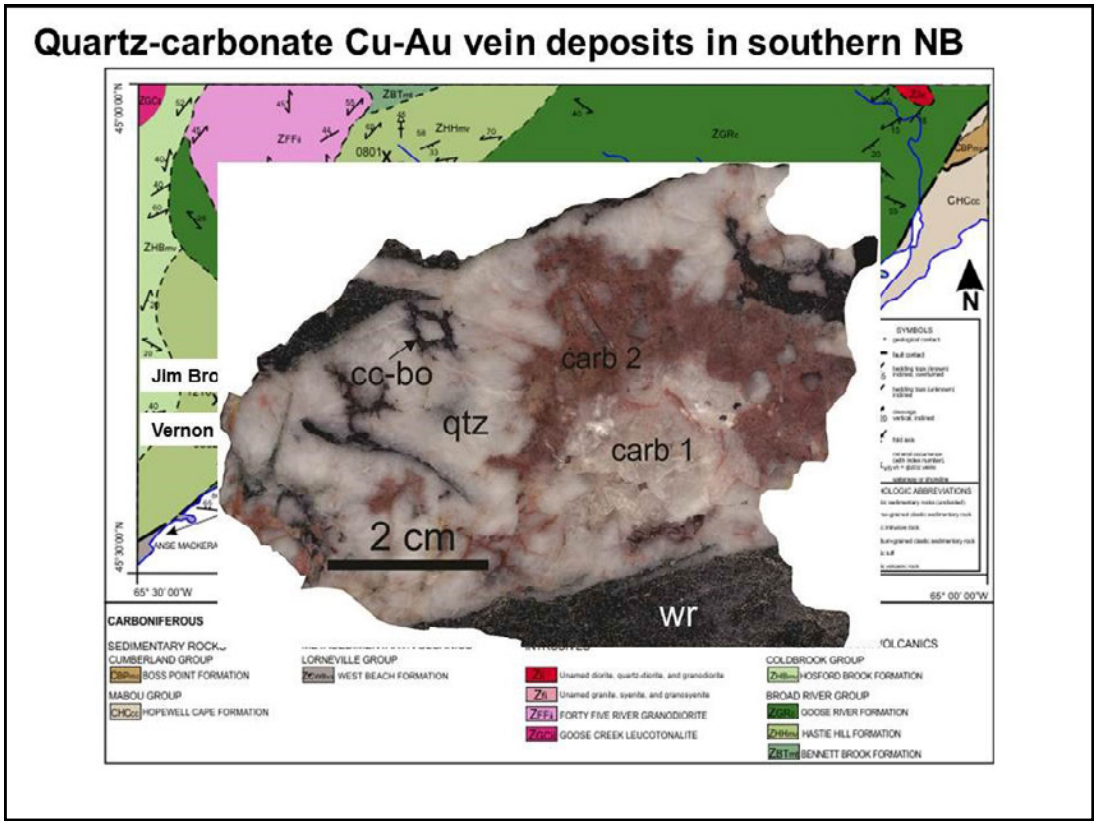
Quartz-carbonate Cu-Au vein deposits in southern NB
cc-bo
carb 2
qtz
carb 1
2 cm
wr
Jim Bro
Vernon
N
CARBONIFEROUS
SEDIMENTARY ROCK
CUMBERLAND GROUP
BOSS POINT FORMATION
MABOU GROUP
HOPEWELL CAPE FORMATION
LORNEVILLE GROUP
WEST BEACH FORMATION
COLDBROOK GROUP
HOSFORD BROOK FORMATION
BROAD RIVER GROUP
GOOSE RIVER FORMATION
HASTIE HILL FORMATION
BENNETT BROOK FORMATION
FORTY FIVE RIVER GRANODIORITE
GOOSE CREEK LEUCOTONALITE

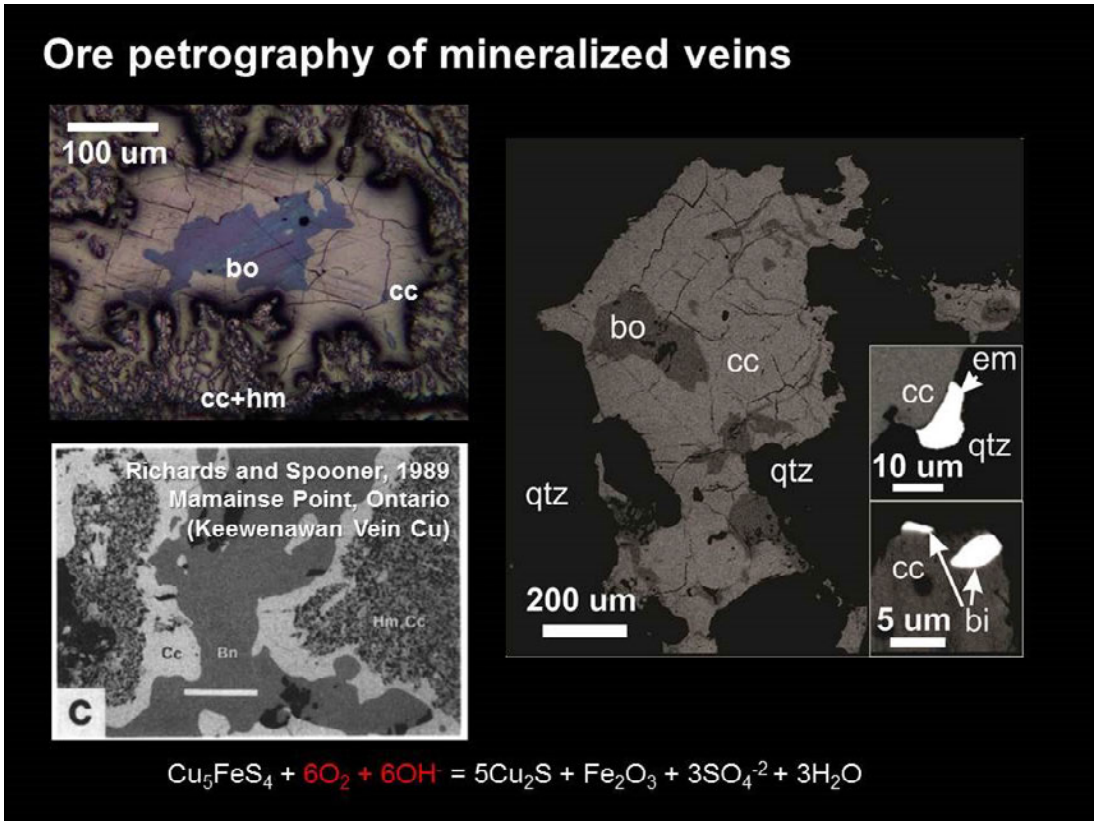
Ore petrography of mineralized veins
100 um
bo
cc
cc+hm
Richards and Spooner, 1989
Mamainse Point, Ontario
(Keewenawan Vein Cu)
Hm,Cc
Cc
Bn
C
bo
cc
qtz
qtz
200 um
em
cc
qtz
10 um
cc
bi
5 um
$Cu_5FeS_4 + 6O_2 + 6OH^- = 5Cu_2S + Fe_2O_3 + 3SO_4^{-2} + 3H_2O$

Fluid inclusion microthermometry

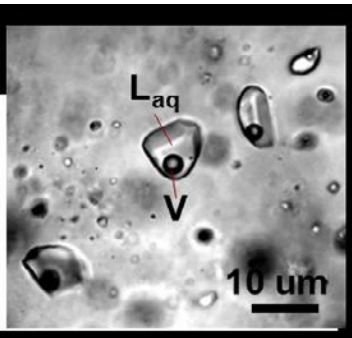

Inter-FIA variations in salinity and Th recognized but ambiguous correlations
Intra-FIA variations in salinity and Th can be large → post-entrapment modification due to oxidation/deformation or fluid P-T-X heterogeneity in single FIA ?

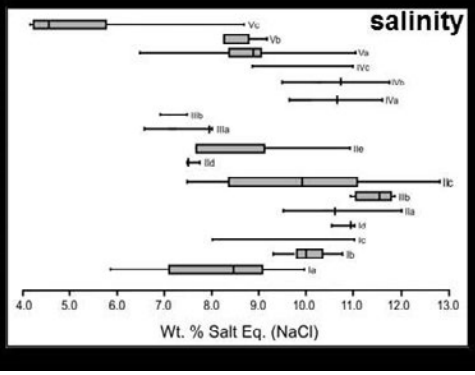

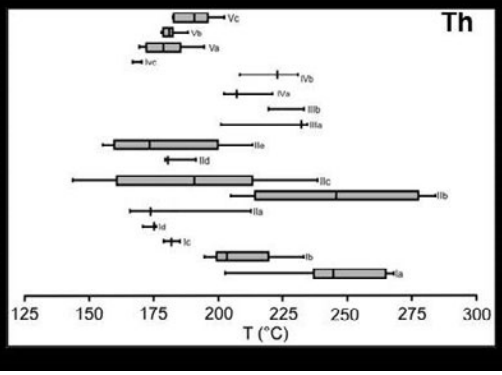

Stable isotopes

Quartz and carbonates
$\delta^{18}O_{bulk}$ = 13.7-15.1‰
$\delta^{13}C_{bulk}$ = -4.4 to -4.6‰
$T_{qtz\text{-}carb}$ ~ 250-270°C

Quartz
$\delta^{18}O_{SIMS}$ = 10.8±1.5‰, 1s, n=32

Variability from 8.2‰ to 16.8‰
→ growth zoning
→ in proximity to sulfides

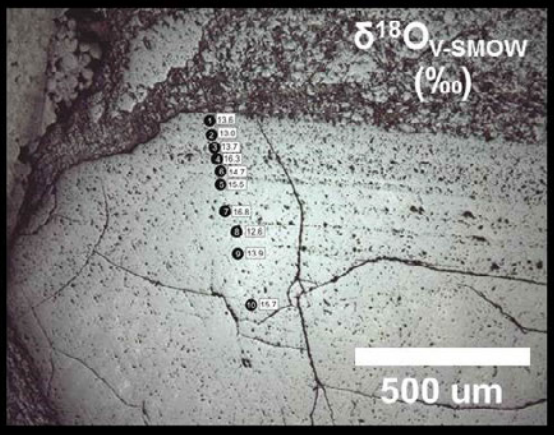

Two possible scenarios considered:

1. Localized mixing of the metal-bearing fluid ($\delta^{18}O$ = 6 to 7 ‰) representing a magmatic or metamorphic fluid with low latitude, formation water ($\delta^{18}O$ = -1 to 0‰), or formation water variably modified by interaction with mafic volcanics
2. Fluctuations in fluid temperature during vein formation, with the lowest T portions of the vein quartz associated with copper-gold precipitation from magmatic/metamorphic fluid or modified formation water

Stable isotopes

Quartz and carbonates

$\delta^{18}O_{bulk}$ = 13.7-15.1‰

$\delta^{13}C_{bulk}$ = -4.4 to -4.6‰

$T_{qtz\text{-}carb}$ ~ 250-270°C

Quartz

$\delta^{18}O_{SIMS}$ = 10.8±1.5‰, 1s, n=32

Variability from 8.2‰ to 16.8‰

→ growth zoning

→ in proximity to sulfides

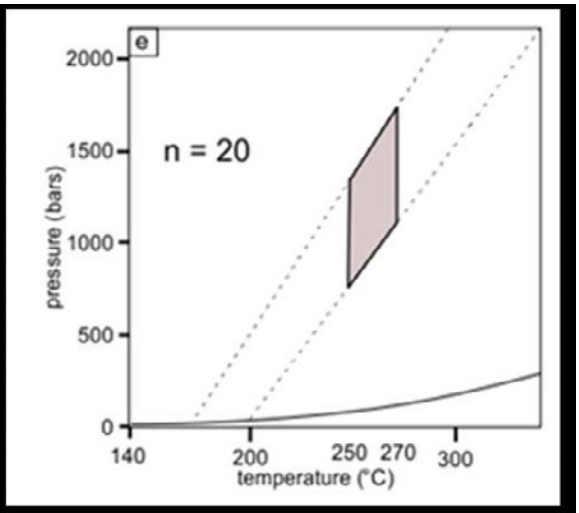

Two possible scenarios considered:

1. Localized mixing of the metal-bearing fluid ($\delta^{18}O$ = 6 to 7 ‰) representing a magmatic or metamorphic fluid with low latitude, formation water ($\delta^{18}O$ = -1 to 0‰), or formation water variably modified by interaction with mafic volcanics
2. Fluctuations in fluid temperature during vein formation, with the lowest T portions of the vein quartz associated with copper-gold precipitation from magmatic/metamorphic fluid or modified formation water

Comparison to other sediment and volcanic-associated Cu deposits

	Richards 1985	Morrison & Parry, 1986	Richards *et al.*, 1988	Anderson *et al*, 2004	Greyling *et al.*, 2005	Bradshaw, 2008	El Desouky *et al.*, 2009
Geographic location	Mamainse Point (Canada)	Paradox basin, (SW USA)	Central African copper belt (Zaire and northern Zambia)	SW Scottish Highlands	Zambian Copperbelt (Africa)		Katanga Copperbelt (Africa)
Deposit (or group) name	Coppercorp mine	Lisbon Valley anticline	Musoshi Minet	Argyll Group	Chambishi deposit		Kamoto and Luiswishi Mines
Deposit type	Fissure/vein-hosted	Fault-related anticline	Stratiform	Vein	stratiform		hypogene strataform
Deposit age	Mesoproterererozoic (Keweenawan)	Post-Laramide (Cretaceous - Eocene)	> 550 m.y.	Carboniferous			
Host rock type	Volcanic/sedimentary (intra-continental)	Sedimentary	Sedimentary (shale) (intracontinental)	Metavolcanic/ Metasedimentary			
Host-rock age	Meso-proterozooic	Permian	1.3 Ga – 602 Ma	Neoproterozoic			
Major ore minerals	Cc	Cc	Ccp, Bn	n/a			
Trace ore minerals	Cp, Py, Hm, Cu, Ag, Bn	Ccp, Cu, Dol Ba-Sr(SO_4), Cv, Dg, Ag	Py	Ccp, Py, Sp, Gn			
FI- bearing mineral	Qtz	Calcite and dolomite	Qtz	Qtz	quartz		quartz
Timing of deposit	Syngenetic	Epigenetic	Epigenetic	Epigenetic	late-diagenetic		early-diagenetic
Fluid compositon (wt.% $NaCl_{equiv}$)	0 – 20	5.0 – 13.4 (vein) 18.5 – 19.7 (veinlets)	39 (high-temp group)* 28 (low temp.)*	4.0 – 12.7	11.9 - 23.1		11.3 - 20.9
T_H(°C)	100 – 450	72 – 113	397 ± 5 [1] 275 ± 13 [1]	223 – 360	86 - 160		115 - 220
P (bar)	X				480 - 800		
T (°C)	X				130 - 270		
O isotope data (SMOW ‰)	10.7 - -1.4	21.2 – 10.7	n/a	+11.7- +16.5 (Qtz) +17.1 - +24.5 (Dol)			
C isotope data (PDB)‰	-4.0 ± 0.9	-11.8 - -0.8	n/a	-3.0 - -0.8 (Dol)			
S isotope data		n/a	n/a	-13.6 - - 1.1 9 (excludes Brt = +7.1 - +8.1))			

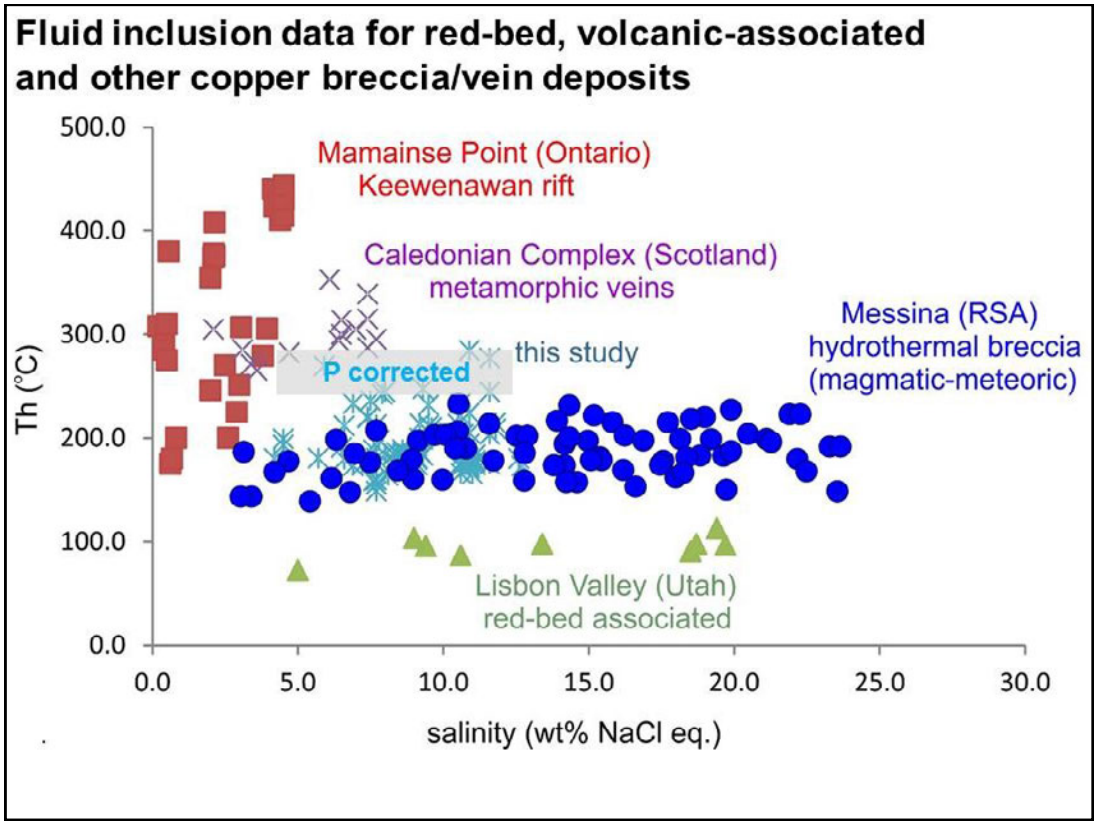
Fluid inclusion data for red-bed, volcanic-associated and other copper breccia/vein deposits
Mamainse Point (Ontario)
Keewenawan rift
Caledonian Complex (Scotland)
metamorphic veins
this study
P corrected
Messina (RSA)
hydrothermal breccia
(magmatic-meteoric)
Lisbon Valley (Utah)
red-bed associated
Th (°C)
500.0
400.0
300.0
200.0
100.0
0.0
0.0
5.0
10.0
15.0
20.0
25.0
30.0
salinity (wt% NaCl eq.)

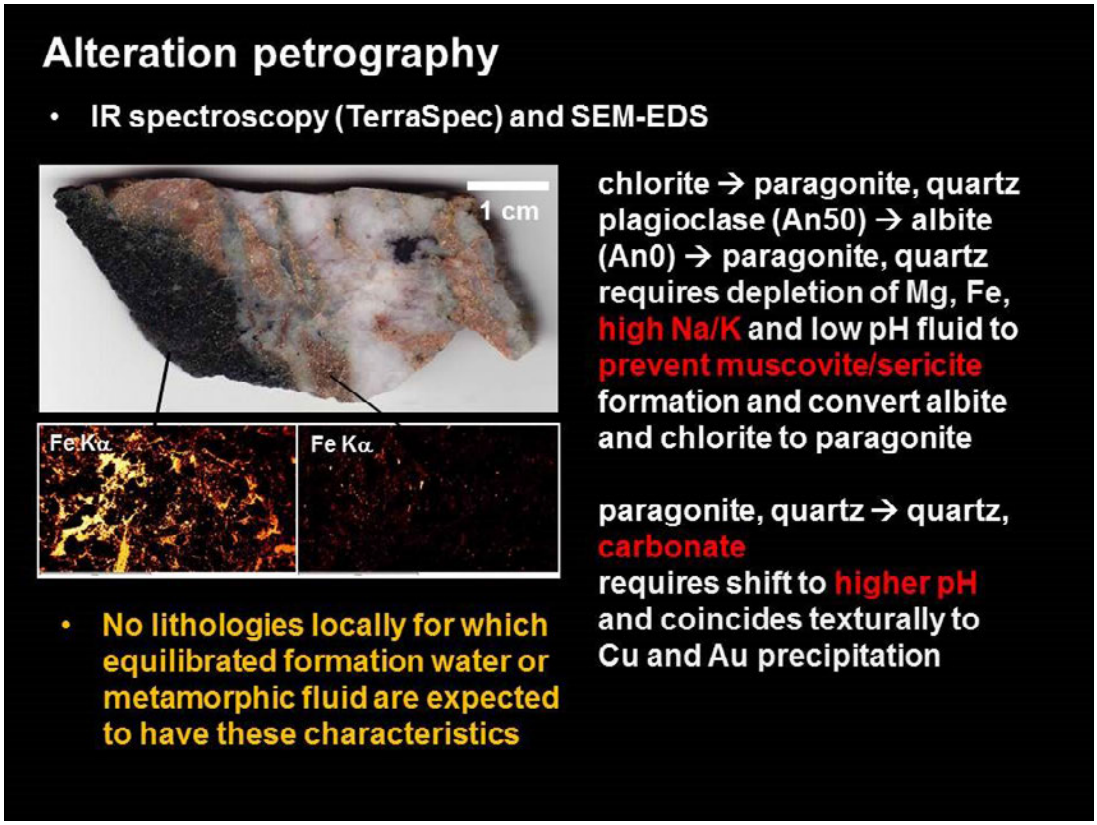
Alteration petrography
• IR spectroscopy (TerraSpec) and SEM-EDS
1 cm
Fe Kα
Fe Kα
chlorite → paragonite, quartz
plagioclase (An50) → albite (An0) → paragonite, quartz
requires depletion of Mg, Fe, high Na/K and low pH fluid to prevent muscovite/sericite formation and convert albite and chlorite to paragonite
paragonite, quartz → quartz, carbonate
requires shift to higher pH and coincides texturally to Cu and Au precipitation
• No lithologies locally for which equilibrated formation water or metamorphic fluid are expected to have these characteristics

Preliminary summary

- Carbonate, Cu-sulfide-Au-Bi vein infilling precipitated from a low salinity (<10 wt% NaCl), low-moderate temperature (<270°C) aqueous fluid at a depth of >3 km with clear inter-FIA variations in bulk salinity and T
- Consistent with other deep-seated qtz-carb Cu vein deposits (Messina, RSA; Mamainse Point, Lake Superior; SW Scottish Highlands
- C and O isotopes of ore co-precipitated quartz-carbonates
  - mixing scenario involving magmatic fluid and meteoric water
  - fluctuations in fluid T, with ore precipitation ~ lowering of T
- Alteration minerals are recording a decrease in pH and influx of high Na/K rich fluid preceding ore precipitation followed by an increase in pH during ore precipitation

Ore precipitation controls

- Ore minerals are recording increasing fO2 and pH
- Increasing fO2 and reduction in T favours formation of neutral Au and Cu bisulfide complexes but eventually leads to bisulfide oxidation
- Increasing pH, reduction in T and salinity destabilizes Au and Cu chloride complexes
- Fluid mixing provides mechanism as does alteration of wall-rock albite to paragonite
- No evidence for boiling or sulfidation reactions with host rocks

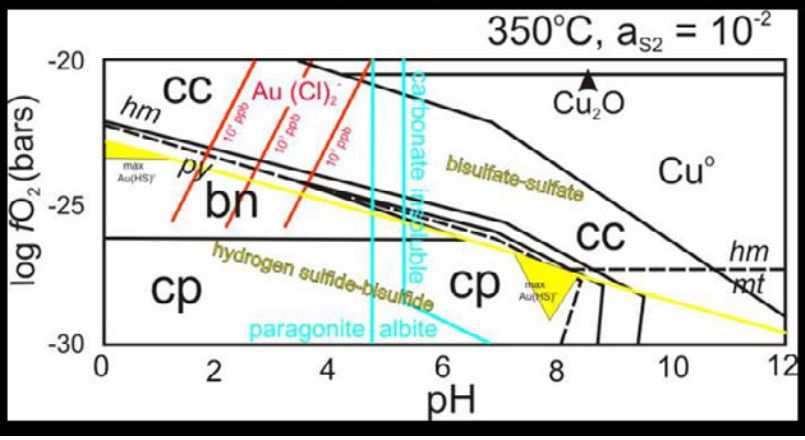

Connections to intrusive activity ?

Barr and White (1999), Park et al., (2008):

- W. Caledonian Highlands: 630-620 Ma dioritic to granitic plutons coeval with subduction-related volcanics in Broad River Group
- E. Caledonian Highlands: 560-550 Ma gabbroic to syenogranitic plutons coeval with extension-related volcanics in Cold Brook Group
- Many plutons show highly anomalous Cu contents (e.g., Point Wolfe River Pluton, Forty Five River Granodiorite near our study area)
- Initiated ~615 Ma regional deformation was prolonged, possibly up to Carboniferous and similar deposits to Mile Brook-Roman Wolfe are hosted in Carboniferous rocks (Mispeck Group), even cross cutting regional deformational fabrics (Ruitenberg, 1979)

→ Dating of monazite in qtz-carb-sulfide veins in progress
→ Regional structural study of deposits to clarify reported field relations
→ LA-ICPMS of fluid inclusions (is the fluid consistent with a contracted magmatic vapour phase ? Cs-B-As-Sb-Au-Cu)

Connections to intrusive activity ?

If so, which of these two suites are more productive for hydrothermal vein deposits at higher stratigraphic levels ? Are these "subepithermal" vein deposits spatially linked to hidden intrusion-related deposits in the Caledonian Highlands ?

Petrographic observations and evaporate mound analysis of quartz-hosted fluid inclusions: Applications to assess metal fertility in granites

F. Tweedale[1], J.J. Hanley[1], D.J. Kontak[2] and N. Rogers[3]

1. Saint Mary's University, 923 Robie St., Halifax, Nova Scotia

2. Laurentian University, 935 Ramsey Lake Rd., Sudbury, Ontario

3. Geological Survey of Canada, 601 Booth St., Ottawa, Ontario

Abstract: The 380 Ma South Mountain Batholith (SMB), Nova Scotia, is a large (~7300 km^2), contiguous, mesozonal granitoid intrusion consisting of 13 coalesced plutons hosting a variety of mineralized zones (e.g., Sn-Zn-Cu-Ag, Mn-Fe-P, U, Cu-Ag). Given the hydrothermal nature of this mineralization, it is expected that a geochemical fingerprint of the mineralizing fluids might be preserved both petrographically and as secondary fluid inclusions (FIs) in the granites on a scale equal to or larger than the mineralized zones. In this unique study, we investigate the possibility of integrating petrographic observations that reflect fluid:rock interaction and the chemistry of secondary, quartz-hosted FIs in samples from the SMB to assess granite fertility and also the scale of this potential vectoring tool. The protocol involved: (1) detailed petrographic study of >500 archived samples and focused on the extent and degree of alteration (e.g., perthite textures, chlorite alteration of biotite, plagioclase alteration, percent of secondary muscovite, abundance of FI in quartz); and (2) determining fluid chemistry of quartz- hosted FIs in >100 samples collected from a 10 × 10 km grid superimposed on the SMB. The petrographic data record highly variable degrees of alteration and the results are being used to design an alteration algorithm that can be used to map the extent of fluid:rock interaction throughout the batholith. The chemistry of FIs, determined using the evaporate mound method, is being used as a proxy for both the mineralizing and altering fluids. At present, results for >600 mounds determined for 68 samples indicate the fluids are dominated by Na-K-Ca-Cl-F, with traces of Fe, Mn, and S, and that two distinct types are present, one Na-rich and the other Ca-rich. Two intriguing results to date include: (1) the pervasive occurrence of F in the mound analysis with up to 40 wt% when normalized to 100%, even in samples distal to known mineralization; and (2) elevated Ca in many samples, including those from chemically evolved, hence Ca-depleted rocks. This latter feature may reflect extensive albitization of plagioclase, hence liberation of Ca, during fluid-mediated alteration. Thus, our preliminary findings clearly indicate that mappable variation in the degree and extent of alteration is retained in the main mineral phases of the granites and that fluid chemistry, preserved as secondary FIs in quartz, is a potential proxy for fluid:rock interaction and hence a measure of metal fertility.

Originally presented Fredericton 2014: Geological Association of Canada - Mineralogical Association of Canada Joint Annual Meeting, Special Session 3: Discovering the Next Generation of Porphyry Deposits: Advancements in Locating and Understanding Hidden Intrusion-related Mineralization. May 21, 2014.

Corresponding author: Fergus M. Tweedale (fergus.tweedale@smu.ca)

Tweedale, F., Hanley, J.J., Kontak, D.J., and Rogers, N., 2015. Petrographic observations and evaporate mound analysis of quartz-hosted fluid inclusions: Applications to assess metal fertility in granites; *in* TGI 4 – Intrusion Related Mineralisation Project: New Vectors to Buried Porphyry-Style Mineralisation, (ed.) N. Rogers; Geological Survey of Canada, Open File 7843, p. 369-381.

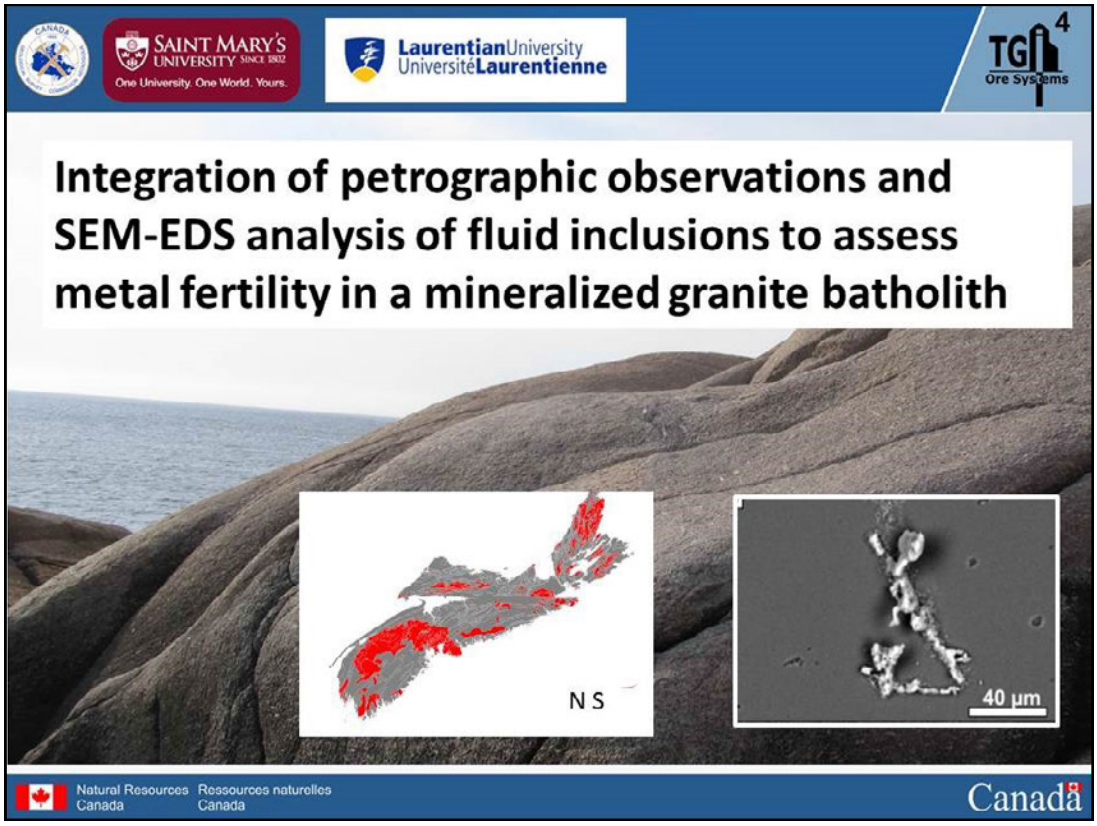

Research objectives

1) Evaluate (i) alteration textures preserved in granitic rocks from the study area and (ii) fluid chemistry of quartz-hosted fluid inclusions.

2) Evaluate the application of alteration indices and fluid chemistry to determine metal fertility of a mineralized batholith (i.e., South Mountain Batholith (SMB)).

As mandated by TGI-4 federal government program, this research provides a protocol and case study that can be exported to assess metal fertility of any mineralized batholith,

Presentation Outline

1) Study area

2) Methods and Analytical Considerations

3) Results

4) Evaluation of results

5) Conclusion

6) References

7) Acknowledgements

1) Study area

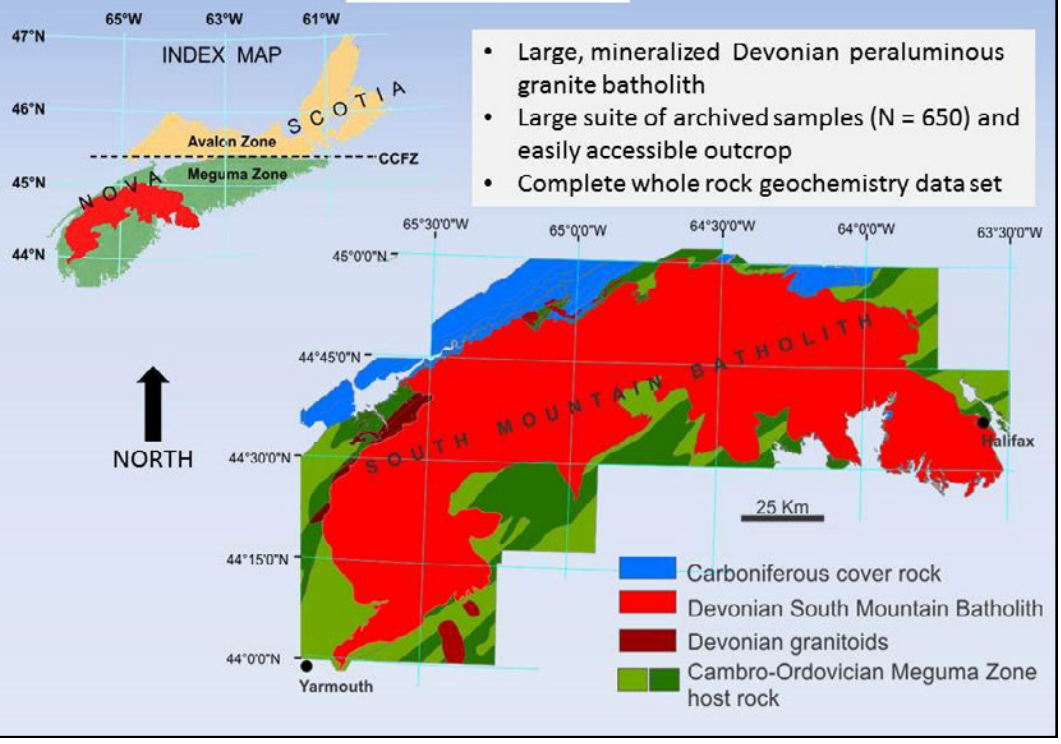

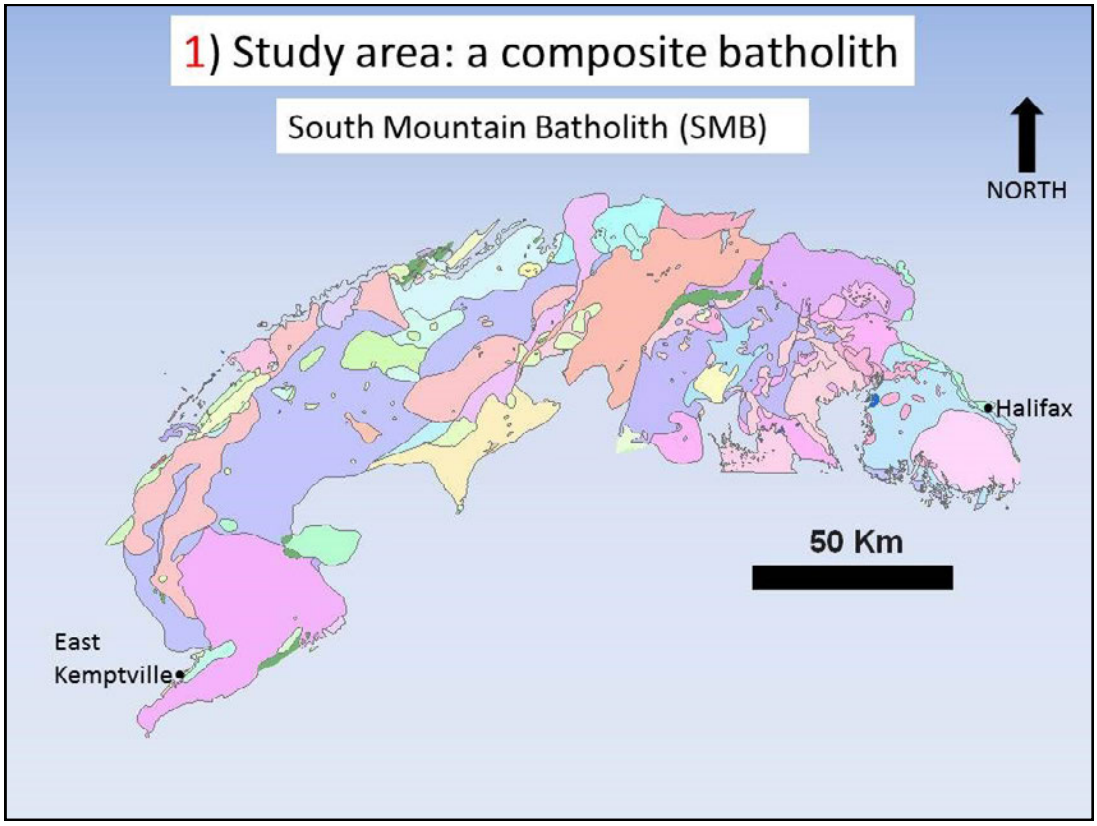
1) Study area: a composite batholith
South Mountain Batholith (SMB)
NORTH
Halifax
50 Km
East
Kemptville

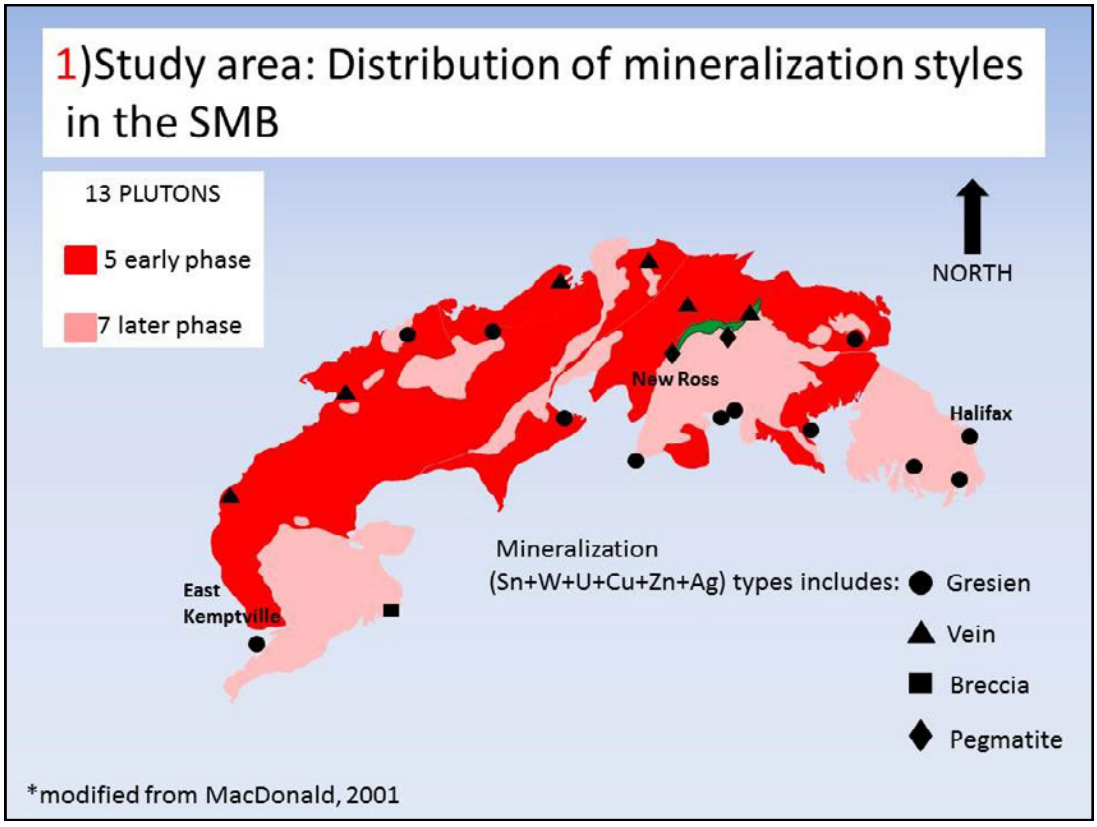
1)Study area: Distribution of mineralization styles in the SMB
13 PLUTONS
5 early phase
7 later phase
NORTH
New Ross
Halifax
East
Kemptville
Mineralization
(Sn+W+U+Cu+Zn+Ag) types includes:
Gresien
Vein
Breccia
Pegmatite
*modified from MacDonald, 2001

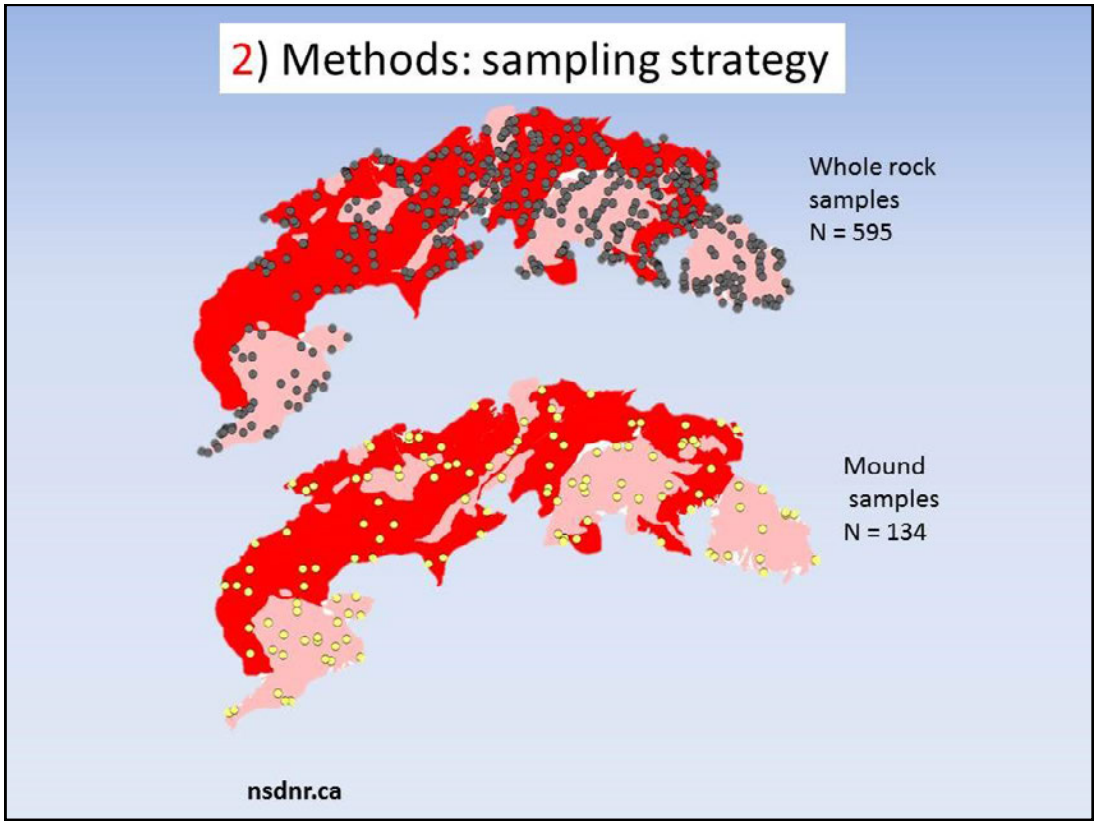
2) Methods: sampling strategy
Whole rock samples N = 595
Mound samples N = 134
nsdnr.ca

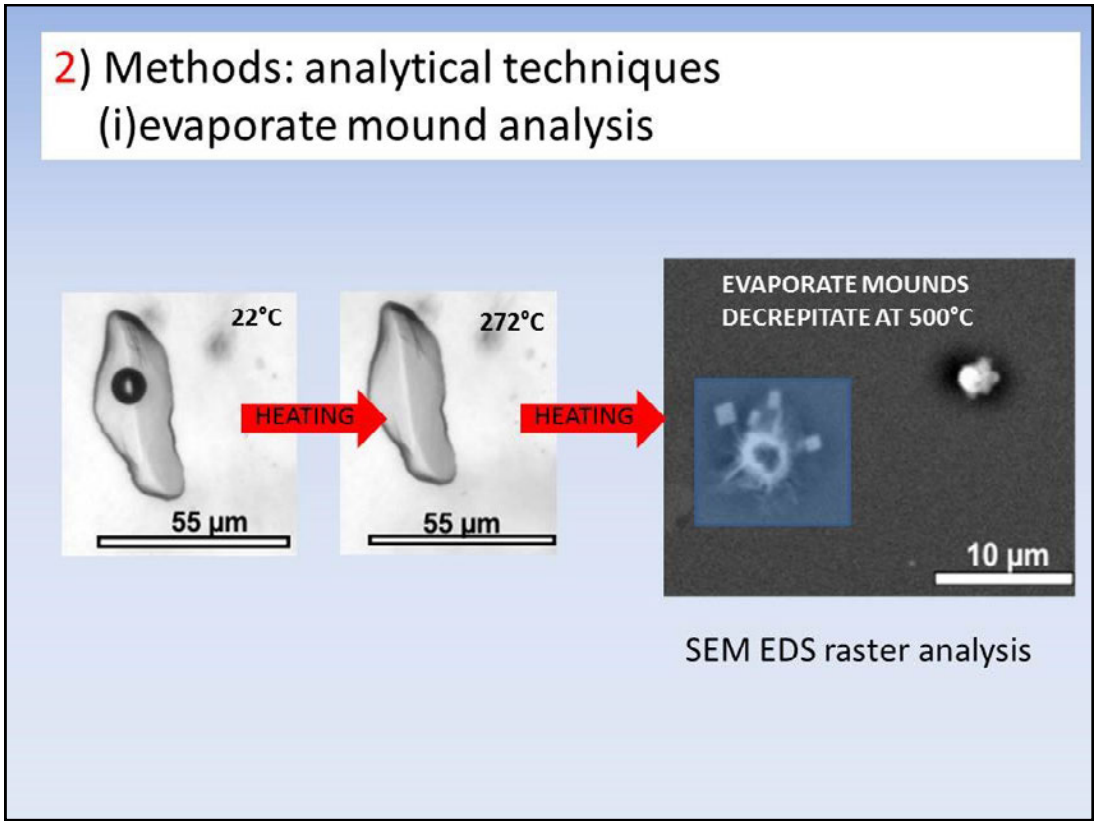
2) Methods: analytical techniques
(i)evaporate mound analysis
22°C
55 µm
HEATING
272°C
55 µm
HEATING
EVAPORATE MOUNDS DECREPITATE AT 500°C
10 µm
SEM EDS raster analysis

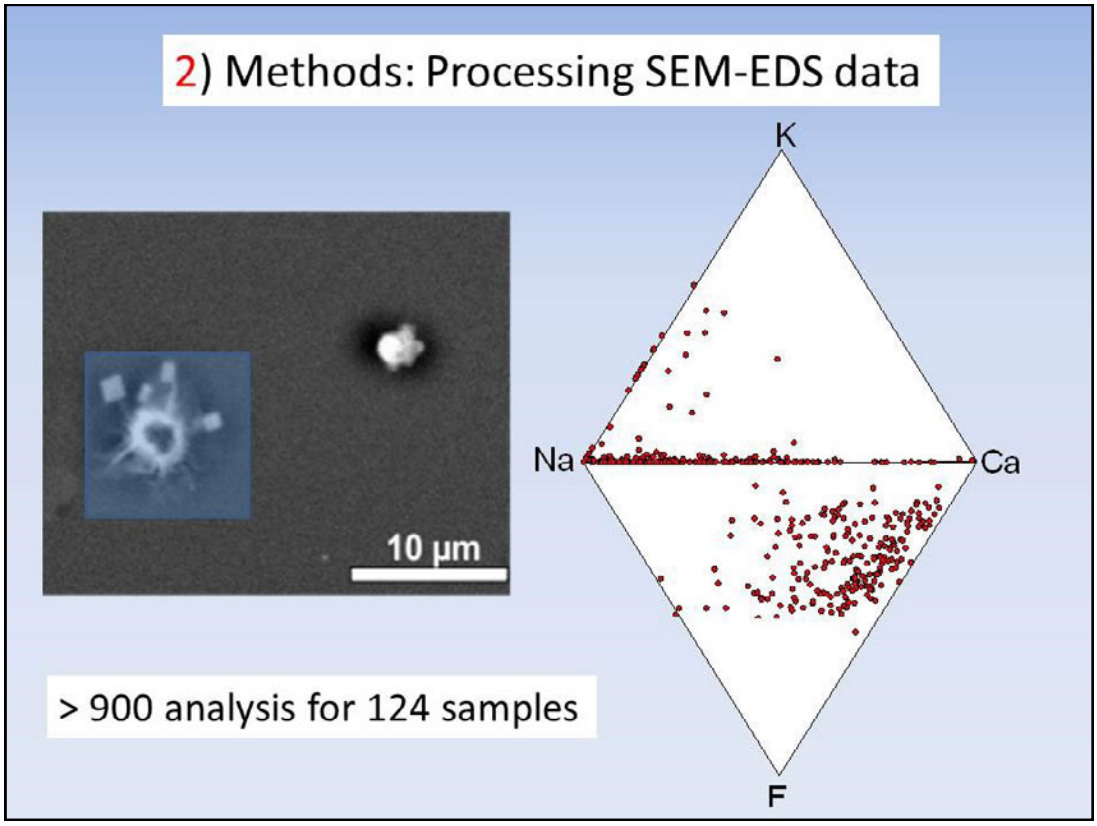
2) Methods: Processing SEM-EDS data
10 µm
K
Na
Ca
F
> 900 analysis for 124 samples

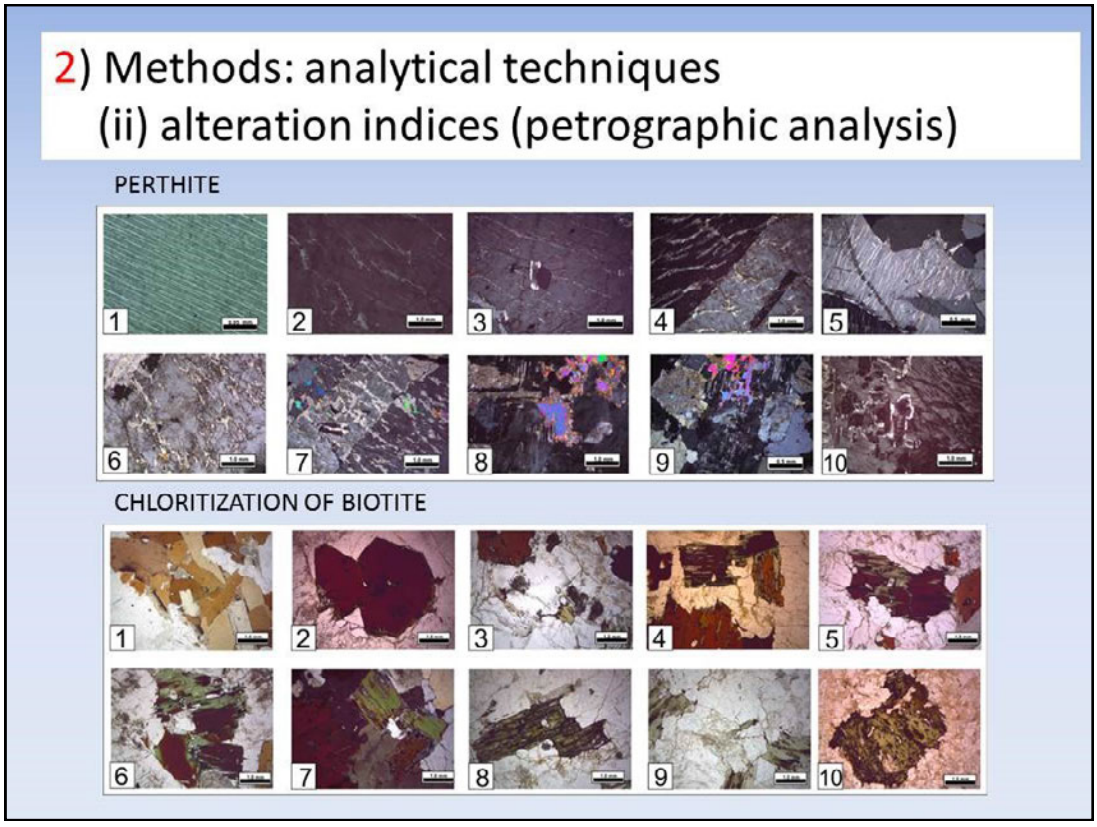
2) Methods: analytical techniques
(ii) alteration indices (petrographic analysis)
PERTHITE
1
2
3
4
5
6
7
8
9
10
CHLORITIZATION OF BIOTITE
1
2
3
4
5
6
7
8
9
10

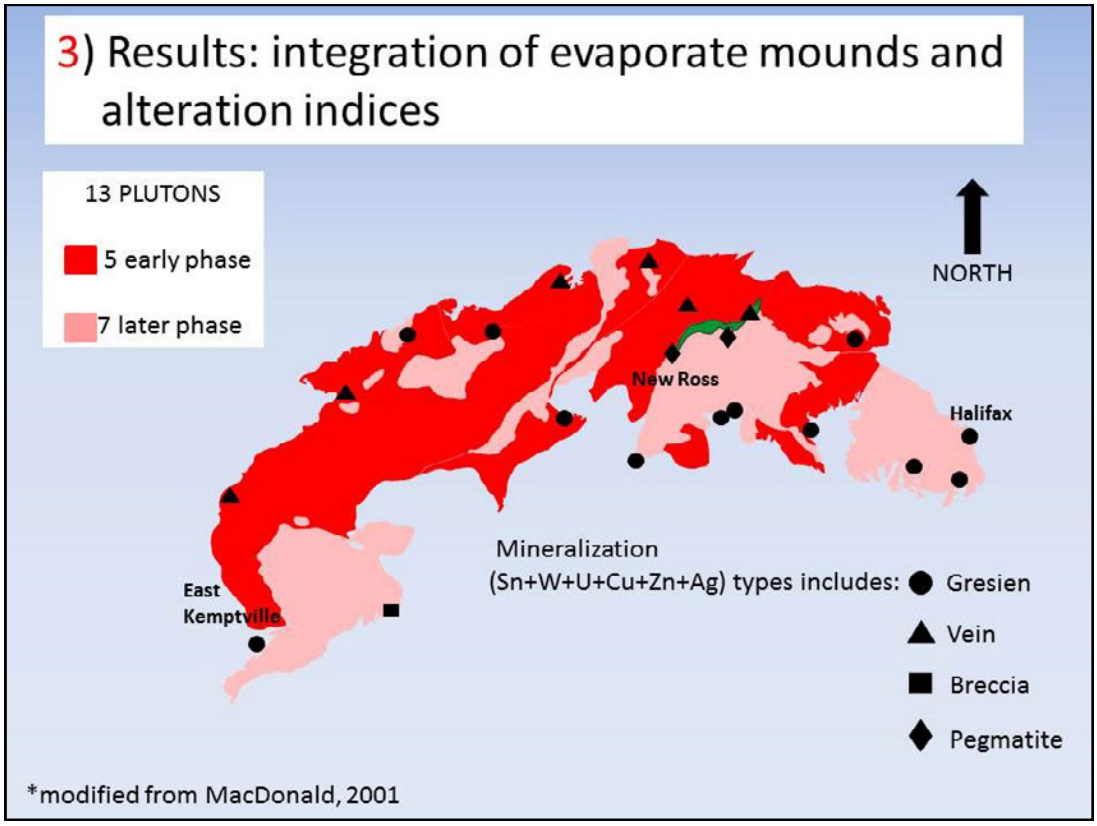
3) Results: integration of evaporate mounds and alteration indices
13 PLUTONS
5 early phase
7 later phase
NORTH
New Ross
Halifax
East Kemptville
Mineralization
(Sn+W+U+Cu+Zn+Ag) types includes:
Gresien
Vein
Breccia
Pegmatite
*modified from MacDonald, 2001

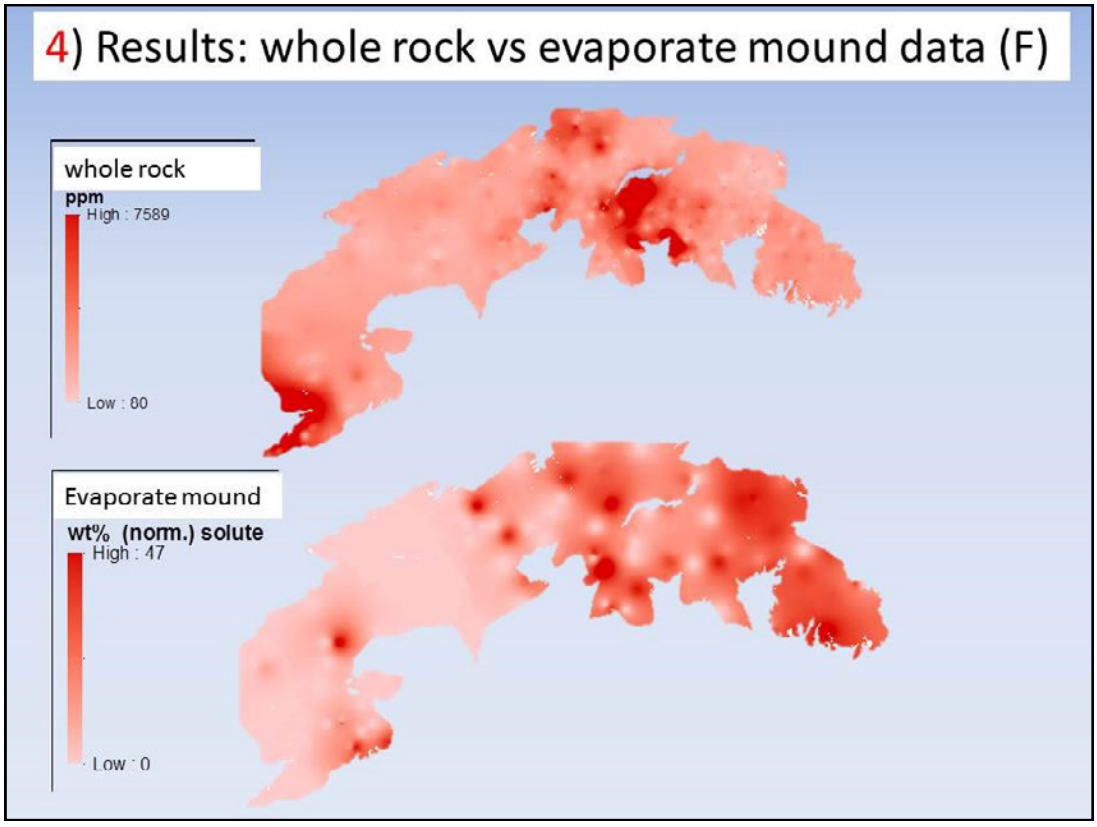
4) Results: whole rock vs evaporate mound data (F)
whole rock
ppm
High : 7589
Low : 00
Evaporate mound
wt% (norm.) solute
High : 47
Low : 0

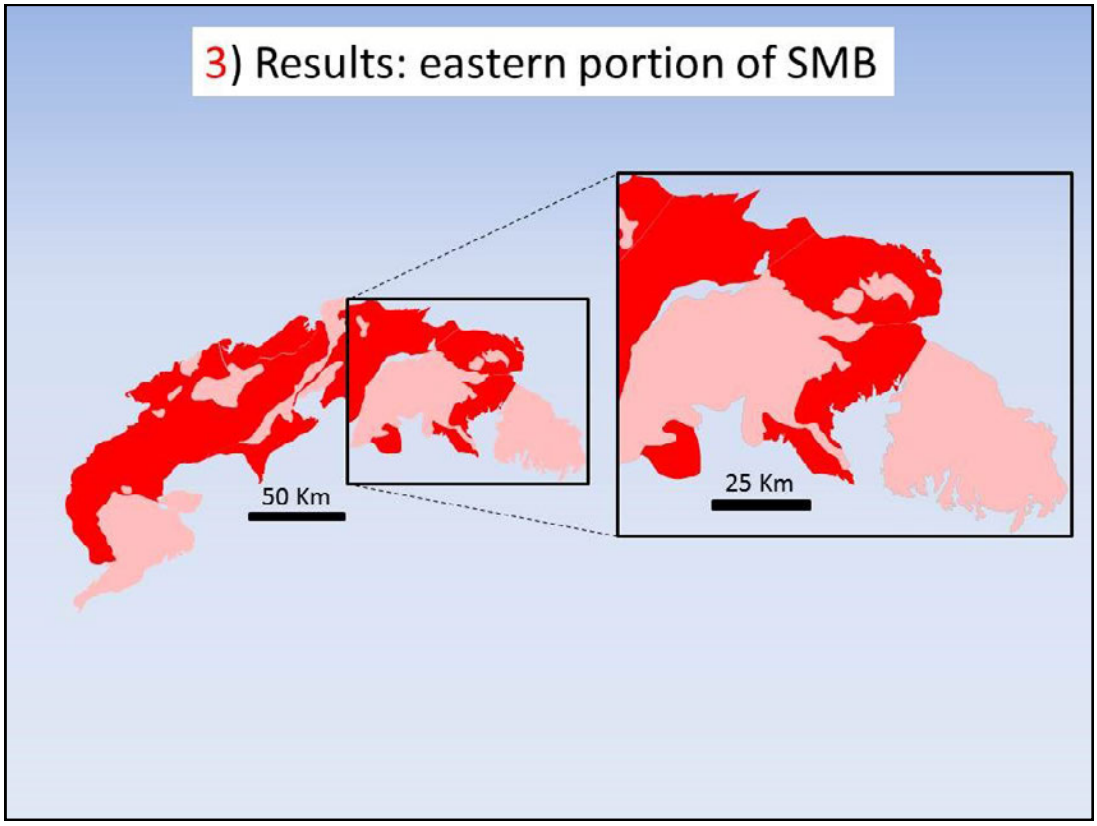
3) Results: eastern portion of SMB
50 Km
25 Km

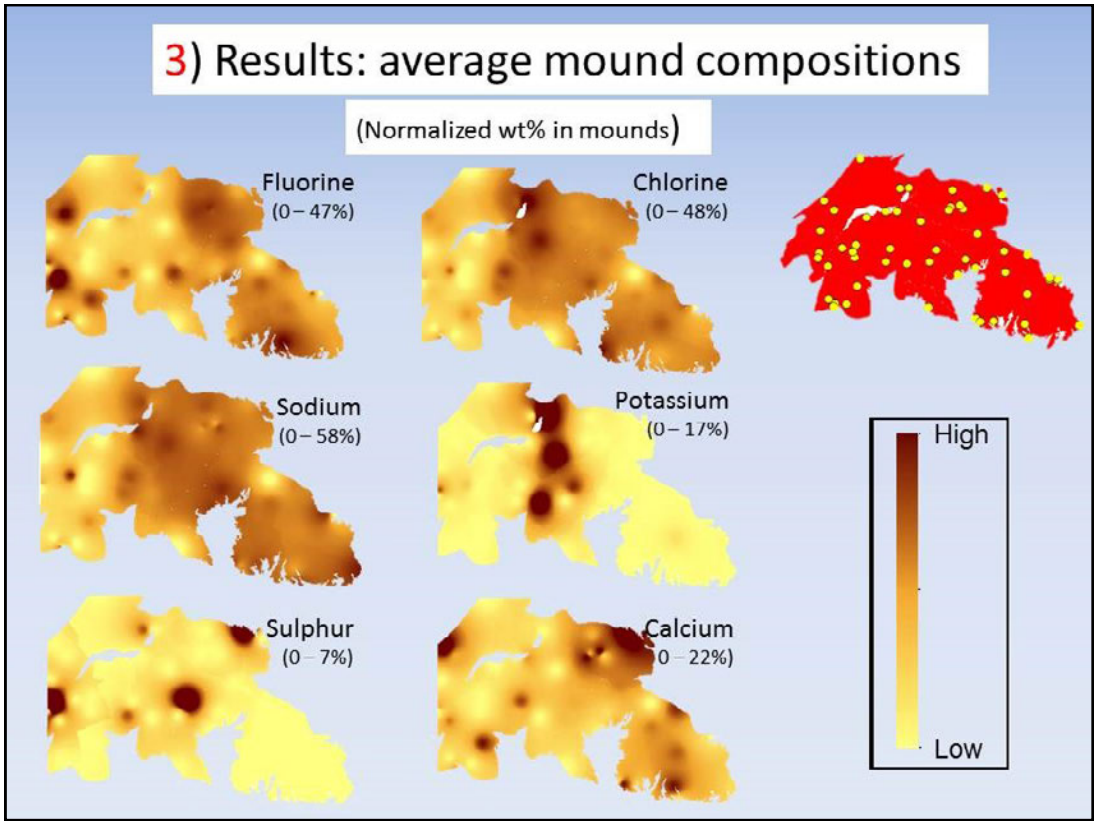
3) Results: average mound compositions
(Normalized wt% in mounds)
Fluorine
(0 – 47%)
Chlorine
(0 – 48%)
Sodium
(0 – 58%)
Potassium
(0 – 17%)
Sulphur
(0 – 7%)
Calcium
(0 – 22%)
High
Low

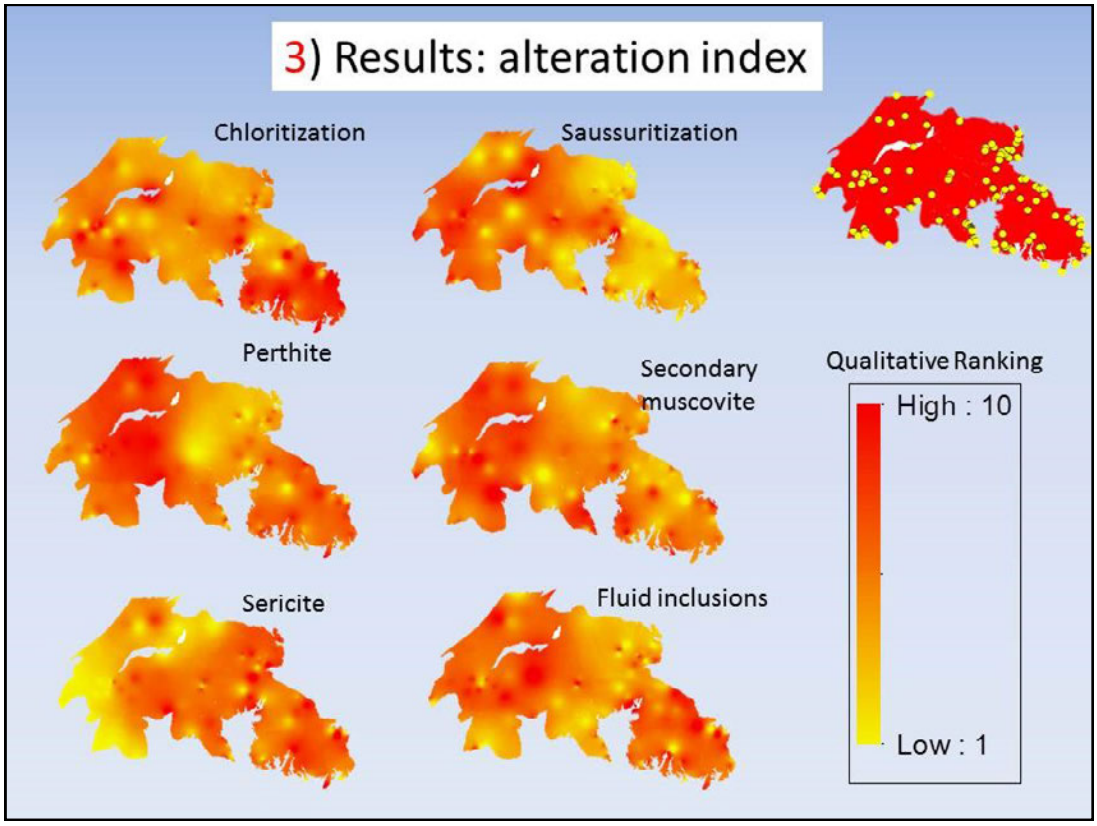
3) Results: alteration index
Chloritization
Saussuritization
Perthite
Secondary muscovite
Sericite
Fluid inclusions
Qualitative Ranking
High : 10
Low : 1

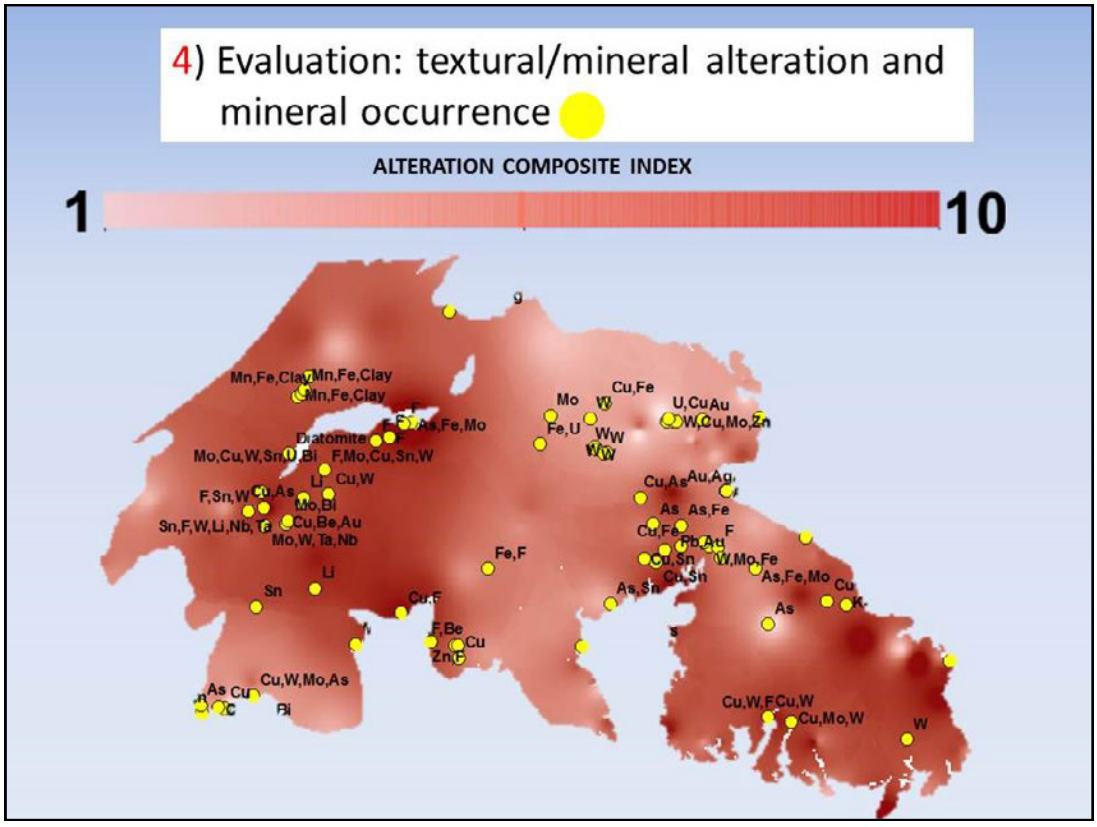
4) Evaluation: textural/mineral alteration and mineral occurrence
ALTERATION COMPOSITE INDEX
1
10

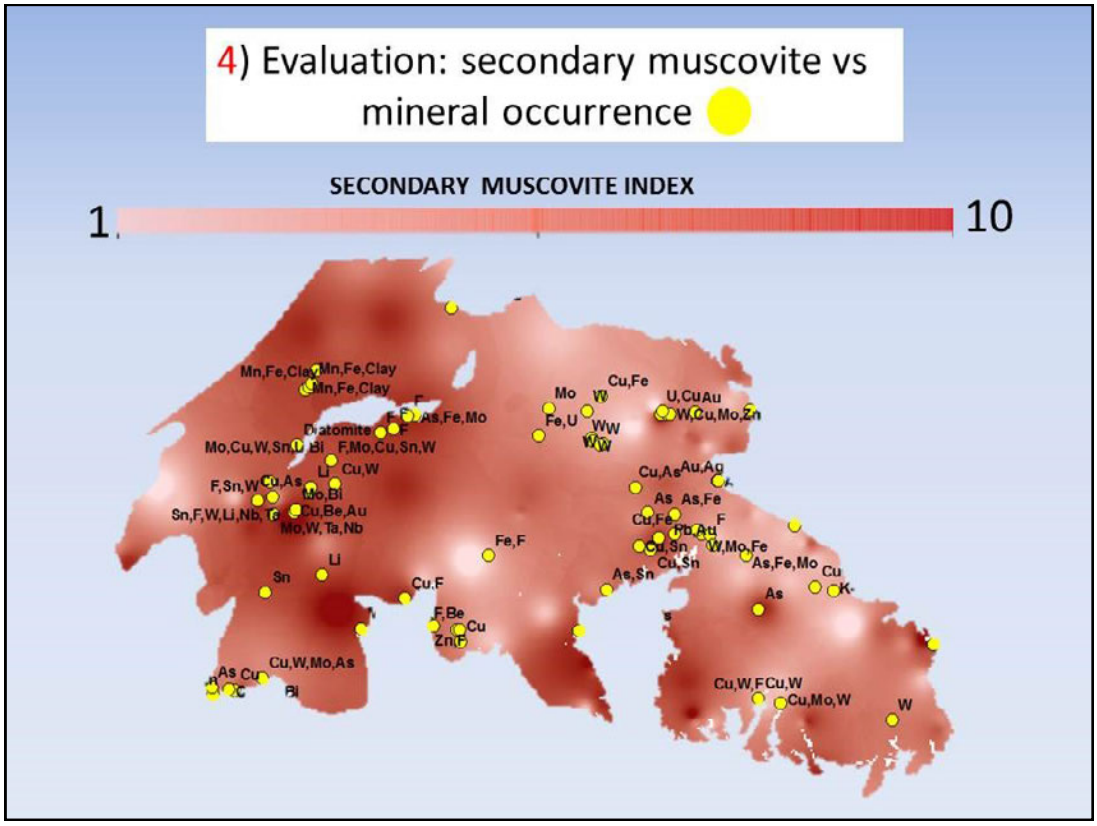
4) Evaluation: secondary muscovite vs mineral occurrence
SECONDARY MUSCOVITE INDEX
1
10
Mn,Fe,Clay
Mn,Fe,Clay
Mn,Fe,Clay
Diatomite
Mo,Cu,W,Sn,U,Bi
F,Mo,Cu,Sn,W
Li
Cu,W
F,Sn,W
Cu,As
Mo,Bi
Sn,F,W,Li,Nb,Ta
Cu,Be,Au
Mo,W,Ta,Nb
Li
Sn
Cu,F
F,Be
Cu
Zn,F
As,Cu
Cu,W,Mo,As
Bi
Fe,F
Mo
Cu,Fe
U,Cu,Au
W,Cu,Mo,Zn
Fe,U
Cu,As
Au,Ag
As
As,Fe
Cu,Fe
F
Pb,Au
W,Mo,Fe
Cu,Sn
As,Fe,Mo
Cu
As,Sn
As
K
Cu,W,F
Cu,W
Cu,Mo,W
W

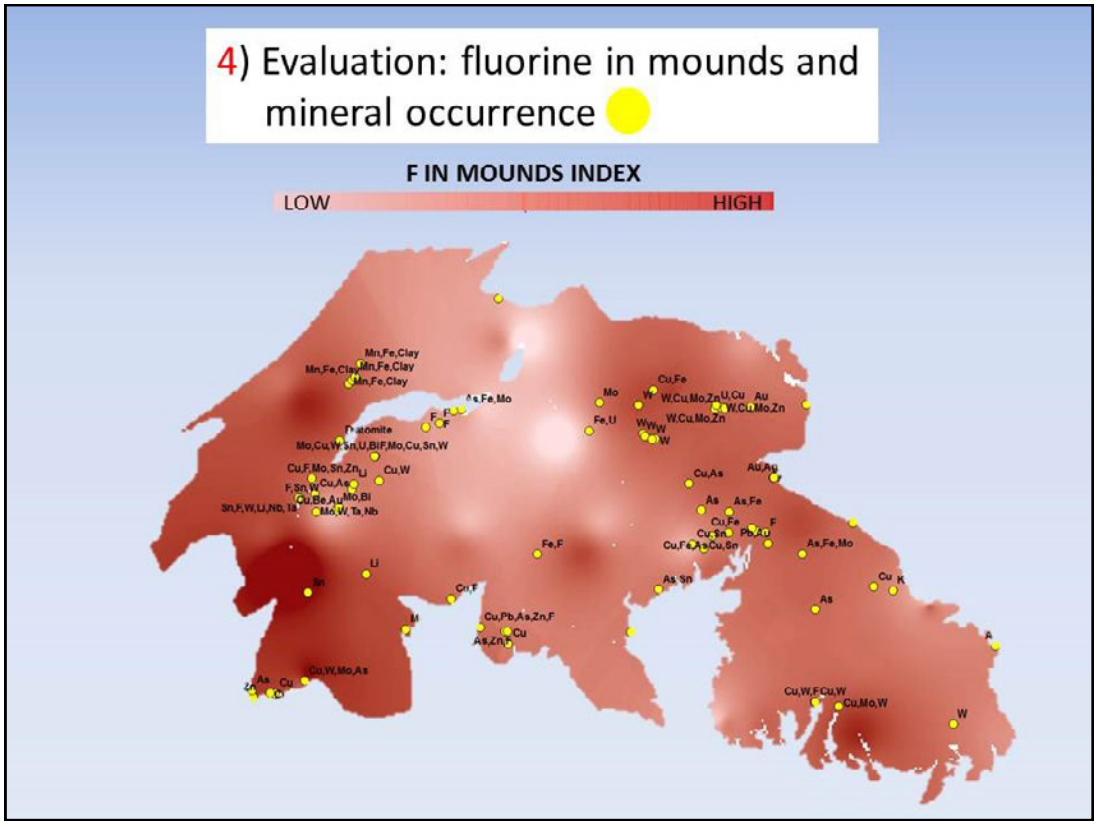
4) Evaluation: fluorine in mounds and mineral occurrence
F IN MOUNDS INDEX
LOW
HIGH
Mn,Fe,Clay
Mn,Fe,Clay
Mn,Fe,Clay
Diatomite
Mo,Cu,W,Sn,U,Bi
F,Mo,Cu,Sn,W
Cu,F,Mo,Sn,Zn
Li
Cu,W
F,Sn,W
Cu,As
Mo,Bi
Sn,F,W,Li,Nb,Ta
Cu,Be,Au
Mo,W,Ta,Nb
Li
Sn
Cu,F
Cu,Pb,As,Zn,F
Cu
As,Zn
As,Cu
Cu,W,Mo,As
Fe,F
Mo
Cu,Fe
W,Cu,Mo,Zn
Li,Cu
Au
W,Cu,Mo,Zn
Fe,Li
W,Cu,Mo,Zn
Cu,As
Au,Ag
As
As,Fe
Cu,Fe
F
Cu,Sn
Pb,Au
Cu,Fe,As,Cu,Sn
As,Fe,Mo
Cu
K
As,Sn
As
A
Cu,W,F
Cu,W
Cu,Mo,W
W

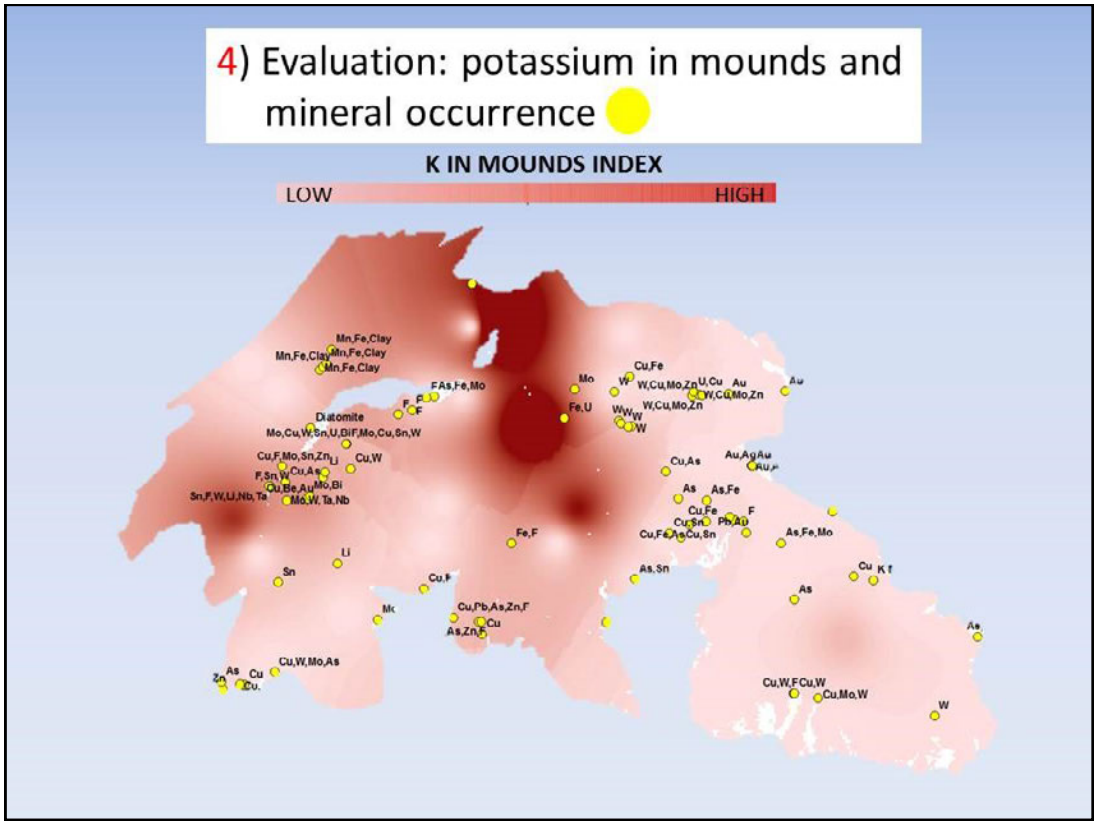
4) Evaluation: potassium in mounds and mineral occurrence
K IN MOUNDS INDEX
LOW
HIGH

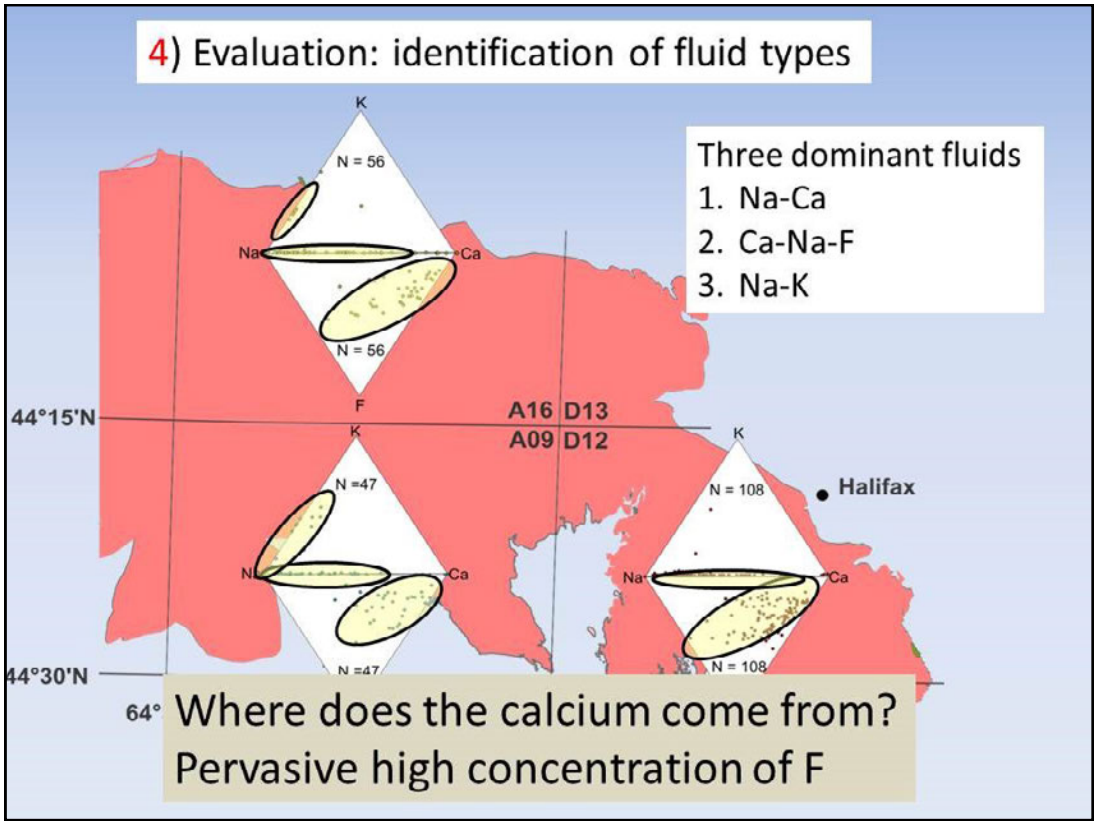
4) Evaluation: identification of fluid types
Three dominant fluids
1. Na-Ca
2. Ca-Na-F
3. Na-K
K
N = 56
Na
Ca
N = 56
F
44°15'N
A16 D13
A09 D12
K
K
N =47
N
Ca
N = 108
Halifax
Na
Ca
44°30'N
N =47
N = 108
64°
Where does the calcium come from?
Pervasive high concentration of F

5) CONCLUSIONS

- Evaluation of metal fertility of a batholith using integration of evaporate mound analysis and alteration indices is feasible
- Strong correlations between mineralized centres and alteration and evaporate mound compositions
- Abundance of calcium-rich fluids suggest batholith-wide albitization
- Abundance of F-rich fluids suggests presence of buried evolved intrusions below current level of exposure

6) References

MacDonald, M.A., 2001, Geology of the South Mountain Batholith, Southwestern Nova Scotia, Nova Scotia Department of Natural Resources, Open File Report ME 2001-2.

7) Acknowledgments

Jacob Hanley, Saint Mary's University
Dan Kontak, Laurentian University
Neil Rogers, GSC, Ottawa

NSDNR: Bob Ryan, Tracy Lenfesty, Chris White

Saint Mary's University: Randy Corney, Victor Owen, Xiang Yang, Greg Baker

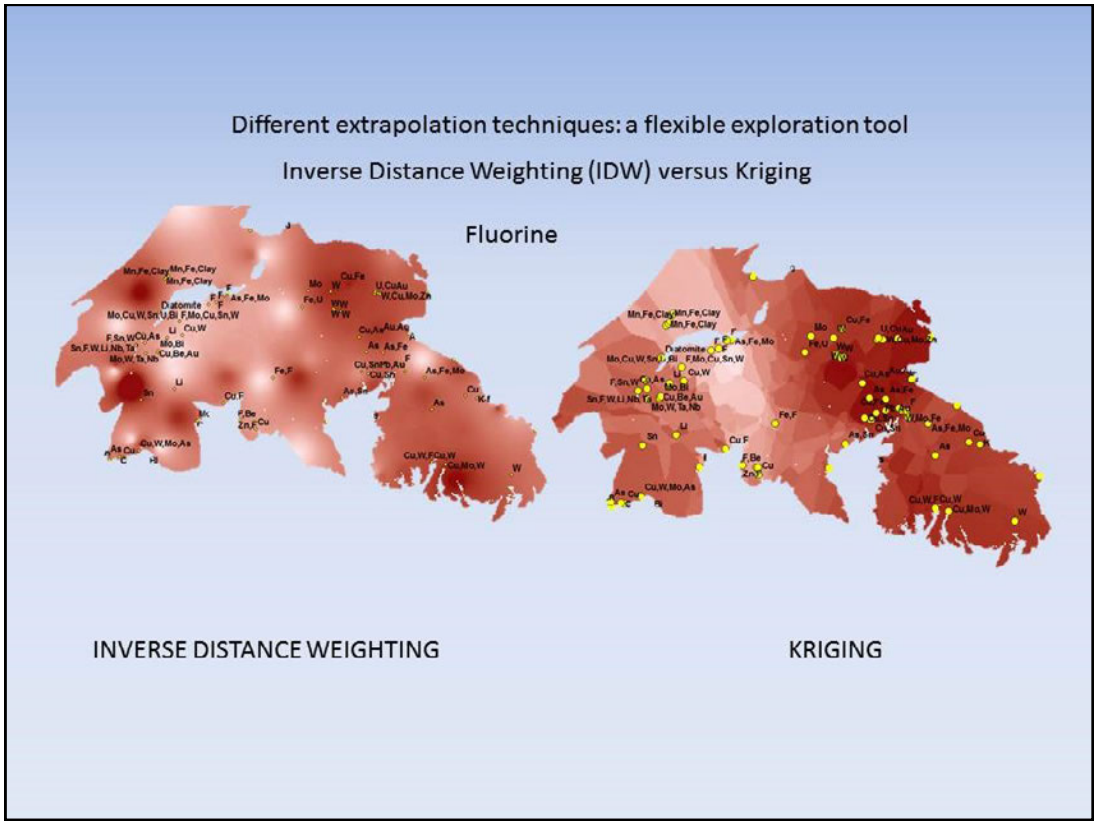
Different extrapolation techniques: a flexible exploration tool
Inverse Distance Weighting (IDW) versus Kriging
Fluorine
INVERSE DISTANCE WEIGHTING
KRIGING

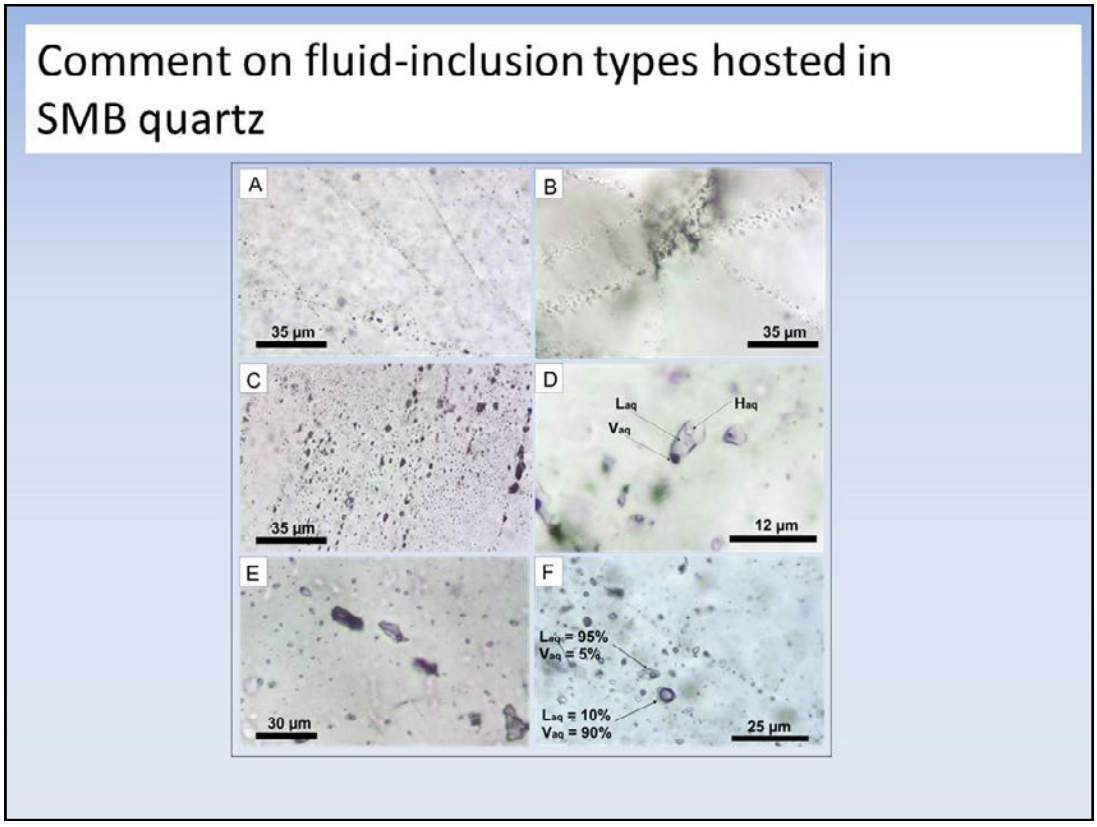
Comment on fluid-inclusion types hosted in SMB quartz
A
35 µm
B
35 µm
C
35 µm
D
Laq
Haq
Vaq
12 µm
E
30 µm
F
Laq = 95%
Vaq = 5%
Laq = 10%
Vaq = 90%
25 µm

The south Newfoundland granophile mineral district: Features and opportunities for research on blind deposits

A. Kerr

St. John's, Newfoundland and Labrador

Abstract: The south coast of the island of Newfoundland is a diverse and potentially important district of granophile mineral deposits, in which several mineralized intrusive complexes span contrasting tectonostratigraphic zones of the Appalachian Orogen. In addition to molybdenum and tungsten deposits that represent potential producers, the district includes one of the world's largest producing fluorspar deposits, at St. Lawrence. The settings of mineral deposits vary, as do their associated commodities, but there is a common magmatic thread throughout the district. All major deposits are associated with evolved, alkali-calcic, siliceous granitoid rocks emplaced within a short time interval from ca. 388 Ma to ca. 375 Ma. Coherent U-Pb and Re-Os geochronology links these deposits to spatially associated plutons, even where direct physical connections are lacking. There are common geochemical themes that link prospective magmas, but these are not always easily visible through the geochemical and isotopic diversity connected to the contrasts in basement terranes along the belt. There is a dire need for other types of diagnostic data (e.g., Pb isotopes, accessory mineral chemistry) that can better unravel the respective contributions of magma sources, contaminants and fractionation histories to regional prospectivity.

There are contrasts in the erosional levels revealed in individual complexes, from endocontact disseminated mineralization in high-level granites, to sheeted vein complexes and related hydrothermal lodes associated with hidden subsurface plutons. The Grey River - Moly Brook area provides the best example of the latter setting, and has all of the expected characteristics of a large zoned hydrothermal system. This area is of particular interest in the context of exploring such blind systems, because high-resolution geophysical data provide potential 3D information to augment the direct data from drilling. Exploring for targets associated with hidden intrusions is never going to be easy, so examples such as this, for which multiple data sets exist, are obvious priorities for expanded research.

Originally presented Fredericton 2014: Geological Association of Canada - Mineralogical Association of Canada Joint Annual Meeting, Special Session 3: Discovering the Next Generation of Porphyry Deposits: Advancements in Locating and Understanding Hidden Intrusion-related Mineralization. May 21, 2014.

Corresponding author: Andy Kerr (akerr@mun.ca)

Kerr, A., 2015. The south Newfoundland granophile mineral district: Features and opportunities for research on blind deposits; *in* TGI 4 – Intrusion Related Mineralisation Project: New Vectors to Buried Porphyry-Style Mineralisation, (ed.) N. Rogers; Geological Survey of Canada, Open File 7843, p. 383-401.

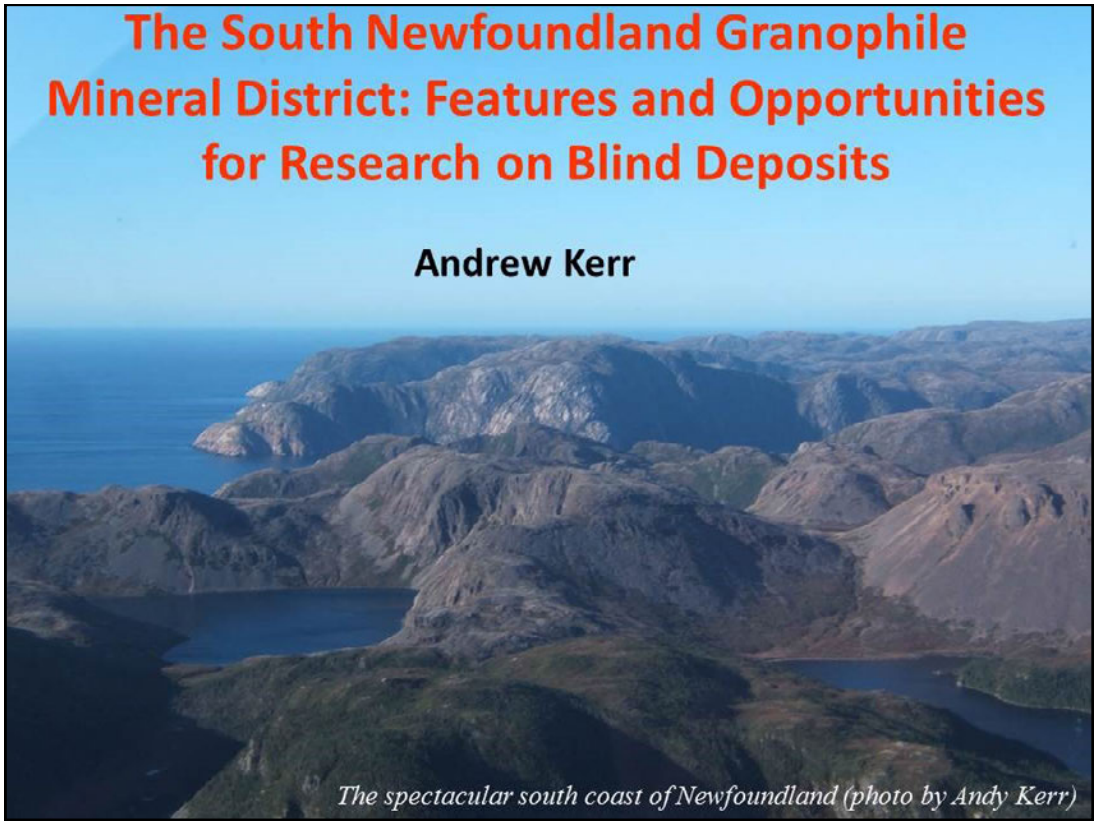
The South Newfoundland Granophile Mineral District: Features and Opportunities for Research on Blind Deposits
Andrew Kerr
The spectacular south coast of Newfoundland (photo by Andy Kerr)

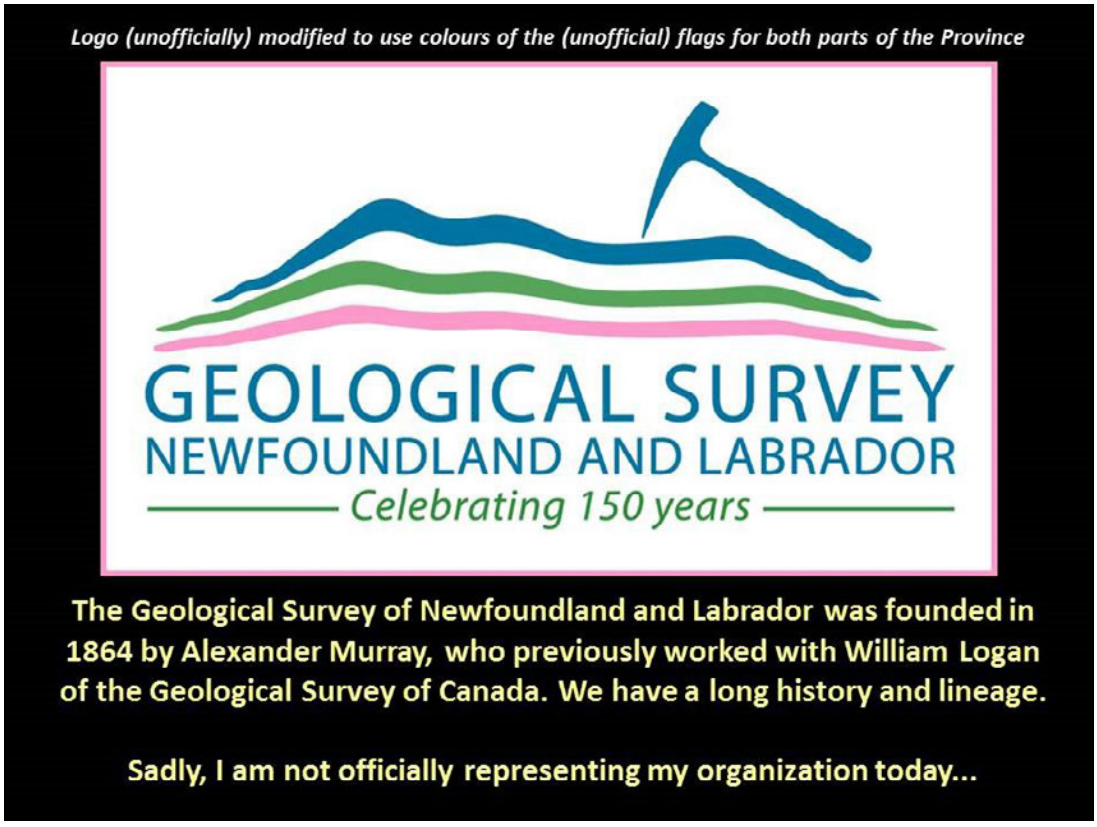
Logo (unofficially) modified to use colours of the (unofficial) flags for both parts of the Province
GEOLOGICAL SURVEY
NEWFOUNDLAND AND LABRADOR
Celebrating 150 years
The Geological Survey of Newfoundland and Labrador was founded in 1864 by Alexander Murray, who previously worked with William Logan of the Geological Survey of Canada. We have a long history and lineage.
Sadly, I am not officially representing my organization today...

The South Newfoundland Granophile District

- This is a district-scale metallogenic province that stretches for some 350 km along the south coast of the island of Newfoundland.
- A common theme appears to be the link between mineralization and late Devonian plutonic activity.
  (sometimes called 'NeoAcadian', although the term is unclear)
- A diverse metal association, including Mo, W, Sn, (Cu + Pb + Zn), Ag, Au (?), fluorite, barite and silica.
- Deposits and occurrences have varied settings that range from disseminated in plutonic rocks, to contact zones, vein swarms, and discrete veins.
- Research on blind deposits/hidden plutons ?

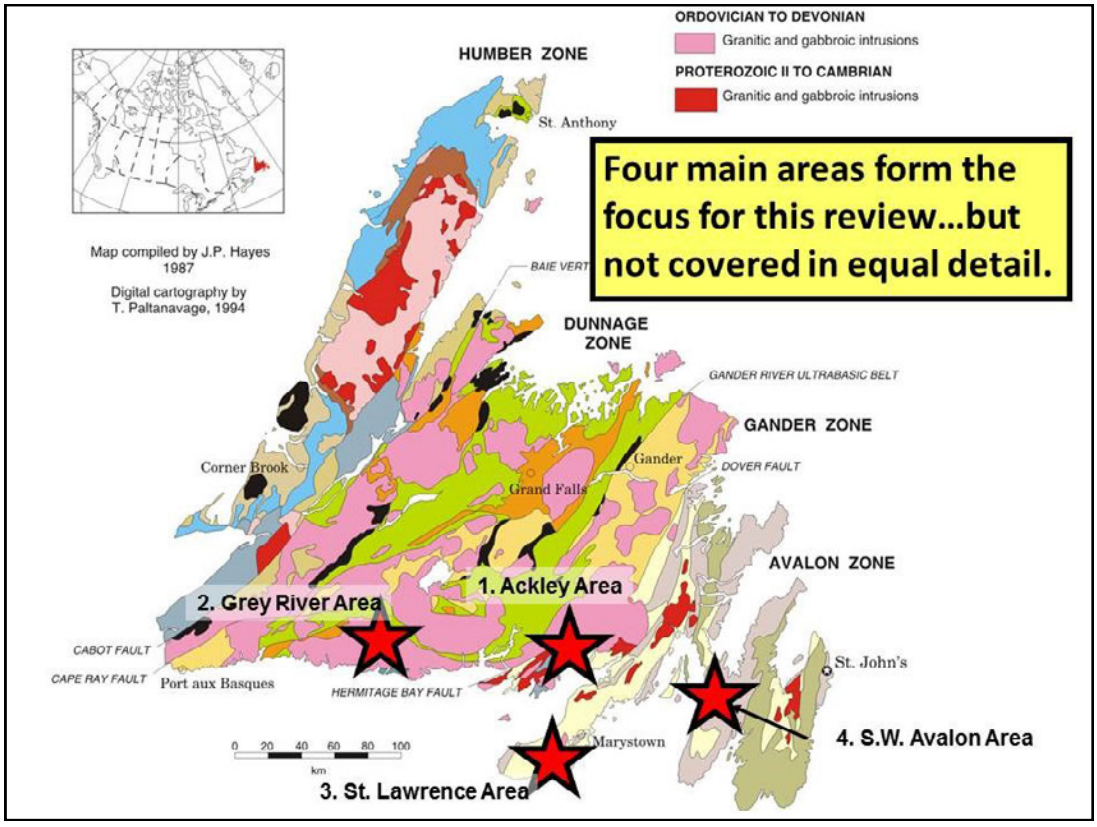

A General Outline for the Presentation

- Some background geology and the regional context of associated magmatic suites.
- Salient points for each of these areas, with emphasis on potential for research work; we proposed some of this for TGI-4, but it now looks more likely for TGI-5.
- There is a general 'upward' progression in the erosion level of these potentially large systems moving away from the Gander-Avalon boundary.
- Presentation includes discussion of U-Pb zircon data, but also Re-Os results from Ed Lynch's work, presently published in abstract form.

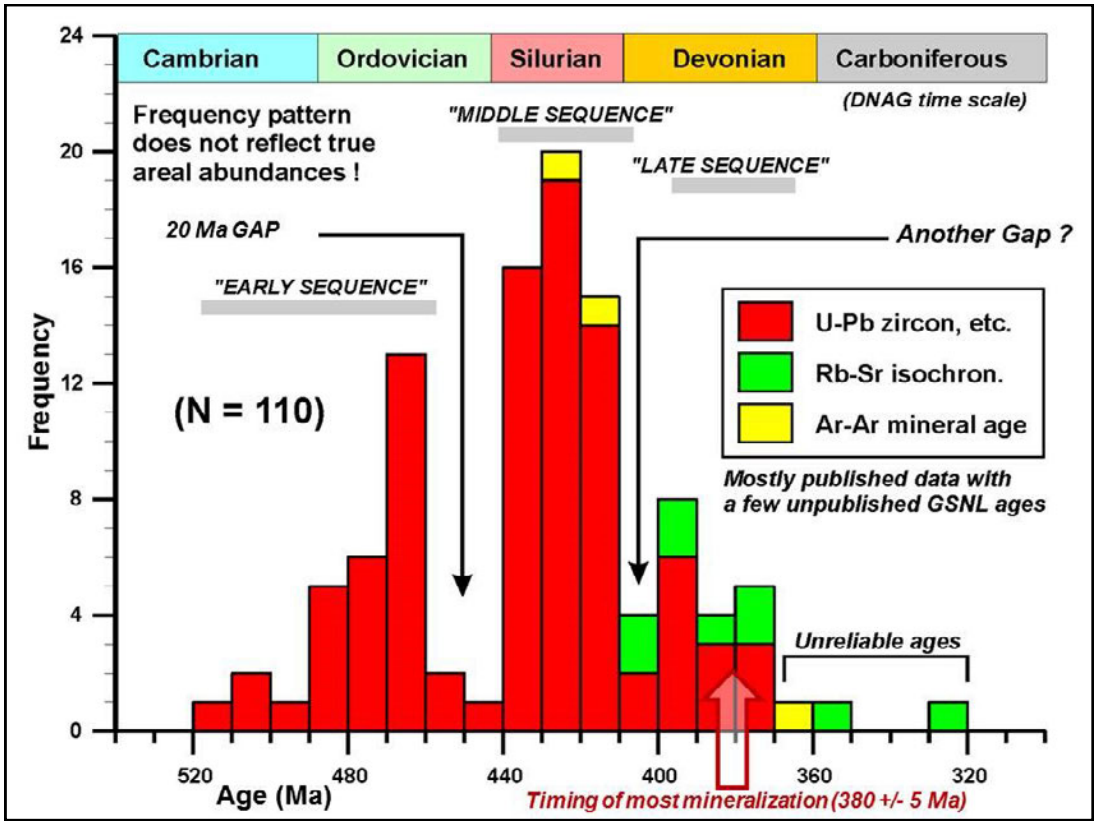

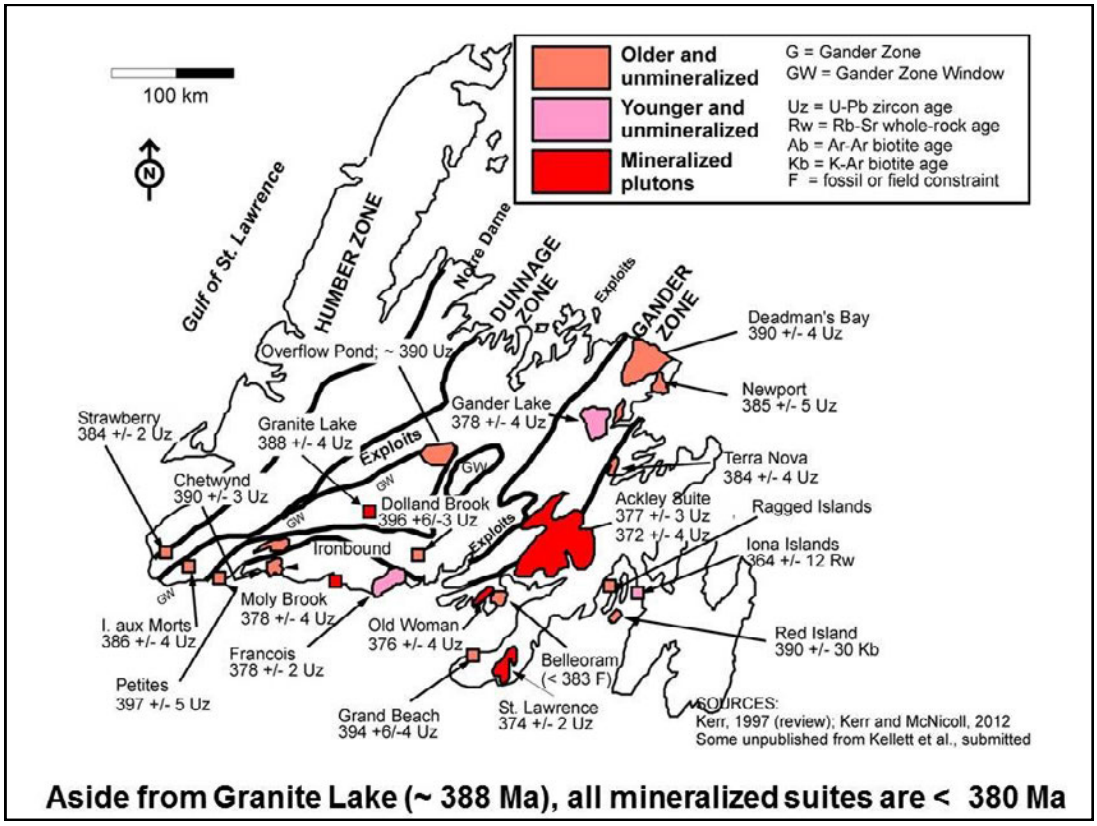
Older and unmineralized
Younger and unmineralized
Mineralized plutons
G = Gander Zone
GW = Gander Zone Window
Uz = U-Pb zircon age
Rw = Rb-Sr whole-rock age
Ab = Ar-Ar biotite age
Kb = K-Ar biotite age
F = fossil or field constraint
100 km
N
Gulf of St. Lawrence
HUMBER ZONE
Notre Dame
DUNNAGE ZONE
Exploits
GANDER ZONE
Deadman's Bay 390 +/- 4 Uz
Overflow Pond; ~ 390 Uz
Newport 385 +/- 5 Uz
Strawberry 384 +/- 2 Uz
Granite Lake 388 +/- 4 Uz
Gander Lake 378 +/- 4 Uz
Terra Nova 384 +/- 4 Uz
Chetwynd 390 +/- 3 Uz
Dolland Brook 396 +6/-3 Uz
Ackley Suite 377 +/- 3 Uz
372 +/- 4 Uz
Ragged Islands
Ironbound
Iona Islands 364 +/- 12 Rw
Moly Brook 378 +/- 4 Uz
I. aux Morts 386 +/- 4 Uz
Old Woman 376 +/- 4 Uz
Red Island 390 +/- 30 Kb
Francois 378 +/- 2 Uz
Belleoram (< 383 F)
Petites 397 +/- 5 Uz
Grand Beach 394 +6/-4 Uz
St. Lawrence 374 +/- 2 Uz
SOURCES:
Kerr, 1997 (review); Kerr and McNicoll, 2012
Some unpublished from Kellett et al., submitted
Aside from Granite Lake (~ 388 Ma), all mineralized suites are < 380 Ma

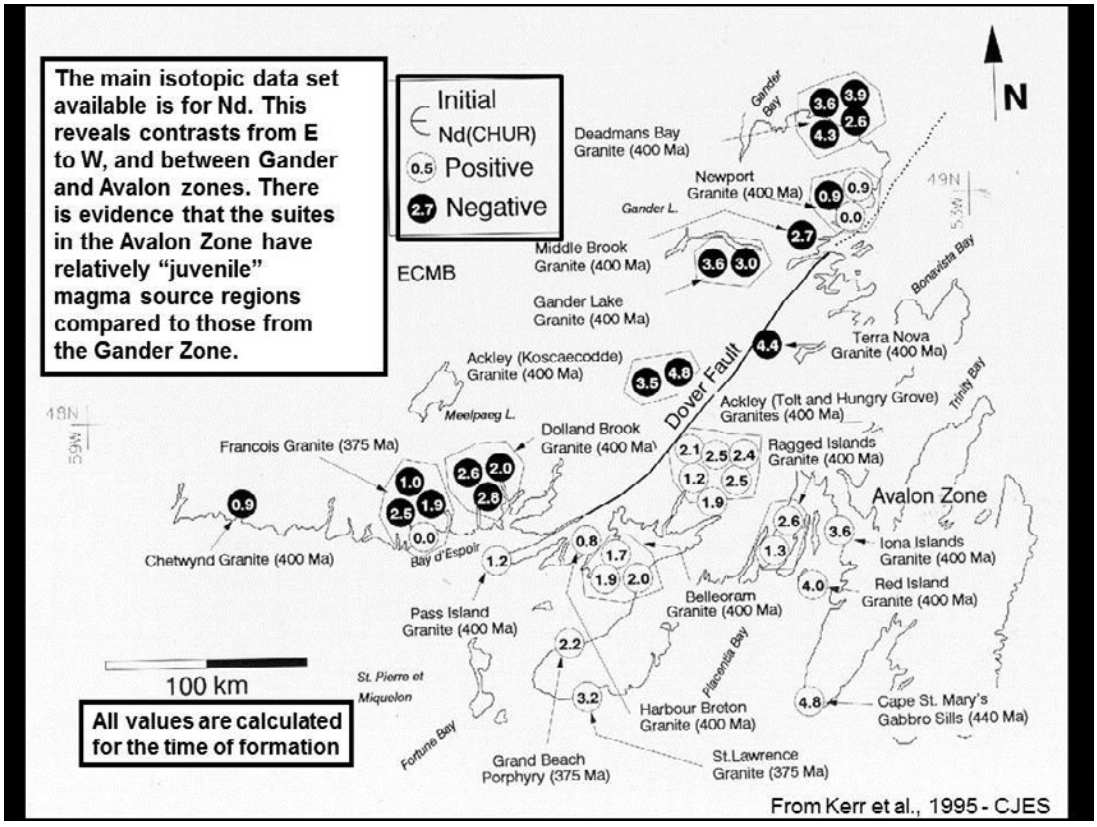
The main isotopic data set available is for Nd. This reveals contrasts from E to W, and between Gander and Avalon zones. There is evidence that the suites in the Avalon Zone have relatively "juvenile" magma source regions compared to those from the Gander Zone.
Initial Nd(CHUR)
0.5 Positive
2.7 Negative
ECMB
N
Deadmans Bay Granite (400 Ma)
Newport Granite (400 Ma)
Middle Brook Granite (400 Ma)
Gander Lake Granite (400 Ma)
Terra Nova Granite (400 Ma)
Ackley (Koscaecodde) Granite (400 Ma)
Ackley (Tolt and Hungry Grove) Granites (400 Ma)
Dover Fault
Dolland Brook Granite (400 Ma)
Francois Granite (375 Ma)
Ragged Islands Granite (400 Ma)
Avalon Zone
Chetwynd Granite (400 Ma)
Iona Islands Granite (400 Ma)
Red Island Granite (400 Ma)
Belleoram Granite (400 Ma)
Pass Island Granite (400 Ma)
Harbour Breton Granite (400 Ma)
Cape St. Mary's Gabbro Sills (440 Ma)
St.Lawrence Granite (375 Ma)
Grand Beach Porphyry (375 Ma)
100 km
All values are calculated for the time of formation
From Kerr et al., 1995 - CJES

Mo (+ Sn) Mineralization in the Ackley Granite and adjacent plutonic suites

- This is largely "endocontact" mineralization that is associated with high-level evolved granites and in some cases greisen-like rocks.
- Little modern exploration – depth potential limited.

Rugged country along the southern edge of the Ackley Granite

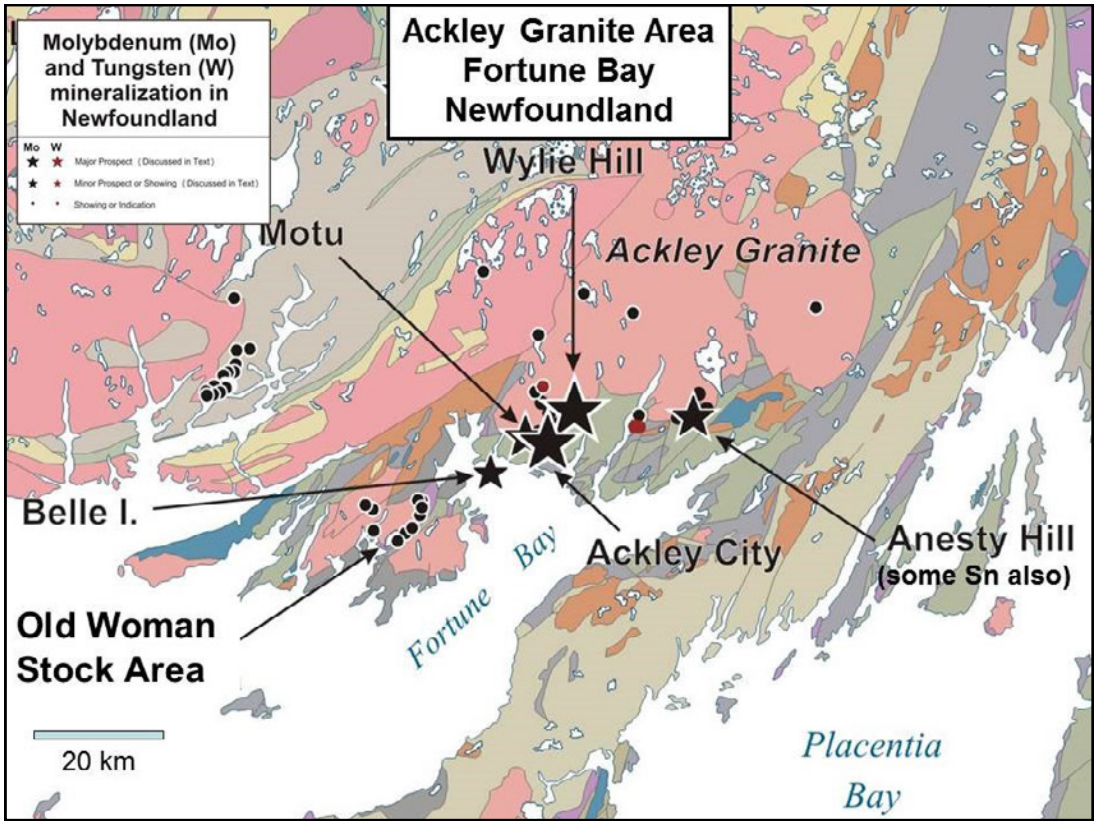

Molybdenum – Ackley Granite and Area

- Discovered in the 1880s, and evaluated through underground exploration in the 1930s. The resource here is small, but grades are locally good - 0.4% Mo.
- Mineralization is located in the roof zone of the granites, at its southern contact – associated with alaskitic granite, pegmatite and greisens.
- Mo is syngenetic, local association with Fe-Cu sulphides. Geochemical gradients in underlying granitic rocks, with no mineralization at depth.
- Low-grade Sn mineralization is associated with topaz greisens, with little Mo present; the relation between these and the Mo zones is not clear.
- Moly in the "Old Woman Stock" is broadly similar.

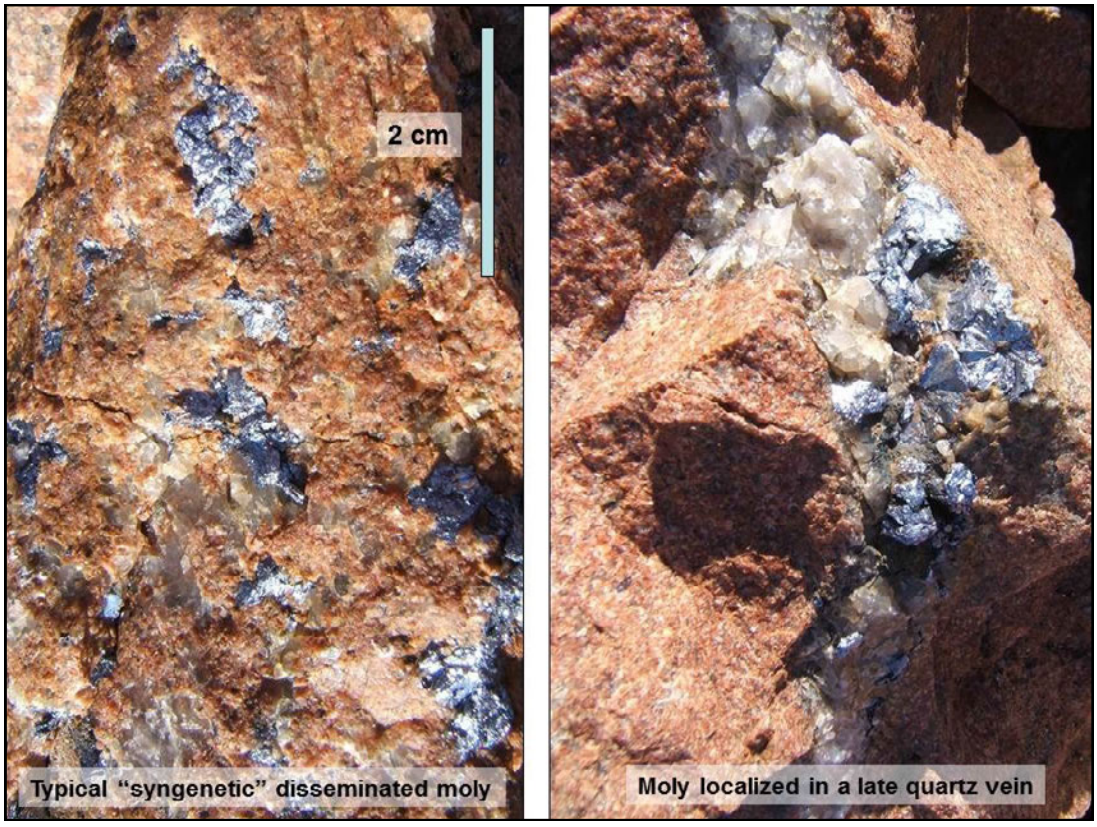

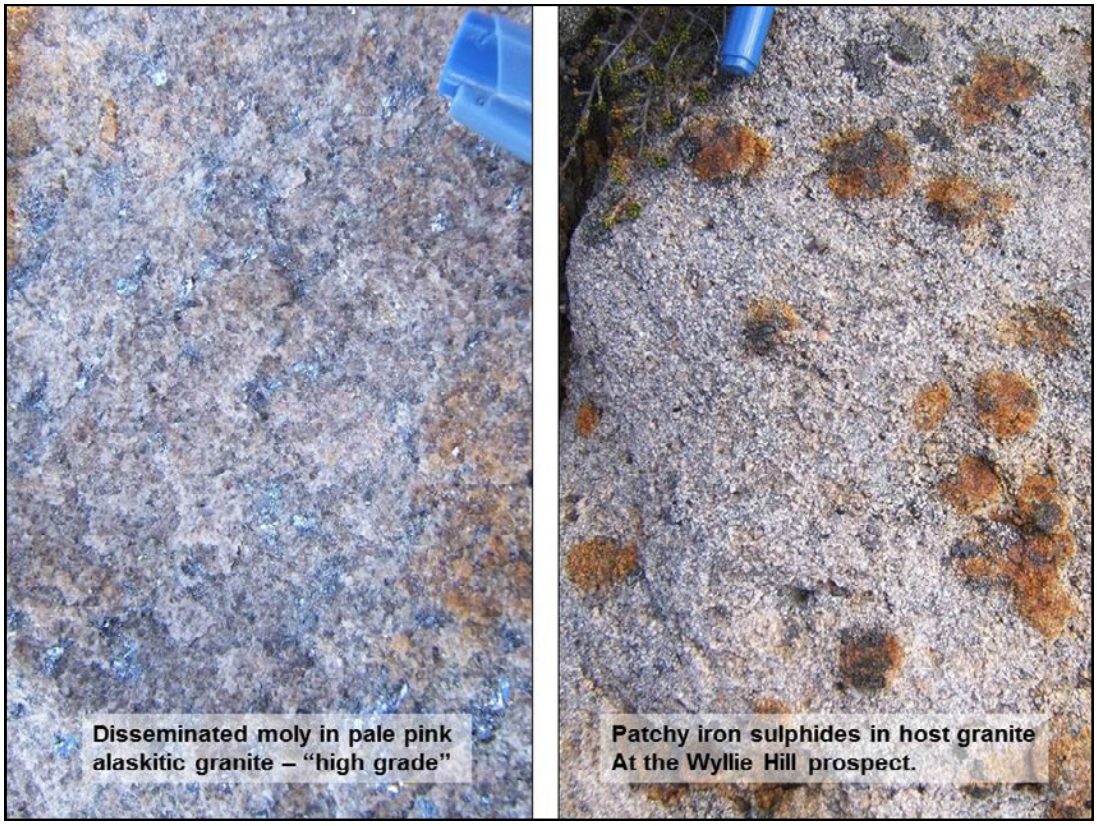

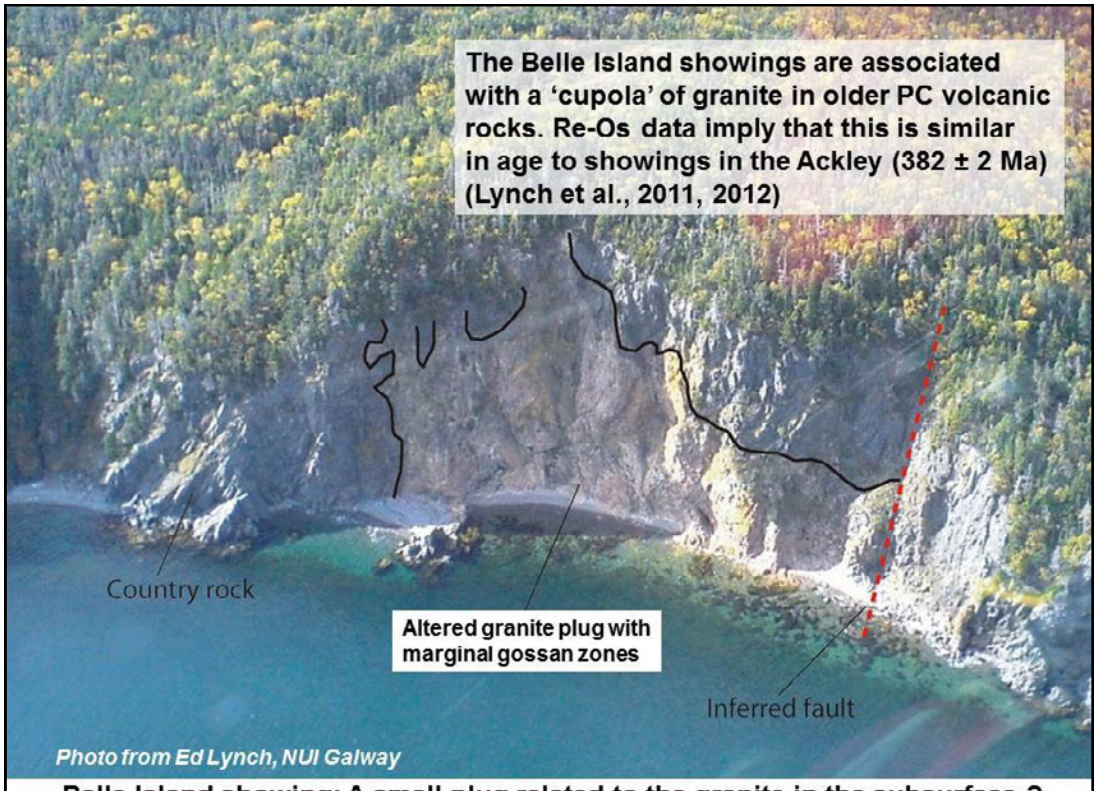

Belle Island showing: A small plug related to the granite in the subsurface ?

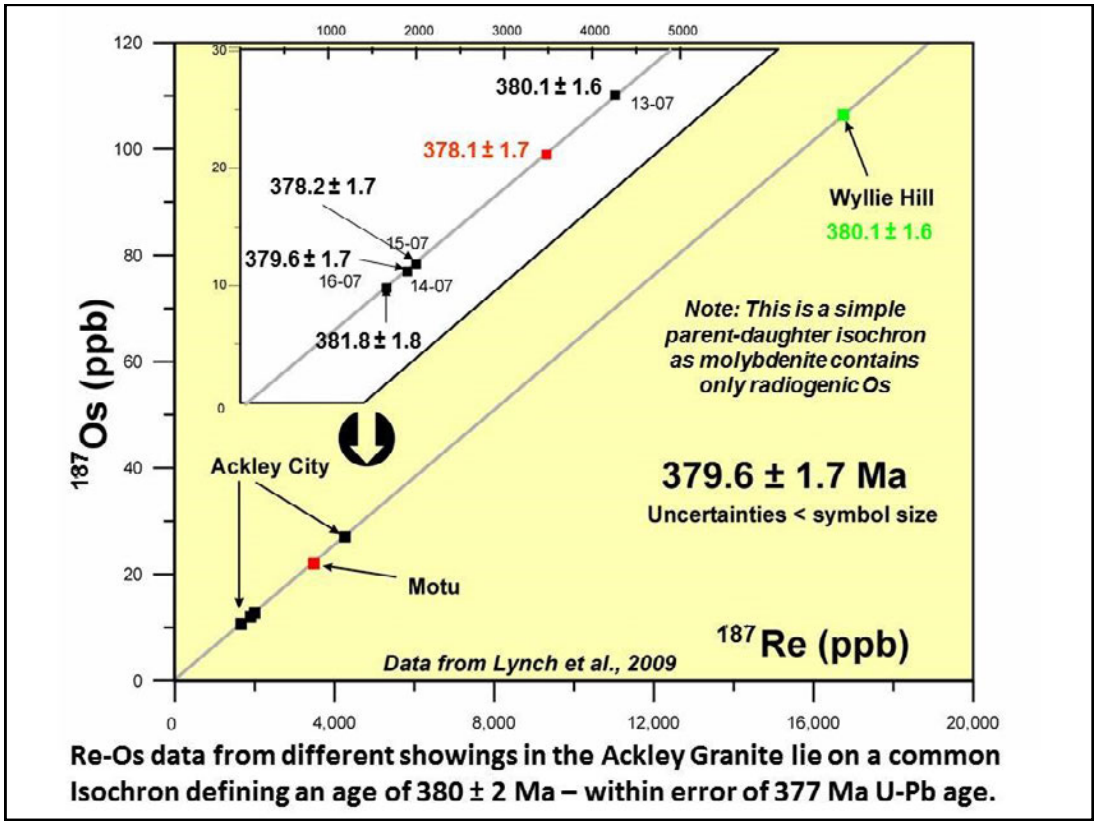

Re-Os data from different showings in the Ackley Granite lie on a common Isochron defining an age of 380 ± 2 Ma – within error of 377 Ma U-Pb age.

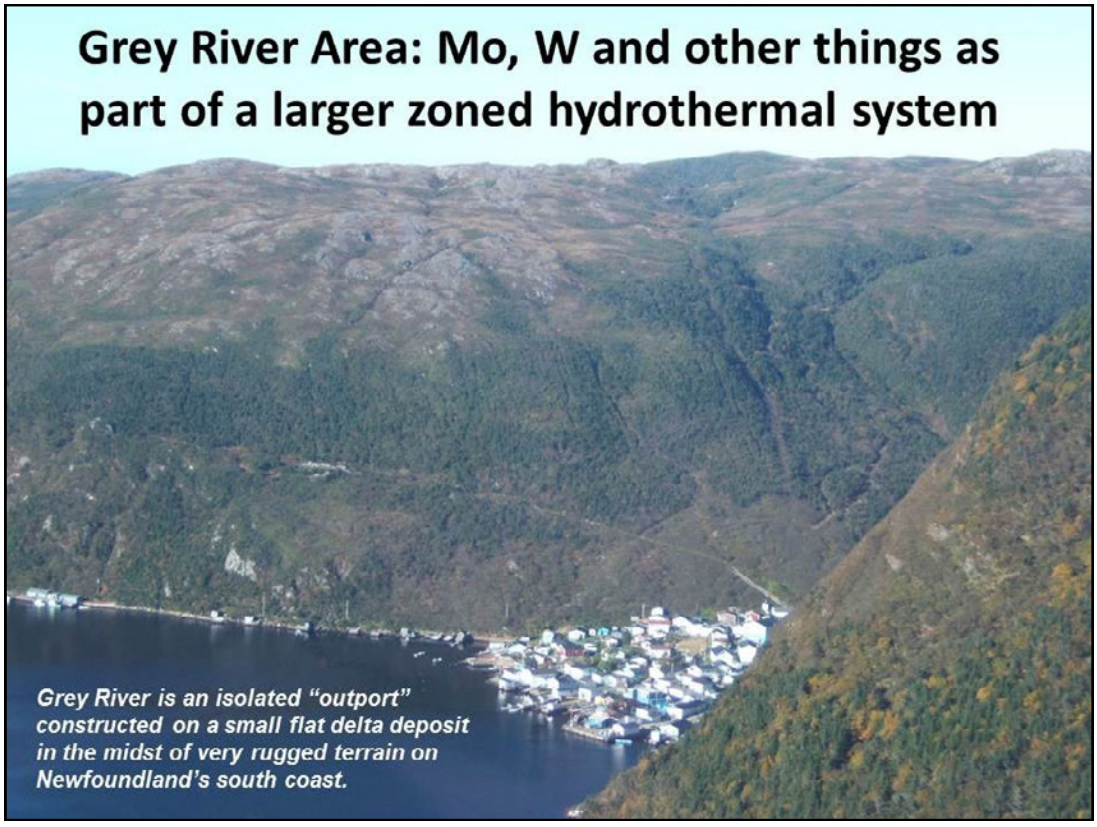

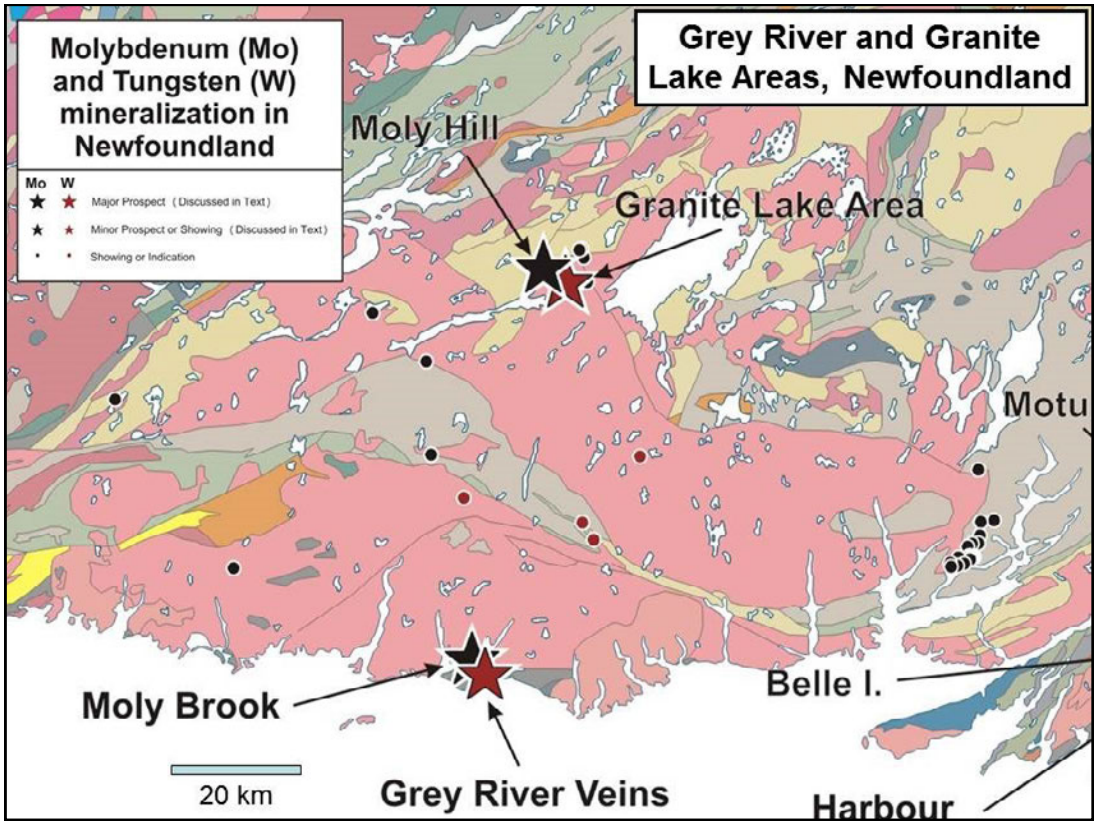

Mineralization in the Grey River Area

- The area is known mostly for wolframite in quartz veins, discovered in the 1950s. Numerous base-metal (± Ba) veins are known. Low-grade Mo-Cu discovered in the 1980s was evaluated in more detail from 2007-09; W veins were also reassessed at that time.
- Mo-Cu associated with sheeted quartz veins/stock-works hosted in older (Early Devonian) granite. Mineralized granite veins imply a younger buried pluton, now confirmed by geochronology.
- The 'Moly Brook' deposit is a large, low-grade resource that remains open – long intersections (e.g., 370 m at 0.084% Mo) suggest potential for growth.
- Total resource of 120 Mt at 0.063% Mo (May 2009).

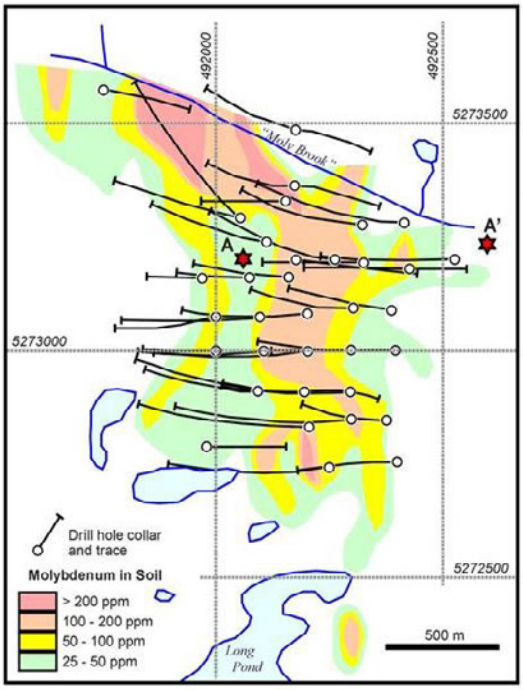

Plan view and generalized cross-section of the Moly Brook Deposit

Modified after Tenajon Resources (press releases and website)

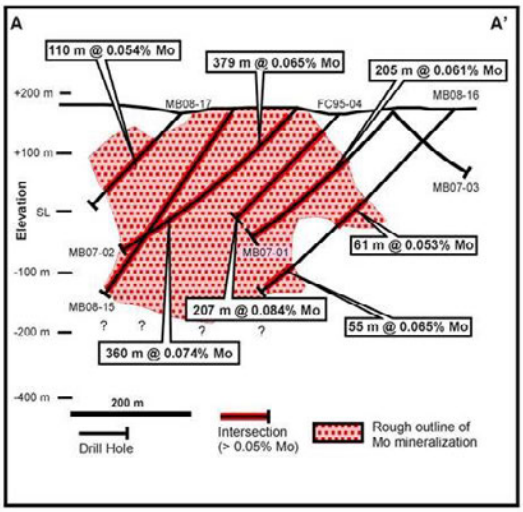

Total resource estimate of about 118 Mt at 0.063% Mo (73% indicated, 151 million lbs of Mo) at a cut off grade of 0.04% Mo (PR, May 2009).

Quartz veins with two main trends cutting altered K-feldspar porphyritic granite at Moly Brook – mineralization is associated almost entirely with vein systems

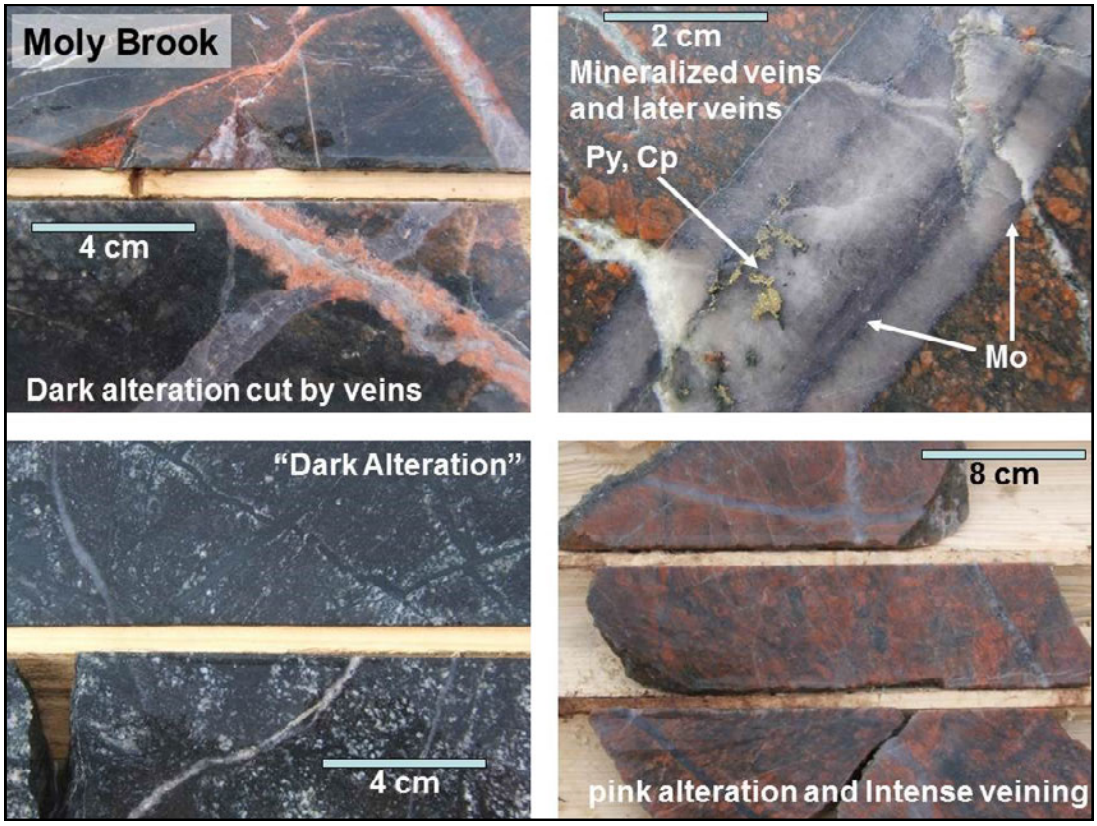

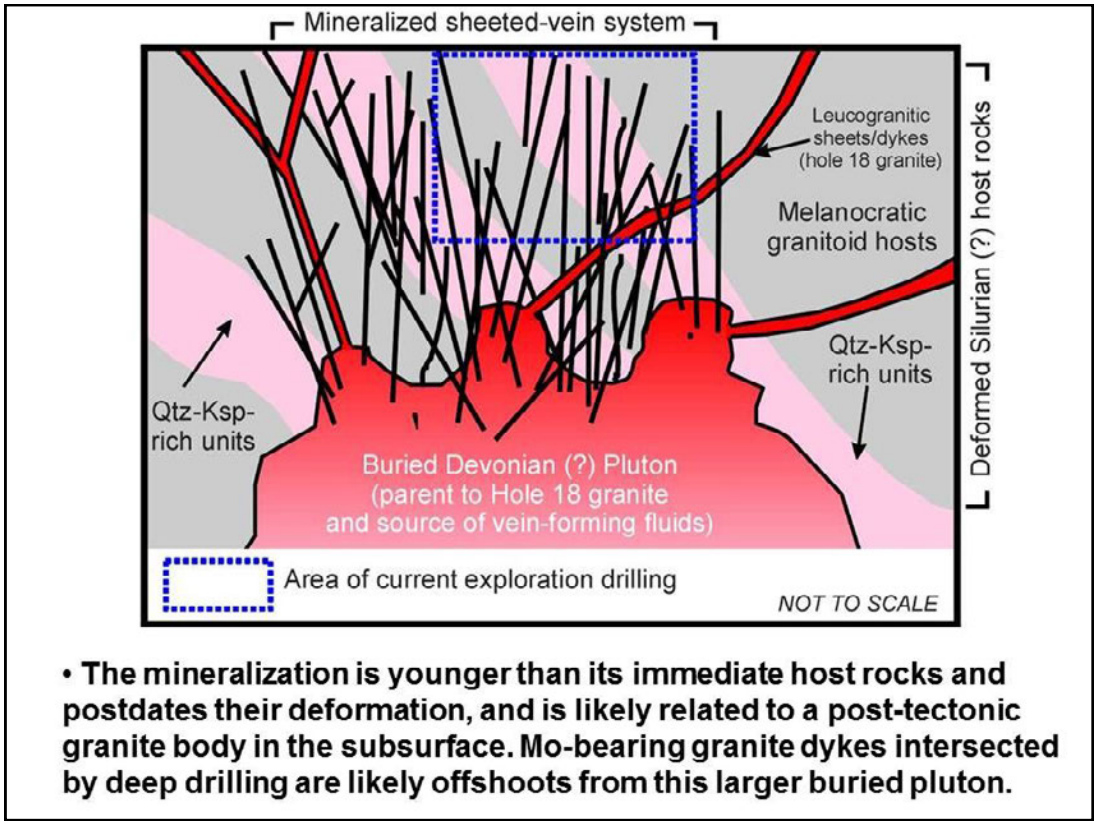

• The mineralization is younger than its immediate host rocks and postdates their deformation, and is likely related to a post-tectonic granite body in the subsurface. Mo-bearing granite dykes intersected by deep drilling are likely offshoots from this larger buried pluton.

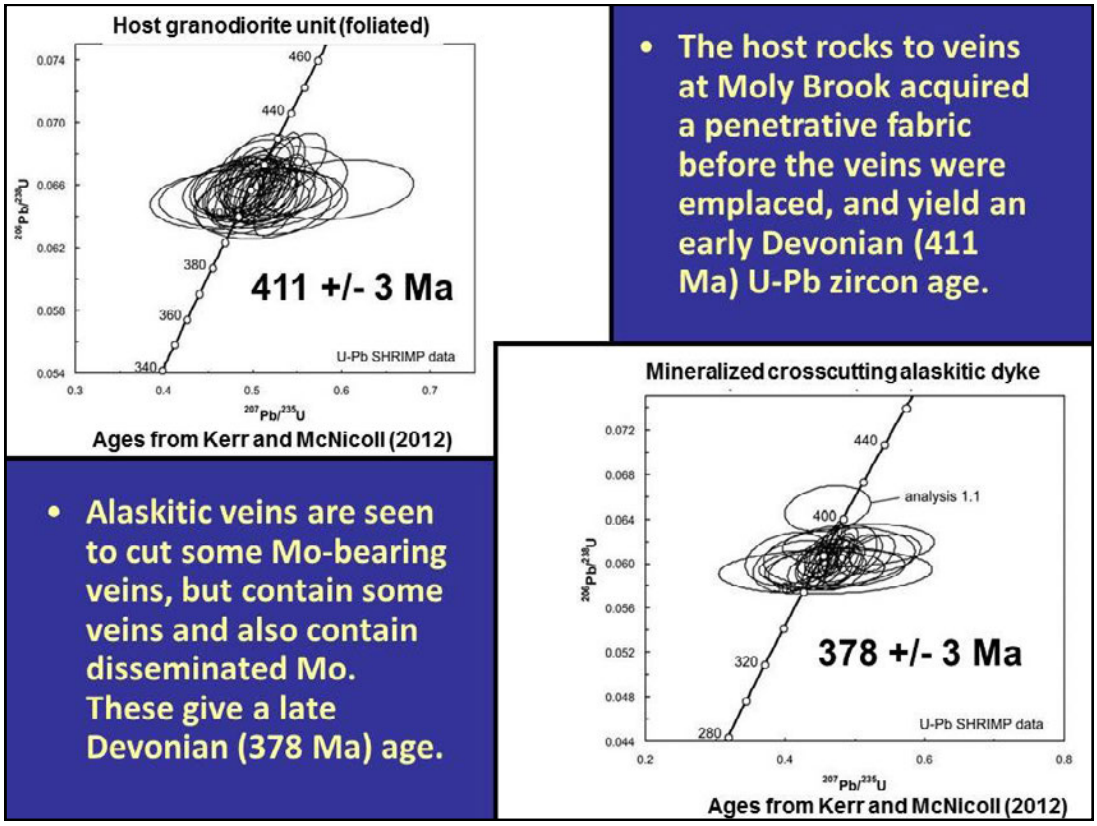
Host granodiorite unit (foliated)
411 +/- 3 Ma
U-Pb SHRIMP data
Ages from Kerr and McNicoll (2012)
• The host rocks to veins at Moly Brook acquired a penetrative fabric before the veins were emplaced, and yield an early Devonian (411 Ma) U-Pb zircon age.
• Alaskitic veins are seen to cut some Mo-bearing veins, but contain some veins and also contain disseminated Mo. These give a late Devonian (378 Ma) age.
Mineralized crosscutting alaskitic dyke
analysis 1.1
378 +/- 3 Ma
U-Pb SHRIMP data
Ages from Kerr and McNicoll (2012)

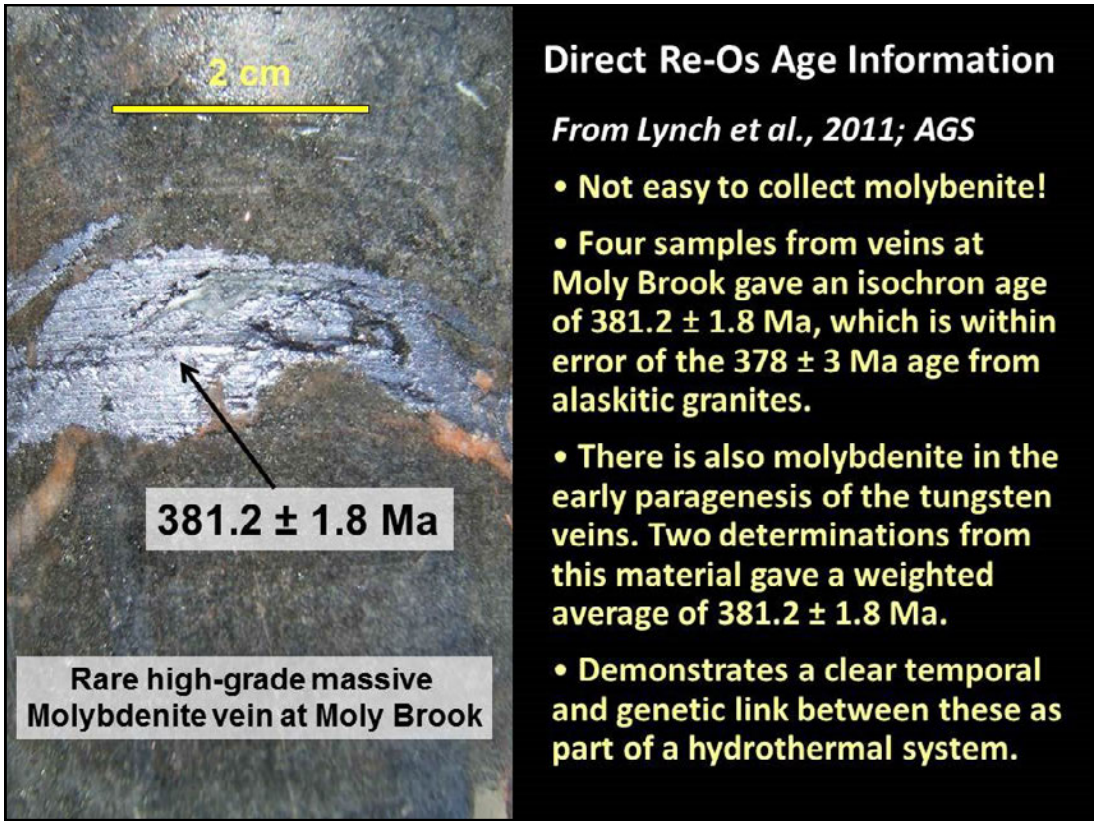
2 cm
381.2 ± 1.8 Ma
Rare high-grade massive Molybdenite vein at Moly Brook
Direct Re-Os Age Information
From Lynch et al., 2011; AGS
• Not easy to collect molybenite!
• Four samples from veins at Moly Brook gave an isochron age of 381.2 ± 1.8 Ma, which is within error of the 378 ± 3 Ma age from alaskitic granites.
• There is also molybdenite in the early paragenesis of the tungsten veins. Two determinations from this material gave a weighted average of 381.2 ± 1.8 Ma.
• Demonstrates a clear temporal and genetic link between these as part of a hydrothermal system.

Research Potential at the Moly Brook Deposit

- This is an area where there is good evidence of a link between Mo-Cu-W and a largely hidden granite body.
- Exploration is now dormant but there is a large amount of geo-chemical and geophysical data available in assessment reports that are now public domain.
- This includes IP data, magnetic data; also large amounts of measured geochemical data from multielement assays.
- Excellent resource for research applications.

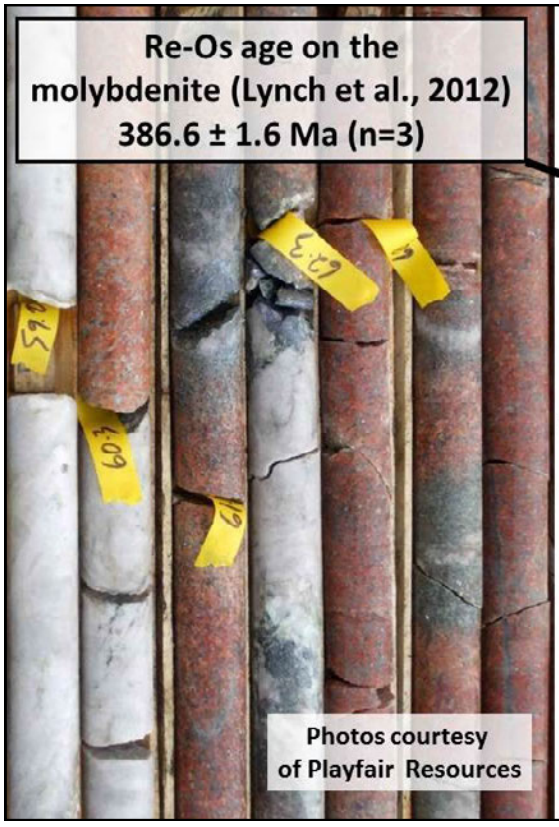

- Mineralization in the Granite Lake area is not as well defined in terms of resources, but seems similar in many respects. Possibly deeper – seems to be as veins in granite (388 ± 4 Ma; U-Pb zr).

Fluorite, St. Lawrence
Galena and fluorite, St. Lawrence
Barite, Cape St. Mary's
Barite,
Collier Point

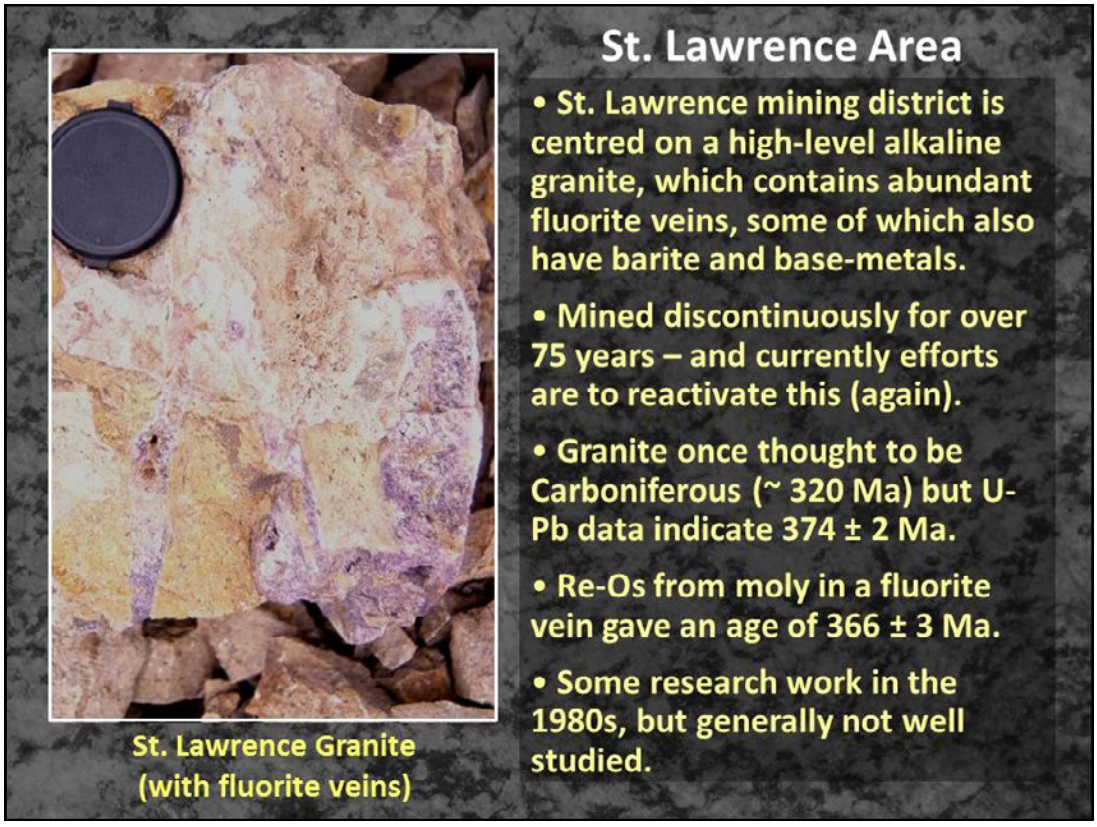
St. Lawrence Area
• St. Lawrence mining district is centred on a high-level alkaline granite, which contains abundant fluorite veins, some of which also have barite and base-metals.
• Mined discontinuously for over 75 years – and currently efforts are to reactivate this (again).
• Granite once thought to be Carboniferous (~ 320 Ma) but U-Pb data indicate 374 ± 2 Ma.
• Re-Os from moly in a fluorite vein gave an age of 366 ± 3 Ma.
• Some research work in the 1980s, but generally not well studied.
St. Lawrence Granite
(with fluorite veins)

Traditionally, most work was conducted where the wall rocks are the granite.....

New resources defined at the Grebes Nest vein occur in sedimentary wall rocks – these open new possibilities for exploration.

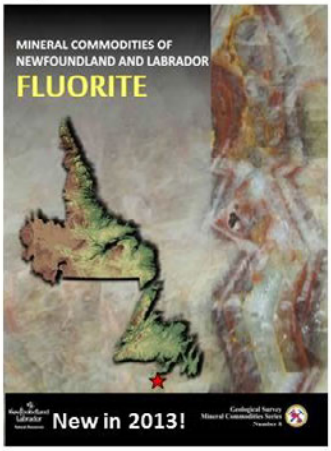

High-grade fluorite intersection in Grebes Nest vein (Canada Fluorspar)

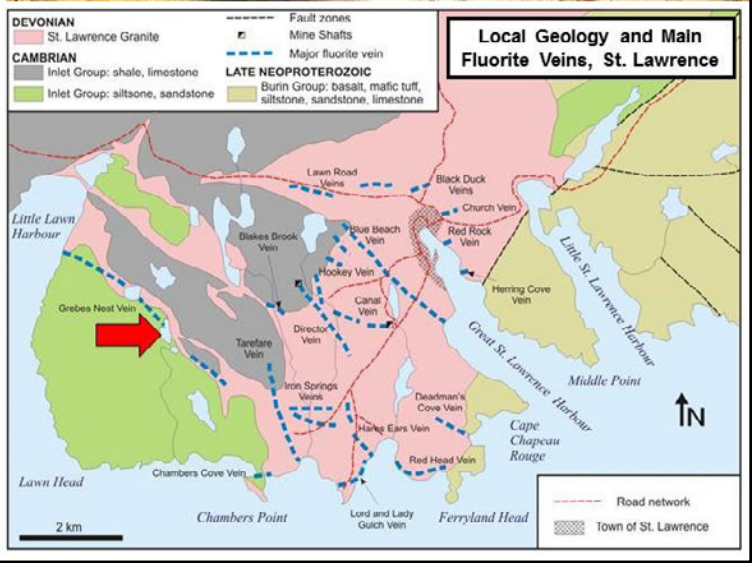

Southwest Avalon Peninsula Area

- The site of some of the earliest mining ventures in Newfoundland – centred on vein-style base metal deposits (mostly Pb-Zn +/- Ag) and barite.
- Geophysical data suggests a large Paleozoic batholith in this area, even though surface expression is limited.
- Minor production from La Manche (Pb) and from Collier Point (Ba); potential remains in the latter.
- Other minor showings across the region (e.g., Mo near St. John's, fluorite in Placentia Bay *might* have some connection to Paleozoic magmatism.
- Much of the research to date is through B.Sc. Theses.

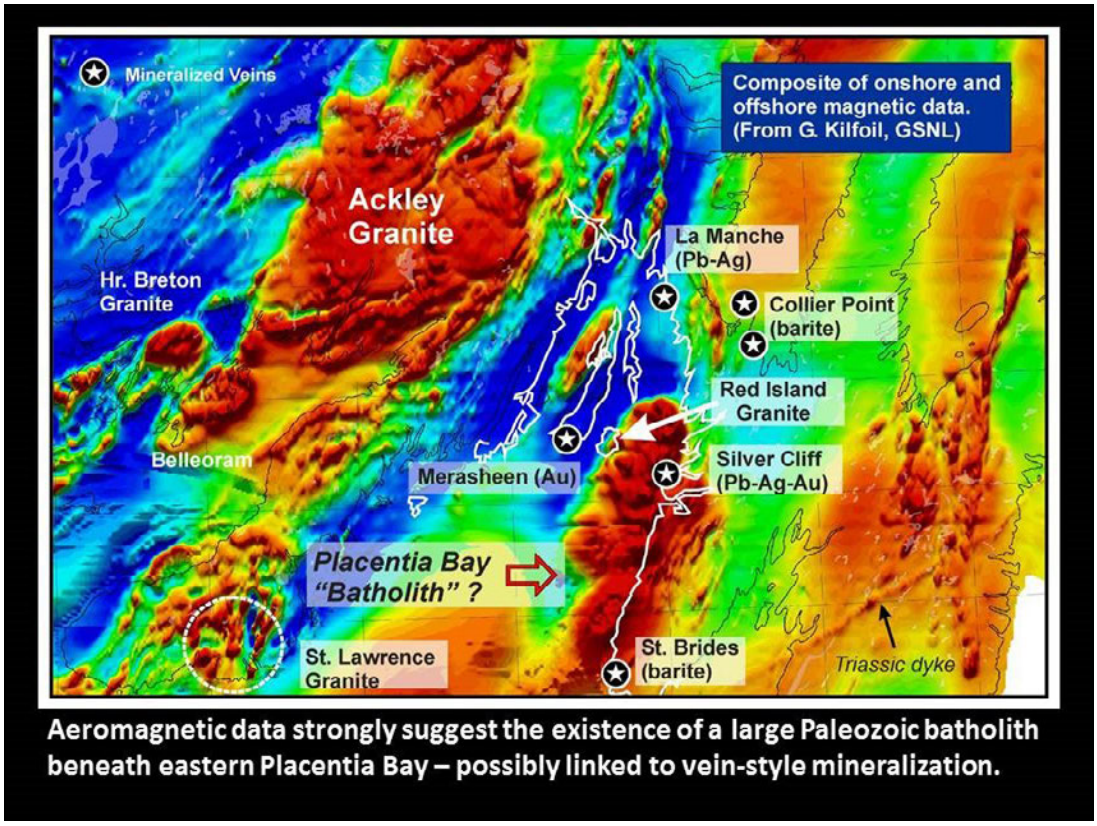

Aeromagnetic data strongly suggest the existence of a large Paleozoic batholith beneath eastern Placentia Bay – possibly linked to vein-style mineralization.

Galena- and sphalerite-bearing vein material, La Manche area.

Barite vein within normal fault cutting Cambrian sedimentary rocks and also Silurian (?) or Devonian (?) dykes , St. Brides.

Summary – Regional Characteristics

- Southern Newfoundland hosts diverse granophile mineralization, most of which seems to be linked to late Devonian (ca. 380 Ma) magmatism.
- The most deeply eroded examples lie in the Ackley Gramite and other areas close to the G-A boundary.
- Elsewhere, associated plutonic suites appear to be in the subsurface – mineralization is largely associated with vein swarms and discrete vein systems.
- Historical production from fluorite and barite veins, but resources occur elsewhere (Moly Brook).
- Moly Brook also represents an interesting research opportunity, in which new work could be linked to an extensive exploration database.

Other Questions and Potential Topics

- The new U-Pb and Re-Os data improve resolution of timing constraints, but some remain unpublished.
- Are there regional controls imposed on fertility by the nature of basement terranes? I think not, but this is difficult to prove. More data needed!
- Understanding of magma sources would be better with regional data for isotopic systems other than Nd. I think I might have suggested this before…..
- Is there potential to use mineral chemistry as a tool for regional exploration?
- Does deeper erosion eliminate mineral potential in the northeast Gander Zone area?

Acknowledgements
Ed Lynch – Geological Survey of Sweden
Sue & Bill Scott – GeoScott Exploration
Dave Visagie – Tenajon Resources
Neil Briggs – Playfair Mining
Derek Wilton – Memorial University
Vicki McNicoll – GSC Geochron Lab
David Selby – Durham University, UK
Connaigre Peninsula,
South coast of Newfoundland
Thank You !

Mineralogy and chemistry of tourmaline in the Woodjam porphyry deposits, British Columbia

J.B. Chapman

Geological Survey of Canada, 605 Robson Street, Vancouver, British Columbia

Abstract: Tourmaline is a common accessory and gangue mineral in a diverse range of hydrothermal ore-forming systems covering a broad spectrum of pressure, temperature and chemical conditions, reflecting tourmaline's wide stability range. Previous studies, dating back into the 1960s, have shown that tourmaline can very closely track changes in physicochemical conditions within the fluid from which it is precipitated. Tourmaline's refractory and resistant physical properties mean that the mineral is able to preserve this information through numerous subsequent phases of metamorphism, alteration and weathering; in many cases tourmaline may be the only robust remaining record of original hydrothermal processes. Although tourmaline's utility in mineral exploration has been demonstrated, very few studies have attempted to measure concentrations of the ore metals themselves. In general, these limitations have been imposed by the common use of EPMA alone to interrogate mineral chemistry at high spatial resolution.

In many porphyry-related deposits of the South American Cordillera, tourmaline occurrences are abundant and extensive, and have attracted much interest for use during mineral deposit exploration. However, owing to various factors including differences in their tectonic settings and magma chemistries, porphyry-related deposits of the Canadian Cordillera rarely report significant tourmaline among their mineral inventory. Consequently, studies of tourmaline associated with Canadian deposits are limited, and almost no data exist on tourmaline occurrences associated with alkalic or hybrid alkalic - calc-alkalic systems. In this study we report mineralogical and LA-ICP-MS trace element analyses of tourmaline minerals from within the hybrid alkalic and calc-alkalic Woodjam porphyry Cu-Au deposits of central British Columbia. These minerals display significant variation in both their major and trace element compositions, reflecting both temporal and spatial evolution of the magmatic- hydrothermal fluids from which the deposit formed. Tourmaline associated with high-temperature potassic alteration has greater schorl (i.e., Fe-rich) component and trace element abundances characteristic of the core of a porphyry hydrothermal system, while tourmaline recovered in association with distal, lower-temperature, albite-rich alteration has an increased dravitic (i.e., Mg-rich) component and a distinct trace element suite. Tourmaline recovered in intimate association with chalcopyrite mineralization has a pronounced blue colour and increased copper content. Hence, within the Woodjam and other similar deposits it may be possible to use tourmaline mineralogy and chemistry as a vector to mineralization. In addition, careful analysis of tourmaline recovered from surficial samples (till, soil, etc.) may provide detailed information on the type and abundance of any concealed mineralized body.

Originally presented Fredericton 2014: Geological Association of Canada - Mineralogical Association of Canada Joint Annual Meeting, Special Session 3: Discovering the Next Generation of Porphyry Deposits: Advancements in Locating and Understanding Hidden Intrusion-related Mineralization. May 21, 2014.

Corresponding author: John B. Chapman (john.chapman@nrcan-rncan.gc.ca)

Chapman, J.B., 2015. Mineralogy and chemistry of tourmaline in the Woodjam porphyry deposits, British Columbia; *in* TGI 4 – Intrusion Related Mineralisation Project: New Vectors to Buried Porphyry-Style Mineralisation, (ed.) N. Rogers; Geological Survey of Canada, Open File 7843, p. 403-413.

GAC-MAC 2014
Fredericton, NB
May 21, 2014

Tourmaline in the Woodjam porphyry deposits, British Columbia

John B. Chapman
Geological Survey of Canada

Natural Resources Canada | Ressources naturelles Canada

Canada

Why use tourmaline?

- 'Tourmaline' is not a single mineral, but a related group
- Common gangue and matrix mineral in porphyry deposits
- Occur over a wide range of temperatures and pressures
- Structurally and chemically complex, versatile geological record
- Chemically and physically resistent, will preserve data

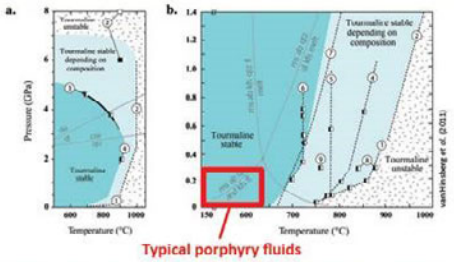

Typical porphyry fluids

Tourmalines are stable over a very wide range of pressures and temperatures. They are therefore well able to record and preserve porphyry-related ore-forming processes.

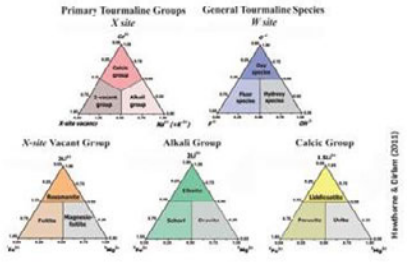

$XY_3Z_6[T_6O_{18}][BO_3]_3V_3W$

The tourmaline crystal structure contains numerous sites that can accommodate a large number of different elements. Major element variation in the Y site results in the major species present in porphyry environments:

Dravite: $NaMg_3Al_6Si_6O_{18}(BO_3)_3(OH)_3(OH)$
Schorl: $NaFe_3Al_6Si_6O_{18}(BO_3)_3(OH)_3(OH)$
Elbaite: $Na(Li_{1.5}Al_{1.5})_3Al_6Si_6O_{18}(BO_3)_3(OH)_3(OH)$

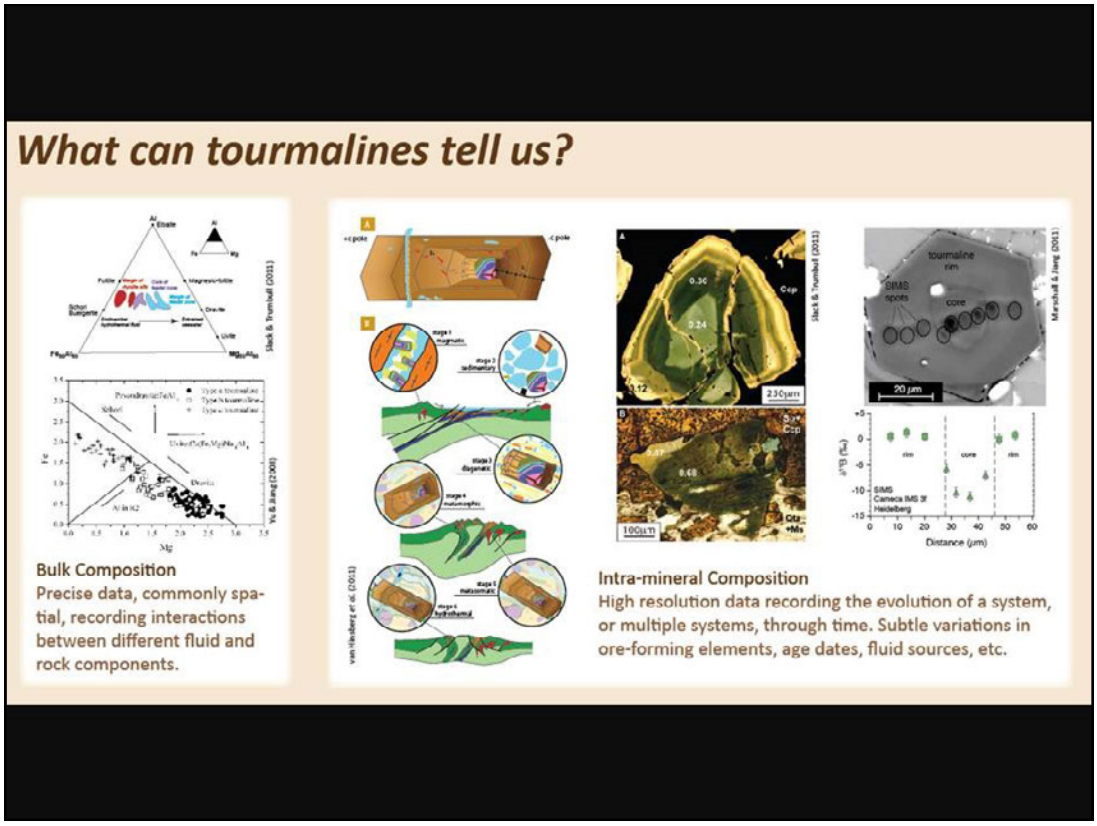
What can tourmalines tell us?
Bulk Composition
Precise data, commonly spatial, recording interactions between different fluid and rock components.
Intra-mineral Composition
High resolution data recording the evolution of a system, or multiple systems, through time. Subtle variations in ore-forming elements, age dates, fluid sources, etc.

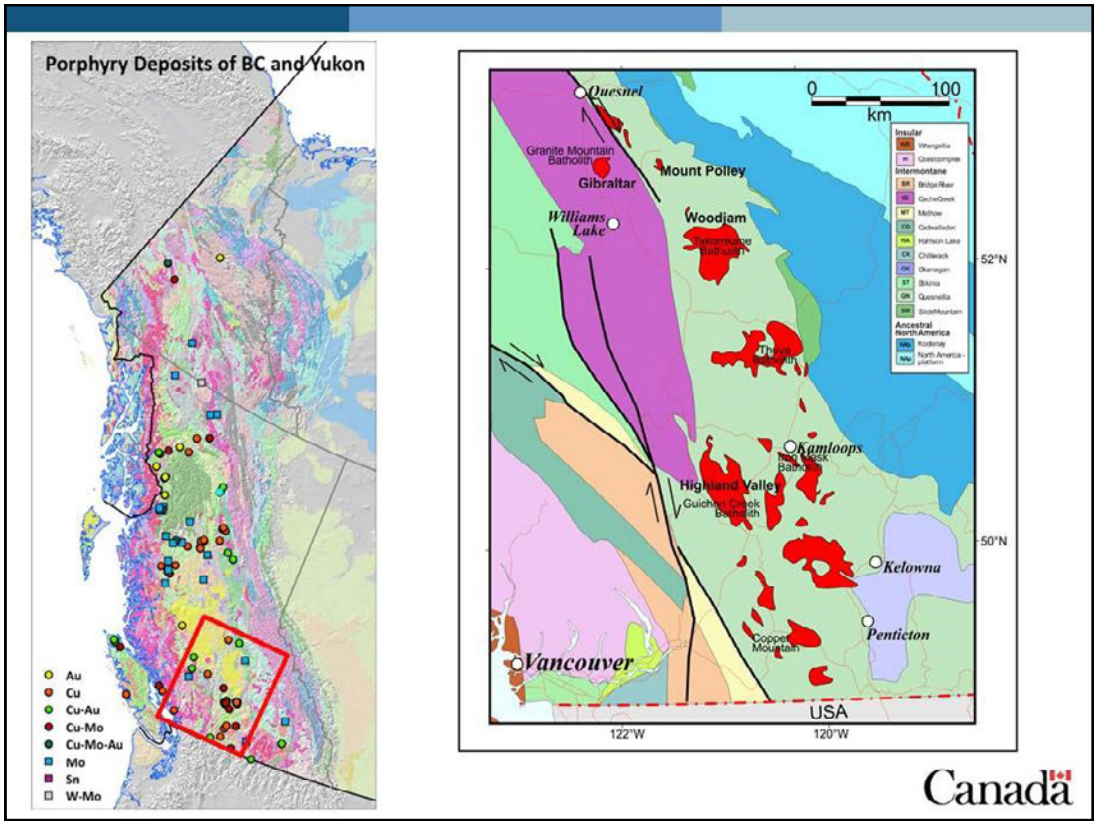
Porphyry Deposits of BC and Yukon
Au
Cu
Cu-Au
Cu-Mo
Cu-Mo-Au
Mo
Sn
W-Mo
Quesnel
Granite Mountain Batholith
Gibraltar
Mount Polley
Williams Lake
Woodjam
Highland Valley
Guichon Creek Batholith
Kamloops
Kelowna
Penticton
Vancouver
Copper Mountain
USA
0
100
km
52°N
50°N
122°W
120°W
Canada

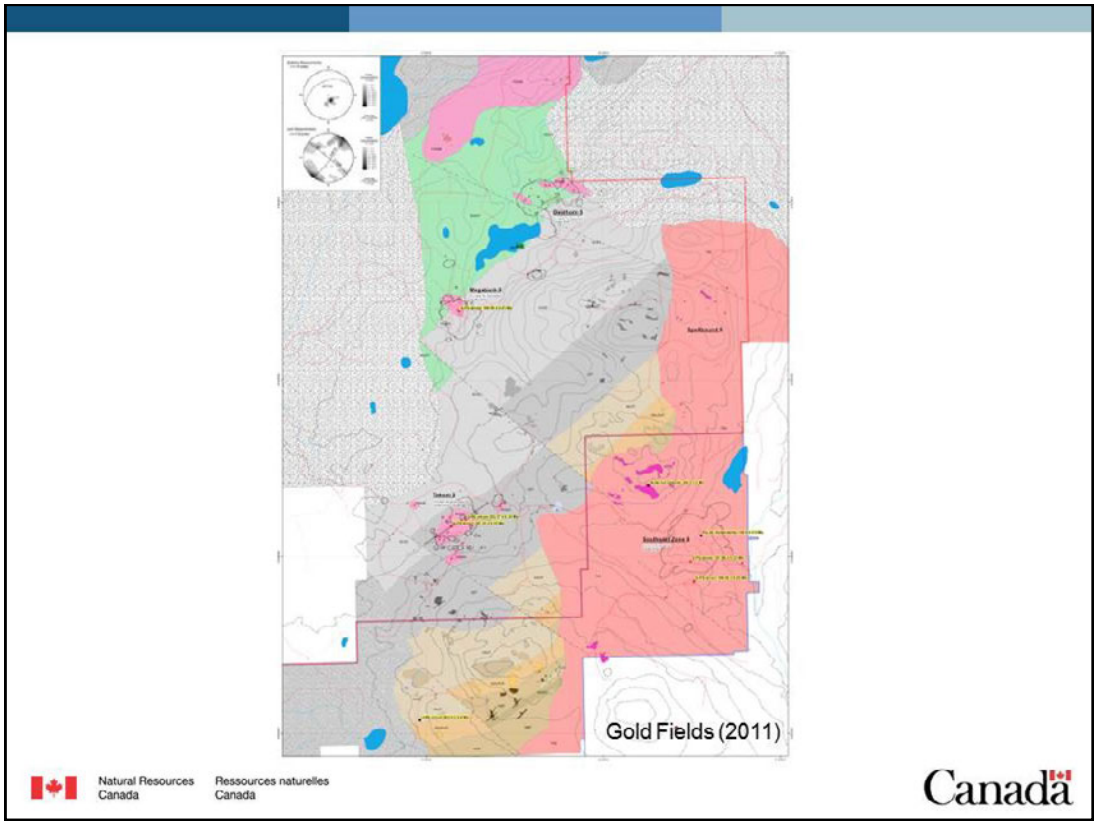
Gold Fields (2011)
Natural Resources Canada
Ressources naturelles Canada
Canada

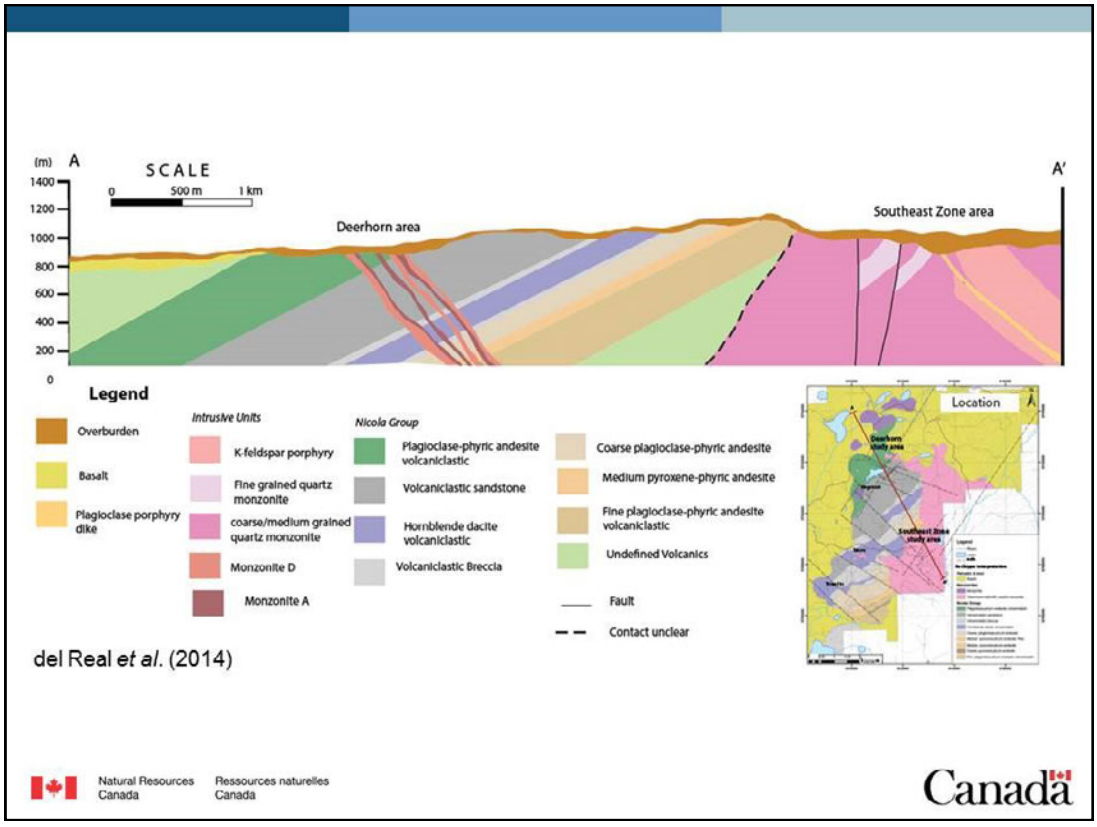
(m)
A
A'
SCALE
0
500 m
1 km
1400
1200
1000
800
600
400
200
0
Deerhorn area
Southeast Zone area
Legend
Overburden
Basalt
Plagioclase porphyry dike
Intrusive Units
K-feldspar porphyry
Fine grained quartz monzonite
coarse/medium grained quartz monzonite
Monzonite D
Monzonite A
Nicola Group
Plagioclase-phyric andesite volcaniclastic
Volcaniclastic sandstone
Hornblende dacite volcaniclastic
Volcaniclastic Breccia
Coarse plagioclase-phyric andesite
Medium pyroxene-phyric andesite
Fine plagioclase-phyric andesite volcaniclastic
Undefined Volcanics
Fault
Contact unclear
Location
del Real *et al.* (2014)
Natural Resources Canada
Ressources naturelles Canada
Canada

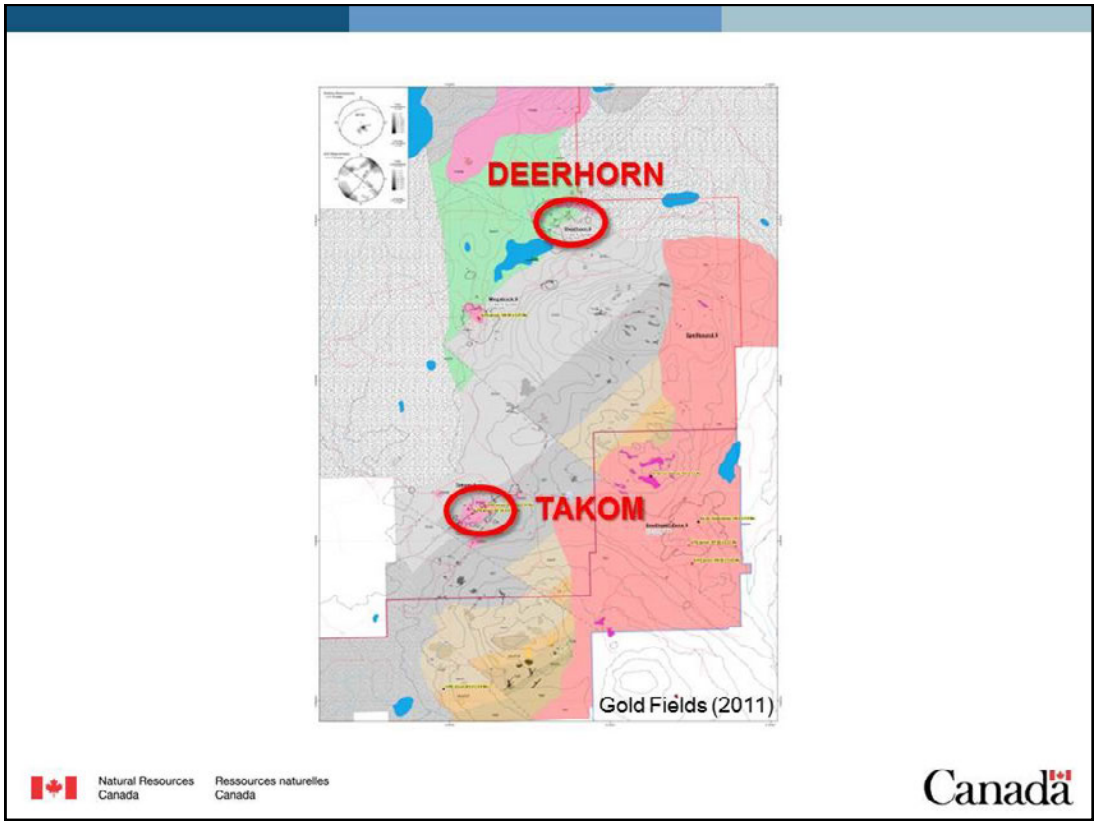
DEERHORN
TAKOM
Gold Fields (2011)
Natural Resources Canada
Ressources naturelles Canada
Canada

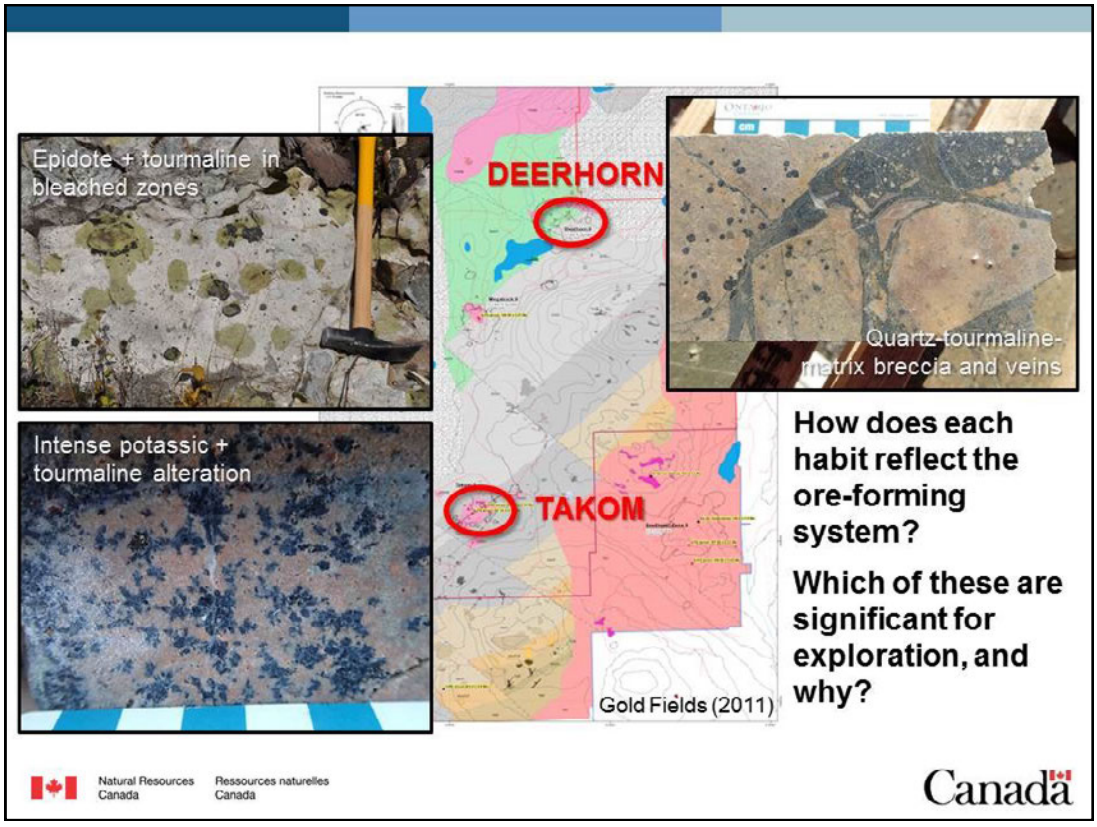
Epidote + tourmaline in bleached zones
Intense potassic + tourmaline alteration
DEERHORN
TAKOM
Quartz-tourmaline-matrix breccia and veins
How does each habit reflect the ore-forming system?
Which of these are significant for exploration, and why?
Gold Fields (2011)
Natural Resources Canada
Ressources naturelles Canada
Canada

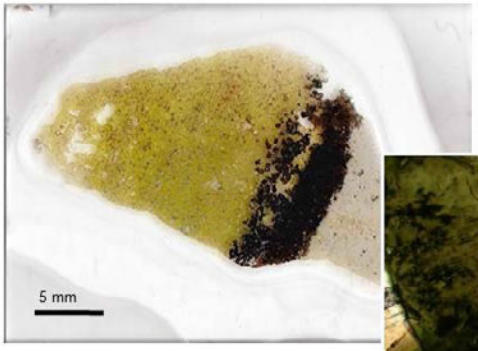

Dense, crystalline epidote (L) replacing bleached igneous host (R), no sulfide. Border between the two marked by dense tourmaline band, appears late.

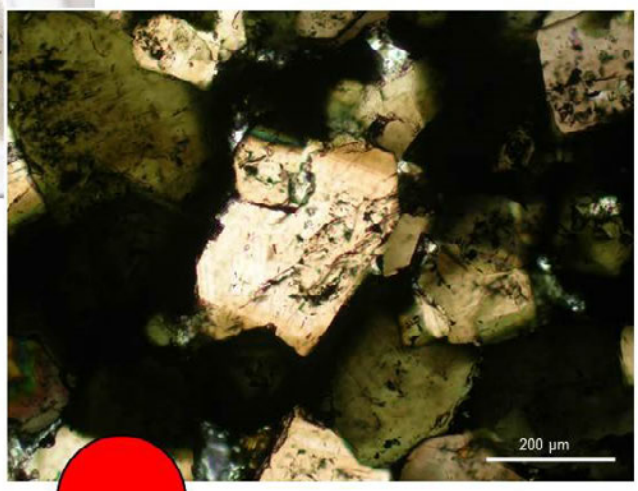

Tourmaline within the band is pale brown to black schorl. Outer growth zones are more intensely coloured.

Natural Resources Canada Ressources naturelles Canada

Canada

Tourmaline-quartz-pyrite veins. Potassic-altered host, with tourmaline-pyrite clots, no chalcopyrite.

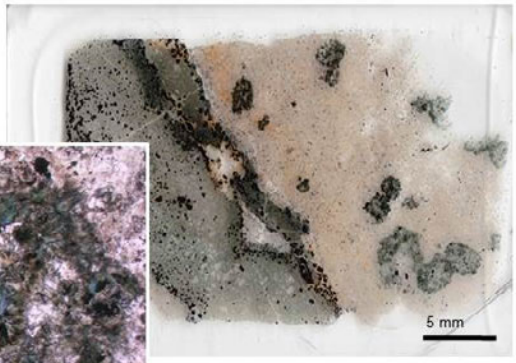

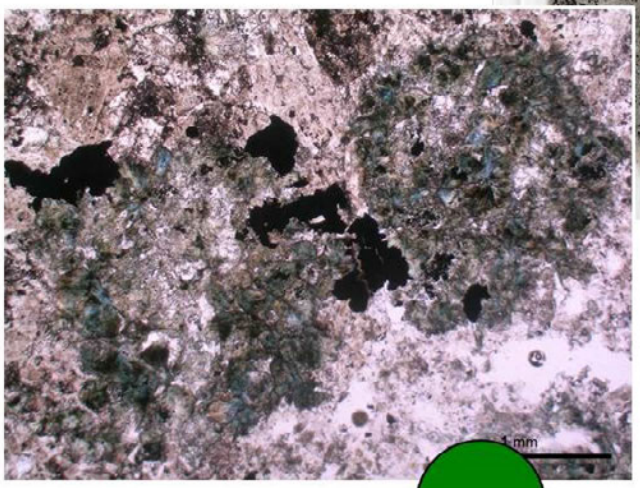

Tourmaline is dominantly fine, felted blue-green to green schorl to dravite.
Pyrite associated with periphery of tourmaline masses.

Natural Resources Canada Ressources naturelles Canada

Canada

Colourless to blue-green to blue tourmaline (species?). Crystals become increasingly blue toward distal terminations. Blue colouration linked to elevated Cu^{2+} content?

Intense potassic + tourmaline alteration. Fine, disseminated py+cpy mineralisation.

Natural Resources Canada Ressources naturelles Canada

Canada

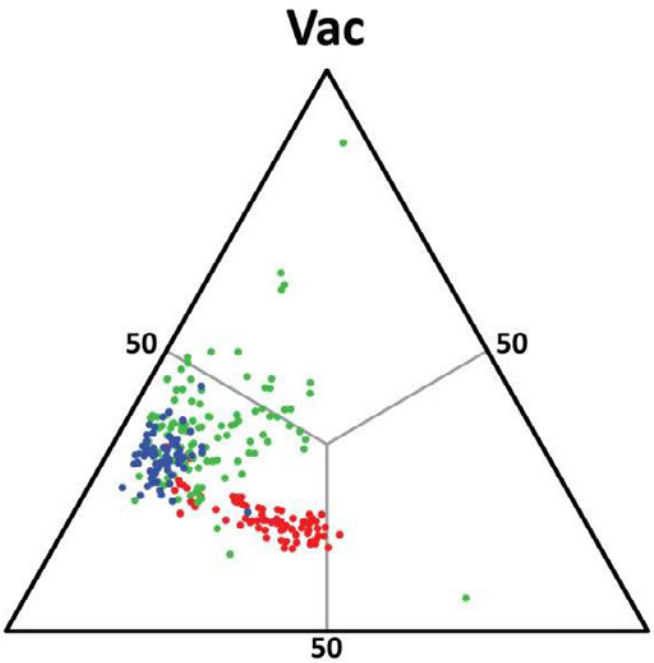

Natural Resources Canada Ressources naturelles Canada

Canada

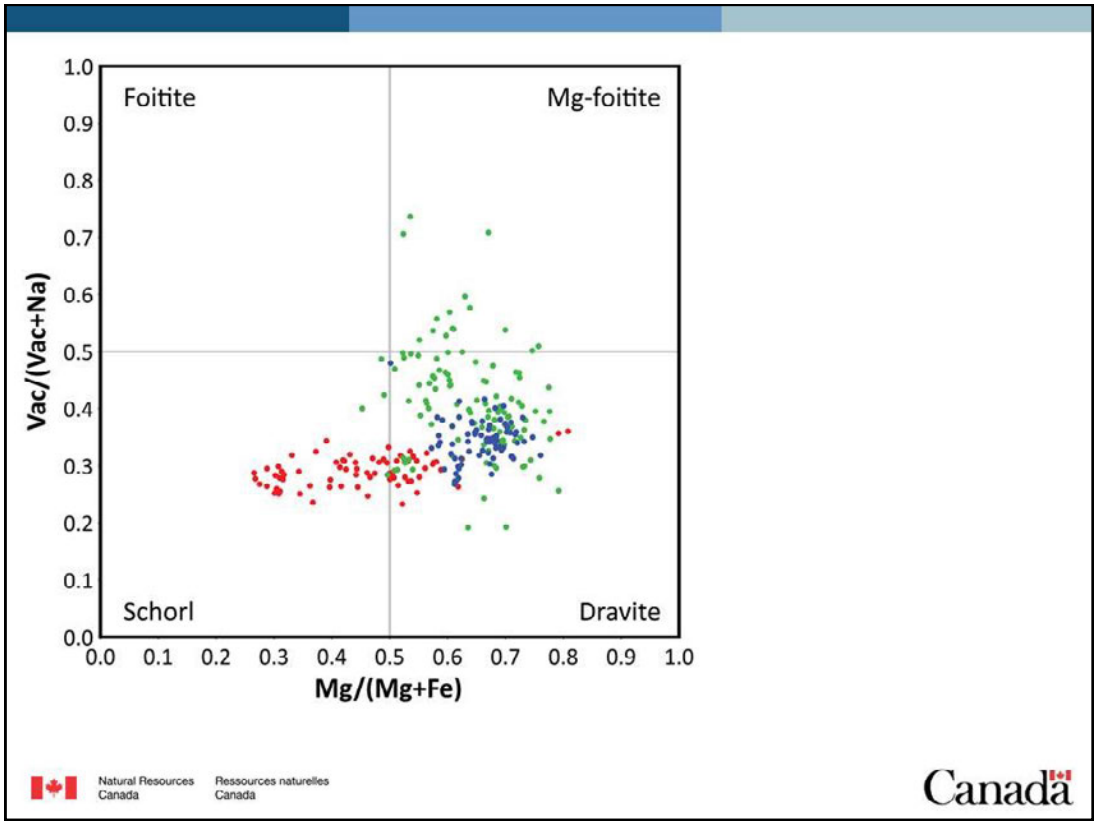
Foitite
Mg-foitite
Schorl
Dravite
Vac/(Vac+Na)
Mg/(Mg+Fe)
0.0
0.1
0.2
0.3
0.4
0.5
0.6
0.7
0.8
0.9
1.0
Natural Resources Canada
Ressources naturelles Canada
Canada

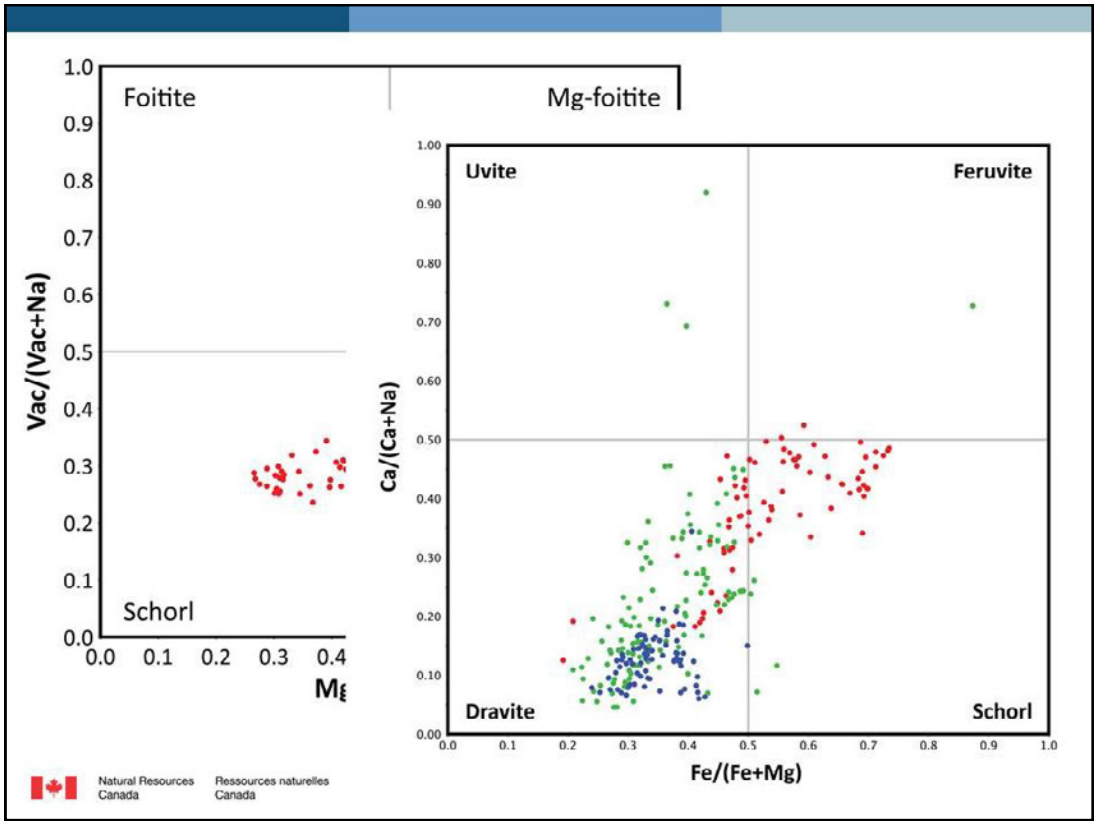
Foitite
Mg-foitite
Schorl
Vac/(Vac+Na)
Uvite
Feruvite
Dravite
Schorl
Ca/(Ca+Na)
Fe/(Fe+Mg)
0.00
0.10
0.20
0.30
0.40
0.50
0.60
0.70
0.80
0.90
1.00
Natural Resources Canada
Ressources naturelles Canada

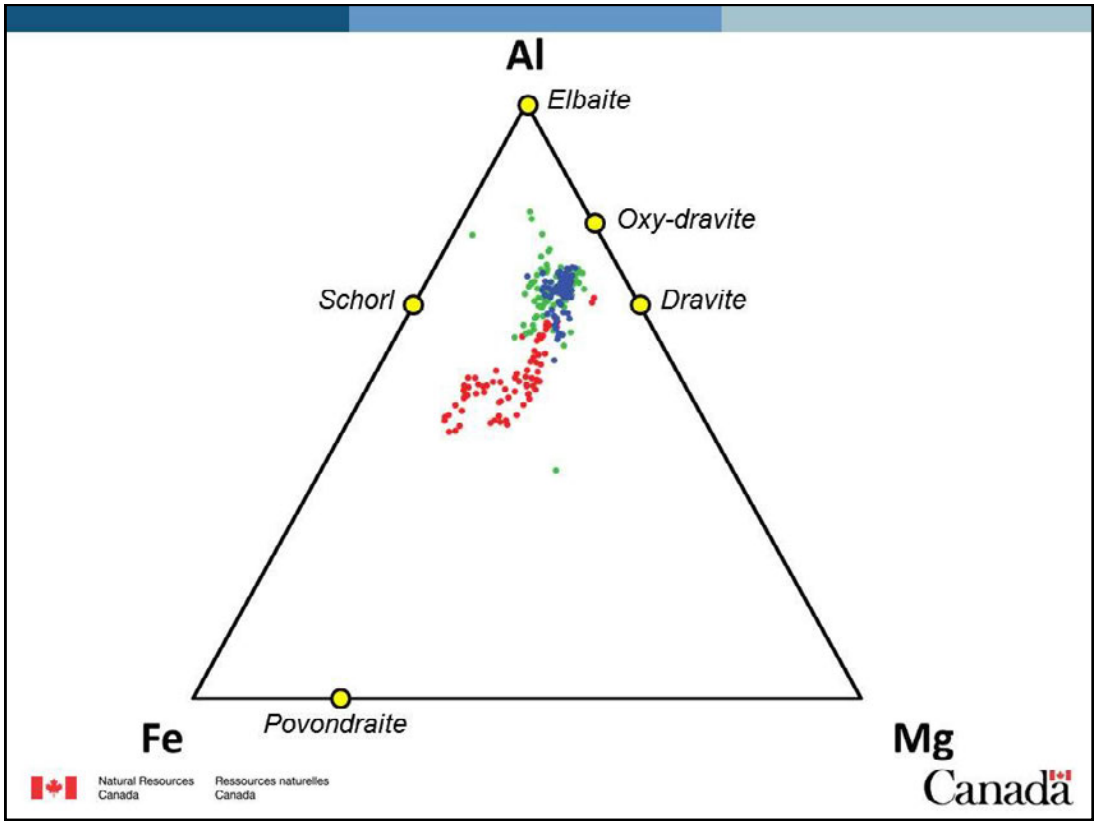
Al
Elbaite
Oxy-dravite
Schorl
Dravite
Fe
Povondraite
Mg
Natural Resources Canada
Ressources naturelles Canada
Canada

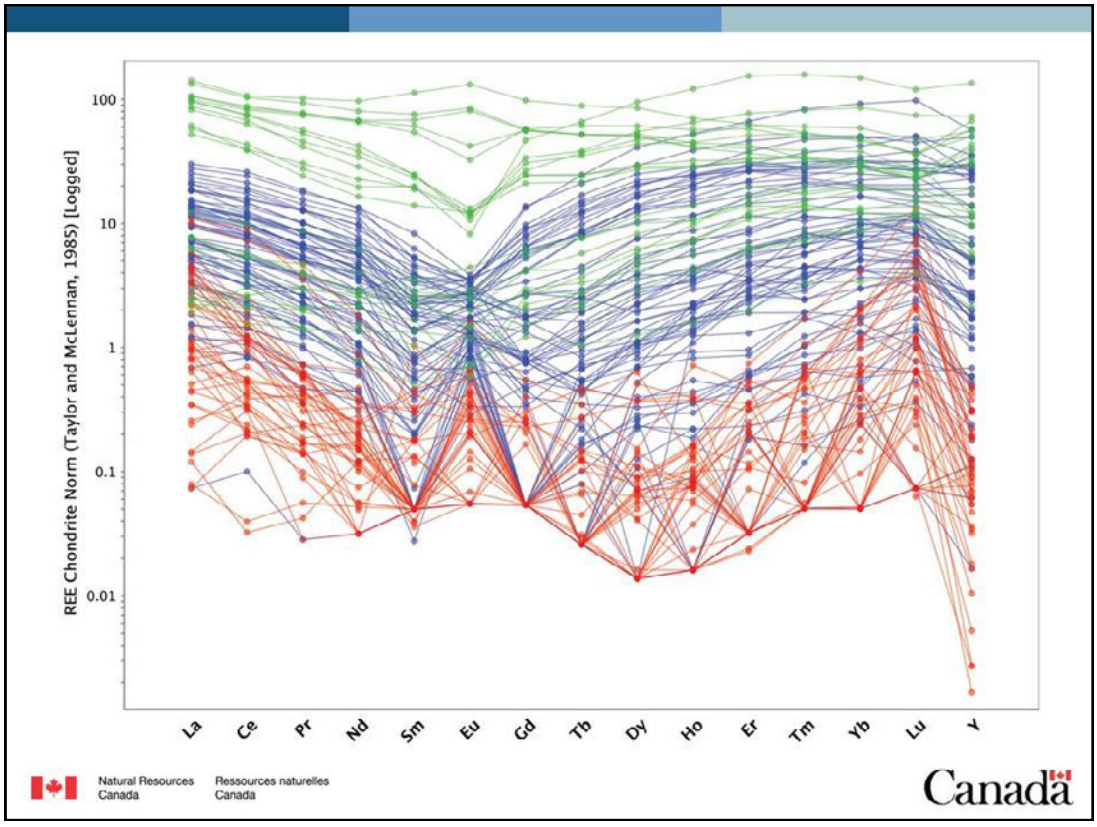
REE Chondrite Norm (Taylor and McLennan, 1985) [Logged]
100
10
1
0.1
0.01
La
Ce
Pr
Nd
Sm
Eu
Gd
Tb
Dy
Ho
Er
Tm
Yb
Lu
Y
Natural Resources Canada
Ressources naturelles Canada
Canada

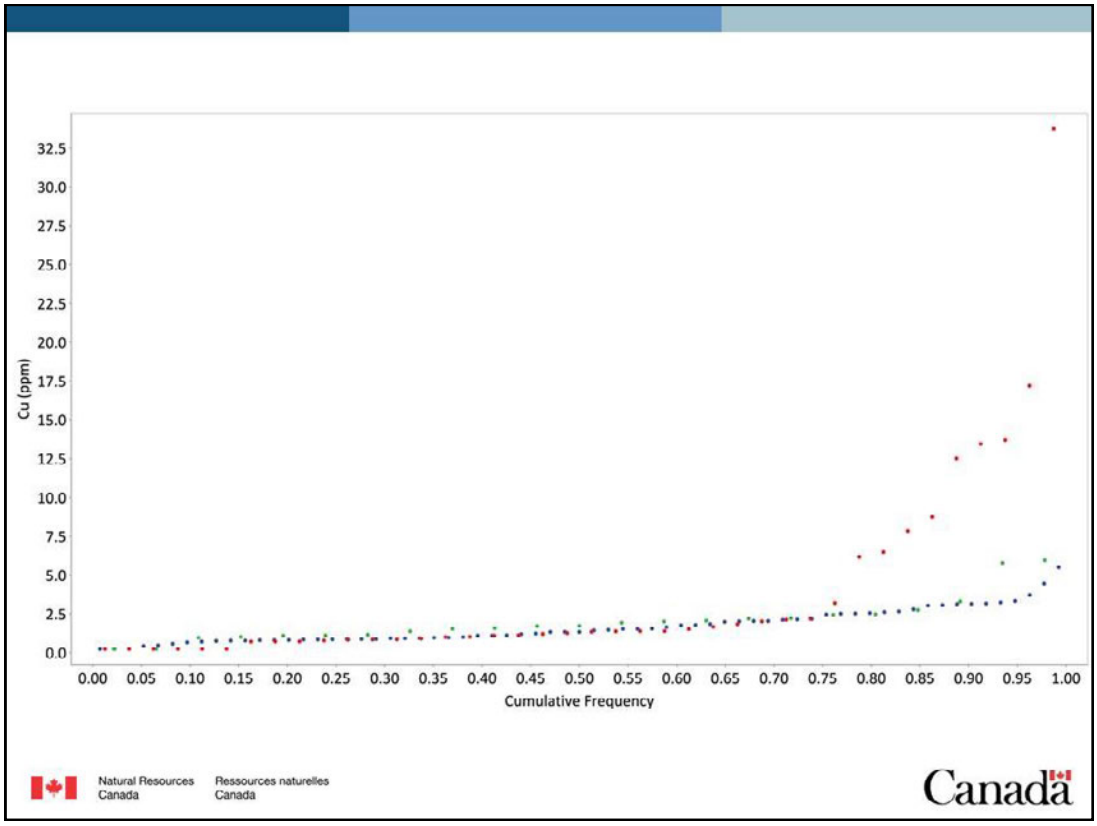
Cu (ppm)
Cumulative Frequency
Natural Resources Canada
Ressources naturelles Canada
Canada

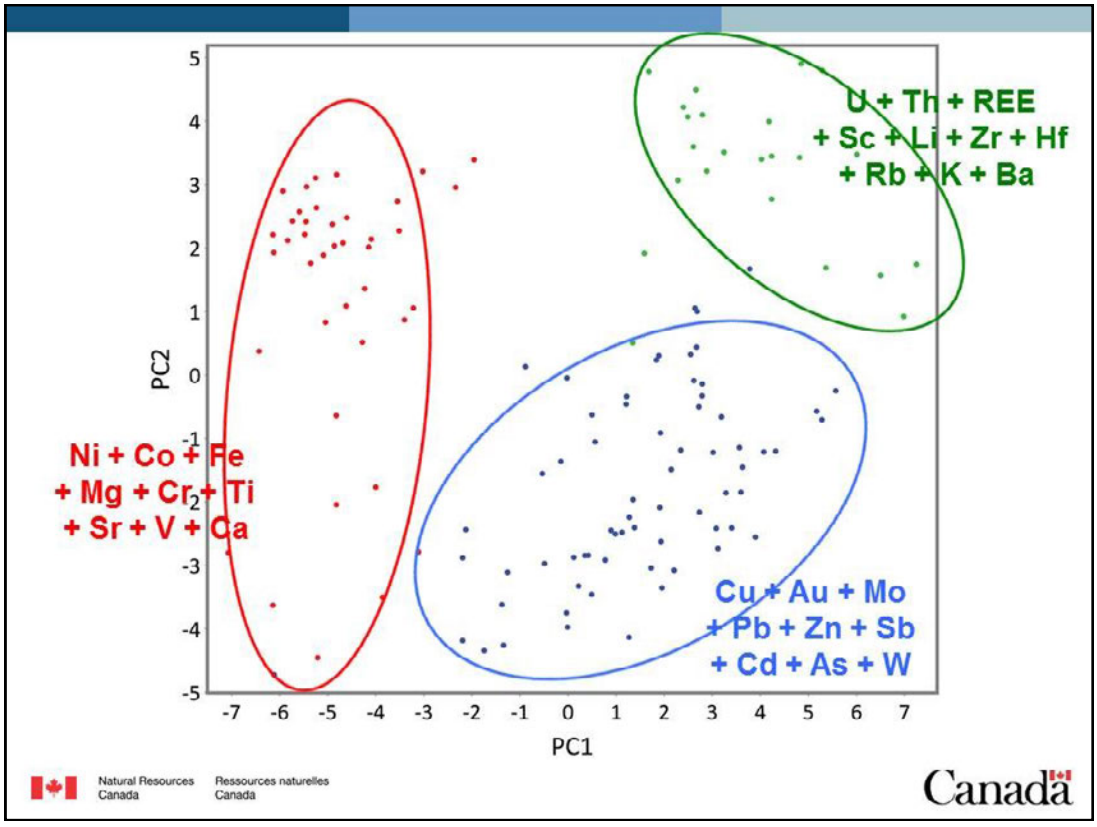
U + Th + REE
+ Sc + Li + Zr + Hf
+ Rb + K + Ba
Ni + Co + Fe
+ Mg + Cr + Ti
+ Sr + V + Ca
Cu + Au + Mo
+ Pb + Zn + Sb
+ Cd + As + W
PC1
PC2
Natural Resources Canada
Ressources naturelles Canada
Canada

Conclusions

- Major element composition and mineralogy can distinguish porphyry from non-porphyry tourmaline, but…
- Barren magmatic-hydrothermal species have very similar major element character to ore associated species

- Trace element chemistry cannot be employed as simple, one-dimensional fingerprint indices, but…
- Multivariate statistics can identify element clusters that can be formed into complex indices, but this may be deposit specific. Needs testing!

Natural Resources Canada Ressources naturelles Canada

Canada

Many thanks!

- To Consolidated Woodjam and Gold Fields for access to samples and data, and particularly Tim Stubley and Jacqueline Blackwell of Gold Fields for all their help.

Gold mineralization in the Cantung W-skarn deposit, Northwest Territories: An examination of distribution, mineralogy, and petrogenesis

E.M. Palmer[1], C.R.M. McFarlane[1], D.R. Lentz[1] and H. Falck[2]

1. University of New Brunswick, 2 Bailey Drive, Fredericton, New Brunswick
2. Northwest Territories Geoscience Office, PO Box 1320, Yellowknife, Northwest Territories

Abstract: The Cantung mine is a world-class W-skarn deposit; it is located just east of the Yukon border in the Selwyn Mountain Range of the Northwest Territories. The deposit area is within the southern extent of the polymetallic Tintina Gold Belt, which has many notable intrusion-related Au deposits. The extensive W skarns at Cantung were developed by hydrothermal fluids that, based on earlier research, were determined to be predominately supercritical magmatic brines with homogenization temperatures ranging from 270-500°C. Mineralization is composed of calcic exoskarn replacement of a clean limestone and lower grade replacements in a calc- silicate/chert unit; these occur in both the operating open pit and underground mine (the E Zone). The main sulphide identified petrographically is pyrrhotite, which is abundant in all skarn facies. Scheelite and chalcopyrite are dominant and there is locally abundant sphalerite. Native Bi exhibits textures indicative of forming later than the silicate assemblage in the paragenetic sequence, and it is decorated by bismuthinite, Bi tellurides, Ag tellurides, and Bi selenides. Tungsten and Cu are the main mine products, but the Au potential of the deposit merits further investigation.

This study characterized the distribution, mineralogy, and petrogenesis of Au mineralization by examining five skarn samples with bulk rock Au assay values >0.5 ppm taken from the E Zone. No free gold or electrum were identified petrographically or by SEM and FEG- SEM analyses. A positive correlation (Spearman's Rank, r') of Au with Bi (0.76), Ag (0.70), Fe (0.64), Cu (0.64), and Mo (0.60) was identified using the bulk rock geochemical data (n = 48). The strong correlation between Bi and Au is suggestive of a liquid bismuth collector mechanism for Au enrichment. However, LA ICP-MS analysis of native Bi and Bi alloys failed to reveal significant Au predicted by the liquid bismuth collector model. In contrast, the highest Au concentration was encountered in hessite (Ag_2Te) and other tellurides. Nano-inclusions within chalcopyrite and silicate minerals were also investigated using FEG-SEM for their Au content, but their composition consisted of native Bi. The decoration of native Bi by bismuthinite, Bi tellurides, Ag tellurides, and Bi selenides provides evidence for a late stage S-, Ag-, and Te-rich fluid. This fluid is thought to have remobilized the Au and deposited it as lattice bound invisible Au within the tellurides. This new data constrains Au exploration targets at Cantung to areas of altered skarn or where there is a presence of telluride minerals

Originally presented Fredericton 2014: Geological Association of Canada - Mineralogical Association of Canada Joint Annual Meeting, Special Session 3: Discovering the Next Generation of Porphyry Deposits: Advancements in Locating and Understanding Hidden Intrusion-related Mineralization. May 21, 2014.

Corresponding author: Emily Palmer (epalmer@unb.ca)

Palmer, E.M., McFarlane, C.R.M., Lentz, D.R., and Falck, H., 2015. Gold mineralization in the Cantung W-skarn deposit, Northwest Territories: An examination of distribution, mineralogy, and petrogenesis; *in* TGI 4 – Intrusion Related Mineralisation Project: New Vectors to Buried Porphyry-Style Mineralisation, (ed.) N. Rogers; Geological Survey of Canada, Open File 7843, p. 415-428.

Gold mineralization in the Cantung W-skarn deposit, NWT:

AN EXAMINATION OF DISTRIBUTION, MINERALOGY, AND PETROGENESIS

EMILY PALMER
BSC STUDENT AT THE
UNIVERSITY OF NEW BRUNSWICK

Regional geology

- Tintina Gold Province (TGP): precious & base metals
  - Spatially & genetically defined to Cretaceous plutons
- Tombstone-Tungsten Belt: felsic, sub-alkalic, reduced intrusions
- S- to I-type granitic plutons of the Selwyn plutonic suite

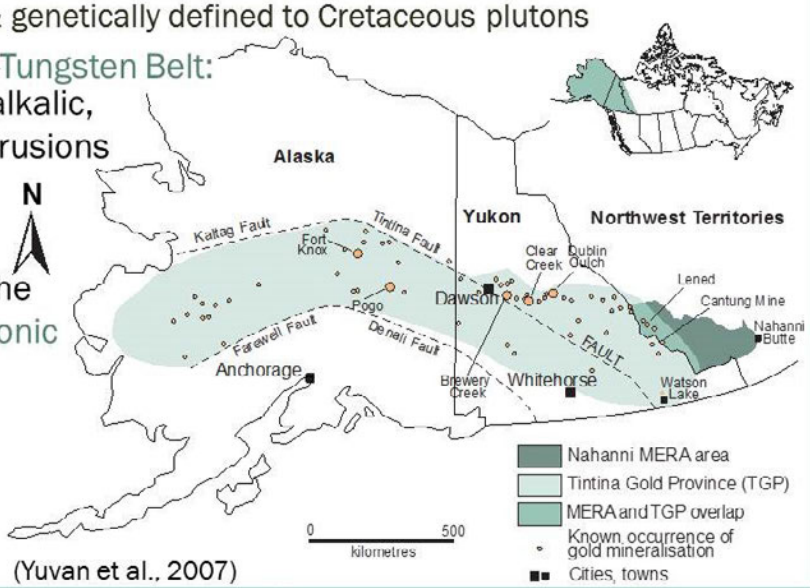

(Yuvan et al., 2007)

Local geology

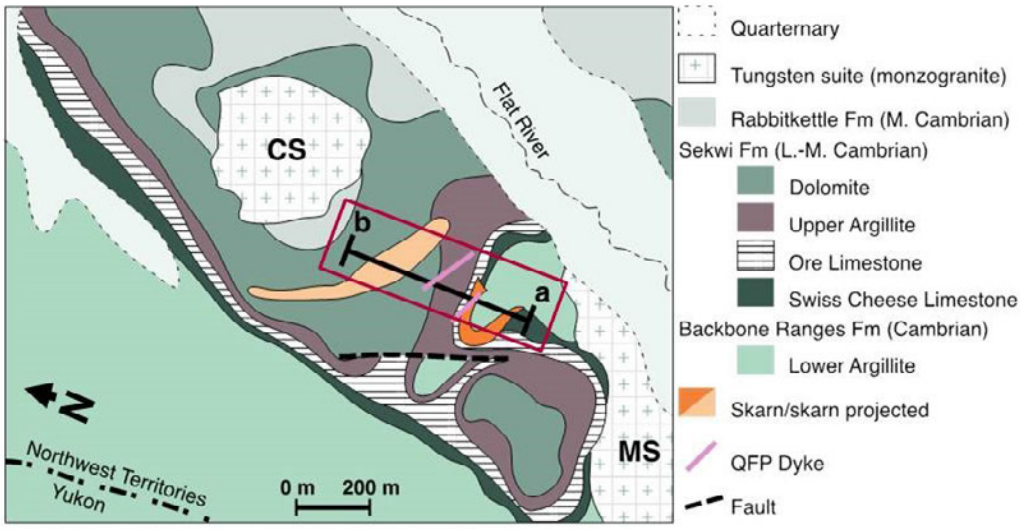

Surface geology at the Cantung mine. CS = circular stock. MS = mine stock (Rasmussen et al., 2011).

2

Local geology

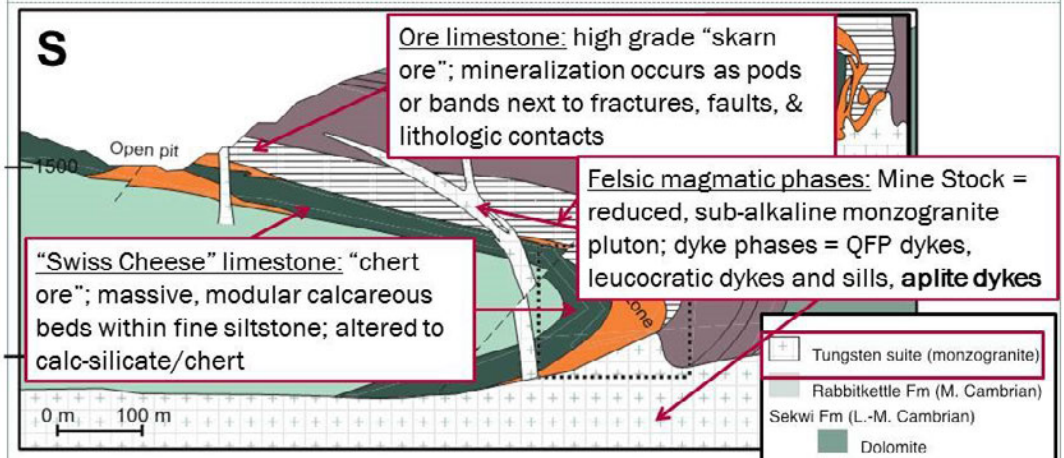

Generalized south to north cross section of the Cantung ore resources illustrating the locations of the open pit & E-zone ore bodies within the folded stratigraphy (Rasmussen et al., 2011).

3

Skarn formation

1. Prograde: contact metamorphism
   - Pluton intrudes country rock
   - Thermal maximum of 600°- 650°C (Mathieson and Clark, 1984)

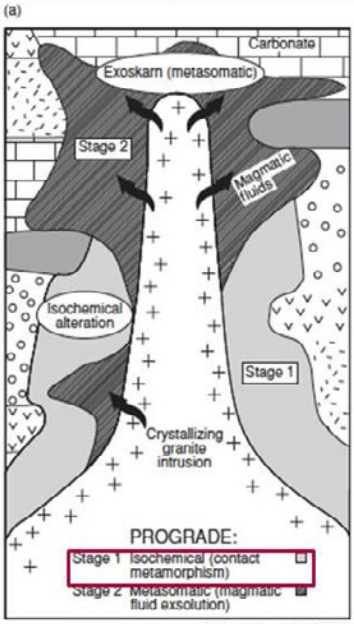

(Robb, 2005)

4

Skarn formation

2. Prograde: metasomatism
   - Magmatic fluid exsolution
     - Enrichment of H_2S, $FeCl_2$, $MgCl_2$, & KCl in main mineralizing fluid
     - Incompatible element enrichment in latest exsolved fluids
   - Egress of fluid phase into contact metamorphosed rock
   - Periodic trapping of fluid at crystallization front = over-pressuring
   - Pervasive metasomatism of aplite dykes (Rasmussen, 2011) = ongoing influx of magmatic fluid

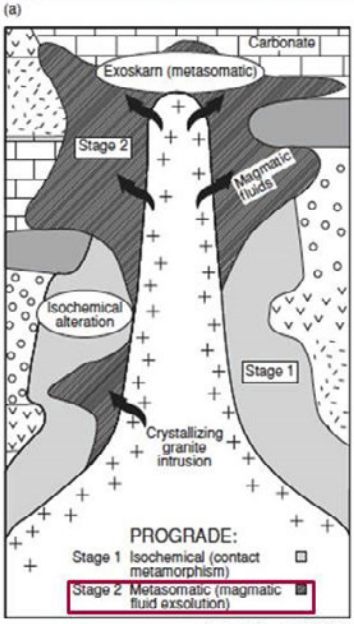

(Robb, 2005)

5

Skarn formation

3. Retrograde: meteoric fluid influx & main metal precipitation
   - Magmatic fluid neutralized by carbonates = increased pH
     - Enhances permeability & fluid flow
   - Decreased temperatures
   - Promotes precipitation of metals + sulphides
     - Pyrrhotite, scheelite, chalcopyrite, native Bi and Bi-minerals

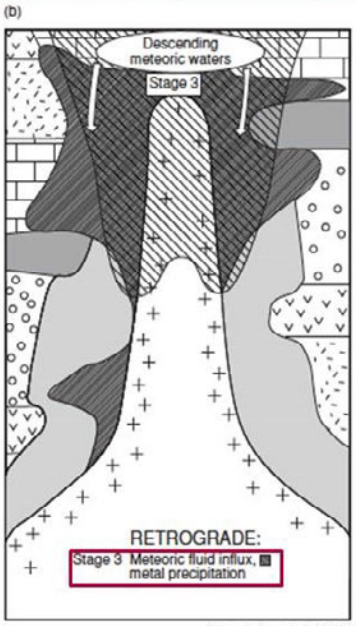

(Robb, 2005)

6

Objectives and purpose

- To characterize:
  - Distribution of Au
  - Petrogenesis of Au
  - Paragenetic sequence
- Purpose: are there economic concentrations of Au in the E-Zone?

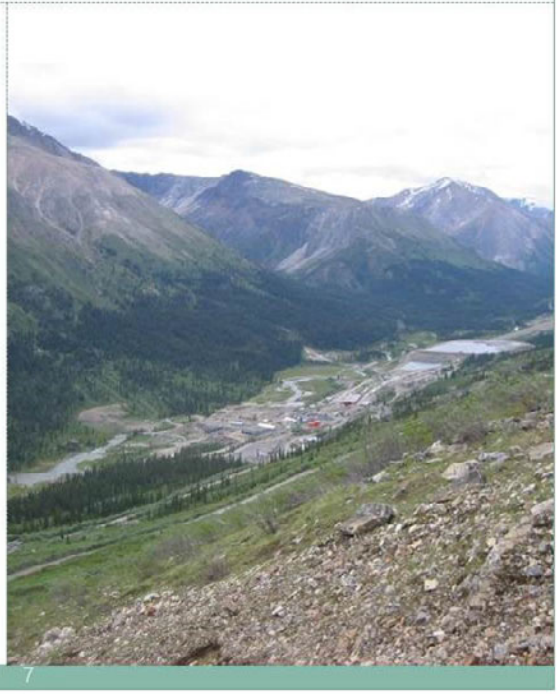

7

Analytical techniques

- Sample E-Zone
  - 46 samples
- Bulk rock geochemistry
  - Acid digestion, ICP-MS
- Petrography
  - Optical microscopy
  - SEM analysis
- FEG-SEM analysis
- LA ICP-MS analysis

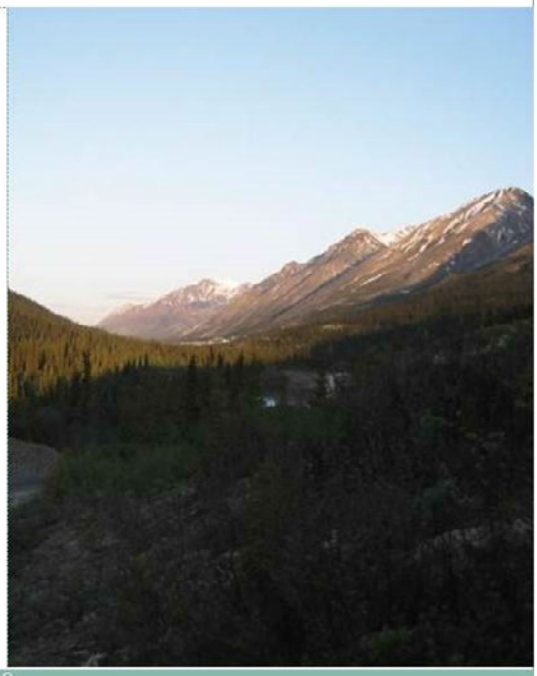

8

Geochemistry results

Sample #	03-DL-03	03-DL-04	03-DL-17a	03-DL-26	03-DL-27
Au (ppm)	0.9	0.6	0.9	1.3	8.0

- Spearman rank correlation coefficient
  - Measures statistical dependence of 2 variables
  - r' = +1: area rich in element 1 is likely to also have Au present
  - r' = -1: area rich in element 1 is likely to have no Au present
- Te and Se were not analyzed

9

Geochemistry results

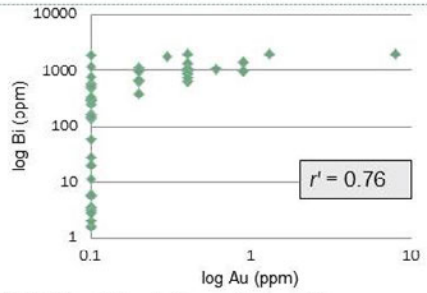

Fig.1: Correlation between Au and Bi

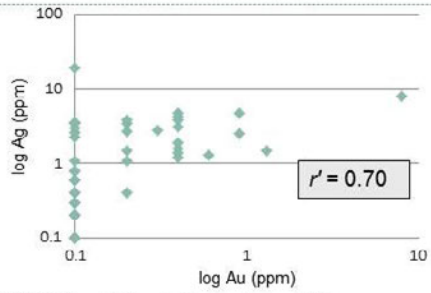

Fig.2: Correlation between Au and Ag

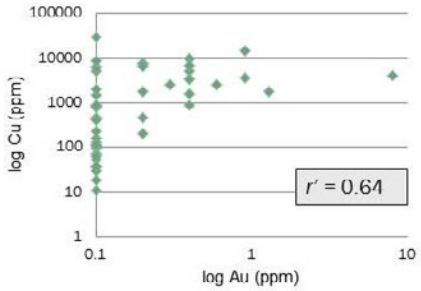

Fig.3: Correlation between Au and Cu

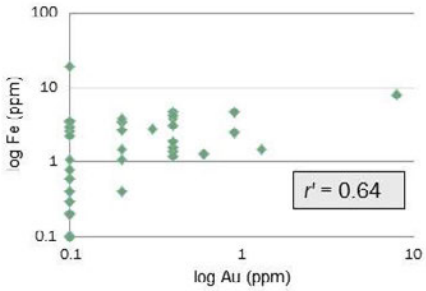

Fig.4: Correlation between Au and Fe

10

Petrography results

- Dominated by scheelite (W) & chalcopyrite (Cu)
- Pyrrhotite is the primary sulphide species
- Actinolite, quartz, chlorite, clinozoisite, clinopyroxene, garnet, biotite, apatite
- Native Bi decorates pyrrhotite grains (A & B)
- Very thin native Bi stringers common (C)

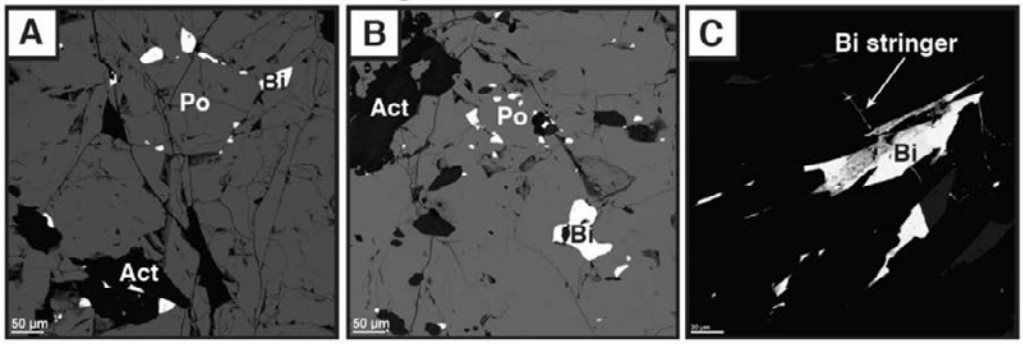

11

Petrography results

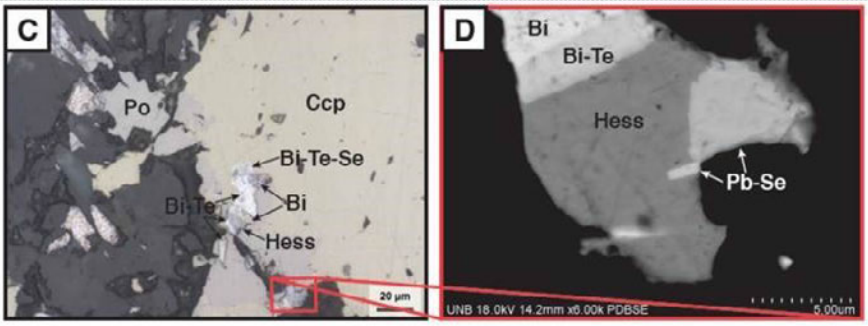

- Bi-sulfosalts, Bi-tellurides surround native Bi
- Native Bi & Bi-minerals found in association with zones of actinolite skarning
  - Hessite (Ag_2Te), Bi-tellurides, bismuthinite (Bi_2S_3) + sulfosalts
- No free Au present

12

FEG-SEM results

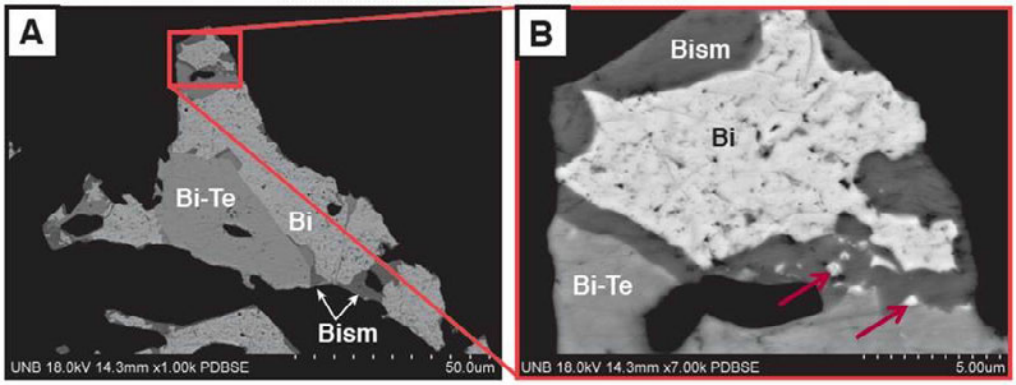

- Nano-inclusions in minerals, interstitial blebs, & stringers
  - Small (<1 µm), rounded to sub-rounded
- All that were analyzed = native Bi

13

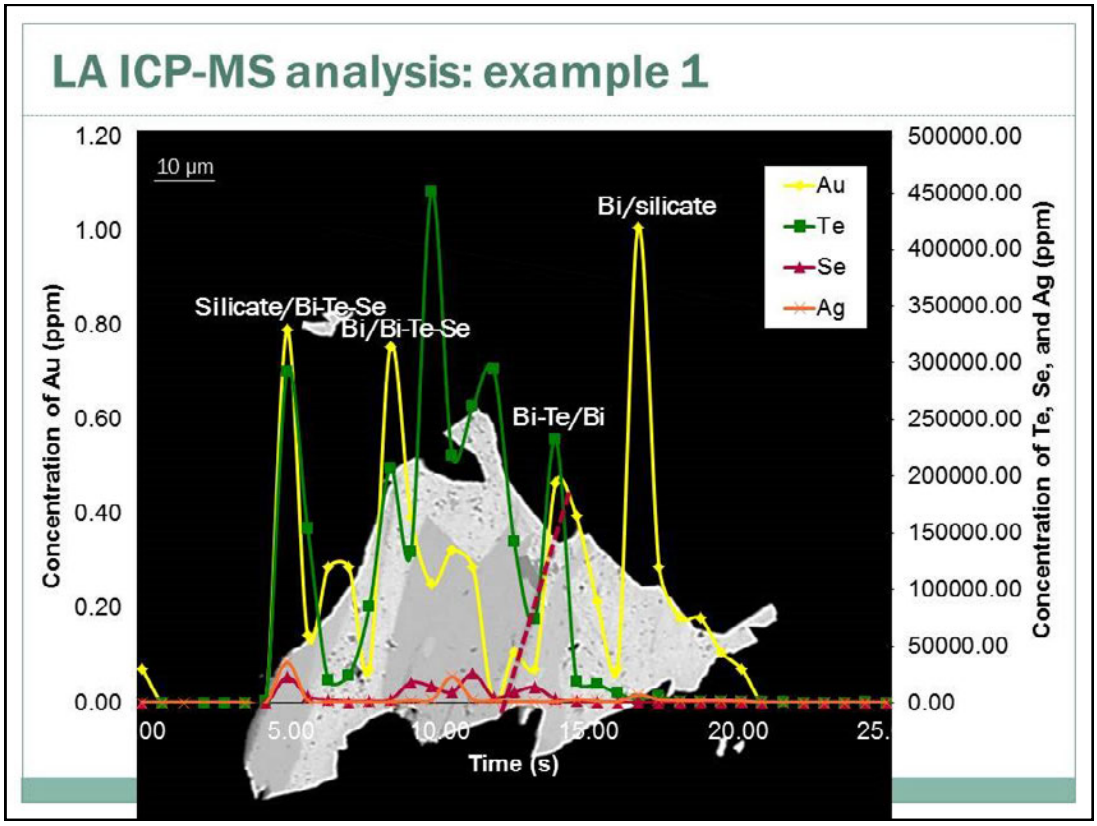
LA ICP-MS analysis: example 1
10 μm
Au
Te
Se
Ag
Bi/silicate
Silicate/Bi-Te-Se
Bi/Bi-Te-Se
Bi-Te/Bi
Concentration of Au (ppm)
1.20
1.00
0.80
0.60
0.40
0.20
0.00
500000.00
450000.00
400000.00
350000.00
300000.00
250000.00
200000.00
150000.00
100000.00
50000.00
0.00
Concentration of Te, Se, and Ag (ppm)
5.00
10.00
15.00
20.00
Time (s)

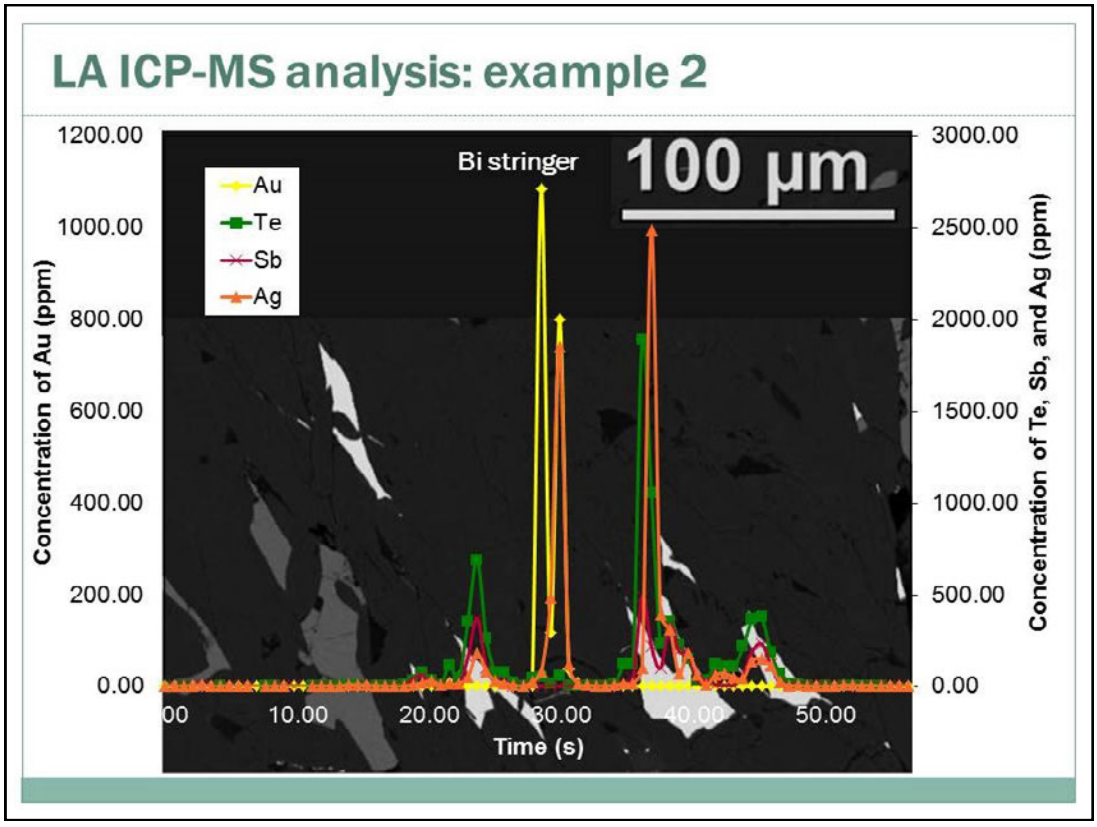
LA ICP-MS analysis: example 2
100 μm
Au
Te
Sb
Ag
Bi stringer
Concentration of Au (ppm)
1200.00
1000.00
800.00
600.00
400.00
200.00
0.00
3000.00
2500.00
2000.00
1500.00
1000.00
500.00
0.00
Concentration of Te, Sb, and Ag (ppm)
10.00
20.00
30.00
40.00
50.00
Time (s)

Distribution of Au

- Au concentrated on outer rim of Bi-mineral grains
- 3 possibilities:

1. Solid solution as invisible Au within outer rim of Bi-minerals
2. Au nano-inclusions within/on edges of native Bi & Bi-minerals
3. Both lattice-bound & included as nano-inclusions

Au petrogenesis

- Au dissolves mainly as $AuCl^{-}_{2}$ at high temperatures
- Model A: high H_2S in fluid
- Solubility highest at high temperatures

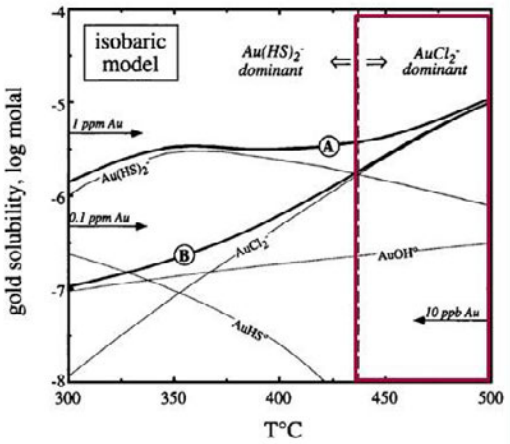

(Gammons and William-Jones, 1997)

17

Au petrogenesis

- Au dissolves mainly as $AuCl^-_2$ at high temperatures
- Model A: high H_2S in fluid
- Solubility highest at high temperatures
- Au precipitation:

1. Neutralization &/or
2. Reduction

- Likely remobilized by Cl^- complexes and later fluid deposited with Bi

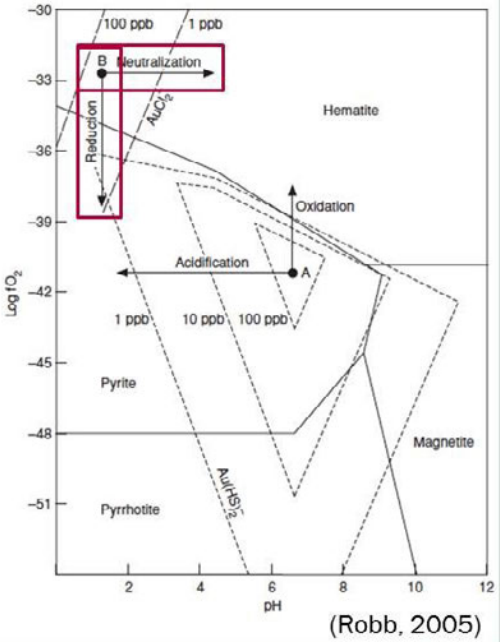

(Robb, 2005)

Au petrogenesis

- Liquid bismuth collector model: potential explanation for Au-Bi deposits (Douglas et al., 2000)
- Au partitions into Bi-melts even from undersaturated aqueous solutions (Tooth et al., 2008)

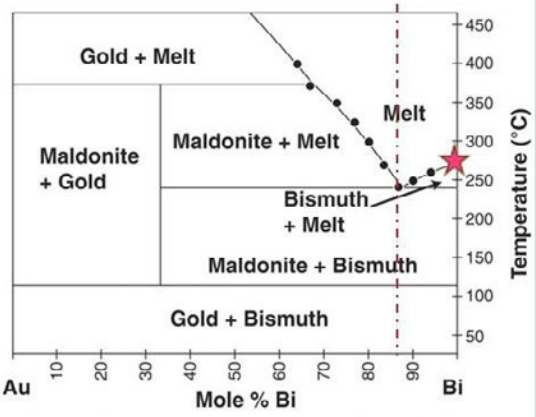

Phase diagram for Au-Bi system at 1 bar (Tooth et al., 2008). Native Bi has a melting temperature of 270ºC. Au-Bi melt has a eutectic with ~12 atomic % Au.

Au petrogenesis

- Likely aqueous Bi complex = $Bi(OH)_3$
  - Precipitation of Fe^{3+} minerals = reduction of Bi^{3+} to Bi^0 (melt)
- Alteration assemblages > 300°C (Mathieson and Clark, 1987)
  - Bi-Bi_2S_3 assemblage partially liquid for much of ore formation (270°C)
  - Liquid Bi reacting with skarn fluid system
- Crystallized at eutectic or lower Bi-Au-Ag-Pb-Te-Se-S eutectic (Cockerton and Tomkins, 2012)

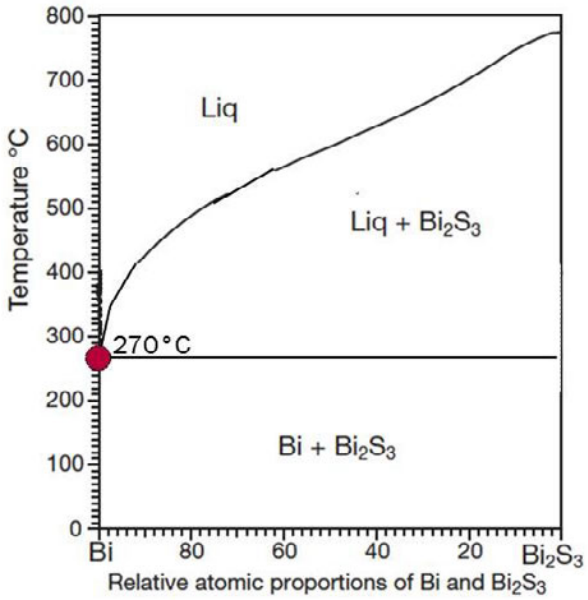

(Cockerton and Tomkins, 2012)

20

Conclusions

- No free Au present
  - Solid solution of Au on rims of Bi-minerals
  - Higher concentrations of Au likely occur as nanoparticles, although none identified
- Au transported from depth as $AuCl^-_2$
- Incorporated in Bi-minerals due to high affinity of Bi and Au
- Area at margin of reaction front more promising for Au exploration where massive sulphides are located
  - Fluid movement and remobilization constant within front until cooled

22

Paragenetic sequence

- Contact metamorphism:
  - Garnet, clinopyroxene
- Silication:
  - Actinolite, epidote, biotite, apatite, chlorite
- Main mineral precipitation:
  - Pyrrhotite, chalcopyrite, scheelite, sphalerite
  - Native Bi, bismuthinite, Bi-tellurides/Bi-Te-Se sulfosalts, hessite
  - Gold

21

Acknowledgements

I would like to thank Chris McFarlane and Dave Lentz for their direction and advice on the direction of the project; Douglas Hall and Steven Cogswell for their helpful expertise using the SEM; and Suporn Boonsue for her time and laughter while on the FEG-SEM.

Funding for this project was provided by the Northwest Territories Geoscience Office (NTGO). A special thank you to Hendrik Falck for pushing my opportunity to visit the NWT for a poster presentation on this project.

23

References

Cockerton, A.B.D., and Tomkins, A.G. (2012). Insights into the liquid bismuth collector model through analysis of the Bi-Au Stormont Skarn Prospect, Northwest Tasmania. *Economic Geology, 107*(4), 667-682.

Ciobanu, C. L., Birch, W. D., Cook, N. J., Pring, A., and Grundler, P. V. (2010). Petrogenetic significance of Au–Bi–Te–S associations: The example of Maldon, Central Victorian gold province, Australia. *Lithos, 116*(1-2), 1–17.

Ciobanu, C. L., Cook, N. J., and Pring, A. (2006). Bismuth tellurides as gold scavengers. *Mineralogy and Petrology, 87*(3-4), 277–304.

Ciobanu, C. L., Cook, N. J., Pring, A., Brugger, J., Danyushevsky, L. V., and Shimizu, M. (2009)."Invisible gold" in bismuth chalcogenides. *Geochimica et Cosmochimica Acta, 73*(7), 1970–1999.

Cook, N. J. and Ciobanu, C. L. (2004). Bismuth tellurides and sulphosalts from the Larga hydrothermal system, Metaliferi Mts, Romania: Paragenesis and genetic significance. *Mineralogical Magazine, 68*(2), 301–321.

Douglas, N., Mavrogenes, J., Hack, A., and England, R. (2000. The liquid bismuth collector model: an alternative gold deposition mechanism [abs.], in Silbeck, G., and Hubble, T.C.T., eds., Understanding planet Earth; searching for a sustainable future; on the starting blocks of the third millennium: 15th Australian Geological Convention Abstracts: Sydney, Geological Society of Australia, p. 135.

Mathieson, G. and Clark, A. (1984). The Cantung E Zone scheelite skarn orebody, Tungsten, Northwest Territories: a revised genetic model. *Economic Geology, 79*, 883–901.

Rasmussen, K. L., Lentz, D. R., Falck, H., and Pattison, D. R. M. (2011). Felsic magmatic phases and the role of late-stage aplitic dykes in the formation of the world-class Cantung Tungsten skarn deposit, Northwest Territories, Canada. *Ore Geology Reviews, 41*(1), 75–111.

Rasmussen, K. L. and Mortensen, J. K. (2013). Magmatic petrogenesis and the evolution of (F:Cl:OH) fluid composition in barren and tungsten skarn-associated plutons using apatite and biotite compositions: Case studies from the northern Canadian Cordillera. *Ore Geology Reviews, 50*, 118–142.

Tooth, B., Brugger, J., Ciobanu, C., and Liu, W. (2008). Modeling of gold scavenging by bismuth melts coexisting with hydrothermal fluids. *Geology, 36*(10), 815.

Yuvan, J., Shelton, K., Falck, H., 2007. Geochemical investigations of the high-grade quartz–scheelite veins of the Cantung Mine, Northwest Territories. In: Wright, D.F., Lemkow, D., Harris, J.R. (Eds.), Mineral and Energy Resource Assessment of the Greater Nahanni Ecosystem under Consideration for the Expansion of the Nahanni National Park Reserve, Northwest Territories. Geological Survey of Canada Open File 5344, pp. 177–190.

24

Feldspar triclinicity, superheating and mineralization

R. Girard[1], C. Potvin-Doucet[2], L.P. Bédard[2] and F. Bouchard[3]

1. IOS Services Géoscientifiques Inc., 1319 Boul. St-Paul, Saguenay, Quebec
2. Université du Québec à Chicoutimi, 555 Boul. de l'Université, Saguenay, Quebec
3. Osisko Mining Corporation, 100 Chemin du Lac Mourier, Malartic, Quebec

Abstract: The association of hydrothermal alteration and gold mineralization with Archean porphyric felsic dykes swarms is a well-known feature. Examples are abundant in the Abitibi greenstone belt, such as Fenn-Gibbs or Lamaque. It has been frequently observed by the authors, in the course of routine petrographic work, that feldspar phenocrysts from such dykes ("FP" or "QFP") are monoclinic sanidine or anorthoclase, rather than the more usual orthoclase. It is estimated that about 50 % of the "QFP" occurrences are apparently sanidine bearing, suggesting an underlying process. Preservation of the high temperature structure of feldspar requires rapid heat dissipation in order to avoid inversion to triclinic feldspar or perthite. In hypabyssal or mesozonal conditions, it requires abundant fluids percolation. Such fluid inflow necessitates permeability, likely by fracturation, as indicated by the coeval pervasive sericite dominated hydrothermal alteration invading in the wallrock of the dyke swarm. Porphyritic felsitic dykes can be seen as the uppermost expression of larger magmatic chambers, linking it with the eruptive complex Superheating evidences are abundant, such as phenocrysts resorbtion, similar to what is commonly seen in rhyolite and dacite.

Feldspars, under magmatic conditions, are monoclinic and form a complete solid solution between albite and orthose. Their inversion into triclinic structure occurs at about 700°C, where microcline and albite end-members exsolve into perthites. Orthose can preserve pseudomonoclinic structure and variable obliquity. The magnitude of this obliquity is potentially related to the cooling history of the intrusion, and is envisaged as a proxy of the cooling gradient.

Recognizing sanidine or anorthoclase from orthoclase can be done under the petrographic microscope, while accurate measurement of obliquity needs time-consuming 5- axis Federov's stage manipulations. The relation between optical obliquity and d_(13 1) - d_131 spacing by XRD are under evaluation, as well is the development of more efficient procedures. The effectiveness of the method is currently tested on a well-documented mineralized system at Osisko's Canadian Malartic deposit. In the event the premise works, it may provide a new tool to test the fertility of porphyritic intrusions.

Originally presented Fredericton 2014: Geological Association of Canada - Mineralogical Association of Canada Joint Annual Meeting, Special Session 3: Discovering the Next Generation of Porphyry Deposits: Advancements in Locating and Understanding Hidden Intrusion-related Mineralization. May 21, 2014.

Corresponding author: Réjean Girard (rejeang@iosgeo.com)

Girard, R., Potvin-Doucet, C., Bédard, L.P., and Bouchard, F., 2015. Feldspar triclinicity, superheating and mineralization; *in* TGI 4 – Intrusion Related Mineralisation Project: New Vectors to Buried Porphyry-Style Mineralisation, (ed.) N. Rogers; Geological Survey of Canada, Open File 7843, p. 429-443.

FELDSPAR TRICLINICITY, SUPERHEATING AND MINERALIZATION

R. GIRARD [1]
C. POTVIN-DOUCET [1,2]
L.P. BÉDARD [2]
F. BOUCHARD [3]

1: IOS Services Géoscientifiques Inc
2: Université du Québec à Chicoutimi
3: Corporation Minière Osisko Inc.

IOS Services Géoscientifiques inc

STARTING POINT

CLASSICAL PORPHYRY MODEL:

HYDROTHERMAL PROCESS WITH A MAGMATIC HEAT SOURCE.

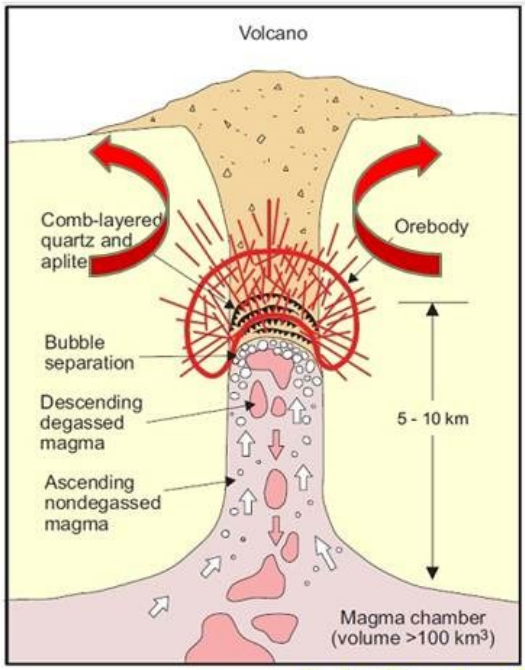

IOS L'innovation comme motivation UQAC

IDEAS!

QUESTION:

IF HYDROTHERMALISM IS DRIVEN BY COOLING OF MAGMATIC BODIES, IS THE MINERALIZATION RELATED TO THE COOLING HISTORY?

IS THE COOLING HISTORY RECORDED IN FELDSPAR CRYSTALLINE STRUCTURE?

CAN WE DEVELOP AN EXPLORATION TOOL FROM THESE PREMISSES?

IOS *L'innovation comme motivation* UQAC

PROSPECTOR'S KNOWLEDGE

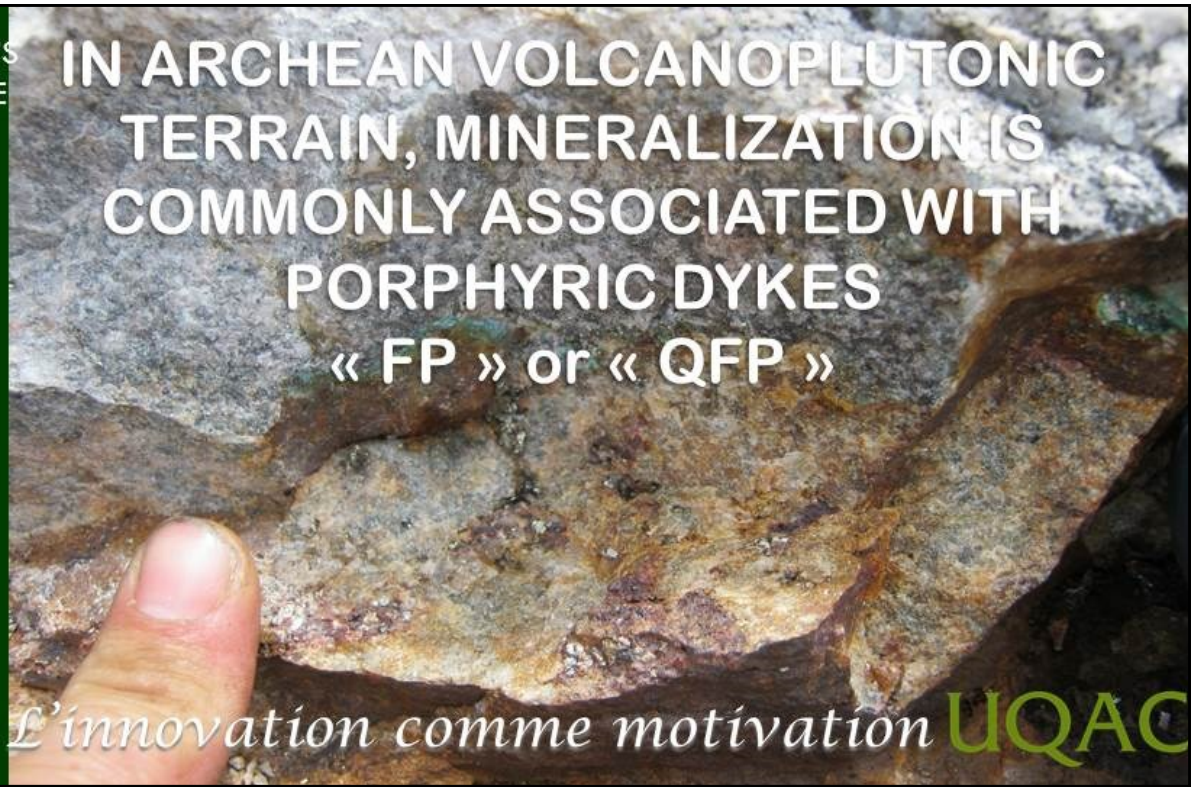

IOS *L'innovation comme motivation* UQAC

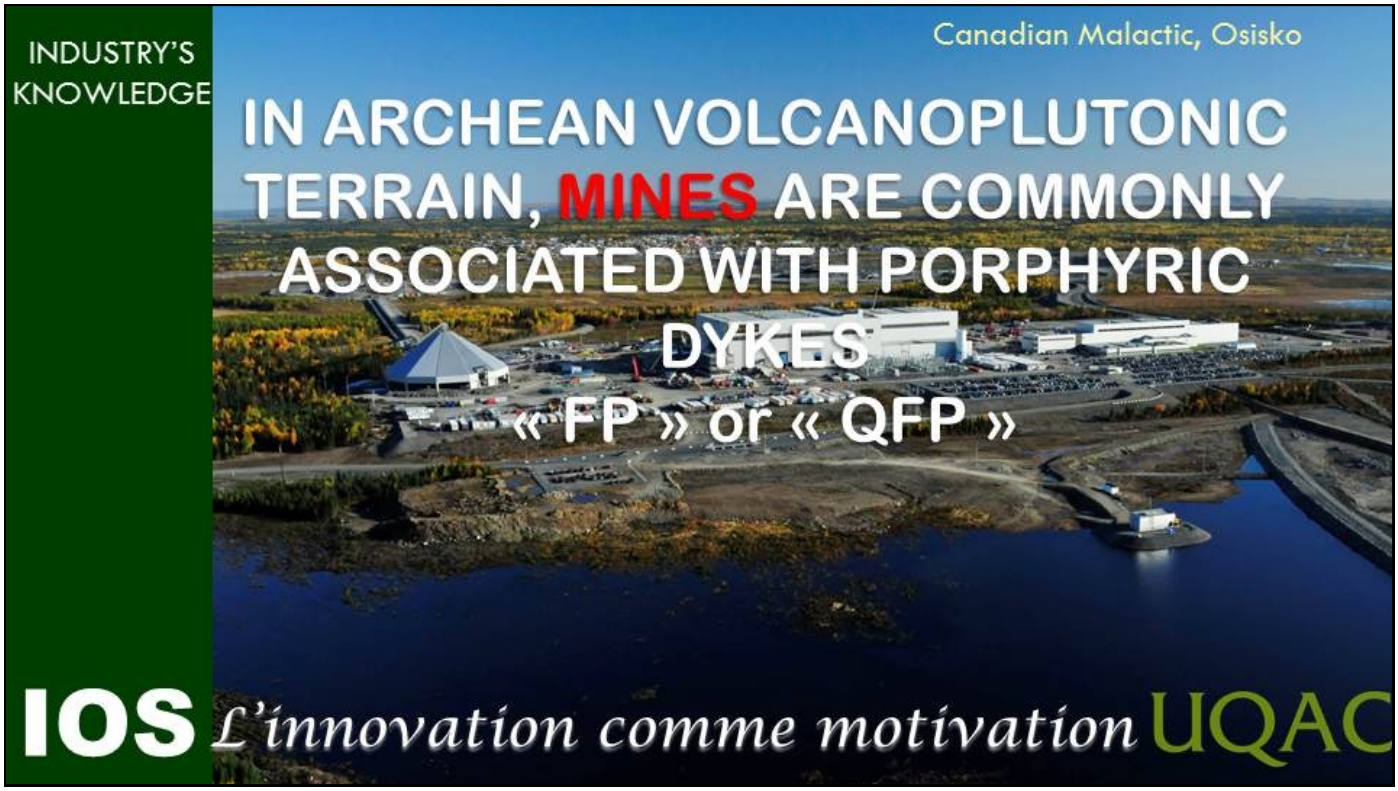
INDUSTRY'S KNOWLEDGE
Canadian Malactic, Osisko
IN ARCHEAN VOLCANOPLUTONIC TERRAIN, MINES ARE COMMONLY ASSOCIATED WITH PORPHYRIC DYKES
« FP » or « QFP »
IOS
L'innovation comme motivation
UQAC

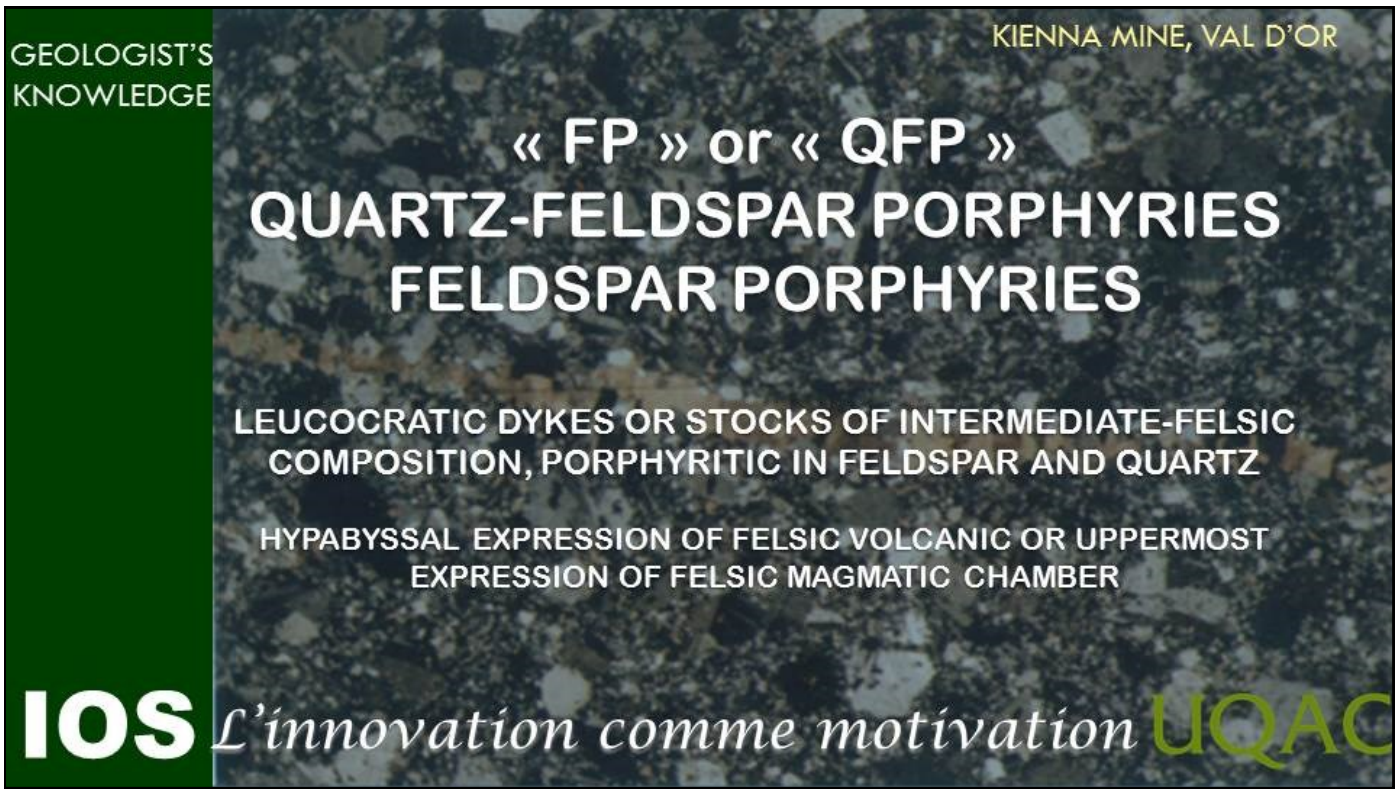
GEOLOGIST'S KNOWLEDGE
KIENNA MINE, VAL D'OR
« FP » or « QFP »
QUARTZ-FELDSPAR PORPHYRIES
FELDSPAR PORPHYRIES
LEUCOCRATIC DYKES OR STOCKS OF INTERMEDIATE-FELSIC COMPOSITION, PORPHYRITIC IN FELDSPAR AND QUARTZ
HYPABYSSAL EXPRESSION OF FELSIC VOLCANIC OR UPPERMOST EXPRESSION OF FELSIC MAGMATIC CHAMBER
IOS
L'innovation comme motivation
UQAC

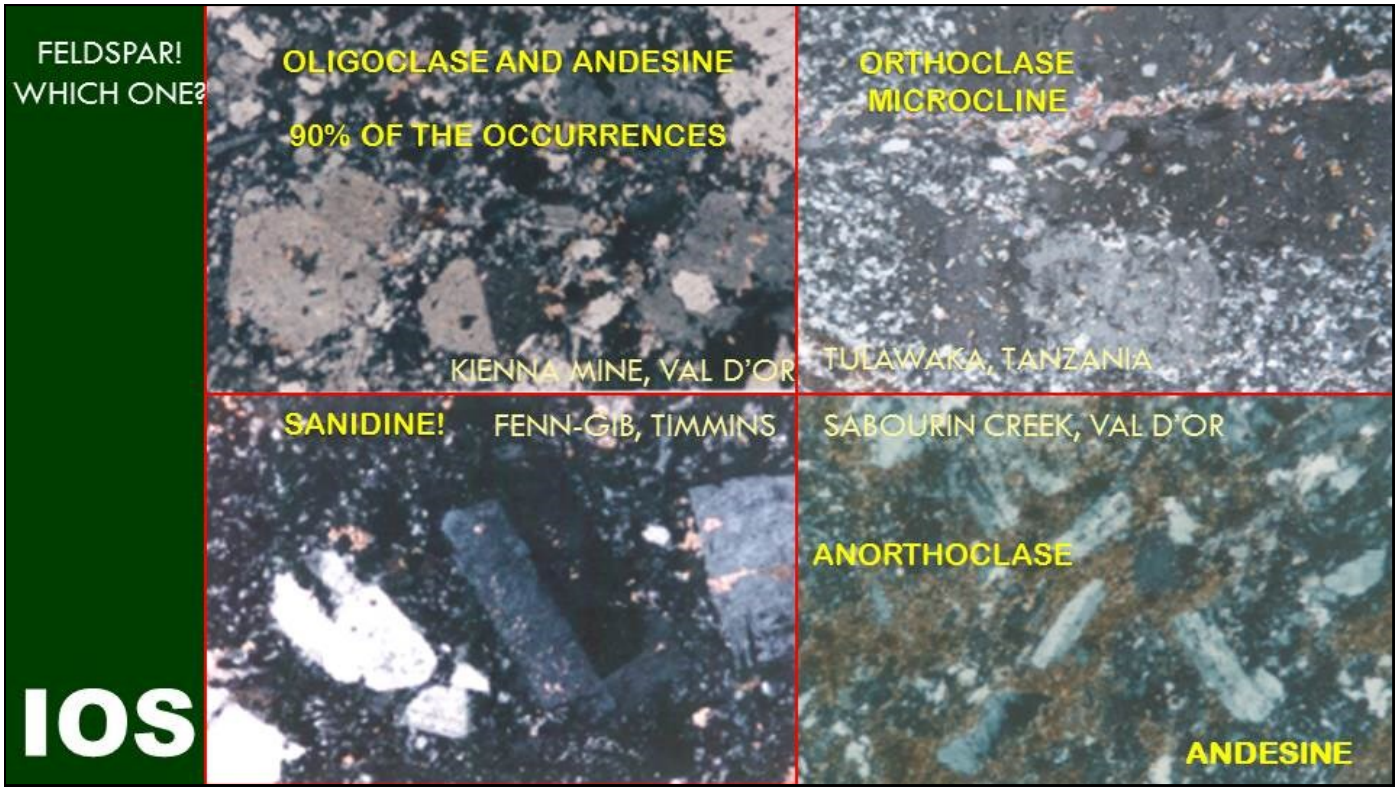
FELDSPAR!
WHICH ONE?
OLIGOCLASE AND ANDESINE
90% OF THE OCCURRENCES
KIENNA MINE, VAL D'OR
ORTHOCLASE
MICROCLINE
TULAWAKA, TANZANIA
SANIDINE!
FENN-GIB, TIMMINS
SABOURIN CREEK, VAL D'OR
ANORTHOCLASE
ANDESINE
IOS

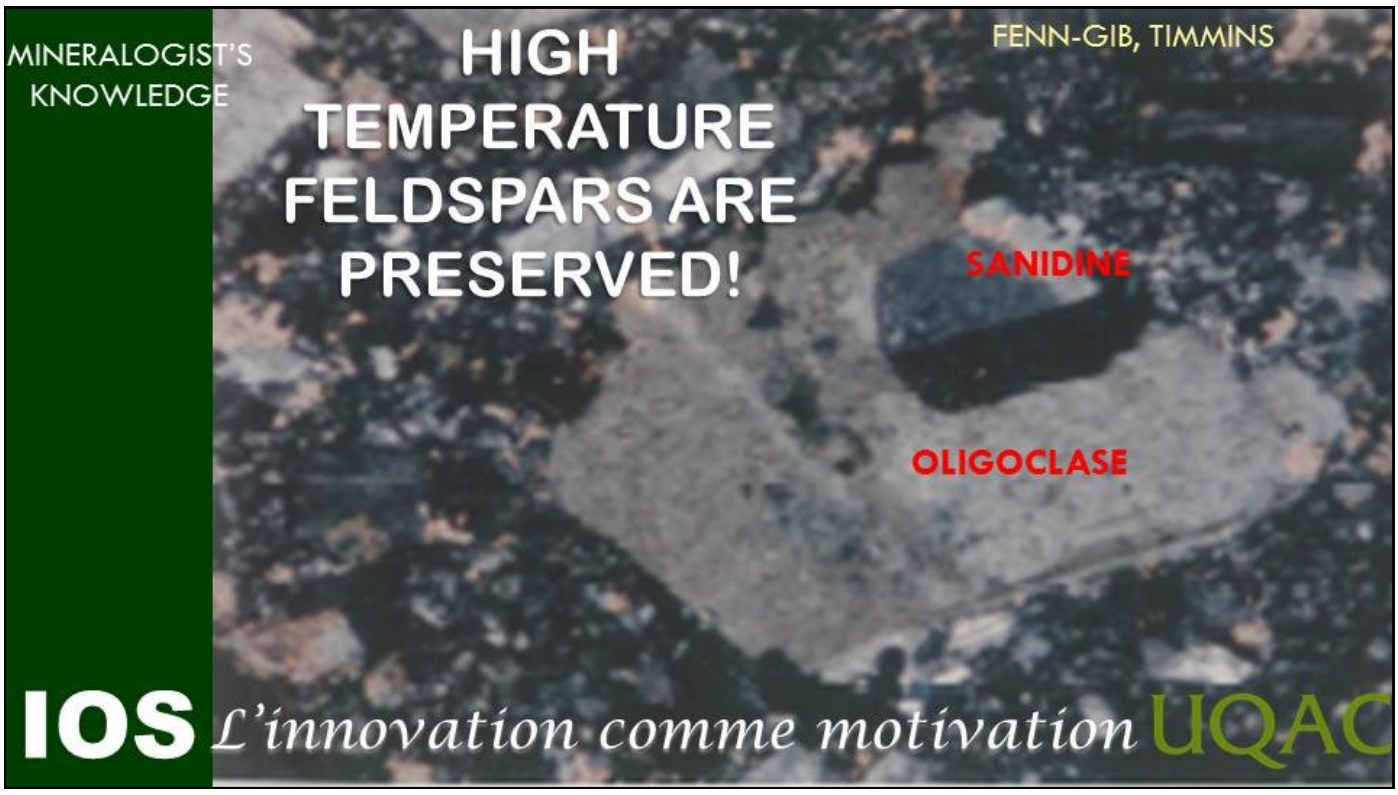
MINERALOGIST'S
KNOWLEDGE
HIGH
TEMPERATURE
FELDSPARS ARE
PRESERVED!
FENN-GIB, TIMMINS
SANIDINE
OLIGOCLASE
IOS
L'innovation comme motivation
UQAC

FELDSPAR SERIES

HIGH TEMPERATURE FELDSPARS

LOW TEMPERATURE: DISCONTINUOUS SOLUTION

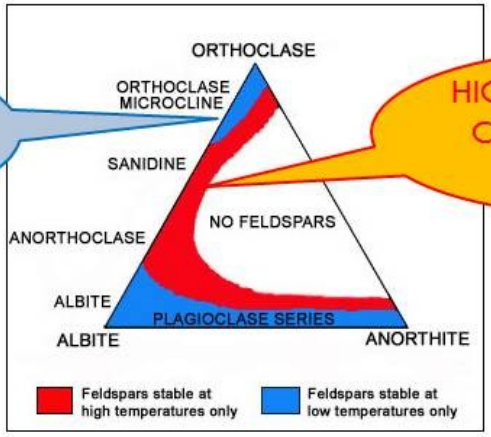

HIGH TEMPERATURE: COMPLETE SOLID SOLUTION

IOS L'innovation comme motivation UQAC

A QUESTION OF POLYMORPHS

SANIDINE

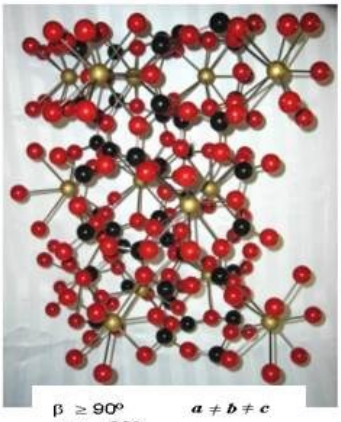

$\beta \geq 90°$ $\alpha, \gamma = 90°$ $a \neq b \neq c$

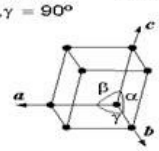

Monoclinique

ORTHOCLASE

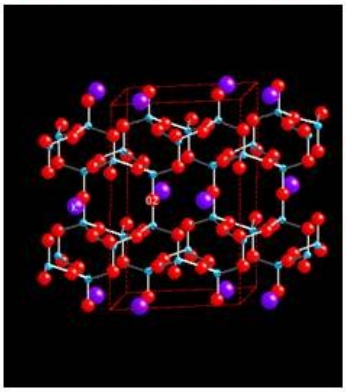

$\alpha, \beta, \gamma \neq 90°$ $a \neq b \neq c$

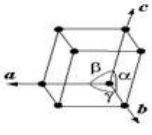

Pseudo-monoclinique

MICROCLINE

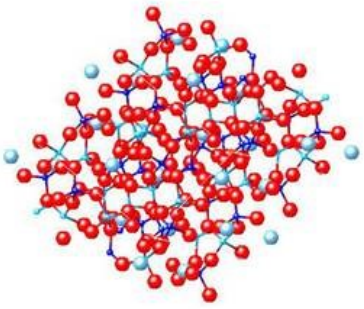

$\alpha, \beta, \gamma \neq 90°$ $a \neq b \neq c$

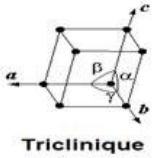

Triclinique

IOS L'innovation comme motivation UQAC

A QUESTION OF DISORDER

DISTRIBUTION OF AL+++

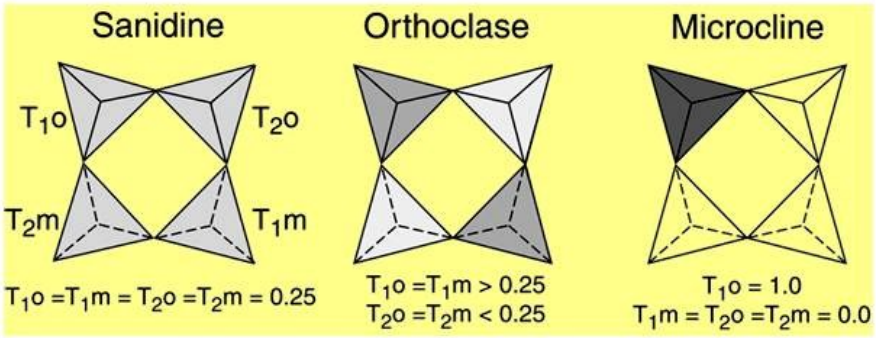

Al^{+++} is randomly distributed among tetrahedron

Al^{+++} always in the same tetrahedral site

IOS L'innovation comme motivation UQAC

A QUESTION OF TEMPERATURE

ORDERING DEPENDS ON TEMPERATURE

MAGMA

METAMORPHISM

HYDROTHERMALISM

SURFACE

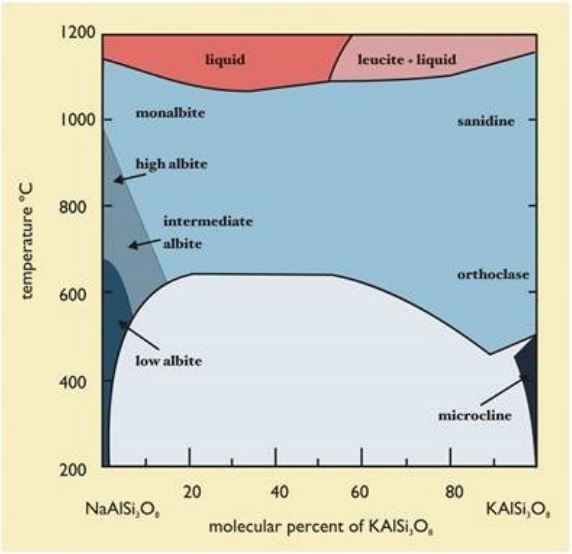

SANIDINE

ORTHOCLASE

MICROCLINE

ORDERING

IOS L'innovation comme motivation UQAC

A QUESTION OF TEMPERATURE

FELDSPAR AND COOLING RATES

Volcanics | **Hypabyssal** | **Plutonic**

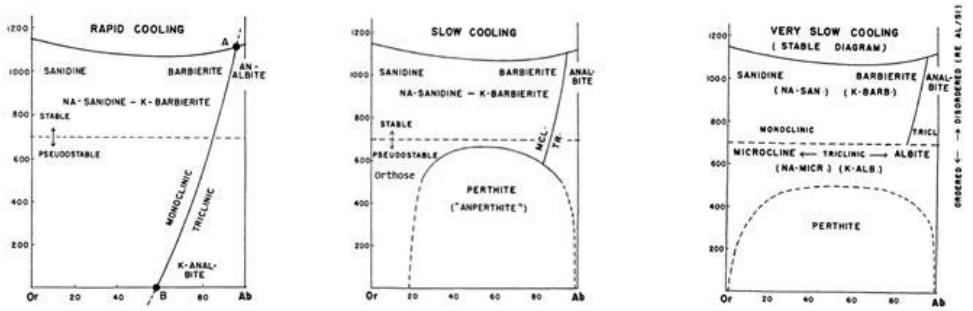

SANIDINE ANORTHOCL. | ORTHOCLASE ALBITE | MICROCLINE ALBITE

Smith 1974, Laves 1952

IOS *L'innovation comme motivation* UQAC

A QUESTION OF DROP

SLOW COOLING: INVERSION SANIDINE → PERTHITE, CRYPTOPERTHITE

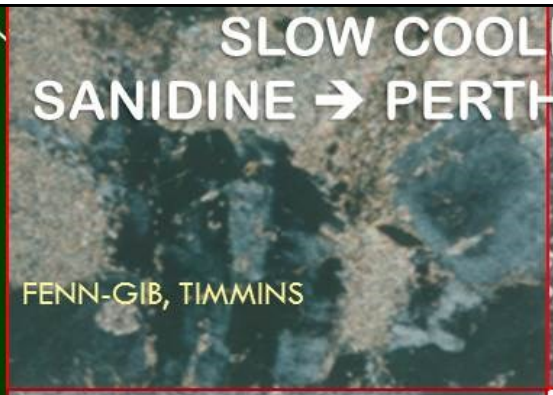

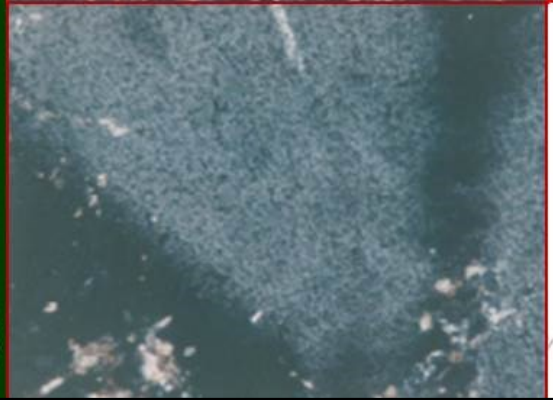

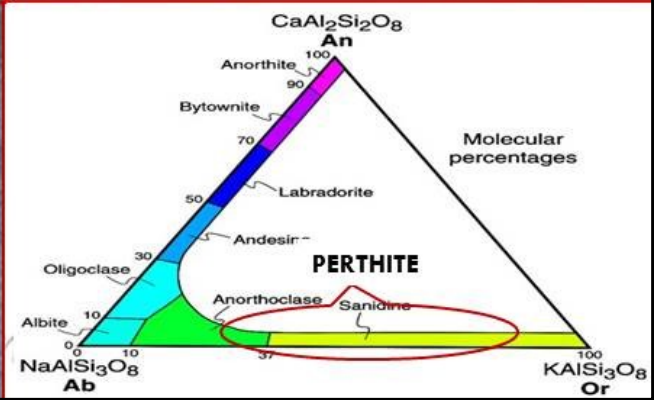

IOS

A QUESTION OF CHARACTER
HOW DO WE DISCRIMINATE FELDSPAR?
ALTERATION AND TWINNING: EASY
CALSBAD TWINNING ONLY: DIFFICULT
VALLEJO: COLUMBIA
IOS
L'innovation comme motivation
UQAC

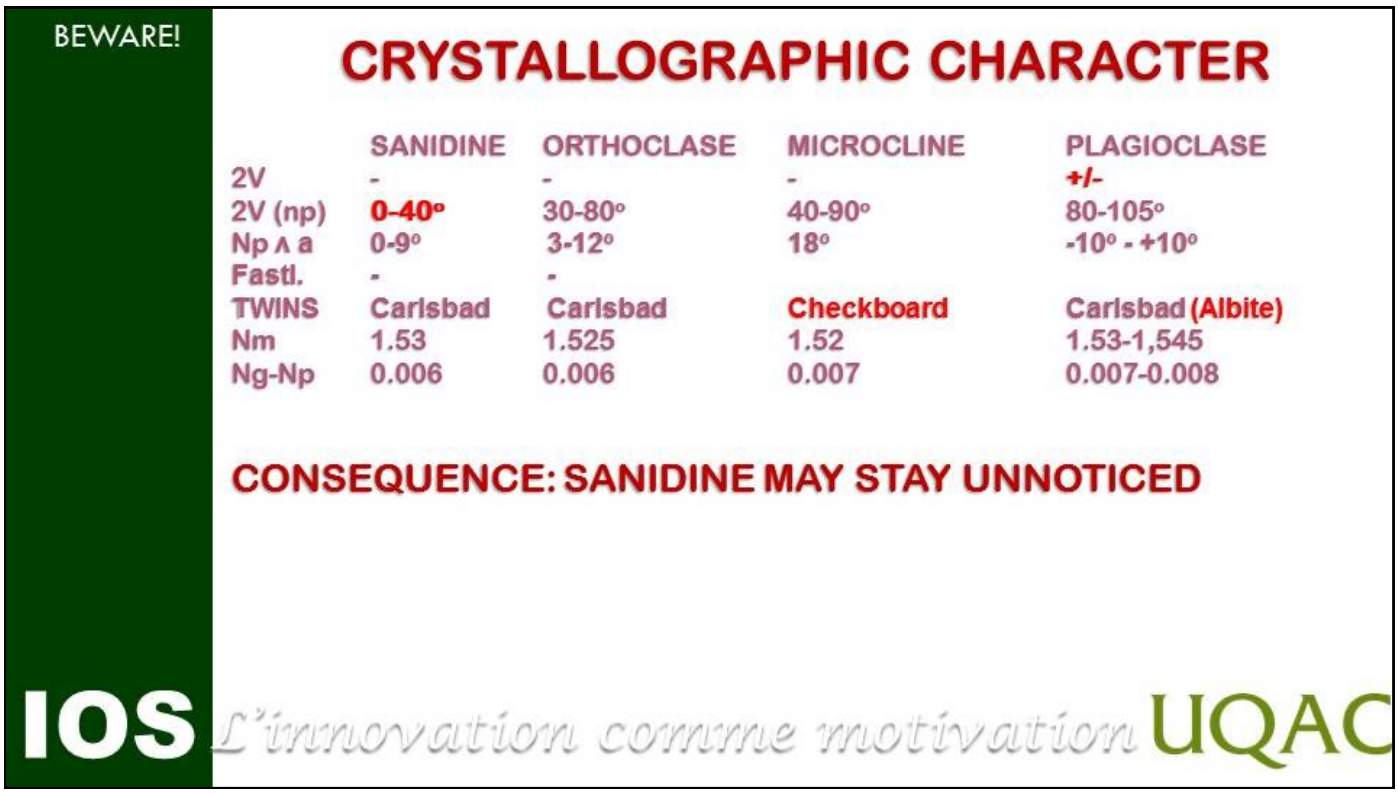
BEWARE!
CRYSTALLOGRAPHIC CHARACTER
SANIDINE ORTHOCLASE MICROCLINE PLAGIOCLASE
2V - - - +/-
2V (np) 0-40° 30-80° 40-90° 80-105°
Np ∧ a 0-9° 3-12° 18° -10° - +10°
Fastl. - -
TWINS Carlsbad Carlsbad Checkboard Carlsbad (Albite)
Nm 1.53 1.525 1.52 1.53-1,545
Ng-Np 0.006 0.006 0.007 0.007-0.008
CONSEQUENCE: SANIDINE MAY STAY UNNOTICED
IOS
L'innovation comme motivation
UQAC

SOLUTION FROM THE MUSEUM

5-AXIS FEDEROV STAGE

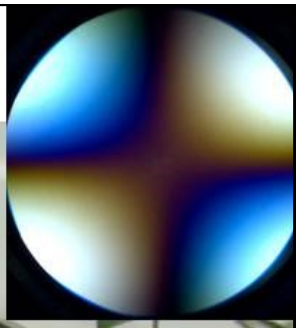

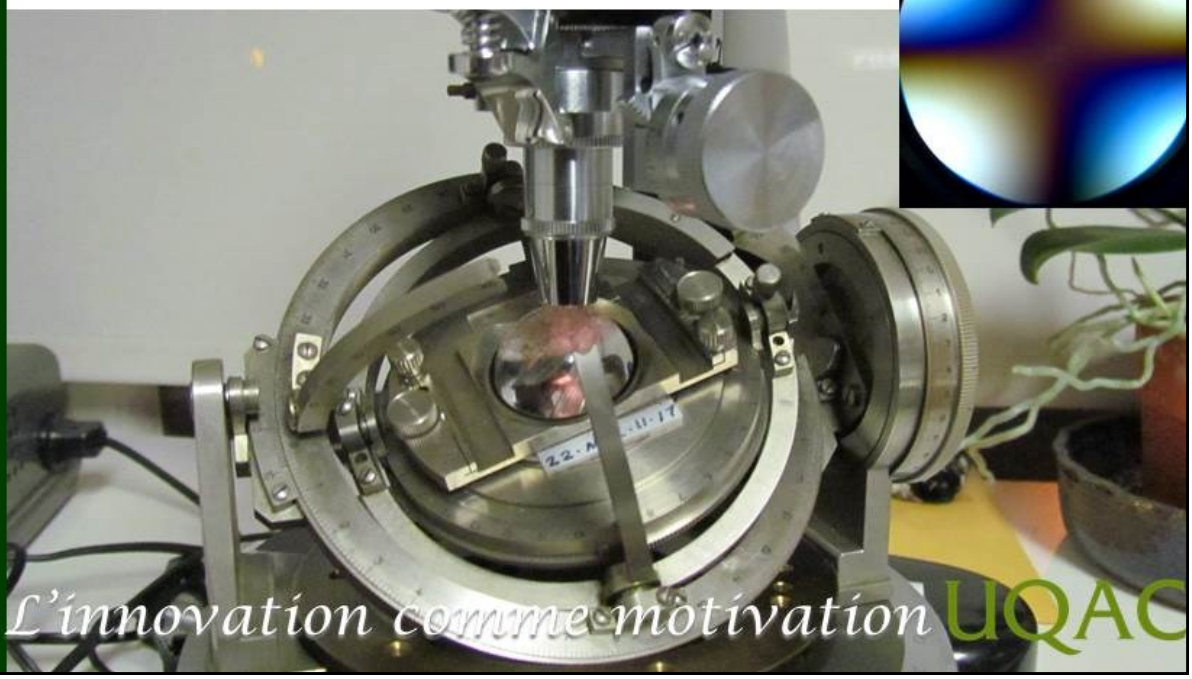

IOS *L'innovation comme motivation* UQAC

OLD KNOWHOW!

DISORDER MEASUREMENT

- DISORDER RELATES TO 2V
- Monoclinic, OAP ∥ (010)

$$\sum T_1 = 2T_1 = 0.665 - 0.711 sin^2 V_x$$

- Mono or triclinic, OAP ⊥ (010)

$$\sum T_1 = T_1o + T_1m = 0.665 + 0.711 sin^2 V_x$$

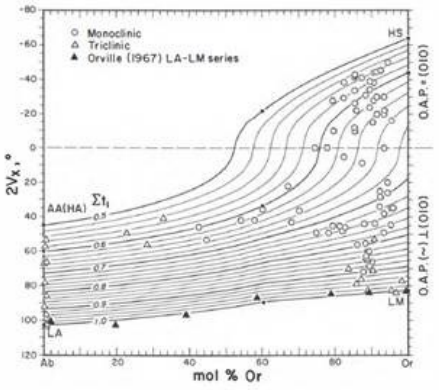

Su (1986)

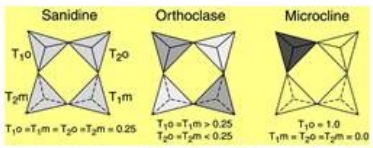

IOS *L'innovation comme motivation* UQAC

OLD KNOWHOW!

MICROCLINE OBLICITY FROM XRD

- Oblicity of feldspar (Δ) is measured by the distance between d_{131} and $d_{1\bar{3}1}$ from X-ray diffraction patterns

$$\Delta = 12.5\,(d_{131} - d_{1\bar{3}1})$$

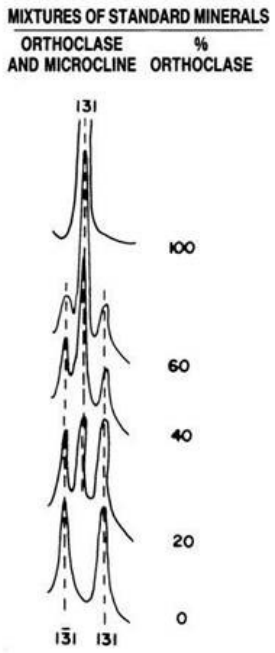

IOS *L'innovation comme motivation* UQAC

TOOL BOX

- 2V from Federov stage
- XRD on powder
- Cathodoluminescence
- Raman spectrometry
- Micro-XRD
- EBSD

IOS *L'innovation comme motivation* UQAC

FRESH
BRAINJUICE!
C. POTVIN-DOUCET
M.Sc Thesis on Canadian Malartic case
Thanks to:
Mitacs
IOS
L'innovation comme motivation
UQAC

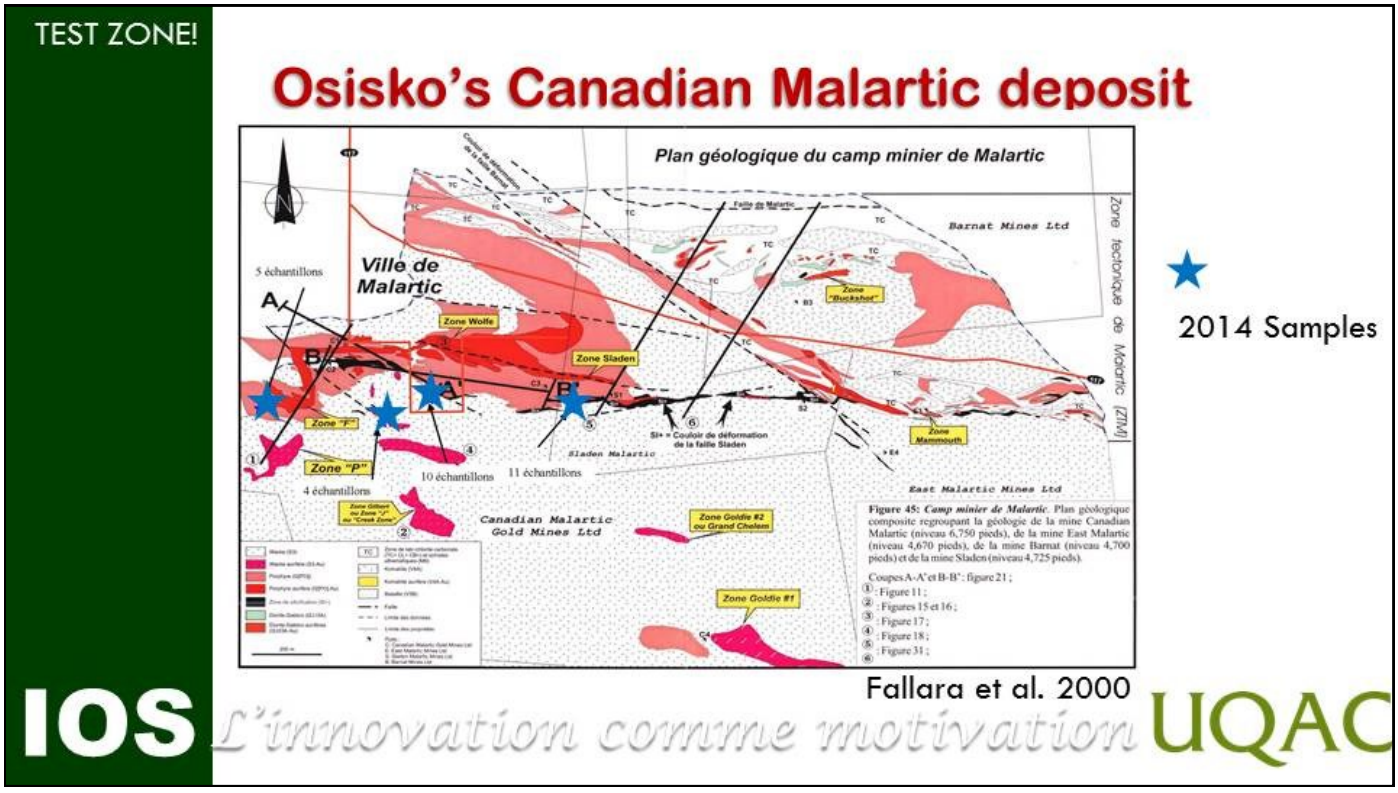
TEST ZONE!
Osisko's Canadian Malartic deposit
Plan géologique du camp minier de Malartic
Ville de Malartic
5 échantillons
4 échantillons
10 échantillons
11 échantillons
Zone Wolfe
Zone Sladen
Zone "F"
Zone "P"
Zone Gilbert ou Zone "J" ou "Creek Zone"
Zone Goldie #2 ou Grand Chelem
Zone Goldie #1
Zone Mammouth
Zone "Buckshot"
Barnat Mines Ltd
East Malartic Mines Ltd
Canadian Malartic Gold Mines Ltd
Sladen Malartic
Zone tectonique de Malartic (ZTM)
2014 Samples
Fallara et al. 2000
IOS
L'innovation comme motivation
UQAC

PRELIMINARY TESTS

1: COMPOSITION OF FELDSPAR: SEM-EDS

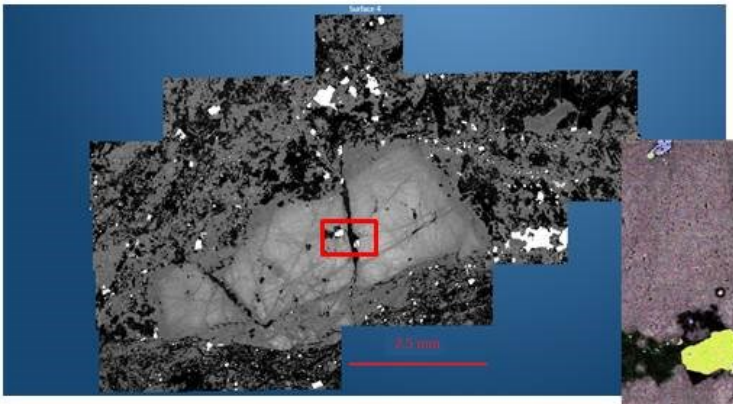

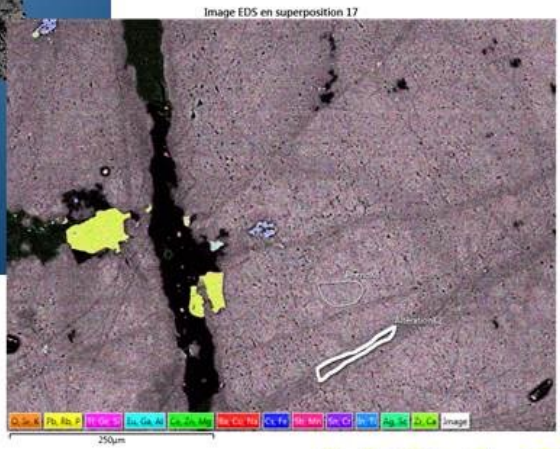

IOS *L'innovation comme motivation* UQAC

ORIGINS MATTER

1: COMPOSITION OF FELDSPAR: SEM-EDS

- CORE
  - No Ca or Na
  - Ba: 1,8% to 2,2%
  - ➔ Magmatic
- Rims: No Ba
  - ➔ Hydrothermal

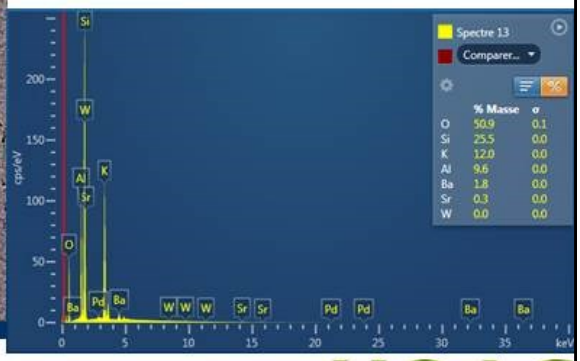

IOS *L'innovation comme motivation* UQAC

WORK IN PROGRESS

3: OBLICITY MEASUREMENT: XRD

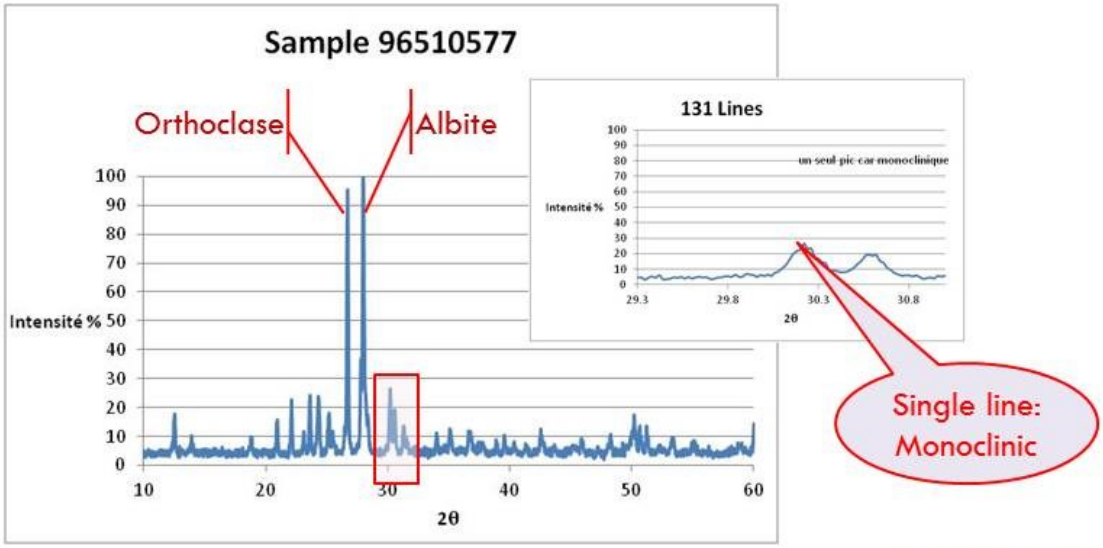

PROBLEM: MIXTURE OF FELDSPARS

IOS L'innovation comme motivation UQAC

THE GREAT QUESTIONS!

PRESERVATION OF HIGH-T FELS → QUENCH

- HOW CAN HIGH-T FELDSPAR BEING PRESERVED IN INTRUSIVE ROCKS?
- HOW CAN FELDSPAR STRUCTURE BE USED AT COOLING INDICATIONS?
- IS COOLING RATES RELATES OR TRIGGS HYDROTHERMAL VIGOR?
  - BECAUSE MINERALIZATION RELATES TO HYDROTHERMALISM!
- HOW DOES HIGH TEMPERATURE STRUCTURE BE PRESERVED DURING HYDROTHERMALISM?

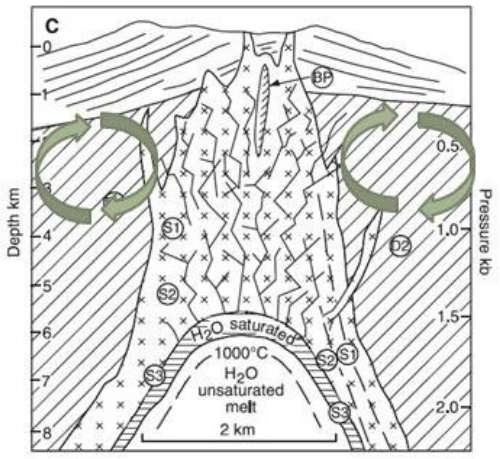

Pirajno 2009

IOS L'innovation comme motivation UQAC

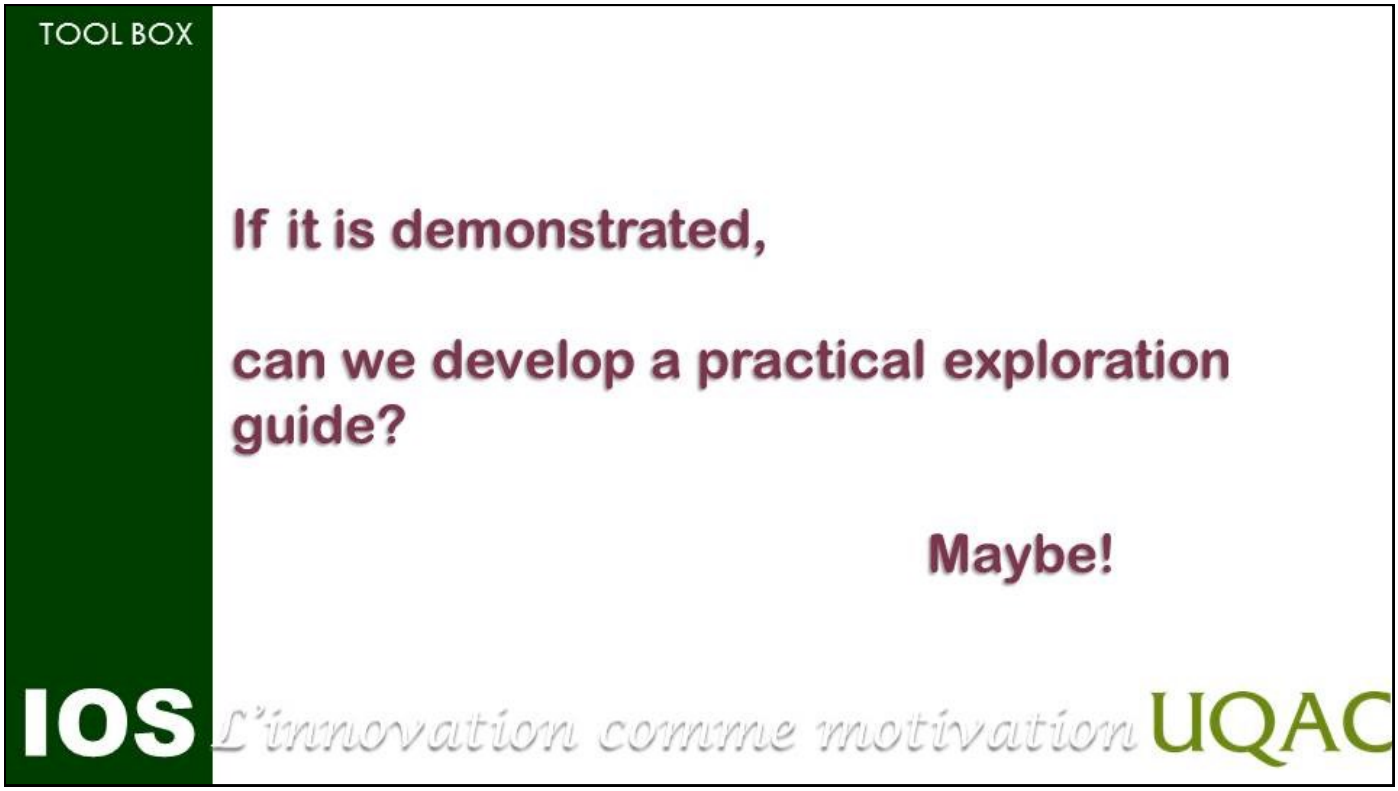
TOOL BOX
If it is demonstrated,
can we develop a practical exploration guide?
Maybe!
IOS
L'innovation comme motivation
UQAC

Chemical fingerprinting of the Archean Côté Gold deposit: A large-tonnage, low-grade intrusion-related deposit system, Ontario, Canada

L.R. Katz[1], D.J. Kontak[1], B. Dubé[2] and J.R. Rogers[3]

1. Laurentian University, Sudbury, Ontario
2. Geological Survey of Canada, 490 rue de la Couronne, Québec, Quebec
3. IAMGOLD Corporation, 401 Bay Street, Toronto, Ontario

Abstract: The Côté Gold intrusion-related Au (-Cu) deposit, in the Archean Swayze greenstone belt of the Abitibi Subprovince, is a large-tonnage, low-grade deposit hosted by ca. 2741 Ma tonalite and diorite of the Chester intrusive complex which formed in a high-level sub-volcanic setting. The deposit contains a resource (indicated + inferred) of 8.3 M oz Au that is centered on a magmatic-hydrothermal breccia. Mineralisation occurs as disseminations or is associated with quartz ± carbonate vein arrays, and is broadly coincident with biotite, silica-sodic and sericite alteration zones. Lithogeochemical and petrographic/SEM-EDS studies (>600 samples) across the deposit are used to assess the petrogenesis of the magmatic host rocks, distinguish between magmatic versus hydrothermal breccia, differentiate alteration types, determine the precursor rock where alteration is most intense, and chemically fingerprint the deposit. Preliminary observations indicate the following: (1) the tonalite suite is characterised by unfractionated CN REE patterns and reflects melt generation in a low-P regime; (2) protolith rocks are best discriminated using CaO, TiO_2 and Zr/TiO_2; (3) the magmatic-hydrothermal breccia is characterised by an Au-Cu-F-Te-Zn association; (4) biotite alteration, often with intergrowth of chalcopyrite, is characterised by Ba and LREE enrichment often accompanied by the presence of allanite-euxenite-bastnaesite; (5) zones of intense sodic alteration, up to 40 m thick and approaching 10 wt% Na_2O are characterised by a red-pink colour and a vuggy texture due to quartz dissolution. In thin section albite is pitted, contains abundant fluid inclusions and is mantled by clear albite. These rocks are considered to be episyenites; (6) sericite alteration zones, up to 150 m and cutting silica-sodic alteration, are characterised by an F ± Au ± Cu association; and (7) the chemistry of biotite in the breccia unit shows a reversal in Mg# after fractionation from diorite to tonalite (i.e., decreasing Mg#) which may indicate either injection of a new primitive melt or an oxidation-sensitive event coincident with formation of the breccia. Many of the features of the Côté Gold deposit suggest derivation of mineralisation and alteration by the flux of high-temperature fluids enriched in K, Fe, F, LREE, CO_2, and Ba, in addition to Au, Te and Cu. The association of Au-Cu mineralisation with a magmatic-hydrothermal breccia and a chemical signature that is atypical for Archean orogenic-type gold deposits indicates a possible affinity with a spatially and temporally related intrusive centre.

Originally presented Fredericton 2014: Geological Association of Canada - Mineralogical Association of Canada Joint Annual Meeting, Special Session 3: Discovering the Next Generation of Porphyry Deposits: Advancements in Locating and Understanding Hidden Intrusion-related Mineralization. May 21, 2014.

This research activity forms part of the TGI 4 - Lode Gold Project and was co-funded by IAMGOLD Corp.

Corresponding author: Laura R. Katz (lkatz@laurentian.ca)

Katz, L.R., Kontak, D.J., Dubé B., and Rogers, J.R., 2015. Chemical fingerprinting of the Archean Côté Gold deposit: A large-tonnage, low-grade intrusion-related deposit system, Ontario, Canada; *in* TGI 4 – Intrusion Related Mineralisation Project: New Vectors to Buried Porphyry-Style Mineralisation, (ed.) N. Rogers; Geological Survey of Canada, Open File 7843, p. 445-458.

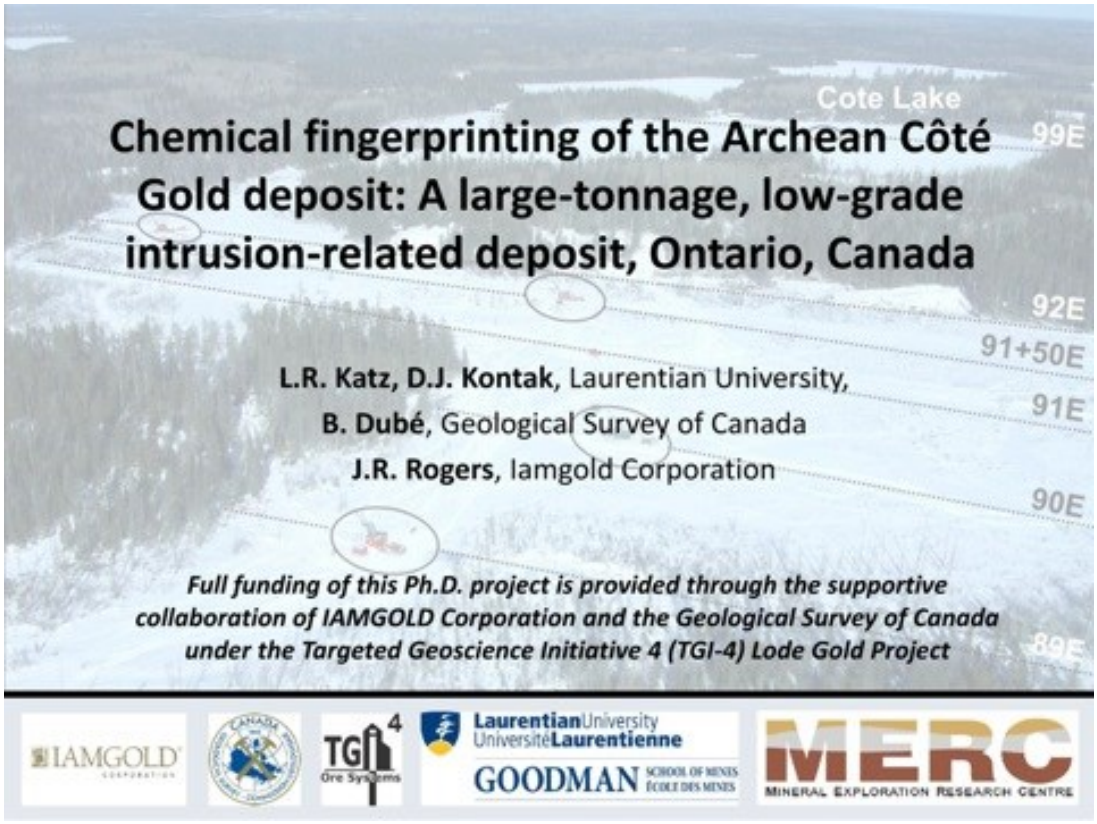

Outline

1) Introduction
2) Regional geological setting
3) Deposit geology
4) Nature of mineralization and alteration
5) Lithogeochemistry
   i. Alteration geochemistry
   ii. Characterization of the breccia unit
   iii. Chemical fingerprinting of the deposit
6) Conclusions

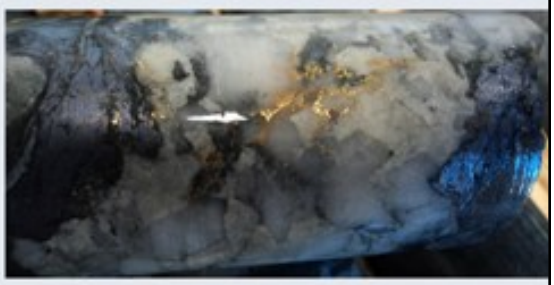

1. Introduction

Côté Gold Deposit

- Discovered in 2009/2010;
- Gold resource: indicated = 296 Mt @ 0.88 g/t Au (7.61 M oz) and inferred = 44 Mt @ 0.74 g/t Au (1.04 M oz);
- Hosted in ca. 2741 Ma, high-level tonalite-diorite complex and centered on a magmatic-hydrothermal breccia body;
- First large gold deposit discovered in the Swayze greenstone belt;
- Represents at new metallogenic event at 2741 Ma.

2. Geological Setting

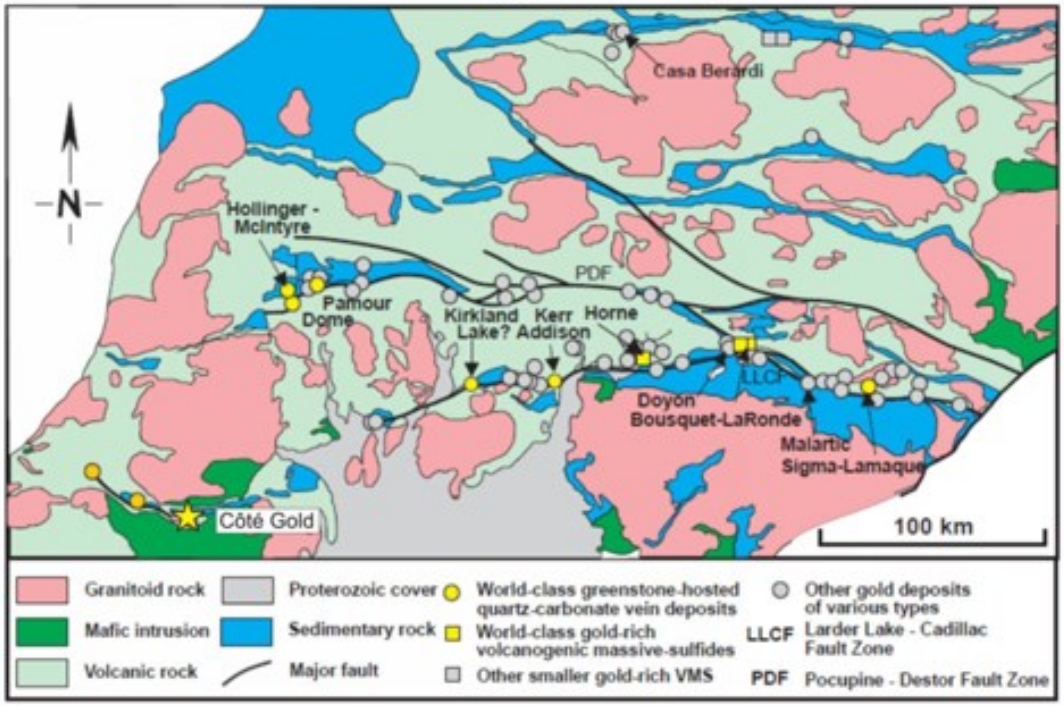

Modified after Dubé and Gosselin (2007)

Geological Setting

- **ca. 2741 Ma Chester Intrusive Complex (CIC): laccolith-shaped, synvolcanic tonalite-diorite intrusion;**
- CIC intrudes mafic metavolcanic rocks of Arbutus Formation and underlies coeval (ca. 2739 Ma) felsic to intermediate metavolcanic unit.

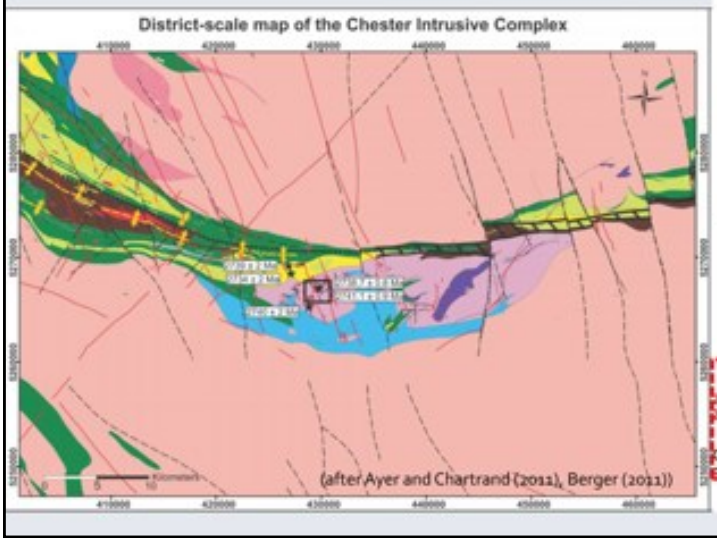

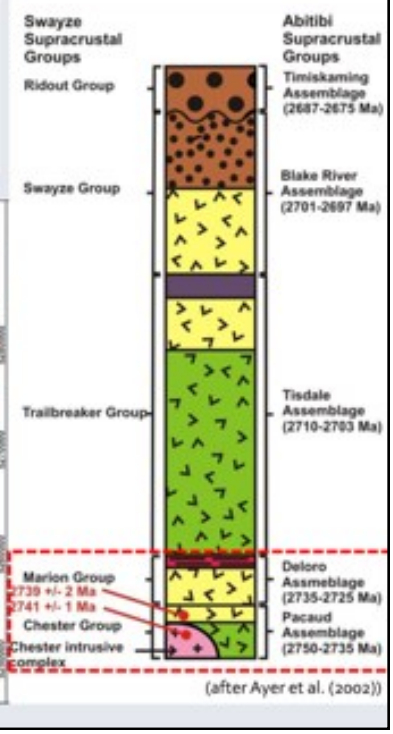

3. Deposit Geology

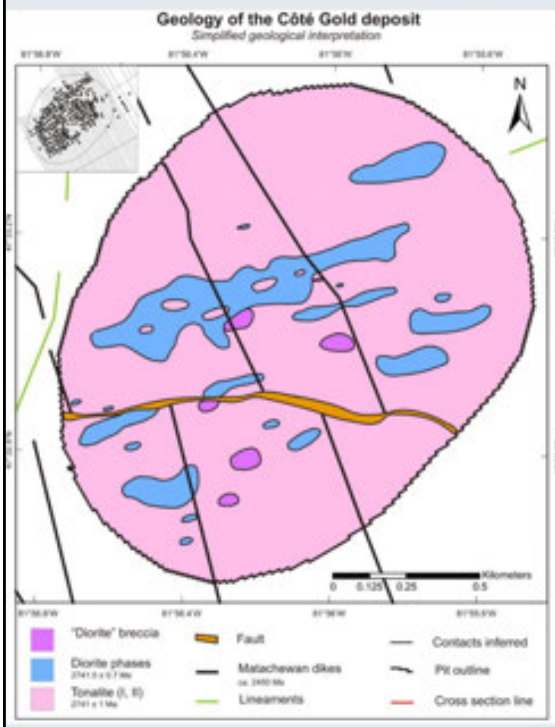

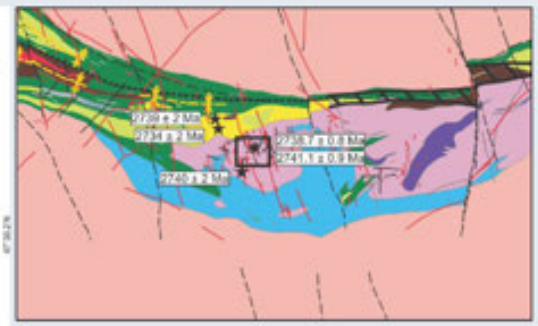

- Hosted in CIC tonalite (I) and diorite (II) → tonalite (II);
- High-level intrusion: mariolitic cavities, granophyric texture, breccia;
- CIC constrained to 2741 Ma
- Mineralization centred on a magmatic-hydrothermal breccia;
- Maximum age of gold mineralization constrained to 2739 ± 7 Ma;
- Late dike rocks and brittle fault cuts through deposit.

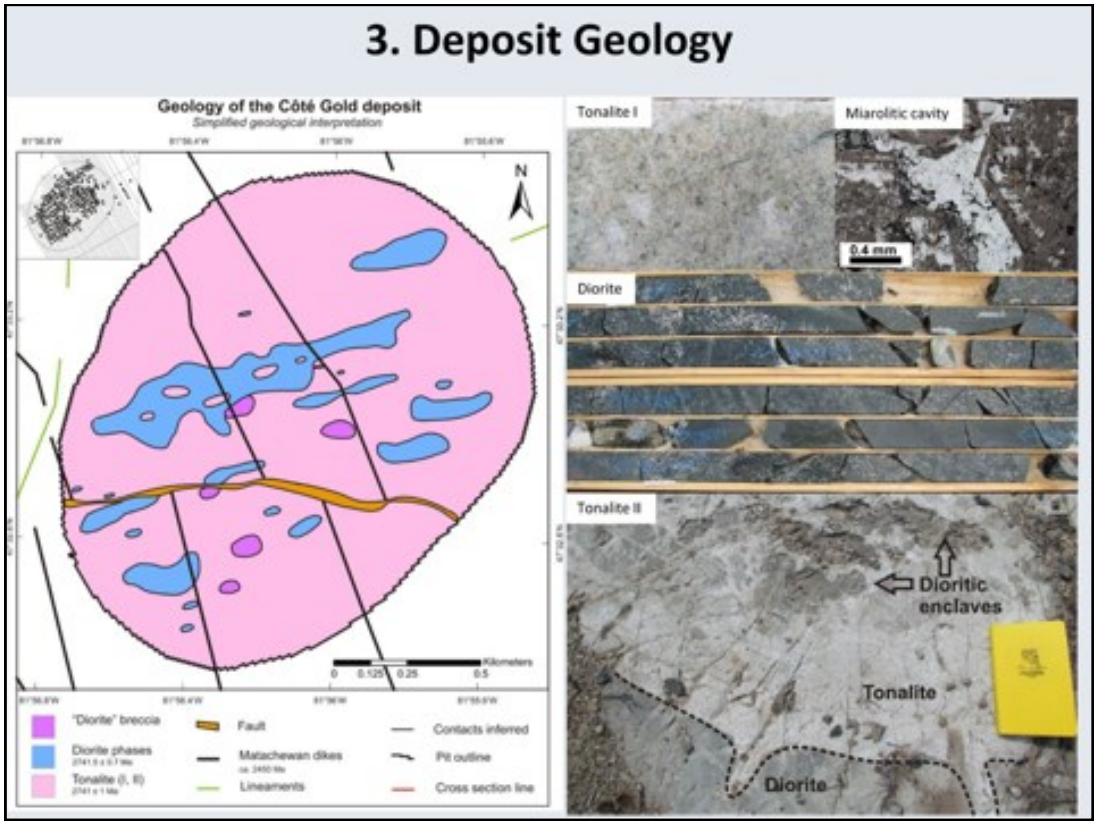
3. Deposit Geology
Geology of the Côté Gold deposit
Simplified geological interpretation
N
Kilometers
0 0.125 0.25 0.5
"Diorite" breccia
Diorite phases
Tonalite (I, II)
Fault
Matachewan dikes
Lineaments
Contacts inferred
Pit outline
Cross section line
Tonalite I
Miarolitic cavity
0.4 mm
Diorite
Tonalite II
Dioritic enclaves
Tonalite
Diorite

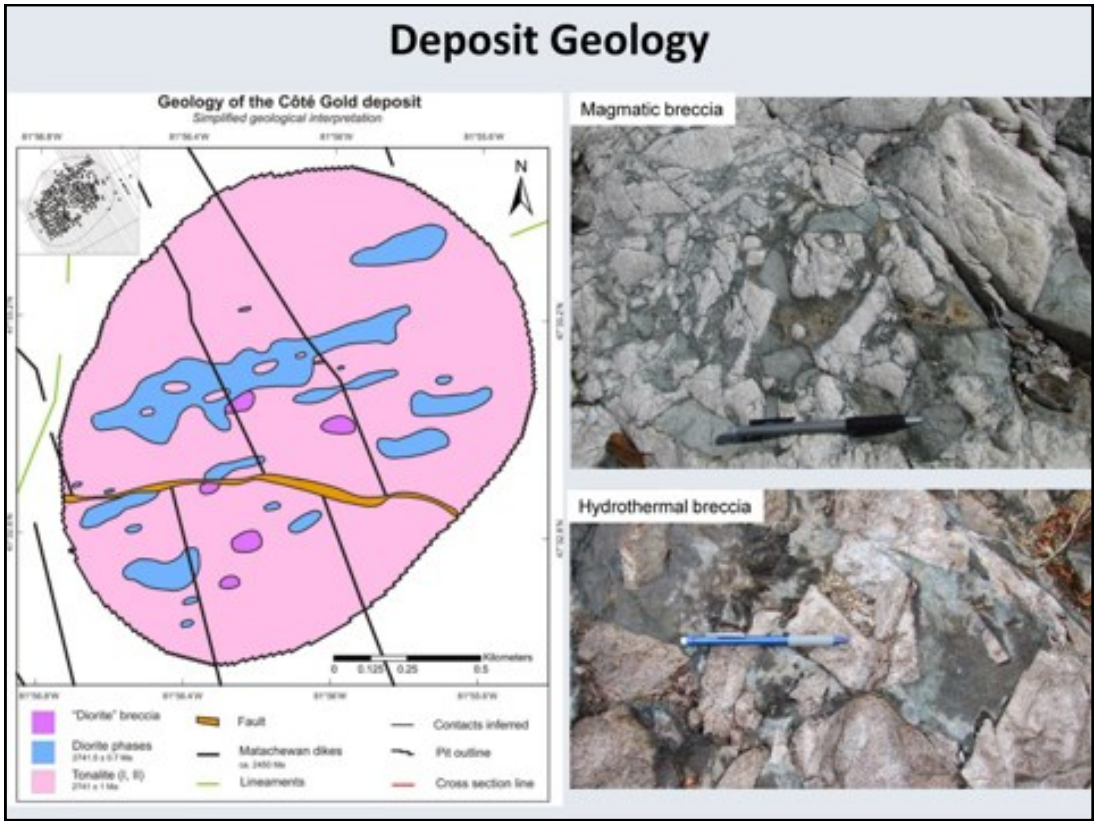
Deposit Geology
Geology of the Côté Gold deposit
Simplified geological interpretation
N
Kilometers
0 0.125 0.25 0.5
"Diorite" breccia
Diorite phases
Tonalite (I, II)
Fault
Matachewan dikes
Lineaments
Contacts inferred
Pit outline
Cross section line
Magmatic breccia
Hydrothermal breccia

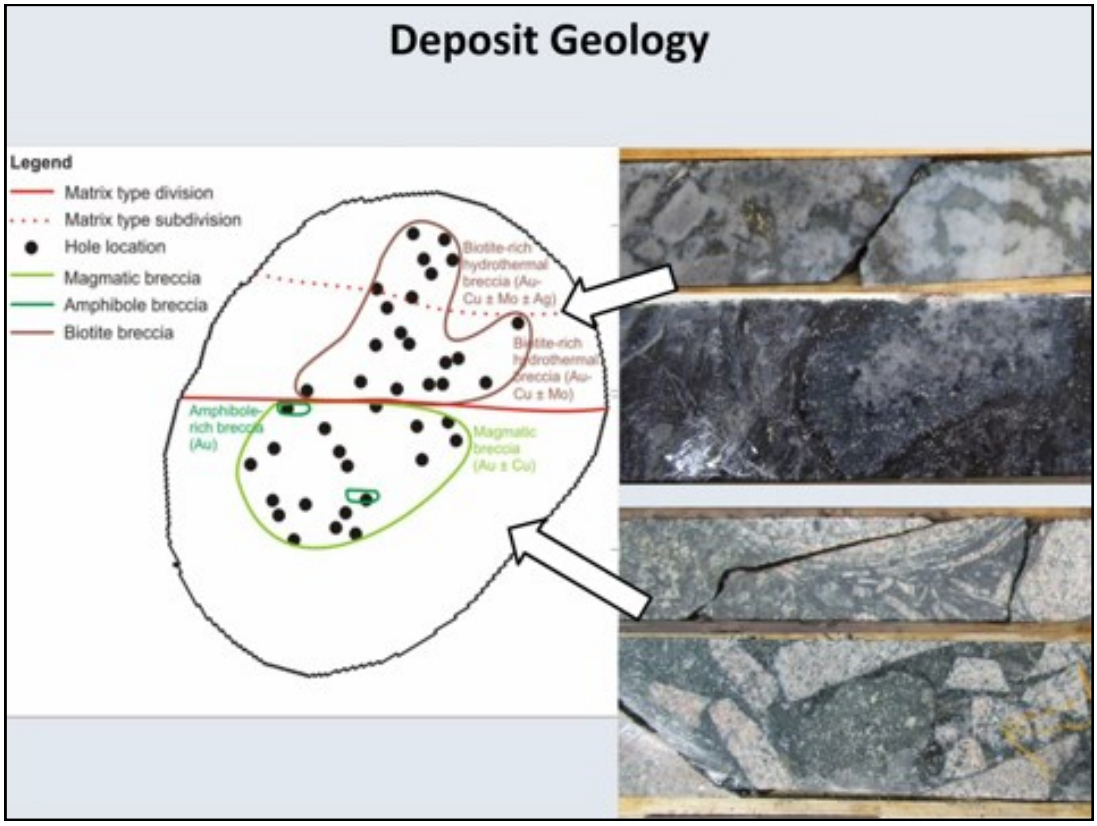

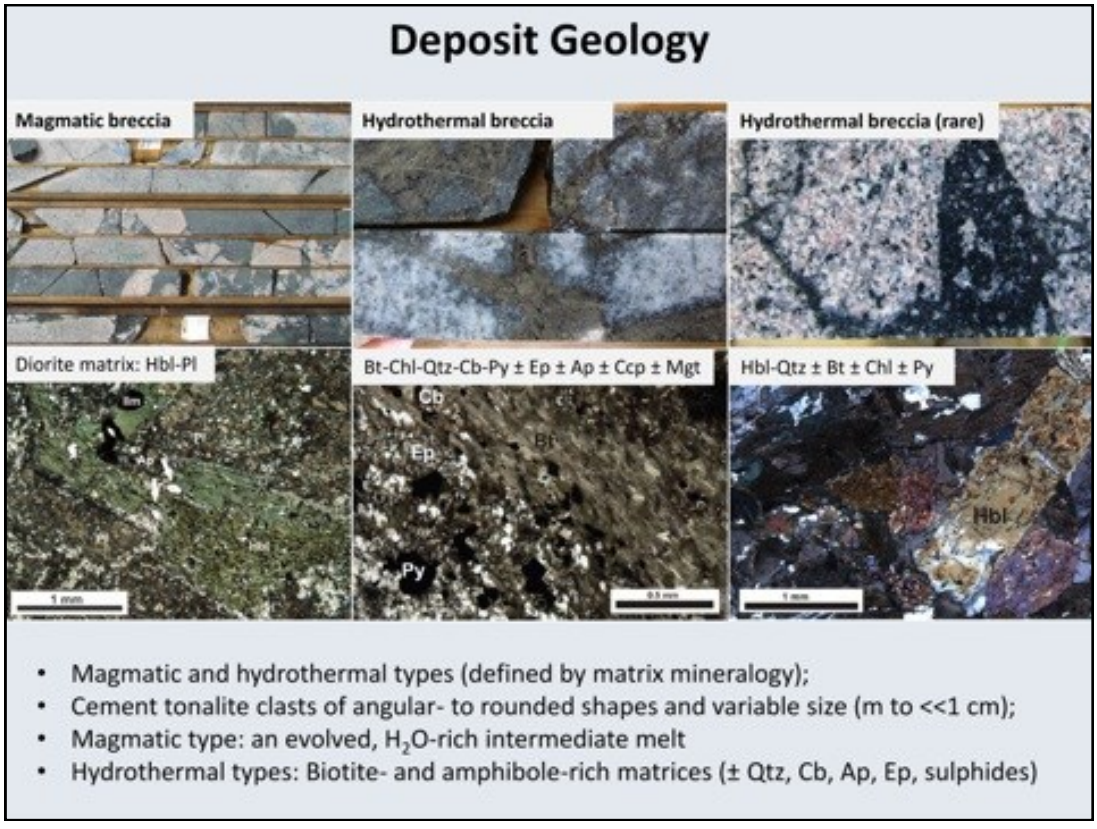

- Magmatic and hydrothermal types (defined by matrix mineralogy);
- Cement tonalite clasts of angular- to rounded shapes and variable size (m to <<1 cm);
- Magmatic type: an evolved, H_2O-rich intermediate melt
- Hydrothermal types: Biotite- and amphibole-rich matrices (± Qtz, Cb, Ap, Ep, sulphides)

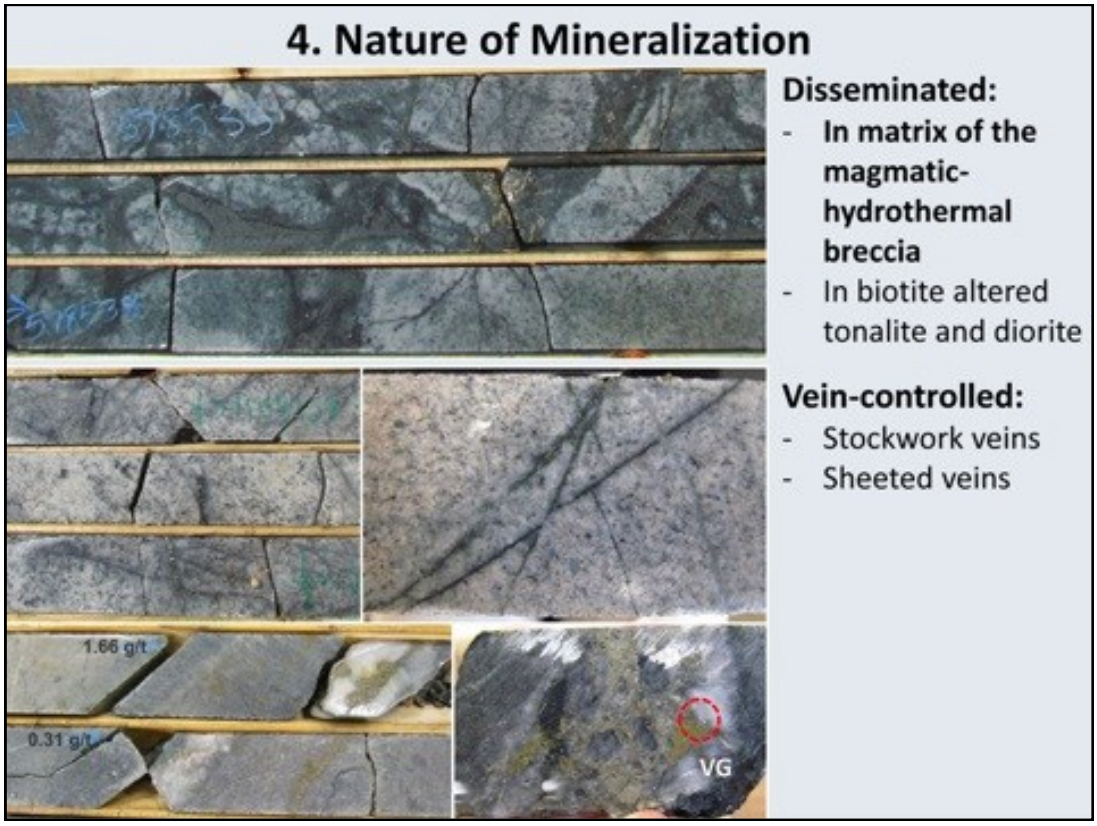
4. Nature of Mineralization
Disseminated:
- In matrix of the magmatic-hydrothermal breccia
- In biotite altered tonalite and diorite
Vein-controlled:
- Stockwork veins
- Sheeted veins
1.66 g/t
0.31 g/t
VG

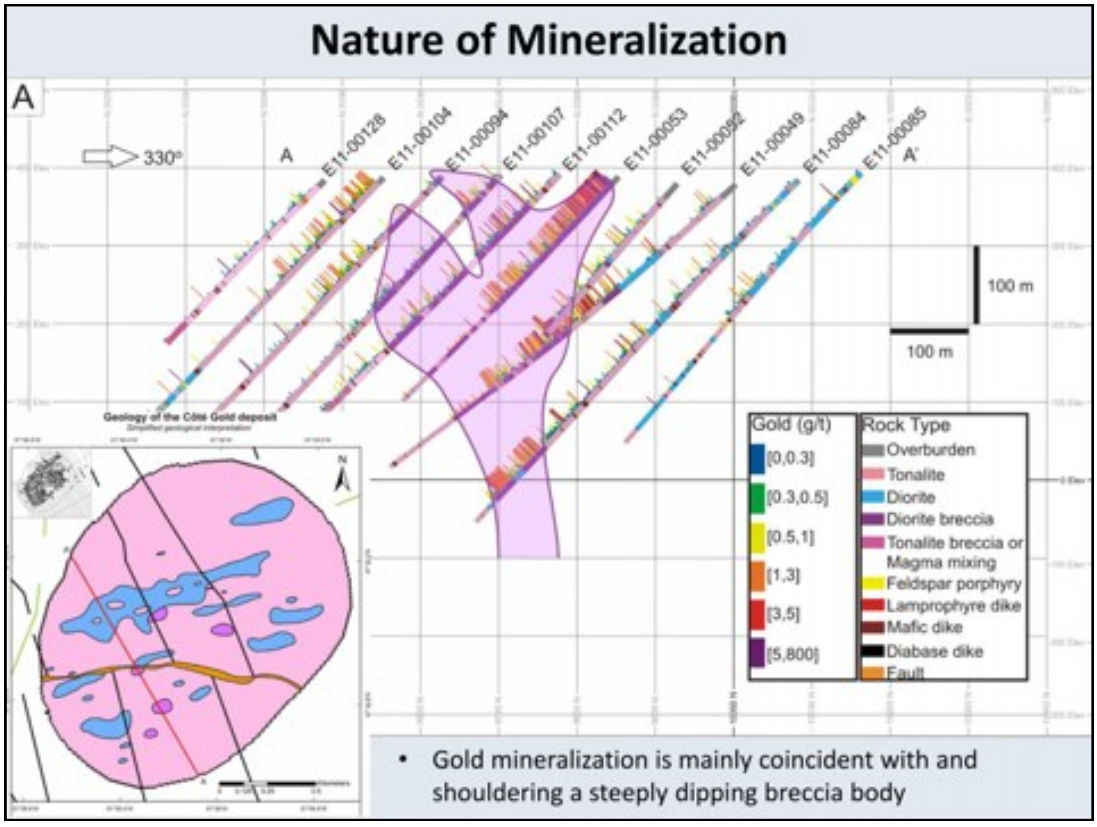
Nature of Mineralization
A
330°
A
E11-00128
E11-00104
E11-00094
E11-00107
E11-00112
E11-00053
E11-00092
E11-00049
E11-00084
E11-00085
A'
100 m
100 m
Geology of the Côté Gold deposit
Gold (g/t)
[0,0.3]
[0.3,0.5]
[0.5,1]
[1,3]
[3,5]
[5,800]
Rock Type
Overburden
Tonalite
Diorite
Diorite breccia
Tonalite breccia or Magma mixing
Feldspar porphyry
Lamprophyre dike
Mafic dike
Diabase dike
Fault
• Gold mineralization is mainly coincident with and shouldering a steeply dipping breccia body

Alteration
Biotite
Sericite
Silica-Sodic
Epidote
Early
Late
Breccia matrix
Tonalite
Breccia
Tonalite

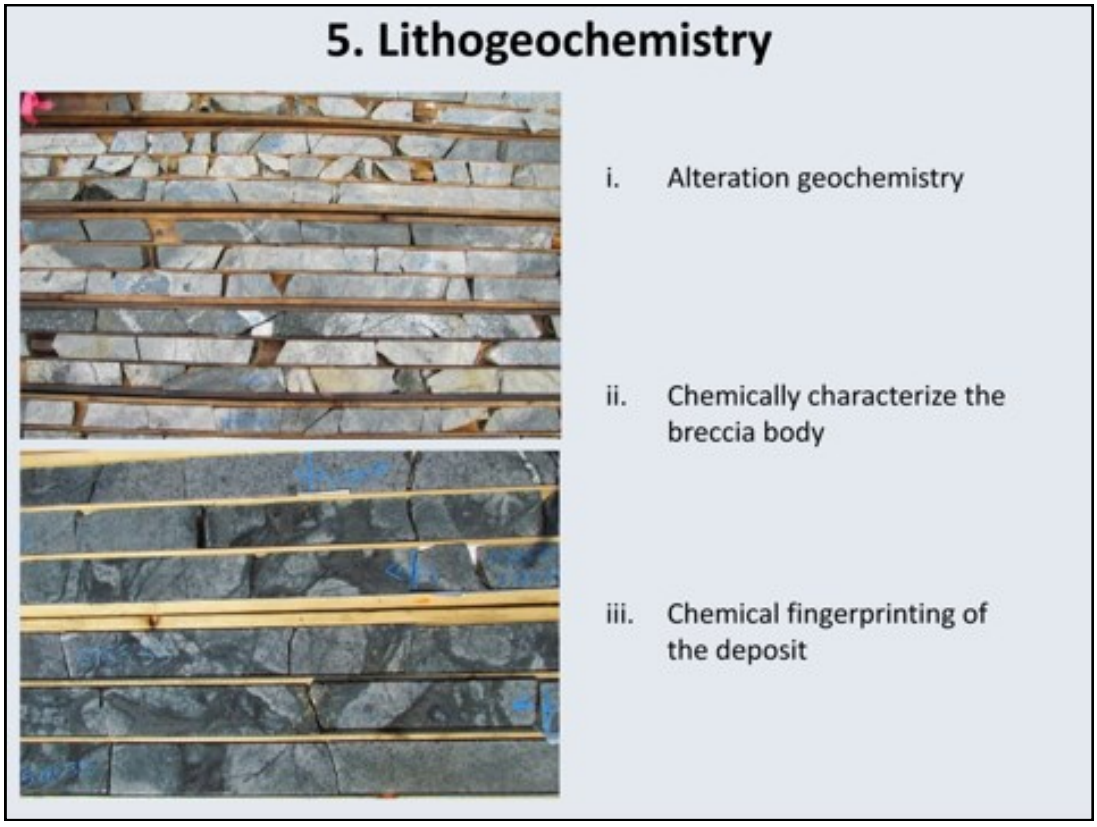
5. Lithogeochemistry
i. Alteration geochemistry
ii. Chemically characterize the breccia body
iii. Chemical fingerprinting of the deposit

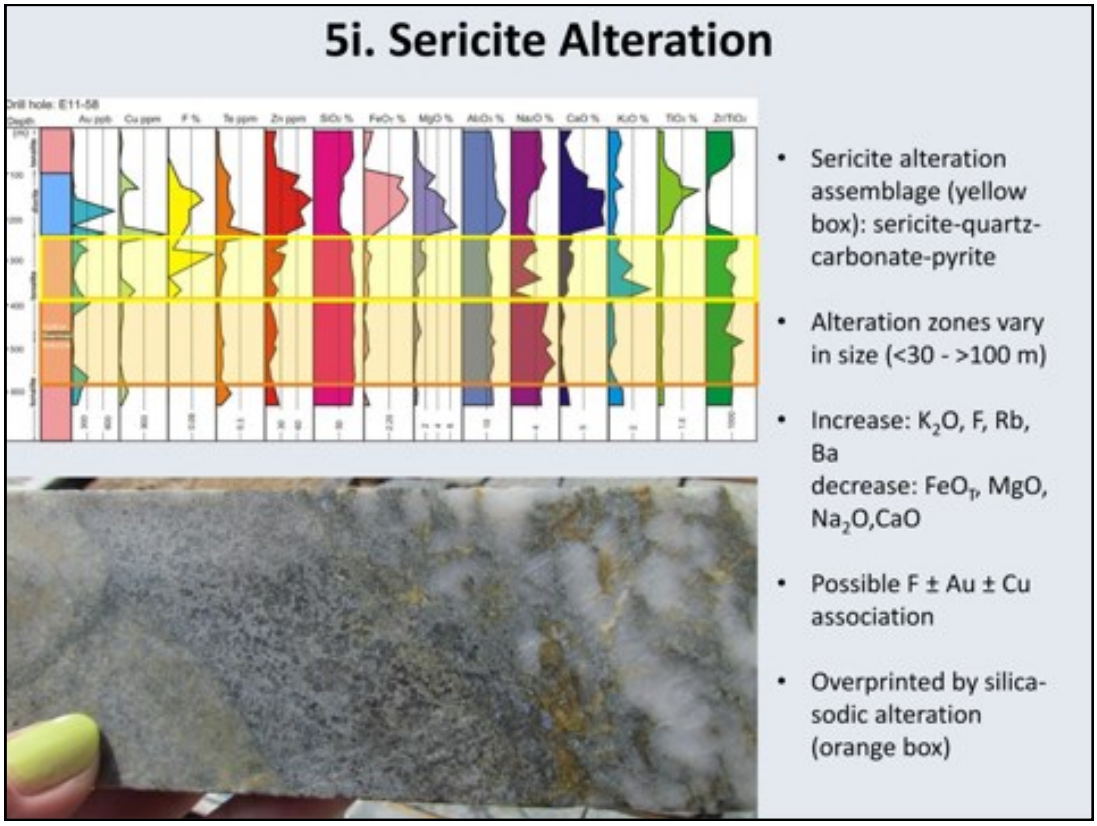
5i. Sericite Alteration
Drill hole: E11-58
Depth
Au ppb
Cu ppm
F %
Te ppm
Zn ppm
SiO2 %
FeOT %
MgO %
Al2O3 %
Na2O %
CaO %
K2O %
TiO2 %
Zr/TiO2
• Sericite alteration assemblage (yellow box): sericite-quartz-carbonate-pyrite
• Alteration zones vary in size (<30 - >100 m)
• Increase: K2O, F, Rb, Ba
decrease: FeOT, MgO, Na2O,CaO
• Possible F ± Au ± Cu association
• Overprinted by silica-sodic alteration (orange box)

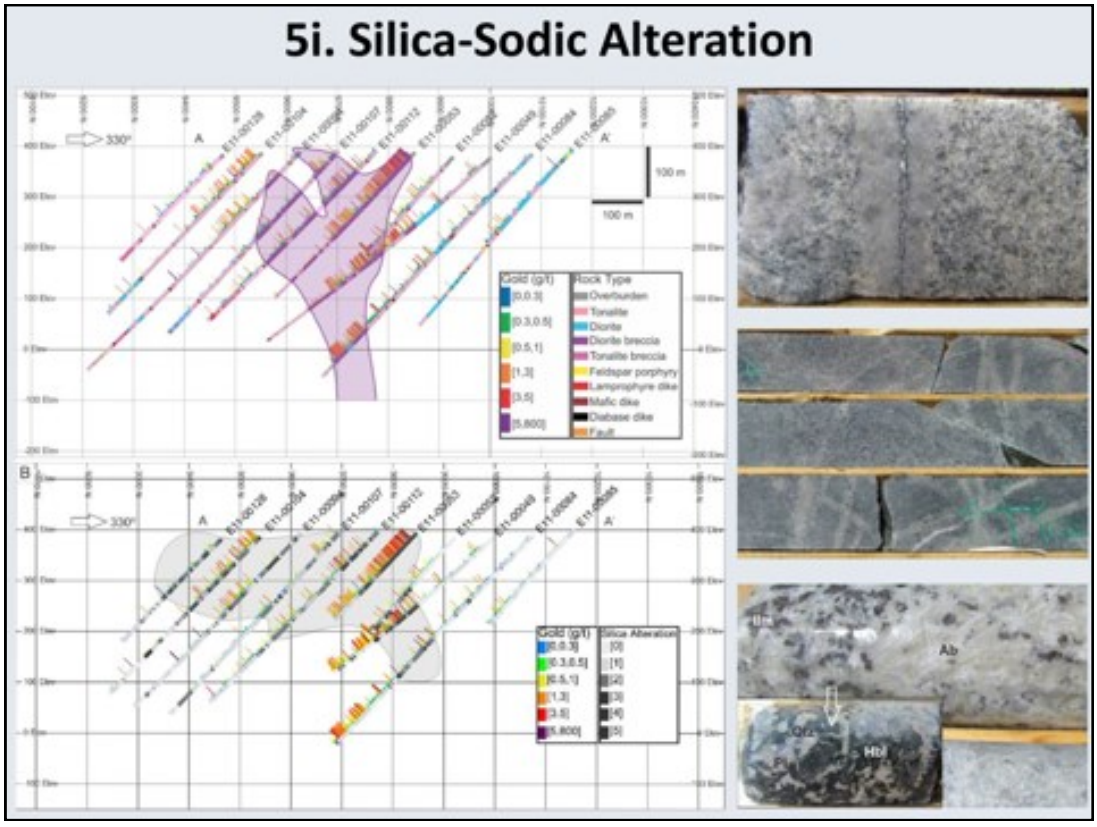
5i. Silica-Sodic Alteration
330°
A
A'
100 m
100 m
Gold (g/t)
[0,0.3]
[0.3,0.5]
[0.5,1]
[1,3]
[3,5]
[5,800]
Rock Type
Overburden
Tonalite
Diorite
Diorite breccia
Tonalite breccia
Feldspar porphyry
Lamprophyre dike
Mafic dike
Diabase dike
Fault
B
330°
A
A'
Gold (g/t)
Silica Alteration
Ab
Qtz
Hbl

5i. Silica-Sodic Alteration

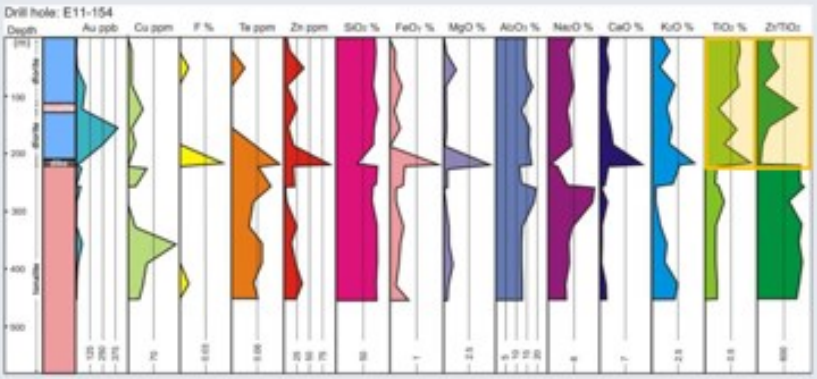

- Increase: SiO_2, Na_2O (up to 10 wt. % Na_2O) decrease: FeO_T, MgO, CaO
- Alteration zones vary in size (~100 - >500 m)
- TiO2 and Zr/TiO2 ratio can distinguish between tonalite and diorite when altered

5i. Sodic Alteration

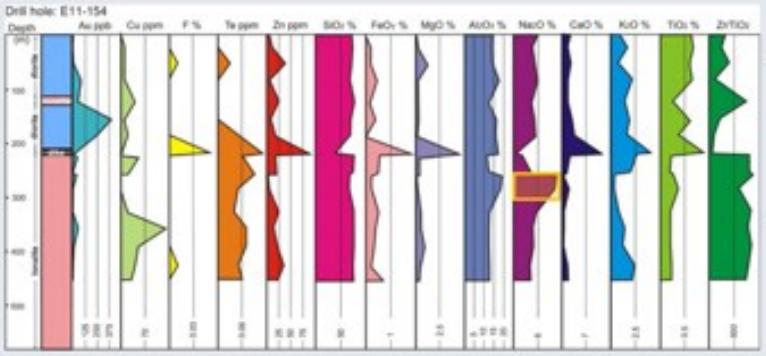

- Rare, localized, intense sodic altered zones (up to 10 wt. % Na_2O)
- <40 m zones of episyenite: characterized by vuggy texture

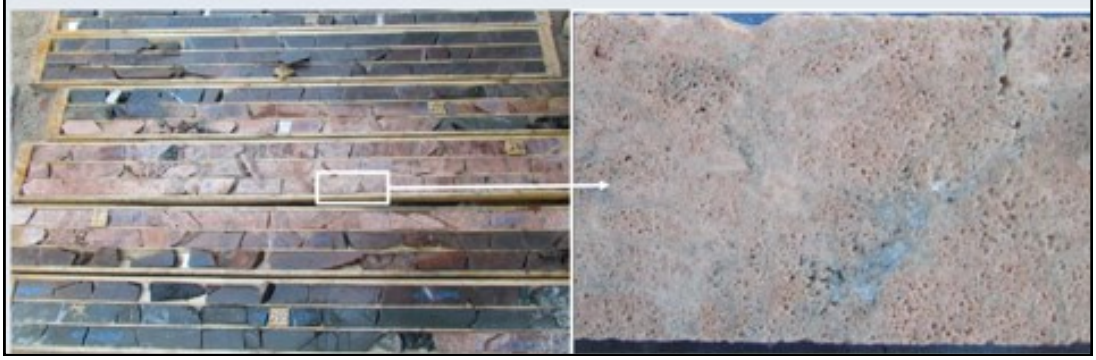

5ii. Breccia Body

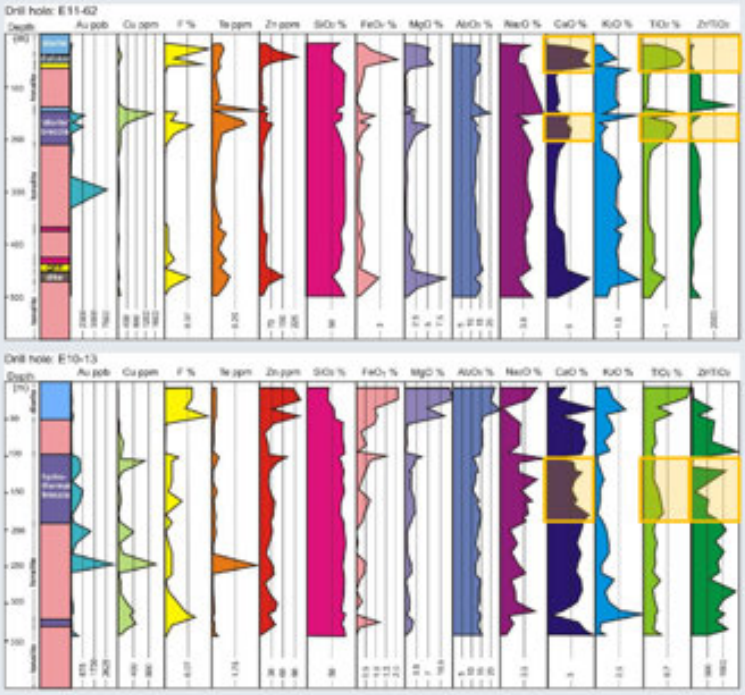

- Magmatic breccia contains elevated CaO, TiO2 and low, Zr/TiO2 similar to diorite
- Hydrothermal breccia contains lower CaO, TiO2 and higher Zr/TiO2, than diorite and magmatic breccia

5ii. Breccia Body

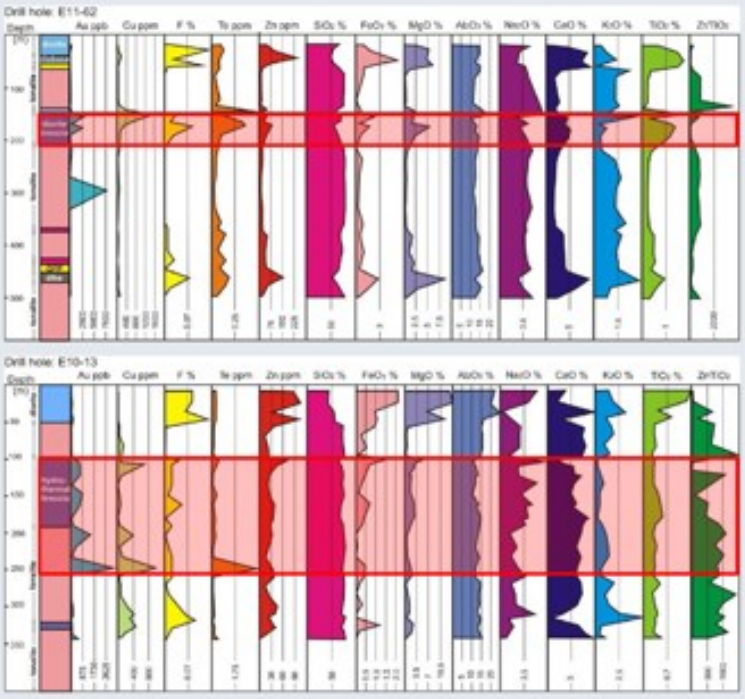

- Au-Cu-Te-F ± Zn ± Mo association in breccia unit
- Less apparent in tonalite and diorite rocks
- Footwall to the breccia unit, gold mineralization extends into altered tonalite and occurs as veins of quartz ± carbonate ± chlorite ± pyrite ± chalcopyrite

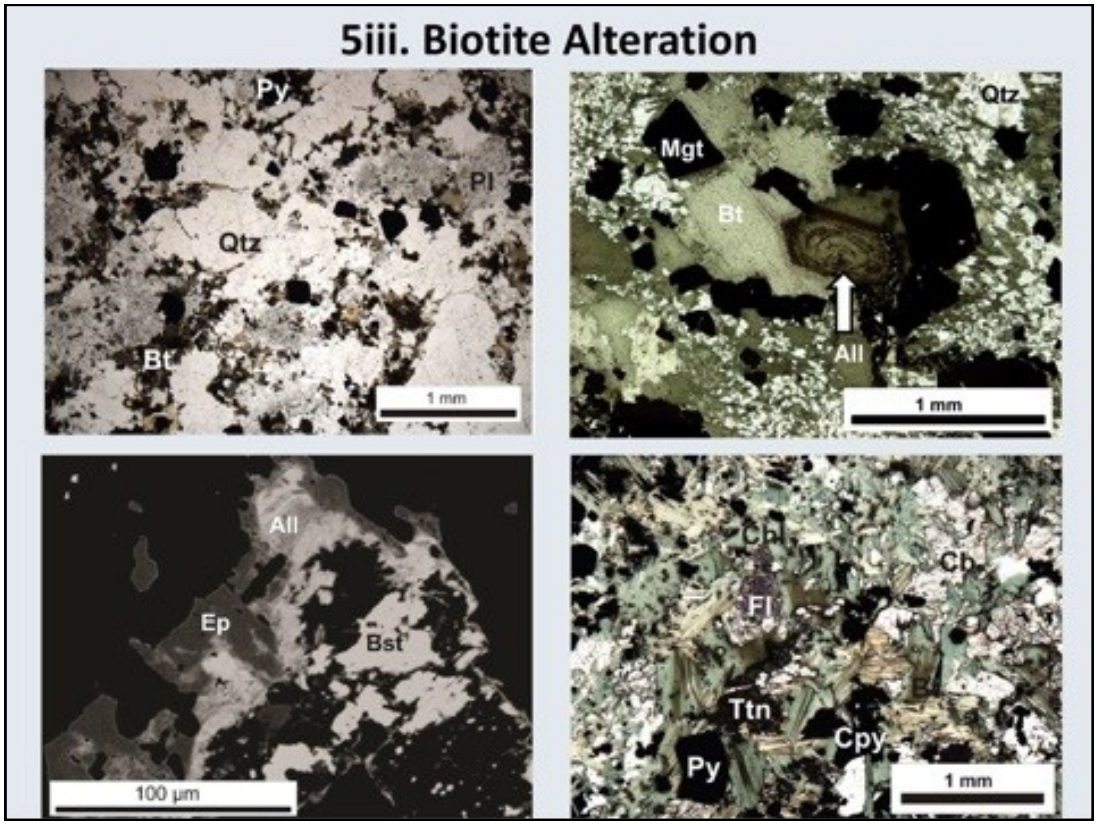
5iii. Biotite Alteration
Py
Pl
Qtz
Bt
1 mm
Qtz
Mgt
Bt
All
1 mm
All
Ep
Bst
100 µm
Chl
Cb
Fl
Ttn
Cpy
Py
1 mm

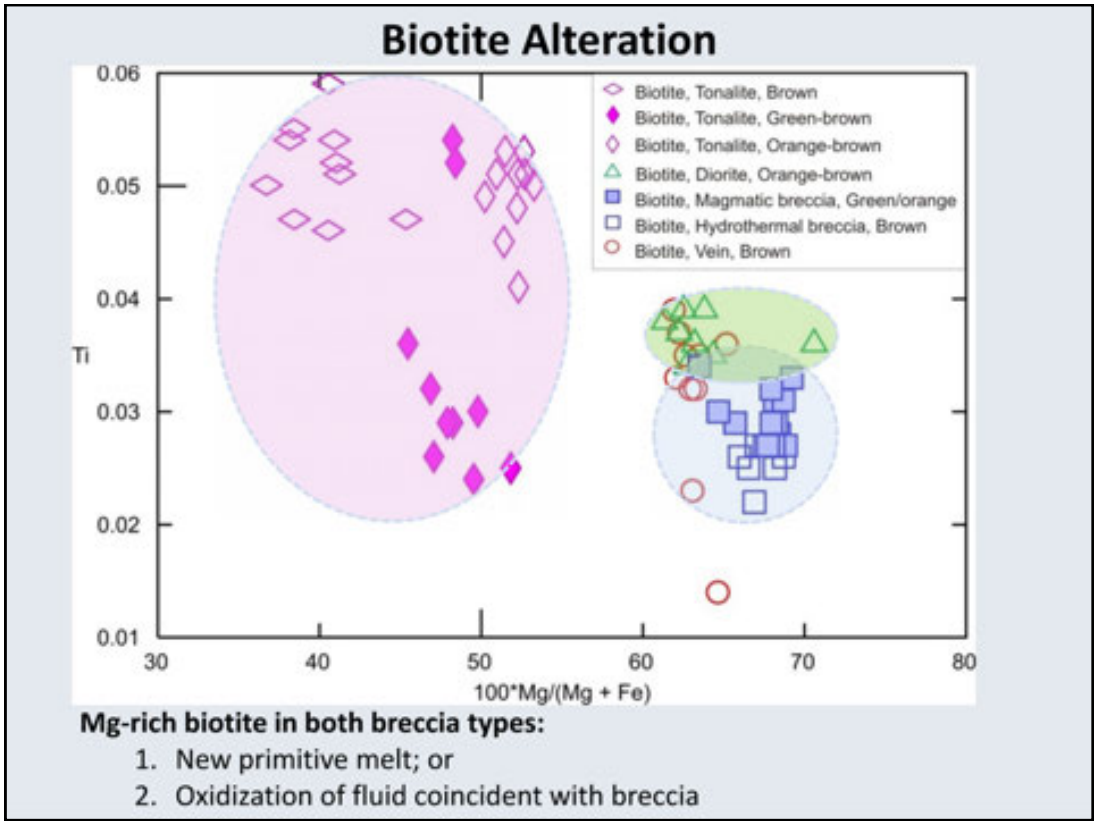
Biotite Alteration
Biotite, Tonalite, Brown
Biotite, Tonalite, Green-brown
Biotite, Tonalite, Orange-brown
Biotite, Diorite, Orange-brown
Biotite, Magmatic breccia, Green/orange
Biotite, Hydrothermal breccia, Brown
Biotite, Vein, Brown
Ti
0.06
0.05
0.04
0.03
0.02
0.01
30
40
50
60
70
80
100*Mg/(Mg + Fe)
Mg-rich biotite in both breccia types:
1. New primitive melt; or
2. Oxidization of fluid coincident with breccia

Biotite Alteration

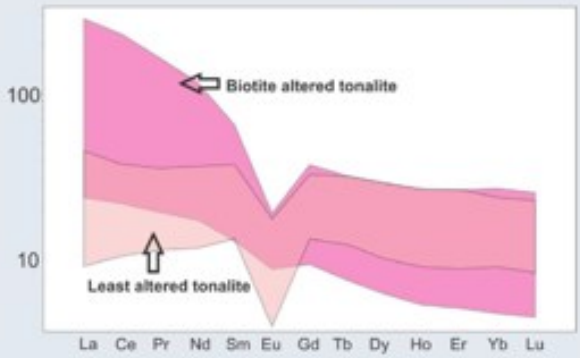

Geochemical fingerprint:

- Increase of LREE due to LREE-bearing minerals (e.g., allanite and bastnaesite)
- Elevated F due to biotite, titanite and fluorite

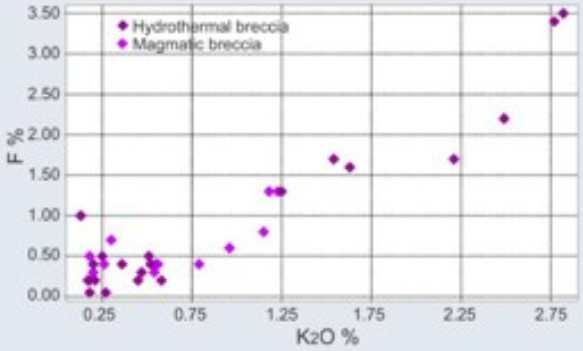

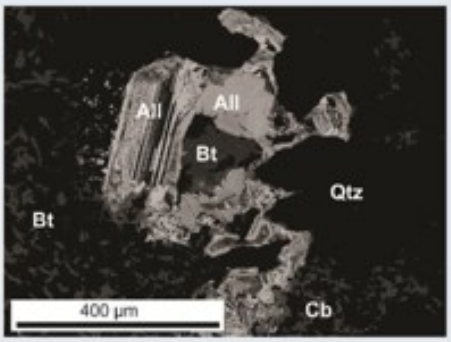

5iii. Metal Association

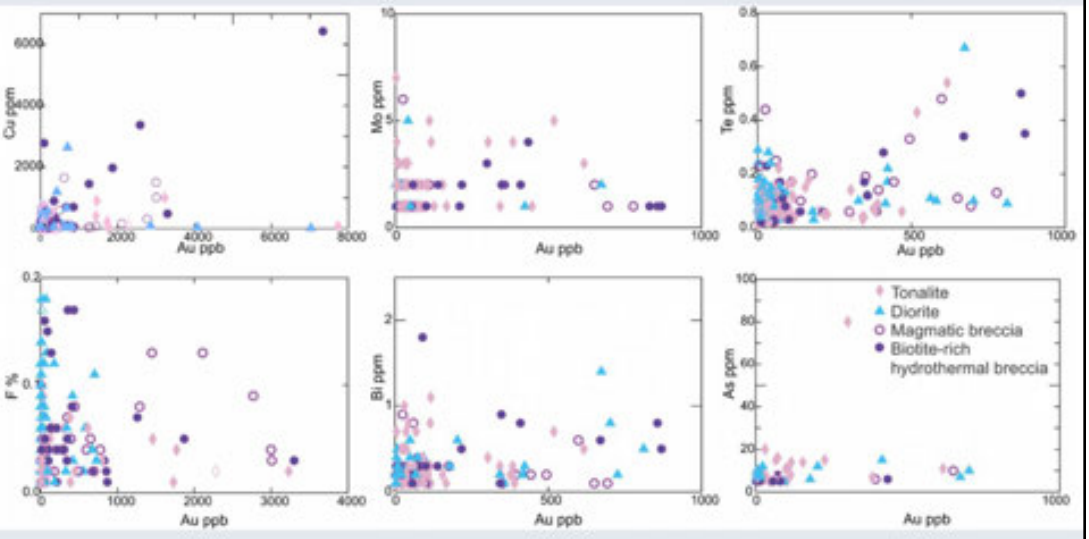

- Moderate Au-Cu and Au-Te association in the breccia unit
- Weak Au-F association in the breccia unit
- No Au-Cu, Au-Te or Au-F association in tonalite or diorite rocks
- Overall lack of elemental associations at the Côté Gold deposit

6. Summary and Conclusions

- Low-grade, large-tonnage Au deposit (Indicated: 296 Mt @ 0.88 g/t Au (7.61 M oz) and inferred: 44 Mt @ 0.74 g/t Au (1.04 M oz));
- Centred on a magmatic-hydrothermal breccia body that intruded a high-level tonalite (ca. 2741 Ma);
- Represents a new metallogenic event at 2741 Ma;
- Mineralization consists of disseminated and stockwork types that are co-spatial with biotite, sericite and silica-sodic alteration styles;
- Breccia body is of magmatic-hydrothermal origin and is characterized by Au, Te, Cu, F association;
- Breccia body has textural and metal zonation;
- Biotite alteration is chemically characterized by enrichment in LREE and F (basnaesite, allanite, fluorite, F-bearing titanite).

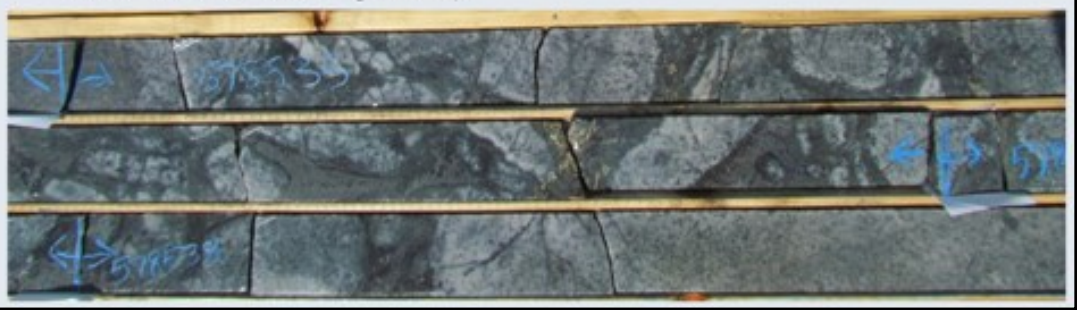

Using biotite composition of the Devonian Lake George granodiorite, New Brunswick, as a case study for W-Mo-Au-Sb mineralized magmatic hydrothermal systems

Z. Azadbakht, D.R. Lentz and C.R.M. McFarlane

University of New Brunswick, Box 4400, 2 Bailey Drive, Fredericton, New Brunswick

Abstract: The granodioritic Lake George polymetallic deposit is located approximately 35 km southwest of Fredericton, New Brunswick. This intrusion is a metaluminous to weakly peraluminous, calc-alkaline body that shows an evolved I-type, volcanic arc affinity. Based on an Early Devonian age determination, (412 +5/-4 Ma, zircon U-Pb) it is related to the Hakshaw granite phase of the Pokiok Batholith. The Lake George stock is cut by Hibbard stibnite -quartz veins and quartz-scheelite-molybdenite veinlets that contain significant amounts of gold. Fresh biotites from this intrusion were analyzed at both the core and rim by electron microprobe, and along rim to rim transects by laser ablation ICP-MS at the University of New Brunswick to build an understanding of the halogens responsible for mineralization and trace element distribution within this deposit.

Biotites of this intrusion are reddish brown in colour (indicative of reduced I-type source) and mostly altered to chlorite. They usually contain apatite, zircon, titanite, ilmenite, rutile, and sulphide minerals as mineral inclusions. Temperature was calculated with the Ti-In-biotite geothermometer, in which the results showed a variation between 583 and 745°C.

Two depths of emplacement were determined based on the Al in hornblende and biotite geobarometries confirming the porphyritic texture of this intrusion (4.3 and 1.5 km, respectively). Forming amphiboles at that depth clearly indicates a high water content of the source magma; in addition, hydroxyl is the most dominant component of the hydroxyl site (Average 1.89 wt%) in biotites. The limited range of IV(F/Cl) values of the Lake George biotites suggested that they all equilibrated with one fluid.

Even though there is no noticeable difference in major elements from core to rims, evidence of magma evolution is recorded by biotite grains by their trace elements. For instance, Cu, Rb, Cr, K, Mo, Sn, Cs and W increase from core to rims, whereas Ba, Ni, Mn, and Li act inversely. Sb has a negligible variation from core to rim. Interestingly, the partition coefficient (biotite/whole-rock) is significantly small for Sb, W, and Mo (main associated mineralization) with 0.06, 0.28 and 0.13 in pure magmatic biotites and increase to 0.77, 1.93 and 0.20 in more altered biotites reflecting enrichment of these elements towards the late stage fluid.

Based on these observations, the concept of using mica composition to help identify fertile Acadian magma systems was proved; this method may be a useful tool to indicate the difference between barren and mineralized granophile-element rich systems.

Originally presented Fredericton 2014: Geological Association of Canada - Mineralogical Association of Canada Joint Annual Meeting. May 25, 2014.

Corresponding author: Zeinab Azadbakht (zeinab.azadbakht@unb.ca)

Azadbakht, Z., Lentz, D.R., and McFarlane, C.R.M., 2015. Using biotite composition of the Devonian Lake George granodiorite, New Brunswick, as a case study for W-Mo-Au-Sb mineralized magmatic hydrothermal systems; *in* TGI 4 – Intrusion Related Mineralisation Project: New Vectors to Buried Porphyry-Style Mineralisation, (ed.) N. Rogers; Geological Survey of Canada, Open File 7843, p. 459-474.

Project Goals

- Document detailed chemistry of coexisting phyllosilicate mineral phases to reveal distinctive element signatures that may be specific to fertile granitoids.
- Provide a geochemical fingerprint for more-specific mineralization styles and prospectivity in the Acadian Plutonic Complex.

Geological and Tectonic Setting

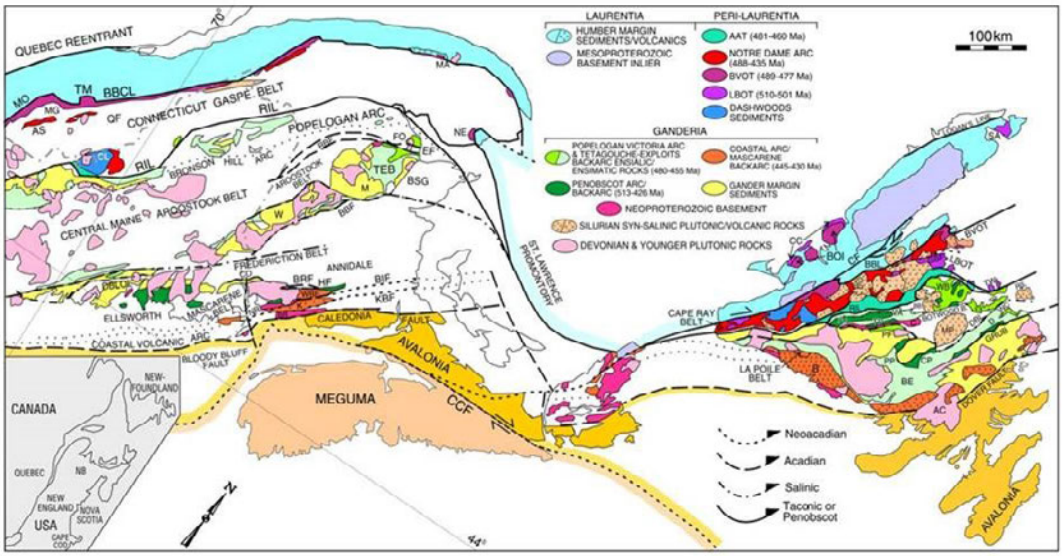

Van Staal et al. (2009)

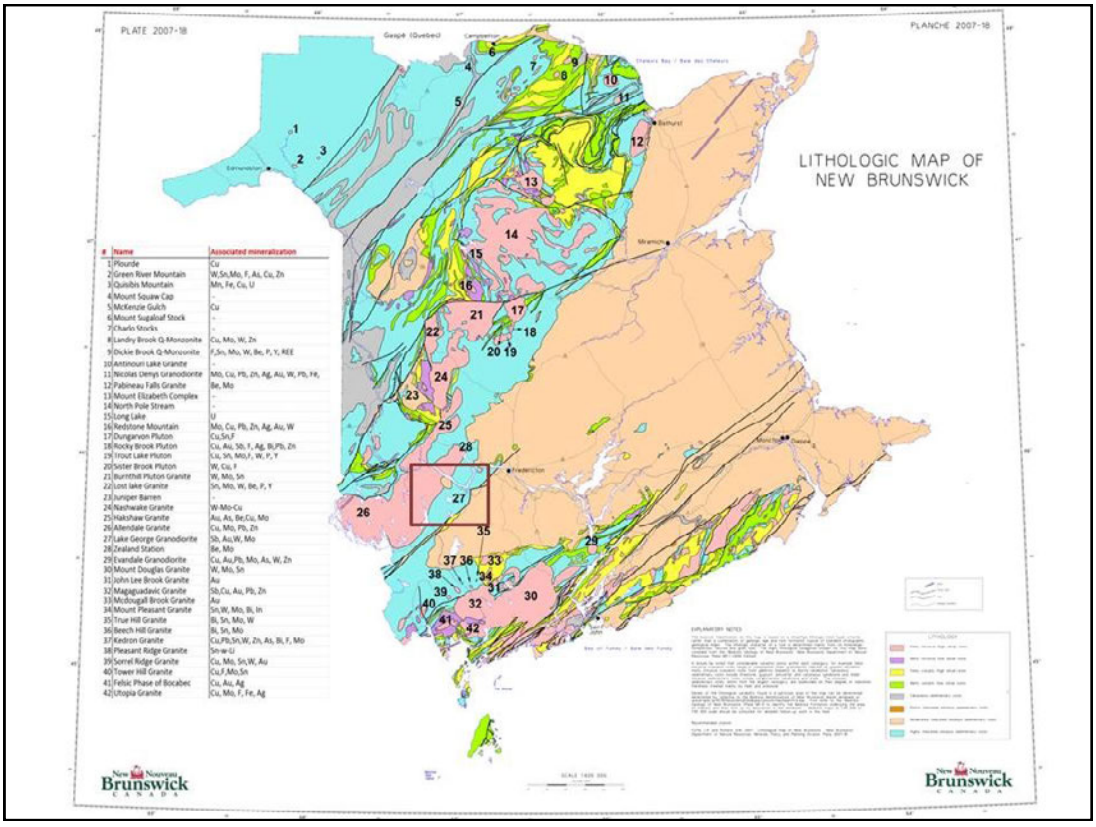

#	Name	Associated mineralization
1	Plourde	Cu
2	Green River Mountain	W,Sn,Mo, F, As, Cu, Zn
3	Quisibis Mountain	Mn, Fe, Cu, U
4	Mount Squaw Cap	-
5	McKenzie Gulch	Cu
6	Mount Sugaloaf Stock	-
7	Charlo Stocks	-
8	Landry Brook Q-Monzonite	Cu, Mo, W, Zn
9	Dickie Brook Q-Monzonite	F,Sn, Mo, W, Be, P, Y, REE
10	Antinouri Lake Granite	-
11	Nicolas Denys Granodiorite	Mo, Cu, Pb, Zn, Ag, Au, W, Pb, Fe,
12	Pabineau Falls Granite	Be, Mo
13	Mount Elizabeth Complex	-
14	North Pole Stream	-
15	Long Lake	U
16	Redstone Mountain	Mo, Cu, Pb, Zn, Ag, Au, W
17	Dungarvon Pluton	Cu,Sn,F
18	Rocky Brook Pluton	Cu, Au, Sb, F, Ag, Bi,Pb, Zn
19	Trout Lake Pluton	Cu, Sn, Mo,F, W, P, Y
20	Sister Brook Pluton	W, Cu, F
21	Burnthill Pluton Granite	W, Mo, Sn
22	Lost lake Granite	Sn, Mo, W, Be, P, Y
23	Juniper Barren	-
24	Nashwake Granite	W-Mo-Cu
25	Hatchaw Granite	Au, As, Be,Cu, Mo
26	Allendale Granite	Cu, Mo, Pb, Zn
27	Lake George Granodiorite	Sb, Au,W, Mo
28	Zealand Station	Be, Mo
29	Evandale Granodiorite	Cu, Au,Pb, Mo, As, W, Zn
30	Mount Douglas Granite	W, Mo, Sn
31	John Lee Brook Granite	Au
32	Magaguadavic Granite	Sb,Cu, Au, Pb, Zn
33	McDougall Brook Granite	Au
34	Mount Pleasant Granite	Sn,W, Mo, Bi, In
35	True Hill Granite	Bi, Sn, Mo, W
36	Beech Hill Granite	Bi, Sn, Mo
37	Kedron Granite	Cu,Pb,Sn,W, Zn, As, Bi, F, Mo
38	Pleasant Ridge Granite	Sn-w-Li
39	Sorrel Ridge Granite	Cu, Mo, Sn,W, Au
40	Tower Hill Granite	Cu,F,Mo,Sn
41	Felsic Phase of Bocabec	Cu, Au, Ag
42	Utopia Granite	Cu, Mo, F, Fe, Ag

Geological Setting

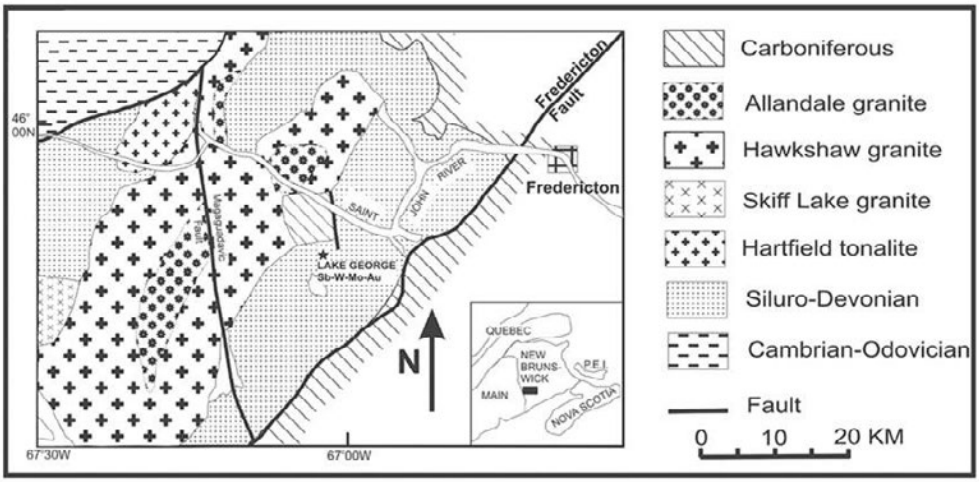

Yang et al. (2002)

Geological Setting

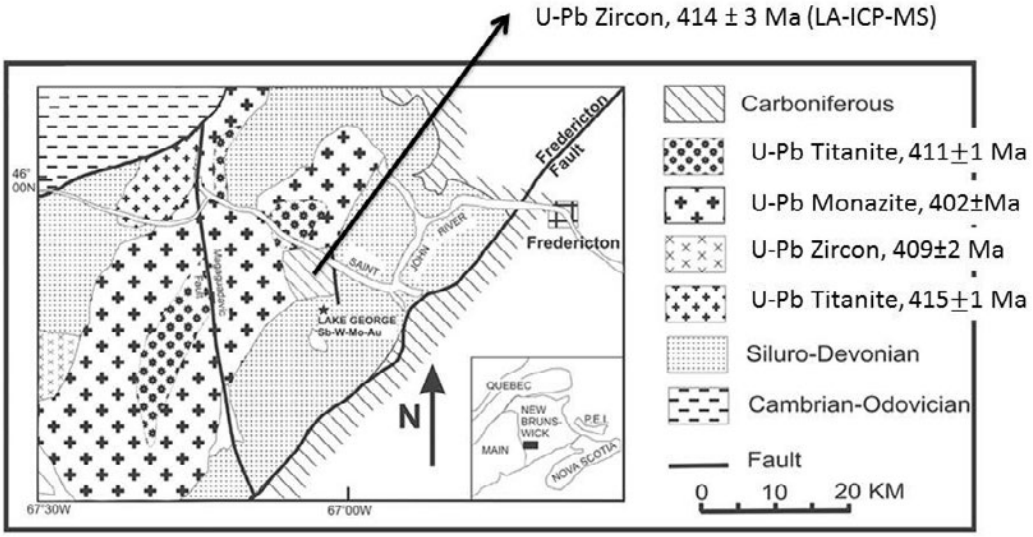

Yang et al. (2002)

Geological Setting

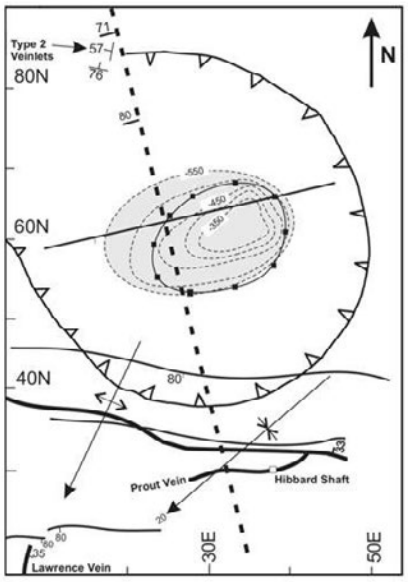

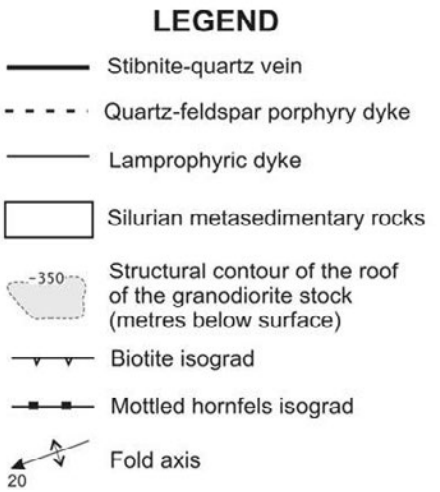

Leonard et al. 2005

Wholerock Geochemistry

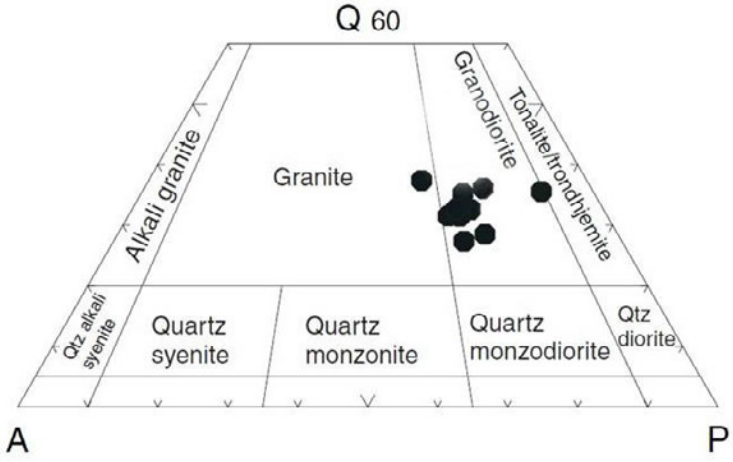

Quartz (Q)-Alkali feldspar (A)- Plagioclase (P) mesonormative classification diagram(after Le Maitre et al., 1989) (Yang et al.(2002)

Tectonic Setting

Yang et al. (2002)

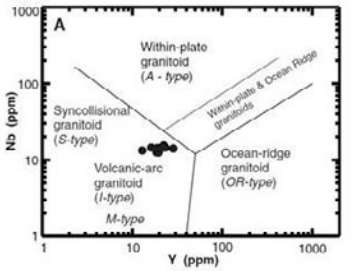

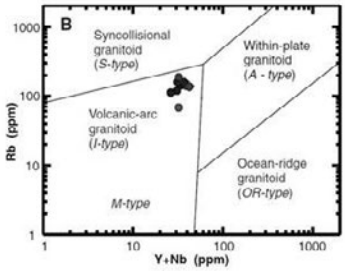

Lalonde and Bernard (1993)

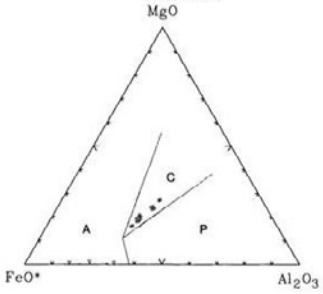

Abdel-Rahman (1994)

Geobarometry

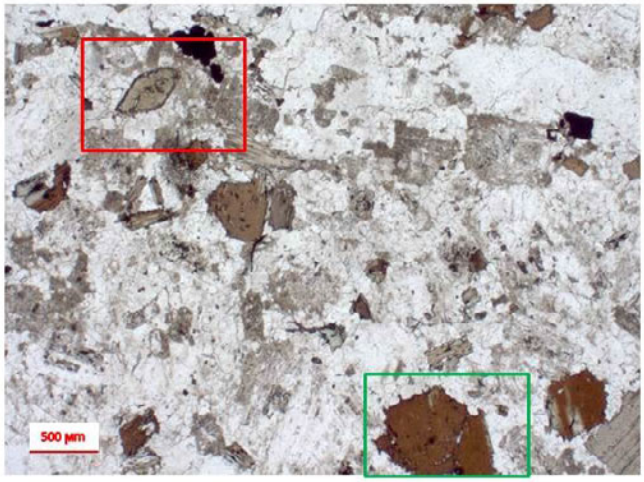

(~3.4 - 4.6 kb)
Done by Yang et al.(2002)

1~2 kb
Uchida et al.(2007)

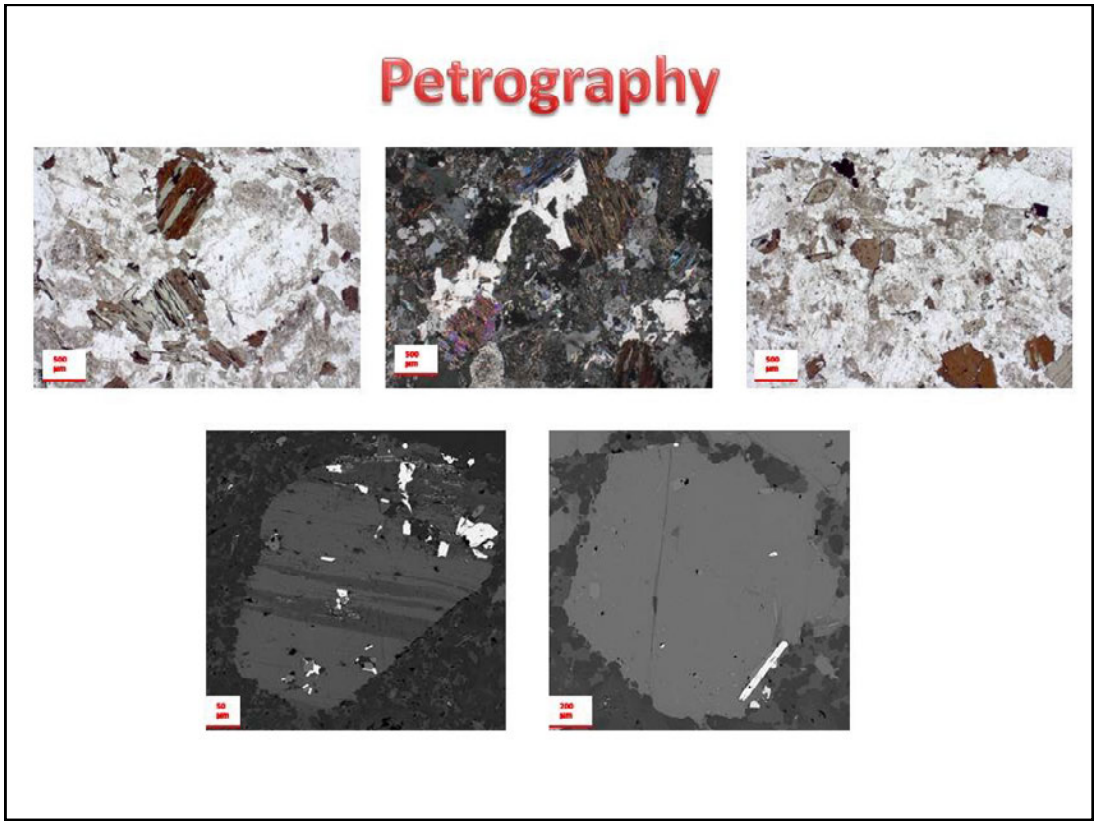
Petrography

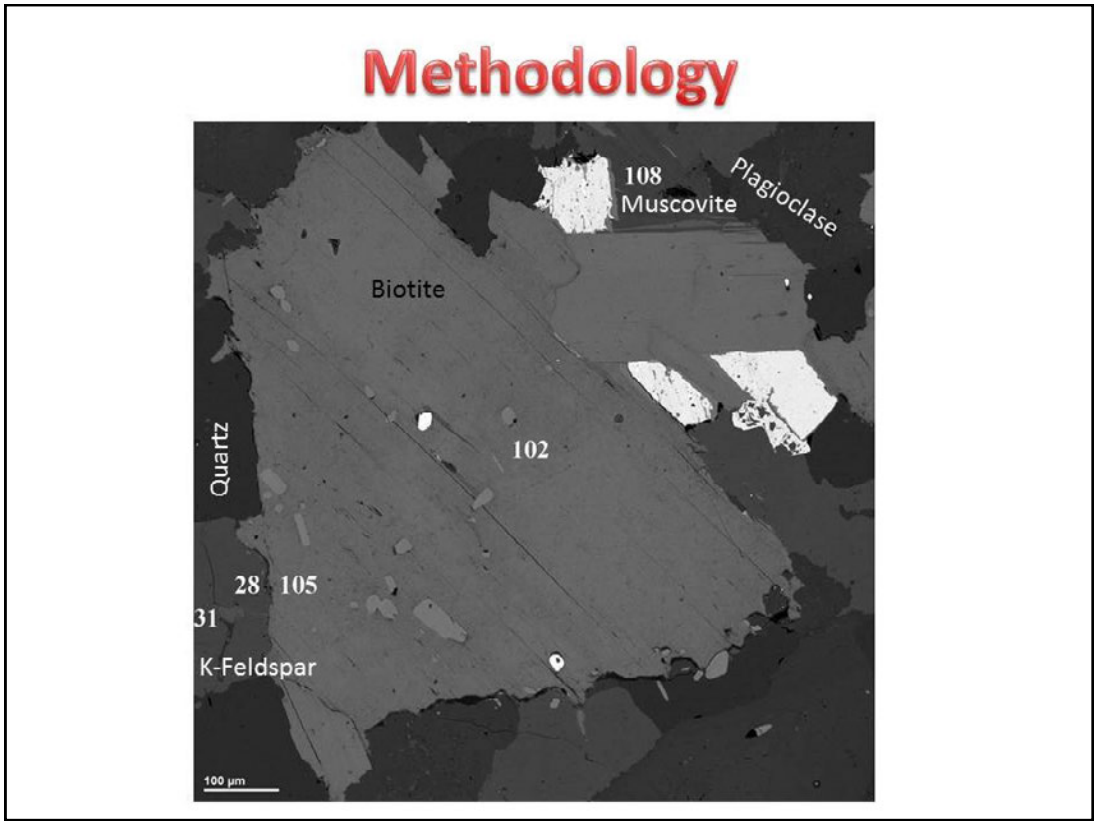
Methodology
108
Muscovite
Plagioclase
Biotite
102
Quartz
28
105
31
K-Feldspar
100 µm

Biotite Classification

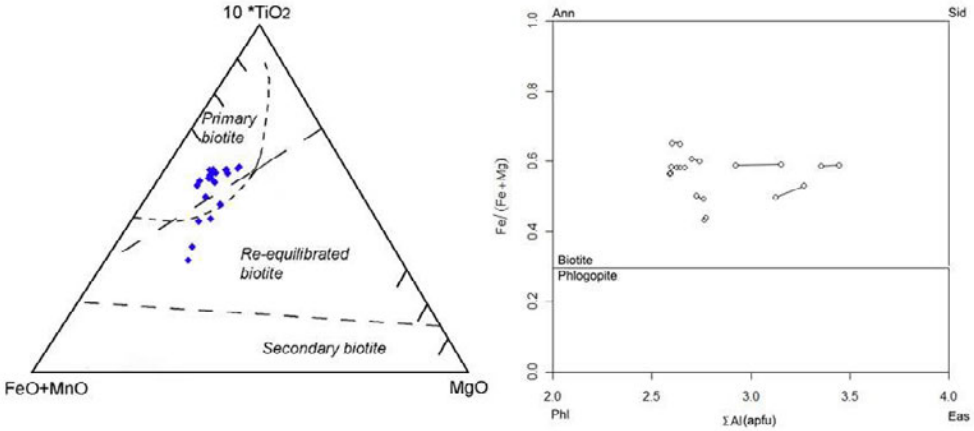

$10 \times TiO_2 - (FeO + MnO) - MgO$ ternary plot of biotite composition from the Lake George granodiorite; the discrimination field boundaries are from Nachit et al. (2005).

Biotite Classification

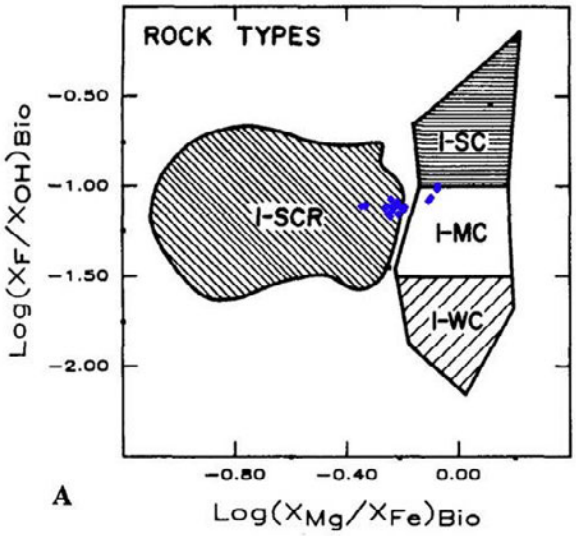

Plot of log (X_{Mg}/X_{Fe}) *and log* (X_F/X_{OH}) *of the magmatic* biotite I-SC, strongly contaminated I-type; I-SCR, strongly contaminated and reduced I-type; I-WC, weakly contaminated I-type; after Ague and Brimhill (1987).

Oxygen Fugacity

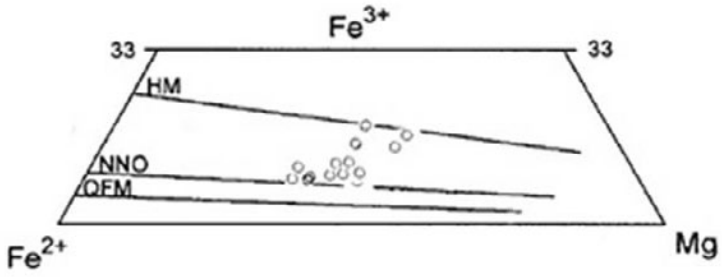

Mica+
Yavuz (2003 a and b)

Biotite Halogen Study

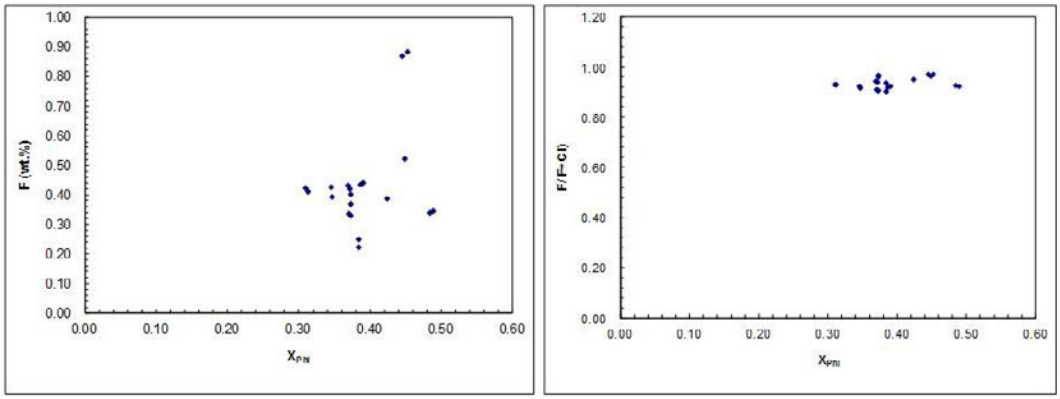

Composition of the biotite plotted with respect to F Wt% vs. X_{phl} for granodiorite samples of Lake George. X_{phl} = Mg/Sum octahedral site

Biotite Halogen Study

Munoz 1984

$IV(F)= 1.25\ X_{phl}+0.42X_{ann}+0.20X_{sid}-\log\ (X_F/X_{OH})$

$X_{sid}=[(3-Si/Al)/1.75]\ (1-X_{phl})$

$X_{ann}= 1-(X_{phl}+X_{sid})$;

X_F and X_{OH}= mole fractions of F and OH respectively on the hydroxyl site

Biotite Halogen Study

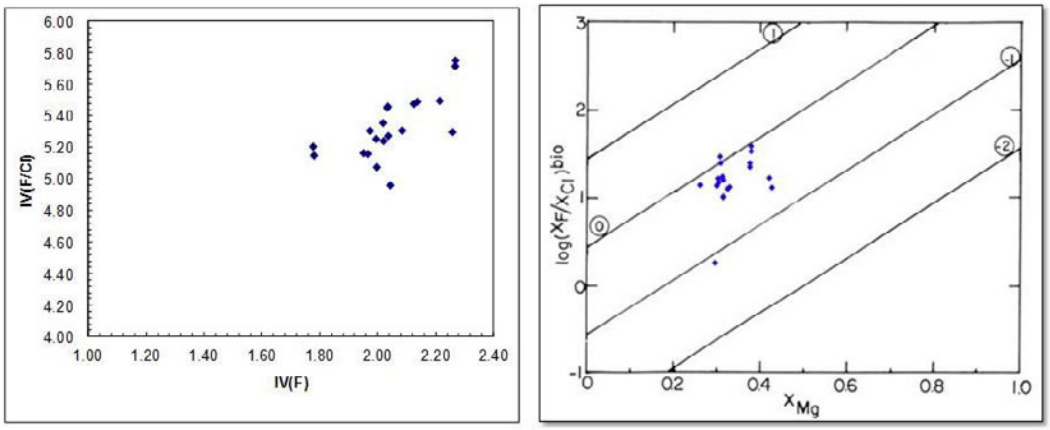

Plot showing values of IV(F) vs. IV(F/Cl) of biotite grains from granodiorite of Lake George

Magmatic Hydrothermal Fluid

$$\log(f\mathrm{H_2O})/(f\mathrm{HF})\text{fluid} = 1000/T[2.37 + 1.1(X_{\mathrm{Mg}})\text{biotite}] + 0.43 - \log(X_{\mathrm{F}}/X_{\mathrm{OH}})\text{biotite},$$

$$\log(f\mathrm{H_2O})/(f\mathrm{HCl})\text{fluid} = 1000/T[1.15 + 0.55(X_{\mathrm{Mg}})\text{biotite}] + 0.68 - \log(X_{\mathrm{Cl}}/X_{\mathrm{OH}})\text{biotite},$$

$$\log(f\mathrm{HF})/(f\mathrm{HCl})\text{fluid} = -1000/T[1.22 + 1.65(X_{\mathrm{Mg}})\text{biotite}] + 0.25 + \log(X_{\mathrm{F}}/X_{\mathrm{Cl}})\text{biotite},$$

Munoz 1992

Magmatic Hydrothermal Fluid

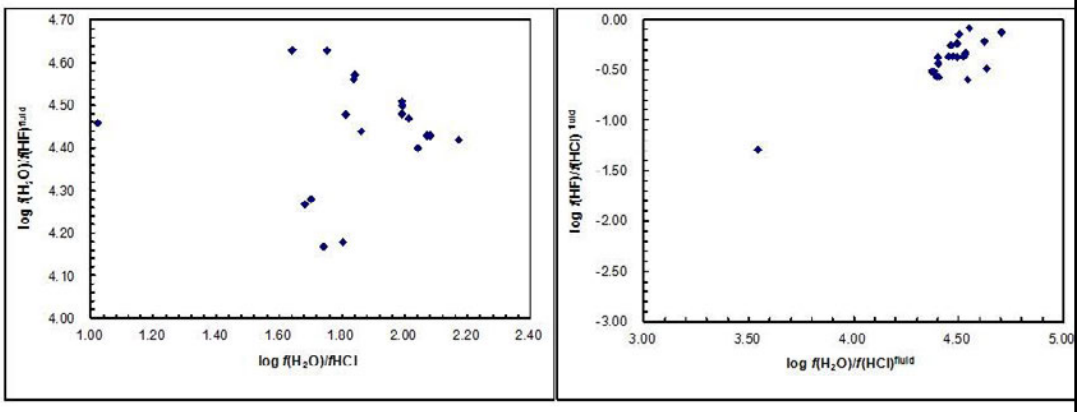

Ti in Biotite Thermometry

#	Core	Rim
1351	725	725
1190	744	746
1886	719	718
1741	726	729
1291	735	729
1647	720	717
80-33-A	710	711
612	748	746
1567	718	716
80-33-B	719	719

Henry et al.2005

Biotite grains containing secondary rutile show a lower calculated temperature following the Henry method.

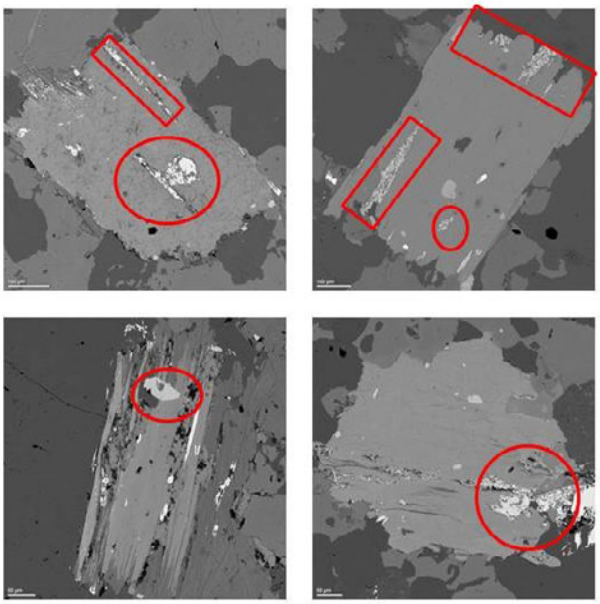

Trace Elements

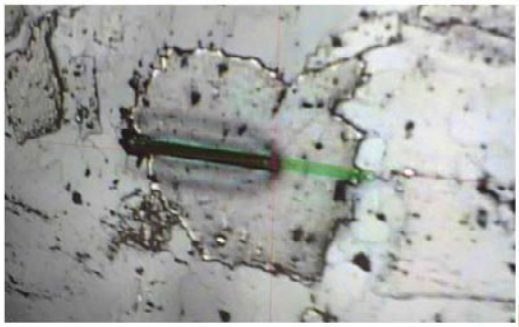

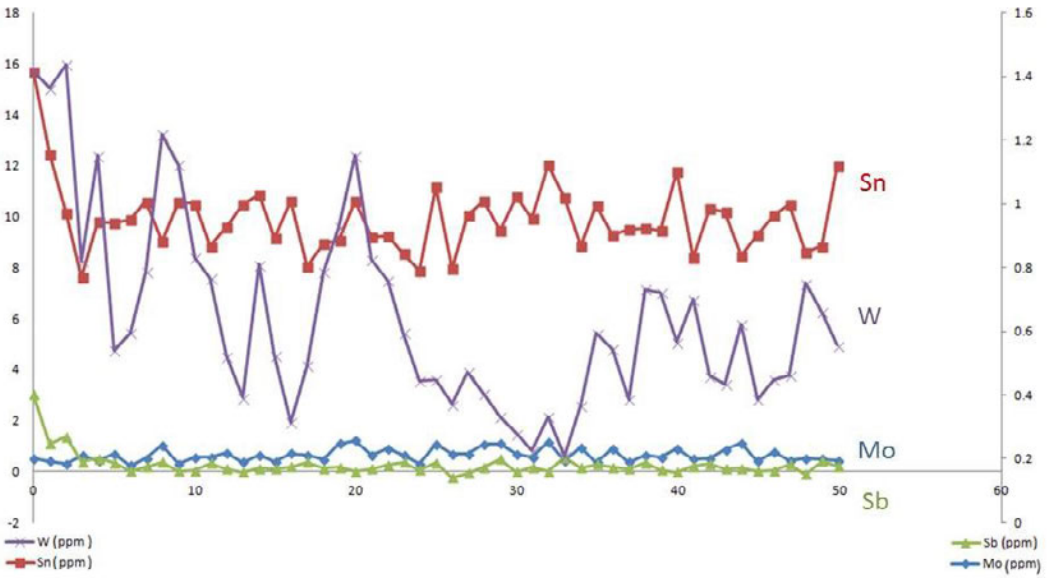

Concentration of W, Sn, Sb, and Mo in a biotite from sample LG81-1647

Trace Elements

(ppm)	80-33A	1291	1351	1647	1741	1886
Li	257.42	265.23	275.35	321.72	281.47	392.44
P	2.93	23.86	14.04	72.06	19.43	2174.51
Ca	292.38	452.92	347.68	266.09	732.63	6141.64
Ti	24872.94	31702.44	27927.93	27990.00	28495.14	27782.75
V	385.32	640.43	454.60	523.67	486.95	544.28
Cr	47.51	130.86	60.52	69.05	70.14	63.88
Mn	6634.01	2263.85	4287.13	4652.31	3940.02	4649.05
Co	44.53	31.43	58.46	49.38	62.84	45.65
Ni	44.84	46.29	61.08	48.67	62.42	40.49
Cu	3.66	4.99	1.15	0.55	3.81	12.50
Zn	531.73	391.19	455.21	476.70	449.32	484.71
Ga	50.72	63.22	46.02	49.68	45.97	50.80
Rb	802.79	843.97	733.01	763.71	755.35	746.56
Sr	1.73	5.65	1.59	1.70	2.32	5.69
Mo	0.97	0.34	0.74	0.35	0.62	0.32
Sn	63.94	18.77	8.02	10.57	8.21	12.11
Sb	0.77	2.36	0.27	0.07	0.33	-0.09
Cs	90.91	58.39	17.94	26.41	20.55	42.73
Ba	1304.40	1439.19	1885.19	2053.30	1466.99	2468.81
W	1.07	1.29	0.78	0.76	0.59	0.84

Yellow: Highest concentration

Orange: lowest concentration

Trace Elements

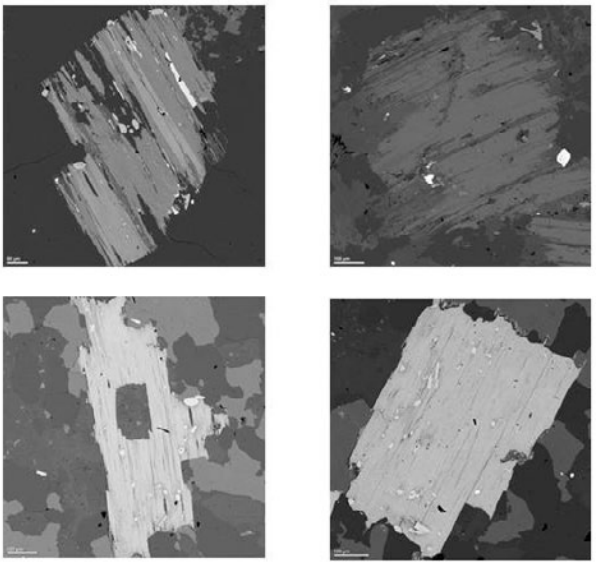

1291- Sb-W

80-33A Sn-Mo

Trace Elements

	Mo	Sn	Sb	W
1351	6	<1	4.8	<1
1741	3	<1	4.3	8
1647	7	<1	6	6
1291	6	1	6.5	<1
1886	2	<1	5.6	5

Whole rock trace element Yang et al. (2002)

Averages of Mo, Sn, Sb and W in biotites of the Lake George granodiorite (Right)

	Mo	Sn	Sb	W
1351-6	0.64	9.91	0.26	0.64
1351-7	0.75	9.31	0.22	0.67
1351-8-1	0.71	6.89	0.33	0.92
1741-2	0.64	8.66	0.47	0.64
1741-4	0.54	8.05	0.75	0.69
1741-5	0.65	8.01	0.4	0.59
80-33-A-2	1.00	66.18	0.76	1.30
80-33-A-3	1.12	62.56	0.66	1.06
80-33-A-5	0.74	62.82	1.16	0.92
1647-3	0.33	10.82	0.06	0.56
1647-4	0.44	10.62	0.01	0.48
1647-5	0.29	10.14	0.16	1.54
1291-2	0.29	20.78	0.32	0.64
1291-7	0.39	16.37	3.59	2.24
1291-8	0.34	17.18	11.14	2.91
1886-4	0.33	11.70	-0.2	0.77
1886-6	0.29	12.56	0.11	0.95

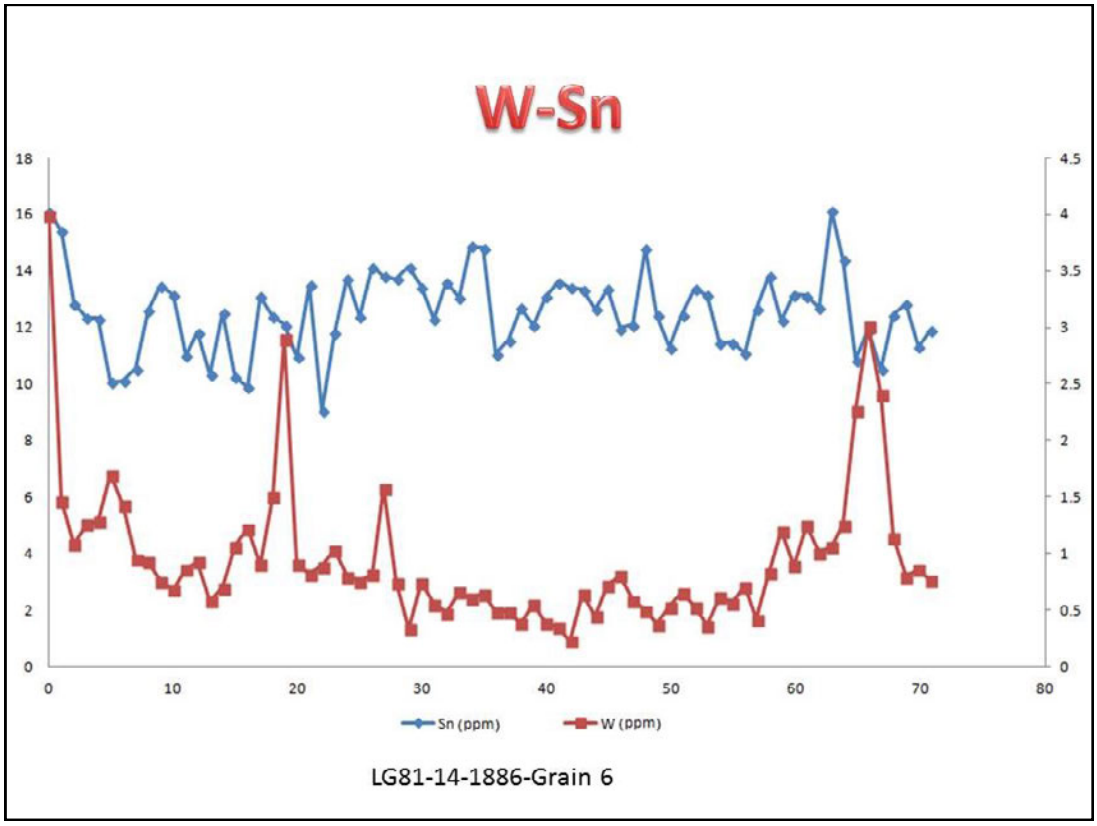

LG81-14-1886-Grain 6

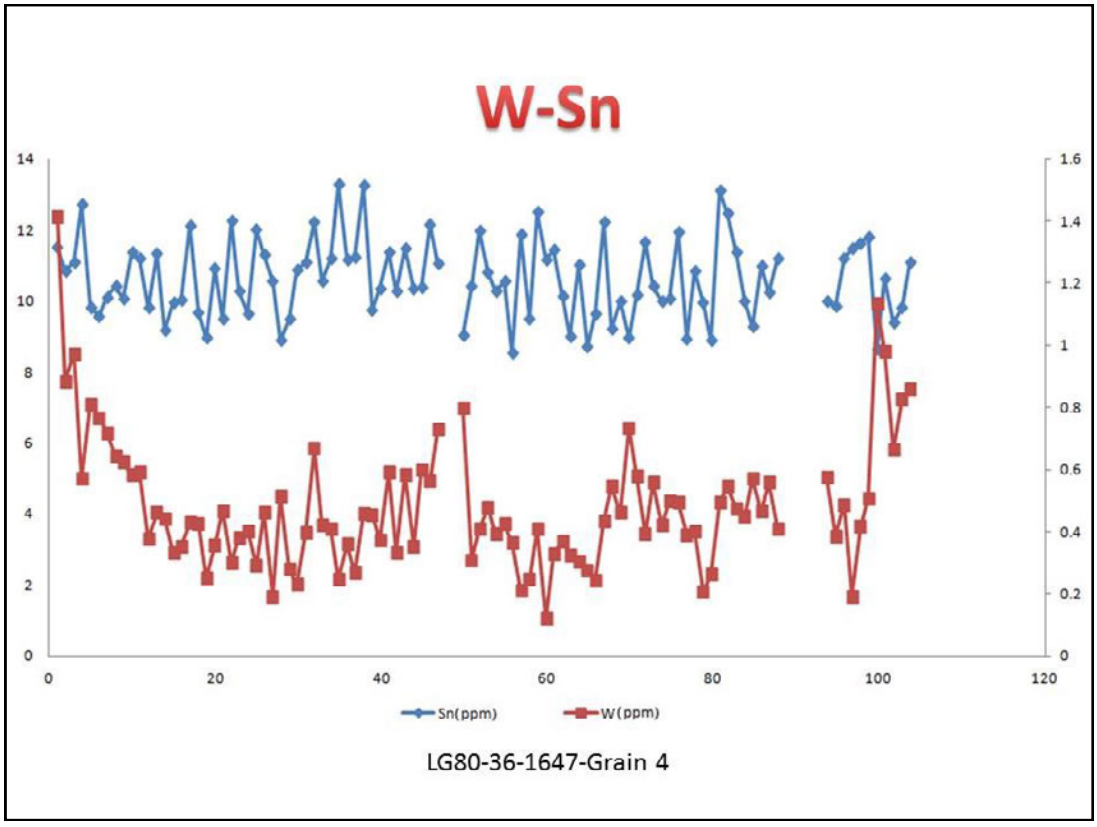

LG80-36-1647-Grain 4

What I think

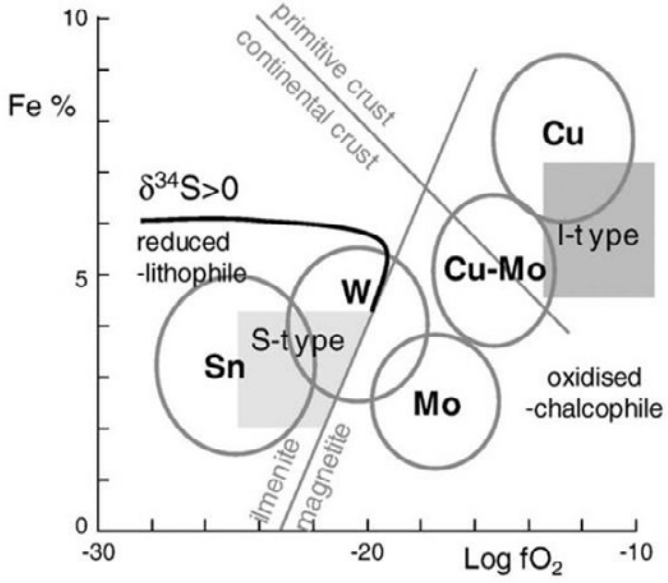

Conclusion

- Biotite chemistry reflects whole rock geochemistry
- fH$_2$O is higher than fHF and fHCl
- Disequilibrium partitioning of halogens and high metal concentrations in biotite, good reflection of contamination?
- Internal zoning of trace element good record of physio-chemical changes during biotite crystallization
- Proof of concept that mica chemistry may aid in identification of fertile Acadian magma systems

Trace elements and oxygen isotope of quartz from the Nashwaak Granite and dykes, and quartz veins related to the Sisson Brook W-Mo-Cu deposit, west-central New Brunswick

W. Zhang[1], D.R. Lentz[1], C.R.M. McFarlane[1] and K.G. Thorne[2]

1. University of New Brunswick, Box 4400, 2 Bailey Drive, Fredericton, New Brunswick
2. Geological Surveys Branch, New Brunswick Department of Energy and Mines, Fredericton, New Brunswick

Abstract: The Sisson Brook W-Mo-Cu deposit, situated in west-central New Brunswick, is hosted by Cambro-Ordovician volcanic and sedimentary rocks of the Miramichi and Tetagouche groups. These rocks have been intruded by the Early Devonian Howard Peak diorite-gabbro, Nashwaak Granite, a phaneritic felsic dyke swarm, and a distinctively younger Late Devonian porphyritic felsic dyke. In order to understand the magma evolution history, the textural and geochemical characteristics of quartz phenocrysts from these felsic rocks were analyzed with the aid of SEM-cathodoluminescence (CL), laser ablation inductively coupled plasma mass spectrometry (LA ICP-MS), and secondary ion mass spectrometry (SIMS).

Four intrusive granitic units in the Sisson Brook deposit area: (1) medium-grained, equigranular two-mica granite with brown biotite that is slightly altered to chlorite; (2) biotite- granite with ca. 20 % greenish brown biotite and accessory zircon, apatite, monazite, magnetite, titanite, sulfide and ilmenite; (3) biotite-granite dykes with similar mineralogical features to the biotite-granite; and (4) porphyry dykes with phenocrysts consisting of approximately 23 % plagioclase, 10 % quartz, 8 % biotite, and 7 % K-feldspar.

Quartz phenocyrsts in two-mica granite and biotite-granite plutonic phases is unzoned indicating that it formed at relatively stable magma chamber. Quartz dissolution textures in the dyke phases might be caused by cooling from 600°C to 300°C at pressure below 1 Kbar. Quartz phenocrysts in porphyry dyke samples are oscillatory-zoned. With the assumption that the activity of Ti in these magmas is 0.8 (based on the presence of ilmenite rather than rutile), Ti-In-quartz geothermometry indicates that the porphyry dykes formed at a temperature above 675°C, two-mica granite and biotite-granite plutons formed at 600°C to 700°C, and the biotite-granite dykes formed at slightly below 600°C. Higher Ge/Ti ratios reflect greater degrees of magma differentiation. This ratio increases from porpyrhy dykes, two-mica granite and biotite-granite pluton phases to biotite dykes. The highest Al content of quartz measured in two-mica granite is consistent with the highest aluminium saturation index of its whole rock. The oxygen isotope of quartz is from 8-8.5 ‰ for biotite-granite, 9-10 ‰ for biotite dykes and porphyry dykes, and 10-10.5 ‰ for the two-mica granites. The later mineralization quartz veins in the dykes have oxygen isotope values between 8.5 ‰ to 9.5 ‰, indicating the hydrothermal fluids related to the Sisson Brook deposit are dominantly magmatic fluids.

Originally presented Fredericton 2014: Geological Association of Canada - Mineralogical Association of Canada Joint Annual Meeting. May 25, 2014.

Corresponding author: Wei Zhang (Wei.Z@unb.ca)

Zhang, W., Lentz, D.R., McFarlane, C.R.M., and Thorne, K.G., 2015. Trace elements and oxygen isotope of quartz from the Nashwaak Granite and dykes, and quartz veins related to the Sisson Brook W-Mo-Cu deposit, west-central New Brunswick; *in* TGI 4 – Intrusion Related Mineralisation Project: New Vectors to Buried Porphyry-Style Mineralisation, (ed.) N. Rogers; Geological Survey of Canada, Open File 7843, p. 475-491.

Trace elements and oxygen isotope of quartz from the Nashwaak Granite and dykes, and quartz veins related to the Sisson Brook W-Mo-Cu deposit, west-central New Brunswick

Wei Zhang, Dave Lentz, Chris McFarlane
Department of Earth Sciences, University of New Brunswick

Kay Thorne
Geological Surveys Branch, New Brunswick Department of Energy and Mines

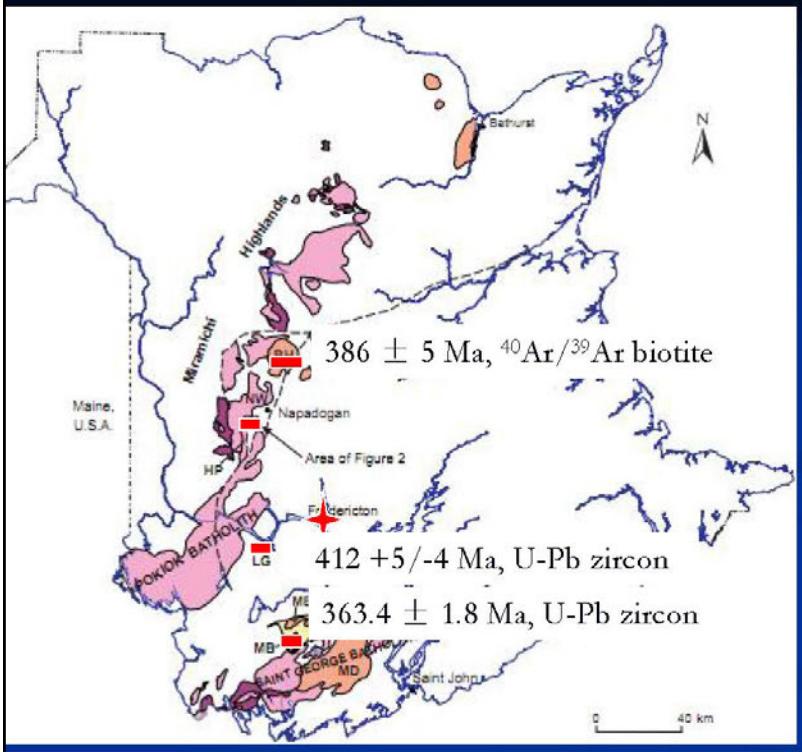

The Sisson Brook W-Mo-Cu deposit is situated in west-central New Brunswick, along the eastern margin of an extensive belt of "Acadian" plutonic rocks that underlie the Miramichi Highlands

Geological setting

Cambrian to Early Ordovician
$\in OTL_{gn}$ - Trousers Lake Metamorphic Suite
$\in OKB_{mc}$, - Miramichi Group
Ordovician
OLC_{fi} - Little Clearwater Brook Granite
OMK_{fi} - McKiel Lake Granite
$OPBD, OHL_{fc}, OHL_{mv}, OTU_{ls}$,OTM,OHL - Tetagouche Group
Silurian
SCR_{fc}, SBU_{mc}, STR_{mc}, SSM_{fc}, $SBOG_{ii}$
Devonian
DHfia - Hawkshaw Granite
DBLmi - Becaguimec Lake Gabbro
DHPii - Howard Peak Granodiorite
DNWfia - Nashwaak biotite Granite
DNWfib - Nashwaak two-mica Granite
Carboniferous
---------- Fault

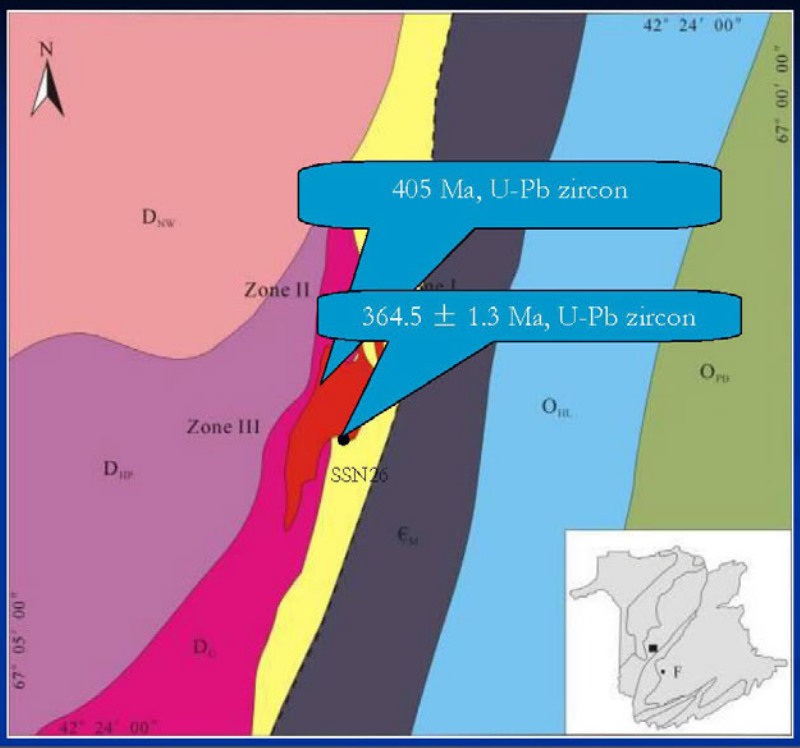

Devonian:
D_{NW} Nashwaak Granite
D_{HP} Howard Peak Diorite
D_G Gabbro

Ordovician:
O_{PB} Push and Be Damned
O_{HL} Hayden Lake
O_{TM} Turnbull Mountain

Cambro-Ordovician:
$\in_M$ Miramichi Group

Taylor et al. (1987)
Whalen and Theriault (1990)
Martin (2006)
Fyffe et al. (2008)

Resource Estimate for Sisson Brook deposit (Zone I, II, and III)

	Tonnage (Mt)	WO_3 (%)	Mo (%)	WO_3 (M mtu)	Mo (m lb)	Agv NSR (US$/t)
Measured	107	0.072	0.024	7.7	56.6	21.11
Indicated	276	0.065	0.020	17.94	121.7	18.76

Resource Estimate: ROSCOE POSTLE ASSOCIATES INC., 43-101, June 29, 2012

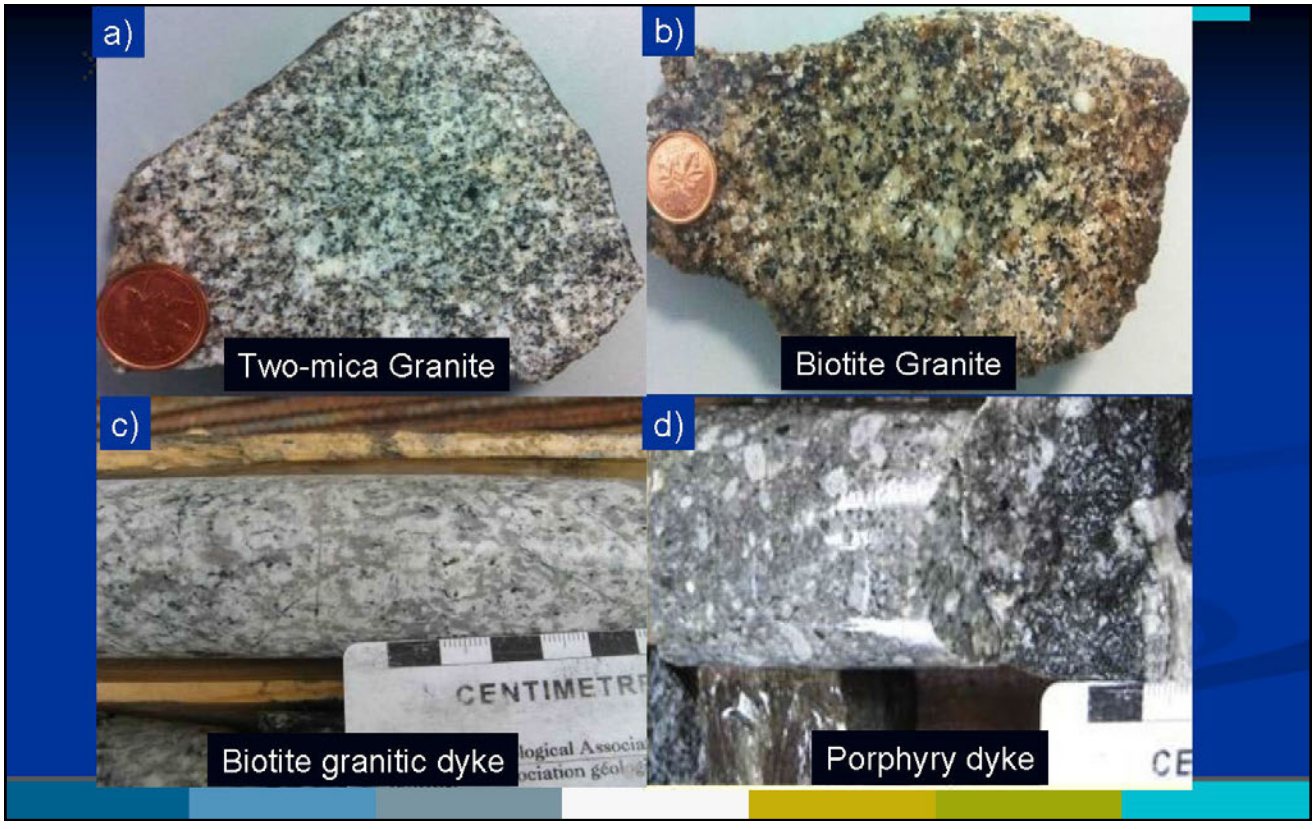

Pegmatoidal dyke

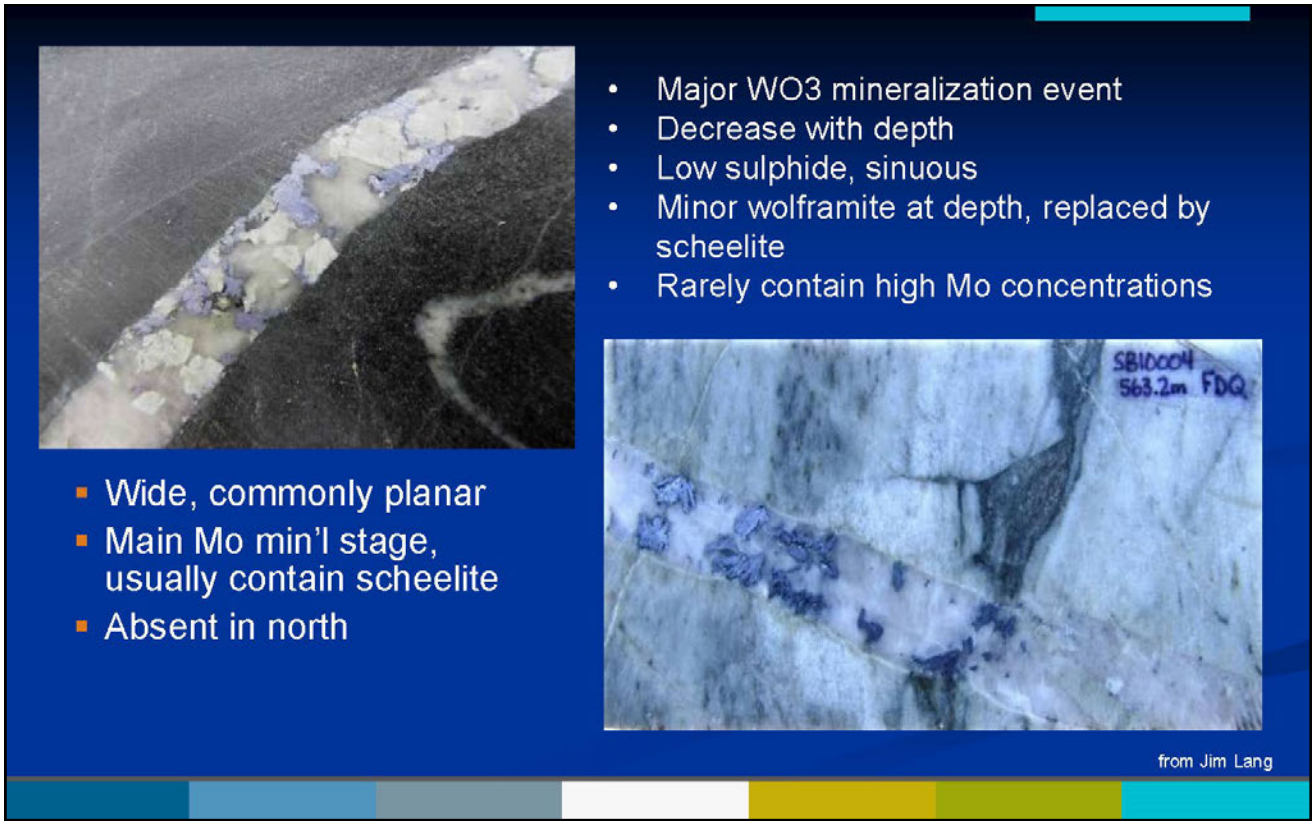
Major WO3 mineralization event
Decrease with depth
Low sulphide, sinuous
Minor wolframite at depth, replaced by scheelite
Rarely contain high Mo concentrations
Wide, commonly planar
Main Mo min'l stage, usually contain scheelite
Absent in north
SB10004
563.2m FDQ
from Jim Lang

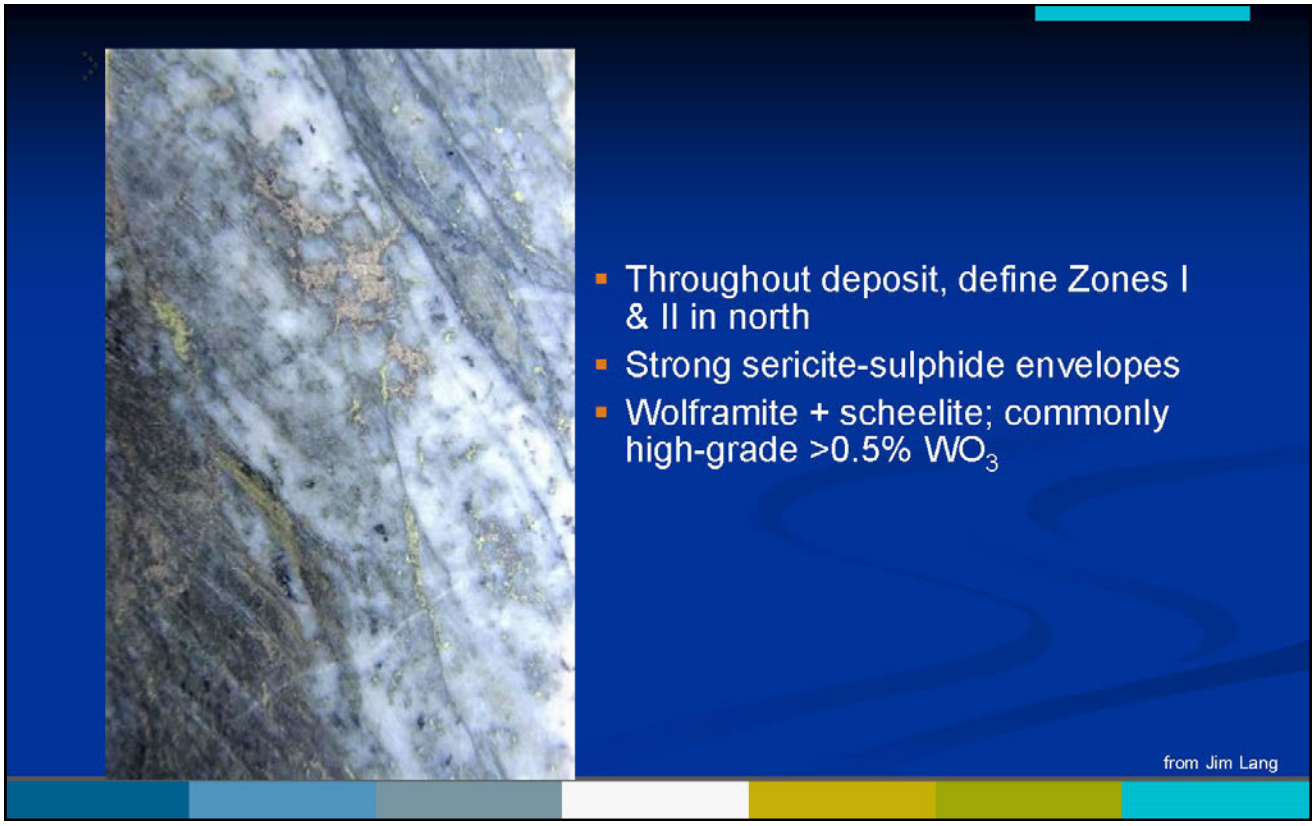
Throughout deposit, define Zones I & II in north
Strong sericite-sulphide envelopes
Wolframite + scheelite; commonly high-grade >0.5% WO_3
from Jim Lang

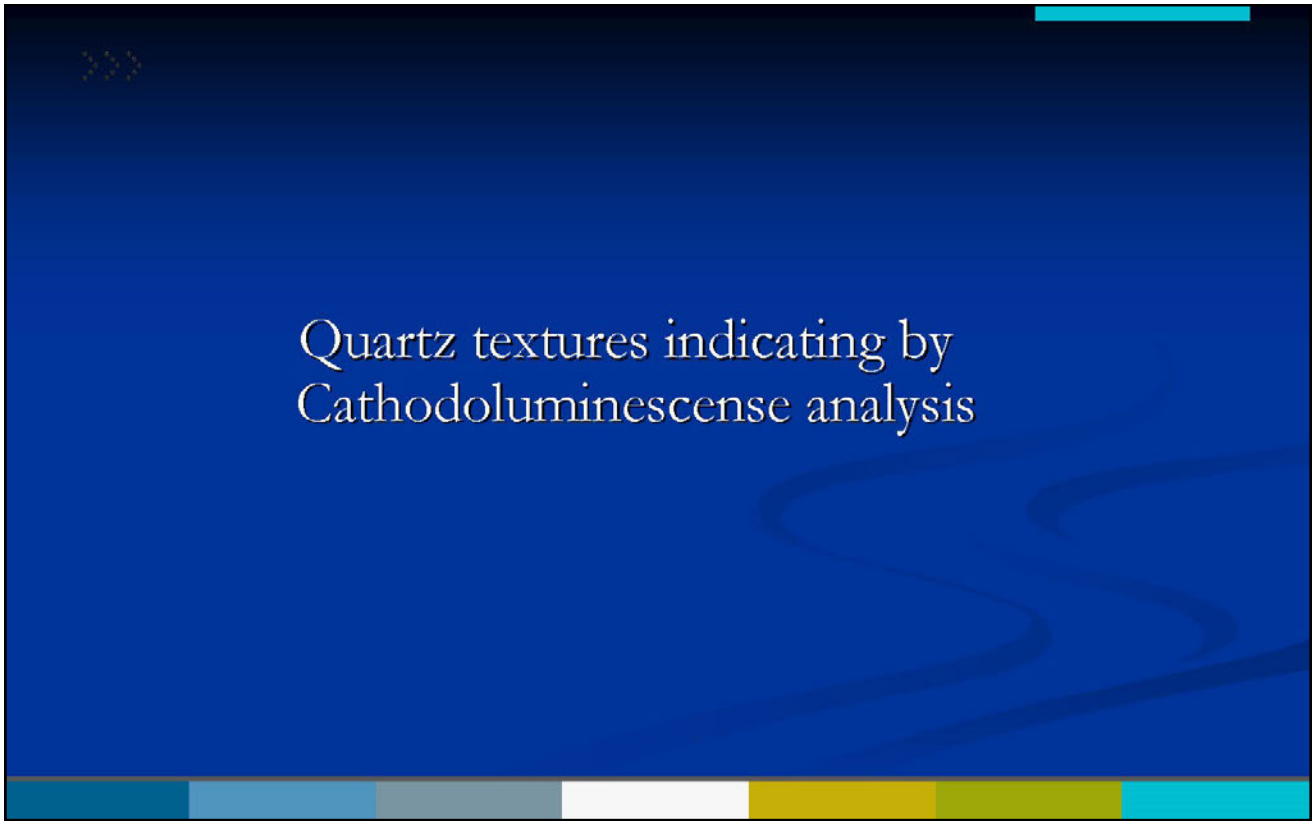
Quartz textures indicating by Cathodoluminescense analysis

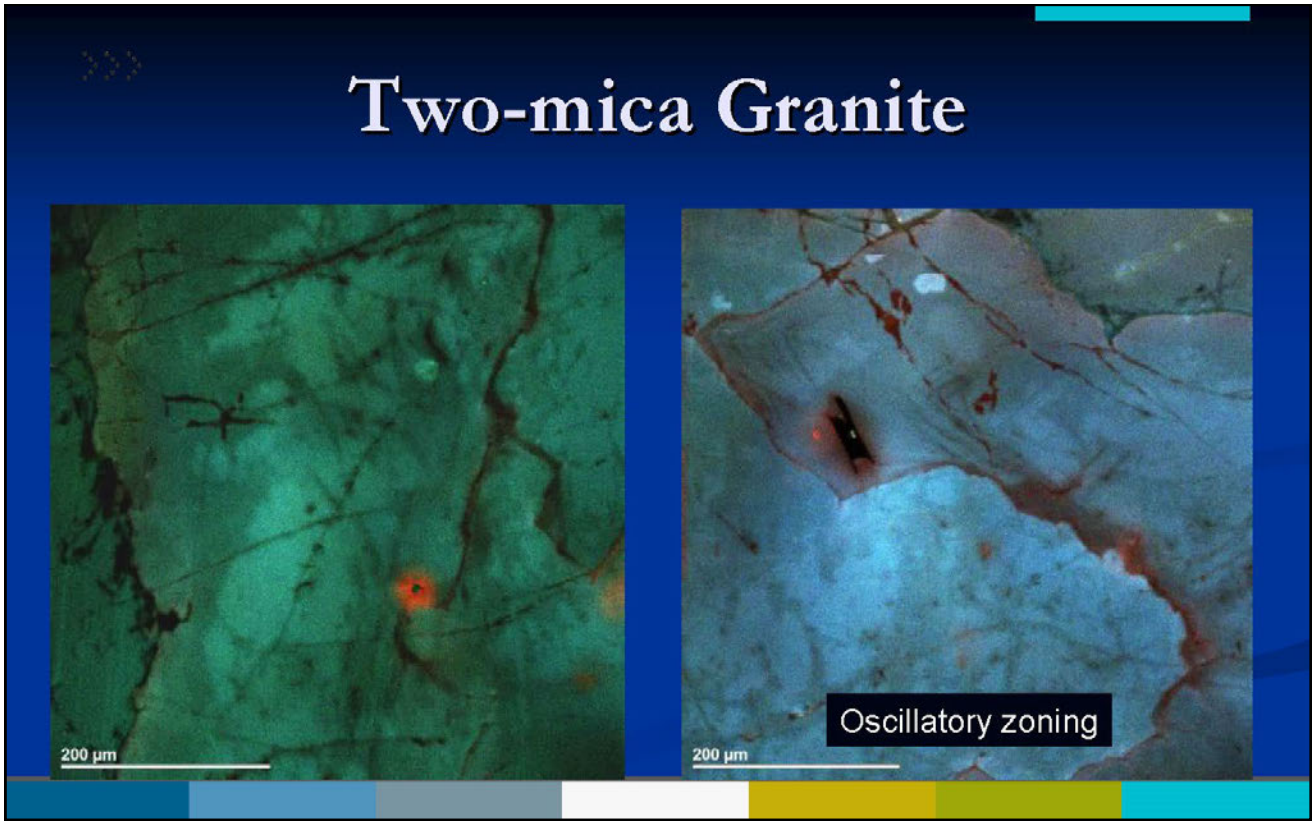
Two-mica Granite
200 µm
Oscillatory zoning
200 µm

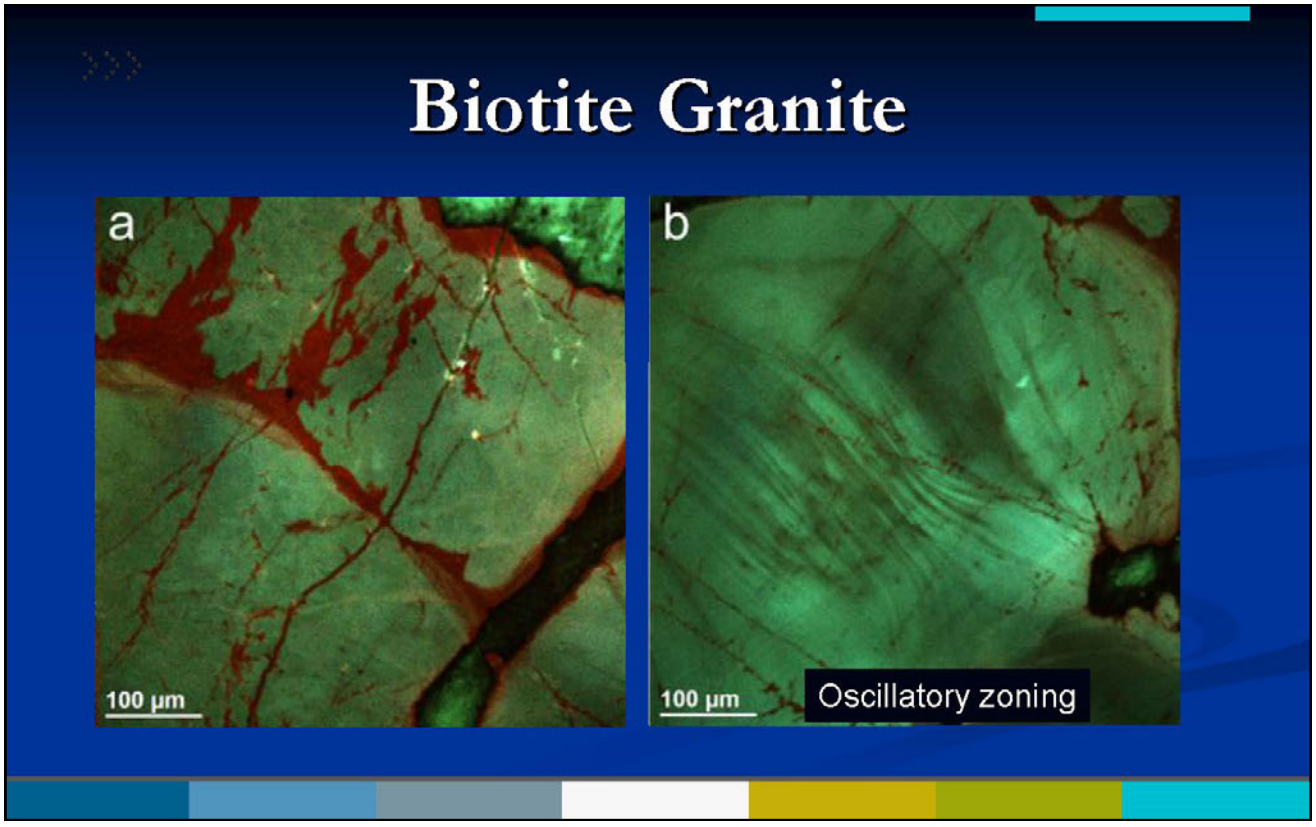
Biotite Granite
a
100 µm
b
100 µm
Oscillatory zoning

Biotite dykes

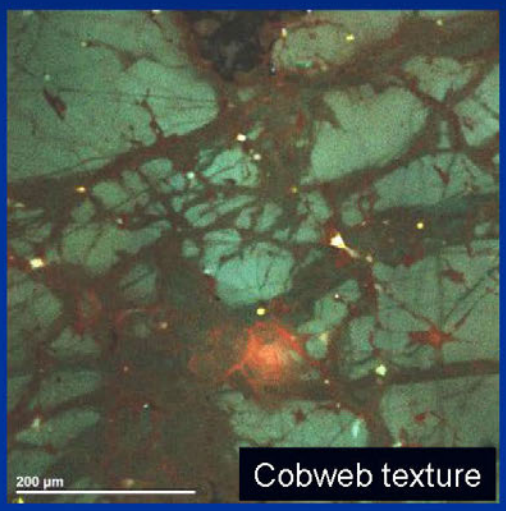

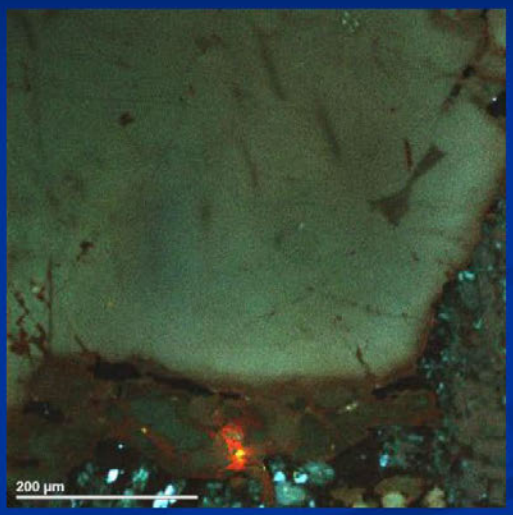

Solubility of quartz in pure water

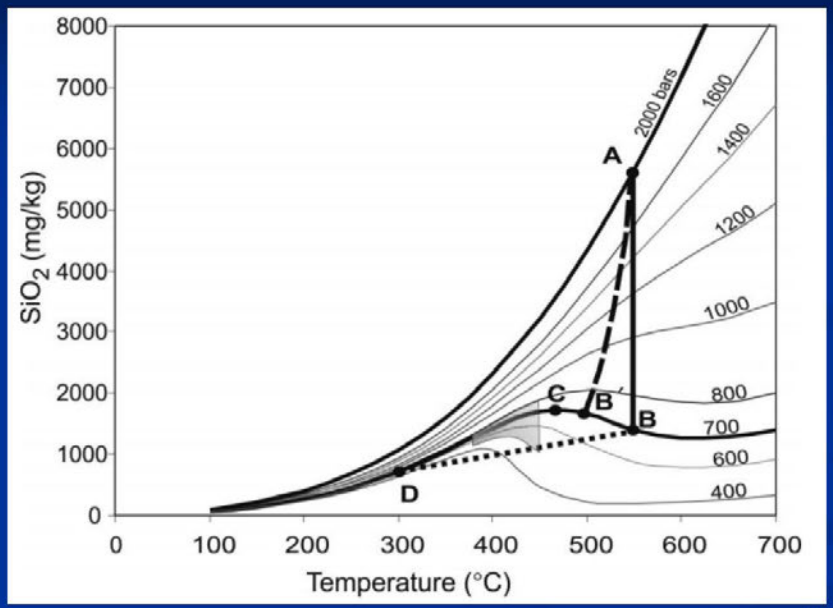

Rusk and Reed, 2002

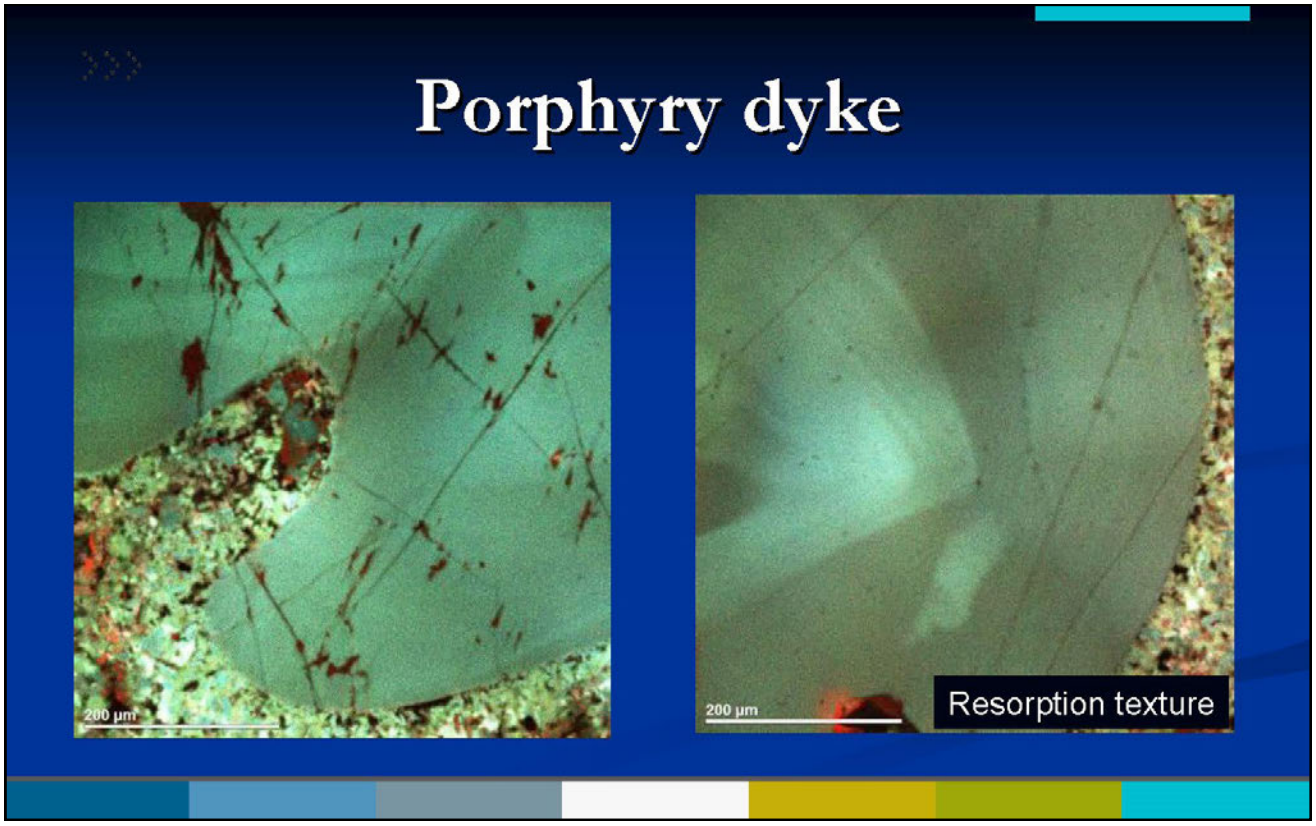
Porphyry dyke
200 µm
200 µm
Resorption texture

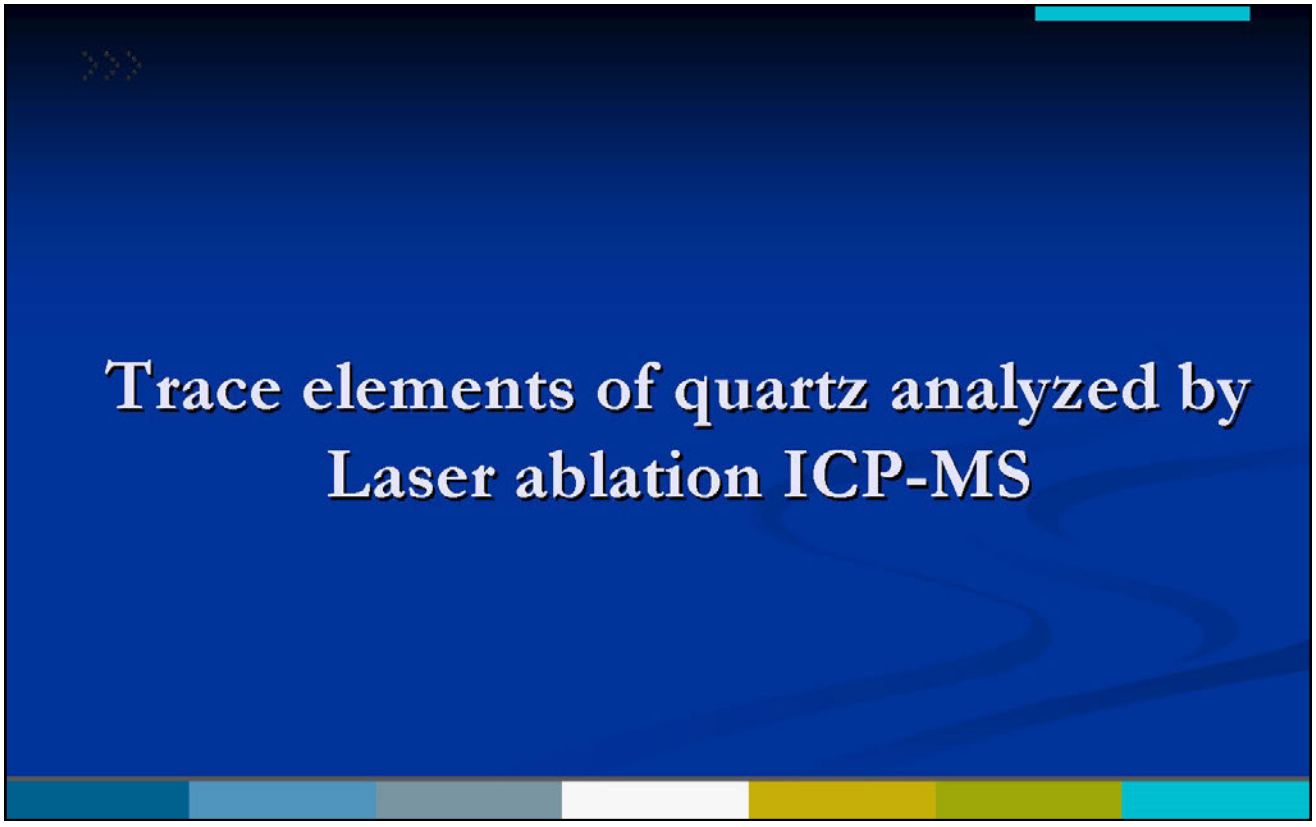
Trace elements of quartz analyzed by
Laser ablation ICP-MS

Substitution Mechanisms

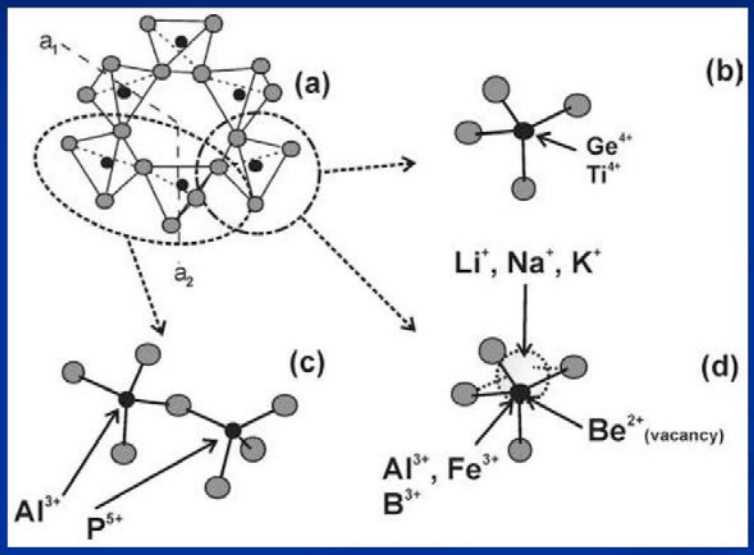

Larsen et al. (2004)

$Ti^{4+}(Ge^{4+}) \longrightarrow Si^{4+}$

Relatively compatible Relatively incompatible

K=>Fe=>Be=>Ti=>P=>Ge=>Li=>Al

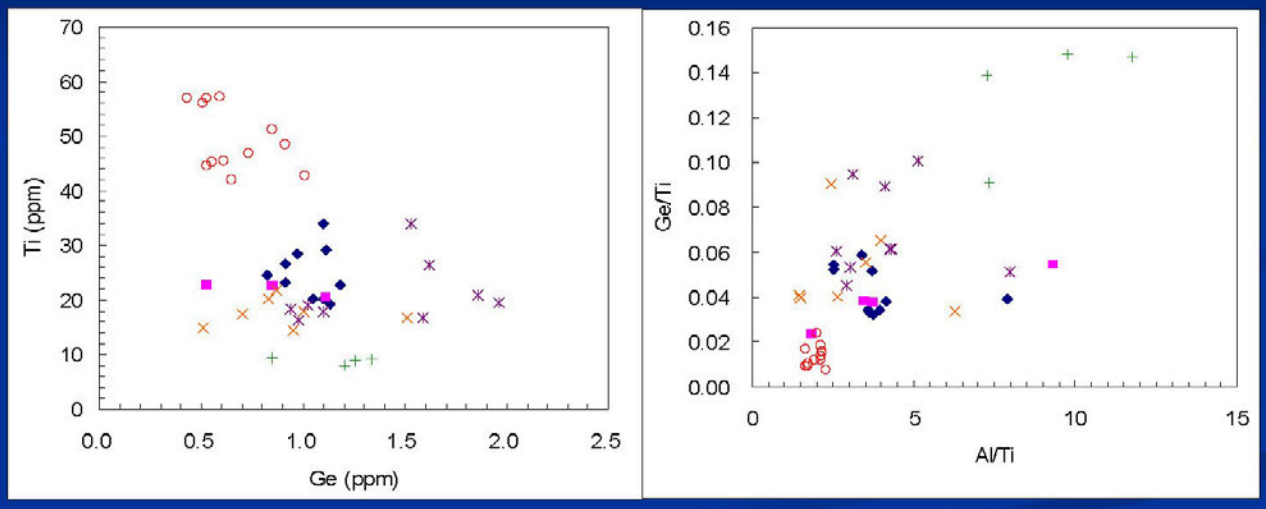

Larsen et al., 2004

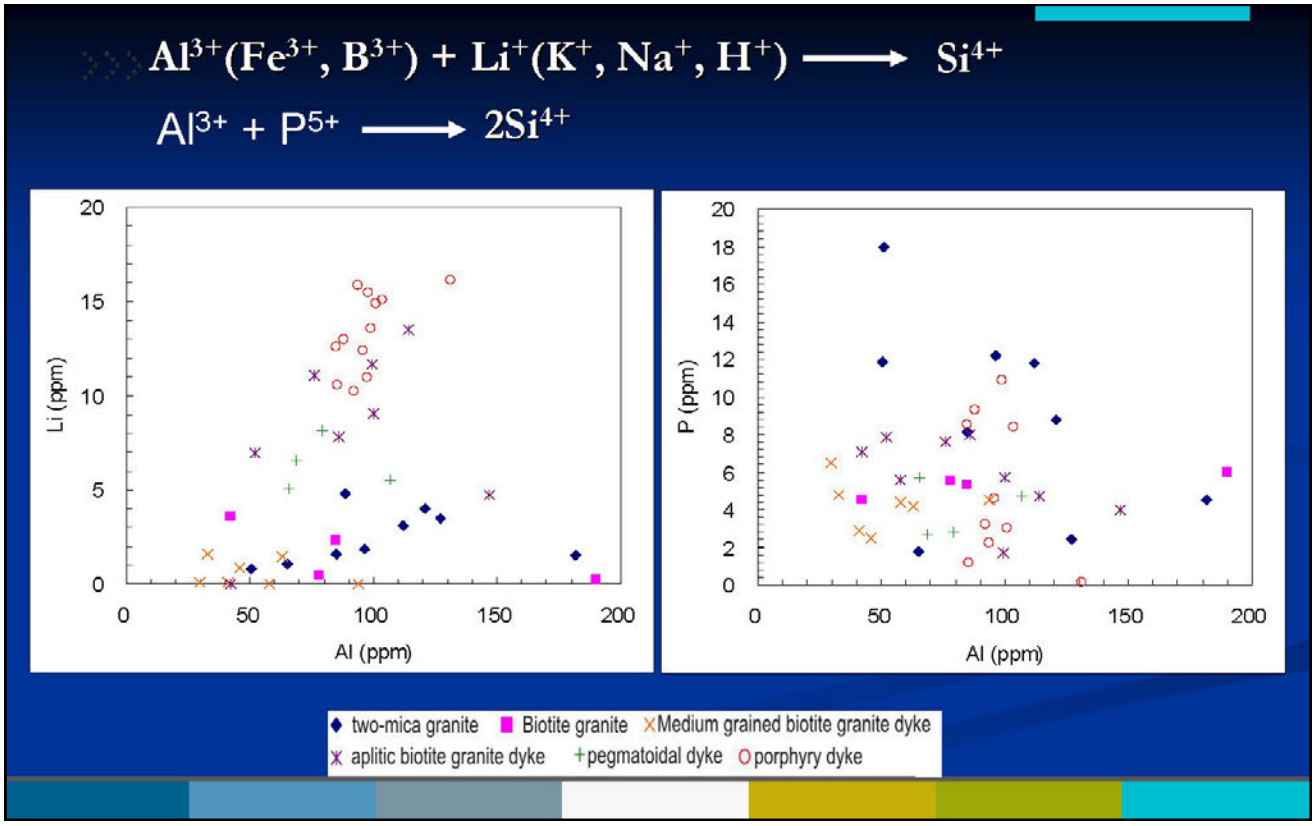
$Al^{3+}(Fe^{3+}, B^{3+}) + Li^{+}(K^{+}, Na^{+}, H^{+}) \longrightarrow Si^{4+}$
$Al^{3+} + P^{5+} \longrightarrow 2Si^{4+}$
Li (ppm)
Al (ppm)
P (ppm)
Al (ppm)
two-mica granite
Biotite granite
Medium grained biotite granite dyke
aplitic biotite granite dyke
pegmatoidal dyke
porphyry dyke

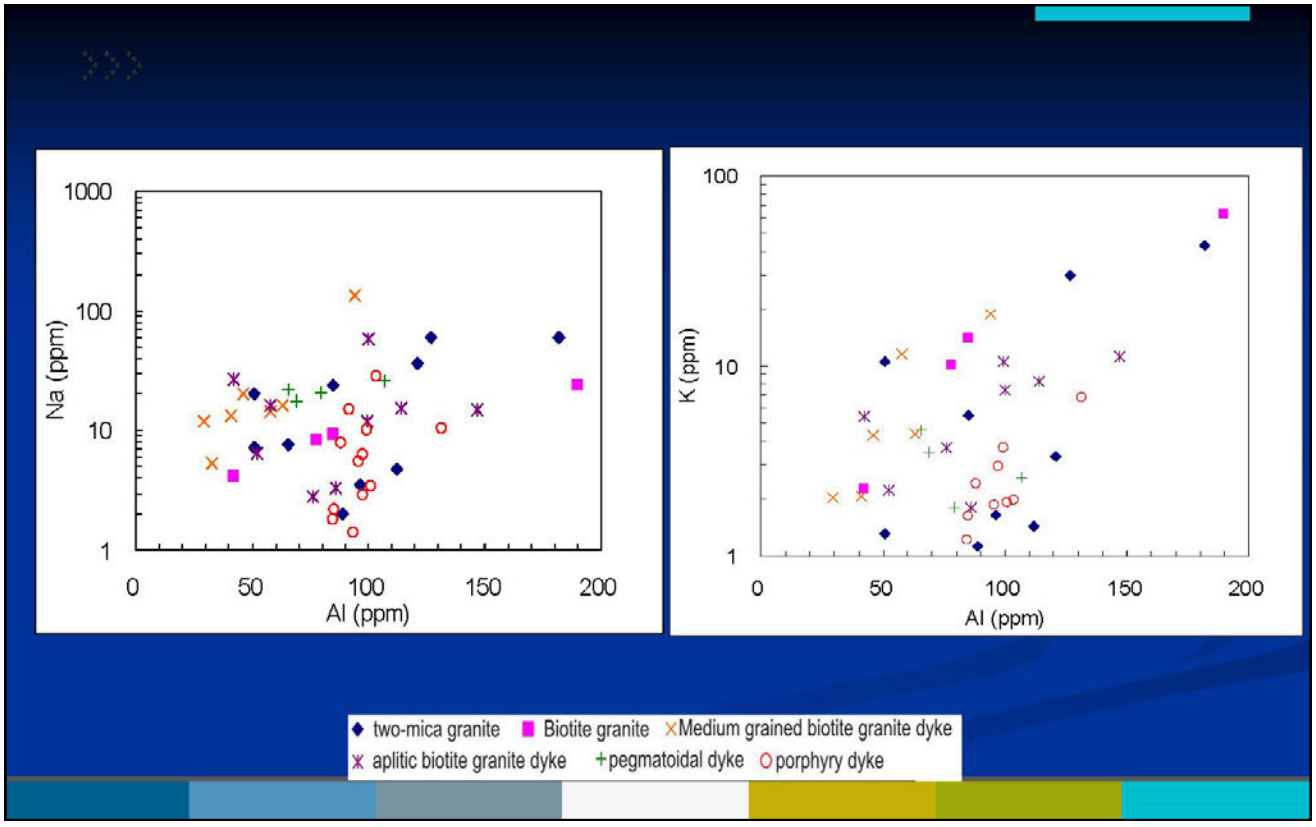
Na (ppm)
Al (ppm)
K (ppm)
Al (ppm)
two-mica granite
Biotite granite
Medium grained biotite granite dyke
aplitic biotite granite dyke
pegmatoidal dyke
porphyry dyke

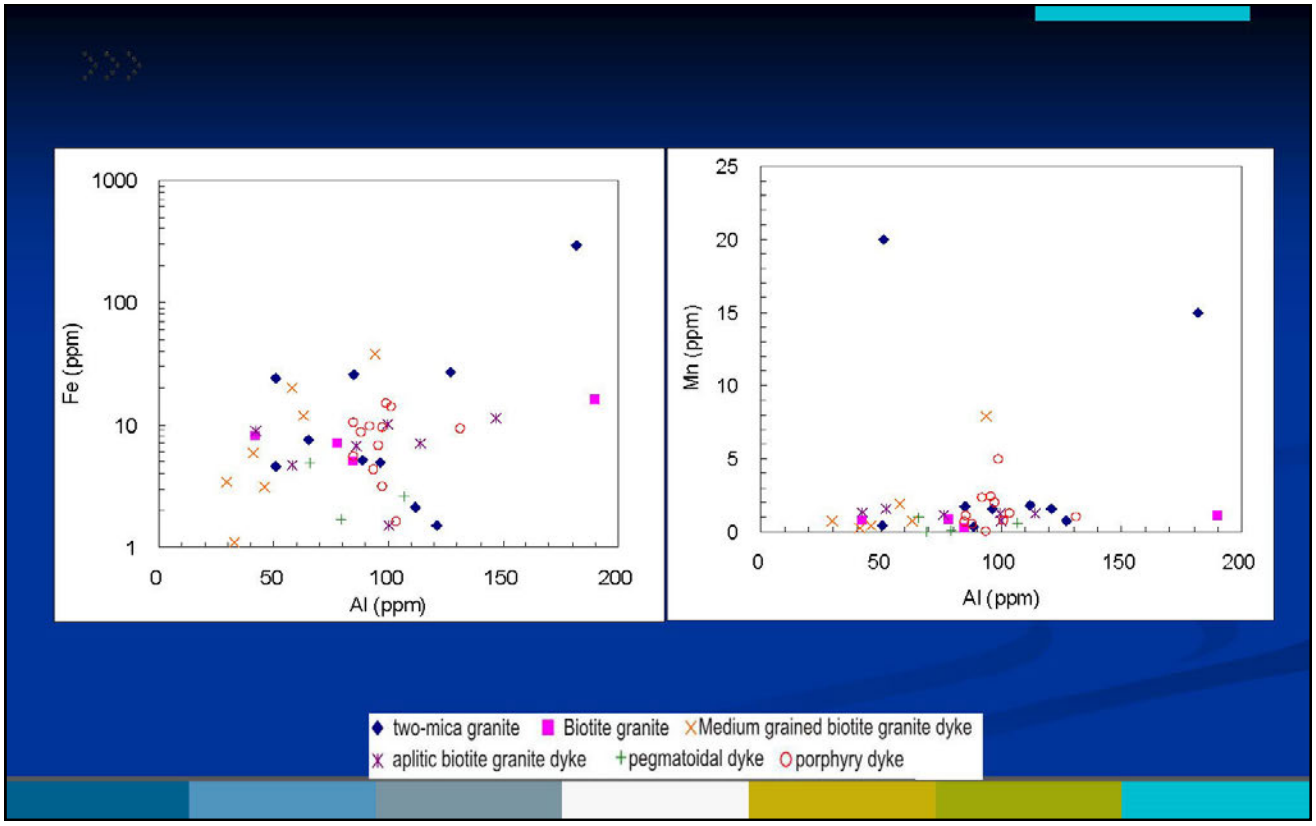
1000
100
10
1
Fe (ppm)
0
50
100
150
200
Al (ppm)
25
20
15
10
5
0
Mn (ppm)
0
50
100
150
200
Al (ppm)
two-mica granite
Biotite granite
Medium grained biotite granite dyke
aplitic biotite granite dyke
pegmatoidal dyke
porphyry dyke

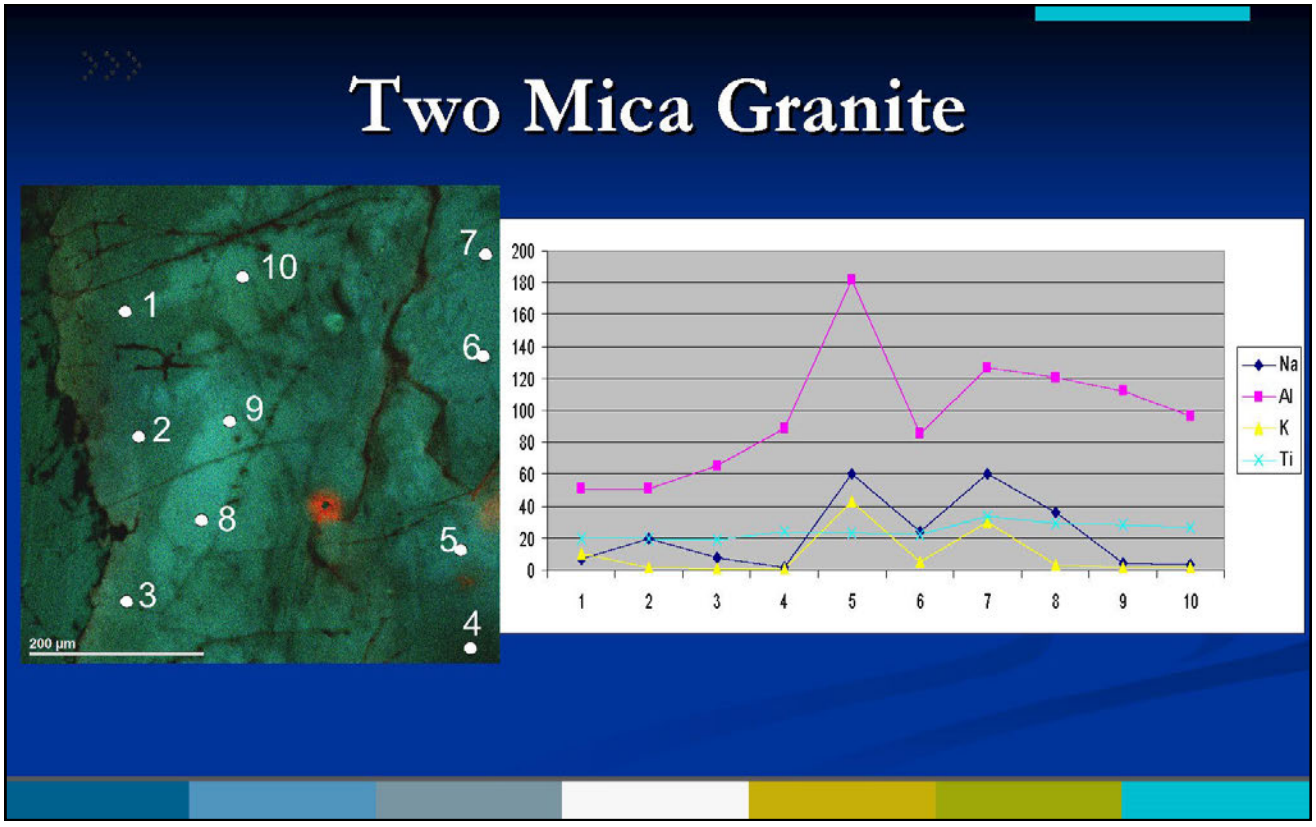
Two Mica Granite
1
2
3
4
5
6
7
8
9
10
200 μm
200
180
160
140
120
100
80
60
40
20
0
1
2
3
4
5
6
7
8
9
10
Na
Al
K
Ti

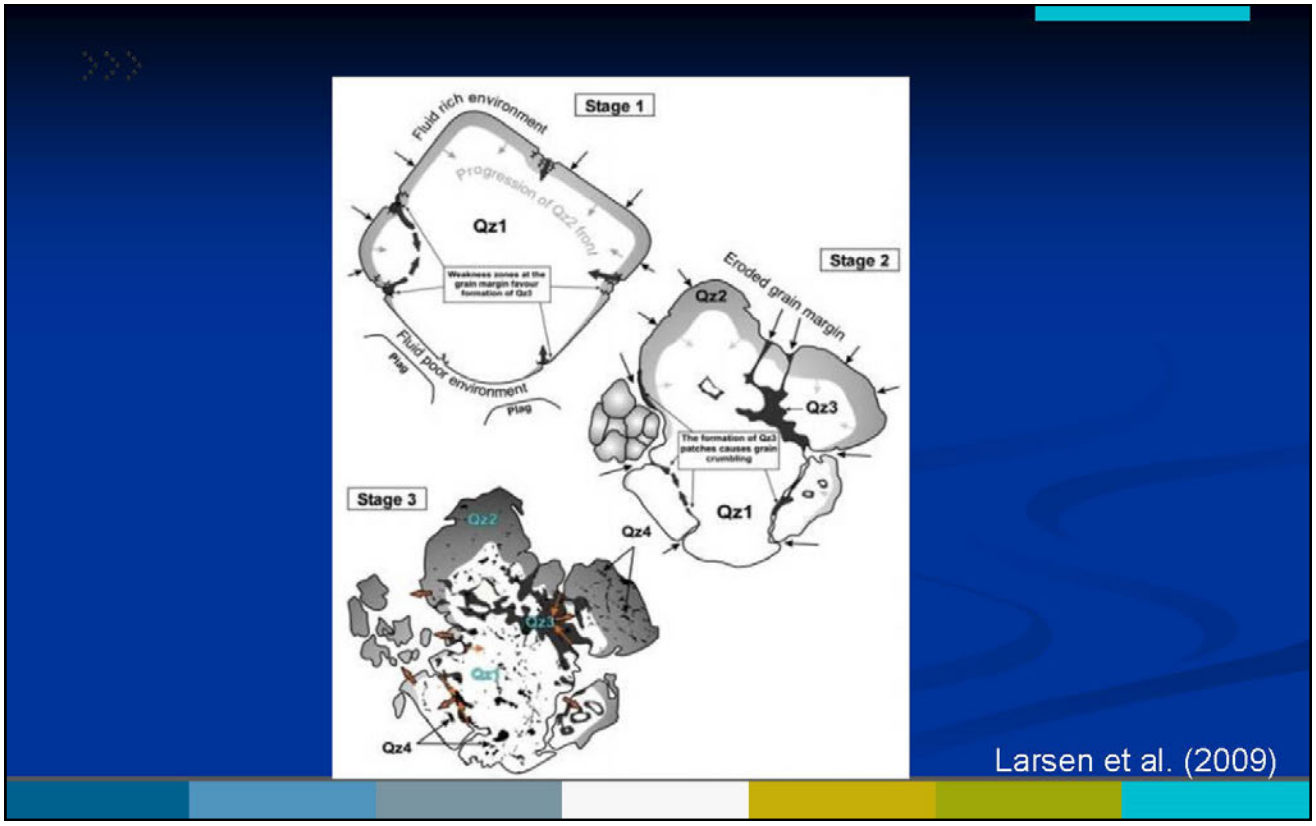
Stage 1
Fluid rich environment
Progression of Qz2 front
Qz1
Weakness zones at the grain margin favour formation of Qz3
Fluid poor environment
Plag
Plag
Stage 2
Eroded grain margin
Qz2
Qz3
The formation of Qz3 patches causes grain crumbling
Qz1
Qz4
Stage 3
Qz2
Qz3
Qz1
Qz4
Larsen et al. (2009)

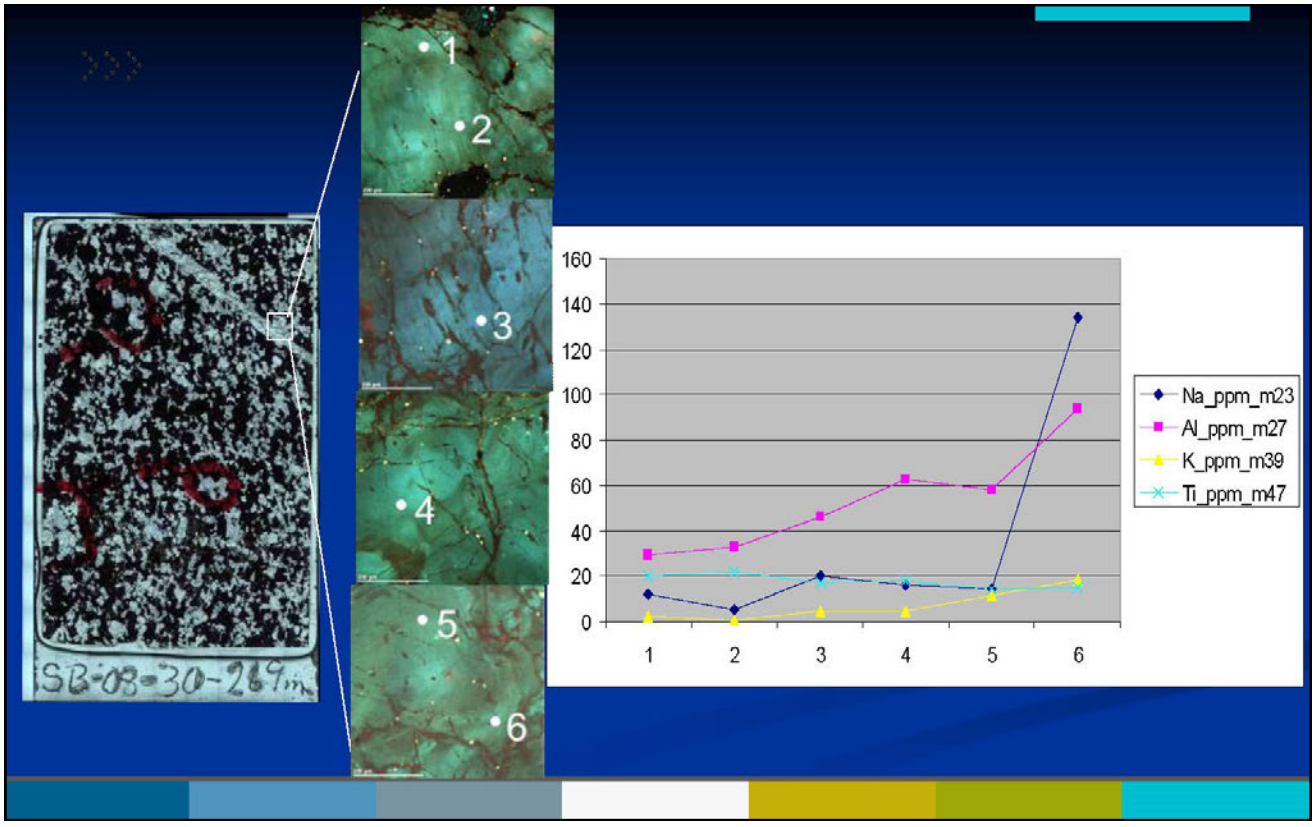
1
2
3
4
5
6
SB-08-30-264m
160
140
120
100
80
60
40
20
0
1
2
3
4
5
6
Na_ppm_m23
Al_ppm_m27
K_ppm_m39
Ti_ppm_m47

Relationship with whole rock geochemistry

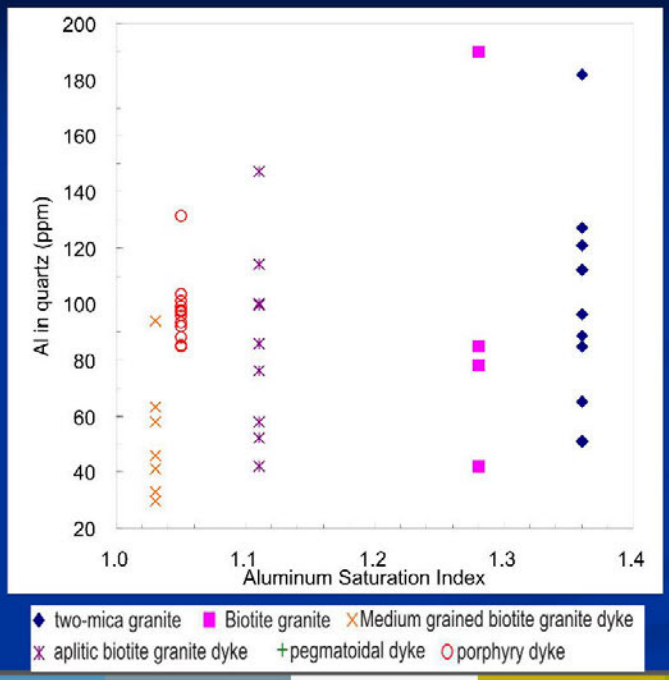

Relationship with whole rock geochemistry

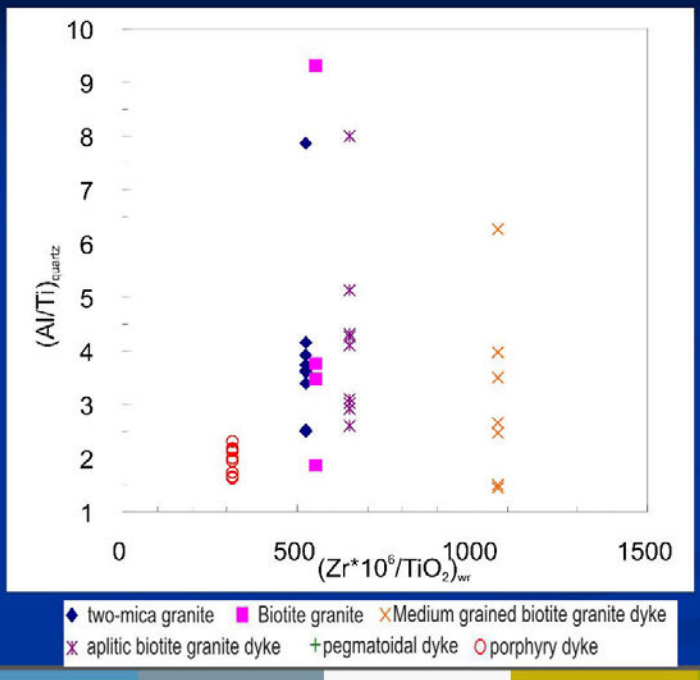

Relationship with whole rock geochemistry

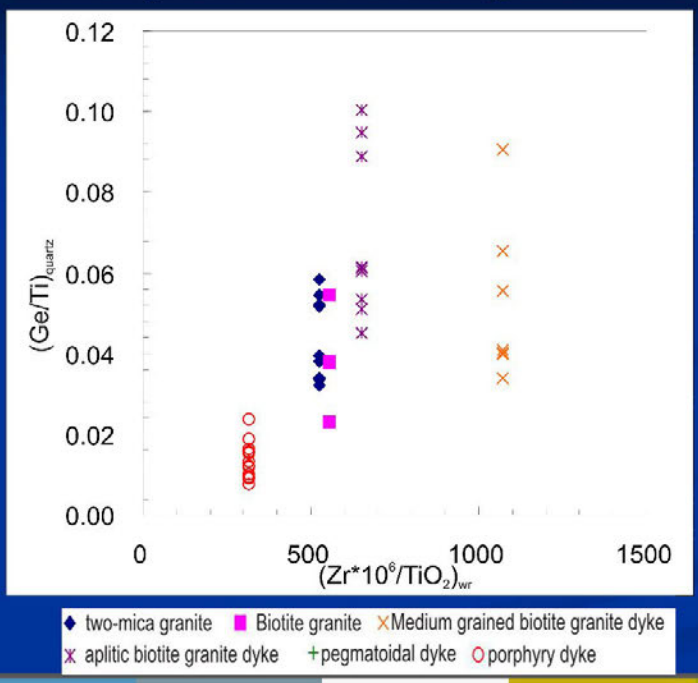

Ti-in-quartz geothermometer

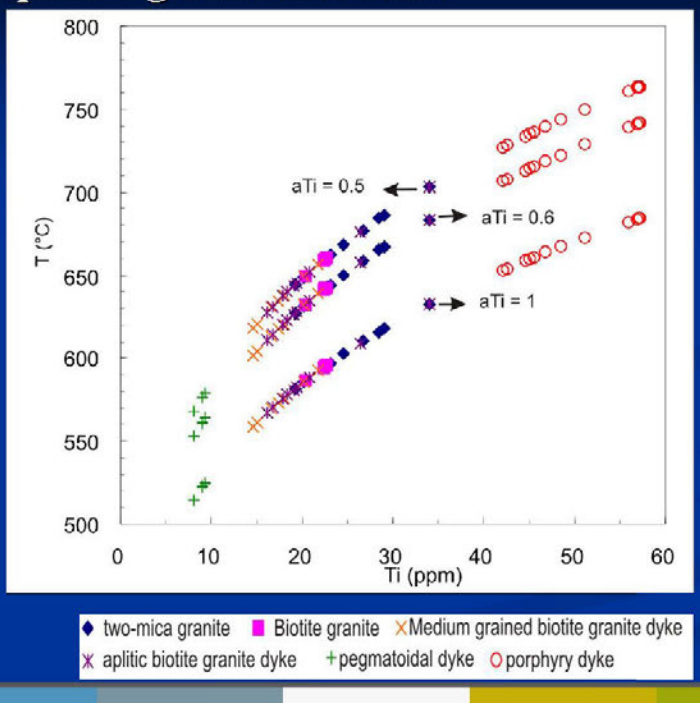

Wark and Watson (2006)

Oxygen Isotope

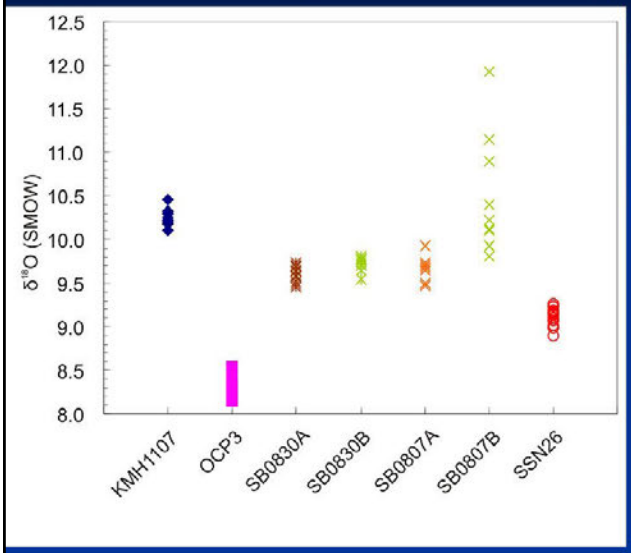

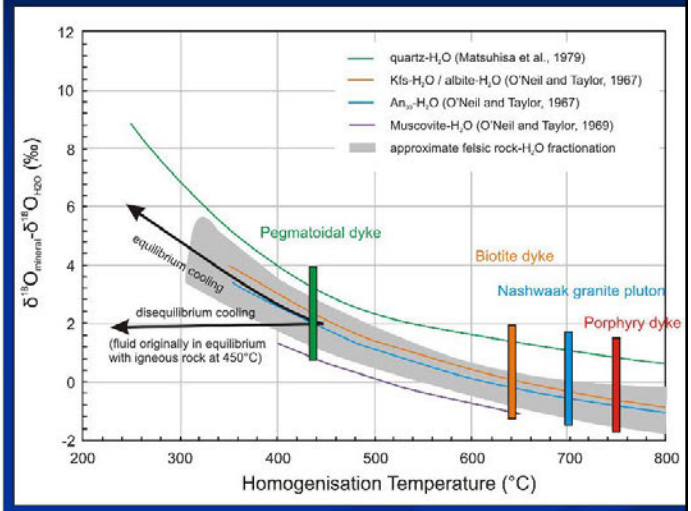

two-mica granite Biotite granite Medium grained biotite granite dyke
aplitic biotite granite dyke pegmatoidal dyke porphyry dyke

Allan and Yardley (2007)

Conclusions

- Ge/Ti ratio of quartz is a reliable index of the magmatic evolution of granitic igneous system. It is consistent with Zr/TiO_2 ratio of whole rock and indicate that porphyry dyke is most primary and biotite dyke is the most fractionated granite.
- During the magmatic hydrothermal transition process, the chemistry of primary aqueous fluids is strongly modified from its primary igneous composition before eventually being expelled from the granitic system
- Based on the Ti-in-quartz thermometer, the calculated oxygen isotope composition of the fluids indicate that these hydrothermal fluids are dominantly originated from magma.

Funded by: New Brunswick Department of Energy and Mines,
Geodex Minerals Ltd. and Northcliff Resources Ltd.
GEODEX MINERALS
HDI NORTHCLIFF
New Nouveau Brunswick
CANADA

Are there elephants hiding in the Jurassic of Yukon? A tectonomagmatic perspective on porphyry prospectivity

J.B. Chapman

Geological Survey of Canada, 605 Robson Street, Vancouver, British Columbia

Abstract: Within British Columbia, Triassic-Jurassic felsic plutonic and intrusive rocks of the Stikinia and Quesnellia terranes are very much considered "elephant country", and are spatially and genetically associated with some of the most significant porphyry Cu-Mo deposits in North America. However, where these terranes meet and merge in central Yukon, little significant mineralization has been discovered in similarly aged felsic plutonic rocks and they host only one operating Cu mine, despite outcrop covering hundreds of square kilometres. The reasons for this discrepancy are not clear. In order to provide assessment of the tectonomagmatic setting and porphyry prospectivity of Jurassic plutonic rocks within Yukon, 65 unmineralized samples from across the district have been analyzed for their whole rock major and trace element geochemistry, and their zircon Ce^{4+}/Ce^{3+} ratios were determined by laser ablation ICP-MS. Most samples plot within calc-alkaline to high K calc-alkaline fields within a plot of SiO_2 vs. K_2O, although data display significant scatter and lack any strong trend, suggestive of later disturbance of the K content. Rocks from all sampling locations show HFSE depletions and negative Nb anomalies characteristic of suprasubduction zone environments, and commonly depleted HREE patterns are suggestive of melt generated below the depth of garnet stability. Plots of Sr/Y vs. Y and La/Yb_N vs. Yb_N both indicate significant adakite-like and adakitic characteristics in a subset of the samples analysed. Taken together, the suprasubduction zone character and presence of adakite-like magmatism have been suggested as strong indicators of high porphyry potential in other parts of the world. Zircon Ce^{4+}/Ce^{3+} values were highly variable and ranged up to more than 2100, an order of magnitude greater than previous studies have suggested as a porphyry prospectivity threshold. However, aluminum-in-hornblende data and Cu and Mo contents well below crustal abundances suggest that Jurassic plutonic rocks may represent the mid-crustal, volatile-depleted residue of porphyry-related magmatism that has been eroded away. Future exploration for Cu-Mo-Au mineralization within Yukon will depend on understanding of tectonic uplift across the region, and better constraint on the genesis of known mineralization.

Originally presented Geological Association of America Annual Meeting 2014, Vancouver, BC. October 21, 2014.

Corresponding author: John B. Chapman (john.chapman@nrcan-rncan.gc.ca)

Chapman, J.B., 2015. Are there elephants hiding in the Jurassic of Yukon? A tectonomagmatic perspective on porphyry prospectivity; *in* TGI 4 – Intrusion Related Mineralisation Project: New Vectors to Buried Porphyry-Style Mineralisation, (ed.) N. Rogers; Geological Survey of Canada, Open File 7843, p. 493 -506.

GSA Annual Meeting 2014
Vancouver, BC, Canada
21st October 2014

Are there elephants hiding in the Jurassic of Yukon? A tectonomagmatic perspective on porphyry prospectivity

John B. Chapman
Geological Survey of Canada

Natural Resources Canada | Ressources naturelles Canada

Canada

Uneven distribution?

- Triassic-Jurassic granitoids host or are linked to most of British Columbia's largest and economically significant porphyry Cu-Mo and Cu-Au ore bodies
- To date, only one operating Cu-Au mine in the Yukon: Minto
- However, the Intermontane Superterrane, including Stikine and Quesnel terranes, has significant outcrop in Yukon.

Natural Resources Canada | Ressources naturelles Canada

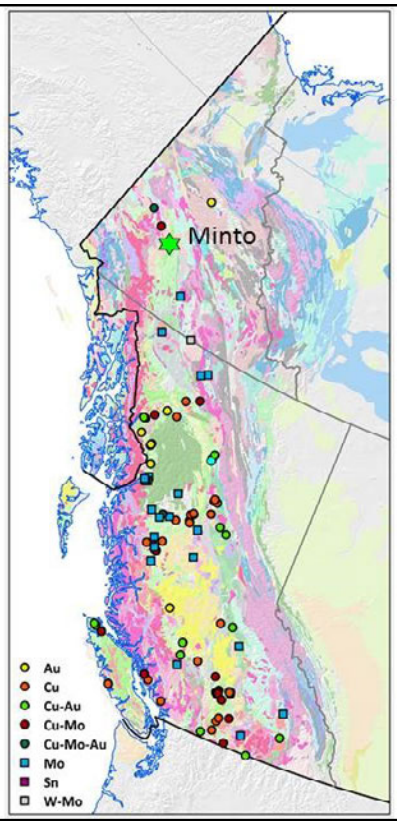

Data from Sinclair (2007)

Yukon plutons

- Abundant granitoid intrusions throughout central and southern Yukon
- Dominantly Triassic-Jurassic, Cretaceous and Tertiary
- Host major mineral occurrences, including Minto mine, Casino, Carmacks Copper, Sonora Gulch and many more...
- BUT... exploration activity is spotty between different plutonic bodies

Natural Resources Canada / Ressources naturelles Canada

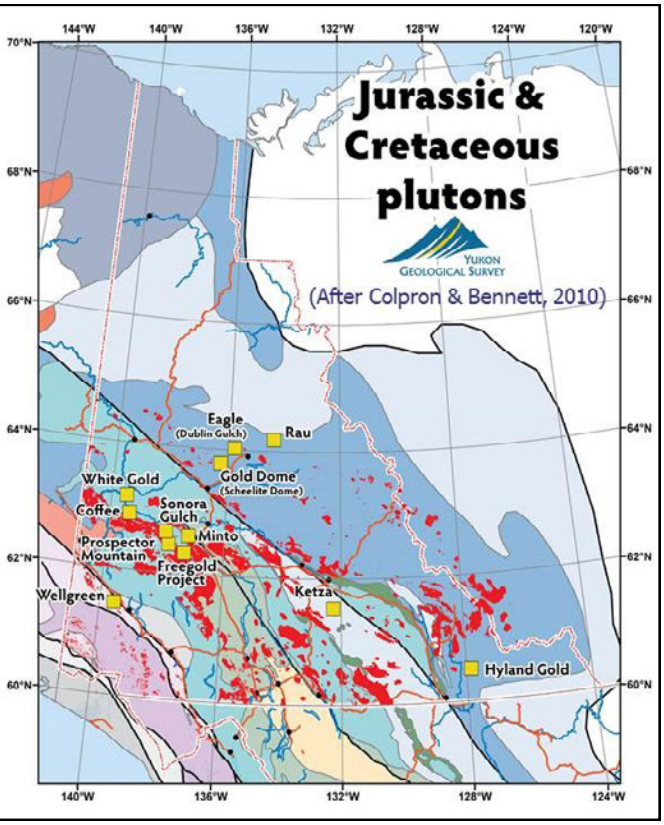

Triassic-Jurassic plutonic outcrop

Plutonic rocks of late Triassic to early Jurassic age (orange) outcrop throughout south-central Yukon, along both the east and western margins of the Whitehorse Trough. The Minto Cu-Au mine sits at the point where the eastern and western belts converge.

(CC BY 3.0, Hwy43)

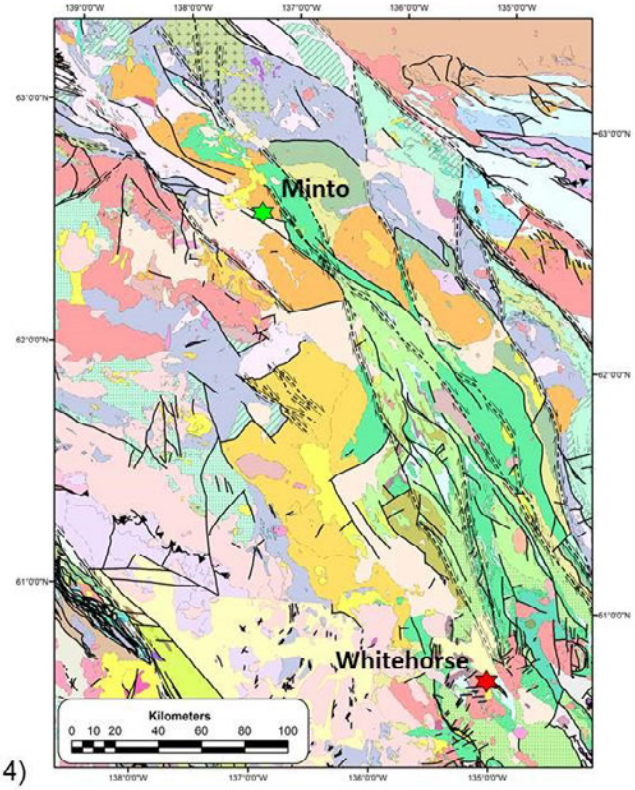

Modified from Colpron (2014)

MINFILE occurrences

While plutonic rocks Cretaceous age (dark pink) west of the Big Creek Fault contain abundant porphyry occurrences listed in the MINFILE database, occurrences recorded for the Triassic-Jurassic suite are sparse, and dominantly located in the Granite Mountain and Minto plutons, in the vicinity of known economic mineralization at the Minto deposit itself and the Carmacks deposit (formerly Williams Creek).
Most occurrences are of the normal calc-alkalic porphyry Cu type (orange stars), but some instances of alkalic Cu (red stars) and porphyry Mo (blue stars) have been reported.

Modified from Colpron (2014)

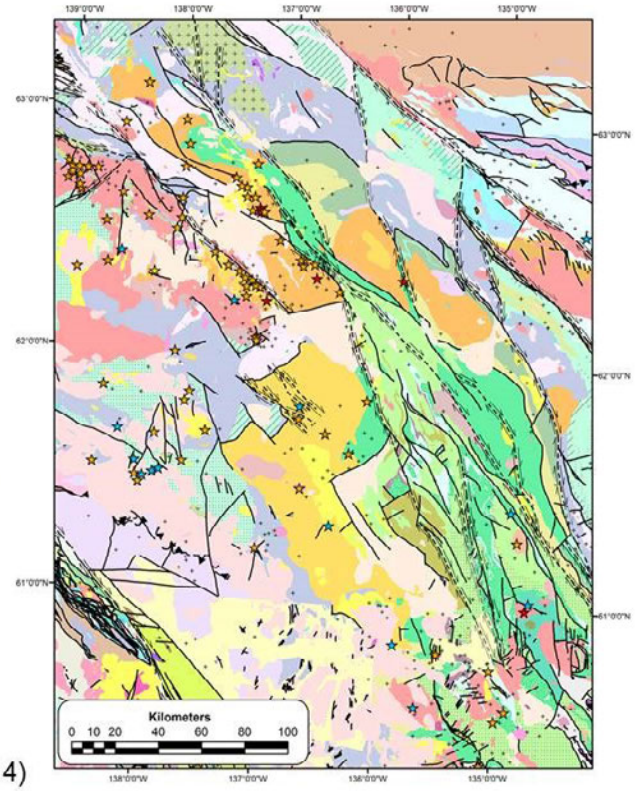

Sampling distribution

In order to examine the tectonomagmatic setting of Triassic-Jurassic plutonic rocks in central Yukon, 65 samples were taken from the surface outcrop locations shown.
Individual pluton and batholith names are used to distinguish sampling locations (below).

Key

- Walhalla Ck.
- Minto
- Granite Mtn.
- Tatchun
- Aishihik
- Teslin Cross.
- Big Creek

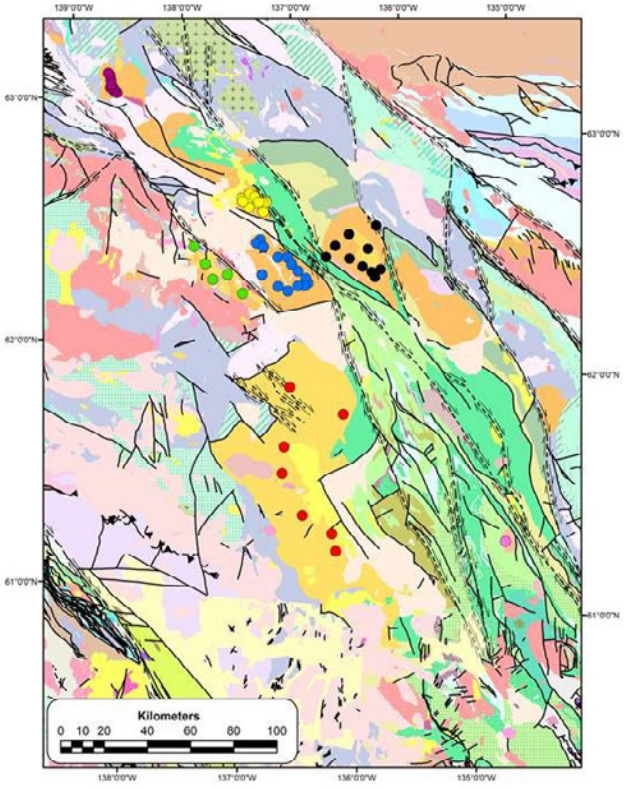

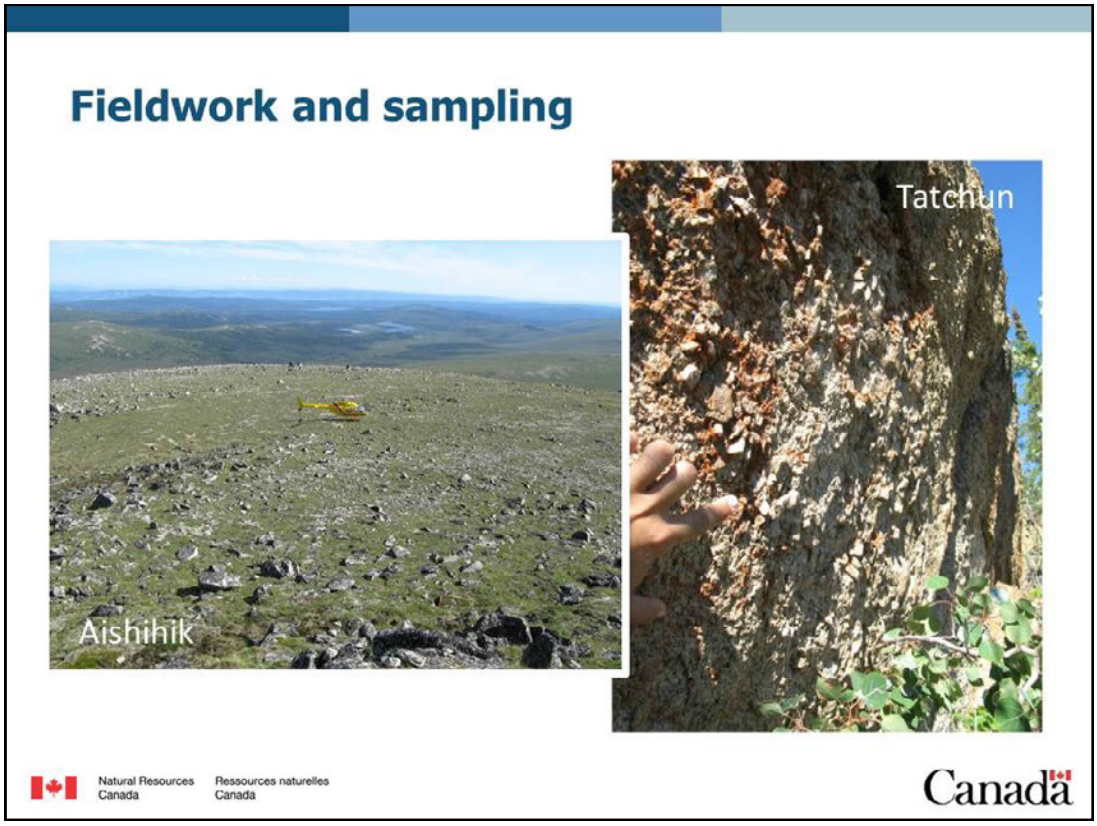
Fieldwork and sampling
Tatchun
Aishihik
Natural Resources Canada
Ressources naturelles Canada
Canada

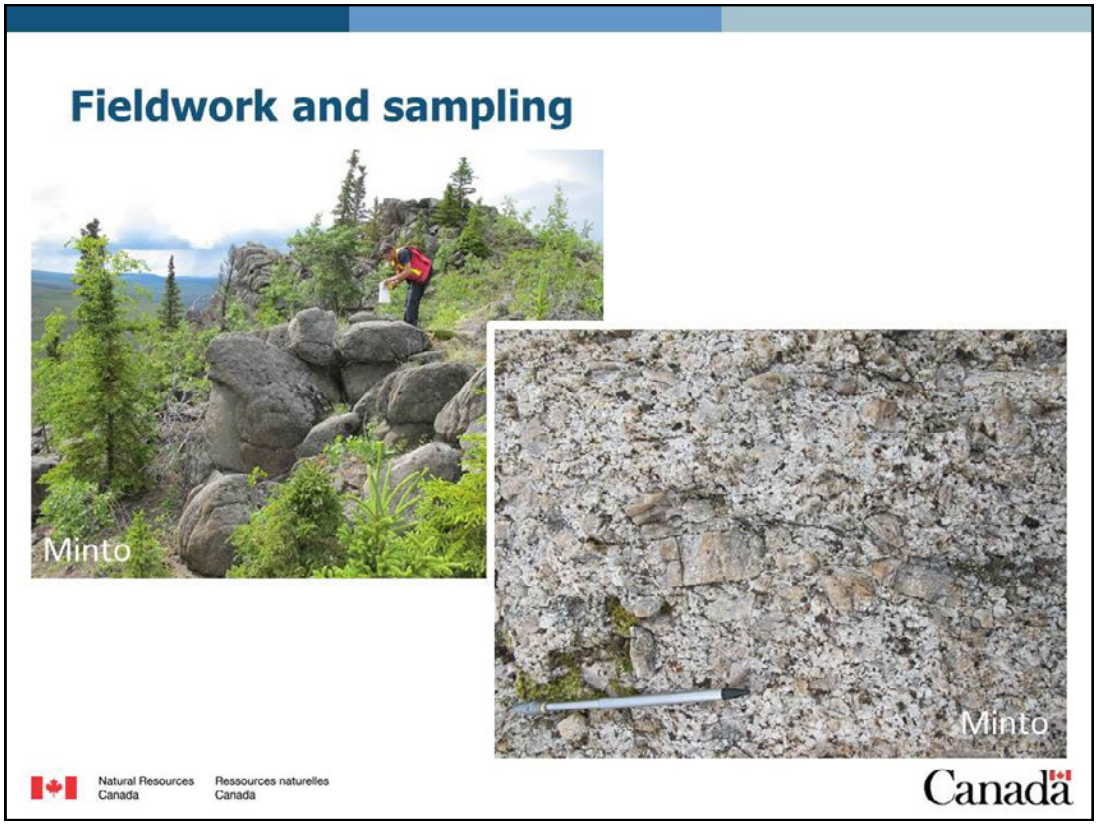
Fieldwork and sampling
Minto
Minto
Natural Resources Canada
Ressources naturelles Canada
Canada

Fieldwork and sampling

Natural Resources Canada Ressources naturelles Canada

Canada

TAS Rock Classification

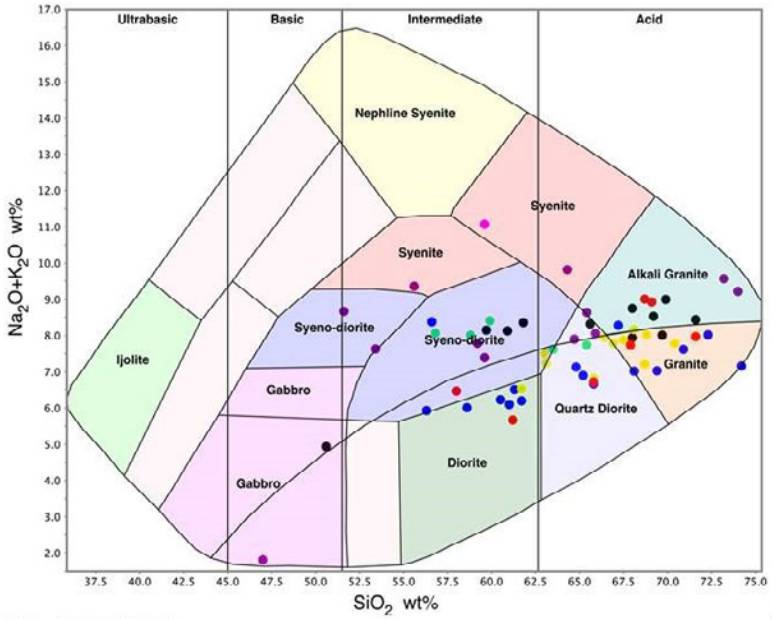

Natural Resources Canada Ressources naturelles Canada

Canada

Classification

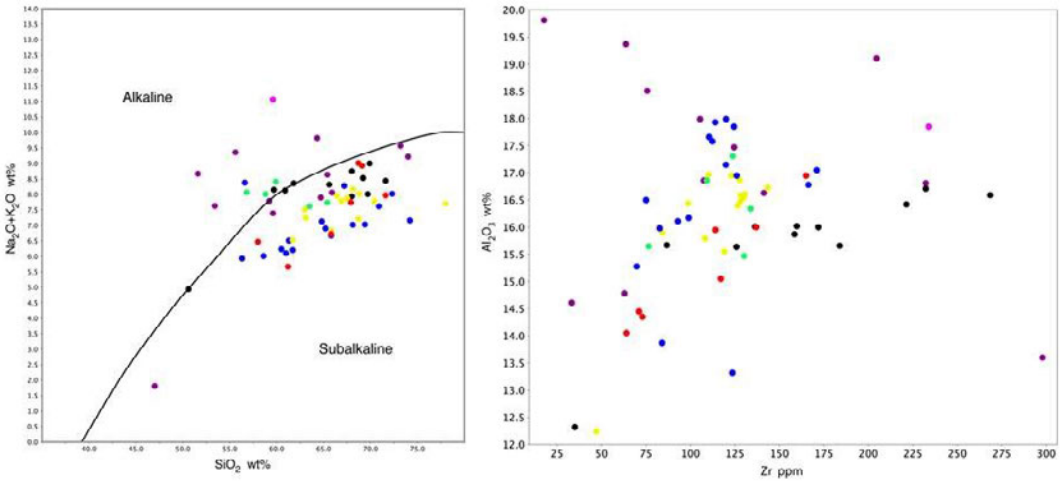

Natural Resources Canada Ressources naturelles Canada

Canada

Pearce tectonic discrimination

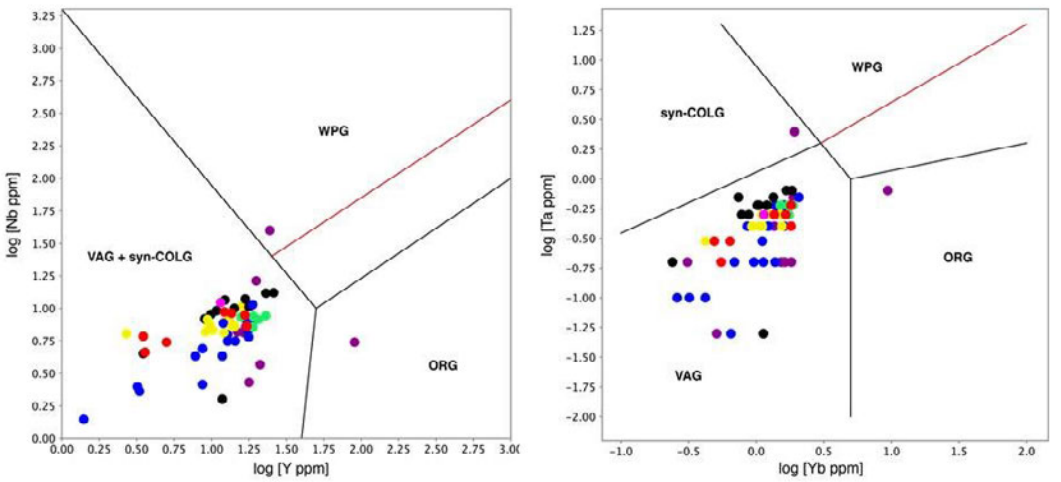

Natural Resources Canada Ressources naturelles Canada

Canada

Pearce tectonic discrimination

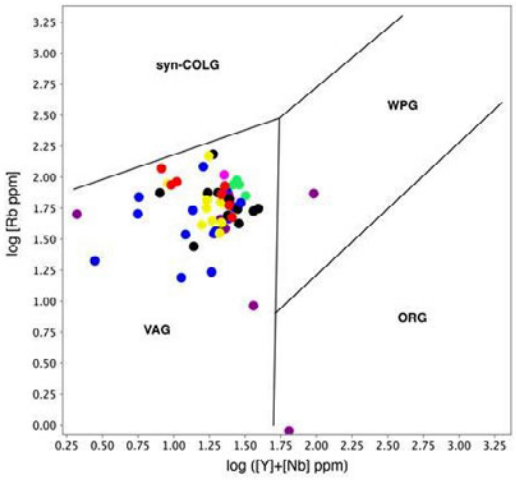

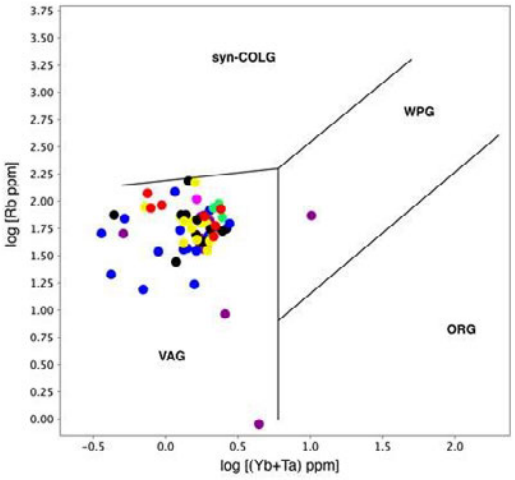

Natural Resources Canada Ressources naturelles Canada

Canada

Harris tectonic discrimination

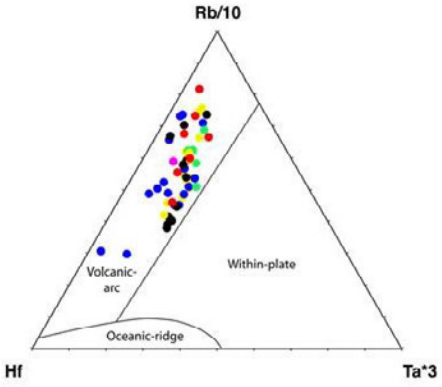

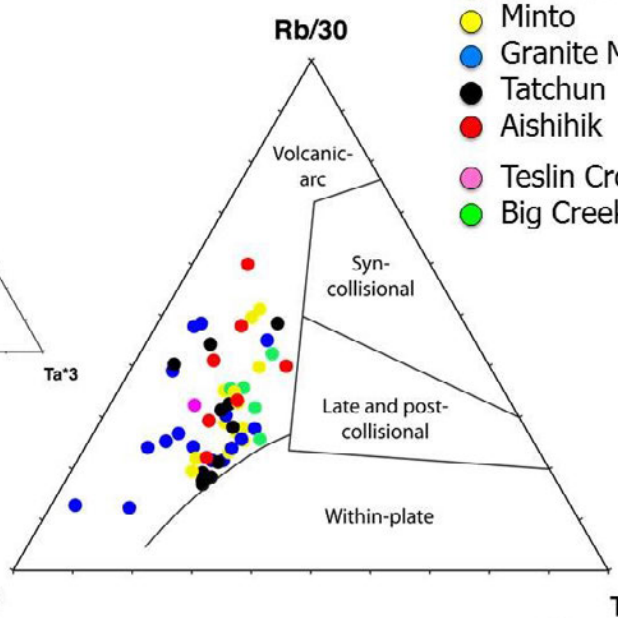

Key

- Walhalla Ck.
- Minto
- Granite Mtn.
- Tatchun
- Aishihik
- Teslin Cross.
- Big Creek

Natural Resources Canada Ressources naturelles Canada

Canada

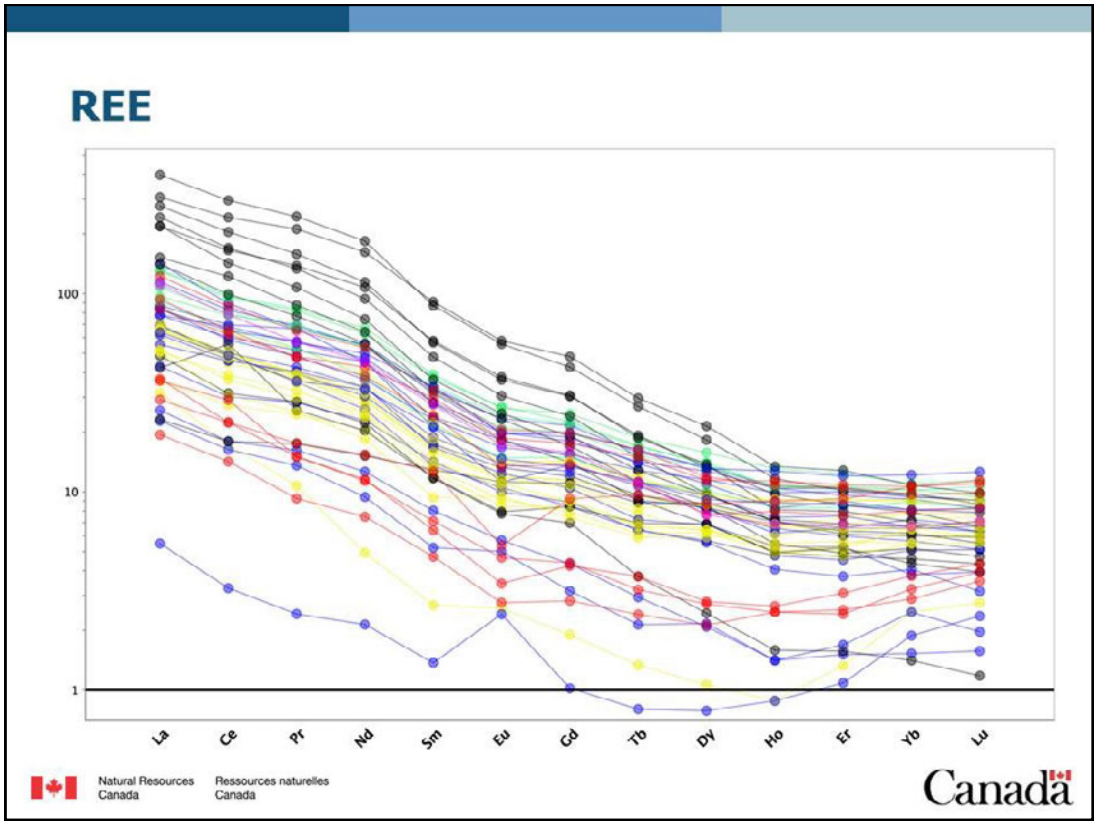
REE
100
10
1
La
Ce
Pr
Nd
Sm
Eu
Gd
Tb
Dy
Ho
Er
Yb
Lu
Natural Resources Canada
Ressources naturelles Canada
Canada

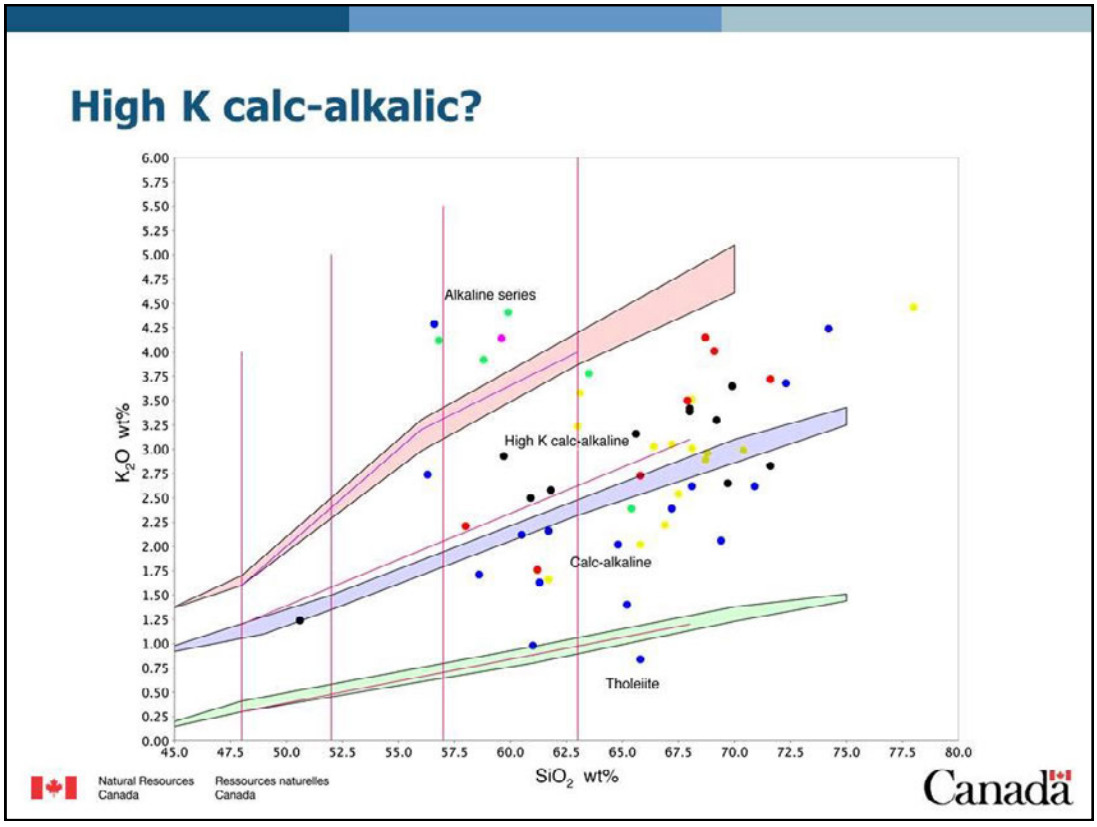
High K calc-alkalic?
Alkaline series
High K calc-alkaline
Calc-alkaline
Tholeiite
K_2O wt%
SiO_2 wt%
Natural Resources Canada
Ressources naturelles Canada
Canada

Other genetic indicators...

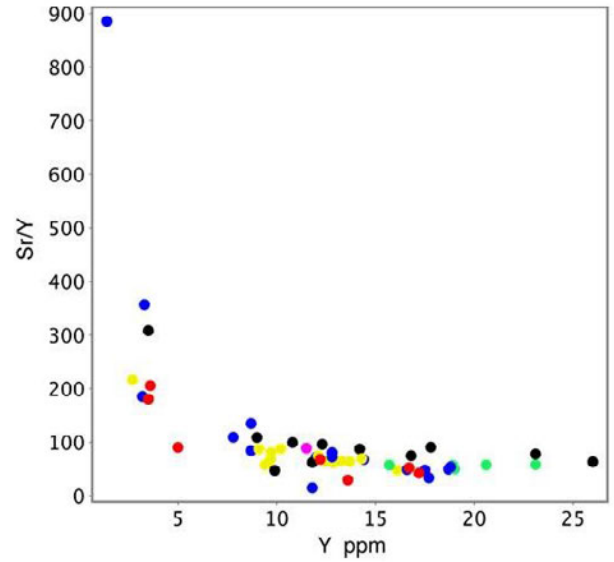

Key

- Walhalla Ck.
- Minto
- Granite Mtn.
- Tatchun
- Aishihik
- Teslin Cross.
- Big Creek

Natural Resources Canada | Ressources naturelles Canada

Canada

Other genetic indicators...

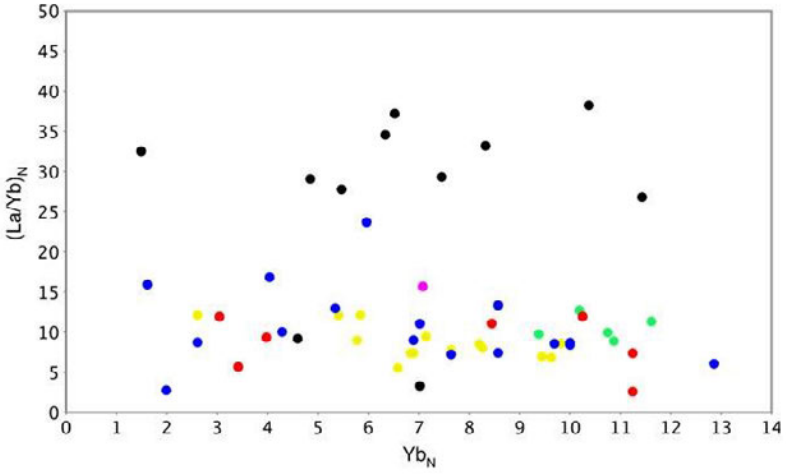

Key

- Walhalla Ck.
- Minto
- Granite Mtn.
- Tatchun
- Aishihik
- Teslin Cross.
- Big Creek

Natural Resources Canada | Ressources naturelles Canada

Canada

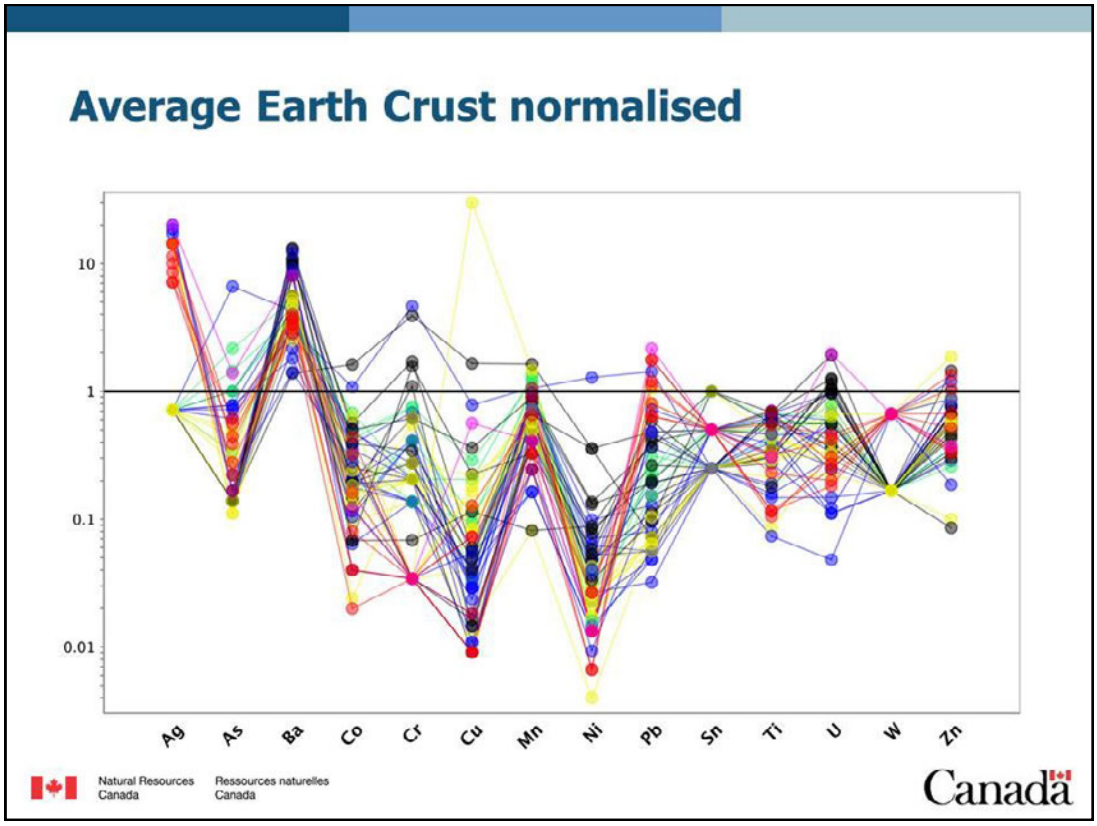
Average Earth Crust normalised
10
1
0.1
0.01
Ag
As
Ba
Co
Cr
Cu
Mn
Ni
Pb
Sn
Ti
U
W
Zn
Natural Resources Canada
Ressources naturelles Canada
Canada

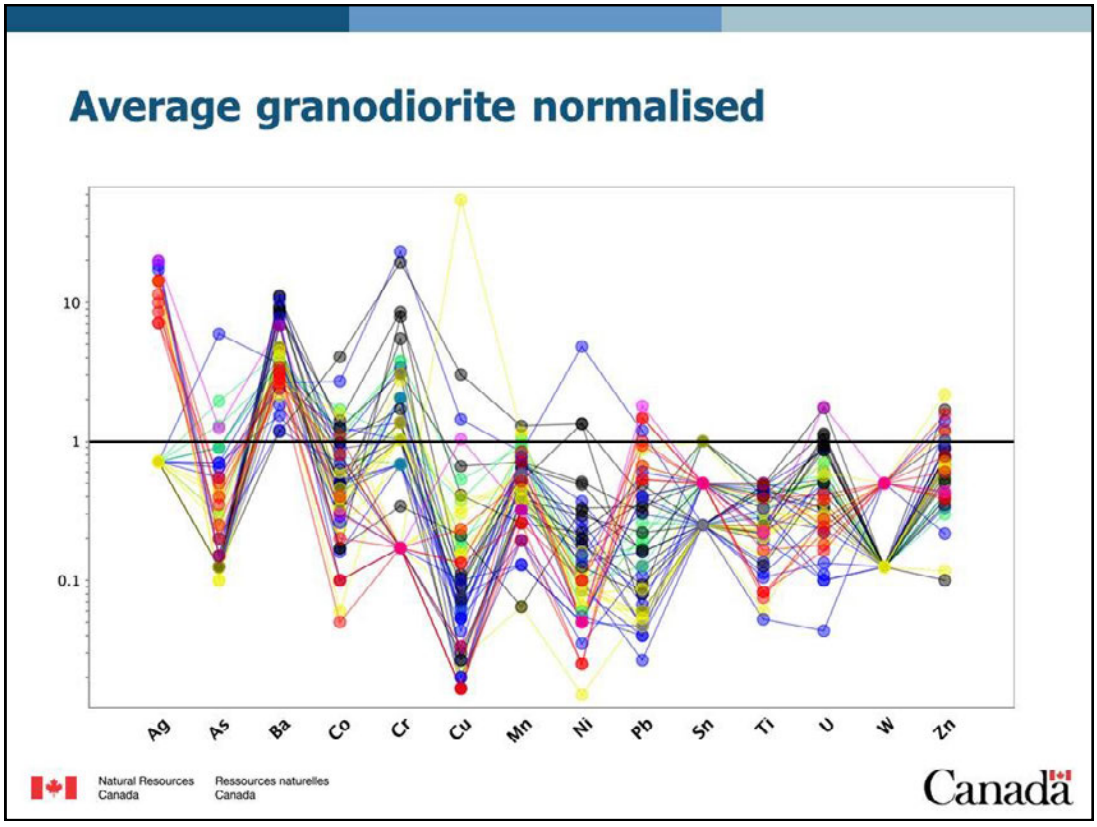
Average granodiorite normalised
10
1
0.1
Ag
As
Ba
Co
Cr
Cu
Mn
Ni
Pb
Sn
Ti
U
W
Zn
Natural Resources Canada
Ressources naturelles Canada
Canada

Zircon Ce^{4+}/Ce^{3+}

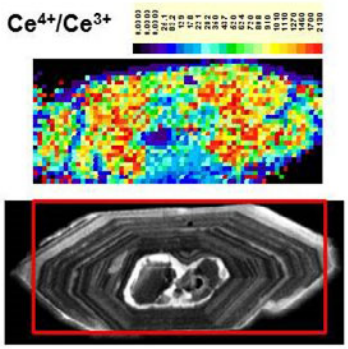

- Oxygen fugacity not the dominant process?
- Pressure and magma polymerization also major controls

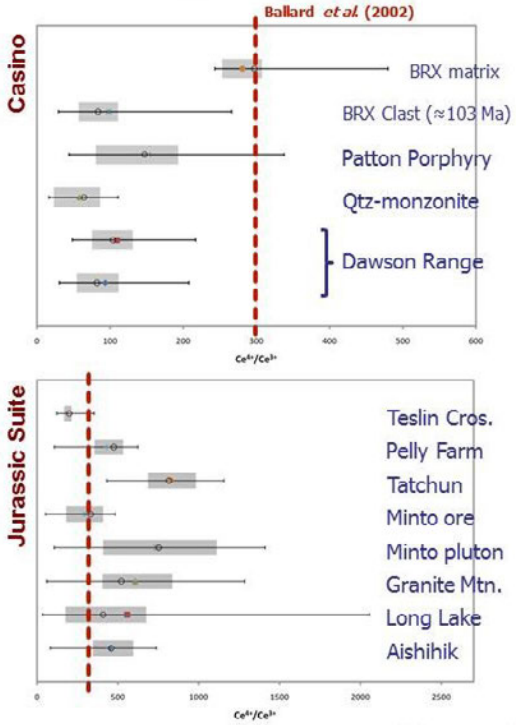

Natural Resources Canada Ressources naturelles Canada

Canada

Summary

- Majority of Triassic-Jurassic suite have volcanic arc geochemical affinities
- Background plutonic rocks appear metal depleted
- High K calc alkaline rocks and evidence for high fO_2 and high H_2O rocks in some areas
- Generally, but not exclusively, deep apparent erosion level: Walhalla Creek possibly cumulate influenced?
- Differential tectonic uplift? Need to understand cooling, exhumation and erosional history in more detail to facilitate exploration

- Are there elephants?

Natural Resources Canada Ressources naturelles Canada

Canada

Minto and Carmacks Copper?

Measured & Indicated Resources:
~49.3 Mt @ 1.10% Cu, 0.40 g/t Au, 3.85 g/t Ag
(Capstone Mining Corp., Dec. 2013)

Photo taken July 2011

Natural Resources Canada | Ressources naturelles Canada

Canada

Minto and Carmacks Copper?

Natural Resources Canada | Ressources naturelles Canada

Canada

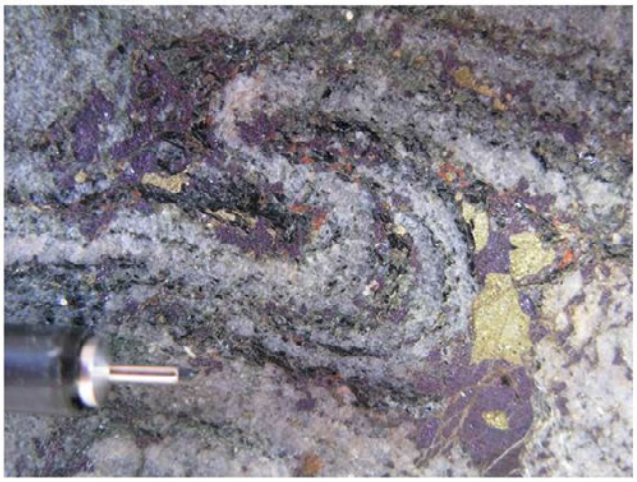

Natural Resources Canada Ressources naturelles Canada

Canada

References

Colpron, M. 2014. Update of the Yukon Bedrock Geology Map – Updated Bedrock Geology Polygons. Yukon Geological Survey.

Sinclair, W.D. 2007. Porphyry deposits. *In:* Goodfellow, W.D. (ed.) *Mineral Deposits of Canada: A Synthesis of Major Deposit-types, District Metallogeny, the Evolution of Geological Provinces, and Exploration Methods.* Mineral Deposits Division, Geological Association of Canada, Special Publication 5. Supplementary GIS data.

Natural Resources Canada Ressources naturelles Canada

Canada

Magmatic evolution in Devonian granitic rocks and relation to granophile mineralization in New Brunswick: Application of biotite trace element mapping with EPMA and LA-ICP-MS

Z. Azadbakht, D.R. Lentz and C.R.M. McFarlane

University of New Brunswick, Box 4400, 2 Bailey Drive, Fredericton, New Brunswick

Abstract: Two suites of felsic intrusions were emplaced during the later parts of the Appalachian orogenic cycle in New Brunswick. However, just those associated with crustal thickening processes of Acadian orogeny, post Acadian uplift, and Neoacadian orogeny are mineralized with granophile elements to form Sn, W, Mo, Cu, Bi, Sb, and Au deposits, as well as Ta, Li, base-metals, and U mineralization. Biotite major element classification indicated that these intrusions are mostly A- and S-type granitoids and their hybrid varieties; some I-type granitoids are also present in the area.

Magmatic biotite from forty-two of these Devonian intrusions was studied by electron microprobe (EPMA) and LA -ICP-MS at the University of New Brunswick. Whereas major elements are typically constant from core to rim, biotite grains can show remarkable trace element zoning. LA-ICP-MS trace element maps were also produced when permitted by the size of the biotite, frequency of the mineral inclusions, degree of alteration, and the laser spot size required to achieve sub-ppm detection limits. In this study, unaltered biotite grains with minor mineral inclusions, and diameters larger than 300 μm, display trace-element zoning patterns. Furthermore, smaller biotite tends to be more susceptible to intracrystalline diffusion. As a result, their elemental zoning should be further studied and cross -checked with other characteristics.

Results of this study showed LILE zoning, including Cs, Ba, and Rb, for most of the biotite grains. As these elements are highly incompatible, any zoning can be a result of the magma evolution history recorded within the biotite crystalline structure. Any other trace element pattern following them will also be of an igneous source. For example, biotite grains from the Pleasant Ridge granite show an increase from core to rim for Cs and Sn and a decrease for W and Sc. Copper is also high along the cleavages where biotite is weakly altered to chlorite. These observations coupled with an increase in F/Cl content from 770 to 1300 indicate that fractional crystallisation of this granite led to Sn mineralization. Tin is positively correlated with Fe/(Fe+Mg), but negatively correlated with Fe_T/Ti; this relationship may indicate that the Sn content of biotite increases with low fo_2 and low temperatures as indicated by the iron/magnesium ratio.

According to the results, the use of biotite as an indicator of trace element changes within granitic systems was achieved; with the help of other types of data, the composition of biotite may be a useful tool to indicate a difference between barren and mineralized granophile-element rich systems.

Originally presented Exploration, Mining and Petroleum New Brunswick Conference 2014. November 3, 2014.

Corresponding author: Zeinab Azadbakht (zeinab.azadbakht@unb.ca)

Azadbakht, Z., Lentz, D.R., and McFarlane, C.R.M., 2015. Magmatic evolution in Devonian granitic rocks and relation to granophile mineralization in New Brunswick: Application of biotite trace element mapping with EPMA and LA-ICP-MS; *in* TGI 4 – Intrusion Related Mineralisation Project: New Vectors to Buried Porphyry-Style Mineralisation, (ed.) N. Rogers; Geological Survey of Canada, Open File 7843, p. 507-519.

Magmatic Evolution in Devonian Granitic Rocks and Relation to Granophile Mineralization in New Brunswick: Application of Biotite Trace Element Mapping with EPMA and LA-ICP-MS

Zeinab Azadbakht , David Lentz, Christopher McFarlane

UNB

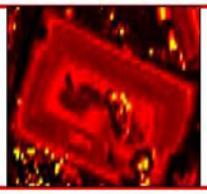

TGI 4 Ore Systems

Project Goals

- Document detailed chemistry of coexisting phyllosilicate mineral phases to reveal distinctive element signatures that may be specific to fertile granitoids.
- Provide a geochemical fingerprint for more-specific mineralization styles and prospectivity in the Acadian Plutonic Complex.

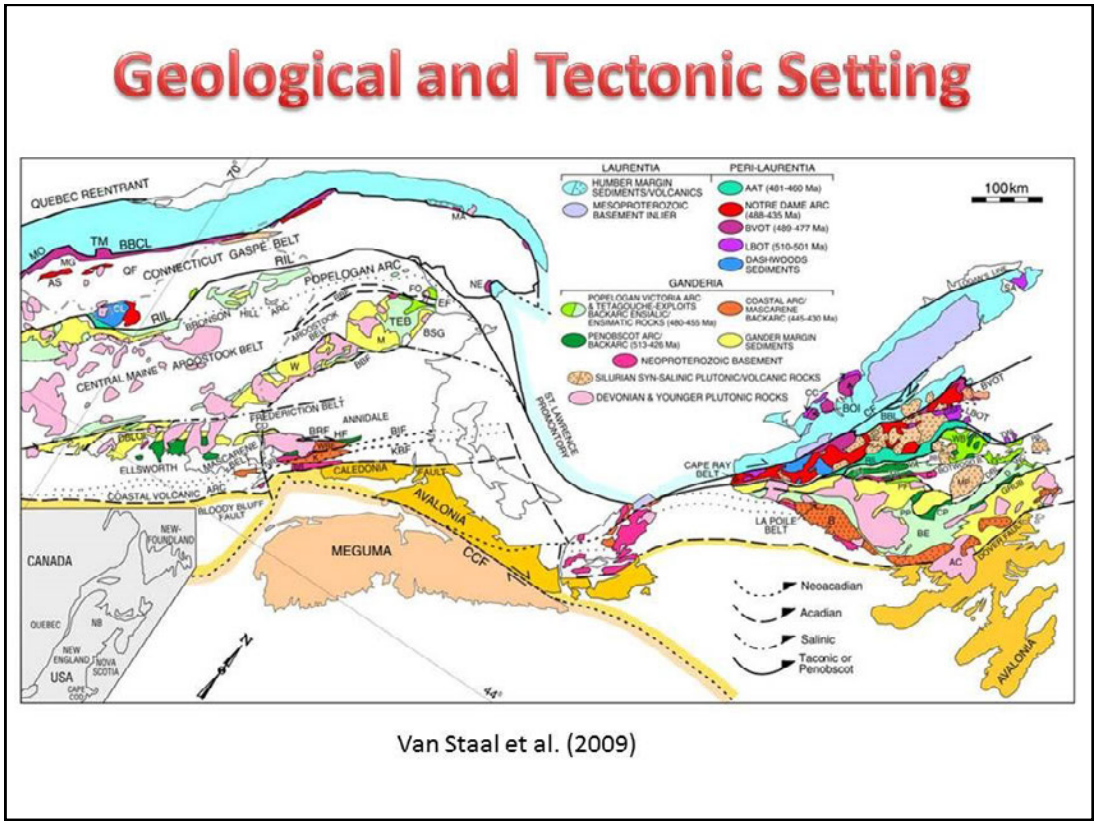
Geological and Tectonic Setting
LAURENTIA
PERI-LAURENTIA
HUMBER MARGIN SEDIMENTS/VOLCANICS
MESOPROTEROZOIC BASEMENT INLIER
AAT (461-460 Ma)
NOTRE DAME ARC (488-435 Ma)
BVOT (489-477 Ma)
LBOT (510-501 Ma)
DASHWOODS SEDIMENTS
GANDERIA
POPELOGAN VICTORIA ARC & TETAGOUCHE-EXPLOITS BACKARC ENSIALIC/ ENSIMATIC ROCKS (480-455 Ma)
COASTAL ARC/ MASCARENE BACKARC (445-430 Ma)
PENOBSCOT ARC/ BACKARC (513-426 Ma)
GANDER MARGIN SEDIMENTS
NEOPROTEROZOIC BASEMENT
SILURIAN SYN-SALINIC PLUTONIC/VOLCANIC ROCKS
DEVONIAN & YOUNGER PLUTONIC ROCKS
100km
QUEBEC REENTRANT
CONNECTICUT GASPÉ BELT
POPELOGAN ARC
CENTRAL MAINE
AROOSTOOK BELT
FREDERICTON BELT
ANNIDALE
ELLSWORTH
COASTAL VOLCANIC ARC
CALEDONIA FAULT
AVALONIA
MEGUMA
CCF
BLOODY BLUFF FAULT
CAPE RAY BELT
LA POILE BELT
CANADA
NEW-FOUNDLAND
QUEBEC
NB
NEW ENGLAND
NOVA SCOTIA
USA
Neoacadian
Acadian
Salinic
Taconic or Penobscot
Van Staal et al. (2009)

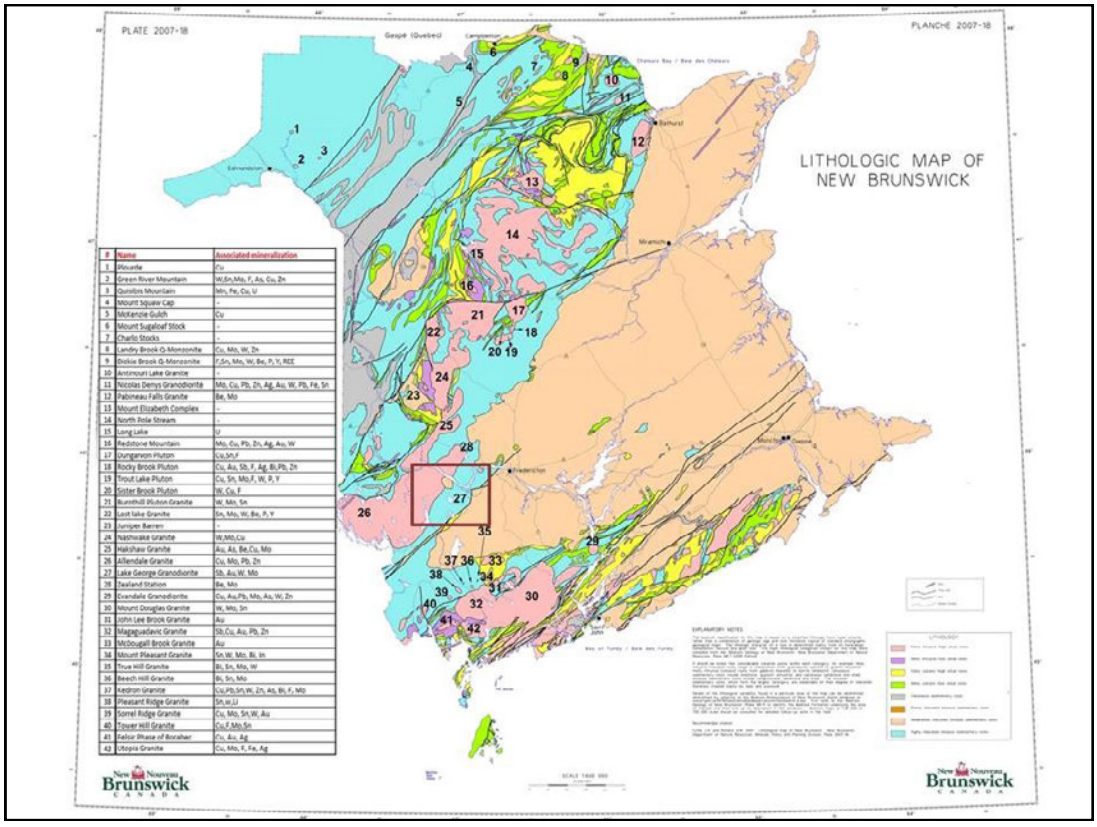
PLATE 2007-18
PLANCHE 2007-18
LITHOLOGIC MAP OF NEW BRUNSWICK
Brunswick

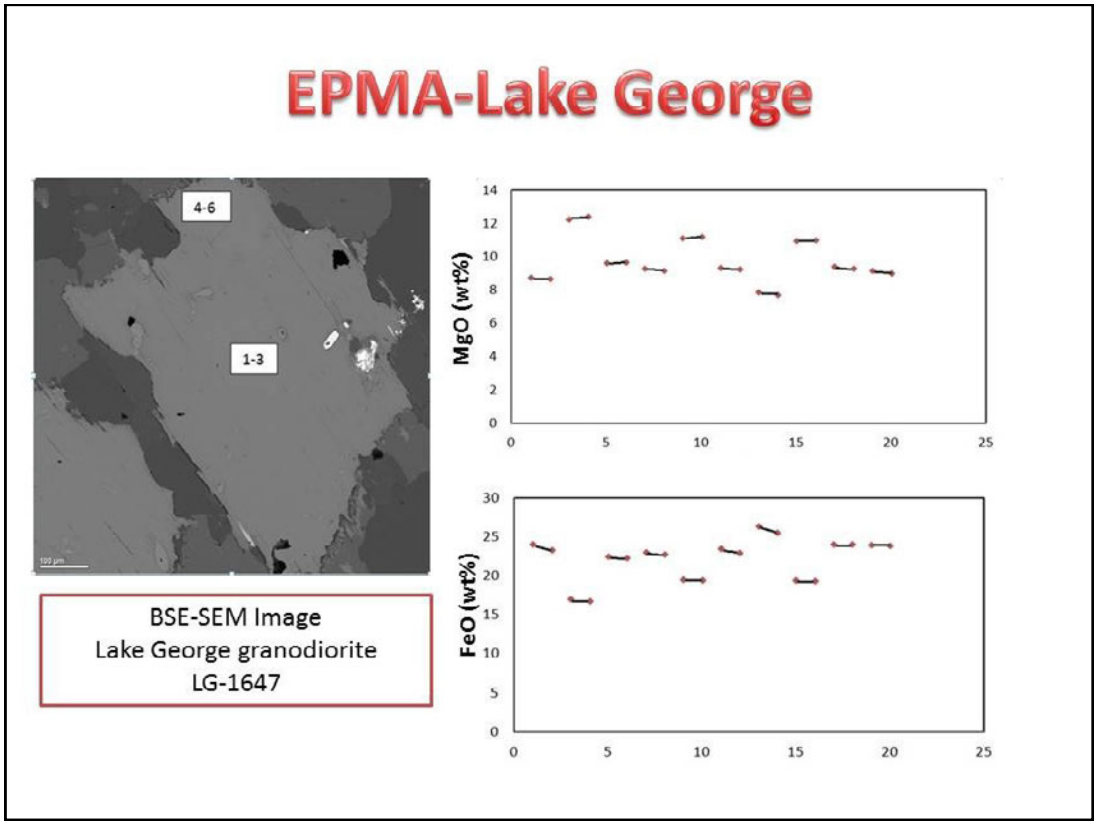
EPMA-Lake George
4-6
1-3
BSE-SEM Image
Lake George granodiorite
LG-1647
MgO (wt%)
FeO (wt%)

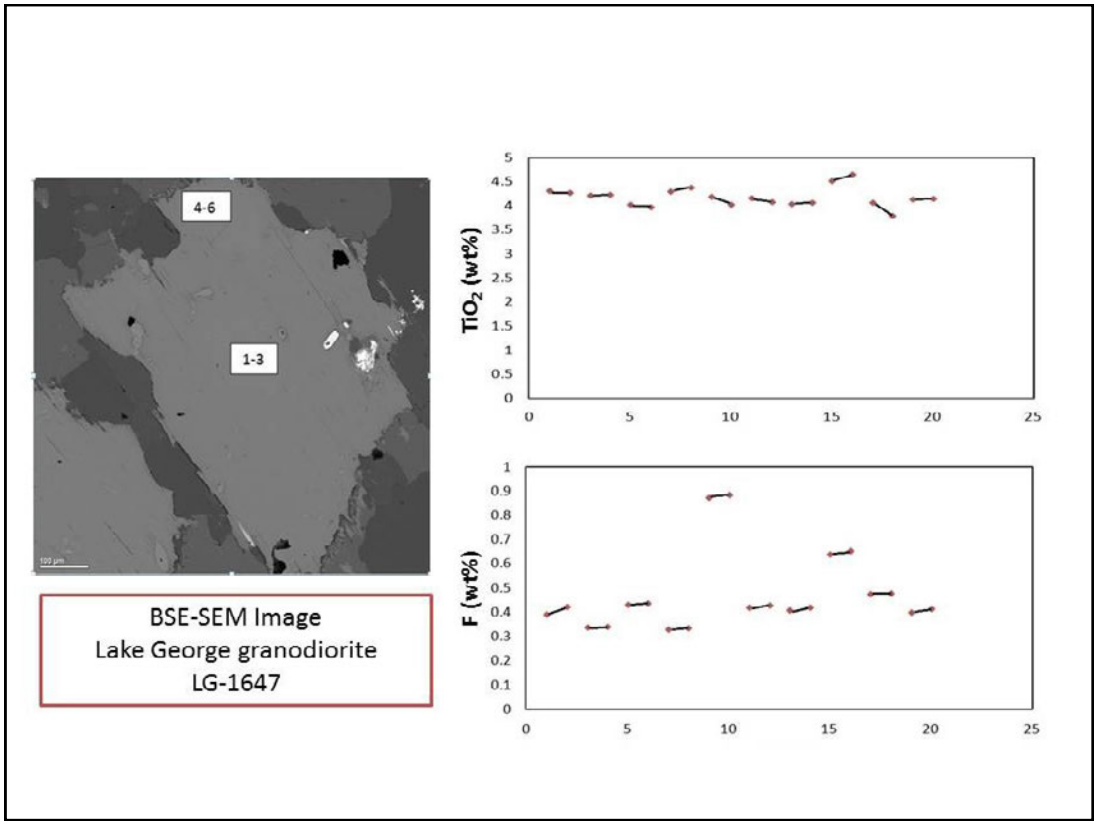
4-6
1-3
BSE-SEM Image
Lake George granodiorite
LG-1647
TiO2 (wt%)
F (wt%)

LA-ICPMS- Lake George

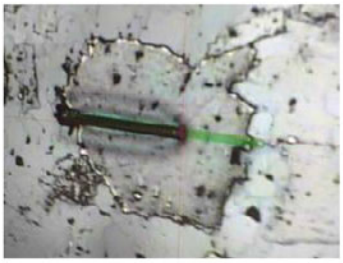

Photomicrograph of a biotite from Lake George granodiorite
LG-1748
(Field of view is 600µ)

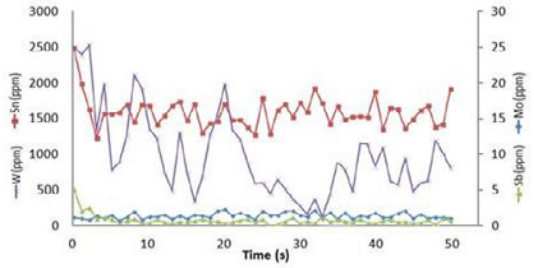

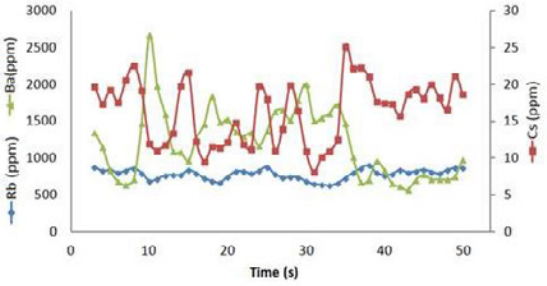

How to make a laser map

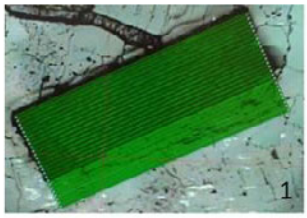

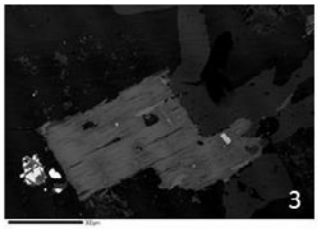

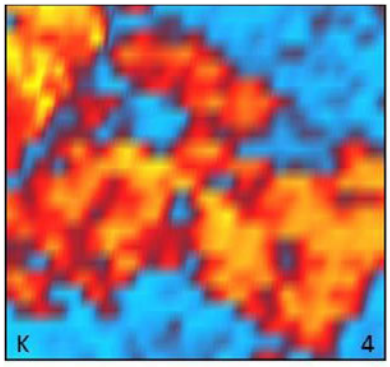

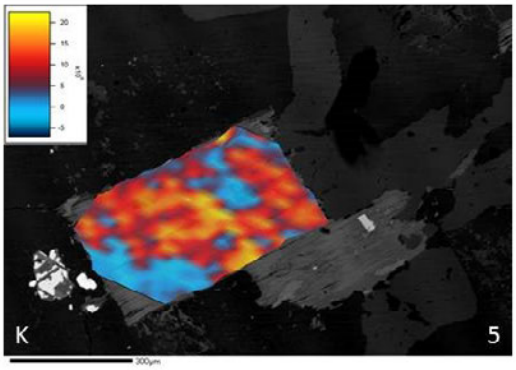

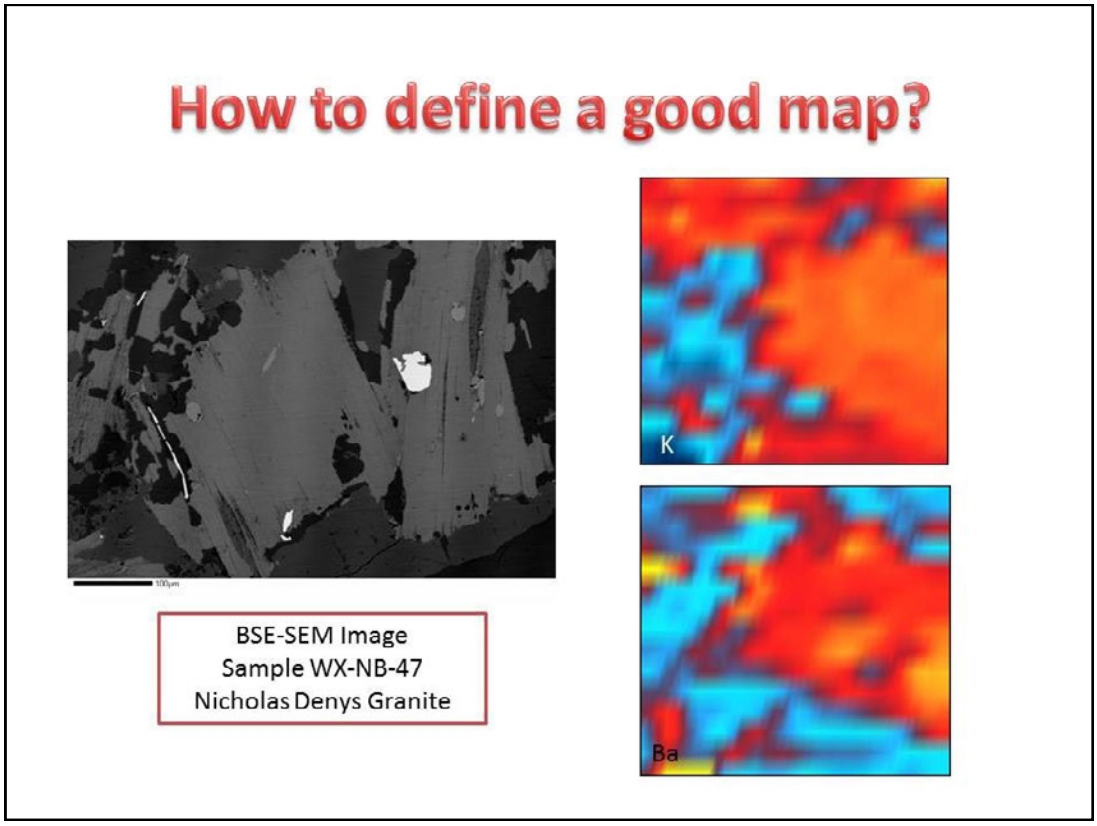
How to define a good map?
K
Ba
BSE-SEM Image
Sample WX-NB-47
Nicholas Denys Granite

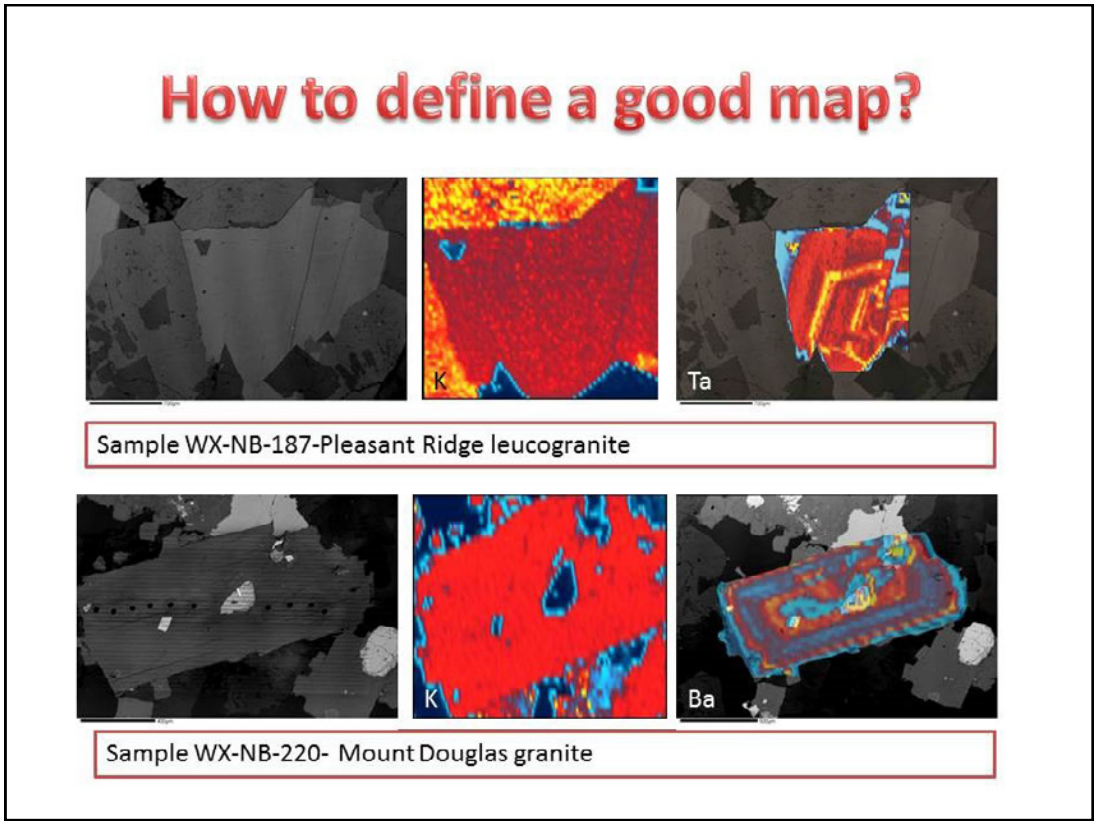
How to define a good map?
K
Ta
Sample WX-NB-187-Pleasant Ridge leucogranite
K
Ba
Sample WX-NB-220- Mount Douglas granite

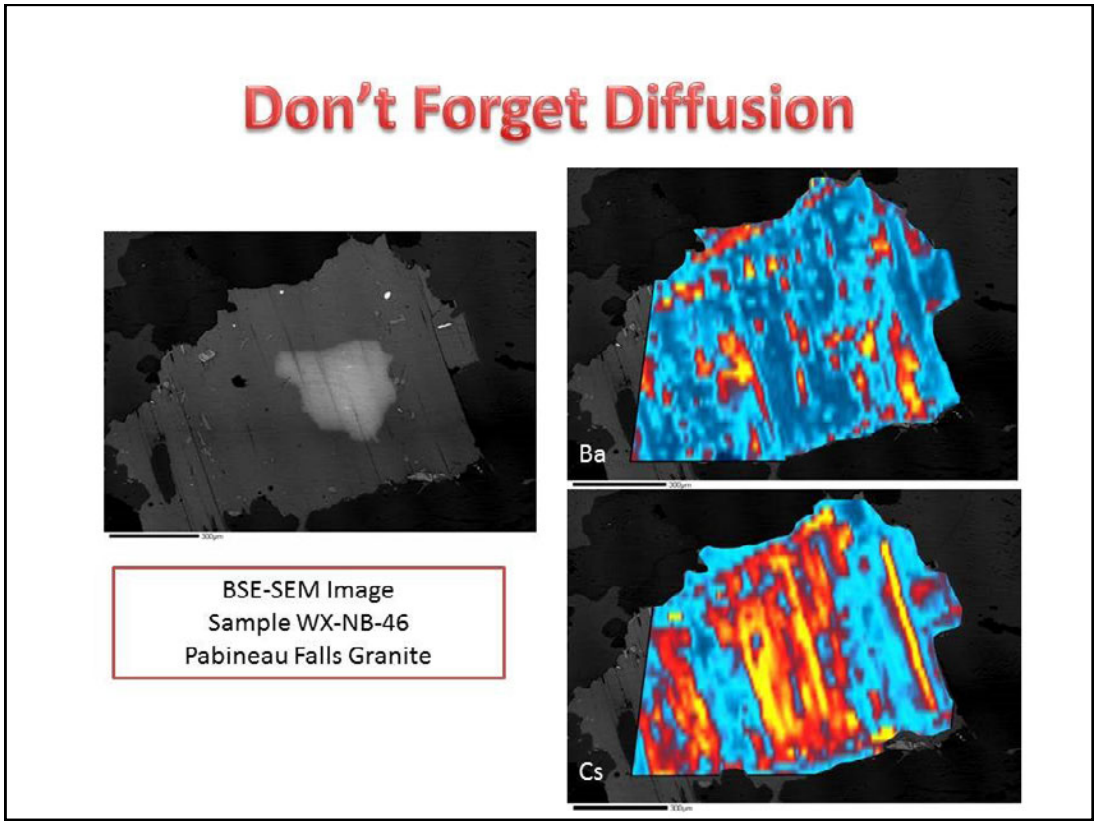
Don't Forget Diffusion
Ba
Cs
BSE-SEM Image
Sample WX-NB-46
Pabineau Falls Granite

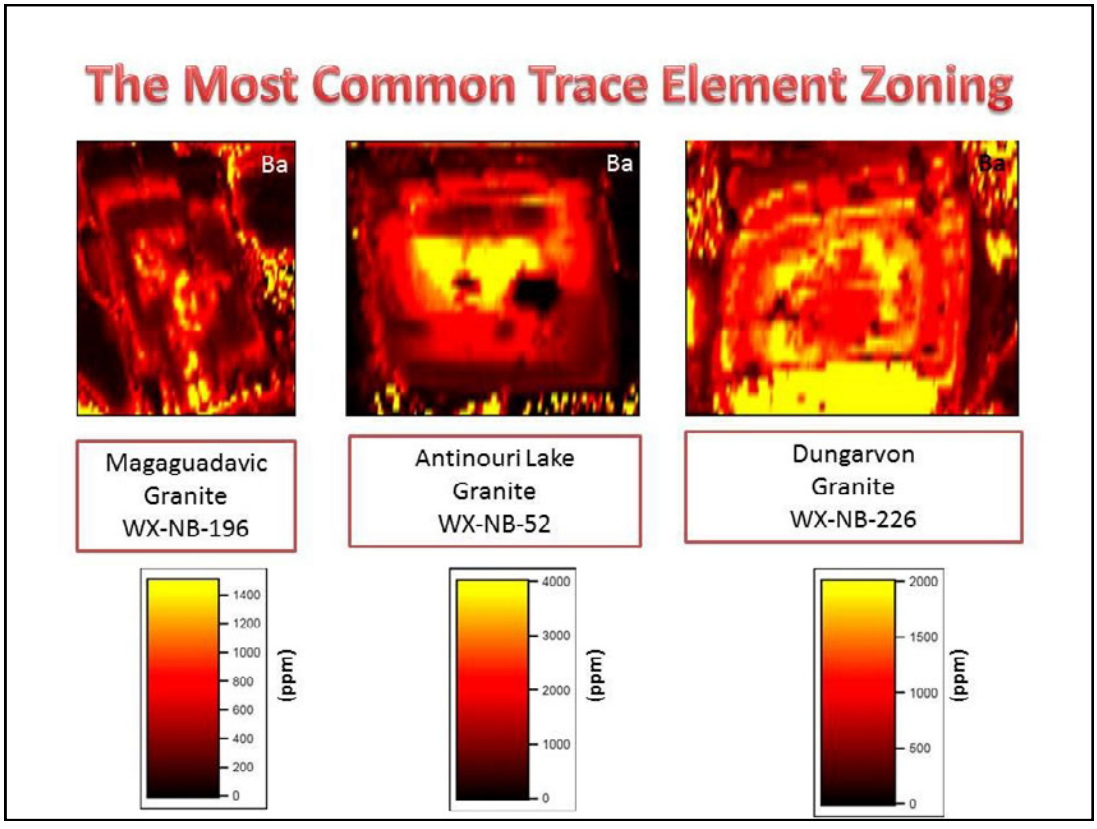
The Most Common Trace Element Zoning
Ba
Ba
Ba
Magaguadavic Granite WX-NB-196
Antinouri Lake Granite WX-NB-52
Dungarvon Granite WX-NB-226
1400
1200
1000
800
600
400
200
0
(ppm)
4000
3000
2000
1000
0
(ppm)
2000
1500
1000
500
0
(ppm)

Element Substitution

	T site	O site	A site
After calculation	8.00	5.65	1.75
Full site	8.00	6.00	2

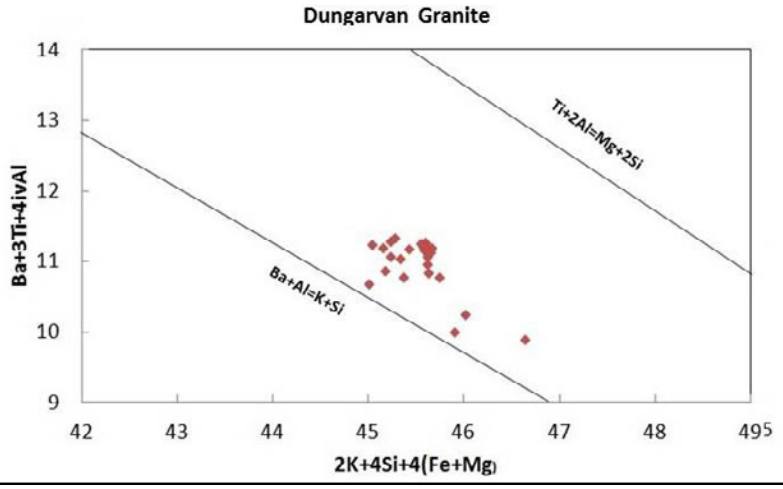

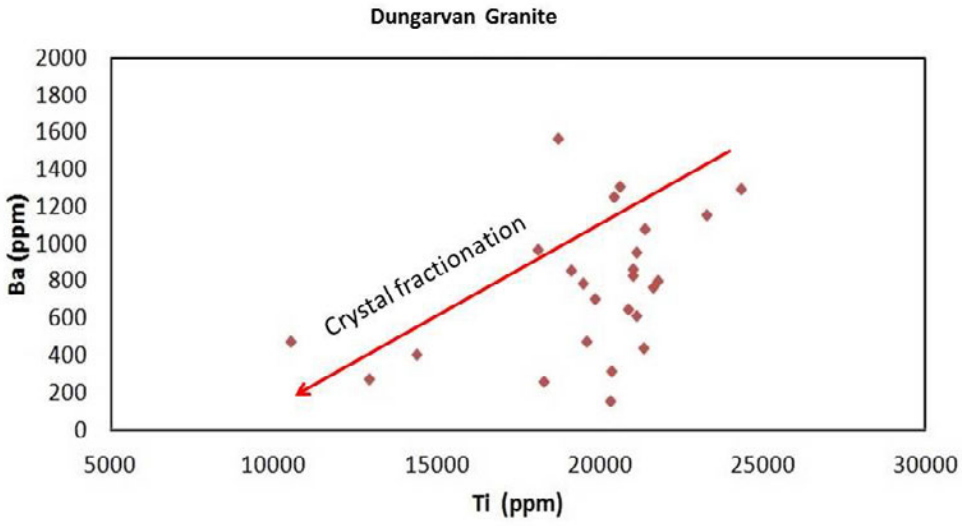

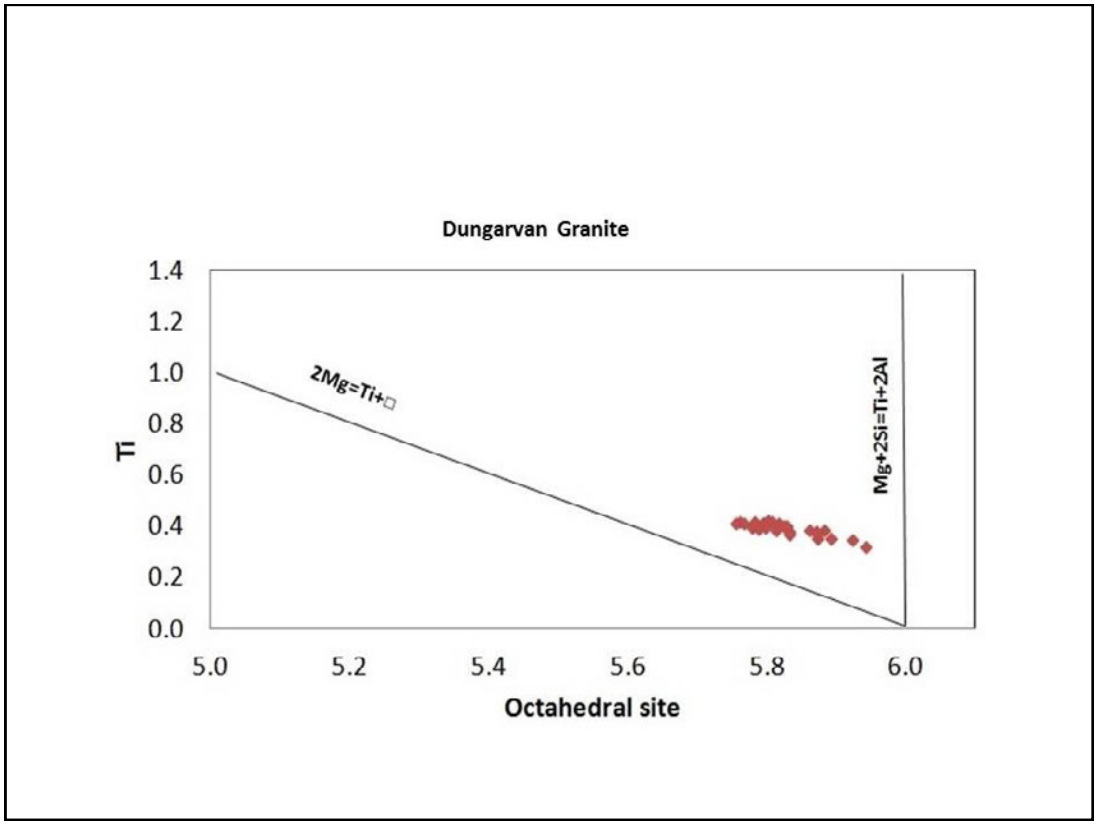
Dungarvan Granite
1.4
1.2
1.0
0.8
0.6
0.4
0.2
0.0
Ti
2Mg=Ti+□
Mg+2Si=Ti+2Al
5.0
5.2
5.4
5.6
5.8
6.0
Octahedral site

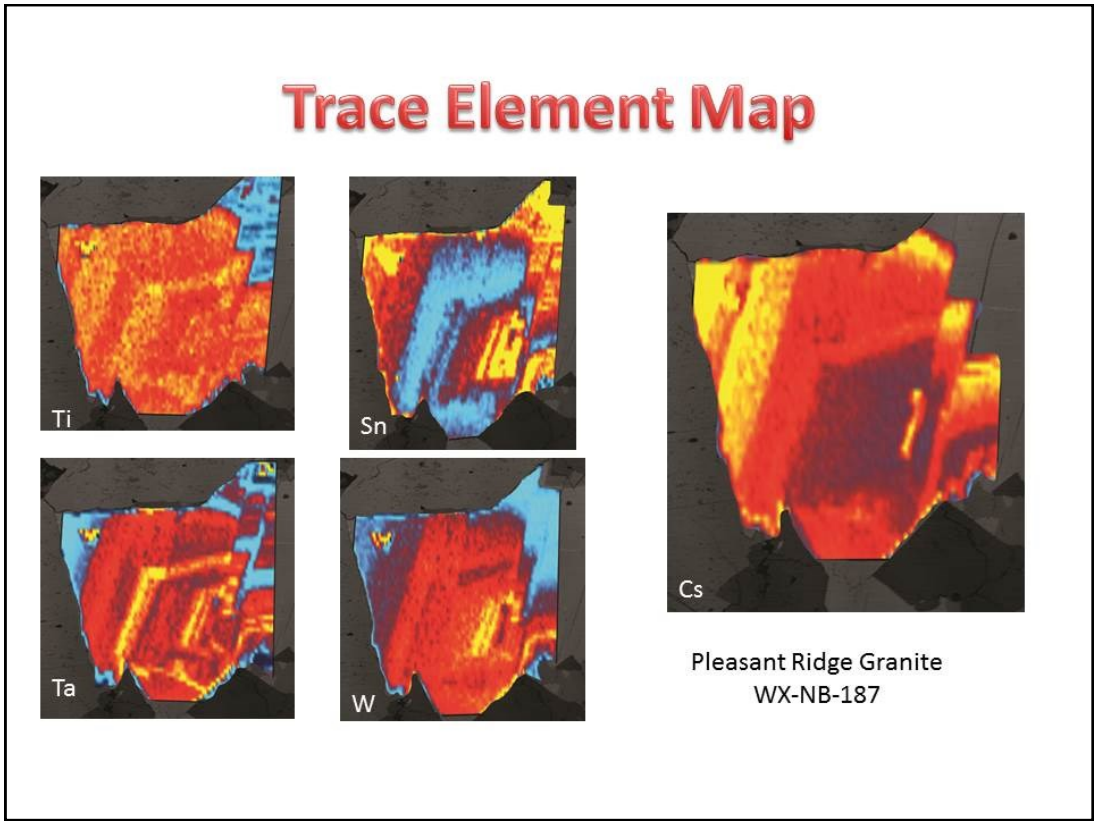
Trace Element Map
Ti
Sn
Cs
Ta
W
Pleasant Ridge Granite
WX-NB-187

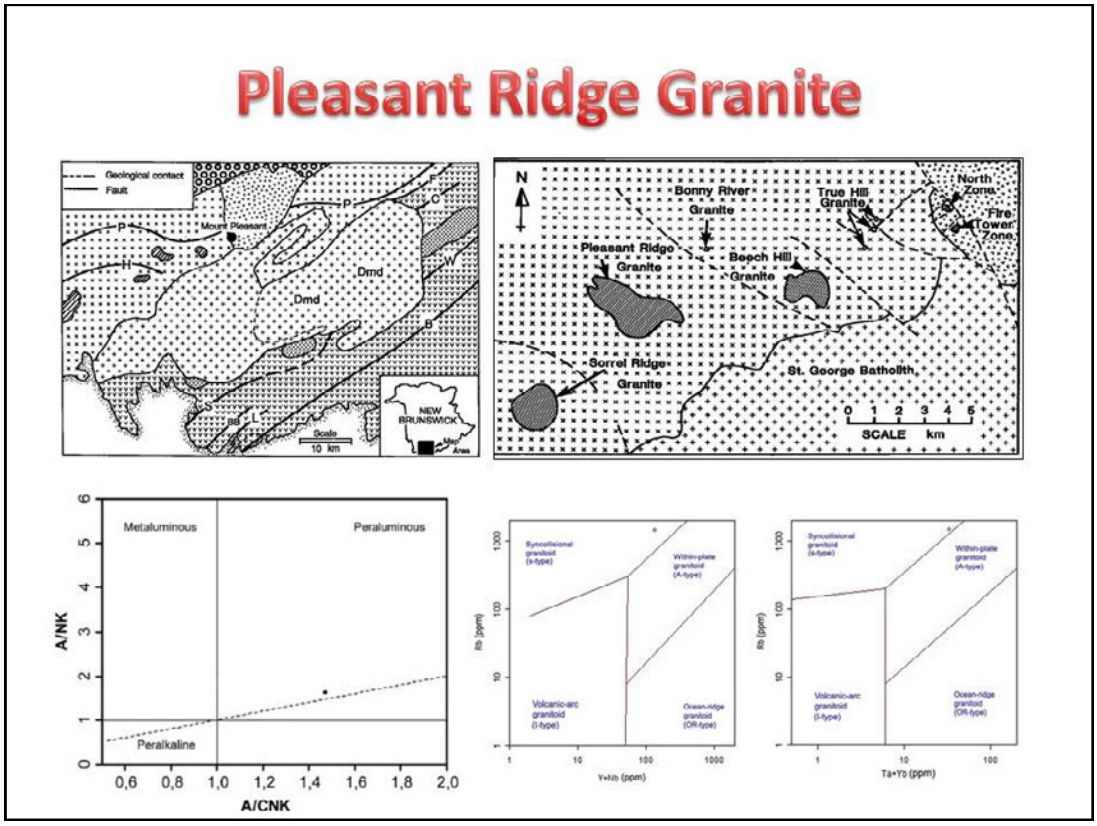
Pleasant Ridge Granite
Geological contact
Fault
Mount Pleasant
Dmd
NEW BRUNSWICK
Scale
10 km
N
Bonny River Granite
True Hill Granite
North Zone
Fire Tower Zone
Pleasant Ridge Granite
Beech Hill Granite
Sorrel Ridge Granite
St. George Batholith
SCALE km
Metaluminous
Peraluminous
Peralkaline
A/NK
A/CNK
Volcanic-arc granitoid (I-type)
Within-plate granitoid (A-type)
Ocean-ridge granitoid (OR-type)
Rb (ppm)
Y+Nb (ppm)
Ta+Yb (ppm)

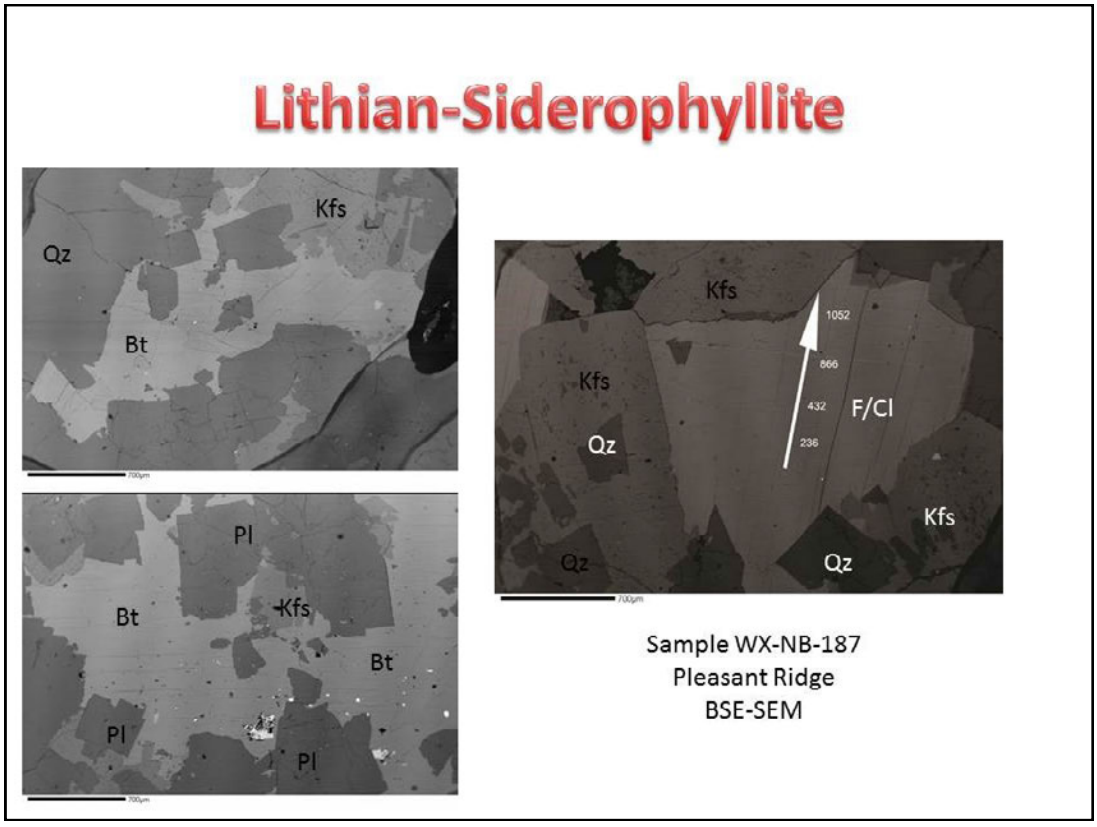
Lithian-Siderophyllite
Kfs
Qz
Bt
Pl
Kfs
Bt
Bt
Pl
Pl
Kfs
Kfs
Qz
1052
866
432
236
F/Cl
Kfs
Qz
Qz
Sample WX-NB-187
Pleasant Ridge
BSE-SEM

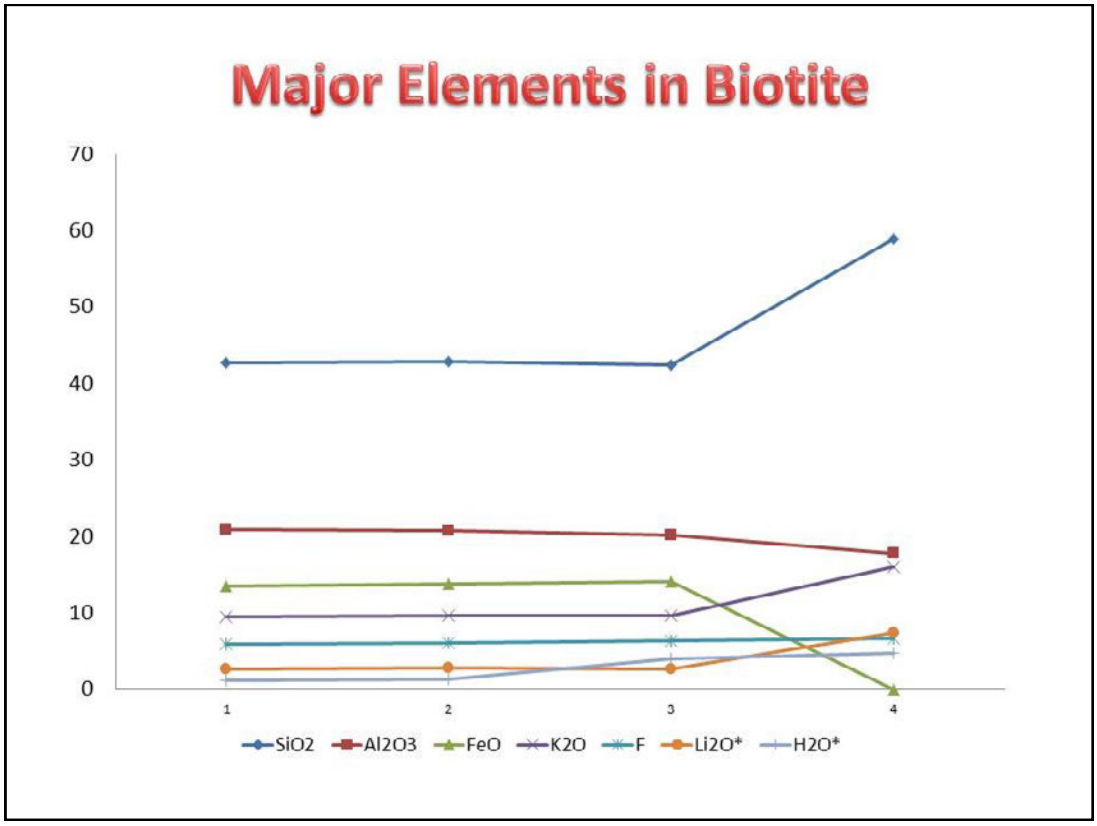
Major Elements in Biotite
70
60
50
40
30
20
10
0
1
2
3
4
SiO2
Al2O3
FeO
K2O
F
Li2O*
H2O*

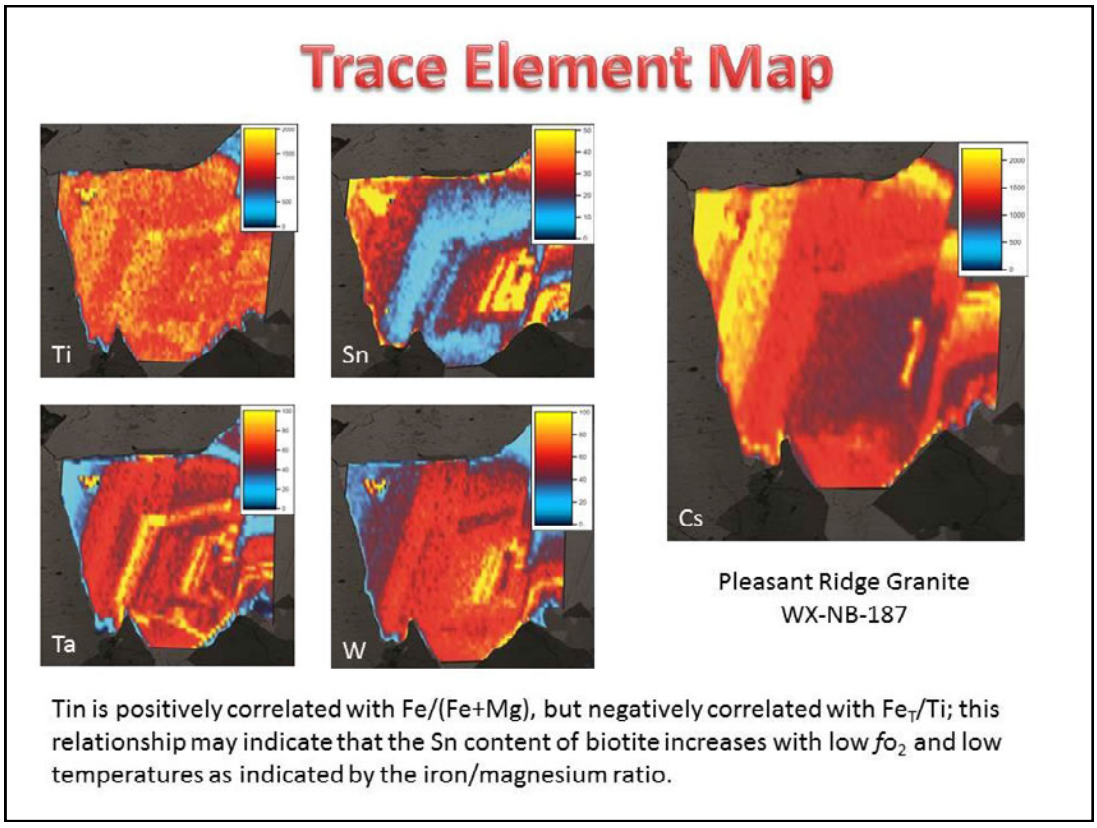
Trace Element Map
Ti
Sn
Cs
Ta
W
Pleasant Ridge Granite
WX-NB-187
Tin is positively correlated with Fe/(Fe+Mg), but negatively correlated with Fe_T/Ti; this relationship may indicate that the Sn content of biotite increases with low fo_2 and low temperatures as indicated by the iron/magnesium ratio.

Future Studies

- Analyze adjacent K-feldspar with laser and study the equilibrium between them and biotite.
- Further study of the apatite , and analyze this mineral with laser
- Comparing the collected data with the biotite result and future explore the granophile mineralization in New Brunswick.

Is biotite a good mineral to study magmatic evolution history?

- Yes

How close is this project to the goal?

- Pretty close

Conclusion

- Laser-ablation ICPMS map is a perfect way to study changes in mica group minerals.
- Size of the grain, frequency of mineral inclusion, degree of alteration, and the laser spot size required are the limitations of this method.
- Mica group minerals and specifically Lithium biotite are good indictor of magma evolution history.

Acknowledgment

- Joseph Whalen
- Cees van Staal
- Les Fyffe
- Neil Rogers
- Dave Lentz
- Christopher McFarlane
- Kathleen Thorne

Mineral markers of porphyry processes: regional and local signatures of porphyry prospectivity

J.B. Chapman[1], A. Plouffe[2], S.E. Jackson[2], J.J. Ryan[1] and T. Ferbey[3]

1. Geological Survey of Canada, 605 Robson St., Vancouver, British Columbia
2. Geological Survey of Canada, 601 Booth St., Ottawa, Ontario
3. British Columbia Geological Survey, 1810 Blanshard St., Victoria, British Columbia

Abstract: Porphyry-style mineralisation occurs chiefly as a consequence of the release of large volumes of metal-bearing aqueous brine during the cooling and crystallization of plutonic and intrusive magmatic systems. In addition to the metals of economic interest, many additional elements are preferentially incorporated into the aqueous fluid during its segregation from the parent magma, or are gained from interactions with proximal county rocks. During its segregation, pooling and ascent, this magmatic-hydrothermal fluid also deposits many of its elemental components; either through direct precipitation of new minerals or by metasomatic interactions with existing minerals.

The elemental and mineralogical signatures of each of these fluid generation, mineral precipitation and hydrothermal alteration processes may be recorded within the resultant mineral residues at each stage, and will likely reflect a complex and evolving suite of physicochemical influences that operated during the formation of each ore deposit. Modern analytical methods are increasingly able to interrogate these signatures at smaller scales and lower cost, thus bringing effective and efficient mineral analysis within the scope of even small scale mineral exploration programs. In this presentation we will discuss a suite of mineralogical and mineral chemistry studies performed in the last few years as part of the Government of Canada's Geomapping for Energy and Minerals and Targeted Geoscience Initiative Programs. All are targeted toward increasing both the efficiency and effectiveness of porphyry mineral exploration within Canada.

Late Triassic to early Jurassic plutonic rocks of British Columbia are genetically associated with the great majority of Canada's porphyry copper, molybdenum and gold resources and producing mines, forming the 'Copper Pine of the Cordillera'. Within Yukon they host the sole currently producing copper-gold mine in the territory. However, additional exploration activity within Yukon has been largely unsuccessful and, away from Minto mine itself, the metal endowment of Triassic-Jurassic plutonic suites remains uncertain. In order to assess the prospectivity of these rocks and to provide a tool whereby future exploration in the region could be focused, our study examined the Ce^{4+}/Ce^{3+} composition of igneous zircon samples taken from across the district, as well as comparative samples from the late Cretaceous Casino deposit. Our results indicate that physicochemical conditions which prevailed during formation of the Minto deposit occurred widely across the Yukon Triassic-Jurassic plutonic suites, but that mineralisation may have occurred at much deeper crustal depths than expected for 'typical' porphyry deposits.

Within central and southern British Columbia, many known porphyry deposits are partly or entirely covered by Quaternary glacial sediments. However, a suite of indicator minerals in till in areas around these deposits can detect diagnostic mineralogical signatures of porphyry mineralisation many kilometres down-ice of the deposit location. In addition to indicator minerals, chemical analysis of the till can be used to fingerprint the type of mineralisation expected. A combination of till geochemistry and mineralogy might potentially be developed to provide preliminary information on the metal endowment of a buried mineralized body. At the Woodjam porphyry Cu-Au±Mo deposits of central BC, we can demonstrate that mineralogical complexity in bedrock tourmaline minerals – associated with both ore-forming and distal hydrothermal alteration processes – can be detected in surficial materials, providing context and refined detail to the broad exploration target produced.

Within porphyry and greisen-style tin-tungsten-base metal systems of the Canadian Appalachian district, zones of high indium content are significant exploration targets. However, despite apparent bulk mineralogy and base metal grade similarities between indium-rich and -poor ore, these zones do not occur evenly throughout the region. As a part of a detailed inventory and mineralogical assessment of indium distribution within southern New Brunswick and Nova Scotia we have identified distinct mineralogical fingerprints associated with indium enrichment.

Originally presented AME-BC Mineral Exploration Roundup 2015, Vancouver, BC. January 26, 2015.

Corresponding author: John B. Chapman (john.chapman@nrcan-rncan.gc.ca)

Chapman, J.B., Plouffe, A., Jackson, S.E., Ryan, J.J., and Ferbey, T., 2015. Mineral markers of porphyry processes: regional and local signatures of porphyry prospectivity; *in* TGI 4 – Intrusion Related Mineralisation Project: New Vectors to Buried Porphyry-Style Mineralisation, (ed.) N. Rogers; Geological Survey of Canada, Open File 7843, p. 521-534.

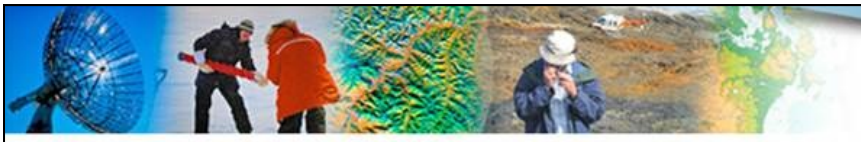

NATURAL RESOURCES CANADA - INVENTIVE BY NATURE

Mineral Markers of Porphyry Processes

John Chapman, Simon Jackson, Jim Ryan, Alain Plouffe,
Katherine Venance, Pat Hunt and Zhaoping Zheng
Natural Resources Canada – Geological Survey of Canada
Christopher Goeddeke and Iain Samson
University of Windsor
Maurice Colpron
Yukon Geological Survey
Travis Ferbey
British Columbia Geological Survey

Natural Resources Canada | Ressources naturelles Canada

Canada

2

Talk Outline

- Mineral research at the Geological Survey of Canada
- Zircon REE chemistry as a marker of magma fertility
  …the Casino and Minto deposits and regional-scale studies in Yukon
- Tourmaline chemistry as a marker of porphyry prospectivity
  …the Woodjam deposits and surrounding regional till mineralogy, BC
- The mineralogy and paragenesis of indium-rich Sn deposits
  …district-scale studies in southern New Brunswick and Nova Scotia

Natural Resources Canada | Ressources naturelles Canada

Canada

3

Zircon as a Redox Proxy

- Zircon ($ZrSiO_4$) is a common accessory mineral in igneous rocks of intermediate to felsic composition.
- Tetravalent cations of similar ionic radius to Zr^{4+} (0.84 Å) substitute readily into the lattice.
  - e.g. U, Th, Hf, etc.
- Trivalent cations (e.g. REE) will do so as well, with distribution coefficients dominated by ionic radius.
- Eu^{3+} will substitute more readily than Eu^{2+}, but abundances are governed by the redox state of the parent magma.
- Similarly, Ce^{4+} will substitute more readily than Ce^{3+}.

Natural Resources Canada Ressources naturelles Canada

Canada

4

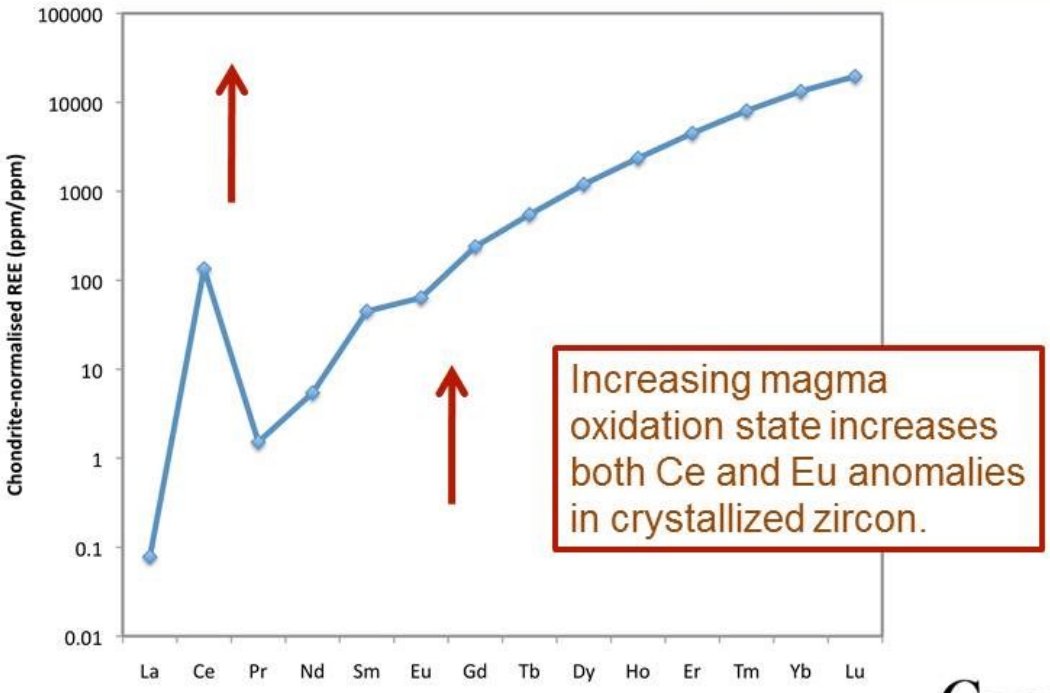

Natural Resources Canada Ressources naturelles Canada

Canada

5

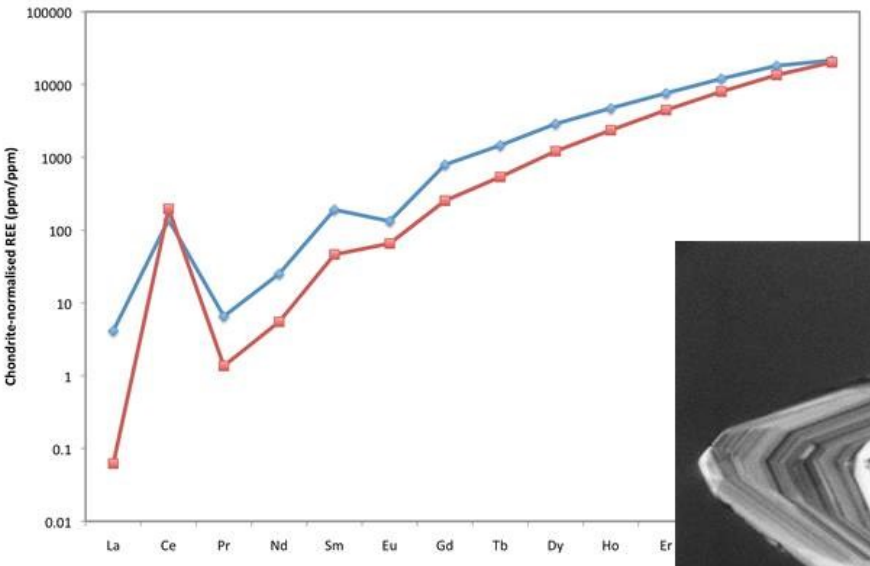

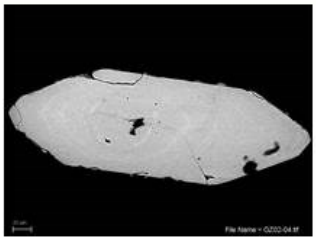

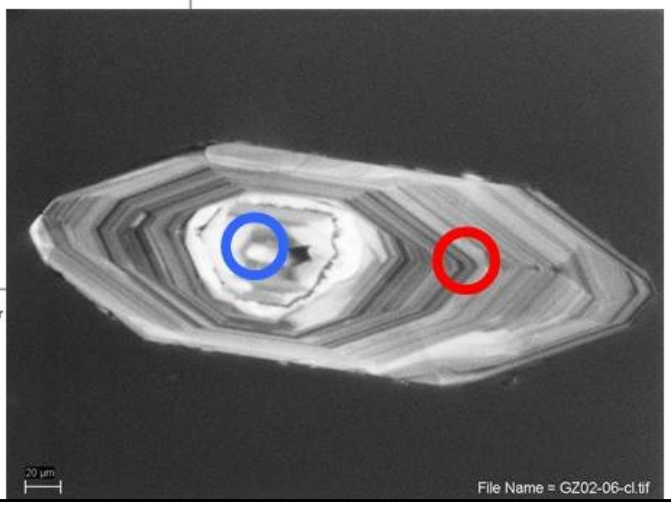

	GZ02-06-1	GZ02-06-2
Ce/Ce*	26.68	674.84
Eu/Eu*	0.341	0.605
Age (Ma)	305	189

6

Calculation of Ce^{4+}/Ce^{3+}

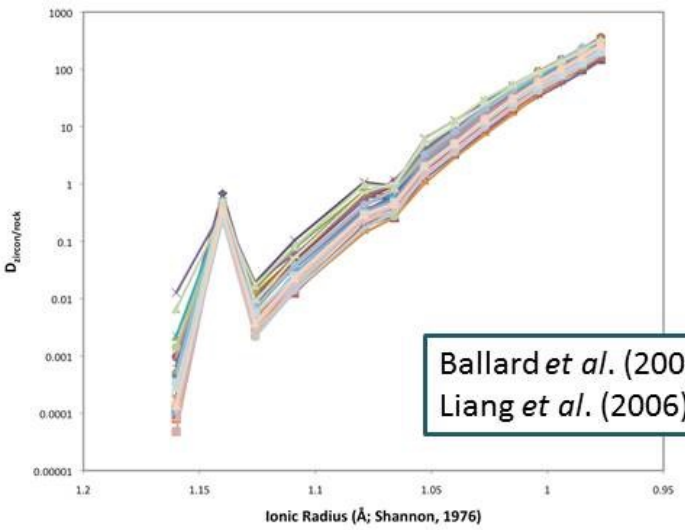

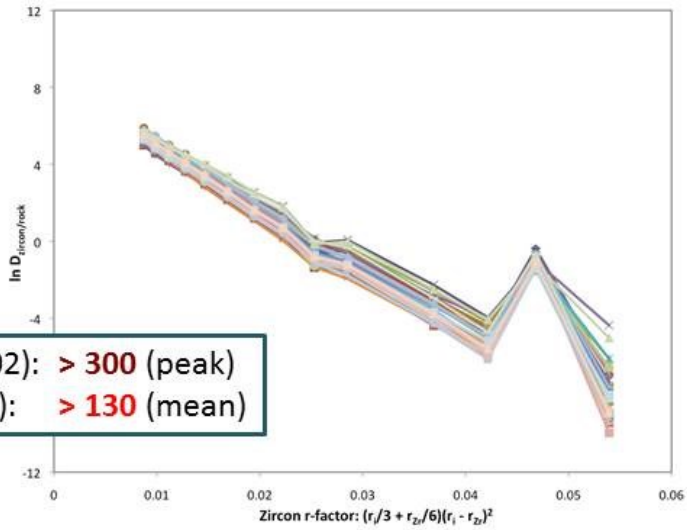

Ballard *et al.* (2002): **> 300** (peak)
Liang *et al.* (2006): **> 130** (mean)

Natural Resources Canada | Ressources naturelles Canada

Canada

7

- Abundant granitoid intrusions throughout central and southern Yukon
- Dominantly Triassic-Jurassic, Cretaceous and Tertiary
- Host major mineral occurrences, including Minto mine, Casino, Carmacks Copper, Sonora Gulch and many more…
- BUT… exploration activity is spotty between different plutonic bodies

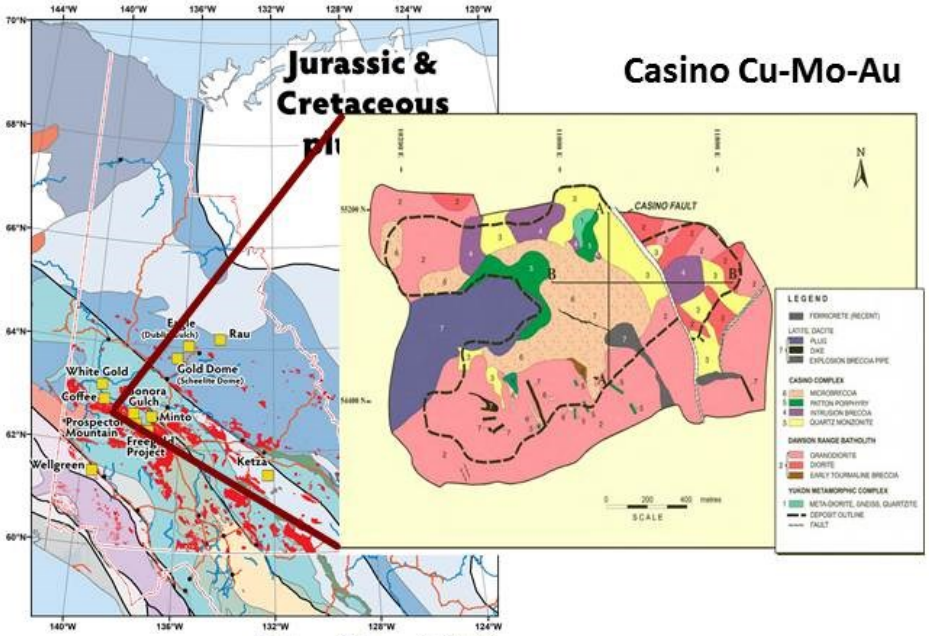

(Colpron & Bennett, 2010)

Natural Resources Canada Ressources naturelles Canada

Canada

8

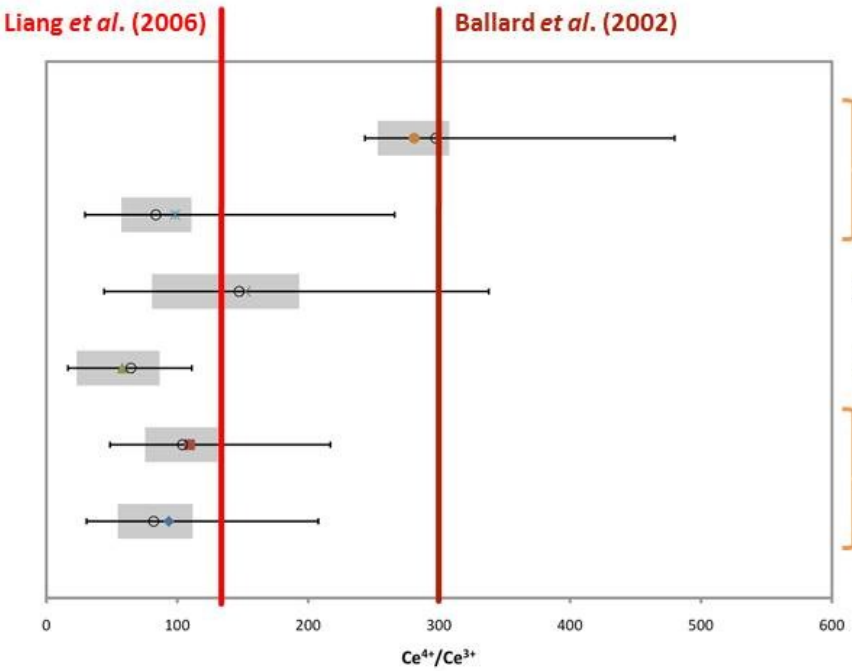

Crackle breccia ≈ 72 Ma

≈ 103 Ma

Patton Porphyry

Qtz-monzonite

Dawson Range

Natural Resources Canada Ressources naturelles Canada

Canada

9

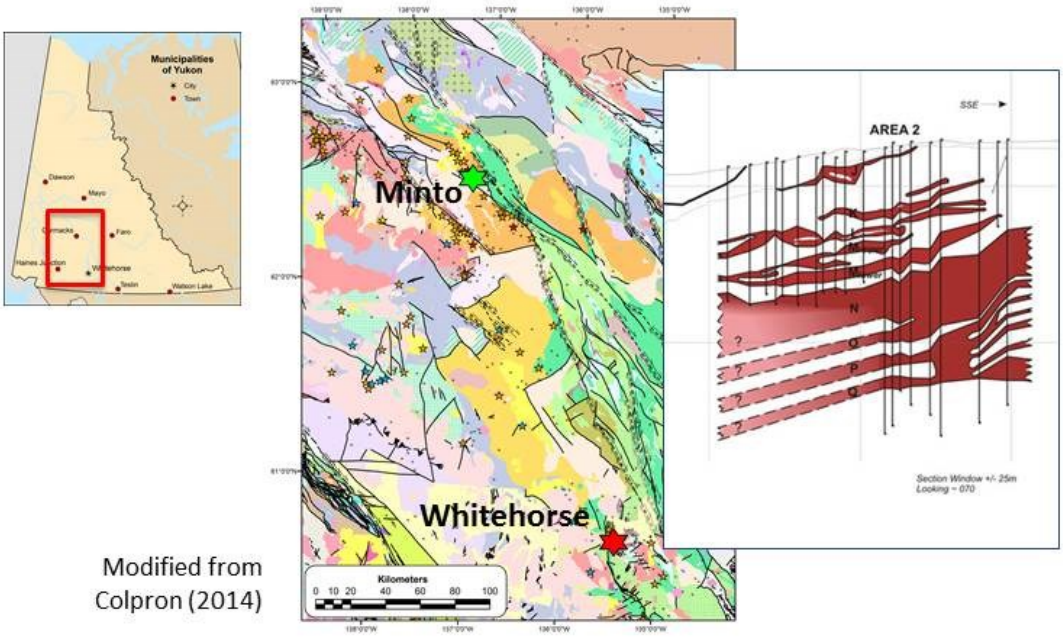

Modified from Colpron (2014)

10

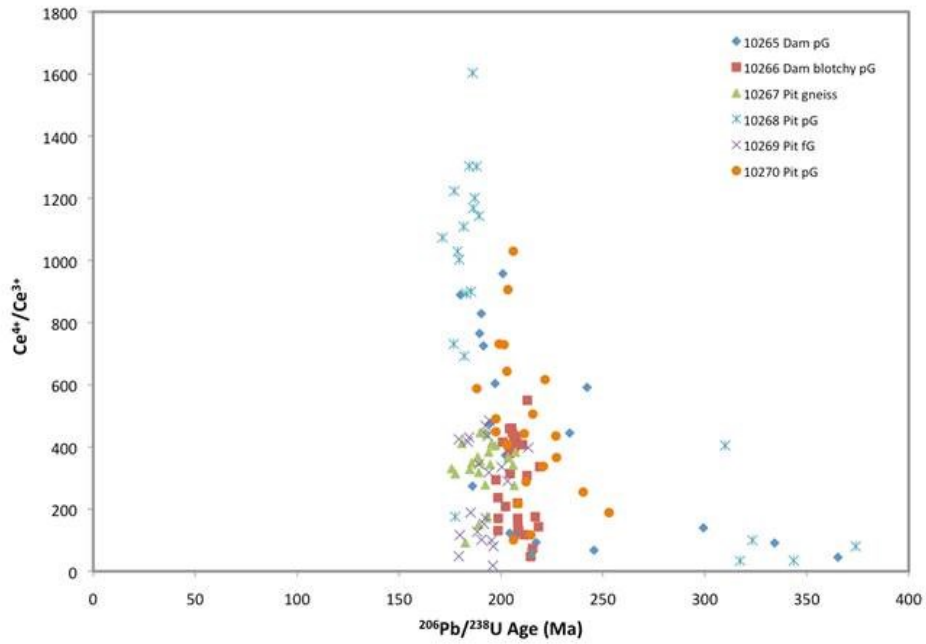

11

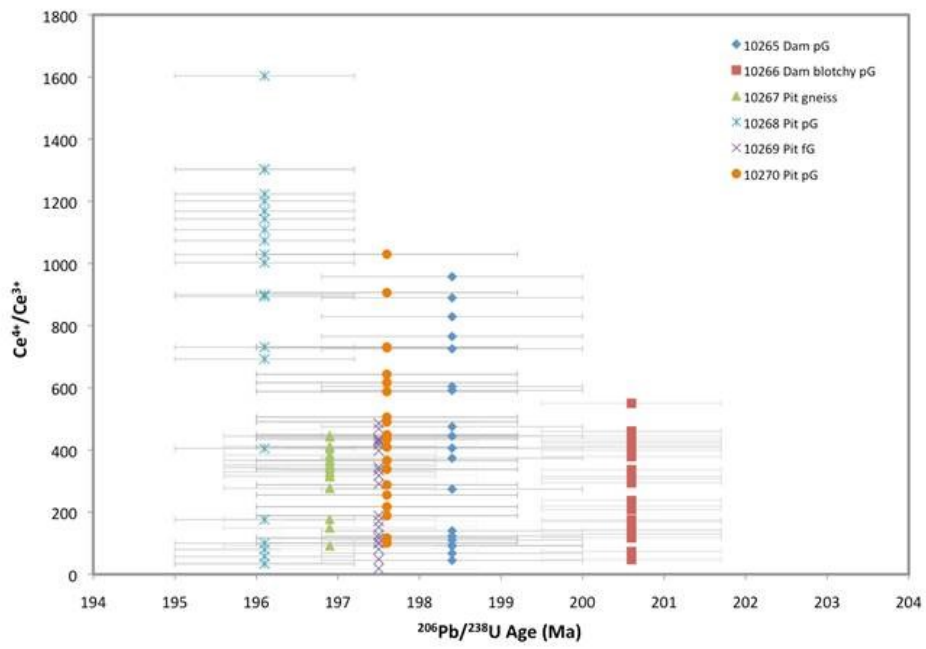

Natural Resources Canada Ressources naturelles Canada

Canada

12

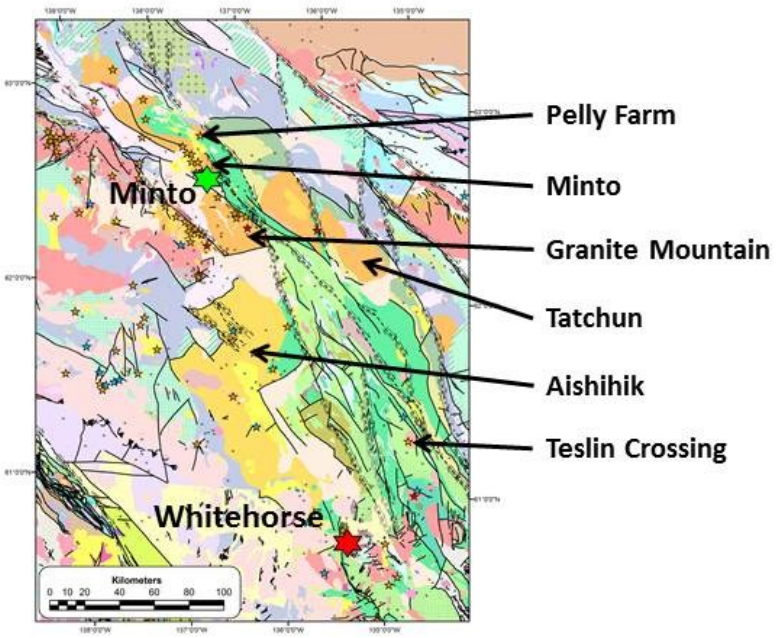

Modified from Colpron (2014)

Natural Resources Canada Ressources naturelles Canada

Canada

13

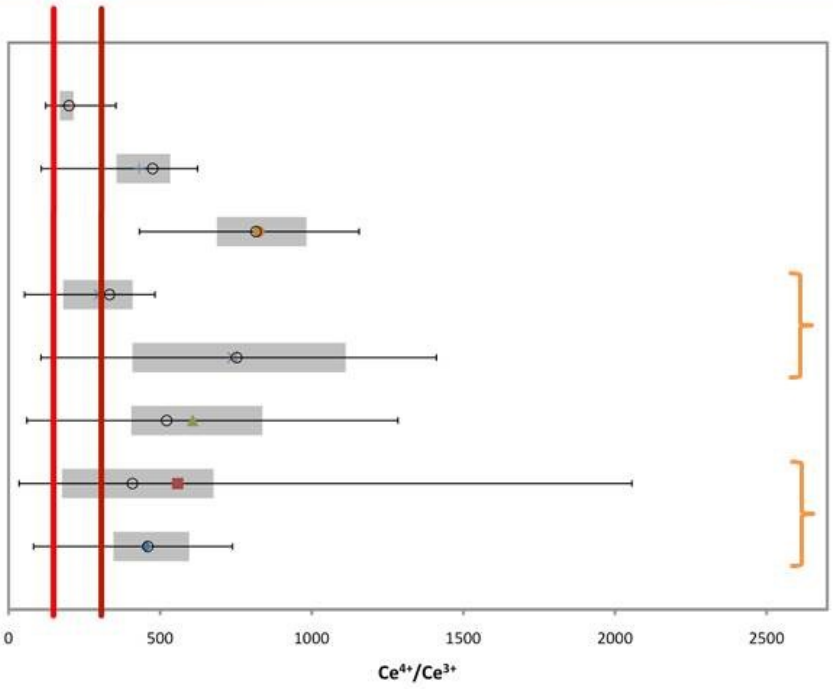

Natural Resources Canada Ressources naturelles Canada

Canada

14

Why use tourmaline?

- 'Tourmaline' is not a single mineral, but a related group
- Common gangue and matrix mineral in porphyry deposits
- Occur over a wide range of temperatures and pressures
- Structurally and chemically complex, versatile geological record
- Chemically and physically resistent, will preserve data

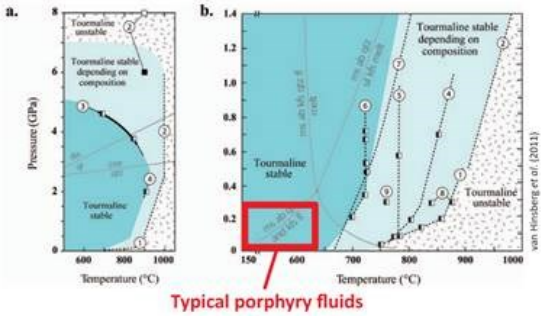

Typical porphyry fluids

Tourmalines are stable over a very wide range of pressures and temperatures. They are therefore well able to record and preserve porphyry-related ore-forming

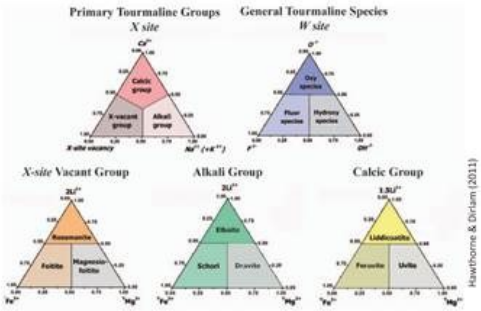

$XY_3Z_6[T_6O_{18}][BO_3]_3V_3W$

The tourmaline crystal structure contains numerous sites that can accommodate a large number of different elements. Major element variation in the Y site results in the major species present in porphyry environments:

Dravite: $NaMg_3Al_6Si_6O_{18}(BO_3)_3(OH)_3(OH)$
Schorl: $NaFe_3Al_6Si_6O_{18}(BO_3)_3(OH)_3(OH)$
Elbaite: $Na(Li_{1.5}Al_{1.5})_3Al_6Si_6O_{18}(BO_3)_3(OH)_3(OH)$

Natural Resources Canada Ressources naturelles Canada

Canada

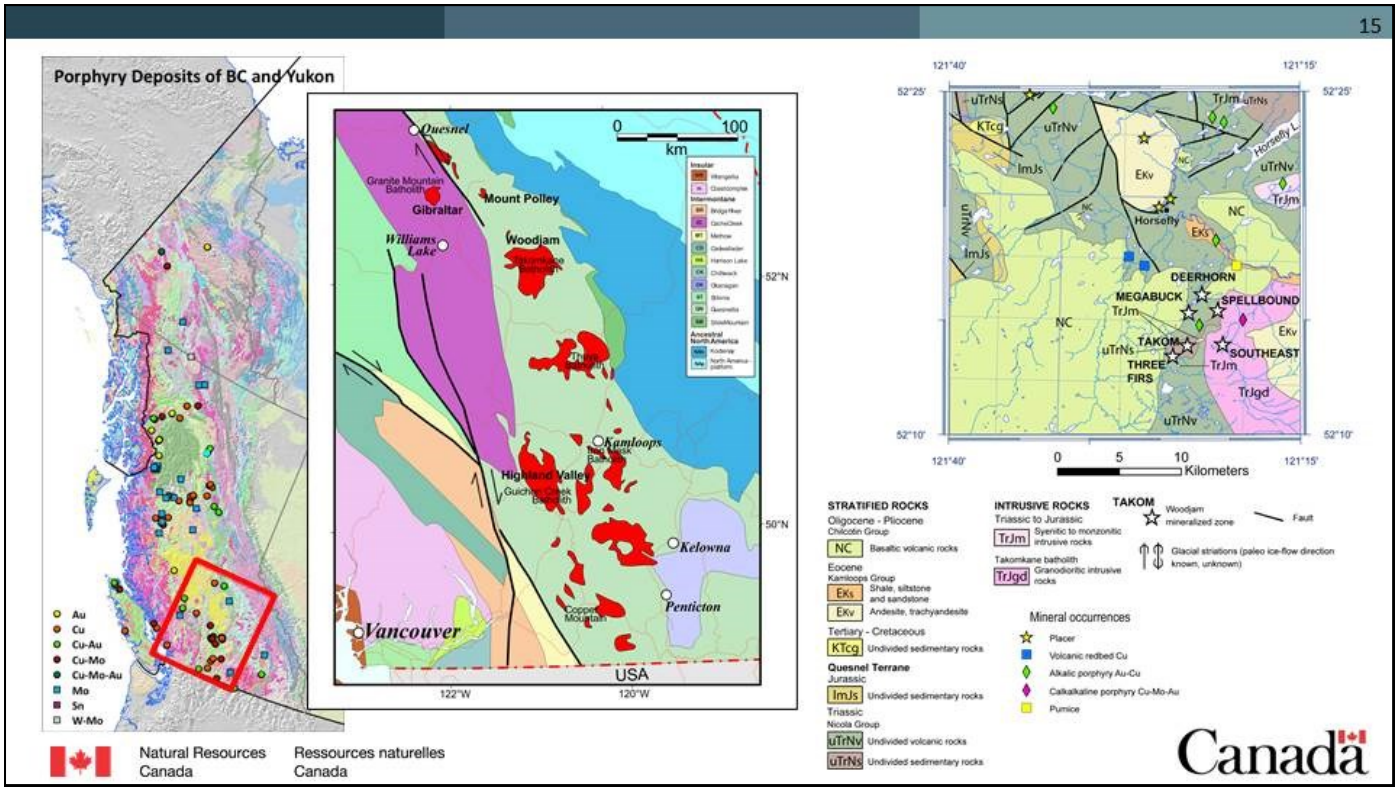
15
Porphyry Deposits of BC and Yukon
Au
Cu
Cu-Au
Cu-Mo
Cu-Mo-Au
Mo
Sn
W-Mo
Quesnel
Granite Mountain Batholith
Gibraltar
Mount Polley
Williams Lake
Woodjam
Highland Valley
Kamloops
Kelowna
Penticton
Vancouver
Copper Mountain
USA
0 100 km
122°W
120°W
52°N
50°N
121°40'
121°15'
52°25'
52°10'
0 5 10 Kilometers
DEERHORN
MEGABUCK
SPELLBOUND
TAKOM
SOUTHEAST
THREE FIRS
Horsefly
Horsefly L.
STRATIFIED ROCKS
Oligocene - Pliocene
Chilcotin Group
NC Basaltic volcanic rocks
Eocene
Kamloops Group
EKs Shale, siltstone and sandstone
EKv Andesite, trachyandesite
Tertiary - Cretaceous
KTcg Undivided sedimentary rocks
Quesnel Terrane
Jurassic
ImJs Undivided sedimentary rocks
Triassic
Nicola Group
uTrNv Undivided volcanic rocks
uTrNs Undivided sedimentary rocks
INTRUSIVE ROCKS
Triassic to Jurassic
TrJm Syenitic to monzonitic intrusive rocks
Takomkane batholith
TrJgd Granodioritic intrusive rocks
TAKOM
Woodjam mineralized zone
Fault
Glacial striations (paleo ice-flow direction known, unknown)
Mineral occurrences
Placer
Volcanic redbed Cu
Alkalic porphyry Au-Cu
Calkalkaline porphyry Cu-Mo-Au
Pumice
Natural Resources Canada
Ressources naturelles Canada
Canada

16
Natural Resources Canada
Ressources naturelles Canada
Canada

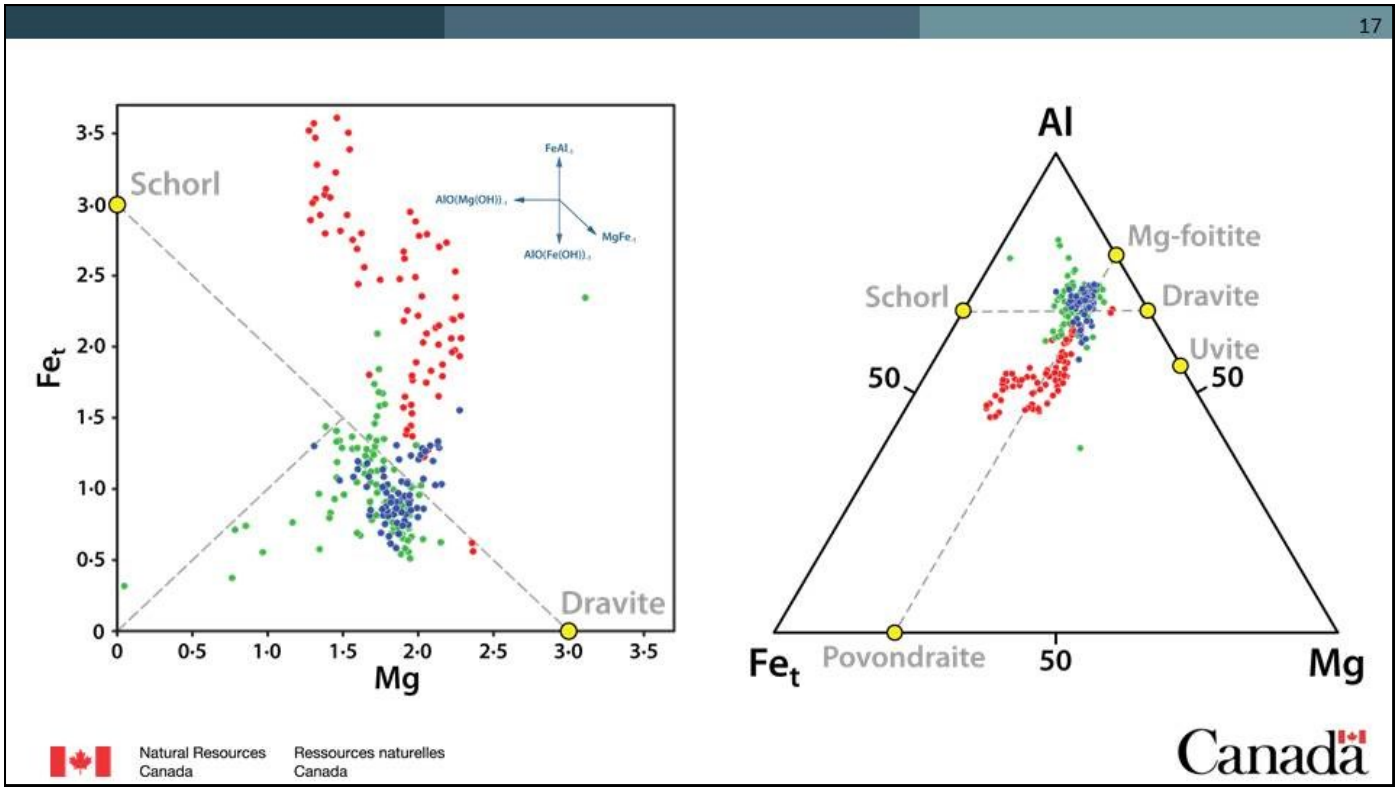
17
Schorl
Dravite
Fe$_t$
Mg
Al
Mg-foitite
Schorl
Dravite
Uvite
50
50
Fe$_t$
Povondraite
50
Mg
Natural Resources Canada
Ressources naturelles Canada
Canada

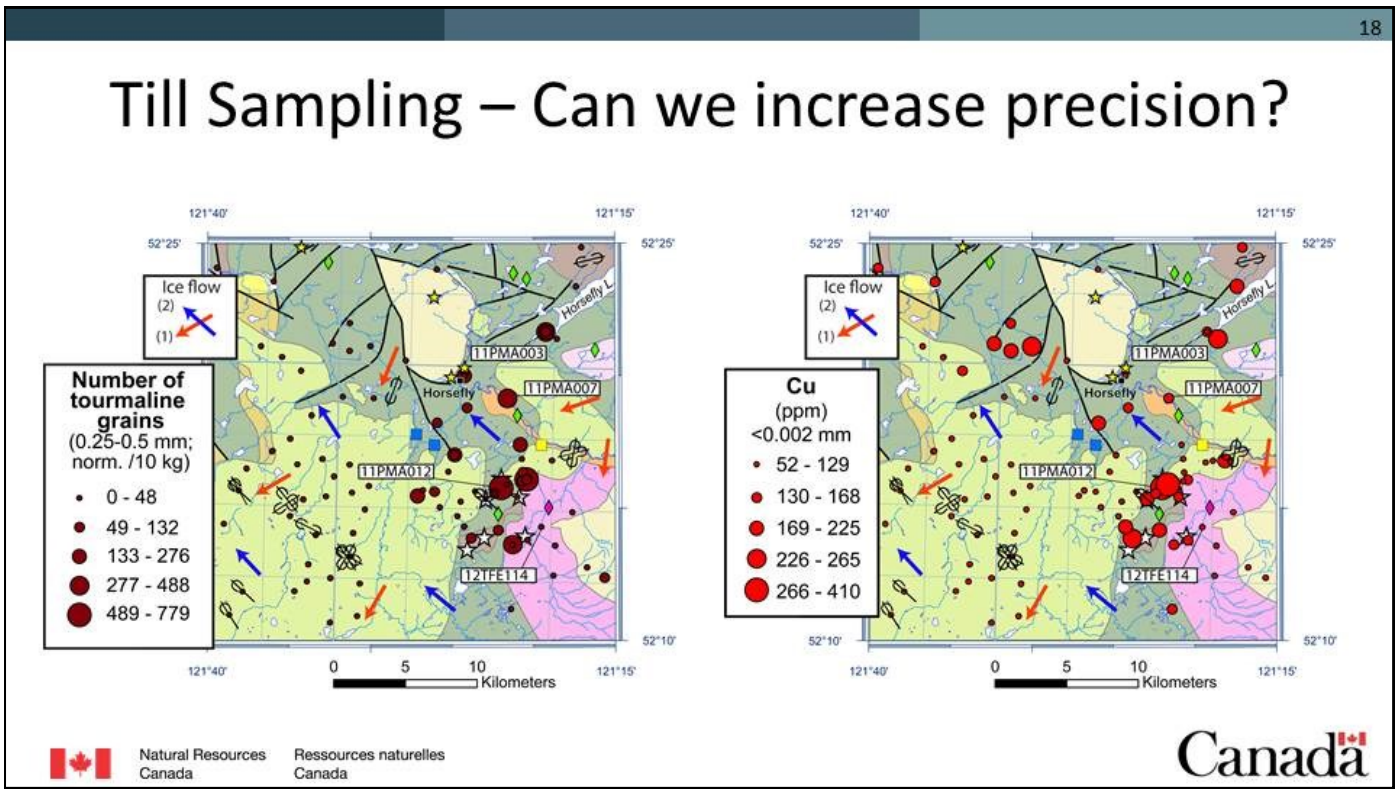
18
Till Sampling – Can we increase precision?
Ice flow
(2)
(1)
Number of tourmaline grains
(0.25-0.5 mm; norm. /10 kg)
0 - 48
49 - 132
133 - 276
277 - 488
489 - 779
Cu
(ppm)
<0.002 mm
52 - 129
130 - 168
169 - 225
226 - 265
266 - 410
11PMA003
11PMA007
11PMA012
12TFE114
Horsefly
Horsefly L
121°40'
121°15'
52°25'
52°10'
0 5 10 Kilometers
Natural Resources Canada
Ressources naturelles Canada
Canada

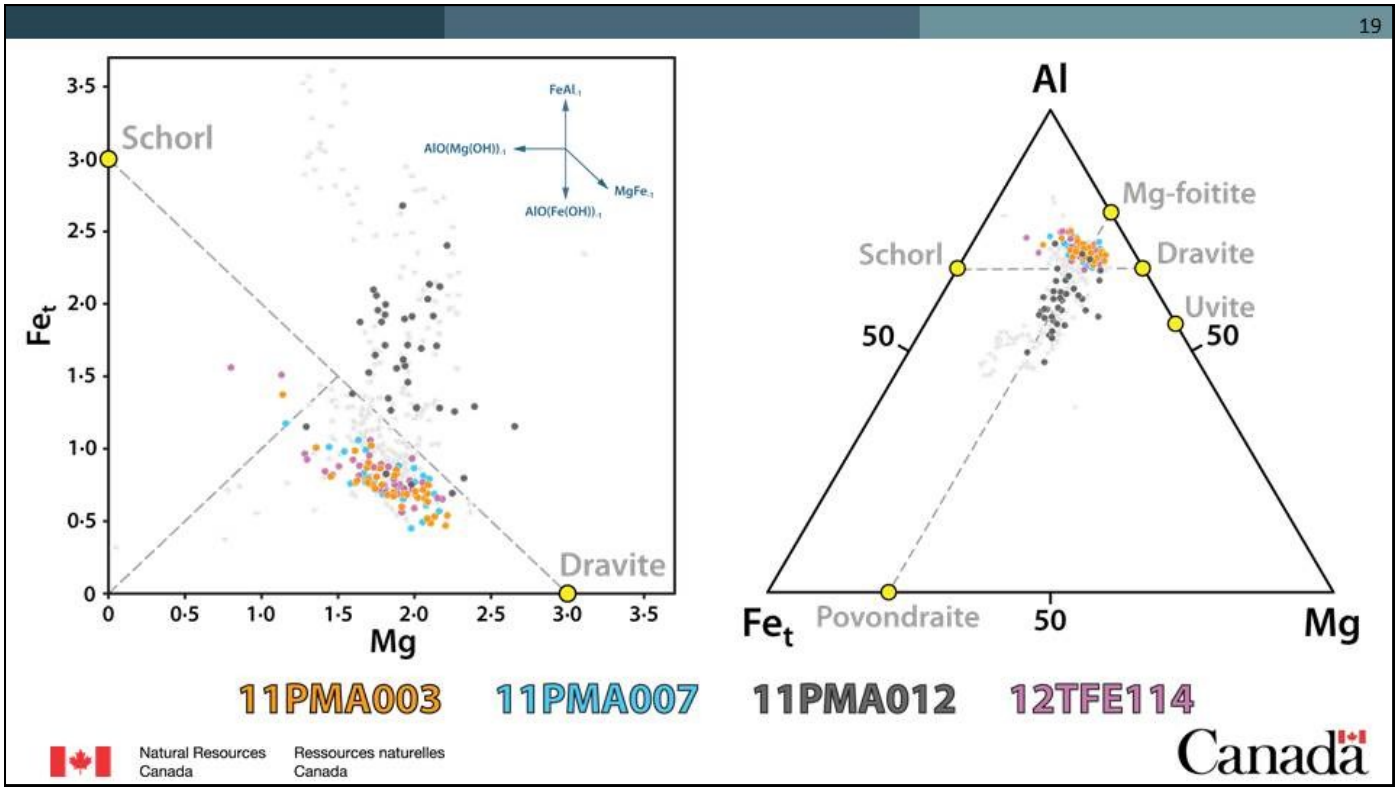
19
Schorl
Dravite
Fe$_t$
Mg
FeAl$_{-1}$
AlO(Mg(OH))$_{-1}$
MgFe$_{-1}$
AlO(Fe(OH))$_{-1}$
Al
Mg-foitite
Schorl
Dravite
Uvite
50
50
Fe$_t$
Povondraite
50
Mg
11PMA003
11PMA007
11PMA012
12TFE114
Natural Resources Canada
Ressources naturelles Canada
Canada

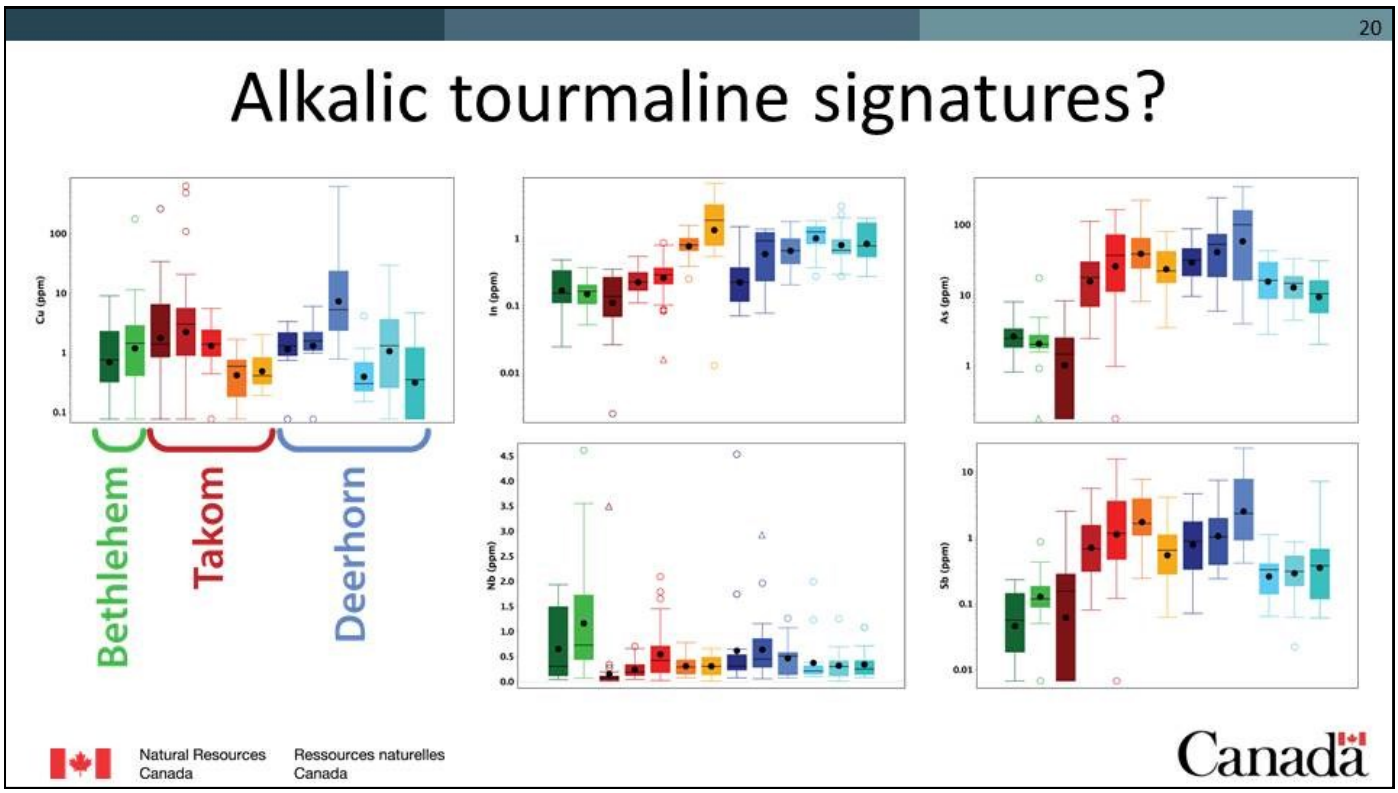
20
Alkalic tourmaline signatures?
Cu (ppm)
In (ppm)
As (ppm)
Nb (ppm)
Sb (ppm)
Bethlehem
Takom
Deerhorn
Natural Resources Canada
Ressources naturelles Canada
Canada

21

Indium in Sn-W Systems

- Global primary ≈ 670 t/yr
- Recycling ≈ 850 t/yr
- 55-60% from China
- Canada 2nd largest producer
- Teck Trail Smelter (BC) produces ≈ 75 t/yr
- Falconbridge (latterly Xstrata) Kidd Met. Site (ON) produced ≈ 40 t/yr
- Adex pilot trials produced Zn con at 5310 ppm In, and hydrometallurgical indium sponge at 96.25%

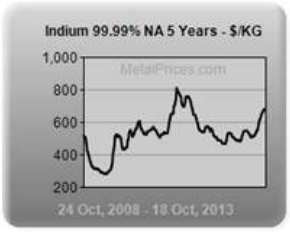

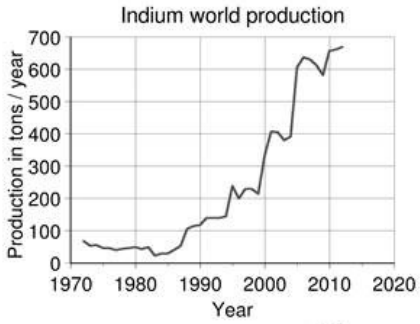

Natural Resources Canada Ressources naturelles Canada

Canada

22

Duck Pond
Metasediment-hosted qtz-sulfide veins and greisen. Zn to wt% levels, no In data

East Kemptville - Baby
Granite-hosted massive greisen. Abundant sphalerite and chalcopyrite, but little In?

Kempt Snare Lake
Metasediment-hosted qtz-sulfide veins. Zn to wt% levels but little/no In

Gardners Meadow
Metasediment-hosted qtz-sulfide veins. DDH assays to 26 ppm In with 1.07 wt% Zn

Dominique
Metasediment-hosted greisen Sn-Zn. DDH assays to 120 ppm In with 1.2 wt% Zn

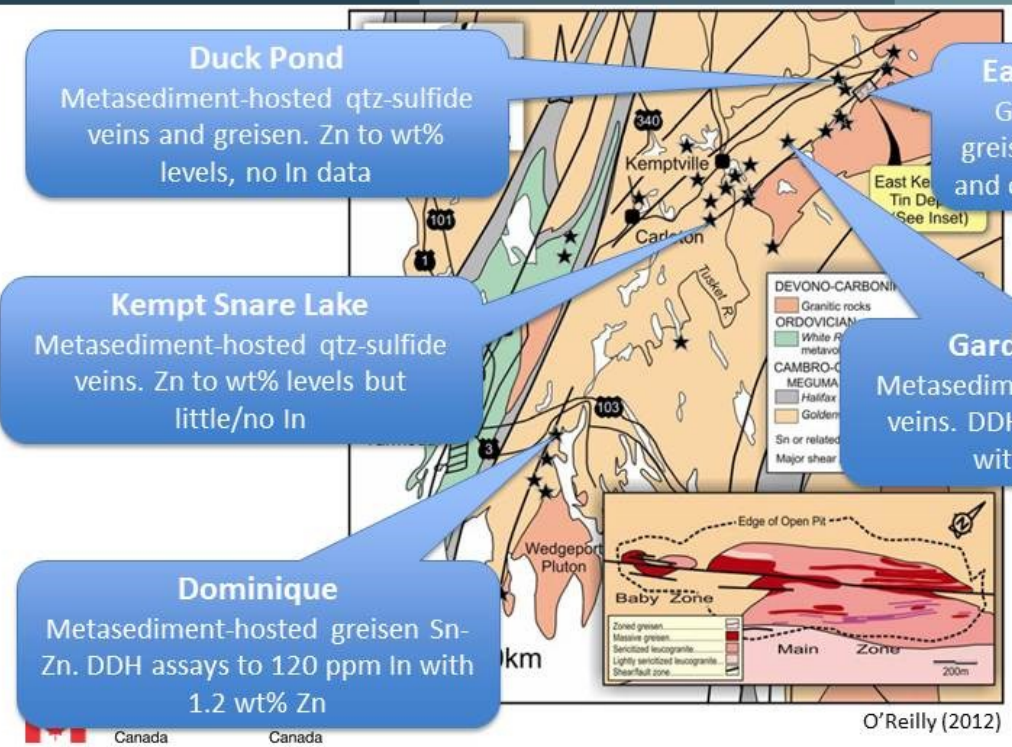

O'Reilly (2012)

Natural Resources Canada Ressources naturelles Canada

Canada

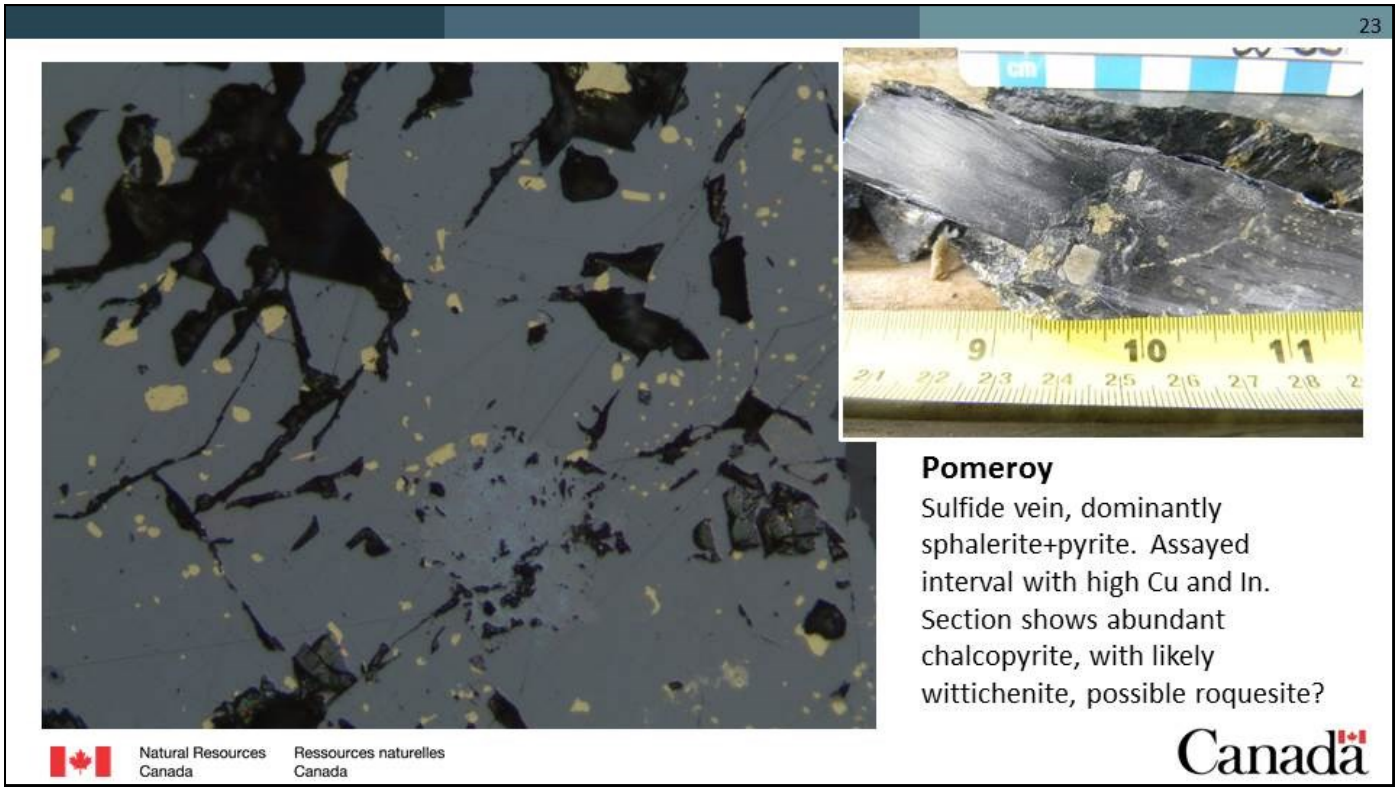
23
Pomeroy
Sulfide vein, dominantly sphalerite+pyrite. Assayed interval with high Cu and In. Section shows abundant chalcopyrite, with likely wittichenite, possible roquesite?
Natural Resources Canada
Ressources naturelles Canada
Canada

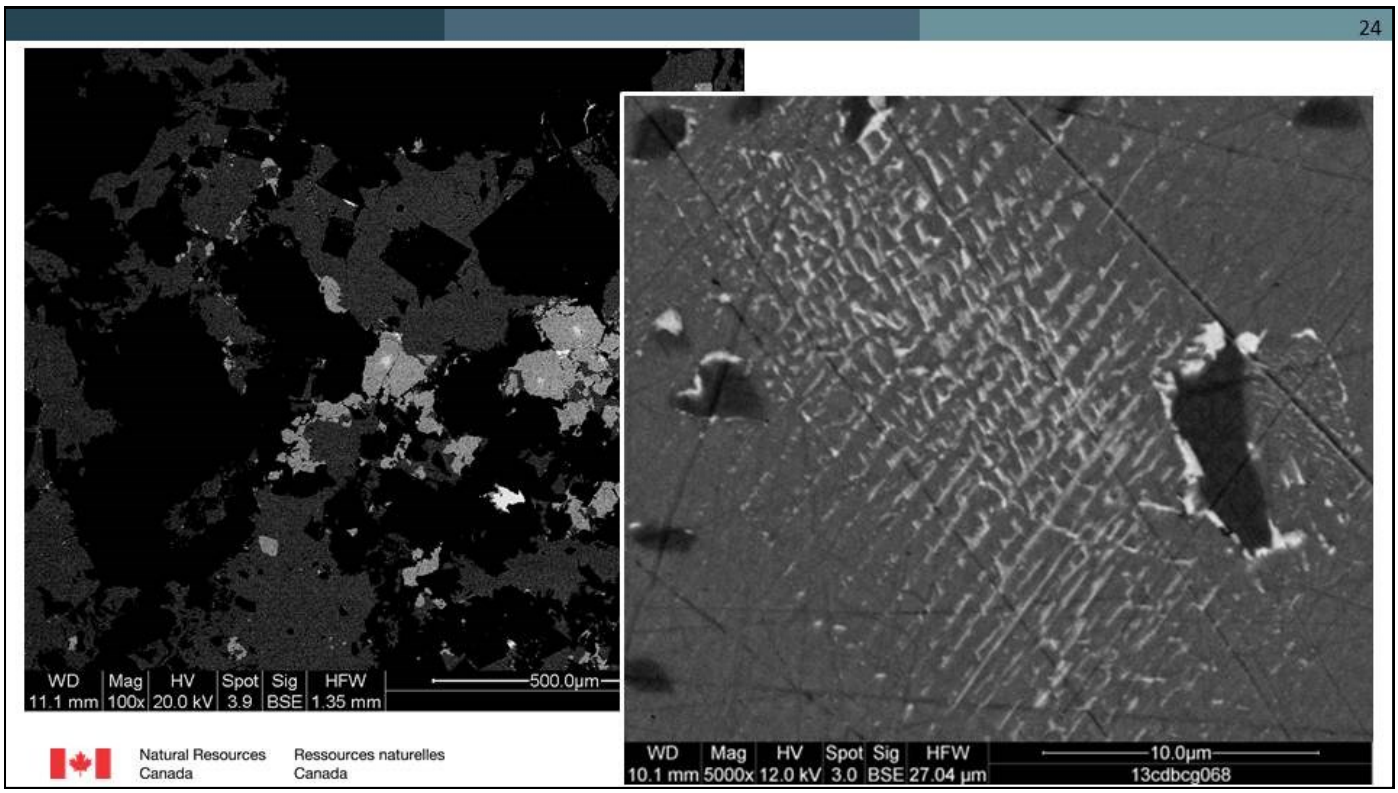
24
WD 11.1 mm | Mag 100x | HV 20.0 kV | Spot 3.9 | Sig BSE | HFW 1.35 mm | 500.0µm
WD 10.1 mm | Mag 5000x | HV 12.0 kV | Spot 3.0 | Sig BSE | HFW 27.04 µm | 10.0µm | 13cdbcg068
Natural Resources Canada
Ressources naturelles Canada

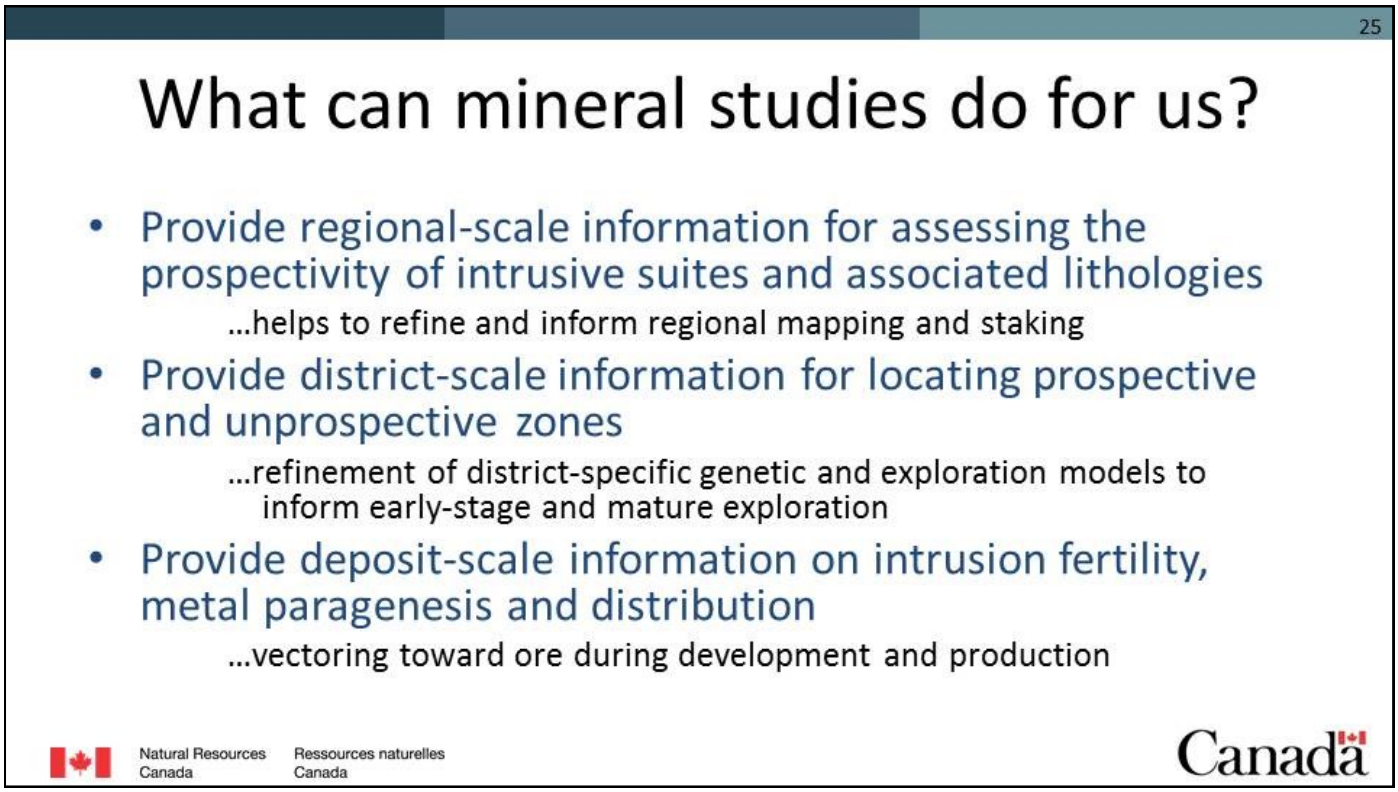
25
What can mineral studies do for us?
• Provide regional-scale information for assessing the prospectivity of intrusive suites and associated lithologies
…helps to refine and inform regional mapping and staking
• Provide district-scale information for locating prospective and unprospective zones
…refinement of district-specific genetic and exploration models to inform early-stage and mature exploration
• Provide deposit-scale information on intrusion fertility, metal paragenesis and distribution
…vectoring toward ore during development and production
Natural Resources Canada
Ressources naturelles Canada
Canada

Using biotite composition of the Devonian Mount Elizabeth Intrusive Complex, New Brunswick, as a proxy for magma fertility and differentiation in W-Mo-Au-Sb mineralized magmatic hydrothermal systems

Z. Azadbakht, D.R. Lentz and C.R.M. McFarlane

University of New Brunswick, Box 4400, 2 Bailey Drive, Fredericton, New Brunswick

Abstract: The Early Devonian (418 ± 1 Ma, monazite U-Pb) Mount Elizabeth intrusive complex, New Brunswick, Canada, is a multiphase metaluminous to weakly peraluminous, high K calc-alkaline body that shows within plate affinity. The complex consists of apparently contemporaneous igneous suites including a mafic suite, an eastern peraluminous granite suite and a western alkali granite suite. The eastern part comprises compositionally and texturally homogenous biotite granite, whereas the western part is mostly heterogeneous and contains five different units. The most abundant phase of the western suite is medium- to coarse-grained alkaline equigranular granite. This complex poorly exposed so that most of the available data, including inferred contact relationships, is based on geophysical data. It should be added that no mineral occurrences have been reported so far from this complex.

Fresh biotite from this intrusion was analysed from core to rim by electron microprobe, and laser ablation ICP-MS at the University of New Brunswick to test whether biotite preserves a record of magma evolution in terms of major and trace-element and halogen compositional variations. Subhedral to elongate biotite phenocrysts are less than 700 μm long and reddish brown in colour indicative of a reduced I-type source. A calc-alkaline affinity is also suggested by biotite major element classification schemes. Biotite is locally altered to chlorite along cleavage planes, and typically contain iron oxides, monazite, ilmenite, apatite, xenotime, and zircon as mineral inclusions.

Results of electron microprobe and laser ablation ICP-MS studies indicate that biotite grains are homogenous in major elements; however, they show variation in trace elements from core to rim. The biotite grains investigated have the highest Sn, W, Sb, and Mo concentrations recorded thus far among Devonian-related granitoid intrusions of New Brunswick (130, 40, 1, 3 ppm, respectively). There is no systematic correlation between major elements including Fe_{Tot}, or Fe_{Tot}/Ti and any of these trace elements. To further study trace-element distribution, a biotite from each of the phases was mapped with laser-ablation ICP-MS revealing patchy Ba, Rb, and Cs zoning. These patterns are interpreted to be a result of localized hydrothermal alteration and intracrystalline volume diffusion in these biotite grains. The intracrystalline distribution of Sn, W, Mo and Sb is homogeneous. Furthermore, halogen contents analysed by EPMA indicate that hydroxyl is the dominant component of hydroxyl site followed by fluorine. It also showed that these biotites formed from strongly contaminated and reduced I-type granite.

As a result, high concentration of Sn in biotite is interpreted to be caused by crustal contamination, and low-temperature hydrothermal processes (sub-solidus) rather than being magmatic in origin.

Originally presented Atlantic Geoscience Society Colloquium and Annual Meeting 2015. January 31, 2015.

Corresponding author: Zeinab Azadbakht (zeinab.azadbakht@unb.ca)

Azadbakht, Z., Lentz, D.R., and McFarlane, C.R.M., 2015. Using biotite composition of the Devonian Mount Elizabeth Intrusive Complex, New Brunswick, as a proxy for magma fertility and differentiation in W-Mo-Au-Sb mineralized magmatic hydrothermal systems; *in* TGI 4 – Intrusion Related Mineralisation Project: New Vectors to Buried Porphyry-Style Mineralisation, (ed.) N. Rogers; Geological Survey of Canada, Open File 7843, p. 535-546.

Using Biotite Composition of the Devonian Mount Elizabeth Intrusive Complex, New Brunswick, as a Proxy for Magma Fertility and Differentiation in W-Mo-Au-Sb Mineralized Magmatic Hydrothermal Systems

Zeinab Azadbakht, David Lentz

Christopher McFarlane

UNB

TGI 4 Ore Systems

Outline

- Project goal
- Geological and tectonic setting
- Mount Elizabeth Intrusive Complex
- Whole Rock Geochemistry
- Tectonic Setting
- Isotopic Characteristics of the Gander Granites

Whalen (1993)

- Petrography
- Biotite Classification
- Biotite Halogen Study
- Magmatic Hydrothermal Fluid
- Trace Element
- Conclusion

My research

Project Goals

- Document detailed chemistry of coexisting phyllosilicate mineral phases to reveal distinctive element signatures that may be specific to fertile granitoids.
- Provide a geochemical fingerprint for more-specific mineralization styles and prospectivity in the Acadian Plutonic Complex.

Geological and Tectonic Setting

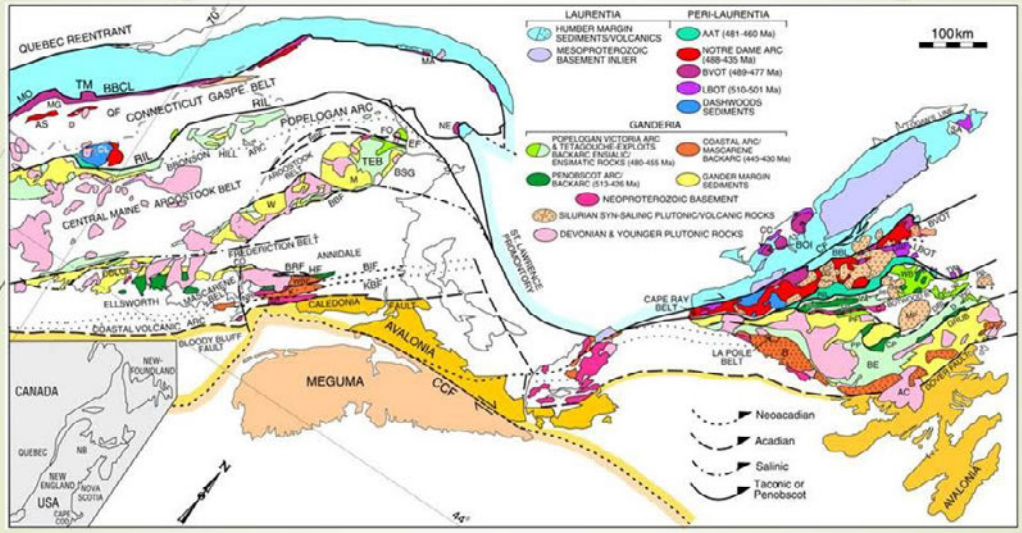

van Staal et al. (2009)

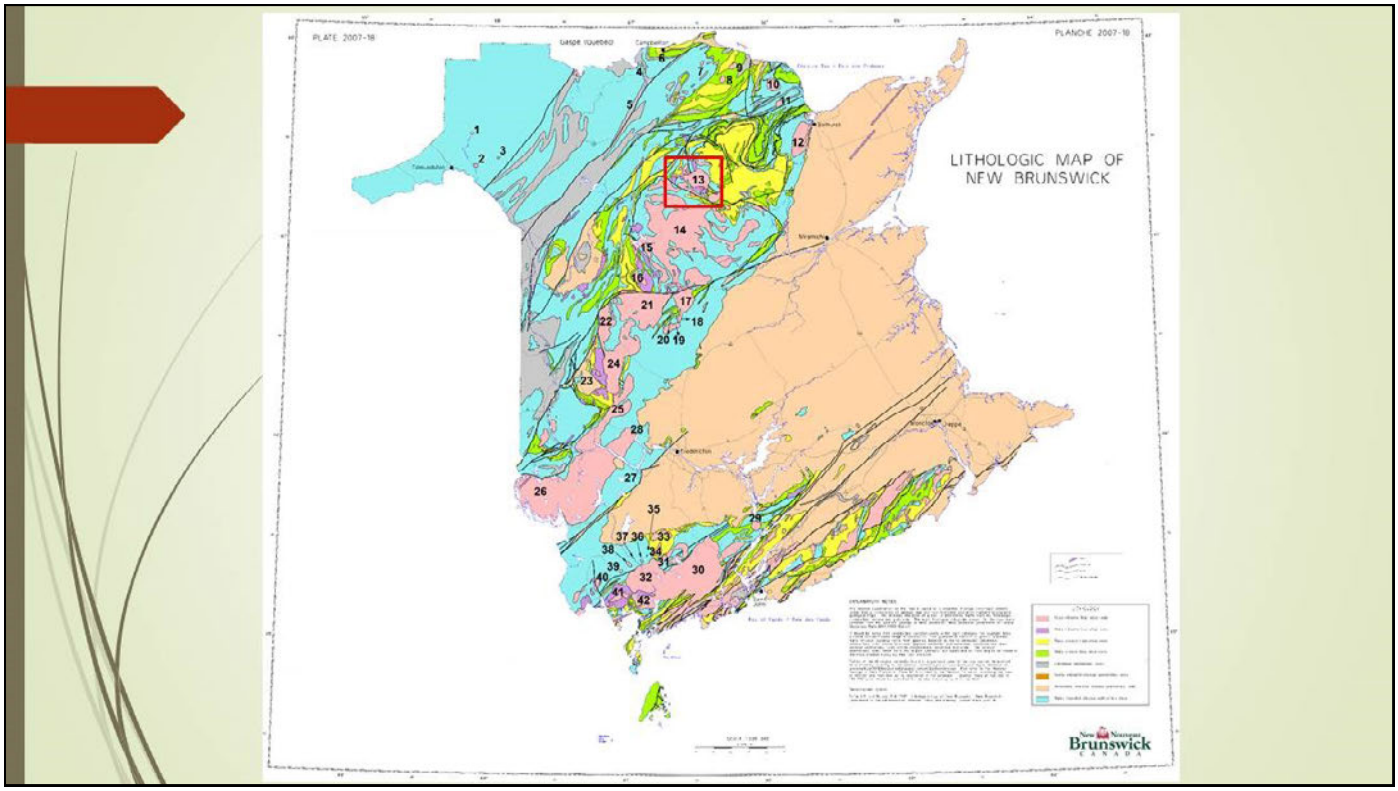
LITHOLOGIC MAP OF
NEW BRUNSWICK
Brunswick

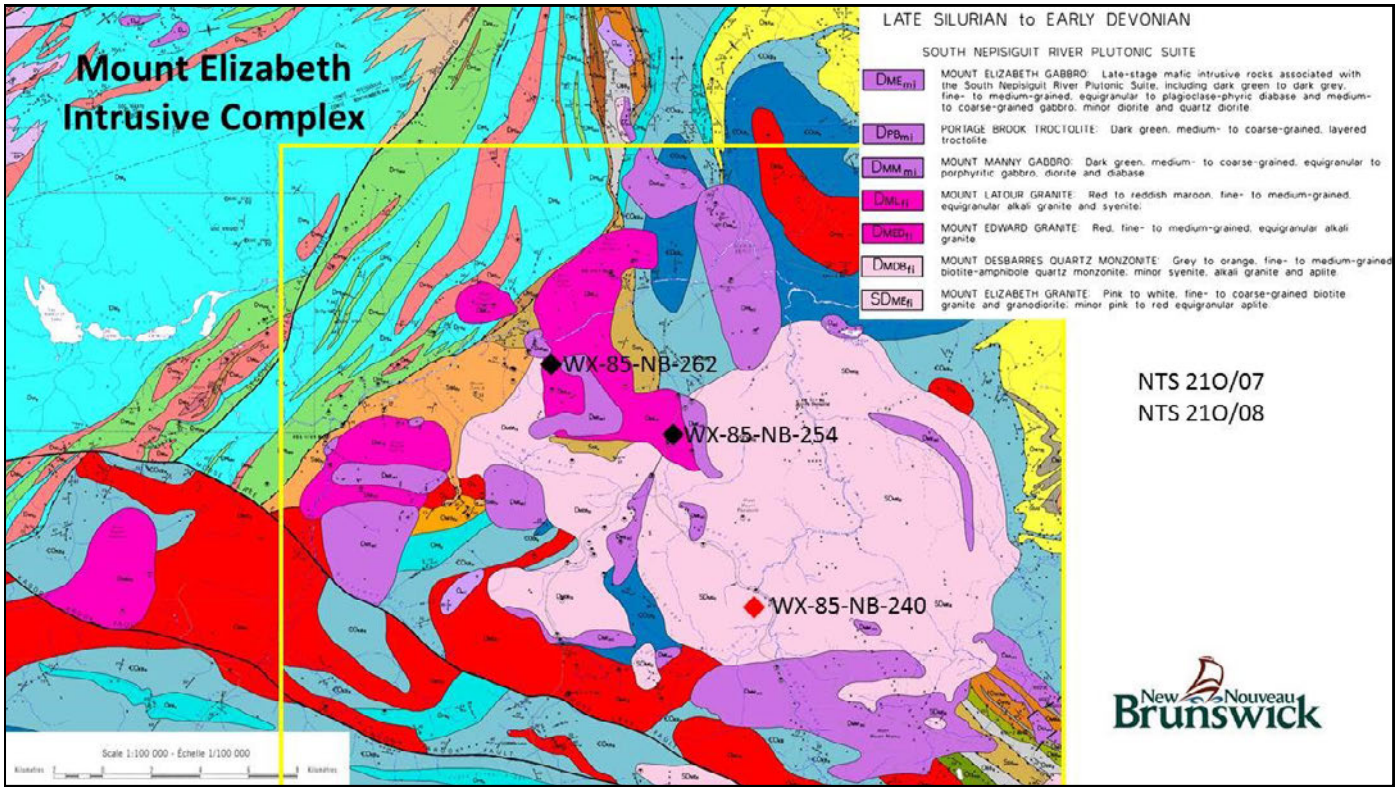
Mount Elizabeth
Intrusive Complex
LATE SILURIAN to EARLY DEVONIAN
SOUTH NEPISIGUIT RIVER PLUTONIC SUITE
DME mi MOUNT ELIZABETH GABBRO: Late-stage mafic intrusive rocks associated with the South Nepisiguit River Plutonic Suite, including dark green to dark grey, fine- to medium-grained, equigranular to plagioclase-phyric diabase and medium- to coarse-grained gabbro, minor diorite and quartz diorite.
DPB mi PORTAGE BROOK TROCTOLITE: Dark green, medium- to coarse-grained, layered troctolite.
DMM mi MOUNT MANNY GABBRO: Dark green, medium- to coarse-grained, equigranular to porphyritic gabbro, diorite and diabase.
DML fi MOUNT LATOUR GRANITE: Red to reddish maroon, fine- to medium-grained, equigranular alkali granite and syenite.
DMED fi MOUNT EDWARD GRANITE: Red, fine- to medium-grained, equigranular alkali granite.
DMDB fi MOUNT DESBARRES QUARTZ MONZONITE: Grey to orange, fine- to medium-grained biotite-amphibole quartz monzonite, minor syenite, alkali granite and aplite.
SDME fi MOUNT ELIZABETH GRANITE: Pink to white, fine- to coarse-grained biotite granite and granodiorite; minor pink to red equigranular aplite.
WX-85-NB-262
WX-85-NB-254
WX-85-NB-240
NTS 21O/07
NTS 21O/08
Scale 1:100 000 - Échelle 1/100 000
New Nouveau Brunswick

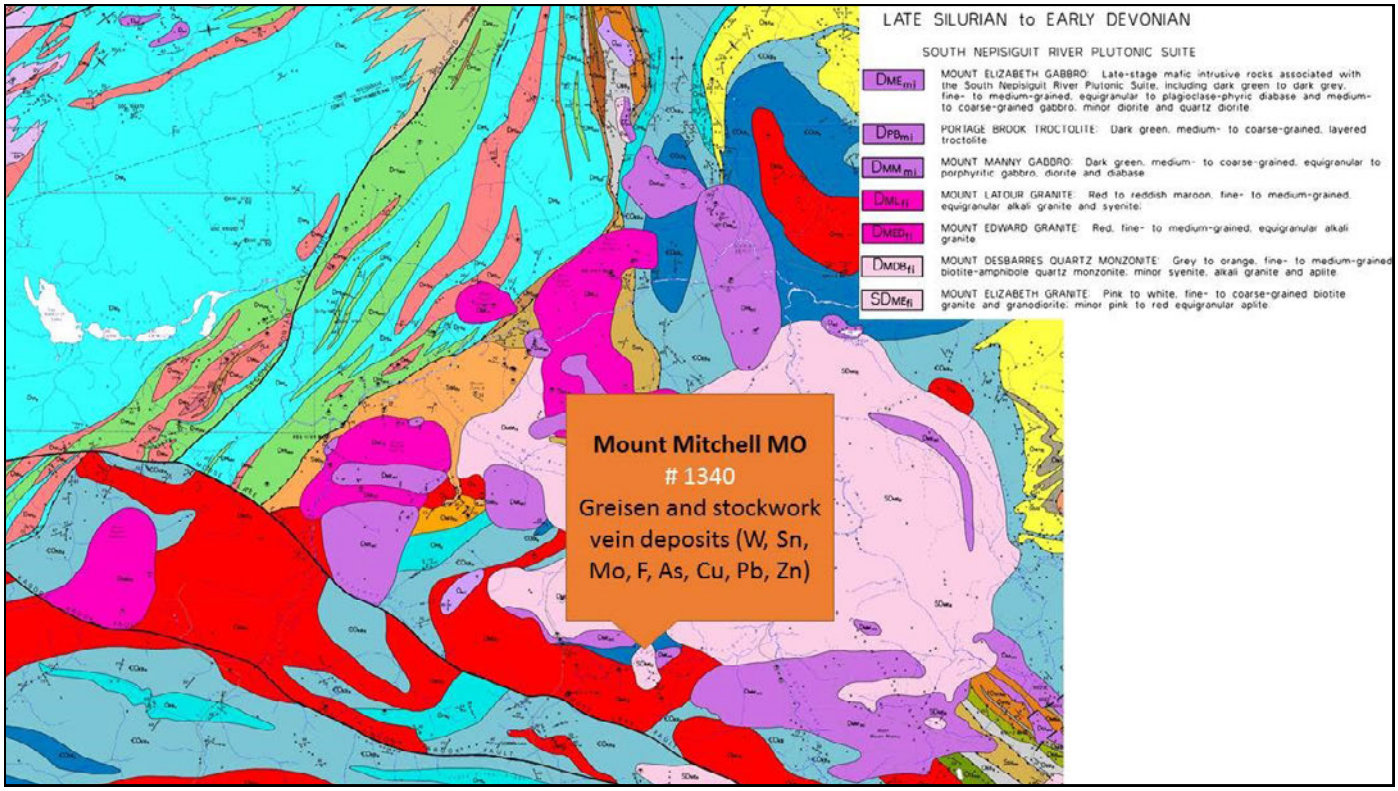
LATE SILURIAN to EARLY DEVONIAN
SOUTH NEPISIGUIT RIVER PLUTONIC SUITE
DME$_{mi}$ MOUNT ELIZABETH GABBRO: Late-stage mafic intrusive rocks associated with the South Nepisiguit River Plutonic Suite, including dark green to dark grey, fine- to medium-grained, equigranular to plagioclase-phyric diabase and medium- to coarse-grained gabbro, minor diorite and quartz diorite
DPB$_{mi}$ PORTAGE BROOK TROCTOLITE: Dark green, medium- to coarse-grained, layered troctolite
DMM$_{mi}$ MOUNT MANNY GABBRO: Dark green, medium- to coarse-grained, equigranular to porphyritic gabbro, diorite and diabase
DML$_{fi}$ MOUNT LATOUR GRANITE: Red to reddish maroon, fine- to medium-grained, equigranular alkali granite and syenite
DMED$_{fi}$ MOUNT EDWARD GRANITE: Red, fine- to medium-grained, equigranular alkali granite
DMDB$_{fi}$ MOUNT DESBARRES QUARTZ MONZONITE: Grey to orange, fine- to medium-grained biotite-amphibole quartz monzonite, minor syenite, alkali granite and aplite
SDME$_{fi}$ MOUNT ELIZABETH GRANITE: Pink to white, fine- to coarse-grained biotite granite and granodiorite; minor pink to red equigranular aplite
Mount Mitchell MO
1340
Greisen and stockwork vein deposits (W, Sn, Mo, F, As, Cu, Pb, Zn)

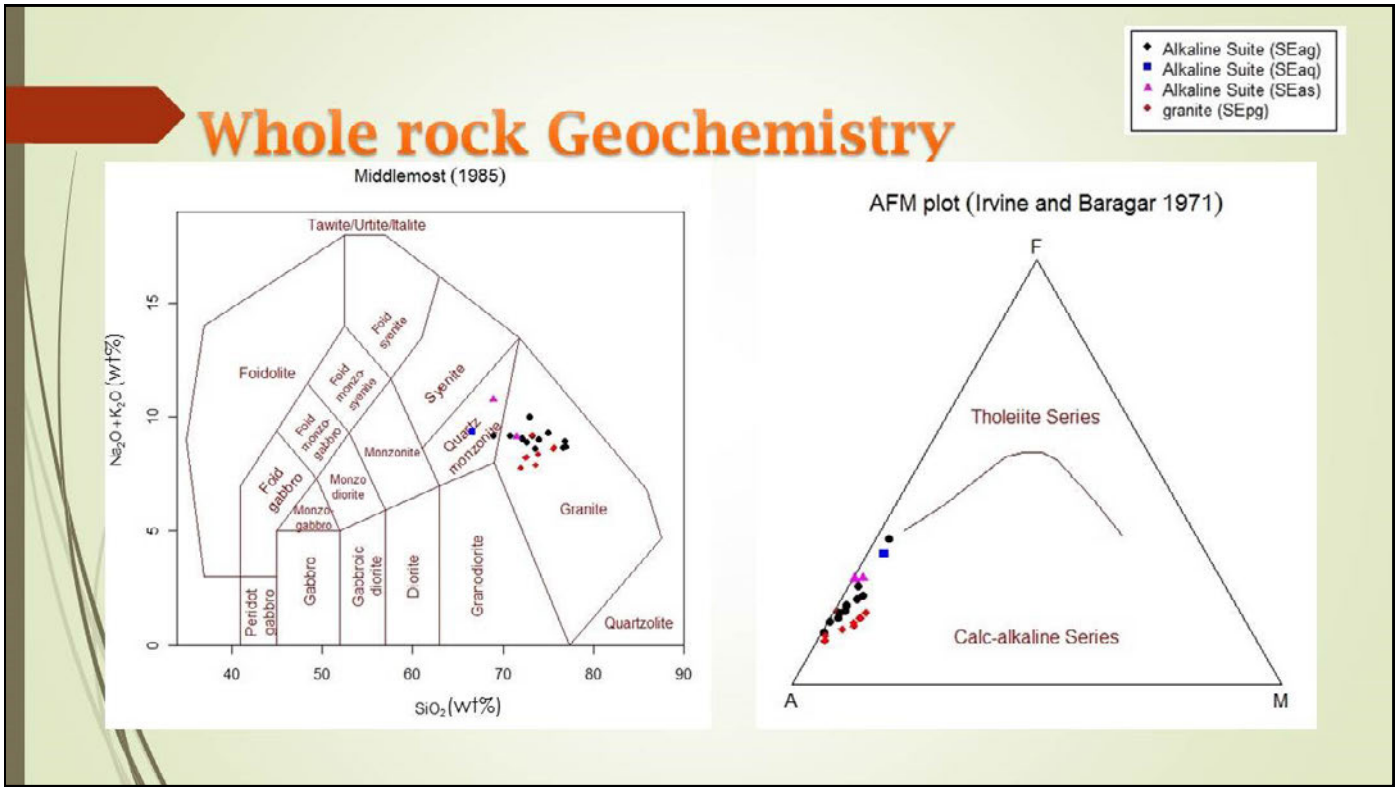
Alkaline Suite (SEag)
Alkaline Suite (SEaq)
Alkaline Suite (SEas)
granite (SEpg)
Whole rock Geochemistry
Middlemost (1985)
Tawite/Urtite/Italite
Foidolite
Fold syenite
Fold monzo-syenite
Syenite
Fold monzo-gabbro
Monzonite
Quartz monzonite
Fold gabbro
Monzo diorite
Monzo-gabbro
Granite
Peridot gabbro
Gabbro
Gabbroic diorite
Diorite
Granodiorite
Quartzolite
Na_2O+K_2O (wt%)
SiO_2(wt%)
AFM plot (Irvine and Baragar 1971)
F
Tholeiite Series
Calc-alkaline Series
A
M

Whole rock Geochemistry

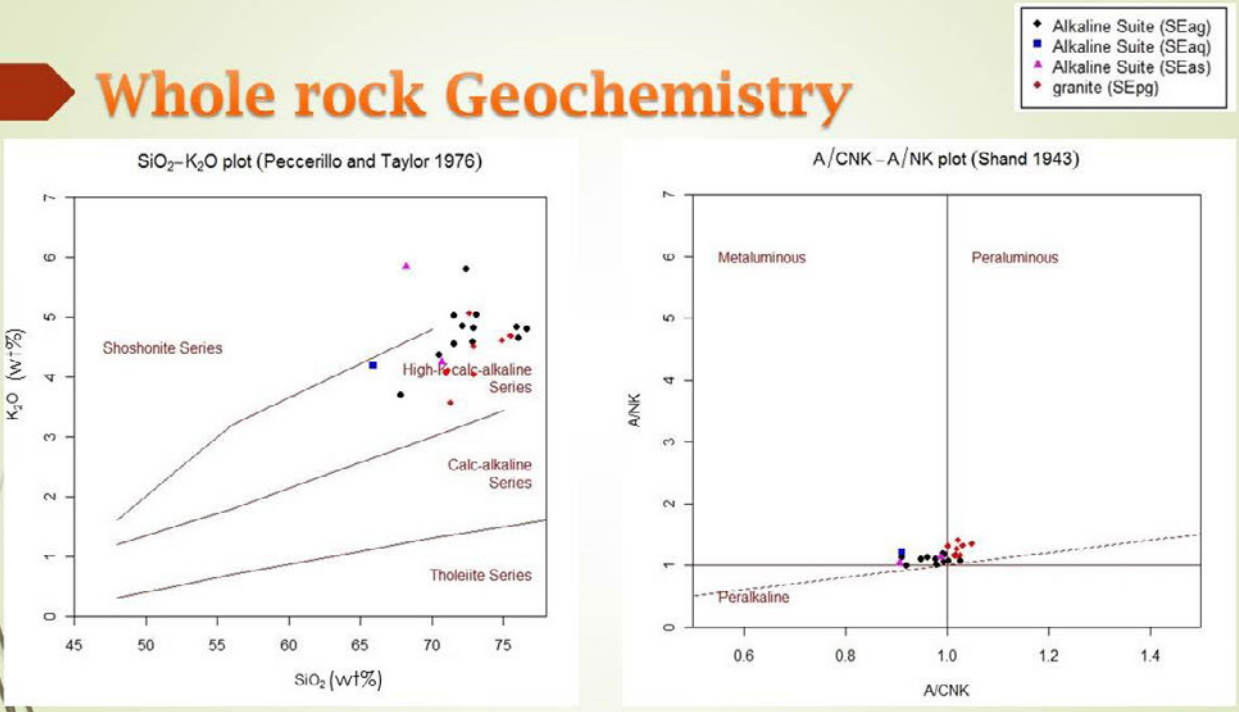

Tectonomagmatic Geochemical Discrimination Diagrams

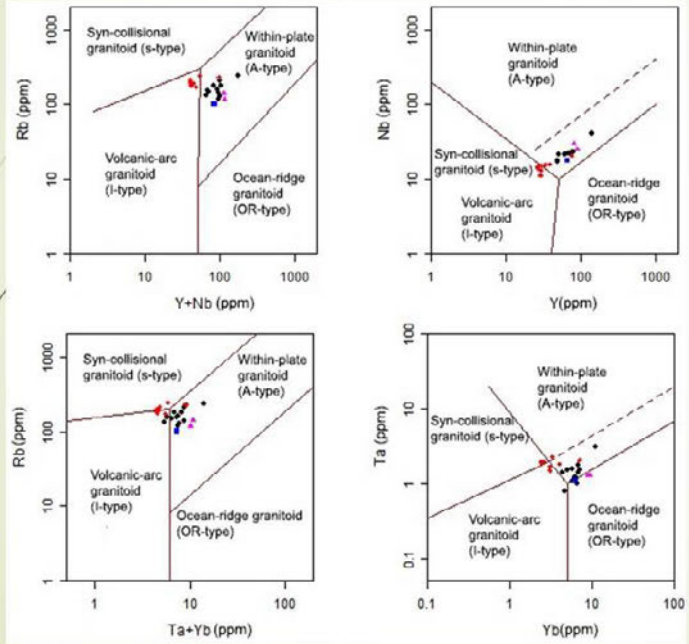

Pearce et al. (1984) as modified by Christiansen and Keith (1996)

Tectonomagmatic Geochemical Discrimination Diagrams

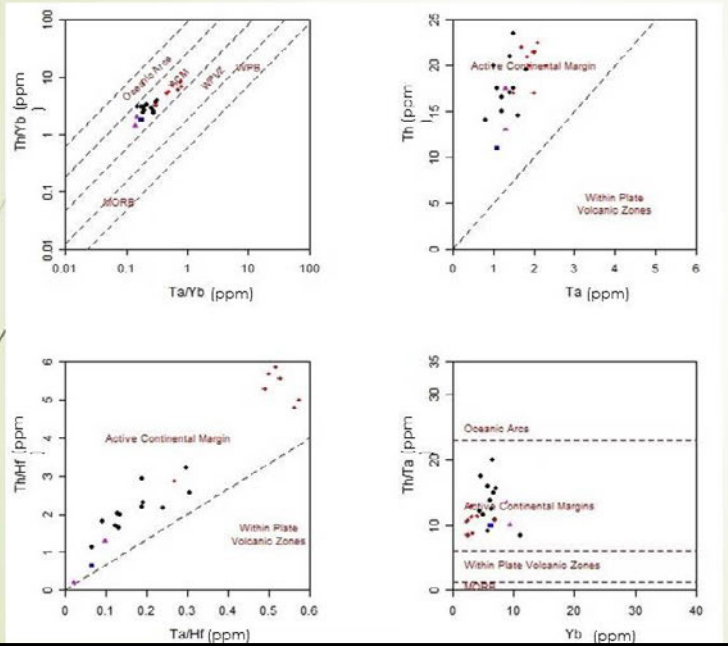

Schandl and Gorton(2002)

Tectonomagmatic Geochemical Discrimination Diagrams

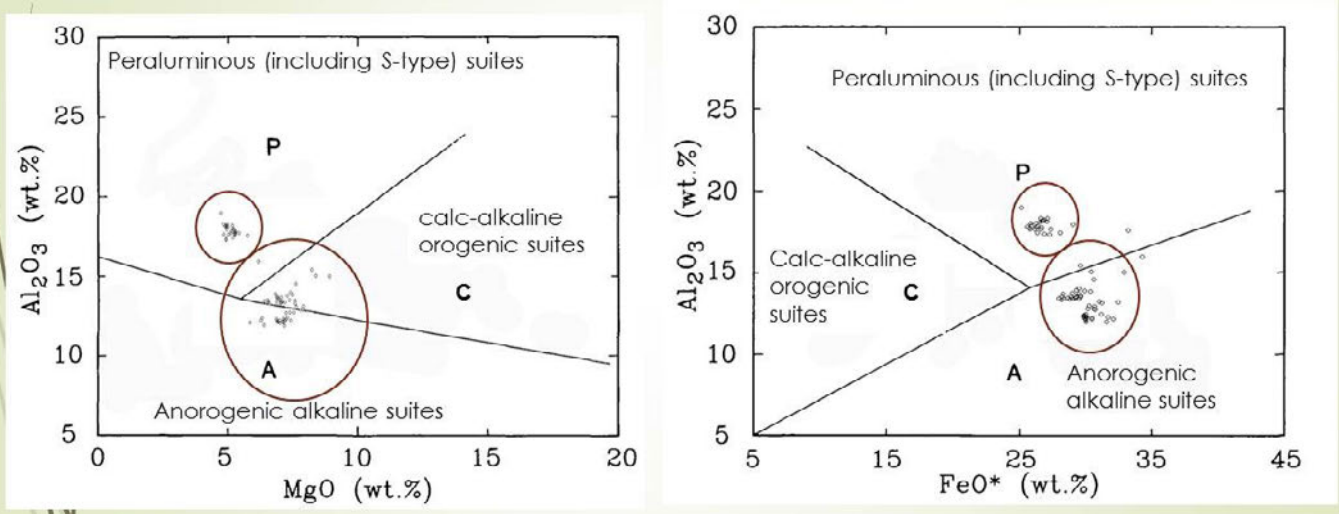

Abdel-Rahman (1994)

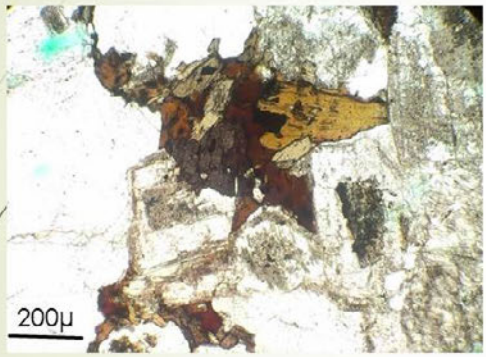

Lalonde and Bernard (1993)

Isotopic Characteristics of the Gander Granites

Zone	Al/(Na+K+Ca)	ε_{Nd}	ε_{Nd} (0.4 Ga)	T_{DM} (Ga)	$\delta^{18}O$	$^{206}Pb/^{204}Pb$	$^{207}Pb/^{204}Pb$	$^{208}Pb/204Pb$
Ordovician	1.02±0.06 (0.89/1.15)	-2.3±1.7 (-5.4/0.1)	-2.8±1.8 (-6.1/-0.2)	1.5±0.2 (1.1/1.7)	9.0±0.7 (8.2/10.1)	18.543±0.137 (18.353/18.770)	15.692±0.010 (15.675/15.709)	38.429±0.144 (38.232/38.707)
Silurian-Devonian	1.03±0.07 (0.85/1.17)	-1.09±1.0 (-4.2/-0.3)	-2.0±1.1 (-4.4/-0.4)	1.4±0.1 (1.1/1.7)	8.6±1.1 (5.6/10.4)	18.391±0.105 (18.276/18.708)	15.667±0.021 (15.628/15.702)	38.284±0.077 (38.089/38.420)

Old Continental crust or enriched mantle

Supracrustal Source

U-Pb monazite age of 418±1 Ma Eastern Peraluminous suite

Negative ε_{Nd} (0.4 Ga) values indicates reworking of the same, significantly older (range in depleted mantle model ages, T_{DM}= 1.1-1.7 Ga), crustal protolith during a number of different partial melting events (Whalen 1993)

The isotopic data indicates that Gander zone granites were generated from older (1.5± 0.5 Ga) crustal source which included a major supracrustal component (Whalen 1993)

Petrography (SEM-BSE Images)

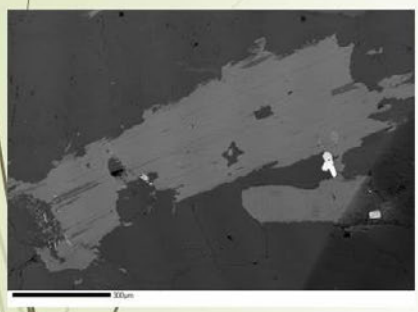

WX-85-NB-240
coarse grained
equigranular biotite
granite
SEpg

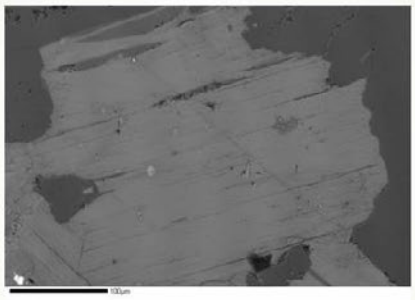

WX-85-NB-254
coarse grained equigranular
white biotite granite
SEag

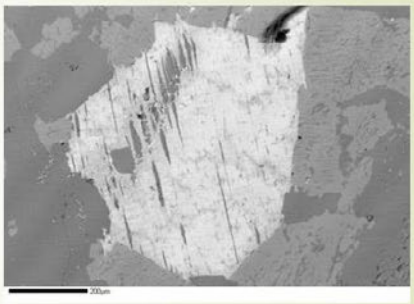

WX-85-NB-262
coarse grained equigranular
red biotite-amphibole
alkali granite
SEag

Biotite Classification

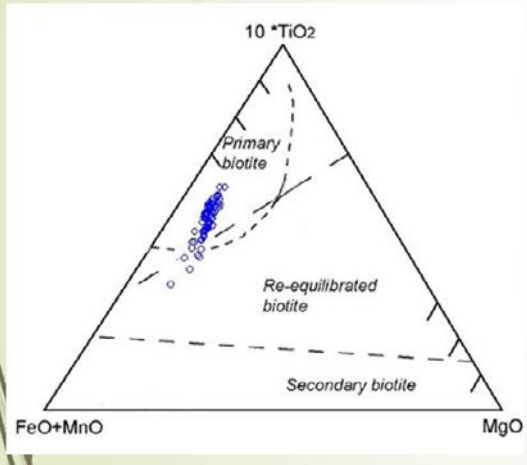

Nachit et al. (2005)

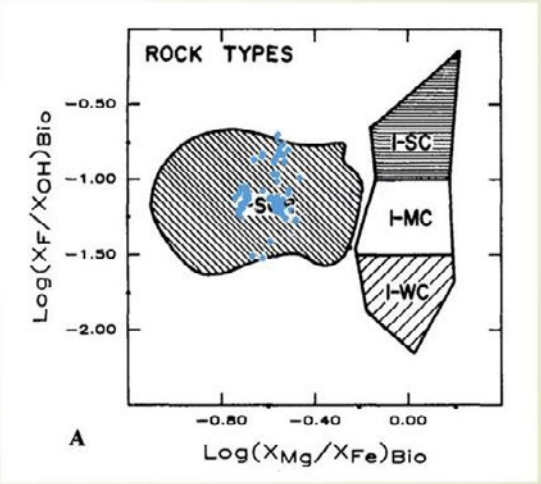

Ague and Brimhall (1987)

Biotite Halogen Study

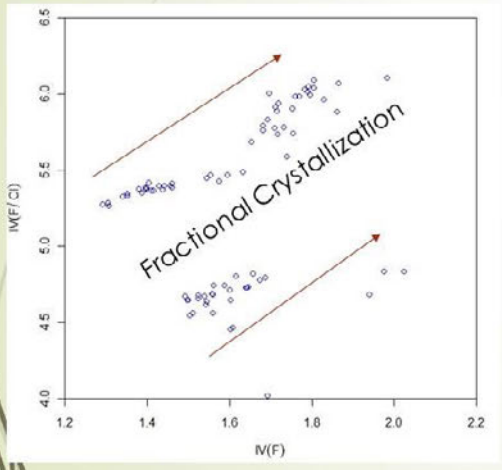

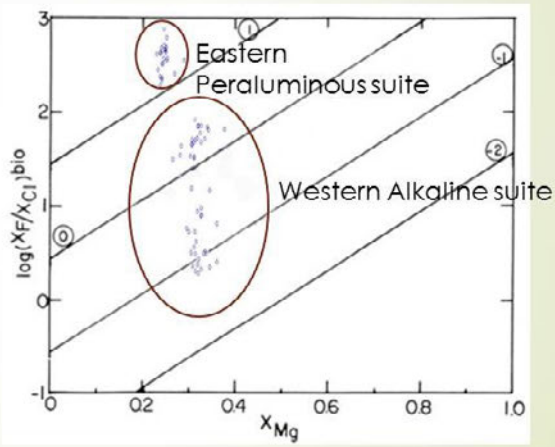

Magmatic Hydrothermal Fluid

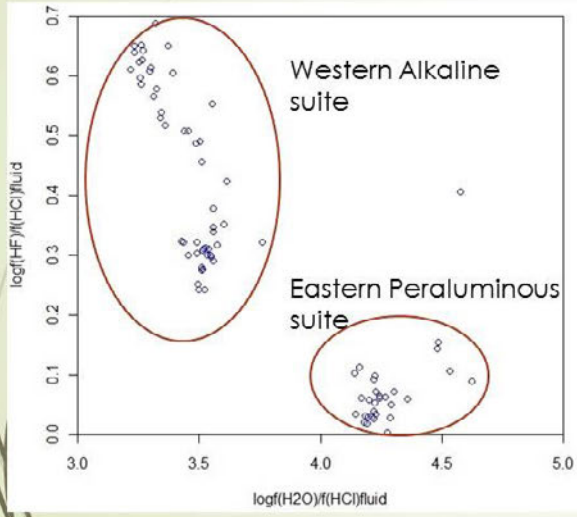

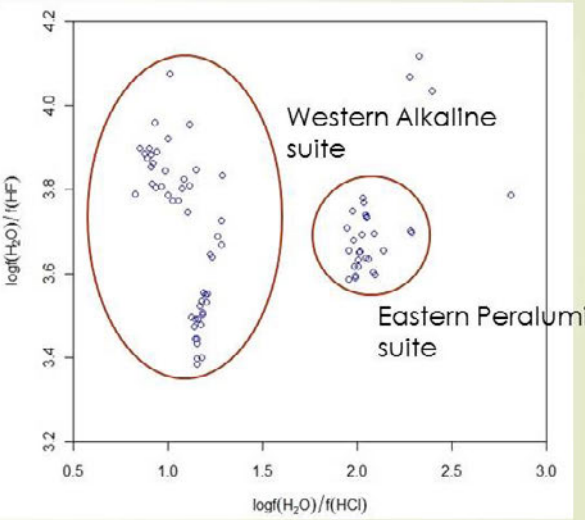

Trace Elements

Sample #	Suite	Mo (ppm)	Sn (ppm)	Sb (ppm)	W (ppm)
WX-85-NB-240	SEpg	2±1	130±10	0.3±0.1	9±2
WX-85-NB-254	SEag	2±1	8±2	1±0.5	2±1
WX-85-NB-262	SEag	2±1	24±5	0.5±0.1	10±2

Conclusion

- Mount Elizabeth Intrusive Complex seems to be fractionally crystalized
- It seems that different suites have been equilibrated with a different hydrothermal fluid (at least two different hydrothermal fluid
- Proof of concept that mica chemistry may aid in identification of fertile Acadian magma systems
- Systematic sampling
- U/Pb Zircon dating of different phases to study the time relationship between them
- Detail mapping of the area
- Geophysical survey

Acknowledgment

- Joseph Whalen
- Cees van Staal
- Les Fyffe
- Neil Rogers
- Dave Lentz
- Christopher McFarlane
- Jim Walker

Magmatic evolution of the Late Devonian Mount Douglas leucogranites, southwestern New Brunswick, Canada; An example of extreme fractional crystallization

N. Mohammadi and D.R. Lentz

University of New Brunswick, Box 4400, 2 Bailey Drive, Fredericton, New Brunswick

Abstract: The Late Devonian Mount Douglas intrusive suite (MD, ~600 km^2) of southwestern New Brunswick, Canada, eastern part of the Saint George Batholith, is a suite of peraluminous leucogranites extended from Red Rock Lake to Mount Douglas. Extreme fractional crystallization associated with formation of this suite is the most important factor affecting the magmatic evolution, producing three compositionally and chronologically different intrusive units, Dmd1, Dmd2, and Dmd3. Petrochemical data show that the subunits of the Mount Douglas Granite have within-plate geochemical character with evidence of hybrid I- and S-type affinity.

Very low K/Rb (average 102.7), Nb/Ta (≤ 6.8), and Zr/Hf (≤ 37.45) ratios in Dmd3 compared to Dmd1 possibly reflect significant involvement of extreme low T crystal fractionation in the last- stages of magmatic differentiation; The continuous variation trends for many major and trace elements (e.g., Zr vs. TiO_2, Zr/Hf vs. K/Rb, F vs. K/Rb, and Pb vs. Ba) suggest that probably Dmd2 and Dmd3 were generated by extensive fractionation of the parental Dmd1 magma. Also, normalized to the least-evolved sample of the MG granites (Dmd1), the Dmd3 unit is the most enriched in Rb, Th, U, Ce, Ta, Pb, Nd, Sm, Dy, Y, Yb, and Lu, and depletion of Cs, Ba, Sr, P, Zr, Eu, and Ti content, reflects their production of the same parental magma by crystal fractionation from Dmd1 to Dmd3. A flat "birdwing shape" REE patterns with the most pronounced negative Eu anomalies and the lowest $(La/Yb)_N$ (ranging from 1.7-7.4) ratios of Dmd3 show the highly evolved attributes of Dmd3. Calculation of zircon saturation temperatures supports an interpretation of crystal fractionation from Dmd1 to Dmd3. Estimated average temperatures using the bulk rock Zr composition for Dmd1, Dmd2, and Dmd3 range 747-826˚C, 733-817˚C, and 729-816˚C, respectively. All above data suggest that they might have a single genetic group with different fractionation originated from a homogenous parental magma, in which this fractionation increases from the early unit (Dmd1) to the latest unit (Dmd3); significant mineral occurrences, such as Sn, W, and Mo, seem to be mostly associated with the latest and most highly differentiated Dmd3 intrusive phases.

Originally presented Atlantic Geoscience Society Colloquium and Annual Meeting 2015. January 31, 2015.

Corresponding author: Nadieh Mohammadi (Nadia.mohammadi@unb.ca)

Mohammadi, N. and Lentz, D.R., 2015. Magmatic evolution of the Late Devonian Mount Douglas leucogranites, southwestern New Brunswick, Canada; An example of extreme fractional crystallization; *in* TGI 4 – Intrusion Related Mineralisation Project: New Vectors to Buried Porphyry-Style Mineralisation, (ed.) N. Rogers; Geological Survey of Canada, Open File 7843, p. 547-557.

Magmatic Evolution of the Late Devonian Mount Douglas Leucogranites, Southwestern New Brunswick, Canada; an Example of Extreme Fractional Crystallization

Nadia Mohammadi

David Lentz

UNB
UNIVERSITY OF
NEW BRUNSWICK

1

This project is supported by:

New Brunswick Energy and Mines

President's Doctoral scholarship (UNB)

New Brunswick Innovation Foundation
(NBIF)

Supervisors:

Dr. David Lentz

Dr. Christopher McFarlane

2

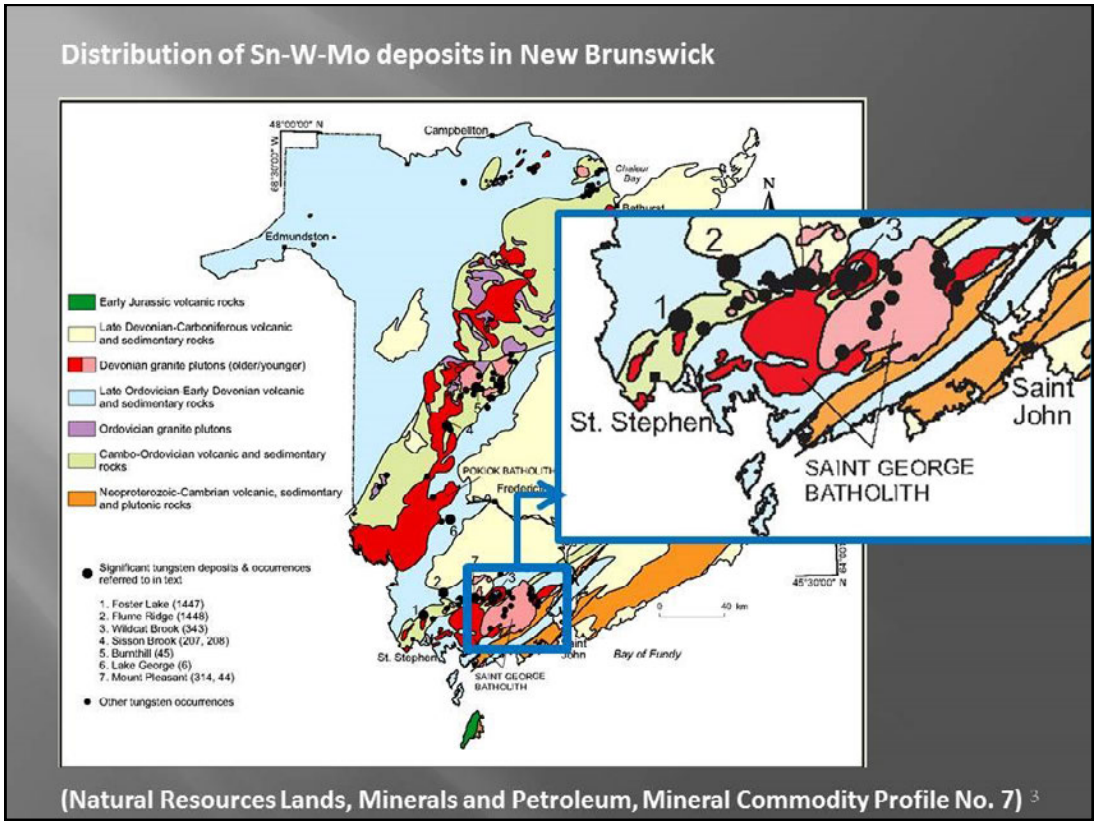
Distribution of Sn-W-Mo deposits in New Brunswick
Campbellton
Edmundston
Chaleur Bay
Bathurst
Fredericton
St. Stephen
Saint John
SAINT GEORGE BATHOLITH
POKIOK BATHOLITH
Ray of Fundy
Early Jurassic volcanic rocks
Late Devonian-Carboniferous volcanic and sedimentary rocks
Devonian granite plutons (older/younger)
Late Ordovician Early Devonian volcanic and sedimentary rocks
Ordovician granite plutons
Cambro-Ordovician volcanic and sedimentary rocks
Neoproterozoic-Cambrian volcanic, sedimentary and plutonic rocks
Significant tungsten deposits & occurrences referred to in text
1. Foster Lake (1447)
2. Flume Ridge (1448)
3. Wildcat Brook (343)
4. Sisson Brook (207, 208)
5. Burnthill (45)
6. Lake George (6)
7. Mount Pleasant (314, 44)
Other tungsten occurrences
0 40 km
(Natural Resources Lands, Minerals and Petroleum, Mineral Commodity Profile No. 7)
3

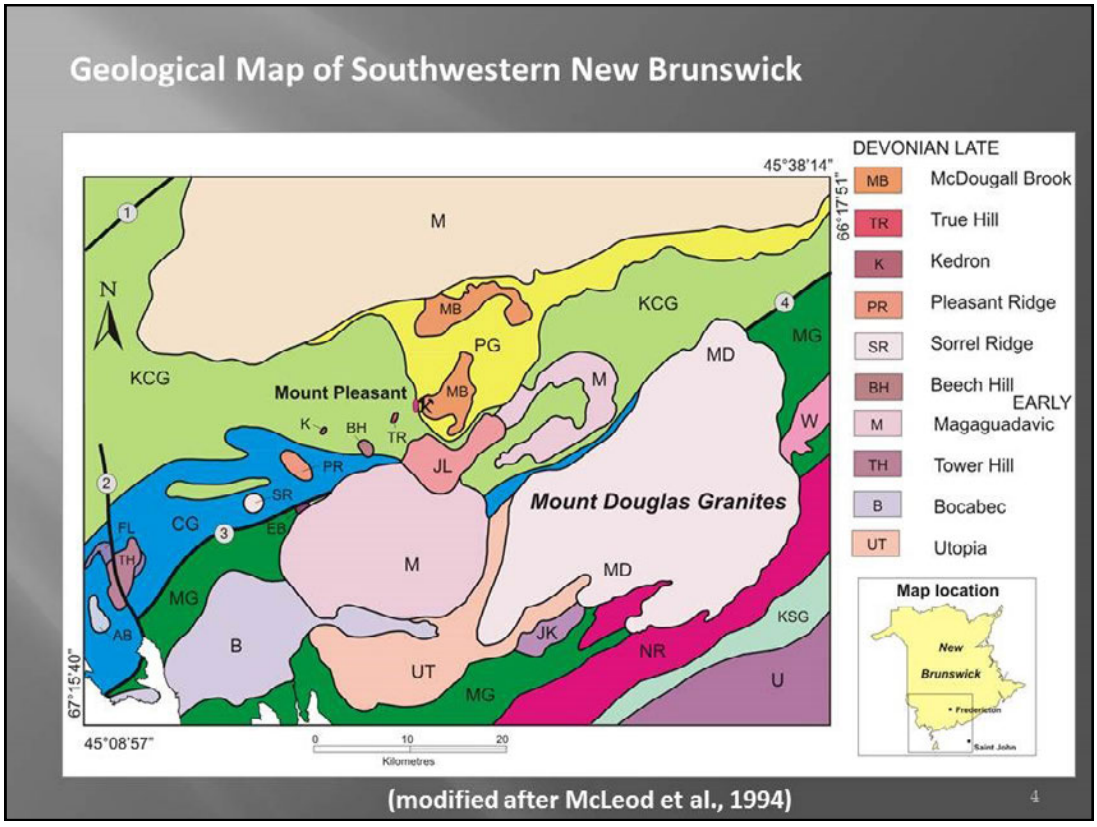
Geological Map of Southwestern New Brunswick
45°38'14"
66°17'51"
67°15'40"
45°08'57"
N
Mount Pleasant
Mount Douglas Granites
M
MB
PG
KCG
MD
MG
JL
PR
SR
BH
TR
K
CG
EB
FL
TH
AB
B
UT
JK
NR
KSG
U
W
0 10 20
Kilometres
DEVONIAN LATE
MB McDougall Brook
TR True Hill
K Kedron
PR Pleasant Ridge
SR Sorrel Ridge
BH Beech Hill
EARLY
M Magaguadavic
TH Tower Hill
B Bocabec
UT Utopia
Map location
New Brunswick
Fredericton
Saint John
(modified after McLeod et al., 1994)
4

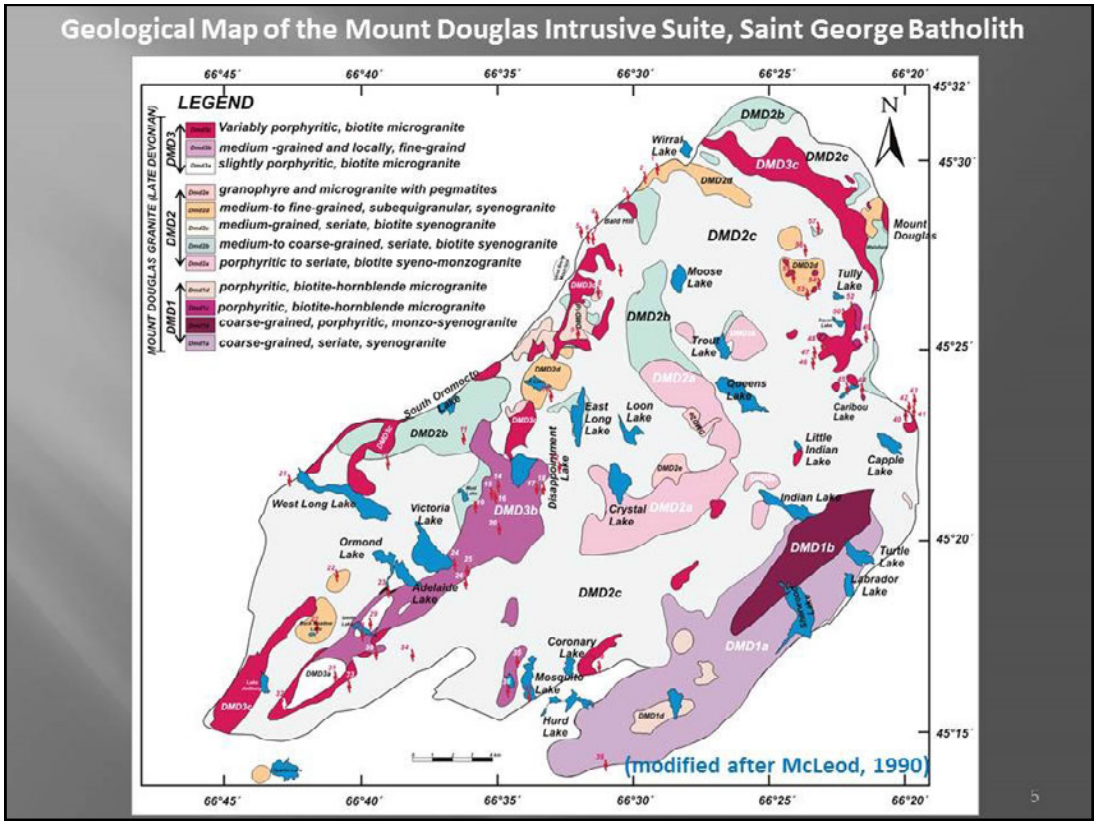
Geological Map of the Mount Douglas Intrusive Suite, Saint George Batholith
LEGEND
MOUNT DOUGLAS GRANITE (LATE DEVONIAN)
DMD3
Variably porphyritic, biotite microgranite
medium -grained and locally, fine-graind
slightly porphyritic, biotite microgranite
DMD2
granophyre and microgranite with pegmatites
medium-to fine-grained, subequigranular, syenogranite
medium-grained, seriate, biotite syenogranite
medium-to coarse-grained, seriate, biotite syenogranite
porphyritic to seriate, biotite syeno-monzogranite
DMD1
porphyritic, biotite-hornblende microgranite
porphyritic, biotite-hornblende microgranite
coarse-grained, porphyritic, monzo-syenogranite
coarse-grained, seriate, syenogranite
N
DMD2b
DMD3c
DMD2c
DMD2a
DMD3b
DMD1b
DMD1a
Wirral Lake
Mount Douglas
Moose Lake
Tully Lake
Trout Lake
Queens Lake
Caribou Lake
East Long Lake
Loon Lake
Little Indian Lake
Capple Lake
South Oromocto Lake
Disappointment Lake
West Long Lake
Victoria Lake
Crystal Lake
Indian Lake
Ormond Lake
Turtle Lake
Labrador Lake
Adelaide Lake
Coronary Lake
Mosquito Lake
Hurd Lake
(modified after McLeod, 1990)

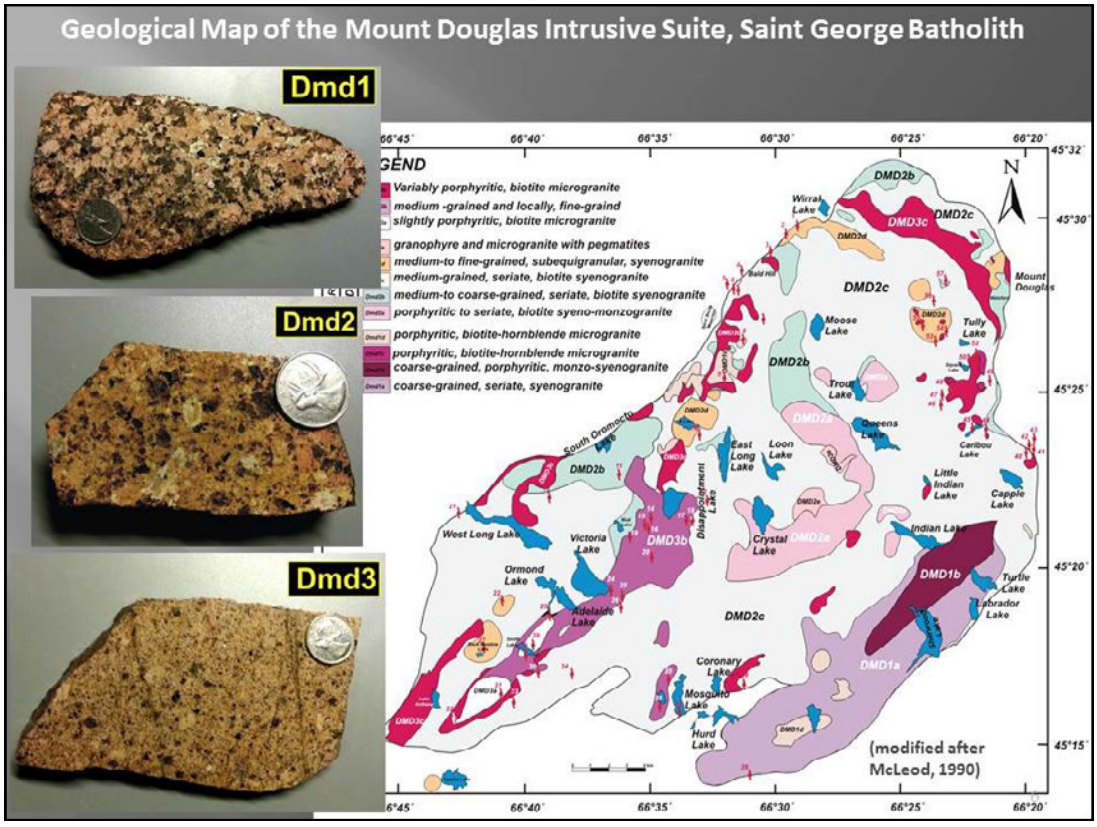
Geological Map of the Mount Douglas Intrusive Suite, Saint George Batholith
Dmd1
Dmd2
Dmd3
Variably porphyritic, biotite microgranite
medium -grained and locally, fine-graind
slightly porphyritic, biotite microgranite
granophyre and microgranite with pegmatites
medium-to fine-grained, subequigranular, syenogranite
medium-grained, seriate, biotite syenogranite
medium-to coarse-grained, seriate, biotite syenogranite
porphyritic to seriate, biotite syeno-monzogranite
porphyritic, biotite-hornblende microgranite
porphyritic, biotite-hornblende microgranite
coarse-grained, porphyritic, monzo-syenogranite
coarse-grained, seriate, syenogranite
N
DMD2b
DMD3c
DMD2c
DMD2a
DMD3b
DMD1b
DMD1a
Wirral Lake
Mount Douglas
Moose Lake
Tully Lake
Trout Lake
Queens Lake
Caribou Lake
East Long Lake
Loon Lake
Little Indian Lake
Capple Lake
South Oromocto Lake
Disappointment Lake
West Long Lake
Victoria Lake
Crystal Lake
Indian Lake
Ormond Lake
Turtle Lake
Labrador Lake
Adelaide Lake
Coronary Lake
Mosquito Lake
Hurd Lake
(modified after McLeod, 1990)

Mineral occurrences associated with the Mount Douglas Suite

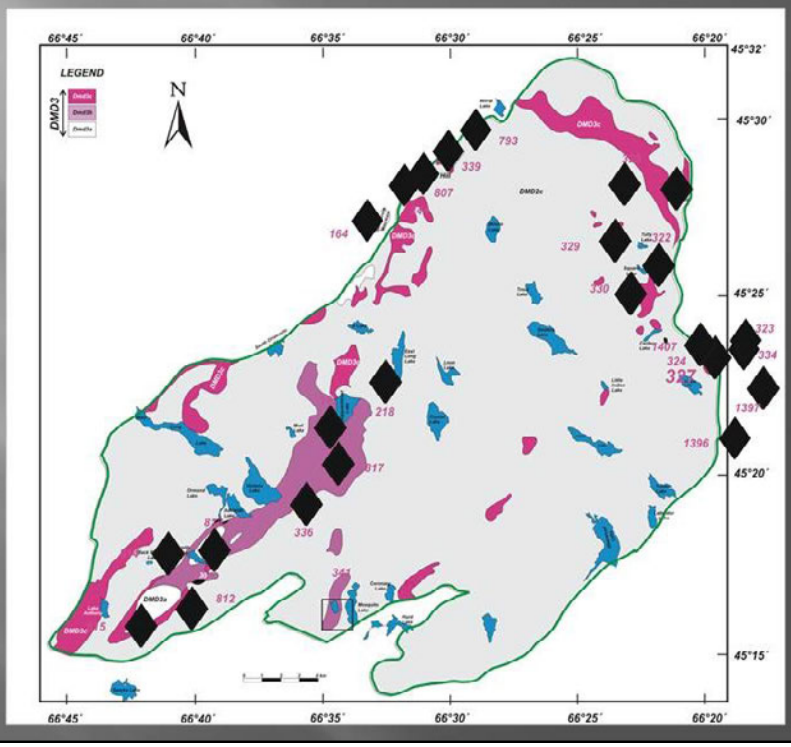

7

Geochemical Studies

McLeod's whole rock analytical data (1990)

high content:

SiO_2 (68-78 wt.%)

K_2O (3.5-7.8)

$(Fe_2O_3+FeO)/MgO$ (average 8.7)

Alkalis

Dmd3
SiO2: 76.4 wt.%

8

Geochemical Studies

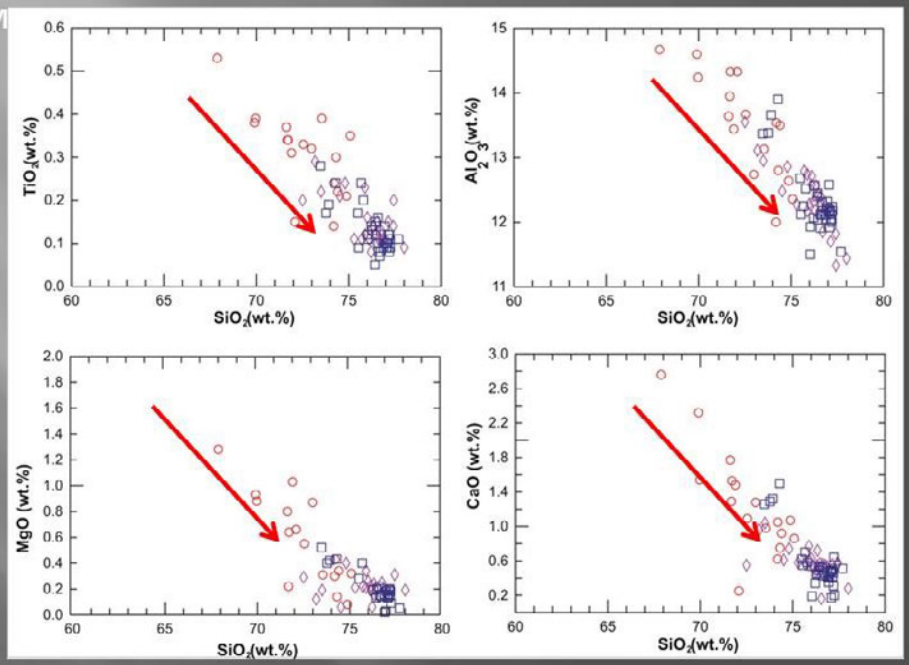

Magma Composition

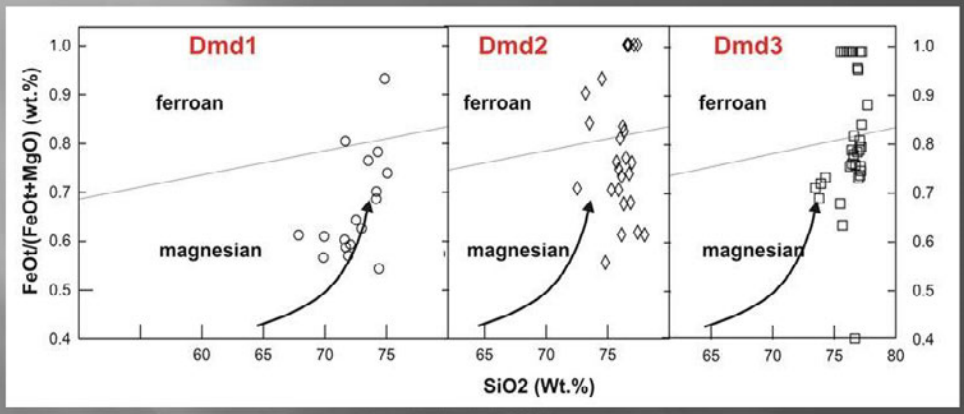

Frost et al. (2001)

Magma Composition

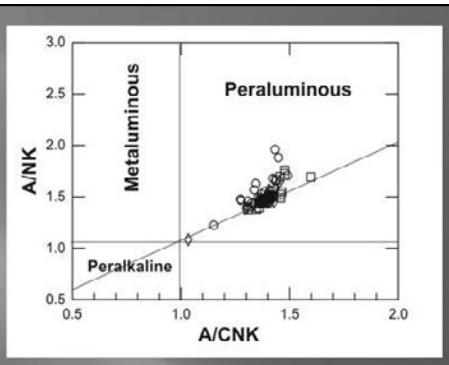

Maniar & Piccoli , 1989

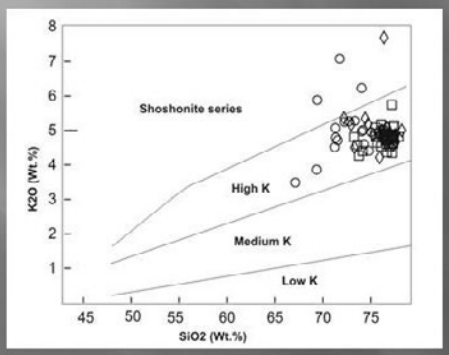

Le Maitre et al. (1989)

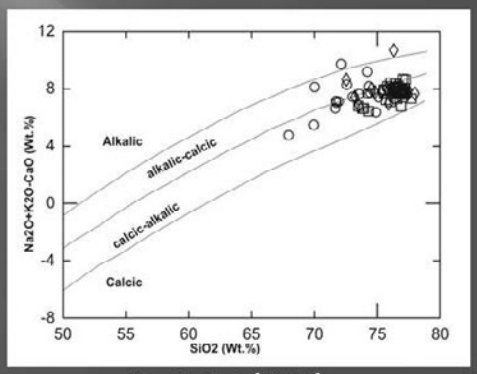

Frost et al. (2001)

11

Petrogenesis and Tectonic Setting

✓ within-plate geochemical character

✓ with possibility of hybrid I- and S-type affinity

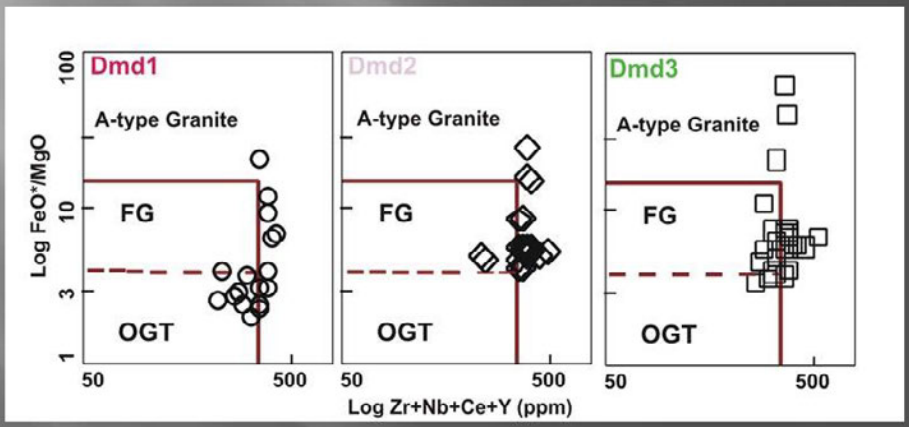

Whalen et al. (1987)

12

Trace Elements Studies

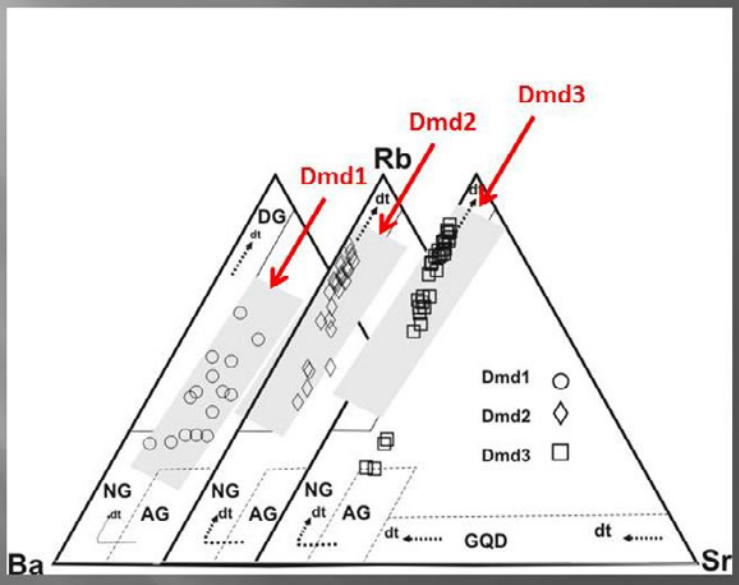

El Bouseilly and Sokkary (1975); modified after McLeod, (1990)

13

Trace Elements Studies

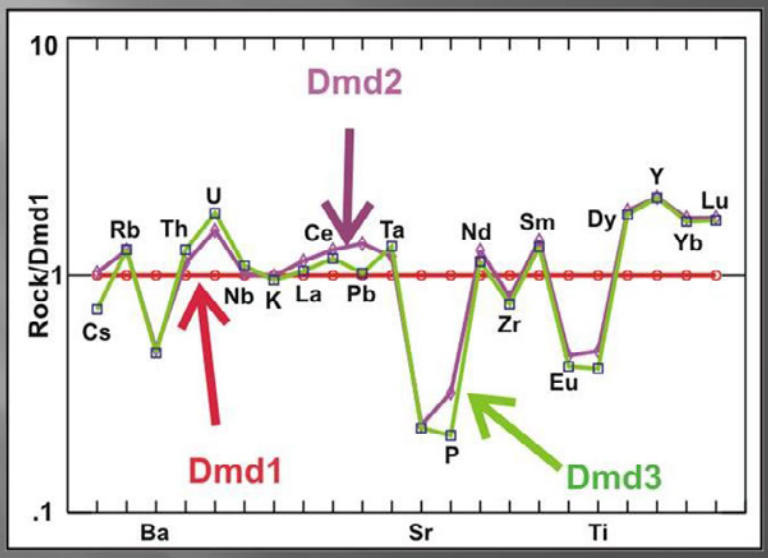

14

Magmatic Temperatures

Zircon-Saturation Temperatures

Watson and Harrison (1983)

$T_{Zr} = 12{,}900/[2.95 + 0.85M + \ln(496{,}000/Zr_{melt})]$

$M = [(Na + K + 2 \cdot Ca)/(Al \cdot Si)]$

	Dmd1	Dmd2	Dmd3
T (˚C)	747-826	733-816	729-815
M	1.28-1.64	1.26-1.78	1.11-1.43

15

Magmatic Temperatures

Zircon-Saturation Temperatures

Watson and Harrison (1983)

$T_{Zr} = 12{,}900/[2.95 + 0.85M + \ln(496{,}000/Zr_{melt})]$

$M = [(Na + K + 2 \cdot Ca)/(Al \cdot Si)]$

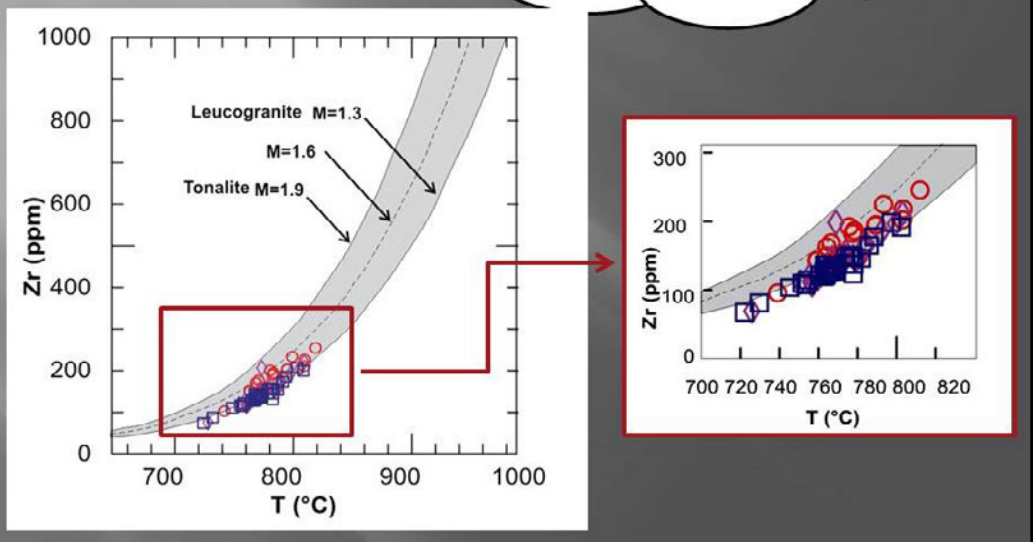

Miller et al. (2012)

16

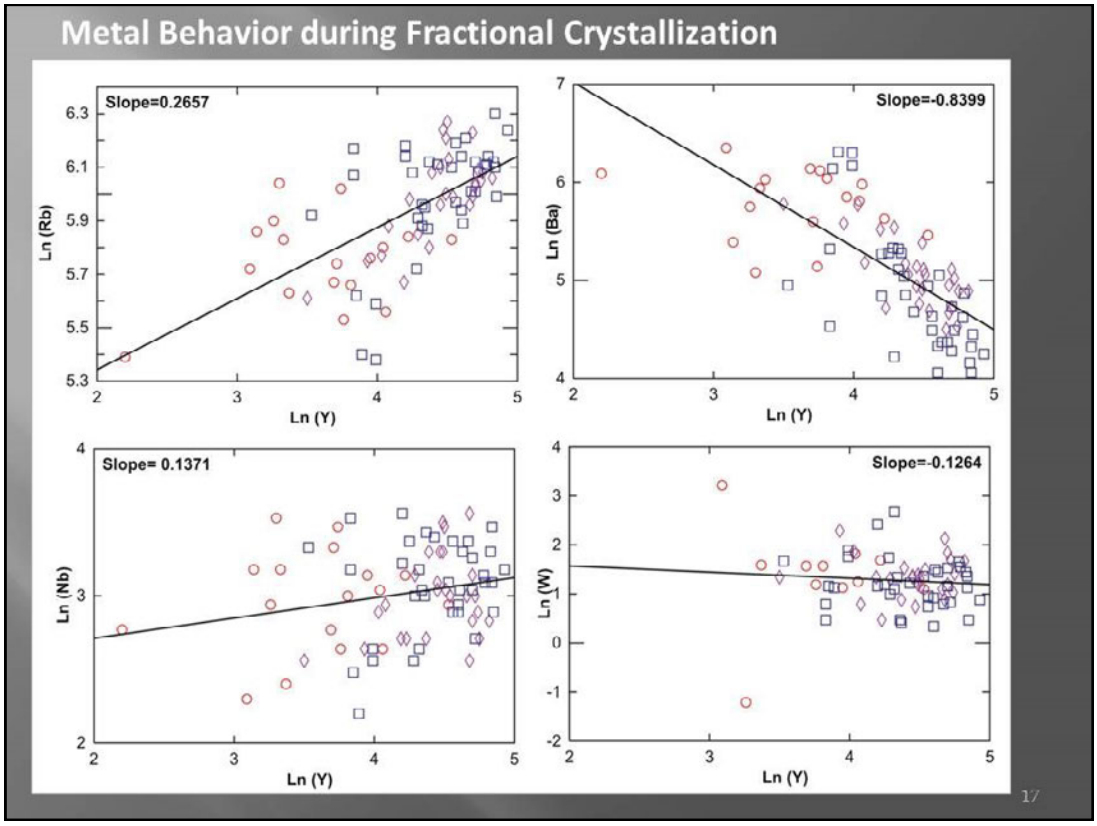
Metal Behavior during Fractional Crystallization
Slope=0.2657
Ln (Rb)
Ln (Y)
Slope=-0.8399
Ln (Ba)
Ln (Y)
Slope= 0.1371
Ln (Nb)
Ln (Y)
Slope=-0.1264
Ln (W)
Ln (Y)
17

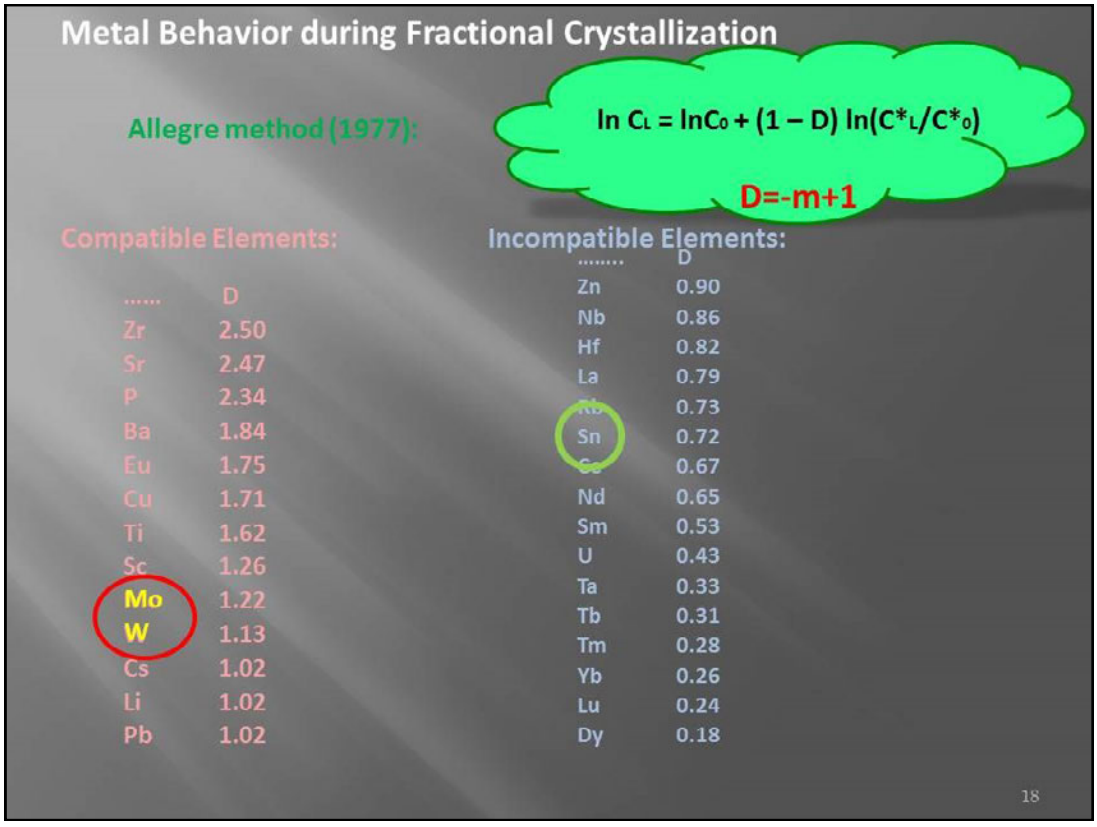
Metal Behavior during Fractional Crystallization
Allegre method (1977):
ln CL = lnC0 + (1 – D) ln(C*L/C*0)
D=-m+1
Compatible Elements:
..... D
Zr 2.50
Sr 2.47
P 2.34
Ba 1.84
Eu 1.75
Cu 1.71
Ti 1.62
Sc 1.26
Mo 1.22
W 1.13
Cs 1.02
Li 1.02
Pb 1.02
Incompatible Elements:
..... D
Zn 0.90
Nb 0.86
Hf 0.82
La 0.79
0.73
Sn 0.72
0.67
Nd 0.65
Sm 0.53
U 0.43
Ta 0.33
Tb 0.31
Tm 0.28
Yb 0.26
Lu 0.24
Dy 0.18
18

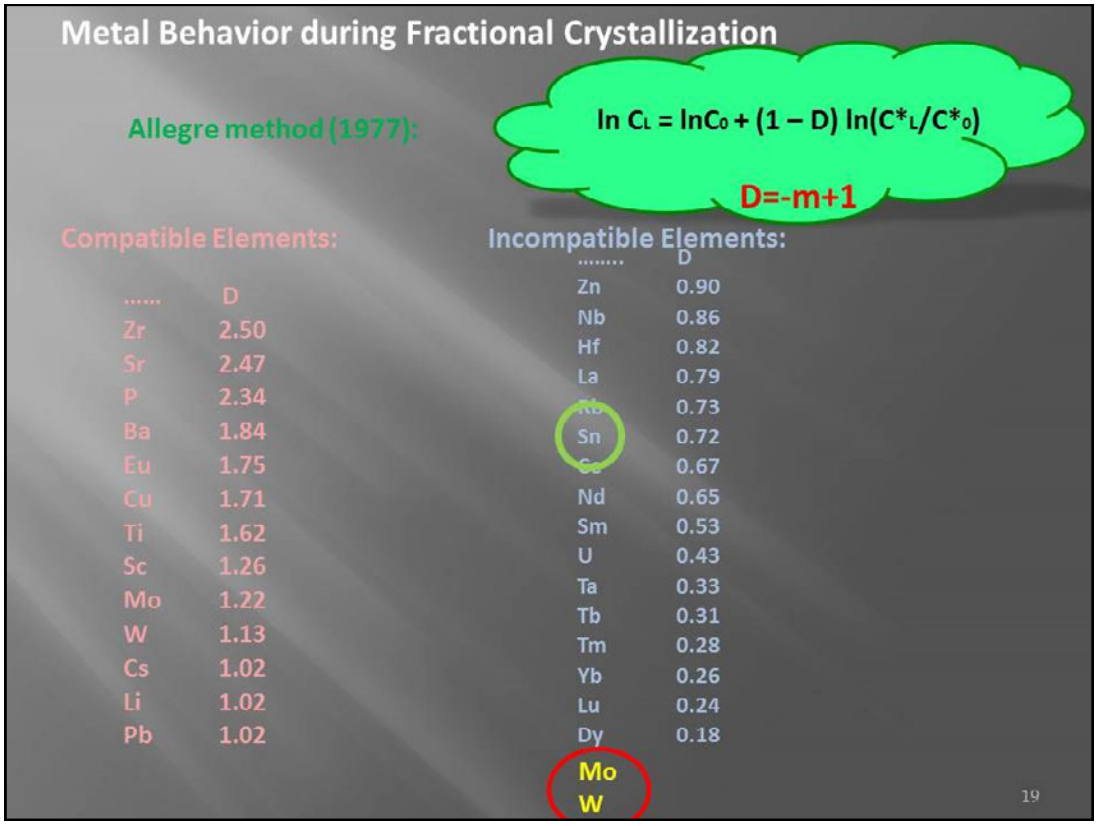
Metal Behavior during Fractional Crystallization
Allegre method (1977):
ln C_L = lnC_0 + (1 – D) ln(C^*_L/C^*_0)
D=-m+1
Compatible Elements:
..... D
Zr 2.50
Sr 2.47
P 2.34
Ba 1.84
Eu 1.75
Cu 1.71
Ti 1.62
Sc 1.26
Mo 1.22
W 1.13
Cs 1.02
Li 1.02
Pb 1.02
Incompatible Elements:
..... D
Zn 0.90
Nb 0.86
Hf 0.82
La 0.79
0.73
Sn 0.72
0.67
Nd 0.65
Sm 0.53
U 0.43
Ta 0.33
Tb 0.31
Tm 0.28
Yb 0.26
Lu 0.24
Dy 0.18
Mo
W
19

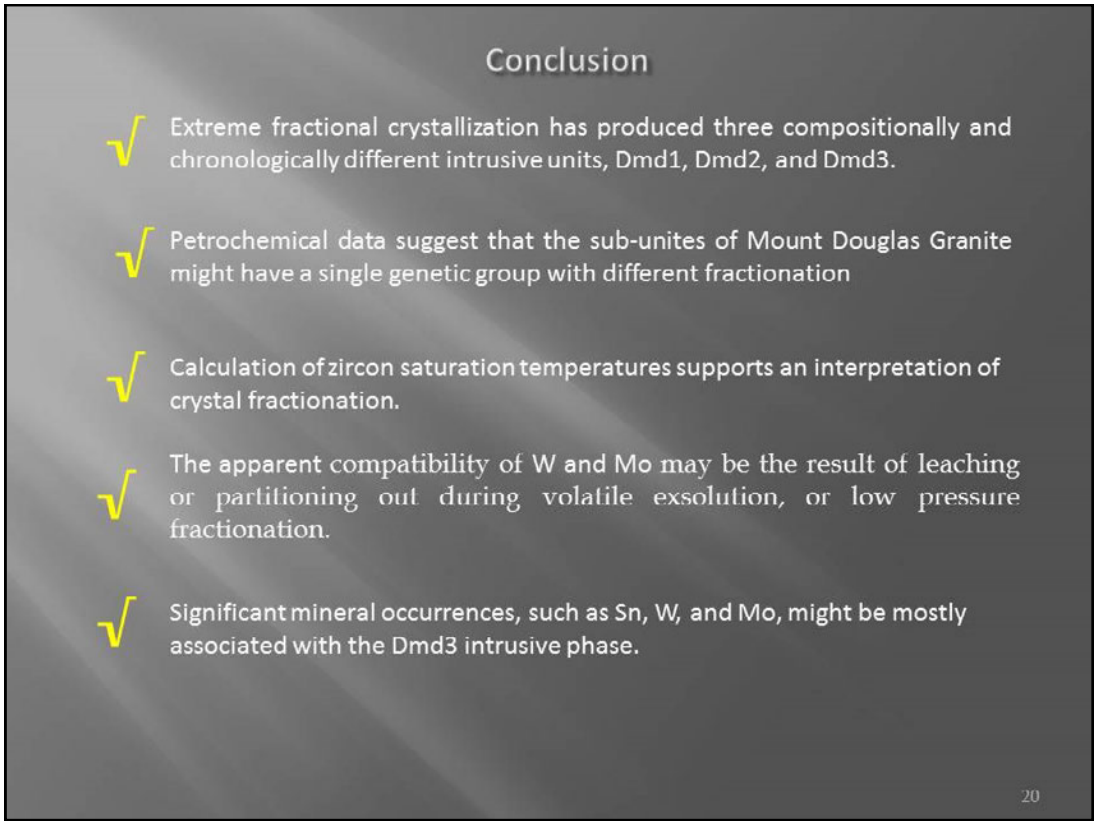
Conclusion
√ Extreme fractional crystallization has produced three compositionally and chronologically different intrusive units, Dmd1, Dmd2, and Dmd3.
√ Petrochemical data suggest that the sub-unites of Mount Douglas Granite might have a single genetic group with different fractionation
√ Calculation of zircon saturation temperatures supports an interpretation of crystal fractionation.
√ The apparent compatibility of W and Mo may be the result of leaching or partitioning out during volatile exsolution, or low pressure fractionation.
√ Significant mineral occurrences, such as Sn, W, and Mo, might be mostly associated with the Dmd3 intrusive phase.
20

Structural and tectonic controls on Devonian intrusion related mineralisation on the Connaigre Peninsula, Newfoundland

G. Ruberti[1], N. Rogers[2], D.A. Kellett[2], C.R. van Staal[3] and J. Hanchar[1]

1. Memorial University of Newfoundland, 300 Prince Philip Drive, St John's, Newfoundland and Labrador
2. Geological Survey of Canada, 601 Booth Street, Ottawa, Ontario
3. Geological Survey of Canada, Vancouver, British Columbia

Abstract: The Canadian Appalachians represent an archetypal ancient, accretionary orogen the study of which has played a substantial role in developing modern geological concepts. From the initial simplistic models of a mountain belt deriving from the closure of the Iapetus Ocean, our understanding has evolved, recognising a richer, more complex geological history. Current models define multiple collisions between arcs and microcontinents due to the closures of interposed oceans and seaways. Delineating specific tectonic events provides context to the various periods and styles of mineralisation produced, which in turn can define new exploration models for the next generation of deposits.

One of the least understood deposit types in the Canadian Appalachians are the Devonian granitoid intrusion-related Sn-W-Mo mineralisation. The Connaigre Peninsula was selected to study such deposits as it contains a variety of supracrustal units plus (apparently) barren and mineralised intrusives within a relatively constrained and accessible area. The distributions of the main lithotectonic packages indicate three distinct tectonic blocks that were amalgamated by the Middle Devonian, and subsequently intruded by Upper Devonian granitoids concurrent with clastic sedimentation.

The ca. 376 Ma Old Woman Stock contains several known Mo occurrences. Molybdenite is disseminated and associated with vugs containing dog-tooth quartz, and intense alteration zones (up to 5 cm wide) are localised along north – south to north-west – south-east trending joints. The distribution of deposits demonstrates a potential linkage between regional structures and the localisation of mineralisation. At the large scale, the Connaigre Peninsula in the Upper Devonian is interpreted to be in extension associated with far removed non-orthogonal accretion of other peri-Gondwanan elements to composite Laurentia. It is notable however that the mineralisation does not occur at a major fault, but rather at the intersection of a prominent north- east to south-west lineament and well-developed north – south to north-west – south-east jointing. The implication is that the high-angle intersection of breaks that are contemporaneous with intrusion but have relatively little motion provide ideal pathways for mineralising fluids.

In contrast to the Old Woman Stock, the adjacent, approximately coeval to slightly younger Belleoram Granite is apparently barren. It remains unclear why the Belleoram Granite contains no known Sn-W-Mo mineralisation. Possible explanations include: i) its hybrid nature makes it compositionally unsuitable; ii) it formed at too shallow a crustal depth; or iii) it was too dry and did not develop fluid pathways.

Originally presented Fredericton 2014: Geological Association of Canada - Mineralogical Association of Canada Joint Annual Meeting, Special Session 3: Discovering the Next Generation of Porphyry Deposits: Advancements in Locating and Understanding Hidden Intrusion-related Mineralization. May 21, 2014.

Corresponding author: Giorgio Ruberti (giorgio.ruberti@mun.ca)

Ruberti, G., Rogers, N., Kellett, D.A., van Staal, C.R., and Hanchar, J., 2015. Structural and tectonic controls on Devonian intrusion related mineralisation on the Connaigre Peninsula, Newfoundland; *in* TGI 4 – Intrusion Related Mineralisation Project: New Vectors to Buried Porphyry-Style Mineralisation, (ed.) N. Rogers; Geological Survey of Canada, Open File 7843, p. 559-560.

Structural and tectonic controls on Devonian intrusion related mineralization on the Connaigre Peninsula, NL

Giorgio Ruberti[1*], Neil Rogers[2], Dawn Kellett[2], Cees van Staal[3] and John Hanchar[2]

[1]Memorial University of Newfoundland, St John's, [2]Geological Survey of Canada, Ottawa, [3]Geological Survey of Canada, Vancouver, *corresponding author - giorgio.ruberti@mun.ca

Intrusion related (e.g., porphyry) deposits are structurally-controlled, low- to medium-grade deposits that provide most of the Cu, Mo, W and Sn extracted worldwide along with significant quantities of Au, Ag, and PGEs. The mineralisation is associated with a variety of igneous rocks, ranging from diorite-granodiorite to high-silica granite, and is typically hosted within stockworks, veins and fractures. Porphyry deposits are associated with a variety of different tectonic settings that determines the metallogenic content.

The Connaigre Peninsula, located at the boundary between two different terranes (Ganderia and Avalonia) that collided during the Acadian orogeny in the Devonian, comprises a variety of collision-related intrusives closely related in space, some of which are barren, others host intrusion-related Sn – W – Mo mineralisations.

Because of these reasons, along with its relatively accessible area, the Connaigre Peninsula has been chosen to study the structural and tectonic controls on the genesis of this family of deposits.

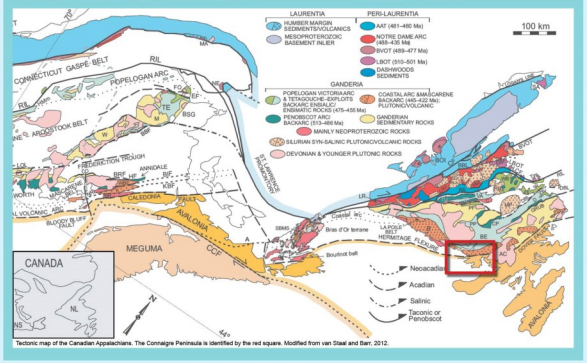

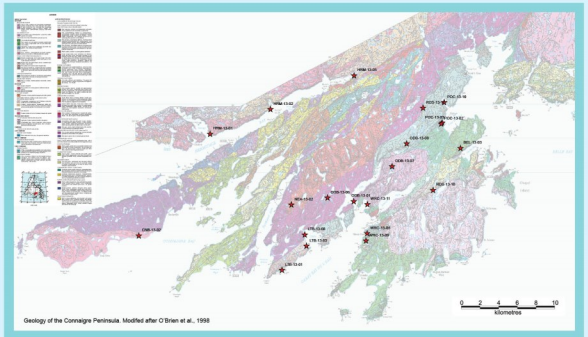

The project involves also the study of the foreland basin of the Acadian orogenic belt, represented in that area by three Devonian formations (Cinq Isles Fm., Pools Cove Fm. and Great Bay de l'Eau Fm.). Dating the sediments, assessing their provenance and deciphering their kinematics should lead to a comprehensive understanding on the collision between Ganderia and Avalonia in Newfoundland.

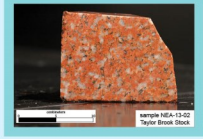

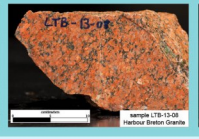

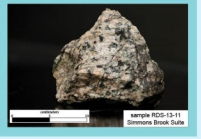

The samples collected so far have been analysed for whole-rock major and trace elements via x-ray fluorescence (XRF) and dilution-inductively coupled plasma mass spectrometry (ICP-MS). They are currently being examined for whole rock tracer isotopes and detrital zircon population via cathodoluminescence (CL) and laser ablation-inductively coupled plasma mass spectrometry (LA-ICP-MS).

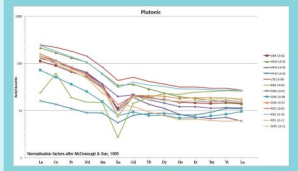

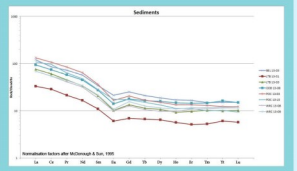

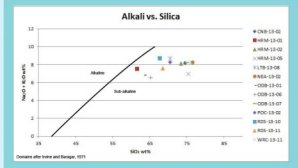

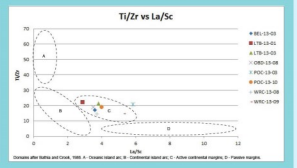

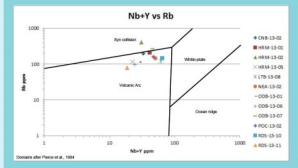

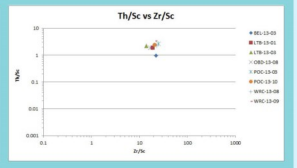

Most of the analysed granitoids show an enrichment in LREE, a generally flat HREE pattern and a variable but ubiquitous negative Eu anomaly.
The alkali vs. silica plot shows the undersaturate nature of the samples while the Nb+Y vs Rb plot highlights the tectonic domain is which they formed. The data are consistent with the tectonic model proposed in the literature (van Staal et al., 2009).

Sediments show a typical Upper Crust REE-chondrite normalized pattern with LREE enrichment, negative Eu anomaly and flat HREE.
The Ti/Zr vs La/Sc values fall in the Active Continental Margin field of Bathia and Crook (1986) and the Th/Sc vs Zr/Sc plot shows moderately high values for Zr/Sc and Th/Sc suggesting a minor component of recycled sediments.

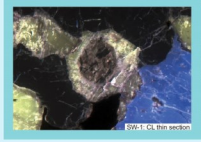

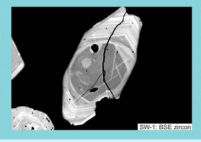

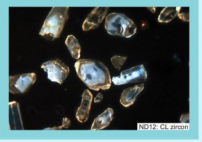

Magmatic mica and its potential as an indicator of magma fertility in the granitoids of New Brunswick

Z. Azadbakht, D.R. Lentz and C.R.M. McFarlane

University of New Brunswick, Box 4400, 2 Bailey Drive, Fredericton, New Brunswick

Abstract: The mineralized intrusions of New Brunswick are related to crustal growth processes that occurred during Acadian Orogeny, post Acadian uplift, and Neo-Acadian Orogeny. They were emplaced pre-, syn-, late-, and post-tectonically between 423 and 360 Ma. These intrusions have affinities ranging from primitive to highly evolved A-, S-, and I-types granitoids, and are associated with Sn, Ta, Li, Sb, W, Mo, Cu, and Au, as well as base-metals and U mineralization.

Biotite crystallizes over a wide range of conditions and reacts very sensitively to physiochemical conditions of the magma; this sensitivity makes mica a great mineral for identifying the petrogenetic, mineralization, and alteration processes of the host granitic rocks. The following features make biotite a valuable probe of magma composition: 1) it is the most important reservoir of any excess aluminium in granites that do not contain modal garnet, cordierite, or the Al_2SiO_5 polymorphs; therefore, it directly reflects the peraluminosity of the host magma in such rocks; 2) it is the most readily available indicator of oxidation state; and 3) it can provide information about the F and Cl content of the magma. Mineralized and barren rocks are characterized by different chemical variations in biotite. For instance, mineralized biotite is characterized by lower Mg and Ti contents relative to biotite from barren rocks; they also have higher amount of Al comparing to biotite from barren phases.

Several studies have shown that biotite, continuously equilibrates with the host liquids. Therefore, core-to-rim study of this mineral and its compositional zoning may provide a record of magma evolution so that the origin and evolution of granitoids can be discerned. Furthermore, the chemical composition and the colour of this mineral strongly reflects the tectonic origin of its host. For instance, the bright red colour of biotite indicates peraluminous collisional granitic pluton and reflects a high total Fe content with low $Fe^{3+}/(Fe^{2+} + Fe^{3+})$ and probably the presence of Ti^{4+}.

In part this study aims to calculate fluoride and chloride activity of aqueous fluids based on F and Cl contents in the minerals containing hydroxyl and halogens determined by combined electron microprobe and LA ICP-MS analysis. The final data will be compared to the whole rock geochemistry. These results are expected to help constrain crystallization conditions, volatile exsolution and fluorine-chlorine activity of fluids associated with these intrusions. They should also indicate the degree of subsolidus re-equilibration via various geothermobarometry techniques.

Originally presented Fredericton 2014: Geological Association of Canada - Mineralogical Association of Canada Joint Annual Meeting. May 23-25, 2014.

Corresponding author: Zeinab Azadbakht (zeinab.azadbakht@unb.ca)

Azadbakht, Z., Lentz, D.R., and McFarlane, C.R.M., 2015. Magmatic mica and its potential as an indicator of magma fertility in the granitoids of New Brunswick; *in* TGI 4 – Intrusion Related Mineralisation Project: New Vectors to Buried Porphyry-Style Mineralisation, (ed.) N. Rogers; Geological Survey of Canada, Open File 7843, p. 561-562.

Magmatic Mica and its Potential as an Indicator of Magma Fertility in the Granitoids of New Brunswick

Zeinab Azadbakht[1], David Lentz[1]
Christopher McFarlane[1], Neil Rogers[2]

[1]University of New Brunswick, Department of Earth Sciences, Fredericton
[2]Geological survey of Canada, Ottawa

Zeinab.azadbakht@unb.ca

Abstract

The mineralized intrusions of New Brunswick are related to crustal growth processes that occurred during Acadian Orogeny, post Acadian uplift, and Neo-Acadian Orogeny. They were emplaced pre-, syn-, late-, and post-tectonically between 423 and 360 Ma. These intrusions have affinities ranging from primitive to highly evolved A-, S-, and I-types granitoids, and are associated with Sn, Ta, Li, Sb, W, Mo, Cu, and Au, as well as base-metals and U mineralization.

Biotite crystallizes over a wide range of conditions and reacts very sensitively to physio-chemical conditions of the magma; this sensitivity makes mica a great mineral for identifying the petrogenetic, mineralization, and alteration processes of the host granitic rocks. The following features make biotite a valuable probe of magma composition: 1) It is the most important reservoir of any excess aluminium in granites that do not contain modal garnet, cordierite, or the Al_2SiO_5 polymorphs; therefore, it directly reflects the peraluminosity of the host magma in such rocks, 2) it is the most readily available indicator of oxidation state, and 3) it can provide information about the F and Cl content of the magma. Mineralized and barren rocks are characterized by different chemical variations in biotite. For instance, mineralized biotite is characterized by lower Mg and Ti contents relative to biotite from barren rocks; they also have higher amount of Al comparing to biotite from barren phases.

Several studies have shown that biotite, continuously equilibrates with the host liquids. Therefore, core-to-rim study of this mineral and its compositional zoning may provide a record of magma evolution so that the origin and evolution of granitoids can be discerned. Furthermore, the chemical composition and the colour of this mineral strongly reflects the tectonic origin of its host. For instance, the bright red colour of biotite indicates peraluminous collisional granitic pluton and reflects a high total Fe content with low $Fe^{3+}/(Fe^{2+}+Fe^{3+})$ and probably the presence of Ti^{4+}.

In part this study aims to calculate fluoride and chloride activity of aqueous fluids based on F and Cl contents in the minerals containing hydroxyl and halogens determined by combined electron microprobe and LA ICP-MS analysis. The final data will be compared to the whole rock geochemistry. These results are expected to help constrain crystallization conditions, volatile exsolution and fluorine-chlorine activity of fluids associated with these intrusions. They should also indicate the degree of subsolidus re-equilibration via various geothermobarometry techniques.

Introduction

Mica group minerals are among the most common mafic minerals of intermediate to felsic igneous rocks; they can also be found in most metamorphic and some sedimentary rocks. Among them, biotite is particularly characteristic of the intermediate rocks of calc alkaline affinities and occurs in a wide range of rocks of hybrid origin (Deer et al. 1992).

Mineralized and barren rocks are characterized by different chemical variations in biotite. For instance, mineralized biotite is characterized by lower Mg and Ti contents relative to biotite from barren rocks; they also have elevated Al contents compared to biotite from barren phases (Boomeri et al. 2010).

Biotite in the granitoids of New Brunswick usually have chlorite and/or muscovite alteration along their cleavages; some are totally replaced by chlorite. They usually contain apatite, zircon, titanite, ilmenite, rutile, and sulfide minerals (e.g., pyrrhotite, pyrite) as mineral inclusions. Their colour also varies from green to brown and reddish brown reflecting differences in their redox conditions (cf. Lalonde and Bernard 1993).

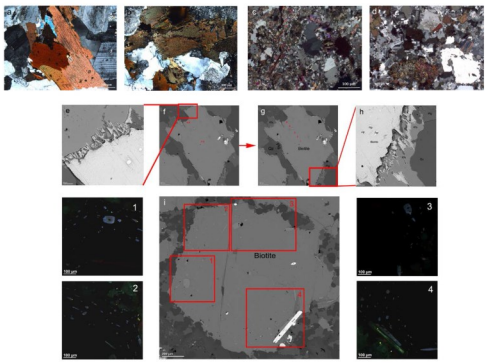

Fig. 1. Photomicrographs, SEM-BSE, and ChromaSEMCL images of some New Brunswick biotite-bearing assemblages illustrating the mineralogy and texture, (a) Olive-green-brown biotite grains show one good cleavage, and contain a pleochroic halo (burn mark) around zircon grains; blue mineral is muscovite. Sample from Skiff Lake granite, (b) Apatite inclusions (gray) in brownish biotite from Redstone granite, (c) Partly altered brownish biotite to muscovite along their cleavages from the Lake George granodiorite, (d) Partly altered brownish biotite to chlorite along their cleavages from the Lake George granodiorite, (e) Mixing texture between potassium feldspar and biotite in a sample from the Lake George granodiorite; this texture was observed in most of the Devonian intrusions of the New Brunswick area, (f) SEM-BSE image of a biotite grain from the Lake George granodiorite indicating the location of microprobe analysing point, (g) The same grain showing the new method of analyzing points for the rest of the intrusions indicated on figure 2, (h) Same texture as e (i) Apatite inclusions in a biotite grain from the Lake George area; boxes 1 to 4 show ChromaSEMCL images of the same grain indicating two different origins for apatite inclusions. Bt= Biotite, Ap= Apatite, Zrn=Zircon, Kfs= Potassium feldspar, Plg=Plagioclase, Qz= Quartz.

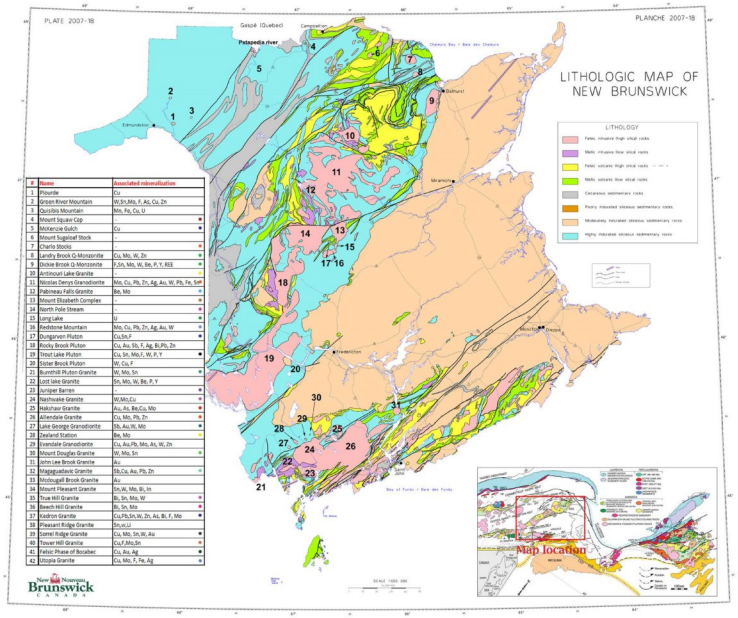

#	Name	Associated mineralization
1	Flourite	Cu
2	Green River Mountain	W,Sn,Mo, F, As, Cu, Zn
3	Quisibis Mountain	Mo, Fe, Cu, U
4	Mount Squaw Cap	-
5	McKenzie Gulch	Cu
6	Mount Sagamaf Stock	-
7	Charlo Stocks	-
8	Landry Brook Q-Monzonite	Cu, Mo, W, Zn
9	Boise Brook Q-Monzonite	F,Sn, Mo, W, Be, P, Y, REE
10	Antinouri Lake Granite	-
11	Nicolas Denys Granodiorite	Mo, Cu, Pb, Zn, Ag, Au, W, Pb, Fe, Sn
12	Palmeau Falls Granite	Be, Mo
13	Mount Elizabeth Complex	-
14	North Pole Stream	-
15	Long Lake	U
16	Redstone Mountain	Mo, Cu, Pb, Zn, Ag, Au, W
17	Dungarvon Pluton	Cu,Sn,F
18	Rocky Brook Pluton	Cu, Au, Sb, F, Ag, Bi,Pb, Zn
19	Trout Lake Pluton	Cu, Sn, Mo,F, W, P, Y
20	Sister Brook Pluton	W, Cu, F
21	Burnthill Pluton Granite	W, Mo, Sn
22	Lost Lake Granite	Sn, Mo, W, Be, P, Y
23	Juniper Barren	-
24	Nashoaka Granite	W,Mo,Cu
25	Hakchaw Granite	Au, As, Be,Cu, Mo
26	Allendale Granite	Cu, Mo, Pb, Zn
27	Lake George Granodiorite	Sb, Au,W, Mo
28	Zealand Station	Be, Mo
29	Irondale Granodiorite	Cu, Au,Pb, Mo, As, W, Zn
30	Mount Douglas Granite	W, Mo, Sn
31	John Lee Brook Granite	Au
32	Magaguadavic Granite	Sb,Cu, Au, Pb, Zn
33	Mcdougall Brook Granite	Au
34	Mount Pleasant Granite	Sn,W, Mo, Bi, In
35	True Hill Granite	Bi, Sn, Mo, W
36	Beech Hill Granite	Bi, Sn, Mo
37	Hodron Granite	Cu,Pb,Sn,W, Zn, Au, Bi, F, Mo
38	Pleasant Ridge Granite	Sn,w,Li
39	Somel Ridge Granite	Cu, Mo, Sn,W, Au
40	Tower Hill Granite	Cu,F,Mo,Sn
41	Felsic Phase of Bocabec	Cu, Au, Ag
42	Utopia Granite	Cu, Mo, F, Fe, Ag

Fig. 2. Geological map of New Brunswick showing the location of Devonian granitoid intrusions and their associated mineralization.

Tectonic setting

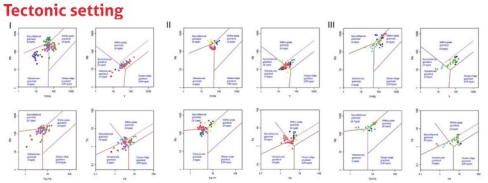

Fig. 3. Tectonomagmatic geochemical discrimination diagrams of New Brunswick Devonian granitoids (data from Whalen (1993)); field boundaries are from Pearce et al. (1984) as modified by Christiansen and Keith (1996); colour code and description is annotated in figure 2 ; (I) 1-16, (II) 17-28 and (III) 29-42.

Laser Ablation ICP-MS

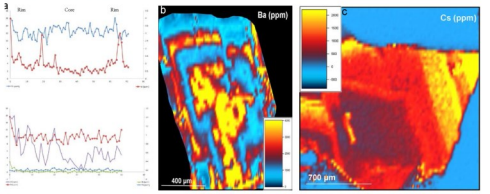

Fig. 4. (a) Trace element results of a laser raster line from rim to rim showing a record of changes in biotite composition during crystallisation, (b) Laser- ICPMS map of a biotite grain from the Mount Douglas granite showing barium zoning, (c) LA-ICPMS map of a biotite grain from the highly fractionated Pleasant Ridge granite showing cesium zoning.

Acknowledgments

The authors thank the many people and organizations who support this PhD research. In particular, we thank Dr. Neil Rogers and Dr. Joseph Whalen of the Geological Survey of Canada and the staff of the NB Dept. of Energy and Mines.

References

Boomeri, M. Nakashima, K. and Lentz, D.R. (2010) The Sarcheshmeh porphyry copper deposit, Kerman, Iran: A mineralogical analysis of the igneous rocks and alteration zones including halogen element systematic related to Cu mineralization processes. Ore Geology Reviews, 38, 367-381.

Christiansen, E.H. and Keith, J.D. (1996) Trace-element systematics in silicic magmas: a metallogenic perspective. In Trace Element Geochemistry of Volcanic Rocks: Applications for Massive Sulfide Exploration. Edited by D.A. Wyman. Geological Association of Canada, Short Course Notes 12, 115– 151.

Deer, W.A., Howie, R.A. and Zussman, J. (1992) An Introduction to Rock Forming Minerals. 2nd edition. Pearson Education Limited.

Lalonde, A. and Bernard, P. (1993) Composition and color of biotite from granites: two useful properties in the characterization of plutonic suites from the Helburn internal zone of Wopmay orogen, Northwest Territories. Canadian Mineralogist, 31, 203-217.

Pearce, J.A., Nigel, B.W. and Tindle, A.G. (1984) Trace Element discrimination diagrams for the tectonic interpretation of granitic rocks. Journal of Petrology, 25, 956-983.

Whalen, J.B. (1993) Geology, Petrography, and Geochemistry of Appalachian Granites in New Brunswick and Gaspesie, Quebec. Geological Survey of Canada Bulletin 436.

Biotite chemistry as a monitor of magma fertility and mineralisation potential: Results from the Devonian granitoids of New Brunswick

Z. Azadbakht[1], D.R. Lentz[1], C.R.M. McFarlane[1] and N. Rogers[2]

1. University of New Brunswick, Box 4400, 2 Bailey Drive, Fredericton, New Brunswick
2. Geological Survey of Canada, 601 Booth Street, Ottawa, Ontario

Abstract: There are over 150 granitoid intrusions in the New Brunswick; however, all the mineralised intrusions formed in relation to Acadian and Neoacadian orogenic phases of Appalachian accretion. These granitoids range in age from 423 to 360 Ma, and include examples of pre-, syn-, late-, and post-tectonic emplacement with affinities ranging from primitive to highly evolved A-, S-, and I-types granitoids along with their hybrid varieties. Many of these are spatially and temporally related to specific styles of mineralization, producing deposits of Sn, Ta, Li, Sb, W, Mo, Cu, and Au, as well as other base-metals and U.

Igneous biotite crystallises over a wide range of conditions and reacts very sensitively to physio-chemical conditions like halogen and oxygen fugacities, pressure, temperature and chemical composition of the magmas. This sensitivity makes biotite a suitable mineral for identifying the petrogenetic processes, mineralization and alteration of the host granitic rocks. The following features make biotite a valuable probe of magma composition: i) It is the most important reservoir of any excess aluminium in granites that do not contain modal garnet, cordierite, or the Al_2SiO_5 polymorphs; therefore, it directly reflects the peraluminosity of the host magma in such rocks; ii) it is the most readily available indicator of oxidation state; and iii) it can provide information about the F and Cl composition of the magma.

Previous studies have shown that biotite, and to lesser extent hornblende and magnetite, continuously equilibrates with host liquids. Consequently, a core-to-rim study of these minerals and their compositional zoning can provide a record of magma evolution so that the origin and evolution of granitoids can be documented.

The aim of this study is to calculate fluoride and chloride activity of aqueous fluids based on measuring F and Cl contents in the minerals containing hydroxyl and halogens, using a combination of electron microprobe and Laser Ablation ICP-MS. These data will be combined and compared with whole-rock trace element geochemistry. The results are expected to help constrain crystallisation conditions, volatile exsolution, and fluorine-chlorine activity of fluids associated with these intrusions, and also to examine the degree of subsolidus re-equilibration using various geothermobarometry techniques. By linking these results to the various styles/types of granitoids and their associated mineralisation it is hoped to establish biotite composition as a robust indicator of an intrusions ore potential.

Originally presented Atlantic Geoscience Society 40th Colloquium and Annual Meeting. Wolfville, NS, February 7-9, 2014.

Corresponding author: Zeinab Azadbakht (zeinab.azadbakht@unb.ca)

Azadbakht, Z., Lentz, D.R., McFarlane, C.R.M., and Rogers, N., 2015. Biotite chemistry as a monitor of magma fertility and mineralisation potential: Results from the Devonian granitoids of New Brunswick; *in* TGI 4 – Intrusion Related Mineralisation Project: New Vectors to Buried Porphyry-Style Mineralisation, (ed.) N. Rogers; Geological Survey of Canada, Open File 7843, p. 563-564.

Biotite Chemistry as a Monitor of Magma Fertility and Mineralisation Potential: Results From the Devonian Granitoids of New Brunswick

Zeinab Azadbakht[1], David Lentz[1]
Christopher McFarlane[1], Neil Rogers[2]

[1]University of New Brunswick, Department of Earth Sciences, Fredericton
[2]Geological survey of Canada, Ottowa

Zeinab.azadbakht@unb.ca

Abstract

There are over 150 granitoid intrusions in the New Brunswick; however, all the mineralised intrusions formed in relation to Acadian and Neo-Acadian orogenic phases of Appalachian accretion. These granitoids range in age from 423 to 360 Ma, and include examples of pre-, syn-, late-, and post-tectonic emplacement with affinities ranging from primitive to highly evolved A-, S-, and I-types granitoids along with their hybrid varieties. Many of these are spatially and temporally related to specific styles of mineralization, producing deposits of Sn, Ta, Li, Sb, W, Mo, Cu, and Au, as well as other base-metals and U.

Igneous biotite crystallises over a wide range of conditions and reacts very sensitively to physio-chemical conditions like halogen and oxygen fugacities, pressure, temperature and chemical composition of the magmas. This sensitivity makes biotite a suitable mineral for identifying the petrogenetic processes, mineralization and alteration of the host granitic rocks. The following features make biotite a valuable probe of magma composition: i) It is the most important reservoir of any excess aluminium in granites that do not contain modal garnet, cordierite, or the Al_2SiO_5 polymorphs; therefore, it directly reflects the peraluminosity of the host magma in such rocks; ii) it is the most readily available indicator of oxidation state; and iii) it can provide information about the F and Cl composition of the magma.

Previous studies have shown that biotite, and to lesser extent hornblende and magnetite, continuously equilibrates with host liquids. Consequently, a core-to-rim study of these minerals and their compositional zoning can provide a record of magma evolution so that the origin and evolution of granitoids can be documented.

The aim of this study is to calculate fluoride and chloride activity of aqueous fluids based on measuring F and Cl contents in the minerals containing hydroxyl and halogens, using a combination of electron microprobe and Laser Ablation ICP-MS. These data will be combined and compared with whole-rock trace element geochemistry. The results are expected to help constrain crystallisation conditions, volatile exsolution, and fluorine-chlorine activity of fluids associated with these intrusions, and also to examine the degree of subsolidus re-equilibration using various geothermobarometry techniques. By linking these results to the various styles/types of granitoids and their associated mineralisation it is hoped to establish biotite composition as a robust indicator of an intrusions ore potential.

Introduction

Mica group minerals are among the most common mafic minerals of intermediate to felsic igneous rocks; they can also be found in most of metamorphic and some of sedimentary rocks. Among them, biotite is particularly characteristic of the intermediate rocks of calc alkaline affinities and occurs in a wide range of rocks of hybrid origin (Deer et al. 1992).

Mineralized and barren rocks are characterized by different chemical variations in biotite. For instance, mineralized biotite is characterized by lower Mg and Ti contents relative to biotite from barren rocks; they also have higher amount of Al comparing to biotite from barren phases (Boomeri et al. 2010).

Biotites in the granitoid of New Brunswick area usually altered to chlorite and to some extent muscovite along their cleavages, and some of them totally replaced by chlorite; they usually contain apatite, zircon, titanite, ilmenite, rutile, and sulfide minerals (e.g., pyrrhotite, pyrite) as mineral inclusions. Their colour also varies from green to brown and reddish brown reflecting differences in their redox conditions (cf. Lalonde and Bernard 1993).

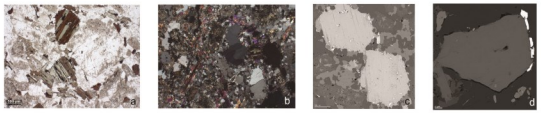

Fig. 1. Photomicrographs and SEM-BSE images of some New Brunswick biotite-bearing assemblages illustrating the mineralogy and texture. (a) Partly altered brownish biotite to chlorite along their cleavages, Lake George granodiorite, sample 1567, PPL, (b) Partly altered brownish biotite to muscovite along their cleavages, Lake George granodiorite, sample 612, XPL, (c) Apatite inclusions (BSE, bright gray) in a biotite grain from the Lake George granodirite, sample 1647, (d) Pyrrhotite crystals (white) adjacent to a biotite grain from the Lake George granodiorite, sample 1190.

Tectonic setting

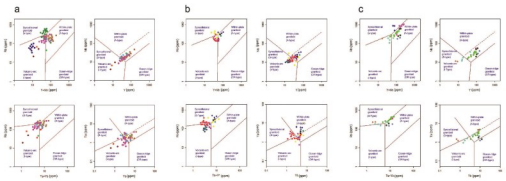

Fig. 2. Tectonomagmatic discrimination diagrams of New Brunswick Devonian granitoids data from Whalen (1993).Field boundaries are from Pearce et al. (1984) as modified by Christiansen and Keith (1996); colour code and description is annotated in figure 3; (a) 1-16, (b) 17-28 and (c) 29-42.

Future studies

(a) Calculating zircon saturation temperature, (b) calculating apatite saturation temperature, (c) studying zoning in plagioclase, (d) apatite, and (e) zircon and trying to correlate their zoning in order to better understanding the history of magma evolution, (f) calculation of the trace element distribution and partition coefficient of elements between K-feldspar and biotite, (g) trace element mapping of the studied grains (h) U-Pb dating of all the intrusions (zircon &/or monazite) that are imaged by SEM-BSE and ChromaSEMCL, (i) analyzing the studied grains using laser from rim to rim, and calculating trace element distribution between whole rock and biotite grains, (j) Advancing the LIBS method done at the University of New Brunswick.

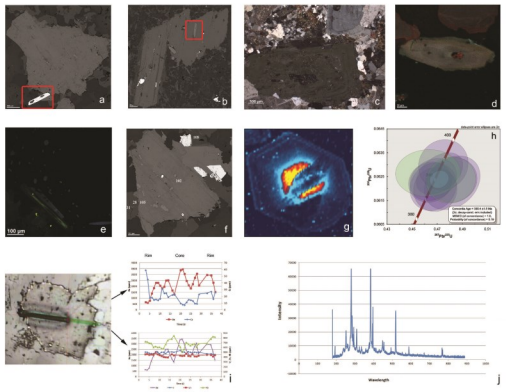

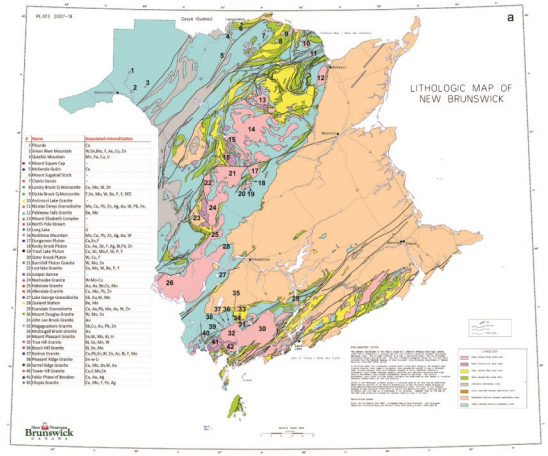

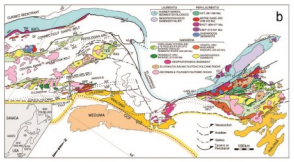

Fig. 3. Geological map of New Brunswick showing the location of Devonian granitoid intrusions and their associated mineralization, (b) Geology of the Canadian and adjacent New England Appalachians with the geographical distribution of the major tectonic elements discussed in text; A, Arisaig Group;AC, Ackley granite; B, Burgeo batholith; BB, Badger basin; BBF, Bamford Brook fault; BBL, Baie Verte Brompton Line; BVDT, Baie Verte oceanic tract; CCF, CobequidChedabucto fault; CF, Cabot fault; CL, Chain Lakes Massif; CO, Cookson Group; DBL, Dog Bay Line; FO,Fournier Group; F, Fogo Island pluton; GBF, Green Bay fault;GRUB, Gander River ultrabasic belt; HH, Hodges Hill pluton; LBDT, Lushs Bight oceanic tract; MP, Mount Peyton pluton; RBF, Rocky Brook–Millstream fault system;RF, Restigouche fault; RIL, Red Indian Line; SGB, St. George batholith; SM, South Mountain batholith; U, Utopia granite; VA, Victoria arc; TP, Tally Pond Group. (van Staal et al. 2009)

Acknowledgment

The authors thank the many people and organizations who support this PhD research. In particular, we thank Dr. Neil Rogers of the Geological Survey of Canada and the staff of the NB Dept. of Energy and Mines.

References

Boomeri, M, Nakashima, K. and Lentz, D.R. (2010) The Sarcheshmeh porphyry copper deposit, Kerman, Iran: A mineralogical analysis of the igneous rocks and alteration zones including halogen element systematic related to Cu mineralization processes. Ore Geology Reviews, 38, 367-381

Christiansen, E.H. and Keith, J.D. (1989) Trace-element systematics in silicic magmas: a metallogenic perspective. In Trace Element Geochemistry of Volcanic Rocks: Applications for Massive Sulfide Exploration. Edited by D.A. Wyman. Geological Association of Canada, Short Course Notes 12, 115– 151

Deer, W.A., Howie, R.A. and Zussman, J. (1992) An Introduction to Rock-Forming Minerals. 2nd edition. Pearson Education Limited

Lalonde, A. and Bernard, P. (1993) Composition and color of biotite from granites: two useful properties in the characterization of plutonic suites from the Hefburn internal zone of Wopmay orogen, Northwest Territories. Canadian Mineralogist, 31, 203-217

Pearce, J.A., Nigel, B.W. and Tindle, A.G. (1984) Trace Element discrimination diagrams for the tectonic interpretation of granitic rocks. Journal of Petrology, 25, 956-983

van Staal, C.R., Whalen, J.B., Valverde-Vaquero, P., Zagorevski, A. and Rogers, N. (2009) Pre-Carboniferous, episodic accretion-related, orogenesis along the Laurentian margin of the northern Appalachians. Geological Society Special Publication 327, 271-316

Whalen, J.B. (1993) Geology, Petrography, and Geochemistry of Appalachian Granites in New Brunswick and Gaspesie, Quebec. Geological Survey of Canada Bulletin 436

Magmatic biotite and its use to distinguish barren and mineralized granitic systems in New Brunswick, Canada

Z. Azadbakht, D.R. Lentz and C.R.M. McFarlane

University of New Brunswick, Box 4400, 2 Bailey Drive, Fredericton, New Brunswick

Abstract: Forty-two different Devonian granitoid intrusions in New Brunswick were studied for this project. They formed by crustal growth processes during the Acadian orogeny, post-Acadian uplift, and Neoacadian orogeny and most are associated with granophile element deposits, such as Sn, W, Mo, Cu, Bi, In, Sb, Au, and possibly Ta and Li, as well as base-metals and U mineralization. These intrusions were emplaced pre-, syn-, late-, and post-tectonically between 423 and 360 Ma with affinities ranging from primitive to highly evolved A-, S-, and I-types granitoids.

The aim of this study is to find a way to differentiate barren and mineralized granitic systems using biotite compositional systematics since it is highly sensitive to physico-chemical changes of its host, and continuously re-equilibrates with host and derivative fluids. Therefore, core to rim studies of this mineral and analysis of its compositional zoning may reveal the origin and evolution history of the hosting granitoid and the different types of associated mineralization. Mineralized and barren granitoids are characterized by different chemical variations in biotite. For instance, biotite from a mineralized granitoid is characterized by lower Mg and Ti, and higher Al content relative to biotite from a barren granitoid. A combination of electron microprobe (EPMA) and laser ablation ICP-MS (LA-ICP-MS) was used to identify major, minor, trace elements, and halogen contents of biotite; these results were used to calculate fluoride and chloride activity of aqueous fluids associated with these intrusions, based on F and Cl contents in the mineral.

Microprobe studies indicated homogeneous intragranular major element composition; crystallization temperature was calculated using Ti-In-biotite geothermometer, which gave a range of 670 to 750 ± 25°C . However, hydroxyl exchange biotite-apatite thermometer confirmed sub-solidus processes disturbed these systems resulting in a lower temperature around 300. Biotite grains from the highly fractionated bodies of the Pleasant Ridge, Mount Pleasant, and Kedron granites show the highest fluorine contents, ranging from 4.5 wt.% to 6.5 wt.%.

Trace element changes within the biotite lattice were measured using LA-ICP-MS. Interestingly, almost all of studied grains show Cs, Ba, and Rb zoning relative to K. These patterns were followed by Co, Cu, K, Li, Be, Sn, W, Ti, Sc, Ni, B, and V. Large ionic charge and radius make it difficult for elements to join or leave any crystalline structure; therefore, any Cs or Ba zoning could be of an igneous origin. As a result, any other elemental pattern following those could be a result of magmatic evolution, which has been recorded by the biotite crystal growth.

Based on the results of this project, the concept of using biotite composition to help identify fertile Acadian magma systems has been established; however, more work needs to be done to define characteristics of different magmatic processes.

Originally presented Exploration, Mining and Petroleum New Brunswick Conference 2014. November 3, 2014.

Corresponding author: Zeinab Azadbakht (zeinab.azadbakht@unb.ca)

Azadbakht, Z., Lentz, D.R., and McFarlane, C.R.M., 2015. Magmatic biotite and its use to distinguish barren and mineralized granitic systems in New Brunswick, Canada; *in* TGI 4 – Intrusion Related Mineralisation Project: New Vectors to Buried Porphyry-Style Mineralisation, (ed.) N. Rogers; Geological Survey of Canada, Open File 7843, p. 565-566.

Magmatic Biotite and Its Use to Distinguish Barren and Mineralized Granitic Systems in New Brunswick, Canada

Zeinab Azadbakht[1], David Lentz[1]
Christopher McFarlane[1], Neil Rogers[2]

[1]University of New Brunswick, Department of Earth Sciences, Fredericton
[2]Geological survey of Canada, Ottawa

Zeinab.azadbakht@unb.ca

Abstract

Forty-two different Devonian granitoid intrusions in New Brunswick were studied for this project. They formed by crustal growth processes during the Acadian orogeny, post Acadian uplift, and Neo-Acadian orogeny and most are associated with granophile element deposits, such as Sn, W, Mo, Cu, Bi, In, Sb, Au, and possibly Ta and Li, as well as base-metals and U mineralization. These intrusions were emplaced pre-, syn-, late-, and post-tectonically between 423 and 360 Ma with affinities ranging from primitive to highly evolved A-, S-, and I-types granitoids.

The aim of this study is to find a way to differentiate barren and mineralized granitic systems using biotite compositional systematics since it is highly sensitive to physico-chemical changes of its host, and continuously re-equilibrates with host and derivative fluids. Therefore, core to rim studies of this mineral and analysis of its compositional zoning may reveal the origin and evolution history of the hosting granitoid and the different types of associated mineralization. Mineralized and barren granitoids are characterized by different chemical variations in biotite. For instance, biotite from a mineralized granitoid is characterized by lower Mg and Ti, and higher Al content relative to biotite from a barren granitoid. A combination of electron microprobe (EPMA) and laser-ablation ICP-MS (LA-ICP-MS) was used to identify major-, minor-, trace-elements, and halogen contents of biotite; these results were used to calculate fluoride and chloride activity of aqueous fluids associated with these intrusions, based on F and Cl contents in the mineral.

Microprobe studies indicated homogeneous intragranular major element composition; crystallization temperature was calculated using Ti-in-biotite geothermometer, which gave a range of 670 to 750±25C. However, hydroxyl exchange biotite-apatite thermometer confirmed sub-solidus processes disturbed these systems resulting in a lower temperature around 300C. Biotite grains from the highly fractionated bodies of the Pleasant Ridge, Mount Pleasant, and Kedron granites show the highest fluorine contents, ranging from 4.5 wt.% to 6.5 wt.%.

Trace element changes within the biotite lattice were measured using LA-ICP-MS. Interestingly, almost all of studied grains show Cs, Ba, and Rb zoning relative to K. These patterns were followed by Co, Cu, K, Li, Be, Sn, W, Ti, Sc, Ni, B, and V. Large ionic charge and radius make it difficult for elements to join or leave any crystalline structure; therefore, any Cs or Ba zoning could be of an igneous origin. As a result, any other elemental pattern following those could be a result of magmatic evolution, which has been recorded by the biotite crystal growth.

Based on the results of this project, the concept of using biotite composition to help identify fertile Acadian magma systems has been established; however, more work needs to be done to define characteristics of different magmatic processes.

Introduction

Mineralized and barren rocks are characterized by different chemical variations in biotite. For instance, biotite grains from mineralized intrusions are characterized by lower Mg and Ti contents relative to biotite from barren intrusions; they also have elevated Al content compared to biotite from barren intrusions (Boomeri et al. 2010).

Biotite in the granitoids of New Brunswick usually have chlorite and/or muscovite alteration along their cleavages; some are totally replaced by chlorite. They usually contain apatite, zircon, titanite, ilmenite, rutile, and sulfide minerals (e.g., pyrrhotite, pyrite) as mineral inclusions. Their colour also varies from green to brown and reddish brown reflecting differences in their redox conditions (cf. Lalonde and Bernard 1993).

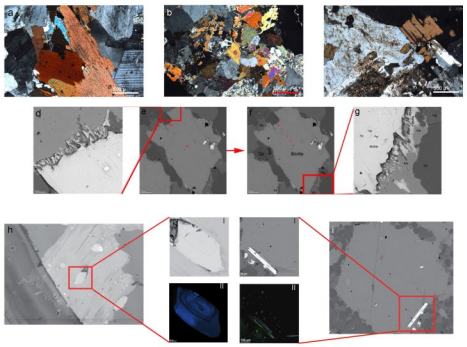

Fig. 1. Photomicrographs, SEM-BSE, and ChromaSEMCL images of some New Brunswick biotite-bearing granitoids illustrating the mineralogy and texture. (a) Olive-green-brown biotite grains showing one good cleavage, and contain a pleochroic halo (burn mark) around zircon grains; blue mineral is muscovite (sample WX-NB-12 from Swift Lake granite). (b) Altered brownish biotite to muscovite (sample WX-NB-8 from Hawkshaw granite). (c) Partly altered brownish biotite to chlorite along their cleavages (sample WX-NB-4 from Hawkshaw granite). (d) Mixing texture between potassium feldspar and biotite in sample LG 80-33A from Lake George granodiorite; this texture was observed in most of the Devonian intrusions of the New Brunswick area. (e) SEM-BSE image of a biotite grain from Lake George granodiorite indicating the location of microprobe analyzing point (1-3, 4-6). (f) The same grain showing the new method of analyzing points for the rest of the intrusions indicated on figure 2. (g) Same texture as d. (h) Apatite inclusions in a biotite grain (sample WX-NB-196 from Magaguadavic granite); SEM-BSE image (I), and ChromaSEMCL image (II) of the same grain indicating six different growth zones for the apatite inclusion. (i) Zircon inclusions in a biotite grain (sample LG-1647 from Lake George granodiorite); SEM-BSE image (I), and ChromaSEMCL image (II) of the same grain indicating different growth zones for the zircon inclusion. Bt= Biotite, Ap= Apatite, Zrn=Zircon, Kfs= Potassium feldspar, Plg=Plagioclase, Qz= Quartz.

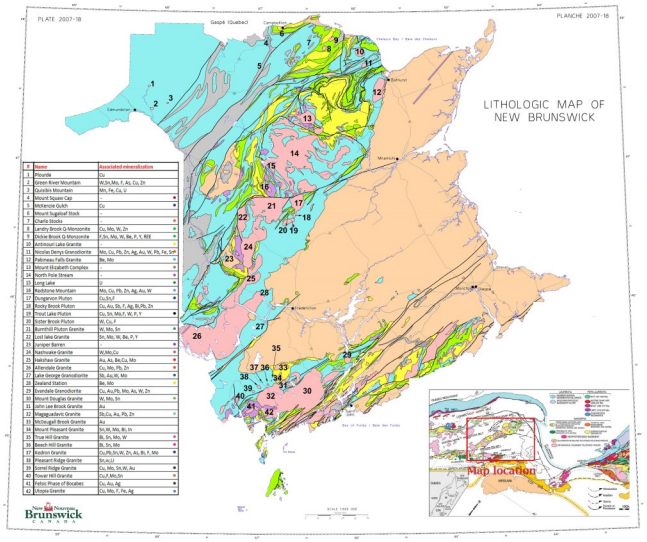

Fig. 2. Geological map of New Brunswick showing the location of Devonian granitoid intrusions and their associated mineralization

Tectonic Settings

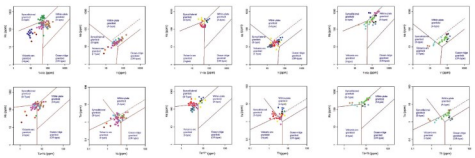

Fig. 3. Tectonomagmatic geochemical discrimination diagrams of New Brunswick Devonian granitoids (data from Whalen (1993)); field boundaries are from Pearce et al. (1984) as modified by Christiansen and Keith (1996); colour code and description is annotated in figure 2 ; (I) 1-16, (II) 17-28 and (III) 29-42.

Laser Ablation ICP-MS

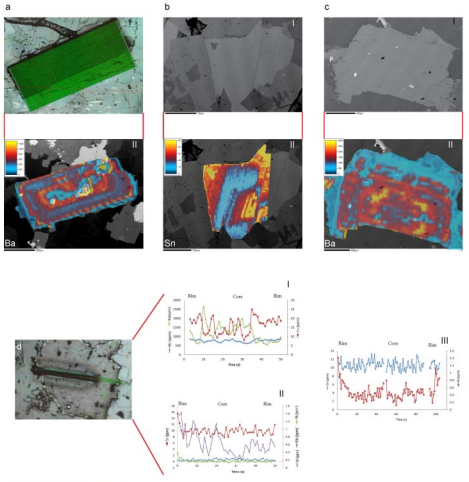

Fig. 4. (a) A photomicrograph of a biotite grain showing the laser ablation-ICPMS pattern (I), and corresponding SEM-BSE image with overlaying Ba laser ablation-ICPMS map of the same grain (II), sample from Mount Douglas granite, (b) SEM-BSE image (I) and the corresponding overlaying Cs laser ablation-ICPMS map (II) of a biotite grain from the highly fractionated Pleasant Ridge granite, (c) SEM-BSE image (I) and the corresponding overlaying Ba laser ablation-ICPMS map (II) of a biotite grain from Dungarvon granite, (d) A biotite grain showing a laser raster line from rim to rim (the green line); results (I to III) represent trace element changes in magma composition during crystallization.

Acknowledgments

The authors thank the many people and organizations who support this PhD research. In particular, we thank Dr. Neil Rogers and Dr. Joseph Whalen of the Geological Survey of Canada and the staff of the NB Dept. of Energy and Mines.

References

Boomeri, M. Nakashima, K. and Lentz, D.R. (2010) The Sarcheshmeh porphyry copper deposit, Kerman, Iran: A mineralogical analysis of the igneous rocks and alteration zones including halogen element systematic related to Cu mineralization processes. Ore Geology Reviews, 38, 367-381.

Christiansen, E.H. and Keith, J.D. (1996) Trace-element systematics in silicic magmas: a metallogenic perspective. In Trace Element Geochemistry of Volcanic Rocks: Applications for Massive Sulfide Exploration. Edited by D.A. Wyman. Geological Association of Canada, Short Course Notes 12, 115– 151.

Lalonde, A. and Bernard, P. (1993) Composition and color of biotite from granites: two useful properties in the characterization of plutonic suites from the Hefburn Internal zone of Wopmay orogen, Northwest Territories. Canadian Mineralogist, 31, 203-217.

Pearce, J.A., Nigel, B.W. and Tindle, A.G. (1984) Trace Element discrimination diagrams for the tectonic Interpretation of granitic rocks. Journal of Petrology, 25, 956-983.

Whalen. J.B. (1993) Geology, Petrography, and Geochemistry of Appalachian Granites in New Brunswick and Gaspesie, Quebec. Geological Survey of Canada Bulletin 436.

Sn-W-Mo polymetallic behaviour during magmatic evolution of Late Devonian Mount Douglas leucogranites, southwestern New Brunswick, Canada

N. Mohammadi[1], D.R. Lentz[1] and K.G. Thorne[2]

1. University of New Brunswick, Box 4400, 2 Bailey Drive, Fredericton, New Brunswick
2. Geological Surveys Branch, New Brunswick Department of Energy and Mines, PO Box 6000, Fredericton, New Brunswick

Abstract: The Mount Douglas intrusive suite consists of an assemblage of peraluminous leucogranites located along the eastern part of the Saint George Batholith in southwestern New Brunswick, Canada. This late Devonian suite extends from Red Rock Lake to Mount Douglas, and is interpreted to represent the subvolcanic portion of the Mount Pleasant Sn-W-Mo-Bi-In-Zn deposits. The magmatic systems in the Mount Douglas suite have undergone extreme differentiation producing three distinct phases, including Dmd1, Dmd2, and Dmd3, and are associated with various granophile-element occurrences, such as Sn, W, and Mo. It seems the three phases might originate from a single source that evolves with increasing fractionation from the earliest unit (Dmd1) to the youngest unit (Dmd3).

Metal behavior during fractional crystallization is one of the most important factors affecting the types of mineral occurrences associated with the Mount Douglas granites. To establish the metal behavior in the Mount Douglas suite, analytical data from Malcolm McLeod's 1990 report was used in this study. The most incompatible element, Ta, has been selected for defining partition coefficients (D) using the Allegre method. Based on their D values, as expected, Sn with Rb, Y, Nb, LREE [La, Ce, Nd, and Sm], HREE [Tb, Dy, Tm, Yb, and Lu], Pb, Th, and U behave as incompatible elements; showing the Mount Douglas Granite could be considered for exploration of Sn deposits as previous studies have mentioned. However, W and Mo accompanied with the other elements, such as Li, P, Sc, Ti, Cu, Zn, Sr, Zr, Cs, Ba, Eu, and Hf seem to act as compatible elements during magmatic evolution, although melt - supercritical fluid evolution can easily affect W, Mo, Cs, and Li abundances. The apparent compatibility of W and Mo is in contrast with the expected results in which they might act as incompatible elements for developing considerable potential for W-Mo deposits. However, W and Mo concentrations increased with the degree of fractionation and show a significant enrichment in the Mount Douglas granites relative to other granitoid suites in the region; thus their compatibility may be the result of leaching or partitioning out during volatile exsolution, or low pressure fractionation. Furthermore, very low K/Rb (average 102.7), Nb/Ta (≤ 6.83), and Zr/Hf (≤ 35.58) ratios, and high Ti/Sc (125.3 ≤) ratio in Dmd3 compared to Dmd1 possibly reflect significant involvement of extreme low T crystal fractionation or even fluid fractionation in the last-stage magmatic differentiation. Consequently, although much more analytical data are needed for exact evaluation of the mineral occurrences in the Mount Douglas Granites, Dmd3 as the most highly differentiated phases might be considered a superior candidate for hosting of Sn-W-Mo deposits.

Originally presented Exploration, Mining and Petroleum New Brunswick Conference 2014. November 1-3, 2014.

Corresponding author: Nadieh Mohammadi (Nadia.mohammadi@unb.ca)

Mohammadi, N., Lentz, D.R., and Thorne, K.G., 2015. Sn-W-Mo polymetallic behaviour during magmatic evolution of Late Devonian Mount Douglas leucogranites, southwestern New Brunswick, Canada; *in* TGI 4 – Intrusion Related Mineralisation Project: New Vectors to Buried Porphyry-Style Mineralisation, (ed.) N. Rogers; Geological Survey of Canada, Open File 7843, p. 567-568.

Sn-W-Mo-Polymetallic Behaviour during Magmatic Evolution of Late Devonian Mount Douglas Leucogranites, Southwestern New Brunswick, Canada

By Nadia Mohammadi,[1] David Lentz[1] and Kathleen Thorne[2]
[1]University of New Brunswick, [2]New Brunswick Department of Energy and Mine

ABSTRACT

Metal behavior during fractional crystallization is one of the most important factors affecting the types of mineral occurrences associated with the Mount Douglas granites. The most incompatible element, Ta, has been selected for defining partition coefficients (D) using the Allegre method. Based on their D values, Sn behaves as incompatible elements; showing the Mount Douglas Granite could be considered for exploration of Sn deposits. However, W and Mo act as compatible elements during magmatic evolution, although melt-supercritical fluid evolution can easily affect W, Mo, Cs, and Li abundances. The apparent compatibility of W and Mo is in contrast with the expected results in which they might act as incompatible elements for developing considerable potential for W-Mo deposits. However, W and Mo concentrations increased with the degree of fractionation and show a significant enrichment in the Mount Douglas granites relative to other granitoid suites in the region; thus their compatibility may be the result of leaching or partitioning out during volatile exsolution, or low pressure fractionation.

CONTACT

Name: Nadia Mohammadi
Organization: University of New Brunswick,
Department of Earth Sciences, Fredericton, NB E3B5A3
Email: nadia.mohammadi@unb.ca

ACKNOWLEDMENTS

This project supported by NB Energy and Mines, a President's Doctoral scholarship (NM), and a NB Innovation Fund award (NM). DL is supported by a NSERC Discovery grant.

INTRODUCTION

The Mount Douglas intrusive suite consists of an assemblage of peraluminous leucogranites located along the eastern part of the Saint George Batholith in southwestern New Brunswick, Canada (Fig. 1). This late Devonian suite extends from Red Rock Lake to Mount Douglas, and is interpreted to represent the subvolcanic portion of the Mount Pleasant Sn-W-M-Bi-In-Zn deposits. The magmatic systems in the Mount Douglas suite have undergone extreme differentiation producing three distinct phases, including Dmd1, Dmd2, and Dmd3, and are associated with various granophile-element occurrences, such as Sn, W, and Mo.

MAJOR AND TRACE ELEMENTS STUDIES

The samples from the Mount Douglas (MD) granites are characterized by high contents (wt.%) of SiO_2 (68-78), K_2O (3.5-7.8), $(Fe_2O_3+FeO)/MgO$ ratio (average 8.7), and alkalis; low CaO and MgO, and very low P_2O_5 and TiO_2. The Dmd3 shows the highest amount of SiO_2 with an average of 76.4 wt. %. With regards to their trace elements, the MD leucogranites are strongly enriched in the incompatible elements, such as F, Li, Rb, Cs, U, Th, and Nb; this enrichment is correlated with an obvious depletion in compatible elements (e.g., Ca, Mg, Ti, Sr, Ba, and Eu). Compared to the Dmd2 and Dmd3, the Dmd1 has the lowest amounts of compatible trace elements, the smallest negative Eu anomalies, as well as Ba, Sr, P, and Ti; however, they have enriched chondrite-normalized REE patterns [$(La/Yb)_N$ = 4.321.8]. Normalized to the least-evolved sample of the MG granites (Dmd1), the Dmd3 unit is the most enriched in Rb, Th, U, Ce, Ta, Pb, Nd, Sm, Dy, Y, Yb, and Lu, and show extreme reduction in Ba, Sr, P, Zr, Eu, and Ti content (Fig. 2), thus reflecting fractionation from Dmd1 to Dmd3. Rb-Ba-Sr diagram (Fig. 3) shows a clear progressive differentiation from Dmd1 to Dmd3. On the plot of Nb vs. Sr (Fig. 4), the samples mainly fall in the field between fractional crystallization and assimilation-fractional crystallization (r= 0.2) curves.

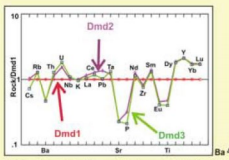

Fig. 2: Enrichment-factor diagram of the three units of the Mount Douglas granites. Dmd1 to Dmd3 data are based on the average composition of all samples from each normalized to Dmd1 as the least-evolved granite.

Fig. 3: A clear progressive differentiation of the Mount Douglas Granites from Dmd1 to Dmd3 on the Rb-Ba-Sr diagram. GQD: granodiorites, quartz diorites, and diorites NG: Normal Granites, DG: Strongly Differentiated Granites, dr: differentiation trend.

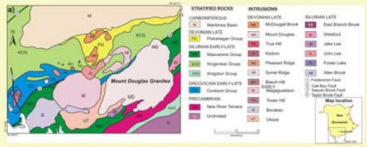

Fig. 1: a. Geological map of southwestern New Brunswick (modified after McLeod et al., 1994) and location of the studied leucogranite suite (Mount Douglas). b. Geological setting of the Mount Douglas suite and the related mineral occurrences (modified after McLeod, 1990).

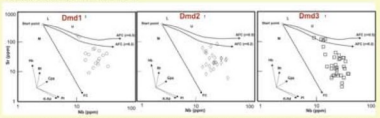

Fig. 4: Nb vs. Sr diagram for granitoid samples of the Mount Douglas Granites. The Mount Douglas samples mainly fall in the field between fractional crystallization and assimilation-fractional crystallization (r=0.2) curves (see Yang et al., 2003).

METAL BEHAVIOUR

To establish the metal behavior in the Mount Douglas suite, analytical data from Malcolm McLeod's report (1990) was used in this study. Ta has been selected for defining partition coefficients (D) using the Allegre method. Based on their D values, Sn with Rb, Y, Nb, LREE [La, Ce, Nd, and Sm], HREE [Tb, Dy, Tm, Yb, and Lu], Pb, Th, and U behave as incompatible elements; however, W and Mo accompanied with the other elements, such as Li, P, Sc, Ti, Cu, Zn, Sr, Zr, Cs, Ba, Eu, and Hf seem to act as compatible elements (Fig. 5). Furthermore, very low K/Rb (average 102.7), Nb/Ta ($\leq$ 6.83), and Zr/Hf ($\leq$ 35.58) ratios, and high Ti/Sc (125.3 $\leq$) ratio in Dmd3 compared to Dmd1 possibly reflect significant involvement of extreme low T crystal fractionation or even fluid fractionation in the last-stage magmatic differentiation.

CONCLUSION

Petrochemical data show that the subunits of Mount Douglas Granites, Dmd1, Dmd2, and Dmd3, have within-plate geochemical character with possibility of hybrid I- and S-type affinity. It seems that they have been produced by fractional crystallization of the same parental magma with different magmatic evolution. Extreme fractional crystallization and fluid involvement during formation of these units have been the most important factors affecting the magma evolution, producing three different units, compositionally. Although W and Mo apparently act as compatible elements comparing to Ta, their concentration increase is accompanied with the degree of fractionation. On the other hand, these metals show a significant enrichment, and their compatibility may be the result of leaching or partitioning out during volatile exsolution. Consequently, although much more analytical data are needed for exact evaluation of the mineral occurrences in the Mount Douglas Granites, Dmd3 as the most highly differentiated phases might be considered for hosting of endogranitic Sn-W-Mo deposits.

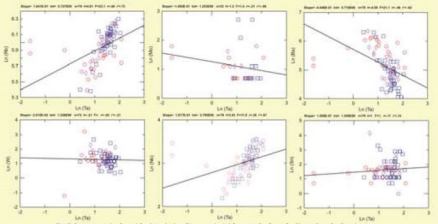

Fig. 5: Representative logarithmic variation diagrams (ppm) for samples from the Mount DouglasGranites.

REFERENCES

Allégre, C.H., Treuil, M., Minster, J.F., Minster, B., and Albarede, F., 1977. Systematic use of trace elements in igneous process, Part I: fractional crystallization processes in volcanic suites. Contributions to Mineralogy and Petrology, 60: 57-75.

Dostal, J., and Chatterjee, A.K., 2000. Contrasting behavior of Nb/Ta and Zr/Hf ratios in a peraluminous granitic pluton (Nova Scotia, Canada). Chemical Geology, 163: 207-218.

El Bouseily, A.M., and El Sokkary, A.A., 1975. The relationship between Rb, Ba and Sr in granitic rocks. Chemical Geology, 16: 207-219.

McLeod, M.J., 1990. Geology, Geochemistry, and Related Mineral Deposits of the Saint George Batholith. Charlotte, Queens, and King Counties, New Brunswick Department of Natural Resources and Energy, Mineral Resources, Mineral report 5, 169 p.

Whalen, J.B., Currie, K.L., and Chappell, B.W., 1987. A-type granites: geochemical characteristics, discrimination and petrogenesis. Contributions to Mineralogy and Petrology, 95: 407-419.

Yang, X.M., Lentz, D.L., and McCutcheon, S.R., 2003. Petrochemical evolution of subvolcanic granitoid intrusions within the Late Devonian Mount Pleasant Caldera, southwestern New Brunswick, Canada: comparison of Au versus Sn-W-Mo-polymetallic mineralization systems. Atlantic Geology, 39: 97-121.

Methodology for solute characterization of fluid inclusions by petrographic and SEM/EDS complementary analysis

F. Tweedale[1], J.J. Hanley[1], D.J. Kontak[2] and N. Rogers[3]

1. Department of Geology, Saint Mary's University, Halifax, Nova Scotia
2. Department of Earth Sciences, Laurentian University, Sudbury, Ontario
3. Geological Survey of Canada, 601 Booth Street, Ottawa, Ontario

Abstract: A cost-effective, simple, and time-efficient method to determine the bulk composition of fluid inclusions is evaporate mound analysis. This method is semi-quantitative and determines inclusion composition by integrating SEM imaging with energy-dispersive analysis of precipitates, or mounds, produced by thermal decrepitation of fluid-inclusions. The method is applicable to magmatic-hydrothermal systems where fluid inclusions contain solute ions (e.g., Na, K, Ca, Cl, F). In order to assess the application of this method for evaluating hydrothermal evolution and metal fertility with regards to intrusion-related mineralisation, a test study is being conducted on the large (7800 km^2) and variably mineralized (e.g., Sn, W, Cu, U, Mo, Ta) South Mountain Batholith (SMB) of Nova Scotia.

Decrepitate mounds were analyzed using a LEO 1450VP (SEM) imaging system linked to an Oxford X-Max 80 mm^2 SDD detector energy-dispersive detector. Based on decrepitating over a range of temperatures, from 325°C to 500°C, it appears that T = 500°C is optimal to produce large, well-shaped, and readily identifiable mounds. To optimize analysis time and, hence, increase research efficiency while maintaining result accuracy, data were collected with 5, 10, and 30 second acquisition times. The number of analyses required to produce representative results was also tested by comparing the results for 4, 8, 16, 32, and 64 mound analyses for individual samples. Results indicate that optimal procedures require multiple (N = 12) point-mode analyses on individual decrepitate mounds to substantiate mound heterogeneity, and that in order to accurately reflect in-situ fractionation a single, 10 second raster-mode analysis is the best approach.

These optimal analytical protocols are being applied to a regional study of the SMB to determine their suitability as mineral fertility indicator and/or vector to ore mineralisation. This test case is the first of its kind conducted on a batholithic scale, with the resulting methodological protocols being readily exportable for the mineral fertility assessment of other regions. Data interpretation protocols integrate a granitic petrographic alteration index, fluid inclusion types, density and evaporate mound chemistry. Samples are chosen such that the entire batholith may be assessed, with all mapped lithologies represented. Fluid compositions determined thus far include brines with 5-20 % fluorine, which is quantitatively indeterminable using other methods, and has been linked as primary control on the transport and deposition of ore in porphyry- and greisen-style mineralisation.

Originally presented Geology Matters - Exploration and Mining Expo Nova Scotia, Halifax, NS, November 12-13, 2014.

Corresponding author: Fergus Tweedale (fergus.tweedale@smu.ca)

Tweedale, F., Hanley, J.J., Kontak, D.J., and Rogers, N., 2015. Methodology for solute characterization of fluid inclusions by petrographic and SEM/EDS complementary analysis; *in* TGI 4 – Intrusion Related Mineralisation Project: New Vectors to Buried Porphyry-Style Mineralisation, (ed.) N. Rogers; Geological Survey of Canada, Open File 7843, p. 569-570.

Methodology for solute characterization of fluid inclusions by petrographic and SEM/EDS complementary analysis

Fergus Tweedale[*1], Jacob Hanley[1], Dan Kontak[2] and Neil Rogers[3]

[1]Saint Mary's University, Halifax (fergus.tweedale@smu.ca); [2]Laurentian University, Sudbury; [3]Geological Survey of Canada, Ottawa

Saint Mary's University Since 1802 — One University. One World. Yours.

Laurentian University / Université Laurentienne

Geological Survey of Canada with Provincial and Territorial Collaboration

TGI 4 Ore Systems

INTRODUCTION

Hydrothermal-magmatic mineral deposits are an important subset of all mineral deposits, and given the nature of these deposits, it is expected that a fingerprint of the mineralizing fluids may be manifested both petrographically and by the chemistry of aqueous fluid inclusions hosted in the rocks on a scale equal to or larger than the mineralized centres. The combination of petrography and SEM/EDS evaporate mound analysis is an effective technique for characterizing fluid inclusion types, and for quantitatively assessing fluid-inclusion solute compositions. The methodology described herein is applied to a granitoid sample suite (N = 66) that is representative of a large (~7500 Km^2), variably mineralized batholith. The integration of results from qualitative petrography and SEM/EDS chemical analysis provides a rigorous assessment of fluid - rock interaction that could help guide future localized research in the South Mountain Batholith. However, the robust nature of the technique makes possible its application to any geological setting in which fluid inclusions occur. Beyond the practical benefits of cost efficiency and of a relatively simple methodology, the technique described in this paper also features particular analytical advantages over other, more costly and time-consuming techniques that are commonly applied to fluid-inclusion research.

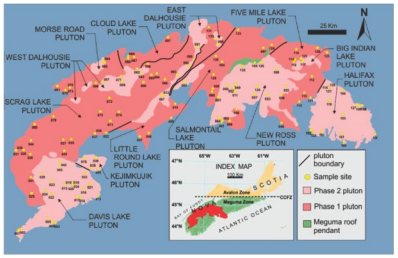

Fig. 1. Geological map of study area. The Devonian South Mountain Batholith of Nova Scotia is a mineralized granitoid complex composed of two contiguous phases of plutons. An objective of this research to evaluate the chemical composition of FIs across the entire SMB. (Map boundaries: NSDNR)

METHODOLOGY

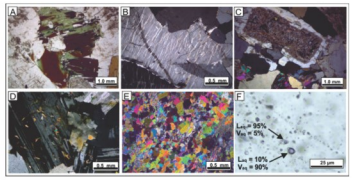

Fig. 2. Photomicrographs of polished thin sections illustrating degree of fluid:rock interaction in the South Mountain Batholith. A. Well-developed chloritization of primary biotite grain. B. K-feldspar megacryst exhibiting flame perthite. C. Coarse-grained feldspar grain exhibiting sericitization of core. D. Saussuritization of Ca-plagioclase. E. Intergrowth of white mica. F. Fluid-inclusion assemblages hosted in annealed quartz

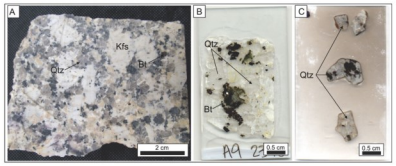

Fig. 3. Preparation of samples for SEM/EDS analysis. A. A slab sample for one hundred 10 x 10 Km2 grid squares covering the study area is collected. B. Fluid inclusion wafers are prepared for petrographic evaluation and identifying of targeted fluid inclusions. C. Chips containing abundant fluid inclusions, hosted by quartz, are cut from the wafer and immediately carbon coated (10 – 20 µm veneer).

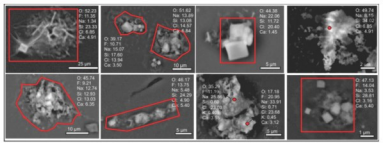

Fig. 4. Evaporate mounds. During sample heating, fluid inclusion decrepitate, or burst, and solute species precipitate within the vicinity of evacuated fluid inclusion pits. Evaporate mounds are amenable to EDS analysis, from which the chemical composition of the fluid inclusions is determined. Red boxes bound areas of raster mode analyses and red circles indicate location of point mode analyses.

RESULTS

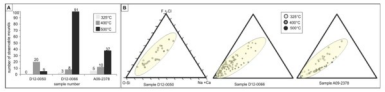

Fig. 5. Optimizing decrepitation temperature. A. Histogram showing number of mounds generated vs oven temperature. B. Composition of evaporate mounds.

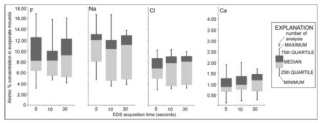

Fig. 6. Optimizing run time. Plots of mound analysis vs EDS acquisition time.

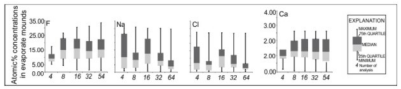

Fig. 7. Optimizing sampling. Plots of mound composition vs number of analysis.

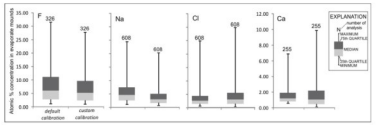

Fig. 8. Calibration of instrument to improve analytical precision.

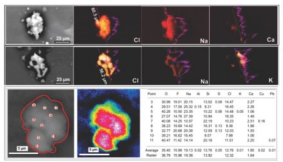

Fig.9. Substantiating mound heterogeneity (fractionation during decrepitation).

DISCUSSION

The results produced from this study suggest two points worthy of discussion: 1) the presence of Ca-bearing fluid, 2) enrichment of fluorine in F-Na-Ca FI populations Fig. 10).

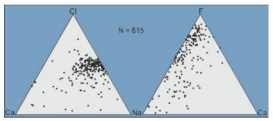

Fig. 10. Ternary plots of major solute compositions of SMB fluid inclusions.

The unexpected enrichment of F is likely the first recognition of this phenomenon in granitic bodies on such a scale anywhere. Enrichment of F suggests the generation of an F-rich fluid is part of the natural evolution of the system and consistent with the presence of topaz in the most evolved magmatic rocks and as part of mineralized greisens. In addition, that F enrichment occurs in the same fluid with Ca indicates a possible cause and effect relationship which we suggest relates to the reactive capacity of the original exsolved Na-F fluid.

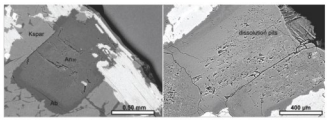

Fig. 11. BSE image images of a SMB monzogranite. A) Plagioclase (An30) grain mantled by albite and surrounded by perthitic K-feldspar. B) Close-up of the plagioclase core showing pitted area surrounded by the fresh plagioclase

The Ca-bearing fluid may reflect the petrographic observation of extensive albitization of plagioclase, which occurs in all samples. This alteration process could explain the distinctive pitted texture in the altered feldspar and the liberation of calcium to the fluid. The process is attributed to the reaction of an orthomagmatic fluid with already crystallized granite.

Natural Resources Canada / Ressources naturelles Canada — Canada

TGI 4: Investigating structural and tectonic controls on Devonian intrusion related mineralisation on the Connaigre Peninsula, Newfoundland

N. Rogers[1], G. Ruberti[2], D.A. Kellett[1], C.R. van Staal[3] and J. Hanchar[2]

1 Geological Survey of Canada, 601 Booth Street, Ottawa, Ontario

2. Memorial University of Newfoundland, St John's, Newfoundland and Labrador

3. Geological Survey of Canada, Vancouver, British Columbia

Abstract: Targeted Geoscience Initiative 4 (TGI 4) is a 5 year Government of Canada program to help produce the next generation of innovative geoscience knowledge and analytical techniques that will result in more effective targeting of buried mineral deposits. The Geological Survey of Canada in collaboration with provincial and territorial surveys, industry and academia will conduct thematic, knowledge-driven projects based around ore systems. The thematic nature of TGI 4 means that individual projects are not defined by geographic region, but instead integrate data and knowledge from multiple sites across Canada, to optimise ore system categorisation.

Intrusion related (e.g., porphyry) deposits are the most important sources for Cu, Mo, W and Sn, along with Au, Ag, and PGEs. Porphyry deposits are large, low- to medium-grade deposits in which mineralisation is hosted within and immediately surrounding distinctive intrusive phases within larger intrusive complexes that commonly have a complex and prolonged emplacement history. The metallogenic contents of intrusion related deposits are diverse, reflecting a variety of tectonic settings.

The Connaigre Peninsula was selected to study the structural and tectonic controls on the formation of granitoid intrusion-related Sn-W-Mo mineralisation as it contains a variety of supracrustal units plus (apparently) barren and mineralised intrusives within a relatively constrained and accessible area. The main mineralised zones are related to the ca. 376 Ma Old Woman Stock and ca. 377 Ma phase of the Ackley Granite (Rencontre Lake facies of Tuach, 1987).

The detailed bedrock map of O'Brien (1992) has been simplified to highlight the main lithotectonic packages. Their distributions indicate three distinct tectonic blocks (herein Gander, Deadman's Bight and Wreck Cove blocks) that were amalgamated during the Devonian along major fault zones. The topographically prominent Hermitage Bay Fault has traditionally been considered to represent the Gander – Avalon boundary in this area. However, the recently obtained Silurian age for the Pass Island Granite indicates against this, as Avalonia (sensu lato) was on the passive margin at that time. In contrast to the Hermitage Bay Fault, the White Horse – East Bay fault zone, although major break, is obscured by younger sequences and so its exact position is unknown. It is interpreted to be positioned to the north-west of the Cambrian passive margin style sequences of the Young's Cove Group. In this model the White Horse – East Bay fault zone also separates the Upper Devonian Poole's Cove and Great Bay De L'Eau formations. As these formations: i) occupy approximately the same stratigraphic position; ii) are both red to buff coloured sandstone to boulder conglomeratic sequences; and iii) both appear to unconformably overlie the likely Lower Devonian Cinq Isles Formation, they are considered as a single map unit for this study.

Originally presented AMEBC Mineral Exploration Roundup 2015, Vancouver, BC, January 25-28, 2015.

Corresponding author: Neil Rogers (nrogers@nrcan.gc.ca)

Rogers, N., Ruberti, G., Kellett, D.A., van Staal, C.R., and Hanchar, J., 2015. TGI 4: Investigating structural and tectonic controls on Devonian intrusion related mineralisation on the Connaigre Peninsula, Newfoundland; *in* TGI 4 – Intrusion Related Mineralisation Project: New Vectors to Buried Porphyry-Style Mineralisation, (ed.) N. Rogers; Geological Survey of Canada, Open File 7843, p. 571-572.

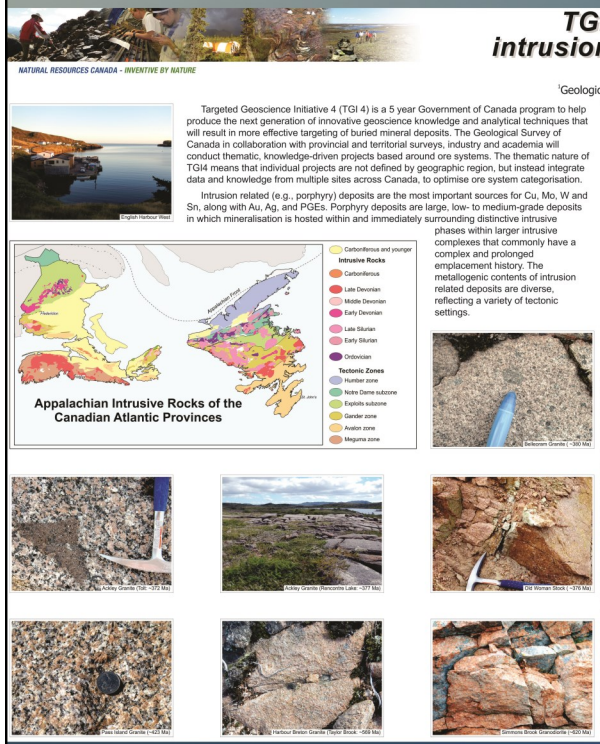

TGI 4: Investigating structural and tectonic controls on Devonian intrusion related mineralisation on the Connaigre Peninsula, Newfoundland

Neil Rogers[1*], Giorgio Ruberti[2], Dawn Kellett[1], Cees van Staal[3] and John Hanchar[2]

[1]Geological Survey of Canada, Ottawa; [2]Memorial University of Newfoundland, St John's; [3]Geological Survey of Canada, Vancouver: *corresponding author - nrogers@nrcan.gc.ca

English Harbour West

Targeted Geoscience Initiative 4 (TGI 4) is a 5 year Government of Canada program to help produce the next generation of innovative geoscience knowledge and analytical techniques that will result in more effective targeting of buried mineral deposits. The Geological Survey of Canada in collaboration with provincial and territorial surveys, industry and academia will conduct thematic, knowledge-driven projects based around ore systems. The thematic nature of TGI4 means that individual projects are not defined by geographic region, but instead integrate data and knowledge from multiple sites across Canada, to optimise ore system categorisation.

Intrusion related (e.g., porphyry) deposits are the most important sources for Cu, Mo, W and Sn, along with Au, Ag, and PGEs. Porphyry deposits are large, low- to medium-grade deposits in which mineralisation is hosted within and immediately surrounding distinctive intrusive phases within larger intrusive complexes that commonly have a complex and prolonged emplacement history. The metallogenic contents of intrusion related deposits are diverse, reflecting a variety of tectonic settings.

Belleoram Granite (~390 Ma)

Ackley Granite (Tick ~372 Ma)

Ackley Granite (Rencontre Lake ~377 Ma)

Old Woman Stock (~378 Ma)

Pass Island Granite (~423 Ma)

Harbour Breton Granite (Taylor Brook ~569 Ma)

Simmons Brook Granodiorite (~420 Ma)

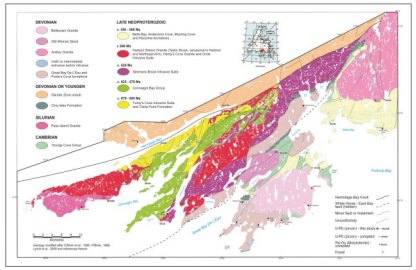

The Connaigre Peninsula was selected to study the structural and tectonic controls on the formation of granitoid intrusion-related Sn – W – Mo mineralisation as it contains a variety of supracrustal units plus (apparently) barren and mineralised intrusives within a relatively constrained and accessible area. The main mineralised zones are related to the ca. 376 Ma Old Woman Stock and ca. 377 Ma phase of the Ackley Granite (Rencontre Lake facies of Tuach, 1987).

The detailed bedrock map of O'Brien (1992) has been simplified (below) to highlight the main lithotectonic packages. Their distributions indicate three distinct tectonic blocks (herein Gander, Deadman's Bight and Wreck Cove blocks) that were amalgamated during the Devonian along major fault zones. The topographically prominent Hermitage Bay Fault has traditionally been considered to represent the Gander – Avalon boundary in this area. However, the recently obtained Silurian age for the Pass Island Granite indicates against this, as Avalonia (sensu lato) was on the passive margin at that time. In contrast to the Hermitage Bay Fault, the White Horse – East Bay fault zone, although major break, is obscured by younger sequences and so its exact position is unknown. It is interpreted to be positioned to the north-west of the Cambrian passive margin style sequences of the Young's Cove Group. In this model the White Horse – East Bay fault zone also separates the Upper Devonian Poole's Cove and Great Bay De L'Eau formations. As these formations: i) occupy approximately the same stratigraphic position; ii) are both red to buff coloured sandstone to boulder conglomeratic sequences; and iii) both appear to unconformably overlie the likely Lower Devonian Cinq Isles Formation, they are considered as a single map unit for this study. That said, field observations of granite clast morphology suggest a significant along strike facies change from Little Bay to Poole's Cove, indicating the primary granitoid detritus source is the ca. 569 Ma Jerseyman's Harbour phase of the Harbour Breton Granite. This determination requires analytical testing, as different aged granites are frequently extremely similar in appearance. To test this, samples are currently being examined for detrital zircon populations at Memorial University via laser ablation - inductively coupled plasma mass spectrometry (LA-ICP-MS) coupled with backscattered electron (BSE) and cathodoluminescence (CL) imaging.

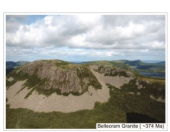

Belleoram Granite (~374 Ma)

Poole's Cove Formation (Upper Devonian)

Great Bay Du L'Eau Formation (Upper Devonian)

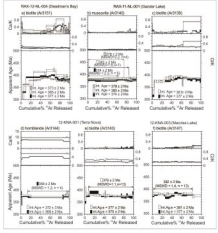

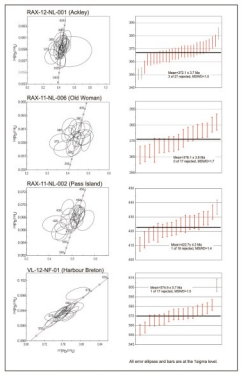

The Old Woman Stock contains several known Mo occurrences; the most accessible is the 376.1 ± 3.8 Ma (U-Pb zircon SHRIMP) Road Cut showing. Molybdenite is disseminated and associated with vugs containing dog-tooth quartz, and intense alteration zones (up to 5 cm wide) localised along N-S to NW-SE trending joints. Based on results from other on-going TGI 4 studies the presence of fluorite is potentially significant, as initial results indicate that HF-rich fluids are an important factor for Sn – W – Mo mineralisation. This site also demonstrates the link between regional structures and the localisation of mineralisation. Macroscopically, the Connaigre Peninsula in the Upper Devonian is in extension due to far removed non-orthogonal accretion of other peri-Gondwanan elements to composite Laurentia. It is notable that the mineralisation does not occur along major faults, but rather at the intersection of a prominent NE to SW lineament and well-developed N-S to NW-SE jointing. The implication is that the high-angle intersection of breaks that are contemporaneous with intrusion but have relatively little motion provide ideal pathways for mineralising fluids.

Pass Island Granite (~423 Ma)

It is hoped that additional age determinations, with chemistry and isotopic analysis, will provide a definitive tectonic association to the Deadman's Bight block. The Silurian Pass Island Granite suggests that this tectonic block was part of composite Laurentia prior to the end of the Salinic Orogen and, as noted by O'Brien et al. (1995), the pre-Devonian sequences are distinct from the Avalon elsewhere in Newfoundland. A possible correlative for the Tickle Point Formation occurs in the Mira Terrane, Cape Breton (Barr et al., 1990; Barr, 1993), whereas the ca. 569 Ma Harbour Breton Granite and Grole Intrusive Suite are (superficially) compositionally similar to the broadly coeval Crippleback Intrusive Suite of central Newfoundland (Rogers et al, 2006).
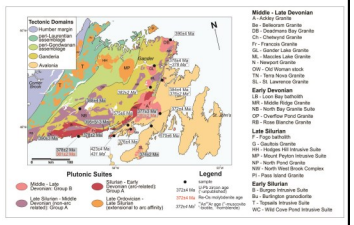
The Belleoram Granite is typified by mafic clots (up to a few centimetres in diameter) that occur throughout the unit, and are taken to indicate hybridisation. An incomplete age of ca. 380 Ma makes the Belleoram geochronologically indistinguishable from the Old Woman Stock. However, clot-bearing granitic dykes that cut mafic dykes, which in turn are correlated to mafic dykes that cut the Old Woman Stock, indicate a somewhat protracted history for Belleoram-type magmatism. Notably some of the Belleoram Granite intrusive contacts appear peperitic (i.e., intruded unlithified sediment). Although it remains unclear why the Belleoram Granite contains no known Sn – W – Mo mineralisation, in stark contrast to the adjacent Old Woman Stock, that it formed at too shallow a level (depositional control) seems most likely.